Radiopharmaceuticals

in Nuclear Pharmacy and Nuclear Medicine

Second Edition

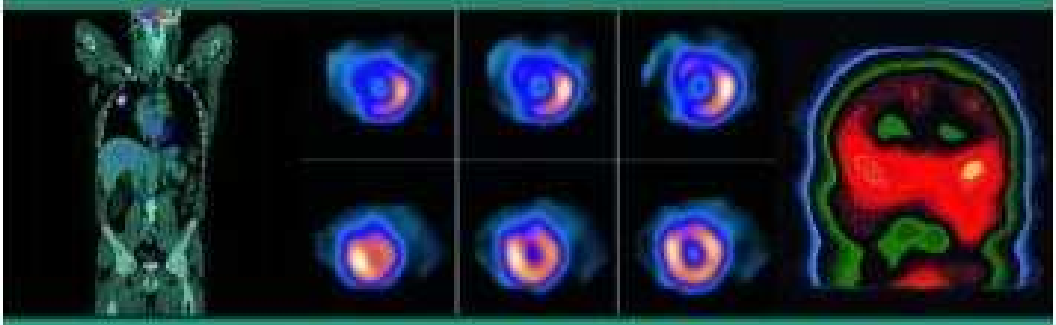

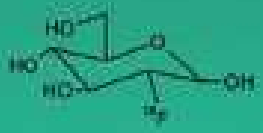

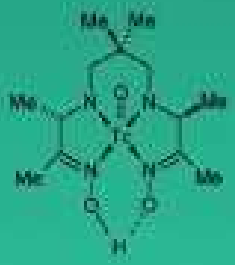

Richard J. Kowalsky
Steven W. Falen

American Pharmacists Association
APhA

Radiopharmaceuticals

in Nuclear Pharmacy and Nuclear Medicine

Second Edition

Radiopharmaceuticals

in Nuclear Pharmacy and Nuclear Medicine

Second Edition

Richard J. Kowalsky, PharmD, BCNP, FAPhA
Associate Professor of Pharmacy
Associate Professor of Radiology
University of North Carolina
Chapel Hill, North Carolina

Steven W. Falen, MD, PhD
Director of Nuclear Medicine and PET Services
Riverside Regional Medical Center
Newport News, Virginia

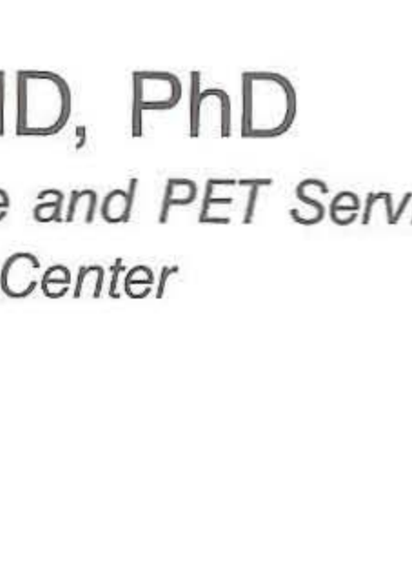

American Pharmacists Association
Washington, D.C.

Editor: Nancy Tarleton Landis
Acquiring Editor: Sandra J. Cannon
Layout and Graphics: Roy A. Barnhill
Proofreading: Kathleen K. Wolter
Indexing: L. Pilar Wyman

APhA was founded in 1852 as the American Pharmaceutical Association.

Published by the American Pharmacists Association
2215 Constitution Avenue, N.W.
Washington, DC 20037-2985

To comment on this book via e-mail, send your message to the publisher at aphabooks@aphanet.org.

Library of Congress Cataloging-in-Publication Data

Kowalsky, Richard J.
Radiopharmaceuticals in nuclear pharmacy and nuclear medicine / Richard J. Kowalsky, Steven W. Falen.-- 2nd ed.
p. ; cm.
Rev. ed. of: Radiopharmaceuticals in nuclear medicine practice. c1987.
Includes bibliographical references and index.
ISBN 1-58212-031-5
1. Radioisotope scanning. 2. Radiopharmaceuticals. 3. Radioisotopes in pharmacology. [DNLM: 1. Radiopharmaceuticals--diagnostic use. 2. Radiopharmaceuticals--therapeutic use. 3. Nuclear Medicine. 4. Radiochemistry--methods. WN 440 K88r 2004] I. Falen, Steven W. II. Kowalsky, Richard J. Radiopharmaceuticals in nuclear medicine practice. III. Title.

RC78.7.R4K69 2004
616.07'575--dc22

2004011196

Acknowledgments

We owe a great debt of gratitude to several individuals who helped to bring this book to fruition. These people include James F. Cooper, PharmD, for his recommendations regarding biologic control testing of radiopharmaceuticals; Marija Ivanovic, PhD, for her recommendations on radiation detection, instrumentation, and statistics; Wenbin Lin, PhD, for his helpful discussions of stereochemistry; Gary Pollack, PhD, for his recommendations and helpful discussions of pharmacokinetic principles; and Stanley Shaw, PhD, for his input on the history of nuclear pharmacy.

We extend our deep appreciation to the nuclear pharmacy students at the University of North Carolina School of Pharmacy who critiqued many of the chapters and provided constructive criticism to improve the clarity. These individuals include Miles Bare, Ben Borders, Song Bui, Thomas Carter, Mark Chen, Radu Ciocan, Chris Cornish, Seboo Dhakhura, Megan Fales, Don Haslam, Sean Hatfield, Hayden Honeycutt, Heather Johnson, Matt Ju, RJ Kulyk, Angie McKeehan, Cecilia Reyes, Lysa Turner, Matt Wead, and Kevin Wiltz.

We also are most grateful to our editor, Nancy Landis, for her insights, constructive suggestions, and attention to detail during the editing of this book, and to Julian Graubart, Director, Books and Electronic Products Department at APhA, for his guidance and patience during the writing of this textbook.

Finally, we would like to acknowledge J. Randolph Perry, MD, now deceased, the coauthor of the previous edition. His material in that edition was useful in the preparation of this one, and several of the images he contributed remain in the current edition.

Contents

Preface

Radiopharmaceuticals in Nuclear Pharmacy and Nuclear Medicine, Second Edition, follows the same basic format as its predecessor, *Radiopharmaceuticals in Nuclear Medicine Practice.* Chapters from that first edition have been rewritten and updated, and new chapters are included. The first 12 chapters deal with the physical and chemical properties of radiopharmaceuticals and their safe handling and control, while the remaining 11 chapters deal with the biologic properties of radiopharmaceuticals and their clinical application in nuclear medicine.

The book begins with an overview of radiopharmaceuticals used in nuclear medicine and pharmacy, followed by discussions of radioactive decay, radiation detection and measurement, radiation protection and risk, radiation safety, radiation biology, licensing and regulatory controls, radionuclide production, radiopharmaceutical chemistry, positron emission tomography (PET) radiopharmaceuticals, the nuclear pharmacy, and quality control. The chapters on radiation biology and PET radiopharmaceuticals are new to this edition. Together, these first 12 chapters present the essential information needed for a pharmacist to become an authorized nuclear pharmacist.

Chapter 1 contains an overview of the general properties of radiopharmaceuticals and their distribution patterns after administration and an introduction to the types of procedures performed in nuclear medicine. New to this edition is a history of the development of nuclear pharmacy as a specialty practice, covering key events in the evolution of nuclear pharmacy practice, the development of programs for training nuclear pharmacists, and the certification process for recognition of nuclear pharmacy as the first pharmacy specialty by the Board of Pharmaceutical Specialties.

The next few chapters expand upon the physical aspects of radiopharmaceuticals, covered in Chapter 2 in the previous edition. Chapter 2 of this edition reviews atomic physics, radioactive decay, and radioactivity. Covered in Chapter 3 are the interactions of radiation with matter and instrumentation for radiation detection, plus a new section on counting statistics. Chapter 4 addresses radiation measurement and protection, radiation dosimetry, and the new topic of radiation risk assessment.

Chapter 5 is a new chapter that expands the topic of radiation safety. It includes a discussion of radiation protection organizations; radiation safety programs; radiation safety terms and units; sources of radiation exposure in nuclear pharmacy and nuclear medicine; personnel and area monitoring; radiation worker notices, reports, and instructions; and the receipt, shipment, and disposal of radioactive material.

Chapter 6 is a new chapter on the biologic effects of ionizing radiation. It begins with a discussion of the effects of radiation on cellular biologic systems and includes genetic effects, effects on cell cycles, radiosensitivity, and the effects of dose fractionation. Also covered are the biologic effects of whole-body irradiation, the carcinogenic and hereditary effects of radiation exposure, radiation effects on the embryo and fetus, and radiation-induced cataractogenesis.

An expanded discussion of licensing and regulatory control of radioactive material is presented in Chapter 7, authored by Neil A. Petry, MS, BCNP, of the Duke University Medical Center in Durham, North Carolina. It begins with a review of nuclear pharmacy practice guidelines, then delves into drug regulation by the Food and Drug Administration and regulation of radioactive material by the Nuclear Regulatory Commission (NRC). Specific regulations on radiopharmaceuticals, including PET drugs, and investigational

new drug (IND), new drug application (NDA), and abbreviated new drug application (ANDA) processes are described. The chapter concludes with a comprehensive review of NRC regulations for the medical use of radiopharmaceuticals, specifically of the newly revised Part 35 regulations in Title 10 of the Code of Federal Regulations.

Chapter 8 deals with the production of radionuclides for medical use. It covers nuclear reactions; radionuclides produced in nuclear reactors, cyclotrons, and linear accelerators; and generator-produced radionuclides. Generator physics, with emphasis on the ^{99m}Tc generator, is also discussed.

Chapter 9 is a greatly expanded discussion of radiopharmaceutical chemistry, presenting many recent developments. This chapter includes ideal properties of radiopharmaceuticals, radiopharmaceutical development and classification, and a basic chemistry review covering bonding concepts, stereochemistry concepts, and radiometal solution chemistry. A discussion of technetium chemistry follows, including the development of first- and second-generation technetium compounds and the preparation and properties of specific technetium radiopharmaceuticals from kits. A discussion of radioiodine radiopharmaceuticals includes the solution chemistry of radioiodine, radioiodination methods, and the preparation and properties of radiopharmaceuticals labeled with iodine isotopes. The remainder of Chapter 9 discusses the chemistry of other radionuclides used in nuclear medicine (gallium, indium, thallium, xenon, chromium, cobalt, phosphorus, strontium, yttrium, and samarium) and the preparation and properties of their radiopharmaceuticals.

Chapter 10 is a new chapter on PET radiopharmaceuticals, authored by Stephen M. Moerlein, PhD, BCNP, of the Mallinckrodt Institute of Radiology in St. Louis, Missouri. It covers the basic concepts of PET, including scanner design and data acquisition, PET/computed tomography (CT) scanners, and imaging applications including blood flow, metabolism, and neuroreceptor studies. Reimbursable PET procedures for oncology, neurology, and cardiology are discussed, as are production of PET nuclides from generators and cyclotrons. A thorough discussion of PET radiopharmaceutical chemistry includes the preparation and properties of radiolabeling precursors, PET radiopharmaceutical synthesis, and systems for preparing PET drugs for clinical use. Also included in the chapter are a discussion of reformulation procedures used in PET radiopharmaceutical preparation and a brief discussion of quality assurance and regulatory issues related to PET radiopharmaceuticals.

Chapter 11, on the nuclear pharmacy, was authored by Kristina M. Wittstrom, BS, BCNP, of the University of New Mexico in Albuquerque and begins with a brief history of the development of nuclear pharmacy. It then covers facilities and equipment necessary to operate a nuclear pharmacy, radiation detection instrumentation, ancillary equipment and supplies, and personnel. Nuclear pharmacist responsibilities are discussed; these include radiopharmaceutical procurement, compounding, quality assurance, dispensing, distribution, health and safety issues in practice, professional consultation, and the monitoring of patient outcomes. The chapter concludes with a discussion of record-keeping issues.

Chapter 12 is an in-depth discussion of radiopharmaceutical quality control, authored by Joseph C. Hung, MS, PhD, BCNP, of the Mayo Clinic in Rochester, Minnesota. An overview of quality control is followed by discussion of specific areas, including radionuclide, radiochemical, pharmaceutical, and biologic considerations. The chapter comprehensively covers the instrumentation and methods used to assess radiopharmaceutical identity, quantity, and purity. A discussion of instrumentation quality control includes dose calibrators and survey instruments. The chapter ends with a discussion of quality control issues specific to PET drug products.

The remaining 11 chapters cover the diagnostic and therapeutic use of radiopharmaceuticals. Chapters on specific body systems (brain; thyroid; heart; lung; liver, spleen, and

gastrointestinal tract; kidney; and bone) are followed by a chapter on total body procedures. Two new chapters cover monoclonal antibodies and therapeutic radiopharmaceuticals. This edition retains the chapter on in vivo function studies from the previous edition, but the chapter on in vitro studies has been removed because these studies are no longer a significant part of nuclear medicine practice.

Chapters 13 through 20, on the major organ systems, follow the same format. Each discusses physiologic processes important to the localization of imaging agents and describes the development of radiopharmaceuticals used to study the particular organ system. The focus is on current agents of choice, their biologic properties, and their mechanisms of localization. The chapters conclude with a discussion of nuclear medicine procedures, including the rationale, pharmaceutical choices, and interpretation of results. Images are included to illustrate normal and abnormal studies.

Chapter 21, on monoclonal antibodies for diagnostic use, begins with a review of the immune system and proceeds with a discussion of antibody structure, classification, development, modification, antibody–antigen interactions, and nomenclature. General antibody labeling methods are discussed, as are specific diagnostic antibodies and their preparation, properties, and use.

Chapter 22 covers in vivo function studies. These nonimaging studies include blood volume measurement and tests for vitamin B_{12} deficiency. The underlying principles involved in each study and the radiopharmaceuticals used are discussed.

Chapter 23 is a new chapter on therapeutic radiopharmaceuticals, including monoclonal antibodies. It begins with a discussion of radioimmunotherapy principles and radionuclide and antibody requirements for treating tumors. This is followed by a discussion of methods used in radioimmunotherapy and a description of the preparation, properties, and use of therapeutic monoclonal antibodies. The chapter concludes with a discussion of non-antibody therapeutic radiopharmaceuticals: radiotherapy of bone pain and ^{32}P therapy for polycythemia, effusions, and radiation synovectomy. The chapter concludes with a brief discussion of brachytherapy for brain tumors using the ^{125}I product Iotrex.

Some 150 tables and 440 figures are included to enrich and illustrate the text. Each chapter is referenced to the primary literature so that readers can find more detailed information on a topic. The comprehensive nature of this book makes it suitable for use as a reference by nuclear pharmacy practitioners, nuclear medicine technologists, and nuclear medicine physicians. The book should also be useful in programs for educating these practitioners.

Although the title of this edition emphasizes nuclear pharmacy, emphasis on radiopharmaceutical use in nuclear medicine has not decreased; the book has expanded in both areas. The work of four co-authors who are both practitioners and educators not only helped us complete the book but enriched its content. We are grateful for their willingness to add this work to their busy professional lives.

Richard J. Kowalsky
Steven W. Falen
2004

Contributors

Joseph C. Hung, MS, PhD, BCNP
Professor of Pharmacy
Professor of Radiology
Mayo Clinic College of Medicine
Director of Nuclear Pharmacy Laboratories and PET Radiochemistry Facility
Mayo Clinic
Rochester, MN

Stephen M. Moerlein, PhD, BCNP
Associate Professor of Radiology and Biochemistry
The Edward Mallinckrodt Institute of Radiology
Washington University School of Medicine
St. Louis, MO

Neil A. Petry, MS, BCNP, FAPhA
Assistant Professor in Radiology
Director, Radiopharmacy and Nuclear Medicine Laboratory
Duke University Medical Center
Durham, NC
Clinical Assistant Professor of Pharmacy Practice
School of Pharmacy
Campbell University
Buies Creek, NC

Kristina M. Wittstrom, BS, BCNP
Research Lecturer
Radiopharmacy
College of Pharmacy
University of New Mexico
Albuquerque, NM

1 Radiopharmaceuticals, Nuclear Medicine, and Nuclear Pharmacy: An Overview

Identifying the beginning of nuclear medicine and defining the field depend upon one's perspective on the application of radiation to human disease. If the focus is on the use of natural radioactive material, then nuclear medicine implicitly started in 1901 when the French physician Henri Danlos used radium (a natural element) to treat a tuberculous skin lesion.[1] If the focus is on artificial radioisotopes, then nuclear medicine started after 1934, when the French radiochemists Frederic Joliot and his wife, Irene Curie Joliot, produced the first artificial radioisotope, phosphorus 30 (^{30}P). In the latter case, nuclear medicine began either with George Hevesy's successful use of radiophosphorus in healthy animals in 1935 or with Joseph Hamilton's attempts to treat leukemic patients with sodium 24 (^{24}Na) in 1936. The cyclotron was introduced around that time, and the resulting investigative ferment produced numerous radionuclides that were applied to diagnosis and therapy. Nuclear medicine as officially defined in 1967 was "the specialty of the practice of medicine dealing with the diagnostic, therapeutic (exclusive of sealed radiation sources) and investigative use of radionuclides." Since that time, however, the field has changed extensively.

The application of magnetic resonance imaging (MRI) methods to allow diagnosis without the use of radioactive material inspired a new definition of nuclear medicine that reflected the use of nuclear properties from stable nuclides. In February 1983 the Society of Nuclear Medicine board of trustees adopted the following definition: "the medical specialty which utilizes the nuclear properties of radioactive and stable nuclides for diagnostic evaluation of the anatomic and/or physiologic conditions of the body and provides therapy with unsealed radioactive sources." With the exception of MRI, the practice of nuclear medicine is accomplished primarily through the application of radiopharmaceutical agents in diagnosis and therapy, which is the focus of this book on radiopharmaceuticals in nuclear pharmacy and nuclear medicine practice.

THE RADIOPHARMACEUTICAL

A radiopharmaceutical can be defined as a chemical substance that contains radioactive atoms within its structure and is suitable for administration to humans for diagnosis or treatment of disease. In short, it is a radioactive drug. Radiopharmaceuticals are formulated in various chemical and physical forms to target radioactivity to particular parts of the body. Gamma radiation emitted from diagnostic radiopharmaceuticals readily escapes from the body, permitting external detection and measurement. The pattern of distribution of radiation in an organ system over time permits the nuclear medicine physician to make a diagnostic evaluation of system morphology and function. A therapeutic radiopharmaceutical emits particulate radiation (beta particles) that deposits energy within the organ

being treated for disease. Some radionuclides, such as ^{32}P, emit only beta radiation, while other radionuclides, such as ^{131}I, emit beta and gamma radiation simultaneously and therefore possess both therapeutic and diagnostic usefulness.

NUCLEAR MEDICINE PROCEDURES

Examining the types of procedures routinely performed in nuclear medicine is helpful in understanding how radiopharmaceuticals are used. These procedures can be divided into three categories: (1) imaging procedures, (2) in vivo function studies, and (3) therapeutic procedures. The first two categories are diagnostic in nature and account for most of the studies performed in nuclear medicine.

Imaging Procedures

Imaging procedures provide diagnostic information based on the distribution pattern of radioactivity in the body. The procedures are either dynamic or static. *Dynamic studies* provide functional information through measurement of the rate of accumulation and removal of the radiopharmaceutical by the organ. *Static studies* provide morphologic information regarding organ size, shape, and position or the presence of space-occupying lesions, and in some cases relative function.

Detection and measurement of organ radioactivity is usually done with a gamma camera, an electronic device with a radiation detector large enough to visualize, in most cases, the entire organ of interest (Figure 1-1). Before the days of gamma cameras, images were made with rectilinear scanners. The rectilinear scanner detector was 3 to 5 inches in diameter and required multiple passes or scans over the area of interest in a rectangular and linear fashion to obtain an image of the entire organ. Because of this technique, imaging procedures are still referred to as "scans."

Dynamic imaging studies require that the camera detector be positioned over the organ of interest before injection of the radiopharmaceutical, so that the camera is able to capture the radioactivity as it enters and leaves the organ. Information collected can be stored in a computer for further analysis or permanently recorded on photographic film. An example of a dynamic study is the renogram, which is performed to assess kidney function. A kidney-localizing radiopharmaceutical, such as ^{99m}Tc-mertiatide, is injected intravenously, and the time course of its transport and excretion by the renal tubular cells is measured. With normal kidney function, the time to peak renal concentration is 3 to 5 minutes after injection and the renal clearance half-life is 12 to 15 minutes. Deviation from these times reflects the presence of varying degrees of kidney disease.

Static imaging studies are performed after a radiopharmaceutical is allowed to accumulate in the organ of interest. Images or "pictures" of the organ are acquired as the camera detector is rotated about the body to obtain multiple-angle views of the organ of interest. Image acquisition requires several minutes to produce a satisfactory image. Making gamma camera images is somewhat analogous to taking a conventional photograph under low-light conditions, where a prolonged shutter speed is required to collect enough light for a clear picture. In both cases, motion artifacts are a concern.

The pattern of radiopharmaceutical distribution in an organ varies with and depends on the particular organ studied and the presence or absence of disease. In some studies, the normal organ readily concentrates the radiopharmaceutical and appears uniformly radioactive or "hot." In these organs, diseased tissue excludes the radiopharmaceutical, and lesions appear as "cold" spots within a "hot" organ. An example is a liver colloid scan obtained after injection of radioactive colloidal particles that localize in the phagocytic

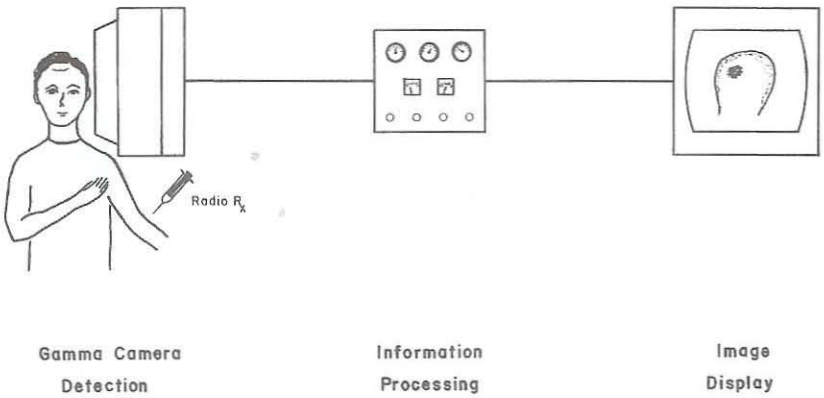

FIGURE 1-1 Schematic of a scintillation gamma camera system demonstrating radiopharmaceutical injection, detection of radioactivity, electronic processing, and image display.

cells of the liver. If a tumor or other lesion is present that displaces colloid-localizing cells, it is visualized as an area of decreased or absent radioactivity. In other types of organ studies the normal organ excludes the radiopharmaceutical, but diseased tissue concentrates it so that lesions appear as "hot" spots within a "cold" organ. An example is a brain scan obtained with an agent normally excluded by the blood–brain barrier. In disease states where the blood–brain barrier is disrupted, however, radioactivity can leave the vascular space to localize in the lesion.

In still other types of studies a normal organ may accumulate the radiopharmaceutical, but diseased tissue may concentrate it either to a greater degree because of increased function or to a lesser degree because of decreased function. An example is thyroid gland imaging with radioactive iodine. The thyroid gland readily accumulates iodine through normal function, but a diseased gland with either hyperfunctioning or hypofunctioning thyroid tissue demonstrates increased or decreased concentration of radioiodine. Examples of these static studies are illustrated in Figure 1-2. They were obtained using a planar imaging camera that produces two-dimensional images. A disadvantage of planar imaging is that lesion detection may be impaired, especially when target-to-background ratios are low or there are overlying structures that obscure view of the lesion. Single-photon emission computed tomography (SPECT) or positron emission tomography (PET) cameras are able to construct computer-generated slice images through an organ in transverse, sagittal, and coronal planes and make possible the visualization of an organ in three dimensions (Figure 1-3). Tomographic imaging, therefore, provides greater depth resolution and delineation of the structural and functional information present.

In Vivo Function Studies

In vivo function studies measure the function of an organ or system based upon the absorption, dilution, concentration, or excretion of radioactivity after administration of a radiopharmaceutical. These studies do not require imaging, but analysis and interpretation is based on counting radioactivity emanating either directly from organs within the body or from blood or urine samples counted in vitro. Some examples of in vivo function studies are (1) the radioactive iodine uptake study to assess thyroid gland function as determined by external measurement of the percentage of a dose of radioiodine taken up by the gland over time, (2) determination of whole blood volume by measuring the dilution of a known amount of intravenously injected ^{51}Cr-labeled red blood cells to determine the red cell

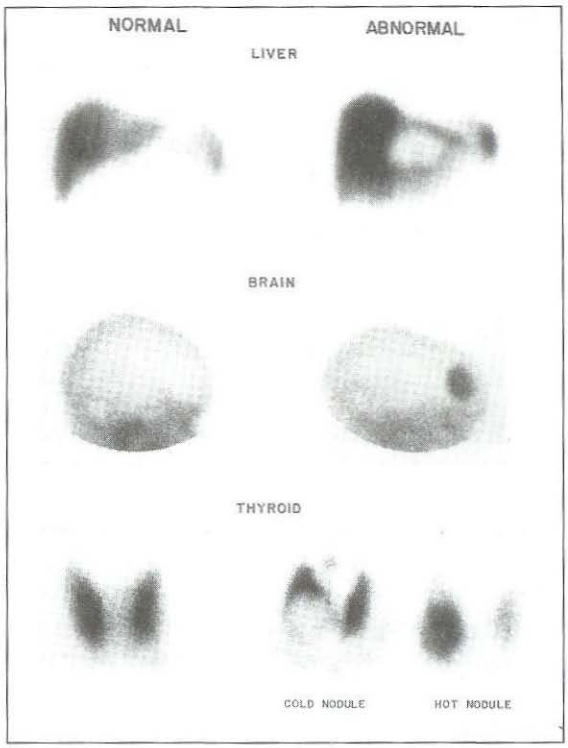

FIGURE 1-2 Typical normal and abnormal static images of organs obtained with a conventional planar imaging gamma camera: anterior view of the liver, lateral view of the brain, and anterior view of the thyroid gland.

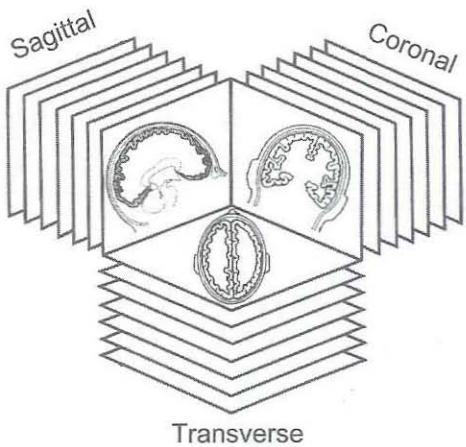

FIGURE 1-3 Diagram of three-dimensional, computer-generated slice images obtained with a gamma camera, showing organ in transverse, sagittal, and coronal planes.

volume, and (3) indirect assessment of vitamin B_{12} absorption from the gastrointestinal tract by measuring the fraction of orally administered radioactive ^{57}Co-labeled vitamin B_{12} that is excreted in the urine over a defined period of time (the Schilling test). An important requirement for in vivo function studies is that the radiopharmaceutical should not alter, in any way, the function of the organ system being measured.

Therapeutic Procedures

Therapeutic procedures in nuclear medicine are on the rise. These procedures are intended to be either curative or palliative and typically rely on the absorption of beta radiation to

destroy diseased tissue. The classic therapeutic procedure is the use of ^{131}I-sodium iodide to treat hyperthyroidism and thyroid cancer. Because ^{131}I is a beta–gamma emitter, it can be used both diagnostically and therapeutically in thyroid disease; however, the therapeutic dosage of radioactivity administered is on average 1,000 to 20,000 times larger than the diagnostic dosage used in measuring thyroid function. Of the radiation dose absorbed by the thyroid gland from ^{131}I, about 90% is from beta radiation and about 10% from gamma radiation. Radioimmunotherapy (RIT) employing radiolabeled antibodies and peptides has achieved some success in treating tumors. Examples of RIT agents are ^{131}I-tositumomab and ^{90}Y-ibritumomab tiuxetan for treating non-Hodgkin's lymphoma. Another significant area of nuclear medicine therapy is palliative procedures for treating pain associated with bone cancer. In this regard agents such as ^{89}Sr-strontium chloride and ^{153}Sm-samarium lexidronam, which are selectively localized in bone, have been used successfully. The therapeutic application of radiation to target tumor-specific tissue will likely become more successful as advances in molecular biologic and chemical techniques are made.

PERSPECTIVE ON RADIOPHARMACEUTICAL USE

The amount of radioactivity administered to a patient in a nuclear medicine study is termed the *dosage* and is typically measured in units of millicuries (mCi, or 10^{-3} Ci). The curie (Ci) is equal to 3.7×10^{10} disintegrations (atoms decaying) per second. In the International System of Units, radioactivity is measured in becquerels (Bq). One Bq is equal to 1 disintegration per second; therefore, 1 mCi = 37 MBq. The amount of radiation absorbed by tissue in the body in which a radioactive substance resides is termed the radiation *dose* and is traditionally measured in rad (radiation absorbed dose). One rad is equal to 100 ergs of energy absorbed in 1 gram of tissue. The International Unit (IU) of absorbed dose, the gray (Gy), is equal to 1 joule of energy absorbed in 1 kg of tissue (1 Gy = 100 rad).

A goal in diagnostic nuclear medicine is to administer the optimum dosage of radioactivity to acquire the desired information with the lowest radiation dose to the patient, that is, to keep the radiation absorbed dose as low as reasonably achievable. This is accomplished, in part, by the use of short-lived radionuclides (radioactive atoms) that decay quickly. Short-lived radionuclides permit larger amounts of radioactivity to be administered without a great increase in radiation absorbed dose.

The radionuclide used in most nuclear medicine studies is ^{99m}Tc. Because of its 6 hour half-life, about 90% of ^{99m}Tc's radioactivity is lost in 1 day. For drug manufacturers supplying ^{99m}Tc radiopharmaceuticals to nuclear medicine facilities in distant locations, this presents significant logistical problems. ^{99m}Tc and other short-lived radiopharmaceuticals therefore require local or in-hospital preparation. Each ^{99m}Tc agent is prepared daily. The preparation and testing procedure includes radiopharmaceutical compounding, measurement of activity, and assessment of radionuclidic purity and radiochemical purity. Aseptic conditions must be maintained during preparation because these agents are administered by intravenous injection. The personnel who perform these functions may be radiochemists, radiopharmacists, or nuclear medicine technologists. Radiochemists and radiopharmacists are usually employed at large medical center hospitals and are instrumental in developing new agents and procedures. Radiopharmacists also practice in centralized nuclear pharmacies located in metropolitan areas, which supply radiopharmaceuticals to nuclear medicine departments at nearby hospitals. Nuclear medicine technologists sometimes have the responsibility of preparing and controlling radiopharmaceuticals in smaller rural hospitals.

Radiopharmaceuticals with longer half-lives are also used in nuclear medicine because of their desirable biochemical properties. A good example is ^{131}I, which has an

TABLE 1-1 Chemical and Physical Forms of Radiopharmaceuticals

Form	Example
Elemental	Xenon 133 (^{133}Xe), krypton 81m (^{81m}Kr)
Simple ions	$^{131}I^-$ (iodide), $^{99m}TcO_4^-$ (pertechnetate)
Labeled small molecules	^{131}I-MIBG (covalently bonded)
	^{99m}Tc-DTPA (chelation compound)
Labeled macromolecules	^{125}I-human serum albumin (protein)
	^{111}In-capromab pendetide (antibody)
Labeled particles	^{99m}Tc-sulfur colloid
	^{99m}Tc-macroaggregated albumin
Labeled cells	^{51}Cr- or ^{99m}Tc-erythrocytes
	^{111}In- or ^{99m}Tc-leukocytes

TABLE 1-2 Routes and Forms of Radiopharmaceutical Administration

Route	Form
Oral	Capsules and solutions
Intravenous injection	Solutions, colloidal dispersions, suspensions
Intrathecal injection	Solutions
Inhalation	Gases and aerosols
Instillation via	Sterile solutions
Eye drops	
Urethral catheter	
Intraperitoneal catheter	
Shunts	

8 day half-life. This is long enough to permit commercial manufacture and testing of ^{131}I radiopharmaceuticals and allows storage in the nuclear medicine laboratory for use when needed. Although ^{131}I has some undesirable physical properties from a radiation dose viewpoint, such as long half-life, high-energy gamma rays, and beta radiation, iodine's physiologic importance in thyroid work and its chemical reactivity, which allows it to be labeled to different chemical molecules, make it a valuable radionuclide in nuclear medicine.

Table 1-1 lists the general classification of chemical and physical forms of radiopharmaceuticals used in nuclear medicine and illustrates the diverse nature of these agents. These include elemental radionuclides such as the inert gases, simple inorganic ions, radiolabeled molecules, and specialized forms such as labeled particles and blood cells.

Table 1-2 lists the usual routes of administration of radiopharmaceuticals. Contrary to the usual requirement that intravenous injections be true solutions, some radiopharmaceuticals are deliberately particulate to achieve site-specific localization of radioactivity in the body. These specialized dosage forms permit imaging of, for example, the principal organs of the reticuloendothelial system (liver, spleen, and bone marrow) with radiolabeled colloidal particles, the cardiac blood pool with radiolabeled red blood cells, and lung perfusion with albumin aggregates. Table 1-3 lists radiopharmaceuticals used in nuclear medicine.

Radiopharmaceuticals have other unique properties when compared with conventional therapeutic drugs. Intrinsically, they are radioactive and have an associated radiation risk. Therefore, before radiopharmaceuticals are marketed for use in humans, tissue distribution studies are performed in animals to identify the critical organs (those that receive the highest radiation absorbed dose) and to estimate the radiation dose. The

TABLE 1-3 Radiopharmaceuticals Used in Nuclear Medicine

Radionuclide	Dosage Form	Use	Typical Dosage (Adult[a])	Route[b]
Carbon C 11	Carbon monoxide	Cardiac: Blood volume measurement	60–100 mCi	Inhalation
Carbon C 11	Flumazenil injection	Brain: Benzodiazepine receptor imaging	20–30 mCi	IV
Carbon C 11	Methionine injection	Neoplastic disease evaluation in brain	10–20 mCi	IV
Carbon C 11	Raclopride injection	Brain: Dopamine D_2 receptor imaging	10–15 mCi	IV
Carbon C 11	Sodium acetate injection	Cardiac: Marker of oxidative metabolism	12–40 mCi	IV
Carbon C 14	Urea	Diagnosis of *Helicobacter pylori* infection	1 μCi	PO
Chromium Cr 51	Sodium chromate injection	Labeling red blood cells (RBCs) for measuring RBC volume, survival, and splenic sequestration	10–80 μCi	IV
Cobalt Co 57	Cyanocobalamin capsules	Diagnosis of pernicious anemia and defects of intestinal absorption	0.5 μCi	PO
Fluorine F 18	Fludeoxyglucose injection	Glucose utilization in brain, cardiac, and neoplastic disease	10–15 mCi	IV
Fluorine F 18	Fluorodopa injection	Dopamine neuronal decarboxylase activity in brain	4–6 mCi	IV
Fluorine F 18	Sodium fluoride injection	Bone imaging	10 mCi	IV
Gallium Ga 67	Gallium citrate injection	Hodgkin's disease, lymphoma	8–10 mCi	IV
		Acute inflammatory lesions	5 mCi	IV
Indium In 111	Capromab pendetide injection	Metastatic imaging in patients with biopsy-proven prostate cancer	5 mCi	IV
Indium In 111	Indium chloride sterile solution	Radiolabeling various ^{111}In radiopharmaceuticals	Various	
Indium In 111	Indium oxine sterile solution	Labeling autologous leukocytes	500 μCi	IV
Indium In 111	Pentetate injection	Cisternography	500 μCi	Intrathecal
Indium In 111	Pentetreotide injection	Neuroendocrine tumors	3 mCi (planar) 6 mCi (SPECT[c])	IV
Indium In 111	Ibritumomab tiuxetan	Biodistribution imaging prior to therapeutic dosing with ^{90}Y Zevalin (Biogen Idec) in the treatment of non-Hodgkin's lymphoma	5 mCi	IV
Iodine I 123	Sodium iodide capsules and solution	Thyroid gland imaging	400–600 μCi	PO
		Thyroid metastases (total body)	2 mCi	PO
Iodine I 123	Iobenguane injection	Pheochromocytoma, carcinoid tumors, nonsecreting paragangliomas, neuroblastoma	0.14 mCi/kg (child) 10 mCi (adult)	IV
Iodine I 125	Albumin injection	Plasma volume determination	5–10 μCi	IV
Iodine I 125	Iothalamate sodium injection	Glomerular filtration rate (GFR) determination	30 μCi	IV
Iodine I 131	Iobenguane injection	Pheochromocytoma, carcinoid tumors, nonsecreting paragangliomas, neuroblastoma	0.5 mCi/1.7m^2	IV

TABLE 1-3 Radiopharmaceuticals Used in Nuclear Medicine (Continued)

Radionuclide	Dosage Form	Use	Typical Dosage (Adult[a])	Route[b]
Iodine I 131	Sodium iodide capsules and solution	Thyroid function	5–10 μCi	PO
		Thyroid imaging (neck)	50–100 μCi	
		Thyroid imaging (substernal)	100 μCi	
		Thyroid metastases (total body)	2 mCi	
		Hyperthyroidism	5–33 mCi	
		Carcinoma	150–200 mCi	
Iodine I 131	Iodohippurate sodium injection	Recoverable renal function	200 μCi (2 kidneys) 75 μCi (1 kidney)	IV
Iodine I 131	Tositumomab	Treatment of refractory low-grade non-Hodgkin's lymphoma	Patient-specific dosing; not >75 cGy whole body	IV
Nitrogen N 13	Ammonia injection	Myocardial perfusion studies	10–20 mCi	IV
Oxygen O 15	Water injection	Cardiac perfusion	30–100 mCi	IV
Phosphorus P 32	Chromic phosphate suspension	Peritoneal and pleural effusions	10–20 mCi	Intraperitoneal or intrapleural (Not for IV use)
Phosphorus P 32	Sodium phosphate injection	Polycythemia	1–8 mCi	IV
Rubidium Rb 82	Rubidium chloride injection	Myocardial perfusion studies	30–60 mCi	IV
Samarium Sm 153	Lexidronam injection	Bone pain palliation in confirmed osteoblastic metastatic bone lesions	1.0 mCi/kg	IV
Strontium Sr 89	Strontium chloride injection	Bone pain palliation in confirmed osteoblastic metastatic bone lesions	4 mCi	IV
Technetium Tc 99m	Albumin injection	Heart blood pool imaging	20 mCi	IV
Technetium Tc 99m	Albumin aggregated injection	Perfusion lung imaging	3 mCi	IV
Technetium Tc 99m	Arcitumomab	Recurrent or metastatic colorectal carcinoma	20 mCi	IV
Technetium Tc 99m	Bicisate injection	Adjunct to CT/MRI[d] in patients with confirmed stroke	20 mCi	IV
Technetium Tc 99m	Disofenin injection	Hepatobiliary imaging	5 mCi	IV
Technetium Tc 99m	Exametazime injection	With or without methylene blue for regional cerebral perfusion in stroke	20 mCi	IV
		Without methylene blue for leukocyte labeling	10 mCi	IV
Technetium Tc 99m	Gluceptate injection	Brain imaging	20 mCi	IV
		Renal perfusion imaging	10 mCi	IV
Technetium Tc 99m	Mebrofenin injection	Hepatobiliary imaging	5 mCi	IV

Technetium Tc 99m	Medronate injection	Bone imaging	20–30 mCi	IV
Technetium Tc 99m	Mertiatide injection	Kidney imaging	5 mCi	IV
		Renogram—renal transplant	1–3 mCi	IV
		Renogram—captopril	1–3 mCi	IV
Technetium Tc 99m	Oxidronate injection	Bone imaging	20–30 mCi	IV
Technetium Tc 99m	Pentetate injection	GFR (quantitative)	3 mCi	IV
		Renogram (diuretic)	3 mCi	IV
		Renal perfusion imaging	10 mCi	IV
Technetium Tc 99m	Pyrophosphate injection	Infarct-avid scan	15 mCi	IV
TechnetiumTc 99m	Red blood cells injection	GI bleed (intermittent)	15 mCi	IV
TechnetiumTc 99m	Sestamibi injection	Myocardial perfusion and function, parathyroid imaging	8–40 mCi	IV
Technetium Tc 99m	Sodium pertechnetate injection	Brain imaging	20 mCi	IV
		Thyroid imaging	10 mCi	IV
		Radionuclide ventriculogram	20 mCi	IV
		Radionuclide cystography	1 mCi	Urethral
		Dacryocystography	0.1 mCi	Eye drops
		Meckel's diverticulum	5 mCi	IV
Technetium Tc 99m	Succimer injection	Renal scan—differential renal function	5 mCi	IV
		Renal scan—cortical anatomy	5 mCi	IV
Technetium Tc 99m	Sulfur colloid injection	Liver–spleen scan	5 mCi	IV
		Lymphoscintigraphy (breast)	0.4–0.6 mCi	Interstitial
		Lymphoscintigraphy (melanoma)	0.5–0.8 mCi	Intradermal
		Gastric emptying (scrambled egg)	1 mCi	PO
		GI bleed (acute)	10 mCi	IV
		Lung aspiration	5 mCi	PO
		Gastroesophageal reflux	0.2 mCi	PO
Technetium Tc 99m	Tetrofosmin injection	Myocardial perfusion and function	8–40 mCi	IV
Thallium Tl 201	Thallous chloride injection	Myocardial perfusion imaging	3–4 mCi	IV
		Parathyroid imaging	2 mCi	IV
Xenon Xe 133	Xenon	Lung ventilation imaging	10–20 mCi	Inhalation
Yttrium Y 90	Ibritumomab tiuxetan	Treatment of refractory low-grade non-Hodgkin's lymphoma	0.3–0.4 mCi/kg	IV

[a] Except where otherwise noted.
[b] IV = intravenous; PO = oral.
[c] SPECT = single-photon emission computed tomography.
[d] CT =computed tomography; MRI =magnetic resonance imaging.

magnitude of this dose estimate sets limits on the amount of radioactivity that can be safely administered to humans in diagnostic studies.

Radiopharmaceuticals are administered in extremely small amounts, so chemical toxicity is not as great a concern as with traditional pharmaceuticals. In fact, the amount of a radiopharmaceutical administered in a standard dosage is not enough to produce a pharmacologic response. Therefore, the premarket testing required to identify acute and chronic toxic effects of traditional drugs is usually not as extensive for radiopharmaceuticals. For example, a typical 10 μCi diagnostic dose of ^{131}I-sodium iodide contains only 8×10^{-11} gram of iodine, one eighty-millionth of the normal total-body iodine stores and about one two-millionth of the daily dietary intake of iodine. It is easy to see that this amount of radioiodine should pose no threat to patients, even to those who may be allergic to iodine-containing substances.

Because of the radioactive nature of radiopharmaceuticals, there are specific requirements for the safe and efficacious use of these agents. Procedures are needed to protect patients from unnecessary radiation exposure, personnel from the radioactive material that they handle, and the general public from unnecessary exposure to radioactive environmental waste. The use of radioactive material is therefore strictly controlled by state and federal agencies. Because radiopharmaceuticals are radioactive drugs, they are regulated by the U.S. Food and Drug Administration in regard to their chemical safety and efficacy and by the U.S. Nuclear Regulatory Commission (NRC) and the appropriate state licensing agencies in regard to radiation safety. The use of radioactive material in human subjects requires that physicians and paramedical personnel be properly trained and experienced in the handling of such materials and be recognized in this regard by specific licensure.

HISTORICAL PERSPECTIVES IN NUCLEAR PHARMACY: PRACTICE, EDUCATION, AND SPECIALTY CERTIFICATION

Nuclear Pharmacy Practice

In 1950, John Christian[2] published an article encouraging hospital pharmacists to become informed about radioisotopes in medical practice and to take the initiative to establish facilities for handling radioactive material. He also put forth a plan for a laboratory design with a separate "hot element" room for storage and handling operations and a measurement room for low-level radioactive counting. Christian could advise and counsel with authority, because in 1946 he received the first shipment of radioactive isotopes for biochemical research from Oak Ridge National Laboratory and used them in pharmaceutical development at Purdue University School of Pharmacy and Pharmacal Sciences. Soon thereafter, in 1947, he initiated the first formal lecture and laboratory courses in the United States for teaching the basic principles of radioisotope methodology.

The roots of a pharmacist-run nuclear pharmacy (radiopharmacy) service can be traced to the University of Chicago Clinics, where a radioisotope laboratory was established by Chief Pharmacist Paul Parker in the early 1950s[3] and continued to be operated by Chief Pharmacist Peter Solyom.[4] The staff pharmacist in charge of the radioisotope laboratory where radioactive medications were procured and dispensed for patient use was Larry Summers. In those days, decay tables and a slide rule were used to make calculations. After the establishment of this laboratory, a report on radioisotopes in hospital pharmacy was published.[3] The report was the work of the Committee on Isotopes appointed by George Archambault, then president of the American Society of Hospital Pharmacists, to study the role of the hospital pharmacist in handling radioisotopes. The committee had specific charges to develop special courses in isotope handling and to assess the feasibility of an isotope section in a pharmacy department and determine its layout and design.

In 1958 William Briner[5] informed hospital pharmacists about radiopharmacy and introduced them to pertinent terminology and basic considerations of radiologic health. This was followed in 1960 by another article strongly promoting the role hospital pharmacists should have in the preparation and handling of radiopharmaceuticals for patient use, citing the U.S. Atomic Energy Commission (AEC) requirement that "byproduct material shall not be used in humans until its pharmaceutical quality and assay have been established."[6] Although the program at the University of Chicago Clinics predated the program at the National Institutes of Health (NIH), it is well recognized in the profession that Briner, at NIH, established and maintained a long-standing, active practice of nuclear pharmacy, stalwartly promoted the involvement of pharmacists in nuclear medicine, and was directly responsible for training many of those pharmacists. Early radiopharmacist colleagues who worked with Briner were Edgar Adams, Robert Chandler, and Raymond Farkas. Briner preached the value of pharmacist involvement in nuclear medicine through his professional presentations and publications for more than 40 years. For his pioneering efforts he is affectionately remembered as the "father of radiopharmacy." Briner's leadership helped to create the regulatory and practice environment within which nuclear pharmacists and nuclear medicine professionals work today.

The introduction of ^{99m}Tc-sodium pertechnetate into nuclear medicine practice changed the face of practice dramatically. Its clinical use began in 1961 at the University of Chicago, where several ^{99m}Tc-labeled radiopharmaceuticals were developed by Paul Harper and radiopharmacist Kathryn Lathrop.[7] Shortly thereafter, the ^{99}Mo–^{99m}Tc generator became available commercially and the national growth of nuclear medicine procedures escalated. The short half-life of ^{99m}Tc demanded local preparation of pharmaceutical agents labeled with this nuclide and increased the demand for nuclear pharmacy services.

The shortage of pharmacists trained in radioisotope methodology stimulated the establishment of a Master of Science in Radiopharmacy training program at the University of Southern California School of Pharmacy in 1968, under the direction of Walter Wolf and Manuel Tubis. This program ran until 1986 and graduated more than 210 students.

The dearth of nuclear pharmacists also inspired the concept of a shared nuclear pharmacy service, the progenitor of today's centralized or commercial nuclear pharmacy practice. The idea was conceived, established, and evaluated by Thomas Gnau in the Nuclear Medicine Division at Bowman Gray School of Medicine in Winston-Salem, North Carolina, in 1969.[8,9] The intent was to reduce cost, improve staffing efficiency, and ensure a high level of quality control in the delivery of radiopharmaceuticals to several nuclear medicine facilities in a metropolitan area.

The centralized nuclear pharmacy concept proved successful, and such pharmacies developed in the early 1970s. Of note were those established at the University of Washington by David Allen, the University of Tennessee (UT) by James Cooper, the University of Nebraska Medical Center by J. William Dirksen, and the Indiana University Medical Center by Michael Kavula, and the radiopharmacy program at the University of New Mexico (UNM) directed by Richard Keesee.

William Baker, who interned with Gnau at Bowman Gray, joined Keesee and set up the UNM radiopharmacy record-keeping system following the Bowman Gray model. Soon thereafter, in 1972, Keesee established the first centralized radiopharmacy to be licensed by a state board of pharmacy and the AEC. In 1973 Baker moved to the University of Utah Medical Center to establish the Intermountain Radiopharmacy program. He was later joined there by Robert Beightol, who had trained under Cooper at UT.

The UNM program graduated several nuclear pharmacists trained in the centralized pharmacy model who themselves went on to establish private centralized radiopharmacies. Notable among these were Nuclear Pharmacy Inc. (Robert Sanchez and Richard Sakasitz), Pharmatopes (Mark Hebner and Monty Fu), and Texatopes (Nunzio Desantis

and Larry Oliver). In 1975 Richard Keesee and David Hurwitz opened Pharmaco Nuclear, which eventually merged with Syncor in 1981. Pharmatopes merged with this company in 1982, followed by Nuclear Pharmacy Inc. in 1984, to become Syncor International Corporation, which is now a part of Cardinal Health. Other large to moderate-sized commercial nuclear pharmacy companies in operation today include Mallinckrodt Medical, Nycomed/Amersham, Geodax Technology Inc., Central Pharmacy Services Inc., and PETNET. While the bulk of nuclear pharmacy service throughout the United States is provided by these operations, there are a few dozen smaller-scale independent nuclear pharmacies that operate in several states. Over 400 centralized nuclear pharmacies staffed by 800 to 1000 nuclear pharmacists provide more than 80% of the radiopharmaceutical dosage forms used in nuclear medicine in the United States today.

Nuclear Pharmacy Education Programs

The initial lecture and laboratory courses created by Christian at Purdue University led eventually to the creation of the Department of Bionucleonics. The educational efforts of this group resulted in the training of many nuclear pharmacy researchers and practitioners, several of whom are recognized as nuclear pharmacy pioneers (see Table 1-4). The Purdue program is still in operation today under the apt leadership of Stanley Shaw, who is head of the Division of Nuclear Pharmacy. The current program was established in 1972 by Shaw and Gordon Born and has produced hundreds of nuclear pharmacists.

In the 1950s and early 1960s, there were few radioisotope programs where pharmacists could receive training. One program available at the time was at the Division of Radiological Health, U.S. Public Health Service, Robert A. Taft Sanitary Engineering Center, Cincinnati, Ohio; another was the course on radioisotope techniques at the Oak Ridge Institute of Nuclear Studies in Oak Ridge, Tennessee.

The tremendous growth of nuclear medicine in the 1960s demanded more nuclear pharmacists and therefore more training programs. The earliest sites (before 1970) for nuclear pharmacy education and training were at the University of Southern California, Purdue University, and the NIH Radiopharmaceutical Service. Other programs to eventually develop courses and training programs for pharmacists were the University of Arkansas, the University of New Mexico, the University of Utah, the University of Nebraska, the University of Pittsburgh, William Beaumont Hospital in Michigan, the University of Minnesota, the University of Wisconsin, the University of Tennessee, the Massachusetts College of Pharmacy, the University of North Carolina, the Medical University of South Carolina, the University of Indiana, the University of Toronto, the University of Cincinnati, Mercer University, Temple University, the University of Michigan, and the University of Oklahoma. These sites offered a variety of programs, including radiopharmacy residencies, short courses, semester courses, condensed (200 hour) authorized nuclear pharmacist programs, and nuclear pharmacy certificate programs.

Despite the apparent large number of institutions offering training, only a few of these programs were turning out pharmacists with training sufficient to obtain licensure as authorized nuclear pharmacists, and the supply of adequately trained nuclear pharmacists could not meet the demand of nuclear pharmacy practice. As a consequence, one nuclear pharmacy company (Syncor) established its own university-associated authorized nuclear pharmacist training program. Other companies utilized certificate programs, such as those directed by Shaw at Purdue University, Kavula at Mercer University, and George Hinkle at Ohio State University, to train their nuclear pharmacists. These programs have proven to be especially useful for pharmacists who wish to make a career change into nuclear pharmacy. More recently a joint program between the University of Arkansas Medical Center (UAMS) and UNM has been developed to train nuclear pharmacists via distance

TABLE 1-4 Nuclear Pharmacy Pioneers

David R. Allen	John E. Christian	Mark T. Hebner	Larry Oliver
William J. Baker	Clyde N. Cole	Kenneth R. Hetzel	William C. Porter
Robert W. Beightol	James F. Cooper	Dennis R. Hoogland	Richard Sakasitz
Gordon S. Born	Nunzio Desantis	David Hurwitz	Robert Sanchez
Barry M. Bowen	J. William Dirksen	Rodney D. Ice	Stanley M. Shaw
Kenneth Breslow	Raymond J. Farkas	Michael P. Kavula	Anne C. Smith
William H. Briner	Monty Fu	Tom K. Kawada	Arthur C. Soloman
Ronald J. Callahan	Thomas R. Gnau	Richard Keesee	Dennis P. Swanson
Robert P. Chandler	Robert F. Gutkowski	Richard J. Kowalsky	Walter Wolf
Henry M. Chilton	Donald R. Hamilton	Geoffrey Levine	A. Michael Zimmer

learning on the Internet. The program is managed by Nicki Hilliard at UAMS and Kristina Wittstrom at UNM. Students completing this program are eligible for NRC certification. A description of nuclear pharmacy education at colleges of pharmacy has been published.[10] Schools of pharmacy that have comprehensive nuclear pharmacy programs are located at Arkansas, Mercer, Purdue, Massachusetts, New Mexico, North Carolina, Oklahoma, Duquesne, Temple, South Carolina, and Toronto.

A Syllabus for Nuclear Pharmacy Training, assembled by the Educational Affairs Committee of the Section on Nuclear Pharmacy, Academy of Pharmacy Practice and Management of the American Pharmaceutical Association (APhA), was published in 1995. The syllabus was based on the NRC requirements for authorized nuclear pharmacist training: 200 didactic hours in the basic areas of radiation physics and instrumentation, radiation protection, math related to radioactivity, radiation biology, and radiopharmaceutical chemistry, and 500 hours of off-campus practical training in a nuclear pharmacy under the direction of an authorized nuclear pharmacist. The syllabus is intended as guidance for pharmacy school faculty and nuclear pharmacy preceptors who are involved in the education and training of nuclear pharmacists. Currently, the Code of Federal Regulations (10 CFR 35.980) specifies that training for an authorized nuclear pharmacist should consist of a structured educational program containing 700 hours of didactic and experiential training in the areas noted above.

Specialty Certification of Nuclear Pharmacists

Specialty certification in nuclear pharmacy became a reality only after nuclear pharmacists organized as a section within APhA. The process began in Chicago in August 1974 during the Nuclear Pharmacy Symposium at the APhA annual meeting. A petition submitted by these nuclear pharmacists was accepted by APhA, and the Section on Nuclear Pharmacy was officially established in 1975 as the first section within the Academy of General Practice, with James Cooper as chairman pro tem.

The section soon established an education committee, directed by Ronald Callahan, which initiated the comprehensive Task Analysis of Nuclear Pharmacy Practice to identify the types and extent of activities in which nuclear pharmacists were involved. These were organized into the following domains: procurement, compounding, quality assurance, dispensing, distribution, health and safety, and provision of information and consultation. This analysis culminated in practice standards that delineated the recognized duties and responsibilities of nuclear pharmacists. These standards were revised and reissued by APhA in 1995 as *Nuclear Pharmacy Practice Guidelines*. The guidelines contain the original practice domains and two more: monitoring patient outcome, and research and development. Each domain identifies a list of tasks and a knowledge statement related to each task.

TABLE 1-5 Nuclear Pharmacy Specialty Petition Committee

Ronald J. Callahan	James F. Cooper	Kenneth R. Hetzel	Geoffrey Levine
Robert P. Chandler	John Coupal	Michael P. Kavula	Susan G. Rowles
Henry M. Chilton	Robert Gutkowski	Tom K. Kawada	Stanley M. Shaw
William J. Christopherson	Donald R. Hamilton	Alan S. Kirschner	Arthur C. Soloman

TABLE 1-6 First Nuclear Pharmacy Specialty Council

David R. Allen	Paul G. Grussing	Sam H. Kalman	Stanley M. Shaw
Ronald J. Callahan	Rodney D. Ice	Richard D. Penna	Arthur C. Soloman
James F. Cooper, Chair			

Shortly after the establishment of the Section on Nuclear Pharmacy, the Board of Pharmaceutical Specialties (BPS) was established in 1976 by APhA. BPS immediately recognized nuclear pharmacy as a likely candidate for specialization. Chairman Cooper assembled 16 volunteers to serve as the nuclear pharmacy specialty petition committee (Table 1-5). This committee used the previously identified nuclear pharmacy practice standards as its guide in the petition to BPS. The petition was approved by BPS in 1978, and nuclear pharmacy became the first recognized specialty within the profession of pharmacy.

After approval of the nuclear pharmacy specialty petition, BPS established a Specialty Council on Nuclear Pharmacy (composed of six nuclear pharmacists, three non–nuclear pharmacist generalists, and a test developer/consultant) and charged it with the task of developing a certification program for the new specialty. The first specialty council members are listed in Table 1-6. The standards were again used in this process, serving as the basis for determining the areas of knowledge and skills to be tested on the certification exam. The process involved item writing, test assembly, test administration, and score interpretation.[11,12] The first nuclear pharmacy specialty certification exam was administered simultaneously in Las Vegas and Atlanta on April 24, 1982. The test resulted in 63 practitioners becoming board certified in nuclear pharmacy (BCNP). Today the *Nuclear Pharmacy Practice Guidelines* are used as the basis for constructing the specialty examination. At the time of this writing there are 475 BCNPs (Figure 1-4).

To ensure the competence of board-certified practitioners, BPS instituted a program of recertification every 7 years after initial certification. Recertification assures the public and the profession that certified practitioners undergo periodic evaluation. A BCNP is recertified by a three-step process: self-assessment, peer review, and formal assessment. Self-assessment involves annual review of the BCNP's nuclear pharmacy practice activities since initial certification or last recertification. Peer review involves the review of documented nuclear pharmacy practice and continuing education activities over the 7 year certification period by the Specialty Council on Nuclear Pharmacy. Formal assessment involves either achieving a passing score on a 100 item recertification exam or completing 70 hours of continuing education in a BPS-approved professional development program. Information on nuclear pharmacy certification and recertification can be obtained from the Board of Pharmaceutical Specialties, 2215 Constitution Ave. N.W., Washington, DC 20037-2985.

As James Cooper[13] remarked in his description of the nuclear pharmacy specialization process, "the unexpected benefit of the process was that it allowed scores of Section members to participate as item writers for the exam and take pride and ownership for the specialty process." The process demonstrated the powerful results that the collaborative effort of a

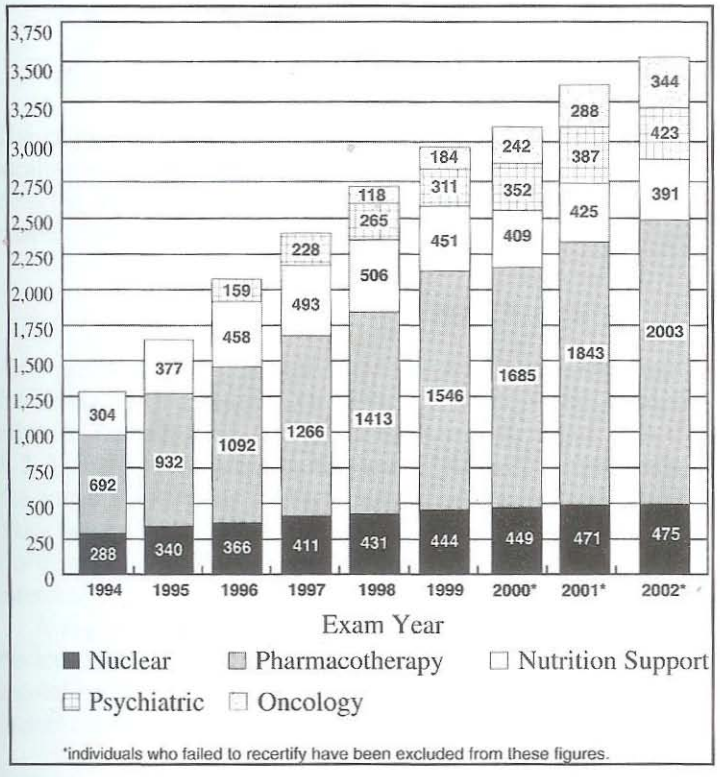

FIGURE 1-4 Pharmacists certified by the Board of Pharmaceutical Specialties (BPS); numbers of pharmacist specialists holding BPS certification in each year. (Used with permission of BPS.)

group of dedicated professionals can have. The ultimate benefit, however, is improved pharmaceutical care of patients through the services provided by nuclear pharmacists.

REFERENCES

1. Grigg ERN. The beginnings of nuclear medicine. In: Gottschalk A, Potchen EJ, eds. *Diagnostic Nuclear Medicine*. Baltimore: Williams & Wilkins; 1976:1-13.
2. Christian JE. Radioactive isotopes in hospital pharmacy. *Bull Am Soc Hosp Pharm*. July-August 1950;7:178-83.
3. Latiolais CJ, Parker PF, Hutchinson GB, et al. Radioisotopes in hospital pharmacy. *Bull Am Soc Hosp Pharm*. 1955;12:372-9.
4. Solyom P. Pharmacy service: University of Chicago Clinics. *Am J Hosp Pharm*. 1958;15:52-7.
5. Briner WH. Certain aspects of radiological health. *Am J Hosp Pharm*. 1958;15:44-51.
6. Briner WH. Nuclear medicine has come of age. *Am J Hosp Pharm*. 1960;17:333-8.
7. Harper PV, Lathrop KA, Gottschalk A. Pharmacodynamics of some technetium-99m preparations. In: Andrews GA, Kniseley RM, Wagner HN, eds. *Radioactive Pharmaceuticals*. Oak Ridge, TN: US Atomic Energy Commission; 1966:335-58.
8. Gnau TR, Maynard CD, Finley CW. Shared radiopharmacy services: a community study. *J Nucl Med*.1971;12:358-9.
9. Gnau TR, Maynard CD. Reducing the cost of nuclear medicine: sharing radiopharmaceuticals. *Radiology*. 1973;108:641-5.
10. Heske SM, Hladik WB 3rd, Laven DL, et al. Status of radiologic pharmacy education at colleges of pharmacy. *Am J Pharm Educ*. 1996;60:152-61.
11. Grussing PG, Allen DR, Callahan RJ, et al. Development of pharmacy's first specialty certification examination: nuclear pharmacy. *Am J Pharm Educ*. 1983;47:11-8.
12. Ponto JA. Nuclear pharmacy and the Board of Pharmaceutical Specialties (BPS). *J Pharm Pract*. 1989; 2:299-301.
13. Cooper JF. The nuclear pharmacy specialization process. In: Cooper JF, ed. *25th Anniversary—Nuclear Pioneers*. Washington, DC: American Pharmaceutical Association; 2000:15-9.

2 Radioactive Decay

The chemical and physical properties of a radiopharmaceutical are responsible for its localization in the body, whereas its radioactive decay properties dictate how it can be detected and measured and whether it has diagnostic or therapeutic applications. This chapter considers the radionuclide decay properties associated with radiopharmaceuticals.

NUCLIDES

An atom is the smallest particle of an element possessing the properties of the element. It is made up of a nucleus consisting of protons and neutrons surrounded by electrons in orbitals, or shells. The electron shells are designated with the principal quantum numbers 1, 2, 3, and so forth or with the letters K, L, or M, respectively, with the K shell closest to the nucleus. Electrons fill the shells in order, with a specified number per shell. A neutral atom has the same number of electrons as protons (Figure 2-1). Removal of one or more electrons produces an ionized atom. Ionization can occur by several processes. One is the interaction of radiation with matter, which is discussed later in this chapter.

A nuclide is an atom characterized by the number of protons and neutrons in its nucleus. Nuclides are designated by the following notation, where X represents the elemental symbol, Z is the number of protons, and N is the number of neutrons. The mass number A is the sum of protons and neutrons:

$$^{A}_{Z}X_{N}$$

Nuclides are classified according to their A, Z, and N values, illustrated by the following examples.

- Isotopes are nuclides with the same Z but different A and N:

$$^{1}_{1}H_{0} \qquad ^{2}_{1}H_{1} \qquad ^{3}_{1}H_{2}$$

- Isobars are nuclides with the same A but different Z and N:

$$^{64}_{28}Ni_{36} \qquad ^{64}_{30}Zn_{34}$$

- Isotones are nuclides with the same N but different Z and A:

$$^{41}_{19}K_{22} \qquad ^{42}_{20}Ca_{22}$$

- Isomers are nuclides with the same A, Z, and N but different nuclear energy states:

$$^{99}_{43}Tc_{56} \qquad ^{99m}_{43}Tc_{56}$$

The lowercase "m" in the mass number denotes the metastable state, an excited nuclear condition that occurs for a measurable period of time.

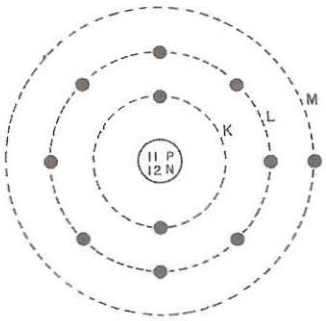

FIGURE 2-1 Bohr model of the sodium atom.

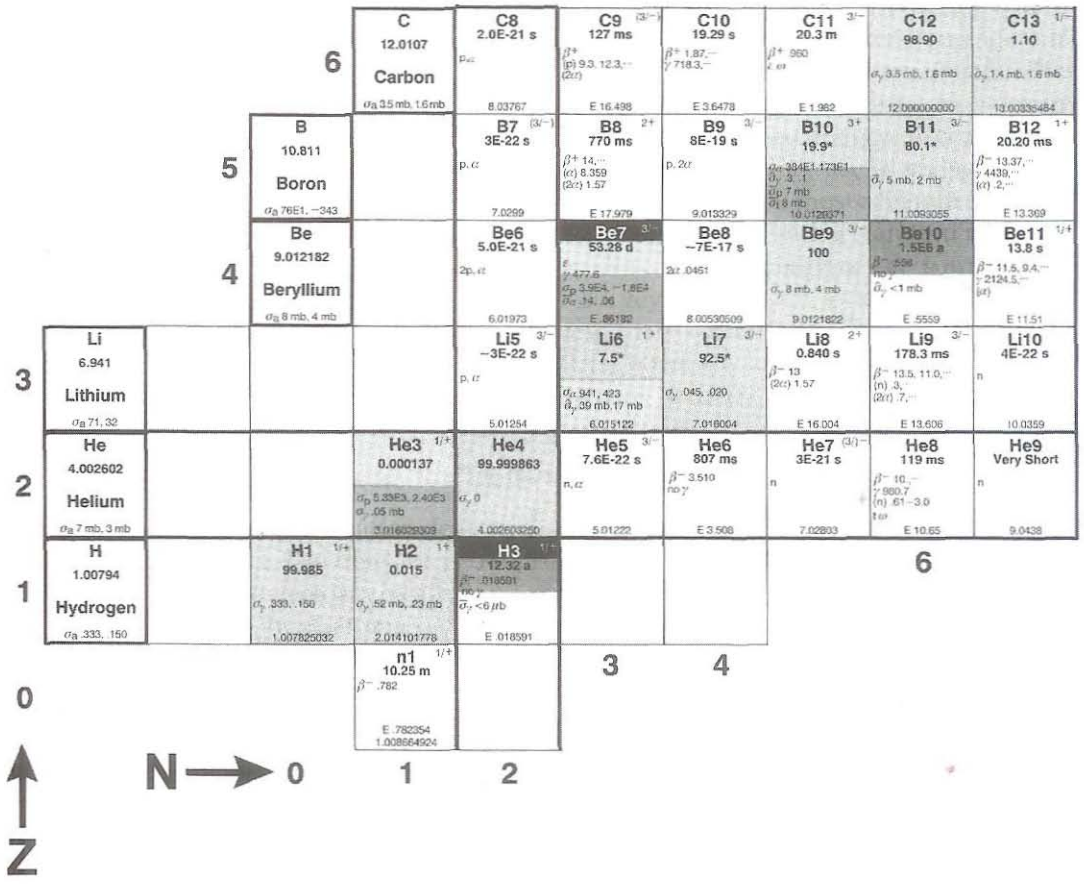

FIGURE 2-2 Chart of the nuclides in the region of the light elements. Reprinted with permission from reference 1. The complete chart is available from Lockheed Martin at http://www.chartofthenuclides.com.

The periodic table lists 103 elements. If the isotopes of each element are included, the total number of nuclides is in excess of 1900, and 266 of them are stable. The remaining unstable species are called radionuclides. A radioisotope is a radionuclide of a particular element. Figure 2-2 illustrates a portion of the chart of the nuclides in the region of the light elements.[1]

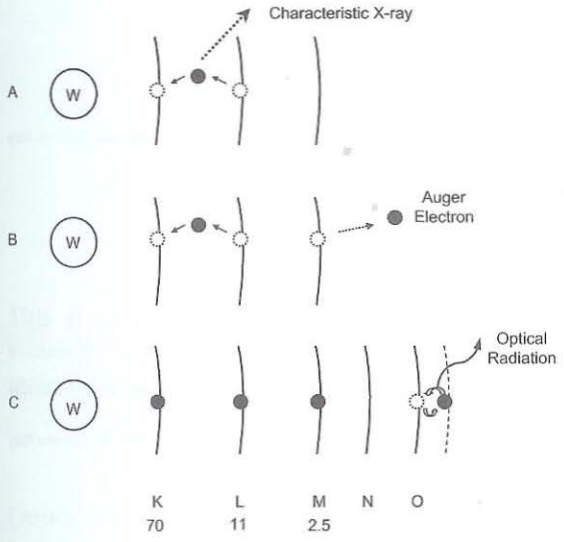

FIGURE 2-3 Perturbations of the tungsten electron shells: (A) characteristic x-ray production after ejection of a K-shell electron after fill-in by an M-shell electron, (B) Auger electron production after ejection of a K-shell electron (as an alternative to x-ray production), (C) optical radiation production after an excited valence electron falls back to its ground state. Numbers are energy in kiloelectron volts, explained in text.

ORBITAL ENERGY LEVELS

Electrons are bound in their shells by an electron-binding energy, which is the energy that must be applied to remove an electron from its shell. The K-shell electrons have the highest binding energy because they reside closest to the positive attractive force of the nucleus. In general, inner shells fill with electrons before outer shells. If an inner-shell electron is removed, an outer-shell electron will fill the vacancy. When this occurs, energy is released from the atom equal to the difference between the binding energies of the two shells. A diagram of the tungsten (W) atom is shown in Figure 2-3. If its K-shell electron is removed and the vacancy is subsequently filled by an L-shell electron, a characteristic x-ray is produced equal to 59 kiloelectron volts (keV), the difference between the K- and L-shell binding energies (Figure 2-3A). The characteristic x-rays released from some radionuclides (e.g., ^{125}I and ^{201}Tl) are the principal radiations used for their detection in nuclear medicine.

An alternative process to characteristic x-ray production is emission of an Auger electron (Figure 2-3B). When this occurs, the available x-ray energy is given to an outer-shell electron, which is ejected from the atom. The Auger electron's kinetic energy is equal to the x-ray energy given to it minus its binding energy. In the case of tungsten, a 59 keV x-ray produces a 56.5 keV Auger electron from its M shell.

Optical radiation may also be produced from an atom (Figure 2-3C). This occurs when outer-shell valence electrons are excited to higher-energy suborbits. When the electrons return to their ground state, visible light is emitted. An example is the excitation of minerals with ultraviolet light, which causes them to fluoresce.

NUCLEAR ENERGY LEVELS

Neutrons and protons (collectively know as nucleons) exist in the nucleus of an atom in discrete energy levels. In a stable atom, nucleons are in their ground state. They may, however, be excited to higher-energy states by interaction with a high-speed particle or during radioactive decay. When these excited nucleons return to their ground state, energy is emitted from the nucleus as a gamma ray. The energy may be released as one discrete gamma ray or in a cascade as multiple gamma rays of different energies (Figure 2-4). The nuclear de-excitation process is analogous to the electron shell changes discussed previously, but certain differences exist. First, the electron shell de-excitation process immediately follows

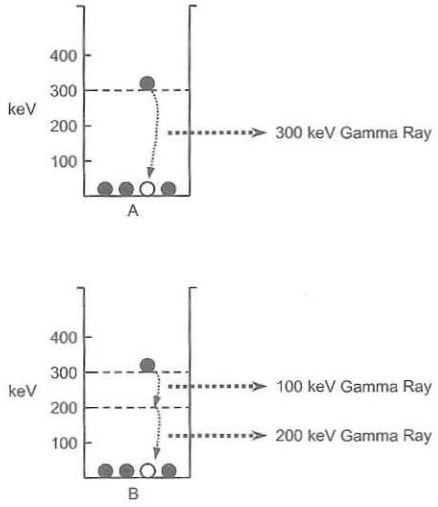

FIGURE 2-4 Nuclear de-excitation by emission of gamma rays after the return of excited nucleons to their ground state. Energy is emitted as a single gamma ray or as a cascade of two gamma rays.

atomic excitation, whereas nuclear de-excitation may be immediate or delayed. When nuclear de-excitation is delayed, the excited nucleus is said to be in the metastable state. Also, although characteristic x-rays and gamma rays are high-energy electromagnetic radiation, they differ in that gamma rays typically have much higher energy and originate from nuclear energy changes, while characteristic x-rays are lower in energy and arise from electron shell energy changes.

NUCLEAR MASS AND ENERGY

In 1905, Albert Einstein proposed his famous equation relating mass to energy: $E = mc^2$, where E is energy in erg units, m is mass in gram units, and c is the velocity of light (2.998×10^{10} cm/sec). The standard atomic mass unit (AMU) is defined as one-twelfth the mass of a ^{12}C atom. The mass of 1 AMU is calculated as

$$\frac{12 \text{ grams}}{6.023 \times 10^{23} \text{ atoms}} \times \frac{1 \text{ atom}}{12 \text{ AMU}} = 1.6603 \times 10^{-24} \text{ gram/AMU}$$

The energy equivalent of this small mass can be calculated from Einstein's equation, where the erg has units of cm^2-g-sec^{-2}:

$$E = \left(1.6603 \times 10^{-24} \text{ gram/AMU}\right)\left(2.998 \times 10^{10} \text{ cm/sec}\right)^2$$

$$E = 1.49228 \times 10^{-3} \text{ erg/AMU}$$

In the radiation sciences, the basic energy unit used is the electron volt (eV) and its multiples, the kiloelectron volt (keV) and the megaelectron volt (MeV). An electron volt is a unit of energy equal to the energy acquired by 1 electron falling through a potential difference of 1 volt (V). The energy equivalent of 1 AMU is

$$\frac{1.49228 \times 10^{-3} \text{ erg/AMU}}{1.602 \times 10^{-6} \text{ erg/MeV}} = 931.5 \text{ MeV/AMU} \qquad (2\text{-}1)$$

TABLE 2-1 Mass–Energy Relationship of Atomic Particles

Particle	Mass (AMU)	Energy (MeV)
Electron	5.48597×10^{-4}	000.511
Proton	1.0072766	938.278
Neutron	1.0086654	939.572
Hydrogen atom	1.0078252	938.789

Source: Reference 2, p. 535.

This simple relationship between mass and energy allows calculation of the energy released in a nuclear reaction or in a radioactive decay process. Some useful atomic mass–energy relationships are listed in Table 2-1.

NUCLEAR FORCES

Opposite poles of a magnet attract and like poles repel. The attractive and repulsive forces become greater as the poles come close together. A similar phenomenon occurs with protons and electrons. Protons, however, can exist in close proximity within the nucleus of an atom without repulsion. This is possible because an attractive force is present in the nucleus. This attractive force is called the nuclear force and is about 100 times greater than the electrostatic repulsive force. It is responsible for holding the neutrons and protons in the nucleus.

The nuclear force is greatest between unlike and uncharged particles (i.e., the attraction between n and p [n,p] > n,n > p,p). The nuclear attractive force is appreciable only over a finite range and is strongest when nucleons are 1×10^{-13} cm apart. The force becomes repulsive at distances less than 0.4×10^{-13} cm and negligible at 2.4×10^{-13} cm.

NUCLEAR BINDING ENERGY

Atoms are created from neutrons, protons, and electrons. When a ^{12}C atom is created, the sum of its individual parts (i.e., six neutrons, six protons, and six electrons) is

$$\begin{aligned} n &= 6\,(1.0086654\ \text{AMU}) = 6.0519924\ \text{AMU} \\ p &= 6\,(1.0072766\ \text{AMU}) = 6.0436596\ \text{AMU} \\ e &= 6\,(0.0005486\ \text{AMU}) = 0.0032916\ \text{AMU} \\ \text{Sum of components} &= 12.0989436\ \text{AMU} \end{aligned}$$

However, the nuclidic mass of a finished atom of ^{12}C is only 12.0000000 AMU, or 0.0989436 AMU less than the sum of its individual components. The mass that is apparently lost is called the *mass defect* and occurs each time atoms are created from individual atomic particles. Because most of the atom's mass is in the nucleus, this mass defect is associated with the nucleus and in actuality is not lost but converted into an equivalent amount of energy called the *nuclear binding energy.* The amount of this energy can be calculated for ^{12}C as follows:

$$(0.0989436\ \text{AMU}) \times (931.5\ \text{MeV/AMU}) = 92.166\ \text{MeV}$$

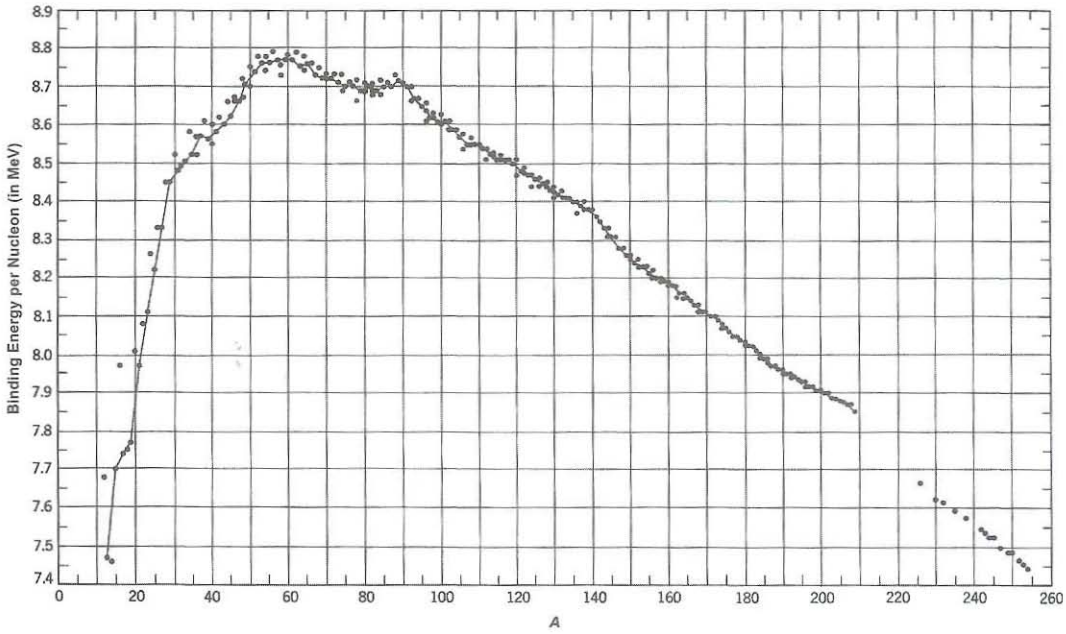

FIGURE 2-5 The average binding energy per nucleon as a function of mass number, *A*. The line drawn connects the odd *A* points. (Reprinted with permission of John Wiley & Sons, Inc., from reference 2.)

The nuclear binding energy is thus defined as the energy released when a nucleus is produced from its component nucleons, or the energy required to separate a nucleus into its individual components. The average binding energy (BE_{avg}) per nucleon for ^{12}C is calculated as

$$BE_{avg} = \frac{92.166 \text{ MeV}}{12 \text{ nucleons}} = 7.68 \text{ MeV/nucleon}$$

The average binding energy per nucleon has been determined for all stable nuclides and is plotted as a function of mass number in Figure 2-5.[2] For mass numbers greater than 11, the BE_{avg} is between 7.4 and 8.8 MeV throughout the table of elements. Maximum values of about 8.8 MeV occur in the vicinity of $A = 60$, for iron and nickel, elements that represent a high percentage of the earth's crust. Higher BE_{avg} nuclides are more stable because it takes more energy to break their nuclei apart. The trend in nature is for elements to achieve the greatest nuclear stability. This is evident from the fission of heavy nuclei to form lighter and more stable ones and from the fusion of light nuclei (occurring in the stars) to form heavier ones with higher nuclear stability.

RADIATION AND RADIOACTIVE DECAY

Radiation can be defined as the emission and propagation of energy through space. Radiation can be particulate or electromagnetic. The principal forms of radiation emitted from radionuclides are alpha particles, beta particles, gamma rays, and x-rays. An alpha particle is a helium nucleus, $^4He^{2+}$, or a helium atom stripped of its two orbital electrons. Alpha particles are emitted primarily from heavier nuclei such as uranium, thorium, plutonium, and radium, but a few lighter nuclides are also alpha emitters. Beta particles are electrons

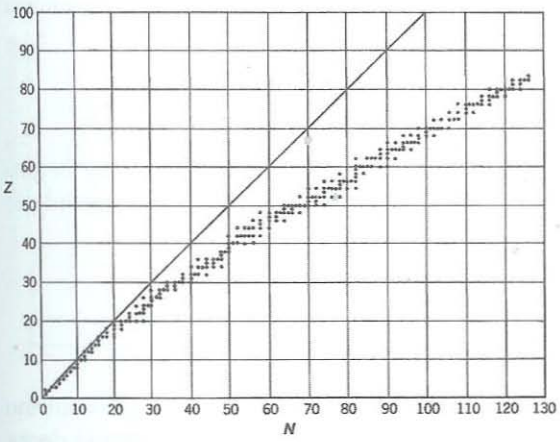

FIGURE 2-6 Plot of Z versus N of the stable nuclei. The solid line represents a neutron-to-proton ratio of unity. Note the increase in this ratio for nuclides of Z greater than 20. (Reprinted with permission of John Wiley & Sons, Inc., from reference 2.)

TABLE 2-2 Carbon Isotopes

Isotope	Neutron:Proton Ratio	Radiation	Half-life	% Isotopic Abundance[a]
^{9}C	0.50	β^+	0.127 sec	–
^{10}C	0.67	β^+	19.29 sec	–
^{11}C	0.83	β^+	20.3 min	–
^{12}C	1.00	None	Stable	98.90
^{13}C	1.17	None	Stable	1.10
^{14}C	1.33	β^-	5715 yr	Trace amounts
^{15}C	1.50	β^-	2.45 sec	–
^{16}C	1.67	β^-	0.75 sec	–
^{17}C	1.83	β^-	0.19 sec	–
^{18}C	2.00	β^-	0.092 sec	–
^{19}C	2.17	β^-	0.05 sec	–
^{20}C	2.33	β^-	0.01 sec	–

[a] Amounts present in Earth's crust; dash indicates isotope is not present in Earth's crust.

emitted from the nuclei of unstable atoms. Negatively charged beta particles are known as *negatrons*; positively charged beta particles are called *positrons*. Beta particles have the same mass as orbital electrons with a rest-mass energy equivalent of 0.511 MeV. Gamma rays are high-energy electromagnetic radiation. They have no mass or charge and are emitted from unstable nuclei secondary to particle decay.

The ratio of neutrons to protons in a nucleus determines whether a nuclide is stable or radioactive. For light nuclei, stability is achieved when the n/p ratio is 1. Above atomic number 20, however, the n/p ratio must be greater than 1 for stability because the repulsive force of additional protons becomes more prominent and extra neutrons are required to "buffer" this proton interaction. Figure 2-6 illustrates a plot of the stable nuclides,[2] which all fall on the *line of beta stability*. Nuclides that have too many protons for stability fall in the region above the line of beta stability, whereas nuclides with too many neutrons fall in the region below the line of beta stability. In either situation, nuclides in these regions are unstable and will undergo radioactive decay until a stable n/p ratio is achieved. Nuclides farther away from the line of beta stability, in general, have shorter half-lives, indicating their tendency toward greater instability than those closer to the line. This is illustrated in Table 2-2, which lists the isotopes of carbon. It demonstrates that proton-rich nuclides with n/p ratios less than 1 undergo positron decay, whereas neutron-rich nuclides undergo negatron decay. In positron decay an excess positive charge is reduced in the

nucleus through the ejection of a positive electron. In negatron decay, the positive nuclear charge is increased through the ejection of a negative electron.

Negatron Decay

Neutron-rich nuclides undergo negatron or beta-minus decay. Negatron decay begins when a neutron is converted into a proton, an electron, and a neutrino (ν) according to the following transformation:

$$n \rightarrow p^{+} + e^{-} + \nu$$

Because the electron is not part of the nucleus, it is ejected as beta radiation. (The neutrino is discussed later.) Consider, for example, the decay of ^{32}P shown in the following decay equation:

$$\underset{31.973908\ \text{AMU}}{{}^{32}_{15}P_{17}} \rightarrow \underset{31.972047\ \text{AMU}}{{}^{32}_{16}S_{16}} + E(\beta, \nu)$$

^{32}P is the parent nuclide and sulfur is the daughter nuclide. We will examine this decay and account for all particles and energy. A ^{32}P atom contains 15 protons and 17 neutrons in its nucleus, and it has 15 orbital electrons. The instant after it decays it no longer is phosphorus; it becomes sulfur. The atom now has 16 protons (atomic number of sulfur), 16 neutrons, and 16 orbital electrons. The beta particle escapes from the ^{32}P nucleus just before it changes into ^{32}S. The ^{32}P atom weighs 31.973908 AMU before decay to ^{32}S and 31.972047 AMU afterward. The difference is a mass defect of 0.001861 AMU and is equivalent to 1.73 MeV of energy. This is known as the transition energy (E_{max}). The transition energy is the total energy released when a parent radionuclide decays to its daughter nuclide. This energy comes from the small amount of mass lost by the parent. Parent nuclides are always "heavier" than their daughter nuclides.

In negatron decay the transition energy is dissipated as the kinetic energy of the beta particle and the neutrino. The maximum energy a ^{32}P beta particle can have is 1.73 MeV. Measurements made by nuclear scientists, however, have demonstrated that on average only about one-third of the transition energy is associated with the beta particle when ^{32}P decays. Because this contradicts the law of conservation of mass and energy, scientists postulated that another particle must carry off the remaining two-thirds of the energy. This particle was subsequently found, and named the neutrino. The neutrino is a chargeless particle of extremely small mass emitted from the nucleus in all beta decay processes, and it carries away the energy not used by the beta particle.[3] If the energy of each particle from thousands of ^{32}P atoms were measured and their frequency of occurrence versus energy plotted, the beta energy spectrum would be similar to the one in Figure 2-7. If a decaying ^{32}P atom emits a 0.73 MeV beta particle, the neutrino carries away 1.00 MeV. The average energy carried away by beta particles is approximately one-third of the maximum beta energy. The average beta energy varies with Z and beta energy, and ranges from about 0.25 to 0.45.[4] Table 2-3 shows the relationship of beta energies for some commonly used beta emitters.

In negatron decay, one need not account for the electron mass lost from the nucleus of the ^{32}P atom because an equivalent electron mass is acquired in the electron shell of ^{32}S to offset it.

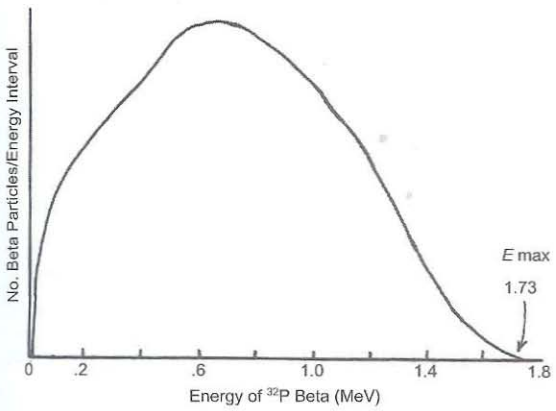

FIGURE 2-7 Beta energy spectrum for ^{32}P decay. The vertical coordinate gives the relative number of beta particles that are emitted at each energy on the horizontal coordinate up to the maximum of 1.73 MeV. For example, about twice as many particles are emitted with an energy of 0.6 MeV as with 1.2 MeV.

TABLE 2-3 Beta-Emitter Energy Profile

		Beta Energy (MeV)		
Radionuclide	Atomic Number	Maximum *E* (*E* max)	Average *E* (*E* avg)	*E* avg/*E* max
^{3}H	1	0.018	0.006	0.33
^{14}C	6	0.155	0.05	0.32
^{32}P	15	1.71	0.70	0.41
^{89}Sr	38	1.49	0.56	0.38
^{90}Y	39	2.28	0.93	0.41
^{131}I	53	0.606	0.19	0.31
^{137}Cs	55	0.512	0.24	0.47

Source: Reference 3.

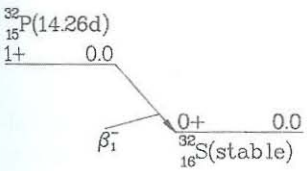

FIGURE 2-8 Decay scheme for ^{32}P. (Reprinted with permission of the Society of Nuclear Medicine from reference 5.)

Decay schemes are often used to provide a ready reference to a variety of data, such as mode of decay, transition energy, radiation energy and abundance, and parent and daughter nuclides. Radiation emissions in decay schemes are indicated by diagonal arrows drawn from the parent to the daughter nuclide, either to the right or to the left. Gamma ray emissions are designated as vertically drawn arrows. By convention, when the daughter nuclide has a higher atomic number than the parent (e.g., in negatron decay), the diagonal arrow depicting transition from parent to daughter is drawn to the right. When the daughter nuclide is of lower atomic number, as occurs in alpha particle decay, positron decay, or electron capture (EC) decay, the arrow is drawn to the left.

The decay scheme for ^{32}P is shown in Figure 2-8. ^{32}P is called a pure beta emitter because all the transition energy is distributed between the beta particle and the neutrino. The nucleus does not receive any of this energy and is therefore not raised to an excited state that would lead to gamma emission. For this reason, ^{32}P is not a useful diagnostic radionuclide but is used for various types of interstitial therapies, in which the tissues absorb all its energy. Other examples of pure beta emitters are ^{14}C, ^{3}H, ^{35}S, and ^{90}Y.

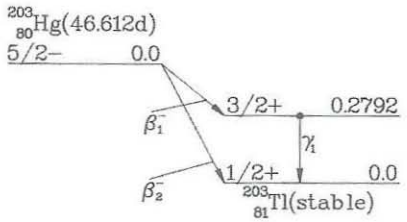

FIGURE 2-9 Decay scheme for ^{203}Hg. (Reprinted with permission of the Society of Nuclear Medicine from reference 5.)

Some radionuclides are beta and gamma emitters. Examples of those that have been used in nuclear medicine are ^{131}I, ^{99}Mo, ^{133}Xe, ^{198}Au, and ^{203}Hg. The latter two are no longer used routinely; however, the decay of ^{203}Hg will be illustrated because of its simplicity. The decay equation for ^{203}Hg is as follows:

$$\underset{202.972857\ \text{AMU}}{{}^{203}_{80}\text{Hg}_{123}} \rightarrow \underset{202.972330\ \text{AMU}}{{}^{203}_{81}\text{Tl}_{122}} + E(\beta, \nu, \gamma)$$

The mass defect for this decay is 0.000527 AMU, equivalent to a transition energy of 0.471 MeV. The decay scheme is shown in Figure 2-9. ^{203}Hg does not decay directly to the ground state of ^{203}Tl but to its excited state of 0.279 MeV. That is, for every atom of ^{203}Hg that decays, 0.192 MeV of the transition energy is distributed between the beta particle and neutrino, and 0.279 MeV is released as a gamma ray when the excited ^{203}Tl nucleus de-excites to its ground state. The gamma ray is emitted simultaneously with the beta particle.

Positron Decay

Positron decay occurs when the n/p ratio is too low for stability. These proton-rich nuclides decay by converting a proton into a neutron and a positron–neutrino pair ejected from the nucleus. The nuclear transformation is

$$p^+ \rightarrow n + e^+ + \nu$$

Because positron emission decreases the atomic number by one unit, the electron orbital must lose one electron as soon as the nucleus ejects the positron. The atomic mass of the daughter nuclide will thus be at least two electron masses less than the parent nuclide. The loss of two electron masses in positron decay requires that at least 1.022 MeV (2 × 0.511 MeV/electron) of transition energy be available for the process to occur. ^{18}F-fluorine is a positron emitter whose decay equation is

$$\underset{18.000950\ \text{AMU}}{{}^{18}_{9}\text{F}_{9}} \rightarrow \underset{17.9991598\ \text{AMU}}{{}^{18}_{8}\text{O}_{10}} + E(\beta, \nu)$$

The mass defect for this decay is 0.0017902 AMU and is equivalent to a transition energy of 1.66757 MeV. Because 1.022 MeV of this energy must be used for the positron–electron pair lost from the atom, the remaining 0.6456 MeV is dissipated between the positron kinetic energy and the neutrino, in roughly a one-third/two-thirds distribution, respectively. The decay scheme is shown in Figure 2-10.

Positrons are considered antimatter, existing only for very short periods of time. After being ejected from the nucleus, the positron traverses a distance of a few millimeters in tissue in about 1 microsecond, after which it has lost most of its energy and will combine

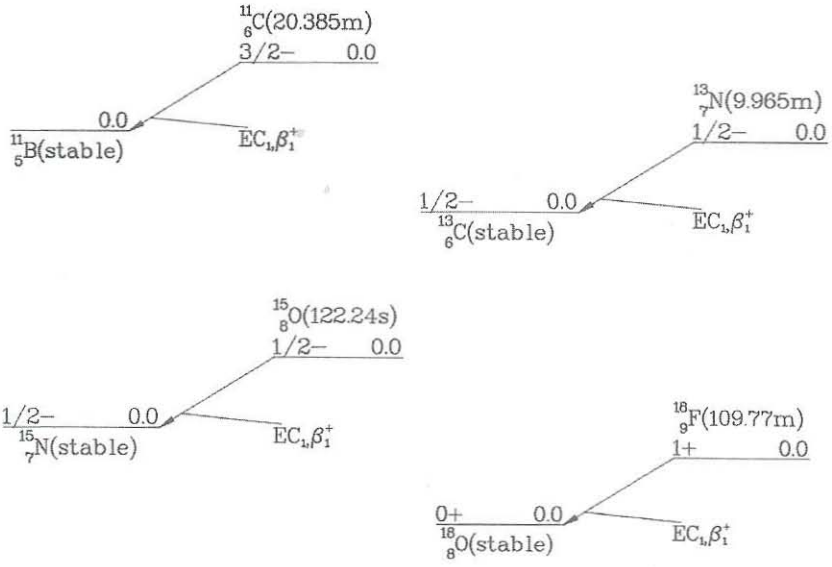

FIGURE 2-10 Decay schemes for ^{11}C, ^{13}N, ^{15}O, and ^{18}F. (Reprinted with permission of the Society of Nuclear Medicine from reference 5.)

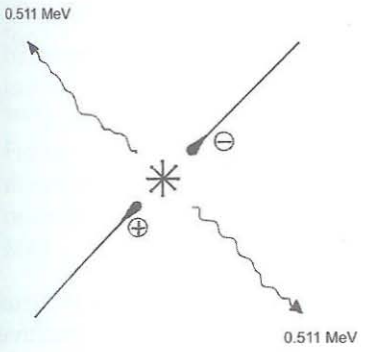

FIGURE 2-11 Positron annihilation reaction. Two electron masses, one positron and one negatron, are converted into their equivalent electromagnetic energy of two 0.511 MeV photons.

with a negative electron. The two electron masses annihilate into two 0.511 MeV photons (annihilation radiation), which are emitted in opposite directions (Figure 2-11). Positron emitters always produce 0.511 MeV photons. Several positron emitters are used in nuclear medicine, including ^{11}C, ^{13}N, ^{15}O, ^{18}F, ^{68}Ga, and ^{82}Rb (Figures 2-10 and 2-12). Positron-emitting radiopharmaceuticals are discussed more thoroughly in Chapter 10. A positron emitter may also decay by EC to excited daughter states and emit gamma rays in addition to annihilation radiation. ^{68}Ga is an example of this type of decay.

Electron Capture Decay

EC is the second way in which proton-rich nuclides decay to decrease an excess positive nuclear charge. The change in nuclear composition is similar to that occurring in positron decay, but the mechanism is different. Therefore, EC and positron decay are competing processes. In fact, both processes of decay can occur in radionuclides with transition energies greater than 1.022 MeV. If a proton-rich nuclide does not have at least 1.022 MeV of transition energy, a positron cannot be created and EC decay will occur.

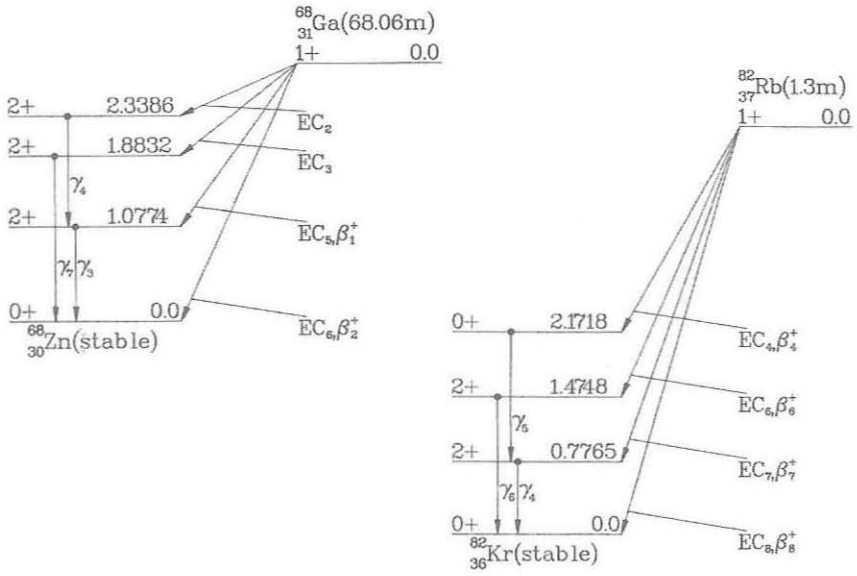

FIGURE 2-12 Decay schemes for ^{68}Ga and ^{82}Rb. (Reprinted with permission of the Society of Nuclear Medicine from reference 5.)

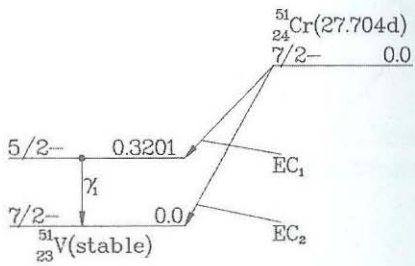

FIGURE 2-13 Decay scheme for ^{51}Cr. (Reprinted with permission of the Society of Nuclear Medicine from reference 5.)

In EC decay, an orbital electron, usually the K-shell electron, is captured by the nucleus and combines with a proton to produce a neutron and a neutrino. This reduces the positive nuclear charge by one unit. The nuclear transformation that occurs is

$$p^+ + e^- \rightarrow n + \nu$$

For most EC decay processes a K-shell electron is captured unless the transition energy is less than the K-shell binding energy, in which case L-shell capture occurs.

The neutrino carries off all the transition energy released in the EC decay process unless an excited daughter nuclide is produced, in which case the energy is shared between the neutrino and the gamma ray emitted by the daughter.

Several radionuclides used in nuclear medicine decay by EC: ^{51}Cr, ^{57}Co, ^{67}Ga, ^{111}In, ^{123}I, ^{125}I, and ^{201}Tl. EC is a desirable decay mode for diagnostic radiopharmaceuticals because no particulate radiation is produced, lowering the patient's radiation absorbed dose. The decay equation for ^{51}Cr is

$$\underset{50.944786\ \text{AMU}}{{}^{51}_{24}\text{Cr}_{27}} \rightarrow \underset{50.943978\ \text{AMU}}{{}^{51}_{23}\text{V}_{28}} + E(\nu, \gamma)$$

The mass defect for this transition is 0.000808 AMU and is equivalent to a transition energy of 0.753 MeV. The decay scheme is shown in Figure 2-13. The scheme demonstrates that 91% of ^{51}Cr atoms decay directly to the ground state of ^{51}V by emitting a 0.753 MeV neutrino. In 9% of the decayed atoms, however, the neutrino carries only 0.433 MeV, and a gamma ray of 0.320 MeV is emitted from the excited ^{51}V daughter. Secondary radiations, such as characteristic x-rays and Auger electrons, are also produced during EC decay.

Each of the decay processes previously discussed is called an isobaric transition because in every case of negatron, positron, or EC decay the parent and daughter nuclides have the same mass number. Only the numbers of protons and neutrons change.

Isomeric Transitions and Metastable States

Isomeric transition occurs when an excited nucleus loses its excess energy by emission of only a gamma ray, with no change in the atomic number or neutron number. This process was referred to in the earlier discussion of nuclear energy levels. A nucleus can become excited in several ways, but the most common way is through a radioactive decay process in which some of the transition energy remains in the nucleus after particle emission. This excess nuclear energy can be emitted either promptly or in a delayed manner. Prompt de-excitation occurs when gamma rays are emitted immediately after particle emission, usually within 10^{-13} seconds. Delayed de-excitation occurs when the excited nucleus persists for a measurable period of time, with half-life in the range of 10^{-9} seconds to several months. These nuclei are called metastable states and are designated by writing a lowercase "m" after the mass number. Most of the radionuclides used in nuclear medicine are prompt gamma emitters (e.g., ^{131}I and ^{51}Cr). Some metastable species have a long enough half-life that they can be separated and isolated from the parent radionuclide. These isolated species are sometimes referred to as pure gamma emitters. A good example is ^{99m}Tc, which is produced by the decay of ^{99}Mo. A simplified decay scheme is shown in Figure 2-14. When ^{99}Mo decays, 13.95% of the atoms decay to the ^{99}Tc ground state, but the other 86.05% yield the metastable isomer ^{99m}Tc, which has a half-life of 6 hours. It will undergo de-excitation to its ^{99}Tc isomer by emitting a monoenergetic gamma ray of 0.140 MeV.

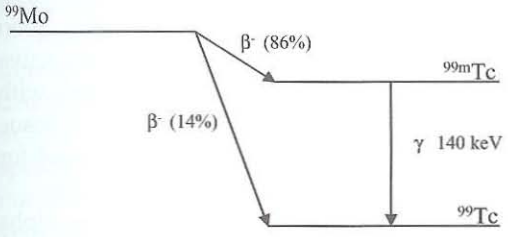

FIGURE 2-14 Simplified decay scheme for ^{99}Mo.

Internal Conversion

In some isomeric transitions the energy released from the nucleus may be transferred to an inner-shell electron instead of being emitted as a gamma ray. According to quantum mechanics, some of the orbital electrons, particularly the K-shell electrons, spend an appreciable amount of time near or actually within the nucleus. If an electron absorbs the nuclear energy that is available, it is ejected from the atom, with a kinetic energy equal to the difference between the energy available in the nucleus and the binding energy of the electron. Such an electron is called a *conversion electron*, and the process is referred to as *internal conversion*. Nuclides in the isomeric state may therefore emit either gamma rays

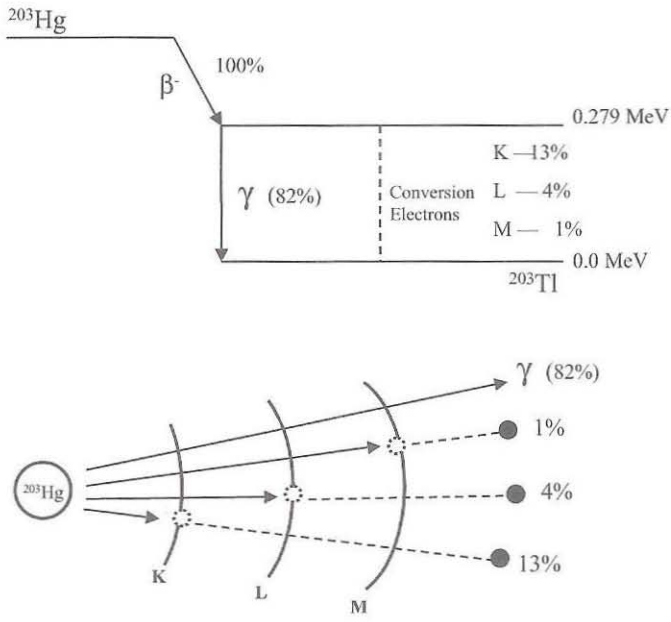

FIGURE 2-15 Simplified decay scheme for ^{203}Hg illustrating the percentage of internal conversion in the K, L, and M shells.

or conversion electrons during their de-excitation. This is illustrated in the decay scheme for ^{203}Hg (Figure 2-15); the internal conversion process is shown as an internal photoelectric effect in which the 0.279 MeV gamma ray may undergo K-, L-, or M-shell conversion. Because 100% of ^{203}Hg atoms decay by beta emission to the excited state of ^{203}Tl, theoretically one should be able to detect 100 gamma rays of 0.279 MeV for every 100 atoms decayed. Only 82 gamma rays are detectable, however, because 18% of the atoms undergo internal conversion in the K, L, and M shells. The number of detectable photons per 100 disintegrations is known as the photon abundance. The photon abundance for ^{203}Hg is 82%.

Alpha Particle Decay

Although alpha radiation holds no current clinical usefulness, some alpha-emitting radionuclides have merit, and some may be used in the future for therapeutic application. Soon after radium's discovery in 1898 by Marie and Pierre Curie, ^{226}Ra and its radioactive daughter, ^{222}Rn, were used in medicine. The most frequent use was radiation therapy with sources sealed in glass or platinum seeds that were implanted in or near cancerous tissue for treatment and removed at the end of treatment. Currently, ^{192}Ir and ^{125}I are used for such purposes. ^{103}Pd seeds have been successfully used for treating prostate cancer.

Alpha emitters have no application in diagnostic nuclear medicine because alpha particles produce dense ionization within tissue, accompanied by severe radiation damage. However, the decay of ^{226}Ra is discussed here because of historical interest. The decay equation is

$$\underset{226.0254\ \text{AMU}}{{}^{226}_{88}\text{Ra}_{138}} \rightarrow \underset{222.0175\ \text{AMU}}{{}^{222}_{86}\text{Rn}_{136}} + \underset{4.0026\ \text{AMU}}{{}^{4}_{2}\text{He}_{2}}$$

Alpha decay usually occurs in heavy nuclei where four nucleons (two protons plus two neutrons) can achieve an energy that exceeds the nuclear binding energy to escape from the nucleus. In the decay equation for ^{226}Ra the alpha particle is shown as a neutral helium

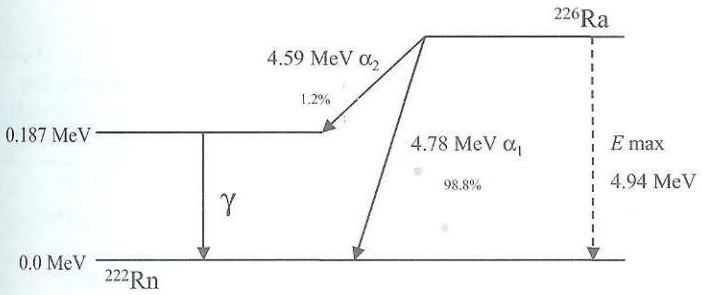

FIGURE 2-16 Simplified decay scheme for ^{226}Ra.

atom with its orbital electrons, but alpha particles do not assume this state until they have almost exhausted their kinetic energy. The sum of the ^{222}Rn and ^{4}He masses is 0.0053 AMU less than the mass of the ^{226}Ra atom. This mass defect is equivalent to a transition energy of 4.94 MeV.

A simplified decay scheme depicting the principal decay routes for ^{226}Ra is shown in Figure 2-16. A branching decay occurs, with 98.8% of the atoms decaying directly to ^{222}Rn and 1.2% to the excited state of ^{222}Rn, which subsequently de-excites by emission of a 0.187 MeV gamma ray. The difference between the alpha-1 energy of 4.78 MeV and the transition energy of 4.94 MeV is 0.16 MeV. This difference is the *recoil energy*, which is given to the nucleus as the massive alpha particle is ejected. This occurs with all alpha emitters and is required for the conservation of energy and momentum. Recoil energy is usually on the order of 0.1 MeV.

Table 2-4 lists some radionuclides used in nuclear medicine and their properties.

RADIOACTIVITY

Up to this point we have discussed some basic properties of all atoms and considered the ways in which unstable atoms transform into stable nuclei. Soon after the discovery of radioactivity by Henri Becquerel in 1896, it was observed that some elements lost their radioactive properties in a consistent fashion that varied from one element to another. In 1900, before atomic structure was understood, Ernest Rutherford used the terms *decay* and *disintegrate* to describe this process. It is now known that radioactivity is a nuclear process involving the transformation of a parent nucleus into a daughter nucleus by radioactive decay.

Radioactivity can be defined as the random process of unstable nuclei undergoing transformation to release excess energy in the form of radiation. The key words in this definition are *random process* and *transformation*. It is not possible to predict at what point in time a single radioactive atom will transform or decay, because radioactive decay is spontaneous. However, when a large number of radioactive atoms of a particular radionuclide decay, some of them decay immediately, some at intermediate times, and some very late. Thus, a certain fraction of the total number of atoms decays within a definite time period. For any radionuclide in pure form, the number of atoms that decay per unit of time, dN/dt, is proportional to the number present, N, and a proportionality constant, λ. This relationship describes the *radioactive decay law* and is expressed as

$$\frac{-dN}{dt} = \lambda N \tag{2-2}$$

The negative sign indicates a decreasing number with time. This first-order differential equation provides the rate of decay for infinitely small periods of time. To obtain the rate of decay for measurable periods of time, the equation must be integrated into the following form:

TABLE 2-4 Radionuclides in Nuclear Medicine

Radionuclide	Decay Mode[a]	Half-life[b]	Photon Energy (MeV) and Abundance (%)	β-Max[c] (MeV)	Half-Value Layer (mm Pb)	Gamma Ray Dose Constant (R/mCi-hr/cm)[d]
^{11}C	β^+	20.3 min	0.511 (200)	0.960	4.0	5.91*
^{13}N	β^+	9.97 min	0.511 (200)	1.198	4.0	5.91*
^{14}C	β^-	5715 yr	None	0.156	None	None
^{15}O	β^+	122 sec	0.511 (200)	1.730	4.0	5.91*
^{18}F	β^+	109.8 min	0.511 (181)	0.635	4.0	5.73*
^{32}P	β^-	14.28 days	None	1.710	None	None
^{51}Cr	EC	27.7 days	320 (10)	None	1.7	0.18
^{57}Co	EC	271.8 days	122 (86) 136 (10)	None	0.2	1.0
^{58}Co	EC, β^+	70.9 days	0.511 (31) 0.810 (99)	None	9.0	5.5
^{67}Cu	β^-	61.9 hr	0.092 (11) 0.185 (49)	0.57	7.0	0.52*
^{67}Ga	EC	78.26 hr	0.093 (38) 0.185 (24) 0.300 (16)	None	0.66	0.8
^{68}Ga	β^+	67.8 min	0.511 (178)	1.899	4.0	5.37*
^{82}Rb	β^+	75.6 sec	0.511 (189) 0.777 (13)	3.4	7.0	6.1
^{81m}Kr	IT	13.1 sec	0.191 (66)	None	0.019	1.6
^{89}Sr	β^-	50.52 days	None	1.488	None	None
^{90}Y	β^-	64.08 hr	None	2.28	None	None
^{99}Mo	β^-	65.94 hr	0.740 (14) 0.778 (4.8)	1.214	6.5	0.18
^{99m}Tc	IT	6.01 hr	0.140 (88)	None	0.17	0.78
^{111}In	EC	2.8 days	0.023 x-rays (68) 0.026 x-rays (15) 0.172 (90) 0.247 (94)	None	0.23	3.21
^{123}I	EC	13.2 hr	0.027 x-rays (71) 0.031 x-rays (16) 0.159 (84)	None	0.05	1.6
^{125}I	EC	59.4 days	0.027 x-rays (115) 0.035 (6.7)	None	0.017	1.43
^{131}I	β^-	8.02 days	0.284 (5.8) 0.364 (82) 0.637 (6.5)	0.606	2.4	2.27
^{133}Xe	β^-	5.24 days	0.081 (36%)	0.346	0.035	0.51
^{137}Cs	β^-	30.07 yr	0.662 (95)	0.512	6.0	3.32*
^{153}Sm	β^-	46.27 hr	0.103 (29)	0.710	0.1	0.46
^{186}Re	β^-	89.2 hr	0.137 (9)	1.07	2.5	0.2
^{201}Tl	EC	72.94 hr	0.068–0.080 x-rays (94) 0.167 (10)	None	0.006	4.7

[a] EC = electron capture, IT = isomeric transition.

[b] Half-life values obtained from reference 1.

[c] β-max = decay transition energy (*E* max) minus any photon energy emitted.

[d] R = roentgen. Values with asterisk are from reference 3, pp. 737–741; other values are from package inserts.

$$N = N_0 e^{-\lambda t} \tag{2-3}$$

where:
N_0 = original number of atoms at $t = 0$
N = number of atoms remaining after decay time $t = t$
N_0–N = number of atoms that decayed in time $t = t$
λ = decay constant in reciprocal time t^{-1}
t = time of decay

The rate of decay of a radionuclide is described by its activity, A, or the number of nuclear transformations or disintegrations per unit of time; therefore, A is equivalent to $-dN/dt$, and we may write

$$A = \lambda N \tag{2-4}$$

where:
A = number of disintegrations per unit time
N = number of radioactive atoms
λ = decay constant

The *decay constant* describes the fraction of atoms that decays per unit of time. For example, a decay constant of 0.01 sec^{-1} means that approximately 1% of the atoms decay per second. A decay constant of 0.15 sec^{-1} means approximately 15% decay per second. This interpretation is only approximate, because radioactive decay is a logarithmic function. A strictly linear interpretation of the decay constant gives a falsely high decay rate, but the interpretation helps to make the decay constant tangible. The decay constant is peculiar to the radionuclide in question. No two radionuclides are identical. As we shall see in a subsequent section, the decay constant is related to the radionuclide half-life.

The activity of a radioactive substance is directly proportional to the decay constant of the radionuclide and the number of radioactive atoms present in the sample, as given by the decay law. Therefore, Equation 2-4 can be used to calculate the amount of a radioactive material from its activity. In working with radioactive material it is convenient to know the amount of activity present in the sample at various periods of time. Because activity is directly proportional to the number of atoms, we can substitute the expression A/λ for N in Equation 2-3 and arrive at an exponential expression for radioactive decay in terms of activity:

$$A = A_0 e^{-\lambda t} \tag{2-5}$$

Units of Activity

Radioactivity can be expressed in three ways: (1) as nuclear transformations per second, frequently referred to as decays or disintegrations per second (dps); (2) as curies, millicuries, microcuries, or nanocuries; and (3) as becquerels. The curie was originally defined as the number of disintegrations per second occurring in 1 gram of ^{226}Ra. In the early days of radiochemistry the decay rate of 1 gram of ^{226}Ra was subject to slight variations because it was affected by the purity of a radium sample. Experiments determined that 1 gram of "pure" radium had a disintegration rate close to 3.7×10^{10} dps, and this value was officially

adopted in 1950. Now, the International System of Units has adopted the becquerel (Bq) as the official SI unit of radioactivity. One Bq is defined as one nuclear transformation per second. Therefore, the following expressions are considered to be equivalent:

1 becquerel (Bq) = 1 dps
1 curie (Ci) = 3.7×10^{10} dps (Bq) or 37 gigabecquerels (GBq)
1 millicurie (mCi) = 3.7×10^{7} dps (Bq) or 37 megabecquerels (MBq)
1 microcurie (μCi) = 3.7×10^{4} dps (Bq) or 37 kilobecquerels (KBq)
1 nanocurie (nCi) = 37 dps (Bq) or 37 Bq

By definition we also have the following equivalent expression:

$$1 \text{ Bq} = 2.7 \times 10^{-11} \text{ Ci}$$

Although the becquerel is the official unit of radioactivity, the traditional curie units are routinely used in practice. By using the previous expressions, conversions can be made readily.

Half-life

In 1902 Rutherford noted in his measurements of ^{234}Th that half of any quantity was gone in 24 days. He coined the term *half-life*, the time for any quantity of radionuclide to decrease to half its original quantity. Mathematically it is expressed as

$$T_{1/2} = \frac{0.693}{\lambda} \tag{2-6}$$

Thus, half-life and the decay constant are inversely proportional. For the derivation of this expression, assume that the time of decay (T) in the expression $A = A_0 e^{-\lambda T}$ is that of the half-life or $T_{1/2}$ so that

$$A = \frac{A_0}{2}$$

$$\frac{A_0}{2} = A_0 e^{-\lambda T_{1/2}}$$

$$\frac{1}{2} = e^{-\lambda T_{1/2}}$$

$$2 = e^{+\lambda T_{1/2}}$$

$$\ln 2 = \lambda T_{1/2}$$

$$\frac{0.693}{\lambda} = T_{1/2}$$

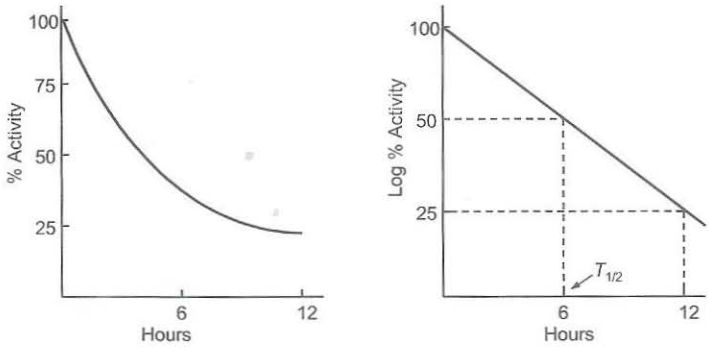

FIGURE 2-17 Half-life determination illustrated by a plot of the decay of ^{99m}Tc over time on linear coordinates (left) and log-linear coordinates (right) that yields a straight line characteristic of a first-order rate process.

The half-life of a radionuclide can be determined experimentally by measuring the activity of a sample over time, assuming that the half-life is reasonably short. Radionuclides with very short or very long half-lives require special techniques. Figure 2-17 shows plots of activity versus time on linear and log-linear coordinates. Because radioactive decay is a first-order rate process, the log-linear plot is a straight line from which the half-life is easily determined.

Radioactivity Calculations

Sample calculations 1A and 1B illustrate the random nature of radioactive decay.

Example 1A. The half-lives of ^{99m}Tc and ^{123}I are 6.01 hours and 13.1 hours, respectively. Which of these two radionuclides has the higher probability for radioactive decay?

The probability for decay is related to the nuclide's decay constant, λ, which is defined as the fraction of radioactivity (and atoms) that decays per unit of time. Thus, the decay constant of ^{99m}Tc is 0.693/6.01 hr = 0.1153 hr^{-1}, or about 11.5% per hour, and the decay constant for ^{123}I is 0.693/13.1 hr = 0.0529 hr^{-1}, or about 5.29% per hour. Therefore, given 100 radioactive atoms of each nuclide, ^{99m}Tc has the probability of decaying about 11 atoms in 1 hour, whereas ^{123}I decays only about 5 atoms in 1 hour.

Example 1B. How many atoms of each radionuclide are in 1 mCi (37 MBq) of ^{99m}Tc and ^{123}I?

The relationship between radioactive atoms and radioactivity is expressed in the formula $A = \lambda N$. Rearranging, we have the following:

$$N = \frac{A}{\lambda} = \frac{A \cdot T_{1/2}}{0.693} = A \cdot T_{1/2} \cdot 1.443$$

$$N_{^{99m}\mathrm{Tc}} = (1\ \mathrm{mCi})(3.7 \times 10^7\ \mathrm{dps/mCi})(6.01\ \mathrm{hr} \times 3600\ \mathrm{sec/hr})(1.443) = 1.16 \times 10^{12}\,\mathrm{d(atoms)}$$

$$N_{^{123}\mathrm{I}} = (1\ \mathrm{mCi})(3.7 \times 10^7\ \mathrm{dps/mCi})(13.1\ \mathrm{hr} \times 3600\ \mathrm{sec/hr})(1.443) = 2.52 \times 10^{12}\,\mathrm{d(atoms)}$$

We can see from these relationships that the number of radioactive atoms is directly proportional to the radionuclide's half-life and inversely proportional to the decay constant. Because

1 mCi (37 MBq) of activity is equal to a defined number of atoms decaying per second, a slower-decaying nuclide must have proportionally more atoms present to be able to decay at the same rate as the faster-decaying nuclide. In this case the ratio of atoms (and half-lives) of ^{123}I to ^{99m}Tc is 2.2. In other words, ^{123}I must have slightly more than twice the number of atoms as ^{99m}Tc to show the same activity.

Mean Life

The expression $N = (A)(1/\lambda)$ describes the total number of atoms in a radioactive source. The term $1/\lambda$ is known as the *mean life* of a radioactive source. The relationship between the mean life and the half-life of a radioactive source is expressed as $1/\lambda = T_{½}/0.693 = (T_{½})(1.443)$. Consider a sample decaying at a rate of 1 mCi (37 MBq). During the first second, 3.7×10^7 atoms decay, but during the next second less than this number decay, and during the third second even less, and so forth (i.e., the decay rate decreases with time). Even though the number of atoms decaying per second decreases, the fraction of radioactive atoms decaying per second remains constant, as defined by λ.

Consider an alternative hypothetical situation in which we assume the sample decay rate does not decrease with time but continues at its initial rate until all the atoms have decayed. The time for this to occur is the mean life. Mean life is a useful term in calculating the radiation absorbed dose to the body, because the dosimetrist must know the total energy that will eventually be deposited after complete decay. This can be calculated from the energy released per atom per decay and the total number of atoms that decay. In the preceding example 1 mCi (37 MBq) of ^{99m}Tc is equal to 1.16×10^{12} atoms. This means that after complete radioactive decay this many atoms of ^{99m}Tc will have transformed into ^{99}Tc. If the gamma ray energy per decay is 140 keV and the photon abundance is 88%, then (140 keV) (0.88) (1.16×10^{12}) or 1.62×10^{14} keV will be emitted as gamma radiation. The remaining 12% of energy will be released as conversion electrons.

Example 2. A vial contains 100 mCi (3700 MBq) of ^{131}I-sodium iodide in a 10 mL volume on Monday at 12 noon. Calculate the volume of solution required for a 12 mCi (444 MBq) dose on Friday at noon.

This problem requires use of exponential decay Equation 2-5. First calculate the radioactive concentration on Monday noon.

$$100 \text{ mCi}(3700 \text{ MBq})/10 \text{ mL} = 10 \text{ mCi}(370 \text{ MBq})/\text{mL}$$

Next, calculate the new concentration on Friday noon (4 days later).

$$A = Ae^{-\lambda t}$$

$$A = 10 \text{ mCi/mL } e^{-\frac{0.693}{8.05 \text{ days}}(4 \text{ days})}$$

$$A = 10 \text{ mCi/mL}(0.7087)$$

$$A = 7.09 \text{ mCi/mL}$$

$$\text{A dose of 12 mCi requires } \left[\frac{12 \text{ mCi}}{7.09 \text{ mCi/mL}}\right] \text{ or } 1.7 \text{ mL}$$

Example 3. A vial contains 50 μCi (1850 kBq) of ^{131}I-sodium iodide capsules. How many days are required for the capsules to decay to 5 μCi (185 kBq)?

The half-life can be used to estimate the time required.

Number of days	0	8	16	24	32
Number of half-lives	0	1	2	3	4
Capsule activity (μCi)	50	25	12.5	6.25	3.125

Thus, between 24 and 32 days is required. To arrive at the exact answer, use Equation 2-5 in logarithmic form.

$$A = A_0 e^{-\lambda t}$$

$$\ln A = \ln A_0 - \lambda t$$

$$\ln(5\ \mu\text{Ci}) = \ln(50\ \mu\text{Ci}) - \frac{0.693}{8.05\ \text{days}}(t)$$

$$1.61 = 3.91 - 0.0861t$$

$$t = \frac{2.3}{0.0861\ \text{days}^{-1}} = 26.7\ \text{days}$$

Decay Tables

When making decay calculations on a routine basis in a nuclear pharmacy, it is more convenient to use decay tables instead of the exponential decay equation. A decay table is a tabulation of specified times and the respective fraction of activity remaining at those times. It is prepared using the exponential decay equation. Rearrangement of Equation 2-5 yields the following expression:

$$\frac{A}{A_0} = e^{-\lambda t} \qquad (2\text{-}7)$$

If A is the activity remaining after an original amount of activity (A_0) decays for a period of time (t), then A/A_0 is the fraction of the original amount remaining. For example, a decay table for ^{131}I can be generated by substituting the values of 1, 2, or 3 days and so forth for t in Equation 2-7 to yield the following:

t (days)	$e^{-\lambda t}$
0	1.0000
1	0.9175
2	0.8418
3	0.7724
4	0.7087
5	0.6502
6	0.5966
7	0.5474
8	0.5022

Example 4. Calculate the activity in a 10 μCi (370 kBq) capsule of ^{131}I-sodium iodide.

a. What is the activity after 5 days' decay?
Answer: 10 μCi (0.6502) = 6.5 μCi (240.5 kBq)

b. What is the activity after 9 days' decay?
Answer: 10 μCi (0.5022) (0.9175) = 4.6 μCi (170.2 kBq)

Radiopharmaceuticals are labeled with the total amount of activity at a specified date and time, referred to as the *calibration time*. Only at this time will the vial contain the labeled activity. After the calibration time it will contain less activity because of radioactive decay, and before the calibration time it will contain proportionately more activity. Radiopharmaceuticals are often received in the nuclear pharmacy before the calibration time.

Example 5. Calculate the activity in a capsule of ^{131}I-sodium iodide at noon on January 1 if the label states "10 μCi (370 kBq) per capsule as of 12 noon January 6."

Since the capsule must obviously contain more than 10 μCi (370 kBq) on January 1, the calibration time activity should be divided by the decay factor for 5 days. Thus, the activity in the capsule on January 1 is (10 μCi)/(0.6502) = 15.38 μCi (569 kBq).

The same answer can be obtained by using the reciprocal of the postcalibration decay factor, 1/0.6502 or 1.538, which is the precalibration decay factor. The answer to the previous question is calculated as follows: 10 μCi × 1.538 = 15.38 μCi (569 kBq). Precalibration factors can be readily calculated for any times before the calibration time using the following rearrangement of Equation 2-5:

$$\frac{A}{A_0} = e^{+\lambda t} \tag{2-8}$$

A precalibration decay table for ^{131}I is

t (days)	$e^{+\lambda t}$
8	1.9912
7	1.8268
6	1.6762
5	1.5380
4	1.4110
3	1.2947
2	1.1870
1	1.0899
0	1.0000

REFERENCES

1. *Chart of the Nuclides*. 15th ed. Cincinnati, OH: Lockheed Martin; 1996.
2. Friedlander C, Kennedy JW, Miller JM. *Nuclear and Radiochemistry*. 2nd ed. New York: Wiley; 1966:28.
3. Johns HE, Cunningham JR. *The Physics of Radiology*. 3rd ed. Springfield, IL: Charles C Thomas; 1969.
4. Quimby EH, Feitelberg S. *Radioactive Isotopes in Medicine and Biology*. 2nd ed. Philadelphia: Lea & Febiger; 1963:92-3.
5. Weber DA, Eckerman KF, Dillman LT, et al. *MIRD: Radionuclide Data and Decay Schemes*. Reston, VA: Society of Nuclear Medicine; 1989.

3 Radiation Detection and Measurement

The type of radiation emitted from a radioactive substance and its particular application in medicine and science determine the method used to detect it. In nuclear medicine and nuclear pharmacy, special types of instruments are used to quantitate the amount of radioactivity in a radiopharmaceutical dosage, to measure the radioactivity present in the body of a patient undergoing a nuclear medicine procedure, and to survey packages of radioactive material and the work environment for health and safety reasons. All of the instruments used in these types of procedures are based on the ability of radiation to ionize matter.

INTERACTIONS OF RADIATION WITH MATTER

Radiation in nature is of two types, particulate and electromagnetic. Both types are emitted from the radiopharmaceuticals used in nuclear medicine. The energy of these radiations is sufficient to cause excitation and ionization of the atoms in matter. During excitation, orbital electrons may be raised to higher-energy suborbits and then emit visible and ultraviolet (UV) light when they return to the ground state. During ionization, electrons are removed from atoms, producing ion pairs. An ion pair is one electron and one positively charged atom from which the electron was removed. The average energy required to produce an ion pair in air (W) is 34 eV. A particular form of radiation will produce thousands of excitations and ionizations in matter, depending on its total energy. Thus, a 340 keV (340,000 eV) beta particle will produce about 10,000 ion pairs in air before it comes to rest.

The number of ion pairs produced per unit path length traveled by radiation is termed *specific ionization* (SI), while the energy dissipated per unit path length is termed the *linear energy transfer* (LET). SI and LET are directly related:

$$\text{LET} = \text{SI} \times \text{W} \qquad (3\text{-}1)$$

SI and LET are directly proportional to particle mass and charge and inversely proportional to particle velocity. Therefore, an alpha particle has higher specific ionization and LET compared with a proton of the same energy because the alpha particle is roughly four times more massive, has twice the charge, and moves more slowly through matter. An electron of similar energy, having a unit negative charge and much smaller mass compared with the proton or alpha particle, moves through matter at a much higher velocity and with a lower specific ionization and LET. Tables 3-1 and 3-2 compare the specific ionization and LET, respectively, of these particles in air.

The interaction of radiation with matter is important because it is the basis for detection and measurement of radiation and is the initiating event that leads to biologic damage in tissue.

TABLE 3-1 Specific Ionization of Radiation in Air

Energy (MeV)	Specific Ionization (ion pairs per 1.0 mg-cm^{-2})		
	Beta Particle	Proton	Alpha Particle
10	53	1,100	13,000
5	49	2,100	22,000
4	48	2,400	26,000
3	47	3,100	32,000
2	46	4,200	41,000
1	46	6,800	54,000
0.5	50	11,200	56,000
0.2	100	16,700	40,000

Adapted from reference 1.

TABLE 3-2 Linear Energy Transfer (LET) of Radiation in Water

Energy (MeV)	LET (keV/μm)		
	Beta Particle	Proton	Alpha Particle
0.1	0.45	90	170
0.5	0.21	47	350
1.0	0.18	27	300
5.0	0.18	9	110

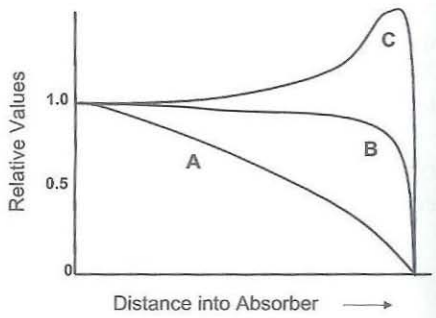

FIGURE 3-1 Composite diagram of alpha particle interactions in matter. (A) particle velocity; (B) particle range; (C) particle specific ionization and linear energy transfer.

Alpha Particles

Alpha particles are fast-moving monoenergetic helium nuclei carrying two positive charges. Relative to other types of radiation they are quite massive, being composed of two protons and two neutrons. Consequently, alpha particles are not easily deflected by interaction with electrons in matter, and they travel in straight-line paths with a definite range in a particular absorber.[1] An alpha particle produces excitation and ionization in matter by electrostatic attraction of electrons. After thousands of excitations and ionizations, an alpha particle eventually comes to rest, acquiring two electrons to become a neutral helium atom. Alpha particles have high SI and LET, as shown in Tables 3-1 and 3-2 and Figures 3-1 and 3-2. SI and LET increase rapidly near the end of the alpha particle's path because of the particle's slower speed in this region, which increases its probability of interaction. In tissue, the dense ionization of an alpha particle with release of energy results in a higher probability for biologic damage compared with low LET radiation. This is a principal reason for not using alpha emitters in diagnostic applications.

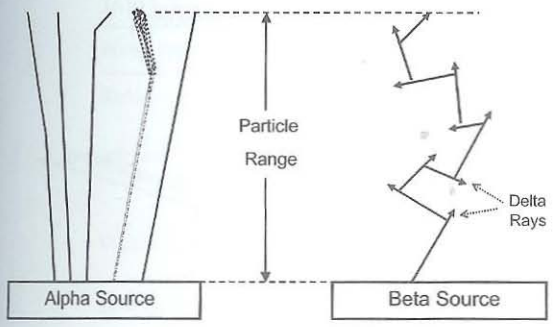

FIGURE 3-2 Pathways of alpha and beta particle interactions in matter.

Positrons

Positrons are positively charged beta particles (electrons) released from the nuclei of proton-rich radionuclides. Positrons produce excitation and ionization of matter by electrostatic attraction of orbital electrons in the matter, similar to alpha particles. However, because of their smaller mass, positrons are easily deflected during their interaction with orbital electrons. The path of a positron through matter is tortuous, similar to that of a negatron (Figure 3-2). After thousands of excitations and ionizations, the positron comes to rest in association with a negative electron to momentarily produce a species called a positronium. The positronium can be thought of as an atom, with the positron acting as the nucleus. The positron then combines with the electron and undergoes an annihilation reaction, converting the two electron masses into two 0.511 MeV annihilation photons (see discussion of positron decay in Chapter 2).

Negatrons

Negatrons are negatively charged beta particles (electrons) released from the nuclei of neutron-rich radionuclides. Negatrons interact with matter by three major processes: excitation, ionization, and bremsstrahlung production. The first two processes involve interaction with orbital electrons and the third process involves an interaction with the nucleus. Negatrons interact with orbital electrons by electrostatic repulsion. During excitation, negatrons in the vicinity of an atom can cause a loosely bound valence electron to be moved to an optical orbit, whereupon the return of the excited electron causes emission of light. Negatrons may ionize atoms by removing an electron from either an outer shell or an inner shell. Removal of inner-shell electrons results in the release of characteristic x-rays as outer-shell electrons fill in the inner-shell deficits. The electrons released from the atom by the ionization process are called *delta rays*. Because the interaction is between particles of equal mass, the path of a negatron is tortuous, being deflected at each interaction (Figure 3-2). A high-energy negatron may undergo a deceleration in the vicinity of the nucleus, releasing electromagnetic radiation called *bremsstrahlung* (braking radiation). The probability of bremsstrahlung production increases directly as the negatron's energy and the atomic number of the absorber increase. For this reason, it is best to shield high-energy beta emitters, such as ^{32}P, with an inner shield of material with a low atomic number (Z), such as Plexiglas, and an outer shield of lead to absorb any bremsstrahlung. The processes of negatron interaction with matter are summarized in Figure 3-3.

Neutrons

The neutron was proposed by Ernest Rutherford in 1920 as a particle of unit mass and charge of zero that could easily penetrate a nucleus and unite with it. In 1932 James

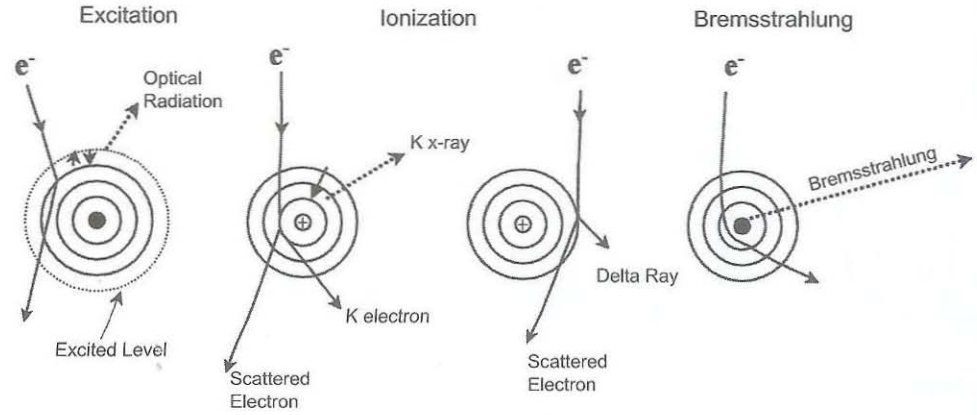

FIGURE 3-3 Beta particle interactions with matter: excitation, ionization, and bremsstrahlung.

Chadwick demonstrated that the neutron could not be deflected in electric and magnetic fields, attesting to its neutral charge.[2]

It is known from beta-minus decay that a neutron is converted into a proton and an electron in the nucleus. Energy is liberated in this process, since the combined mass of a proton and electron is less than the mass of a neutron. Using the example of a hydrogen atom, the neutron mass (1.0086654 AMU) exceeds the combined proton and electron mass (1.0078252 AMU) by 0.0008402 AMU, so an energy equivalent to 0.782 MeV is liberated in the process; therefore, a free neutron should decay spontaneously as follows:

$$^{1}_{0}n \rightarrow {}^{1}_{1}H + {}^{0}_{-1}e + \nu$$

Experiments have demonstrated that a neutron decays spontaneously with a half-life of 700 seconds.[2]

Although neutron emitters are not used in nuclear medicine, their interactions with matter are of interest. Neutrons can be classified by their energies as being thermal (approximately 0.025 eV), slow (0.03 eV–100 eV), intermediate (100 eV–10 keV), and fast (10 keV–20 MeV). Neutrons interact with matter in three ways: (1) scatter by nuclear collision, (2) capture by a nucleus, and (3) decay of a free neutron. Typical scatter and capture reactions that may occur in biologic systems are as follows:[3]

Scatter reactions

$$^{1}_{0}n + {}^{1}_{1}H \rightarrow {}^{1}_{1}H + {}^{1}_{0}n' \left(\text{elastic scatter}\right)$$

$$^{1}_{0}n + {}^{12}_{6}C \rightarrow {}^{12}_{6}C + {}^{1}_{0}n' + \gamma \left(\text{inelastic scatter}\right)$$

Capture reactions

$$^{1}_{0}n + {}^{14}_{7}N \rightarrow {}^{14}_{6}C + {}^{1}_{1}H$$

Scatter reactions are nonionizing events typical of neutron moderation reactions that occur in water or graphite reactors. *Elastic scatter* collisions are those in which the total kinetic energy and momentum of the neutron and nucleus remain constant. This is most likely to occur between two bodies of equal mass, as in a billiard ball collision. Paraffin, water, and other materials rich in hydrogen are good moderators of neutrons by the elastic

TABLE 3-3 Properties of the Electromagnetic Wave Spectrum

Wave Type	Frequency[a]	Wavelength[b]	Photon Energy
Radio	1×10^5	3×10^5 cm	4.13×10^{-10} eV
	3×10^{10}	1.0 cm	1.24×10^{-4} eV
Infrared	3×10^{12}	0.01 cm	0.0124 eV
	3×10^{14}	0.0001 cm (10,000 Å)	1.24 eV
Visible light	4.3×10^{14}	7000 Å	1.77 eV
	7.5×10^{14}	4000 Å	3.1 eV
Ultraviolet	7.5×10^{14}	4000 Å	3.1 eV
	3×10^{16}	100 Å	124 eV
Soft x-rays	3×10^{16}	100 Å	124 eV
	3×10^{18}	1 Å	12.4 keV
Diagnostic x-rays, gamma rays	3×10^{18}	1 Å	12.4 keV
	3×10^{20}	0.01 Å	1.24 MeV
Cosmic rays	3×10^{20}	0.01 Å	1.24 MeV
	3×10^{23}	0.00001 Å	1240 MeV

[a] Waves/second.

[b] Photon emitters in nuclear medicine generally range from 0.155 Å (80 keV) to 0.031 Å (400 keV).

scatter process. In the reaction with hydrogen, a portion of the neutron's energy is transferred to the nucleus and the remaining energy is retained by the scattered neutron. *Inelastic collisions* result in a loss of energy from the system. The reaction is (n,n'γ) where n is the incident neutron and n' is the slower neutron released by the nucleus, the energy difference being emitted as a gamma ray. Moderation of fast neutrons by carbon is primarily by this process.

Neutron capture reactions are ionizing events because a proton is ejected from the collision with a nucleus. This type of reaction obviously has more biologic consequence than a scatter reaction. Thermal and slow neutrons can more easily be captured by a nucleus because the probability of capture is inversely related to neutron speed. Nuclei with high capture cross-sections have a higher probability of capturing fast neutrons. Boron or cadmium rods in nuclear reactors are used to control or shut down the reactor because they have high neutron capture cross-sections. Capture reactions are an important means of producing artificial radionuclides (see Chapter 8). An interesting proposed medical application is boron neutron capture therapy. This simple yet elegant technique involves targeting a boron-containing drug to a tumor and irradiating the tumor with thermal neutrons. The capture of neutrons by boron generates alpha particles that intensely irradiate the tumor. The success of this technique has been limited because of the difficulty in delivering boron-containing drugs and thermal neutrons specifically to tumor cells.

Gamma and X-Rays

Electromagnetic radiation exhibits properties characterized by frequency, wavelength, and energy. This is shown in Table 3-3 and described by the following equations:

$$\nu = \frac{c}{\lambda} \tag{3-2}$$

$$E = h\nu = \frac{hc}{\lambda} \tag{3-3}$$

where
ν = frequency (waves/sec)
c = speed of light (2.998×10^{10} cm/sec)
λ = wavelength (in angstroms $\times 10^{-8}$ cm)
E = energy in ergs
h = Planck's constant (6.626×10^{-27} erg-sec)

Thus, the energy of a 1-angstrom photon is

$$E = \frac{\left(6.626 \times 10^{-27}\ \text{erg–sec}\right)\left(2.998 \times 10^{10}\ \text{cm/sec}\right)}{1 \times 10^{-8}\ \text{cm}} = 1.986 \times 10^{-8}\ \text{erg}$$

and its equivalent energy in electron volt units is

$$E = \frac{1.986 \times 10^{-8}\ \text{erg}}{1.602 \times 10^{-9}\ \text{erg/keV}} = 12.4\ \text{keV}$$

Thus,

$$E_{\text{keV}} = \frac{12.4}{\lambda} \tag{3-4}$$

Long-wavelength low-energy electromagnetic radiation that occurs in the visible light spectrum exhibits wavelike properties; however, short-wavelength high-energy radiation such as x-rays and gamma rays does not behave as waves but more as discrete packets of energy. These discrete packets are called *quanta* or *photons*, and they interact with matter as if they were small particles. The three processes of photon interaction with matter are the photoelectric effect, Compton scatter, and pair production. Each of these interactive processes causes ionization of matter.

Photoelectric Effect

Absorption of photons by the photoelectric effect is illustrated in Figure 3-4. This process involves a relatively low-energy photon interacting with and ejecting an inner-shell electron, usually from the K shell. The photon disappears, with all of its energy expended to overcome the electron's binding energy and to impart kinetic energy to the ejected electron. For example, a 50 keV photon interacting with a K-shell electron having a binding energy of 40 keV ejects a photoelectron with 10 keV of energy. The photoelectric interaction produces ion pairs. Additionally, characteristic x-rays and Auger electrons are emitted from the ionized atom when electron shell vacancies are filled in by outer-shell electrons. The total energy emitted by an ionized atom from all processes is equal to the incident photon energy.

In soft tissue, the photoelectric effect is the predominant interactive process for photon energies up to 50 keV. The probability for the interaction increases as the photon energy decreases below 50 keV and as the atomic number and density of the absorber increase. Bone, with a Z of 13.8 and a density of 1.92, will absorb about six times more energy than soft tissue, which has an average Z of 7.4 and density of 1. Radionuclides with photon

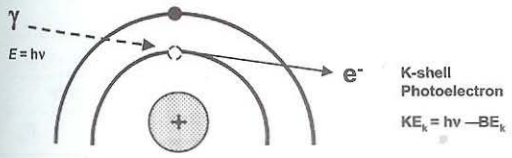

FIGURE 3-4 Photoelectric absorption. The entire photon energy is transferred to the ejected electron. The kinetic energy of the ejected electron, KE_k, is equal to the initial photon energy, hv, minus the electron's binding energy, BE_k.

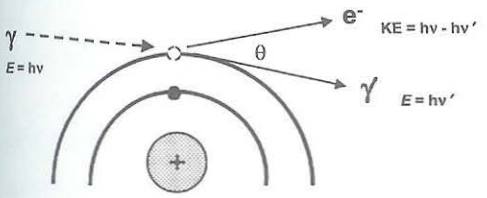

FIGURE 3-5 Compton effect. An incident photon transfers part of its energy to a loosely bound electron that is ejected from the atom. The remaining energy is associated with the scattered photon. The kinetic energy of the ejected electron (KE_m) is equal to the difference between the incident and scattered photon energies. The electron binding energy is insignificant.

energies below 50 keV, such as ^{125}I (30 keV), are unsatisfactory for diagnostic imaging because of high tissue absorption by the photoelectric effect.

Compton Scatter

The process of Compton scatter involves the interaction of a medium-energy photon with a loosely bound outer-shell electron. The electron is ejected and an ion pair is produced. As shown in Figure 3-5, only a portion of the incident photon energy is transferred to the electron, depending on the angle of scatter (θ). The energy of the scattered photon (in kiloelectron volts) can be calculated from the following relationship:

$$E_s = \frac{E_i}{1 + \frac{E_i}{511}(1 - \cos\theta)} \tag{3-5}$$

The kinetic energy given to the Compton electron also depends on the angle of interaction. A direct hit with a scatter angle of 180° transfers the largest amount of energy to the Compton electron. In any event, the energy of the ejected electron is the difference between the energies of the incident photon (E_i) and the scattered photon (E_s) given by

$$E_{ce} = E_i - E_s \tag{3-6}$$

The secondary or Compton-scattered photon continues to undergo additional Compton interactions until the photon is eventually absorbed by the photoelectric effect. The relationships between the energies of the incident photon, scattered photon, and Compton electron at various angles of interaction for ^{125}I, ^{99m}Tc, and ^{131}I photons are given in Table 3-4. The very small energy required to overcome electron-binding energy has been ignored in these calculations.

The probability for photon interaction by the photoelectric effect and Compton scatter is about equal at photon energies between 10 and 50 keV. The Compton process predominates at energies higher than 50 keV (Table 3-5).[4] Most radionuclides used in nuclear medicine, because of their higher energies, interact in tissue initially by Compton scatter. The probability of a Compton interaction depends upon electron density. High-density

TABLE 3-4 Energy of Compton-Scattered Photons and Electrons[a]

Radionuclide	Photon Energy (keV)	Angle of Scatter, θ							
		45°		90°		135°		180°	
		E_s	E_{ce}	E_s	E_{ce}	E_s	E_{ce}	E_s	E_{ce}
^{125}I	27.5	27.1	0.4	26.1	1.4	25.2	2.3	24.8	3.3
^{99m}Tc	140.5	130.5	10.5	110.5	30.5	95.9	45.1	90.9	50.1
^{131}I	364	301.1	62.9	212.6	151.4	164.3	199.7	150.1	213.9

[a] E_s = energy of the scattered photon, E_{ce} = energy of the Compton-scattered photon.

TABLE 3-5 Relative Importance of Different Types of Absorption in Water

Photon Energy	Percent Absorption	
	Photoelectric	Compton
Up to 10 keV	95	5
25 keV	50	50
50 keV	11	89
80 keV	3	97
100 keV	1	99
150–1000 keV	0	100

Source: Reference 4.

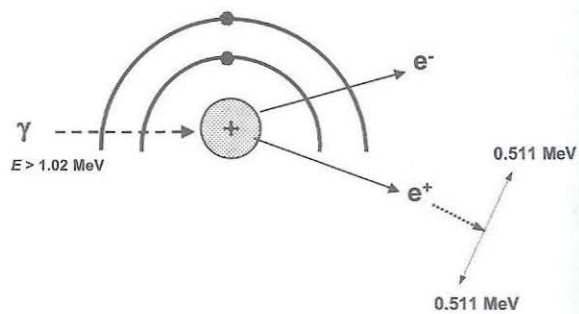

FIGURE 3-6 Pair production. An incident photon of at least 1.022 MeV in the vicinity of the nuclear force field is transformed into two electrons, one negative and one positive. The positron eventually is annihilated outside the atom, producing two 0.511 MeV photons.

material provides more stopping power for photons undergoing photoelectric and Compton interactions, because more atoms (and electrons) are present per unit volume of absorber compared with low-density material. For this reason, lead (density 11.35) is a good absorber of gamma radiation.

Pair Production

The pair production process involves the interaction of a very high energy photon within the nuclear force field with conversion of the photon into two electronic particles: one positron and one negatron (Figure 3-6). Because the particles produced are equivalent to the mass of two electrons, the minimum energy required for this process to occur is 1.022 MeV. Photon energy in excess of 1.022 MeV is distributed to the particles as kinetic energy. The probability for pair production increases with increasing atomic number of the absorber because of the increased nuclear force field present with high-Z material. Pair

production begins to be significant in soft tissue, with photon energies between 5 and 10 MeV, and therefore is not an important mode of photon absorption with the radionuclides used in nuclear medicine.

RADIATION DETECTION INSTRUMENTATION

Detection and measurement of radiation in nuclear pharmacy and nuclear medicine is important for radiation protection purposes and for accurate assessment of radiopharmaceutical activity for imaging procedures. Proper use of radiation detection equipment requires an understanding of its construction and operation. This section covers the two basic methods of radiation detection and measurement: ion collection and scintillation.

Ion Collection Methods of Radiation Detection

Ion collection methods of radiation detection are based on the ability of radiation to ionize atoms of gas. Typical gases used are air, helium, and argon. The gas is contained in a sealed chamber with a positive and negative electrode pair (Figure 3-7). A power supply creates a voltage potential across the electrodes. An ammeter measures the current produced by electrons released from the ionization process. The current generated is directly proportional to the number of ion pairs produced by the radiation source.[3]

Figure 3-8 illustrates the relationship between applied voltage and current in a gas-filled detector. The change in current with change in voltage can be understood by considering a constant source of activity exposed to a chamber that contains a definite number of ionizable gas molecules. In this situation a given amount of ionizing radiation enters the chamber and ionizes a given number of the gas molecules. When no voltage is applied, the ion pairs recombine (*recombination region*) and no current is generated. However, as the voltage is increased, some of the electrons in the ion pairs are collected at the anode, generating a current. A greater proportion of these electrons are collected with a proportional increase in current as the voltage continues to increase. When the voltage applied is high enough, all of the primary electrons are collected and a plateau known as the *saturation current* is reached. Additional increases in voltage do not cause an appreciable increase in current over the plateau; the primary electrons are simply collected at a faster rate as voltage is increased. Over this voltage range simple ionization occurs. Beyond the plateau, however, additional increases in voltage produce an increase in current proportional to

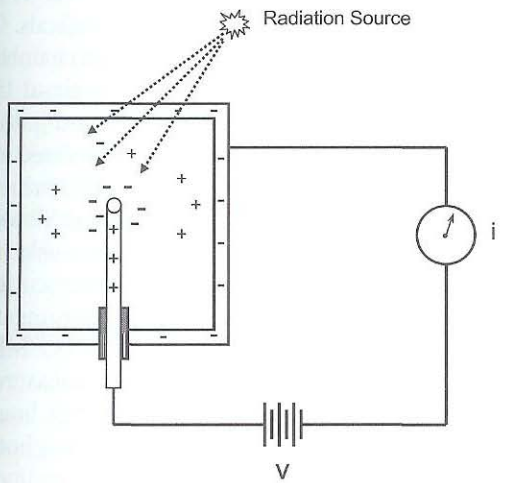

FIGURE 3-7 A simple gas-filled radiation detector. Electrons released by ionization of the detector gas molecules are collected at the central anode, producing a current proportional to the amount of ionization; i = current, v = voltage.

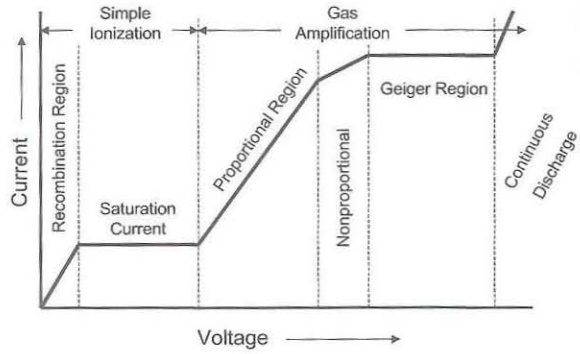

FIGURE 3-8 Current–voltage curve for gas-filled ionization detectors. See text for explanation.

voltage because of secondary ionizations. This is known as the *proportional region*, in which fast-moving primary electrons produce secondary ionizations on their way to the anode. Eventually, most of the gas molecules in the chamber are ionized, and a region of nonproportionality is reached. As voltage is increased further above this point, another current saturation plateau is reached, known as the *Geiger region*. The voltage in this region is high enough that the initial ionizing event in the tube will result in an avalanche of ion pairs because of ionization of all available gas molecules. In the Geiger region the same current output is produced whether the ionizing event initially produces 1, 100, or 1000 ion pairs. At still higher voltages, a continuous discharge or arcing of current across the electrodes occurs and should be avoided because this will damage the tube.

Three types of ion collection instruments are represented in this current/voltage response curve: ionization chambers, proportional counters, and Geiger-Müller (GM) counters. *Ionization chambers* are useful for measuring medium- to high-intensity sources of radioactivity and have operating voltages in the range of 50 to 150 volts (saturation current plateau region). Examples of instruments include the hand-held "Cutie Pie" ionization chamber survey meter, which is useful for measuring output from high-activity sources, and the dose calibrator, which is used to measure the activity of radiopharmaceuticals in the microcurie to curie range. GM detectors are used to measure low-intensity radiation, such as in radiation surveys of the work environment. Their operating voltages are usually set near 1000 volts (Geiger region).

Radionuclide Dose Calibrator

The dose calibrator is used routinely to measure the activity of radiopharmaceuticals. Its output is directly proportional to the amount of activity placed into the ionization chamber. Figure 3-9 is a block diagram of its essential components.[5] Operating voltage is about 150 volts. The electrode elements are configured in a sealed chamber of pressurized gas. A typical chamber may contain approximately 12 atmospheres of argon to increase detection sensitivity. The chamber is constructed with a central well for accepting radiopharmaceutical vials and syringes. The current-to-voltage amplifier in the circuit of the dose calibrator converts the small current generated by the ionizations into a voltage. The range selector is a variable resistor circuit that adjusts the instrument for the activity range (microcuries, millicuries, curies) being measured. This adjustment is automatic in newer instruments. The useful activity range of a dose calibrator is 0.1 mCi to approximately 10 Ci (3.7 MBq to 3.7×10^5 MBq), although activities below 0.1 mCi (3.7 MBq) can be accurately measured if background activity is low. The chamber sensitivity of a dose calibrator is not linear with photon energy (Figure 3-10); sensitivity increases below 200 keV because of photoelectric interactions and above 200 keV because of an increase in Compton interactions.

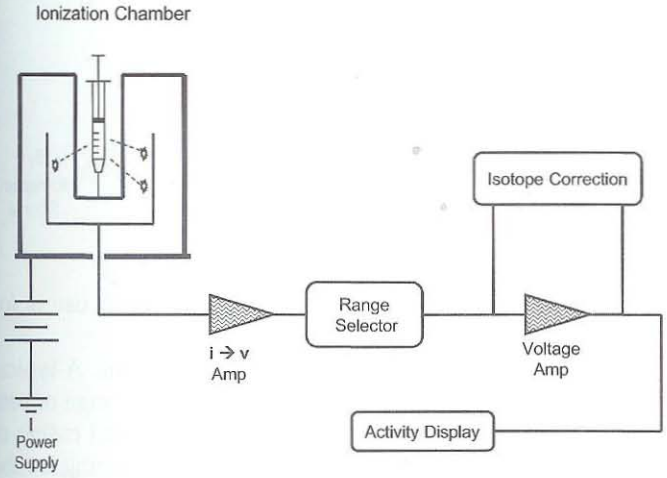

FIGURE 3-9 Block diagram of an ionization chamber detector (dose calibrator); i = current, v = voltage.

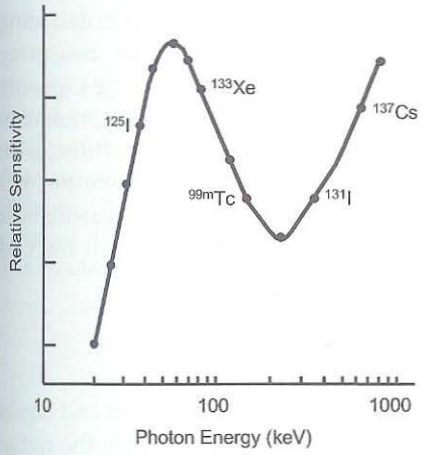

FIGURE 3-10 Relative change in dose calibrator ion chamber response with photon energy.

Therefore, an isotope correction amplifier is necessary to adjust the detector's output, compensating for the different currents generated by radionuclides with different photon energies and intensities.[6] Instruments typically employ preset radionuclide pushbuttons or a calibration dial for this compensation. This adjustment permits the instrument to display the correct activity of the radionuclide being measured.

In measuring the activity of a particular radionuclide, its calibration setting is selected and the instrument's display is "zeroed" to remove any background activity. The source is then placed in the chamber well and its activity is automatically displayed on the readout. Before each day's use, the dose calibrator's operation is checked with a long-lived reference source, such as ^{137}Cs. The full complement of quality control tests required for dose calibrators is discussed in Chapter 12.

Geiger-Müller Detectors

A GM detector is used to detect and measure low-level beta and gamma radiation. Some units can also detect alpha radiation through a thin end-window. The GM counter's response is independent of the amount of ionization occurring within the detector, because a single ionization event is all that is needed to produce a current pulse. This makes the

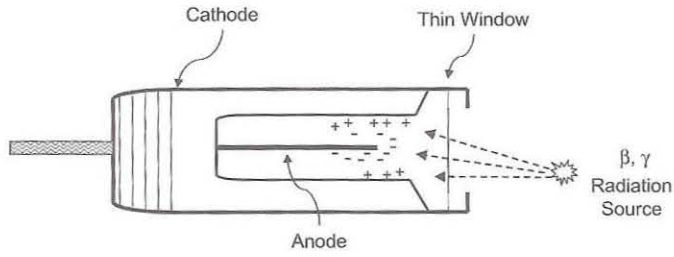

FIGURE 3-11 Cutaway diagram of an end-window Geiger-Müller detector.

GM counter suitable for low-level radioactivity detection; its most common use is for surveying work areas for radioactive contamination.

GM tubes are supplied with end-window or side-window configurations. A typical end-window tube is shown in Figure 3-11. The thin mica window allows passage of beta particles and weak gamma rays that normally would be stopped by the metal casing of the tube. Because of the high operating voltage in GM tubes, radiation entering a tube produces primary ionizations that proceed to ionize the entire gas. A quenching agent in the gas absorbs energy to momentarily stop discharge between ionizing events. This alternating ionization–quenching sequence produces current pulses that drive an exposure meter and are audible as ticking sounds. GM detectors have no energy-discriminating ability but, if calibrated against a reference source such as ^{137}Cs, are useful for measuring exposure rate in roentgens per hour from gamma ray sources. The most accurate exposure measurements, however, require calibration of the GM detector with a standard radiation source whose gamma energy is identical to or close to the energy of the source to be measured. By contrast, an ionization chamber survey meter, such as the Cutie Pie, has low energy dependence and will therefore give a more accurate exposure measurement over a wide range of radionuclide energies. It is, however, less sensitive than the GM counter and has more application with high-intensity sources.

Scintillation Methods of Radiation Detection

There are two types of scintillation detectors: solid-crystal scintillation detectors and liquid scintillation detectors. The detector is the primary medium that interacts with the radiation. A solid-crystal detector typically is a sodium iodide (NaI) crystal that is hermetically sealed in a metal casing. Gamma radiation of sufficient energy can readily penetrate this casing to interact with the crystal, but particulate radiation cannot do so. Consequently, the counting of pure beta emitters such as ^{3}H and ^{14}C is best accomplished by liquid scintillation. With liquid scintillation, the sample to be counted is dissolved or suspended in a scintillation "cocktail" that consists of a solvent with scintillator compounds. The intimate admixture of sample and scintillator provides efficient detection of beta radiation. Except for the difference in detector material, the operating principles of liquid and solid-crystal scintillation detectors are basically the same. Liquid scintillation detection is illustrated in Figure 3-12.

The basic instrument used for counting gamma radiation in nuclear medicine is the scintillation counter. It consists of a sodium iodide crystal/photomultiplier tube detector and an electronic processing unit (Figure 3-13). The crystal may be flat-surfaced or contain a well for test-tube samples. The sodium iodide detector converts photon energy into visible light after absorption of gamma rays by Compton scatter and photoelectric interactions. The photomultiplier (PM) tube converts the visible light photons into electrical pulses. The processing unit consists of an amplifier for adjusting the magnitude of electrical pulses and a pulse height analyzer (PHA) for selection or rejection of pulses for

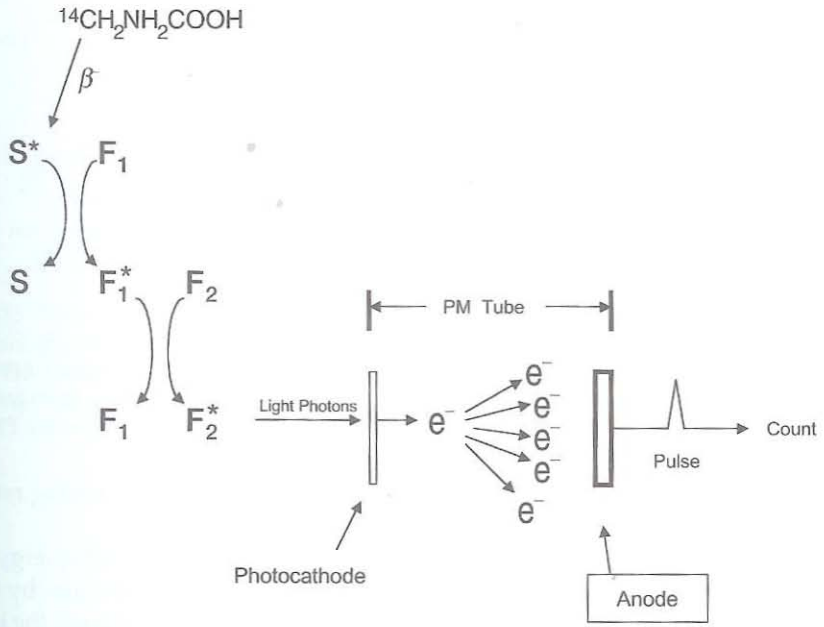

FIGURE 3-12 Liquid scintillation detection. Decay of a beta-emitting radiochemical in the scintillation "cocktail" releases beta particles (electrons) which, through a series of interactions, transfer energy to the solvent molecules. Excited solvent molecules (S*) then transfer their energy to the fluor molecules (F). Excited fluor molecules (F*) release their energy as visible light photons (scintillations). The light photons strike the photocathode of the photomultiplier (PM) tube, releasing electrons. These electrons are multiplied, generating an electrical pulse that is registered as a count. The number of pulses counted is proportional to the amount of radioactivity in the sample.

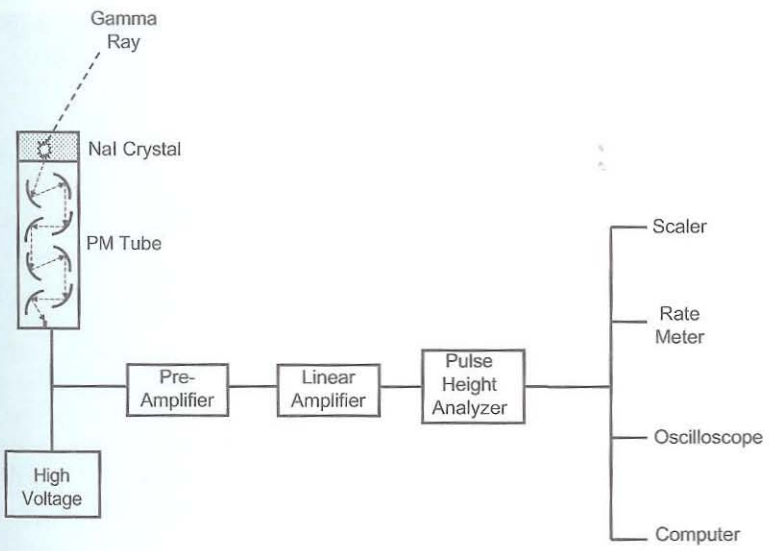

FIGURE 3-13 Block diagram of a scintillation counter. See text for explanation.

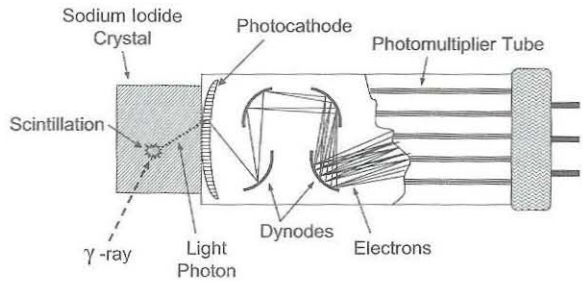

FIGURE 3-14 Sodium iodide crystal–PM tube scintillation detector. Total light output is proportional to gamma ray energy deposited in the crystal. If one electron ejects four electrons from each dynode, 10 dynodes will result in 4^{10} or about 1 million electrons collected at the anode of the PM tube.

counting. A variety of devices are used for recording output pulses, including rate meters, scalers, oscilloscopes, and computers.

Figure 3-14 shows the sodium iodide detector and PM tube. High-energy photons interacting with the crystal transfer energy to the sodium iodide molecules by Compton scatter and photoelectric interactions. The energy of electrons released from the ionization process is mostly absorbed as heat, because pure sodium iodide crystals do not scintillate well. However, if the crystal is activated with 0.1% thallium, designated NaI(Tl), some of the excited electrons become trapped in the vicinity of the thallium atoms, whereupon their energy is released as visible light photons of about 3 eV. This is the scintillation event. It takes about 30 eV absorbed to generate a single 3 eV light photon. About 20 to 30 of these light photons are produced per kiloelectron volt of energy transferred to the crystal.[7] The number of scintillations and thus the amount of light generated is proportional to the amount of gamma energy deposited in the crystal. The light photons cause electrons to be ejected from the photosensitive cathode of the PM tube, which is optically coupled to the sodium iodide crystal. The electrons are then attracted to a series of dynodes, each about 100 V more positive than the previous one. An average of four electrons are ejected for each incident electron on a dynode so that electron multiplication occurs. A series of 10 dynodes will result in 4^{10} or about 1 million electrons, which produce a small electrical pulse at the collecting anode. The magnitude of the output pulse of the PM tube is proportional to the gamma ray energy deposited in the crystal. Thus a 200 keV gamma ray produces a pulse twice the height of a 100 keV gamma ray.

Processing of the output pulse from the PM tube involves amplification and discrimination. A preamplifier matches impedance between the PM tube and the amplifier. The amplifier permits adjustment of the pulse height, increasing or decreasing it proportionately, to facilitate analysis. The PHA is an electronic circuit consisting of an upper-level energy discriminator (ULD) and a lower-level energy discriminator (LLD) configured in an anticoincidence circuit. Only those pulses that fall within the "window" created between the LLD and ULD settings are counted (Figure 3-15). The PHA permits radionuclides with different photon energies to be counted independently by adjustment of the window (Figure 3-16).

A variety of devices can record events. A scaler is a digital counter that totals the number of counts detected. A rate meter displays counts per unit time. An oscilloscope provides a visual display of a radionuclide's gamma-energy spectrum in a multichannel analyzer (Figure 3-17). The computer monitor of a gamma camera system displays the distribution of radioactive material in the patient's body. Detector output can also be stored in computer memory for data analysis and image processing.

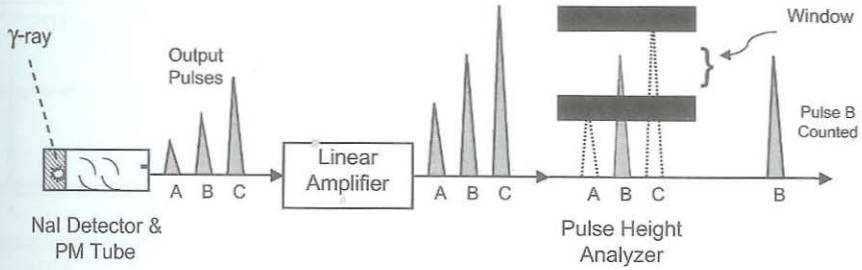

FIGURE 3-15 Schematic of pulse height analysis in a scintillation counter. Pulses A, B, and C are amplified linearly before processing by the pulse height analyzer. Pulse B falls within the "window" created by the lower-level discriminator (LLD) and upper-level discriminator (ULD) and is counted. Pulse A is rejected by the LLD and pulse C by the ULD.

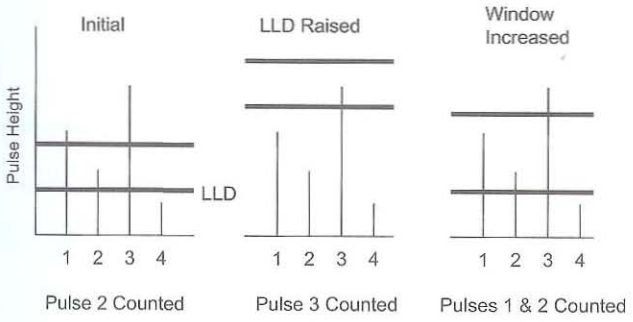

FIGURE 3-16 Effect of pulse height analyzer settings on acceptance or rejection of various pulse heights.

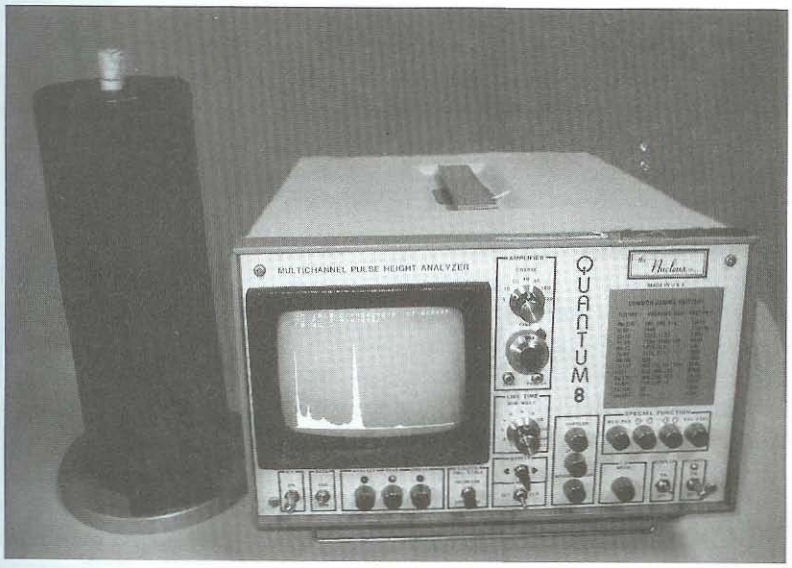

FIGURE 3-17 Sodium iodide well counter and multichannel analyzer.

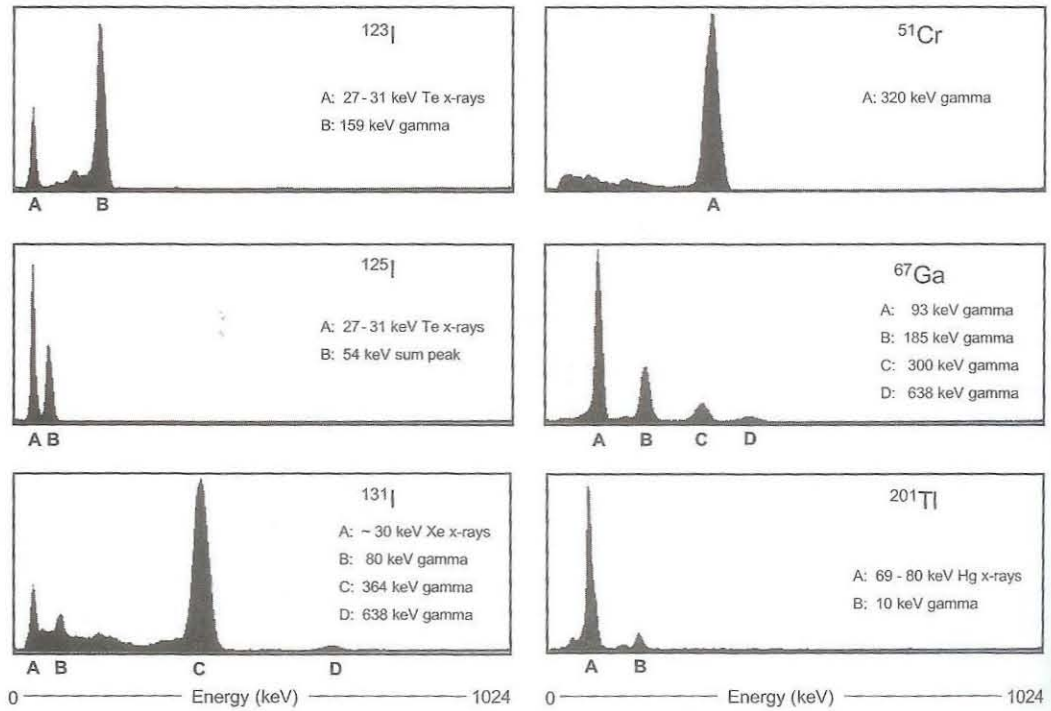

FIGURE 3-18 Gamma energy spectra for ^{123}I, ^{125}I, ^{131}I, ^{51}Cr, ^{67}Ga, and ^{201}Tl in a 2 × 2-inch sodium iodide crystal.

Gamma Energy Spectrum

When a radionuclide is counted with a scintillation counter and the count rate plotted versus energy, a gamma-energy spectrum is produced (Figures 3-18 and 3-19). Each radionuclide has a unique spectrum that identifies its photon energy peaks. This "gamma fingerprint" can be used to identify radionuclides in an unknown source. The gamma-energy spectrum can also be used to establish the best instrument settings for counting or imaging. The instruments most frequently used in nuclear medicine for counting gamma radiation are the scintillation well counter, probe, and gamma camera.

Well Counter

The scintillation well counter is designed for counting test tube samples. It is a sensitive device, typically used for counting samples containing less than 1 μCi (37 kBq). The sodium iodide crystal may vary in size but generally is 1.5 to 2 inches in diameter and about inches deep. A cylindrical well is drilled into it for accepting tubes (Figure 3-20). The majo advantage of this arrangement is the increased counting efficiency that results from su rounding the sample by the detector. The detector is shielded with lead to reduce bac ground radiation.

Scintillation Probe

A scintillation probe is similar to the well counter except that the sodium iodide detec is flat-faced and has no well. The crystal may be of various sizes depending on the intend

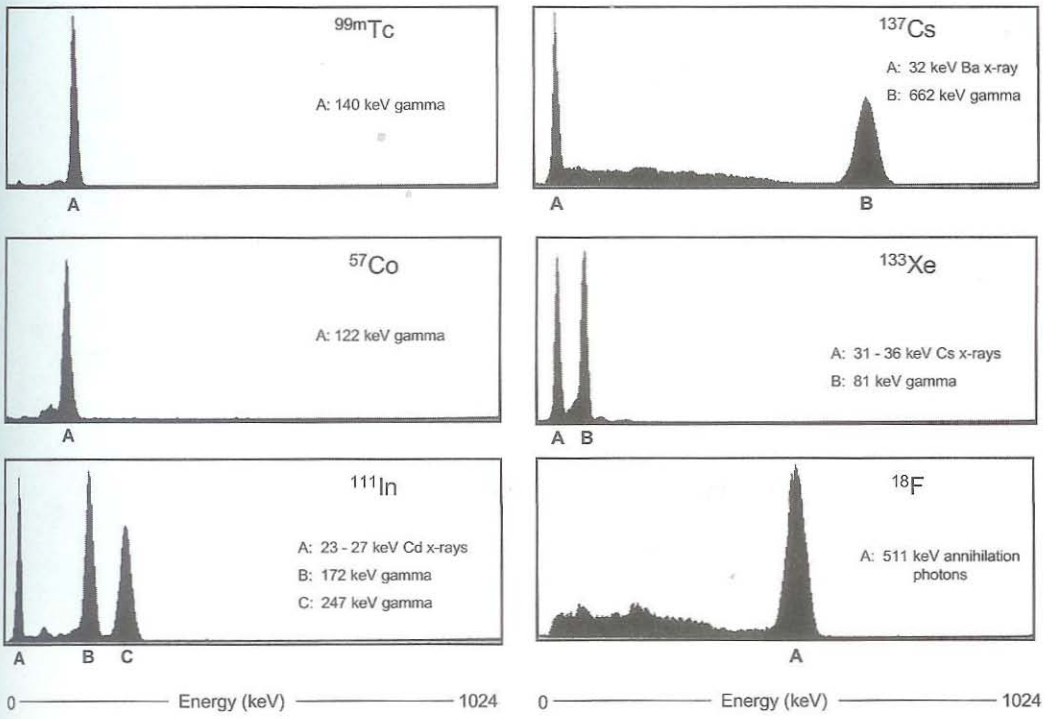

FIGURE 3-19 Gamma energy spectra for ^{99m}Tc, ^{57}Co, ^{111}In, ^{137}Cs, ^{133}Xe, and ^{18}F in a 2 × 2-inch sodium iodide crystal.

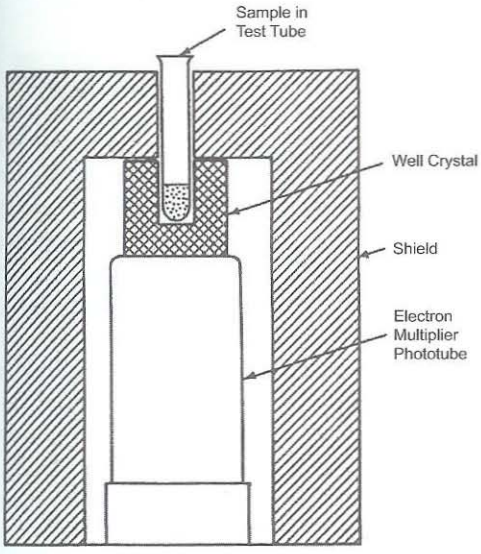

FIGURE 3-20 Scintillation well counter. (Reprinted from *Handbook 80, A Manual of Radioactivity Procedures*, U.S. Department of Commerce, National Bureau of Standards, 1963.)

use. Thicker crystals are more efficient detectors and are necessary for high-energy gamma rays. Probes with crystals 1.5 to 2 inches in diameter and 1 inch thick are routinely used for thyroid uptake measurements. Smaller hand-held portable probes are used to monitor radioactivity over various body parts and as survey instruments in radiation safety operations. An example of a probe detector used in thyroid uptake studies is shown in Figure 3-21.

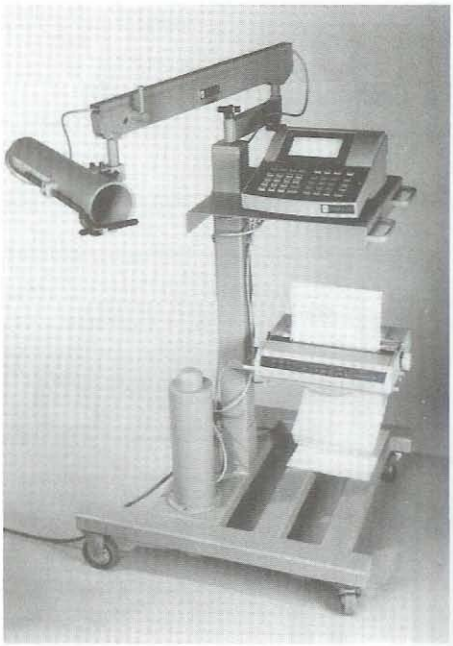

FIGURE 3-21 Stationary scintillation thyroid uptake probe and counter. (Used with permission of Capintec Inc., Ramsey, NJ.)

Gamma Cameras

Three types of gamma cameras are used in nuclear medicine: planar cameras, single-photon emission computed tomography (SPECT) cameras, and positron emission tomography (PET) cameras.

Planar Cameras

The early system used in nuclear medicine for imaging procedures was the rectilinear scanner. This imaging device had a sodium iodide crystal 3 to 5 inches in diameter and 2 to 3 inches thick. Images were made by moving the detector down and across the region of interest, recording information line by line as the detector scanned across the organ (Figure 3-22). The images obtained were called "scans." Modern-day imaging employs gamma cameras whose detectors are large enough to view the entire organ of interest in most instances. The images obtained are often referred to as "scans," even though the method of acquisition no longer involves scanning.

The planar camera was the first type of gamma camera to replace the rectilinear scanner. It acquires a two-dimensional image of a three-dimensional distribution of radioactivity in an organ. Lesion detection is improved by acquiring images in different planes around the patient, typically in anterior, posterior, oblique, and right and left lateral projections. However, with this technique of image acquisition, a deep-seated lesion within an organ may be obscured by overlying normal tissue.

The camera system includes a detector consisting of a 12 to 20 inch diameter sodium iodide crystal ¼ inch or ⅜ inch thick backed by an array of PM tubes and faced with a lead collimator. The detector is wired to the camera's electronic processing unit, which consists of a PHA, a scaler–timer, a positioning logic system, a monitor, and a computer. The sodium iodide crystal detects the radioactivity in the patient's body and produces the primary scintillation events used to generate an image. The PHA permits energy discrimination of pulses and is used to set appropriate windows for acquiring information.

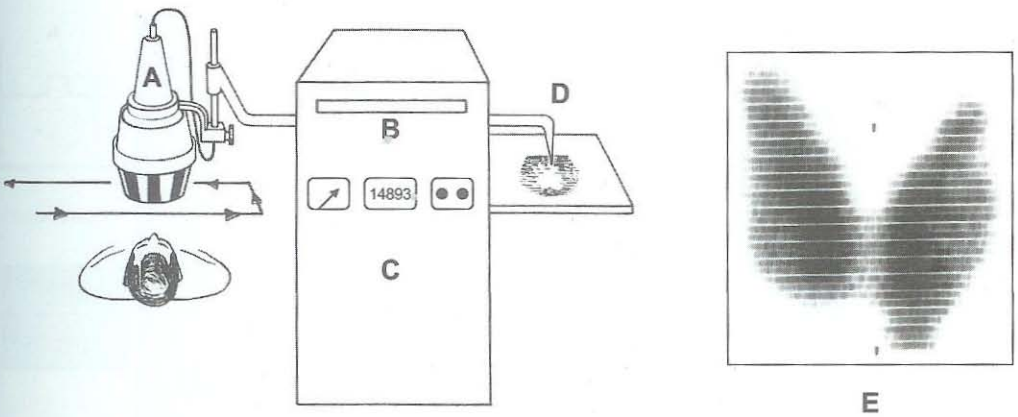

FIGURE 3-22 Diagram of a rectilinear scanner, an imaging device used in nuclear medicine before gamma cameras came into use. (A) sodium iodide detector, consisting of a collimator, sodium iodide crystal, and PM tube assembly that moved laterally back and forth and vertically over the area to be scanned, creating an image line by line; (B) photographic film recording device; (C) electronic processing unit; (D) "dot" image recording device; (E) example of a thyroid gland scan made with a rectilinear scanner.

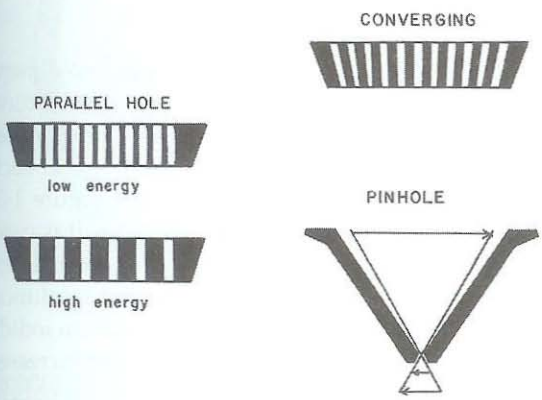

FIGURE 3-23 Diagram of types of gamma camera collimators.

The scaler–timer records the number of counts and sets the desired time required for image acquisition. The collimator is a lead disk with an array of holes drilled through it. It is positioned immediately in front of the sodium iodide crystal and limits detection to only those photons emitted from the patient within the angle of view of the collimator's holes. Any photon emitted from the patient outside the angle of view (greater than or less than 90°) will be absorbed by the lead septa between the holes and not be counted. Without the collimator, a photon could hit the crystal at a position unrelated to its point of origin in the patient, which would result in an image with incorrect activity distribution. In short, a collimator limits the field of view of the crystal so that detail can be resolved. Types of collimators are shown in Figure 3-23. In general, higher-energy nuclides require collimators with thicker lead septa to achieve acceptable image resolution. A positioning logic system produces x- and y-coordinates of the pulses generated in the crystal. In essence it determines the location of each gamma ray interaction within the crystal that, in turn, is related to its site of origin within the organ. The acquired image is stored in computer memory for data analysis and can be displayed on a monitor for viewing. The monitor display is useful for patient positioning during image acquisition.

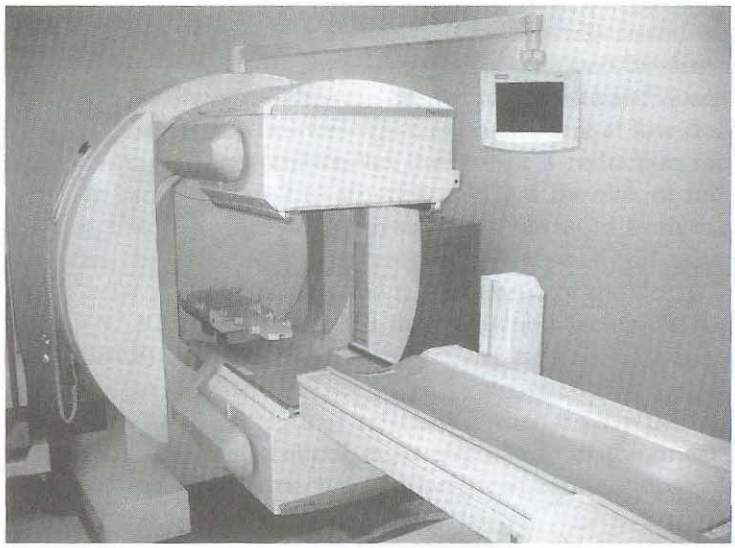

FIGURE 3-24 Single-photon emission computed tomography (SPECT) dual-head gamma camera.

SPECT Cameras

In a SPECT camera system, the detector rotates around the patient to acquire two-dimensional images over 360°, similar to a planar imaging camera. Computer reconstruction algorithms permit display of stored information in three orthogonal planes: transverse, sagittal, and coronal. In essence electronic "slices" are made through the organ in each plane so that the activity distribution can be seen in three dimensions (see Figure 1-3, Chapter 1). A SPECT camera can be used both for planar and SPECT imaging. It is used mostly to detect photons emitted singly from radionuclides, as opposed to the coincidence detection of dual annihilation photons in PET imaging. However, the spatial resolution of SPECT is inferior to that of dedicated PET systems. SPECT cameras use sodium iodide crystals and can be configured with one, two, or three detecting heads. Sensitivity increases in proportion to the number of heads. The detector typically rotates 360° about the patient in a continuous or stepwise manner. A typical dual-head SPECT camera system is shown in Figure 3-24.

A significant advantage of SPECT over planar imaging is an improved target-to-nontarget ratio.[8] In planar imaging, nontarget foreground and background activity around the target is recorded with the target activity, degrading image quality. In SPECT imaging this nontarget activity is reduced significantly by the image reconstruction process (Figure 3-25).

PET Cameras

The emission of a positron from a radionuclide distributed within the body produces two 511 keV annihilation photons that travel in opposite directions 180° apart in accordance with the momentum conservation principle. This colinear property of the photons allows them to be detected simultaneously by opposing detectors coupled to a coincidence device (Figure 3-26). Because only coincident photons are detected, there is no need for a lead collimator to determine the line of origin, and that is why this process is referred to as electronic collimation. Lines of response (coincidence lines) for coincidence events are stored in computer memory and processed by an image reconstruction algorithm to

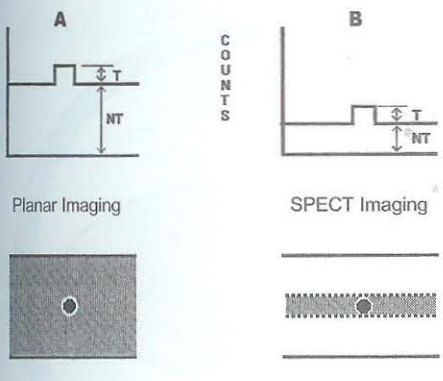

FIGURE 3-25 Schematic showing the value of SPECT imaging (B), versus planar imaging (A), for improving target to nontarget ratios. With SPECT, a substantial amount of background and foreground information is removed while information from the area of interest is retained. (Reprinted with permission from reference 8.)

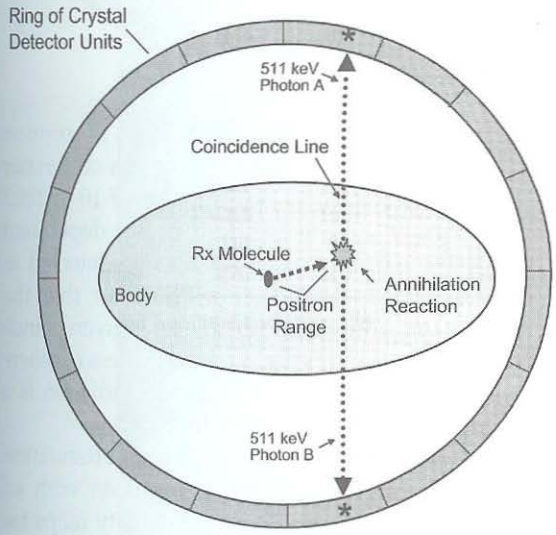

FIGURE 3-26 Diagram of a PET detector demonstrating position of positron release (Rx molecule), its travel to a point of annihilation, and the coincident detection of the two 511 keV photons along the coincidence line. The coincidence line is also referred to as the line of response (LOR) or line of origin.

generate cross-sectional images of the activity distribution. Theoretically, the two detectors will detect an event at precisely the same time only if annihilation has occurred precisely in the middle of the line between the two detectors. Because events occur at other points along the coincidence line, the coincidence window must be adjusted to accommodate these events. To accomplish this, the average coincidence time for PET cameras is set at approximately 6 to 12 nanoseconds.[9] This resolving time is long enough to record a significant number of true coincidence events that occur "off-center" on the coincident line but short enough to limit the number of random coincidence events that strike the crystal detector coincidently with true events.

A number of possible coincidence events can be recorded with PET (Figure 3-27). A true coincidence event (T) is one where the photons recorded by opposing detectors belong to the same annihilation event. Unwanted events, such as random (R) and scattered (S) photons, may be recorded simultaneously with true events. Random coincidence events are those in which two photons from unrelated annihilation events are detected simultaneously. Scatter coincidence events are those events in which one or both photons from the same annihilation event are scattered prior to detection. In random and scattered coincidence events, the recorded line of response does not correspond to the true line of response. Such events act to degrade image quality, and correction factors must be applied to diminish their effect.

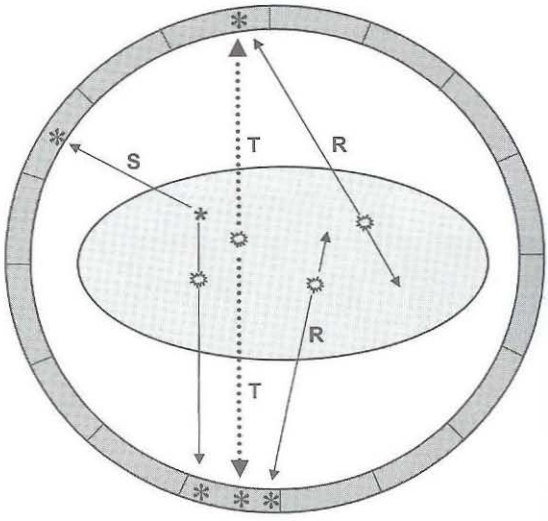

FIGURE 3-27 Random (R), scattered (S) and true (T) events detected in a PET detector. See text for explanation.

One advantage of PET imaging over planar or SPECT cameras is that no absorption collimator is required because coincidence detection is used. The absence of a collimator significantly increases the detection sensitivity of PET cameras, by a factor of 10 to 100.[9] Another important factor with coincidence detection is that sensitivity is not dependent on depth, because two photons must always cross a total path length to be detected in coincidence. Thus, if one 511 keV photon travels a short distance to one detector, then the other photon must travel the long distance to the opposing detector. Along a given coincidence line the total distance two photons travel to be detected is the same regardless of where along the line the annihilation occurs. Thus, the attenuation of annihilation radiation is a function only of the total length of travel, independent of the depth of its origin.[10]

Another major advantage of coincidence detection is that precise photon attenuation correction is possible. This is typically accomplished by a transmission scan with an external radioactive source (e.g., $^{68}Ge/^{68}Ga$ or ^{137}Cs) to determine tissue density maps for attenuation correction. Some PET cameras use a computed tomography (CT) x-ray source to accomplish attenuation correction. Attenuation correction permits accurate quantitation of the amount of activity at a given location and is a major advantage of PET.

Spatial resolution in PET is affected by detector size and design. Modern cameras have a resolution of 4 to 6 mm, which is near the maximum resolution physically possible.[9] Resolution is limited by the distance positrons travel in tissue from their point of origin to their point of annihilation. Positron emitters that have a short mean linear range in tissue have better resolution than those with a longer range (Table 3-6). Additionally, because the positron may have some residual kinetic energy when it annihilates with an electron, the two 511 keV photons emitted will not travel in precisely opposite directions, that is, at exactly 180°. This results in a small angular deviation from colinearity that degrades spatial resolution.

A PET camera consists of a gantry with a patient portal and detector system, a patient bed, and electronic components to control the unit. Different types of detectors are used. Common detector materials in modern PET cameras are bismuth germanate (BGO), lutetium oxyorthosilicate (LSO), and gadolinium silicate (GSO), which have high detection efficiency of annihilation photons and high signal-to-noise ratio. Cesium fluoride and barium fluoride detectors offer high time resolution capability but are no longer used. Sodium iodide detectors offer high sensitivity but poor detection efficiency. PET imaging

TABLE 3-6 Positron Emitter Energy and Range in Tissue

Radionuclide	Maximum Energy of Positron (MeV)	Maximum Linear Range (mm)	Mean Linear Range (mm)
^{11}C	0.96	5.0	0.3
^{13}N	1.19	5.4	1.4
^{15}O	1.72	8.2	1.5
^{18}F	0.64	2.4	0.2
^{68}Ga	1.89	9.1	1.9
^{82}Rb	3.35	15.6	2.6

Source: Reference 9, p. 5.

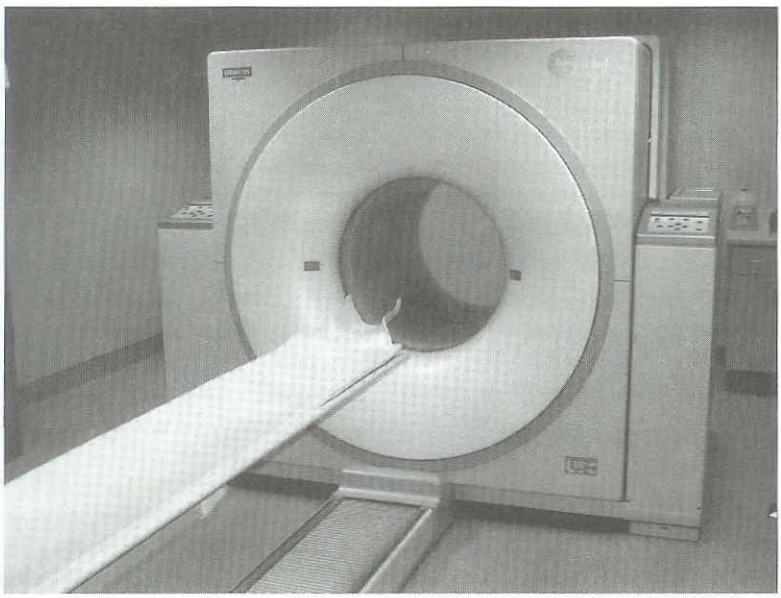

FIGURE 3-28 A CT/PET camera.

employs computer reconstruction algorithms to display images in transverse, sagittal, and coronal planes, providing three-dimensional imaging capability similar to SPECT.

There are dedicated PET cameras and combined CT/PET cameras. A CT/PET camera is shown in Figure 3-28. The advantage of the CT/PET camera is the ability to acquire an anatomic image with CT and a functional image with PET sequentially. Computer programs permit exact coregistration or overlaying of the CT image with the PET image to confirm if functional activity is associated with a suspected lesion. This combined imaging modality provides a powerful diagnostic means of determining, for example, if a previously treated tumor is still viable.

Some SPECT cameras can also be used to image 511 keV positron annihilation photons, either singly, with the use of special collimators, or in coincidence mode, employing dual heads without collimators, similar to PET cameras. In coincidence mode they differ from PET cameras in that the dual-head SPECT camera must rotate around the patient and this requires more time for image acquisition. In summary, the advantages of PET over SPECT imaging are increased sensitivity; precise attenuation correction, which permits quantitative

TABLE 3-7 Gamma Camera Properties

Camera Type	Properties			
	Images	Detector[a]	Collimation	Utility
Planar	2-D	NaI Single and dual head	Yes	Manually reposition detector
SPECT	2-D, 3-D Tomographic slices (transverse, coronal, sagittal)	NaI Single, dual, triple head	Yes	Detector rotates continuously or stepped 360° around patient[b]
PET	2-D, 3-D Tomographic slices (transverse, coronal, sagittal)	BGO, LSO(Ce), GSO(Ce), NaI, BaF_2, CsF Circular detector	None Electronic collimation Coincidence detection 10–100-fold ↑ sensitivity[c]	Patient moves slowly through a stationary detector[b]

[a] NaI = sodium iodide, BGO = $Bi_3Ge_4O_{12}$, bismuth germanate, LSO(Ce) = $Lu_2(SiO_4)O$:Ce, lutetium oxyorthosilicate, GSO(Ce) = $Gd_2(SiO_4)O$:Ce, gadolinium silicate, BaF_2 = barium fluoride, CsF = cesium fluoride.

[b] Uses computer-based image reconstruction algorithms.

[c] Short positron range = higher resolution.

measurements; higher resolution; and the use of isotopically labeled compounds that permit physiologic tracer studies.

Table 3-7 compares the characteristics of planar, SPECT, and PET camera systems.

COUNTING RADIOACTIVE SAMPLES

Counting Statistics

Two types of errors are associated with counting radioactive samples: determinate errors and indeterminate errors.[3] Determinate (systematic) errors are errors determined not by chance but by bias. They are errors caused by, for example, malfunctioning equipment or inconsistent methods of making measurements (e.g., variation in geometry between samples). Such errors are avoidable and can be controlled by the experimenter. Indeterminate (random) errors are errors not under the control of the experimenter that are caused by the random variability of the system being studied. Determining the activity of a radioactive sample is associated with random error because of the spontaneous nature of radioactive decay.

Determinate errors in counting radioactive samples can be minimized by the worker's awareness of good laboratory practices. The first step in minimizing errors is to confirm that all counting equipment is in good working order. This is accomplished by calibrating equipment with standard radioactive sources and applying statistical tests to ensure proper operation. Additionally, the experimenter must be aware of the limitations of counting equipment, such as the maximum and minimum activity levels that can be counted accurately. The second step in minimizing determinate errors is to confirm that all samples to be counted are configured in identical geometry, that is, they must have the same volume and container type.

Indeterminate errors in counting radioactive samples can be minimized by being familiar with the random nature of radioactive decay and applying statistical parameters and tests to ensure accuracy within acceptable limits of error.

Accuracy is defined as the closeness of a measurement to the true value. Precision is defined as reproducibility of measurement. A measurement may be precise but not accurate. For example, you may count a sample multiple times and obtain a similar count each

TABLE 3-8 Counting Data for a Nominal Source Count Rate of 150 Counts per Minute (cpm)

Observation	Sample Count (cpm)	Sample Deviation[a]	Square of Sample Deviation
1	159	+12	144
2	155	+8	64
3	141	–6	36
4	130	–17	289
5	177	+30	900
6	150	+3	9
7	144	–3	9
8	123	–24	576
9	129	–18	324
10	162	+15	225
Total	1470	0	2576

[a] Difference from the mean of the 10 counts.

time, and thus be precise, but if the sample was pipetted incorrectly, the activity of the sample will be inaccurate. The goal of good scientific measurement is to be both precise and accurate.

It is not possible to predict the exact time a single radioactive atom will undergo decay, but a given fraction of a large quantity of atoms will decay in a specified period of time. The larger the sample of atoms, the greater the accuracy in determining the exact fraction that will decay in a given time. The decay of radioactive atoms is a spontaneous or random process, and therefore multiple independent counts of a source will typically yield a different count in a given time. Thus it is difficult to identify the true count rate of the source. Confidence can be gained in estimating the true value by making several 1-minute counts of a source and finding an average count per minute. Consider the counting data in Table 3-8, which shows 10 1-minute counts of a source with nominal activity of 150 counts per minute (cpm). The average or mean cpm is expressed by

$$\bar{n} = \frac{\sum n_i}{N} \tag{3-7}$$

where $\bar{n}$ is the mean cpm, $\sum n_i$ is the sum of individual 1-minute counts (n_i), and N is the number of observations. In the example in Table 3-8, $\bar{n}$ is 147 cpm. If the experiment were repeated, $\bar{n}$ might be 145 cpm. One could then estimate from the two sets of data that the true mean count rate was between 145 cpm and 147 cpm, or 146 cpm. Still another series of counts might produce a different mean cpm. It is obvious from such experimentation that the true count lies somewhere near the mean count and that the individual counts are equal to the mean count plus or minus a few counts. Such results exemplify the nature of a random variable. That is, for a very large number of sample counts, a plot of each count on the x-axis versus the probability of that count on the y-axis would give a Poisson distribution. The Poisson distribution, however, is not symmetric about the mean. Therefore, a normal or Gaussian distribution is typically used to describe counting statistics because it is symmetric about the mean and is very close to the Poisson distribution.[11] A normal distribution curve is shown in Figure 3-29 and is described by the Gaussian probability equation as

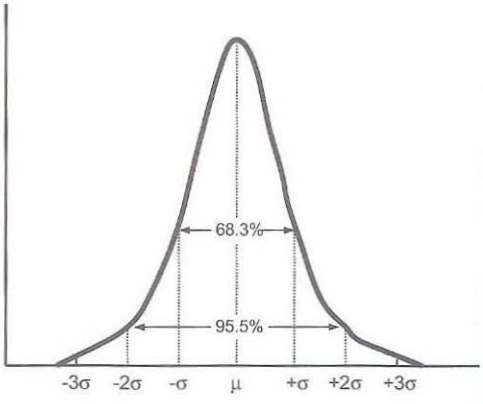

FIGURE 3-29 Normal (Gaussian) distribution curve displaying the mean count and random distribution of counts about the mean from a radioactive source.

$$G_n = \frac{1}{\sqrt{2\pi\mu}} e^{-\frac{(n-\mu)^2}{2\mu}} \tag{3-8}$$

where μ is the true mean value of the source count, n is the experimental value of the source count, and G_n is the probability of an individual count n occurring. If μ is 30, the probability of obtaining a count of 28 is 0.0681, or 6.81%.

$$G_n = \frac{1}{\sqrt{2\pi(30)}} e^{-\frac{(28-30)^2}{2(30)}} = 0.0681$$

The further away a count is from μ, the lower its probability of occurring. The probability of a count of 20 occurring is 0.0138, or 1.38%. Since the Gaussian distribution is symmetric, the probability of a count of 32 is also 6.81% and the probability of a count of 40 is 1.38%.

The Gaussian distribution is defined by the parameters μ, which defines the center of the distribution, and σ, the standard deviation, which defines the spread or dispersion of data about the mean. The experimental or sample mean ($\bar{n}$) and the sample standard deviation (s) are used to estimate μ and σ.

The usefulness of statistics in dealing with random events is that it describes the magnitude of error introduced by randomness and helps to establish conditions that will minimize the error between μ and its estimator $\bar{n}$. Figure 3-29 can be interpreted to mean that, for multiple counts of a single source, 68.3% of all observed counts are expected to occur within one standard deviation of the mean count and 95.5%, within two standard deviations.

The sample standard deviation, s, for multiple counts is expressed as

$$s = \sqrt{\frac{\sum(n-\bar{n})^2}{N-1}} \tag{3-9}$$

For the data in Table 3-8

$$\bar{n} = \frac{1470}{10} = 147 \quad s = \sqrt{\frac{2576}{10-1}} = 16.9$$

Thus, the sample count is expressed as $\bar{n} \pm s$ or 147 ± 16.9 cpm. In terms of the Gaussian distribution, 68.3% of the 1-minute counts would be expected to fall within the range of 130 to 164 cpm.

Counting Error

The standard deviation gives the numerical (absolute) spread of counts about the mean count. A useful parameter for expressing the error associated with the standard deviation is the coefficient of variation. The coefficient of variation (CV) is the ratio of the sample standard deviation to the sample mean, or $CV = s/\bar{n}$. The percent error (%CV) in a count is

$$\%CV = \frac{s \times 100}{\bar{n}} \tag{3-10}$$

In the example above, the percent error is

$$\frac{16.9 \text{ cpm} \times 100}{147 \text{ cpm}} = 11.5\%$$

In a single 10-minute count of the source, the mean count rate (R) is 147 cpm (1470 counts/10 minutes). For a single count n, the standard deviation is $\sqrt{n}$ and in terms of the count rate is

$$s_R \text{ cpm} = \frac{\sqrt{n}}{t} \quad \text{or} \quad \sqrt{\frac{R}{t}} \tag{3-11}$$

In the example above, s_R cpm is

$$s_R \text{ cpm} = \frac{\sqrt{1470 \text{ counts}}}{10 \text{ min}} = 3.8 \text{ cpm}$$

The sample count rate is expressed, therefore, as the mean count rate $R \pm s_R$ cpm or in this case 147 ± 3.8 cpm. The percent error of standard deviation in the single sample count rate is

$$s_R\% = \frac{s_R \times 100}{R} = \frac{3.8 \text{ cpm} \times 100}{147 \text{ cpm}} = 2.6\%$$

It is obvious that the error in the standard deviation of a single count is much smaller than that of taking multiple counts on the same sample. Consider, for example, counting a source with a nominal count rate of 1000 cpm for a single count of 0.1, 1.0, 5.0, 10, and

TABLE 3-9 Sample Counting Error

Time (min)	Net Count	Standard Deviation	Percent Error in Standard Deviation (Confidence Level)		
			68.3	95.5	99.7
0.1	100	10	10	20	30
1.0	1000	31.6	3.2	6.3	9.5
5.0	5000	70.7	1.4	2.8	4.2
10.0	10,000	100	1.0	2.0	3.0
100.0	100,000	316	0.32	0.63	0.95

100 minutes. The data shown in Table 3-9 demonstrate that a longer single sample counting time yields a smaller error and therefore a mean count that is closer to the true count rate of the sample. As a general rule in nuclear medicine, samples should be counted for a minimum of 10,000 counts. This produces a 3% error at the 99.7% confidence level, which is quite acceptable for clinical work. The error is actually a measure of the range of counts about the mean caused by the randomness of radioactive decay, and the greater the number of counts in the sample, the smaller the effect of randomness in the count rate. At this confidence level there is only a 0.3% chance that the true count rate of the sample falls outside the mean count plus or minus three standard deviations. Another way of saying this is that if the source were counted 1000 times, 3 times out of 1000 the count rate would be expected to fall outside this range and 997 times it would fall within this range.

Counting Efficiency

In its simplest form counting efficiency is counts per minute recorded by an instrument divided by the disintegrations per minute (dpm) occurring in the sample being counted (efficiency = cpm/dpm). Counting efficiency is typically below 100%; for a number of reasons, the detector may not be able to capture all of the disintegrations occurring in a radioactive sample. The main factors that affect counting efficiency are the intrinsic efficiency of the detector and geometry factors.

Intrinsic efficiency is the number of radiations interacting within the detector divided by the number of radiations incident on the detector.[12] It is affected by the type of radiation and its energy and the size and composition of the detector. For example, the intrinsic efficiency of solid-crystal sodium iodide detectors for pure beta emitters, such as ^{3}H and ^{14}C, is zero because the weak beta particles cannot penetrate into and interact with the sodium iodide crystal. However, if a beta emitter is dispersed within a liquid scintillation fluid, essentially all of the emitted radiation is absorbed by the scintillation fluid and counting efficiency is quite high, depending on the energy of the beta particles. For example, the counting efficiency of low-energy beta particles from ^{3}H, having a maximum beta particle energy (beta max) of 12.3 keV, is approximately 60%, whereas the efficiency of higher-energy beta particles from ^{14}C (beta max 156 keV) is closer to 90%. The counting efficiency of a beta emitter is easily determined with liquid scintillation by counting an accurate aliquot of a calibrated standard of the beta source and dividing the net counts per minute observed by the known disintegrations per minute in the sample.

The intrinsic efficiency of a gamma emitter in a sodium iodide detector must be adjusted for the photon abundance. The counting efficiency of a gamma emitter is determined by counting an aliquot of a calibrated sample of the gamma source and dividing the net counts per minute observed by the known disintegrations per minute in the sample and the photon abundance (mean number per disintegration). The photon abundance

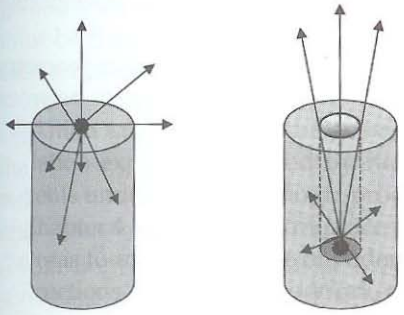

FIGURE 3-30 The counting geometry of a flat-field sodium iodide (NaI) detector is less efficient than that of a well-type NaI detector, which almost completely surrounds the radioactive source.

must be considered because a detectable photon will not be emitted after each disintegration. Thus

$$\text{Efficiency} = \frac{\text{Net cpm}}{(\text{Source } \mu\text{Ci})(2.22 \times 10^6 \text{ dpm}/\mu\text{Ci})(\text{Photon abundance})} \quad (3\text{-}12)$$

Photon energy and geometry factors, such as detector size, distance of the source from the detector, and absorption and scatter of radiation within the source itself and in any material between the source and the detector, can affect counting efficiency.[12] The attenuation coefficient of photons in sodium iodide is inversely related to photon energy. Thus, for a sodium iodide detector of a given thickness, higher gamma energy sources will be less efficiently detected than lower energy sources, and for a given photon energy large-diameter crystals will be more efficient detectors than small-diameter crystals. A typical sodium iodide well counter crystal is 1.75 inches in diameter and 2 inches thick and contains a well that is 0.7 inch in diameter and 1.6 inches deep. Crystal detectors without wells (flat-field detectors) range in size from 0.5 to 3 inches in diameter and 1 to 3 inches in thickness. Higher counting efficiencies are achieved using a well counter because the source is almost completely surrounded by the detector, thus minimizing absorption losses, compared with counting the source using a flat-field detector, in which a greater fraction of disintegrations escape detection (Figure 3-30).

If a radioactive source is moved farther away from the detector, fewer emissions will reach the detector and efficiency will fall. This can be a useful technique for counting sources that are "too hot" and would exceed the dead time of the detector.

The configuration of the source container can also affect counting efficiency. Counts may escape detection when the volume of a sample placed in a scintillation well detector is nearly equal to the volume of the well. In this situation, disintegrations occurring near the surface of the sample at the top of the well are more apt to escape detection by the crystal. It is best to keep the sample volume small and near the bottom of the well so that most of the sample is surrounded by the crystal detector. The source container is important. A source counted in a plastic tube will count with a different efficiency compared with the same source counted in a glass tube, especially if the gamma energy of the source is weak (<50 keV). This is particularly true for low-energy photon emitters, such as the 27 keV x-rays of ^{125}I.

Counting instrument settings, particularly the window of the PHA, can also affect counting efficiency. Wider windows allow more of the incident radiation to be counted.

However, narrow windows may be needed to exclude unnecessarily high background counts.

The most important consideration in radioactive counting is keeping source geometry and counting instrument settings consistent when making relative counts between unknown samples and standards.

Example: A 1.0 μCi (37 kBq) source of ^{133}Xe gas in a 3 mL glass vial is counted in a scintillation counter to yield 486,508 net cpm. The photon abundance for the 81 keV gamma ray for ^{133}Xe is 36%. Calculate the counting efficiency for ^{133}Xe in this configuration.

$$\text{Efficiency} = \frac{486{,}508 \text{ cpm}}{(1.0\ \mu\text{Ci})(2.22\times10^{-6}\ \text{dpm}/\mu\text{Ci})(0.36)} = 0.61$$

If one knows the detector efficiency for a particular radionuclide in a given geometry, the source's activity can be determined as follows:

$$\text{Activity}\ (\mu\text{Ci}) = \frac{\text{Net cpm}}{(\text{Efficiency})(2.22\times10^{6}\ \text{dpm}/\mu\text{Ci})(\text{Photon abundance})} \qquad (3\text{-}13)$$

Example: A "grab-sample" of exhaust gas from a charcoal trap in a ^{133}Xe lung ventilation machine yields 350 net cpm in a 3 mL vial. How many microcuries of ^{133}Xe are in the sample?

$$\text{Activity}\ (\mu\text{Ci}) = \frac{350 \text{ cpm}}{(0.61)(222\times10^{6}\ \text{dpm}/\mu\text{Ci})(0.36)} = 7.19\times10^{-4}\ \mu\text{Ci}$$

If the maximum permissible concentration (MPC) of ^{133}Xe in the work environment is 1×10^{-4} μCi/mL, does this charcoal trap need to be changed?

The concentration of ^{133}Xe in the sample is (7.19×10^{-4} μCi/3 mL or 2.4×10^{-4} μCi/mL). Since this is 2.4 times higher than the MPC, the trap does need to be changed.

Resolving Time and Maximum Detectable Activity

The resolving time of a detector is the time required, between two successive interactions in the detector, for the interactions to be recorded as separate events. It is also known as dead time, because during this time the instrument is unable to record an interaction occurring in the detector. For example, a detector whose resolving time is 10 microseconds theoretically can resolve 100,000 counts per second. If the detector's efficiency for ^{133}Xe is 61%, the theoretical maximum activity it could count accurately is

$$\frac{6\times10^{6}\ \text{cpm}}{0.61(2.22\times10^{6}\ \text{dpm}/\mu\text{Ci})(0.36)} = 12.3\ \mu\text{Ci}$$

In this example, any sample containing more than 12.3 μCi (455 kBq) would record a count that is erroneously low because the number of detector interactions per second would be

greater than its ability to resolve them as individual events. In practice, each instrument must be challenged to determine the actual maximum detectable activity it can count for each radionuclide.

Sometimes a source is too "hot" for counting in a scintillation well counter. Techniques employed to not exceed instrument dead time are (1) increasing the source distance from the detector, (2) partially shielding the source, and (3) diluting the source. Dead-time problems are most likely to occur in a nuclear pharmacy during chromatographic analysis of high-activity radiopharmaceuticals. For example, a ^{99m}Tc bone kit containing 200 mCi (7400 MBq) in 10 mL contains 100 μCi (3.7 MBq) in a 5 μL spot. This amount of activity surely exceeds the dead time of a scintillation counter. As a rule of thumb not more than 1 μCi should be counted in a well counter. The *maximum detectable activity* for a scintillation counter can be determined by counting a series of sources of increasing activity and plotting the counts per minute versus activity on linear graph paper. The point on the graph where the plotted line deviates from linearity is the maximum detectable activity for that radionuclide.

Minimum Detectable Activity

In some circumstances it is necessary to measure low levels of activity, for example, in assessing the concentration of radioactive material released into restricted or unrestricted environments. An example is the release of ^{133}Xe into the workroom or the outside environment. Such releases should not exceed the MPC for ^{133}Xe defined in the Code of Federal Regulations (10 CFR Part 20). The MPC for ^{133}Xe is 1×10^{-4} μCi/mL for restricted areas (work environment) and 5×10^{-7} μCi/mL for unrestricted areas (effluent air). In monitoring released concentrations of ^{133}Xe the question becomes, "Is the scintillation counter sensitive enough to detect these low concentrations?" This is where determination of the minimum detectable activity (MDA) is important. In monitoring ^{133}Xe release, for example from a lung ventilation machine, one method is to collect a sample of gas effluent from the charcoal trap into a 3 mL vial and count it in a scintillation counter to determine if it exceeds the MPC. The following discussion and examples illustrate the calculations involved.

Minimum sensitivity (MS) is defined as the net count rate above background that must be exceeded before a sample is said to contain any measurable radioactivity. MS is essentially three times the standard deviation of the background count rate. It is calculated as follows:

$$\text{MS} = \frac{3\sqrt{\text{Background count}}}{\text{Count time}} \tag{3-14}$$

Example: A background of 400 counts in 5 minutes gives a SD of 4 cpm ($\sqrt{400}$ counts/5 min). The MS is therefore 12 cpm. From Gaussian statistics, the mean count rate is 80 cpm, and 99.7% of background counts would be expected to fall within three standard deviations of the mean, or 80 ± 12 cpm. There is only a 0.3% chance that a true background count would exceed this. A sample whose count is 12 cpm above an average background of 80 cpm (>92 cpm) is considered to contain radioactivity.

The *minimum detectable activity* (MDA) is defined as the smallest quantity of radioactivity that can be measured under specific conditions of MS and counting efficiency. It is calculated as follows:

$$\text{MDA} = \frac{\text{MS}_{\text{cpm}}}{\left(\text{Efficiency}_{\text{cpm/dpm}}\right)\left(2.22\times10^{6}\ \text{dpm}/\mu\text{Ci}\right)\left(\text{Photon abundance}\right)} \tag{3-15}$$

Example: A 3 mL vial is counted for background in a scintillation counter with a baseline set at 60 keV and a window of 40 keV to center on the ^{133}Xe photopeak of 81 keV. The background count was 523 counts in 5 minutes. The MS is

$$\text{MS} = \frac{3\sqrt{523}\ \text{counts}}{5\ \text{min}} = \frac{3(23)}{5} = 3(4.57) = 14\ \text{cpm}$$

The MDA for ^{133}Xe in this counter is

$$\text{MDA} = \frac{14\ \text{cpm}}{(0.61\ \text{cpm/dpm})(2.22\times10^{6}\ \text{dpm}/\mu\text{Ci})(0.36)} = 2.87\times10^{-5}\ \mu\text{Ci}$$

If this activity was acquired in a 3 mL sample vial, the minimum detectable concentration of ^{133}Xe would be 9.57×10^{-6} μCi/mL. This value is 9.6% of the MPC for a restricted area; therefore, the scintillation counter can easily measure ^{133}Xe activity below the MPC and be used to monitor effluent from the lung ventilation machine. Efficiency for ^{133}Xe can be obtained by placing a known number of microcuries in a 3 mL vial measured in a dose calibrator and allowing it to decay down to an amount that can be counted without exceeding the instrument dead time.

REFERENCES

1. Friedlander G, Kennedy JW, Miller JM. *Nuclear and Radiochemistry.* 2nd ed. New York: Wiley; 1964;90-103.
2. Glasstone S. *Sourcebook on Atomic Energy.* 3rd ed. New York: Van Nostrand Reinhold; 1967:395-431.
3. Chase CD, Rabinowitz JL. *Principles of Radioisotope Methodology.* 3rd ed. Minneapolis: Burgess; 1967:244-8.
4. Quimby EH, Feitelberg S. *Radioactive Isotopes in Medicine and Biology.* 2nd ed. Philadelphia: Lea & Febiger; 1963:85.
5. Kowalsky RJ, Johnston RE, Chan FH. Dose calibrator performance and quality control. *J Nucl Med Technol.* 1977;5:35-40.
6. Suzuki A, Suzuki MN, Weis AM. Analysis of a radioisotope calibrator. *J Nucl Med Technol.* 1976;4:193-8.
7. Hine GJ. Sodium iodide scintillators. In: Hine GJ, ed. *Instrumentation in Nuclear Medicine.* Vol 1, chap 6. New York: Academic Press; 1967.
8. Early PJ. SPECT Imaging: single photon emission computed tomography. In: Early PJ, Sodee BD, eds. *Principles and Practice of Nuclear Medicine.* 2nd ed. St Louis: Mosby; 1995:291-313.
9. Newiger H, Hamisch Y, Oehr P, et al. Physical principles. In: Ruhlmann J, Oehr P, Biersack HJ, eds. *PET in Oncology: Basics and Clinical Applications.* Berlin: Springer-Verlag; 1999:1-34.
10. Phelps ME, Hoffman EJ, Nizar AM, et al. Application of annihilation coincidence detection to transaxial reconstruction tomography. *J Nucl Med.* 1975;16:210-24.
11. Chase CD, Rabinowitz JL. *Principles of Radioisotope Methodology.* 3rd ed. Minneapolis: Burgess; 1967:75-108.
12. Cherry SR, Sorenson JA, Phelps ME. *Physics in Nuclear Medicine.* 3rd ed. Philadelphia: WB Saunders; 2003.

4 Radiation Protection and Risk

The biologic effects of ionizing radiation were experienced soon after the discovery of radioactivity. In one of the first instances, Henri Becquerel noticed skin erythema after keeping a radioactive preparation in his side coat pocket. In another, Pierre Curie noted that an ulcer on his hand from radium exposure was slow to heal. Such early experiences caused scientists to begin using radiation more cautiously. Methods for measuring radiation dose and techniques of radiation protection were eventually developed. This chapter covers the principal issues in radiation protection and risk as they relate to the use of radiation in nuclear medicine and nuclear pharmacy. The topics discussed include the units used in radiation measurement, techniques for protection against radiation exposure, radiation dosimetry, and radiation risk assessment.

RADIATION MEASUREMENT UNITS

The two principal factors to be considered in radiation measurement are the ionization of matter by radiation and the energy absorbed by matter from radiation. These are directly related to the biologic consequences of the interaction of radiation with the human body. Several types of units are used in the measurement of radiation: the curie (Ci) and the becquerel (Bq) for measuring radioactivity in a source; the roentgen (R) for measuring exposure from electromagnetic radiation; the radiation absorbed dose (rad) and the gray (Gy) for measuring absorbed dose; and the roentgen equivalent man (rem) and the sievert (Sv) for measuring biologic dose.

The Curie and the Becquerel

The curie and becquerel were defined in Chapter 2. Either of these activity terms can be used in measuring the quantity of radioactive material present in a source. The activity term is related to a defined number of atoms decaying per unit of time. The older term, curie, is equivalent to 3.7×10^{10} disintegrations or atoms decaying per second. Dosages of radiopharmaceuticals are typically measured in subunits of the curie: the millicurie and microcurie. The becquerel is the SI unit of radioactivity and is equal to one disintegration per second or 2.7×10^{-11} Ci.

The Roentgen

In the past, the roentgen was defined as the quantity of x or gamma radiation that produces 1 electrostatic unit (esu) of charge in 1 cm^3 (0.001293 gram) of air at standard temperature and pressure (STP). By current definition, 1 R equals 2.58×10^{-4} coulombs per kilogram of air. The 1 esu is produced by the photoelectrons and Compton electrons released by a photon's interaction with the atoms of air. The passage of 1 R of radiation results in the production of 2.082×10^9 ion pairs per cubic centimeter of air at STP. It is important to note that the roentgen relates only to x-rays and gamma radiation and does not include particulate radiation. Additionally, the roentgen relates only to an exposure quantity, with no qualification of the time of exposure or the amount of radiation absorbed.

Radiation Absorbed Dose and the Gray

The rad is the quantity of any ionizing radiation equivalent to 100 ergs of energy absorbed per gram of absorber. This term is more inclusive and quantitative because it relates to all types of radiation, not just x-rays or gamma radiation, and to the amount of radiation deposited in matter, not just exposure. The value of 1 R in rad is obtained by the following conversion.

$$1\text{R} = \frac{2.082 \times 10^{9}\ \text{Ion pairs}}{0.001293\ \text{gram air}} \cdot \frac{33.7\ \text{eV}}{1\ \text{Ion pair}} \cdot \frac{1.602 \times 10^{-12}\ \text{erg}}{1\ \text{eV}} \cdot \frac{1\ \text{rad}}{100\ \text{ergs/gram}} = 0.869\ \text{rad} \quad (4\text{-}1)$$

Because tissue is denser than air, the absorbed dose in tissue is greater by a factor of 1.108. Thus, 1 R is equivalent to 1.108 × 0.869 rad, or 0.96 rad, in tissue. The gray is the SI unit of absorbed dose and is equal to 100 rad. One rad is equal to 1 centigray (cGy). These relationships allow conversion of an exposure dose to an absorbed dose; however, they still do not indicate the biologic effects of x-ray or gamma radiation exposure or how such exposure compares with an equivalent amount of particulate radiation exposure.

Relative Biologic Effectiveness and Quality Factors

The biologic effect of radiation relates not only to how much energy is absorbed but to how it is distributed within the absorber. It is fairly easy to understand that if 100 ergs of energy is deposited within 1 gram of tissue the damage that may occur within the cells of that tissue will be greater if the 100 ergs are concentrated in a small portion of the 1 gram than if they are spread uniformly throughout the 1 gram. A simple analogy illustrates this concept: If you expose your hand to the noonday sunlight for a few minutes, you will notice a feeling of warmth on your skin. But if you interpose a magnifying glass between the sunlight and your hand so that the incident photons of sunlight are focused on a point on your skin, you will feel a different effect, even though the same amount of sunlight interacts with your hand. The biologic effect differs because of the distribution of energy.

Different types of radiation may deposit the same amount of energy in tissue but have different patterns of distribution. Relative biologic effectiveness (RBE) is a term used to describe the degree of biologic effect produced by different types of radiation at the same absorbed dose. RBE is defined as the dose in rad of x or gamma radiation required to produce a given biologic effect divided by the dose in rad of any ionizing radiation required to produce the same biologic effect.

Gamma rays of ^{60}Co (average energy 1.25 MeV) and 200 to 300 keV x-rays have been used as the reference radiation in determining RBE. The RBE depends on the linear energy transfer (LET) of a given radiation. Generally, the larger the LET, the greater will be the biologic effect of a given absorbed dose. Energy absorbed over a short distance causes more injury than energy absorbed over a long distance. Some radiations produce more ionization per path length traveled. They have high specific ionization and therefore deposit more energy over this same path; that is, they have high LET. In general, 0.05 rad of alpha radiation in tissue produces the same biologic effect as 1 rad of x-ray or gamma radiation. The RBE for alpha particles is therefore 20. One rad of beta particles produces the same biologic effect as 1 rad of x-ray or gamma radiation and therefore has an RBE of 1.

In radiation protection, it is convenient to sum the dose contributions from different types of radiation, and a modifier known as the radiation quality factor (Q) is used. Q is related to the type and energy of the radiation and its LET, and is assigned a value based

TABLE 4-1 Radiation Weighting (Quality) Factors

Radiation Type and Energy	Weighting Factor (Q)
Photons, all energies	1
Electrons, all energies	1
Neutrons <10 keV	5
Neutrons 10 keV to 100 keV	10
Neutrons >100 keV to 2 Mev	20
Protons >2 MeV	5
Alpha particles	20

Adapted from reference 1.

on the RBE. Q values are now known as *radiation-weighting factors* by the International Commission on Radiological Protection (ICRP 60) and are listed in Table 4-1.

Roentgen Equivalent Man and the Sievert

The product of the absorbed dose in rad and the radiation-weighting factor (Q) is called the *equivalent dose*, expressed in rem.[1] The equivalent dose is used in radiation protection and personnel radiation monitoring; the current SI unit of equivalent dose is the sievert (Sv). One sievert is equivalent to 100 rem. One rem is equal to one centisievert (cSv). The practical value of the equivalent dose is that it accounts for the different biologic effects produced by equivalent doses of radiations with different LET. For example, the dose in rem and sievert for 2.5 rad of thermal neutrons would be calculated as follows:

$$\text{Equivalent dose} = \text{Dose}\left(\text{rad}\right) \times Q$$

$$= 2.5 \text{ rad} \times 5 = 12.5 \text{ rem}\left(0.125 \text{ Sv}\right)$$

In summary, the roentgen (and its subunit milliroentgen) is considered a unit of exposure dose and is a measure of the number of electrons produced in a defined quantity of air. It is the unit measured with a Geiger-Müller survey meter. The rad and gray are units of absorbed dose and are measures of the amount of energy absorbed in a defined quantity of matter. These units are used in estimating organ dose from an administered radiopharmaceutical or in the therapeutic application of radiation by any means. The rem and sievert are units of equivalent dose, which takes into consideration the sensitivity of the organ irradiated and the relative importance of that organ to the well-being of the human body. These units are used in radiation protection to report exposures recorded by radiation monitoring devices such as film badges and dosimeters. As a general rule, for beta and gamma ray sources used in nuclear medicine, 1 R is approximately equal to 1 rad or 1 rem. Some useful conversions are given in Table 4-2.

RADIATION PROTECTION

Table 4-3 compares the absorption ranges of electrons and alpha particles in air and water with the attenuation of photons of similar energy.[2] In nuclear pharmacy the primary concern about external exposure relates to gamma and x-ray emissions, because of their ability to penetrate tissue and cause ionization. The data in Table 4-3 demonstrate that low-energy photon emitters, such as ^{125}I (27–35 keV), are absorbed close to 50% per

TABLE 4-2 Radiation Dosimetric Conversions

1 R (tissue) = 0.96 rad
1 Gy = 100 rad
1 rad = 1 cGy or 10 mGy
1 Sv = 100 rem
1 rem = 1 cSv or 10 mSv
1 Bq = 1 dps
1 mCi = 3.7×10^7 dps (Bq)
1 mCi = 37 MBq
1 Bq = 2.7×10^{-11} Ci

TABLE 4-3 Radiation Absorption in Air and Water

Energy (MeV)	Maximum Range into Absorber (mm)				% Photons Absorbed per cm[a]	
	Electrons		Alpha Particles			
	Air	Water	Air	Water	Air	Water
0.025	12	0.013	0.6	0.0006	<0.1	45
0.050	41	0.04	0.9	0.0009	<0.1	20
0.1	135	0.14	1.4	0.0014	<0.1	16
0.2	422	0.45	2.1	0.0022	<0.1	13
0.3	791	0.84	2.6	0.0027	<0.1	11
0.5	1656	1.77	3.5	0.0037	<0.1	9
1.0	4076	4.37	5.6	0.0059	<0.1	7

[a] % Absorbed = $100(1 - e^{-\mu x})$, where x = 1 cm.

Source: http://physics.nist.gov/ (Particle Range and Photon Attenuation Coefficient Tables).

centimeter in water (similar to soft tissue) and therefore could deposit a significant radiation dose to tissue. The high level of tissue absorption limits detectable photons and is the primary reason why ^{125}I is not used for diagnostic imaging. The data in Table 4-3 also indicate that the short range of particulate radiation in water would cause the particles to be completely absorbed after internal administration, producing a significant radiation body burden.

There appears to be little hazard to the body from external exposure to particulate radiation, because electrons and alpha particles are readily absorbed by air or a few millimeters of skin. However, a few high-energy beta emitters such as ^{32}P (1.7 MeV), ^{90}Y (2.28 MeV), and ^{89}Sr (1.46 MeV) can pose an external threat because of the range these betas have in air and tissue. The maximum range in air, water, and plastic of some typical beta emitters used in nuclear medicine is listed in Table 4-4. The maximum range of beta particles of various energies in different absorbers, in grams per square centimeter, has been tabulated (http://physics.nist.gov/). Table 4-4 lists these ranges for water. The range or distance in centimeters that a beta particle travels into an absorber is of practical interest. The range (R) in centimeters and grams per square centimeter is related to the density (d) of an absorber as follows: R (cm) = R (grams/cm^2)/d (grams/cm^3). Since the density of water is 1.0 gram/cm^3, the range in centimeters that a beta particle travels in water is the same as its range in grams/cm^2. Therefore, the range of a similar-energy beta particle in a different absorber can be found by dividing its range in water in grams/cm^2 by the density of the absorber. Thus, for example, the maximum range of a 2.28 MeV ^{90}Y beta particle in Lucite is 1.13 grams/cm^2 divided by 1.19 grams/cm^3, or 0.95 cm. ^{90}Y beta particles have a maximum range in air of about 8.7 m, which creates an external exposure

TABLE 4-4 Beta Particle Range in Matter

Nuclide	Beta Max (MeV)	Beta Range in Water (g/cm^2)	Maximum Beta Particle Range into Absorber (cm)		
			Water $d = 1\ g/cm^3$	Air $d = 1.293 \times 10^{-3}\ g/cm^3$	Plastic[a] $d = 1.19\ g/cm^3$
^{3}H	0.018	0.0007	0.0007	0.58	0.0006
^{14}C	0.155	0.03	0.03	23	0.03
^{32}P	1.71	0.83	0.83	642	0.70
^{89}Sr	1.46	0.69	0.69	534	0.58
^{90}Y	2.28	1.13	1.13	874	0.95
^{153}Sm	0.81	0.34	0.34	263	0.29

[a] Polymethylmethacrylate (Lucite, Plexiglas, Perspex).

Source of beta particle range in water: http://physics.nist.gov/.

threat from ^{90}Y. However, these beta particles are completely absorbed in about 1 cm of Lucite. This exemplifies the well-known use of low-Z material for shielding high-energy beta particles. However, bremsstrahlung production by high-energy beta particles necessitates overwrapping the plastic shield with a layer of lead to absorb these photons.

Potential sources of internal radiation exposure are ingestion of contaminated food or water and inhalation of airborne radionuclides. The most common threat in nuclear medicine is inhalation of radioiodine vapor during administration of therapeutic radioiodine solution or during radioiodination procedures. Other examples are radioaerosols and radioactive gases used in lung imaging studies. For the most part, however, radiation exposure of workers in nuclear medicine is from working with unshielded sources in the lab and from patients receiving radiopharmaceuticals. Protection from all these sources requires vigilance and the use of various techniques. Airborne contamination can be controlled by using exhaust hoods during dose preparation and radioiodination procedures. Imaging rooms for lung ventilation studies with radioactive xenon gas should have dedicated exhaust to the outside. Additionally, functional charcoal traps should be used on lung ventilation machines to limit room contamination from radioactive xenon during lung ventilation studies. In general, the three most important considerations for protection from external exposure to gamma radiation are time, distance, and shielding.

Time of Exposure

The shorter the time of exposure, the lower will be the radiation dose. This means that work with radioactive material must be planned well and performed as quickly as possible, especially when workers are handling unshielded sources.

NRC regulations (10 CFR 20.1301) state that the total effective dose equivalent to individual members of the public must not exceed 0.1 rem in a year and that the dose in any unrestricted area from external sources must not exceed 2 mrem in any 1 hour. These dose rate limits are intended only for short-term, nonoccupational exposures over periods of not more than 50 hours (i.e., 100 mrem divided by 50 hours = 2 mrem/hour). These limits apply particularly to "nonoccupational personnel"—persons such as hospital nurses, visitors, and non–radiation-treated patients who may be exposed to a patient treated with radioactive material. Listed in Table 4-5 (from NCRP Report 37, 1970[3]) are approximate times for an exposure of 100 mrem from 100 mCi of various radionuclides at specific distances.

In particular circumstances, such as in some NRC agreement states (described in Chapter 5), the total dose to a nontreated patient near a treated patient may exceed 100

TABLE 4-5 External Exposure from Radionuclides

	Approximate Time (hours) for 100 mrem per 100 mCi	
Radionuclide	At 2 Feet (0.61 m)	At 6 Feet (1.83 m)
^{137}Cs	1	10
^{60}Co	0.33	3
^{125}I	12	115
^{131}I	1.5	15
^{192}Ir	0.75	7

mrem. In North Carolina, for example, the regulations permit a 125 mrem dose limit for the duration of a brachytherapy procedure. NCRP Report 37 provides guidance on precautions in managing patients who have received therapeutic amounts of radionuclides. If nonoccupational personnel will have chronic exposure longer than 50 hours, the hourly dose rate must be reduced below 2 mrem so that the total exposure does not exceed 100 mrem.

Regarding exposure from patients released from an institution after receiving radioactive materials, NRC regulations (10 CFR 35.75 and Regulatory Guide 8.39) state that a licensee may "release from its control any individual who has been administered radiopharmaceuticals or permanent implants containing radioactive material if the total effective dose equivalent (TEDE) to any other individual from exposure to the released individual is not likely to exceed 5 mSv (500 mrem)." Since the TEDE in this situation can exceed 100 mrem, the licensee must provide the released patient with oral and written instructions on how to maintain doses as low as reasonably achievable to other individuals. The instructions should contain guidance on limiting the time other individuals are exposed to the patient. The licensee must apply to NRC for exposure of members of the public up to 500 mrem, according to 10 CFR 20.1301.

Hospital personnel may also be at risk for chronic radiation exposure if their workplace is adjacent to a radiation therapy department that uses a linear accelerator for patient treatment. Another example of chronic radiation exposure is a nuclear pharmacy where the business office is adjacent to the radiation preparation or storage area. Adequate shielding of floors, walls, and ceiling around an accelerator or high-radiation area must be provided so that exposure does not exceed 100 mrem per year to nonradiation workers.

Distance

Maintaining as much distance as practical from a radiation source is an effective method for reducing exposure because of the *inverse square law.* This law, which applies only to gamma and x-rays, states that the amount of radiation from a point source is inversely proportional to the square of the distance from the source. Simply stated, doubling the distance from a source reduces the exposure to one-fourth. This principle of exposure reduction works only if the source is small relative to the exposed body.

The specific gamma ray constant (Γ) of a radionuclide must be known to apply the inverse square law. This constant is the exposure rate in R/hour at a distance of 1 cm from a 1 mCi (37 MBq) source of radionuclide. The units of Γ are R-cm^2/mCi hour. Table 4-6 lists the specific gamma ray constants for several radionuclides used in nuclear medicine. For any given number of millicuries, N, the dose rate at distance d from the source is given by the following equation:

TABLE 4-6 Radionuclide-Specific Gamma Ray Constants (Γ) and Half-Value Layers in Lead

Radionuclide	Half-Value Layer (mm Pb)	Γ (R-cm²/mCi hr)
^{18}F	4.0	5.73
^{51}Cr	1.7	0.18
^{57}Co	0.2	1.0
^{58}Co	9.0	5.5
^{67}Ga	0.66	0.8
^{99m}Tc	0.17	0.78
^{111}In	0.23	3.21
^{123}I	0.05	1.6
^{125}I	0.017	1.43
^{131}I	2.4	2.20
^{133}Xe	0.035	0.51
^{137}Cs	6.0	3.32
^{201}Tl	0.006	4.7

$$R/hr = \frac{N\Gamma}{d^2} \tag{4-2}$$

Example 1: What is the dose rate from a 100 mCi (3700 MBq) ^{131}I source at 1 cm and at 2 feet (61 cm)?

$$R/hr\ @\ 1\ cm = \frac{N\Gamma}{d^2} = \frac{(100\ mCi)(2.2\ R\cdot cm^2/mCi\cdot hr)}{(1\ cm)^2} = 220\ R/hr$$

$$R/hr\ @\ 61\ cm = \frac{N\Gamma}{d^2} = \frac{(100\ mCi)(2.2\ R\cdot cm^2/mCi\cdot hr)}{(61\ cm)^2} = 0.059\ R/hr$$

Example 2: How much time would it take to accumulate a 100 mR (0.1 R) exposure dose from 100 mCi (3700 MBq) of ^{131}I at the distance of 2 feet?

$$\text{Time to accumulate } 0.1\ R = \frac{0.1\ R}{0.059\ R/hr} = 1.7\ hr$$

Example 3: What distance would lower the dose rate to 2 mR/hr from the 100 mCi (3700 MBq) ^{131}I source?

$$\frac{N\Gamma}{d^2} = 2\ mR/hr$$

$$d(cm) = \sqrt{\frac{100\ mCi \times 2.2\ R/hr/mCi \times 1000\ mR/R}{2\ mR/hr}} = 332\ cm \text{ or about } 11\ feet$$

TABLE 4-7 Photon Attenuation Coefficients

Energy (keV)	Linear Attenuation Coefficients, μ (cm^{-1})[a]			
	Soft Tissue $d = 1.06$	Bone $d = 1.92$	Copper $d = 8.94$	Lead $d = 11.35$
20	0.87	7.68	302.1	980.2
30	0.40	2.56	97.6	374.8
50	0.24	0.81	23.4	91.3
100	0.18	0.36	4.1	63.0
150	0.16	0.28	2.0	22.9
200	0.14	0.25	1.4	11.3
300	0.12	0.21	1.0	4.6
500	0.10	0.17	0.7	1.8
1000	0.07	0.13	0.5	0.8

[a] μ (cm^{-1}) = mass attenuation coefficient (cm^2/gram) × absorber density (gram/cm^3).

Source: http://physics.nist.gov/ (X-ray Mass Attenuation Coefficient Tables).

Maintaining distance from a source reduces exposure significantly, but this alone does not provide adequate safety in the handling of high-activity sources. These sources must be shielded. Practical applications of the inverse square law in the handling of radioactive sources in nuclear pharmacy are discussed in Chapter 5.

Shielding

The effectiveness of any shielding material depends upon its atomic number, density, and thickness. Material of high density and high Z has many atoms (and electrons) packed into a small volume, producing high stopping power. As the energy of gamma photons increases, thicker shields are required to stop them. If one interposes an absorber between a radiation source and a Geiger-Müller counter, the fraction of the original intensity transmitted through the shield will be a function of the absorber thickness, x, and the linear attenuation coefficient, μ. The attenuation coefficient depends on the atomic number (Z) of the absorber and the photon energy (E), but for given values of Z and E, μ has a constant value. The linear attenuation coefficients of various photon energies in several absorbers are listed in Table 4-7. The following formula shows the relationship between original intensity and transmitted intensity after shielding:

$$I = I_0 e^{-\mu x} \tag{4-3}$$

where I is the transmitted intensity after shielding, I_0 is the original intensity before shielding, and μ is the linear attenuation coefficient (mm^{-1}).

If one plots transmitted intensity (I) values for various absorber thicknesses, a linear relationship is obtained on semi-log graph paper as shown in Figure 4-1. The absorber thickness required to reduce the original intensity to half its value is known as the *half-value layer* (HVL). HVL values for several radionuclides are listed in Table 4-6. Mathematically, the HVL is inversely related to the linear attenuation coefficient as follows:

$$\mu = \frac{0.693}{\text{HVL}} \tag{4-4}$$

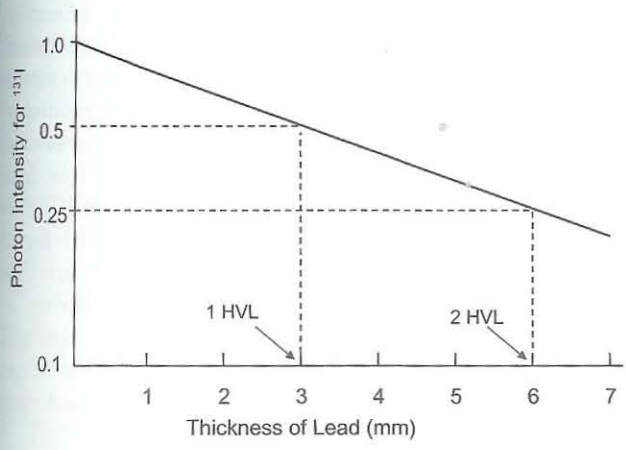

FIGURE 4-1 Plot of log-transmitted gamma ray intensity (ordinate) versus absorber thickness (abscissa) for ^{131}I in lead. HVL = half-value layer.

For example, the thickness of lead required to reduce the radiation intensity from a 100 mCi (3700 MBq) point source of ^{99m}Tc from its original intensity to 2 mR/hour can be calculated. From Table 4-6, Γ (^{99m}Tc) = 0.78 R-cm^2/mCi hour. Using the natural log form of Equation 4-3 we have:

$$I_0 = \frac{(0.78\ \text{R}\cdot\text{cm}^2/\text{mCi}\cdot\text{hr})(100\ \text{mCi})(1000\ \text{mR/R})}{1\ \text{cm}^2} = 78{,}000\ \text{mR/hr}$$

$$\ln I = \ln I_0 - \mu x$$

$$\ln 2\ \text{mR/hr} = \ln 78{,}000\ \text{mR/hr} - \frac{0.693}{0.17\ \text{mm}}(x)$$

$$0.693 = 11.26 - 4.08x$$

$$x = 2.59\ \text{mm}$$

RADIATION DOSIMETRY

The radiation dose to the whole body and to individual organs from an administered radiopharmaceutical is important for several reasons. The amount of radiation absorbed must be known in order to assess the risk to the patient. This information can then be relayed to the patient in a way that compares the risk of a radiologic procedure with other types of risky activities that are familiar to the patient. The radiation dose information also determines the maximum amount of administered activity for a nuclear medicine procedure.

A radiopharmaceutical is distributed throughout the body, but not necessarily in a uniform manner. Different organs absorb different amounts of radiation. The organ receiving the highest radiation dose is termed the *critical organ*. In some instances it is the target organ, the one being imaged. Sometimes the critical organ is not the target organ. For example, ^{99m}Tc-exametazime (^{99m}Tc-HMPAO) is used for brain imaging, but the critical organ is the lacrimal glands.

Radiation Dose Terms and Units

It is necessary to understand the terms used in radiation dosimetry and radiation protection. The fundamental term is the *absorbed dose (D)*, the mean energy imparted by ionizing

radiation to a given mass of tissue. The traditional unit of absorbed dose defined earlier is the rad, equivalent to 100 ergs absorbed per gram of matter. The SI unit of absorbed dose is the gray (Gy), equivalent to 100 rad. Because the biologic effect of radiation depends not only on the absorbed dose but on the type and energy of the radiation, the term *dose equivalent* (H) was instituted by ICRP 30 in 1977.[4] The dose equivalent is the absorbed dose multiplied by the appropriate radiation quality factor (Q) (Table 4-1). The dose equivalent is the traditional term used by radiation protection programs. In 1991 ICRP 60 renamed the dose equivalent as the *equivalent dose* (H_T) and the radiation quality factor term as the *radiation-weighting factor* (W_R).[1] Both terms have units of rem or sievert. One sievert (Sv) is equivalent to 100 rem. The relationships of these terms are as follows:

$$\text{Absorbed dose}\left(\text{rad}\right) = \frac{\text{Total energy absorbed}\left(\text{ergs}\right)}{\text{Mass of absorber}\left(\text{grams}\right)} \tag{4-5}$$

$$\text{Dose equivalent}\left(\text{H}\right)\text{ in rem}\left(\text{ICRP 30}\right) = D \times \text{Q} \tag{4-6}$$

$$\text{Equivalent dose}\left(\text{H}_\text{T}\right)\text{ in rem}\left(\text{ICRP 60}\right) = D \times \text{W}_\text{R} \tag{4-7}$$

There is a conceptual difference between the dose equivalent and equivalent dose. The dose equivalent (H) was based on the absorbed dose at a "point" in tissue, weighted by a distribution of quality factors that are related to the LET distribution of the radiation at that point. The equivalent dose is based on an average absorbed dose in the tissue and weighted by the radiation-weighting factor for the type of radiation impinging on the body or emitted by an internal source.[1]

Radiation Dose Calculation

The radiation dose to an organ from an internally administered radionuclide is given by the expression

$$\bar{D}\left(r_k \leftarrow r_h\right) = \tilde{A}_h \cdot S\left(r_k \leftarrow r_h\right) \tag{4-8}$$

where $\bar{D}$ is the mean absorbed dose in rad to a target organ (r_k) from a radionuclide distributed uniformly in a source organ (r_h). The absorbed dose to an organ depends on several factors; those of significance are the

- Amount of radioactivity in the organ
- Type and energy of the radiation
- Amount of energy absorbed by the organ
- Residence time of radiation in the organ
- Distribution of radiation in the organ and
- Organ mass

It must be kept in mind that the target organ will receive the radiation dose from radioactivity within it and from neighboring organs.

In Equation 4-8 $\tilde{A}_h$ (pronounced "A tilde") is the cumulated activity, in units of microcurie-hour (μCi hr), in the source region (r_h). It is the sum, or accumulation, of all the nuclear transitions occurring in the organ h during the time interval of interest, usually taken as infinity when complete decay has occurred. For complete nuclide decay $\tilde{A}_h$ is determined by the amount of activity in the organ and its effective half-life, T_{eff}, as follows:

$$\tilde{A}_h(\mu\text{Ci-hr}) = \frac{A_0(\mu\text{Ci})}{\lambda_e} = A_0(\mu\text{Ci}) \cdot 1.443 \cdot T_{\text{eff}}(\text{hr}) \tag{4-9}$$

The value of $\tilde{A}_h$ is influenced by the fraction of administered activity taken up by the organ, which is governed by normal physiologic factors and any alterations due to organ pathology.

The S in Equation 4-8 relates to physical data regarding the radionuclide and the organ mass because the dose will be expressed in rad. It is given by the expression

$$S(r_k \leftarrow r_h) = \frac{\Sigma \Delta_i \Phi_i (r_k \leftarrow r_h)}{m_k} \tag{4-10}$$

where

$$\Delta_i = 2.13 \cdot n_i \cdot E_i \tag{4-11}$$

In Equation 4-11, the 2.13 is a unit conversion constant, n_i is the mean number of particles or photons per nuclear transformation, and E_i is the mean energy of the radiation in megaelectron volts. The units of Δ_i are gram-rad/μCi hr. In Equation 4-10, the term m_k is the mass in grams of the target organ, making the S unit rad/μCi hr. The term Φ_i is the absorbed fraction of radiation in the target organ and is unitless. For nonpenetrating radiations such as beta particles, the fraction absorbed is 1. For photons the fraction absorbed is usually less than 1 and depends on photon energy.

The Medical Internal Radiation Dose (MIRD) Committee of the Society of Nuclear Medicine has tabulated values of S for several radionuclides, greatly facilitating radiation dose calculations using Equation 4-8. Table 4-8 lists the S values for ^{99m}Tc.[5]

Example: An investigational ^{99m}Tc radiopharmaceutical for spleen imaging has the following distribution after intravenous administration: 80% spleen, 15% liver, and 5% total body. Estimate the radiation dose to the spleen from a 1 mCi (37 MBq) dose. Assume very slow biologic elimination, that is, $T_{eff} = T_p$ (physical half-life) or 6 hours.

The first step in the process is to calculate the cumulated activities in the source organs (spleen, liver, total body). Thus

$$\tilde{A}\ \text{spl} = (1000\ \mu\text{Ci})(0.80)(1.443)(6\ \text{hr}) = 6926\ \mu\text{Ci-hr}$$

$$\tilde{A}\ \text{liv} = (1000\ \mu\text{Ci})(0.15)(1.443)(6\ \text{hr}) = 1299\ \mu\text{Ci-hr}$$

$$\tilde{A}\ \text{tb} = (1000\ \mu\text{Ci})(0.05)(1.443)(6\ \text{hr}) = 433\ \mu\text{Ci-hr}$$

TABLE 4-8 MIRD *S* Values for ^{99m}Tc

S, ABSORBED DOSE PER UNIT CUMULATED ACTIVITY, (RAD/UCI-H)
TECHNETIUM-99M HALF-LIFE 6.03 HOURS

TARGET ORGANS	SOURCE ORGANS									
	ADRENALS	BLADDER CONTENTS	INTESTINAL TRACT				KIDNEYS	LIVER	LUNGS	OTHER TISSUE (MUSCLE)
			STOMACH CONTENTS	SI CONTENTS	ULI CONTENTS	LLI CONTENTS				
ADRENALS	3.1E-03	1.5E-07	2.7E-06	1.0E-06	9.1E-07	3.6E-07	1.1E-05	4.5E-06	2.7E-06	1.4E-06
BLADDER WALL	1.3E-07	1.6E-04	2.7E-07	2.6E-06	2.2E-06	6.9E-06	2.8E-07	1.6E-07	3.6E-08	1.8E-06
BONE (TOTAL)	2.0E-06	9.2E-07	9.0E-07	1.3E-06	1.1E-06	1.6E-06	1.4E-06	1.1E-06	1.5E-06	9.8E-07
GI (STOM WALL)	2.9E-06	2.7E-07	1.3E-04	3.7E-06	3.8E-06	1.8E-06	3.6E-06	1.9E-06	1.8E-06	1.3E-06
GI (SI)	8.3E-07	3.0E-06	2.7E-06	7.8E-05	1.7E-05	9.4E-06	2.9E-06	1.6E-06	1.9E-07	1.5E-06
GI (ULI WALL)	9.3E-07	2.2E-06	3.5E-06	2.4E-05	1.3E-04	4.2E-06	2.9E-06	2.5E-06	2.2E-07	1.6E-06
GI (LLI WALL)	2.2E-07	7.4E-06	1.2E-06	7.3E-06	3.2E-06	1.9E-04	7.2E-07	2.3E-07	7.1E-08	1.7E-06
KIDNEYS	1.1E-05	2.6E-07	3.5E-06	3.2E-06	2.8E-06	8.6E-07	1.9E-04	3.9E-06	8.4E-07	1.3E-06
LIVER	4.9E-06	1.7E-07	2.0E-06	1.8E-06	2.6E-06	2.5E-07	3.9E-06	4.6E-05	2.5E-06	1.1E-06
LUNGS	2.4E-06	2.4E-08	1.7E-06	2.2E-07	2.6E-07	7.9E-08	8.5E-07	2.5E-06	5.2E-05	1.3E-06
MARROW (RED)	3.6E-06	2.2E-06	1.6E-06	4.3E-06	3.7E-06	5.1E-06	3.8E-06	1.6E-06	1.9E-06	2.0E-06
OTH TISS (MUSC)	1.4E-06	1.8E-06	1.4E-06	1.5E-06	1.5E-06	1.7E-06	1.3E-06	1.1E-06	1.3E-06	2.7E-06
OVARIES	6.1E-07	7.3E-06	5.0E-07	1.1E-05	1.2E-05	1.8E-05	1.1E-06	4.5E-07	9.4E-08	2.0E-06
PANCREAS	9.0E-06	2.3E-07	1.8E-05	2.1E-06	2.3E-06	7.4E-07	6.6E-06	4.2E-06	2.6E-06	1.8E-06
SKIN	5.1E-07	5.5E-07	4.4E-07	4.1E-07	4.1E-07	4.8E-07	5.3E-07	4.9E-07	5.3E-07	7.2E-07
SPLEEN	6.3E-06	6.6E-07	1.0E-05	1.5E-06	1.4E-06	8.0E-07	8.6E-06	9.2E-07	2.3E-06	1.4E-06
TESTES	3.2E-08	4.7E-06	5.1E-08	3.1E-07	2.7E-07	1.8E-06	8.8E-08	6.2E-08	7.9E-09	1.1E-06
THYROID	1.3E-07	2.1E-09	8.7E-08	1.5E-08	1.6E-08	5.4E-09	4.8E-08	1.5E-07	9.2E-07	1.3E-06
UTERUS (NONGRVD)	1.1E-06	1.6E-05	7.7E-07	9.6E-06	5.4E-06	7.1E-06	9.4E-07	3.9E-07	8.2E-08	2.3E-06
TOTAL BODY	2.2E-06	1.9E-06	1.9E-06	2.4E-06	2.2E-06	2.3E-06	2.2E-06	2.2E-06	2.0E-06	1.9E-06

S, ABSORBED DOSE PER UNIT CUMULATED ACTIVITY, (RAD/UCI-H) (CONTINUED)
TECHNETIUM-99M HALF-LIFE 6.03 HOURS

TARGET ORGANS	SOURCE ORGANS									
	OVARIES	PANCREAS	SKELETON			SKIN	SPLEEN	TESTES	THYROID	TOTAL BODY
			R MARROW	CORT BONE	TRA BONE					
ADRENALS	3.3E-07	9.1E-06	2.3E-06	1.1E-06	1.1E-06	6.8E-07	6.3E-06	3.2E-08	1.3E-07	2.3E-06
BLADDER WALL	7.2E-06	1.4E-07	9.9E-07	5.1E-07	5.1E-07	4.9E-07	1.2E-07	4.8E-06	2.1E-09	2.3E-06
BONE (TOTAL)	1.5E-06	1.5E-06	4.0E-06	1.2E-05	1.0E-05	9.9E-07	1.1E-06	9.2E-07	1.0E-06	2.5E-06
GI (STOM WALL)	8.1E-07	1.8E-05	9.5E-07	5.5E-07	5.5E-07	5.4E-07	1.0E-05	3.2E-08	4.5E-08	2.2E-06
GI (SI)	1.2E-05	1.8E-06	2.6E-06	7.3E-07	7.3E-07	4.5E-07	1.4E-06	3.6E-07	9.3E-09	2.5E-06
GI (ULI WALL)	1.1E-05	2.1E-06	2.1E-06	6.9E-07	6.9E-07	4.6E-07	1.4E-06	3.1E-07	1.1E-08	2.4E-06
GI (LLI WALL)	1.5E-05	5.7E-07	2.9E-06	1.0E-06	1.0E-06	4.8E-07	6.1E-07	2.7E-06	4.3E-09	2.3E-06
KIDNEYS	9.2E-07	6.6E-06	2.2E-06	8.2E-07	8.2E-07	5.7E-07	9.1E-06	4.0E-08	3.4E-08	2.2E-06
LIVER	5.4E-07	4.4E-06	9.2E-07	6.6E-07	6.6E-07	5.3E-07	9.8E-07	3.1E-08	9.3E-08	2.2E-06
LUNGS	6.0E-08	2.5E-06	1.2E-06	9.4E-07	9.4E-07	5.8E-07	2.3E-06	6.6E-09	9.4E-07	2.0E-06
MARROW (RED)	5.5E-06	2.8E-06	3.1E-05	4.1E-06	9.1E-06	9.5E-07	1.7E-06	7.3E-07	1.1E-06	2.9E-06
OTH TISS (MUSC)	2.0E-06	1.8E-06	1.2E-06	9.8E-07	9.8E-07	7.2E-07	1.4E-06	1.1E-06	1.3E-06	1.9E-06
OVARIES	4.2E-03	4.1E-07	3.2E-06	7.1E-07	7.1E-07	3.8E-07	4.0E-07	0.0	4.9E-09	2.4E-06
PANCREAS	5.0E-07	5.8E-04	1.7E-06	8.5E-07	8.5E-07	4.4E-07	1.9E-05	5.5E-08	7.2E-08	2.4E-06
SKIN	4.1E-07	4.0E-07	5.9E-07	6.5E-07	6.5E-07	1.6E-05	4.7E-07	1.4E-06	7.3E-07	1.3E-06
SPLEEN	4.9E-07	1.9E-05	9.2E-07	5.8E-07	5.8E-07	5.4E-07	3.3E-04	1.7E-08	1.1E-07	2.2E-06
TESTES	0.0	5.5E-08	4.5E-07	6.4E-07	6.4E-07	9.1E-07	4.8E-08	1.4E-03	5.0E-10	1.7E-06
THYROID	4.9E-09	1.2E-07	6.8E-07	7.9E-07	7.9E-07	6.9E-07	8.7E-08	5.0E-10	2.3E-03	1.5E-06
UTERUS (NONGRVD)	2.1E-05	5.3E-07	2.2E-06	5.7E-07	5.7E-07	4.0E-07	4.0E-07	0.0	4.6E-09	2.6E-06
TOTAL BODY	2.6E-06	2.6E-06	2.2E-06	2.0E-06	2.0E-06	1.3E-06	2.2E-06	1.9E-06	1.8E-06	2.0E-06

The second step is to multiply these cumulated activities by the appropriate S values from Table 4-8 to calculate the total dose to the spleen:

$$D\ \text{spl} = \tilde{\text{A}}\ \text{spl}\cdot S(\text{spl} \leftarrow \text{spl}) + \tilde{A}\ \text{liv}\cdot S(\text{spl} \leftarrow \text{liv}) + \tilde{A}\ \text{tb}\cdot S(\text{spl} \leftarrow \text{tb})$$

$$= (6926\ \mu\text{Ci-hr})(3.3\times10^{-4}\ \text{rad}/\mu\text{Ci-hr}) +$$

$$(1299\ \mu\text{Ci-hr})(9.2\times10^{-7}\ \text{rad}/\mu\text{Ci-hr}) +$$

$$(433\ \mu\text{Ci-hr})(2.2\times10^{-6}\ \text{rad}/\mu\text{Ci-hr})$$

$$= 2.286\ \text{rad} + 0.001\ \text{rad} + 0.001\ \text{rad}$$

$$D\ \text{spl} = 2.288\ \text{rad}$$

Example: Estimate the radiation dose to the lungs from a ^{99m}Tc-DTPA aerosol used for lung ventilation imaging. Assume instantaneous uptake in lungs of 1 mCi (37 MBq) with biologic removal from the lungs into blood of 1.5% per minute.

Because there is a biologic clearance component, the effective half-life will need to be calculated as a first step. Thus, if λ_b, λ_p, and λ_{eff} are, respectively, the biologic, physical, and effective decay constants:

$$\lambda_b = 0.015\ \text{min}^{-1}\cdot 60\ \text{min/hr} = 0.900\ \text{hr}^{-1}$$

$$\lambda_p = 0.693/6.02\ \text{hr} = 0.1151\ \text{hr}^{-1}$$

$$\lambda_{eff} = 0.9000 + 0.1151 = 1.015\ \text{hr}^{-1}$$

The cumulated activity and dose to the lung is as follows:

$$\tilde{A}_{lu} = \frac{1000\ \mu\text{Ci}}{1.015\ \text{hr}^{-1}} = 985\ \mu\text{Ci-hr}$$

$$\bar{D}_{lu} = \tilde{A}_{lu}\cdot S(lu \leftarrow lu)$$

$$= (985\ \mu\text{Ci-hr})(5.2\times10^{-5}\ \text{rad}/\mu\text{Ci-hr})$$

$$= 0.051\ \text{rad}$$

RADIATION RISK ASSESSMENT

Risk is defined as the possibility of loss or injury. In regard to radiation it refers to the probability of a defined deleterious outcome from radiation exposure. Key questions that can be asked about the risks of ionizing radiation are, What physical harm can result from exposure to radiation? and What is the risk of getting cancer or causing a genetic mutation? These questions cannot be answered precisely, mainly because there is no ethical way of experimentally exposing humans to radiation to measure its effects. However, data on radiation-induced biologic effects are available from cell and animal irradiation experiments,

accidental human exposure incidents, patients with adverse effects of exposure to radiation for medical treatment, and Japanese survivors of atomic bombs dropped during World War II. Even with these data, in most instances estimations and extrapolations must be made about the risks of radiation at the low levels typical of occupational and medical exposure.

Stochastic and Deterministic Effects of Radiation

Stochastic effects of ionizing radiation exposure are those effects whose probability of occurrence increases with dose but whose severity is independent of dose. Examples of stochastic effects are cancer (a somatic risk of ionizing radiation exposure) and hereditary disorders (a genetic risk of ionizing radiation exposure). A stochastic effect is an all-or-none effect that can arise from damage to the DNA of a single cell; there is no threshold dose required to produce it. This is because there is a finite probability for the occurrence of a stochastic event even at very small doses so that, unless all such events can be repaired up to some level of dose, there can be no threshold. As radiation dose increases, the frequency of stochastic effects increases but the severity of the effect is not expected to increase.[1] Thus, the severity of cancer caused by 1 Gy of radiation is no different from that caused by 0.1 Gy, but the chance of developing cancer is increased at 1 Gy.

Deterministic effects of ionizing radiation exposure are somatic and genetic effects whose severity does increase with dose because of a proportional increase in damage or death to cells. Radiation-induced cell killing plays a crucial role in the pathogenesis of tissue injury. Nonlethal damage can also contribute significant detriment by, for example, interfering with the inflammatory response of cells or with the natural migration of cells in developing organs. A threshold dose exists for deterministic effects. The threshold dose is the dose below which no measurable effect is detected and above which an effect is observed because tissue damage exceeds repair. Examples of deterministic effects from radiation exposure are lens opacification, bone marrow depression, decrease in sperm count, skin erythema, epilation, and mental retardation. Previously, these effects were termed *nonstochastic* effects. However, the meaning of the term deterministic is "causally determined by preceding events," and ICRP 60 changed the term, considering it a more appropriate description of the events that occur. Thus, the death of an individual cell may be considered a random or stochastic effect, but the composite effect of killing a high proportion of cells in an organ, altering its structure or function, is deterministic.[1] Figure 4-2 shows idealized dose–response curves for stochastic and deterministic effects of ionizing radiation.

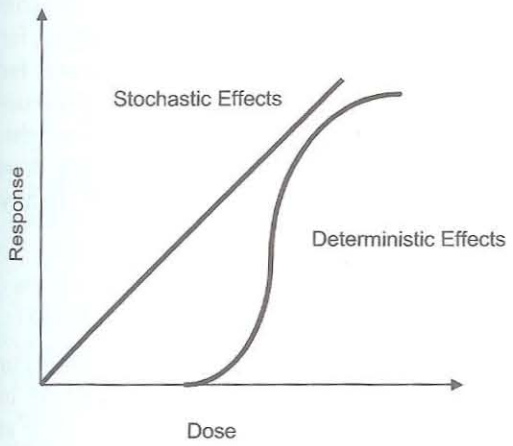

FIGURE 4-2 Idealized plot of stochastic and deterministic responses to ionizing radiation dose.

Effective Dose

The equivalent dose, discussed previously, is the product of the absorbed dose and a radiation-weighting factor. It takes into consideration the radiation dose absorbed by tissue and the relative biologic effectiveness of the particular radiation, which is related to its LET. Because the risk of stochastic effects to an individual from exposure to ionizing radiation depends not only on the absorbed dose and the radiation's RBE but on the radiosensitivity of the particular organ or tissue exposed, a tissue-weighting factor is applied to the equivalent dose. For example, the risk to an individual from gonadal irradiation or lung irradiation is greater than the risk from irradiation of the hand or skin. The factor by which the equivalent dose in a tissue or organ (T) is weighted is termed the *tissue-weighting factor* (W_T). It represents the relative contribution of that organ or tissue to the total detriment if the total body is irradiated uniformly. The weighted dose equivalent was termed the *effective dose equivalent* (H_E) by ICRP 26. The weighted equivalent dose is now termed the effective dose (E) by ICRP 60. The effective dose equivalent is the sum of the products of the dose equivalents (H) to the organs or tissues and the weighting factors (W_T) applicable to each organ or tissue irradiated; it is given by the following ICRP 26 expression:

$$H_E = \sum W_T \cdot H \tag{4-12}$$

The equivalent expression for effective dose by ICRP 60 is

$$E = \sum W_T \cdot H_T \tag{4-13}$$

To simplify terminology, ICRP 60 changed the name from effective dose equivalent to effective dose. ICRP 60 also expanded the list of tissue-weighting factors and modified their values from those of ICRP 26. This was done because in the 1980s new information became available from the Life Span Study in Japan. The data available from extended follow-up of survivors of the atomic bombings indicated that new risk estimates would allow improvements in dosimetry calculations. Table 4-9 lists the tissue-weighting factors for both ICRP 26 and ICRP 60. Confusion often occurs when terminology is changed; Table 4-10 compares the radiation dose terms and units.

To understand how these weighting factors might be used, consider the data in Table 4-11, which lists the radiation absorbed doses (dose equivalents, H) to various organs for ^{99m}Tc-medronate (^{99m}Tc-MDP). These absorbed doses are found in the package insert for the MDP kit. To calculate the effective dose equivalent for ^{99m}Tc-MDP using ICRP 26 tissue-weighting factors, each of the organ dose equivalents is multiplied by the organ's weighting factor. The sum of these is the effective dose equivalent. Similarly, the effective dose can be calculated by using tissue-weighting factors from ICRP 60, which are slightly different from those of ICRP 26.

Risk Assessment

For acute whole-body exposures above a few gray of low LET radiation, early effects occur primarily because of cell killing. This can give rise to organ and tissue damage and, in extreme cases, death. These are deterministic effects. A second type of effect can occur at later times after exposure. This type is from damage to cellular nuclear material (DNA),

TABLE 4-9 Tissue Weighting Factors

ICRP 26 (1977)		ICRP 60 (1990)	
Tissue or Organ	W_T	Tissue or Organ	W_T
Gonads	0.25	Gonads	0.20
Breast	0.15	Breast	0.05
Red marrow	0.12	Red marrow	0.12
Lung	0.12	Lung	0.12
Thyroid	0.03	Thyroid	0.05
Bone	0.03	Bone surface	0.01
Remainder[a]	5 @ 0.06	Colon	0.12
Total	1.00	Stomach	0.12
		Liver	0.05
		Esophagus	0.05
		Bladder	0.05
		Skin	0.01
		Remainder[b]	0.05
		Total	1.00

[a] Remainder is equally divided between the five organs or tissues with the highest doses.

[b] Remainder = adrenals, brain, upper large intestine, small intestine, kidney, muscle, pancreas, spleen, thymus, and uterus. If a remainder organ dose is greater than any organ listed, use W_T of 0.025 for that organ and 0.025 to average the dose of the rest of the remainder.

TABLE 4-10 Radiation Dose Terminology

Dose Equation	Conventional Unit	SI Unit	Symbol and Description
$D = \tilde{A} \cdot S$	rad	gray	$\tilde{A}$ = Cumulated activity in organ (μCi-hr)
$H = D \cdot Q$	rem	sievert	S = Mean dose/unit cumulated activity (rad/μCi-hr)
$H_T = D \cdot W_R$	rem	sievert	D = Absorbed dose
$H_E = \sum W_T \cdot H$	rem	sievert	H = Dose equivalent (ICRP 26)
$E = \sum W_T \cdot H_T$	rem	sievert	H_T = Equivalent dose (ICRP 60)
			H_E = Effective equivalent dose (ICRP 26)
			E = Effective dose (ICRP 60)
			Q = Radiation quality factor (ICRP 26)
			W_R = Radiation-weighting factor (ICRP 60)
			W_T = Tissue-weighting factor (ICRP 26, 60)

resulting in radiation-induced cancer in exposed individuals (somatic effects) or hereditary disease in their descendants (genetic effects). These effects are stochastic.

Epidemiologic studies of Japanese survivors of radiation exposure from atomic bombs are the source of much of the data used to estimate the somatic risk of developing cancer. This is considered a good model for risk estimation because exposure of the survivors was uniform over the total body and people of all ages were exposed. Although exposures of this population were spread over a wide range, from low dose to high dose, all exposures were at high dose rate. Therefore, for radiation protection purposes the effects of this type of exposure must be extrapolated down to the low dose and low dose rate conditions typical of occupational exposures.

TABLE 4-11 Absorbed Dose (Dose Equivalent) and Effective Dose Equivalent for ^{99m}Tc-Medronate[a]

Organ	Dose Equivalent (H) in rad/20 mCi	W_T	$W_T \cdot H$
Kidneys	0.80	0.06	0.048
Ovaries	0.24	0.25	0.060
Red marrow	0.56	0.12	0.067
Bone surfaces	0.70	0.03	0.021
Bladder wall	3.40	0.06	0.204
Liver	0.06	0.06	0.004
Total body	0.13	1.00	0.130

Effective dose equivalent (rem/20 mCi) $H_E = \Sigma W_T \cdot H = 0.534$.

[a] Based on ICRP 26 tissue weighting.

For radiation-induced hereditary disease, risk estimates are made primarily on the basis of animal studies, mostly in mice, but only after exposures at intermediate to high dose levels. Limited human data are available from studies carried out on the children of Japanese survivors who were irradiated.

Radiation Risk Models

The chief sources of information on the risks of radiation-induced cancer are the Japanese survivors of the atomic bombings, who were exposed to whole-body irradiation, and patients treated with radiation. Follow-up of these populations has shown that there is a minimum period of time between irradiation and the appearance of a radiation-induced tumor, although this latency period varies with age and from one tumor type to another. For example, the latency period for acute myeloid leukemia is about 2 years, compared with 5 to 10 years for other cancers. Many solid tissue tumors (e.g., liver and lung) have latency periods of 10 years or more.[1]

Because of the unknown effects over time, and the effects of other factors such as age and sex, empiric models have been postulated that extrapolate data based on only a limited portion of the lives of exposed individuals. Two models have been proposed.[1,6] The first is the *additive* or *absolute risk model*. This model postulates that radiation will induce cancer independently of the spontaneous rate and that variations in risk due to age and sex at exposure may occur. It predicts a constant excess of induced cancer throughout life, unrelated to the natural spontaneous rate of cancer. The second model is the *multiplicative* or *relative risk model*. It postulates that radiation exposure will increase the natural incidence of cancer by a constant factor and will consequently increase with age. Both forms of response occur after a minimum latency period.

Most organizations in the 1970s used the absolute risk model for risk assessment. This model produces predictions of eventual probability of death that are about half the values predicted by the relative risk model. ICRP 60 has since favored the relative risk model and a modified relative risk model proposed by the Biologic Effects of Ionizing Radiation committee (BEIR V) that considers sex, age, age at exposure, and time since exposure.[7] The United Nations Scientific Committee on the Effects of Atomic Radiation (UNSCEAR) used both models, absolute and relative, for its estimates of lifetime probability of cancer death.[8]

Compared with previous ICRP 26 estimates, the ICRP 60 estimates of the probability of death from cancer for the period 1950 to 1985 were higher because of several factors, including an increase in the number of excess solid tumors observed between 1975 and

1985, new dosimetry estimates for survivors, and preference for the relative risk model rather than the absolute model for projecting the observed numbers of solid cancers to lifetime values.[1] ICRP 60 selected data from the atomic bomb survivors as the most complete set of information on which to base quantitative risk estimates, following the lead of BEIR V[7] and UNSCEAR.[8] The Japanese study group is large (75,991 with dosimetry data) and includes both sexes, all ages, and an extensive dose range with uniform whole-body exposure. Of the total survivors, 34,272 serve as an internal control group; their radiation doses were negligible (<0.5 rad) because they were so far from the hypocenter. The remaining 41,719 survivors had doses greater than 0.5 rad and, of these, 3,435 died of some form of cancer between 1950 and 1985.

Dose–Response Relationship

Experimental information on dose–response relationships and the influence of dose rate on radiation-induced cancer incidence has been comprehensively reviewed by the National Council on Radiation Protection and Measurements (NCRP, 1980).[9] The general conclusion was that the shape of the dose–response relationship for low-LET radiation, in most biologic systems, was curvilinear with dose, that is, linear–quadratic in form given by the relationship $E = \alpha D + \beta D^2$. This is shown as curve A in Figure 4-3. This relationship had its origins in the 1930s, when it was used to fit data for radiation-induced chromosome aberrations. At low doses, the slope of the dose–response curve is less than at high doses. At low doses and low dose rates, it is unlikely that more than one ionizing event will occur in the critical parts of a cell (DNA) while repair mechanisms in the cell are operational. Under these conditions the effect per unit dose is constant ($E/D = \alpha$). At higher doses and dose rates, however, the effect increases more rapidly; it increases linearly with dose squared as the quadratic term becomes operative, that is, $E = \beta D^2$. This response is consistent with two or more events combining to produce an enhanced effect. At still higher doses, the effect often declines because cell killing reduces the number of cells at risk.

The ratio α/β, which is the dose at which the linear and quadratic contributions to the biologic effect are equal, can vary from about 1 Gy to more than 10 Gy. Fitted dashed line B in Figure 4-3 is a high dose and high dose rate linear response derived from the available data from Japanese survivors (data points shown). The low dose and low dose rate linear response (dotted line C) is an extrapolation of the low dose portion of the sigmoid curve A.

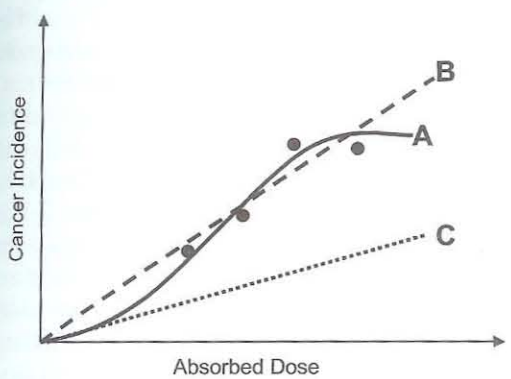

FIGURE 4-3 Schematic curves of cancer incidence versus absorbed dose. (Adapted from reference 7.)

From a radiation protection perspective, most exposures of the general public, patients undergoing radiologic procedures, and radiation workers involve low dose, low dose rate radiation. Estimates of risk for these groups have been obtained by direct extrapolation from epidemiologic studies of populations exposed at high doses and dose rates. To obtain risk estimates for radiation-induced cancer when exposures are at low doses or low dose rates, most organizations have recommended the use of a reduction factor. Suggested reduction factors have ranged from 2 to 10, meaning that the risk of radiation-induced cancer from low dose, low dose rate radiation should be reduced from that of high dose, high dose rate radiation by one-half to one-tenth. NCRP termed the reduction factor the *dose rate effectiveness factor* (DREF) and defined it as the ratio of the slopes of curves C and B shown in Figure 4-3.[9] ICRP prefers to call this reduction factor the *dose and dose rate effectiveness factor* (DDREF). To provide a conservative risk coefficient for radiation protection purposes, ICRP 60 has applied a DDREF of 2 for doses below 0.2 Gy (20 rad) at any dose rate and for higher doses if the dose rate is less than 0.1 Gy per hour. These dose rates apply to curve C, which is, in effect, an extrapolation of the linear portion of the actual dose–response relationship expected at a low dose and low dose rate.

Cancer Risk Estimates

Studies have shown that the risk of cancer depends on the particular kind of cancer, the age and sex of the person exposed, the magnitude of the dose to a particular organ, the quality of the radiation, the nature of the exposure, whether brief or chronic, the presence of other factors such as exposure to carcinogens and promoters that may interact with the radiation, and individual characteristics of the person.[7] Since nearly 20% of all deaths in the United States result from cancer, the estimated number of cancers attributable to low-level radiation is only a small fraction of the total number of deaths that occur from all causes. Furthermore, the cancers that result from radiation have no special features by which they can be distinguished from those having other causes. Thus, the probability of cancer resulting from a small dose of radiation can be estimated only by extrapolation from the increased rates of cancer that have been observed in individuals after larger doses, on the basis of assumptions about the dose–incidence relationship at low doses.

The BEIR V report based its cancer risk estimates on the data gathered from Japanese atomic bomb survivors. It used a time-dependent relative risk model that considered not only how risk increases with dose but also how it varies as a function of time for persons exposed at various ages. Only the atomic bomb survivor cohort contains persons of all ages at exposure. Survivors who were young when exposed are just now reaching the age at which cancer becomes an appreciable cause of death in the general population. The number of excess cancer deaths in this group to date has been small. Estimates of how the radiation-induced excess changes over time for those exposed as children introduce a great deal of uncertainty into attempts to project lifetime risks for the population as a whole.

Although the number of excess cases of cancer has increased as exposed groups have been followed for longer periods, the data are not strong when stratified into different dose, age, and time categories for all cancers at specific sites in the body. Reliance on data for all types of cancer has been limited, and attention has been focused on estimating the risk for leukemia, breast cancer, thyroid cancer, and cancers of the respiratory and digestive systems, of which the numbers of excess cases are substantial. However, to obtain an estimate of the total risk of mortality from all cancers, the BEIR V committee also modeled cancers other than those in Japanese survivors. The committee used epidemiologic data from patients treated with radiation for ankylosing spondylitis, cervical cancer, and postpartum mastitis and women who received multiple fluoroscopies in conjunction with artificial pneumothorax treatment for tuberculosis.

TABLE 4-12 Excess Cancer Mortality Estimates per 100,000 Exposed Persons

Type of Exposure	Male	Female
Single exposure to 0.1 Sv (10 rem)	770	810
Continuous lifetime exposure to 1 mSv/yr (0.1 rem/yr)	520	600
Continuous exposure to 0.01 Sv/yr (1.0 rem/yr) from age 18 to 65	2880	3070

Adapted from reference 5, pp. 172–173.

TABLE 4-13 Excess Cancer Mortality by Age at Exposure and Site for 100,000 Males of Each Age Exposed to 0.1 Sv (10 rem)

Age (yr) at Exposure	Total	Leukemia	Non-Leukemia	Respiratory	Digestive	Other
5	1276	111	1165	17	361	787
15	1144	109	1035	54	369	612
25	921	36	885	124	389	372
35	566	62	504	243	28	233
45	600	108	492	353	22	117
55	616	166	450	393	15	42
65	481	191	290	272	11	7
75	258	165	93	90	5	–
85	110	96	14	17	–	–
Average	770	110	660	190	170	300

Adapted from reference 5, p. 175.

Risks were calculated for the following patterns of exposure to low-LET radiation: (1) instantaneous exposure causing a dose equivalent to all body organs of 0.1 Sv (10 rem), varying the age at exposure by 10-year intervals, (2) continuous lifetime exposure causing a dose equivalent in all body organs of 1 mSv (0.1 rem) per year, and (3) continuous exposure from age 18 to 65 causing a dose equivalent to all body organs of 10 mSv (1 rem) per year. The excess cancer risks associated with these exposure assumptions are summarized in Table 4-12. The BEIR V committee stratified by age at exposure (in 10-year intervals) the excess cancer mortality for males and females by site for a single exposure of 10 rem (10 cSv), as summarized in Tables 4-13 and 4-14. In general, individuals exposed at a younger age are more susceptible to radiation-induced cancer. This is especially significant for females exposed before the age of 15; those exposed at age 45 or older show little or no excess. Susceptibility to radiation-induced leukemia is relatively constant throughout life, whereas susceptibility to respiratory cancers increases in middle age. The nonleukemia cancers listed in the tables are simply the sum of respiratory, digestive, and other risks.

From the data in Tables 4-13 and 4-14 it is estimated that if 100,000 persons of all ages received a whole-body dose of 0.1 Gy (10 rad) of gamma radiation in a single brief exposure (high dose rate), about 800 extra cancer deaths would be expected to occur during these persons' remaining lifetimes in addition to the nearly 20,000 cancer deaths that would occur naturally in the absence of the radiation. Therefore, the 10 rad radiation exposure increases the cancer mortality risk to 20.8% or an excess of 0.8%. Because exposures of radiation workers and patients are considered low dose, low dose rate, the DDREF would reduce the excess risk by one-half, to 0.4%. Thus, according to BEIR V estimates, the excess risk of death from radiation-induced cancer would be about 0.04% per 1 rem effective dose equivalent (EDE) for low-LET radiation exposure associated with medical procedures.

TABLE 4-14 Excess Cancer Mortality by Age at Exposure and Site for 100,000 Females of Each Age Exposed to 0.1 Sv (10 rem)

Age (yr) at Exposure	Total	Leukemia	Non-Leukemia	Breast	Respiratory	Digestive	Other
5	1532	75	1457	129	48	655	625
15	1566	72	1494	295	70	653	476
25	1178	29	1149	52	125	679	293
35	557	46	511	43	208	73	187
45	541	73	468	20	277	71	100
55	505	117	388	6	273	64	45
65	386	146	240	–	172	52	16
75	227	127	100	–	72	26	3
85	90	73	17	–	15	4	–
Average	810	80	730	70	150	290	220

Adapted from reference 5, p. 175.

TABLE 4-15 Probability Coefficients for Cancer Lethality by Radiation

Exposed Group	High Dose/High Dose Rate (10^{-2} per Sv)	Low Dose/Low Dose Rate (10^{-2} per Sv)
Working population[a]	8	4
Whole population	10	5

[a] Adult workers (age 25–64 years), of both sexes.

Source: Reference 1.

ICRP 60 considered all the risk estimates of its committees and others, namely BEIR and UNSCEAR, and developed overall risk coefficients for radiation-induced cancer. Table 4-15 summarizes these coefficients for the population of all ages and the working population (ages 25–64) at high dose and high dose rate and at low dose and low dose rate applying a DDREF of 2. These coefficients indicate, for example, that for the whole population exposed to low dose, low dose rate radiation the risk of cancer above the spontaneous incidence is 5×10^{-2} per sievert per person. Another way of expressing this risk coefficient is to say that an excess of 1 person out of 20 people exposed to 100 rem (or an excess of 1 person in 2000 exposed to 1 rem) of low dose, low dose rate radiation is estimated to die from radiation-induced cancer. This is an excess risk of 0.05% above the natural incidence of cancer, similar to the BEIR V estimate discussed above. This total risk coefficient was derived from the number of radiation-induced cancers that developed in each organ in the body. Table 4-16 compares the fatal probability coefficients for organ cancers developed by ICRP 26 and ICRP 60. The risk coefficients of ICRP 60 (5×10^{-2} Sv^{-1}) are four times higher than those of ICRP 26 (1.25×10^{-2} Sv^{-1}). The difference is due principally to new data on the increased probability of cancer acquired from Japanese survivors, new dosimetry methods used, and use of the relative rather than the absolute risk model for projecting the observed number of solid cancers to lifetime values.

Hereditary Risk Estimates

Estimation of the probability of radiation-induced hereditary effects in humans is based primarily on genetic studies in animals, mainly mice, exposed to ionizing radiation.

TABLE 4-16 Nominal Risks in a Population[a] from Specific Types of Fatal Cancer after Exposure to Low Dose/Low Dose Rate Low LET Radiation

	Nominal Risk (Fatal Probability Coefficient $\times 10^{-2}$ Sv^{-1})	
Organ	ICRP 26	ICRP 60
Bladder	–	0.30
Bone marrow	0.20	0.50
Bone surface	0.05	0.05
Breast	0.25	0.20
Colon	–	0.85
Liver	–	0.15
Lung	0.20	0.85
Esophagus	–	0.30
Ovary	–	0.10
Skin	–	0.02
Stomach	–	1.10
Thyroid	0.05	0.08
Remainder[b]	0.50	0.50
Total	1.25[c]	5.00[d]

[a] Nominal risks are average values for a population of equal numbers of males and females of all ages; breast and ovary are for females only.

[b] The composition of the remainder is quite different in the two cases.

[c] This total was used for both workers and the general public.

[d] General public only. The total fatal cancer risk for a working population only is taken to be 4.00×10^{-2} Sv^{-1}.

Animal studies provide information for estimating mutation rates; these data and certain assumptions are used to estimate the probability of radiation-induced hereditary disorders in humans. A hereditary disorder is a pathologic condition arising as a consequence of a mutation or chromosomal aberration transmitted from one human generation to the next. The disorders are classified into three groups: (1) X-chromosome-linked gene mutations and autosomal dominant and recessive gene mutations occurring on all other chromosomes, (2) chromosome number or structural abnormalities such as deletions, duplications, and translocations, and (3) multifactorial effects resulting from a combination of genetic and environmental factors, including congenital abnormalities present at birth and common disorders of adult life.

Two models are used to estimate hereditary risks of radiation, the doubling dose method and the direct method. These are similar to the relative and absolute carcinogenic risk models, respectively. The *doubling dose model* compares radiation-induced mutations with those that occur spontaneously and then expresses the result in terms of the doubling dose, that is, the dose of radiation that will double the spontaneous mutation rate. The *direct model* looks at the incidence of disorders that occur in the first generation exclusive of the spontaneous rate. It ignores the natural mutation rate and looks for new mutations. ICRP 60 prefers the doubling dose model. The estimate of doubling dose is 1 Gy (100 rad) and is based on mouse data and low dose rate, low LET exposure.[1] This is a calculated rather than measured quantity, based on the measured mutation rate per gene locus in mice, adjusted for the estimated comparable number of loci in humans.[10]

TABLE 4-18 Recommended Values of Tissue-Weighting Factors and Risk Coefficients[a] from which They Were Derived (ICRP 26)

Tissue (T)	Risk Coefficient 10^{-2} Sv^{-1}	W_T
Gonads	0.40	0.25
Breast	0.25	0.15
Red marrow	0.20	0.12
Lung	0.20	0.12
Thyroid	0.05	0.03
Bone surfaces	0.05	0.03
Remainder[b]	0.50	0.30
Total[c]	1.65	1.00

[a] The risk coefficient is the probability of developing fatal cancer per person for 100 rem (1 Sv) of exposure.

[b] A W_T of 0.06 is assigned to each of the five remainder tissues receiving the highest dose equivalents, and the other remainder tissues are to be neglected.

[c] The total somatic risk alone is 1.25×10^{-2} Sv^{-1}. The genetic risk is 0.4×10^{-2} Sv^{-1}, making the total risk 1.65×10^{-2} Sv^{-1}.

sex chromosome abnormality. Analysis of the data showed a difference in these two groups in the direction of higher radiation, but the difference was not statistically significant. However, an average doubling dose calculated from these data was found to be 156 rem (1.56 Sv).

From the results of all types of genetic studies conducted, ICRP 60 considers the nominal hereditary probability coefficients for severe genetic effects for the whole population to be 1×10^{-2} per sievert per individual and for workers to be 0.6×10^{-2} per sievert. When weighted further for years of life lost if harm occurs, the corresponding numbers are 1.3×10^{-2} per sievert and 0.8×10^{-2} per sievert.[1] Another way of expressing this is to say that there would be 60 excess genetic disorders above the normal incidence in the working population or 100 excess disorders in the whole population per million people exposed to 1 rem (1 cSv) effective dose.

Tissue-Weighting Factors and Detriment

When the whole body is uniformly irradiated, the probability of the occurrence of cancer and genetic effects is assumed to be proportional to the dose equivalent to the whole body, and the risk can be represented by a single value.[11] Because irradiation from internally administered radionuclides is not uniform, the concept of effective dose equivalent was developed by a scientific committee of NCRP in 1967 and subsequently adopted by ICRP. Tissue-weighting factors, recommended by ICRP 26, were derived from organ risk coefficients. These factors and their risk coefficients appear in Table 4-18. Thus, for example, the breast receives a tissue-weighting factor (W_T) of 0.15 (0.25/1.65), because its risk coefficient is 15% of the total risk coefficient. In 1990 ICRP 60 considered organ risk coefficients, weighting factors, and detriment. The revised tissue-weighting factors based on these data are listed in Table 4-9, which compares the factors of ICRP 26 and ICRP 60.

ICRP noted that detriment is a measure of the total harm that would eventually be experienced by an exposed group and its descendants as a result of the group's exposure to ionizing radiation. ICRP 60 considers four main components of detriment: (1) risk of

TABLE 4-17 Estimated Genetic Effects of 1 rem Exposure per Generation

Type of Exposure	Current Spontaneous Incidence/ 10^6 Liveborn Offspring	Additional Cases/10^6 Liveborn Offspring/rem/Generation	
		First Generation	Equilibrium
Autosomal dominant			
Severe	2500	5–20	25
Mild	7500	1–15	75
X-linked	400	<1	<5
Recessive	2500	<1	Very slow increase
Chromosomal			
Translocations	600	<5	Very little increase
Trisomies	3800	<1	<1
Congenital abnormalities	20,000–30,000	10	10–100
Totals	37,300–47,300	20–40	115–200

Adapted from reference 5.

The induced hereditary burden from radiation exposure based on the doubling dose method is estimated from the following equation:[7]

$$\text{Induced burden} = \text{Spontaneous burden} \times \left(\text{Doubling dose}\right)^{-1} \times \text{Mutation component} \times \text{Dose}$$

For example, if the spontaneous burden is 20,000 per million liveborn humans for some class of genetic disease, and the doubling dose is 100 rem (1 Sv), and the average mutational component for the disease is 50%, then for parents in each generation exposed to 100 rem (i.e., 100 rem/30 years) the induced burden will be 10,000 cases/10^6 liveborn/generation, or 100 additional cases per rem exposure.[5]

On the assumption of a doubling dose of 100 rem (1 Sv), the BEIR V committee has estimated the genetic effects of 1 rem exposure per generation. Table 4-17 lists the type and number of mutations that occur spontaneously, together with those that are produced by radiation per million live births. The total number of spontaneous defects averages 42,300 (37,300 to 47,300), or about 4.2% of all live births. The right columns in the table list the expected increase in the respective spontaneous mutations resulting from 1 rem (1 cSv) of radiation exposure per 30-year generation. The number of mutations in the first generation is small because only dominant mutations are manifested at this time. At equilibrium, after several generations have been irradiated and there is sufficient time for all types of mutations to become manifest, the number of mutations is larger, giving the full measure of the radiation-induced burden. Thus, for example, the number of clinically severe autosomal dominant mutations per million live births at equilibrium is 25 per rem, which is predicted by the induced burden formula previously described. That is, a doubling dose of 100 rem (1 Sv) will induce a mutation rate equal to the spontaneous rate of 2500 mutations at equilibrium.

Heritable effects of radiation have yet to be clearly demonstrated in humans, but the absence of a statistically significant increase in genetically related disease in the children of atomic bomb survivors is not inconsistent with animal data.[1] The only data available are from Japanese offspring of atomic bomb survivors; parents of these offspring exposed to low-dose (1 to 9 rad) and high-dose (≥100 rad) radiation were studied.[10] In this study the following genetic risk factors were considered: untoward pregnancy outcomes (stillbirths, congenital defects, death in the first week), childhood mortality, and frequency of

TABLE 4-19 Nominal Probability Coefficients for Stochastic Effects

	Detriment[a] (10^{-2} Sv^{-1})			
Population Exposed	Fatal Cancer	Nonfatal Cancer	Severe Hereditary Effects	Total
Adult workers	4.0	0.8	0.8	5.6
Whole population	5.0	1.0	1.3	7.3

[a] Fatal cancer or hereditary effects in excess of spontaneous or naturally occurring effects.

Source: Reference 1, p. 22, and reference 10, page 31.

fatal cancer, (2) risk of serious hereditary disease in future generations, (3) morbidity from nonfatal cancer, and (4) life lost due to fatal cancer. The probability coefficients for stochastic effects from fatal cancer and hereditary effects, as previously discussed, are listed in Table 4-19.[12–14] These values were also endorsed by NCRP in 1993.[15]

Comparison of Radiation Risk and Other Risks

The concept of effective dose equivalents permits comparison of radiation risk with other risks people are exposed to in their daily lives. This can be particularly helpful on patient consent forms, which require disclosure of the amount of radiation risk a patient or research subject will be exposed to during a radiologic procedure. A comparison between various types of risky activities can facilitate a patient's understanding of the degree of risk involved in undergoing a radiologic procedure. For example, the estimated risk of smoking is 1.37×10^{-7} deaths per cigarette; that is, one death will occur for every 7,299,270 cigarettes smoked. The risk of dying in an automobile accident in North America is 5.6×10^{-8} deaths per mile driven; that is, one death will occur for every 17,857,143 miles driven.[16] The stochastic risk of death from radiation is 1.65×10^{-4} (somatic, 1.25×10^{-4} and genetic, 0.4×10^{-4}) per rem effective dose equivalent (ICRP 26); that is, one extra death above natural causes is expected to occur for every 6060 people exposed to 1 rem EDE. Thus, if one follows the ICRP 26 risk estimate, the risk of dying from cancer or from a severe genetic defect due to exposure to 1 rem EDE is similar to the risk of dying from smoking one pack of 20 cigarettes per day for 2 months (about 1200 cigarettes) or driving about 2900 miles. According to ICRP 60, the stochastic risk of death from fatal cancer and severe hereditary effects from radiation is 6.3×10^{-4} per rem EDE (Table 4-19); that is, one death is expected to occur for about 1600 people exposed to 1 rem EDE. This would mean that the risk of dying from 1 EDE is equivalent to smoking about 4600 cigarettes or driving about 11,250 miles. Thus, the ICRP 60 risk estimates are about four times greater than ICRP 26 risk estimates for exposure to radiation. As an example of communicating risk factors in nuclear medicine, if a patient were to undergo a ^{99m}Tc-MDP bone scan (EDE about 0.5 rem or 0.5 cSv), the procedure would carry the same risk of dying as smoking about 2300 cigarettes or driving about 5600 miles, using ICRP 60 risk guides.

Other ways of discussing radiation risk with patients are to compare the EDE for a procedure with the average annual amount of natural background radiation of about 0.3 rem (0.3 cSv), the annual allowable whole-body exposure for a radiation worker of 5 rem (5 cSv), or the EDE of another radiologic procedure, such as a chest x-ray. Common radiologic procedures and their effective dose equivalents are listed in Table 4-20. A patient undergoing a ^{99m}Tc-MDP bone scan could be told that the amount of radiation exposure from the study is about one and one-half times the average annual background radiation or about one-tenth the annual exposure allowed for a radiation worker. Or, as previously discussed, the patient could simply be told that the increased risk of radiation-induced cancer from 1 rem EDE is 20.4%, whereas the natural incidence of cancer without radiation exposure is 20%.

TABLE 4-20 Effective Dose Equivalents of Radiologic Exposures

Radiation Source	Effective Dose Equivalent (rem)
Annual occupational exposure limit[12]	5.0
Average annual natural background radiation in the United States[13]	0.3
X-ray procedures (average doses)[13]	
Chest (digital x-ray, PA and lateral)	0.138
Chest (standard, nondigital)	0.06
Cervical spine	0.020
Kidneys, ureter, bladder	0.055
Pelvis and hip	0.065
Lumbar spine	0.130
Intravenous pyelogram	0.160
Upper GI	0.245
Barium enema	0.405
^{99m}Tc radiopharmaceuticals[14]	
Disofenin, mebrofenin 5 mCi	0.47
Exametazime 20 mCi	1.02
Gluceptate 20 mCi	0.76
Human serum albumin 20 mCi	0.58
Macroaggregated albumin 3 mCi	0.14
Medronate, pyrophosphate, RBCs 20 mCi	0.54
Mertiatide (MAG3) 5 mCi	0.22
Oxidronate 20 mCi	0.46
Pentetate (DTPA) 20 mCi	0.60
Pertechnetate 20 mCi	0.78
Sestamibi 30 mCi (rest study)	0.45
Succimer (DMSA) 5 mCi	0.30
Sulfur colloid 5 mCi	0.25
White blood cells 10 mCi	0.74

REFERENCES

1. International Commission of Radiological Protection. *1990 Recommendations of the International Commission of Radiological Protection*. ICRP Publication 60. New York: Pergamon Press; 1991.
2. Quimby EH, Feitelberg S. *Radioactive Isotopes in Medicine and Biology*. 2nd ed. Philadelphia: Lea & Febiger; 1963:85.
3. National Council on Radiation Protection and Measurements. *Precautions in the Management of Patients Who Have Received Therapeutic Amounts of Radionuclides*. NCRP Report No. 37. Washington, DC: National Council on Radiation Protection and Measurements; 1970.
4. International Commission of Radiological Protection. *Limits for Intakes of Radionuclides by Workers*. ICRP Publication 26. New York: Pergamon Press; 1977.
5. Snyder WS, Ford MR, Warner GG, et al. *"S,"Absorbed Dose per Unit Cumulated Activity for Selected Radionuclides and Organs*. MIRD Pamphlet No. 11. New York: Society of Nuclear Medicine; 1975.
6. United Nations Scientific Committee on the Effects of Atomic Radiation. *Sources and Effects of Ionizing Radiation. Vol II: Effects*. UNSCEAR 2000 Report to the General Assembly. New York: United Nations; 2000.
7. National Academy of Sciences. *Health Effects of Exposure to Low Levels of Ionizing Radiation*. BEIR V Report. Washington, DC: National Academy Press; 1990.
8. United Nations Scientific Committee on the Effects of Atomic Radiation. Radiation carcinogenesis in man. In: *Sources, Effects and Risks of Ionizing Radiation*. Annex F. New York: United Nations; 1988.
9. National Council on Radiation Protection and Measurements. *Influence of Dose and Its Distribution in Time on Dose-Response Relationships for Low-LET Radiations*. NCRP Report No. 64. Bethesda, MD: National Council on Radiation Protection and Measurements; 1980.

10. Hall EJ. *Radiobiology for the Radiologist*. 4th ed. Philadelphia: JB Lippincott; 1994.
11. National Council on Radiation Protection and Measurements. *Recommendations on Limits for Exposure to Ionizing Radiation*. NCRP Report No. 91. Bethesda, MD: National Council on Radiation Protection and Measurements; 1987.
12. Standards for Protection Against Radiation, Occupational Dose Limits for Adults. 10 CFR 20.1201 (2003).
13. National Council of Radiation Protection and Measurements. *Ionizing Radiation Exposure of the Population of the United States*. NCRP Report No. 93. Bethesda, MD: National Council of Radiation Protection and Measurements; 1987.
14. Stabin MG, Stubbs, JB, Toohey RE. *Radiation Dose Estimates for Radiopharmaceuticals*. Oak Ridge, TN: Radiation Internal Dose Information Center, Oak Ridge Institute for Science and Education; 1996.
15. National Council on Radiation Protection and Measurements. *Limitation of Exposure to Ionizing Radiation*. NCRP Report No. 116. Bethesda, MD: National Council on Radiation Protection and Measurements; 1993.
16. Huda W. Nuclear medicine dose equivalent: a method for determination of radiation risk. *J Nucl Med Technol*. 1986;14:199-201.

5 Radiation Safety

Radiation safety refers to the activities and control measures used to limit the amount of radiation exposure received by radiation workers, members of the general public, and patients undergoing radiologic procedures. The radiation protection techniques described in Chapter 4 are used in workplace radiation safety practices. Guidance on radiation safety issues is found in the Code of Federal Regulations under Title 10: Energy, Part 19: Notices, Instructions and Reports to Workers: Inspections and Investigations (10 CFR 19); Part 20: Standards for Protection Against Radiation (10 CFR 20); and Part 35: Medical Use of Byproduct Material (10 CFR 35). Helpful information related specifically to nuclear pharmacies is contained in NUREG 1556, Volume 13, Program Specific Guidance about Commercial Radiopharmacy Licenses. These documents are available in the U.S. Nuclear Regulatory Commission (NRC) reference library on the Web at http://www.nrc.gov/. Additional information regarding transport of radioactive material is found in U.S. Department of Transportation (DOT) regulations, which can be accessed at http://www.access.gpo.gov/nara/cfr/.

This chapter discusses important points related to the safe handling of radioactive material in nuclear medicine and nuclear pharmacy.

RADIATION PROTECTION ORGANIZATIONS

The population at risk from exposure to ionizing radiation is roughly divided into two groups: (1) the general public (nonoccupational exposure group) and (2) radiation workers (occupational exposure group). A number of organizations are involved in studying the effects of ionizing radiation on biologic systems to assess the risks associated with such exposure. This chapter focuses on those groups that monitor and analyze investigational studies and reports and make recommendations regarding radiation dose limits.

Two principal scientific committees conduct this type of assessment. The first is the United Nations Scientific Committee on the Effects of Atomic Radiation (UNSCEAR), whose mandate is to assess and report levels and effects of exposure to ionizing radiation to the General Assembly of the United Nations. The last report by this international organization appeared in 2000.[1] The second committee is the Biologic Effects of Ionizing Radiations (BEIR) Committee, appointed in the United States by the National Academy of Sciences. This committee advises the U.S. government, through periodic reports, on the health consequences of radiation exposure. Its last report (BEIR V) appeared in 1990.[2] These committees analyze and summarize data and suggest risk estimates for radiation-induced cancer and genetic effects, but they are not obligated to make recommendations on dose limits.

Two principal committees make recommendations regarding radiation dose limits. The first is the International Commission on Radiological Protection (ICRP). This committee is well respected by the scientific community and often takes a leadership role in formulating concepts in radiation protection and in recommending dose limits. Its most recent report is ICRP 60, published in 1991.[3] The second committee is the National Council on Radiation Protection and Measurements (NCRP), a U.S. organization. NCRP often follows the recommendations of ICRP. Its most recent report on dose limits is NCRP 116, published in 1993.[4]

The principal regulatory body in the United States is NRC. It was established in 1974 by the Energy Reorganization Act and replaced the Atomic Energy Commission, the

(B) Appoint a radiation safety officer (RSO) who agrees, in writing, to be responsible for implementing the radiation protection program.
(C) Permit an authorized user or qualified individual to serve as a temporary RSO.
(D) Appoint more than one temporary RSO.
(E) Establish, in writing, the authority, duties, and responsibilities of the RSO.
(F) Establish a radiation safety committee if two or more different types of uses of byproduct material or types of units are authorized; this committee must include an authorized user of each type of use permitted in the license, the RSO, a representative of the nursing service, and a representative of management.
(G) Provide the RSO with authority and resources to conduct the radiation safety program to (1) identify radiation safety problems, (2) initiate, recommend, or provide corrective actions, (3) stop unsafe operations, and (4) verify implementation of corrective actions.
(H) Retain records of action taken in (A), (B), and (E) of part 35.24 for 5 years.

In a nuclear pharmacy the RSO must have a level of basic technical knowledge sufficient to understand the work to be performed with byproduct material and be qualified by training and experience to perform the duties noted above. Any individual who has sufficient training and experience to be named as an authorized nuclear pharmacist is also considered qualified to serve as the facility RSO.[5] Typical duties and responsibilities of an RSO in a nuclear pharmacy are outlined in Appendix H of NUREG-1556.

OCCUPATIONAL DOSE LIMITS AND RISK

An occupational dose is a radiation dose received by an individual in the course of employment in which the individual's assigned duties involve exposure to ionizing radiation. An occupational dose does not include doses received from background radiation, from any medical administration, or from voluntary participation in medical research. Occupational dose limits and dose limits for the public are enforced by NRC and agreement states and are found in 10 CFR 20. These limits are derived from recommendations made by ICRP and NCRP. Table 5-1 lists the annual dose limits for exposure to ionizing radiation. The occupational dose limits have changed considerably over the years. The annual limit for whole-body dose was reduced by a factor of about 3 between 1934 and 1950 and by another factor of 3, to the equivalent of 50 mSv (5 rem), by 1958.[1] The lower

TABLE 5-1 Annual Radiation Dose Limits

A. Occupational dose limits for adults (10 CFR 20.1201)	
A licensee must establish controls to not exceed the following:	
1. An annual limit, which is the more limiting of	
a. Total effective dose equivalent	5 rem (50 mSv)
Or	
b. Sum of deep-dose equivalent and committed dose equivalent to any organ or tissue except lens of eye	50 rem (500 mSv)
2. The annual limits to lens of the eye, to the skin, and to the extremities, which are	
a. Lens dose equivalent	15 rem (150 mSv)
b. Shallow-dose equivalent to skin or any extremity	50 rem (500 mSv)
3. Cumulative exposure (NCRP limit)	1 rem × age in yr
B. Occupational dose limits for minors (10 CFR 20.1207)	10% of adult limits
C. Limits for embryo or fetus of occupational worker (10 CFR 20.1208)	0.5 rem (5 mSv)
D. Total effective dose equivalent (public) (10 CFR 20.1301)	0.1 rem (1 mSv)

organization that previously regulated byproduct material in the United States. NRC is composed of five members and is responsible for licensing and regulating nuclear facilities and materials. It establishes and enforces rules and regulations concerning the safe use of radiation and radioactive byproduct material in the United States. Its regulations are published in 10 CFR.

Naturally occurring and accelerator-produced radionuclides are regulated by individual states. NRC may grant regulatory authority for byproduct material to individual states, in which case these so-called agreement states regulate all forms of radioactive material: naturally occurring material, byproduct material, and accelerator-produced material. A state's regulation of byproduct material must be compatible with NRC regulations.

AS LOW AS REASONABLY ACHIEVABLE

The goal of any radiation protection program is to prevent the occurrence of radiation-induced hazardous conditions. This goal is met by (1) preventing or limiting the development of deterministic (nonstochastic) effects of radiation by setting equivalent dose limits well below the threshold limits for a person's working lifetime and (2) limiting the risk of stochastic effects to a frequency no greater than the risks seen in nonradiation occupations.[4] Deterministic effects of radiation exposure are those effects that become more severe with increasing dose but manifest themselves only above a threshold dose. Some examples are skin erythema, cataract formation, and reduction in sperm count. Stochastic effects are those that occur without a threshold dose and whose probability of occurrence increases with dose. Such effects include the development of cancer and genetic defects.

As stated in 10 CFR 20.1101, a licensee must establish a radiation protection program so that occupational doses and doses to members of the public are as low as reasonably achievable (ALARA). Additionally, the program must establish air emission limits for the general public, and the program must be reviewed annually to ensure compliance with ALARA. With such radiation protection programs in place, the public is assured that radiation will be used in a safe manner.

To keep radiation exposure ALARA, access to areas that house radiation sources must be controlled. A restricted area is one to which access is limited for the purpose of protecting individuals against undue risks from exposure to radiation and radioactive materials, such as the areas in a nuclear pharmacy or nuclear medicine laboratory where sources are stored, a radiopharmaceutical compounding and dispensing area, a nuclear medicine imaging room, or a hospital room where a patient is being treated with radionuclide therapy. Restricted areas are typically posted with signs to warn people of the potential for exposure to ionizing radiation. An unrestricted area is one to which access is neither limited nor controlled by the licensee, such as a nuclear pharmacy office, a nuclear medicine waiting room, or a nuclear medicine reading room.

RADIATION SAFETY PROGRAM

The authority and responsibilities for a radiation protection program are outlined in 10 CFR 35.24. The regulation states that a licensee's management must

(A) Approve in writing (1) license applications, renewals, or amendments before submission to NRC, (2) individuals who work as authorized users, authorized nuclear pharmacists, or authorized medical physicists, and (3) any radiation protection program changes permitted under 35.26.

dose limits became feasible mainly because radiation protection techniques and methods were developed that workers could use in their practices to keep exposures ALARA.

The philosophy of NCRP is that, for occupational exposure, the level of protection provided should ensure that the risk of developing fatal cancer from exposure to radiation be no greater than that of fatal accidents in safe industries.[4] Quantitatively, this can be viewed as follows. It is estimated that the average nominal lifetime excess risk from a single, uniform whole-body equivalent dose of 1 Sv (100 rem) is 4×10^{-2} for fatal cancer, 0.8×10^{-2} for severe genetic effects, and 0.8×10^{-2} for nonfatal cancer, for a total detriment of 5.6×10^{-2} (see Table 4-19, Chapter 4). The average fatal accident rate in all industries is 1×10^{-4} per year or 1 death in 10,000, with a range of 0.2×10^{-4} to 5×10^{-4}.[4] NCRP data from 1980 indicate that the average equivalent dose of monitored workers was approximately 2.1 mSv (0.21 rem) per year, which would suggest a total detriment of about 1.1×10^{-4} per year (2.1×10^{-3} Sv per year $\times$ 5.6×10^{-2} detriment Sv^{-1}).[4] This suggests, therefore, that the occupational risk of the average radiation worker is roughly comparable to the average risk of accidental death for all industries.

NCRP considers further what the risks might be for the radiation worker who is exposed to maximum permissible doses of radiation. The NCRP limits on occupational radiation exposure are listed in Table 5-1: not more than 50 mSv (5 rem) per year, and a cumulative exposure not to exceed a person's age $\times$ 10 mSv (1 rem). Using these limits and a hypothetical worst-case scenario of acceptable maximal exposure, the lifetime fatal cancer risk is approximately 3×10^{-2}.[4] The worst-case scenario for accidental death in a safe industry is 5×10^{-4} per year $\times$ 50 years, which results in a lifetime fatal accident risk of 2.5×10^{-2}. Thus, the risk of a fatal outcome from maximal allowable exposure for a radiation worker is consistent with the maximal risk of accidental death for all industries.

RADIATION DOSE TERMS

In addition to the absorbed dose, dose equivalent, and effective dose equivalent discussed in Chapter 4, there are other radiation dose terms used in the area of radiation protection. Some of these, as defined in 10 CFR 20, are as follows:

- Committed dose equivalent (CDE, or $H_{T,50}$). The dose equivalent to organs or tissues of reference that will be received from an intake of radioactive material by an individual during the 50 year period after the intake. This term considers internally deposited radionuclides whose dose will be determined by the time course of radiation residing in the body. It differs from an external dose received over a short exposure time. ICRP considers what the committed dose equivalent will be over a person's working lifetime of 50 years. Radionuclides with effective half-lives of 2.5 months or less are essentially decayed in 1 year, and the committed dose equivalent is essentially equal to the annual dose equivalent in the year of the intake.
- Committed effective dose equivalent (CEDE or $H_{E,50}$). The sum of the products of the weighting factors applicable to each of the body organs or tissues that is irradiated and the committed dose equivalent to these organs or tissues.

$$H_{E,50} = \sum W_T \cdot H_{T,50}$$

- Deep-dose equivalent (DDE or Hd). The dose equivalent at a tissue depth of 1 cm from whole-body external exposure.

- Lens dose equivalent (LDE). The dose equivalent from external exposure of the lens of the eye at a tissue depth of 0.3 cm (300 mg/cm^2).
- Shallow-dose equivalent (SDE or Hs). The dose equivalent from external exposure of the skin of the whole body or the skin of an extremity at a tissue depth of 0.007 cm (7 mg/cm^2) averaged over an area of 10 cm^2.
- Total effective dose equivalent (TEDE). The sum of the deep-dose equivalent (for external exposures) and the committed effective dose equivalent (for internal exposures).

DOSE LIMITS FOR VOLUNTEER SUBJECTS

Radiation safety concerns typically involve monitoring the exposure of radiation workers (occupational exposure), the general public (nonoccupational exposure), and patients undergoing diagnostic or therapeutic procedures. A fourth exposure group consists of human subjects who volunteer to undergo experimental procedures that involve exposure to ionizing radiation during research studies. Such studies are typically conducted at universities or research centers and monitored by institutional review boards (IRBs) in compliance with FDA regulations. The main purpose of an IRB is to ensure that the research is conducted in an ethical manner and that the volunteer subject has been informed of the benefits and risks of participating in the study and has consented to do so. If the subject will receive a radioactive drug or be exposed to external beam radiation from a source such as an x-ray or computed tomography (CT) machine, a human-use radioisotope committee must also approve the research. The two main purposes of this committee are to ensure that the radiation dose received by the subject is within the acceptable guidelines for radiation exposure and that no female subject is or might be pregnant during the study.

NCRP Report 70, Nuclear Medicine Factors Influencing the Choice and Use of Radionuclides in Diagnosis and Therapy (1982), contains guidelines for radiation exposure for adult volunteer subjects who receive radionuclides for investigative purposes. These guidelines, which are listed in 21 CFR 361 (April 1, 2000), state that the limits for radiation exposure of the whole body, active blood-forming organs, lens of the eye, and gonads are 3 rem per year for a single dose and 5 rem per year for an annual and total dose commitment; for other organs the limits are 5 rem and 15 rem for single dose and annual and total dose commitment, respectively. For research subjects under 18 years of age, the radiation dose is not to exceed 10% of these limits. These guidelines can be used by a human-use radioisotope committee in evaluating the radiation safety of proposed research and by the principal investigator of the study in drafting the consent form that informs the subject of the radiation risk.

SOURCES OF RADIATION EXPOSURE

Everyone is exposed to some form of ionizing radiation. In the United States, the average annual effective dose equivalent from natural background radiation is 3 mSv (300 mrem). About one-third of this exposure comes from radiation in the cosmos and terrestrial sources, and about two-thirds comes from radon. Additional sources of ionizing radiation exposure, principally from medical procedures, increase the annual exposure to about 3.6 mSv (360 mrem) (Table 5-2).[6]

TABLE 5-2 Annual Effective Dose Equivalent in the U.S. Population, 1980–1982

Source	Average Annual H_E (mrem)
Natural sources	
Radon	200
Cosmic, terrestrial, body	100
Medical	
Diagnostic x-rays, nuclear medicine	53
Nonmedical	7
Total	360

Source: Reference 5.

Background Radiation

The natural sources of background radiation include cosmic, terrestrial, and human body sources. Cosmic radiation, mostly from high-energy protons, varies with altitude and latitude. The average annual dose in the United States is 26 mrem. It doubles with every 6562 feet of altitude. At 39,000 feet, which is representative of airline altitude, it is 0.5 mrem/hour.[6] Cosmic radiation is higher at the North and South Poles, where charged particles are attracted, and lower at the equator. Terrestrial radiation is from the earth and building materials and varies geographically. In the Rocky Mountains, where rocks are rich in thorium and uranium, the average annual effective dose equivalent is 63 mrem/year; in the Atlantic and Gulf Coast regions it is 16 mrem/year; and for the remainder of the country it is 30 mrem/year.[6] Natural bodily exposure comes mainly from inhaled radon gas, with a small component from ingested nuclides, principally ^{14}C, ^{210}Po, and ^{40}K.[6]

Manufactured sources of background radiation include medical procedures in diagnostic radiology and nuclear medicine and nonmedical sources of exposure such as consumer products (e.g., smoke detectors) and radioactive fallout from the atmosphere.

The average natural background radiation exposure varies around the world. For example, in the United States it is 300 mrem, in the Brazilian coastal region it is 500 mrem, in Niue Island in the Pacific it is 1000 mrem, and in Kerala, India, it is 1300 mrem. Interestingly, despite the wide variation in these background dose rates, there appears to be no significant difference in the rate of stochastic effects of radiation between these populations.

Radiation Exposure in Nuclear Medicine and Nuclear Pharmacy

The primary exposure to ionizing radiation in professional practice occurs while handling radioactive material during transport and receipt, during radiopharmaceutical compounding and dispensing operations, during patient dose administration, and during patient imaging procedures. Patient procedures pose a radiation risk to both nuclear medicine personnel and the patients themselves. Radiation workers wear whole-body film badges and extremity dosimeters that are processed monthly to assess exposure. The results are reviewed by the RSO for compliance with regulations. In general, radiation worker exposure is well below the occupational dose limits. A few principal areas are reviewed here to identify the sources and magnitude of worker exposures from procedures in nuclear medicine and nuclear pharmacy, as described in NCRP Report 124.[7]

Transport and Receipt of Radioactive Material

As a general rule, radiation sources should be shielded so that the external exposure does not exceed 20 μGy (2 mrem)/hour. For example, a 3700 MBq (100 mCi) source of ^{131}I requires 5 cm (2 inches) of lead to achieve 20 μGy/hour. Thus, for example, it is important that the cart used to transport doses of ^{131}I-sodium iodide to a patient's room provide adequate shielding to the transporter to keep exposure ALARA. After the patient receives a dose of ^{131}I-sodium iodide, exposure increases significantly because the patient is not shielded. For example, the dose rate at 1 m from a patient immediately after receiving 100 mCi of ^{131}I is approximately 0.2 mGy (20 mrem)/hour. A typical dose rate from a shielded radiopharmaceutical package containing 100 mCi of ^{131}I is about 60 mrem/hour at the surface and 0.2 mrem/hour at 1 m.[7] This dose rate, of course, varies depending on the amount of lead used to shield the source.

Hospital inpatients are sometimes injected with a radiopharmaceutical in their rooms when the nuclear medicine procedure requires a waiting period between dose administration and imaging. This typically occurs with bone imaging. In this circumstance the radiopharmaceutical dosage should be transported to the patient room in a lead-lined syringe carrier to minimize exposure of the technologist and others along the way. This ensures that ALARA exposure is maintained in nonoccupational areas.

Dose Preparation and Patient Injection

NRC regulations require that a syringe shield be used in compounding radiopharmaceutical kits, because hand exposure can be quite high when large amounts of radioactivity are handled in such operations. Figure 5-1 illustrates the exposure from ^{99m}Tc with and without lead shielding. It demonstrates that 0.3 cm (⅛ inch) of lead reduces the exposure rate by a factor of 1000.

Exposure rate to the hands has been assessed by several investigators. The equivalent doses reported vary because of the differing conditions of exposure and monitoring, but they provide a guide to the potential magnitude of the exposure. Anderson et al.,[8] using thermoluminescent dosimeters (TLDs) taped to the fingers, found that the average dose

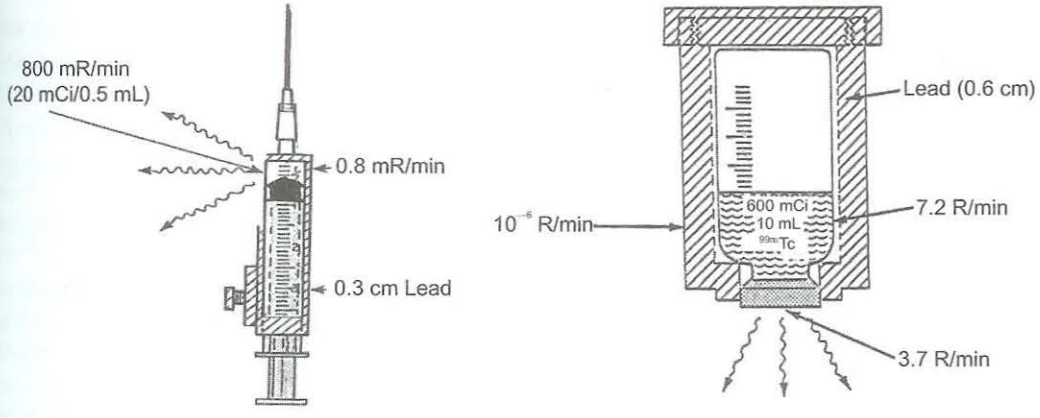

FIGURE 5-1 Rates of film exposure from a ^{99m}Tc source in a syringe and a generator elution vial. Syringe contains 20 mCi of ^{99m}Tc activity emitting a dose rate of 800 mR/minute (unshielded) and 0.8 mR/minute (shielded with 0.3 mm of lead). Generator elution vial contains 600 mCi of ^{99m}Tc emitting 3.7 R/minute at the unshielded entrance port of the vial and 10^{-6} R/minute at the surface of a lead shield 0.6 cm thick. (Courtesy of Dr. John Howley, Radiation Safety Branch, National Institutes of Health, Bethesda, MD.)

Volume (mL)	A	B	C
0.5	55	1.25	0.30
1.0	40	1.75	0.25
2.0	25	5.95	0.20

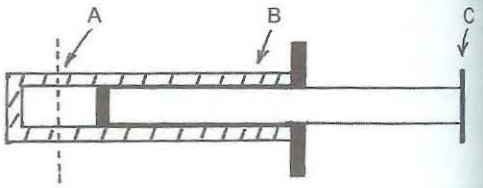

FIGURE 5-2 Exposure rate (in mrem per mCi per minute) of fingers at various positions on an unshielded 2 mL plastic syringe containing ^{99m}Tc. (Compiled from reference 9.)

to the index finger was 1600 mrem per curie of ^{99m}Tc injected using unshielded syringes, with a significantly smaller dose to the other fingers. For personnel who performed only generator elution, calibration, and dose preparation (no patient injection), the average dose was only 200 mrem per curie eluted. This report indicates that the majority of exposure comes from patient injection and averages about 1400 mrem per curie or about 28 mrem per 20 mCi (740 MBq) dose injected.

Use of syringe shields during patient injection is considered optional by NRC regulations, but dose rates, as just noted, can be high if precautions are not taken. Henson,[9] using a computer analysis and calculation method, assessed the exposure rate from unshielded radiopharmaceutical syringes at various positions on the syringe. Figure 5-2 summarizes the dose rates from syringes containing ^{99m}Tc and illustrates that there is a significant difference in dose depending on how close the finger is to the volume of activity. Figure 5-2 indicates that the dose rate decreases considerably when the finger is moved away from the active volume in the syringe. For example, if the average dose administered is 0.5 mL in a 2 mL syringe, the dose rate is 55 mrem per millicurie per minute at position A. Considering that finger contact time with the syringe during patient injection averages 15 seconds,[8] a 20 mCi (740 MBq) dose would deliver 275 mrem to the finger at position A, 6.25 mrem at position B, and 1.5 mrem at position C. The occupational dose limit for extremity exposure is 50 rem per year or an average of 1 rem per week. From the example just cited it is clear that one could easily exceed this limit after administering only 4 unshielded doses with the fingers held at position A and after 160 doses at position B. Based on an average dose rate from radiopharmaceuticals, noted previously by Anderson, of 28 mrem per 20 mCi (740 MBq) dose injected, 35 doses per week (1000 mrem per week limit divided by 28 mrem per dose) would be the maximum allowed in order to avoid exceeding the 50 rem per year limit of extremity exposure.

It is obvious that the position of the fingers on the syringe relative to the radioactive volume is an important factor in reducing exposure of the hands. This points out the advantage of using the inverse square law (see Chapter 4) when handling syringes, especially if they are not shielded. It is important also to recognize that hand radiation badges worn on the ring finger will not give a true estimate of exposure at the fingertips. On the basis of these data, technologists who inject patients and nuclear pharmacists who routinely prepare patient doses should monitor hand and finger exposure rates during these procedures. Syringe shields may be necessary to keep exposures within the acceptable dose limit. The design of syringe shields has improved over the years to make them less bulky and easier to handle. Figure 5-3 illustrates a shield constructed of tungsten, which is 50% denser than lead.

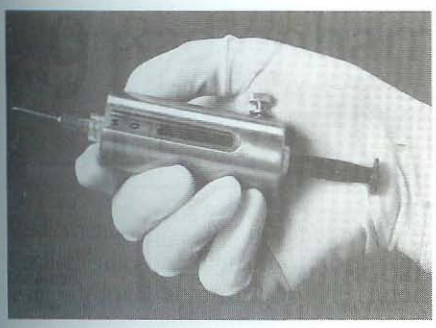

FIGURE 5-3 Tungsten syringe shield with leaded-glass viewing window. (Used with permission of Biodex Medical Systems, Shirley, NY.)

TABLE 5-3 Dose Rates from Patients Injected with 20 mCi ^{99m}Tc-Medronate

Time after Injection	Patient Condition	Position of Measurement	Dose Rate in mR/hr (patient's waist)	
			At Surface	At 1 Meter
5 min	With and without bone metastases	Anterior	9	0.9
		Posterior	9	1.0
4 hr	Without metastases	Anterior	3	0.3
		Posterior	5	0.6
	With metastases	Anterior	14	2
		Posterior	49	4

Source: Reference 7, p. 21.

Skin contamination can be a potential problem. Kereiakes[10] reported that complete decay of 1 μCi of ^{99m}Tc on the skin can range from 200 Gy from a point source to 0.07 Gy if it is spread out over 1 cm^2. The potential for such a high dose rate emphasizes the importance of wearing disposable gloves while handling radioactive material.

Beta-emitting sources can also produce significant exposure of the hands. It has been estimated that a dose of 4.5 rad is delivered to a finger held for 30 seconds in contact with a syringe containing 10 mCi (370 MBq) of ^{32}P in a 5 mL volume.[9] This high dose rate is possible because of the penetrating power of high-energy beta particles. With the increased use of beta emitters for radionuclide therapy, the handling of these doses should be given careful consideration. See Table 4-4, Chapter 4, for physical data on beta emitters used in nuclear medicine.

Patient Procedures

Several studies have reported on exposures of nurses and nuclear medicine technologists from patients who have received a radiopharmaceutical, and these have been summarized.[7] Some of the highest exposure doses to technologists arise from patients injected with a ^{99m}Tc bone agent. For example, the dose rates from a 20 mCi (740 MBq) dose of ^{99m}Tc-medronate are summarized in Table 5-3. NCRP Report 124 states that the exposure from diagnostic nuclear medicine patients is typically less than 1 mR/hour at 1 m. Benedetto et al.[11] estimated that the dose per year to nuclear medicine personnel exposed to patients is about 400 mrem.

Summary

In summary, the following recommendations will reduce radiation dose to the hands and body.

- Time: Work quickly and efficiently.
- Distance:
  - Hold syringes at a safe distance from the active volume.
  - Make venipuncture with a butterfly set and stopcock for difficult injections to reduce handling time of the dose.
  - Handle "hot" sources with tongs.
- Shielding: Use syringe shields, especially with large-activity sources.
- Protectives: Wear disposable gloves.
- Monitors:
  - Monitor hands with Geiger-Müller (GM) counter frequently to detect contamination.
  - Wear ring badges on index finger or finger likely to receive the highest dose on the basis of syringe handling technique.

PERSONNEL MONITORING

Radiation workers are monitored for exposure with whole-body badges and extremity badges such as finger dosimeters. Persons who should be badged are outlined in 10 CFR 20.1502 as follows.

External exposure monitoring is required for

1. Adults likely to receive an annual dose in excess of any of the following:
   - 5 mSv (0.5 rem) deep-dose equivalent
   - 15 mSv (1.5 rem) lens-dose equivalent
   - 50 mSv (5 rem) shallow-dose equivalent to the skin or any extremity
2. Minors likely to receive an annual dose in excess of any of the following:
   - 1 mSv (0.1 rem) deep-dose equivalent
   - 1.5 mSv (0.15 rem) lens-dose equivalent
   - 5 mSv (0.5 rem) shallow-dose equivalent to the skin or any extremity
3. Declared pregnant women likely to receive an annual dose during their entire pregnancy of 1.0 mSv (0.1 rem) deep-dose equivalent

Internal exposure monitoring is required for

1. Adults likely to receive in 1 year in excess of 10% of the applicable annual limit on intake (ALI) for ingestion and inhalation. The ALI is the intake of a given radionuclide per year that results in a committed effective dose equivalent of 5 rem or a committed dose equivalent to an organ or tissue of 50 rem.
2. Minors and declared pregnant women likely to receive in 1 year a committed effective dose equivalent in excess of 1.0 mSv (0.1 rem).

Beyond these regulations, a person may be badged at any time for any reason if he or she is concerned about risk from radiation exposure during work involvement.

Whole-body badges, which monitor for deep-dose and shallow-dose equivalent exposure, must be worn on the body where they are likely to receive the highest exposure (10 CFR 20.1201c). Typically, this is the chest area or the waist.

Investigational Levels

During implementation of the radiation safety program, the RSO establishes personnel exposure investigational levels to help identify potential areas of excessive radiation

TABLE 5-4 Investigational Levels for Radiation Exposure Monitoring

Body Part	Investigational Level (mrem per monthly monitoring period)	
	Level 1	Level 2
Whole body: head, trunk, gonads, or eye lens	100	400
Extremities: elbow, arm below elbow, foot, knee, leg below knee, or skin	1000	3000
Conceptus	30	40

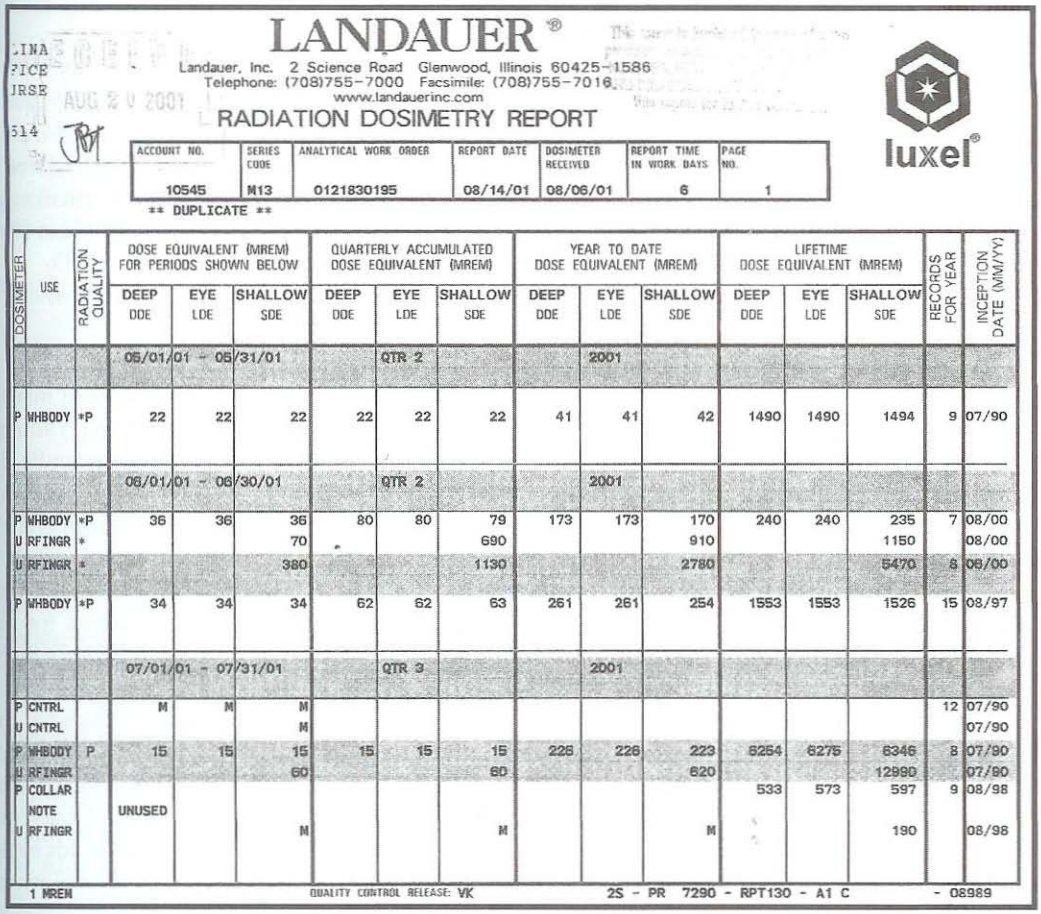

LANDAUER®

Landauer, Inc. 2 Science Road Glenwood, Illinois 60425-1586
Telephone: (708)755-7000 Facsimile: (708)755-7016
www.landauerinc.com

RADIATION DOSIMETRY REPORT

luxel®

ACCOUNT NO.	SERIES CODE	ANALYTICAL WORK ORDER	REPORT DATE	DOSIMETER RECEIVED	REPORT TIME IN WORK DAYS	PAGE NO.
10545	M13	0121830195	08/14/01	08/06/01	6	1

** DUPLICATE **

DOSIMETER	USE	RADIATION QUALITY	DOSE EQUIVALENT (MREM) FOR PERIODS SHOWN BELOW			QUARTERLY ACCUMULATED DOSE EQUIVALENT (MREM)			YEAR TO DATE DOSE EQUIVALENT (MREM)			LIFETIME DOSE EQUIVALENT (MREM)			RECORDS FOR YEAR	INCEPTION DATE (MM/YY)
			DEEP DDE	EYE LDE	SHALLOW SDE	DEEP DDE	EYE LDE	SHALLOW SDE	DEEP DDE	EYE LDE	SHALLOW SDE	DEEP DDE	EYE LDE	SHALLOW SDE		
			05/01/01 - 05/31/01				QTR 2			2001						
P	WHBODY	*P	22	22	22	22	22	22	41	41	42	1490	1490	1494	9	07/90
			06/01/01 - 06/30/01				QTR 2			2001						
P	WHBODY	*P	36	36	36	80	80	79	173	173	170	240	240	235	7	08/00
U	RFINGR	*			70			690			910			1150		08/00
U	RFINGR	*			380			1130			2780			5470	8	08/00
P	WHBODY	*P	34	34	34	62	62	63	261	261	254	1553	1553	1526	15	08/97
			07/01/01 - 07/31/01				QTR 3			2001						
P	CNTRL		M	M	M										12	07/90
U	CNTRL				M											07/90
P	WHBODY	P	15	15	15	15	15	15	226	226	223	6254	6275	6346	8	07/90
U	RFINGR				60			60			620			12990		07/90
P	COLLAR											533	573	597	9	08/98
	NOTE		UNUSED													
U	RFINGR				M			M			M			190		08/98

1 MREM QUALITY CONTROL RELEASE: VK 2S - PR 7290 - RPT130 - A1 C - 08989

FIGURE 5-4 Personnel radiation dosimetry report.

exposure and to initiate an investigation into the cause of an exposure. Investigational level 1 exposures are typically set well below (about one-fourth) the occupational exposure limits to identify exposure level trends in the work environment and to provide a level of control that keeps doses ALARA. Table 5-4 gives examples of investigational levels at an institution. If level 1 exposure is exceeded, the RSO may send the person a written report with a request to review radiation safety procedures to keep exposure ALARA. If level 2 exposure is exceeded, the RSO may conduct a direct investigation and an interview with personnel involved and prepare a written report with suggested corrective actions. Figure 5-4 illustrates a typical radiation dosimetry report for personnel exposures.

Film Badges and Thermoluminescent Dosimeters

Film Badges

Film badges consist of radiation-sensitive photographic film housed in a plastic holder that can be clipped to clothing. They are typically worn on the chest or waist areas for 1 month periods. The badge contains filters that selectively absorb radiation to permit identification of the radiation type and energy. For example, an area with no filter detects weak betas and gammas. The badge is sent to a laboratory that develops the film and reads the exposure. The greater the exposure, the darker is the film. It is compared with a standard known exposure to assess the person's exposure level. The typical sensitivity range for film badges is 30 to 1000 mrem.

Thermoluminescent Dosimeters

TLDs are small devices that contain calcium or lithium fluoride crystals. The crystals absorb energy released in them by ionizing radiation and the molecules achieve a metastable state. When heated under controlled conditions the crystals release their "stored" energy in the form of visible light, which is analyzed for exposure intensity. The sensitivity range is 10 mrem to 100 rem. TLDs are typically used in finger badges, but they are also used in some body badges. Figure 5-5 shows examples of a film badge and a TLD.

Bioassays

In accordance with 10 CFR 20.1502, a licensee is required to monitor occupational intake of radioactive material by and assess the committed effective dose equivalent to (1) adults who are likely to receive in 1 year greater than 10% of ALI in 10 CFR 20, Appendix B, Table 1, columns 1 and 2, and (2) minors and declared pregnant women likely to receive a committed effective dose equivalent in excess of 0.05 rem in 1 year. A recommended time of monitoring is within 24 hours of exposure.

A critical area of concern for nuclear medicine and nuclear pharmacy personnel is the handling of radioiodine. The performance of thyroid bioburden measurements for all occupationally exposed individuals involved in the preparation or administration of therapeutic dosages of ^{131}I (capsules and solutions) is addressed in 10 CFR 20.1204 and 20.1501. Each licensee must monitor (20.1204) the occupational intake of radioactive material by and assess the committed effective dose equivalent to adults likely to receive, in 1 year, an intake in excess of 10% of the applicable ALI(s) in 10 CFR 20.1001–20.2402, Appendix B, Table 1, columns 1 and 2. Additionally, Regulatory Guide 8.9 (Acceptable Concepts, Models, Equations and Assumptions for a Bioassay Program) provides guidance for evaluating a thyroid burden of radioiodine. The guide recommends an evaluation level when any thyroid measurement exceeds 2% of the ALI and an investigational level when it exceeds 10% of the ALI. The ALI values for a few radionuclides are given in Table 5-5.

FIGURE 5-5 Radiation monitoring devices: finger ring badge (left) and body badge (right).

TABLE 5-5 Annual Limits on Intake (ALI), Derived Air Concentrations (DAC), and Maximum Permissible Concentrations (MPC) for Selected Radionuclides, from 10 CFR 20, Appendix B

	Table 1 Occupational Values			Table 2 Effluent MPC		Table 3 Release to Sewers
	Oral Ingestion	Inhalation (Restricted Areas)		Unrestricted Areas		
Radionuclide	Column 1 ALI (μCi)	Column 1 ALI (μCi)	Column 2 DAC (μCi/mL)	Column 1 Air (μCi/mL)	Column 2 Water (μCi/mL)	Avg Conc/Month (μCi/mL)
^{123}I	3000	6000	3×10^{-6}	2×10^{-8}	1×10^{-4}	1×10^{-3}
^{125}I	40	60	3×10^{-8}	3×10^{-10}	2×10^{-6}	2×10^{-5}
^{131}I	30	50	2×10^{-8}	2×10^{-10}	1×10^{-6}	1×10^{-5}
^{133}Xe			1×10^{-4}	5×10^{-7}		

An example of how the evaluation procedure works follows, taken from Appendix A of NRC Regulatory Guide 8.9.

A technologist prepared a dose of ^{131}I-sodium iodide for thyroid therapy. A bioassay of the technologist's thyroid indicated a thyroid content of 0.08 μCi 24 hours after dosage preparation. Does this thyroid bioburden require further evaluation?

Determine if the thyroid intake of ^{131}I exceeds 2% of the ALI.

$$\text{Intake} = \frac{\text{A } \mu\text{Ci } (\text{thyroid content at time of measurement})}{\text{IRF for } ^{131}\text{I}}$$

$$= \frac{0.080 \ \mu\text{Ci}}{0.133} = 0.60 \ \mu\text{Ci}$$

The intake retention fraction (IRF) for ^{131}I after 24 hours is 0.133 (from the table of IRF thyroid values in NUREG/CR 4884, Interpretation of Bioassay Measurements). The evaluation level for ^{131}I is 2% (1 μCi) of the ALI (50 μCi). Since the intake for this technologist (0.6 μCi) does not exceed this level, no further evaluation is needed. If a person's thyroid content is greater than 0.133 μCi, the intake value is greater than 1 μCi, and the RSO is required to evaluate the situation by, for example, repeating measurements to verify the results. If a person's thyroid uptake exceeds 0.665 μCi, the intake value exceeds 10% of 50 μCi ALI, and the RSO needs to conduct a more thorough investigation (level 2) with multiple measurements, air sampling, and so on. A thyroid content of 6.65 μCi reaches the ALI, and the person should be excluded from further exposure to radioiodine for the year. Preferably, the person should be removed from radioiodine exposure before the ALI is reached.

Pregnant Radiation Workers

A licensee must develop a pregnancy policy to ensure that the dose equivalent to the embryo or fetus during the entire pregnancy of a declared pregnant radiation worker does not exceed 0.5 rem (10 CFR 20.1208). NCRP 91 (1987) also recommends a total dose limit of 0.5 rem and no more than 0.05 rem in any month once a pregnancy becomes known. The policy should require a woman to voluntarily declare her pregnancy in writing and include the estimated date of conception (10 CFR 20.1003). The records may be maintained in a separate file for privacy (10 CFR 20.2106e). Without this declaration, the licensee

cannot be held responsible for the radiation safety of the fetus. If the dose equivalent to the embryo or fetus is found to have exceeded the 0.5 rem limit, or to be within 0.05 rem of this dose by the time of declaration, the licensee must take measures to ensure that any additional dose does not exceed 0.05 rem for the remainder of the pregnancy.

AREA MONITORING

Surveys

In accordance with the new 10 CFR 35.70 (July 10, 2003), at the end of each day of use a licensee must survey with a radiation detection instrument all areas where unsealed byproduct material requiring a written directive was prepared for use or administered. Records of the survey must be kept for 3 years. This requirement is less descriptive than the previous Part 35 regulation. Therefore, the older regulations are described here because they delineate the types of surveys and exposure level or surface contamination limits that are practical and likely to be followed at most facilities.

1. The licensee must survey for ambient radiation levels at the end of each day of use all areas where radiopharmaceuticals are routinely prepared and administered and at the end of each week all areas where radiopharmaceuticals and radiopharmaceutical waste are stored. The licensee must conduct these surveys with an instrument capable of detecting 0.1 mR hour. The licensee must establish dose rate trigger levels for each area surveyed and notify the RSO if trigger levels are exceeded.
2. The licensee must survey for removable contamination (wipe test) each week areas where radiopharmaceuticals are prepared for use, administered, and stored. The wipe test detection method must be capable of detecting 2000 disintegrations per minute (dpm). The licensee must establish removable contamination trigger levels for each area surveyed and notify the RSO if trigger levels are exceeded.
3. The licensee must retain records of these surveys for 3 years, to include the following information: (1) date of survey and plan of the area surveyed, (2) trigger levels established for each area, (3) results of the surveys obtained, reported in mR/hour or dpm per 100 cm^2, and (4) the instruments used and initials of the person who conducted the surveys.

An example of survey trigger levels established at an educational institution for monitoring ambient and removable contamination is shown in Table 5-6.

TABLE 5-6 Trigger Levels for Workplace Surveys for Ambient and Removable Contamination

Unrestricted Areas		Restricted Areas	
Radiation Exposure	**Surface Contamination**	**Radiation Exposure**	**Surface Contamination**
Not >2 mR/hr Not >100 mrem/ 5 consecutive days Not >500 mrem in any 1 year	Not >200 dpm/100 cm^2	Not >2 mR/hr in frequently occupied areas	Not >0.1 mrem at 5 cm from surface of interest Not >600 dpm per 100 cm^2

Effluent Monitoring

In accordance with regulations stated in 10 CFR 20.1301, a licensee's operation must be conducted so that (1) the total effective dose equivalent to the public does not exceed 0.1 rem per year, and (2) the dose rate from an external source to an unrestricted area does not exceed 2 mrem in any 1 hour. Concerning compliance with these limits, 10 CFR 20.1302 states that the licensee must make measurements or calculations to demonstrate that the total effective dose equivalent to any member of the public does not exceed 0.1 rem per year or that (1) the average concentrations of radioactive material released in gaseous or liquid effluents to an unrestricted area do not exceed the values in 10 CFR 20, Appendix B, Table 2, and (2) if an individual is continuously present, the dose from external sources does not exceed 2 mrem in any 1 hour and 0.05 rem in a year.

An example of demonstrating compliance with these regulations is a calculation used to determine that the effluent concentration of ^{133}Xe gas exhausted to the outside of a facility does not exceed the maximum permissible concentration (MPC) of ^{133}Xe in the air exhausted, as follows.

A nuclear medicine facility conducts lung ventilation studies with ^{133}Xe gas. On average, 10 doses of 20 mCi each are administered per week. Determine if the expected levels of ^{133}Xe released outside the facility exceed the MPC to an unrestricted area given in 10 CFR 20, Appendix B, Table 2.

The room exhaust rate is 1714 ft^3/minute $\times$ 2.83 $\times$ 10^4 mL/ft^3 = 4.85 $\times$ 10^7 mL/minute. Assume 20% spillage of ^{133}Xe. The MPC of ^{133}Xe to an unrestricted area is 5×10^{-7} µCi/mL (see Table 5-5).

$$^{133}\text{Xe } \mu\text{Ci/mL exhausted/wk} = \frac{20{,}000 \ \mu\text{Ci/dose} \times 10 \ \text{doses/wk} \times 0.20}{4.85 \times 10^7 \ \text{mL/min} \times 10{,}080 \ \text{min/wk}}$$

$$= 8.09 \times 10^{-8} \ \mu\text{Ci/mL} \ (16\% \text{ of DAC})$$

Regulatory Guide 8.37 (ALARA Levels for Effluents) recommends aiming for only 20% of derived air concentration (DAC) in effluents as a conservative limit for radioactive material release.

DAC is the concentration of radionuclide breathed for 2000 working hours per year that results in an intake of 1 ALI; 1 DAC = ALI/2.4 $\times$ 10^9 mL. Note: 2.4 $\times$ 10^9 mL = (2000 hours) $\times$ (60 minutes/hour) $\times$ (2 $\times$ 10^4 mL/minute). The following determination must consider the DAC used in occupational exposure:

What is the evacuation time for a radiation worker in the imaging room if a 20 mCi (740 MBq) dose of ^{133}Xe is spilled in the room (restricted area)?

Regulatory Guide 10.8 (Guide for Preparation of Applications for Medical Use) states in Appendix 0.4 a model procedure for calculating spilled gas clearance times (t), where

A = highest activity of gas in a single container, in microcuries
= 20,000 µCi
V = volume of room, in milliliters
= (5628 ft^3) $\times$ (2.83 $\times$ 10^4 mL/ft^3) = 1.59 $\times$ 10^8 mL
Q = exhaust rate, in mL/minute
= (1714 ft^3/minute) $\times$ (2.83 $\times$ 10^4 mL/ft^3) = 4.85 $\times$ 10^7 mL/minute
C = DAC ^{133}Xe restricted area = 1 $\times$ 10^{-4} µCi/mL (Table 5-5)

$$t(\text{clearance time}) = -\frac{V}{Q} \times \ln\left(C \times \frac{V}{A}\right)$$

$$= -\frac{1.59 \times 10^8 \text{ mL}}{4.85 \times 10^7 \text{ mL/min}} \times \ln\left(1 \times 10^{-4} \text{ μCi/mL} \frac{1.59 \times 10^8 \text{ mL}}{20{,}000 \text{ μCi}}\right)$$

$$= 0.75 \text{ min}$$

Note that this is the time until the concentration reaches the DAC for ^{133}Xe in a restricted area, and workers must leave the room during this period.

In a comprehensive radiation safety program, dose equivalents are assessed from surveys or other measuring devices to ensure compliance. DAC and ALI values from 10 CFR 20, Appendix B, Table 1 can be used to demonstrate compliance. This is particularly useful for volatile nuclides such as radioiodines and radioxenons. A partial list of radionuclides given in 10 CFR 20, Appendix B, is shown in Table 5-5.

Sealed Source Monitoring

A licensee must wipe test a sealed source every 6 months to ensure that not more than 0.005 μCi (185 Bq) of removable contamination is present (10 CFR 35.67 and 35.2067). This procedure does not apply to sources with half-lives of less than 30 days, gases, and 100 μCi (3.7 MBq) or less of beta- or gamma-emitting radionuclides. Typical sources that apply in nuclear pharmacy would be reference standards, such as ^{137}Cs, ^{133}Ba, and ^{57}Co, used to check the dose calibrator. Records of the leak test must be retained for 3 years.

CAUTION SIGNS

Signs are used to warn individuals that radiation is present in a container, work area, or room. In general, all signs and labels bear the radiation symbol shown in Figure 5-6. Caution signs for various doses of radiation, as listed in 10 CFR 20.1902, are as follows:

- Caution, Radiation Area: >5 mrem in 1 hour at 30 cm
- Caution, High Radiation Area: >100 mrem in 1 hour at 30 cm
- Grave Danger, Very High Radiation Area: >500 rad in 1 hour at 1 m

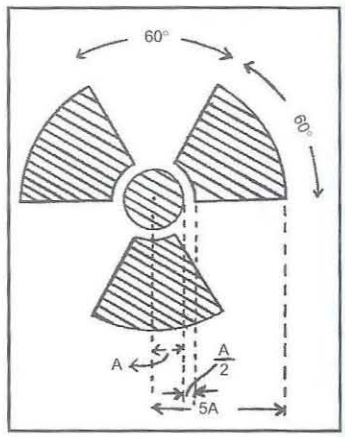

FIGURE 5-6 Standard radiation symbol. The cross-hatched area is magenta or purple; the background is yellow. (Reprinted from 10 CFR 20.1901.)

Because of the types and amounts of radioactive material used and stored in nuclear medicine and nuclear pharmacy laboratories, these areas are likely to require no more than the Caution, Radiation Area sign.

NOTICES, INSTRUCTIONS, AND REPORTS TO RADIATION WORKERS

The regulations in 10 CFR 19 list the requirements for information transfer by the licensee to workers who participate in radiation-associated activities, as well as the rights of workers during NRC or agreement state inspections.

Posting Requirements (10 CFR 19.11)

1. Each licensee must post the following documents or a notice stating where they may be examined:
   a. Current copies of the regulations in 10 CFR 19 and 20.
   b. The radioactive materials license.
   c. The operating procedures applicable to licensed activities.
2. A licensee must post, for 5 days or until the violation is corrected, any notice of violation involving working conditions within 2 days of receipt of the violation notice.
3. A licensee must post NRC Form 3, "Notice to Employees," in a sufficient number of places to be observed by workers.

Instruction to Workers (10 CFR 19.12)

Any person likely to receive an occupational dose higher than 100 mrem per year must be

1. Informed of storage, transfer, or use of radioactive material.
2. Instructed in radiation safety procedures.
3. Instructed to report any violations to the licensee.
4. Instructed on how to respond to warnings in case of radiation exposure occurrences.
5. Instructed about requesting radiation exposure reports.

Notification and Reports to Individuals (10 CFR 19.13)

A licensee must provide each worker with the following reports:

1. A written report of radiation exposure data, analyses, and calculations of an individual's exposure.
2. An annual report of a worker's radiation dose.
3. A radiation exposure record upon a former worker's request.
4. A report of any radiation exposure incident report sent to NRC.
5. A radiation exposure report upon termination of employment.

Presence of Individuals during Inspections (10 CFR 19.14)

A licensee must comply with the following conditions of inspection:

1. A licensee must allow NRC to inspect facilities annually.
2. A licensee must notify NRC of any individual authorized to represent workers at inspection.

3. The workers' representative must be actively engaged in radiation work.
4. A consultant may accompany the inspection.

Consultation with Workers during Inspection (10 CFR 19.15)

The following conditions must prevail during inspections:

1. NRC may consult with workers privately.
2. Workers may bring any perceived violations of regulations, overexposures, and so on to NRC's attention.

Request for Inspections (10 CFR 19.16)

The following conditions must prevail regarding requests for inspection:

1. Any worker may submit a written request to the NRC regional office to inspect a licensee regarding any perceived violation. The complainant may request anonymity,
2. NRC will determine if inspection is warranted.

RECEIPT OF RADIOACTIVE MATERIAL

Regulations describing the procedures and monitoring limits for receiving and opening packages of radioactive material are found in 10 CFR 20.1906, 10 CFR 71.87 and 71.47, and 49 CFR 172 and 173. The regulations for some agreement states may differ and may be more stringent than NRC regulations. Part 20 requires a survey only for packages containing greater than Type A quantities (which are typically >10 Ci), but all packages bearing White-I, Yellow-II, or Yellow-III labels must be wipe tested for surface contamination (see Warning Labels section). Table 5-7 summarizes the package receipt requirements for NRC. The GM survey for external radiation levels is made at the package surface and at 1 m distance. The 1 m survey is the transport index. Wipe testing of the external surface is typically made with a 1 inch filter paper disk rubbed over at least 300 cm^2 of multiple surfaces. The disk is counted, corrected for counter efficiency to convert counts per minute (cpm) to dpm, and the results reported as dpm per 100 cm^2. Monitoring of packages must be performed as soon as practicable but not later than 3 hours after receipt. If measured levels exceed the limits stated in Table 5-7, the licensee must immediately notify (1) the final delivery carrier and (2) the NRC operations center by telephone.

TABLE 5-7 Nuclear Regulatory Commission Monitoring Requirements for Radioactive Material Packages upon Receipt

Limit Type	Qualifications	Requirements
External radiation limits (Geiger-Müller survey)	Only radioactive materials with Radioactive White-I, Yellow-II, or Yellow-III label containing > Type A quantities or if crushed, wet, or damaged. Most radionuclide Type A quantities are >10 Ci (see Table 5-8)	Package surface levels (not >200 mR/hr) Transport index (not >10 mR/hr at 1 m)
Surface contamination limits (wipe test)	All packages with Radioactive White-I, Yellow-II, or Yellow-III label except if a gas or special form. All nuclear medicine radioactive materials are normal form	Averaged over 300 cm^2 must be not greater than 2200 dpm (0.001 μCi) per 100 cm^2 of package surface

Each licensee must establish and maintain written procedures for safely opening radioactive material packages, ensure that they are followed, and give any special instructions for the type of package being opened. In addition to the monitoring requirements, the package-opening procedures should include the following good practice guides listed in NUREG 1556:

1. Open the outer package and remove the packing slip; open the inner package to verify contents, comparing requisition, packing slip, and label on the container.
2. Check integrity of container, inspecting for breaks in seals, loss of liquid, and high count rates on wipes.
3. Survey packing material and packages for contamination before discarding, treating any contaminated materials as radioactive waste.
4. Obliterate any radiation labels prior to discard of materials.
5. Maintain records of receipt, survey, and wipe tests for 3 years.

SHIPMENT OF RADIOACTIVE MATERIAL

For the most part the regulations in this section apply to pharmaceutical manufacturers and nuclear pharmacies that ship radiopharmaceuticals to hospitals and clinics. Requirements for packaging and transportation of radioactive material are described in DOT regulations (49 CFR) and in an NRC-adapted version (10 CFR 71) and are summarized in a DOT publication.[12] Specifically, 10 CFR 71.5 states that "each licensee who transports licensed material outside the confines of its plant or other place of use, or who delivers licensed material to a carrier for transport, must comply with the applicable requirements of the regulations appropriate to the mode of transport of DOT in 49 CFR 170 through 189." The parts that particularly relate to packaging and shipment of radioactive materials are

1. Packaging: 49 CFR 173: subparts A, B, and I, and 173.400 through 173.476
2. Marking and labeling: 49 CFR 172: subpart D, 172.400 through 172.407, 172.436 through 172.440, and subpart E
3. Placarding: 49 CFR 172: subpart F, 172.500 through 172.519, 172.556, and Appendices B and C
4. Accident reporting: 49 CFR 171.15 and 171.16
5. Shipping papers and emergency information: 49 CFR 172: subparts C and G
6. Hazardous material employee training: 49 CFR 172: subpart H
7. Hazardous material shipper/carrier registration: 49 CFR 107: subpart G

DOT requirements do not apply when radiopharmaceuticals are being transported by a physician for his or her medical practice, as outlined in 10 CFR 71.9, but the physician must be licensed according to 10 CFR 35.

For purposes of transportation, radioactive materials are defined as those materials that spontaneously emit ionizing radiation and have a specific activity in excess of 0.002 μCi/gram (74 Bq/gram) of material. All materials are radioactive to some degree. The demarcation of 0.002 μCi/gram (74 Bq/gram) allows a distinction between materials not normally considered radioactive and those that are regulated as radioactive in transportation.

Packaging Requirements

Packaging requirements for radioactive material are determined by the form, type, and quantity being shipped. The two forms of radionuclide are special form and normal form. Special form radioactive material is material that may present a direct radiation hazard if

released from the package but causes little hazard resulting from contamination because it is in a nondispersible solid form or sealed in a durable capsule. Special form materials are much less likely to spread contamination in the event of package failure. The regulations therefore generally allow substantially larger quantities of special form materials than of normal form materials to be placed in a given package. Normal form radioactive materials may be solid, liquid, or gaseous and include any material that has not been qualified as special form. Radiopharmaceuticals are normal form materials.

The principal types of package used to ship radioactive material are Type A, Type B, and "excepted" packages. The criteria for testing the integrity of Type A packages are found in 49 CFR 173.465 and those for excepted packages in 49 CFR 173.410. Packaging normally used by nuclear pharmacies is military ammunition boxes. Radiopharmaceutical manufacturers typically ship in cardboard or fiberboard boxes. Shippers are not required to personally test the package, only to ensure that the testing was performed before use.

The quantity of particular radionuclides that can be shipped in a Type A package is listed in Table 5-8. Every radionuclide is assigned an A_1 and an A_2 value. These values are simply the maximum activity (in curies) of that radionuclide that may be shipped in a Type A package. The A_1 values are for special form and A_2 values for normal form radionuclides. Quantities exceeding Type A package limits require Type B packages. Radiopharmaceuticals are shipped in Type A packages and excepted packages. The activity limits for these packages are shown in Table 5-8.

TABLE 5-8 Type A Package Activity Limits for Radionuclides in Nuclear Medicine

	Package Activity Limits		
Radionuclide	A_1 (Special Form)[a] (curies)	A_2 (Normal Form)[a] (curies)	Excepted Quantity Package Limits[b] (millicuries)
^{11}C	27	13.5	1.35
^{57}Co	216	216	21.6
^{58}Co	27	27	2.7
^{51}Cr	811	811	81.1
^{137}Cs	54.1	13.5	1.35
^{18}F	27	13.5	1.35
^{67}Ga	162	162	16.2
^{123}I	162	162	16.2
^{125}I	541	54.1	5.41
^{131}I	81.1	13.5	1.35
^{111}In	45.1	54.1	5.41
^{99}Mo	16.2	13.5	1.35
^{13}N	16.5	13.5	1.35
^{32}P	8.11	8.11	0.811
^{186}Re	108	13.5	1.35
^{188}Re	5.41	5.41	0.541
^{81}Rb	54.1	24.3	2.43
^{153}Sm	108	13.5	1.35
^{89}Sr	16.5	13.5	1.35
^{99m}Tc	216	216	21.6
^{99}Tc	1080	24.3	2.43
^{201}Tl	270	270	27
^{117m}Sn	162	54.1	5.41
^{133}Xe	541	541	541
^{90}Y	5.41	5.41	0.541

[a] From 49 CFR 173.425

[b] From 49 CFR 173.435 (liquids = $A_2 \times 10^{-4}$; gases = $A_2 \times 10^{-3}$)

An excepted package is usually one used for returned waste, such as used patient syringes. Certain quantities of radioactive material are excepted from some of the DOT requirements that apply to Type A packages. These exceptions include not having to provide specification packaging, shipping papers, certification, marking, or labeling. There are a number of conditions, however, that must be met, outlined in 49 CFR 173.421 as follows:

1. Package may not exceed excepted quantity package limits (see Table 5-8).
2. Material must be packed in strong, tight packages that will not leak any radioactive material during normal transport conditions.
3. External radiation at any point on the external surface cannot exceed 0.5 mR/hour.
4. Removable external contamination cannot exceed 22 dpm/cm^2.
5. The outside of the inner packaging, or if there is no inner packaging the outside of the packaging itself, bears the marking "Radioactive."
6. A description of the contents must be on a document that is in or on the package or forwarded with it. The document must include the name of the consignee or consignor and the statement, "This package conforms to the conditions and limitations specified in 49 CFR 173.421 for excepted radioactive material, limited quantity, N.O.S., UN 2910."

Marking and Labeling

Transport Index

The transport index (TI) is the highest dose rate at 1 m from any accessible exterior surface of the package of radioactive material. The TI limits are listed in Table 5-9. All TI values are rounded to the nearest tenth, and no package offered for transport may have a TI greater than 10. The total of all packages in any single transport vehicle or storage location may not exceed 50. The TI system provides control over radiation exposure of personnel handling packages and of casually exposed persons in the immediate vicinity, as well as the exposure of fast photographic film in close proximity to radioactive material.

Warning Labels

Each package of radioactive material, unless excepted, must be labeled on two opposite sides with a distinctive warning label (Figure 5-7). Each of the three label types bears the unique trefoil symbol recommended by NCRP. The labels alert persons that the package contains radioactive materials and that the package may require special handling. A label with an all-white background (White-I) indicates that the external radiation level is low and no special handling is required. If the upper half of the label is yellow (Yellow-II and Yellow-III), it signifies higher radiation levels and the need for more precautions. Radiation level limits for these labels are given in Table 5-9.

TABLE 5-9 Labeling, Transport Index, and Radiation Limits for Radioactive Packages

	Limits of Radiation Exposure from Package	
Label Required	**Transport Index**	**At Package Surface**
White-I	Not applicable	≤0.5 mR/hr
Yellow-II	<1.0 mR/hr	>0.5 mR/hr and ≤50 mR/hr
Yellow-III	>1.0 mR/hr	>50 mR/hr

FIGURE 5-7 U.S. Department of Transportation (DOT) labels for radioactive material packages. The I, II, or III referring to level of radiation emanating from the package is in red. Each label is diamond shaped, 4 inches on each side, and has a black solid-line border one-fourth inch from the edge. The background color of the upper half is white for the I label and yellow for the II and III labels. The 7 is the DOT hazardous material classification number for radioactive material.

FIGURE 5-8 Radioactive placard for transport vehicles if any radioactive material package on board bears a radioactive Yellow-III label. The background color of the black trefoil in the upper half of this 12 × 12 inch placard is yellow.

The following items must be entered in the blank spaces on the warning label:

1. Contents: The name of the radionuclide or its symbol (e.g., molybdenum 99 or ^{99}Mo)
2. Activity: The activity contained in the package, expressed in curies, millicuries, microcuries, or their abbreviations (Ci, mCi, or μCi), or becquerels (Bq)
3. Transport index: The value measured with a calibrated survey meter at 1 m from the external surface, rounded up to the nearest tenth (not required for White-I labels)

Most packages shipped from nuclear pharmacies are either White-I or Yellow-II. Yellow-III is rarely required but typically is found on ^{99m}Tc generators and ^{131}I-sodium iodide therapy packages.

Placarding

The shipper of radioactive material packages, by rail or highway, must apply a "radioactive" placard (Figure 5-8) to the transport vehicle if any package on board bears a radioactive Yellow-III label. The placard must appear on four sides of the transport vehicle. Placarding is usually not of concern for nuclear pharmacies because they rarely offer Yellow-III packages for transport.

Monitoring

Any package of radioactive material offered for transportation must be wipe tested for removable contamination on its external surface in accordance with 49 CFR 174.443. The

wipe must occur over at least 300 cm^2 of surface and not exceed a level of 2200 dpm per 100 cm^2. Common sites for radioactive contamination on nuclear pharmacy shipping containers are the handles and closure clasps on ammunition boxes.

Other Package Requirements

A package in excess of 110 pounds must have its gross weight marked on the outside of the package; the words Type A or Type B when appropriate must be lettered (½ inch high) on the outside of the package; and exported packages must be marked "U.S.A." The proper shipping name for most radiopharmaceuticals is "Radioactive Material, N.O.S., UN 2982." Other shipments, involving primarily small quantities of radioactive material, and especially return shipments by nuclear pharmacy clients, are labeled as excepted packages of limited quantity, as previously noted. Requirements for excepted shipments are found in 49 CFR 173.421 and 173.422. A package containing more than the reportable quantity (RQ) listed in the Hazardous Materials Table in 49 CFR 172.101 must have the letters RQ noted on the package and shipping papers. Most radionuclides in nuclear pharmacy shipments are less than the hazardous materials limit; however, ^{131}I has a limit of 10 mCi and "RQ" must appear on the package markings and shipping papers (e.g., RQ Radioactive Material, N.O.S., UN 2982).

If a package contains liquid radioactive material, it must be packed with enough absorbent material to absorb at least twice the volume of liquid. Additionally, the outside of each package must contain a security seal that is not readily breakable and that will give evidence that the package has not been illicitly opened.

Shipping Papers

Shipping papers must be included with transported radioactive material as described in 49 CFR 173.200 through 173.204. Items included are

- Proper shipping name (e.g, Radioactive Materials, N.O.S.)
- Hazard class: For radiopharmaceuticals, the hazard class is 7
- ID number: For the shipping name "Radioactive Material, N.O.S.," the ID number is UN 2982
- Package type: This is typically Type A
- Name or abbreviation of each radionuclide in the shipment
- Physical and chemical form of the radioactive material
- Category of label applied to each package (e.g., White-1, Yellow-II)
- TI of each package
- Emergency response telephone number
- Shipper's certification and signature

An excepted quantity package needs no shipping papers, but the verbatim statement noted earlier under excepted packages (49 CFR 173.422) must be included on or in the package.

Accident Reporting

According to 49 CFR 171.15 and 171.16, the carrier of radioactive material must ensure that DOT and the shipper are notified in the event of fire, breakage, spillage, or suspected radioactive contamination involving the shipment. Carriers must also ensure that vehicles, areas, or equipment in which radioactive material may have spilled are not placed in

service again until surveyed and decontaminated. An emergency response telephone number must be included in the shipping papers and the number monitored at all times that the material is being transported by a person knowledgeable of the hazardous material being shipped. Emergency response information must be included with the shipping papers.

Training

Subpart H of DOT regulations, 49 CFR 172.700, 172.702, and 172.704, describes the purpose and scope, applicability, and responsibility for training of employees involved in the transport of radioactive material. The training must include

1. Familiarization with DOT requirements and ability to identify hazardous materials
2. Training for each specific function the employee performs
3. Safety training concerning emergency response information, including measures to protect the employee, and methods to avoid accidents, such as proper procedures for handling packages containing radioactive material

Quality Control Measures

The following are important measures the shipper must attend to before and during a shipment of radioactive material.

1. Ensure that the package is proper for the contents.
2. Determine that the package is in good physical condition.
3. Check that the external radiation and contamination levels are within allowable limits.
4. Conduct vehicle inspections for proper operation.
5. Review requirements pertaining to vehicle attendance and incident reporting.
6. Establish a procedure for loading and unloading radioactive material, including securing packages by blocking or bracing so that packages will not move during transport.
7. Maintain shipping papers within accessible reach while driving.

Summary of Radioactive Material Shipment

Packages that contain less than the limited quantities for excepted packages shown Table 5-8 and that have less than 0.5 mR/hour at the surface with no significant exter contamination may be shipped in an excepted package. The container must be capabl preventing leakage during normal shipment. No outer label is required, but the ir container must be labeled "Radioactive."

Packages that contain more than a limited quantity or no more than the A_2 quar must be shipped in a Type A package. A surface wipe test must be performed and package surveyed at the surface and at 1 m to determine the TI. The package shou labeled with two warning labels (White-I, Yellow-II, or Yellow-III), one each on opp sides of the package. The labels must contain the name or symbol of the radionuclic activity, and the TI. The package must contain the marking "Radioactive, N.O.S 2982." It must have a security seal and be accompanied by shipping papers.

Empty, reusable packages such as those used to deliver radiopharmaceutical doses must be surveyed inside and out before they are returned to the shipper and should have any external "Radioactive" signs removed if no activity is present.

DISPOSAL OF RADIOACTIVE WASTE

The following methods are acceptable for the disposal of radioactive waste according to 10 CFR 20.2001: (1) transfer to an authorized recipient, (2) decay in storage, (3) effluent release, (4) release to sanitary sewer, (5) incineration, and (6) burial in the soil. Of these, the first four methods are the most practical for nuclear medicine and nuclear pharmacy practice.

Transfer to an Authorized Recipient

Radioactive material may be transferred to an authorized commercial radiation waste dump, but this is very costly and is rarely, if ever, used for nuclear medicine waste because of the relatively short half-lives of the material. Transfer of waste applies mostly in situations in which a hospital participates in a return shipment program with a radiopharmaceutical manufacturer that reuses the lead shielding material. A typical example is the ^{99m}Tc generator return program. Another example is a nuclear medicine lab returning used syringes to the nuclear pharmacy that supplied the patient doses. Of course, DOT regulations for shipment must be followed if radioactive material is returned.

Decay in Storage

Since most radionuclides used in nuclear medicine have short half-lives, a licensee may allow a radioactive material with a physical half-life of less than 120 days to decay in storage before disposal (10 CFR 35.92). If this option is chosen, the licensee must survey the vial to confirm background levels of radioactivity and obliterate all radiation labels before discarding into ordinary trash. This method is particularly suitable if sufficient storage space for waste is available.

Effluent Release

This method applies to the release to an unrestricted area of volatile radionuclide waste such as ^{131}I and ^{133}Xe. The requirements under 10 CFR 20.1301 must be followed. See the previous section on Effluent Monitoring.

Release to Sanitary Sewer

In accordance with 10 CFR 20.2003, the following conditions must be met in order to dispose of radioactive waste to a sanitary sewer: (1) The radioactive material must be readily soluble or dispersible in water, (2) the monthly release must not exceed the concentration listed in 10 CFR 20, Appendix B, Table 3, and (3) the total quantity released in a year cannot exceed 5 Ci of ^{3}H, 1 Ci of ^{14}C, and 1 Ci of all other radioactive material combined. All radioactive excreta are exempt from this regulation.

Example: How much ^{131}I can be disposed of in the sewer each month from a 200 bed hospital?

The monthly limit for ^{131}I in 10 CFR 20, Appendix B, Table 3 is 1×10^{-5} μCi/mL (see Table 5-6). Sewer release, based on 10^{6} mL/bed/day),[13] is (1×10^{6} mL/bed/day) (30 days/

TABLE 5-10 Radionuclide Activities above Which Major Spill Procedure Is Used

Radionuclide	Millicuries	Radionuclide	Millicuries
^{32}P	10	^{111}In	10
^{51}Cr	100	^{123}I	10
^{57}Co	100	^{125}I	1
^{67}Ga	100	^{131}I	1
^{99m}Tc	100	^{201}Tl	100

Source: Regulatory Guide 10.8.

month) (200 beds) = 6×10^9 mL/month. So the allowed release is 1×10^{-5} μCi/mL × 6×10^9 mL/month = 60,000 μCi (2220 MBq)/month.

Incineration and Burial in Soil

Each of these methods requires a special license and is not generally applicable to nuclear medicine or nuclear pharmacy.

RADIATION EMERGENCY PROCEDURES

The most common radiation emergency in nuclear medicine or nuclear pharmacy is accidental spill of radioactive material. Spills may be minor or major depending on the amount of activity released. The general guide to follow in the event of any spill is confinement and shielding of the spilled activity to protect personnel from exposure. NRC Regulatory Guide 10.8 provides a model spill procedure in Appendix J and lists items that can be used to assemble a spill kit.

The decision to implement a major spill procedure instead of a minor spill procedure depends on several variables, including the number of individuals affected, the radiation energy and exposure rate, the likelihood of spread of contamination, and the radiotoxicity of the spilled material. For some short-lived radionuclides the best spill procedure is to simply restrict access to the area until complete decay occurs. Shielding spilled material that has a low gamma energy, such as ^{99m}Tc, is an effective way to limit exposure of workers. In any event the RSO should be consulted. Regulatory Guide 10.8 lists several radionuclides and the amounts above which a major spill procedure should be instituted; these are reproduced in Table 5-10. These amounts can be used as a guide for developing any laboratory spill procedure guidelines. The model procedures for minor and major spills recommended by Regulatory Guide 10.8 are as follows.

Minor Spill Procedure (Liquids and Solids)

1. Notify persons in the area that a spill has occurred.
2. Prevent spread by covering with absorbent material.
3. Clean spill using disposable gloves and absorbent paper, placing material into a plastic bag.
4. Survey area with a survey meter, also checking hands, clothing, and shoes for contamination. Shield nonremovable contamination.
5. Report the incident to the RSO.
6. The RSO will follow up and complete the necessary reports.

Major Spill Procedure (Liquids and Solids)

1. Clear the area. Notify all persons not involved in the spill to vacate the room.
2. Prevent spread by covering with absorbent material, but do not attempt to clean up the spilled material. Limit the movement of any personnel who may be contaminated.
3. Shield the source if possible.
4. Close the room and lock or secure the area to prevent entry.
5. Notify the RSO immediately.
6. Decontaminate personnel by removing contaminated clothing, flushing contaminated skin with water, and washing with mild soap.
7. The RSO will supervise cleanup of the spill and completion of necessary reports.

REFERENCES

1. United Nations Scientific Committee on the Effects of Atomic Radiation. *Sources and Effects of Ionizing Radiation*. Vol I: Sources and Vol II: Effects. UNSCEAR 2000 Report to the General Assembly. New York: United Nations; 2000.
2. National Academy of Sciences. *Health Effects of Exposure to Low Levels of Ionizing Radiation*. BEIR V Report. Washington, DC: National Academy Press; 1990.
3. International Commission of Radiological Protection. *1990 Recommendations of the International Commission of Radiological Protection*. ICRP Publication 60. New York: Pergamon Press; 1991.
4. National Council on Radiation Protection and Measurements. *Limitation of Exposure to Ionizing Radiation*. NCRP Report No. 116. Bethesda, MD: National Council on Radiation Protection and Measurements; 1993.
5. US Nuclear Regulatory Commission. *Consolidated Guidance about Materials Licenses: Program-Specific Guidance about Commercial Radiopharmacy Licenses*. NUREG-1556, vol 13. Washington, DC: US Nuclear Regulatory Commission; 1999.
6. National Council on Radiation Protection and Measurements. *Ionizing Radiation Exposure of the Population of the United States*. NCRP Report No. 93. Bethesda, MD: National Council on Radiation Protection and Measurements; 1987.
7. National Council on Radiation Protection and Measurements. *Sources and Magnitude of Occupational and Public Exposures from Nuclear Medicine Procedures*. NCRP Report No. 124. Bethesda, MD: National Council on Radiation Protection and Measurements; 1996.
8. Anderson DW, Richter CW, Ficken VJ, et al. Use of TLD for measurement of dose to the hands of nuclear medicine technicians. *J Nucl Med* 1972;13:627-9.
9. Henson PW. Radiation dose to the skin in contact with unshielded syringes containing radioactive substances. *Br J Radiol* 1973;46:972-6.
10. Kereiakes JG. *Biophysical Aspects: Medical Uses of Technetium-99m*. American Association of Physicists in Medicine Topical Review Series. New York: American Institute of Physics Inc; 1992.
11. Benedetto AR, Dziuk TW, Nusynowitz ML. Population exposure from nuclear medicine procedures: measurement data. *Health Phys*. 1989;57:725-31.
12. US Department of Transportation. *A Review of the Department of Transportation (DOT) Regulations of Transportation of Radioactive Materials*. Washington, DC: US Department of Transportation; 1983.
13. *A Manual of Radioactivity Procedures*. Handbook 80. Washington, DC: US Department of Commerce, National Bureau of Standards; 1961: 133.

6 Radiation Biology

Scientists learned in their earliest experiments with ionizing radiation that it had the capacity to produce biologic effects. A radium source that Henri Becquerel carried in his vest pocket produced skin erythema. Pierre Curie's exposure of his hand to radium caused an ulcer that was slow to heal. We now know that electromagnetic and particulate radiation interacts with matter to produce excitation and ionization of atoms, and during such interactions part or all of the radiation's energy is released and deposited within the volume of interaction. This fact has been put to good use in tailoring radiation treatment regimens for patients with cancer.

Biologic tissue is composed of various substances held together by chemical bonds, principally those between carbon, hydrogen, oxygen, and nitrogen. The average energy dissipated per ionizing event is about 34 eV, more than enough to break a covalent bond. Scientists studying the interactions of ionizing radiation with biologic material have discovered that the energy deposited can produce a variety of effects on cells and tissue. Tissues vary in their radiosensitivity to radiation, some tissues being more resistant than others. Survival studies after irradiation of cells at low doses have demonstrated that cells have the ability to repair damage from radiation, but that cells can be killed by radiation if the dose is large enough. These findings come from experimental work carried out in scientific laboratories by radiobiologists and in hospitals by radiotherapists.

This chapter covers the basic principles of radiation biology, including the effects of ionizing radiation on normal living cells and on tumors.

BIOLOGIC EFFECTS OF IONIZING RADIATION

Figure 6-1 is a flow diagram of the significant elements to be considered in a discussion of the biologic effects of radiation. We are concerned only with ionizing radiation, that is, alpha, beta, gamma, and neutron radiation. These are penetrating types of radiation that pose a potential risk from internal and external exposure. Although ultraviolet radiation has potential for biologic damage, primarily to the skin or the eyes, it is not an ionizing radiation and will not be included in this discussion.

The primary interactions of ionizing radiation within cells of the body cause excitation and ionization, releasing high-speed electrons that cause further interactions with biologic molecules. Energy is transferred, by direct or indirect action, to critical components of the cell during these events. The energy deposited may break the bonds of molecules that are necessary for cellular function or reproduction. The most critical target is DNA. If the radiation dose is small and the damage slight, the cell may be able to repair the damage and return to health. Higher doses and dose rates may cause harm that exceeds the cell's ability to repair, and permanent damage will become evident within days or weeks of exposure. Such results are known as deterministic effects. If the dose is high enough, deterministic effects can be life threatening, as in the deaths caused by the Chernobyl nuclear reactor accident in 1986. Some examples of non–life-threatening deterministic effects are skin erythema caused by x-ray exposure, loss of hair (epilation) in a patient being treated with radiation therapy for a brain tumor, and the development of cataracts several years after high-dose radiation exposure of the eye. Deterministic effects have a threshold dose below which no effect is observed but above which the severity of effect

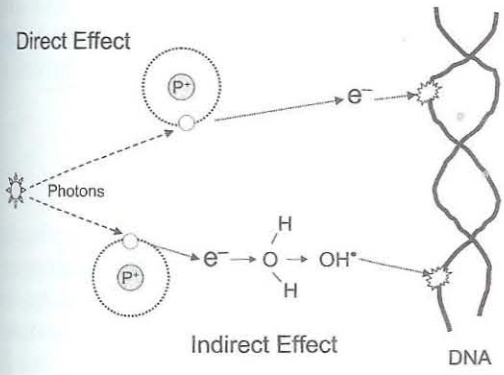

FIGURE 6-2 Mechanisms of direct and indirect effects of ionizing radiation on biologic systems. Gamma ray photons from an ionizing radiation source release free electrons by photoelectric or Compton interactions. The electrons then interact directly with DNA or indirectly via free radicals.

The direct and indirect processes of radiation interaction are illustrated in Figure 6-2. In each situation the primary event is the same: release of a high-speed electron from an ionizing event. In the direct effect, this primary electron deposits its energy directly within the DNA molecule. In the indirect effect, the primary electron interacts first with water, producing a free radical that then goes on to deposit its energy within DNA.

The reactions between radiation and water molecules to produce free radicals are

$$H_2O \leftrightarrow H^+ + OH^- \tag{6-1a}$$

$$H_2O \xrightarrow{h\nu} H^\cdot + OH^\cdot \tag{6-1b}$$

$$RH \xrightarrow{h\nu} R^\cdot + H^\cdot \tag{6-1c}$$

Equation 6-1a describes, for comparison, the normal dissociation of water into hydrogen ions and hydroxyl ions. This process does not involve any interaction with radiation. When the water molecule dissociates, all the electrons involved in the covalent bond between oxygen and hydrogen are possessed by the hydroxyl group. This leaves it with one more electron than its number of protons and, therefore, with a single negative charge. The hydrogen atom, having no electrons, remains as a positively charged proton.

Equation 6-1b describes the production of hydrogen and hydroxyl free radicals. The radiation interaction with a water molecule separates the atoms so that the hydrogen retains its lone unshared electron, leaving the hydroxyl group with an unshared electron. Both, therefore, have neutral ionic charges. Equation 6-1c shows a similar reaction with a biologic molecule (represented by RH).

The stepwise mechanism for the radiolysis of water into hydrogen and hydroxyl free radicals is shown in Equations 6-2a, b, and c.

$$H_2O \xrightarrow{h\nu} H_2O^+ + e^- \tag{6-2a}$$

$$H_2O^+ + H_2O \rightarrow H_3O^+ + OH^\cdot \tag{6-2b}$$

$$e^- + H_2O \rightarrow OH^- + H^\cdot \tag{6-2c}$$

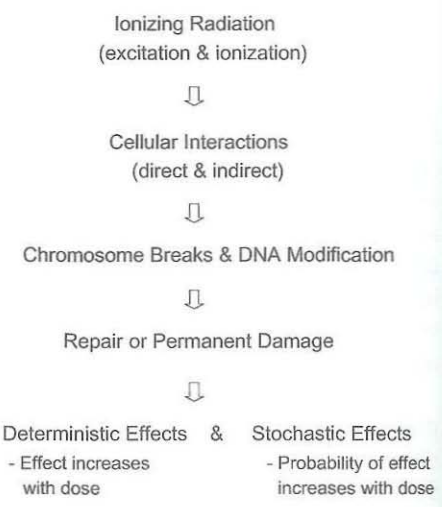

FIGURE 6-1 Overview of biologic effects of ionizing radiation.

increases in proportion to the dose. Radiation protection practices to keep exposure as low as reasonably achievable are designed to prevent deterministic effects.

If any repair process from radiation-induced damage is incomplete or defective, the cell may be altered in such a way that it will become cancerous or contain a heritable defect. These late effects are known as stochastic effects. Stochastic effects do not have a threshold dose, that is, a particular cancer may occur after a low dose or a high dose of radiation exposure, but the likelihood is greater after a high dose. Stochastic effects can be somatic or genetic. The development of cancer is a somatic stochastic effect. Genetic stochastic effects occur when germinal cells (oocytes or spermatogonia) sustain radiation-induced damage resulting in a mutation that is passed on to future generations.

The International Commission of Radiological Protection (ICRP) has estimated that the risk of fatal cancer to the general population from uniform whole-body exposure is 5% per sievert.[1] The chance of anyone receiving this magnitude of exposure is extremely rare, so the risk to the general population and radiation workers from typical radiation exposure in the environment or on the job, in general, is much smaller.

DIRECT AND INDIRECT EFFECTS OF RADIATION

Experiments have shown that the sensitive target within cells for interactions with ionizing radiation is DNA. Two principal mechanisms are involved in this interaction. Direct effects occur when radiation produces primary ionization, releasing a high-speed electron in the vicinity of a chromosome that interacts directly within DNA. For example, photons may interact by the photoelectric effect or Compton effect, releasing a free electron that then deposits its energy within the DNA molecule and causes a bond to break. The critical points are the bonds between base, sugar, and phosphate molecules in the DNA chain. Direct effects are more probable with high linear energy transfer (LET) radiation, such as alpha particles, protons, and neutrons, because the high ionization density of their tracts releases many electrons as the radiation passes through the DNA molecule.

Indirect effects of radiation are mediated by free radicals produced secondarily in the interaction of radiation with water molecules. The free radical, which carries an unpaired electron, is highly reactive and may interact with DNA, causing bond breakage. Indirect effects are more probable with low-LET radiation, such as beta particles, gamma rays, and x-rays. Since water constitutes such a high percentage of biologic matter, about two-thirds of x-ray damage in mammalian cells is due to the hydroxyl radical ($OH^{\cdot}$).[2]

In the first step, a photon ionizes a water molecule, producing a fast electron and an ion radical. In the second step, the ion radical combines with another water molecule to produce the hydronium ion and a hydroxyl radical. Finally, the fast electron combines with a water molecule to produce a hydroxide ion and the hydrogen radical.

Free-Radical Reactions

The radiolysis of water is a significant event in radiobiology because of the free radicals formed. Electrons not only orbit around the nucleus of an atom but also spin on their own axes. The most stable atoms have electrons paired and spinning in opposite directions. If one electron is removed from the pair, for example by a radiation interaction, an unpaired electron remains, creating a free radical. The free radical is much less stable, making it very reactive chemically as it seeks to pair with another electron of opposite spin. If the free radical is produced in the vicinity of a cell's DNA, it may react with the DNA helix, breaking one of its bonds. If the broken bond is not repaired correctly, the cell may not be able to replicate, may fail to produce a critical protein required for cell viability, or may produce conditions that lead eventually to the development of cancer or a genetic mutation.

A number of free-radical reactions are possible. Some of the more significant ones are

$$R^{\cdot} + H^{\cdot} \rightarrow RH \quad (\text{restored organic molecule}) \tag{6-3a}$$

$$R^{\cdot} + O_2 \rightarrow RO_2^{\cdot} \quad (\text{restoration blocked}) \tag{6-3b}$$

$$H^{\cdot} + O_2 \rightarrow HO_2^{\cdot} \quad (\text{hydroperoxy radical}) \tag{6-3c}$$

$$RH + HO_2^{\cdot} \rightarrow R^{\cdot} + H_2O_2 \quad (\text{molecule inactivated}) \tag{6-3d}$$

$$HO_2^{\cdot} + H^{\cdot} \rightarrow H_2O_2 \quad (\text{hydrogen peroxide}) \tag{6-3e}$$

$$OH^{\cdot} + OH^{\cdot} \rightarrow H_2O_2 \quad (\text{hydrogen peroxide}) \tag{6-3f}$$

Equation 6-3a demonstrates the possibility of restoration of a biologic molecule after it interacts to form free radicals, and Equation 6-3b shows how the presence of oxygen can combine with a free-radical molecule to block its restoration. Oxygen can also combine with a hydrogen radical to produce the reactive hydroperoxy radical shown in Equation 6-3c. The hydroperoxy radical can in turn inactivate a biologic molecule, as shown in Equation 6-3d. If the inactivated molecule plays a significant role in the cell's metabolism, the cell's viability may be threatened. The hydroperoxy radical can combine with a hydrogen radical (Equation 6-3e) or two hydroxyl radicals can combine (Equation 6-3f) to produce hydrogen peroxide, a known cell toxicant. Thus, multiple mechanisms that may cause detrimental biologic consequences are possible.

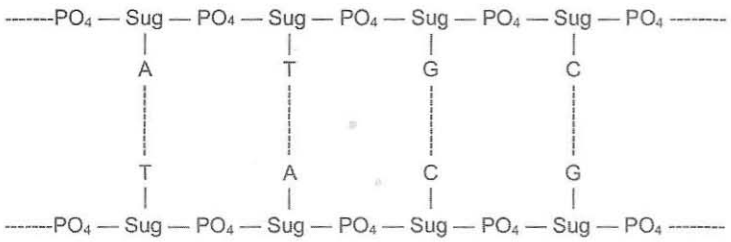

FIGURE 6-3 Ladder structure of a portion of the DNA molecule illustrating the two phosphate–sugar backbone rails covalently bonded to the bases: adenine, thymine, guanine, and cytosine. The two rails are connected by hydrogen bonds (dashed lines) between the base pairs.

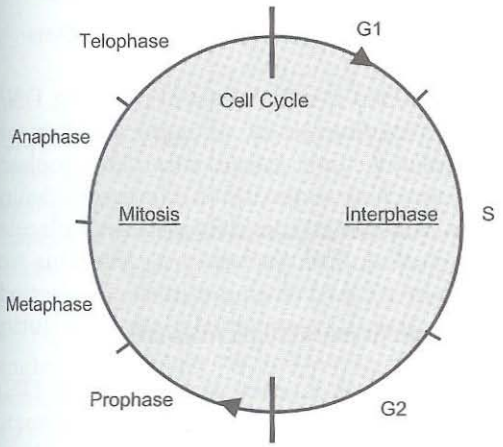

FIGURE 6-4 Phases of the cell cycle. See text for description.

THE CELL CYCLE

Before we discuss the effects of radiation on biologic systems, a review of the chemical composition and structure of DNA and the functions occurring during the cell cycle is in order. DNA appears in the nucleus of the cell as a coiled double helix of the sugar molecule deoxyribose, a phosphate, and the bases adenine, thymine, guanine, and cytosine. If the DNA helix is uncoiled and flattened out, it resembles a ladder (Figure 6-3). The covalently bonded sugar–phosphate groups form the rails or backbone of the ladder, and the rungs are formed by hydrogen bonding of the base pairs attached to the sugar molecules in each rail. The bases bond in specific pairs: adenine with thymine and guanine with cytosine. The DNA molecule is replicated in the nucleus of every cell that undergoes mitosis. If it is damaged in any way, by either chemicals or radiation, it may not be able to replicate or may replicate in a way that creates a mutant gene. Extensive research has been done to study the effect of radiation on cell growth, DNA, and the cell cycle.

The cell cycle is divided into two main segments: interphase and mitosis, or M phase (Figure 6-4). These, in turn, are divided into additional phases. Interphase is the period from the end of cell division to the beginning of a new mitosis. During this time the cell appears to be quiescent, in part because the chromosomes in the nucleus are not readily visible because the DNA strands are uncoiled and filamentous. However, during the S phase of interphase DNA synthesis occurs. This is the event that allows each new daughter

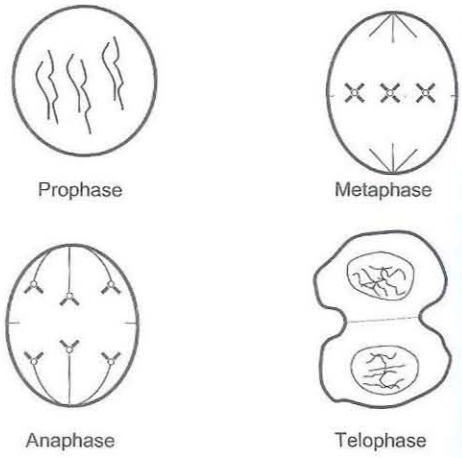

FIGURE 6-5 Four phases of mitosis in the cell cycle, illustrating movement of the chromosomes.

cell formed during mitosis to acquire exactly the same genetic makeup. During DNA synthesis the hydrogen bonds holding the base pairs together break, allowing the filaments to separate. Each filament serves as a template. Available "free" bases in the cell cytoplasm then match up with their complementary bases attached to the DNA filament (adenine with thymine and guanine with cytosine). New phosphate and deoxyribose molecules follow base pairing and the DNA strand is duplicated. The nucleus now contains two identical chromatids, one for each daughter cell to be formed during mitosis. The periods just before and immediately after the S phase, G1 and G2 respectively, are gaps during interphase when DNA is not replicating.

The cell cycle enters mitosis at prophase (Figure 6-5). During this phase the DNA filaments of each chromatid shorten and condense into coils, thickening the chromatin material and making it visible after staining procedures. The nuclear membrane disappears, and a centromere appears between the two chromatids. Spindle fibers begin to form at the opposite ends of the cell. The beginning of chromatid movement toward the center of the cell initiates metaphase. During this phase the centromeres divide, the chromatids align themselves at the center of the cell, and each centromere attaches itself to a spindle fiber. During anaphase the chromatids repel each other, with half the number migrating along the spindle toward one end of the cell and the other half migrating toward the opposite end of the cell. When they reach the opposite poles of the cell, telophase begins. During telophase the chromosomes uncoil and elongate into filamentous strands once again, and a nuclear membrane is formed around them. The center of the cell indents, separating the cytoplasm into two distinct cells after the formation of a new cell membrane. The two new daughter cells, each with a complete set of identical chromosomes, enter interphase and the cell cycle is complete.

The length of the cell cycle and the various phases for a particular type of cell can be determined by labeling techniques. One method uses a radioactive substrate (tritiated thymidine) that is taken up during DNA synthesis. Cells labeled with tritiated thymidine are allowed to grow for a period of time and then are fixed, stained, and subjected to autoradiography. If the cells are analyzed immediately after incorporation of the label, those cells that incorporate the radioactive thymidine are in the S phase of DNA synthesis. If staining and autoradiography is delayed for several hours after labeling, some cells will move on to mitosis, in which cells incorporate radioactivity at the various stages of cell division depending on how much time has passed between labeling and the analysis. By using this technique, the lengths of various phases of the cell cycle can be determined.

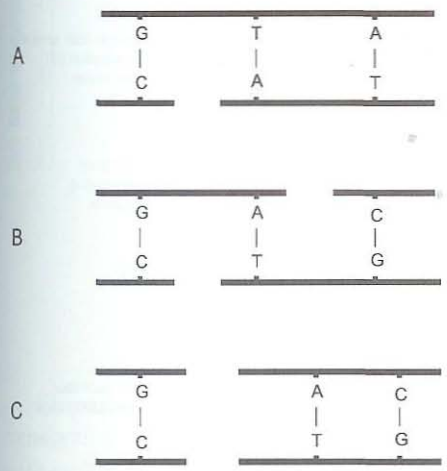

FIGURE 6-6 Radiation-induced breaks in DNA molecule. (A) single-strand break, (B) double-strand separated break, (C) double-strand opposite break.

EFFECTS OF RADIATION ON GENETIC MATERIAL

Ample evidence from radiobiologic experiments demonstrates that DNA is the critical target for the biologic effects of radiation in cellular systems. Other molecules and organelles in the cell may also exhibit detrimental effects from radiation, such as structural changes in proteins, alterations in enzyme activity, and increased permeability of membranes, but the most critical target is DNA. When radiation interacts with DNA, breaks can occur in its backbone. If a break occurs in a single rail of the backbone, repair enzymes can repair it easily, using the opposite rail as a template. Such a break in DNA is called a single-strand break (Figure 6-6A). However, the effectiveness of enzymes in repairing a break may be thwarted if a free radical binds to the broken strand of DNA, blocking the enzyme's access to the break. If both rails of the DNA molecule break in such a way that base pairing holds them together, the strands may still be easily repaired. This is called a separated double-strand break (Figure 6-6B). If the rails break directly opposite each other, the DNA backbone may separate. This is called an opposite double-strand break (Figure 6-6C). This type of break is more difficult to repair and can lead to misrepair and chromosomal aberrations that may cause lethal effects in the cell.

Radiobiologic studies on irradiated cells have demonstrated various types of chromosome abnormalities resulting from opposite double-strand breaks in DNA in which the chromosome breaks in two. These abnormalities typically result from breaks occurring in two separate chromosomes, followed by misrepair of the breaks. Examples of aberrations that cause cell death are shown in Figure 6-7. A *dicentric chromosome* is formed when a double-strand break occurs in two different chromosomes during the G1 phase. A misrepair can occur when the broken fragment from one chromosome is exchanged with the fragment from the other chromosome, resulting in one chromosome with two centromeres (a dicentric chromosome) and one with no centromere (an acentric chromosome). Subsequent duplication of these chromosomes in the S phase yields an aberrant dicentric chromosome and two acentric chromosomes (Figure 6-7A). The acentric chromosomes lack a centromere, cannot attach to a spindle fiber, and will not be transmitted to the daughter cell. A *ring chromosome* is formed when a double-strand break occurs in the same chromosome in the G1 phase (Figure 6-7B). Misrepair occurs when the two broken ends attach to each other, forming a ring chromosome with one centromere and an acentric chromosome. When these replicate during the S phase, a ring chromosome is transmitted to each daughter cell minus the pieces lost in the acentric chromosome. A *dicentric chromatid* forms when a cell is irradiated immediately after DNA synthesis during the G2 phase.

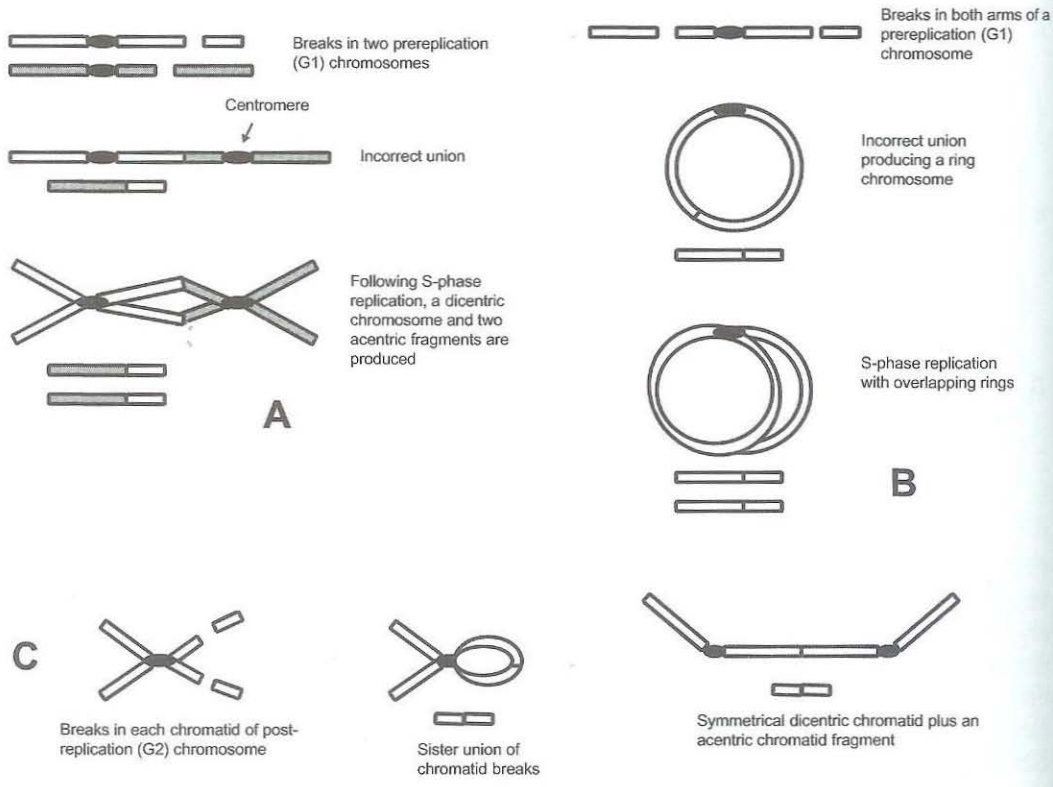

FIGURE 6-7 Chromosome aberrations induced by radiation. (A) Breaks in two irradiated G1-phase chromosomes before replication followed by illegitmate union of the broken fragments. After S-phase replication a dicentric chromosome and two acentric fragments are formed. (B) Breaks in both arms of the same irradiated G1-phase prereplication chromosome followed by incorrect union forming a chromosome ring. After replication, overlapping ring chromosomes form. (C) Breaks in each chromatid of a G2-phase irradiated postreplication chromosome followed by sister union of the broken ends. During anaphase a dicentric chromatid is formed and each centromere migrates to a pole, stretching the chromatid between the two poles to form an anaphase bridge.

Breaks occurring in each chromatid of the same chromosome are misrepaired by sister union of the two ends (Figure 6-7C). After centromere duplication, a dicentric chromatid attempts to migrate toward opposite poles at anaphase and the chromatid stretches across the cell, forming an anaphase bridge, preventing individual daughter cells from forming.

An important distinction should be made regarding chromosome breaks induced by radiation. During the S phase of the cell cycle DNA replicates, producing an exact duplicate of itself. These two identical sister chromosomes are called chromatids. If cells are irradiated at this point of the cell cycle, one of the chromatids may be damaged. If it is not repaired, the chromatid aberration produced will be passed on to the daughter cell receiving that chromatid. The other daughter cell will receive the normal chromatid. Chromatid aberrations, therefore, are produced in individual chromatids when irradiation occurs after DNA synthesis. Chromosome aberrations are produced when cells are irradiated prior to DNA synthesis in the G1-phase. If successful repair of the damage is completed before DNA synthesis occurs, each daughter cell receives normal chromosomes. If the repair is not completed or if there is a misrepair, it will be duplicated in the S phase and the damaged chromatids will be passed on to both daughter cells.

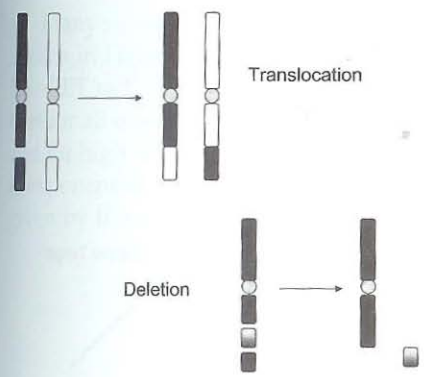

FIGURE 6-8 Double-strand breaks in adjacent chromosomes. Translocation misrepair results in exchange of broken pieces between chromosomes. Deletion misrepair causes loss of a piece of genetic material after a double-strand break in the same chromosome.

Chromosome breaks that lead to nonlethal aberrations are shown in Figure 6-8. A *translocation* aberration involves a double-strand break in two G1-phase chromosomes, with exchange of the broken ends between the two chromosomes. This type of break and misrepair has been shown to cause activation of an oncogene, which leads to malignancy. Burkitt's lymphoma is an example. A *deletion* aberration can result when two double-strand breaks occur in the same arm of a chromosome, causing a piece of genetic material to be removed. If the piece of genetic material that is lost is associated with the production of a suppressor gene in the cell, cancer can develop.

CELL SURVIVAL CURVES

Cell killing by radiation is defined as a loss of proliferative ability. It may result from any number of causes, such as point mutations, chromosome breakage, and rupture of vital cellular membranes. The magnitude of cell killing is measured by the fraction of cells that survive after radiation exposure, the end point being the ability of cells to form colonies in growth media. Therefore, survival curve analysis is limited to cells that undergo mitosis.

Much of the information known about the effects of ionizing radiation on biologic systems comes from studies in which viruses, bacteria, yeasts, and mammalian cells are irradiated and the fraction of cells that survive as a function of dose is measured. A survival curve is generated by irradiating cells at various doses, plating them on growth media, and counting the number of cell colonies that survive after a given time. Unirradiated cells are also plated as a baseline to determine the fraction of untreated cells that will grow. This is the plating efficiency (PE). The survival fraction of treated cells at each dose of radiation is determined by the following formula:

$$\text{Survival fraction} = \frac{\text{Number of colonies}}{\text{Number of cells plated} \times \text{PE}}$$

The first survival curve for mammalian cells was from measurements after x-ray irradiation of cells derived from human squamous cell carcinoma of the cervix (HeLa cells).[3] The curve had a shoulder region at low doses up to 150 rad and became exponential at higher doses. Survival curves, in general, are of two types: exponential and sigmoid (Figure 6-9). An exponential curve indicates that there is a single target in the cell that must be hit or inactivated to kill the cell. With this type of survival, the fraction of cells killed is constant as the dose increases, but the number of cells killed per unit of dose diminishes because the starting number of live cells at higher doses is smaller, similar to exponential decay of a radionuclide. This type of curve has been observed after irradiation

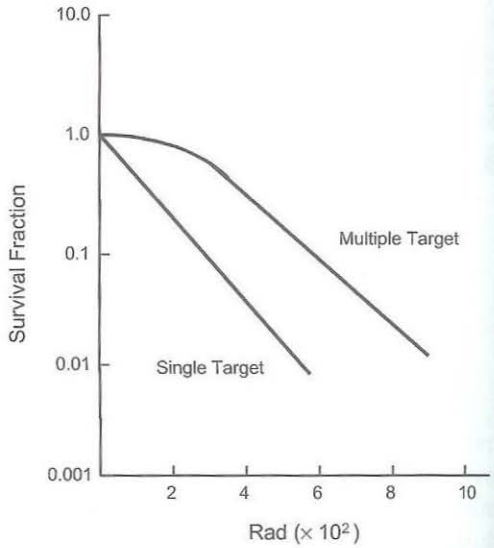

FIGURE 6-9 Survival curves resulting from radiation interaction in cells. The exponential curve shows that cell killing increases proportionally with dose, implying that a single target must be inactivated to kill the cell. The sigmoid curve implies that there are multiple targets that must be hit (inactivated) to kill the cell. A shoulder region is evident at lower doses (cell killing not proportional to dose), signifying that damage must be accumulated before a cell is killed or that repair processes are in effect. At higher doses cell killing is exponential, signifying that all targets in a cell that is hit are inactivated and repair is not possible. As dose increases, the probability of more cells being inactivated increases, and the survival fraction declines.

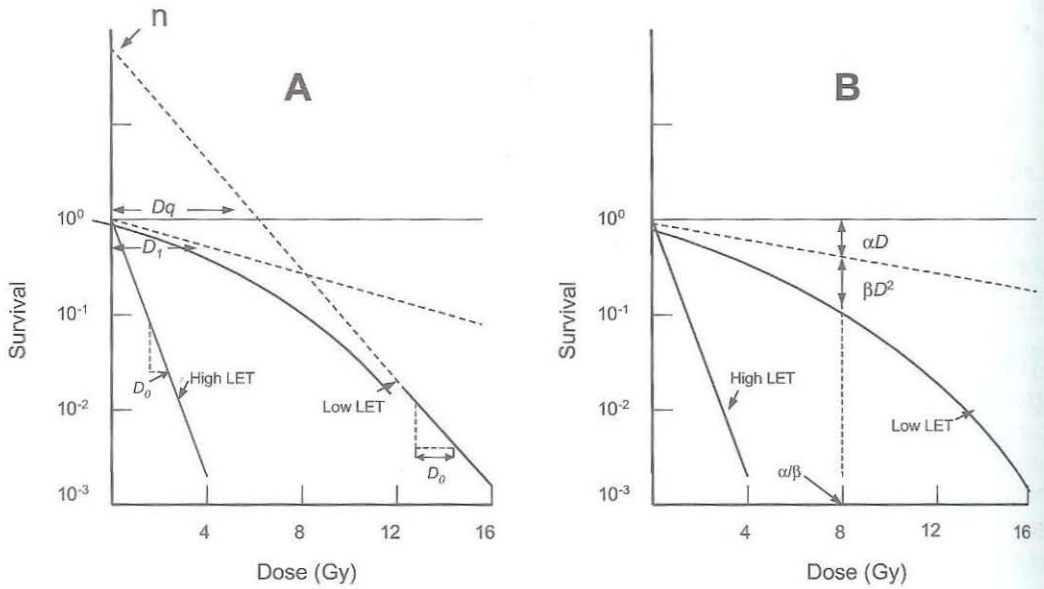

FIGURE 6-10 Survival curves for mammalian cells exposed to high-LET and low-LET ionizing radiation at high dose rates (>0.1 Gy/min). D is the applied dose of radiation, D_0 is the mean lethal dose, and D_q is the quasi-threshold dose. (Adapted from reference 1, p. 100.)

of viruses and certain bacteria and yeasts. A sigmoid curve indicates that multiple targets must each be hit (inactivated) to kill the cell. This is the multitarget, single-hit theory of cell survival kinetics. In the sigmoid curve a shoulder region is evident at lower doses (cell killing is not proportional to dose), signifying that damage must be accumulated before a cell is killed (i.e., sublethal damage occurs in this region). However, as the radiation dose increases, a point is reached at which the amount of sublethal damage is eventually maximized. At this point, cell killing becomes proportional to dose, and the survival curve becomes exponential. A sigmoid curve is typically observed after irradiation of mammalian cells.

Many studies conducted over the years have yielded survival curves typified by those shown in Figure 6-10, which demonstrate the response of mammalian cells to high- and low-LET radiation at high dose rates (>0.1 Gy/minute).[1] Looking at curve A, it is evident that for all doses of densely ionizing radiation of high LET (alpha particles and neutrons) and for high doses of low-LET radiation (x-rays or gamma rays), the dose–response curve is exponential, that is, linear on a semilog plot. Survival of cells under these conditions is given by the equation

$$\frac{N}{N_0} = e^{-D/D_0} \tag{6-4}$$

where N is the number of cells surviving, N_0 is the number of cells initially, N/N_0 is the surviving fraction, D is the applied dose of radiation, and D_0 is the mean lethal dose. D_0 is the dose considered to provide, on average, one inactivating event per cell. According to this equation, when the applied dose is equal to the mean lethal dose (i.e., $D = D_0$), then $N = 0.37N_0$. Therefore, the D_0 dose is the dose at which 37% of cells survive (i.e., 63% of cells are killed).

The question then is, if the applied dose is sufficient to kill all cells, why do 37% survive? The answer is related to the random nature of radiation interaction with matter. When the D_0 dose is applied, some cells will sustain a lethal event more than once and some will escape being hit at all. Another way of saying this is that the random nature of radiation interaction dictates that

- Some cells will sustain hits in all targets (lethal damage).
- Some cells will sustain hits in a few targets (sublethal damage).
- Some cells will sustain no hits in a cell (cells not affected).

The survival curve in Figure 6-10A for low-LET radiation is characterized by the parameters n (the extrapolation number), D_0 (the D_{37} dose), and D_q (the quasi-threshold dose). The extrapolation number is obtained by extrapolating the linear portion of the high-dose curve to the ordinate. This was originally regarded as the number of targets required to be hit to inactivate a cell, but it is now called simply the extrapolation number. For mammalian cells, n ranges from 2 to 10. The D_0 dose was previously defined. The quasi-threshold dose is the dose at which the straight portion of the survival curve, extrapolated backward, intersects the dose axis drawn through a survival fraction of unity. It can be viewed as the dose during which most of the sublethal damage occurs after a large dose of radiation. The D_q and n terms are measures of the size of the shoulder region typically seen in the early part of the curve and are related by the following equation:[2]

$$\frac{D_q}{D_0} = \log_e n \tag{6-5}$$

The survival curve in Figure 6-10A for low-LET radiation shows a shallower initial slope (shoulder) that increases with dose. This response is explained by the multitarget theory, which states that only sublethal damage occurs in the cell, allowing the cell to repair the damage. The repair of cellular damage has been demonstrated in mammalian cell experiments involving two doses of radiation separated by intervals of time.[4] It was shown that when the same total dose of radiation is administered in fractions, separated by a period of time, the number of cells surviving increases with the time between fractions and the survival curve after the second fraction exhibits the same D_0, n, and D_q as the previous survival curve (Figure 6-11). Cells surviving the first dose fraction respond as

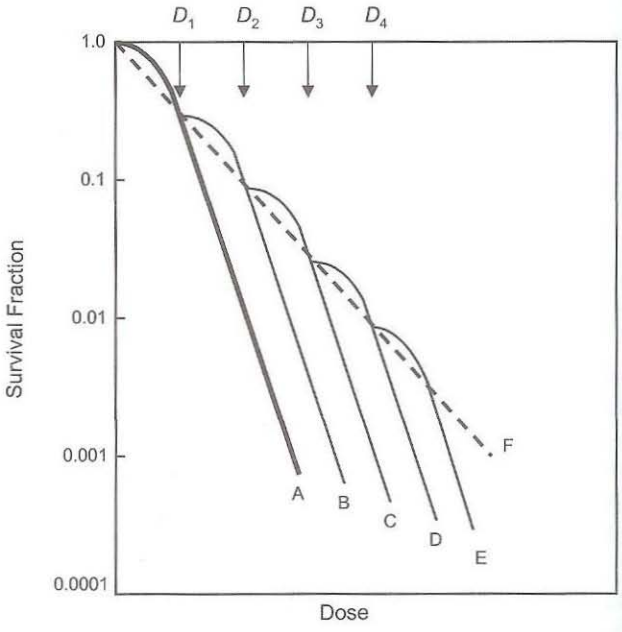

FIGURE 6-11 Effect of dose fractionation on the survival of cells irradiated with successive fractions of ionizing radiation separated by a set time interval. Each curve exhibits the same shoulder, slope, and extrapolation number, indicating that repair of damage has occurred between doses. Curve A represents survival from a single large dose. Curves B–E represent survival after equal fractions of the large dose. The dotted line F connecting single points on curves B–E has a shallower slope than line A and therefore a larger D_0 compared with curve A, demonstrating repair. (Adapted from reference 4, p. 287.)

unirradiated cells to the second fraction. This was interpreted to mean that sublethal radiation damage had been repaired by the time the second dose was administered.

Another way of explaining what is happening in cell survival curves is shown in Figure 6-10B. The low-LET curve in B is similar to the one in curve A, but it is continuously bending, with no final straight portion. This curve is fitted to a linear–quadratic function that assumes there are two components to cell killing, where the frequency of lethal events is given by $F(D) = \alpha D + \beta D^2$, indicating that cellular effects are proportional to dose and dose squared, depending on the magnitude of the dose. This concept is similar to the induction of cancer and hereditary effects caused by low-dose and high-dose radiation discussed in Chapter 4. Survival of cells is given by the equation

$$S = e^{-(\alpha D + \beta D^2)}$$

where S is the surviving fraction (N/N_0) from applied dose (D), and α and β are constants of proportionality. The dose at which the linear and quadratic components are equal is the ratio of α/β. This ratio has significance in radiotherapy.

According to the linear–quadratic model, radiation response in cells is related, in a simplified way, to radiation-induced chromosome aberrations.[2] Recall that lethal aberrations are likely the result of misrepair of double-strand breaks occurring in two separate chromosomes. A double-strand break can be caused by a single track of radiation passing through DNA of each chromosome, such as an electron released from a single ionizing event. A double-strand break in each chromosome can also be caused by two electrons produced from two separate ionizing events, one electron causing a double-strand break in one chromosome and the other electron causing a double-strand break in the second chromosome (Figure 6-12). At low doses, the two breaks may result from the passage of a single electron set in motion by an x-ray, and the probability of an interaction between the two breaks is proportional to dose. This makes the dose–response curve for chromosomal aberrations linear at low doses. At higher doses the two chromosome breaks may result from two separate electrons, and the probability is then proportional to dose

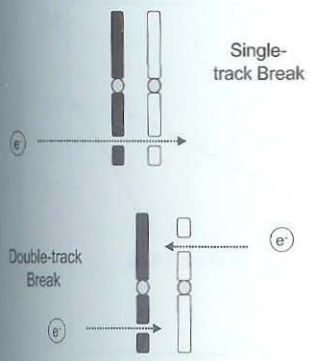

FIGURE 6-12 Double-strand breaks in two adjacent chromosomes by one electron from a single ionizing event (single-track break) and by two electrons from separate ionizing events (double-track break).

squared. The quadratic effect causes the dose–response line to become curved. It is therefore reasonable to link the linear–quadratic relationship characteristic of the induction of chromosome aberrations to the cell survival curve.[2]

RADIOSENSITIVITY

Not too many years after the discovery of x-rays and radioactivity, physicians observed that rapidly growing tissue such as tumors appears to be more readily affected by radiation than nearby normal tissue. To gain more objective evidence of cellular sensitivity, Bergonie and Tribondeau[5] exposed rodent testicles to radiation, reporting their results in 1906. Testicles contain cells at various stages of maturity, and Bergonie and Tribondeau's experiments demonstrated that ionizing radiation is more effective against immature spermatogonia undergoing mitosis than against mature differentiated sperm cells. Their conclusions were that dividing cells are more sensitive than cells that do not divide and that a cell's sensitivity is determined by the cell's characteristics rather than the radiation.

In 1925 Ancel and Vitemberger[6] modified the law of Bergonie and Tribondeau; they proposed that the damage to any cell from radiation is the same but the appearance of damage is influenced by two factors. They suggested that mitosis is an important factor because radiation-induced damage is expressed only when the cell attempts to divide, and that damage is more apparent when various conditions are present during and after irradiation, changing the cell's sensitivity.

In 1968 Casarett[7] classified cells into five categories of radiosensitivity, ranging from vegetative, undifferentiated stem cells, which are the most radiosensitive, to differentiated mature cells, which are the most radioresistant. These categories are summarized in Table 6-1. It is clear from this classification that cells actively undergoing division are the most radiosensitive and are at greatest risk from excessive radiation exposure.

One of the first clinical symptoms to arise from high-dose whole-body exposure to ionizing radiation, such as occurred in the Chernobyl nuclear reactor accident, is nausea and vomiting caused by the effects of radiation on the gastrointestinal cells. In calculating effective dose from radiopharmaceuticals, the cells of the body given the greatest risk weighting factor are the gonadal cells because of their potential for passing on radiation-induced genetic defects when they divide.

FACTORS AFFECTING RADIOSENSITIVITY

As mentioned previously, several factors have a role in determining the sensitivity of cells to radiation. The significant factors are LET, dose rate, the presence of oxygen, and the phase of the cell cycle during irradiation.

TABLE 6-1 Relative Radiosensitivity of Cell Populations

Radiosensitivity	Cell Type
High sensitivity	Lymphocytes
	Erythroblasts
	Spermatogonia
Relative sensitivity	Myelocytes
	Intestinal crypt cells
	Epidermal basal cells
Intermediate	Endothelial cells
	Osteoblasts
Relatively resistant	Granulocytes
	Osteocytes
	Erythrocytes
	Spermatozoa
Highly resistant	Fibroblasts
	Muscle cells
	Nerve cells

Source: Reference 7.

Linear Energy Transfer

High-LET radiation, such as neutrons and alpha particles, has a high specific ionization and therefore produces dense ionization along its tracks, in contrast to x-rays or gamma rays. The high density of ion pairs increases the probability for interaction within the critical target centers of a cell. Rad for rad, biologic damage is greater than with sparsely ionizing radiation. The shoulder region seen on survival curves for low-LET radiation, which is associated with cellular repair of sublethal damage, is reduced or absent with high-LET radiation because of the increased efficiency for inflicting lethal damage (more double-strand breaks) (see Figure 6-10). The quasi-threshold dose, D_q, is absent on the survival curve, resulting in an extrapolation number of 1.

Dose Rate

For low-LET x-rays or gamma radiation, a high dose rate is more damaging to cells than a low dose rate because low dose rates produce more single-strand breaks, which allow for repair of sublethal damage. Therefore, the shoulder of the survival curve is broader with radiation at a low dose rate (Figure 6-13). High dose rates deliver more ionizing tracks per unit of time, thus producing more double-strand breaks, and also allow less time for repair of sublethal damage. There is no dose-rate effect with high-LET radiation because of its dense ionization.

Oxygen Effect

Oxygen has been shown to be an effective radiosensitizer; its presence during irradiation of cells and tissue can enhance the killing effect of radiation. The magnitude of oxygen's effect can be measured and is known as the *oxygen enhancement ratio* (OER). The OER is the ratio of the radiation dose required to produce a given effect without oxygen to that required to produce the same effect with oxygen. Experiments have shown that administration of oxygen during irradiation enhances the effect more than administration before

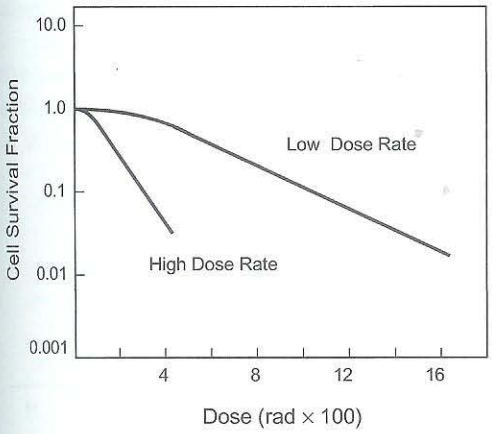

FIGURE 6-13 Effect of dose rate on cell survival from low-LET radiation. Low dose rate (10 rad/min) produces a broad shoulder and shallow slope compared with high dose rate (100 rad/min), which produces a smaller shoulder and steeper slope.

or after irradiation. Oxygen is most effective when it is present over a range of 0 to 20 mm Hg tension, but effectiveness falls off at oxygen tensions in the 20 to 40 mm Hg range. Because the effect is most pronounced during irradiation, it is postulated that the mechanism of action is related to free radical formation of biologic molecules that combine with oxygen, preventing the molecules from restoring themselves (see Equation 6-3b).[8] This effectively increases cell damage and lethality at a lower dose than if oxygen were absent.

For mammalian cells the OER averages approximately 2.5. This means that a 100 rad dose in the presence of oxygen will produce the same killing effect as 250 rad in the absence of oxygen. The oxygen effect is most pronounced with x-rays or gamma rays; it is absent or diminished with high-LET radiation (alpha and neutron) because the damage produced by densely ionizing radiation is not repairable.

Tumors have a distinct architectural pattern consisting of a central region of necrosis (dead cells) surrounded by a rim of viable well-oxygenated cells. In between are viable cells that have a relative deficiency in oxygen (hypoxic cells). Hypoxic viable cells pose the biggest problem in radiotherapy because they are relatively radioresistant compared with well-oxygenated cells. The presence of these cells will result in tumor regrowth and treatment failure. Exogenous methods of increasing the oxygen titer in hypoxic tumor cells, thus increasing their radiosensitivity, have not met with much success. There is evidence, however, that the proportion of hypoxic cells decreases after a dose of radiation because as oxygenated cells are killed their oxygen supply is made available to the hypoxic cells. Thus, these cells become more radiosensitive at subsequent doses of radiation (dose fractions), and this phenomenon is believed to play a role in the effectiveness of fractionated radiation treatment plans.

Cell Cycle Effects

Experiments have shown that the radiosensitivity of cells is different at different phases of the cell cycle. The most sensitive phases are the G2 phase immediately after DNA synthesis and the M phase. The G1 phase is less sensitive to radiation, and the S phase is the most resistant.

When mammalian cells grown in culture are irradiated at 37°C, more cells in the G2 and M phases are killed than cells in the S phase. The surviving cells tend to become partly synchronized in the cell cycle. In this situation, most surviving cells will be in the S phase of the cell cycle. If the length of the cell cycle for the particular cell type is known, radiobiologists can irradiate a group of synchronized cells when they reach another phase of the cycle. In this way the relative radiosensitivities of the cell cycle can be determined.

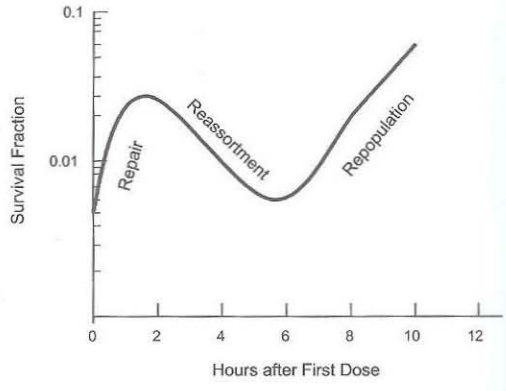

FIGURE 6-14 Survival of hamster cells exposed to two fractions of x-radiation separated by various time intervals. Repair of cells is evident in the first phase of the curve between 0 and 2 hours. Cells synchronized in the S phase from the first dose cycle to more sensitive G2–M phases by 6 hours, causing a fall in survival when the second dose is given here. If the second dose is given at 10–12 hours, cells show an increase in survival, having exceeded their cycle time and repopulated by mitosis. (Adapted from reference 9.)

The total cell cycle time for Chinese hamster cells in vivo is 11 hours. The times for the phases of the cycle are M phase, 1 hour; S phase, 6 hours; G2 phase, 3 hours; and G1 phase, 1 hour. Elkind et al.[9] studied the growth of hamster cells in vitro, which have a shorter cycle time (about 9 hours). These cells were irradiated at various times during the cell cycle with a total dose of 1551 rad of x-rays fractionated into two doses (747 rad and 804 rad) (Figure 6-14). After the first dose, cells in the more sensitive phases have been killed but cells in the S phase, being more resistant, are spared. The remaining cell population, then, is synchronized in the S phase of the cycle and can undergo repair before the second dose is given. If 6 hours elapses before the second dose, this cohort of cells cycle around (reassortment) to the G2 and M phases, where they become more radiosensitive. If the second dose is given at this time in the cycle, the increased radiosensitivity exceeds the effect of repair, and the surviving fraction will decrease. If the second dose is not given until 10 to 12 hours after the first dose (i.e., more than the length of the cell cycle), the cells will have cycled through mitosis and increased in number (repopulation). This triad of repair, reassortment, and repopulation, coupled with reoxygenation, is known as the "4 Rs" of radiobiology and plays a significant role in the treatment of tumors with radiation.

DOSE FRACTIONATION IN TUMOR TREATMENT

Soon after its discovery, radiation was applied to treat cancer. The treatment schedules that were developed fall into two main groups. Single-dose therapy involves large radiation doses at one time, and multiple-dose therapy involves smaller (fractionated) doses over a longer time.[10] The information gained from clinical experience and radiobiology research has shown that dose fractionation has several inherent advantages that enhance the treatment of cancer with radiation.

A key factor in treating a cancerous tumor with radiation is the effect of the radiation on surrounding normal tissue. The amount of radiation used to treat a tumor is limited by the tolerance of normal tissue. The dose of radiation that will cause total destruction of tumor cells is called the tumor lethal dose (TLD), while the dose that begins to cause normal tissue necrosis is called the normal tolerance dose (NTD). The ratio of NTD to TLD is called the therapeutic ratio. It is desirable that this ratio be large in order to spare normal tissue and reduce morbidity. Therapeutic ratios vary by tumor type because of the differences in tumor and normal cell radiosensitivities. The total tumor dose and

fractionation schedule are selected to maximize tumor killing and minimize normal tissue damage.

Dose fractionation is an important factor in planning radiation treatment. Ultimately, the benefit of radiotherapy depends on a therapeutic gain between the responses of the tumor and that of the normal tissue. A gain from fractionation is realized because a number of factors are operational during therapy:

- Repair of sublethal and potentially lethal damage; normal cells often have a greater capacity to repair intracellular effects than tumor cells do;
- Repopulation of cells between fractions, allowing regrowth of normal cells;
- Redistribution of cells throughout the cell cycle, which tends to sensitize the more rapidly dividing cells in tumors; and
- Reoxygenation effects; repeated fractions permit reduction of the number of hypoxic cells in tumors while little change in oxygenation occurs in normal tissues, permitting a gradual increase in the tumor's sensitivity to radiation.[11]

Survival curves of normal and tumor cells have provided insight into the effects of different fractionation schemes on tumor destruction. In general, more rapidly dividing tissues (skin, mucosal cells, rapidly dividing tumors) have relatively greater α/β ratios, about 10 Gy, while more slowly dividing tissues (kidney, brain) have smaller α/β ratios, about 2 Gy, representing their greater capacity to repair at lower doses.[11] The greater the α/β value in tumor cells and the lower the value in adjacent normal tissue cells, the more fractionation will help the therapeutic ratio. If the radiation dose is divided into several fractions, each with a smaller dose, more slowly dividing tissues like normal organ tissues can be preferentially spared from the effects of radiation. More rapidly dividing tissues like tumors show a relatively greater radiation effect during fractionation because they have a greater chance of being irradiated during sensitive phases of the cell cycle. More rapidly dividing normal cells like skin and mucosa will show a greater effect as well, but these tissues have an excellent capacity to replenish themselves. After each treatment both normal cells and tumor cells recover, but if normal cells recover more, a differential is achieved and eventually a dose can be reached at which normal cells can recover but tumor cells cannot. Thus, sometimes a greater tumor cell kill with relatively fewer late normal tissue effects can be achieved by reducing the fraction size and increasing the total number of fractions to create a greater therapeutic gain.[11]

ACUTE EFFECTS OF WHOLE-BODY IRRADIATION

The acute effects that occur after whole-body irradiation are well described.[2,12] These effects are deterministic in that they result in a measurable loss of cell and tissue function as a direct consequence of radiation's inactivation of vital elements within cells. Information on these effects is derived mostly from Japanese atomic bomb survivors, patients who undergo radiotherapy, and victims of nuclear reactor accidents. The effects become evident after exposures in excess of 1 to 2 Gy (100 to 200 rad), and the sequence of effects is known as the acute radiation syndrome.

Three principal syndromes may occur, based on the organ system principally involved in causing death: the hematopoietic, gastrointestinal, and cerebrovascular or acute incapacitation syndromes. Each of these is preceded by a prodromal phase and a latency phase. The prodromal phase lasts about 24 hours, with peak symptoms occurring 6 to 8 hours after exposure. The most frequent prodromal symptoms are anorexia, nausea, and vomiting. The time of onset and the severity of symptoms are dose dependent. The frequency

of prodromal symptoms is about 25% in persons exposed to 150 rad and about 95% in those exposed to 300 rad.[12] The latency phase is an asymptomatic period following the prodromal phase. Its length is inversely proportional to the magnitude of exposure. This phase may not be evident at doses in excess of 10 Gy (1000 rad) because of the severity of prodromal symptoms. At lower doses the latency period is the result of the time required for the deleterious consequences of cell depletion in mitotically active tissues to become clinically evident. This is most important for cells in the gastrointestinal tract and bone marrow. Thus, after an exposure event, the stem cells of these systems may be killed but the mature cells that are present will continue to function for a time until they die. When this occurs, clinical symptoms and signs of stem cell deficiency will become evident. The symptoms include chills and fever due to neutropenia and infection and the development of petechiae and hemorrhage, which are consequential signs of thrombocytopenia.

Hematopoietic Syndrome

This syndrome results from an exposure in the range of 2 to 8 Gy. At higher doses in this range, stem cells in the bone marrow that produce the blood cellular elements are killed and thus are no longer available to replace the circulating cells as they are lost to senescence. As a result, the victim experiences lymphopenia, neutropenia, thrombocytopenia, and anemia. The characteristic signs are petechiae, bleeding from mucous membranes, and infection. If death occurs, it will be within 2 to 4 weeks after exposure. The cause of death is bone marrow suppression and hematopoietic failure.

The likelihood of death during the hematopoietic syndrome depends on the dose received. Experiments in monkeys exposed to a single dose of x-rays showed that no animals died with doses up to 200 rad, whereas a dose of about 800 rad killed all the animals exposed.[2] The $LD_{50/30}$, which is the dose that kills 50% in 30 days, is about 530 rad for monkeys. For humans the peak time of death from hematopoietic failure is also 30 days, but the time can be as long as 60 days. Therefore, the LD_{50} for humans is expressed as $LD_{50/60}$. Dose estimates of Japanese survivors of the atomic bombs indicate an average $LD_{50/60}$ of 3.1 Gy, with a range of 2.7 to 4.0 Gy, depending on the circumstances of exposure.[12] The available data indicate that the $LD_{50/60}$ for healthy humans after an acute total-body exposure in the absence of medical care is in the range of 2.5 to 3.5 Gy, increasing to 4.5 Gy when supportive medical care is applied and 10 to 11 Gy with a successful bone marrow transplant.[12] After the nuclear reactor accident at Chernobyl in 1986, an estimated 203 workers received an exposure of more than 100 rad. Of these, 35 workers had severe bone marrow failure and 13 died. The remainder recovered after medical care.[2]

Gastrointestinal Syndrome

This syndrome results from an exposure of 10 to 50 Gy. The most frequent symptoms of gastrointestinal damage are nausea, vomiting, and bloody diarrhea. Without specific therapy, the loss of body fluids and electrolytes results in dehydration, with death typically occurring 5 to 12 days after exposure. The cause of death is necrosis and mitotic arrest of mucosal stem cells. The cells most affected are the stem cells in the crypts of the small intestine. As the mature cells lining the intestine become senescent and slough, no cells are available to replace them. Thus, the intestinal wall becomes denuded and is unprotected, permitting invasion of bacteria into the body. Hemorrhage and fluid loss ensue. Similar effects occur in the stomach, colon, and rectum but at a slower rate because these cells turn over more slowly.[12]

Cerebrovascular Syndrome

This syndrome results from an exposure of more than 50 Gy. Soon after exposure the principal symptoms are apathy, lethargy, somnolence, tremors, convulsions, and coma. Death occurs within 10 to 36 hours after exposure.[12] This syndrome is so named because the most consistent lesions involve the arterioles and venules. Hemorrhage and leakage of fluid occur from the vascular space. The exact cause of death is unknown, but it is speculated to be cerebral edema from small vessel leakage, which is typically found at autopsy.[12] The high-dose exposure in this syndrome is also sufficient to cause severe damage to the hematopoietic and gastrointestinal systems, so that if the victim lives long enough death occurs because of failure of one or both of these systems.

Prognosis and Treatment

Recovery from acute radiation exposure depends on the dose received, the health of the victim, and the medical care provided. If the prodromal phase is short and the latency period long with milder symptoms, the prognosis for recovery is better than if the latency period is short or absent and symptoms are severe. Supportive medical treatment can improve the outcome. Typical measures include reverse isolation to protect against infection and aggressive replacement of fluids, electrolytes, and blood products. In some instances bone marrow transplantation may be indicated. In general, if the dose received is less than 400 to 500 rad, treatment of symptoms should be instituted. Antibiotics for infection and platelets for bleeding are recommended, but blood transfusions should be withheld because they suppress regeneration of new blood cells.[2] Animal experimentation has shown that the use of antibiotics to control infection raises the LD_{50} by a factor of 2. The patient should be isolated in a sterile environment. After higher doses (800 to 1000 rad), bone marrow transplantation may be useful.[2]

The magnitude of radiation exposure may not be known in some cases. The blood levels of cellular elements can provide some measure of exposure, because lymphopenia, neutropenia, thrombocytopenia, and anemia occur in that order. The absolute lymphocyte count is especially useful in this context.

Despite the severity of effects from acute radiation exposure, heavily irradiated survivors of radiation accidents in the nuclear industry who have been followed for as long as 30 years have shown no remarkable difference from the normal aging population in terms of shortened life span, early malignancies, or rapidly growing cataracts.[2] Although this is encouraging information for victims who survive acute exposure, it cannot be considered definitive of the actual level of risk because of the small study population.

CARCINOGENIC EFFECTS OF RADIATION

The preceding section discussed the deterministic effects of acute large-dose radiation exposure in which radiation terminates the reproductive and metabolic functions of cells and causes the victim to die. The carcinogenic as well as the hereditary effects of radiation (discussed in the next section) are known as stochastic effects because they arise from random modifications (mutations) in somatic or germ cells. Because the cells are not killed, the mutation produced may eventually cause somatic cells to become cancerous or germ cells to produce genetic defects in offspring from the parent cell. As was discussed in Chapter 4, the risk of stochastic effects increases with radiation dose, and the chance for repair of radiation-induced alterations improves as dose and dose rate decrease.

Many reports in the literature from the early years of radiation use document the increased incidence of cancer in persons exposed to radiation in the work environment

which decays to long-lived alpha-particle emitters of high LET.[13] Even though there is a clearly increased incidence of lung cancer among mine workers, it is difficult to separate the effects of radiation from those of other contributing factors, such as cigarette smoke. The excess cancer mortality is slightly higher for males than females and is greatest between the ages of 25 and 65 for both sexes (see Tables 4-13 and 4-14).

- *Bone cancer.* The ingestion of long-lived, alpha-emitting radium isotopes, which have metabolism similar to calcium and localize in bone, has been associated with the development of bone cancer. One of the two known populations affected was the painters of luminous dials on clocks and watches who licked their radium paint brushes to achieve a fine point. Small amounts of radium ingestion (^{226}Ra and ^{228}Ra) over several years produced a radiation bone burden. Bone sarcomas and carcinomas of the epithelial cells lining the paranasal sinuses and nasopharynx developed in these workers. The other affected population was patients given injections of ^{224}Ra for treatment of tuberculosis and ankylosing spondylitis. These cancers were induced by high-LET radiation in bone with very slow turnover.
- *Skin cancer.* The first person to die of radiation-induced cancer in the United States was Clarence Madison Dally, Thomas Edison's assistant, whose hand was exposed to x-rays from a fluoroscope.[13] He developed radiation dermatitis and finally died from metastatic epidermoid carcinoma. In the years that followed, many such cases occurred among physicists, physicians, x-ray technologists, and dentists before safety standards were instituted. Squamous cell and basal cell carcinomas were observed frequently. Radiation-induced skin cancers are readily diagnosed and treated, and there is a large difference between incidence and mortality.[2]

Mechanisms of Carcinogenesis

Radiation exposure does not cause a unique type of tumor; it simply increases the incidence of tumors that will form spontaneously. In Chapter 4 it was shown that the incidence of radiation-induced cancer follows a linear–quadratic relationship with dose (see Figure 4-3). This relationship is based on data from the Japanese survivors of the atomic bombs, who were exposed at high dose and dose rates. At low dose and dose rate the relationship is linear, being proportional to dose. At high dose and dose rate the relationship is exponential, being proportional to dose squared. The incidence of cancer induction falls off at very high dose because of cell killing. This dose–response relationship for cancer induction is similar to that for induction of chromosome aberrations and therefore links the induction of cancer to radiation's alteration of genetic material.

A plot of cell survival and neoplastic transformation in mammalian cells as a function of radiation dose from ^{60}Co gamma-ray exposure is shown in Figure 6-15. The plot shows that the frequency of neoplastic transformation per surviving cell increases with dose up to a few gray and reaches a plateau at higher doses, representing a balance between transformation in surviving cells and cell killing. At still higher doses the curve falls exponentially, paralleling the survival curve of normal cells, indicating that cells destined to become transformed have a survival response similar to that of untransformed normal cells.

It is known from experimental studies that control of cell proliferation is the consequence of signals affecting cell division and differentiation, and if a cell turns cancerous it is because of a change in the signaling system. The conversion of a normal cell into a malignant state may result from activation of an oncogene, loss of a suppressor gene, or a combination of these two mechanisms.[2,13]

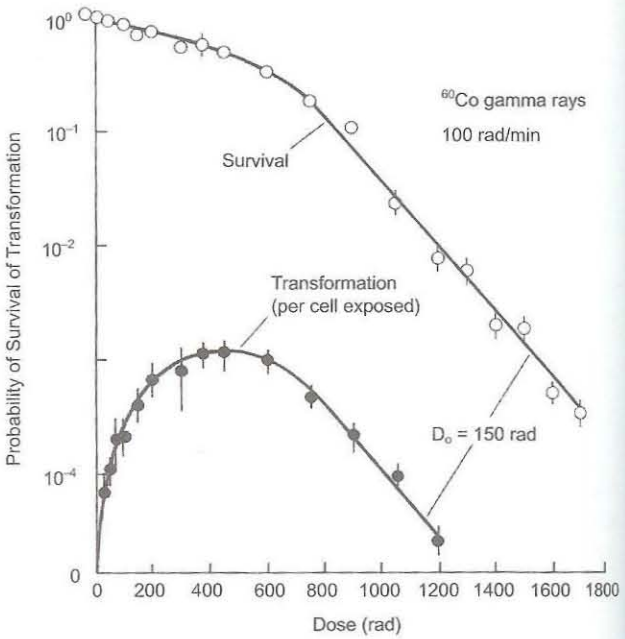

FIGURE 6-15 Probability of survival of 10T1/2 mammalian cells (top curve) and neoplastic transformation per irradiated cell (bottom curve) as a function of radiation dose. See text for explanation. (Reprinted with permission of the American Association for Cancer Research, Inc., from Han A, Hill CK, Elkind MM. Repair of cell killing and neoplastic transformation at reduced rates of Co-60 gamma rays. *Cancer Res.* 1980;40:3329.)

Oncogenes

Cells in their normal state contain proto-oncogenes that function to regulate cell growth. Studies have shown that proto-oncogenes may be activated to the corresponding oncogene by various means, causing the cell to become cancerous. Activation can be induced by chemicals, viruses, and radiation, which each can produce tumors that are indistinguishable from one another. The three principal mechanisms by which proto-oncogenes are activated to produce a malignant cell are as follows:[2,13]

- *Point mutation.* The change of a single base pair, resulting in a protein with a single amino acid change. An example is the point mutation in the oncogene N-*ras* found in cancer cells of acute leukemia.
- *Chromosome translocation.* Radiation breaks occurring in two separate chromosomes with translocation of the pieces. For example, breaks in chromosomes 2 and 8 with translocation activate the *myc* oncogene that is responsible for Burkitt's lymphoma.
- *Gene amplification.* Extra copies (overexpression) of a proto-oncogene can lead to activation of the oncogene. For example, gene amplification in the N-*myc* oncogene produces neuroblastoma.

Suppressor Genes

Normal cells may contain tumor suppressor genes that are associated with various chromosomes. Hybridization studies have demonstrated that when these cells are combined with certain tumor cells, tumorigenicity of the tumor cells is suppressed.[14] One example is chromosome 11 in normal human fibroblasts, which contains a suppressor gene for the malignant phenotype of HeLa cells (a human tumor cell line). Studies have shown that when HeLa cells are fused with human fibroblasts the hybrid cells do not produce the malignant phenotype of HeLa cells. However, when chromosome 11 is removed from the hybrid cells, the tumor is expressed again.

Radiation may inactivate suppressor genes in chromosomes of human cells, resulting in cancer. Some examples of suppressor genes whose inactivation or loss is associated with human cancer are the p105-RB gene on chromosome 13, which is associated with retinoblastoma, and the p53 gene on chromosome 17, which is associated with breast cancer, small cell lung cancer, cervical cancer, and bladder cancer.[2] The risks of radiation-induced cancer are discussed in Chapter 4.

HEREDITARY EFFECTS OF RADIATION

Radiation does not produce unique genetic effects; it simply increases the probability of effects that would occur naturally, similar to the induction of carcinogenic effects by radiation. While the carcinogenic effects of radiation arise from transformational changes in the DNA of somatic cells, thereby affecting the person who received the radiation exposure, the hereditary effects of radiation arise from transformations in the DNA of germ cells, which will manifest themselves in the offspring of those irradiated. If a radiation-induced mutation affects a dominant gene, the defect will be expressed in the first generation. If, however, the mutation occurs in a recessive gene of one parent, the defect will be expressed only if there is no dominant complementary gene from the other parent. For example, a mutation occurring on the X chromosome of a mother will not be expressed in a daughter who receives a normal X chromosome from her father. However, the defective gene will remain with the daughter as a sex-linked recessive defect, and it may be expressed in her son if the Y chromosome from his father does not carry a dominant complementary gene. Examples of sex-linked recessive defects are hemophilia and color blindness. The hereditary risks associated with exposure to ionizing radiation are discussed in Chapter 4.

Genetic Effects

The effects of radiation on the DNA of reproductive cells are similar to those in somatic cells. Gene mutations that are not lethal to the cell can be passed on to offspring, whereas lethal chromosome breaks will not be passed on. However, some chromosome translocations resulting from breaks are not lethal and will be passed on. Offspring will have a defective chromosome from one parent and a normal complementary chromosome from the unaffected parent. If the defective chromosome does not cause embryonic death, the offspring will likely have some physical or mental abnormality as a result of the defective chromosome.

Radiation Effects on Testes and Ovaries

The male produces sperm from puberty to death. Mature sperm are the result of several developmental stages. Spermatogonial stem cells progress to become primary and secondary spermatocytes, then spermatids, and finally mature spermatozoa. The average time from the immature stem cell stage to mature spermatozoa is 10 weeks. Since the first studies by Bergonie and Tribondeau, exposure of male germ cells to radiation has shown that spermatogonia are most sensitive to radiation and mature spermatozoa are most radioresistant. Temporary and permanent sterility can be caused by gonadal exposure to radiation. Because these cells undergo continual cell division and are at various stages of maturity, a moderate dose of radiation may kill the more sensitive immature spermatocytes. Reproductive potency will remain as long as the unaffected mature sperm are viable; however, a risk of mutation will be present in these cells. When these sperm die, a period of temporary sterility will ensue until the viable stem cells can repopulate by division.

TABLE 6-2 Threshold Doses for Deterministic Effects in Human Germ Cells

Tissue and Effect	Acute Single Dose (rad)	Prolonged Exposure[a] (rad/yr)
Testes		
Temporary sterility	15	40
Permanent sterility	350–600	200
Ovaries		
Permanent sterility	250–600	20

[a] Annual dose rate if received in highly fractionated or protracted exposures.

Source: Reference 1.

The ovary has its full complement of oocytes at birth; by 3 days of age the oocytes are in a resting phase and no further cell division occurs. Thus, there is no possibility of temporary sterility as with spermatogonia. The radiation exposures necessary to confer temporary and permanent sterility to human reproductive cells are shown in Table 6-2.

Some interesting and useful findings have come from what is known as the "mega-mouse project." In this study millions of specially bred mice were irradiated under various conditions and the effects were measured. Hall[2] summarized the findings as follows:

- Radiosensitivities of mice for different mutations vary widely.
- Dose fractionation results in a reduced mutation rate from acute exposure.
- The male mouse is much more radiosensitive than the female mouse, so much so that at low dose rate almost all the genetic burden in a population is carried by males.
- The genetic consequences of a given dose can be greatly reduced if a time interval is allowed between irradiation and conception. The decrease in mutation rate with time after irradiation is likely due to some repair process.

The last point is relevant in the genetic counseling of persons who receive gonadal exposure to radiation. It is recommended that persons exposed to 10 rad or more allow a period of 6 months to elapse between exposure to radiation and a planned conception, to permit repair processes to minimize the risk of genetic mutation.

RADIATION EFFECTS ON THE EMBRYO AND FETUS

The principal effects of irradiation on the mammalian fetus are lethal effects on the embryo, malformations, mental retardation, and induction of malignancy.[1] The most important factors in causing these effects are dose, dose rate, and stage of gestation during irradiation.

Russell and Russell[15,16] divided the developmental period in utero into three stages. (1) *Preimplantation* is the time from fertilization to when the embryo attaches to the uterine wall. This period is about 9 days in human development. During this time the fertilized ovum repeatedly divides, forming a ball of cells that are highly undifferentiated. (2) *Organogenesis* begins after the embryo implants in the uterine wall at around day 9 of gestation. During this stage the cells of the embryo differentiate into the various stem cells that will eventually form the major organs of the body. This process continues for about 6 weeks, at which point the embryo is termed a fetus. (3) The *fetal stage* is the period during which growth of the formed structures takes place. At this stage the central nervous system (CNS) is developing. The CNS in adults consists of nondividing highly differentiated cells,

but in the fetus the cells forming the CNS are continually dividing, migrating, and differentiating. The neuroblasts appear by the 18th day of gestation in the human. As the fetus develops, the neuroblasts disperse throughout the body and become more differentiated. Neuroblasts continue to exist throughout fetal development of the CNS and until at least 2 weeks after birth. The CNS continues to develop until 10 to 12 years of age.[8] Much of the evidence for radiation effects on the embryo and fetus has been obtained from experiments in animals, notably mice. Therefore, it is useful to compare the time spans of gestational stages in mice and humans:

- Preimplantation: Mouse, 0 to 5 days; human, 0 to 9 days
- Organogenesis: Mouse, 5 to 13 days; human, 10 days to 6 weeks
- Fetal period: Mouse, 13 days to full term (20 days); human, 6 weeks to 9 months

Effects of Radiation: Animal Studies

The principal effects seen from irradiation of mice and rats are growth retardation, congenital malformations, and embryonic, neonatal, or fetal death.

Irradiation during the preimplantation period results in either embryonic death or normal development if the embryo survives. At this stage the cells of the conceptus are few and are not yet specialized. Damage to one cell, the progenitor of many descendant cells, has a high probability of being fatal; growth retardation or malformations are not seen at this stage of development. In mice, doses as low as 10 rad can kill a fertilized egg.[2]

Irradiation during early organogenesis produces severe growth retardation, seen as low birth weight at term. Animals can recover, however, and go on to attain full growth as adults. A dose of 100 rad will produce growth retardation. Another principal effect during this sensitive stage is the development of congenital anomalies. Some anomalies observed in mice are exencephaly (imperfect cranium with protrusion of the brain outside the skull), anencephaly (absence of a cranial vault and cerebral hemispheres), stunted development, and evisceration. Since various organs form on specific gestational days, irradiation on those days produces specific abnormalities. For example, radiation exposure of the mouse embryo on the 9th day results in a high frequency of ear and nose abnormality, whereas exposure on the 10th day results in bone abnormalities.[8] The neuroblasts in the fetus are highly undifferentiated, mitotically active, and highly radiosensitive if irradiated at this time. Some of the common abnormalities observed in mice after in utero irradiation are microcephaly (small brain), hydrocephaly (water on the brain), and eye deformities such as microphthalmia (small eyes).[8] A dose of 200 rad in mice during the period of maximum sensitivity 8 to 12 days after conception can result in a nearly 100% rate of malformations at birth. A 200 rad dose on day 10 after conception carries a 70% death rate because of gross fetal abnormalities.[2]

The fetal growth stage is less sensitive to radiation, because the organs are formed and cells are more differentiated. Higher doses are required to produce effects, mostly on formed organ systems. Any growth retardation at this stage, however, is permanent. Irradiation during this period may result in stochastic effects such as cancer later in life.

Effects of Radiation: Human Studies

Information about irradiation of humans in utero comes primarily from studies of Japanese atomic bomb survivors and exposure of pregnant women during medical procedures.

In Japanese survivors and their offspring, no birth defects were found as a result of irradiation before 15 days of gestation; this is consistent with animal data. That is, any

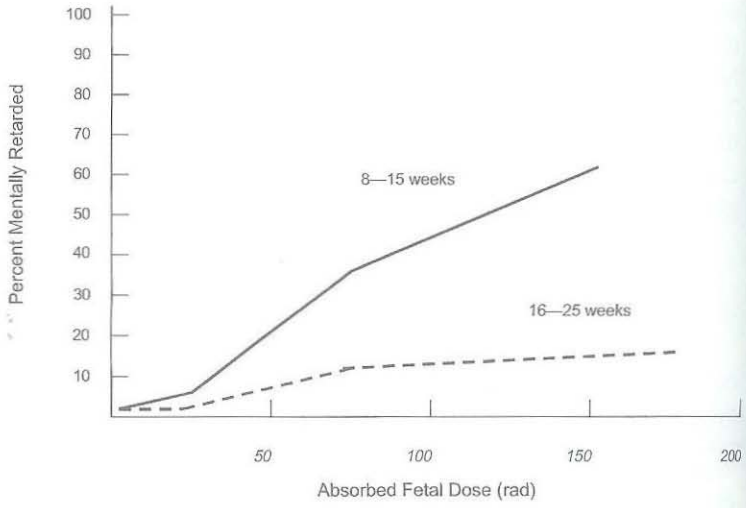

FIGURE 6-16 Frequency of mental retardation as a function of dose and gestational age from atomic bomb radiation exposure in utero. (Adapted from reference 17.)

damage that occurs during this stage will likely result in embryonic death. The embryos that escape damage develop normally.[2] The principal effects of irradiation in utero are microcephaly and mental retardation. The most pronounced microcephaly was seen with 150 rad of in utero exposure, but effects were also seen with maternal exposure of 10 to 19 rad.[2] Mental retardation was not observed to be induced by radiation before 8 weeks from conception or after 25 weeks.[1] During the most sensitive period, 8 to 15 weeks after conception, the fraction of those exposed who became severely mentally retarded increased by approximately 0.4 per sievert (i.e., approximately 40% of women exposed to 100 rem produced retarded offspring). For exposure during weeks 16 to 25, the risk is only one-fourth as great (0.1 per sievert).[1] Mental retardation is thought to be associated with decreased migration of cells from their place of origin to their site of function in the brain; the highest risk is during the gestational stage when the brain cortex is being formed.[2] Pooled data from Hiroshima and Nagasaki for children exposed at 8 to 15 weeks of gestation demonstrate that the dose–response relationship for mental retardation is linear, with a threshold of 12 to 20 rad (Figure 6-16).[16] This is consistent with the deterministic nature of retardation, which requires the killing of a minimum number of cells to be manifest.

Less severe mental retardation in children exposed to ionizing radiation before birth has been shown by intelligence test scores.[17,18] With exposure during the sensitive period 8 to 15 weeks after conception, the observed shift in IQ scores is about 30 IQ points per Gy (100 rad).

One of the first studies of medical exposure of pregnant women, demonstrating the adverse effects of x-irradiation in utero, was performed by Goldstein,[19] who reported microcephaly and mental retardation and other defects. Dekaban[20] surveyed the literature on abnormalities in children exposed to x-irradiation during various stages of gestation and reported several findings:

- Doses higher than 250 rad to the embryo before 2 to 3 weeks of gestation may cause embryos to abort but are not likely to produce severe abnormalities in fetuses that survive to term.
- Irradiation between 4 and 11 weeks of gestation may produce severe abnormalities of many organs, particularly in the skeleton and CNS.

- Irradiation between weeks 11 and 16 of gestation may cause a few eye, skeletal, and genital abnormalities and frequently causes microcephaly, retardation, and stunting of growth.
- Mild microcephaly, mental retardation, and growth stunting may result from irradiation during weeks 16 to 20 of gestation.
- After 20 weeks, the fetus is more radioresistant, but irradiation during this time may produce some functional defects.

Children who were exposed to radiation in utero seem to be susceptible to childhood leukemias and other cancers that are expressed during approximately the first decade of life.[1] Studies in England[21] and the United States[22,23] of x-ray exposure in utero and subsequent malignancies show an association between exposure and the subsequent development of childhood malignancies. Stewart and Kneale[21] performed an analysis of the Oxford Survey of Childhood Cancers. The survey analyzed 15,298 children. Fifty percent (7649) died of malignancy before age 10 (case group); of these, 1141 had been x-rayed in utero. There were 7649 children who did not die and were cancer-free (control group), and of these 774 had been x-rayed before birth. The case/control ratio of those who were x-rayed (1.48) was significantly greater than the ratio of those who were not x-rayed (0.95). The case/control ratio increased with fetal radiation dose from 1.26 with one x-ray exam to 2.24 for more than five exams. When the groups were stratified by trimester of irradiation, it was found that the case/control ratio was 8.25 in the first trimester, 1.49 in the second, and 1.43 in the third. Thus, the excess of cancer risk from x-ray examination in utero was directly related to fetal dose, and the risk of cancer was greatest when exposure occurred during the first trimester. Another way to analyze these data is to look at the rate of death from cancer of those x-rayed versus those not x-rayed. Of the 1915 children x-rayed, 1141 (59.3%) died of cancer, whereas of the 13,383 not x-rayed, 6508 (48.6%) died of cancer. This demonstrates a 22% increase in cancer death after x-ray exposure in utero.

Additional evidence that in utero irradiation causes childhood malignancy comes from a study that showed the same incidence of leukemia and other cancers in twins of irradiated women as in single children of such women, with a clear excess over children who were not exposed to radiation.[24] ICRP estimates that the risk of fatal childhood cancer due to prenatal exposure throughout pregnancy is 2.8×10^{-2} per sievert.[1] This corresponds to an excess over the spontaneous rate of 280 malignancies per 10,000 person-Sv.

NCRP recommends that the total dose to the fetus during gestation not exceed 0.5 rem, with a monthly limit of 0.05 rem.[25] Once pregnancy is declared, the duties of a radiation worker should be reviewed to ensure that this limit is not exceeded.

The most critical stage of gestational development for radiation-induced congential malformations, including microcephaly and mental retardation, extends from 10 days to 26 weeks. The data from Japan suggest a threshold of 12 to 20 rad for retardation. On the basis of this threshold, 10 rad is often considered the cutoff point above which an anomaly may occur in a child irradiated in utero.[2]

RADIATION-INDUCED CATARACT FORMATION

A cataract is an opacification of the normally transparent lens of the eye. Cataracts may be caused by aging, family history (genetic), medical problems such as diabetes, injury, medication such as steroids, and ionizing radiation. The lens contains cells that continue to divide and replenish the lens tissue. Radiation injures the dividing cells, making them nontranslucent. Accumulation of these injured cells leads to cataract development, which is a deterministic effect.

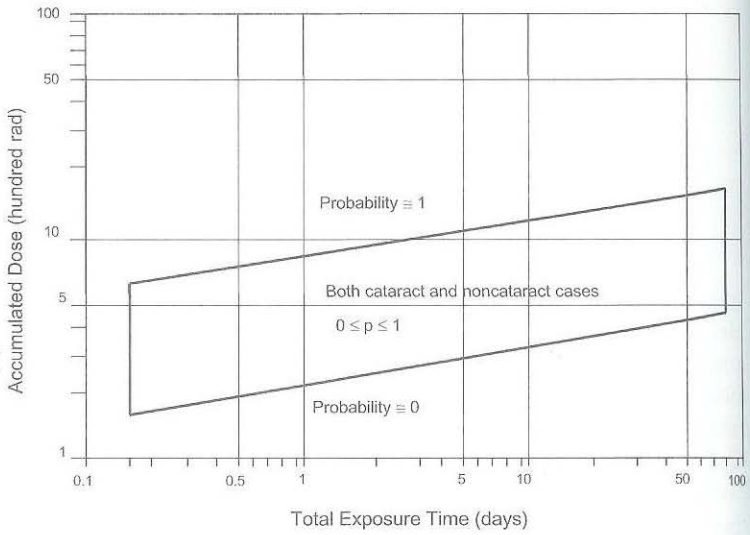

FIGURE 6-17 Time–dose relationship for cataract formation in humans. (Reprinted with permission of S. Karger AG, Basel, from reference 26.)

Radiation Injury to the Lens

Studies in humans, principally radiation therapy patients, and in animals have shown that ionizing radiation can cause cataracts.[26,27] A cataract may be stationary at a defined locus or it may progress to cloud a larger portion of the lens (progressive cataract).

The minimum dose required to produce a progressive cataract is about 2 Gy (200 rad) in a single exposure, with larger doses necessary in a fractionated regimen.[26] The latent period between irradiation and the appearance of lens opacity is dose related.[2] The latency period is about 8 years after exposure to a dose in the range of 2.5 to 6.5 Gy (250 to 600 rad). In one study of radiotherapy patients who had received low doses to the eye (220 to 650 rad), progressive cataracts developed in only about 12%, compared with 88% of those who received high doses (650 to 1150 rad).[2] Radiation-induced cataracts are a deterministic late effect. There is a practical threshold dose below which cataracts are not produced and above which the severity of the biologic response is dose related (Figure 6-17).

What are the potential risks for those who handle large amounts of activity, particularly ^{99m}Tc generator eluates? The following simple example provides some guidance on the amount of exposure possible and demonstrates the small probability of cataract induction from this type of exposure.

What time of exposure is required to accumulate 200 rad from the unshielded injection port on a ^{99m}Tc elution vial containing 7 Ci of activity?

$$\frac{7000 \text{ mCi} \times 0.8 \text{ R/hr/mCi/cm}}{60 \text{ min/hr}} = 93 \text{ R/min at 1 cm}$$

$$\frac{200 \text{ rad}}{93 \text{ R/min}} = 2.15 \text{ min at 1 cm from unshielded end of vial}$$

Applying the inverse square law we have

$$\frac{93\ \text{R/min}}{(30\ \text{cm})^2} = 0.1\ \text{R/min at 1 foot}$$

$$\frac{200\ \text{rad}}{0.1\ \text{R/min}} = 2000\ \text{min}\ (\sim 33\ \text{hr exposure required at 1 foot from unshielded end of vial})$$

REFERENCES

1. International Commission of Radiological Protection. *1990 Recommendations of the International Commission of Radiological Protection*. ICRP Publication 60. New York: Pergamon Press; 1991.
2. Hall EJ. *Radiobiology for the Radiologist*. 4th ed. Philadelphia: JB Lippincott; 1994.
3. Puck TT, Marcus TI. Action of x-rays on mammalian cells. *J Exp Med*. 1956;103:653-66.
4. Elkind MM, Whitmore GF. *The Radiobiology of Cultured Mammalian Cells*. New York: Gordon and Breach; 1967.
5. Bergonie J, Tribondeau L. De quelques resultats de la radiotherapie et essai de fixation d'une technique rationelle. *C R Acad Sci* (Paris). 1906;143:33-983.
6. Ancel P, Vitemberger P. Sur la radiosensibilite cellulaire. *C R Soc Biol*. 1925;92:517.
7. Casarett AP. *Radiation Biology*. Englewood Cliffs, NJ: Prentice Hall; 1968.
8. Travis EL. *Primer of Medical Radiobiology*. Chicago: Year Book; 1975.
9. Elkind MM, Sutton-Gilbert H, Moses WB, et al. Radiation response of mammalian cells in culture. V: Temperature dependence of the repair of x-ray damage in surviving cells (aerobic and hypoxic). *Radiat Res*. 1965;25:359-76.
10. Thames HD. On the origin of dose fractionation regimens in radiotherapy. *Semin Radiat Oncol*. 1992;2:3-9.
11. Meyer JL. Techniques and technology in the practice of radiotherapy. In: Fajardo L-G LF, Berthrong M, Anderson RE, eds. *Radiation Pathology*. New York: Oxford University Press; 2000:143-54.
12. Fajardo L-G LF, Berthrong M, Anderson RE, eds. *Radiation Pathology*. New York: Oxford University Press; 2000:43-51.
13. National Academy of Sciences. *Health Effects of Exposure to Low Levels of Ionizing Radiation*. BEIR V Report. Washington, DC: National Academy Press; 1990.
14. Stanbridge EJ. Suppression of malignancy in human cells. *Nature*. 1976;260:17-20.
15. Russell LB, Russell WL. Radiation hazards to the embryo and fetus. *Radiology*. 1952;58:369-76.
16. Russell LB, Russell WL. An analysis of the changing radiation response of the developing mouse embryo. *J Cell Physiol*. 1954;43(suppl 1):1030-1149.
17. Otake M, Schull WJ. In utero exposure to A-bomb radiation and mental retardation: a resssessment. *Br J Radiol*. 1984;57:409-11.
18. Otake M, Schull WJ, Fujukoshi Y, et al. *Effect on School Performance of Prenatal Exposure to Ionizing Radiation in Hiroshima*. RERF TR2-88. Hiroshima, Japan: Radiation Effects Research Foundation; 1988.
19. Goldstein L, Murphy DP. Microcephalic idiocy following radium therapy for uterine cancer during pregnancy. *Am J Obstet Gynecol*. 1929;18:189-95, 281-82.
20. Dekaban AS. Abnormalities in children exposed to x-irradiation during various stages of gestation: tentative timetable of radiation to the human fetus. *J Nucl Med*. 1968;9:471-7.
21. Stewart A, Kneale GW. Radiation dose effects in relation to obstetric x-rays and childhood cancers. *Lancet*. 1970;1:1185-8.
22. MacMahon B. Prenatal x-ray exposure and childhood cancer. *J Natl Cancer Inst*. 1962;28:1173-91.
23. MacMahon B, Hutchinson GB. Prenatal x-ray and childhood cancer: a review. *Acta Univ Int Contra Cancrum*. 1964;20:1172-4.
24. Harvey EB, Boice JD, Honeyman M, et al. Prenatal x-ray exposure and childhood cancer in twins. *N Engl J Med*. 1985;312:541-5.
25. National Council on Radiation Protection and Measurements. *Recommendations on Limits for Exposure to Ionizing Radiation*. NCRP Report No. 91. Bethesda, MD: National Council on Radiation Protection and Measurements; 1987.
26. Merriam GR, Szechter A, Focht EF. The effects of ionizing radiations on the eye. *Front Radiat Ther Oncol*. 1972;6:346-85.
27. Bateman JL, Bond VP. Lens opacification in mice exposed to fast neutrons. *Radiat Res*. 1967;7(suppl):239-49.

7 Licensing and Regulatory Control

Neil A. Petry

Radiopharmaceuticals are radioactive prescription drug products that are internally administered and intended for use in the diagnosis, treatment, and mitigation of disease. These unique drug products are required for the practice of nuclear medicine, the clinical and laboratory medical specialty that utilizes the measured nuclear properties of radioactive and stable nuclides in diagnosis, therapy, and research and in evaluating metabolic, physiologic, and pathologic conditions of the body.[1] The term radiopharmaceutical is also applicable to nonradioactive reagent kits and radionuclide generators intended for use in the preparation of radioactive drugs and radioactive biologic drug products used in nuclear medicine practice. However, the definition of radiopharmaceuticals does not include substances that contain trace quantities of naturally occurring radionuclides or sealed radionuclide sources intended for brachytherapy.

Because radiopharmaceuticals have both a drug component and a radioactive or nuclear component, the two federal agencies with major responsibility for licensing and regulatory control of radioactive drug products are the Food and Drug Administration (FDA) and the Nuclear Regulatory Commission (NRC). Other federal agencies, including the Occupational Safety and Health Administration (OSHA), the Environmental Protection Agency (EPA), and the Department of Transportation (DOT), primarily regulate the safe industrial production, handling, and transportation of radiopharmaceuticals, rather than issues related to their use in the course of medical or pharmacy practice.

Well-established legal precepts support the rights of states to regulate both the practice of medicine and the practice of pharmacy. Consequently, FDA authority over physicians and pharmacists and their use of drugs products, including radiopharmaceuticals, is attenuated at the state level. Exactly where federal and state authority intersect continues to be controversial. In contrast, NRC, through mutual agreement and with little controversy, most often delegates its authority to radiation control agencies within the various states.

This chapter focuses on issues related to the direct regulation of radiopharmaceuticals by FDA and NRC at the federal level. Before considering the specifics of federal regulation of radioactive drugs, the chapter presents an overview of the regulated products and practice environments, a brief introduction to existing nuclear pharmacy practice guidelines, and a historical perspective on drug regulations in general. The current regulatory framework should be viewed in the context of the evolution of nuclear medicine and nuclear pharmacy practice into vital components of today's high-quality health care systems.[2–7]

REGULATED PRODUCTS AND PRACTICE ENVIRONMENTS

Most of the radiopharmaceutical products used in nuclear medicine are procured from pharmaceutical companies that specialize in the manufacturing, marketing, and distribution of FDA-approved radioactive drug dosage forms. A majority of the radiopharmaceuticals

used clinically are small-volume parenterals; however, oral solutions and capsules, aerosols, gases, and other unique dosage forms are also important. Some of these manufactured radiopharmaceutical products are provided as finished dosage forms ready to be dispensed for patient administration. However, most of the radiopharmaceutical products used in nuclear medicine must be prepared or compounded by a variety of methods just before administration to the patient, largely because of their short physical half-life (i.e., rapid radioactive decay of the radionuclide component) and in some cases because of limited radiochemical stability (i.e., dissociation of the radionuclide from the drug or molecular component).

Usually, radiopharmaceuticals are prepared by nuclear pharmacists practicing in community-based, centralized (i.e., commercial) nuclear pharmacies. Less frequently, they are prepared in hospital pharmacies or institutional nuclear medicine departments. In all practice settings, nuclear pharmacists strive to provide patient-specific unit doses of the highest quality. This typically requires a professional support staff that often includes pharmacy technicians.

Centralized nuclear pharmacies provide service to most hospitals and private clinics offering nuclear medicine services. Large medical institutions typically have an in-house nuclear pharmacy service to facilitate clinical research with both FDA-approved and investigational radiopharmaceutical products. Thus, nuclear pharmacy services are widely available in almost all practice settings and geographic areas. Occasionally, however, nuclear medicine technologists may perform the basic pharmacy function under the direct supervision of a qualified nuclear medicine physician. This arrangement is still permissible in any clinical practice setting, as it constitutes the practice of medicine. Usually, however, centralized unit dose radiopharmaceutical services are used because this is more economical in terms of personnel and cost. Regardless of the model used for providing radiopharmaceutical services, it is important that hospital pharmacy directors be aware of their responsibility for monitoring all drug product use in their institutions, including use in the nuclear medicine department. A basic understanding of the associated licensing and regulatory controls, as summarized here, will be useful in that regard.

NUCLEAR PHARMACY PRACTICE GUIDELINES

The American Pharmacists Association's *Nuclear Pharmacy Practice Guidelines* are well established.[8] They supplement competency-based pharmacy practice standards and identify those areas of responsibility that are unique to nuclear pharmacy. In addition to functioning as standards for nuclear pharmacy practitioners, the guidelines provide a practice-oriented foundation for the competency-based Board of Pharmaceutical Specialties (BPS) certification exam.[9] These standards may also be useful to nuclear medicine physicians and technologists involved in the clinical use of radiopharmaceuticals; however, the standards are not intended to govern the practices of those individuals. Many of these standards of practice are derived from current regulations governing the medical use of both drugs and radioactive materials; thus, there may be specific legal requirements for the activities described.

Nuclear pharmacy practice is a basic patient-oriented pharmaceutical service that embodies the scientific knowledge and professional judgment required to improve and promote health through assurance of the safe and efficacious use of radioactive drugs for diagnosis and therapy.[8] The most readily identifiable areas of responsibility, or domains, that constitute the practice of nuclear pharmacy are the procurement, compounding, quality control, dispensing, and distribution of radiopharmaceuticals and pharmaceutical drug products used in nuclear medicine. Additional domains of responsibility include

health and safety, provision of information and consultation, monitoring patient outcome, and research and development.

Nuclear pharmacists work in a variety of practice settings; therefore, their responsibilities may vary significantly. For example, a nuclear pharmacist working in a centralized facility dedicated primarily to the procurement, compounding, quality control, dispensing, and distribution of unit dose radiopharmaceuticals may have a set of regulatory responsibilities that differ substantially from those of the clinical nuclear pharmacist providing service in an institutional medical center where distribution may not be undertaken at all. On the other hand, the institution-based nuclear pharmacist invariably bears responsibility for regulatory issues associated with the use of radiopharmaceuticals in clinical research and drug development projects. Regardless of practice setting, nuclear pharmacists must be knowledgeable about the many regulations governing each domain of responsibility. Furthermore, nuclear pharmacists may supervise a variety of individuals who assist in the provision of these specialized pharmacy services, so they are responsible for the activities of all such support personnel and for ensuring that they are appropriately trained and credentialed.

DRUG REGULATION: HISTORICAL PERSPECTIVE ON FDA

Current regulations on the medical use of drug products, including radiopharmaceuticals, can best be understood in the context of a series of federal regulatory actions over the past 100 years. A 2003 book by health and science reporter Philip J. Hilts[10] tells the fascinating story of FDA's maturation from its start in the Teddy Roosevelt administration through various crises and triumphs to the deregulatory climate of more recent years. With its many references and annotations, the book is a useful guide to understanding the inner workings of FDA and how the agency regulates food and drug products in the United States.

Until the early 1900s, a plethora of largely unregulated patent medicines of questionable value and safety were sold to the public. The Pure Food and Drugs Act of 1906 was signed into law as a result of unscrupulous manufacturing practices, adulterated foods and drugs, and unfounded claims of the therapeutic efficacy of patent medicines. The act prohibited interstate sales of misbranded and adulterated foods and drugs and paved the way for the establishment of FDA in 1931. The Act did not, however, require premarket testing of drugs to determine their safety. When 107 people died after ingesting sulfanilamide elixir formulated with diethylene glycol, a substance now known to be toxic to both humans and animals, revisions in the 1906 act culminated in passage of the federal Food, Drug, and Cosmetic Act (FDCA) of 1938.

FDCA is the basis of drug regulation in the United States today, and a working knowledge of this law is important for ensuring regulatory compliance of drug use in any clinical setting, including nuclear medicine practice. FDCA is both simple and complex.[11] It is simple in that it specifies only three illegal acts: adulteration, misbranding, and the placing of unapproved drug products into interstate commerce. At the same time, it is complex because many activities are included under the umbrella of these three illegal acts. When challenged to explain why something known to be illegal is in fact illegal under FDCA, stating that the activity is adulteration, misbranding, or the placing of an unapproved new drug into interstate commerce is a safe response. As passed in 1938, FDCA required premarket testing of new drugs for safety and presentation of safety data to FDA prior to approval of a new drug product for marketing. The act also eliminated the requirement for FDA to prove intent to defraud in drug misbranding cases.

In 1962, the Kefauver-Harris amendments to the 1938 FDCA increased federal control over methods of production and testing of drugs before their release for purchase by the

public. The emotional impetus for these amendments came from another medical tragedy. An FDA medical officer, Frances Kelsey, blocked marketing approval of the drug thalidomide because of unexplained adverse effects; the subsequent discovery that thousands of deformed infants had been born to mothers in Europe and South America who had taken this supposedly safe sleeping pill during pregnancy caused Congress to vote for strong new drug controls in 1962. The most important change was the requirement that the efficacy of a new drug, as well as its safety, be established by "substantial evidence" before marketing approval. Among several new concepts contained in the amendment, the most important were investigational new drug (IND) procedures and procedures for the approval of a new drug application (NDA) prior to marketing of the product.

RADIOISOTOPE REGULATION: HISTORICAL PERSPECTIVE ON NRC

The potential medical significance of radioisotopes was well recognized before World War II; nevertheless, the distribution of these radioactive materials was unregulated by the government.[12] Then, in 1942, the Manhattan Project was initiated by the United States Army to conduct atomic research for the purpose of providing new technology to facilitate an end to World War II. The postwar program for radioisotope distribution grew out of the Manhattan Project Isotopes Division, which during the war years had developed top technical expertise for producing and handling radioisotopes at the division's facilities in Oak Ridge, Tennessee. In 1946, the Manhattan Project formally publicized its groundbreaking program for distribution of radionuclides for peaceful research purposes. This new radioisotope distribution program for the first time placed nominal constraints on the procurement of radionuclides for research. Thus, radionuclides for medical research could not be ordered casually; an application for each proposed purchase had to be submitted, reviewed, and approved. A special subcommittee had to review and approve each application for human medical use.

Subsequently, with congressional passage of the Atomic Energy Act of 1946, the authority to continue radioisotope research was transferred from the Army to the United States Atomic Energy Commission (AEC). The Atomic Energy Act gave AEC exclusive governmental control over atomic research and the development of related technologies. The existing AEC radioisotope distribution review subcommittee was then renamed the Subcommittee on Human Applications. On June 28, 1946, the subcommittee held its first meeting, during which a system of local isotope committees was recommended. According to the recommended action plan, each local committee would include (1) a physician well versed in the physiology and pathology of the blood-forming organs, (2) a physician well versed in metabolism and metabolic disorders, and (3) a competent biophysicist, radiologist, or radiation physiologist qualified in the techniques of radioisotopes. By October 1946, radioisotope distribution was well under way, with over 200 radioisotope requests received, reviewed, and approved. Of those approved, nearly 100 were for use in medical research in humans. In 1959, the subcommittee was absorbed into the Advisory Committee on Medical Uses of Isotopes.

As the subcommittee gained experience in developing specific procedures for review and approval of a variety of radioisotope applications, it began to recognize that only a few of the requests for radioisotope use represented unusual cases; most applications were routine and did not require continuous review. The subcommittee delegated review of the routine radioisotope applications to the AEC Isotopes Division, and the Isotopes Division developed a procedure whereby an individual wishing to procure byproduct material had to file an application and receive an Authorization for Radioisotope Procurement prior to obtaining and using byproduct materials. This authorization functioned in much the same way as a license for a byproduct material does today. In 1951, an additional technical

adjustment was made to the approval process with the introduction of "general authorizations" that delegated more authority to local radioisotope committees of approved research institutions. As a result, research institutions possessing general authorizations could for the first time obtain specified radioisotopes for approved purposes pursuant to filing a single application each year, thus eliminating the need to file a separate application for each radioisotope order.

During the 1950s a series of regulatory changes affected many administrative procedures governing radioisotope use. In 1954, licensing and regulation were added to AEC's authority. Concerns about radioisotope procedures were disseminated through various communications made public by the Isotopes Division. Throughout the 1960s and early 1970s, administrative procedures governing the licensing and regulation of radioisotope use continued to evolve. In 1975, as a result of congressional passage of the Energy Reorganization Act of 1974, a major change was implemented when AEC was split into the Energy Research and Development Administration, which later became the Department of Energy, and the Nuclear Regulatory Commission.

At several junctures during the development of procedures for licensing and regulating byproduct material intended for medical use, these government units published official circulars or guidance documents for use by the regulated community. A guidance document published in 1948 was only a few pages long and was simple to comprehend and follow. By 1957, that initial guidance was replaced by a 26 page AEC document entitled The Medical Use of Radioisotopes—Recommendations and Requirements. Then in 1965, AEC published its Guide for the Preparation of Applications for the Medical Use of Radioisotopes, followed in 1980 by NRC Regulatory Guide 10.8, entitled Guide for the Preparation of Applications of Medical Programs.[13] Many additional changes in NRC regulations and licensing guidance have occurred since Regulatory Guide 10.8, including major revisions to Title 10 of the Code of Federal Regulations (CFR), Parts 20 and 35, and publication of NUREG-1556, Volume 9, entitled Consolidated Guidance About Material Licenses: Program-Specific Guidance About Medical Use Licenses.[14] Most important, NUREG-1556 provided valuable guidance on the recently revised 10 CFR 35 rule.

REGULATORY CONTROL OF RADIOPHARMACEUTICALS

The regulation of radiopharmaceuticals has a complicated history. The 1938 FDCA applied to all drugs, including radiopharmaceuticals, which were a unique and promising new class of products. Six years later, the Public Health Services Act of 1944 authorized the FDA Bureau of Biologics to regulate radioactive biologic drug products. However, because of their unique radioactive properties, radiopharmaceuticals were also under the control of AEC. During these formative years of nuclear medicine, radiopharmaceuticals were controlled chiefly by AEC. The 1954 Atomic Energy Act authorized AEC to license the possession, use, and transfer of byproduct material (i.e., radioisotopes produced in a nuclear reactor).

In 1963, after enactment of the Kefauver-Harris amendments, FDA began implementing IND procedures and requirements. These posed a substantial threat to the availability of radiopharmaceuticals and the emergence of nuclear medicine practice as a clinical specialty. FDA began to recognize both the potential clinical value of radiopharmaceuticals and the possibility that their safety and efficacy were not adequately controlled by the agency as required for all drugs by the 1962 FDCA amendments. Fortunately, AEC regulatory controls were adequate to ensure radiation safety in the possession, use, and transfer of radioactive materials for medical use. However, FDA's overriding concern related to the medical safety and efficacy of radioactive drugs once administered to patients. FDA also had to come to terms with the fact that, as an agency, it was not prepared to be the

sole regulator of radioactive drugs. The immediate problem was addressed in 1963 when FDA allowed a temporary exemption for radioactive new drugs and biologics from the IND regulations, provided these agents were distributed in complete compliance with existing AEC regulations.[15] The main purpose of the temporary exemption was to allow the continued availability of radioactive drugs manufactured from reactor-produced radionuclides until FDA and AEC could reach agreement on the establishment of effective regulations that would minimize unnecessary duplication of regulatory control. The exemption did not include naturally occurring or accelerator-produced radionuclides. The temporary exemption was rescinded, in part, on November 3, 1971, when FDA actively entered the regulatory arena by publishing NDA requirements for radioactive drugs.[16] The new regulations, as outlined in 21 CFR 310.503, identified specific reactor-produced radioisotopes that for certain stated uses were no longer exempt from the new drug regulations because they were considered well-established drugs in nuclear medicine practice. Both FDA and AEC concluded that it was inappropriate for these radioactive drugs to be distributed under a claimed IND exemption when they were clearly intended for routine clinical use.[16] Therefore, manufacturers and distributors of these drug products were required to submit adequate evidence of safety and effectiveness for use as recommended in the product labeling.

During the regulatory transition period that followed, radiopharmaceutical manufacturers were allowed to distribute only those radioactive drug products for which FDA had approved an NDA or biologic product license or accepted an IND application. Accordingly, 52 NDAs for radiopharmaceuticals alone were submitted and approved by FDA between 1971 and 1975, compared with a total of 31 drug (pharmaceutical) NDA approvals between 1951 and 1970.[17] On July 25, 1975, FDA issued a final rule that totally revoked the 1963 IND exemption and placed radiopharmaceuticals completely under FDA regulatory authority, as are all other drug products.[18]

Another regulatory milestone was reached on January 19, 1975, when NRC and the Energy Research and Development Administration (which later became the Department of Energy) superseded AEC under the Energy Reorganization Act of 1974. Thus, NRC is now responsible for all licensing and regulatory functions originally assigned to AEC by the Atomic Energy Act of 1954 as amended. Even though NRC's authority covers radioactive drug products containing reactor-produced byproduct materials, it does not include the regulation of such products that contain naturally occurring or accelerator-produced radionuclides, because these two categories are regulated by the states.

In most cases NRC has transferred its authority to control the use of reactor-produced material to individual "agreement" states. Currently, there are 32 agreement states, 14 "nonagreement" states, and 2 states that have filed letters of intent with NRC to become agreement states.[19] (The District of Columbia is treated as a nonagreement state.) Under the current regulatory scheme, the agreement states regulate both reactor- and accelerator-produced radioactive materials, the nonagreement states regulate only accelerator-produced materials, and NRC regulates only reactor-produced materials. It is important for nuclear pharmacists to understand how this regulatory scheme applies to a wide variety of medical and pharmacy practice settings.

REGULATORY AUTHORITY OF FDA AND NRC

After the termination of the 1963 exemption for radiopharmaceuticals from IND regulations, FDA stated that it would regulate the safety and efficacy of radioactive drugs with respect to patients. At the same time, NRC withdrew from regulating radioactive drug safety and efficacy and stated that it would regulate the radiation safety of workers and the general public.

1979 NRC published the following three-part policy statement that it developed to the regulation of medical uses of radioisotopes (44 FR 8242, effective February 9,

NRC will continue to regulate the medical uses of radioisotopes as necessary to provide for the radiation safety of workers and the general public.
NRC will regulate the radiation safety of patients where justified by the risk to patients and where voluntary standards or compliance with these standards is inadequate.
NRC will minimize intrusion into medical judgments affecting patients and into other areas traditionally considered to be part of the practice of medicine.

policy states further in 44 FR 8242 that

The NRC intends not to exercise regulatory control in those areas (regarding patients) where, upon careful examination, it determines that there are adequate regulations by other Federal or State agencies or well administered professional standards. The Commission recognizes that the FDA regulates the manufacture, interstate distribution, investigational, and research use of drugs, including radiopharmaceuticals, but does not have authority to restrict the routine use of drugs to the procedures (described in the product labeling) that the FDA has approved as safe and effective. The NRC sees itself as the only Federal Agency that is currently authorized to regulate the routine use of radioactive drugs from the standpoint of reducing unnecessary radiation exposure to patients.

REGULATION OF POSITRON EMISSION TOMOGRAPHY DRUGS

itron emission tomography (PET) drugs are by definition radiopharmaceuticals that e a radionuclide component consisting of a short-lived positron-emitting radioisotope. most common positron emitters currently used in the production of PET drugs are . ^{13}N, ^{15}O, and ^{18}F; however, there are longer-lived positron emitters that may be used clinical PET imaging in the near future. PET radiopharmaceuticals are discussed in ail in Chapter 10 of this book.

The development of a suitable regulatory framework for PET drugs and the associated aging technology has been quite challenging, owing to the unique nature of PET as a dical imaging technology and the attempts of the federal government to apply regulory policy devised for other, and often quite different, applications of medical technoly. The struggle to regulate PET drugs and imaging technology and the emerging regitory framework have been well documented. In 1998 Keppler and associates[20] blished an excellent case study on PET regulation. The authors provide valuable theoical perspective on why regulations exist, as well as analysis of why regulation of the aturing PET industry has unfolded as it has. The insights provided in that article will pport efforts to expand clinical PET and introduce new imaging technologies into health re. The section of the article that summarizes the history of PET regulation is included re, with permission. (To facilitate identification of the regulatory documents cited in the iginal publication, the reference numbers have been edited to correlate with the reference t provided at the end of this chapter.)

Before 1975, the Food and Drug Administration (FDA) had delegated the regulation of the radiopharmaceutical industry to the Nuclear Regulatory Commission. When

the FDA asserted its jurisdiction in 1975, it chose to regulate the industry substantially the same way as the traditional drug industry. Therefore, the FDA began evaluating new drugs—that is, radiopharmaceuticals—through investigational drug applications. New drugs then were approved for use on the basis of sufficient information provided in new drug applications.[21] The FDA would then enforce current good manufacturing practices for production of the approved drug to ensure quality. Early on, however, it was clear that the short half-lives of many of the PET and other radiopharmaceuticals limited the traditional application of production and manufacturing regulations.

In the late 1970s, the FDA established a subcommittee to evaluate the special circumstances of these short-lived radiopharmaceuticals. Exemption from manufacturing regulations at the site of final use was considered for sites qualifying as a nuclear pharmacy or a medical facility under the provisions of the Durham-Humphrey amendment to the Food, Drug and Cosmetic Act. Thus, facilities preparing radiopharmaceuticals could operate under these provisions, eliminating the need to register with the FDA as a drug manufacturer for these activities. The report detailing the exemption requirements, titled "Nuclear Pharmacy Guideline: Criteria for Determining When to Register as a Drug Establishment" (Nuclear Pharmacy Guidelines), was adopted by FDA in 1984.[22] These guidelines not only covered production activities for traditional nuclear medicine isotopes but also described activities consistent with the preparation of PET isotopes.[22] The activities detailed affirmed the practice of medicine and pharmacy.

In the 1980s, the concept of the "clinical" PET center developed because of the promise of clinical usefulness shown with early trials of F-18 fluorodeoxyglucose (FDG). At about the same time, the health care industry was in the midst of transition. Hospitals were concerned about reductions in revenues because of Medicare Diagnostic Related Group payment schemes and managed care. Private sector insurance providers were faced with a rapidly rising cost base and were cutting reimbursement rates. The capital commitment ($5–$7.25 million) required to develop a clinical PET center made PET an unlikely venture for hospitals fearing the future contraction of the industry.[23] Furthermore, the revenues that could be proposed to offset the more than $2 million per year in operating expenses were viewed as risky in part because its regulatory path and reimbursement potential remained unclear.[23,24]

Many of those attending to these early clinical activities proposed using the Nuclear Pharmacy Guidelines and the practice of medicine and pharmacy as the basis for operations at the new or planned clinical centers. Concern centered only on isotope approvals because PET scanners and the subsequently developed dual-use or coincidence imaging devices received FDA clearance for marketing as "PET devices," grandfathered in with changes in device regulations. The concept of the practice of medicine and pharmacy would allow a fast-track mechanism for clinical utilization of these new PET compounds. Many in the physician and pharmacist communities believed rationale existed for this approach, citing case law, the amendments to the Food, Drug and Cosmetic Act, as well as the Nuclear Pharmacy Guidelines and other FDA publications in support of the exemption for drugs not intended for interstate commerce.[24] But as Coleman et al. pointed out, the FDA contended then—and now—that the practice of medicine and pharmacy cannot be applied to unapproved drugs.[24] The physician and pharmacist communities' assertion that the practice of medicine and pharmacy should be the course of regulations did not convince many hospitals to invest in this new technology.

Industry representatives recognized that clarification of the regulatory, and thus the reimbursement pathway for PET, was essential to commercial growth. A dialogue was initiated with the FDA, ostensibly to seek clarification of their position. A less visible, but nonetheless plausible, concern of industry may have been that if the FDA did not regulate the end drug, then it might instead regulate the equipment used to produce the isotopes.

In 1989, members of the PET industry reached consensus with the FDA on a mechanism to regulate PET; the end users would develop new drug applications for all PET radiopharmaceuticals. At that time, the user community did not want the responsibility of organizing the data to obtain FDA approval, nor were prospective data on the clinical use of PET available to submit for evaluation. Moreover, the community feared that the costs of filing the new drug applications as well as bringing operations in line with manufacturing guidelines would be prohibitive, limiting the clinical proliferation of the technology. Despite appeals from the user community that an alternative approach be devised, the FDA began laying out its plan for regulation. The FDA had little rationale to change its course. Individual cyclotron sites would be expected to obtain new drug applications or abbreviated new drug applications (the generic equivalent) and register as drug manufacturing sites. In exchange for agreeing to their regulatory method, the FDA promised to consider retrospective data in their review of the drug master file, to review the data expeditiously, and to develop modifications of drug manufacturing guidelines so they would be better suited to PET. The FDA clearly stated their position: the practice of medicine and pharmacy would not be an acceptable method of practice; it could be used only until the initial new drug application was approved.

That the user community would be forced to comply with the FDA's plans was clear by 1991. It was believed that the Health Care Financing Administration would not act on a petition for PET reimbursement until FDG was approved, which led to a continued lack of Medicare reimbursement. Therefore, the Institute of Clinical PET, with funding from industry, led efforts to develop a single drug master file for FDG. With the continued support of industry and the diligent efforts of members of the community, a single PET site in Peoria, IL, filed a new drug application in 1992.

Neither the clinical drug master file nor the new drug application was reviewed expeditiously, as promised. Additional prospective data reaffirming earlier conclusions were required. Finally, the FDA approved the efficacy of FDG for a single application (epilepsy) and, in 1994, the new drug application from the Peoria PET facility. The FDA published a notice in the [*Federal Register*] in February 1995, which detailed the process that sites should follow in filing their own new drug applications or abbreviated new drug applications. An approved status for sites would be required or sites would face closure, a stance the FDA may have believed necessary because of the degree of opposition already expressed by the community.

Fluorine-18-fluorodeoxyglucose was now approved by the FDA, but Medicare reimbursement was still not forthcoming. In fact rubidium-82, previously approved by the FDA, at that time still had not been approved for coverage by the Health Care Financing Administration. The status of FDA approval for PET did not bring the reimbursement hoped for. Moreover, the technical requirements placed on the Peoria facility by compliance with the new drug application and the FDA's manufacturing requirements were stringent and required substantial additional operating monies to sustain. The community and industry had serious concerns whether, as now required by the FDA, PET sites could file abbreviated new drug

Finished Pharmaceuticals: Positron Emission Tomography" published in the *Federal Register* on April 22, 1997.[27–29] The rescission was published December 19, 1997, in the *Federal Register*.[30,31] Effectively the legislation reverts regulatory guidelines to those provided in the 1984 Nuclear Pharmacy Guidelines until new guidelines are established. In the interim, *United States Pharmacopeia* standards are to be met for drugs to be considered unadulterated.

Most importantly, a new Medicare approval process also resulted from the political efforts. Despite lack of FDA approval, the Health Care Financing Administration agreed that Medicare would begin to cover PET scans for characterization of solitary pulmonary nodules and initial staging of lung cancer as of January 1, 1998. It was agreed that a fast-track review of several other indications for PET, including evaluation of brain tumors, myocardial viability, colorectal cancer, head and neck cancer, Hodgkin's lymphoma and ovarian cancer, would be initiated over the next 18 months.

In late May 1998, although the prescribed regulatory process had not started in earnest, discussions between the PET community and the Health Care Financing Administration (HCFA) were under way to seek broader approval for use of ^{18}F-fludeoxyglucose (^{18}F-FDG, previously referred to as ^{18}F-fluorodeoxyglucose) in oncology, neurology, and cardiology applications. As a result of the persistent collaborative efforts between the PET community and HCFA, PET imaging reimbursement approvals have been dramatically expanded over the past 5 years.[32] (HCFA was renamed the Centers for Medicare and Medicaid Services [CMS] in 2000.[33]) The reimbursement approvals have allowed clinical PET to grow substantially. More than 95,000 PET procedures were performed in the United States during the fourth quarter of 2002, up 70% from the fourth-quarter 2001 estimate of 55,800 procedures.[34] Although the use of PET imaging in routine health care is expanding rapidly, significant regulatory issues persist.

As required by the FDA Modernization Act of 1997 (FDAMA), representatives from the Institute of Clinical PET (ICP), United States Pharmacopoeia (USP), Society of Nuclear Medicine (SNM), and Council on Radionuclides and Radiopharmaceuticals (CORAR) have maintained a continuing collaborative dialogue with FDA in an attempt to define the future approval process and requirements for all radiopharmaceuticals.[26] FDAMA gave FDA 2 years, and not more than 4 years, from November 1997 to establish new guidelines for the manufacture of PET drugs. The implied FDA deadline of November 2001 has passed, and the agency has not finalized such new guidelines. Consequently, the PET community continues to prepare PET drugs according to applicable USP standards without being required to file NDAs or abbreviated new drug applications (ANDAs) with FDA. However, when the new FDA guidelines are published as a final rule in the *Federal Register*, the medical community will have 2 years to bring itself into compliance with the new regulations. Concerted efforts have been made to develop standards for regulating PET drug production sites that take into account the genuine differences between commercial production centers and nonprofit hospitals compounding PET drugs for on-site use; however, FDA has consistently resisted, and these important differences will probably be overlooked in the final rule. Clearly, there are still many regulatory issues to be resolved regarding the production and clinical use of PET drugs, and the PET community must continue to monitor regulatory developments and prepare for compliance in the near future. It is particularly important that nuclear pharmacists monitor new developments in the regulation of PET drugs. Descriptions of the current IND, NDA, and ANDA submission processes are available on FDA's Web site.[35–37]

ROLE OF FDA IN PUBLIC HEALTH PROTECTION

FDAMA (Public Law 105-115) affirmed FDA's public health protection role and defined the agency's mission as follows: (1) to promote the public health by promptly and efficiently reviewing clinical research and taking appropriate action on the marketing of regulated products in a timely manner; (2) with respect to such products, to protect the public health by ensuring that foods are safe, wholesome, sanitary, and properly labeled; human and veterinary drugs are safe and effective; there is reasonable assurance of the safety and effectiveness of devices intended for human use; cosmetics are safe and properly labeled; and public health and safety are protected from electronic product radiation; (3) to participate through appropriate processes with representatives of other countries to reduce the burden of regulation, harmonize regulatory requirements, and achieve appropriate reciprocal arrangements; and, (4) as determined to be appropriate by the Secretary, carry out items (1) through (3) in consultation with experts in science, medicine, and public health, and in cooperation with consumers, users, manufacturers, importers, packers, distributors, and retailers of regulated products.

FDA's public health protection role as defined in FDAMA is extremely broad. With respect to the practices of medicine and pharmacy, the essence of the FDA mission is to ensure the safety and efficacy of marketed drugs and medical devices. The process by which this mission is achieved is authorized by Congress; formalized by codes, regulations, and guidelines; and interpreted and implemented by scientists, lawyers, biostatisticians, engineers, and project managers of varied backgrounds.[38] Thus, FDA plays a significant role in the development and approval of all radiopharmaceuticals in clinical use. FDA's Center for Drug Evaluation and Research regulates formats for clinical trials and review of radiopharmaceuticals prior to their approval for marketing.

INVESTIGATIONAL NEW DRUG PROCEDURES FOR RADIOPHARMACEUTICALS

From the viewpoint of FDA, a "new drug" may be a new molecular (i.e., chemical) entity that requires proof of safety and efficacy for its intended clinical use (i.e., an investigational new drug) or a known entity that has been recently shown to be safe and efficacious for an intended clinical use (i.e., an approved new drug). A new drug may also be a new dosage form or new route of administration for an old drug (i.e., an approved drug that has been marketed or sold on a prescription basis for a significant period of time), or an old drug being used for a new clinical indication or purpose. Situations involving new forms, routes, or uses of approved drugs occur only occasionally in clinical nuclear medicine practice.

Before 1962, there was no requirement to notify FDA that drugs were being tested in humans. However, since the 1962 FDCA amendments, new drugs lacking NDA approval and intended for investigational use in human subjects may not enter into interstate commerce (commercial distribution) unless a responsible individual or a pharmaceutical company sponsors well-controlled, scientifically designed safety and efficacy studies under an FDA-accepted IND application (referred to simply as an IND). FDA authorization must be secured in advance of the interstate shipment and administration of the new drug to humans enrolled in the planned clinical studies.

The applicant, or "drug sponsor," is the person or entity that assumes responsibility for the marketing of a new drug, including responsibility for compliance with applicable provisions of FDCA and all related regulations. The sponsor is typically an individual, partnership, corporation, government agency, manufacturer, or scientific institution. In many medical practice settings, including nuclear medicine, there is frequently no drug

company interested in sponsoring and conducting important clinical investigations; therefore, the sponsor may be an institution-based physician, who is referred to as the "physician-sponsor" or "investigator-sponsor." As an alternative, the investigator-sponsor may be a clinical radiopharmacologist or nuclear pharmacist qualified by training and experience in the evaluation of new radioactive drug products.

PRECLINICAL RADIOPHARMACEUTICAL STUDIES

In the earliest phase of development of a radioactive drug product, data from animal studies and data on manufacturing and quality control are collected and summarized for eventual inclusion in an IND if the drug shows promise for use in humans. The data must clearly establish that the radioactive drug is reasonably safe for administration to human subjects during the proposed clinical trials. Additionally, the actual procedures and methods used for generating and gathering the preliminary safety data must be described in detail. Preclinical studies are conducted in relevant animal models to assess the drug's relative safety rather than its efficacy, although some potentially relevant efficacy data may be obtained. Characterization and quantification of the radiochemical and radionuclidic purity of the radioactive drug are essential for the evaluation of radiation dosimetry; any trace radiocontaminants (including daughter radionuclides) and altered chemical forms that might significantly influence biodistribution and radiation absorbed dose estimates must be identified. Preclinical studies usually include studies of both biodistribution and toxicity in animals. Animal biodistribution studies are used to determine normal organ distribution patterns, assess translocation, and identify the routes and extent of radiopharmaceutical excretion. These data are essential for obtaining meaningful radiation absorbed dose estimates, the principal measure of radiopharmaceutical safety. Animal toxicity studies usually focus on the potential chemical toxicities of components other than the radionuclide, since only trace amounts of the radioactive element are typically present. Acute toxicity tests are usually required in at least two animal species to determine the acute LD_{50} (amount sufficient to kill 50% of a population of animals) and to demonstrate the lack of acute toxicity at doses several orders of magnitude higher on a dose-per-kilogram basis than those proposed for human studies using the same route of administration. Subacute toxicity testing over a 2 to 3 week period in two animal species, a rodent and a nonrodent, at several dosage levels is required to demonstrate adequate safety margins relative to equivalent maximum clinical dosage. Chronic toxicity studies are typically not required for radiopharmaceuticals, which are administered on a one-time basis to most patients.

Investigators may obtain the required data from their own experiments, but gathering the data can be quite challenging, costly, and time consuming. It may be advantageous to use data from the literature or other valid sources when possible, if the investigator can demonstrate that those data are applicable to the drug product under consideration (i.e., similar dosage form, same route of administration).

RADIOACTIVE DRUG RESEARCH COMMITTEE STUDIES

Limited use of radioactive drug products in human research subjects prior to FDA acceptance of an IND is allowed under specific conditions set forth in 21 CFR 361.1. Radioactive drugs, as defined in 21 CFR 310.3(n), are generally recognized as safe and effective when administered to human research subjects, under the conditions set forth in 21 CFR 361.1(b), during the course of a research project intended to characterize the basic pharmacodynamic and pharmacokinetic properties of the radioactive drug product. Data regarding

the metabolism (including kinetics, distribution, and localization) of the radioactive drug or regarding human physiology, pathophysiology, or biochemistry are extremely valuable. However, such studies must not be intended for immediate therapeutic, diagnostic, or similar purposes or intended to determine the safety and effectiveness of the radioactive drug in humans. In other words, an investigator must not have clinical intent regarding the medical care of subjects receiving the radioactive drug or carry out a clinical trial under this set of regulations. Certain basic research (e.g., studies to determine whether a drug localizes in a particular organ or fluid space and to describe the kinetics of that localization) may have eventual diagnostic or therapeutic implications; however, the initial studies are considered basic research within the meaning of this specific set of regulations.

Before these limited human studies are conducted, approval must be obtained from a local or contract radioactive drug research committee (RDRC). The RDRC is composed and approved by FDA in accordance with the regulations set forth in 21 CFR 361.1(c) that govern committee membership, function, reports, approvals, and monitoring responsibilities. Under the section describing reports that the RDRC must provide to FDA, there is an important federal control point regarding the number of research subjects that may be studied under these regulations. If at any time the RDRC approves a research proposal that involves exposure of more than 30 research subjects, or of any research subject under 18 years of age, the committee must immediately submit a special informational summary to FDA. The reporting of such RDRC approvals thus provides an opportunity for FDA to intervene if necessary. This may explain why most committees encourage protocols requesting fewer than 30 adult research subjects when appropriate and discourage the use of individuals under age 18 unless absolutely necessary. As a practical rule, the RDRC may choose to approve studies in only a few subjects (e.g., six) and require the investigator to report these results before additional studies are approved. In this way, the RDRC can ensure that the number of subjects is kept to the minimum needed to answer pertinent scientific questions. Standards set forth in 21 CFR 361.1(d) are used by the RDRC to determine if the pharmacologic dose and radiation dose are within the required limits and that the radiation exposure is justified by the quality of the proposed study and the importance of the information it seeks to obtain. The RDRC must also ensure that other requirements are in place regarding qualifications of the investigator, proper radioactive material licensure, selection and consent of research subjects, quality of radioactive drug product used, research protocol design, reporting of potential adverse reactions, and approval by an appropriate local or contract institutional review board (IRB).

Compliance with strict pharmacologic dose limits is compulsory in the conduct of human research under an RDRC approval. The amount of active ingredient or combination of active ingredients to be administered must be known not to cause any clinically detectable pharmacologic effect in humans. This fundamental regulatory principle implies that, in the absence of any known human pharmacology data, the study cannot be approved by the RDRC nor conducted by the investigator simply because there are no human data, and the active ingredient will be administered only in minuscule trace amounts. The lack of human data is most often the single reason why potential RDRC studies cannot be approved. In a few isolated cases, investigators have successfully undertaken IRB-approved subpharmacologic dose studies in humans using a nonradioactive form of the active ingredient to demonstrate the lack of clinically detectable pharmacologic effects. Once a subpharmacologic dose was determined and made available to the RDRC, it served as the basis for approval of studies that had otherwise satisfied all RDRC requirements. If such a pathway is approved by the RDRC and undertaken by the investigator, both must recognize that without proper operational controls and safeguards, the dose of active ingredient could theoretically exceed the established subpharmacologic threshold. For example, if short half-life positron-emitting ^{11}C is the radionuclide component of a very

nt study drug, the actual mass of active ingredient in the administered human dose d vary dramatically with time after synthesis, resulting in the potential administra- of a pharmacologic dose. In this case, it is critically important to require that the amount of the active ingredient in any batch of the radioactive drug be substantially than the established subpharmacologic threshold. Finally, when the same active edient without the radionuclide component is administered simultaneously under ND or in accordance with the approved labeling for a therapeutic drug, the total unt of active ingredients including the radionuclide must be known not to exceed dose limitations applicable to the separate administration of the active ingredients uding the radionuclide.

The regulations governing RDRC studies also impose important limits on acceptable ation dose. These limits are significantly more restrictive than those allowed under -approved studies, perhaps because normal volunteer populations are most frequently cted and enrolled in RDRC studies. The key here is that the amount of radioactive erial to be administered must be such that human research subjects receive the mini- m practical radiation dose necessary to perform the study without jeopardizing the efits to be gained from each study. If the single-study or cumulative multiple-study iation dose to an adult research subject in a given year is below the levels specified in se regulations, the study can be recognized as safe and thus approved by the RDRC. cordingly, the whole body, active blood-forming organs, lens of the eye, and gonads y not receive more than 3 rem from a single dosage or an annual and total dose nmitment of 5 rem. Other organs may not receive more than 5 rem from a single dosage an annual and total dose commitment of 15 rem. Occasionally, investigators may wish conduct studies in research subjects less than 18 years of age. This is possible; however, radiation dose cannot exceed 10% of the specifications for adult subjects. All sources radiation exposure associated with each study must be included in the determination total radiation doses and dose commitments. Therefore, exposures from all radioactive mponents in the drug product must be included in this determination, whether they e essential or present as significant contaminants or impurities. Radiation doses from x- procedures that are part of the research protocol must be included. Finally, the numer- l definitions of dose must be based on an absorbed-fraction method of radiation sorbed dose calculation. The RDRC is required to use either the Medical Internal Radi- ion Dose (MIRD) or the International Commission on Radiological Protection (ICRP) stem for these calculations.

Investigators who decide to conduct studies under RDRC approval must realize there e valid reasons for ensuring that such studies are well designed, controlled, and man- ged, since the data could become critically important at some later date. According to 21 FR 361.1 (e), the results of any research conducted under an RDRC approval become art of any clinical evaluation of the radioactive drug product pursuant to 21 CFR 312, hich specifies the requirements for submitting INDs. Therefore, if at any point the intent f an RDRC-approved study is altered in any way to begin use of the radioactive drug in clinical trial, the RDRC must immediately call for the termination of the study and equire the investigator to obtain an IND before additional human subjects are studied. A summary of all study results must be reported to the RDRC, and this report must be nade part of the IND submitted to FDA.

According to 21 CFR 361.1(f), radioactive drugs prepared, packaged, distributed, and primarily intended for use in RDRC studies are exempt from misbranding (FDCA 502(f)(1)) and requirements for adequate directions for use (21 CFR 201.5, 201.100) if the packaging, label, and labeling are in compliance with federal, state, and local law regarding radioactive materials and if the label of the immediate container and shielded container, if any, either separate from or as part of any label and labeling required for radioactive

potent study drug, the actual mass of active ingredient in the administered human dose could vary dramatically with time after synthesis, resulting in the potential administration of a pharmacologic dose. In this case, it is critically important to require that the total amount of the active ingredient in any batch of the radioactive drug be substantially less than the established subpharmacologic threshold. Finally, when the same active ingredient without the radionuclide component is administered simultaneously under an IND or in accordance with the approved labeling for a therapeutic drug, the total amount of active ingredients including the radionuclide must be known not to exceed the dose limitations applicable to the separate administration of the active ingredients excluding the radionuclide.

The regulations governing RDRC studies also impose important limits on acceptable radiation dose. These limits are significantly more restrictive than those allowed under IND-approved studies, perhaps because normal volunteer populations are most frequently selected and enrolled in RDRC studies. The key here is that the amount of radioactive material to be administered must be such that human research subjects receive the minimum practical radiation dose necessary to perform the study without jeopardizing the benefits to be gained from each study. If the single-study or cumulative multiple-study radiation dose to an adult research subject in a given year is below the levels specified in these regulations, the study can be recognized as safe and thus approved by the RDRC. Accordingly, the whole body, active blood-forming organs, lens of the eye, and gonads may not receive more than 3 rem from a single dosage or an annual and total dose commitment of 5 rem. Other organs may not receive more than 5 rem from a single dosage or an annual and total dose commitment of 15 rem. Occasionally, investigators may wish to conduct studies in research subjects less than 18 years of age. This is possible; however, the radiation dose cannot exceed 10% of the specifications for adult subjects. All sources of radiation exposure associated with each study must be included in the determination of total radiation doses and dose commitments. Therefore, exposures from all radioactive components in the drug product must be included in this determination, whether they are essential or present as significant contaminants or impurities. Radiation doses from x-ray procedures that are part of the research protocol must be included. Finally, the numerical definitions of dose must be based on an absorbed-fraction method of radiation absorbed dose calculation. The RDRC is required to use either the Medical Internal Radiation Dose (MIRD) or the International Commission on Radiological Protection (ICRP) system for these calculations.

Investigators who decide to conduct studies under RDRC approval must realize there are valid reasons for ensuring that such studies are well designed, controlled, and managed, since the data could become critically important at some later date. According to 21 CFR 361.1 (e), the results of any research conducted under an RDRC approval become part of any clinical evaluation of the radioactive drug product pursuant to 21 CFR 312, which specifies the requirements for submitting INDs. Therefore, if at any point the intent of an RDRC-approved study is altered in any way to begin use of the radioactive drug in a clinical trial, the RDRC must immediately call for the termination of the study and require the investigator to obtain an IND before additional human subjects are studied. A summary of all study results must be reported to the RDRC, and this report must be made part of the IND submitted to FDA.

According to 21 CFR 361.1(f), radioactive drugs prepared, packaged, distributed, and primarily intended for use in RDRC studies are exempt from misbranding (FDCA 502(f)(1)) and requirements for adequate directions for use (21 CFR 201.5, 201.100) if the packaging, label, and labeling are in compliance with federal, state, and local law regarding radioactive materials and if the label of the immediate container and shielded container, if any, either separate from or as part of any label and labeling required for radioactive

materials by NRC or by state or local radiologic health authorities, bear certain specific information. Two important legal statements are required in the labeling: "Caution: Federal law prohibits dispensing without prescription" and "To be administered in compliance with the requirements of Federal regulations regarding radioactive drugs for research use (21 CFR 361.1)." There are numerous other requirements that may seem impractical but nevertheless must be satisfied to ensure full compliance. The published regulations provide details and list all labeling requirements for radioactive drugs used under RDRC approval.

THE INVESTIGATIONAL NEW DRUG APPLICATION

The IND is an application that a drug sponsor must submit to FDA before beginning a clinical trial with a new drug in humans. It is not an application for marketing approval. Technically, it is a request for exemption from the federal statute that prohibits an unapproved drug product from being shipped in interstate commerce. Federal law requires that a drug be the subject of an approved marketing application before it is transported or distributed across state lines. Because a drug sponsor will almost certainly ship the investigational drug to several clinical sites in multiple states, an exemption must be obtained to satisfy this legal requirement. The IND is the means through which a sponsor obtains an exemption from FDA.

The main purpose of the IND is to provide detailed plans for well-controlled clinical drug studies in human subjects. It gives an overview of all that is currently known about the investigational drug product, including its structural formula, animal test results, human data, if any, and manufacturing information. Thus, an IND is typically quite lengthy and is labor intensive despite the use of innovative electronic processing systems. Most important, the IND serves as the basic documentation for FDA's acceptance of proposals to initiate clinical investigations in human subjects.

There are several types of INDs. Pharmaceutical companies submit commercial INDs with the ultimate goal of obtaining marketing approval for a new drug product. Most INDs, however, are noncommercial; they are filed in support of conducting clinical research, with no intent to obtain marketing approval. Three types of noncommercial INDs may be submitted to FDA for acceptance prior to conducting clinical investigations: the investigator IND, the emergency use IND, and the treatment IND.

A physician who wishes to both initiate and conduct a clinical investigation with a new drug product submits the investigator IND. For this reason, the investigator IND is sometimes referred to as a physician-sponsored IND. Under this type of IND the physician also accepts immediate responsibility for directing the preparation, dispensing, and administration of the investigational drug product. A physician might also wish to submit an investigator IND to conduct studies of an unapproved drug, or an approved product for a new indication or in a new patient population.

A physician may obtain an emergency use IND when urgent medical conditions occur and patients may benefit from the use of an investigational drug product. With this type of IND, FDA authorizes use of an investigational drug in an emergency situation when time is insufficient for submission and review of an IND in accordance with 21CFR 312.23 or 312.24. The emergency use IND may also be useful for patients who do not meet the inclusion criteria of an existing clinical study protocol, or when there is no approved study protocol.

A treatment IND may be submitted for investigational drugs showing promise in clinical testing for serious or immediately life-threatening conditions during the period when the final clinical work is being conducted and FDA review takes place. The treatment IND is thus a mechanism that allows promising investigational drugs to be used in

"expanded-access" protocols—relatively unrestricted studies whose intent is both to learn more about the drugs, especially their safety, and to provide treatment for people with immediately life-threatening or otherwise serious diseases for which there is no real alternative. These expanded-access protocols require researchers to formally investigate the drugs in well-controlled studies and to supply some evidence that the drugs are likely to be helpful. Of course, the drugs cannot expose patients to unreasonable risk. There are only a few therapeutic radiopharmaceuticals in development, and treatment INDs for these important orphan therapy agents have been accepted by FDA.

THE IND PROCESS

The current general regulatory dicta for all IND submissions are found in CFR 21, Subparts 312.1 through 312.70. FDA's Center for Drug Evaluation and Research (CDER) has several on-line resources that summarize IND content, format, and classification and the IND review process.[35]

Given the nature of this set of regulations, securing an IND approval is a lengthy, labor-intensive process that is underappreciated by the novice who has never before accepted this responsibility. Novices may wonder where and how to initiate the intricate process of preparing and submitting an IND; two key FDA regulatory forms not only guide the process well but serve as both the starting and ending points. The process of securing an IND approval should in all cases revolve around the creation and assembly of the required documentation identified in Form FDA-1571, Investigational New Drug Application (IND) (21 CFR 312.23(a)(1)), and Form FDA-1572, Statement of Investigator (21 CFR 312.53(c)(1)). Both of these forms, with supporting documentation, must be part of the IND submission, and both are available from the FDA Web site.[39] Form FDA-1571 serves as the cover sheet for the entire IND submission document. Table 7-1 lists the information requested by the January 2003 version of this form. Form FDA-1572 serves as a means for the IND sponsor to document that investigators are appropriately qualified and sufficiently informed to begin participation in the clinical investigations. Table 7-2 lists the information requested by the January 2003 version of this form. Both forms warn that a willfully false statement is a criminal offense in accordance with U.S.C. Title 18, Section 1001.

Each of these forms states that the estimated "public reporting burden" for collecting the information is 100 hours, including the time for reviewing instructions, searching existing data sources, gathering and maintaining the data needed, and completing and reviewing the collected information. However, the time required can easily surpass this estimate, and the novice sponsor or investigator should plan accordingly and consider seeking assistance from someone experienced in IND applications.

After the completed IND is submitted to CDER, the sponsor must wait 30 calendar days before initiating any clinical trials. During this period, CDER must review the IND for safety to ensure that research subjects will not be subjected to unreasonable risk. If CDER concludes that the clinical trials present unreasonable risk to subjects, or if the data are insufficient to make such a determination, the IND will be placed on clinical hold and the reviewing division will contact the sponsor within the 30-day period. Customarily, drug review divisions do not contact the sponsor if no concerns arise about drug safety and the proposed clinical trials. Therefore, if the sponsor hears nothing from CDER by day 31 after submission of the IND, the study may proceed. Figure 7-1 presents an overview of this review process; a detailed, interactive version of this chart, including an explanation of how CDER determines if a drug product is suitable for use in clinical trials, is available online.[40]

TABLE 7-1 Information Requested by Form FDA-1571, Investigational New Drug Application

1. Name of sponsor
2. Date of submission
3. Address (number, street, city, state, and ZIP code)
4. Telephone number
5. Name(s) of drug, including all available names such as trade, generic, chemical, and code
6. IND number if previously assigned
7. Indication(s) covered by the submission
8. Phase(s) of clinical investigation to be conducted
9. List of numbers of all INDs (21 CFR Part 312), new drug or antibiotic applications (21 CFR Part 314), drug master files (21 CFR 314.420), and product license applications (21 CFR 601) referenced in the application
10. Consecutive or serial number assigned to the submission
11. Checklist indicating purpose of submission. If the submission includes a request for a treatment IND (21 CFR 312.35(b)), treatment protocol (21 CFR 312.35(a)), or charge request/notification (21 CFR 312.7(d)), a justification must be attached satisfying the elements specified in the cited CFR section
12. Checklist identifying items included in the initial application. Form FDA-1571 (21 CFR 312.23(a)(1)), the table of contents (21 CFR 312.23(a)(2)), and several other critical documentation sections are necessary to facilitate both the clinical review and the nonclinical review of the IND submission. The introductory statement (21 CFR 312.23(a)(3)), the general investigational plan (21 CFR 312.23(a)(3)), the investigator's brochure (21 CFR 312.23(a)(5)), and the protocol(s) (21 CFR 312.23(a)(6)) are the main subject of the clinical review. The key protocols for *clinical review* include study protocol(s) (21 CFR 312.23(a)(6)), investigator data (21 CFR 312.23(a)(6)(iii)(b)) or completed Form FDA-1572, facilities data (21 CFR 312.23(a)(6)(iii)(b)) or completed Form FDA-1572, and IRB data (21 CFR 312.23(a)(6)(iii)(b)) or completed Form FDA-1572. The *nonclinical review* focuses primarily on the chemistry, manufacturing, and control (CMC) data (21 CFR 312.23(a)(7)), the pharmacology and toxicology data (21 CFR 312.23(a)(8)), previous human experience data (21 CFR 312.23(a)(9)), and any additional information (21 CFR 312.23(a)(10)).
13. Statement identifying contract research organization (CRO) involvement or transfer of sponsor obligations to CRO. The attached statement should contain the name and address of the CRO, identification of the clinical study, and a list of the obligations transferred. If all obligations governing the conduct of the study have been transferred, a general statement of this transfer—in lieu of a list of the specific obligations transferred—may be submitted.
14. Name and title of person responsible for monitoring the conduct and progress of the clinical investigations
15. Name(s) and title(s) of person(s) responsible for review and evaluation of information relevant to the safety of the drug. The form lists the following sponsor commitments: agreement not to begin clinical investigations until 30 days after FDA's receipt of the IND unless otherwise notified by FDA that studies may begin; not to begin or continue clinical investigations covered by the IND if those studies are placed on clinical hold; that an institutional review board (IRB) that complies with the requirements set forth in 21 CFR Part 56 will be responsible for the initial and continuing review and approval of each of the studies in the proposed clinical investigation; and to conduct the investigation in accordance with all other applicable regulatory requirements
16. Name of sponsor or sponsor's authorized representative
17. Signature of sponsor or sponsor's authorized representative
18. Address (number, street, city, state and ZIP code). If the person signing the application does not reside or have a place of business within the United States, the IND is required to contain the name and address of, and be countersigned by, an attorney, agent, or other authorized official who resides or maintains a place of business within the United States.
19. Telephone number
20. Date of signature

CLINICAL RADIOPHARMACEUTICAL STUDIES

Clinical research in human subjects must be conducted under an FDA-accepted IND generally consisting of three temporal phases. These developmental phases may be combined for a number of practical reasons and therefore may not be distinct. Phase 1 studies,

TABLE 7-2 Information Requested by Form FDA-1572, Statement of Investigator

1. Name and address of investigator
2. Education, training, and experience that qualifies the investigator as an expert in the clinical investigation of the drug for the use under investigation. A curriculum vitae or other statement of qualifications must be provided as an attachment.
3. Name and address of any medical school, hospital, or other research facility where the clinical investigation(s) will be conducted
4. Name and address of any clinical laboratory facilities to be used in the study
5. Name and address of the IRB responsible for review and approval of the study(ies)
6. Names of subinvestigators (e.g., research fellows, residents, associates) who will be assisting the investigator
7. Name and code number, if any, of the protocol(s) in the IND identifying the study(ies) to be conducted by the investigator
8. As attachments, the clinical protocol(s) for each planned phase of study. For Phase 1 investigations, a general outline of the planned investigation, including the estimated duration of the study and the maximum number of subjects that will be involved. For Phase 2 or 3 investigations, an outline of the study protocol, including an approximation of the number of subjects to be treated with the drug and the number to be employed as controls, if any; the clinical uses to be investigated; characteristics of subjects by age, sex, and condition; the kind of clinical observations and laboratory tests to be conducted; the estimated duration of the study; and copies or a description of case report forms to be used.
9. A commitment by the investigator agreeing to do the following: conduct the study(ies) in accordance with the relevant, current protocol(s) and make changes in a protocol only after notifying the sponsor, except when necessary to protect the safety, rights, or welfare of subjects; personally conduct or supervise the described investigation(s); inform any patients, or any persons used as controls, that the drugs are being used for investigational purposes and ensure that the requirements relating to obtaining informed consent in 21 CFR Part 50 and IRB review and approval in 21 CFR Part 56 are met; report to the sponsor adverse experiences that occur in the course of the investigation(s) in accordance with 21 CFR 312.64; read and understand the information in the investigator's brochure, including the potential risks and side effects of the drug; ensure that all associates, colleagues, and employees assisting in the conduct of the study(ies) are informed about their obligations in meeting the above commitments; maintain adequate records in accordance with 21 CFR 312.62 and make those records available for inspection in accordance with 21 CFR 312.68; ensure that an IRB that complies with the requirements in 21 CFR Part 56 will be responsible for the initial and continuing review and approval of the clinical investigation and that the investigator will promptly report to the IRB all changes in the research activity and all unanticipated problems involving risks to human subjects or others, and will not make any changes in the research without IRB approval, except where necessary to eliminate apparent immediate hazards to the human subjects; and comply with all requirements regarding the obligations of clinical investigators and all other pertinent requirements in 21 CFR Part 312.
10. Signature of investigator
11. Date of signature

known as clinical pharmacology studies, are carefully controlled and well documented, because they most often involve the initial administration of the radioactive drug product to a limited number of human subjects. Children and pregnant or lactating females must be excluded from Phase 1 studies. For diagnostic radiopharmaceuticals, normal volunteers may be ideal; however, it may also be desirable and appropriate to enroll diseased subjects in the study. When therapeutic radiopharmaceuticals are being evaluated, only diseased patients should be enrolled. The goal of these initial human studies is to determine absorption, normal biodistribution patterns, organs receiving maximal concentrations, extent of metabolism, route of excretion and half-life, potential toxicity, preferred route of administration, optimum imaging and sampling times, and optimal and safe dosage range. A variety of clinical laboratory tests may be required for the assessment of safety. Radiation absorbed dose should be kept as low as practical for these studies; however, an adequate number of usable particles or photons should be available to ensure that statistically significant images or counting results are obtained with the instrumentation used. When

applications and bring their operations into similar good manufacturing practices at a reasonable cost. Although the new drug application, sponsored by a consortium of industry, was now available to PET sites, no easy path existed for centers to comply with FDA oversight.

Since then, the business, physician, and pharmacist communities petitioned the FDA to modify their position. State boards of pharmacy have supported the practice of medicine and pharmacy approach, and most of the commonly used cyclotron-produced clinical compounds have been added to the *United States Pharmacopeia*. Individuals and professional societies, such as the Institute of Clinical PET, proposed alternative regulatory mechanisms to the FDA directly, methods not requiring hospital pharmacies to register as manufacturing facilities. A commercial radiopharmacy company filed a citizen's petition requesting that the FDA evaluate equipment approvals rather than manufacturing site approvals. This same company filed a lawsuit against the FDA for alleged rule-making violations and for not responding to the community's stated concerns. The initial ruling on this lawsuit was in favor of FDA, stating that the FDA acted within its purview to create rules. Recently, the United States Court of Appeals overturned the earlier ruling, affirming that the FDA had indeed violated rule-making requirements.[25]

Efforts such as these had failed to modify the FDA's stance. Although indications were forthcoming from the FDA that some modifications to manufacturing process would be possible, they would not willingly retreat from their overall position. As anticipated in the December 1994 citizen's petition, the regulatory challenges have dramatically impeded the clinical practice of PET. Nearly 10 years after use of FDG became acceptable clinical practice in the minds of experienced physicians, FDG was still not broadly available.

Relief came through attempts to influence regulatory policy through legislative initiatives. Efforts focused on both circumventing one of the levers that the FDA was using to force compliance (Health Care Financing Administration approval for reimbursement of Medicare patients) and legislating changes in the mandate to the FDA with respect to PET. Reform of the process for the approval and oversight of the manufacturing of radiopharmaceuticals was accomplished legislatively through the recently passed FDA Modernization Act of 1997 ("FDA reform" act).[26] The legislation contains specific language requiring the FDA to adopt "appropriate" procedures for approval of PET new drug applications and abbreviated new drug applications and "appropriate" current good manufacturing practices. These procedures and practices are to be determined jointly by the FDA, industry, and the user community. In addition, the FDA is required to take "due account of any relevant differences between commercial PET centers and not-for-profit PET facilities, with the hope of reducing the costs of coming into regulatory compliance at the hospital level." During the time period that these new processes are developed and for 2 years thereafter, neither new drug applications nor abbreviated new drug applications are required as the medical community brings itself into compliance with the new regulations.[26]

The legislation rescinded all of the recent rules published by the FDA on PET, including the notices entitled "Regulation of Positron Emission Tomography Radiopharmaceutical Drug Products: Guidance," published in the *Federal Register* on February 27, 1995; "Draft Guidelines on the Manufacture of Positron Emission Tomography Radiopharmaceutical Drug Products: Availability," published February 27, 1995; and a final rule entitled "Current Good Manufacturing Practice for

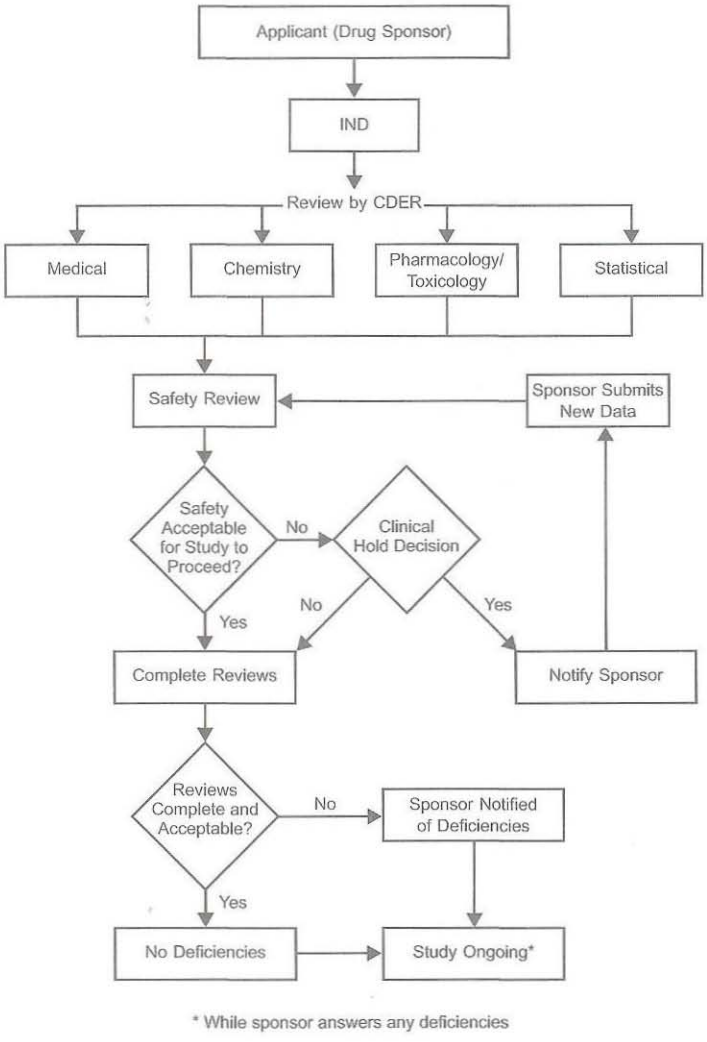

FIGURE 7-1 Process for reviewing investigational new drug applications (INDs) (http://www.fda.gov/cder/handbook/ind.htm).

imaging is performed, imaging times must be reasonable to prevent potential image degradation due to patient motion.

Phase 2 studies, known as clinical investigations, are designed to extend the safety evaluation of the radioactive drug product in a larger but controlled number of subjects for a specific disease state and to provide initial evidence of diagnostic or therapeutic efficacy. Phase 2 studies often require extensive laboratory testing, but somewhat less than is required for Phase 1.

Phase 3 studies, known as clinical trials, require the study of sufficient numbers of patients by two or more investigators to expand the evidence of the drug's safety and effectiveness and desirable dosage and to establish directions for use in the diagnosis or treatment of a specific disease. A risk-versus-benefit assessment is also made during this phase. Phase 3 studies typically require significantly less laboratory testing than is required in Phase 1 and 2 testing. The Phase 3 clinical trial protocol, with minor to moderate

modification, often becomes the recommended clinical protocol once the radioactive drug product is approved by FDA for general marketing.

Upon completion of all required studies for each phase of development, the sponsor of the new drug (the pharmaceutical company) submits supporting data to FDA in the form of a new drug application (NDA), which must be approved before the drug may be sold for routine clinical use. Phase 4 studies, also known as therapeutic use or postmarketing studies, may be required by FDA as a condition of approval, or they may be conducted on a voluntary basis by the drug sponsor wishing to get to market efficiently with a single approved indication and then seek approval for additional indications after marketing. Thus, Phase 4 studies relate to the original approved indication but go beyond the prior demonstration of the drug's safety, effectiveness, and dose range definition. FDA seldom requires Phase 4 studies of new diagnostic radiopharmaceuticals, and sponsors rarely conduct them on a voluntary basis because economic incentives are insufficient. However, it is reasonable and highly likely that Phase 4 studies with new therapeutic radiopharmaceuticals, such as the newly approved radioimmunotherapy drugs for non-Hodgkin's lymphoma, will be undertaken either as a condition for approval or in an effort to optimize the drug's use and maximize the market potential of the original indication.

PHYSICIAN-SPONSORED IND APPLICATIONS

As stated previously, an IND is usually sponsored either by a pharmaceutical company that enlists a group of investigators to conduct the study or by a physician. Often the physician-sponsored IND is a necessary pathway for the investigator who wishes to conduct human studies with a drug product that otherwise has no true sponsor. Such so-called "orphan drugs" have medical applications but have potential utility in very limited numbers of patients with relatively rare conditions or diseases, making the drugs unappealing candidates for the costly and time consuming IND–NDA approval process. Radiopharmaceuticals can easily fall into the orphan drug category, and this issue has been identified and addressed in the literature.[41] In 2002, it cost an estimated $802 million and took about 15 years to get a drug product from the laboratory to the marketplace.[42] If a "blockbuster" radioactive drug product could be brought to market rapidly for only 10% of this estimated cost, it would still be a challenge to attract a company to sponsor the drug's commercial development. For orphan drugs, an abbreviated form of IND submission is acceptable, and the sponsoring physician can deal directly with FDA. This enables both the investigator and FDA to accumulate data on safety and efficacy that can be shared with other physicians. If these studies can demonstrate potential utility in additional medical conditions or diseases, there is greater likelihood of a pharmaceutical company sponsor bringing the drug product to market. As a further economic incentive, and as specified in the Orphan Drug Act (Public Law 97-414), which amended the Food, Drug, and Cosmetic Act as of January 4, 1983, companies that sponsor orphan drugs and bring them to market may qualify for certain tax breaks and a guarantee of market exclusivity for up to 7 years after drug approval.[43] FDA approval of diagnostic iobenguane sulfate I 131 (^{131}I-MIBG) is an example of how this process can facilitate the commercial development of orphan radiopharmaceutical drug products.

The need to use a radiopharmaceutical without an approved NDA or to use an approved agent for an unapproved use or by a different route of administration occasionally arises in nuclear medicine practice. In such cases the question of the need to file a physician-sponsored IND also arises. Depending on the circumstances of use, composition of the radiopharmaceutical, and type of radioactive materials license, an IND may or may not be required. Such questions are difficult to resolve because of the numerous regulations and regulatory bodies (Figure 7-2) that govern the use of radiopharmaceuticals and the

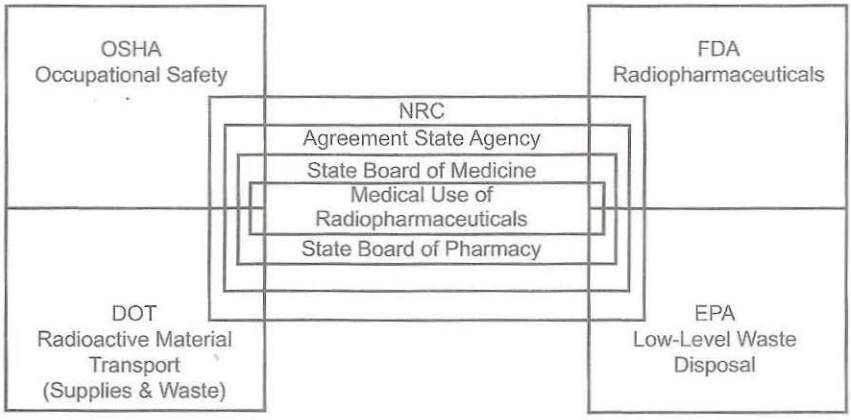

FIGURE 7-2 Regulatory environment for the medical use of radiopharmaceuticals, involving the federal Nuclear Regulatory Commission (NRC), Food and Drug Administration (FDA), Environmental Protection Agency (EPA), Occupational Safety and Health Administration (OSHA), and Department of Transportation (DOT).

overlap and inconsistencies among regulations.[44] These issues are addressed in an article by Swanson and Lieto,[45] which provides specific examples that help clarify when and why a radiopharmaceutical IND may be required.

THE NDA PROCESS

Since 1938, the regulation and control of new drugs by FDA has been based on the new drug application (NDA). Thus, for many decades every new drug in the United States has been subject to NDA approval prior to marketing. The NDA is the vehicle through which drug sponsors formally propose that FDA approve a new drug for human use and for sale and marketing in U.S. interstate commerce. The goal of the NDA is to provide enough well-organized information to permit FDA reviewers to conclude that (1) the product is safe and effective for its proposed use(s), and potential benefits outweigh the associated risks, (2) the proposed product labeling (i.e., the package insert) is suitable and contains sufficient information to promote safe use, and (3) the methods used in manufacturing the drug and the controls used to maintain the drug's quality are adequate to preserve the drug's identity, strength, quality, and purity. The documentation required in the NDA must convey the entire developmental history of the drug product. The data gathered in preclinical studies in animals and clinical trials in humans under the IND become a substantial part of the NDA. In addition, the NDA must identify the drug product ingredients, how the drug behaves in the body, and how it is manufactured, processed, and packaged. General requirements for an NDA submission are specified in 21 CFR, Subparts 314.1 through 314.170. To facilitate understanding of this complicated process, FDA's CDER has on-line resources that summarize NDA content, format, and classification and the NDA review process.[36] Figure 7-3 provide an overview of this review process; a detailed, interactive version of this chart, including an explanation of how CDER determines the benefit-to-risk profile of a drug product prior to marketing approval, is available online.[46]

Pharmacists and nuclear pharmacists are well qualified to participate in the complex but necessary U.S. drug approval process. Traditionally, however, most nuclear pharmacists practice in settings that neither require nor provide the occasion for their direct

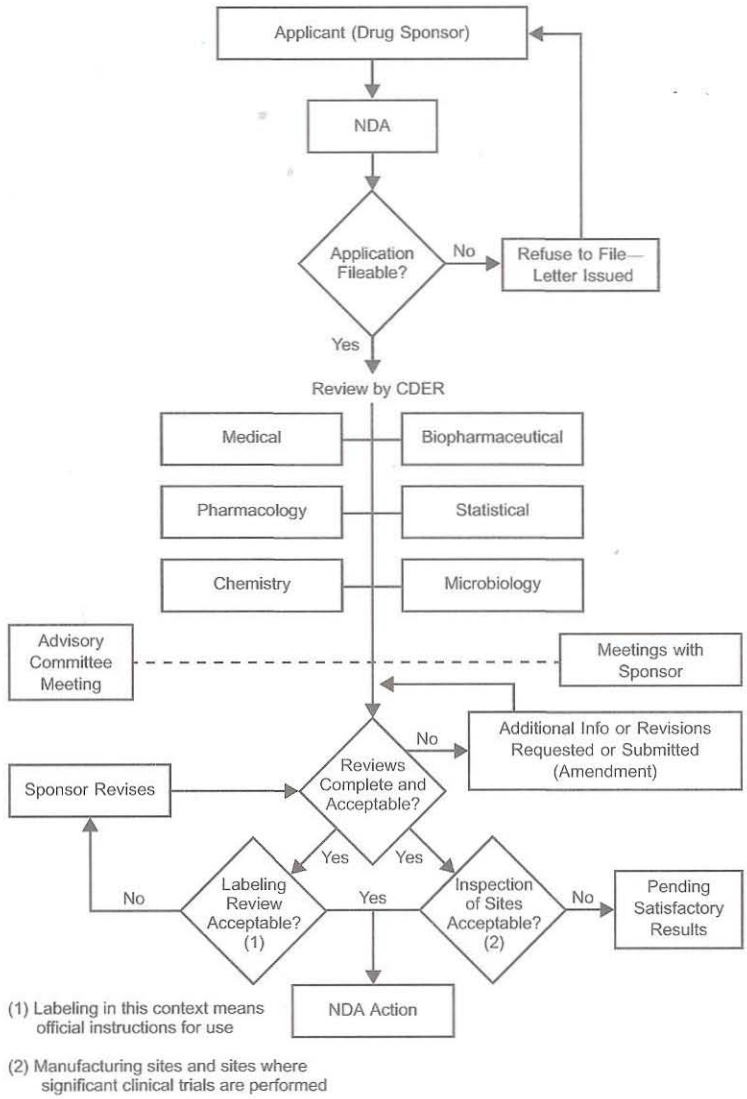

FIGURE 7-3 The new drug application (NDA) approval process (http://www.fda.gov/cder/handbook/nda.htm).

participation in IND–NDA preparation, approval, and management. Nevertheless, growing numbers of experienced nuclear pharmacists working for commercial companies, academic medical centers, and the federal government are playing key roles in a vital translational regulatory process that is being applied to PET drug products, a unique and important class of radiopharmaceuticals that is key to developing and expanding the potential of molecular imaging technologies. Therefore, nuclear pharmacists should consider participating in the preparation of FDA IND–NDA applications for a variety of PET drugs, especially those with current USP monographs (Table 7-3).

Since the Peoria, Illinois, ^{18}F-FDG NDA already exists, the potential next step for other ^{18}F-FDG manufacturing facilities will be to prepare, submit, and gain approval of site-specific abbreviated new drug applications (ANDAs), since each facility will be seeking approval to produce what FDA will view as a generic PET drug product.

TABLE 7-3 PET Radiopharmaceuticals with Monographs in *The United States Pharmacopeia*

Ammonia N 13 Injection
Carbon Monoxide C 11
Fludeoxyglucose F 18 Injection
Flumazenil C 11 Injection
Fluorodopa F 18 Injection
Mespiperone C 11 Injection
Methionine C 11 Injection
Raclopride C 11 Injection
Sodium Acetate C 11 Injection
Sodium Fluoride F 18 Injection
Water O 15 Injection

ABBREVIATED NEW DRUG APPLICATIONS FOR PET DRUGS

An ANDA for submission to the CDER Office of Generic Drugs provides for the review and approval of a generic drug product.[37] After approval, an applicant may manufacture and market the generic product to provide the public with a safe, effective, and potentially lower-cost alternative. By definition, a generic drug product is comparable to an innovator drug product in dosage form, strength, quality, administration route, performance characteristics, and intended clinical use. Generic drug applications are termed "abbreviated" because they are generally not required to include preclinical (animal) and clinical (human) data to establish safety and effectiveness. Instead, ANDA applicants must scientifically demonstrate that their product is bioequivalent (i.e., performs in the same manner as the innovator drug). Bioequivalence is most often demonstrated by measuring the time it takes the generic drug to reach the bloodstream in healthy volunteers. These studies provide data on the rate of absorption, or bioavailability, of the generic drug, which can then be compared with that of the innovator drug. To be considered bioequivalent, the generic version must deliver the same amount of active ingredients into the bloodstream in the same amount of time as the innovator drug. Since radiopharmaceuticals are different from other drug products, FDA has provided guidance documents regarding the content and format of NDAs and ANDAs for PET radiopharmaceutical drug products.[47,48]

IND–NDA–ANDA REVIEW PROCESS FOR RADIOPHARMACEUTICALS

A team of FDA medical officers at CDER initiates the extensive review process for each submitted radiopharmaceutical IND and NDA. In the near future, the FDA medical team will also be responsible for reviewing each submitted PET drug ANDA, most of which will be for ^{18}F-FDG. FDA medical officers have previously described the pathway for FDA review and approval of new radiopharmaceuticals.[38] The guidance, concepts, and principal elements identified by these experts can be of great assistance to individuals charged with the task of gaining FDA clearance for production, clinical evaluation, and eventual marketing of new or generic radiopharmaceutical products.

Radiopharmaceuticals, whether intended for diagnostic imaging procedures or therapeutic applications, differ significantly from other pharmaceuticals used for therapeutic interventions. The most obvious and important differences between these two types of drugs are the frequency of administration, pharmacologic response, pharmacokinetics, and pharmacodynamics. The FDA review team will pay particular attention to the unique aspects of radiopharmaceuticals.

The IND-NDA review process generally has two parts, the nonclinical review and the medical or clinical review. The nonclinical review includes assessment of pharmacology and toxicology, chemistry, and safety and efficacy biostatistics, whereas the clinical review focuses on overall study safety, rights of human subjects, and quality of the scientific evaluation to be conducted during Phases 1, 2, and 3 of the planned clinical trials.

Nonclinical Review

Pharmacology and Toxicology Review

Both pharmacologists and toxicologists serve on the review team to evaluate the results of animal testing and attempt to relate drug effects in animals to potential effects in humans. 21 CFR 312.23(8) and 314.50(2) require the inclusion of a section describing the pharmacologic effects and mechanism(s) of action of the drug in animals and information regarding the absorption, distribution, metabolism, and excretion of the drug, if known. The regulations do not further describe the data to be presented, in contrast to the more detailed description of how to submit toxicologic data. A pharmacology summary report, without individual animal records or individual study results, usually satisfies this requirement. Diagnostic radiopharmaceuticals seldom elicit a detectable pharmacologic response, because only a trace mass of the radiopharmaceutical is typically required. For essentially the same reason, the toxicity of diagnostic agents due to the radionuclide moiety is seldom a significant concern; however, the potential toxicity of a chemical moiety or other chemical components must still be adequately addressed. Therefore, the customary biodistribution and excretion studies in separate animal species are principally designed to obtain essential data for the required calculation of radiation dosimetry estimates that establish relative safety. The ideal approach to estimating dosimetry is to determine the concentration of the radiopharmaceutical in all major organs, tissues, and blood at selected times subsequent to administration of the radioactive drug product to selected test animal species. From the cumulative animal data, the organs receiving the highest radiation absorbed dose can be identified, the blood-to-organ ratios can be calculated, and, for imaging purposes, target-to-nontarget concentrations can be readily established. The evaluation process for therapeutic radiopharmaceuticals is similar to that for conventional therapeutic drugs designed to yield pharmacologic effects. In addition to evaluation of the pharmacokinetics and pharmacodynamics of the therapeutic radiopharmaceutical, changes in vital signs, serum biochemistry, hematogram, and renal function after therapy must be documented. (A hematogram includes measurement of hemoglobin, hematocrit, mean corpuscular volume, and mean corpuscular hemoglobin.) All adverse reactions, regardless of degree of severity, must be evaluated, recorded, and reported. In the end, a complete, integrated summary of the pharmacologic and toxicologic effects of the drug must be provided for review.

Chemistry Review

Each FDA review division employs a team of chemists responsible for reviewing the chemistry, manufacturing, and control (CMC) sections of submitted INDs, NDAs, and ANDAs. The chemistry reviewers consider issues related to drug identity, manufacturing controls, and analysis. The reviewing chemist evaluates the manufacturing and processing procedures associated with each drug product to make certain the drug formulation is adequately reproducible and stable. If the drug were either unstable or not reproducible, the validity of any clinical trial would be significantly undermined because the investigators

would not know precisely what chemical entities were actually administered to the human subjects; more important, the study could pose significant risks to the subjects.

At the beginning of the CMC section, the drug sponsor should state whether it believes the chemistry of either the drug substance or the drug product, or the manufacturing of either the drug substance or the drug product, presents any indicators of potential human risk.[40] If so, these indicators should be completely discussed, with steps proposed to monitor for the associated risks. In addition, sponsors should describe any chemistry and manufacturing differences between the drug product proposed for clinical use and the drug product used in the animal toxicology trials that formed the basis for the sponsor's conclusion that it was safe to continue with the proposed clinical study.[40] Likewise, the sponsor should describe how the known differences might affect the overall safety profile of the drug product as formulated for clinical trials. If there are no differences in the products, this should be stated.

21 CFR 312.23(7) states that sufficient required information is to be submitted to ensure the proper identification, quality, purity, and strength of the investigational drug. The documentation that satisfies this regulatory requirement is commonly referred to as the CMC section of the IND application and is often a primary responsibility of a nuclear pharmacist. The CMC section should include all relevant information to show that the drug product can be prepared with sufficient purity and quality to be safe for administration to human subjects. The essential parts of a suitable CMC section are specified in the applicable regulations and have also been summarized as guidance for industry.[49] The four major elements of the CMC section describe the control processes related to the drug substance, drug product, quality controls, and container and closure system for the final drug product. The NDA will generally have the same documentation format as the IND CMC section; however, there are differences regarding the level of detail required. For example, the NDA requires additional emphasis on structure proofs and establishment of purity profiles and quality controls for raw materials, starting materials, intermediates, drug substance excipients, and the finished drug product. More extensive stability data must be provided, and the data must clearly support the assignment of a valid expiration date or time.

Biostatistics Review

Biostatisticians evaluate the potential statistical significance of data to be collected under an IND and compute the statistical relevance of data submitted in an NDA. Thus, the biostatistics reviewer takes full responsibility for the main tasks of evaluating the methods used to conduct clinical studies and to analyze the acquired data. The overall purpose of these statistical evaluations is to provide the medical officers with enhanced information about the power of the findings as they are extrapolated to the larger patient populations.

21 CFR 314.126(a) indicates that the purpose of conducting clinical investigations of a drug is to distinguish the effect of a drug from other influences, such as spontaneous change in the course of disease, placebo effect, or biased observation. Data submitted to substantiate the safety and efficacy of a new radiopharmaceutical must undergo valid statistical analysis to help authenticate claims made and to confirm the degree to which a hypothesis has been proved or disproved.[50] The elements of the required statistical analysis are identified in 21 CFR 314.50(d)(5, 6). The requisite elements of a well-designed protocol have also been identified and explained in a guidance document on the format and content of the clinical and statistical section of an application.[50] More recently, regulatory experts have summarized these requisite elements for biostatistics evaluations as they apply to the review of radiopharmaceutical drug products.[38]

Clinical Review

Clinical reviewers, also called medical officers, are almost exclusively physicians; consequently, the term medical review may also be used. Nonphysician professionals may be used as medical officers to evaluate certain types of drug data. Clinical reviewers are held responsible for fully evaluating the clinical sections of submissions, such as the overall safety of the clinical protocols described in an IND and the clinical test results as submitted in an NDA. In most divisions, clinical reviewers take the lead role in IND or NDA review and are thus responsible for synthesizing the results of the animal toxicology, human pharmacology, and clinical reviews to formulate the overall basis for a recommended agency action on the application.[40]

Throughout the IND clinical review process, the reviewer evaluates each clinical trial protocol to determine (1) if the research subjects will be protected from unwarranted risks and (2) if the study design will provide data pertinent to the overall safety and effectiveness of the investigational drug product. Under federal regulations, proposed Phase 1 studies are evaluated almost exclusively for overall safety. Since the late 1980s, FDA reviewers have been instructed to provide drug sponsors with greater freedom during Phase 1, as long as the investigations do not expose research subjects to undue risks.[40] In evaluating Phase 2 and Phase 3 investigations, however, clinical reviewers must also provide assurance that proposed studies are of sufficient scientific quality to be capable of yielding significant data that can support final marketing approval.

21 CFR 312.11 describes the customary framework applied to the clinical review of each IND. FDA's primary objectives in reviewing an IND are, in all phases of the investigation, to ensure the safety and rights of subjects and, in Phases 2 and 3, to help ensure that the quality of the scientific evaluation of drugs is adequate to permit an evaluation of the drug's effectiveness and safety. In describing the design of the clinical trial investigational plan, the proposed indication for use of the new radiopharmaceutical should be clearly stated, along with the methods to be used for gathering the necessary data to support the proposed clinical use.[51]

Phase 1

This opening phase of study includes the first introduction of the investigational new drug into human subjects.[51] The purpose of this phase is to validate safety of the new drug or radiopharmaceutical product. These early studies must determine several key radiopharmaceutical characteristics, including blood clearance half-life, normal biologic distribution, critical organ(s) (i.e., those receiving maximum radiopharmaceutical concentration), routes of excretion, and optimal times for sampling and imaging. Additional requisites include descriptive information about the planned subject populations, dosage ranges, radiation absorbed dose ranges, clinical laboratory tests, vital signs, and radiopharmaceutical biodistribution.

Phases 2 and 3

Typically, the differences between Phase 2 and Phase 3 for diagnostic radiopharmaceuticals are minimal in comparison with the differences between these study phases for therapeutic radiopharmaceuticals or drugs. Diagnostic radiopharmaceutical safety evaluations require less detailed pharmacologic toxicity assessments and have a primary focus of establishing valid radiation absorbed dose estimates. Diagnostic efficacy can be established if use of the radiopharmaceutical contributes to making effective decisions about the presence, absence, or extent of disease. Although the exact nature of the disease or abnormality may

not be specified, the clinical utility of the diagnostic radiopharmaceutical must be clearly demonstrated. Diagnostic value is a function of a radiopharmaceutical's biodistribution and the character of its emitted radiation. The extent to which radiopharmaceutical biodistribution is altered by disease, as defined by imaging studies, in vivo uptake studies, and in vitro tests helps to validate efficacy of the agent. Each phase of the study may require fewer research subjects to satisfy the statistical determinants set for each study. Depending on the clarity of response, as few as 20 to 60 subjects may suffice for Phase 2 protocols and 200 to 300 for Phase 3 studies, in contrast to the much larger numbers of subjects often needed for therapeutic drug evaluations. In diagnostic radiopharmaceutical clinical trials the time required to collect the necessary pharmacokinetic, pharmacodynamic, and imaging data is often much shorter because of the nature of these studies and the usual ease of demonstrating presence or lack of efficacy. One of the most critical requirements for Phase 3 evaluations is the performance of studies under a common protocol by at least two separate and independent institutional sites and investigators.[38] The separate studies validate the ability to replicate the safety and efficacy determinants of the new agent with the particular dosage form and for the proposed indication.[52] The critical elements required by FDA for all clinical study designs have been outlined and the common specific elements for all phases of IND–NDA protocols have been summarized elsewhere.[38,53]

NDA SUBMISSIONS

Although nuclear pharmacists and other nuclear medicine professionals rarely become involved in the process of gaining FDA marketing approval for diagnostic and therapeutic radiopharmaceuticals, it is still useful for these individuals to know the NDA submission process as defined by drug law. 21 CFR 314.50 outlines the elements needed to meet the legal requirements for NDA approval to market a new radiopharmaceutical. As indicated previously, the submitted application collates and summarizes all of the nonclinical and clinical data derived to validate the safety and efficacy of the new radioactive drug product. The principal segments of the NDA, as identified in 21 CFR 314.50(c)(I-ix), include summary sections devoted to CMC, nonclinical pharmacology and toxicology, human pharmacokinetics and bioavailability, and clinical data, including the results of statistical analysis of the clinical trials, plus a concluding discussion that presents the benefit and risk considerations related to use of the drug. The final distillation of information that must accompany the NDA during the review and approval process is the label or package insert. The package insert, as specified in 21 CFR 201.50, 201.56, and 201.57, provides a summary of the essential scientific information needed for the safe and effective use of the drug product. This labeling information must be both accurate and informative and cannot be promotional, misleading, or false. Information included in the package insert should be based on proven data that are presented in the NDA. The package insert must also have a prescribed format that includes (1) indication(s) and approved clinical uses, (2) dosage and administration, and (3) warnings and adverse reactions documented during the clinical trials. There are additional considerations regarding the evaluation, summarization, and presentation of completed studies in the NDA, along with several modifications that are appropriate for therapeutic radiopharmaceuticals.[38]

Every IND, NDA, or ANDA submission is a distinctive document because of the unique physical and chemical properties associated with each diagnostic or therapeutic radiopharmaceutical product and the variation in the facilities used and personnel employed for their production. This chapter and its referenced sources will be useful to individuals who take responsibility for preparing and maintaining the various regulatory applications. To optimize the challenging process of gaining radiopharmaceutical drug

product approvals, FDA, the nuclear medicine community, commercial sponsors, and investigators must focus on effective communication at many levels. When questions or potential problems arise at any stage in the drug development process, it is often best to contact FDA to obtain answers or identify a means of resolving problems in the marketing approval process. Recent experience has shown that improved communication can help decrease the time required to review and bring new radiopharmaceuticals into clinical trials and onto the market. Copies of the regulations, further guidance regarding IND procedures, and relevant forms are available from the FDA Legislative, Professional, and Consumer Affairs Branch (HFN-365), 5600 Fisher's Lane, Rockville, MD 20857. Multiple resources and the required forms are also available online.[35–37,39,40,46]

NRC REGULATIONS APPLICABLE TO THE MEDICAL USE OF RADIOPHARMACEUTICALS

The stated mission of NRC is to regulate the civilian use of byproduct, source, and special nuclear materials to ensure adequate protection of public health and safety, to promote the common defense and security, and to protect the environment.[54] This regulatory mission covers three main areas: (1) reactors—commercial reactors for generating electric power and nonpower reactors used for research, testing, and training, (2) materials—uses of nuclear materials in medical, industrial, and academic settings and facilities that produce nuclear fuel, and (3) waste—transportation, storage, and disposal of nuclear materials and waste, and decommissioning of nuclear facilities from service. NRC thus has extremely broad legislative authority regarding radioactive materials. The following discussion, however, focuses on specific issues related to NRC regulation of the medical use of radiopharmaceuticals and the related implications for nuclear pharmacy and nuclear medicine practice.

All NRC regulations are published in the *Federal Register* (FR) and codified in 10 CFR Chapter 1. The specific NRC regulations pertaining to the medical use of byproduct materials are also identified in NRC Regulatory Guide 10.8[13] and listed here in Table 7-4. The medical use of radionuclides requires specific licensure, since it involves the intentional internal or external administration of byproduct material, or the radiation therefrom, to human beings. The regulations that most directly affect nuclear pharmacy and nuclear medicine practice are found in 10 CFR 35 (Medical Use of Byproduct Material), 10 CFR 20 (Standards for Protection Against Radiation), and 10 CFR 71 (Packaging and Transportation of Radioactive Materials). The other regulations listed in the table are equally important in that nuclear pharmacies and nuclear medicine clinics must operate in total compliance with all applicable sections of each part; however, those regulations are primarily administrative and do not directly affect routine practice activities. Important issues

TABLE 7-4 Nuclear Regulatory Commission Rules Pertaining to Medical Use of Byproduct Materials

10 CFR Part 19	Notice, Instructions, and Reports to Workers; Inspections and Investigations
10 CFR Part 20	Standards for Protection Against Radiation
10 CFR Part 21	Reporting of Defects and Noncompliance
10 CFR Part 30	Rules of General Applicability to Domestic Licensing of Byproduct Material
10 CFR Part 35	Medical Use of Byproduct Material
10 CFR Part 71	Packaging and Transportation of Radioactive Material
10 CFR Part 170	Fees for Facilities, Materials, Import and Export Licenses, and Other Regulatory Services Under the Atomic Energy Act of 1954, as Amended
10 CFR Part 171	Annual Fees for Reactor Licenses and Fuel Cycle Licenses and Materials Licenses, Including Holders of Certificates of Compliance, Registrations, and Quality Assurance Program Approvals and Government Agencies Licensed by the NRC

related to 10 CFR 20 and 10 CFR 71 are addressed in Chapters 4 and 5 of this book, so the following discussion will focus on sections of 10 CFR 35 in an effort to characterize the regulatory relationship between NRC and the practice of nuclear pharmacy and nuclear medicine.

MEDICAL USE OF BYPRODUCT MATERIAL

Historically, the regulations contained in 10 CFR 35 have set forth requirements and provisions for the medical use of byproduct material, the issuance of specific licenses authorizing the medical use of this material, and the radiation safety of workers, the general public, patients, and human research subjects. The requirements and provisions of Part 35 are in addition to, and not a substitution for, others in 10 CFR. Unless specifically exempted, Parts 19, 20, 21, 30, 71, 170, and 171 of 10 CFR apply to applicants and licensees subject to Part 35. The nuclear pharmacy practice guidelines are based in part on these federal regulations, and the practice standards state that nuclear pharmacists have a professional responsibility to ensure compliance with NRC and state licenses under which the nuclear pharmacy operates and with federal, state, and institutional rules regulating radiation and radiopharmaceuticals.

A revision of 10 CFR 35 was published in the *Federal Register* (67 FR 20249) on April 24, 2002, and became effective on October 24, 2002.[55] This most recent revision was an effort to create a risk-informed and performance-based regulation that focuses on those medical procedures that pose the highest radiologic risk to workers, patients, and the public. Information is presented here about regulatory requirements pertinent to most nuclear pharmacy practice settings. (In the following discussion of those requirements, "this chapter" means 10 CFR Chapter 1.) For some practice settings, the regulatory requirements may not be adequately addressed here. The complete Part 35 is available on the NRC Web site.[56]

General Information

The stated purpose and scope of the revised regulations is to identify requirements and provisions for medical use of byproduct material and for issuance of specific licenses authorizing medical use of this material. These requirements and provisions provide for the radiation safety of workers, the general public, patients, and human research subjects. Part 35.2 defines key terms used in the regulations; the definitions most directly applicable to the practice of nuclear pharmacy and nuclear medicine follow.

An *authorized medical physicist* (AMP) is an individual who (1) meets the requirements in §§35.51(a) and 35.59; or (2) is identified as an AMP or teletherapy physicist on a specific medical use license issued by NRC or an agreement state, a medical use permit issued by an NRC master material licensee, a permit issued by an NRC or agreement state broad scope medical use licensee, or a permit issued by an NRC master material license broad scope medical use permittee.

An *authorized nuclear pharmacist* (ANP) is a pharmacist who (1) meets the requirements in §§35.55(a) and 35.59; or (2) is identified as an ANP on a specific license issued by NRC or an agreement state that authorizes medical use or the practice of nuclear pharmacy, a permit issued by an NRC master material licensee that authorizes medical use or the practice of nuclear pharmacy, a permit issued by an NRC or agreement state broad scope medical use licensee that authorizes medical use or the practice of nuclear pharmacy, or a permit issued by an NRC master material license broad scope medical use permittee that authorizes medical use or the practice of nuclear pharmacy; or (3) is identified as an

ANP by a commercial nuclear pharmacy that has been authorized to identify ANPs; or (4) is designated as an ANP in accordance with §32.72(b)(4).

An *authorized user* (AU) is a physician, dentist, or podiatrist who (1) meets the requirements in §35.59 and 35.190(a), 35.290(a), 35.390(a), 35.392(a), 35.394(a), 35.490(a), 35.590(a), or 35.690(a); or (2) is identified as an AU on an NRC or agreement state license that authorizes the medical use of byproduct material, a permit issued by an NRC master material licensee that is authorized to permit the medical use of byproduct material, a permit issued by an NRC or agreement state specific licensee of broad scope that is authorized to permit the medical use of byproduct material, or a permit issued by an NRC master material license broad scope permittee that is authorized to permit the medical use of byproduct material.

A *dedicated check source* is a radioactive source that is used to ensure the constant operation of a radiation detection or measurement device over several months or years.

A *medical event* is an event that meets the criteria in §35.3045(a), which states that a licensee must report any event, except for an event that results from patient intervention, in which the administration of byproduct material or radiation from byproduct material results in (1) a dose that differs from the prescribed dose or dose that would have resulted from the prescribed dosage by more than 0.05 Sv (5 rem) effective dose equivalent, 0.5 Sv (50 rem) to an organ or tissue, or 0.5 Sv (50 rem) shallow dose equivalent to the skin, and the total dose delivered differs from the prescribed dose by 20% or more, the total dosage delivered differs from the prescribed dosage by 20% or more or falls outside the prescribed dosage range, or the fractionated dose delivered differs from the prescribed dose, for a single fraction, by 50% or more; (2) a dose that exceeds 0.05 Sv (5 rem) effective dose equivalent, 0.5 Sv (50 rem) to an organ or tissue, or 0.5 Sv (50 rem) shallow dose equivalent to the skin from any of the following: administration of a wrong radioactive drug containing byproduct material, administration of a radioactive drug containing byproduct material by the wrong route of administration, administration of a dose or dosage to the wrong individual or human research subject, administration of a dose or dosage delivered by the wrong mode of treatment, or a leaking sealed source; (3) a dose to the skin or an organ or tissue other than the treatment site that exceeds by 0.5 Sv (50 rem) to an organ or tissue and 50% or more of the dose expected from the administration defined in the written directive (excluding, for permanent implants, seeds that were implanted in the correct site but migrated outside the treatment site).

Medical use is the intentional internal or external administration of byproduct material or the radiation from byproduct material to patients or human research subjects under the supervision of an authorized user.

A *pharmacist* is an individual licensed by a state or territory of the United States, the District of Columbia, or the Commonwealth of Puerto Rico to practice pharmacy.

A *physician* is a medical doctor or doctor of osteopathy licensed by a state or territory of the United States, the District of Columbia, or the Commonwealth of Puerto Rico to prescribe drugs in the practice of medicine.

A *prescribed dosage* is the specified activity or range of activity of unsealed byproduct material as documented (1) in a written directive or (2) in accordance with the directions of the authorized user for procedures performed pursuant to §§35.100 (use of unsealed byproduct material for uptake, dilution, and excretion studies for which a written directive is not required) and 35.200 (use of unsealed byproduct material for imaging and localization studies for which a written directive is not required). According to this definition, the term prescribed dosage is reserved for indicating the amount of radioactivity (e.g., μCi or mCi) to be administered. Thus, the term prescribed dosage is distinct from the term "prescribed dose," which refers to the radiation absorbed dose to be administered.

A *prescribed dose* is (1) for gamma stereotactic radiosurgery, the total dose as documented in the written directive; (2) for teletherapy, the total dose and dose per fraction as documented in the written directive; (3) for manual brachytherapy, either the total source strength and exposure time or the total dose, as documented in the written directive; and (4) for remote brachytherapy afterloaders, the total dose and dose per fraction as documented in the written directive. According to this definition, the term prescribed dose is reserved for indicating the radiation absorbed dose to be administered. Thus, the term prescribed dose is distinct from the term "prescribed dosage," which refers to the activity amount of radiopharmaceutical to be administered.

A *radiation safety officer* (RSO) is an individual who (1) meets the requirements in §§35.50(a) and 35.59; or (2) is identified as an RSO on a specific medical use license issued by NRC or an agreement state or on a medical use permit issued by an NRC master material licensee.

A *sealed source* is any byproduct material that is encased in a capsule designed to prevent leakage or escape of the byproduct material.

A *therapeutic dosage* is a dosage of unsealed byproduct material (e.g., a radiopharmaceutical) that is intended to deliver a radiation dose to a patient or human research subject for palliative or curative treatment.

A *therapeutic dose* is a radiation dose delivered from a source containing byproduct material to a patient or human research subject for palliative or curative treatment.

A *unit dosage* is a dosage prepared for medical use for administration as a single dosage to a patient or human research subject without any further manipulation of the dosage after it is initially prepared.

A *written directive* is an authorized user's written order for the administration of byproduct material or radiation from byproduct material to a specific patient or human research subject, as specified in §35.40.

Part 35.5 specifies requirements for *maintaining applicable records*. The records required by this part must be kept in a readily retrievable, legible form throughout the retention period specified by regulation. Records may be original or reproduced copies or a microform, provided that authorized personnel authenticate the copy or microform and that the microform is capable of producing a clear copy. Records may also be stored in electronic media with the capability for producing legible, accurate, and complete records. Records such as letters, drawings, and specifications must include all pertinent information such as stamps, initials, and signatures. The licensee must maintain adequate safeguards against tampering with and loss of all pertinent records.

Part 35.6 delineates provisions for the *protection of human research subjects* and therefore is an immensely important set of regulations for licensees involved, directly or indirectly, in human research involving radioactive drug products. Consequently, even the nuclear pharmacy licensee that participates only indirectly in such studies by providing radiopharmaceutical service must be aware of the regulatory requirements for protecting human subjects. A licensee may conduct research involving human subjects only if the byproduct materials to be used are specified in the current license and the uses are authorized by this license. If the research is conducted, funded, supported, or regulated by another federal agency that has implemented the federal policy for the protection of human subjects (Federal Policy), the licensee must, before conducting research (1) obtain review and approval of the research from an institutional review board (IRB), as defined and described in the Federal Policy; and (2) obtain informed consent, as defined and described in the Federal Policy, from the human research subject. If the research will not be conducted, funded, supported, or regulated by another federal agency that has implemented the Federal Policy, the licensee must, before conducting research, apply for and receive a specific amendment to its NRC medical use license. The amendment request

must include a written commitment that the licensee will, before conducting research, (1) obtain review and approval of the research from an IRB, as defined and described in the Federal Policy; and (2) obtain informed consent, as defined and described in the Federal Policy, from the human research subject. Nothing in this section relieves licensees from complying with the other requirements in this part.

Part 35.11 specifies that a person *shall not manufacture, produce, acquire, receive, possess, use or transfer* byproduct material for medical use except in accordance with a specific license issued by NRC or an agreement state that authorizes such activities. This licensure requirement is clearly reflected in the procurement practice guidelines that obligate nuclear pharmacists to act with proper authority (i.e., under a valid radioactive materials license) to purchase radioactive material. A specific license is not needed for an individual who (1) receives, possesses, uses, or transfers byproduct material in accordance with the regulations in this chapter under the supervision of an AU as provided in §35.27, unless prohibited by license condition; or (2) prepares unsealed byproduct material for medical use in accordance with the regulations in this chapter under the supervision of an ANP or AU as provided in §35.27, unless prohibited by license condition.

The requirements for *license application, amendment, or renewal* relative to nuclear medicine are specified in §35.12. The applicant or licensee's management must sign each license application. An application for a license for medical use of byproduct material as described in §35.100 (use of unsealed byproduct material for uptake, dilution, and excretion studies for which a written directive is not required), §35.200 (use of unsealed byproduct material for imaging and localization studies for which a written directive is not required), or §35.300 (use of unsealed byproduct material for which a written directive is required) must be made by filing an original and one copy of NRC Form 313, Application for Material License, that includes the facility diagram, equipment, and training and experience qualifications of the RSO, AU(s), ANP(s), and AMP(s) if any. Requests for a license amendment or renewal must be made by submitting an original and one copy of either NRC Form 313 or a letter requesting the amendment or renewal. The applicant or licensee must also provide any other information requested by NRC in its review of the application. An applicant satisfying the requirements specified in §33.13 governing specific domestic licenses of broad scope for byproduct material may apply for a Type A specific license of broad scope.

License amendments are addressed further in §35.13: A licensee must apply for and receive an approved license amendment (a) before it receives, prepares, or uses byproduct material for a type of use that is permitted under this part, but that is not authorized on the licensee's current license issued under this part; or (b) before it permits anyone to work as an AU, ANP, or AMP under the license. Important exceptions are allowed to §35.13(b). For example, exception may be made for AUs who meet the training requirements specified in §§35.190(a) for uptake, dilution, and excretion studies, 35.290(a) for imaging and localization studies, 35.390(a) for use of unsealed byproduct material for which a written directive is required, 35.392(a) for the oral administration of ^{131}I-sodium iodide requiring a written directive in quantities not exceeding 1.22 GBq (33 mCi), and 35.394(a) for the oral administration of ^{131}I-sodium iodide requiring a written directive in quantities greater than 1.22 GBq (33 mCi). To qualify for the exception, the AU must be certified by a medical specialty board, the board certification process must adequately address all of the NRC training requirements, and the board certification must be recognized by NRC or an agreement state. An exception may also be made for ANPs who meet the training requirements specified in §35.55(a) or 35.980(a) and 35.59. Likewise, exceptions may be made for AMPs who meet the training requirements specified in §§35.51(a) or 35.961(a) or (b) and 35.59. Finally, exceptions may be made for an individual who is identified as an AU, an ANP, or an AMP on an NRC or agreement state license or other

equivalent permit or license recognized by NRC that authorizes the use of byproduct material in medical use or in the practice of nuclear pharmacy; on a permit issued by NRC or an agreement state specific license of broad scope that is authorized to permit the use of byproduct material in medical use or in the practice of nuclear pharmacy; on a permit issued by an NRC master material licensee that is authorized to permit the use of byproduct material in medical use or in the practice of nuclear pharmacy; or by a commercial nuclear pharmacy that has been authorized to identify ANPs.

According to §35.13(c), the licensee must apply for and receive a license amendment before it changes RSOs, except as provided in §35.24(c). This exception allows the licensee to permit a qualified individual to serve as a temporary RSO and to perform the associated functions under the prescribed conditions for up to 60 days each year, provided the NRC is properly notified in accordance with §35.14(b). In accordance with 35.13(d), the licensee must apply for and receive a license amendment before it receives byproduct material in excess of the amount or in a different form, or receives a different radionuclide, than is authorized on the license. Further, in accordance with §35.13(e), a licensee must apply for and receive a license amendment before it adds to or changes the areas of use identified in the application or on the license, except for areas of use where byproduct material is used only in accordance with either §§35.100 (uptake, dilution, and excretion studies) or 35.200 (imaging and localization studies). Finally, §35.13(f) requires licensees to apply for and receive a license amendment prior to changing the address(es) of use identified in the application or on the radioactive materials license.

Licensees are obligated under §35.14 to provide several types of timely *notification to NRC*. Part 35.14(a) requires the licensee to provide a copy of the board certification, the NRC or agreement state license, the permit issued by an NRC master material licensee, the permit issued by an NRC or agreement state licensee of broad scope, or the permit issued by an NRC master material license broad scope permittee for each individual no later than 30 days after the date that the licensee permits the individual to work as an AU, ANP, or AMP under §35.13 (b)(1) through (b)(4). Additionally, in accordance with §35.14(b), the licensee must notify NRC by letter no later than 30 days after (1) an AU, ANP, RSO, or AMP permanently discontinues performance of duties under the license or has a name change; (2) the licensee's mailing address changes; (3) the licensee's name changes but the name change does not constitute a transfer of control of the license as described in §30.34(b); or (4) the licensee has added to or changed the areas of use identified in the application or on the license where byproduct material is used in accordance with either §§35.100 (uptake, dilution, and excretion studies) or 35.200 (imaging and localization studies).

General Administrative Requirements

The general administrative requirements associated with properly managing a radioactive materials license in compliance with applicable regulations are quite significant and must be adequately addressed by the licensee. Part 35.24 identifies the authority and responsibilities of the required radiation protection program that each licensee must maintain. These radiation protection program requirements are in addition to those specified elsewhere under §20.1101.

According to §35.24(a), a licensee's management must approve in writing (1) requests for a license application, renewal, or amendment before submittal to NRC; (2) any individual before allowing that individual to work as an AU, ANP, or AMP; and (3) radiation protection program changes that do not require a license amendment and are permitted under §35.26 (radiation protection program changes).

Pursuant to §35.24(b), a licensee's management must appoint an RSO who agrees in writing to be responsible for implementing the radiation protection program. The licensee, through the RSO, must ensure that radiation safety activities are being performed in accordance with licensee-approved procedures and regulatory requirements. As mentioned earlier, §35.24(c) allows the licensee to permit a qualified individual to serve as a temporary RSO and to perform the associated functions under the prescribed conditions for up to 60 days each year, provided the NRC is properly notified. This arrangement can be extended under §35.24(d) to the simultaneous appointment of more than one temporary RSO if needed to ensure that the licensee satisfies the requirements for each of the different types of uses of byproduct material permitted by the license. The licensee must establish the authority, duties, and responsibilities of the RSO in writing as required by §35.24(e).

In accordance with §35.24(f), licensees authorized for two or more different types of uses of byproduct material under Subpart E (Unsealed Byproduct Material—Written Directive Required) must establish a *radiation safety committee* (RSC) to oversee all uses of byproduct material permitted by the license. The RSC must include an AU for each type of use permitted, the RSO, a representative of the nursing service, and a representative of management who is neither an AU nor an RSO. The RSC may include other members the licensee considers appropriate, such as an ANP. The RSO, according to §35.24(g), must be provided sufficient authority, organizational freedom, time, resources, and management prerogative to (1) identify radiation safety problems; (2) initiate, recommend, or provide corrective actions; (3) stop unsafe operations; and (4) verify implementation of corrective actions. Finally, §35.24(h) states that the licensee must retain a record of actions taken under (a), (b), and (e) of this section in accordance with §35.2024.

Part 35.27 addresses the important issue of *proper supervision* of individuals involved in the medical use of licensed materials. As stipulated in §35.27(a), a licensee that permits the receipt, possession, use, or transfer of byproduct material by an individual under the supervision of an AU, as allowed by §35.11(b)(1), must (1) in addition to the requirements in §19.12, instruct the supervised individual in the licensee's written radiation protection procedures, written directive procedures, regulations of this chapter, and license conditions with respect to the use of byproduct material; and (2) require the supervised individual to follow the instructions of the supervising AU, written radiation protection procedures established by the licensee, written directive procedures, regulations of this chapter, and license conditions with respect to the medical use of byproduct material. Likewise, according to §35.27(b), a licensee that permits the preparation of byproduct material for medical use by an individual under the supervision of an ANP or physician who is an AU, as allowed by §35.11(b)(2), must (1) in addition to the requirements in §19.12, instruct the supervised individual in the preparation of byproduct material for medical use, as appropriate to that individual's involvement with byproduct material; and (2) require the supervised individual to follow the instructions of the supervising AU or ANP regarding the preparation of byproduct material for medical use, written radiation protection procedures established by the licensee, the regulations of this chapter, and license conditions. §35.27(c) stipulates that the licensee that permits supervised activities under (a) and (b) is responsible for the acts and omissions of the supervised individual.

AUs must write orders for the administration of byproduct material or radiation from byproduct material to a specific patient or human research subject in the form of a *written directive*. In many ways these directives are analogous to the written prescription required in the customary practice of medicine and pharmacy. According to §35.40(a), a written directive must be dated and signed by an AU prior to the administration of ^{131}I-sodium iodide in amounts greater than 1.11 MBq (30 μCi), any therapeutic dosage of unsealed byproduct material, or any therapeutic dose of radiation from byproduct material. If, because of the emergent nature of the patient's condition, a delay for the purpose of

providing a written directive would jeopardize the patient's health, an oral directive is acceptable. The information contained in the oral directive must be documented as soon as possible in writing in the patient's record. A written directive must be prepared within 48 hours of the oral directive. Additionally, according to §35.40(b), the written directive for a radiopharmaceutical must contain the patient or human research subject's name and the following information: (1) for any administration of quantities greater than 1.11 MBq (30 μCi) of ^{131}I-sodium iodide, the dosage; and (2) for administration of a therapeutic dosage of unsealed byproduct material other than ^{131}I-sodium iodide, the radioactive drug, dosage, and route of administration. Revisions to existing written directives may be made under §35.40(c) if the revision is dated and signed by an AU before administration of the dosage of unsealed byproduct material. If, because of the patient's condition, a delay for the purpose of providing a written revision to an existing written directive would jeopardize the patient's health, an oral revision to an existing written directive is acceptable. The oral revision must be documented as soon as possible in the patient's record. The AU must sign a revised written directive within 48 hours of the oral revision. As is customary with written prescriptions, the licensee must retain a copy of the written directive in accordance with §35.2040.

§35.41(a) requires that the procedures for administration requiring a written directive be well documented. The licensee must develop, implement, and maintain written procedures to provide high confidence that (1) the patient's or human research subject's identity is verified before each administration; and (2) each administration is in accordance with the written directive. At a minimum, these required procedures must address the following items that are applicable to the licensee's use of byproduct material: (1) verifying the identity of the patient or human research subject; (2) verifying that the administration is in accordance with the treatment plan, if applicable, and the written directive; and (3) checking both manual and computer-generated dose calculations. Finally, as is customary in medical and pharmacy practice, the licensee must retain a copy of the procedures required under paragraph (a), in accordance with §35.2041.

RSO training requirements, as delineated in §35.50, are important to consider, since nuclear pharmacists and nuclear medicine physicians may bear responsibility for these associated duties. Except as provided in §35.57, the licensee must require an individual fulfilling the responsibilities of the RSO as provided in §35.24 to be an individual who (a) is certified by a specialty board whose certification process includes all of the requirements in (b) and whose certification has been recognized by NRC or an agreement state; or (b)(1) has completed a structured educational program consisting of both 200 hours of didactic training in the following areas: radiation physics and instrumentation, radiation protection, mathematics pertaining to the use and measurement of radioactivity, radiation biology, and radiation dosimetry; and 1 year of full-time radiation safety experience under the supervision of the individual identified as the RSO on an NRC or agreement state license or permit issued by an NRC master material licensee that authorizes similar types of uses of byproduct material involving the following: shipping, receiving, and performing related radiation surveys; using and performing checks for proper operation of instruments used to determine the activity of dosages, survey meters, and instruments used to measure radionuclides; securing and controlling byproduct material; using administrative controls to avoid mistakes in the administration of byproduct material; using procedures to prevent or minimize radioactive contamination and using proper decontamination procedures; using emergency procedures to control byproduct material; and disposing of byproduct material; and (2) has obtained written certification, signed by a preceptor RSO, that the individual has satisfactorily completed the requirements in (b)(1) and has achieved a level of radiation safety knowledge sufficient to function independently as RSO for a

medical use licensee; or (c) is an AU, ANP, or AMP identified on the licensee's license and has experience with the radiation safety aspects of types of use of byproduct material for which the individual has RSO responsibilities.

The *AMP training requirements*, as delineated in §35.51, may be important to consider. Except as provided in §35.57, the licensee must require the AMP to be an individual who (a) is certified by a specialty board whose certification process includes all of the training and experience requirements in (b) and whose certification has been recognized by NRC or an agreement state; or (b)(1) holds a master's or doctor's degree in physics, biophysics, radiologic physics, medical physics, or health physics and has completed 1 year of full-time training in therapeutic radiologic physics and an additional year of full-time work experience under the supervision of an AMP at a medical institution that includes the tasks listed in §§35.67, 35.433, 35.632, 35.633, 35.635, 35.642, 35.643, 35.645, and 35.652, as applicable; and (2) has obtained written certification that the individual has satisfactorily completed the requirements in (b)(1) and has achieved a level of competency sufficient to function independently as an AMP for each type of therapeutic medical unit for which the individual is requesting AMP status. A preceptor AMP who meets the requirements in §35.51 or equivalent agreement state requirements must sign the written certification for an AMP for each type of therapeutic medical unit for which the individual is requesting AMP status.

The *ANP training requirements*, as delineated in §35.55, are of obvious importance to nuclear pharmacists and nuclear pharmacy operations in any practice setting. Except as provided in §35.57, the licensee must require the ANP to be a pharmacist who (a) is certified as a nuclear pharmacist by a specialty board whose certification process includes all of the requirements in (b) and whose certification has been recognized by NRC or an agreement state; or (b)(1) has completed 700 hours in a structured educational program consisting of both didactic training in the following areas: radiation physics and instrumentation, radiation protection, mathematics pertaining to the use and measurement of radioactivity, chemistry of byproduct material for medical use, and radiation biology; and supervised practical experience in a nuclear pharmacy involving shipping, receiving, and performing related radiation surveys; using and performing checks for proper operation of instruments used to determine the activity of dosages, survey meters, and, if appropriate, instruments used to measure alpha- or beta-emitting radionuclides; calculating, assaying, and safely preparing dosages for patients or human research subjects; using administrative controls to avoid medical events in the administration of byproduct material; and using procedures to prevent or minimize radioactive contamination and using proper decontamination procedures; and (2) has obtained written certification, signed by a preceptor ANP, that the individual has satisfactorily completed the requirements in (b)(1) and has achieved a level of competency sufficient to function independently as an ANP.

§35.57 addresses *exceptions to the training requirements* for experienced RSOs, medical physicists, AUs, and nuclear pharmacists. According to §35.57(a), an individual identified as an RSO, medical physicist, or nuclear pharmacist on an NRC or agreement state license or a permit issued by an NRC or agreement state broad scope licensee or master material license permit or by a master material license permittee of broad scope before October 24, 2002, need not comply with the training requirements of §§35.50, 35.51, or 35.55, respectively. Additionally, according to §35.57(b), physicians, dentists, or podiatrists identified as AUs for the medical use of byproduct material on a license issued by NRC or an agreement state, a permit issued by an NRC master material licensee, a permit issued by an NRC or agreement state broad scope licensee, or a permit issued by an NRC master material license broad scope permittee before October 24, 2002, who perform only those medical uses for which they were authorized on that date need not comply with the training requirements of Subparts D through H of this part.

The issue of the *recentness of professional training* often surfaces in regard to the medica use of byproduct materials. §35.59 states that the training and experience specified i Subparts B, D, E, F, G, H, and J must have been obtained within the 7 years preceding th date of application or the individual must have had related continuing education an experience since the required training and experience was completed.

General Technical Requirements

Because of the importance of safety in the medical use of radioactive materials, numerou technical requirements must be satisfied to remain in regulatory compliance. Part 35.6 addresses the *possession, use, and calibration of instruments* used to measure the activity o unsealed byproduct material. For direct measurements performed in accordance wit §35.63, a licensee must possess and use instrumentation to measure the activity of unseale byproduct material before it is administered to each patient or human research subject Additionally, the licensee must calibrate the required instrumentation in accordance wit nationally recognized standards or the manufacturer's instructions. Finally, the licensee must retain a record of each required instrument calibration in accordance with §35.2060

Radiation survey instruments are used for a number of purposes in complying wit regulations for the use of radioactive materials. Part 35.61 deals with the calibration o such survey instruments. The licensee must calibrate the survey instruments used to show compliance with this part and 10 CFR Part 20 (Standards for Protection Against Radiation) before first use, annually, and after a repair that affects the calibration. The licensee must (1) calibrate all scales with readings up to 10 mSv (1000 mrem) per hour with a radiation source; (2) calibrate two separate readings on each scale or decade that will be used to show compliance; and (3) conspicuously note on the instrument the date of calibration. A licensee may not use survey instruments if the difference between the indicated exposure rate and the calculated exposure rate is more than 20%. The licensee must retain a record of each survey instrument calibration in accordance with §35.2061.

According to §35.63, licensees must make an accurate determination of the *dosages of unsealed byproduct material* for medical use. Thus, the licensee must determine and record the activity of each dosage before release for medical use. For a unit dosage, this determination must be made by (1) direct measurement of radioactivity; or (2) a decay correction, based on the activity or activity concentration determined by a manufacturer or preparer (e.g., nuclear pharmacy) licensed under §32.72 or equivalent agreement state requirements, or by an NRC or agreement state licensee for use in research in accordance with a radioactive drug research committee (RDRC) approved protocol or an investigational new drug (IND) protocol accepted by FDA. For other than unit dosages, this determination must be made by (1) direct measurement of radioactivity; (2) combination of measurement of radioactivity and mathematical calculations; or (3) combination of volumetric measurements and mathematical calculations, based on the measurement made by a manufacturer or preparer licensed under §32.72 of this chapter or equivalent agreement state requirements. It is important to note that unless otherwise directed by the AU, the licensee may not use a dosage if the dosage does not fall within the prescribed dosage range or if the dosage differs from the prescribed dosage by more than 20%. Once again, the licensee must retain a record of the dosage determination required by this section in accordance with §35.2063.

Part 35.65 provides authorization for certain *calibration, transmission, and reference sources* needed to ensure the safe medical use of byproduct materials. Any person authorized by §35.11 for medical use of byproduct material may receive, possess, and use any of the following byproduct materials for check, calibration, transmission, and reference use: (a) sealed sources, not exceeding 1.11 GBq (30 mCi) each, manufactured and distributed by

a person licensed under §32.74 of this chapter or equivalent agreement state regulations; (b) sealed sources, not exceeding 1.11 GBq (30 mCi) each, redistributed by a licensee authorized to redistribute the sealed sources manufactured and distributed by a person licensed under §32.74 of this chapter, provided the redistributed sealed sources are in the original packaging and shielding and are accompanied by the manufacturer's approved instructions; (c) any byproduct material with a half-life not longer than 120 days in individual amounts not to exceed 0.56 GBq (15 mCi); (d) any byproduct material with a half-life longer than 120 days in individual amounts not to exceed the smaller of 7.4 MBq (200 μCi) or 1000 times the quantities in Appendix B of 10 CFR Part 30 (Rules of General Applicability to Domestic Licensing of Byproduct Material); or (e) ^{99m}Tc in amounts as needed.

Sealed sources are routinely used in nuclear pharmacy and nuclear medicine practice, and brachytherapy sources may on rare occasions be in the possession of a nuclear pharmacy licensee. According to §35.67, certain requirements concerning the possession of sealed sources and brachytherapy sources must be satisfied. A licensee in possession of any sealed source or brachytherapy source must follow the radiation safety and handling instructions supplied by the manufacturer. A licensee in possession of a sealed source must (1) test the source for leakage before its first use unless the licensee has a certificate from the supplier indicating that the source was tested within 6 months before transfer to the licensee; and (2) test the source for leakage at intervals not to exceed 6 months or at other intervals approved by NRC or an agreement state in the Sealed Source and Device Registry. To satisfy the leak test requirements, the licensee must measure leak test samples in a manner that will allow for detecting the presence of 185 Bq (0.005 μCi) of radioactive material in the sample. The licensee must retain leak test records in accordance with §35.2067(a) for a period of 3 years. Additional requirements come into play if the leak test reveals the presence of 185 Bq (0.005 μCi) or more of removable contamination. If this occurs, the licensee must (1) immediately withdraw the sealed source from use and store, dispose, or cause it to be repaired in accordance with the requirements in 10 CFR Parts 20 and 30; and (2) file a report within 5 days of the leak test in accordance with §35.3067. The licensee does not need to perform a leak test on (1) sources containing only byproduct material with a half-life of less than 30 days; (2) sources containing only byproduct material as a gas; (3) sources containing 3.7 MBq (100 μCi) or less of beta- or gamma-emitting material or 0.37 MBq (10 μCi) or less of alpha-emitting material; (4) seeds of ^{192}Ir encased in nylon ribbon; and (5) sources stored and not being used. However, the licensee must test each such source for leakage before any use or transfer unless it has been leak tested within 6 months before the date of use or transfer. Licensees in possession of sealed sources or brachytherapy sources, except for gamma stereotactic radiosurgery sources, must conduct a semiannual physical inventory of all such sources in their possession. Finally, licensees must retain each inventory record in accordance with §35.2067(b) for a period of 3 years.

The proper *labeling of radioactive materials* is key to their safe handling and appropriate use. According to §35.69, each syringe and vial that contains unsealed byproduct material must be labeled appropriately to adequately identify the radioactive drug. Each syringe shield and vial shield must also be labeled unless the label on the syringe or vial is visible when shielded. This issue is also dealt with in §32.72(a)(4)(ii); accordingly, the licensee must affix a label to each syringe, vial, or other container used to hold a radioactive drug that is to be transferred for commercial distribution. The label must include the radiation symbol and the words "Caution, Radioactive Material" or "Danger, Radioactive Material" and an identifier that ensures that the syringe, vial, or other container can be correlated with the information on the transport radiation shield label. Beyond this, nuclear pharmacy services label radioactive drugs with the standard elements of required prescription labeling.

Surveys of ambient radiation exposure rates are required according to §35.70, and this requirement is in addition to the surveys required by 10 CFR Part 20. The licensee must survey with a radiation detection survey instrument at the end of each day of use all areas where unsealed byproduct material requiring a written directive were prepared for use or administered. However, the licensee does not need to perform such surveys in areas where patients or human research subjects are confined when they cannot be released under §35.75. The licensee must retain a record of each survey in accordance with §35.2070 for a period of 3 years.

A revised §35.75 was published in the *Federal Register* (62 FR 4120) on January 29, 1997, and became effective on May 29, 1997. This revision delineates the *criteria for release* of individuals containing unsealed byproduct material or implants containing byproduct material. The licensee may authorize the release of any individual from its control who has been administered unsealed byproduct material or implants containing byproduct material if the total effective dose equivalent (TEDE) to any other individual from exposure to the released individual is not likely to exceed 5 mSv (0.5 rem). The required methods for calculating such doses to other individuals and tables of activities not likely to cause doses exceeding this imposed limit can be found in NUREG-1556, Vol. 9 (draft). If the requirements for release are satisfied, the licensee must provide the released individual, or the individual's parent or guardian, with instructions, including written instructions, on actions recommended to maintain radiation doses to other individuals as low as reasonably achievable if the TEDE to any other individual is likely to exceed 1 mSv (0.1 rem). If the TEDE to a nursing infant or child could exceed 1 mSv (0.1 rem) assuming there were no interruption of breast-feeding, the instructions must also include (1) guidance on the interruption or discontinuation of breast-feeding and (2) information on the potential consequences, if any, of failure to follow the guidance. To be fully compliant, the licensee must maintain a record of the basis for authorizing the release of an individual in accordance with §35.2075(a) and the instructions provided to a breast-feeding female in accordance with §35.2075(b). These records must be maintained for a period of 3 years after the date of release of each individual.

In some practice settings licensees may be involved in the provision of *regional mobile medical services*. A licensee involved in providing such services must satisfy the conditions set forth in §35.80. The licensee must (1) obtain a letter signed by the management of each client for which services are rendered that permits the use of byproduct material at the client's address and clearly delineates the authority and responsibility of the licensee and the client; (2) check instruments used to measure the activity of unsealed byproduct material for proper function before medical use at each client's address or on each day of use, whichever is more frequent; at a minimum, the check for proper function must include a constancy check; (3) check survey instruments for proper operation with a dedicated check source before use at each client's address; and (4) before leaving a client's address, survey all areas of use to ensure compliance with the requirements in 10 CFR Part 20. Mobile medical services may not have byproduct material delivered from a manufacturer or a distributor (e.g., a nuclear pharmacy) to the client unless the client has a license allowing possession of the byproduct material. Byproduct material delivered to the client must be received and handled in conformance with the client's license. In addition, the licensee providing such services must retain each signed management letter that permits the provision of service and must record the results of the required radiation area surveys in accordance with §35.2080(a) and (b), respectively.

Holding short-lived radioactive materials for *decay-in-storage* is a very attractive and cost-effective management practice for both nuclear pharmacies and nuclear medicine clinics. Part 35.92(a) identifies the requirements associated with this practice. A licensee may hold byproduct material with a physical half-life of less than 120 days for decay-in-

storage before disposal without regard to its radioactivity if the licensee (1) monitors byproduct material at the surface before disposal and determines that any residual radioactivity cannot be distinguished from the background radiation level as determined with an appropriate radiation detection survey meter set on its most sensitive scale and with no interposed shielding; and (2) removes or obliterates all radiation labels, except for radiation labels on materials that are within containers and that will be managed as biomedical waste after their release by the licensee. Thus, according to (a)(2), radiation labels on biomedical waste (e.g., sharps containers or individual needles and syringes) do not have to be removed or obliterated where there is a biohazard associated with retrieving such material from their outer container. In many cases, biomedical waste containers are packaged in barrels and incinerated, but this may not be done in all cases. Licensees must ensure that released biomedical waste either is incinerated or contains no legible radioactive labels that could otherwise cause a potential incident upon discovery by the general public. Regardless of this new flexibility to support occupational safety, good practice still necessitates the obliteration of all radioactive labels possible, by using safe measures that do not constitute a biohazard to personnel. To be fully compliant, the licensee must retain a record of each disposal permitted in accordance with §35.2092 for a period of 3 years.

Unsealed Byproduct Material—Written Directive Not Required

According to §35.100, unsealed byproduct material may be used for uptake, dilution, and excretion studies without a written directive under certain circumstances. Except for quantities that require a written directive under §35.40(b), a licensee may use any unsealed byproduct material prepared for medical use for uptake, dilution, or excretion studies that is (a) obtained from a manufacturer or preparer licensed under §32.72 or equivalent agreement state requirements; or (b) prepared by an ANP, a physician who is an AU and who meets the requirements specified in §§35.290 or 35.390, or an individual under the supervision of either as specified in §35.27; or (c) obtained from and prepared by an NRC or agreement state licensee for use in research in accordance with an RDRC-approved protocol or an IND protocol accepted by FDA; or (d) prepared by the licensee for use in research in accordance with an RDRC-approved application or an IND protocol accepted by FDA.

As specified in §35.190, appropriate training is required for uptake, dilution, and excretion studies. Except as provided in §35.57, the licensee must require an AU of unsealed byproduct material for the uses authorized under §35.100 to be a physician who (a) is certified by a medical specialty board whose certification process includes all of the requirements in (c) and whose certification has been recognized by NRC or an agreement state; or (b) is an AU under §§35.290 or 35.390 or equivalent agreement state requirements; or (c)(1) has completed 60 hours of training and experience in basic radionuclide handling techniques applicable to the medical use of unsealed byproduct material for uptake, dilution, and excretion studies. The training and experience must include classroom and laboratory training in the following areas: radiation physics and instrumentation, radiation protection, mathematics pertaining to the use and measurement of radioactivity, chemistry of byproduct material for medical use, and radiation biology; and work experience, under the supervision of an AU who meets the requirements in §35.190, §35.290, or §35.390 or equivalent agreement state requirements, involving ordering, receiving, and unpacking radioactive materials safely and performing the related radiation surveys; calibrating instruments used to determine the activity of dosages and performing checks for proper operation of survey meters; calculating, measuring, and safely preparing patient or human research subject dosages; using administrative controls to prevent a medical event involving the use of unsealed byproduct material; using procedures to contain spilled byproduct

material safely and using proper decontamination procedures; and administering dosages of radioactive drugs to patients or human research subjects; and (2) has obtained written certification, signed by a preceptor AU who meets the requirements in §§35.190, 35.290, or 35.390 or equivalent agreement state requirements, that the individual has satisfactorily completed the requirements in (c)(1) and has achieved a level of competency sufficient to function independently as an AU for the medical uses authorized under §35.100.

In accordance with §35.200, unsealed byproduct material may be used for imaging and localization studies without a written directive under certain conditions. Except for quantities that require a written directive under §35.40(b), a licensee may use any unsealed byproduct material prepared for medical use for imaging and localization studies that is (a) obtained from a manufacturer or preparer licensed under §32.72 or equivalent agreement state requirements; or (b) prepared by an ANP, a physician who is an AU and who meets the requirements specified in §§35.290 or 35.390, or an individual under the supervision of either as specified in §35.27; or (c) obtained from and prepared by an NRC or agreement state licensee for use in research in accordance with an RDRC-approved protocol or an IND protocol accepted by FDA; or (d) prepared by the licensee for use in research in accordance with an RDRC-approved application or an IND protocol accepted by FDA.

^{99}Mo is a potential, and the most probable, radionuclidic impurity found in ^{99}Mo–^{99m}Tc generator eluates. If the generators are functioning properly, their eluates should contain ^{99m}Tc as the sole radioactive component. However, if ^{99}Mo "breakthrough" were to occur, excessive amounts of the radionuclide in the administered dosage would contribute unnecessary radiation dose to patients. §35.204 identifies the permissible ^{99}Mo concentration for ^{99}Mo–^{99m}Tc generator eluates. According to this imposed limit, a licensee may not administer to humans a radiopharmaceutical that contains more than 0.15 kBq of ^{99}Mo per megabecquerel of ^{99m}Tc (0.15 μCi of ^{99}Mo per millicurie of ^{99m}Tc). In addition, a licensee that uses ^{99}Mo–^{99m}Tc generators for preparing a ^{99m}Tc radiopharmaceutical must measure the ^{99}Mo concentration of the first eluate after receipt of a generator to demonstrate compliance with paragraph (a) of this section. Previously, licensees were required to check for ^{99}Mo breakthrough after each elution of the ^{99}Mo–^{99m}Tc generator; this is another example of increased regulatory flexibility. Finally, if a licensee is required to measure the ^{99}Mo concentration, the licensee must retain a record of each measurement in accordance with §35.2204 for a period of 3 years. The record must include, for each measured elution of ^{99m}Tc, the ratio of the measures expressed as kilobecquerels of ^{99}Mo per megabecquerel of ^{99m}Tc (or microcuries of ^{99}Mo per millicurie of ^{99m}Tc), the time and date of the measurement, and the name of the individual who made the measurement.

As spelled out in §35.290, AUs must be properly trained to take responsibility for imaging and localization studies. Except as provided in §35.57, the licensee must require an AU of unsealed byproduct material for the uses authorized under §35.200 to be a physician who (a) is certified by a medical specialty board whose certification process includes all of the requirements in (c) and whose certification has been recognized by NRC or an agreement state; or (b) is an AU under §35.390 or equivalent agreement state requirements; or (c)(1) has completed 700 hours of training and experience in basic radionuclide handling techniques applicable to the medical use of unsealed byproduct material for imaging and localization studies; the training and experience must include, at a minimum, classroom and laboratory training in the following areas: radiation physics and instrumentation, radiation protection, mathematics pertaining to the use and measurement of radioactivity, chemistry of byproduct material for medical use, and radiation biology; and work experience, under the supervision of an AU who meets the requirements in §§35.290 or 35.390 or equivalent agreement state requirements, involving ordering, receiving,

and unpacking radioactive materials safely and performing the related radiation surveys; calibrating instruments used to determine the activity of dosages and performing checks for proper operation of survey meters; calculating, measuring, and safely preparing patient or human research subject dosages; using administrative controls to prevent a medical event involving the use of unsealed byproduct material; using procedures to safely contain spilled radioactive material and using proper decontamination procedures; administering dosages of radioactive drugs to patients or human research subjects; and eluting generator systems appropriate for preparation of radioactive drugs for imaging and localization studies, measuring and testing the eluate for radionuclidic purity, and processing the eluate with reagent kits to prepare labeled radioactive drugs; and (2) has obtained written certification, signed by a preceptor AU who meets the requirements in §§35.290 or 35.390 or equivalent agreement state requirements, that the individual has satisfactorily completed the requirements in (c)(1) and has achieved a level of competency sufficient to function independently as an AU for the medical uses authorized under §§35.100 and 35.200.

Unsealed Byproduct Material—Written Directive Required

According to §35.300, a licensee may use any unsealed byproduct material prepared for medical use and for which a written directive is required that is (a) obtained from a manufacturer or preparer licensed under §32.72 or equivalent agreement state requirements; or (b) prepared by an ANP, a physician who is an AU and who meets the requirements specified in §§35.290 or 35.390, or an individual under the supervision of either as specified in §35.27; or (c) obtained from and prepared by an NRC or agreement state licensee for use in research in accordance with an IND protocol accepted by FDA; or (d) prepared by the licensee for use in research in accordance with an IND protocol accepted by FDA.

The provision of safety instructions is a key component of any required radiation safety program. As required in §35.310, the licensee must provide radiation safety instruction, initially and at least annually, for all personnel caring for the patient or the human research subject receiving radiopharmaceutical therapy and hospitalized for compliance with §35.75 of this chapter. To satisfy this requirement, the instruction must describe the licensee's procedures for (1) patient or human research subject control; (2) visitor control; (3) contamination control; (4) waste control; and (5) notification of the RSO, or his or her designee, and the AU if the patient or the human research subject has a medical emergency or dies. The licensee must retain a record of individuals receiving instruction in accordance with §35.2310 for a period of 3 years.

Proper safety precautions, as required under §35.315, must be used with each patient or human research subject who cannot be released under §35.75. Accordingly, the licensee must (1) quarter these individuals either in a private room with a private sanitary facility, or in a room with a private sanitary facility with another individual who also has received therapy with unsealed byproduct material and who also cannot be released under §35.75; (2) visibly post the therapy room with a "Radioactive Materials" sign; (3) note on the door or in the individual's chart where and how long visitors may stay in the therapy room; and (4) either monitor material and items removed from the therapy room to determine that their radioactivity cannot be distinguished from the natural background radiation level with a radiation detection survey instrument set on its most sensitive scale and with no interposed shielding, or handle the material and items as radioactive waste. The licensee must notify the RSO, or his or her designee, and the AU as soon as possible if a patient or human research subject has a medical emergency or dies.

Appropriate training, as stipulated in §35.390, is necessary for use of unsealed byproduct material for which a written directive is required. Except as provided in §35.57, the licensee must require an AU of unsealed byproduct material for the uses authorized under §35.300 to be a physician who (a) is certified by a medical specialty board whose certification process includes all of the requirements in (b) and whose certification has been recognized by NRC or an agreement state; or (b)(1) has completed 700 hours of training and experience in basic radionuclide handling techniques applicable to the medical use of unsealed byproduct material requiring a written directive; the training and experience must include (i) classroom and laboratory training in the following areas: radiation physics and instrumentation, radiation protection, mathematics pertaining to the use and measurement of radioactivity, chemistry of byproduct material for medical use, and radiation biology; and (ii) work experience, under the supervision of an AU who meets the requirements in §35.390(a), §35.390(b), or equivalent agreement state requirements [A supervising AU who meets the requirements in §35.390(b) must have experience in administering dosages in the same dosage category or categories (i.e., §35.390(b)(1)(ii)(G)(1), (2), (3), or (4)) as the individual requesting AU status. The work experience must involve (A) ordering, receiving, and unpacking radioactive materials safely and performing the related radiation surveys; (B) calibrating instruments used to determine the activity of dosages, and performing checks for proper operation of survey meters; (C) calculating, measuring, and safely preparing patient or human research subject dosages; (D) using administrative controls to prevent a medical event involving the use of unsealed byproduct material; (E) using procedures to contain spilled byproduct material safely and using proper decontamination procedures; (F) eluting generator systems, measuring and testing the eluate for radionuclidic purity, and processing the eluate with reagent kits to prepare labeled radioactive drugs; and (G) administering dosages of radioactive drugs to patients or human research subjects involving a minimum of three cases in each of the following categories for which the individual is requesting AU status: (1) oral administration of no more than 1.22 GBq (33 mCi) of ^{131}I-sodium iodide; (2) oral administration of more than 1.22 GBq (33 mCi) of ^{131}I-sodium iodide (experience with at least three cases in category (G)(2) also satisfies the requirement in category (G)(1)); (3) parenteral administration of any beta emitter or a photon-emitting radionuclide with a photon energy less than 150 keV; and (4) parenteral administration of any other radionuclide]; and (b)(2) has obtained written certification that the individual has satisfactorily completed the requirements in (b)(1) and has achieved a level of competency sufficient to function independently as an AU for the medical uses authorized under §35.300. A preceptor AU who meets the requirements in §35.390(a), §35.390(b), or equivalent agreement state requirements must sign the written certification. The preceptor AU, who meets the requirements in §35.390(b), must have experience in administering dosages in the same dosage category or categories (i.e., §35.390(b)(1)(ii)(G)(1), (2), (3), or (4)) as the individual requesting AU status.

Specific training is required, as delineated in §35.392, for the oral administration of ^{131}I-sodium iodide requiring a written directive in quantities not exceeding 1.22 GBq (33 mCi). The requirements are essentially equivalent to those specific to §35.394 for the oral administration of ^{131}I-sodium iodide requiring a written directive in quantities greater than 33 mCi except for specified dosage limits. The purpose of these new sections is to identify requirements for physicians (e.g., endocrinologists) who seek only limited authorization for oral administration of ^{131}I-sodium iodide in dosages not exceeding or dosages greater than 33 mCi and do not seek authorization to prepare radioactive drugs using generators and reagent kits. In limited-authorization settings, except as provided in §35.57, the licensee must require an AU to be a physician who (a) is certified by a medical specialty board whose certification process includes all of the requirements in (c) and whose certification has been recognized by NRC or an agreement state; or (b) is an AU under

§35.390(a), §35.390(b) for uses listed in §35.390(b)(1)(ii)(G)(2), or equivalent agreement state requirements; or (c)(1) has successfully completed 80 hours of classroom and laboratory training applicable to the medical use of ^{131}I-sodium iodide for procedures requiring a written directive; the training must include radiation physics and instrumentation, radiation protection, mathematics pertaining to the use and measurement of radioactivity; chemistry of byproduct material for medical use, and radiation biology; and (c)(2) has work experience, under the supervision of an AU who meets the requirements in §35.390(a), §35.390(b), §35.392, §35.394, or equivalent agreement state requirements [A supervising AU who meets the requirements in §35.390(b) must have experience in administering dosages as specified in §35.390(b)(1)(ii)(G)(1) or (2) or (2) alone. The work experience must involve ordering, receiving, and unpacking radioactive materials safely and performing the related radiation surveys; calibrating instruments used to determine the activity of dosages and performing checks for proper operation for survey meters; calculating, measuring, and safely preparing patient or human research subject dosages; using administrative controls to prevent a medical event involving the use of byproduct material; using procedures to contain spilled byproduct material safely and using proper decontamination procedures; and administering dosages to patients or human research subjects, including at least three cases involving the oral administration of no more than, or greater than, 33 millicuries of ^{131}I-sodium iodide]; and (c)(3) has obtained written certification that the individual has satisfactorily completed the requirements in (c)(1) and (c)(2) and has achieved a level of competency sufficient to function independently as an AU for medical uses authorized under §35.300. A preceptor AU who meets the requirements in §35.390(a), §35.390(b), §35.392, §35.394, or equivalent agreement state requirements must sign the written certification. Finally, a preceptor AU who meets the requirement in §35.390(b) must have experience in administering dosages as specified in §35.390(b)(1)(ii)(G)(1) or (2) or (2) alone.

Training and Experience Requirements

An individual must satisfy certain training and experience requirements, as specified under §35.900, in order to be given the responsibilities and duties of *RSO*. Except as provided in §35.57, the licensee must require an individual fulfilling the responsibilities of RSO as provided in §35.24 to (a) be certified by the American Board of Health Physics in comprehensive health physics, American Board of Radiology, American Board of Nuclear Medicine, American Board of Science in nuclear medicine, Board of Pharmaceutical Specialties (BPS) in nuclear pharmacy, American Board of Medical Physics (ABMP) in radiation oncology physics, Royal College of Physicians and Surgeons of Canada (RCPSC) in nuclear medicine, American Osteopathic Board of Radiology (AOBR), or American Osteopathic Board of Nuclear Medicine (AOBNM); or (b) have had classroom and laboratory training and experience as follows: (1) 200 hours of classroom and laboratory training that includes radiation physics and instrumentation, radiation protection, mathematics pertaining to the use and measurement of radioactivity, radiation biology, and radiopharmaceutical chemistry; and (2) 1 year of full-time experience as a radiation safety technologist at a medical institution under the supervision of the individual identified as the RSO on an NRC or agreement state license that authorizes the medical use of byproduct material; or (c) be an AU identified on the licensee's license.

A physician must satisfy certain training and experience requirements, as specified under §35.910, in order to be given the responsibilities and duties of an *AU for uptake, dilution, and excretion studies*. Except as provided in §35.57, the licensee must require the AU of a radiopharmaceutical in §35.100(a) to be a physician who (a) is certified in (1) nuclear medicine by the American Board of Nuclear Medicine (ABNM), (2) diagnostic

radiology by the American Board of Radiology (ABR), (3) diagnostic radiology or radiology by AOBR, (4) nuclear medicine by RCPSC, or (5) nuclear medicine by AOBNM; or (b) has had classroom and laboratory training in basic radioisotope handling techniques applicable to the use of prepared radiopharmaceuticals and supervised clinical experience as follows: (1) 40 hours of classroom and laboratory training that includes radiation physics and instrumentation; radiation protection; mathematics pertaining to the use and measurement of radioactivity, radiation biology, and radiopharmaceutical chemistry; and (2) 20 hours of supervised clinical experience under the supervision of an AU that includes examining patients or human research subjects and reviewing their case histories to determine their suitability for radioisotope diagnosis, limitations, or contraindications; selecting the suitable radiopharmaceuticals and calculating and measuring the dosages; administering dosages to patients or human research subjects and using syringe radiation shields; collaborating with the AU in the interpretation of radioisotope test results; and patient or human research subject follow-up; or (c) has successfully completed a 6 month training program in nuclear medicine as part of a training program that has been approved by the Accreditation Council for Graduate Medical Education (ACGME) and that included classroom and laboratory training, work experience, and supervised clinical experience in all the topics identified in (b).

A physician must satisfy certain training and experience requirements, as specified under §35.920, in order to be given the responsibilities and duties of an *AU for imaging and localization studies*. Except as provided in §35.57, the licensee must require the AU of a radiopharmaceutical, generator, or reagent kit in §35.200(a) to be a physician who (a) is certified in (1) nuclear medicine by ABNM, (2) diagnostic radiology by ABR, (3) diagnostic radiology or radiology by AOBR, (4) nuclear medicine by RCPSC, or (5) nuclear medicine by AOBNM; or (b) has had classroom and laboratory training in basic radioisotope handling techniques applicable to the use of prepared radiopharmaceuticals, generators, and reagent kits, supervised work experience, and supervised clinical experience as follows: (1) 200 hours of classroom and laboratory training that includes radiation physics and instrumentation, radiation protection, mathematics pertaining to the use and measurement of radioactivity, radiopharmaceutical chemistry, and radiation biology; and (2) 500 hours of supervised work experience under the supervision of an AU that includes ordering, receiving, and unpacking radioactive materials safely and performing the related radiation surveys; calibrating dose calibrators and diagnostic instruments and performing checks for proper operation of survey meters; calculating and safely preparing patient or human research subject dosages; using administrative controls to prevent the medical event of byproduct material; using procedures to contain spilled byproduct material safely and using proper decontamination procedures; and eluting ^{99m}Tc from generator systems, measuring and testing the eluate for ^{99}Mo and alumina contamination, and processing the eluate with reagent kits to prepare ^{99m}Tc-labeled radiopharmaceuticals; and (3) 500 hours of supervised clinical experience under the supervision of an AU that includes examining patients or human research subjects and reviewing their case histories to determine their suitability for radioisotope diagnosis, limitations, or contraindications; selecting the suitable radiopharmaceuticals and calculating and measuring the dosages; administering dosages to patients or human research subjects and using syringe radiation shields; collaborating with the AU in the interpretation of radioisotope test results; and patient or human research subject follow-up; or (c) has successfully completed a 6 month training program in nuclear medicine that has been approved by ACGME and that included classroom and laboratory training, work experience, and supervised clinical experience in all the topics identified in (b).

A physician must satisfy certain training and experience requirements, as specified under §35.930, in order to be given the responsibilities and duties of an *AU for therapeutic*

se of unsealed byproduct material. Except as provided in §35.57, the licensee must require ne AU of radiopharmaceuticals in §35.300 to be a physician who (a) is certified by (1) ABNM, (2) ABR in radiology, therapeutic radiology, or radiation oncology, (3) RCPSC in nuclear medicine, or (4) AOBR after 1984; or (b) has had classroom and laboratory training n basic radioisotope handling techniques applicable to the use of therapeutic radiopharmaceuticals, and supervised clinical experience as follows: (1) 80 hours of classroom and laboratory training that includes radiation physics and instrumentation, radiation protection, mathematics pertaining to the use and measurement of radioactivity, and radiation biology; and (2) supervised clinical experience under the supervision of an AU at a medical institution that includes use of ^{131}I for diagnosis of thyroid function and the treatment of hyperthyroidism or cardiac dysfunction in 10 individuals and use of ^{131}I for treatment of thyroid carcinoma in 3 individuals.

A physician must satisfy certain training and experience requirements, as specified under §35.932, in order to be given the responsibilities and duties of an *AU for treatment of hyperthyroidism*. Except as provided in §35.57, the licensee must require the AU of only ^{131}I for the treatment of hyperthyroidism to be a physician with special experience in thyroid disease who has had classroom and laboratory training in basic radioisotope handling techniques applicable to the use of ^{131}I for treating hyperthyroidism, and supervised clinical experience as follows: (a) 80 hours of classroom and laboratory training that includes radiation physics and instrumentation, radiation protection, mathematics pertaining to the use and measurement of radioactivity, and radiation biology; and (b) supervised clinical experience under the supervision of an AU that includes the use of ^{131}I for diagnosis of thyroid function and the treatment of hyperthyroidism in 10 individuals.

A physician must satisfy certain training and experience requirements, as specified under §35.934, in order to be given the responsibilities and duties of an *AU for treatment of thyroid carcinoma*. Except as provided in §35.57, the licensee must require the AU of only ^{131}I for the treatment of thyroid carcinoma to be a physician with special experience in thyroid disease who has had classroom and laboratory training in basic radioisotope handling techniques applicable to the use of ^{131}I for treating thyroid carcinoma, and supervised clinical experience as follows: 80 hours of classroom and laboratory training that includes radiation physics and instrumentation, radiation protection, mathematics pertaining to the use and measurement of radioactivity, and radiation biology; and (b) supervised clinical experience under the supervision of an AU that includes the use of ^{131}I for the treatment of thyroid carcinoma in three individuals.

An individual must satisfy certain training and experience requirements, as specified under §35.961, in order to be given the responsibilities and duties of an *AMP*. The licensee must require the AMP to be an individual who (a) is certified by ABR in (1) therapeutic radiological physics, (2) roentgen ray and gamma ray physics, (3) x-ray and radium physics, or (4) radiological physics; or (b) is certified by ABMP in radiation oncology physics; or (c) holds a master's or doctor's degree in physics, biophysics, radiological physics, or health physics, and has completed 1 year of full-time training in therapeutic radiological physics and an additional year of full-time work experience under the supervision of a medical physicist at a medical institution that includes the tasks listed in §§35.67, 35.632, 35.633, 35.635, 35.642, 35.643, 35.644, 35.645, and 35.652, as applicable.

A pharmacist must satisfy certain training and experience requirements, as specified under §35.980, in order to be given the responsibilities and duties of an *ANP*. The licensee must require the ANP to be a pharmacist who (a) has current board certification as a nuclear pharmacist by BPS or (b)(1) has completed 700 hours in a structured educational program consisting of both didactic training in the following areas: radiation physics and instrumentation, radiation protection, mathematics pertaining to the use and measurement of radioactivity, chemistry of byproduct material for medical use, and radiation biology;

and supervised experience in a nuclear pharmacy involving the following: shipping, receiving, and performing related radiation surveys; using and performing checks for proper operation of dose calibrators, survey meters, and, if appropriate, instruments used to measure alpha- or beta-emitting radionuclides; calculating, assaying, and safely preparing dosages for patients or human research subjects; using administrative controls to avoid mistakes in the administration of byproduct material; using procedures to prevent or minimize contamination and using proper decontamination procedures; and (2) has obtained written certification, signed by a preceptor ANP, that the above training has been satisfactorily completed and that the individual has achieved a level of competency sufficient to independently operate a nuclear pharmacy.

A pharmacist must satisfy certain training requirements, as specified under §35.981, in order to be recognized as an *experienced nuclear pharmacist*. A licensee may apply for and must receive a license amendment identifying an experienced nuclear pharmacist as an ANP before it allows this individual to work as an ANP. A pharmacist who has completed a structured educational program as specified in §35.980(b)(1) before December 2, 1994, and who is working in a nuclear pharmacy would qualify as an experienced nuclear pharmacist. An experienced nuclear pharmacist need not comply with the requirements for a preceptor statement (§35.980(b)(2)) and recentness of training (§35.59) to qualify as an ANP.

Records

According to §35.2024, records of authority and responsibilities for the radiation protection program must be maintained. The licensee must retain a record of actions taken by the licensee's management in accordance with §35.24(a) for 5 years. The record must include a summary of the actions taken and a signature of licensee management. Additionally, the licensee must retain a copy of authority, duties, and responsibilities of the RSO as required by §35.24(e) and a signed copy of each RSO's agreement to be responsible for implementing the radiation safety program, as required by §35.24(b), for the duration of the license. The records must include the signature of the RSO and licensee management.

Records regarding radiation protection program changes must be maintained according to §35.2026. The licensee must retain a record of each radiation protection program change made in accordance with §35.26(a) for 5 years. The record must include a copy of both the old and new procedures, the effective date of the change, and the signature of the licensee management that reviewed and approved the change.

According to §35.2040, the licensee must retain a copy of each written directive as required under §35.40 for a period of 3 years. Additionally, according to §35.2041, the licensee must retain a copy of the procedures for administrations requiring a written directive, as required by §35.41(a), for the duration of the license.

Records regarding calibrations of instruments used to measure the activity of unsealed byproduct material must be kept as required by §35.2060. The licensee must maintain a record of instrument calibrations, as required by §35.60, for 3 years. In addition, the records must include the model and serial number of the instrument, the date of the calibration, the results of the calibration, and the name of the individual who performed the calibration.

Records of radiation survey instrument calibrations are required under §35.2061. The licensee must maintain a record of the radiation survey instrument calibrations, required by §35.61, for 3 years. In addition, the record must include the model and serial number of the instrument, the date of the calibration, the results of the calibration, and the name of the individual who performed the calibration.

Records of dosages of unsealed byproduct material for medical use must be maintained according to §35.2063. The licensee must maintain a record of dosage determinations required by §35.63 for 3 years. The record must contain (1) the radiopharmaceutical, (2) the patient's or human research subject's name, or identification number if one has been assigned, (3) the prescribed dosage, the determined dosage, or a notation that the total activity is less than 1.1 MBq (30 μCi), (4) the date and time of the dosage determination, and (5) the name of the individual who determined the dosage.

According to §35.2067, records associated with leaks tests and the inventory of sealed sources and brachytherapy sources must be maintained. The licensee must retain records of leak tests required by §35.67(b) for 3 years. The records must include the model number, and serial number if one has been assigned, of each source tested; the identity of each source by radionuclide and its estimated activity; the results of the test; the date of the test; and the name of the individual who performed the test. In addition, the licensee must retain records of the semiannual physical inventory of sealed sources and brachytherapy sources required by §35.67(g) for 3 years. The inventory records must contain the model number of each source, and serial number if one has been assigned; the identity of each source by radionuclide and its nominal activity; the location of each source; and the name of the individual who performed the inventory.

The records of ambient radiation exposure rate surveys, as required under §35.2070, must be maintained. The licensee must retain a record of each survey required by §35.70 for 3 years. The record must include the date of the survey, the results of the survey, the instrument used to make the survey, and the name of the individual who performed the survey.

Records of the release of individuals containing unsealed byproduct material or implants containing byproduct material must be maintained according to §35.2075. The licensee must retain a record of the basis for authorizing the release of an individual, in accordance with §35.75, if TEDE is calculated by (1) using the retained activity rather than the activity administered, (2) using an occupancy factor less than 0.25 at 1 m, (3) using the biologic or effective half-life, or (4) considering the shielding by tissue. In addition, the licensee must retain a record that the instructions required by §35.75(b) were provided to a breast-feeding female if the radiation dose to the infant or child from continued breast-feeding could result in a TEDE exceeding 5 mSv (0.5 rem). These records must be retained for 3 years after the date of release of the individual.

Mobile medical services must keep records according to §35.2080. The licensee must retain a copy of each letter that permits the use of byproduct material at a client's address, as required by §35.80(a)(1). Each letter must clearly delineate the authority and responsibility of the licensee and the client and must be retained for 3 years after the last service is provided. A licensee must retain the record of each survey required by §35.80(a)(4) for 3 years. The record must include the date of the survey, the results of the survey, the instrument used to make the survey, and the name of the individual who performed the survey.

Decay-in-storage records are also required according to §35.2092. The licensee must maintain records of the disposal of licensed materials, as required by §35.92, for 3 years. The record must include the date of the disposal, the survey instrument used, the background radiation level, the radiation level measured at the surface of each waste container, and the name of the individual who performed the survey.

According to §35.2204, records of determined ^{99}Mo concentrations must be maintained. In this regard, the licensee must maintain a record of the ^{99}Mo concentration tests required by §35.204(b) for 3 years. The record must include, for each measured elution of ^{99m}Tc, the ratio of the measures expressed as kilobecquerels of ^{99}Mo per megabecquerel of ^{99m}Tc (or

microcuries of ^{99}Mo per millicurie of ^{99m}Tc), the time and date of the measurement, and the name of the individual who made the measurement.

Safety instruction records must be maintained according to §35.2310. The licensee must maintain a record of safety instructions required by §§35.310, 35.410, and 35.610 for 3 years. The record must include a list of topics covered, the date of instruction, the names of the attendees, and the names of the individuals who provided the instruction.

Reports

Medical Events

Medical events must be managed properly, as stipulated in §35.3045, to ensure regulatory compliance. The licensee must report any event, except for an event that results from patient intervention, in which the administration of byproduct material or radiation from byproduct material results in (1) a dose that differs from the prescribed dose or dose that would have resulted from the prescribed dosage by more than 0.05 Sv (5 rem) effective dose equivalent, 0.5 Sv (50 rem) to an organ or tissue, or 0.5 Sv (50 rem) shallow dose equivalent to the skin; and the total dose delivered differs from the prescribed dose by 20% or more, the total dosage delivered differs from the prescribed dosage by 20% or more or falls outside the prescribed dosage range, or the fractionated dose delivered differs from the prescribed dose, for a single fraction, by 50% or more; (2) a dose that exceeds 0.05 Sv (5 rem) effective dose equivalent, 0.5 Sv (50 rem) to an organ or tissue, or 0.5 Sv (50 rem) shallow dose equivalent to the skin from any of the following: administration of a wrong radioactive drug containing byproduct material, administration of a radioactive drug containing byproduct material by the wrong route of administration, administration of a dose or dosage to the wrong individual or human research subject, administration of a dose or dosage delivered by the wrong mode of treatment, or a leaking sealed source; (3) a dose to the skin or an organ or tissue other than the treatment site that exceeds by 0.5 Sv (50 rem) to an organ or tissue and 50% or more of the dose expected from the administration defined in the written directive (excluding, for permanent implants, seeds that were implanted in the correct site but migrated outside the treatment site).

A licensee must report any event resulting from intervention of a patient or human research subject in which the administration of byproduct material or radiation from byproduct material results or will result in unintended permanent functional damage to an organ or a physiologic system, as determined by a physician. The licensee must notify by telephone the NRC operations center no later than the next calendar day after discovery of the medical event. The licensee must submit a written report to the appropriate NRC regional office (listed in §30.6 of this chapter) within 15 days after discovery of the medical event. The written report must include the licensee's name, the name of the prescribing physician, a brief description of the event, why the event occurred, (v) the effect, if any, on the individual(s) who received the administration, what actions if any have been taken or are planned to prevent recurrence, and certification that the licensee notified the individual (or the individual's responsible relative or guardian), and if not, why not. The report may not contain the individual's name or any other information that could lead to identification of the individual.

The licensee must provide notification of the event to the referring physician and also notify the individual who is the subject of the medical event no later than 24 hours after its discovery, unless the referring physician personally informs the licensee either that he or she will inform the individual or that, in his or her medical judgment, telling the individual would be harmful. The licensee is not required to notify the individual without first consulting the referring physician. If the referring physician or the affected individual

cannot be reached within 24 hours, the licensee must notify the individual as soon as possible thereafter. The licensee may not delay any appropriate medical care for the individual, including any necessary remedial care as a result of the medical event, because of any delay in notification. To meet these requirements, notification of the individual who is the subject of the medical event may be made instead to that individual's responsible relative or guardian. If oral notification is used, the licensee must inform the individual, or appropriate responsible relative or guardian, that a written description of the event can be obtained from the licensee upon request. The licensee must provide such a written description if requested.

Aside from the notification requirement, nothing in this section affects any rights or duties of licensees and physicians in relation to each other, to individuals affected by the medical event, or to the individual's responsible relatives or guardians. A licensee must (1) annotate a copy of the report provided to NRC with the name of the individual who is the subject of the event and the Social Security number or other identification number, if one has been assigned, of the individual who is the subject of the event; and (2) provide a copy of the annotated report to the referring physician, if other than the licensee, no later than 15 days after discovery of the event.

Leaking Source

Occasionally, licensees discover leaking sealed sources in the course of conducting required leak tests. According to §35.3067, a licensee must file a report within 5 days if a leak test required by §35.67 reveals the presence of 185 Bq (0.005 μCi) or more of removable contamination. The report must be filed with the appropriate NRC regional office (listed in §30.6 of this chapter), with a copy to the Director, Office of Nuclear Material Safety and Safeguards, U.S. Nuclear Regulatory Commission, Washington, DC 20555-0001. The written report must include the model number and serial number if assigned, of the leaking source; the radionuclide and its estimated activity; the results of the test; the date of the test; and the action taken.

NRC Requirements and Nuclear Pharmacy Practice Standards

10 CFR 35.24 specifies that each licensee must develop and implement a written radiation protection program that includes provisions for keeping radiation exposures of employees, patients, visitors, and the public as low as reasonably achievable (ALARA). The ALARA concept is embraced throughout the practice standards; nuclear pharmacists are obligated to work jointly with the RSO, health physicist, and nuclear medicine physician in developing radiation protection procedures that comply with this legal standard. Numerous radiation protection procedures, such as the use of time, distance, and shielding techniques, are prescribed in the practice standards, and many of these procedures are specifically required by regulation. For example, 10 CFR 35.60 specifies that the licensee must require each individual who prepares (i.e., compounds) a radiopharmaceutical kit to use a syringe radiation shield and must also require individuals to use a syringe radiation shield when administering a radiopharmaceutical by injection unless the use of the shield is contraindicated for the given patient. This regulation also requires each syringe or syringe radiation shield that contains a syringe with a radiopharmaceutical to be conspicuously labeled so that the contents can be readily identified; however, this requirement is limited to providing the radiopharmaceutical name or its abbreviation, the clinical procedure to be performed, or the patient's name. In this regard, it is interesting to note that nuclear pharmacists are obligated, under both federal and state laws and pharmacy practice standards, to provide for each radiopharmaceutical dosage an appropriate prescription label

containing all legally required information.[17] In addition to this required information, radiopharmaceutical prescription labels must include the amount of radioactivity, the calibration and expiration time, and a cautionary statement and symbol indicating that the dosage is radioactive in order to further ensure that the dosage is used in a safe and efficacious manner.

In some instances conflict may exist between NRC regulations and the standards of nuclear pharmacy practice. For example, 10 CFR 35.200 specifies that a licensee may use any byproduct material in a diagnostic radiopharmaceutical or any generator or any reagent kit for the preparation and diagnostic use of a radiopharmaceutical containing byproduct material that has an FDA-accepted IND or FDA-approved NDA. The regulation also specifies that a licensee must elute generators and prepare kits in accordance with the manufacturer's instructions. This latter requirement is seldom a problem, because nuclear pharmacists usually adhere to the manufacturer's instructions. However, as professional practitioners, nuclear pharmacists must reserve the right to exercise professional judgment as appropriate to the provision of quality nuclear pharmacy services and the overall safety of nuclear medicine procedures. Thus, according to a physician's prescription, patient needs, and individual experience with the prescribed radiopharmaceutical, nuclear pharmacists may modify the manufacturer's instructions or in some cases develop acceptable compounding procedures that are not otherwise described by the manufacturer. As a classic example, nuclear pharmacists may establish specialized procedures for preparing pediatric dosages of ^{99m}Tc-albumin aggregated for pulmonary perfusion studies, because the instructions for preparing the radiopharmaceutical for pediatric patients in a reasonable volume of administration or desired particle number are not provided in the product labeling. Obviously, nuclear pharmacists must consider the legal ramifications associated with this course of action or any other practice activities that may deviate from applicable NRC regulations.

REGULATORY OUTLOOK

NRC's recently amended regulations, discussed above, are one component of the agency's overall program for adjusting its regulatory scheme for the medical use of radioactive byproduct materials. NRC's goals are to focus regulations on those medical procedures that pose the highest risk to workers, patients, and the public and to structure the regulations to be risk-informed and performance-based, consistent with the agency's strategic plan.[54] In the future, all regulated stakeholders will be expected to focus their compliance improvement efforts on high-risk procedures and to continue to adjust their practices to this new risk-informed, performance-based approach to regulation.

FDA is implementing FDAMA, which was passed by Congress after 3 years of FDA scrutiny.[26] In this act, which is very broad and covers all of the agency's activities and programs, Congress recognized that protecting the public health is a responsibility shared by the entire health care community. The law directs the agency to carry out its mission in consultation and cooperation with all FDA stakeholders, including consumer and patient groups, the regulated industry, health care professionals, and FDA's regulatory counterparts abroad. FDA is currently working to cooperate with its stakeholders in the United States and abroad to continue protecting consumers and the public health in a new era of unprecedented technologic and scientific advances.

Progress in clarifying the FDA regulatory framework for PET, the lead imaging technology in nuclear medicine practice, has been much slower than mandated by FDAMA, but a variety of challenging new FDA regulations are sure to be applied to the production of PET drugs in the near future. All facilities engaged in the production of PET drugs, whether for commercial sale or on-site use, will be required to comply. PET industry

stakeholders are moving toward compliance even though FDA has not yet delineated the specific requirements. Implementation of these anticipated regulations will continue to be a major area of concern for PET stakeholders well into the future.

Nuclear pharmacists and other health care professionals must continuously strive to increase their working knowledge of the numerous regulations on the possession and use of radioactive materials and radiopharmaceuticals intended for medical use. Federal regulations promulgated by NRC and FDA are most important; however, other federal, state, and local regulations must also be considered. Nuclear pharmacists, by virtue of their professional licensure and unique practice setting, bear a major responsibility for ensuring that regulatory requirements are satisfied in the course of providing the services necessary for the safe and efficacious use of all radiopharmaceuticals and drugs in nuclear medicine practice. To fulfill this professional obligation, nuclear pharmacists must constantly monitor regulatory changes and modify the practice environment to maintain a comprehensive compliance program.

REFERENCES

1. Accreditation Council for Graduate Medical Education, Suite 2000, 515 North State Street, Chicago, IL 60610-4322, 2004.
2. Croll MN. Mileposts in nuclear medicine history. In: Henkin RE, Boles MA, Dillehay GL, et al., eds. *Nuclear Medicine*. St Louis: Mosby-Year Book; 1996:3-9.
3. Rhodes BA, Hladik WB, Norenberg JP. Clinical radiopharmacy: principles and practices. *Semin Nucl Med*. 1996;26:77-84.
4. Callahan RJ. The role of commercial nuclear pharmacy in the future practice of nuclear medicine. *Semin Nucl Med*. 1996;26:85-90.
5. Shaw SM, Ice RD. Nuclear pharmacy. I: Emergence of the specialty of nuclear pharmacy. *J Nucl Med Technol*. 2000;28:8-11.
6. Ponto JA, Hung JC. Nuclear pharmacy. II: Nuclear pharmacy practice today. *J Nucl Med Technol*. 2000;28:76-81.
7. McCready VR. Milestones in nuclear medicine. *Eur J Nucl Med*. 2000:27(1 suppl):S49-79.
8. American Pharmaceutical Association. *Nuclear Pharmacy Practice Guidelines*. Washington, DC: American Pharmaceutical Association; 1995.
9. Board of Pharmaceutical Specialties, 2215 Constitution Ave NW, Washington, DC, 20037-2985. http://www.bpsweb.org/.
10. Hilts PJ. *Protecting America's Health: The FDA, Business and One Hundred Years of Regulation*. New York: Knopf; 2003.
11. Brushwood DB. Federal pharmacy laws: an overview. 1998. Available at: http://www.continuingeducation.com/pharmacy/fpl-overview/fpl-overview.pdf.
12. Siegel, JA. History and organization of regulation of nuclear medicine. In: *Nuclear Regulatory Commission Regulation of Nuclear Medicine: Guide for Diagnostic Nuclear Medicine*. Reston, VA: Society of Nuclear Medicine; 2001:7-8.
13. US Nuclear Regulatory Commission. *Regulatory Guide 10.8: Guide for the Preparation of Applications of Medical Programs*. Revision 2. August 1987. Available at: http://www.nrc.gov/reading-rm/doc-collections/reg-guides/general/active/10-008/index.html.
14. US Nuclear Regulatory Commission. *Consolidated Guidance About Material Licenses: Program-Specific Guidance About Medical Use Licenses*. NUREG-1556, vol 9. August 1998. Available at: http://www.nrc.gov/reading-rm/doc-collections/nuregs/staff/sr1556/v9/index-old.html.
15. US Food and Drug Administration. Radioactive new drugs for investigational use. 28 *Federal Register* 183 (1963).
16. US Food and Drug Administration. Radioactive new drugs: new drug application requirements. 36 *Federal Register* 21026 (1971).
17. Halperin JA, Stringer SA, Eastep RD. Regulation of radiopharmaceuticals: analysis of radiopharmaceuticals approved for marketing in the United States 1951-1978. In: *Radiopharmaceuticals II: Proceedings of the Second International Symposium on Radiopharmaceuticals*. New York: Society of Nuclear Medicine; 1979:xxi.
18. US Food and Drug Administration. Radioactive new drugs and radioactive biologics: termination of exemptions. 40 *Federal Register* 31298 (1975).

19. US Nuclear Regulatory Commission. State and tribal programs: agreement and non-agreement states. Available at: http://www.hsrd.ornl.gov/nrc/home.html.
20. Keppler JS, Thornberg CF, Conti PS. Regulation of positron emission tomography: a case study. *AJR Am J Roentgenol.* 1998;171:1187-92.
21. Kessler DA. The regulation of investigational drugs. *N Engl J Med.* 1989;320:281-8.
22. US Food and Drug Administration. *Nuclear Pharmacy: Criteria for Determining When to Register as a Drug Establishment.* Rockville, MD: Division of Drug Labeling Compliance, Center for Drugs and Biologics, Food and Drug Administration; 1984.
23. Conti PS, Keppler JS, Halls JM. Positron emission tomography: a financial and operational analysis. *AJR Am J Roentgenol.* 1994;162:1279-86.
24. Coleman RE, Robbins MS, Siegel BA. The future of positron emission tomography in clinical medicine and the impact of drug regulation. *Semin Nucl Med.* 1992;22:193-201.
25. *Syncor v Shalala*, 96-5371 (DC Cir 1997).
26. US Food and Drug Administration Modernization Act (FDAMA). Bill S. 830, Pub L No. 105-115 §121, 11 Stat 2296 (1997). Available at: http://www.fda.gov/cder/guidance/105-115.htm.
27. Regulation of positron emission tomography radiopharmaceutical drug products: guidance. 60 *Federal Register* 10594 (1995).
28. Draft guideline on the manufacture of positron emission tomography radiopharmaceutical drug products: availability. 60 *Federal Register* 10593 (1995).
29. Current good manufacturing practice for finished pharmaceuticals: positron emission tomography. 62 *Federal Register* 19493 (1997).
30. Revocation of certain guidance documents on positron emission tomography drug products. 62 *Federal Register* 66636 (1997).
31. Revocation of regulation on positron emission tomography drug products. 62 *Federal Register* 66522 (1997).
32. Centers For Medicare & Medicaid Services. National coverage determinations (NCDs): positron emission tomography scans. October 1, 2002. Available at: http://www.cms.gov/ncd/searchdisplay.asp?NCD_ID=211&NCD_vrsn_num=1.
33. Centers For Medicare & Medicaid Services. Introducing the CMS. March 6, 2002. Available at: http://www.cms.gov/about/reorg.asp.
34. AuntMinnie.com. PET procedures surge 70%. Available at: http://www.auntminnie.com/default.asp?Sec=sup&Sub=mol&Pag=dis&ItemId=57975.
35. US Department of Health and Human Services, Food and Drug Administration, Center for Drug Evaluation and Research (CDER). Investigational new drug application (IND) process. Available at: http://www.fda.gov/cder/regulatory/applications/ind_page_1.htm.
36. US Department of Health and Human Services, Food and Drug Administration, Center for Drug Evaluation and Research (CDER). New drug application (NDA) process. Updated January 20, 2004. Available at: http://www.fda.gov/cder/regulatory/applications/nda.htm.
37. US Department of Health and Human Services, Food and Drug Administration, Center for Drug Evaluation and Research (CDER). Abbreviated new drug application (ANDA) process for generic drugs. Updated December 30, 2003. Available at: http://www.fda.gov/cder/regulatory/applications/anda.htm.
38. Woodbury DH, Leiberman L, Leutzinger E, et al. Pathway for FDA approval of new radiopharmaceuticals. In: Henkin RE, Boles MA, Dillehay GL, et al., eds. *Nuclear Medicine.* St Louis: Mosby-Year Book; 1996:350-6.
39. US Department of Health and Human Services. Administrative operations, Program Support Center (PSC), PSC forms download site, Food and Drug Administration forms. Available at: http://forms.psc.gov/forms/FDA/fda.html.
40. US Department of Health and Human Services, Food and Drug Administration, Center for Drug Evaluation and Research (CDER). IND review process. Available at: http://www.fda.gov/cder/handbook/ind.htm.
41. Swanson DP. Radiopharmaceuticals as orphan drugs. *Semin Nucl Med.* 1996;36:91-5.
42. Koppal T. Inside the FDA: How CDER's Janet Woodcock helps companies achieve compliance, speed the drug review process and improve time to market for new drugs. *Drug Discovery Dev.* November 2002;5:32-8.
43. US Department of Health and Human Services, Food and Drug Administration. Office of Orphan Products Development (OOPD). Available at: http://www.fda.gov/orphan/index.htm.
44. Petry NA. NRC and FDA regulations affecting nuclear pharmacy practice. *J Pharm Pract.* 1989;2:306-13.
45. Swanson DP, Lieto RP. The submission of IND applications for radiopharmaceutical research: when and why. *J Nucl Med.* 1984;25:714-9.

46. US Department of Health and Human Services, Food and Drug Administration, Center for Drug Evaluation and Research (CDER). NDA review process. Available at: http://www.fda.gov/cder/handbook/ nda.htm.
47. US Department of Health and Human Services, Food and Drug Administration, Center for Drug Evaluation and Research (CDER). Guidance for industry: content and format for an abbreviated new drug application (ANDA)—positron emission tomography (PET) drug products with specific information for ANDAs for fludeoxyglucose F18 injection. Draft guidance, April 1997. Available at: http://www.fda.gov/cder/guidance/andapet.pdf.
48. US Department of Health and Human Services, Food and Drug Administration, Center for Drug Evaluation and Research (CDER). Guidance for industry: PET drug applications—content and format for NDAs and ANDAs. March 2000. Available at: http://www.fda.gov/cder/guidance/3453dft.htm.
49. US Department of Health and Human Services, Food and Drug Administration, Center for Drugs and Biologics. Guidance for industry: guidance for the format and content of the chemistry, manufacturing and controls section of an application. February 1987. Available at: http://www.fda.gov/cder/guidance/old030fn.pdf.
50. US Department of Health and Human Services. Guidelines for format and content of the clinical and statistical section of an application. Washington, DC: US Government Printing Office; 1988.
51. US Department of Health and Human Services. General guidelines for the clinical evaluation of drugs. Washington, DC: US Government Printing Office; 1977. USPHS/FDA 77-3040.
52. Johnson JR, Temple R. Food and Drug Administration requirements for approval of new anticancer drugs. *Cancer Treat Rep.* 1985;69:1155-7.
53. US Department of Health and Human Services. Guidelines for the clinical evaluation of radiopharmaceutical drugs. Washington, DC: US Government Printing Office; 1981. USPHS/FDA 81-3120. Available at: http://www.fda.gov/cder/guidance/old064fn.pdf.
54. US Nuclear Regulatory Commission. Who we are, our mission. August 26, 2003. Available at: http://www.nrc.gov/who-we-are.html.
55. US Nuclear Regulatory Commission. Medical use of byproduct material: *Federal Register* notice April 24, 2002. Available at: http://www.nrc.gov/reading-rm/do99c-collections/cfr/fr/2002/20020424.html.
56. US Nuclear Regulatory Commission. Part 35: medical use of byproduct material. April 24, 2002. Available at: http://www.nrc.gov/reading-rm/doc-collections/cfr/part035/.

19. US Nuclear Regulatory Commission. State and tribal programs: agreement and non-agreement states. Available at: http://www.hsrd.ornl.gov/nrc/home.html.
20. Keppler JS, Thornberg CF, Conti PS. Regulation of positron emission tomography: a case study. *AJR Am J Roentgenol.* 1998;171:1187-92.
21. Kessler DA. The regulation of investigational drugs. *N Engl J Med.* 1989;320:281-8.
22. US Food and Drug Administration. *Nuclear Pharmacy: Criteria for Determining When to Register as a Drug Establishment.* Rockville, MD: Division of Drug Labeling Compliance, Center for Drugs and Biologics, Food and Drug Administration; 1984.
23. Conti PS, Keppler JS, Halls JM. Positron emission tomography: a financial and operational analysis. *AJR Am J Roentgenol.* 1994;162:1279-86.
24. Coleman RE, Robbins MS, Siegel BA. The future of positron emission tomography in clinical medicine and the impact of drug regulation. *Semin Nucl Med.* 1992;22:193-201.
25. *Syncor v Shalala,* 96-5371 (DC Cir 1997).
26. US Food and Drug Administration Modernization Act (FDAMA). Bill S. 830, Pub L No. 105-115 §121, 11 Stat 2296 (1997). Available at: http://www.fda.gov/cder/guidance/105-115.htm.
27. Regulation of positron emission tomography radiopharmaceutical drug products: guidance. 60 *Federal Register* 10594 (1995).
28. Draft guideline on the manufacture of positron emission tomography radiopharmaceutical drug products: availability. 60 *Federal Register* 10593 (1995).
29. Current good manufacturing practice for finished pharmaceuticals: positron emission tomography. 62 *Federal Register* 19493 (1997).
30. Revocation of certain guidance documents on positron emission tomography drug products. 62 *Federal Register* 66636 (1997).
31. Revocation of regulation on positron emission tomography drug products. 62 *Federal Register* 66522 (1997).
32. Centers For Medicare & Medicaid Services. National coverage determinations (NCDs): positron emission tomography scans. October 1, 2002. Available at: http://www.cms.gov/ncd/searchdisplay.asp?NCD_*ID=211&NCD_vrsn_num=1.*
33. Centers For Medicare & Medicaid Services. Introducing the CMS. March 6, 2002. Available at: http://www.cms.gov/about/reorg.asp.
34. AuntMinnie.com. PET procedures surge 70%. Available at: http://www.auntminnie.com/default.asp?Sec=sup&Sub=mol&Pag=dis&ItemId=57975.
35. US Department of Health and Human Services, Food and Drug Administration, Center for Drug Evaluation and Research (CDER). Investigational new drug application (IND) process. Available at: http://www.fda.gov/cder/regulatory/applications/ind_page_1.htm.
36. US Department of Health and Human Services, Food and Drug Administration, Center for Drug Evaluation and Research (CDER). New drug application (NDA) process. Updated January 20, 2004. Available at: http://www.fda.gov/cder/regulatory/applications/nda.htm.
37. US Department of Health and Human Services, Food and Drug Administration, Center for Drug Evaluation and Research (CDER). Abbreviated new drug application (ANDA) process for generic drugs. Updated December 30, 2003. Available at: http://www.fda.gov/cder/regulatory/applications/anda.htm.
38. Woodbury DH, Leiberman L, Leutzinger E, et al. Pathway for FDA approval of new radiopharmaceuticals. In: Henkin RE, Boles MA, Dillehay GL, et al., eds. *Nuclear Medicine.* St Louis: Mosby-Year Book; 1996:350-6.
39. US Department of Health and Human Services. Administrative operations, Program Support Center (PSC), PSC forms download site, Food and Drug Administration forms. Available at: http://forms.psc.gov/forms/FDA/fda.html.
40. US Department of Health and Human Services, Food and Drug Administration, Center for Drug Evaluation and Research (CDER). IND review process. Available at: http://www.fda.gov/cder/handbook/ind.htm.
41. Swanson DP. Radiopharmaceuticals as orphan drugs. *Semin Nucl Med.* 1996;36:91-5.
42. Koppal T. Inside the FDA: How CDER's Janet Woodcock helps companies achieve compliance, speed the drug review process and improve time to market for new drugs. *Drug Discovery Dev.* November 2002;5:32-8.
43. US Department of Health and Human Services, Food and Drug Administration. Office of Orphan Products Development (OOPD). Available at: http://www.fda.gov/orphan/index.htm.
44. Petry NA. NRC and FDA regulations affecting nuclear pharmacy practice. *J Pharm Pract.* 1989;2:306-13.
45. Swanson DP, Lieto RP. The submission of IND applications for radiopharmaceutical research: when and why. *J Nucl Med.* 1984;25:714-9.

8 Radionuclide Production

All radionuclides used in nuclear medicine are produced by artificial means. The production methods involve bombarding target nuclei with high-energy particles, thereby transforming stable nuclides into radioactive ones. This process of nuclear transmutation occurs in two stages. In the first stage, the bombarding particle penetrates and is captured by the target nucleus, adding its kinetic energy and binding energy to the nucleus. The extra allotment of energy in the newly formed "intermediate nucleus" is transferred among its nucleons. In the second stage, one or more nucleons may overcome the nuclear binding energy, by chance, and escape. The escaping particle(s) may carry off all the available energy or only enough to escape. Any energy not carried off by escaping particles is released as gamma radiation from the new nucleus. Note that this process is not radioactivity but is simply the second stage of the nuclear reaction. Escaping particles may vary but typically include protons ($^{1}H^{+}$), deuterons ($^{2}H^{+}$), neutrons (n), and alpha particles ($^{4}He^{2+}$).

In 1934, Frederick Joliot and Irene Curie Joliot performed a nuclear reaction by bombarding a piece of aluminum foil with alpha particles emitted from a polonium source. When the polonium source was removed, radiation still emanated from the target material. They recognized that the aluminum target underwent a transformation into some new elemental form that was radioactive. This experiment produced one of the first artificially made radionuclides, ^{30}P, according to the following reaction:

$$^{27}_{13}Al + ^{4}_{2}He \rightarrow ^{1}_{0}n + ^{30}_{15}P$$

The shorthand notation for this reaction is $^{27}Al(\alpha,n)^{30}P$.

Radionuclides in nuclear medicine are produced in either a nuclear reactor or a particle accelerator.

NUCLEAR REACTORS

A nuclear reactor contains fuel rods of enriched fissionable ^{235}U positioned in the reactor core. The fuel rods are surrounded by a moderator such as heavy water (D_2O). Each fissioning uranium atom releases fast neutrons that are slowed to thermal energy by their interactions with D_2O. A thermal neutron is one that has the same average kinetic energy as the atoms of the surrounding medium. This energy, which is only a fraction of an electron volt at ordinary temperatures, is referred to as the thermal energy, since it depends on the temperature. Thermal neutrons are easily captured by other uranium atoms. When the uranium atoms fission, they release more neutrons that sustain the chain reaction. The rate of thermal neutron capture by the uranium nuclei determines the fission rate in the reactor. This rate is controlled by the use of boron or cadmium control rods, which serve as inert absorbers of neutrons. For a fast reaction, the rods are pulled away from the reactor core. To shut the reaction down, the rods are pushed completely into the core. The fission process generates heat that is carried off by water or other coolants through heat exchangers.

Nuclear reactors are designed for different purposes. Power reactors convert the heat generated from the fission process into electricity. Isotope production reactors have specialized ports where target material may be introduced into the neutron flux, causing neutron activation of stable nuclides into radioactive nuclides.

TYPES OF NUCLEAR REACTIONS

The (n,γ) Reaction

This is the most common type of reaction with neutrons. It has the following characteristics: (1) the reaction requires low-energy thermal neutrons (approximately 0.025 eV), the energy equivalent of an air molecule in equilibrium with its surroundings, and (2) the product nuclide is an isotope of the target nuclide, and chemical separation of target and product nuclides is not possible. This results in a low specific activity product. Example reactions include $^{98}Mo(n,\gamma)^{99}Mo$ and $^{50}Cr(n,\gamma)^{51}Cr$.

The A(n,γ)A*→B Reaction

In some instances radionuclide product separation from stable target material may be possible with (n,γ) reactions if the primary product nuclide (A*) has a short half-life and decays to a longer-lived radionuclide (B) that can be isolated. Some examples are as follows:

$$^{124}Xe(n,\gamma)^{125}Xe \xrightarrow{\beta^-,\ 18\ hr} {}^{125}I\ (59\ days)$$

$$^{130}Te(n,\gamma)^{131}Te \xrightarrow{\beta^-,\ 25\ min} {}^{131}I\ (8\ days)$$

The A(n,p)B Reaction

If fast neutrons are captured by the target, an (n,p) reaction is possible. This nuclear reaction imparts an extra allotment of energy to the intermediate nucleus, enabling a proton to escape. Escape of a proton changes the atomic number of the target nuclide; therefore, the radionuclide produced is not an isotope of the target, but an isobar. A benefit of this reaction is that chemical separation of target and product nuclides is possible, and high specific activities can be achieved. The following reaction is an example:

$$^{32}S(n,p)^{32}P$$

The $^{235}U(n,f)$Byproducts Reaction

When ^{235}U captures a thermal neutron, the intermediate nucleus is very unstable and fissions into radioactive fragment nuclides as follows:

$$^{235}U + {}^{1}n \rightarrow {}^{236}U$$

$$\downarrow$$

$$^{131}Sn + {}^{103}Mo + 2\ {}^{1}n$$

$$\downarrow \qquad \downarrow$$

$$^{131}Sb \qquad {}^{103}Te$$

$$\downarrow \qquad \downarrow$$

$$^{131}Te \qquad {}^{103}Ru$$

$$\downarrow \qquad \downarrow$$

$$^{131}I \qquad {}^{103}Rh$$

$$\downarrow$$

$$^{131}Xe$$

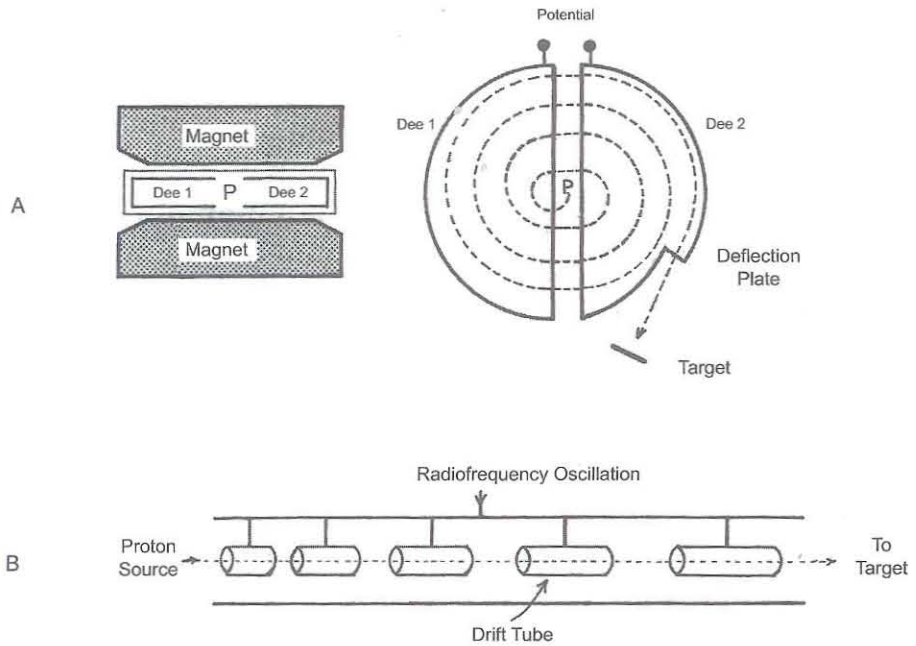

FIGURE 8-1 Schematic diagram of a cyclotron (A) and a linear accelerator (*B*).

The initial fission fragments and the nuclides to which they decay are not isotopes and can be separated chemically to achieve high specific activities. Many radionuclides are made by this process. Some examples are ^{99}Mo (used in the production of the ^{99m}Tc generator), ^{133}Xe, and ^{131}I.

CYCLOTRONS AND LINEAR ACCELERATORS

A cyclotron consists of two hollow, semicircular chambers called Dees placed in a magnetic field. The Dees are coupled to a high-frequency electrical system that alternates the electrical potential on each Dee during cyclotron operation, changing sign about 10^7 times per second. The Dees are heavily shielded and configured so that they can be evacuated to low pressure (Figure 8-1). An arrangement is made at the center of the space between the Dees for releasing protons or deuterons. When a proton is generated, it is attracted into the negatively charged Dee and repelled by the positive Dee. This causes the proton to accelerate into the negative Dee. The magnetic field causes the proton path to bend as it moves through the Dee. When the proton again reaches the gap, the charge on each Dee is reversed. This causes the proton to be accelerated across the gap into the opposite Dee, where the radius of its circular path will increase. Because the proton is moving faster, it will again arrive at the gap precisely when the Dee polarity is reversed, causing further acceleration of the proton. This process is repeated until the proton gains great energy. At this point the proton exits from the Dee and is deflected onto a target where the desired nuclear reaction takes place.

Two types of cyclotrons are used: positive-ion machines, which accelerate protons, and negative-ion machines, which accelerate a proton associated with two electrons, called a positronium. When the positronium ion exits the cyclotron it passes through a carbon foil, which strips away the electrons, allowing a free proton to bombard the target. New-generation cyclotrons are negative-ion machines and have the advantage of less activation of cyclotron components. Chapter 10 covers cyclotron applications in more detail.

When a proton attains speeds approaching the speed of light, its mass becomes relativistic, increasing with energy. As a result the proton slows somewhat and begins to arrive at the gap late, after the Dee polarity has changed. This limits the energy a proton can achieve in a cyclotron. Because of this problem, alternative methods of producing very high energy particles were conceived. One of these methods is the linear accelerator, or linac (Figure 8-1). The linac is a series of cylindrical drift tubes through which electromagnetic waves pass, along with their associated oscillating electric and magnetic fields. A charged particle such as a proton injected into the drift tube will be carried forward by the traveling wave. The lengths of the drift tubes are designed to accommodate relativistic changes in the accelerated particle. In this way the particle arrives at the gap between drift tubes always in phase, and very high energy particles can be achieved, upwards of 200 MeV.

Accelerator Methods of Radionuclide Production

Cyclotrons and linear accelerators are both used in production, but most proton-rich nuclides are generated in a cyclotron. The machine used depends upon the nuclear reaction and the yield desired. Generally, cyclotrons can accelerate charged ions up to about 30 MeV before relativistic problems become a concern. Higher-energy particles require the use of linear accelerators. Linear accelerators can produce particles in the 100 to 200 MeV range. A positively charged bombarding particle requires high energy to overcome the repulsive coulomb barrier of the target nucleus.

Nuclides produced by charged-particle nuclear reactions are not isotopes of the target nuclide. Consequently, chemical separation of product and target nuclides is possible and a high specific activity product can be achieved. Some typical accelerator-produced radionuclides used in nuclear medicine are as follows:

$$^{58}\mathrm{Ni}(\mathrm{p,pn})^{57}\mathrm{Ni} \xrightarrow{\mathrm{EC,\ 37\ hr}} {}^{57}\mathrm{Co}$$

$$^{127}\mathrm{I}(\mathrm{p,5n})^{123}\mathrm{Xe} \xrightarrow{\mathrm{EC,\ 2\ hr}} {}^{123}\mathrm{I}$$

$$^{111}\mathrm{Cd}(\mathrm{p,n})^{111}\mathrm{In}$$

$$^{133}\mathrm{Cs}(\mathrm{p,2p5n})^{127}\mathrm{Xe}(\textit{linear accelerator})$$

Many radionuclides produced in nuclear reactors and particle accelerators have half-lives long enough to allow time for processing and shipment by a manufacturer to nuclear medicine facilities across the country. However, some radionuclides with very short half-lives, such as ^{11}C, ^{13}N, and ^{15}O, require fabrication into radiopharmaceuticals at the site of use. This necessitates an in-house cyclotron. For positron emission tomography (PET), which uses radiopharmaceuticals labeled with longer-lived nuclides such as ^{18}F-fludeoxyglucose (^{18}F-FDG), regional cyclotron facilities located near the site of use are workable. Several PET nuclear pharmacies are being established across the country at strategic sites to supply PET agents to nearby hospitals and clinics. A more comprehensive discussion of PET radiopharmaceuticals appears in Chapter 10.

Some radionuclides can be produced from generator systems that make the production of short-lived radionuclides possible in the hospital. Because the majority of radio-

TABLE 8-1 Radionuclide Generator Systems

Parent (half-life)	Decay Mode	Daughter (half-life)
^{99}Mo (66 hours)	Beta minus	^{99m}Tc (6 hours)
^{113}Sn (115 days)	Electron capture	^{113m}In (1.7 hours)
^{68}Ge (270 days)	Electron capture	^{68}Ga (68 minutes)
^{81}Rb (4.5 hours)	Electron capture	^{81m}Kr (13 seconds)
^{82}Sr (25 days)	Electron capture	^{82}Rb (75 seconds)
^{62}Zn (9.3 hours)	Electron capture	^{62}Cu (9.7 minutes)

pharmaceuticals used in nuclear medicine are labeled with generator-produced ^{99m}Tc, generators will be discussed in some detail.

RADIONUCLIDE GENERATORS

Radionuclide generators were introduced into nuclear medicine practice because of the need to administer large amounts of radioactivity for better-quality images. Large dosages of activity necessitate the use of short-lived nuclides to keep radiation burden low. A practical way to obtain and use short-lived radionuclides is by means of a generator. A generator consists of a long-lived parent that decays to a short-lived daughter. Because the parent and daughter nuclides are not isotopes, it is possible to chemically isolate the daughter nuclide. After separation, new daughters are generated from the decay of the parent atoms remaining in the generator. A generator provides a fresh supply of short-lived daughter nuclides as needed until the parent activity is depleted. The useful life of a generator depends on the parent half-life. Table 8-1 lists several parent–daughter generator systems.

The generator most prominent in nuclear medicine is the ^{99m}Tc generator. This generator was developed in 1957 at the Brookhaven National Laboratory and first used clinically in 1961 at the University of Chicago.[1,2] The ^{99}Mo parent has a 2.75 day half-life and provides a useful generator life of about 2 weeks. Typically, a new generator is received weekly to meet the activity needs of a hospital or nuclear pharmacy.

Production of the ^{99m}Tc Generator

Figure 8-2 outlines the production of a ^{99m}Tc generator. The ^{99}Mo in contemporary generators is obtained as a uranium fission byproduct. Radiochemical techniques separate ^{99}Mo from the other radionuclides in the reactor product. The purified ^{99}Mo is used to prepare the generator. In one method, ^{99}Mo is adjusted to an acidic pH, forming various anionic species such as molybdate (MoO_4^{2-}) and paramolybdate ($Mo_7O_{24}^{6-}$).[3] The anionic molybdate solution is then loaded onto a generator column containing alumina (Al_2O_3). The alumina, which is previously washed in pH 5 saline, acquires a positive charge and is able to firmly adsorb the molybdate ions. The loading capacity of molybdenum on alumina at pH 5 to 6 is approximately 2 mg of molybdenum per gram of alumina.[3] After assembly, generators are autoclaved to render them sterile. They are assembled under aseptic conditions into their final form in a lead-shielded container. Each generator is eluted with normal saline (0.9% sodium chloride solution), and the eluate is subjected to several tests before release of the generator.

Generators typically are tested by the manufacturer for elution efficiency, eluate volume, radionuclidic purity to detect the presence of ^{99}Mo and other radionuclide contaminants,

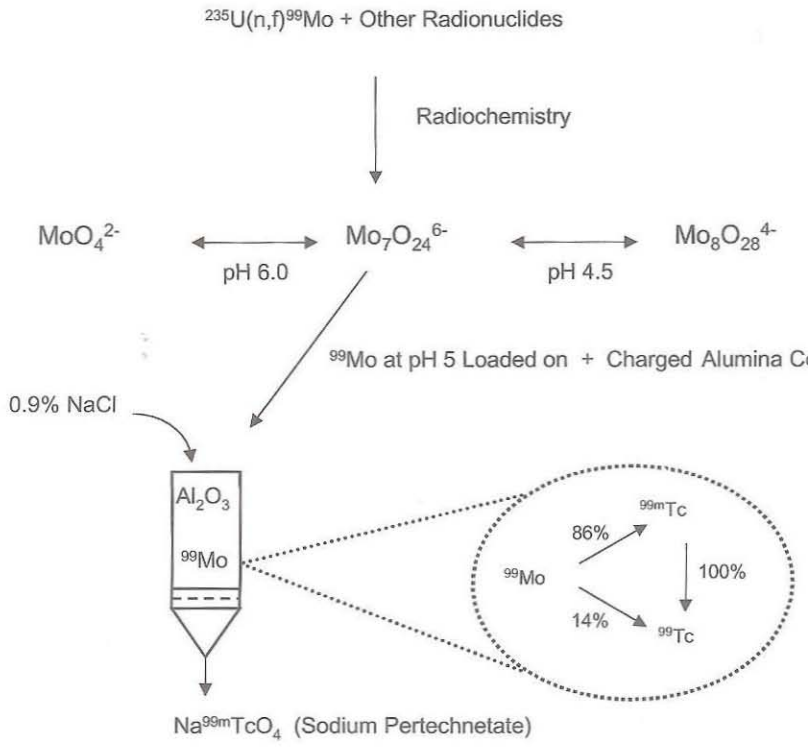

FIGURE 8-2 Schematic diagram of the steps involved in the production of a ^{99m}Tc generator. Fission-produced ^{99}Mo is radiochemically isolated and purified to the anionic molybdate and paramolybdate species, which are loaded on the positively charged alumina (Al_2O_3) generator column previously washed in pH 5 saline.

radiochemical purity to ensure the proper chemical form of ^{99m}Tc as pertechnetate, aluminum ion concentration in the eluate, pH of the eluate, and, finally, pyrogenicity and sterility. Figure 8-3 illustrates a commercial generator system.

Generator Operation

Figure 8-2 illustrates the simplified decay scheme for ^{99}Mo to ^{99m}Tc and ^{99}Tc in the generator. Figure 8-4 shows the relative amounts of ^{99}Mo and ^{99m}Tc activity in the generator over time and illustrates the gradual decay of ^{99}Mo with subsequent buildup of ^{99m}Tc. Maximum buildup of ^{99m}Tc activity is achieved in about 23 hours. About 50% of the maximum value is reached in 4.5 hours and 75% by 8.5 hours after generator elution.[4] Accumulated activity is eluted by washing normal saline solution through the column. The ^{99}Mo activity remains firmly bound to the alumina, but the ^{99m}Tc activity, as the pertechnetate ion (TcO_4^-), is easily displaced by the chloride ion (Cl^-) in the saline solution. Typically 70% to 90% of the available ^{99m}Tc activity is removed in one 5 mL elution. The ^{99}Mo activity remaining on the column continues to decay, generating more ^{99m}Tc activity, whose amount will be less on each subsequent day. The generator in use is replaced when insufficient ^{99m}Tc activity is obtained. Weekly replacements are the norm. ^{99m}Tc activity builds up rapidly after generator elution, and the generator may be eluted several times during the same day to obtain more activity. This is more likely to occur at week's end.

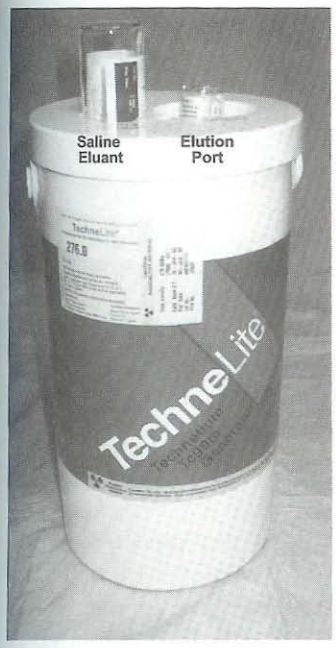

FIGURE 8-3 A commercial ^{99m}Tc generator.

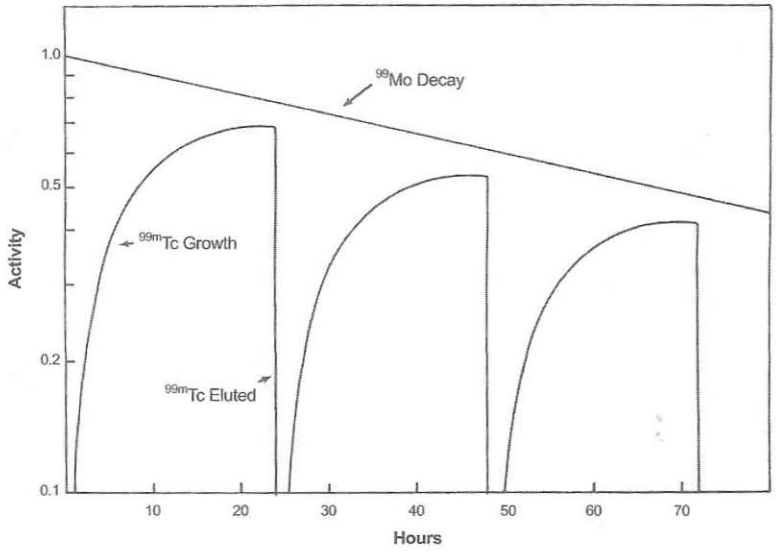

FIGURE 8-4 Decay of ^{99}Mo and growth of ^{99m}Tc activity over time in a ^{99m}Tc generator.

^{99m}Tc Generator Systems

There are two basic types of generator systems: the wet system and the dry system (Figure 8-5). In the wet system, a large reservoir of saline is connected to the generator, which remains continuously bathed in saline. Technetium activity is eluted after attachment of an evacuated sterile vial to the elution port. The vacuum draws the saline–pertechnetate solution into the vial. At the end of elution, the generator column remains bathed in saline. In the dry system, a 5 to 20 mL saline charge is attached to the system before elution. A

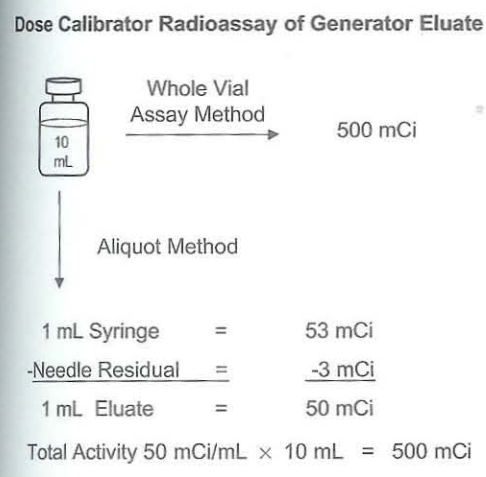

FIGURE 8-6 Generator eluate radioactivity measured in a dose calibrator by (1) the whole-vial method or (2) the aliquot method of assay.

Dry system generators were developed to alleviate the poor elution problem of wet systems by removing saline from the column after elution. This significantly reduced the formation of radiolysis products, because the dry systems introduced air into the column to maintain an oxidized pertechnetate species. Today the problem of incomplete elution rarely occurs with dry generator systems. However, elution problems may still occur if residual eluant remains on the generator column. This might happen if the evacuated vial is removed early before all the eluant has been drawn through the column or if the evacuated vial has a vacuum strength that is insufficient to complete the elution. Therefore, it is important to ensure that the entire eluant volume is drawn through the column and that a sufficient amount of air is introduced after elution.

Quality Control of the Generator Eluate

Three tests should be performed on each generator eluate. The first test is a *radioactivity calibration* (Figure 8-6). This is done with a dose calibrator to determine the activity eluted and the radioactive concentration. This can be accomplished in two ways: (1) assaying the whole elution vial to obtain the total activity and determining the concentration from the total volume eluted or (2) drawing a 1 mL aliquot into a syringe and assaying its contents. In the second method, returning the 1 mL volume to the eluate vial and reassaying the syringe will give the needle activity; the difference between these two measurements provides the activity per milliliter. The total activity in the vial is obtained by multiplying the activity per milliliter by the total volume in the vial. The aliquot method has the advantages of reduced operator exposure and an accurate assessment of the radioactive concentration.

The second test of a generator eluate is a *chemical purity test* for the concentration of aluminum ion present. A colorimetric spot test is typically used. A small drop of generator eluate is placed on a strip of filter paper impregnated with the aluminum-specific indicator aluminon (the ammonium salt of aurintricarboxylic acid) (Figure 8-7). A spot of a standard aluminum ion solution of known concentration (10 μg Al^{3+}/mL) is placed next to the eluate spot. The aluminum ion present reacts with the indicator to produce a pink color whose intensity is proportional to the amount of Al^{3+} present. If the color of the eluate spot is less intense than the aluminum standard spot, the eluate passes the test. The Nuclear Regulatory Commission (NRC) and the United States Pharmacopeia (USP) place the aluminum concentration limit at not more than 10 μg Al^{3+} per milliliter of eluate.

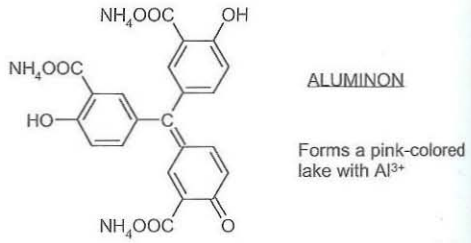

FIGURE 8-7 Colorimetric spot test of generator eluate for aluminum ion. One drop of generator eluate is compared with one drop of aluminum standard solution (10 μg Al^{+3}/mL) applied to a test paper. Aluminon indicator in the test paper reacts with aluminum ion to form a pink-colored lake, with color intensity proportional to Al^{3+} ion concentration.

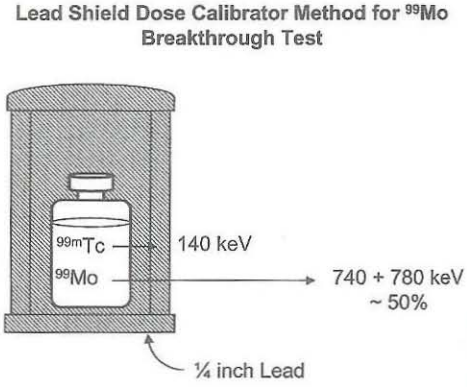

FIGURE 8-8 Generator eluate test for molybdenum breakthrough by the lead shield method in a dose calibrator.

The third test of a generator eluate is the *radionuclidic purity test* for the presence of ^{99}Mo contamination (Figure 8-8). This so-called moly-99 breakthrough test is accomplished with a specialized lead shield and a dose calibrator.[8] In this technique, the whole vial of generator eluate is placed into a tightly sealed lead shield, which is then placed into the dose calibrator adjusted to read ^{99}Mo activity. The shield is designed so that all of the 140 keV ^{99m}Tc photons are absorbed by the lead but approximately 50% of the more energetic ^{99}Mo photons (740 and 780 keV) penetrate the shield. The photons that penetrate the shield are measured in the dose calibrator. The microcuries of ^{99}Mo are read directly from the readout or after application of a correction factor. The only deficiency in this method is that any radionuclide contaminant present that has gamma energies capable of penetrating the lead shield will be counted along with ^{99}Mo, because the dose calibrator has no energy-discriminating capability. This produces an erroneous reading. One report has shown this to be a problem with generators contaminated with ^{132}Te because it decays to ^{132}I, which has gamma energies similar to those of ^{99}Mo.[9] ^{132}I has gamma energies ranging from 668 keV to 1398 keV. Fortunately, ^{132}I has a short half-life and the contamination quickly diminishes with time. A method for identifying ^{132}I or other high-energy contaminants by the lead-shield technique or with a scintillation counter has been suggested.[9]

The limits for ^{99}Mo contamination in ^{99m}Tc eluates have been set by NRC and USP to be not more than 0.15 μCi (5.55 kBq) ^{99}Mo per 1 mCi (37 MBq) ^{99m}Tc in the administered dose. Accordingly, a 20 mCi (740 MBq) dose of ^{99m}Tc may contain no more than 3 μCi (111 kBq) of ^{99}Mo. A convenient method for determining the expiration time for ^{99m}Tc eluates has been devised on the basis of these limits.[10] Table 8-2 lists the expiration time in hours for ^{99m}Tc based on the initial ratio of the microcuries of ^{99}Mo to the millicuries of ^{99m}Tc at generator elution time. For example, if the initial ratio of ^{99}Mo microcuries to ^{99m}Tc millicuries is 0.058, the ^{99m}Tc eluate cannot be used more than 9 hours after the time of elution. The default expiration time for any ^{99m}Tc generator eluate is 12 hours, according to the manufacturer's package insert.

TABLE 8-2 Expiration Times for ^{99m}Tc-Sodium Pertechnetate after Generator Elution

Initial Ratio (microcuries of ^{99}Mo/millicuries of ^{99m}Tc)	Expiration Time (hr)	Initial Ratio (microcuries of ^{99}Mo/millicuries of ^{99m}Tc)	Expiration Time (hr)
0.135	1	0.072	7
0.122	2	0.065	8
0.109	3	0.058	9
0.098	4	0.052	10
0.089	5	0.047	11
0.080	6	0.042	12

Source: Reference 10.

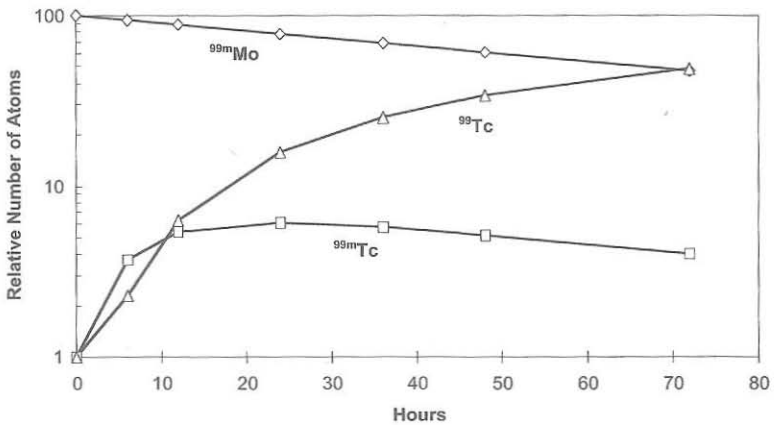

FIGURE 8-9 Relative number of atoms over time of ^{99}Mo, ^{99m}Tc, and ^{99}Tc in a ^{99m}Tc generator.

Results of the moly-99 breakthrough test are typically negative, indicating no significant ^{99}Mo contamination. However, a positive test with significant levels (7 mCi [259 MBq] of ^{99}Mo) in the generator eluate has been reported.[11] In this instance the moly-99 breakthrough was caused by an improperly assembled generator.

Technetium Content in Generator Eluates

The half-lives of the nuclides in the ^{99m}Tc generator are 65.95 hours for ^{99}Mo, 6.01 hours for ^{99m}Tc, and 2.13×10^5 years for ^{99}Tc.[12] Because of its long half-life, ^{99}Tc will build up over time in the generator. In a practical sense this means that eluates from all ^{99m}Tc generators contain both ^{99m}Tc and ^{99}Tc atoms. The relative amounts of ^{99}Mo, ^{99m}Tc, and ^{99}Tc in a generator are shown in Figure 8-9. The mole fraction of the ^{99m}Tc isomer in the eluate is given by the following relationship, where N represents the number of atoms:[13]

$$\frac{N_{^{99m}\mathrm{Tc}}}{N_{(\mathrm{total})}} = \frac{N_{^{99m}\mathrm{Tc}}}{N_{^{99m}\mathrm{Tc}} + N_{^{99}\mathrm{Tc}}} \tag{8-1}$$

The mole fractions, listed in Table 8-3, can be determined at various times from the following equation:[13]

TABLE 8-3 Mole Fractions of ^{99m}Tc in Generator Eluates

Days since Prior Elution	Hours since Prior Elution							
	0	3	6	9	12	15	18	21
0		0.727	0.619	0.532	0.460	0.401	0.352	0.311
1	0.277	0.248	0.223	0.202	0.184	0.168	0.154	0.142
2	0.131	0.122	0.113	0.105	0.098	0.092	0.087	0.081
3	0.077	0.072	0.068	0.065	0.061	0.058	0.055	0.052
4	0.050	0.047	0.045	0.043	0.041	0.039	0.038	0.036

Source: Reference 4.

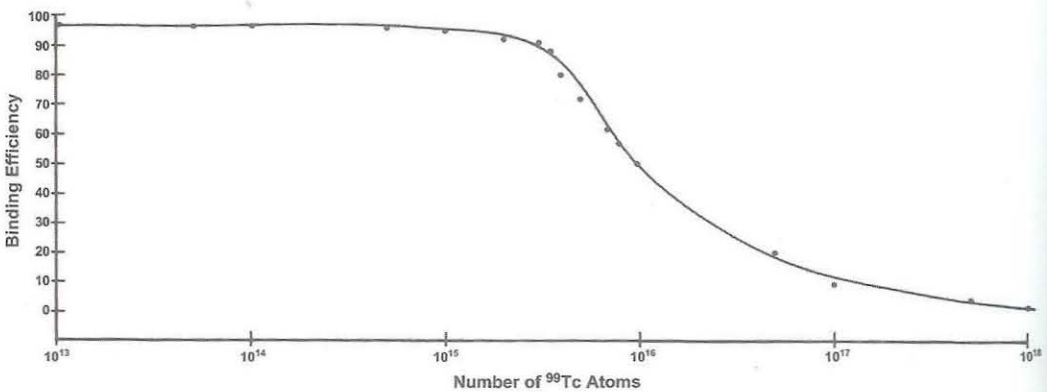

FIGURE 8-10 Effect of carrier technetium on the labeling efficiency of ^{99m}Tc-labeled human serum albumin. (Reprinted with permission from reference 14.)

$$\frac{N_{^{99m}\mathrm{Tc}}}{N_{(\mathrm{total})}} = \frac{0.86\,\lambda_1\left(e^{-\lambda_1 t} - e^{-\lambda_2 t}\right)}{\lambda_2 - \lambda_1\left(1 - e^{-\lambda_1 t}\right)} \tag{8-2}$$

In this equation, λ_1 and λ_2 are the decay constants for ^{99}Mo and ^{99m}Tc, respectively. With increasing time of decay, the mole fraction of ^{99m}Tc decreases because of the buildup of ^{99}Tc atoms. For example, after 1 day of decay the mole fraction of ^{99m}Tc in the generator is 0.2769, or about 28% of the total number of technetium atoms in the generator eluate; the remaining atoms (approximately 72%) are ^{99}Tc. The amount of ^{99m}Tc in generator eluates is therefore not "carrier-free," and its specific activity continuously decreases as the period of time between generator elutions increases. This has the potential of decreasing labeling efficiency in ^{99m}Tc radiopharmaceutical kits that contain small amounts of reducing agent (Sn^{2+} ion). This becomes most critical when, for example, a generator manufactured on a Friday is not eluted until the following Monday. The effect of carrier technetium on the preparation of ^{99m}Tc-labeled human serum albumin is a noteworthy example (Figure 8-10).[14]

Because the labeling yield of some ^{99m}Tc radiopharmaceuticals depends on the total number of atoms present in the reaction mixture, it may be desirable to determine the total number of technetium atoms present in the generator eluate. This determination can be made from the ^{99m}Tc activity and its mole fraction by using the following equation:[13]

$$N(\mathrm{total})\frac{A_{^{99m}\mathrm{Tc}}\left(T_{1/2}\right)(1.443)}{^{99m}\mathrm{Tc\ mole\ fraction}} \tag{8-3}$$

TABLE 8-4 Total Technetium Atoms (^{99}Tc and ^{99m}Tc) $\times 10^{12}$ per Millicurie of ^{99m}Tc Eluted from a ^{99m}Tc Generator

Days since Prior Elution	Hours since Prior Elution							
	0	3	6	9	12	15	18	21
0		1.59	1.87	2.18	2.52	2.89	3.29	3.72
1	4.18	4.67	5.18	5.73	6.30	6.89	7.51	8.16
2	8.83	9.52	10.25	10.99	11.76	12.56	13.38	14.23
3	15.11	16.03	16.97	17.91	18.91	19.95	21.00	22.12
4	23.23	24.41	25.60	26.85	28.15	29.44	30.86	32.23

Thus, the total number of technetium atoms, N (total), per millicurie of ^{99m}Tc is

$$N(\text{total}) = \frac{(1\text{ mCi})(3.7\times10^{7}\text{ dps/mCi})(6.01\text{ hr}\times3600\text{ sec/hr})(1.443)}{^{99m}\text{Tc mole fraction}}$$

or

$$N(\text{total}) = \frac{(\text{mCi }^{99m}\text{Tc eluted})(1.16\times10^{12}\text{ disintegrations/mCi})}{^{99m}\text{Tc mole fraction}} \qquad (8\text{-}4)$$

Example: A generator is eluted 6 hours after the previous elution and yields 500 mCi (18,500 MBq). How many atoms of ^{99m}Tc and ^{99}Tc, total, are contained in the eluate?

$$N(\text{total}) = \frac{(500\text{ mCi})(1.16\times10^{12}\text{ disintegrations (atoms)/mCi})}{0.619} = 9.37\times10^{14}\text{ atoms}$$

Note that each disintegration per second is equivalent to one atom decaying per second.

Table 8-4 lists the total number of technetium atoms per millicurie of ^{99m}Tc eluted from a generator for various periods of time, calculated from Equation 8-4 and the mole fraction values listed in Table 8-3. Table 8-4 simplifies the determination of how much ^{99m}Tc eluate should be used for kit preparation in situations in which the technetium atoms should be limited. Note that Table 8-3 indicates that the highest mole fraction of ^{99m}Tc is achieved when the generator elution interval is short. Thus, in preparing kits requiring small amounts of technetium, a practical method is to re-elute the generator within a few hours of the first elution and use this eluate for kit preparation.

Example: Efficient labeling of a red blood cell kit requires that no more than 1.48×10^{14} technetium atoms be used because of the small amount of stannous ion in the kit.[15] What is the maximum volume of generator eluate that can be used to label the kit if the generator was eluted 24 hours after the previous elution and the eluate contained 800 mCi (29,600 MBq) ^{99m}Tc in a 20 mL volume?

From Table 8-4, the total amount of technetium eluted per 800 mCi (29,600 MBq) ^{99m}Tc in 24 hours is

$$4.18\times10^{12}\text{ atoms/mCi}\times800\text{ mCi} = 3.34\times10^{15}\text{ atoms}$$

The amount of eluate that can be used is

$$\frac{1.48\times10^{14}}{3.34\times10^{15}}\times 20\text{ mL} = 0.9\text{ mL}$$

GENERATOR PHYSICS

In Chapter 2 we considered single-step radioactive decay processes in which the daughter products were stable nuclides. With generators, we must consider the situation in which daughter atoms are radioactive, represented by the following decay sequence:

$$N_1 \xrightarrow{\lambda_1} N_2 \xrightarrow{\lambda_2} N_3$$

N_1 and N_2 are parent and daughter radionuclides, respectively, and N_3 is stable or very long-lived. Because we are interested in the daughter radionuclide, its decay rate (dN_2/dt) is described by the following expression:

$$\frac{dN_2}{dt} = \lambda_1 N_1 - \lambda_2 N_2 \tag{8-5}$$

The net rate at which daughter atoms build up is the difference between the rate of their formation by the parent, $\lambda_1 N_1$, and the rate of their own decay, $\lambda_2 N_2$. For the ^{99m}Tc generator, N_1 is the number of ^{99}Mo atoms and λ_1 is its decay constant; N_2 is the number of ^{99m}Tc atoms and λ_2 is its decay constant. Even though the third product, ^{99}Tc (N_3), is radioactive, its half-life is so long (2.13×10^5 years) that it is essentially stable and does not need to be considered in the decay calculations.

After appropriate rearrangement of Equation 8-5, solution of the first-order differential equation yields the following relationship:[16]

$$N_2 = \underbrace{\frac{\lambda_1}{\lambda_2 - \lambda_1} N_1^0 \left(e^{-\lambda_1 t} - e^{-\lambda_2 t}\right)}_{[------\text{A}------]} + \underbrace{N_2^0 e^{-\lambda_2 t}}_{[--\text{B}--]} \tag{8-6}$$

The expressions in bracket A describe the rate of production and decay of daughter ^{99m}Tc atoms, and the expression in bracket B describes the contribution to N_2 from any daughter ^{99m}Tc atoms present initially or remaining after generator elution. The last term is significant only if generator elution efficiency is low or if the generator is re-eluted within a few hours after the previous elution. Recalling the expression $N = A/\lambda$, one can substitute the appropriate activity expression into Equation 8-6 and derive the following activity equation:

$$A_2 = \frac{\lambda_2}{\lambda_2 - \lambda_1} A_1^0 \left(e^{-\lambda_1 t} - e^{-\lambda_2 t}\right) + A_2^0 e^{-\lambda_2 t} \tag{8-7}$$

Equation 8-7 presumes that 100% of the parent decays to the daughter. For the ^{99}Mo–^{99m}Tc generator, only 86% of ^{99}Mo decays to ^{99m}Tc; therefore, Equation 8-7 is modified as follows:

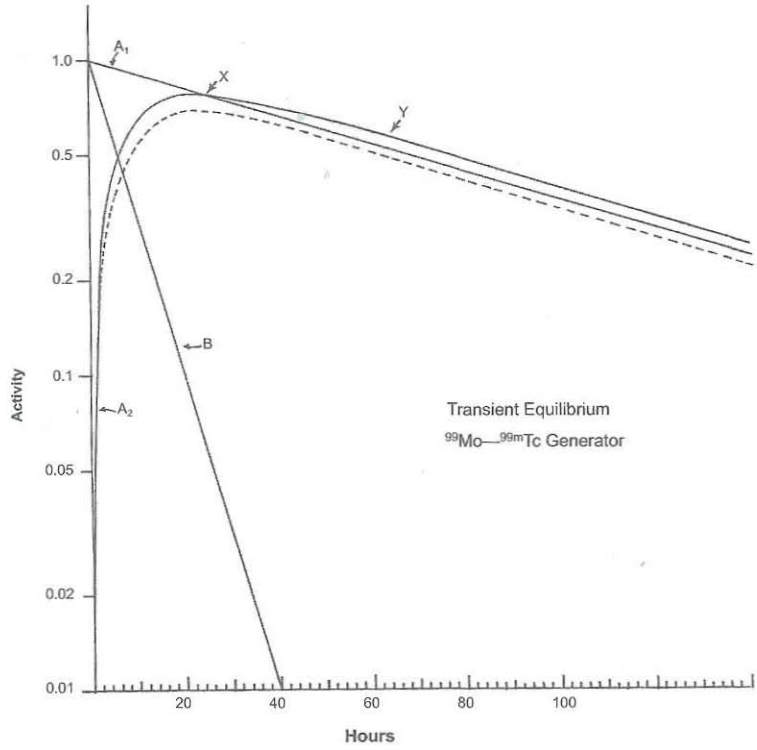

FIGURE 8-11 Transient equilibrium in the ^{99}Mo–^{99m}Tc generator (see text for description).

$$A_2 = \frac{0.86\lambda_2}{\lambda_2 - \lambda_1} A_1^0 \left(e^{-\lambda_1 t} - e^{-\lambda_2 t}\right) + A_2^0 e^{-\lambda_2 t} \qquad (8\text{-}8)$$

Equation 8-8 permits calculation of the theoretical ^{99m}Tc activity (A_2) present in the generator at any time (t) after the previous elution if one knows the ^{99}Mo activity A_1^0 present at the time of the previous elution.

Transient Equilibrium Generators

If the half-life of the parent radionuclide is significantly (say 10 to 100 times) longer than the daughter half-life, and a sufficient period of time is allowed to elapse before the generator is eluted, a condition of transient equilibrium is established between the parent and daughter. This is illustrated in Figure 8-11, in which line A_2 represents daughter ingrowth and line A_1 is parent decay. Immediately after generator elution, the rate of daughter production is greater than its rate of decay, and daughter activity increases rapidly with time. As daughter atoms accumulate, they begin to decay such that their rate of decay is equal to the rate of production and a maximum activity is reached, that is, $dN_2/dt = 0$ and $A_1 = A_2$ (point X on the graph). It should be noted that $A_1 = A_2$ only if 100% of the parent decays to the daughter. The broken line A_2 represents the situation that occurs in the ^{99m}Tc generator, where 86% of the ^{99}Mo decays to ^{99m}Tc. The time required to reach the maximum daughter activity in a generator is derived from Equation 8-6 and is given by the following relationship:

$$t_{max} = \frac{1}{\lambda_2 - \lambda_1} \ln \frac{\lambda_2}{\lambda_1} \tag{8-9}$$

In the ^{99m}Tc generator, the time to reach the maximum ^{99m}Tc activity is 23 hours.[4] After this point in time, the daughter activity exceeds that of the parent and eventually reaches the point of *transient equilibrium*, the point at which the ratio of the daughter and parent activities is a constant (point Y on the graph). From this point on the daughter appears to decay with the parent half-life (65.95 hours), but only for a parent–daughter mixture in equilibrium. If the daughter is separated from the parent and its own activity plotted with time, line B is obtained, whose slope gives the true half-life of the daughter (6.01 hours for ^{99m}Tc). The time required to achieve transient equilibrium in the ^{99}Mo–^{99m}Tc generator is on the order of 48 to 72 hours. At this point, the time of decay since the previous elution has become so large that the value of the exponential term $e^{-\lambda_2 t}$ in Equations 8-7 and 8-8 becomes very small compared with $e^{-\lambda_1 t}$, because λ_2 is much greater than λ_1. Equation 8-8 therefore simplifies to the following expression at transient equilibrium:

$$A_2 = \frac{0.86\lambda_2}{\lambda_2 - \lambda_1} A_1^0 e^{-\lambda_1 t} \tag{8-10}$$

The ratio $\lambda_2 / (\lambda_2 - \lambda_1)$ numerically is 1.1, making the constant term in Equation 8-10 0.946 (0.86×1.1). Furthermore, the term $A_1^0 e^{-\lambda_1 t}$ is equal to the activity of ^{99}Mo present in the generator after transient equilibrium is established. The actual ^{99m}Tc activity present in the generator at transient equilibrium is therefore given as 0.946 times the ^{99}Mo activity present. ^{99m}Tc activity can also be determined from broken line A_2 in Figure 8-11. It should be kept in mind that Equation 8-10 is valid for the calculation of ^{99m}Tc activity only after extended decay time (48 to 72 hours) since the previous generator elution. For times less than 48 hours, Equation 8-8 should be used, although ^{99m}Tc activities calculated with Equation 8-10 at 24 hours will be about 90% of those calculated with Equation 8-8. Table 8-5 lists various relationships between ^{99m}Tc and ^{99}Mo activities in the generator at various times after elution.

Example 1: A ^{99m}Tc generator is manufactured on a Friday, calibrated for 2.5 Ci (92,500 MBq) of ^{99}Mo at 8:00 pm. Calculate the theoretical ^{99m}Tc activity in the generator on the following Monday at 8:00 am if no previous elutions have been made. The decay constants are as follows:

$$\lambda_1\left(^{99}\text{Mo}\right) = \frac{0.693}{65.95 \text{ hr}} = 0.0105 \text{ hr}^{-1}$$

$$\lambda_2\left(^{99m}\text{Tc}\right) = \frac{0.693}{6.01 \text{ hr}} = 0.1153 \text{ hr}^{-1}$$

The time of decay is 60 hours, so Equation 8-10 can be used to make the calculation. Thus,

TABLE 8-5 Relationship between ^{99m}Tc and ^{99}Mo in the Generator at Various Times after Elution

Time (hr)	Curies ^{99}Mo ×	Ratio ^{99m}Tc:^{99}Mo =	Curies ^{99m}Tc[a]
0	1.000		0
1	0.990	0.094	0.093
2	0.979	0.179	0.175
3	0.969	0.255	0.247
4	0.959	0.324	0.311
5	0.949	0.386	0.366
6	0.940	0.441	0.414
12	0.883	0.677	0.598
18	0.829	0.803	0.666
24	0.779	0.870	0.678
36	0.688	0.924	0.636
48	0.607	0.940	0.571
60	0.536	0.944	0.506
72	0.473	0.946	0.448
78	0.445	0.946	0.421

[a] Actual ^{99m}Tc present based on 86.05% ^{99}Mo decay to ^{99m}Tc.

$$A\left(^{99m}Tc\right)=\frac{(0.86)0.1153}{0.1153-0.0105}\,2.5\text{ Ci}\,e^{-0.0105\text{ hr}^{-1}(60\text{ hr})}$$

$$A\left(^{99m}Tc\right)=(0.86)(1.1)(2.5\text{ Ci})(0.533)=1.26\text{ Ci}(46{,}620\text{ MBq})$$

Alternatively, the data in Table 8-5 can be used to solve this problem. ^{99}Mo activity after 60 hours of decay is

$$2.5\text{ Ci}(0.533)=1.33\text{ Ci}(49{,}210\text{ MBq})$$

This value is multiplied by the $^{99m}Tc/^{99}Mo$ ratio at 60 hours; thus,

$$1.33\text{ Ci}(0.944)=1.26\text{ Ci}(46{,}620\text{ MBq})$$

Example 2. If the activity actually eluted from the generator in Example 1 is 1.07 Ci (39,590 MBq), what is the elution efficiency?

$$\text{Percent elution efficiency}=\frac{\text{Measured activity}\times 100}{\text{Theoretical activity}}=\frac{1.07\text{ Ci}\times 100}{1.26\text{ Ci}}=85\%$$

Example 3. If the generator above is re-eluted at 1:00 pm, what is the expected ^{99m}Tc activity?

Because transient equilibrium was not reestablished after the previous elution, Equation 8-8 must be used for this calculation. The residual ^{99m}Tc activity remaining on the column after the 8:00 am elution is

$$(1.26\ \text{Ci available}) - (1.07\ \text{Ci eluted}) = 0.19\ \text{Ci}(7{,}030\ \text{MBq})\ \text{retained}$$

From Equation 8-8, the ^{99m}Tc activity present on the column at 1:00 pm is

$$A(^{99m}\text{Tc}) = (0.86)(1.1)1.33\ \text{Ci}\left(e^{-0.0105\,(5)} - e^{-0.1153\,(5)}\right) + 0.19\ \text{Ci}\, e^{-0.1153\,(5)}$$

$$A(^{99m}\text{Tc}) = 0.487\ \text{Ci} + 0.107\ \text{Ci} = 0.594\ \text{Ci}\ (21{,}978\ \text{MBq})$$

Alternatively, Table 8-5 can be used to solve the problem. ^{99m}Tc activity from 5 hours of ^{99}Mo decay is

$$(1.33\ \text{Ci})(0.949)(0.386) = 0.487\ \text{Ci}(18{,}019\ \text{MBq})$$

^{99m}Tc activity from 5 hours of residual ^{99m}Tc decay is

$$(0.19\ \text{Ci})(0.562) = 0.107\ \text{Ci}(3{,}959\ \text{MBq})$$

Total ^{99m}Tc activity present in the generator at 1:00 pm is

$$(0.487\ \text{Ci} + 0.107\ \text{Ci}) = 0.594\ \text{Ci}(21{,}978\ \text{MBq})$$

Because the elution efficiency is 85%, the expected ^{99m}Tc activity in the generator eluate is

$$(0.594\ \text{Ci})(0.85) = 0.505\ \text{Ci}(18{,}685\ \text{MBq})$$

Secular Equilibrium Generators

If the half-life of the parent is much longer (say 1000 times or more) than the daughter half-life, the parent does not decay appreciably during several daughter half-lives, and a condition of secular equilibrium is established. Figure 8-12 illustrates a secular equilibrium generator in which lines A_1 and A_2 are the parent and daughter activities, respectively. As in the case with transient equilibrium generators, the rate of daughter production initially is greater than its rate of decay, and daughter activity increases rapidly over time. When the rate of production equals the rate of decay, secular equilibrium is established (intersection of lines A_1 and A_2). In this condition the daughter appears to decay with the parent half-life. Because of the large difference in decay constants ($\lambda_2 >> \lambda_1$), the value of λ_1 is insignificant compared with λ_2, and the constant term $\lambda_2/(\lambda_2 - \lambda_1)$ in Equation 8-7 approaches unity. Additionally, at secular equilibrium the $e^{-\lambda_2 t}$ terms approach zero; therefore, Equation 8-7 is simplified to

$$A_2 = A_1^0 e^{-\lambda_1 t} \tag{8-11}$$

That is to say, at secular equilibrium the daughter activity is equal to the parent activity present in the generator.

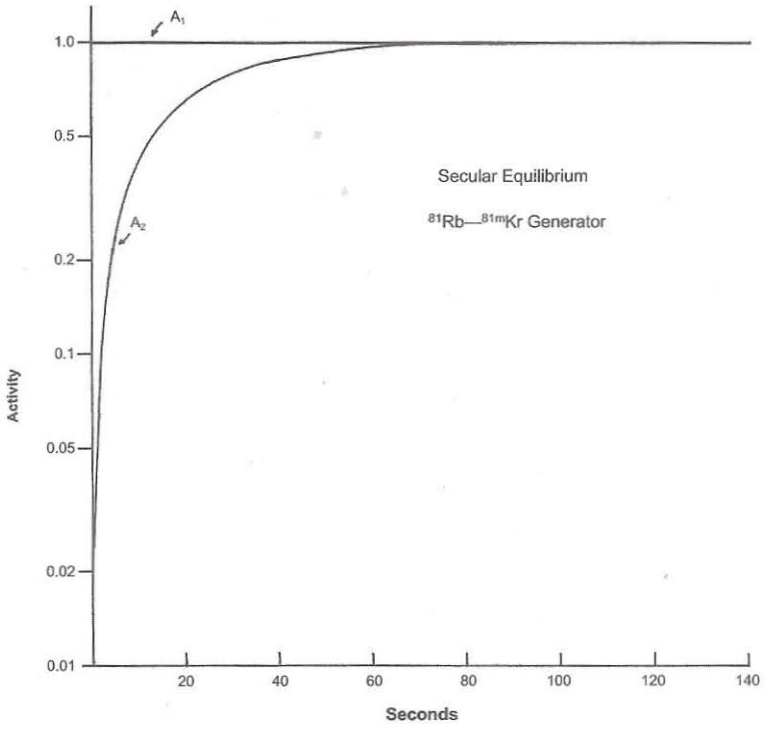

FIGURE 8-12 Secular equilibrium in the ^{81}Rb–^{81m}Kr generator (see text for description).

Some examples of secular equilibrium generators are as follows:

$$^{226}Ra \xrightarrow{1600\ \text{years}} {}^{222}Rn \xrightarrow{3.8\ \text{days}} {}^{218}Po$$

$$^{113}Sn \xrightarrow{115\ \text{days}} {}^{113m}In \xrightarrow{99.4\ \text{minutes}} {}^{113}In$$

$$^{81}Rb \xrightarrow{4.7\ \text{hours}} {}^{81m}Kr \xrightarrow{13\ \text{seconds}} {}^{81}Kr$$

Secular equilibrium for the ^{81}Rb–^{81m}Kr generator is illustrated in Figure 8-12.

DISPOSAL OF THE ^{99M}TC GENERATOR

Generator manufacturers provide a return program for used ^{99m}Tc generators. Usually when the new generator is received, the old one is placed in the empty shipping carton, sealed, surveyed, and shipped back to the manufacturer for credit. A certain amount of paperwork is involved in the proper shipment of used generators to comply with Department of Transportation regulations. Some hospitals choose to decay the old generators to background levels of radioactivity, dismantle them, and discard the generator columns in regular trash. Because fission-moly generators may contain long-lived radiocontaminants such as ^{103}Ru (39.5 day half-life), it has been determined that old generators should be held for 14 weeks before discarding. After that time the generator columns can be removed,

surveyed with a Geiger-Müller counter, and disposed of in regular trash if the surface exposure rate is below background (approximately 0.2 mR/hour).

OTHER GENERATOR SYSTEMS

While the ^{99m}Tc generator system has widespread application in routine nuclear medicine, other generator systems have been used for biomedical applications.[17] Several of these generators have played an important part in the development of imaging agents over the years, some are no longer available, and some may find more application in the future. The properties of several of these generators are briefly discussed in this section. All of them are secular equilibrium generators except for ^{188}W–^{188}Re, which is a transient equilibrium generator.

^{113}Sn–^{113m}In Generator

The ^{113}Sn–^{113m}In generator was used mostly in the 1960s and 1970s for preparing ^{113m}In-labeled radiopharmaceuticals for imaging many of the major organ systems, including the brain, lung, liver, kidney, and blood pool. ^{113}Sn is produced in a nuclear reactor by neutron activation of stable enriched ^{112}Sn through the nuclear reaction ^{112}Sn(n,γ)^{113}Sn. It can also be produced in a cyclotron. The ^{113}Sn is adsorbed on a hydrous zirconium oxide column and the $^{113m}InCl_3$ is eluted with 0.05 M hydrochloric acid. The trivalent cationic indium ($^{113m}In^{3+}$) readily forms chelates. At the time, this was an advantage over ^{99m}Tc, which has to be reduced to a cationic species before chelation. When injected intravenously, indium quickly binds to plasma transferrin, forming a blood pool imaging agent. ^{113m}In is also incorporated into a variety of other compounds, including diethylenetriaminepentaacetic acid (DTPA), hydroxide and phosphate colloids, and albumin aggregates.

^{113}Sn decays with a half-life of 115 days by electron capture (EC) to ^{113m}In. ^{113m}In decays by isomeric transition to stable ^{113}In with a half-life of 1.7 hours, emitting a gamma ray of 393 keV. The long half-life of the parent permits a long shelf life of the generator, but the short half-life of the daughter requires radiopharmaceuticals to be prepared more than once daily.

^{82}Sr–^{82}Rb Generator

After production by a proton spallation reaction on molybdenum, ^{82}Sr is purified and loaded onto a hydrous stannic oxide column with an activity in the range of 90 to 150 mCi (3330 to 5550 MBq). ^{82}Sr decays by EC with a half-life of 25 days to ^{82}Rb. The rubidium daughter is eluted as ^{82}Rb-rubidium chloride from the generator with normal saline.[18] ^{82}Rb decays by positron emission with a half-life of 75 seconds. Because of this short half-life, the system regenerates a full charge of ^{82}Rb activity within 10 minutes of elution, and studies can be repeated frequently. The monovalent cationic $^{82}Rb^+$ is used primarily for cardiac PET imaging, but it is also used for brain tumor imaging.

^{68}Ge–^{68}Ga Generator

After its production in a cyclotron by the proton bombardment of stable gallium, ^{68}Ge in hydrochloric acid solution is neutralized in ethylenediaminetetraacetic acid (EDTA) solution and loaded onto an alumina column. ^{68}Ge decays with a 275 day half-life by EC to ^{68}Ga. The accumulated ^{68}Ga activity is eluted as gallium EDTA from the generator by 0.005 M EDTA solution. ^{68}Ga decays by positron emission with a half-life of 68 minutes. ^{68}Ga

must be separated from EDTA if other radiopharmaceuticals are to be prepared. Alternative methods have been used to elute ^{68}Ga as the trichloride in hydrochloric acid, whereupon the ionic form can be readily used to label other ligands. In this form it can be used to prepare many of the compounds labeled with ^{113m}In because of their similar chemistry. A current application of this generator is as a transmission source in PET for attenuation correction of 511 keV photons.

^{81}Rb–^{81m}Kr Generator

The parent radionuclide, ^{81}Rb, can be produced by several nuclear reactions in a cyclotron by the alpha-particle bombardment of a bromine target, as a bromide salt. This secular equilibrium generator is prepared by adsorbing ^{81}Rb on columns of zirconium phosphate, Bio-Rad Ag50 (Bio-Rad, Richmond, Calif.), or Dowex 50-X8 (Dow Chemical, Midland, Mich.), from which ^{81m}Kr is eluted with approximately 2 mL of distilled water. ^{81}Rb decays by EC with a half-life of 4.5 hours, which greatly limits its clinical utility. ^{81m}Kr decays by isomeric transition with a 13-second half-life, emitting a 191 keV gamma ray. ^{81m}Kr has been used in pulmonary ventilation imaging and to measure tissue blood flow.

^{90}Sr–^{90}Y Generator

^{90}Sr is produced as a fission byproduct of ^{235}U in a nuclear reactor. A convenient radiochemical procedure for separation and purification involves precipitation of strontium as the nitrate and subsequent purification by anion exchange chromatography.[17] ^{90}Y-yttrium chloride is a sterile, aqueous solution of yttrium chloride in 0.05 M hydrochloric acid. It is produced by solvent extraction of ^{90}Y from a ^{90}Sr generator solution and purified into the chloride form, $^{90}YCl_3$. It is available from MDS Nordion (Ontario, Canada) in 5, 10, 20, and 50 mCi amounts per vial with 20 μCi or less of ^{90}Sr radionuclide impurity per curie of ^{90}Y at expiration.

^{188}W–^{188}Re Generator

The ^{188}W parent is produced in a high-flux nuclear reactor by double neutron capture on ^{186}W as the trioxide or metal as follows: $^{186}W(n,\gamma)^{187}W(n,\gamma)^{188}W$.[17,19] ^{188}W decays by beta decay (0.349 MeV E_{max}) with a half-life of 69.4 days to ^{188}Re. ^{188}Re decays also by beta decay (2.12 MeV E_{max}) and gamma emission (0.155 MeV, 15%) with a half-life of 16.98 hours. This transient equilibrium generator has been prepared by packing zirconyl tungstate ^{188}W gel into a column similar to that used for ^{99m}Tc generators. The ^{188}Re is eluted from the generator as perrhenate with water or normal saline in 3 mL fractions with approximately 90% eluted in the first fraction.[19] ^{188}Re has been used to label antibody fragments with diamide dithiolate technology in yields and purity virtually identical to those with ^{99m}Tc.[20]

REFERENCES

1. Stang LG Jr, Tucker WD, Doering RF, et al. Development of methods for the production of certain short-lived radioisotopes. In: *Proceedings of the First UNESCO Conference*. Vol 1. London: Pergamon Press; 1958:50-70.
2. Harper PV, Andros G, Lathrop K. *Preliminary Observations on the Use of Six-hour Tc-99m as a Tracer in Biology and Medicine*. Washington, DC: US Atomic Energy Commission; 1962:77-88. Report ACRH-18.
3. Arino H, Kramer HH. Fission product Tc-99m generator. *Int J Appl Radiat Isot*. 1975;26:301-3.

4. Lamson M III, Hotte CE, Ice RD. Practical generator kinetics. *J Nucl Med Technol.* 1976;4:21-7.
5. Molinski VJ. A review of Tc-99m generator technology. *Int J Appl Radiat Isot.* 1982;33:811-9.
6. Steigman J. Chemistry of the alumina column. *Int J Appl Radiat Isot.* 1982;33:829-34.
7. Vesely P, Cifka J. Some chemical and analytical problems connected with technetium-99m generators. In: *Radiopharmaceuticals from Generator-Produced Radionuclides.* Vienna, Austria: International Atomic Energy Agency; 1971:71-82.
8. Richards P, O'Brien MJ. Rapid determination of Mo-99 in separated Tc-99m. *J Nucl Med.* 1969;10:517.
9. Briner WH, Harris CC. Radionuclidic contamination of eluates from fission product molybdenum-technetium generators [letter]. *J Nucl Med.* 1974;15:466-7.
10. Ponto JA. Expiration times for Tc-99m. *J Nucl Med Technol.* 1981;9:40.
11. Kowalsky RJ, Preslar J. Report of a positive Mo-99 breakthrough test. *J Nucl Med Technol.* 1979;2:108.
12. *Chart of the Nuclides.* 15th ed. Cincinnati, OH: Lockheed Martin, 1996.
13. Lamson ML III, Kirschner AS, Hotte CE, et al. Generator-produced 99m $TcO4^-$: carrier free? *J Nucl Med.* 1975;16:639-41.
14. Porter WC, Dworkin HJ, Gutkowski RF. The effect of carrier technetium in the preparation of Tc-99m-human serum albumin. *J Nucl Med.* 1976;17:704-6.
15. Smith TD, Richards P. A simple kit for the preparation of Tc-99m-labeled red blood cells. *J Nucl Med.* 1976;17:126-32.
16. Friedlander G, Kennedy JW, Miller JM. *Nuclear and Radiochemistry.* 2nd ed. New York: Wiley; 1966:71-5.
17. Finn RD, Molinski VJ, Hupf HB, et al. *Radionuclide Generators for Biomedical Applications.* Oak Ridge, TN: US Department of Energy; 1983. NAS-NS-3202.
18. Gennaro GP, Neirinckx RD, Bergner B, et al. A radionuclide generator and infusion system for pharmaceutical quality Rb-82. In: Knapp FF Jr, Butler TA, eds. *Radionuclide Generators: New Systems for Nuclear Medicine Applications.* ACS Symposium Series No. 241. Washington, DC: American Chemical Society; 1984:135-50.
19. Ehrhardt GJ, Ketring AR, Turpin TA, et al. A convenient tungsten-188/rhenium-188 generator for radiotherapeutic applications using low specific activity tungsten-188. In: Nicolini M, Bandoli G, Mazzi U, eds. *Technetium and Rhenium in Chemistry and Nuclear Medicine 3.* Verona, Italy: Cortina International; 1990:631-4.
20. Vanderheyden JL, Fritzberg AR, Rao TN, et al. Rhenium labeling of antibodies for radioimmunotherapy [abstract]. *J Nucl Med.* 1987;28:656.

9 Radiopharmaceutical Chemistry

A radiochemical is a chemical substance containing radioactive atoms within its structure. A radiochemical becomes a radiopharmaceutical when it has been tested in humans for an intended use, according to U.S. Food and Drug Administration (FDA) requirements, and found to be safe and effective in the diagnosis and treatment of disease. Radiopharmaceuticals come in various physicochemical forms ranging from simple elemental substances to complex radiolabeled molecules, blood cellular elements, and particles. They are administered to patients in oral dosage forms such as capsules and solutions, by inhalation as gases and aerosols, and by various routes of injection, most often intravenous.

Radiopharmaceuticals possess a few unique characteristics. Because only trace amounts are administered, radiopharmaceuticals are subpharmacologic and do not produce physiologic effects in the body, unlike traditional drugs. This also means that their chemical toxicity risk is essentially nil. However, radiopharmaceuticals do possess an inherent radiation risk, and this limits the amounts that can be administered. Radiopharmaceuticals are used most frequently for diagnostic purposes, although several therapeutic applications have been developed.

ACTIVITY–MASS RELATIONSHIP

Although radiopharmaceuticals are typically administered in microcurie or millicurie amounts of activity, it is sometimes useful to know the chemical amount of substance present in a given amount of activity. This can be determined from the activity–mass relationship, $A = \lambda N$, which relates the activity of a substance to its equivalent number of atoms, modified by the decay constant, λ. Since the decay constant varies inversely with half-life, radionuclides with long half-lives, and therefore small decay constants, require more atoms per millicurie than those with short half-lives. A question that might be asked in this regard is "How much iodine is present in a 10 μCi (370 kBq) dose of ^{131}I-sodium iodide for a thyroid uptake study?" The answer can be determined by using the activity–mass relationship to calculate the number of atoms of ^{131}I present in 10 μCi (370 kBq) and converting this to an equivalent mass from Avogadro's number. The calculation is as follows:

$$T_{½} \text{ of } ^{131}\text{I} = (8.02 \text{ days})(24 \text{ hr/day})(3600 \text{ sec/hr}) = 6.93 \times 10^5 \text{ sec}$$

$$N = \frac{A}{\lambda} = \frac{(A)(T_{½})}{0.693} = (A)(T_{½})(1.443)$$

$$N = (10 \text{ μCi})(3.7 \times 10^4 \text{ dps/μCi})(6.93 \times 10^5 \text{ sec})(1.443)$$

$$N = 3.70 \times 10^{11} \text{ disintegrations or atoms}$$

Recall that, by definition, 1 gram atomic weight (GAW) of ^{131}I (131 grams) = 6.023×10^{23} atoms of ^{131}I. Therefore,

$$\frac{3.70\times10^{11}\ \text{atoms}\times131\ \text{grams/GAW}}{6.023\times10^{23}\ \text{atoms/GAW}} = 8.05\times10^{-11}\ \text{gram}$$

The total amount of iodine in the human body is approximately 6.5 mg. Thus, a 10 μCi (370 kBq) dose of ^{131}I is only about one eighty-millionth of the body's iodine stores, demonstrating the extremely small amounts of radionuclide required for a diagnostic study.

RADIOACTIVE CONCENTRATION AND PURITY EXPRESSIONS

The concentration of radioactivity is expressed in several ways. *Radioactive concentration* is the radioactivity per unit weight or volume of diluent. The diluent is typically a liquid, such as water or normal saline, but it may be a solid. Radioactive concentration is expressed, for example, as millicuries or microcuries per milliliter of solution or milligrams of solid diluent. *Specific activity* is the radioactivity per unit weight of radionuclide or labeled compound. It is expressed in units appropriate to the sample in question, for example, millicuries per milligram or micromoles of element or compound.

Theoretically, the highest specific activity of an elemental substance is achieved if every atom in the sample is that of the radionuclide of interest; for a labeled compound, the highest specific activity is achieved if every potential labeling site in the molecule contains only the radionuclide of interest. The theoretical specific activity can be calculated using the formula $A = \lambda N$, which is modified to yield Equation 9-1.

Example: Calculate the specific activity of isotopically pure ^{14}C in millicuries per milligram.

$$A\left(\text{mCi/mg}\right) = \frac{\lambda N}{3.7\times10^{7}\ \text{dps/mCi}}$$

$$\lambda = \frac{0.693}{5715\ \text{yr}\left(3.15\times10^{7}\ \text{sec/yr}\right)} = 3.85\times10^{-12}\ \text{sec}^{-1}$$

$$N = \frac{6.023\times10^{23}\ \text{d/mole}}{14\ \text{grams/mole}\times10^{3}\ \text{mg/gram}} = 4.3\times10^{19}\ \text{d/mg} \qquad (9\text{-}1)$$

$$A = \frac{\left(3.85\times10^{-12}\ \text{sec}^{-1}\right)\left(4.3\times10^{19}\ \text{d/mg}\right)}{3.7\times10^{7}\ \text{dps/mCi}}$$

$$A = 4.47\ \text{mCi}\left(165.4\ \text{MBq}\right)/\text{mg}\ ^{14}\text{C}$$

Carbon in nature contains mostly stable ^{12}C and ^{13}C atoms, so its specific activity with respect to the trace amount of ^{14}C present is extremely low. Note that specific activity is inversely related to half-life. This is illustrated in Table 9-1, which lists the theoretical maximum specific activities of iodine radioisotopes.

TABLE 9-1 Specific Activities (SA) of Radioiodines

Isotope	Half-life	SA (mCi/μg)
^{123}I	13.2 hours	1930.0
^{131}I	8.02 days	124.0
^{125}I	59.4 days	17.6

The labels on the vials of most radiopharmaceuticals provide information on the radioactive concentration and specific activity. From this information one can determine the amount of labeled compound in a unit volume. Thus,

$$\frac{\text{Radioactive concentration } (\text{mCi/mL})}{\text{Specific activity } (\text{mCi/mg})} = \text{Drug concentration } (\text{mg/mL})$$

In the field of radiochemistry, the small chemical amount of a radioisotope in a sample can create a problem with its recovery during chemical processing, primarily because of adsorption losses on glassware surfaces. To mitigate this problem, radiochemists add an amount of stable isotope of the radionuclide being analyzed to the radioactive sample to "carry" it through the chemical process. The stable isotope added is called a "carrier." The term "carrier-free" originally indicated radioactive preparations with no isotopic carrier intentionally added and containing no isotopic material detectable by chemical or spectrographic means.[1] Over time the term carrier-free became misunderstood and misused in relation to its original definition. It was applied to radionuclide samples that contained only the radionuclide of interest, one of absolute theoretical specific activity. It is questionable whether such samples can actually be achieved, given the limitations of radiochemical methods. Consequently, new terminology was proposed.[1] *Carrier-free* (CF) now indicates a radionuclide or stable nuclide that is not contaminated with any other stable or radioactive nuclide of the same element. *No carrier added* (NCA) indicates an element or compound to which no carrier of the same element has been intentionally or otherwise added during preparation. *Carrier added* (CA) indicates any element or compound to which a known amount of carrier has been added. Thus, a preparation that is termed CF is, by definition, NCA. However, one that is designated NCA may not necessarily be CF, because it may contain stable or radioactive isotopic contaminants that were not intentionally added but are present because of limitations of the production and purification processes. Most radiotracer nuclide preparations are NCA.

IDEAL PROPERTIES OF DIAGNOSTIC RADIOPHARMACEUTICALS

Diagnostic agents can be divided into two categories of use: in vivo function agents and imaging agents.

An in vivo function agent traces a physiologic process without altering it in any way, so that a true measure of function can be obtained. Noteworthy examples are measurement of thyroid gland function with ^{131}I-sodium iodide, assessment of vitamin B_{12} metabolism with ^{57}Co-cyanocobalamin, measurement of glomerular filtration rate (GFR) with ^{99m}Tc-diethylenetriaminetetraacetic acid (^{99m}Tc-DTPA or ^{99m}Tc-pentetate) or ^{125}I-iothalamate, and determination of blood volume with ^{51}Cr-labeled red blood cells and ^{125}I-labeled human serum albumin. During in vivo function studies, the radioactive agent is administered to the patient and the specific bodily function is assessed by measuring radiation emitted

TABLE 9-2 Ideal Properties of Radionuclides for Diagnostic Imaging

1. *Decay mode:* Electron capture or isomeric transition from metastable isomers; no particulate radiation; gamma or x-rays only
2. *Photon energy:* 100–200 keV is ideal
   Below 100 keV = tissue absorption and scatter (decreases resolution)
   Above 200 keV = lower detection efficiency (decreases sensitivity)
3. *Half-life:* Effective half-life = 1 to 1.5 times the imaging time
4. *Chemical properties:* Can be compounded into different chemical forms

TABLE 9-3 Photon Detection Efficiency in Half-Inch Sodium Iodide Crystal

Radionuclide	Photon Energy (keV)	Detector Efficiency (%)
^{133}Xe	81	92
^{99m}Tc	140	86
^{111}In	172	73
	247	45
^{131}I	364	23
Positron emitters	511	13

Source: Anger HO. Radioisotope cameras. In: Hine GJ, ed. *Instrumentation in Nuclear Medicine*. New York: Academic Press; 1967: 485.

directly from the organ of interest or by analyzing urine or blood samples. For valid in vivo function measurements, the radiotracer must be physiologic; that is, it must participate in the biologic function being assessed without altering the function in any way.

Diagnostic imaging agents are designed to localize in specific organs. Gamma-camera images of radiotracer distribution within the organ can then be obtained to assess organ morphology (size, shape, position, or presence of space-occupying lesions) and function. An ideal imaging agent should rapidly and avidly localize in the organ of interest, remain there for the duration of the study, and be quickly excreted from the body thereafter. No single agent currently meets these stringent requirements, and a judicious selection of radionuclide and chemical form must be combined to achieve the best compromise. Table 9-2 lists several properties of an ideal radionuclide for diagnostic imaging.

Decay Mode and Energy

Electromagnetic radiations (gamma rays, characteristic x-rays) are the most suitable forms for external detection. Particulate radiation, being completely absorbed by tissue, cannot be detected externally and only increases radiation burden. The most desirable decay modes for diagnostic imaging are electron capture (EC) and isomeric transition, which have no primary particulate emissions associated with them. Additionally, to ensure a high yield of detectable photons (high photon abundance), the extent of internal conversion should be minimal. For example, the 10% photon abundance of the 320 keV gamma ray from ^{51}Cr makes it a poor radionuclide for imaging studies, whereas the 89% abundance of the 140 keV gamma ray from ^{99m}Tc is quite satisfactory.

The energy of gamma rays should be high enough to readily penetrate and escape from the body with minimal scatter, yet be low enough for efficient detection by the gamma camera detector. Table 9-3 lists the detection efficiencies of various radionuclide photon energies in a sodium iodide detector.

Half-life

The effective rate of loss (R_{eff}) of radioactivity from an organ or the body is directly proportional to the rates of physical decay (R_p) of the radionuclide and of biologic excretion (R_b) of the radiopharmaceutical, as shown in Equation 9-2:

$$R_{eff} = R_p + R_b \tag{9-2}$$

In accordance with Equation 9-3, the rate of removal by either process is inversely proportional to the half-life of the process:

$$R(\text{removal rate}) \propto \frac{1}{T_{1/2}} \tag{9-3}$$

Combining Equations 9-2 and 9-3, we have the following relationships:[2]

$$\frac{1}{T_{eff}} = \frac{1}{T_p} + \frac{1}{T_b} \tag{9-4}$$

or

$$T_{eff} = \frac{T_p \times T_b}{T_p + T_b} \tag{9-5}$$

The effective half-life is therefore the time required to remove half of the radioactivity from an organ by a combination of physical decay and biologic elimination. The T_{eff} is always less than either the T_p or T_b, but it will be nearly equal to the smaller function when the other is very large. The following example illustrates the effective half-life for a radiopharmaceutical when (1) T_p is 1 hour and T_b is 10 hours, (2) T_p and T_b are both 10 hours, and (3) T_p is 10 hours and T_b is 1 hour:

1. $T_{eff} = \frac{1 \times 10}{1+10} = \frac{10}{11} = 0.91 \text{ hr}$

2. $T_{eff} = \frac{10 \times 10}{10+10} = \frac{100}{20} = 5.0 \text{ hr}$

3. $T_{eff} = \frac{10 \times 1}{10+1} = \frac{10}{11} = 0.91 \text{ hr}$

From an imaging standpoint, the optimum effective half-life should be about 1 to 1.5 times the period of observation or study time. This time provides enough radioactivity for acceptable counting statistics and a removal rate that diminishes the radiation dose to the patient. In practice, however, it is difficult to achieve an optimum balance between imaging time and T_{eff}. Typically, many radiopharmaceuticals have a prolonged biologic retention, and use of a short-lived radionuclide is the best way to limit radiation dose. Fortunately,

most of the clinical procedures performed in nuclear medicine employ ^{99m}Tc, which has a short physical half-life of 6 hours.

The type of study sometimes dictates the half-life of the radionuclide selected for use. For example, cisternography studies may require 2 to 3 days for completion, in which case the agent of choice would be ^{111}In-DTPA, which has a 2.8 day T_p. Six hour ^{99m}Tc agents are generally unsatisfactory for studies beyond 1 day, although ^{99m}Tc-DTPA may be a satisfactory choice for cerebrospinal fluid (CSF) leak studies, which require only a few hours to complete.

Radiopharmaceuticals with a long T_{eff} have lingering radioactivity levels in the body that may interfere with subsequent diagnostic studies. For example, when performing in vivo function studies that require blood or urine samples, it is a standard of practice to obtain background blood or urine samples before administration of the radiopharmaceutical. This will allow any residual radioactivity in the body to be accounted for during the analysis.

Radionuclide Chemistry

A radionuclide ideally should have chemical properties that allow it to be compounded into a variety of chemical forms useful as biologic tracers. Radionuclides such as radioiodine have been quite useful because iodine's diversified chemistry permits its use as radioiodide for thyroid studies and its incorporation into other molecules. For example, ^{123}I- or ^{131}I-labeled meta-iodobenzylguanidine (MIBG, or iobenguane sulfate) is used for neuroendocrine studies, while radioiodinated proteins and antibodies are used for a variety of biologic applications. Technetium has been incorporated into a large number of chemical compounds that are used in most nuclear medicine studies. Indium's chemistry has permitted it to be complexed into several radiopharmaceuticals, and it is particularly suited for labeling antibodies that require imaging over several days.

RADIOPHARMACEUTICAL DEVELOPMENT

Figure 9-1 illustrates a number of elements having radioisotopes that possess the necessary physical and chemical properties for incorporation into useful radioactive drugs. Because the list of useful radionuclides is somewhat limited, the approach to development of radiopharmaceuticals has often been empiric. In this approach, a radionuclide with favorable nuclear properties is selected and compounded into various chemical and physical forms. Biodistribution studies are then conducted in animals and human subjects with

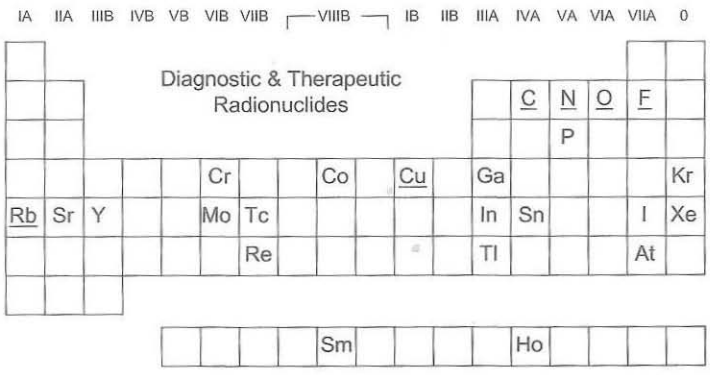

FIGURE 9-1 Elements that have radioisotopes useful for diagnostic and therapeutic applications in nuclear medicine. Positron-emitting nuclides are underlined.

TABLE 9-4 Properties of Isotopic Labels for Biologic Molecules

Nuclide	Decay Mode	Half-life	Photon Energy
^{3}H	β^-	12.32 yr	No photons
^{14}C	β^-	5715 yr	No photons
^{32}P	β^-	14.28 days	No photons
^{35}S	β^-	87.2 days	No photons
^{11}C	β^+	20.3 min	511 keV
^{13}N	β^+	9.97 min	511 keV
^{15}O	β^+	2.04 min	511 keV
^{18}F	β^+	109.8 min	511 keV

the purpose of finding a useful tracer. Examples are radioiodinated albumin for plasma volume measurement, complexation of radiometals with DTPA for GFR measurement, and adjustment of the pH of radiometal solutions to form colloidal particles that localize in the reticuloendothelial system (RES). This approach was moderately successful with the earlier technetium and indium radiopharmaceuticals. A more specific systematic approach is to combine knowledge of organ system physiology and biochemistry with the properties of specific radiotracer compounds to create a suitable diagnostic agent. The classic example is the use of radioiodide for imaging the thyroid gland.

Isotopic labeling is the replacement of a stable atom in a compound with its radioisotope. It results in a radiotracer molecule with structural and biologic properties intact, similar to the nonradioactive "parent" molecule. Although this approach is ideal, the number of desirable imaging radionuclides is a limiting factor. Biologic molecules and drugs are composed mostly of the elements carbon, hydrogen, oxygen, nitrogen, phosphorus, and sulfur. However, the radioisotope properties of these elements, with a few exceptions, are unsatisfactory for diagnostic studies. The primary limitations are half-life, decay mode, photon energy, and availability. One bright spot in recent years has been the development of positron emission tomography (PET), which has made possible the use of ^{11}C, ^{13}N, ^{15}O, ^{18}F, and other positron emitters for isotopic labeling. Although the number of potential molecules that can be synthesized with these isotopes is virtually unlimited, a principal limitation is the availability of rapid synthesis methods for routine production. Table 9-4 lists the physical properties of nuclides available for isotopic labeling.

The limited number of radionuclides available for isotopic labeling necessitates labeling molecules with radionuclides not native to the compound of interest. This process is called *nonisotopic* or "foreign" labeling. Nonisotopic labeling is not ideal because the presence of a foreign atom in a molecule often changes its biologic properties. However, labeling methods can sometimes circumvent potential problems in this regard, and many useful radiopharmaceuticals have been developed with this approach.

Some examples of radiopharmaceuticals that have been developed for nuclear medicine studies, using various approaches to design, are as follows.

1. Many metallic radionuclides will readily hydrolyze in neutral aqueous solution to form insoluble hydrated oxides or hydroxides as colloidal dispersions. After intravenous injection, these radiocolloids localize in organs of the RES to permit imaging of the liver, spleen, and bone marrow. Some early examples include indium hydroxide, indium phosphate colloid, and technetium tin-reduced colloid.
2. The labeling of red blood cells with ^{51}Cr-sodium chromate has allowed the measurement of red cell mass by isotope dilution analysis. Limiting the amount of chromium by use of high specific activity ^{51}Cr minimizes denaturation of the red cells.

3. Radioiodinated human serum albumin was one of the first agents for imaging the blood pool and measuring plasma volume by isotope dilution analysis.
4. The normal process of splenic sequestration of effete red blood cells provides a mechanism for imaging the spleen after the administration of ^{99m}Tc-labeled, heat-denatured red blood cells.
5. Heat denaturation of radiolabeled human serum albumin produces aggregate particles that, upon intravenous injection, temporarily lodge in the arterial capillaries of the lung, creating a lung-scanning agent useful in the detection of pulmonary emboli.
6. Ion-exchange and biochemical transport mechanisms in the body permit evaluation of various organ systems. A few of these:
   A. Cationic $^{201}Tl^{+}$ ion (a potassium ion analogue) is used to evaluate myocardial perfusion because it is extracted from blood into heart muscle cells by the Na-K ATPase pump in the myocyte membrane.
   B. ^{99m}Tc-phosphonate complexes chemisorb to calcium ions on bone surfaces, permitting evaluation of diseases associated with the skeleton.
   C. Imaging the thyroid gland is possible with pertechnetate ion, which is actively trapped in the gland because its molecular size and ionic charge are similar to those of the iodide ion.[3]
   D. Agents for evaluating kidney and liver function were developed on the basis of the ability of these organs to excrete certain ionic substances. When no suitable label for para-aminohippurate could be prepared to measure kidney function, ortho-iodohippurate (OIH) was developed because it could be labeled with radioiodine. After being used for over 30 years, OIH was replaced by the technetium agent ^{99m}Tc-mercaptoacetyltriglycine (^{99m}Tc-MAG3 or ^{99m}Tc-mertiatide), which has properties similar to those of OIH. Similarly, the anionic excretory pathway on the liver's hepatocyte membrane was exploited. The first agent developed to evaluate hepatobiliary function was the anionic red dye ^{131}I-rose bengal. It was eventually replaced in the 1970s by ^{99m}Tc-labeled N-substituted iminodiacetic acid (IDA) analogues, namely, ^{99m}Tc-labeled lidofenin (^{99m}Tc-HIDA), disofenin (^{99m}Tc-DISIDA), and mebrofenin (^{99m}Tc-BRIDA).
   E. The ability to image the adrenal cortex was made possible with ^{131}I-19-iodocholesterol. Its development was based on the natural incorporation of cholesterol precursors into steroid hormones in the adrenal gland. ^{131}I-iobenguane sulfate (^{131}I-MIBG) was then developed to image the adrenal gland because it is taken up by the norepinephrine reuptake mechanism in medullary cells.
   F. The radiolabeled glucose analogue ^{18}F-fludeoxyglucose (^{18}F-FDG) has found widespread use in imaging disease processes associated with increased glucose metabolism, such as epilepsy and tumor growth.
7. Many radiopharmaceuticals are chelates of radionuclide metals. For example, the ^{99m}Tc and ^{111}In chelates of DTPA were developed for kidney studies because of the well-known excretion of metallic chelates by glomerular filtration in the treatment of heavy-metal poisoning. The biodistribution of these metallic chelates is determined by the properties of the chelate molecule and the chelating agent. Thus, in the case of DTPA, biodistribution is not necessarily restricted very much by the type of metal ion chelated to it because ^{99m}Tc-DTPA and ^{111}In-DTPA have similar distributions after intravenous injection. These types of radiopharmaceuticals, for which there are several examples, are considered

"tagged compounds" in that the radioactive atom localizes primarily because of the biologic properties of the chelating agent.

8. An extension of this approach was the development of bifunctional chelates. Bifunctional chelates contain a chelating moiety that binds the radionuclide metal and a biochemical moiety that can be modified to alter the molecule's biodistribution properties. The first important group of agents in this class was the ^{99m}Tc-labeled N-substituted IDA analogues for hepatobiliary imaging. An interesting finding during the development of these agents was that biliary excretion would not occur unless the technetium atom was present in the complex. Structural analysis of these compounds demonstrated that a bis complex is formed with a technetium atom bridging two IDA molecules. Thus, a class of compounds was developed that became known as technetium-essential chelates.

As knowledge and experience grew in the area of technetium chemistry, new ^{99m}Tc complexes were developed with technetium as a core atom that is essential for complex formation and a molecular partner in the determination of biologic localization. Technetium's ability to exist in various oxidation states has made possible the development of numerous ^{99m}Tc complexes with desirable biologic properties. Some noteworthy examples are ^{99m}Tc-mertiatide (^{99m}Tc-MAG3) for kidney imaging, ^{99m}Tc-exametazime (^{99m}Tc-hexamethylpropyleneamine oxime, or ^{99m}Tc-HMPAO) and ^{99m}Tc-bicisate (^{99m}Tc-ethylcysteinate dimer, or ^{99m}Tc-ECD) for brain imaging, and ^{99m}Tc-sestamibi and ^{99m}Tc-tetrofosmin for heart imaging.

RADIOPHARMACEUTICAL CLASSIFICATION

The desire for site-specific localization of radiotracers placed emphasis on a receptor-specific approach to the development of agents. This approach is based on the structure–activity relationship, in which a drug molecule reacts with a specific biologic receptor because of their complementary structures. The development of receptor-binding radiotracers for the autonomic nervous system and radiolabeled antibodies for tumor-associated antigens are examples. A useful classification of radiopharmaceuticals into two groups on the basis of their mechanism of localization has been suggested: substrate nonspecific and substrate specific.[4] Substrate nonspecific agents do not participate in a specific chemical reaction. Radiopharmaceuticals that localize by diffusion (^{99m}Tc-HMPAO), compartmental confinement (^{125}I-human serum albumin [^{99m}Tc-HSA]), capillary blockade (^{99m}Tc-macroaggretated albumin [^{99m}Tc-MAA]), cell sequestration (heat-denatured ^{99m}Tc-red blood cells [^{99m}Tc-RBCs]), and phagocytosis (^{99m}Tc-sulfur colloid) are examples. Substrate-specific agents must participate in a definite chemical reaction or take part in a specific ligand–substrate interaction. Examples are radiotracers that localize by entering into biochemical or metabolic processes involving enzyme systems, such as ^{201}Tl ion in the Na-K ATPase pump for heart imaging, or involving antigen-antibody reactions, such as ^{90}Y-ibritumomab tiuxetan (Zevalin, Biogen Idec) antibody for radiation treatment of non-Hodgkin's lymphoma.

Additional approaches to radiopharmaceutical design have been used; a more complete discussion of this topic can be found in other sources.[3,5]

CHEMISTRY REVIEW

This section reviews some fundamental chemistry concepts that may be helpful to nonchemists who work with radiopharmaceuticals. It includes a discussion of electron

TABLE 9-5 Properties of Atomic Energy Levels

	Principal Energy Level, n			
Property	1	2	3	4
Number of sublevels	1(s)	2 (s,p)	3 (s,p,d)	4 (s,p,d,f)
Number of orbitals, n^2	1	4	9	16
Number of electrons (two per orbital)	2	8	18	32

configuration in atomic orbitals because electrons play a key role in the types of chemical bonding and this knowledge is helpful in understanding the chemistry involved in radiolabeling reactions. Stereochemistry concepts are also reviewed, because many second-generation technetium compounds possess asymmetry and contain chiral centers that yield stereoisomers. Finally, a brief discussion of the solution chemistry of metal ions is included because most radionuclides are metals. This very basic overview of these topics is meant only to acquaint or reacquaint readers with concepts and terminology that now appear in the literature, primarily in regard to technetium compounds. Detailed information can be found in standard texts on chemistry and stereochemistry.

Bonding Concepts

Electrons reside in atoms in energy levels. The possible energy levels are classified into principal energy levels and sublevels. The principal energy levels are numbered consecutively: 1, 2, 3, and so forth. Within each principal energy level are sublevels designated by the letters s, p, d, and f. The number of sublevels in a given principal energy level is equal to the number of that level, and the total number of atomic orbitals in a principal energy level is equal to the square of the number of that level. Thus, the first principal level has one sublevel (s) and one (i.e., 1^2) atomic orbital (s). The second principal level has two sublevels (s and p) and four (i.e., 2^2) atomic orbitals (s, p_x, p_y, and p_z). The electrons at each energy level are confined to a certain space termed the atomic orbital. No more than two electrons may occupy an orbital. Since an orbital can accommodate two electrons, the first principal energy level can have only two electrons, the second principal level can have eight electrons, and so forth (Table 9-5).

The s atomic orbital is spherical, and the s electrons can be randomly located anywhere within the spherical space surrounding the nucleus of the atom. The p orbitals are designated with subscript letters *x*, *y*, and *z* to indicate that they have direction about the nucleus as well as form. The p-orbital electrons travel in a figure 8 pattern about the nucleus in three planes along x-, y-, and z-coordinates that pass directly through the nucleus.

The first 10 elements in the periodic table and their electronic configurations are listed in Table 9-6. As a general rule, an atom seeks to achieve its lowest energy state, and it does this by filling an incomplete principal energy level. The table indicates that of the 10 elements listed, only helium and neon have filled principal energy levels, making these elements inert. Inertness is achieved because these elements cannot increase their stabilities further by combining with other elements. The remaining elements, however, have unfilled energy levels and must combine with other elements to satisfy their electron deficiencies and achieve a lower energy state. This can be accomplished in two ways: by donating or acquiring electrons, or by sharing electrons. These two processes result in different types of chemical bonds. The two basic types of chemical bonds are electrovalent (ionic) bonds and covalent bonds.

TABLE 9-6 Electronic Configurations of Selected Elements

Element	Atomic Number	Electronic Configuration	Electronegativity
H	1	$1s^1$	2.1
He	2	$1s^2$	–
Li	3	$1s^2, 2s^1$	1.0
Be	4	$1s^2, 2s^2$	1.5
B	5	$1s^2, 2s^2, 2p_x^1$	2.0
C	6	$1s^2, 2s^2, 2p_x^1, 2p_y^1$	2.5
N	7	$1s^2, 2s^2, 2p_x^1, 2p_y^1, 2p_z^1$	3.0
O	8	$1s^2, 2s^2, 2p_x^2, 2p_y^1, 2p_z^1$	3.5
F	9	$1s^2, 2s^2, 2p_x^2, 2p_y^2, 2p_z^1$	4.0
Ne	10	$1s^2, 2s^2, 2p_x^2, 2p_y^2, 2p_z^2$	–

Electrovalent Bonds

As the name implies, an electrovalent bond is associated with an electrical charge on atoms. A neutral atom has a positive valence if it loses one or more of its electrons and a negative valence if it gains one or more electrons. For example, a lithium atom can easily donate its single 2s electron to a fluorine atom, resulting in a positively charged lithium ion and a negatively charged fluoride ion. The lithium atom is left with its only remaining principal energy level filled with electrons, and the fluorine atom has both of its principal energy levels filled with electrons. Thus, the lithium fluoride molecule forms because it provides a more stable state for lithium and fluorine.

An electrovalent bond tends to form between atoms that have large differences in electronegativity. Electronegativity is the relative tendency of an atom to attract electrons. The electrovalent bond is a relatively weak bond, however, and in solution lithium fluoride readily dissociates to form free lithium and fluoride ions. Examples of electrovalent radiopharmaceuticals are ^{131}I-sodium iodide, ^{99m}Tc-sodium pertechnetate, ^{201}Tl-thallous chloride, and ^{111}In-indium chloride.

Covalent Bonds

A covalent bond is characterized by the sharing of a pair of electrons between two atoms, one electron donated from each atom. Covalent bonds are stronger than ionic bonds and are favored between atoms with similar electronegativity. The shared electrons go into molecular orbitals, that is, orbitals encompassing two positive nuclei. Because the electrons are attracted by two nuclei, the bond is stronger and the molecule more stable (lower energy state). In the representation of the chemical structures of organic molecules, a single covalent bond is conventionally written as a dash or single line (representing two electrons) between bonding atoms. An example of a covalently bonded radiopharmaceutical is ^{131}I-MIBG, in which the radioiodine atom is covalently bound to a carbon atom at the *meta* position of the aromatic ring.

Carbon is a basic constituent of all organic molecules and is an interesting case in point regarding covalent bonding. In the normal state of elemental carbon, only two covalent bonds may form, since only the two p electrons, p_x and p_y, are unpaired. However, when carbon enters into covalent bonding with other atoms, the 2s electron is "promoted" to the $2p_z$ orbital, making four unshared electrons available for bonding, that is, one electron each in the 2s, $2p_x$, $2p_y$, and $2p_z$ orbitals. The formation of single covalent bonds via these

four sp^3 hybridized orbitals is more profitable in terms of energy and results in a molecule that has greater stability than if carbon bonded only through the use of two p orbitals.

When two carbon atoms bond via a double bond, one of the p electrons does not become hybridized but remains in a separate orbital. The remaining three electrons (one s and two p) become hybridized to form three sp^2 orbitals. These sp^2 orbitals form covalent bonds that are in one plane, as compared with the x, y, and z planes of sp^3 orbitals. In this situation, the unhybridized p electron occupies a separate orbital at right angles to the plane of the sp^2 orbitals. When two carbon atoms form an sp^2 bond, two p-orbital electrons, one from each carbon atom, orient at right angles to the sp^2 orbitals. In this situation the p electrons may enter into a type of molecular orbital known as the pi-orbital, and these electrons form what is known as the pi-bond. Thus, the double bond between two carbon atoms is made up of one sp^2 bond and one pi-bond. Pi-bonds are important in the coordination of radionuclide metals in organometallic chelates.

Coordinate Covalent Bonds

Coordinate covalent bonds are frequently present in organic molecules and are characteristically present in organometallic chelates, such as technetium compounds. The coordinate covalent bond is characterized by the donation of a pair of unshared electrons by one of the atoms involved in the covalent bond. Nitrogen is frequently involved in coordinate covalent bonding. Nitrogen's electronic configuration shows that it has three p orbitals, each with a single unshared electron available for covalent bonding. When these three p-orbital electrons are used in covalent bonding, the pair of 2s-electrons remain and are available for coordinate bonding, being donated as a pair of electrons. The coordinate covalent bond is sometimes written as an arrow in chemical structures to distinguish it from a standard covalent bond.

Complex Compound

A complex (or coordination) compound is defined as a species formed by the association of two or more simpler species, each capable of independent existence. When one of the species is a metal ion, the resulting entity is known as a metal complex. The metal atom acts as an electron acceptor and is referred to as the central atom. Electron-donor atoms that bond with the metal are called coordinating groups, or ligands. The number of bonds formed by a metal with a ligand is known as the coordination number. It is typically 4, 5, or 6. If the complexing agent coordinating with a metal does so through one donor atom, donating one electron pair (i.e., is monodentate), a simple metal–ligand complex is formed. If the complexing agent contains two or more donor atoms (i.e., is multidentate), forming a ring structure with the metal, the complex is called a metal chelate and the complexing agent is called a chelating agent. There is often coordination between a radionuclide metal and an organic ligand, the result being an organometallic complex. Typical donor atoms in these complexes are nitrogen, oxygen, and sulfur. The reactions shown in Figure 9-2 illustrate these complexation processes between a metal (M) and a ligand (L).

Metal chelates may involve ionic and covalent interactions. A good example is the hexadentate chelating agent ethylenediaminetetraacetic acid (EDTA), which possesses two nitrogen donor atoms and four oxygen donor atoms. Not all the potential donor atoms are used in some complexation reactions. Such is the case in Figure 9-2, which shows the coordination of calcium with Na_2EDTA. Many natural substances are chelates: chlorophyll, hemoglobin, vitamin B_{12}, and insulin, for example. Metal chelates, including technetium chelates, are a mix of electrovalent and covalent bonds, depending on the properties of the metal and coordinating groups.

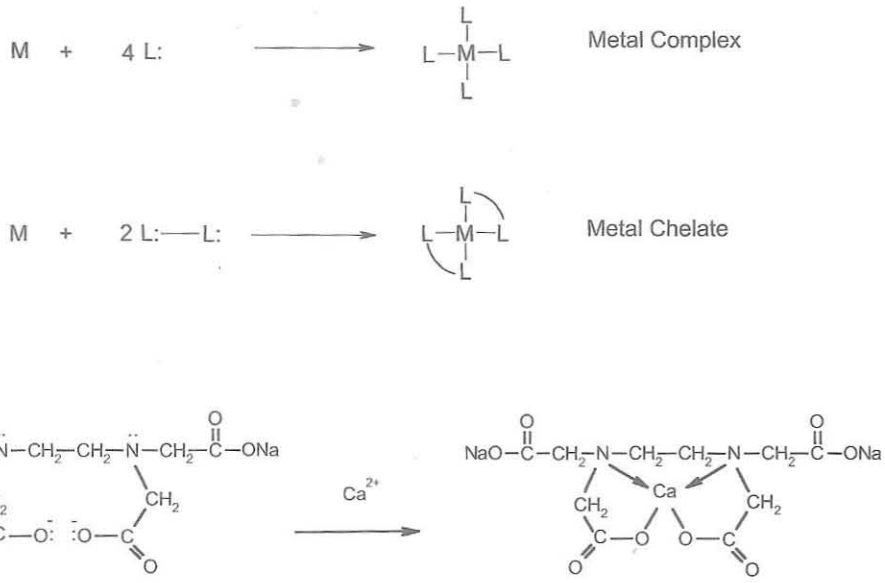

FIGURE 9-2 Generalized complexation reactions between a metal and a ligand with formation of a simple metal complex or a metal chelate. Calcium EDTA chelate shown for illustration.

Stereochemistry Concepts

It has long been known that the biologic localization of a drug molecule is determined by many factors, including lipid solubility, molecular size, ionic charge, and structure, and that the stereochemical configuration of the molecule plays an important part in the structure–activity relationship (SAR). During the design and testing of second-generation technetium radiopharmaceuticals, it became evident that the stereoisomeric form of certain radiopharmaceuticals was important for distribution and localization. Since a radiopharmaceutical does not elicit a pharmacologic response upon interaction with a receptor, its interaction with the receptor is referred to as a structure–distribution relationship (SDR). This concept was brought home during the development of a technetium-labeled radiopharmaceutical replacement for ^{131}I-OIH, for example, when it was shown that the *syn* isomer of ^{99m}Tc-N,N′-bis(mercaptoacetyl)-2,3-diaminopropanoate (^{99m}Tc-CO_2-DADS) had superior renal localization properties as compared with the *anti* isomer. Several second-generation technetium compounds are now discussed in the literature in terms of their stereospecific configurations; therefore, this section will review the terminology and concepts associated with stereochemistry.

Stereoisomers

Compounds that have the same molecular formula with identical numbers and types of atoms but distinctly different arrangement of the atoms are called *isomers*. Isomers can be of two types: constitutional isomers and stereoisomers. Isomers that have different bonding connectivities of their atoms are called *constitutional isomers*. For example, ethanol (CH_3CH_2OH) and acetone (CH_3COCH_3) both have the molecular formula C_3H_6O, but they differ in the nature of the functional group. Likewise, 1-propanol ($CH_3CH_2CH_2OH$) and 2-propanol ($CH_3CHOHCH_3$) have the molecular formula C_3H_8O but differ in the location of the OH group. Isomers that differ only in the relative spatial orientation of atoms or

groups are called *stereoisomers*. There are several types of stereoisomers, but those of greatest interest in regard to the SDR of radiopharmaceuticals are known as enantiomers.

Enantiomers are pairs of molecular species that are mirror images of each other. Additionally, they are nonsuperimposable, which means that their three-dimensional configuration cannot be arranged so that one enantiomer can be overlaid upon the other. Enantiomers are nonsuperimposable because they have chirality. A chiral molecule is one that lacks symmetry. In organic compounds, a tetrahedral carbon atom becomes chiral when the four groups attached to it are different. The different possible spatial arrangement of groups on a chiral carbon atom create the enantiomers. While enantiomers have identical physicochemical properties, their different molecular configurations may cause them to have different biologic properties. The molecular configuration of an enantiomer is designated by letter descriptors, either with a small capital (D) or (L) or with a large, italicized capital (*R*) or (*S*), as described in a later section.

One property of chiral molecules is that they are optically active. When enantiomers are separated and their solutions exposed to plane-polarized light, each enantiomer will cause the light to rotate by opposite but equal amounts. The enantiomer that rotates the plane of light clockwise, to the right, is said to be dextrorotatory and is designated with a plus sign (+) before its name. The enantiomer that rotates the plane of light counterclockwise, to the left, is said to be levorotatory and is designated with a minus sign (–) before its name. An equimolar mixture of enantiomers, designated as (±), is called a racemic mixture or a racemate. Racemates are devoid of optical activity. While enantiomers have identical physicochemical properties, their different optical properties provide a means of identifying the enantiomer that has a desired biologic activity.

Each chiral atom in a molecule can give rise to two optical isomers. If n is the number of asymmetric carbons in a molecule, the number of optical isomers is 2^n unless the molecule as a whole is symmetrical. Figure 9-3 illustrates the relationship between the possible isomers of tartaric acid. The figure shows that (D)-(–)-tartaric acid is the mirror image of (L)-(+)-tartaric acid. Therefore they are enantiomers and optically active. *Meso*-tartaric acid, however, is not a mirror-image of the (D) and (L) forms and is therefore a diastereomer of these forms. *Diastereomers* are stereoisomers that are not mirror images. They have completely different properties. *Meso*-tartaric acid melts at 140°C (D and L forms melt at 170°C), is less dense, and is less soluble in water than the (D) and (L) forms. Also, the *meso* molecule is symmetrical as a whole; that is, even though it contains two asymmetric carbon atoms, the top half and bottom half of the molecule are identical. This plane of symmetry in the molecule makes the *meso* form optically inactive.

Since the only difference in enantiomers is their optical properties, their physicochemical properties such as melting point, boiling point, and solubility are identical and cannot

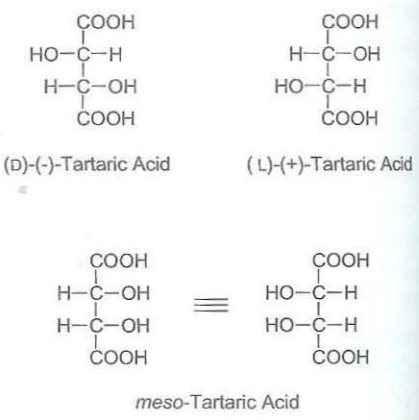

FIGURE 9-3 Enantiomers of tartaric acid: (D) and (L) forms and their diastereomer (*meso*-tartaric acid). See text for details.

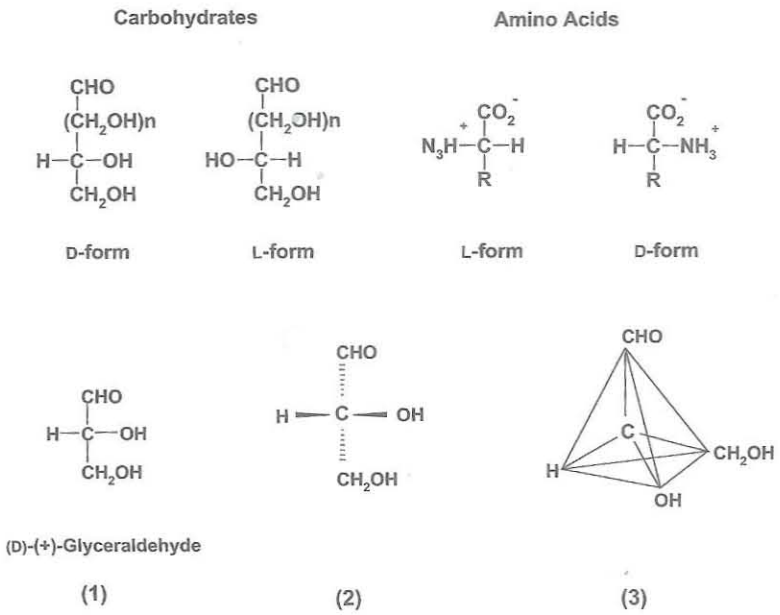

FIGURE 9-4 Upper panel shows the Fischer (D) and (L) configurations for carbohydrates and amino acids. Lower panel shows the structure of (D)-(+)-glyceraldehyde (1), its Fischer projection formula (2), and its three-dimensional pyramidal structure (3). See text for details.

be used to separate them. However, high-performance liquid chromatography (HPLC) using a chiral column packing material has been used to resolve enantiomers on both an analytic and a preparative scale.

Configuration

The spatial arrangement of atoms in a chiral molecule that distinguishes it from its mirror image is known as the absolute configuration. Specific conventions are used to assign configuration. The convention established by Fischer for assigning the configuration of amino acids and carbohydrates is that the longest carbon chain is written vertically with the most oxidized end placed at the top of the chain (e.g., CHO in a carbohydrate). Figure 9-4 illustrates this assignment for carbohydrates and amino acids. If the OH group at the bottommost (highest numbered) chiral center is on the right-hand side, the molecule is given a (D) or dextro configuration, and if it is on the left-hand side, it is given an (L) or levo configuration. With amino acids, the (L) designation is used for amino acids whose α-amino group is on the left-hand side of the carbon chain, and the (D) designation is used if the α-amino group is on the right-hand side. This convention has been applied to other molecules that are closely related to amino acids and carbohydrates. It must be remembered, however, that the (D) and (L) configurational descriptors have nothing to do with the signs of optical rotation. For example, naturally occurring glucose has a (D) configuration and just happens to be dextrorotatory. Therefore, it is written as (D)-(+)-glucose. However, naturally occurring tartaric acid has an (L) configuration and happens to also be dextrorotatory. It is written as (L)-(+)-tartaric acid, as shown in Figure 9-3.

Molecules are three-dimensional, and Fischer developed a two-dimensional projection formula to help visualize the three-dimensional structure. This is illustrated in the bottom panel of Figure 9-4 for (D)-glyceraldehyde. By convention, the projection formula, shown as structure (2) in Figure 9-4, illustrates that the solid wedged groups bonded to the chiral

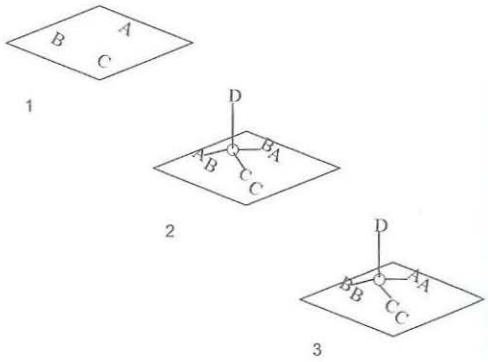

FIGURE 9-5 Stereochemical interaction of a drug molecule (D-ABC) and its receptor (ABC) demonstrating drug–receptor mismatch (2) and match (3).

carbon atom project out of the plane of paper and the dashed wedge groups project behind the plane of paper. The three-dimensional pyramidal structure of (D)-glyceraldehyde is shown for comparison.

Many biologic interactions rely on precise stereochemical matching between the three-dimensional structure of a receptor and its substrate. Thus, in many instances only one enantiomeric form of a drug will be biologically active because its configuration exactly complements the receptor configuration (Figure 9-5). Naturally occurring amino acids are of the (L) form, which is the configuration typically recognized by enzymes in biochemical reactions. This fact can have important consequences in the localization of radiopharmaceuticals in the body. For example, peptide radiopharmaceuticals that contain a naturally occurring (L)-form amino acid in their structure may exhibit poor localization properties because of rapid in vivo metabolism by native enzymes. Consequently, it is sometimes necessary to incorporate the (D)-form isomer of an amino acid in the peptide to retard metabolism. The somatostatin analogue Indium In 111 pentetreotide (OctreoScan, Mallinckrodt) is a prime example of this labeling approach. This radiopharmaceutical contains (D)-phenylalanine and (D)-tryptophan in its structure to inhibit metabolism by amino- and carboxy-peptidases.

A more universal system of configurational nomenclature is the Cahn-Ingold-Prelog (CIP) convention, which is based on the three-dimensional structures of molecules. According to this system, the configuration of a molecule is described as either (*R*) (from *rectus*, Latin for right) or (*S*) (from *sinister*, Latin for left). The assignment is made by considering a hierarchy of assigned values of various ligand groups bonded to a chiral carbon. Priority is given to groups with highest atomic number. The chiral center in a three-dimensional structure is viewed from the side opposite the lowest-ranked ligand. If, from this view, the arrangement of the three remaining ligands (in order of highest to lowest ranking) appears in a clockwise direction (right-handed), the configuration is (*R*) and if the arrangement of ligands is counterclockwise (left-handed), the configuration is (*S*). This is known as the sequence rule. The CIP descriptors for (D)-glucose are shown in Figure 9-6. The benefit of this system is that it permits a compound's structure to be drawn correctly by anyone who understands the sequence rule. As with (D) and (L) descriptors, (*R*) and (*S*) descriptors have nothing to do with signs of optical rotation. Thus, an (*R*)- or (*S*)-configured compound may be dextrorotatory or levorotatory.

In some instances, when an organic molecule contains several different functional groups it is desirable to describe the spatial configuration of one group relative to another group. *Syn* (synperiplanar) and *anti* (antiperiplanar) designations denote the relative configuration of any two stereogenic centers in a chain. A stereogenic center is a focus in a molecule whereby the interchange of two ligands attached to an atom leads to a stereoisomer. A stereogenic center may not be chiral, but all chiral centers are stereogenic. If

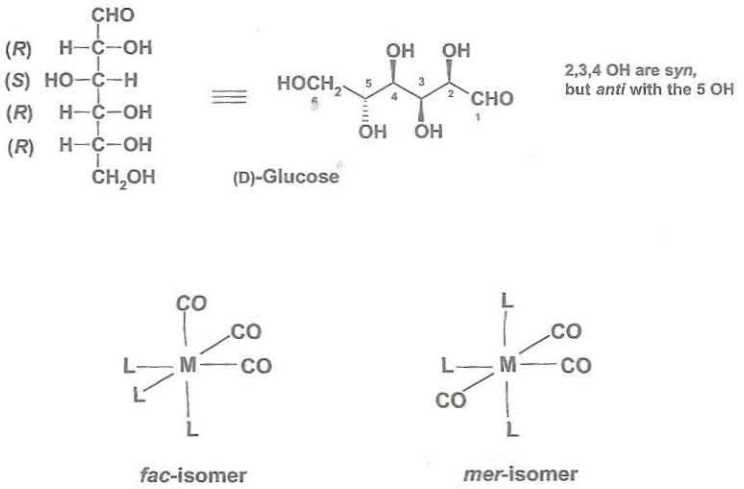

FIGURE 9-6 Upper panel, left, shows the (*R*) and (*S*) configuration for asymmetric carbon atoms in (D)-glucose. To its right is illustrated the zig-zag projection of (D)-glucose indicating the use of *syn* and *anti* descriptors for designating the spatial configuration of one group relative to another. Lower panel illustrates the facial (*fac*) and meridional (*mer*) isomers of an octahedral metal complex. See text for complete description.

ligands on the stereogenic centers are on opposite sides of the plane, the relative configuration is *anti*. If they are on the same side of the plane, they are *syn*. The *syn* and *anti* configurations for hydroxyl groups in (D)-glucose are shown in Figure 9-6. The *syn/anti* designation is used in technetium radiopharmaceuticals to describe the configuration of functional groups relative to the technetium oxo core. A good example is the *syn* and *anti* forms of ^{99m}Tc-CO_2-DADS.

Another type of isomerism found in octahedral complexes having three identical groups coordinated to a metal atom is meridional/facial isomerism. The meridional (*mer*) isomer has the three identical groups bound to the metal in the same plane, whereas the facial (*fac*) isomer has the three groups occupying the same face (Figure 9-6). An example of this type of isomerism in technetium chemistry is the technetium tricarbonyl compounds, which have three carbonyl groups coordinated in a facial configuration.

Solution Chemistry of Metal Ions

In general, metal ions are not soluble in aqueous solution unless the pH is quite low. For example, when stannous chloride is dissolved in hydrochloric acid, a hexacoordinate tin–chloro coordination complex is formed, which keeps the tin soluble:

$$SnCl_2 + 4Cl^- \rightarrow \left[SnCl_6\right]^{4-}$$

When the pH is raised to between 1.2 and 4.5, the insoluble hydrolysis product tetratin (II) hexahydroxide dichloride, $Sn_4(OH)_6Cl_2$, is formed. At pH higher than 5.5, an amorphous hydrous oxide, $Sn_5O_3(OH)_4$, is formed.[6] Formation of these insoluble hydroxide complexes can be prevented by the addition of a chelating agent to sequester the stannous ion as a metal chelate.

Radionuclide metals suffer a similar fate in aqueous solution. In fact, in the early years of radiopharmaceutical development, the hydrolysis reaction was deliberately used to

produce particulate diagnostic tracers. Some examples are the hydrolysis of ^{113m}In-chloride with sodium hydroxide or sodium phosphate to produce insoluble ^{113m}In-hydroxide or phosphate colloids for liver imaging.[7,8] Another example is the production of ^{113m}In-iron hydroxide macroaggregates for lung imaging by raising the pH of ^{113m}In-chloride with sodium hydroxide in the presence of ferric chloride.[8]

Chelation suppresses certain reactions of a metal ion without removing the metal from the system. Trace metal ion contamination of drug products may contribute to oxidative degradation of the drug molecule. EDTA and sodium citrate are often used in traditional nonradioactive pharmaceutical products to sequester these metal ions. An example is the use of EDTA in epinephrine injection to retard metal ion–induced oxidative catalysis of epinephrine to adrenochrome. An example in nuclear pharmacy is the chelation of aluminum ion by EDTA in ^{99m}Tc-sulfur colloid injection. The chelation effectively retards the potential reaction of any aluminum ion present in ^{99m}Tc generator eluates with phosphate buffers in the sulfur colloid kit, which could form insoluble aluminum phosphate that would coprecipitate the sulfur colloid particles. Another example is the chelation of tin (stannous and stannic ions) in ^{99m}Tc radiopharmaceutical kits to suppress unwanted hydrolysis of these metal ions during labeling reactions in neutral or alkaline solutions. Still another example, shown below, is the use of a transfer ligand (TL) that forms a weak intermediate complex of reduced technetium (Tc) while it is being coordinated with the radiopharmaceutical ligand (Rx) in the kit. This technique is used in the MAG3 kit, with tartrate functioning as the transfer ligand.

$$TcO_4^- + TL \xrightarrow{Sn^{2+}} Tc\text{-}TL \xrightarrow{Rx} Tc\text{-}Rx + TL$$

Many radiopharmaceuticals used in nuclear medicine are complexes of metals, for example, gallium, indium, yttrium, and copper radionuclides. Specific examples include ^{99m}Tc, ^{111}In, and ^{67}Ga coordination compounds of complexing agents such as citrate, DTPA, and oxine. Some complexation reactions proceed directly with the simple addition of the metal to the ligand. If the pH compromises a reactant, some adjustment in the formulation is made. For example, in the production of ^{111}In-labeled antibodies, ^{111}In-indium chloride is often mixed with sodium acetate buffer before addition to the antibody. This keeps indium soluble (as indium acetate) while it coordinates with the antibody. Inadequate labeling and antibody degradation occur if the acidic indium chloride is added directly to the antibody. Understanding the chemistry involved is important to radiolabeling success.

TECHNETIUM CHEMISTRY

Element 43, technetium, was discovered in 1937 by Perrier and Segrè[9] in a sample of molybdenum that had been irradiated by deuterons. The new element's name came from the Greek word *technetos*, meaning artificial, because technetium was the first element previously unknown on earth and made artificially.[10] There are 21 isotopes of technetium, ranging from ^{90}Tc to ^{110}Tc. ^{110}Tc has the shortest half-life (0.86 second) and ^{97}Tc the longest (2.6×10^6 years). All the isotopes are radioactive. In 1939, Seaborg and Segrè[11] observed that ^{98}Mo irradiated with slow neutrons gave rise to ^{99}Tc through decay of the metastable isomer, ^{99m}Tc.

The decay scheme for ^{99m}Tc is shown in Figure 9-7. The scheme indicates that its metastable state is 0.1427 MeV above the ground state of ^{99}Tc. This energy is released as gamma rays, conversion electrons, beta particles, characteristic x-rays, and Auger electrons. Three gamma photons (γ_1, γ_2, and γ_3), of 0.0022, 0.1405, and 0.1427 MeV, respectively,

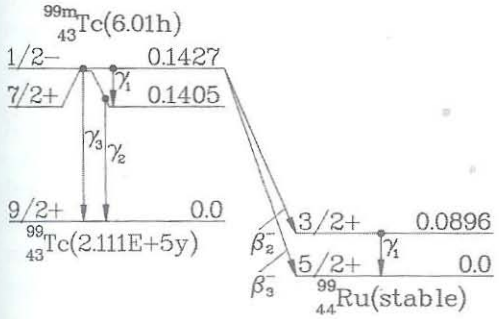

FIGURE 9-7 Decay scheme for ^{99m}Tc. (Reprinted with permission from reference 149.)

are released in the decay to ^{99}Tc, and an 0.0896 MeV gamma ray is emitted in one of the two β^- particle transitions to ^{99}Ru. The beta decay directly to ^{99}Ru is insignificant. The 0.0022 MeV photon is entirely converted to M- and N-shell electrons, and the 0.1427 MeV photon is converted to K-, L-, and M-shell electrons. The primary gamma photon of 0.1405 MeV is released in 89.1% of nuclear transitions of ^{99m}Tc.

In the 1950s, purification work on the ^{132}Te–^{132}I generator at Brookhaven National Laboratory turned up a contaminant that proved to be technetium. The technetium contaminant was the result of the decay of ^{99}Mo, which was also present because it had followed tellurium in the chemical separation process.[12] The discovery eventually led to the production of the ^{99}Mo–^{99m}Tc generator in 1957 at Brookhaven. Final improvements were made by Powell Richards.[12] The simplified decay scheme for ^{99m}Tc production is shown below. ^{99}Mo is now obtained as a fission byproduct of ^{235}U.

$$^{99}\text{Mo} \xrightarrow{86\%} {}^{99m}\text{Tc} \longrightarrow {}^{99}\text{Tc}$$
$$\ddots\ldots 14\% \ldots\ldots\ldots\ldots \triangleright \ddots$$

Technetium was introduced into clinical use at the University of Chicago by Harper et al.[13] The generator used yielded technetium as pertechnetate ion, $^{99m}TcO_4^-$. In mice, the activity was found to localize in the thyroid and salivary glands, stomach, and urinary bladder, similar to the iodide ion. These early studies identified the following advantages of ^{99m}Tc:

1. Short but reasonable half-life of 6 hours.
2. High photon yield (89%) of 140 keV gamma gives good tissue penetration but is easily collimated and stopped by the detector.
3. No beta radiation, resulting in low radiation dose.
4. Availability in a generator for in-hospital use.
5. Chemically reactive, yielding other chemical forms.

Although the 6 hour half-life was advantageous from an imaging standpoint, it created the necessity for daily radiopharmaceutical preparation, purification, and testing in the nuclear medicine laboratory. This led to the employment of radiochemists and radiopharmacists in nuclear medicine, and they subsequently developed new technetium-labeled radiopharmaceuticals, kits, and labeling methods.

Technetium Oxidation States

Technetium is positioned in the periodic table near manganese and rhenium, but its chemistry is more similar to that of rhenium. The electronic configuration of the neutral

technetium atom in the ground state is $1s^2 2s^2 2p^6 3s^2 3p^6 4s^2 4p^6 4d^6 5s^1$. As a transition metal in group VIIB, technetium has seven electrons beyond krypton's noble gas configuration and readily loses these electrons to yield the 7+ oxidation state of pertechnetate, TcO_4^-. Although this is the most stable state in aqueous solution, oxidation states from 1– to 7+ have been identified. For this reason technetium exhibits a diverse chemistry, allowing it to be incorporated into a variety of chemical forms to be used as radiopharmaceuticals.

As the pertechnetate anion, technetium does not bind effectively to other chemical species. Being an oxidizing agent, however, it can be reduced to a positively charged state that will complex with a variety of ligands. An exception to this is ^{99m}Tc-sulfur colloid, in which technetium is considered to maintain the 7+ oxidation state by virtue of its stability as insoluble technetium hepta-sulfide, Tc_2S_7.[14]

Reduced states of technetium can be achieved with suitable reducing agents. Some of the early agents used were ascorbic acid, ferrous iron, and hydrochloric acid, but these substances often led to incomplete reduction, requiring a purification step to remove unreacted pertechnetate. More powerful agents have also been used, including sodium borohydride ($NaBH_4$) and sodium dithionite ($Na_2S_2O_4$), which are useful in alkaline pH, and stannous chloride in acidic pH. The latter has been shown to be a powerful reducing agent capable of producing quantitative yields of technetium-labeled compounds, eliminating the need to remove free pertechnetate. Its use led to the introduction of "instant kits" for the preparation of ^{99m}Tc radiopharmaceuticals.[15] Other stannous salts, such as stannous fluoride and stannous tartrate, are also used in kit formulations.

The most common reducing agent used in ^{99m}Tc kits is stannous chloride dihydrate, $SnCl_2 \cdot 2H_2O$. Commercial sources typically are not pure and may contain 5% or more Sn(IV).[6] The standard reduction potential of the Sn(IV)–Sn(II) couple in hydrochloric acid is +0.15 volts relative to the standard hydrogen electrode at 25°C, but the presence of Sn(IV) in Sn(II) solutions will lower this to about 0.11 to 0.12 volts. It is important, therefore, to use as pure a product as possible in preparing kits. Dissolving high-purity tin wire in concentrated hydrochloric acid under nitrogen purge has been used to ensure high purity and concentrations of Sn(II). Stannous chloride is readily soluble in concentrated hydrochloric acid but will easily hydrolyze as the pH is raised toward neutrality unless a suitable complexing agent is present. Typically, very little Sn(II) is present as free ions in radiopharmaceutical solutions, most of it being complexed with ligand and some of it as colloidal tin aggregates.[6] As a powerful reducing agent, stannous chloride is readily oxidized in the presence of air and by dissolved oxygen in aqueous solution. Typically, a large excess of stannous chloride is present with respect to pertechnetate in radiopharmaceutical solutions, with the ratio of $SnCl_2$ to $^{99m}TcO_4^-$ being as high as 10^8 to 10^9.[14] Very little of the Sn(II) present will be oxidized by pertechnetate per se, and most of its reducing power is lost because of oxidation by oxygen and free radicals generated by radiolysis. Thus, except for a few special situations, it is important to exclude air from most technetium radiopharmaceuticals during and after preparation.

Since ^{99m}Tc is used in the nanomolar range in diagnostic radiopharmaceuticals, information about technetium's chemistry was gained mostly from studying its behavior in aqueous systems at millimolar concentrations, using its more stable isomer ^{99}Tc.[6] In general, while pertechnetate is quite soluble in aqueous solution, at lower oxidation states it may hydrolyze, forming insoluble reduced technetium. The best example of this is Tc(IV) as the hydrated dioxide ($TcO_2 \cdot xH_2O$). Typically, a complexing agent is necessary to keep technetium soluble and stable in the reduced state. Figure 9-8 illustrates several examples of complexing agents used in kits for preparing some of the earliest technetium radiopharmaceuticals in nuclear medicine. Most of them are still in use today.

The oxidation state of technetium and the stability of its compounds are controlled by several factors, such as pH, the Sn(II)/Sn(IV) concentration, and the type of complexing

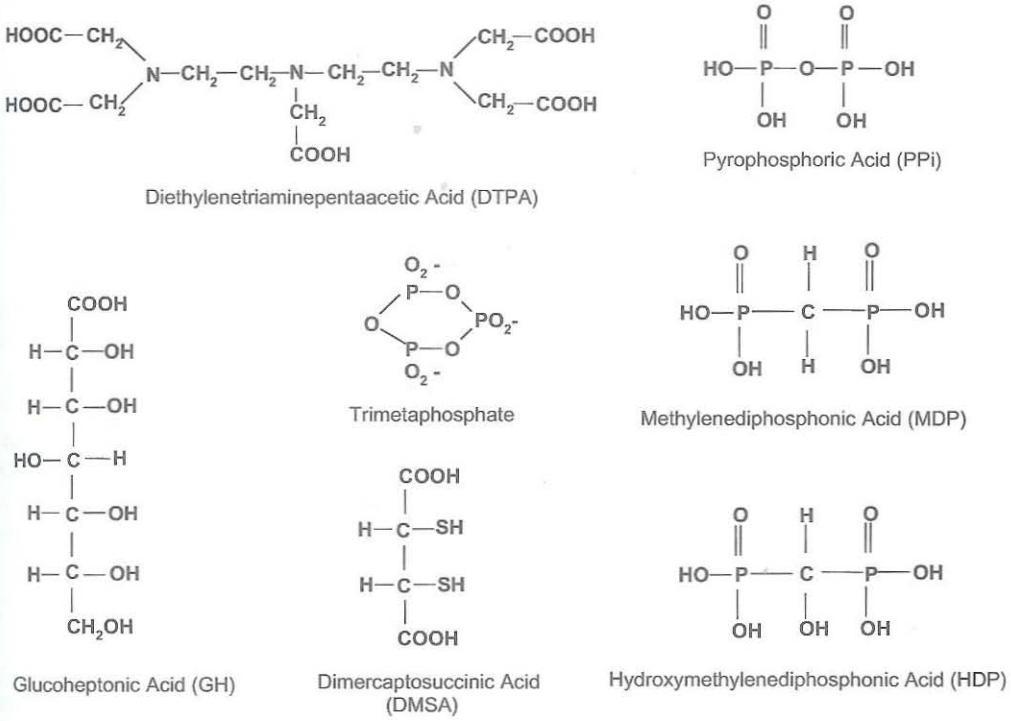

FIGURE 9-8 Chemical structures of several complexing agents (ligands) used in ^{99m}Tc kits.

agent present (ligand type). The most stable states in water are TcO_4(VII) and the insoluble TcO_2(IV).[6] Reduction/titration experiments have shown that some ligands can achieve complexes with technetium in more than one oxidation state depending on the number of electrons, n, acquired by pertechnetate; that is, when $n = 2$, 3, or 4, technetium is reduced to the (V), (IV), or (III) state, respectively. Ligands such as DTPA, pyrophosphate, and tripolyphosphate can form Tc(III) complexes initially, which then oxidize to Tc(IV).[6] Compounds in the (–I), (I), (II), and (III) oxidation states can readily oxidize to that of (IV) and finally to that of (VII). Oxidation states of (V) and (VI) frequently disproportionate to (IV) and (VII), as follows:

$$3\mathrm{Tc(VI)} \rightarrow \mathrm{Tc(IV)} + 2\mathrm{Tc(VII)}$$
$$3\mathrm{Tc(V)} \rightarrow 2\mathrm{Tc(IV)} + \mathrm{Tc(VII)}$$

For example, during the synthesis of a ^{99m}Tc radiopharmaceutical, initial reduction of pertechnetate ($^{99m}TcO_4^-$) leads rapidly to the formation of the Tc(VI) intermediate $^{99m}TcO_4^{2-}$, which is unstable and disproportionates to $^{99m}TcO_4^-$ and $^{99m}TcO_2$. Additionally, rapid reduction of pertechnetate to Tc(IV) can also produce the insoluble colloidal species TcO_2. These types of reactions may compromise labeling yields of the final radiopharmaceutical complex. The presence of a chelating agent can serve to stabilize intermediate oxidation states of technetium. Sometimes a weak, preformed technetium chelate is used as a technetium transfer agent in the reaction scheme for labeling biologic molecules to control the oxidation state of technetium.

Some complexes are quite stable to oxidation (e.g., DTPA, IDA analogues, gluceptate), while others are more labile (e.g., bone agents like hydroxymethylene diphosphonate

TABLE 9-7 Oxidation State of Technetium in Various Compounds

Oxidation State	Chemical Form
Tc(VII)	Pertechnetate, sulfur colloid
Tc(V)	DMSA (high pH), ECD, gluceptate, gluconate, HMPAO, MAG3, tetrofosmin
Tc(IV)	Citrate, DTPA, EHDP, HDP, MDP, PPi (PYP), $TcO_2 \cdot H_2O$
Tc(III)	DMSA (low pH), HIDA, furifosmin, teboroxime
Tc(I)	Sestamibi

Source: Reference 6

[HDP]) and may require an antioxidant in the formulation. The oxidation states of technetium in several useful compounds are listed in Table 9-7.[6] The table should be used with some caution. Electron transfer studies to identify the oxidation state of technetium in first-generation complexes, such as dimercaptosuccinic acid (DMSA), DTPA, and pyrophosphate (PPi or PYP), have not always been conclusive. On the other hand, technetium's oxidation state in many second-generation complexes (e.g., ECD, HMPAO, MAG3, sestamibi, tetrofosmin) has been well characterized. The oxidation states listed in Table 9-7 are considered to be the usual state present in technetium radiopharmaceuticals prepared from kits.

DEVELOPMENT OF TECHNETIUM COMPOUNDS

A principal goal in nuclear medicine has been the development of target-specific localizing radiopharmaceuticals. First-generation technetium agents achieved this goal mainly through the use of simple ^{99m}Tc-labeled species (complexes, particles, and cells) that could exploit normal physiologic processes in the body. Technetium was "tagged" to a variety of molecular species that delivered it to specific organs via a non–substrate-specific localization mechanism. In essence, technetium was a passenger atom not essential for localization. These agents were not well characterized chemically because their technetium concentration (approximately 10^{-8} to 10^{-9} M, e.g., 10 mCi ^{99m}Tc = 1.9 ng) was below that required for conventional chemical methods of analysis. In response to this deficiency, technetium radiopharmaceutical development in the mid-1970s used ^{99}Tc (as NH_4TcO_4) in preparing CA compounds in amounts that permitted structural characterization by conventional means such as infrared spectroscopy, mass spectroscopy, nuclear magnetic resonance spectroscopy, and x-ray crystallography. This also made it possible to demonstrate the equivalence of technetium complexes in CA (macroscopic) and NCA (tracer) quantities.[16–18] Over time, all the lower oxidation states of technetium were examined, and technetium oxidation state cores were identified. An important consideration in the design of technetium radiopharmaceuticals was the development of ligands that not only would stabilize technetium in its lower oxidation state but could be modified to influence site-specific localization in vivo.

The efforts made by chemists to characterize technetium's chemistry and to design new radiopharmaceuticals in the 1970s and 1980s led to some significant findings. Loberg and Fields,[17] in their quest to develop a technetium heart imaging agent, serendipitously discovered the ^{99m}Tc-IDA compounds for hepatobiliary imaging. Their elegant work in characterizing the structure of the dimethyl-substituted IDA analogue (^{99m}Tc-HIDA) led to two important contributions to the future development of technetium radiopharmaceuticals. The first was the finding that the technetium atom in the ^{99m}Tc-HIDA complex was essential for its uptake and excretion by the liver.[17,19] Without technetium, the IDA analogues exhibited renal excretion after intravenous injection. However, when technetium

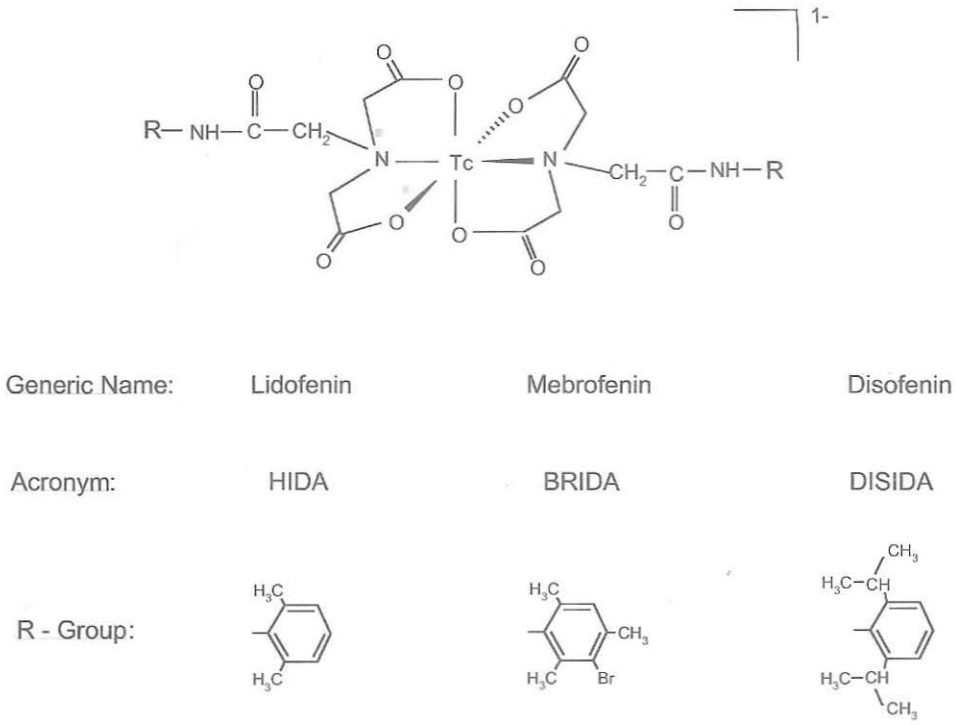

FIGURE 9-9 Chemical structure of iminodiacetic analogues.

was coordinated with two IDA molecules, the principal excretion pathway was hepatobiliary.[20] Figure 9-9 illustrates the chemical structures of several Tc-IDA analogues. The second important contribution from this work was the concept of bifunctional chelators, which are ligands that not only chelate technetium but can be modified with functional groups to control biodistribution of the final technetium complex. This concept was expanded in the 1990s to include the introduction of a reactive site on the bifunctional chelator, enabling binding of the technetium complex to another molecule for targeting purposes.

A number of other contributions were made in the 1970s and 1980s to the development of technetium compounds in use today. With the ability to structurally characterize technetium compounds, efforts were directed toward examining ligands that could stabilize technetium in lower oxidation states, previously thought to be unstable. Davison, Jones, and colleagues,[16] at the Massachusetts Institute of Technology, demonstrated that Tc(V) oxo complexes with bisdithiolate (S_4) and diamidedithiolate (N_2S_2) ligands could produce oxidation-stable square pyramidal complexes, with the oxygen atom at the apex and the sulfur and nitrogen atoms forming the basal plane and with the technetium atom displaced toward the apex. Work with these ligands laid the foundation for introducing ligand backbone substitutions with noncoordinating functional groups that could direct in vivo localization. This permitted the development of a new generation of technetium-labeled radiopharmaceuticals. Deutsch and co-workers,[18] at the University of Cincinnati, contributed significantly to an understanding of technetium's basic chemistry through their efforts to develop a technetium-labeled myocardial imaging agent. Their design and characterization of CA Tc(III) monocationic complexes with the diars, or *o*-phenylenebis(dimethylarsine), ligand, namely $[^{99m}Tc(diars)_2Cl_2]^+$ and $[^{99m}Tc(diars)_2Br_2]^+$, developed

further the concept of technetium-essential compounds designed around a technetium core. Many other investigators made significant contributions to the development of these second-generation technetium compounds that are used routinely in nuclear medicine. Important among these agents are complexes of Tc(I) (sestamibi) and Tc(V) (bicisate, exametazime, mertiatide, and tetrofosmin).[21–26] Through the development of these agents, a number of technetium (V) oxo cores were identified.[27,28] Extensive experience was gained regarding the chemistry of bifunctional chelating agents (BFCAs), many of which are now being developed further in the design of second-generation technetium-tagged compounds that localize by substrate-specific localization mechanisms.

As a result of this developmental history, technetium-labeled compounds are considered to be of two types: technetium-essential and technetium-tagged.[18] *Technetium-essential* compounds have technetium as a necessary core atom around which other components are arranged. Neither of the separated components (coordinating ligands or technetium) localizes the same way that the integrated molecule does. The ligands that coordinate with the core may be monodentate or multidentate and are designed to stabilize technetium in its oxidation state, providing desirable pharmacokinetic properties to the final complex. Technetium's coordination number may be satisfied by multiple monodentate ligands (such as the six individual isonitrile ligands in ^{99m}Tc-sestamibi), one or two multidentate BFCAs (such as those in ^{99m}Tc-bicisate and ^{99m}Tc-tetrofosmin, respectively), or a combination of a multidentate BFCA and individual monodentate ligands (such as that found in ^{99m}Tc-furifosmin). The functional groups on the ligands are chosen to confer certain properties to the final complex, such as lipophilicity, ionic charge, and molecular size. Such modifications alter the pharmacokinetic properties of the technetium complex to enhance its localization and excretion.[28] For example, the design of ^{99m}Tc-MAG3 involves not only careful selection of the coordinating ligand (N_3S), but also the strategic location of a carboxylate substituent in the peptide sequence to give it the necessary renal excretion properties that mimic OIH.[25] Another example is the rearrangement of two methyl groups on the propyleneamine oxime (PnAO) ligand in ^{99m}Tc-PnAO in order to increase its brain retention properties, producing the configuration found in ^{99m}Tc-HMPAO.[24]

Technetium-tagged compounds have technetium bound to a transporting moiety that delivers technetium to a specific site in the body determined by the properties of the transporter. First-generation technetium-tagged compounds have transporters that are relatively simple. They include complexing agents (e.g., DTPA), particles (e.g., sulfur colloid), blood cellular elements (e.g., leukocytes), and proteins (e.g., human serum albumin). Second-generation technetium-tagged compounds have transporters that are receptor-specific (targeting molecules), such as peptides and antibodies, and covalently linked to technetium via a BFCA. The design and labeling methods of these compounds are more sophisticated than those for first-generation technetium-tagged radiopharmaceuticals.

SECOND-GENERATION TECHNETIUM-TAGGED RADIOPHARMACEUTICALS

Two approaches have been used to design second-generation technetium-tagged radiopharmaceuticals: the integrated approach and the bifunctional chelate approach.[29–32]

The integrated approach incorporates technetium into a binding site built into the molecule; technetium thus becomes an integral part of the molecule, affecting its conformation and localization in vivo. This approach has been used to design radiotracers that mimic the three-dimensional configuration of biologically important steroids (testosterone, progesterone, and estradiol) with limited success, but it may prove more successful in the future.[29,32]

A more widely explored direction is the bifunctional chelate approach, in which the key component in the design of technetium-tagged radiopharmaceuticals is a BFCA. The extensive experience gained from the development of technetium-essential radiopharmaceuticals with BFCAs, particularly with the tripeptide MAG3, made the BFCA approach to peptide labeling a natural extension of that work. Furthermore, it instilled the idea of incorporating a technetium-binding amino acid sequence into an active peptide biomolecule. The peptide sequence allows the introduction of coordinating donor groups to facilitate the formation of a stable complex with a technetium oxo core.

Technetium-tagged compounds have the following general structure: targeting molecule–linker–BFCA–^{99m}Tc.[30] The targeting molecule is typically a peptide, antibody, or some other small molecule designed to target a specific receptor in vivo. The linker is usually a simple hydrocarbon chain of variable length; its inclusion modifies the pharmacokinetics or distances the technetium chelate region from the receptor-binding region of the molecule. The BFCA serves two main purposes: to coordinate the technetium and to provide a molecular backbone that can be modified with functional groups for attachment to the targeting molecule. Some examples of BFCAs are the N_2S_2 ligands diaminedithiol, diamidedithiol, and monoaminemonoamide dithiol; triamidethiol (N_3S); N_4 PnAO; and hydrazine nicotinamide (HYNIC).[30] The functional group on the BFCA is the conjugation site where it covalently attaches to the targeting molecule, either directly or through the linker molecule. With this design, the technetium chelate is often far removed from the receptor-binding motif to minimize possible interference with binding at the biologic receptor site. In most instances, technetium will act as a "passenger" to be transported to the receptor site. However, in some situations, such as with small peptides, the biodistribution and target uptake will be influenced by the metal chelate because the technetium atom may contribute greatly to the overall size and molecular weight of the radiopharmaceutical.[30] In such cases the technetium is not entirely passive, and such radiopharmaceuticals could also be considered as technetium-essential.

The principal targeting molecules employed as transporters in technetium-tagged radiopharmaceuticals are antibodies and peptides.[30] They differ primarily in molecular weight and structure. Antibodies are analogous to large and small proteins in size. Whole antibodies have molecular weights on the order of 150,000, and antibody fragments about 50,000 to 100,000. By contrast, peptides usually contain less than 100 amino acids and have molecular weights of about 10,000 or less. Peptides consisting of less than 30 amino acids or having a molecular weight less than 3500 are considered small peptides. In general, whole antibodies have slow blood clearance and only modest target-to-background ratios. Although they exhibit high receptor-binding affinity and specificity, their effectiveness is limited. This has been attributed to their lack of access to tumor cells in solid masses and to the heterogeneous distribution of tumor-associated antigens on the tumor surface. By contrast, the affinities of many peptides for their receptors are significantly greater than those of antibodies or their fragments. Also, they can tolerate harsher chemical conditions for modification or radiolabeling. Peptides are relatively easy to synthesize, exhibit rapid blood clearance, and are less likely to be immunogenic. In most cases, the receptors for peptides are readily accessible on the external surface of cell membranes. One disadvantage of peptides is that they are prone to enzymatic degradation by plasma proteases and peptidases and therefore must be modified to protect against degradation. In some cases this can be accomplished by use of a D-amino acid in place of the L-form (e.g., D-tryptophan in OctreoScan [Mallinckrodt] and NeoTect [Diatide]) and use of alternative amino acids. Another confounding problem is the potential loss of receptor-binding affinity when the peptide is conjugated to the BFCA and labeled with a radionuclide. Small peptides with only four to six amino acid residues are particularly vulnerable in this regard.

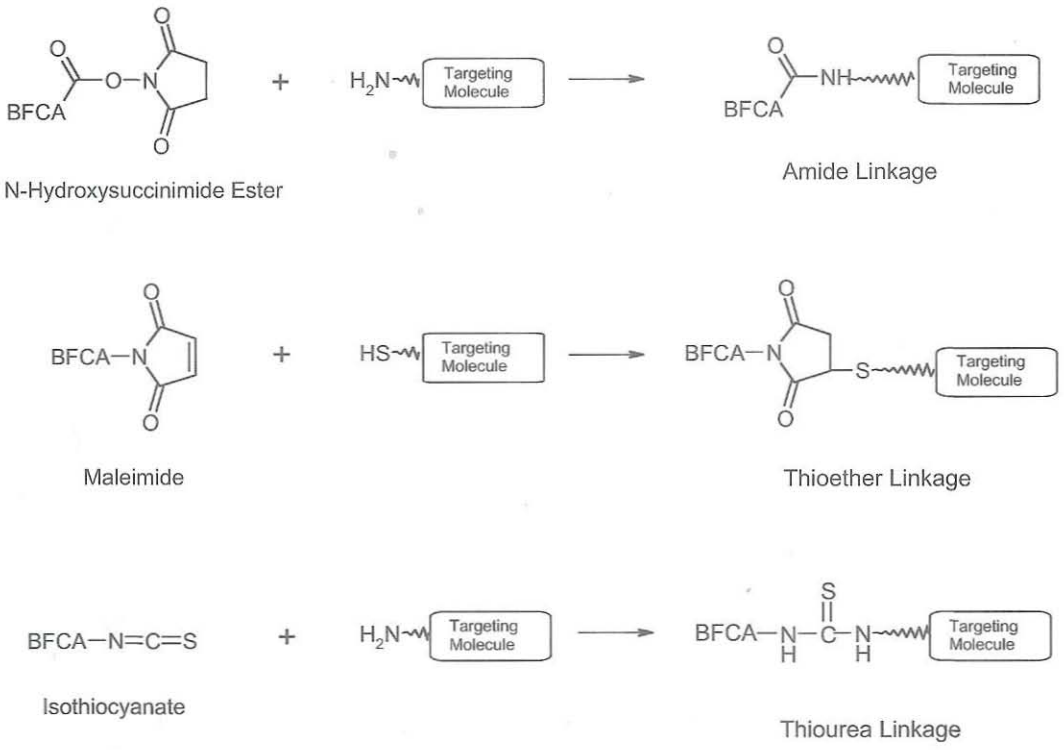

FIGURE 9-10 Typical methods of conjugating bifunctional chelating agents (BFCAs) with targeting molecules.

LABELING APPROACHES

Conjugation of the peptide, protein, or antibody targeting molecule (TM) with the BFCA occurs through a reaction between a primary amino group on the TM and an activated ester group or an isothiocyanate group attached to the BFCA, or between a sulfhydryl group on the TM and a maleimide group on the BFCA (Figure 9-10).[30] Conjugation can occur either after coordination with technetium (prelabeling approach) or before coordination with technetium (postlabeling approach) (Figure 9-11).

The prelabeling approach involves technetium chelation with the BFCA, activation of the BFCA, and conjugation with the TM. In this approach, the technetium chelate is formed before conjugation with the TM. The advantage of the prelabeling approach is that the TM is not subjected to the sometimes harsh labeling conditions (e.g., low pH, high temperature) necessary for coordination of technetium with the BFCA. The disadvantage of this approach is that it is not particularly amenable to simple kit formulation. The postlabeling approach involves activation of the BFCA, conjugation with the TM, and chelation with technetium. An advantage is that this approach permits a carefully worked out chemistry for conjugation of the TM with the BFCA. Also, this approach has particular appeal for kit formulation if the chelation reaction conditions with technetium are not detrimental to the TM. Radiolabeling can be accomplished with either approach by direct reduction of pertechnetate in the presence of the BFCA-TM complex or via ligand exchange with an intermediate technetium complex such as Tc-glucoheptonate. The postlabeling approach is used with the preparation of ^{99m}Tc-apcitide and ^{99m}Tc-depreotide.

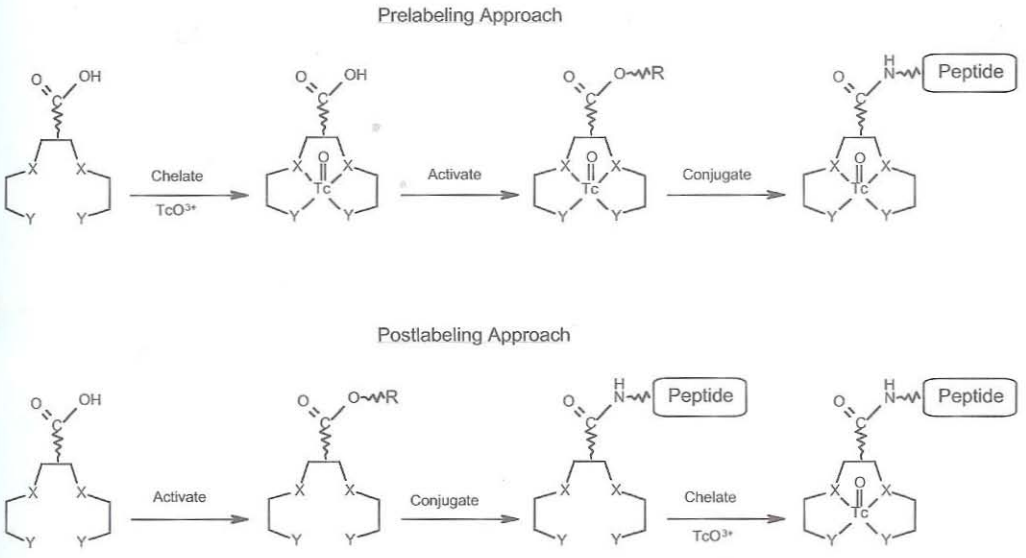

FIGURE 9-11 Prelabeling and postlabeling approaches for coordinating technetium to a targeting molecule (peptide). See text for details.

Technetium-Labeled Peptides

Synthetic peptide ligands have been designed to complex with the $Tc{=}O^{3+}$ core. Two useful technetium-labeled biochemical markers in this group are ^{99m}Tc-apcitide, a platelet receptor-binding peptide for imaging acute venous thrombosis, and ^{99m}Tc-depreotide, a somatostatin receptor marker for imaging malignant lung tumors.[33,34]

^{99m}Tc-apcitide was designed to mimic the peptide sequence -Arg-Gly-Asp (RGD), which recognizes and binds to glycoprotein (GP) IIb/IIIa receptors on activated platelets. Apcitide contains the mimetic sequence -Apc-Gly-Asp (-ApcGD). The synthetic amino acid Apc (S-aminopropyl-L-cysteine) is an arginine surrogate that not only replaces arginine in the receptor-binding sequence but also confers additional selectivity on the molecule.[34] The chemical structures of apcitide and ^{99m}Tc-apcitide have been characterized as shown in Figure 9-12.[33] Apcitide contains a receptor-binding region consisting of the peptide (-Apc-Gly-Asp-) and the technetium-binding region consisting of the peptide (-Gly-Gly-Cys-NH_2-). The apcitide kit for labeling with technetium is formulated with the bibapcitide dimer (Figure 9-13), which is split during labeling to release two apcitide molecules for complexation with technetium.

Depreotide is a 10 amino acid, bifunctional synthetic peptide consisting of a somatostatin receptor-binding region (-tyrosine-D-tryptophan-lysine-valine-) and a tripeptide domain (-β-diaminopropionyl-lysine-cysteine-), which forms an N_3S monoaminediamidethiol chelating unit to complex with ^{99m}Tc (Figure 9-14).[33] During labeling a pair of isomers is formed. Both the *syn* and *anti* isomer bind with high affinity to the somatostatin receptors in vivo.[33] The complex is neutral because the three negative charges formed during coordination (two on nitrogen, one on sulfur) balance the three positive charges on the $Tc{=}O^{3+}$ core.

A significant amount of work is being devoted to developing peptide-based radiopharmaceuticals using BFCAs. Exciting new agents have already been developed and approved for routine use, and many are in the pipeline of investigation. Excellent, comprehensive reviews of the chemistry involved have been presented.[28–34]

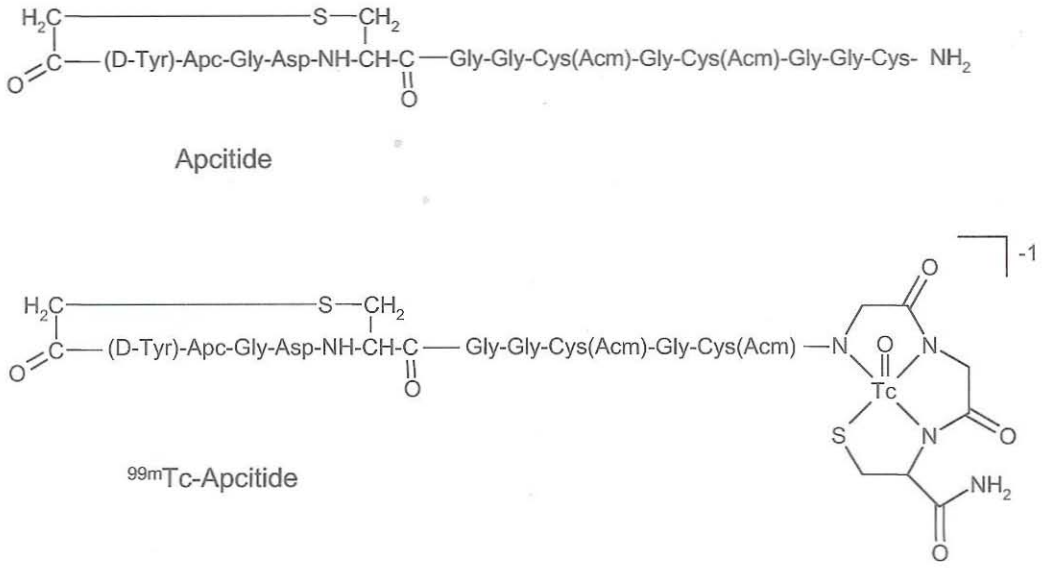

FIGURE 9-12 Chemical structures of the apcitide ligand and ^{99m}Tc-apcitide.

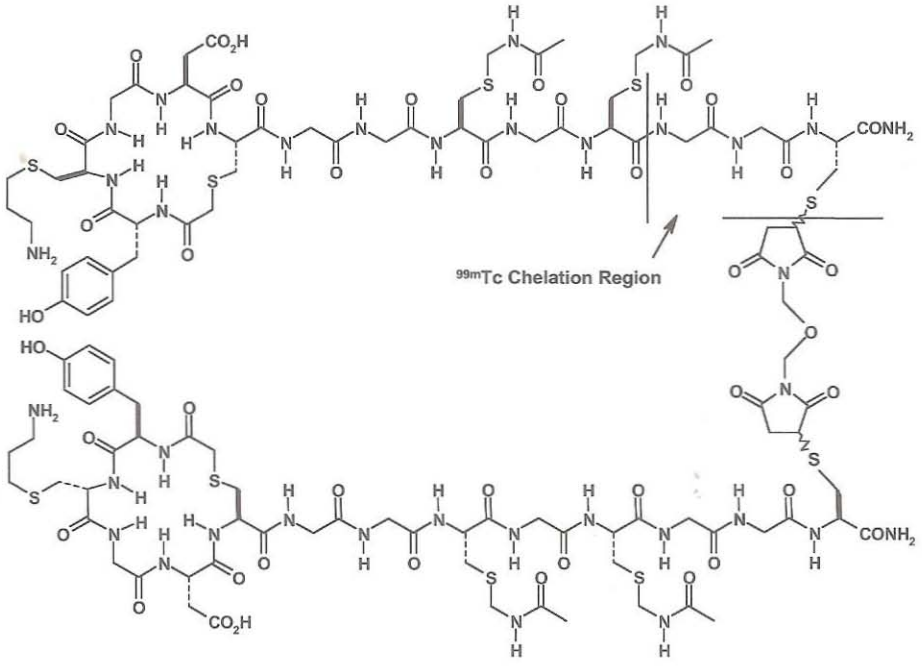

FIGURE 9-13 Chemical structure of the bibapcitide dimer molecule from which the apcitide ligand is derived in the ^{99m}Tc-apcitide kit.

Technetium-Labeled Antibodies

Several approaches have been used to label technetium to antibodies. A direct method relies on the reduction of disulfide bridges within the antibody to generate endogenous sulfhydryl groups (Figure 9-15). Using this approach, Rhodes et al.[35] incubated $F(ab')_2$

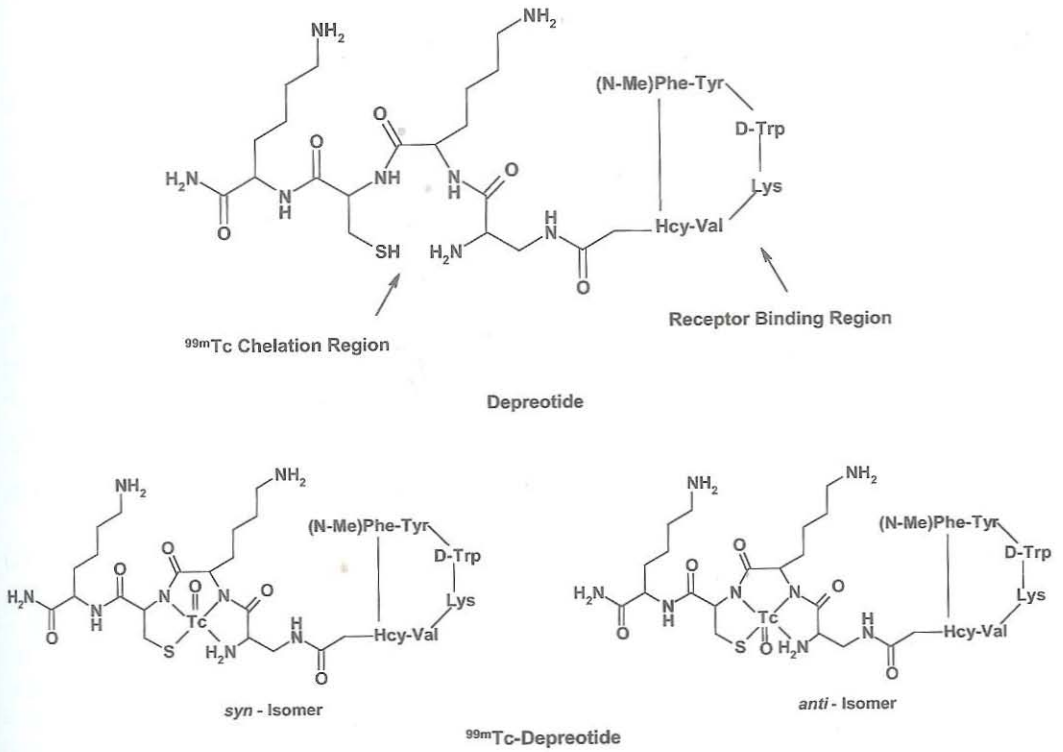

FIGURE 9-14 Chemical structures of the depreotide ligand and the *syn* and *anti* isomers of ^{99m}Tc-depreotide.

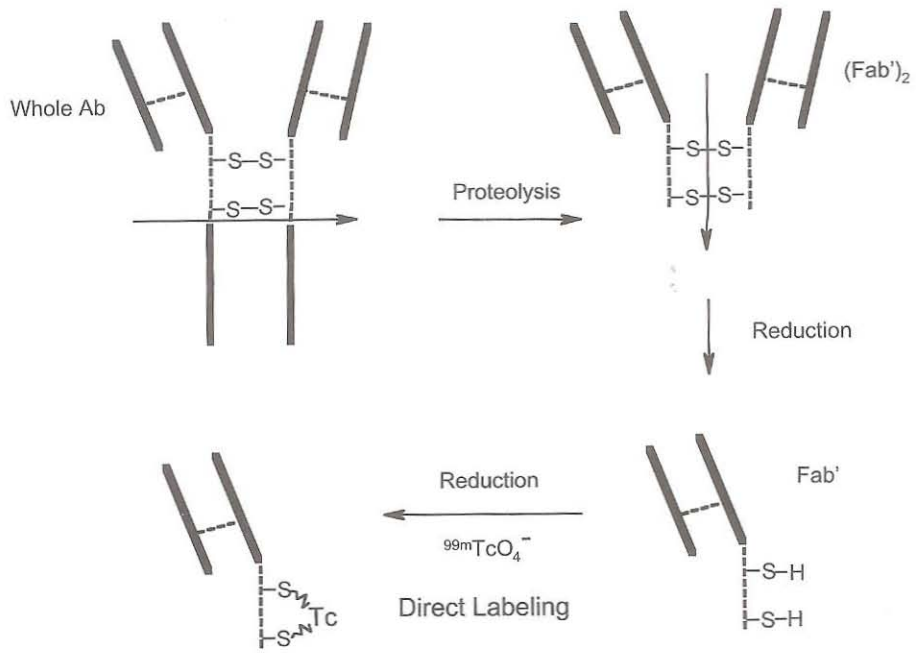

FIGURE 9-15 Generation of antibody fragments, reduction of their disulfide bonds, and direct labeling of fragments with technetium.

antibody fragments with a reducing agent (e.g., stannous tartrate/phthalate mix) and labeled them with ^{99m}Tc-sodium pertechnetate. Technetium's binding affinity with the antibody was found to be both strong and weak, with the strong-affinity bond being a function of exposure time of antibody to stannous ion. A disadvantage of this method is indiscriminate labeling of the antibody; technetium labels both low-affinity sites and high-affinity sites. Additionally, the $F(ab')_2$ antibody fragments split to release the monomeric Fab' fragments. Labeling efficiency can be high (approaching 90%), but immunoreactivity is low (approximately 55%).[35] Schwarz[36] used 2-mercaptoethanol to reduce disulfide bonds and used a novel approach by labeling whole antibody via ligand exchange after adding technetium-labeled bone agents to the antibody. Thakur et al.[37] compared several reducing agents (stannous ion, ascorbic acid, 2-mercaptoethanol, dithiothreitol, and dithioerythritol) to reduce disulfide bonds and found that ascorbic acid produced the highest labeling efficiency (>95%) after addition of dithionite-reduced pertechnetate to the reduced antibody. Immunoreactivity was around 82%. It appears from these studies that the labeling mechanism involves technetium binding to thiol (SH) ligands in the reduced antibody.[37,38] Because $F(ab')_2$ fragments tend to be cleaved during disulfide reduction, Fab' fragments appear to be more suitable to labeling with technetium.

An indirect method of labeling antibodies involves conjugation of a BFCA (e.g., DTPA) to the antibody first and then the addition of reduced technetium to the conjugate, whereupon the technetium is complexed to the antibody through the BFCA.[38] This is the postlabeling approach. In the bifunctional chelate approach, there is competition for technetium between weak- and strong-affinity direct binding to antibody and binding via the covalently bound chelating agent; therefore, this approach does not achieve high radiochemical purity.[38] Additionally, in a comparison of direct- and indirect-labeled antibody, it was shown that a ^{99m}Tc-DTPA conjugated antibody was cleared more slowly from the blood than a direct-labeled Tc-antibody, but that the ^{99m}Tc-DTPA conjugated antibody cleared faster than the ^{111}In-DTPA conjugated antibody.[39] Thus, the ^{99m}Tc-DTPA conjugate appears to provide a more stable bond with the antibody than does the direct-labeled antibody. However, the data suggest that a higher level of protein degradation occurs in the ^{99m}Tc-DTPA conjugate than in the ^{111}In-DTPA conjugate.[39]

Another indirect technique is to modify the antibody with a HYNIC group and label it by ligand exchange with ^{99m}Tc-glucoheptonate.[40] With this postlabeling approach, a ^{99m}Tc-labeled immunoglobulin G (IgG) polyclonal antibody showed similar biodistribution parameters in rats compared with ^{111}In-labeled IgG. When this same method was compared with a direct-labeling method for preparing ^{99m}Tc-IgG, greater instability and faster blood clearance were observed with the direct-labeled antibody.[41]

The results of multiple studies show that antibodies can be labeled with technetium successfully by both direct and indirect methods, but there are differences in the properties of antibodies produced. These differences may depend in part on the type of antibody labeled. A fair amount of evidence, however, suggests that direct labeling of antibodies is less satisfactory than indirect labeling that employs a BFCA attached to the antibody.

A third approach to labeling antibodies with technetium is to use a prelabeled ligand (prelabeling approach). In this method (Figure 9-16), dithionite-reduced technetium is complexed to an N_2S_2 ligand functionalized with a carboxylate group, which is then activated with an ester group through which it is bound efficiently to the antibody via acylation with lysine amine residues.[42] This labeling approach offers the advantage of obviating the nonspecific binding of technetium to the antibody found with direct labeling or postlabeling approaches. While this method produces a stable antibody label without nonspecific binding, the method of preparation is somewhat cumbersome and less adaptable to simple kit formulation.

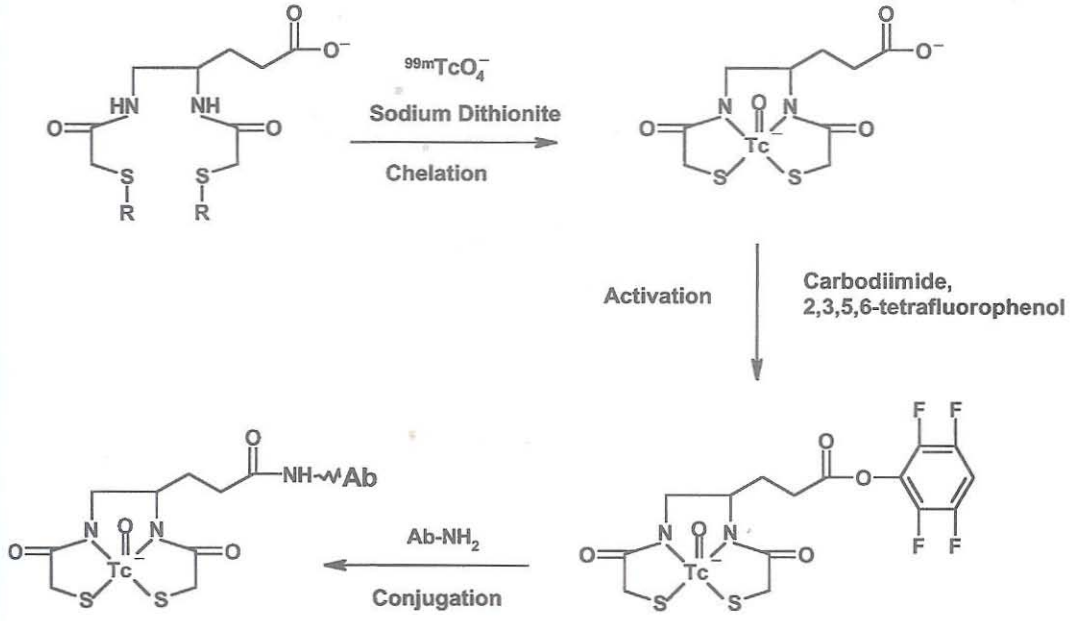

FIGURE 9-16 Method of labeling antibodies with technetium using the prelabeling approach (i.e., technetium chelation, activation, and conjugation to antibody).

A few new technetium-labeled antibodies have been developed. One of these, presently in clinical trials, is ^{99m}Tc-sulesomab (LeukoScan, Immunomedics, Morris Plains, NJ), which is designed to label white blood cells in vivo. It is a Fab' antigranulocyte monoclonal antibody fragment that is indicated for localizing infection in bone in patients with suspected osteomyelitis. Another agent is a technetium-labeled anti-CD15 immunoglobulin M monoclonal antibody (LeuTech, Palatin Technologies, Princeton, NJ), which is another infection-imaging agent. Technetium-labeled antibodies are covered in more detail in Chapter 21.

TECHNETIUM COMPOUNDS OF SPECIFIC OXIDATION STATES AND CORES

The advancement of technetium chemistry in the development of technetium-labeled radiopharmaceuticals has utilized several technetium oxidation states and technetium cores around which compounds are built.[28] Some of these cores and their associated ligands are shown in Figure 9-17.[32]

Tc(I) Compounds

Reduction of Tc(VII), as pertechnetate, to the Tc(I) oxidation state creates a technetium atom with six additional electrons (d^6 configuration) that must be stabilized by ligands that are electron deficient. Some of the coordinating groups that will stabilize Tc(I) are the phosphines (P), diphosphines (P-P), and isonitriles (CNR) because of their pi-electron acceptor properties.[28] The cores most frequently explored with Tc(I) are the Tc^+ core and the $Tc(CO)_3^+$ tricarbonyl core.

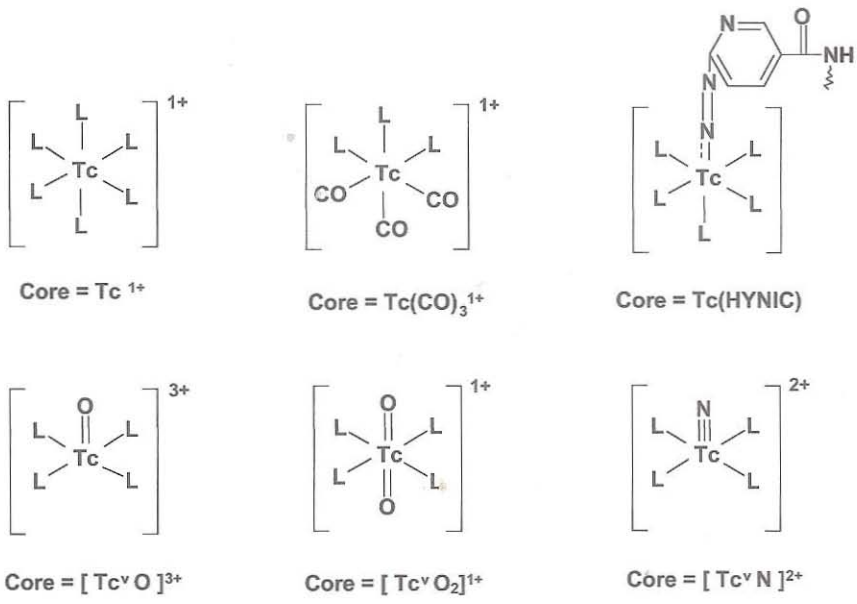

FIGURE 9-17 Technetium cores and the general structures of technetium complexes with ligands. L = a neutral, two-electron donor ligand.

Tc^+ Core

Tc(I) complexes are very stable when six coordination sites are occupied. This is readily accomplished under standard NCA labeling conditions because the excess ligand available in kits forces complete coordination around the metal to maintain reducing conditions. The ligand in Tc(I) complexes can be functionalized with different substituent groups to alter biologic properties, such as lipophilicity, without affecting the stability of the complex. A prime example of a radiopharmaceutical with this core is ^{99m}Tc-sestamibi, a lipophilic heart imaging agent, in which the Tc(I) atom is coordinated by six monodentate 2-methoxy-isobutylisonitrile (MIBI) ligands (Figure 9-18). Since the MIBI ligands are neutral, the sestamibi complex retains the single positive charge of the Tc^+ core.

$Tc(CO)_3^+$ Core

A variety of technetium (and rhenium) complexes can be made starting with the tricarbonyl core. This core can produce complexes that are especially stable because of the low-spin d^6 configuration of Tc(I). They can be reacted with BFCAs possessing residual functional groups that allow them to be coupled with receptor-avid molecules for the preparation of diagnostic agents labeled with technetium and therapeutic agents labeled with $^{186/188}$Re.

Radiopharmaceuticals with the $Tc(CO)_3^+$ core form stable octahedral organometallic complexes of two subtypes: (1) *fac*-$Tc(CO)_3^+$, in which Tc^+ can accommodate a variety of ligands besides the three carbonyls, to complete the octahedral sphere, and (2) $CpTc(CO)_3^+$, in which, in addition to the three carbonyls, Tc^+ is coordinated to a functionalized cyclopentadiene ligand that can attach the complex to a targeting molecule.[29] A novel synthon of *fac*-$Tc(CO)_3^+$ is the water- and air-stable organometallic aqua complex $[Tc(H_2O)_3(CO)_3]^+$. (A synthon is a molecular unit designed to facilitate the synthesis of a desired complex.) The $[Tc(H_2O)_3(CO)_3]^+$ complex can be produced directly from pertechnetate by reduction with sodium borohydride in saline at pH 11 under 1 atm of CO at 75°C.[43] The complex is

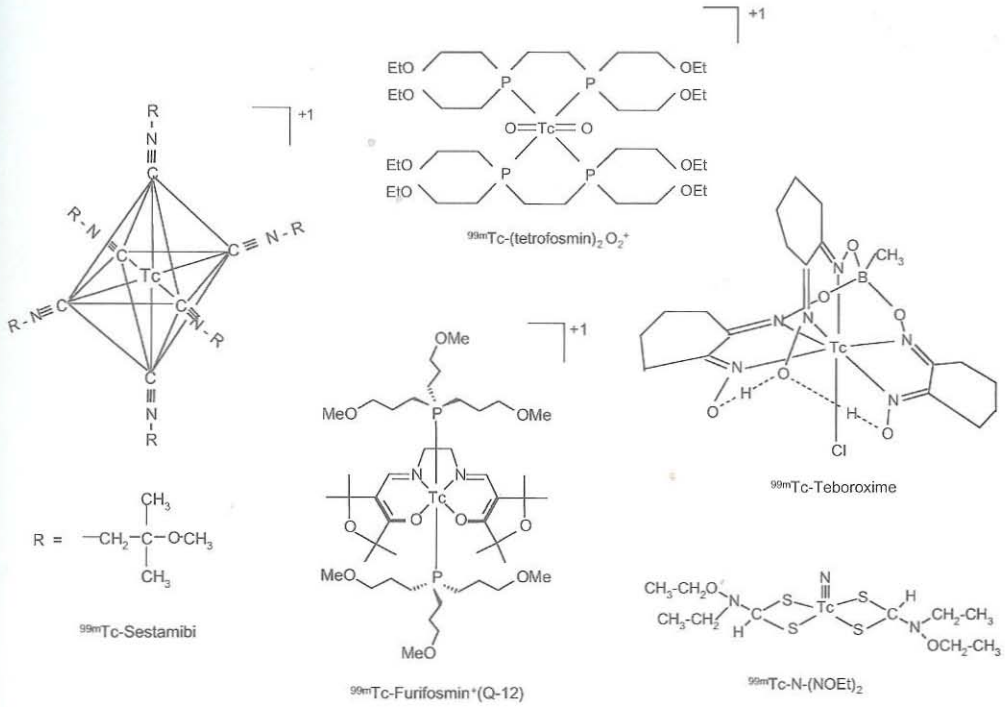

FIGURE 9-18 Chemical structures of various technetium coordination compounds for cardiac imaging. See text for details.

stable from pH 1 to pH 13. The labile water ligands can be readily substituted with donor ligands provided by a BFCA that can be derivatized to attach to an appropriate targeting biomolecule. The synthon $[Tc\text{-}Cl(H_2O)_2(CO)_3]$ has been used to prepare a neutral lipophilic complex, TROTEC-1 (Figure 9-19), in which two water ligands are displaced by sulfur in a dithioether-derivatized tropane analogue. The complex is neutral because of the chloride. TROTEC-1 has been shown to target the dopamine transporter (DAT) in the brain.[44]

The $CpTc(CO)_3^+$ core is interesting because it is highly stable, lipophilic, and can be readily derivatized for conjugation to bioactive molecules. This core has been used to prepare diagnostic technetium or therapeutic rhenium compounds. The method was originally designed to accomplish the reduction, carbonylation, and cyclopentadienylation of pertechnetate in a relatively mild, one-pot reaction termed a double ligand transfer reaction because two ligands (Cp and CO) are transferred together from two different metals (Fe and Mn) to a third metal, Tc.[45] Following the BFCA prelabeling approach, this method has been used to produce a methyl ester-derived Cp preformed chelate. The methyl ester group is subsequently saponified to carboxylic acid and derivatized with an appropriate active ester, leaving a group that readily undergoes acylation with lysine amino groups on proteins and peptides.[46] This method was applied to produce a $Cp^{99m}Tc(CO)_3$-octreotide conjugate (Figure 9-19) that demonstrated receptor-mediated uptake in the adrenal glands and pancreas.[47]

Tc(V) Compounds

Somewhat opposite the Tc(I) oxidation state in terms of electron configuration is Tc(V), which is only two electrons reduced from Tc(VII) in pertechnetate. As such, Tc(V) has a

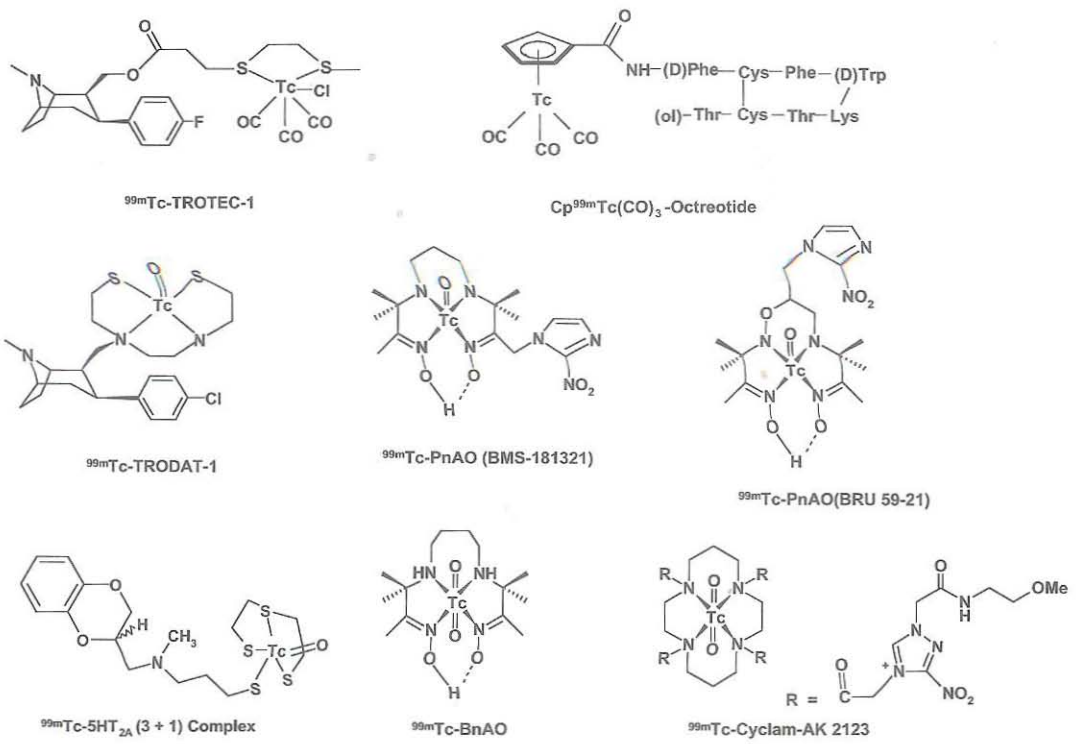

FIGURE 9-19 Chemical structures of various novel technetium coordination compounds. See text for details.

high electron deficiency (5–) and requires good electron-donating ligands to confer stability in its complexes.[28] Tc(V) complexes often have technetium oxo cores, such as $Tc{=}O^{3+}$ and $O{=}Tc{=}O^{+}$ (Figure 9-17).

$Tc{=}O^{3+}$ Core

Many technetium compounds have been designed using this core. In radiopharmaceuticals that contain this core, technetium is five-coordinate and forms square pyramidal complexes with various ligands. Ligands that have produced stable in vivo complexes with the $Tc{=}O^{3+}$ core are PnAO and its hexamethyl-functionalized derivative HMPAO, the diaminedithiol N_2S_2 ligand (N,N'-1,2-ethenediylbis-L-cysteine diethylester, otherwise known as ethylcysteinate dimer [ECD]) found in ^{99m}Tc-bicisate, and the triamidethiol (N_3S) ligand (N-[mercaptoacetyl]glycylglycylglycine) found in ^{99m}Tc-mertiatide (^{99m}Tc-MAG3). The N_2S_2 and N_3S ligands form very stable technetium complexes and can be fitted with functional groups to alter biodistribution. The PnAO ligand is more difficult to functionalize and only the lipophilicity of the complex has been varied.[28]

^{99m}Tc-PnAO was developed as a potential brain imaging agent. It proved to be stable in aqueous solution and is neutral and lipophilic.[48] The technetium-labeled complex ends up neutral because when the nitrogen groups coordinate with technetium, the two amine nitrogens and one oxime nitrogen ionize by loss of hydrogen ions. An intermolecular hydrogen bond forms with the oxygens, and the three negative charges on the nitrogens cancel the three positive charges on the technetium-oxo group (Figure 9-20). An advantage of the PnAO type of BFCA is that radiolabeling can be performed at ambient temperature. Disadvantages are low specific activity for labeling biomolecules, solution instability, and

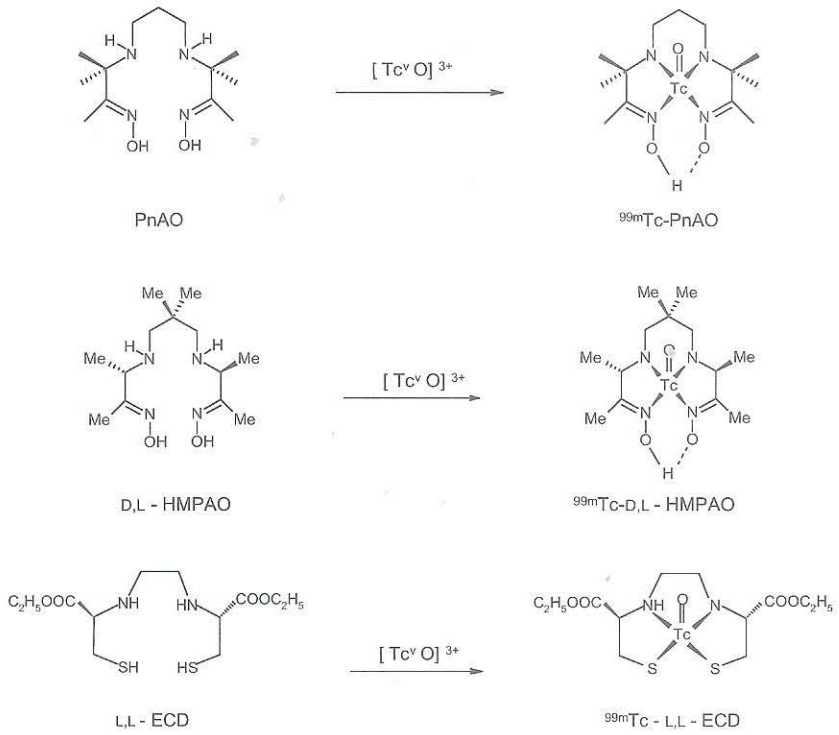

FIGURE 9-20 Chemical structures of brain imaging ligands and their technetium coordination compounds: ^{99m}Tc-PnAO, ^{99m}Tc-HMPAO, ^{99m}Tc-ECD.

extremely high lipophilicity.[30] The PnAO ligand has been used to develop several radiopharmaceuticals, some of which are discussed below.

Some interesting findings related to stereoreactivity surfaced in the development of the Tc(V) complexes. While the ^{99m}Tc-PnAO complex demonstrated rapid brain uptake after intravenous administration, its rapid washout precluded its use for SPECT imaging.[48] Consequently, several derivatives of PnAO were synthesized with methyl groups on the amineoxime backbone, in the hope of finding an agent that remained fixed in the brain. One of these was HMPAO, which exists in two diastereomeric forms, D,L- and *meso*- (Figure 9-21).[49] Because HMPAO has two chiral carbons it can form up to four stereoisomers; however, only three forms exist since the *meso*-isomers are identical and the D,L- isomers are enantiomers. The commercial kit contains the D,L-racemate. In the technetium-labeled complexes, each enantiomer has one of the methyl groups *syn* and the other methyl group *anti* to the Tc=O core. Studies with this complex have demonstrated that it is neutral and lipophilic but unstable in aqueous solution. The instability was found to be a conversion from the primary lipophilic complex to a secondary hydrophilic complex and was mediated by reducing agents.[50,51] Studies in animals and humans demonstrated that the *meso* form had greater in vitro stability but little brain retention, while the D,L form had poor in vitro stability but high brain retention. It was then surmised that brain uptake was caused by the lipophilic complex and brain retention was due to its intracellular conversion to the nondiffusible hydrophilic complex. The brain conversion was shown to be caused by the intracellular reducing agent glutathione, with much faster conversion of the D,L form than the *meso* form.[50] The slow conversion of the *meso* form was believed responsible for its low brain retention, which necessitated its separation from the D,L form prior to labeling with technetium. In other studies, Neirinckx et al.[49] demonstrated that the

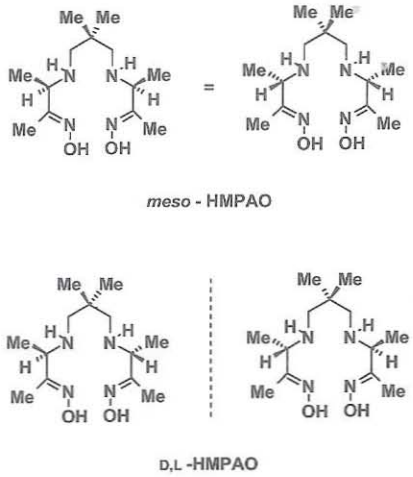

FIGURE 9-21 Chemical structures of the D,L-HMPAO enantiomers and their *meso* diastereomer.

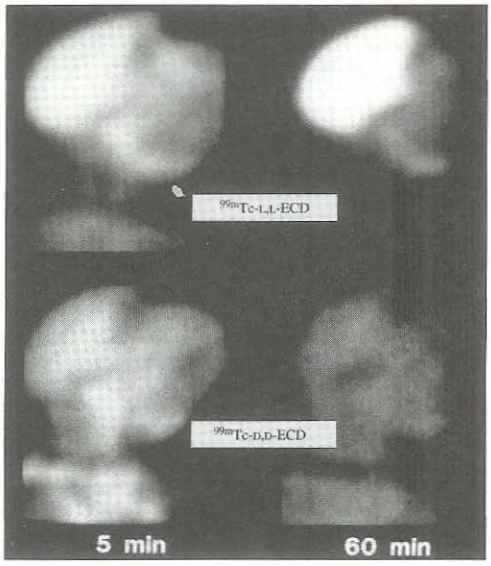

FIGURE 9-22 One-minute lateral planar images of an anesthetized monkey at 5 and 60 minutes after injection of 20 mCi (740 MBq) of ^{99m}Tc-L,L- or D,D-ECD to the same monkey on two different days. Brain retention is observed only with the L,L-complex. (Reprinted with permission from reference 53.)

^{14}C-labeled HMPAO D,L isomer without technetium did not cross the blood–brain barrier, contrary to the identical compound labeled with technetium. Thus, the technetium complex with D,L-HMPAO is considered to be a technetium-essential radiopharmaceutical (Figure 9-20).

The instability of the lipophilic ^{99m}Tc-HMPAO complex in vitro, mediated by a reducing agent, necessitated the use of small amounts of stannous ion in the kit formulation. This instability limited the useful life of the reconstituted kit to 30 minutes. The kit was eventually modified by incorporating a stabilizing buffer and radical scavenger (methylene blue) that extended the useful life of the labeled complex to 4 hours.

Two N_2S_2 ligands, diaminedithiol and diamidedithiol, produce very stable complexes with the $Tc{=}O^{3+}$ core.[52] The diaminedithiol ligand ECD loses three of four ionizable hydrogens (1 N and 2 S) upon complexation with $Tc{=}O^{3+}$ to yield the neutral complex ^{99m}Tc-bicisate, which is lipophilic and stable in aqueous solution (Figure 9-20). The ECD ligand exists as the L,L and D,D isomers; both isomers demonstrate brain uptake but only the L,L isomer exhibits brain retention (Figure 9-22).[53] Brain retention is not only stereospecific but also species specific; ^{99m}Tc-ECD localizes only in the brains of primates (monkeys and humans). While the carbon backbone of the ligand system is quite stable, substitution on this backbone with two ester functionalities makes it labile to enzymatic hydrolysis. The slow hydrolysis in blood and rapid hydrolysis in brain tissue results in high brain uptake and retention of the more hydrophilic metabolite.

The development of ^{99m}Tc-mertiatide (^{99m}Tc-MAG3), as a ^{99m}Tc replacement for ^{131}I-orthoiodohippurate (^{131}I-OIH), followed a long and patient course. The creation of ^{99m}Tc-MAG3 grew out of seminal investigations in which the N_2S_2 diamidedithiol ligand N,N'-bis(mercaptoacetyl)ethylenediamine (DADS) was characterized and identified as a potentially viable backbone for technetium radiopharmaceuticals.[54] The initial technetium complex,

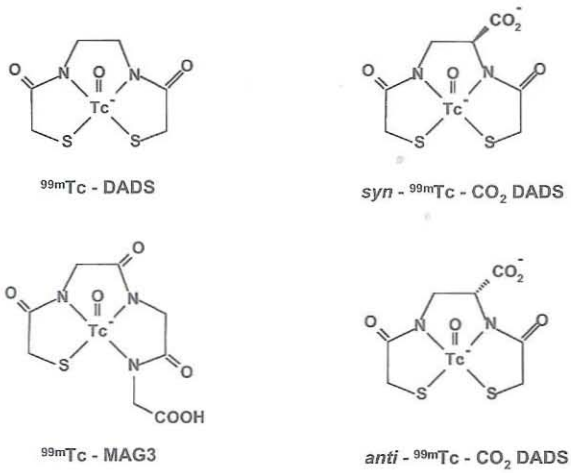

FIGURE 9-23 Structures of technetium-labeled DADS, CO_2-DADS (*syn* and *anti* forms), and MAG3.

^{99m}Tc-DADS), had good renal excretion but was inferior to ^{131}I-OIH. This led to the structural modification of adding a carboxylate group to the ethylene bridge of the DADS ligand to produce N,N'-bis(mercaptoacetyl)-2,3-diaminopropanoate (CO_2-DADS). Subsequent labeling with ^{99m}Tc-sodium pertechnetate yielded ^{99m}Tc-CO_2-DADS (Figure 9-23).[25,55] This modification, however, created an asymmetric carbon atom and resulted in two chelate ring stereoisomers. Renal handling was affected by the orientation of the carboxyl group relative to the technetium oxo core, with the *syn* isomer having better renal excretion than the *anti* isomer.[55,56] Changing the core donor ligand from N_2S_2 to N_3S and placement of the carboxyl group on the third amido nitrogen produced a radiochemically pure product without an asymmetric carbon. The simplest ligand having the necessary groups for renal excretion was MAG3 (Figure 9-23).

Subsequently, a kit formulation was developed that contains an S-benzoyl mercaptoacetyltriglycine donor ligand (betiatide), stannous chloride as the reducing agent, and sodium tartrate.[57] Since the SH group is very reactive and may not be stable in a lyophilized kit, it is protected with the benzoyl group. The sodium tartrate transfer ligand allows formation of a precursor ^{99m}Tc-tartrate complex, keeping reduced technetium soluble during the labeling reaction. Addition of ^{99m}Tc-sodium pertechnetate and heating causes hydrolysis of the protective group and transfer of reduced technetium from tartrate to MAG3 in quantitative yield (Figure 9-24). An alternative rapid method for preparation and quality control of ^{99m}Tc-MAG3 has been described.[58]

Many novel Tc(V) compounds with interesting ligands are being developed, some that are newly designed and others that have achieved a more advanced stage of development, but all of which hold promise for future use in nuclear medicine.

A compound that targets the DAT is ^{99m}Tc-TRODAT-1 (Figure 9-19). TRODAT is [2-[[2-[[[3-(4-chlorophenyl)-8-methyl-8-azabicylo[3.2.1]oct-2-yl]methyl](2-mercaptoetyl)amino]ethyl]amino] ethanethiolato(3-)-N2,N2',S2,S2']oxo-[1R-(exo-exo)], a diaminedithiol complex of the TcO^{3+} core with a tropane analogue derivatized from one nitrogen molecule. The ^{99m}Tc-TRODAT-1 complex is prepared by reacting the preformed TRODAT-1 ligand dissolved in ethanolic hydrochloric acid with sodium pertechnetate in the presence of stannous glucoheptonate and sodium EDTA. The mixture is sterilized by autoclaving, phosphate-buffered to pH 6 to 7, and purified by solvent extraction and HPLC separation.[59] Two diastereomers are formed, both of which bind to DAT receptors in rat striatum. Human imaging studies have demonstrated localization in the basal ganglia consistent with DAT receptor binding.[60]

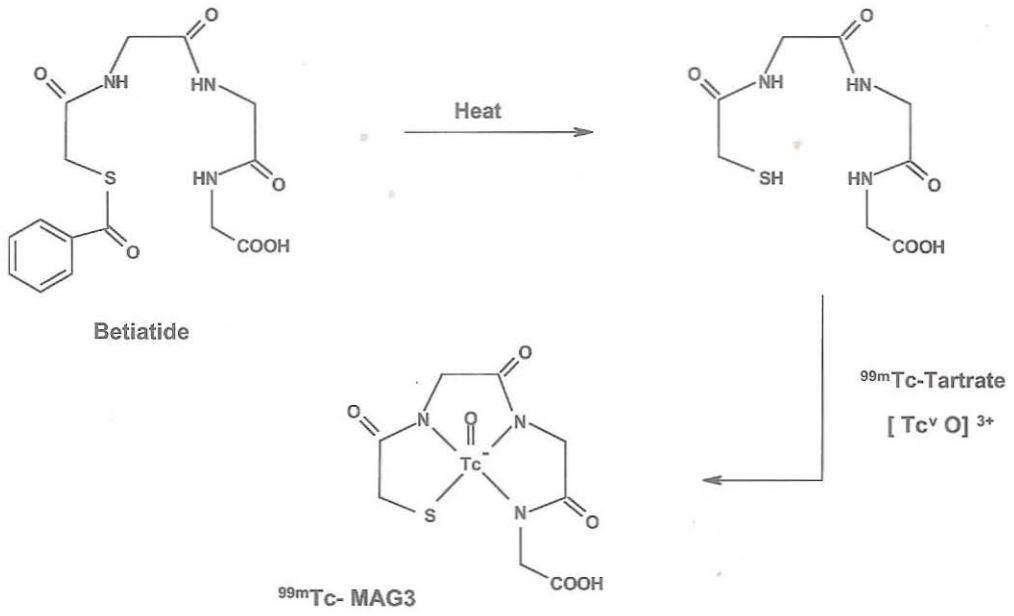

FIGURE 9-24 Synthetic pathway for labeling ^{99m}Tc-mertiatide (^{99m}Tc-MAG3).

Another novel ligand approach to designing technetium complexes for specific receptor imaging is the 3 + 1 concept.[61] A complex formed by coordination of the TcO^{3+} core with a tridentate ligand and a monodentate ligand constitutes a 3 + 1 mixed-ligand complex. The technetium complex is of the type TcO-[(HS-(C_2H_5)-X-(C_2H_5)-SH) + (R-SH)], where X = S or NCH_3 and R is the receptor-binding molecule. In principle, the method consists of saturating three of the four available coordination sites on the TcO^{3+} core with a small tridentate ligand and filling the fourth site with a monodentate coligand that is the receptor-targeting molecule. The manner in which these complexes are constructed puts them into the category of the integrated approach to labeling with technetium. The general labeling sequence is shown below; it begins with a precursor Tc(V)-gluconate complex.[62]

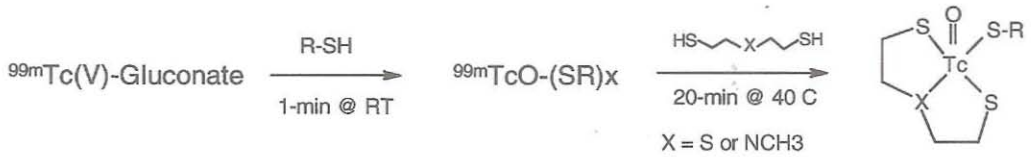

One requirement of the 3 + 1 approach is that the coligand must contain a thiol group to coordinate with technetium. The method has been used to prepare technetium-labeled dopamine-, serotonin-, estrogen-, and androgen-receptor complexes. Johannsen et al.[61,62] used this approach in designing a brain receptor imaging agent to mimic ketanserin, a prototype serotonin-receptor (5-HT) antagonist. By preparing different fragments of ketanserin as the monodentate coligand, this group produced a series of technetium complexes that target the serotonin receptor in the brain. The method lends itself to controlling biodistribution by altering the structural elements of the coligand. These same investigators demonstrated that by modification of the coligand to change pKa, brain uptake of

the complex can be increased significantly with the particular 5-HT_{2A} (3+1) complex shown in Figure 9-19.[63] One concern that has arisen with these compounds is the lability of the thiol coligand group to displacement in vivo by glutathione.[64] This effect was found to be dependent on small structural variations, especially in the S-X-S tridentate ligand, with X = N-CH_3 complexes being significantly more stable than X = S complexes.

A number of compounds labeled with different radionuclides have been investigated for imaging hypoxic tissue, with particular interest in imaging hypoxic myocardium and the hypoxic regions of tumors.[65,66] Several different complexes of technetium have been investigated in vitro and in animals (Figure 9-19). Two of these compounds are 2-nitroimidazole analogues of the PnAO ligand, namely, BMS 181321 and BRU 59-21 (Bracco), each of which has a TcO^{3+} core. Two are nonnitroimidazole derivatives. One of these is ^{99m}Tc-BnAO (HL-91, Prognox, Nycomed Amersham), which has a butylene backbone and a TcO_2^+ core (its structure has not been confirmed), and the other is ^{99m}Tc-cyclam-AK-2123, a derivative of the hypoxic cell radiosensitizer AK-2123.[67]

Most work with hypoxia markers so far has been restricted to in vitro models and animal studies. These studies have shown that it is important from an imaging viewpoint that these agents not be too lipophilic, in order to enhance their blood clearance. The octanol-to-water partition coefficients of the two Tc-PnAO complexes are significantly higher than that of the Tc-BnAO or the Tc-cyclam AK-2123 complexes.[66,67] Therefore, Tc-BnAO and Tc-cyclam-AK-2123 appear to have more favorable target-to-background ratios. Additionally, it has been shown that BMS 181321, BRU-59-21, and Tc-BnAO exhibit trapping in hypoxic tissue over a narrow range of 20 to 40 ppm of oxygen, which is two orders of magnitude lower than what is usually classified as radiobiologic hypoxia. Therefore, these agents may not completely map the extent of radiobiologically significant hypoxia within a tumor because only regions that have extreme hypoxia will trap the tracer.[66] Thus, the ability to modify the oxygen sensitivity of the technetium complex may be a key point in the future development of tissue hypoxia markers.

^{99m}Tc-ethylenedicysteine (^{99m}Tc-EC) is a member of the diaminedithiol family of chelating agents. It is the diacid metabolite produced from the de-esterification of ^{99m}Tc-ECD. The serendipitous observation of high renal excretion of ECD metabolites led to an investigation that identified ^{99m}Tc-EC as a possible renal imaging agent.[68] Formation of the technetium-labeled complex was studied by mixing the EC complexing agent with stannous chloride at differing pH, whereupon it was shown that labeling yields varied from about 50% at pH 7 to 97% to 99% in the pH range of 10 to 12. The yield at pH 7 is low because of protonation of the amine groups, which compete with technetium for the nitrogen ligands. Once the complex is formed, however, the pH can be lowered to 7.4, where it is stable for 8 hours.[68] A kit has been formulated that contains a lyophilized mixture of 1 mg L,L-EC and 100 μg $SnCl_2 \cdot 2H_2O$ in 1 mL of 0.05 M phosphate buffer at pH 12. Labeling is accomplished by adding up to 100 mCi ^{99m}Tc-sodium pertechnetate in 2 to 8 mL followed by neutralization with 0.2 mL of 0.5 M phosphate buffer at pH 5.[68] This complex contains the $Tc{=}O^{3+}$ core as shown in Figure 9-25. When compared with ^{99m}Tc-MAG3, ^{99m}Tc-L,L-EC produces a similar renogram curve but its plasma protein binding is threefold less, giving it much higher plasma clearance.[68,69] Tc-EC complexes can exist in four different stereoisomeric forms, ^{99m}Tc-D,D-EC, ^{99m}Tc-L,L-EC, ^{99m}Tc-*syn* D,L-EC, and ^{99m}Tc-*anti* D,L-EC.[69] When the D,D, L,L, and D,L isomers were compared with ^{131}I-OIH in human subjects, their respective clearances, relative to ^{131}I-OIH, were 82%, 70%, and 40%. The pharmacokinetics of ^{99m}Tc-D,D-EC appear to be closer to ^{131}I-OIH than ^{99m}Tc-L,L-EC, but both complexes exist at physiologic pH in monoanionic and dianionic forms, which likely causes their differences in protein binding and clearance. Further work is needed to determine if any of these complexes will become useful renal imaging agents.

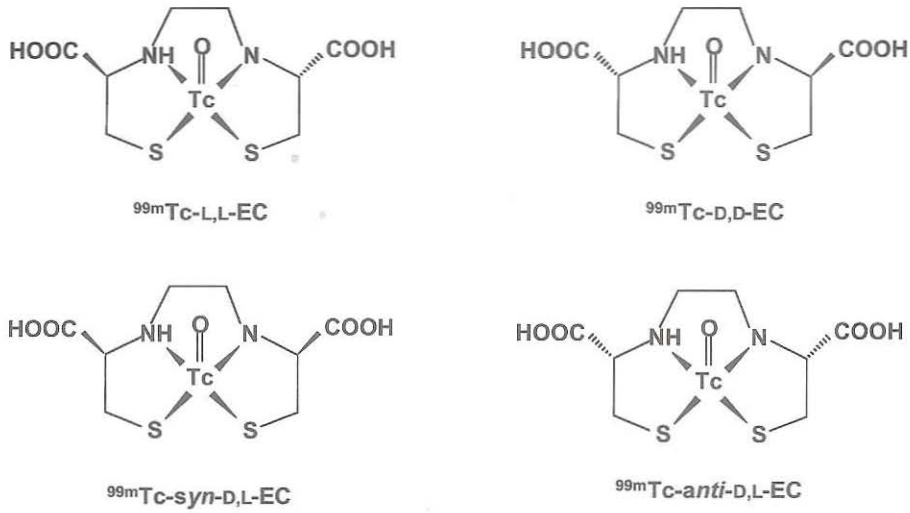

FIGURE 9-25 Stereoisomeric forms of ^{99m}Tc-ethylenedicysteine (^{99m}Tc-EC).

O=Tc=O⁺ Core

The diphosphine (P-P) ligand has been successfully used to produce stable complexes with the O=Tc=O$^+$ core, the most important one to date being 1,2-bis[bis(2-ethoxyethyl)phosphino] ethane (tetrofosmin). ^{99m}Tc-tetrofosmin is a phosphine complex used for myocardial perfusion imaging. Structural characterization of [Tc-(tetrofosmin)$_2$O$_2$]$^+$ has shown that the ^{99m}Tc and ^{99}Tc complexes are identical and possess the O=Tc=O$^+$ core complexed with two 1,2-bis[bis(2-ethoxyethyl)phosphino]ethane (tetrofosmin) donor ligands (Figure 9-18).[26,70] Because the donor ligand is neutral, the Tc complex has a net charge of 1+. The complex is labeled at room temperature and has a long shelf life. The original formulation, which had a pH range of 8.3 to 9.1 and was prepared without adding air to the reaction vial, had a shelf life of 8 hours. Stability work at Amersham revealed that the complex was sensitive to autoradiolytic decomposition and that admission of 2 mL of air at the time of pertechnetate addition and a change in final pH to a range of 7.5 to 9.0 resulted in a product stable for 12 hours.[71] This increase in stability is attributed to the ability of oxygen to scavenge reducing species (the hydrated electron e^-_{aq} and the hydrogen radical H$^\cdot$).[71]

Tc≡N²⁺ Core

The nitrido atom N^{3-} was developed by Baldas et al.[72,73] to complex with Tc(V). Subsequently, a Tc-nitrido compound, [bis (N-ethyl-N-ethoxydithiocarbamato)nitrido ^{99m}Tc(V), was developed, and it has shown promise for myocardial perfusion imaging.[74] It is a neutral lipophilic myocardial imaging agent with a Tc≡N^{2+} core whose chemical structure is shown in Figure 9-18, demonstrating a Tc(V) atom triple-bonded to a strong pi-electron donor nitride atom (N^{3-}) and four sulfur atoms. The complex is prepared in a two-step procedure.[74] The first step involves reduction of ^{99m}Tc-sodium pertechnetate in acidic conditions by trisodium tri(*m*-sulfophenyl) phosphine in the presence of S-methyl N-methyl dithiocarbazate, $H_2NN(CH_3)C(=S)SCH_3$, as the nitrido nitrogen donating agent. This mixture is heated at 100°C for 20 minutes, producing an intermediate species bearing the Tc≡N^{2+} core. The mixture is cooled and neutralized with buffer, and the dithiocarbamate ligand is added, whereupon ligand exchange occurs immediately to form the final

Tc-nitrido dithiocarbamate complex, ^{99m}Tc-N-$(NOEt)_2$. A lyophilized kit has been developed (^{99m}Tc-N-$(NOEt)_2$, CIS Bio-International) using stannous chloride that permits labeling at neutral pH.[74]

After intravenous injection, ^{99m}Tc-N-$(NOEt)_2$ localizes in the myocardium in proportion to blood flow. After myocardial uptake, ^{99m}Tc-N-$(NOEt)_2$ redistributes from the heart and has been compared with ^{201}Tl for myocardial perfusion imaging.[75]

Tc-HYNIC Core

The HYNIC functional group in the Tc-HYNIC core was first utilized by Abrams et al.[40] to label polyclonal IgG. Since then it has been used to label chemotactic peptides, somatostatin analogues, and other biologically interesting molecules.[30] This core forms complexes of the general form [^{99m}Tc(HYNIC-peptide)$(L)_2$], where the HYNIC group satisfies one coordination site and the remaining sites are completed by various coligands, such as tris(hydroxymethyl)methylglycine (tricine) or ethylenediamine-N,N'-diacetic acid (EDDA). During the development of peptide radiopharmaceuticals with this core, a binary ligand system was evaluated that used two tricine coligands. The problem with this approach was that stability of the complex was achieved only in the presence of excess coligand, and multiple isomers were formed.[76] A ternary ligand system was then explored having the general form [^{99m}Tc(HYNIC-peptide)(tricine)(L)], which contains three different ligands: the bifunctional coupling group (HYNIC), a monodentate phosphine (L), and the tetradentate tricine coligand. It was thought that use of a phosphine coligand might impose constraints on the possible coordination modes of the tricine and hydrazine ligands and this would reduce the number of isomers. Following this idea, a complex of the [^{99m}Tc(HYNIC-peptide)(tricine)(L)] type, using tricine and a monodentate triphosphine coligand (TPPTS, trisodium triphenylphosphine-3,3',3''-trisulfonate), was developed (Figure 9-26).[77] Technetium labeling with the HYNIC ternary ligand system follows the post-labeling approach, in which the peptide-HYNIC conjugate is formed prior to coordination with technetium and the coligands. The complex is a GP IIb/IIIa platelet receptor antagonist that is produced in high specific activity (20 Ci/μmol) and high yield (>90%) in a

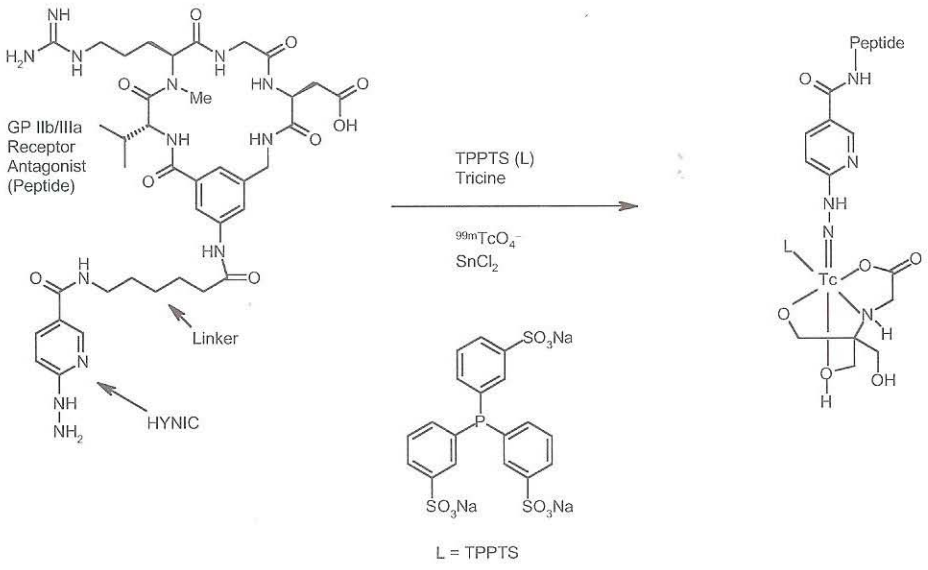

FIGURE 9-26 General scheme for the production of ^{99m}Tc-HYNIC-peptide conjugates.

one-step synthesis, performed by mixing together in one vial an aqueous solution of 10 μg of HYNIC-peptide, 20 to 40 mg of tricine, 1.0 mg of phosphine coligand, 50 mCi (1850 MBq) of $^{99m}TcO_4^-$, and 25 μg of $SnCl_2 \cdot 2H_20$ at pH 4 to 5, then heating at 50°C for 30 minutes. Analysis of this product demonstrated that equal mixtures of two isomers were formed, each of which was stable for at least 6 hours in solution between pH 4 and 8.[77]

The oxidation state of technetium in HYNIC complexes is not clear and may depend on the type of coligand, taking into account that some ligands, such as phosphines, have reducing capability.[30,77] The components in the GP IIb/IIIa ternary ligand complex exist in a 1:1:1:1 ratio of Tc:HYNIC-peptide:tricine:phosphine. This complex demonstrated arterial and venous thrombi in a canine model with thrombus-to-muscle ratios at 2 hours of approximately 10:1.[78] The ternary ligand system has been shown to produce complexes with extremely high specific activity, high solution stability, fewer isomers (2) than the binary tricine system (>10), and the ability to control the radiopharmaceutical's properties through alteration of functional groups on the tricine or phosphine coligands.[30,77]

Tc(III) Compounds

Reduction of pertechnetate, Tc(VII), to the Tc(III) oxidation state creates a technetium atom with four additional electrons (d^4 configuration). In some complexes with Tc(III), this state is reached in multiple reduction steps, first to Tc(V) and then to Tc(III). Coordination numbers of five, six, and seven are possible.[28]

Several interesting technetium compounds with a Tc^{3+} core have been developed for use in nuclear medicine. The Tc-IDA analogues, which contain the Tc(III) core atom, were discussed earlier. Other compounds of interest include ^{99m}Tc-DMPE, ^{99m}Tc-teboroxime, and ^{99m}Tc-furifosmin.

The development of technetium-labeled radiopharmaceuticals for heart imaging began with the design of monovalent cationic complexes, the first being Tc-dichlorobis(1,2-dimethylphosphine)ethane (Tc[III] DMPE) by Nishiyama et al.[79] Animal studies demonstrated promise with this agent, but human studies identified an unsatisfactory heart-to-background activity ratio. Nonetheless, this effort laid important groundwork for the development of other, more successful technetium agents for heart imaging.

^{99m}Tc-teboroxime, [bis[1,2-cyclohexanedione dioximato(1-)-O]-[1,2-cyclohexanedione-ioximato(2-)-O]methylborato(-)-N,N',N'',N''',N'''',N''''']-chlorotechnetium, is a neutral lipophilic complex of the general class of compounds known as boronic acid adducts of technetium dioxime.[80] This complex is prepared by the general method of template synthesis, in which a metal ion (Tc) serves as a template to organize the course of complex multistep reactions. ^{99m}Tc-teboroxime is unique among the technetium complexes in that the ligand is not present in the reaction vial before the addition of pertechnetate but is formed around technetium as the template atom. The essential reactants in the kit are cyclohexanedione dioxime, chloride as the axial ligand, methyl boronic acid, and stannous chloride. After heating (15 minutes at 100°C), the final complex contains a heptacoordinate Tc(III) atom bound to a chlorine atom and to the six nitrogens of the three vicinal dioximes (Figure 9-18). One end of the molecule is capped by a boron atom covalently bound to one oxygen atom from each of the dioximes. ^{99m}Tc-teboroxime exhibits very high first-pass extraction by the myocardium and rapid back-diffusion into the vascular space. The rapid in vivo myocardial kinetics created temporal problems during imaging procedures with this agent and led to its removal from the market.

^{99m}Tc-furifosmin (Q-12) is a phosphine compound with a Tc(III) core coordinated by a bidentate SWL ligand via N and O atoms and two monodentate TMPP ligands (Figure 9-18).[81] The SWL ligand is 1,2-bis[dihydro-2,2,5,5-tetramethyl-3(2H)-furanone-4-methyl-eneamino]ethane, a Schiff base, and the TMPP ligand is tris(3-methoxy-1-propyl)phosphine.

The overall charge on the technetium complex is 1+. The original labeling procedure is a two-step process.[81] The first step involves a stannous reduction of pertechnetate in the presence of the SWL ligand in ethanol to produce the Tc(V) intermediate $[Tc^{V}(O)(SWL)]^{+}$, followed by addition of the TMPP in ethanol in a substitution/reduction reaction to form the final product $[Tc(III)(SWL)(TMPP)_2]^{+}$. Alkyl phosphines are reducing agents, and TMPP reduces the Tc(V) to a stable, nonreducible Tc(III).[82] The mixture is then diluted to 20 mL with water, loaded on a prewet Sep-Pak C18 (Waters) column, and washed with water to remove excess ligands (SWL, TMPP). The product is then eluted in approximately 60% yield with 2 mL of 80:20 ethanol:saline. Reverse-phase HPLC yields a radiochemical purity of more than 95%. The final product is stable for at least 8 hours. A one-step kit preparation has been developed.

Initial biodistribution studies in humans have demonstrated that the lipophilic Tc-Q-12 complex has good heart uptake at rest (2.2% injected dose at 1 hour) with no detectable myocardial washout or redistribution up to 5 hours. Rapid hepatobiliary clearance permits imaging as early as 15 minutes postinjection. In a correlation study, Tc-Q-12 was able to demonstrate perfusion defects in 26 of 27 patients with angiographically proven coronary artery disease,[82] and it is comparable to ^{201}Tl for the detection of coronary artery disease.[83]

Tc(IV) Compounds

Many of the first-generation technetium compounds that were discussed earlier have technetium in the Tc(IV) oxidation state. These are listed in Table 9-7 and include technetium complexes with citrate, DTPA, the phosphonates (ethanehydroxydiphosphonate [EHDP], methylene diphosphonic acid [MDP], hydroxymethylene diphosphonate [HDP]), pyrophosphate (PPi), and the insoluble dioxide TcO_2.

TECHNETIUM TC 99M KITS

Kits are used to prepare ^{99m}Tc radiopharmaceuticals. A radiopharmaceutical kit consists of a sterile reaction vial containing the nonradioactive chemicals required to produce a specific radiopharmaceutical after reaction with ^{99m}Tc-sodium pertechnetate. The primary chemical substances present in the kit are the complexing agent (ligand) and a reducing agent, typically stannous chloride. Stannous fluoride and stannous tartrate are also used. Other substances, such as stabilizers, dispersing agents, transfer ligands, and buffers, may be present.

Radiopharmaceutical kits are supplied by several manufacturers. Formulating a kit usually involves adding an acidified solution of stannous chloride to a ligand solution at a defined pH (Figure 9-27). This was the process followed in many of the early technetium kits (e.g., DTPA, DMSA, MDP, and PPi), in which excess ligand keeps the tin soluble through complexation. An aliquot of the final mixture of ingredients is dispensed into presterilized serum vials. The solution is frozen and lyophilized under vacuum to remove all water. The vials are backfilled with nitrogen or argon gas before sealing. In some of the newer kits, additional complexing agents, such as gluceptate, gluconate, and tartrate, are added to the formulation as solubilizing agents for tin and reduced technetium during the radiolabeling process.

The complexing agent in a kit is usually present in a large molar excess over the amount of tin to ensure that all of the tin (Sn[II] and Sn[IV]) will be complexed and to minimize competition between reduced technetium and tin for the ligand during the labeling reaction. Complexation sequesters the tin, thus preventing its hydrolysis at higher pH. Complexation does not prevent the tin from entering into reduction/oxidation reactions.

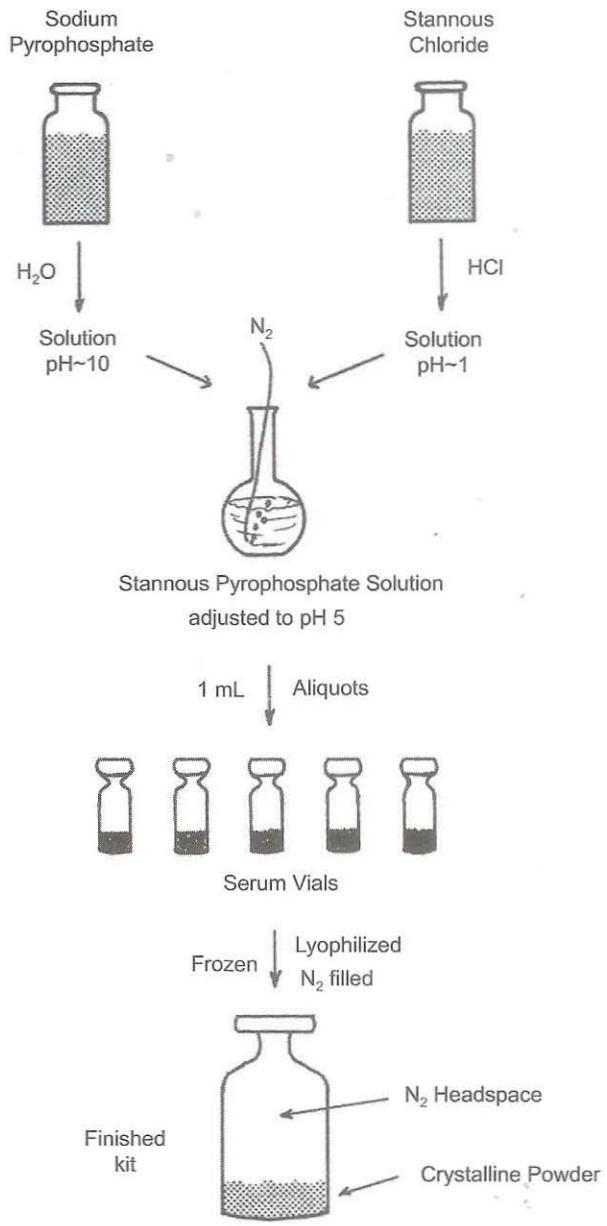

FIGURE 9-27 Procedure for the production of a stannous pyrophosphate kit.

Because stannous ion is easily oxidized, all solutions used to prepare kits must have their oxygen purged with nitrogen or another inert gas. For example, Figure 9-28 demonstrates that a nitrogen flow rate of 83 cc per minute through 450 mL of water will reduce the dissolved oxygen concentration from 6.7 ppm to 0.2 ppm in 30 minutes.

As an example of some common techniques and problems associated with the preparation of kits containing stannous tin, consider the production of stannous pyrophosphate kits. During kit production a solution of stannous chloride is prepared. This can be accomplished by dissolving either stannous chloride or high-purity tin wire in concentrated hydrochloric acid followed by dilution with deoxygenated water. Some initial heating of the hydrochloric acid/tin solution may be required to facilitate dissolution of

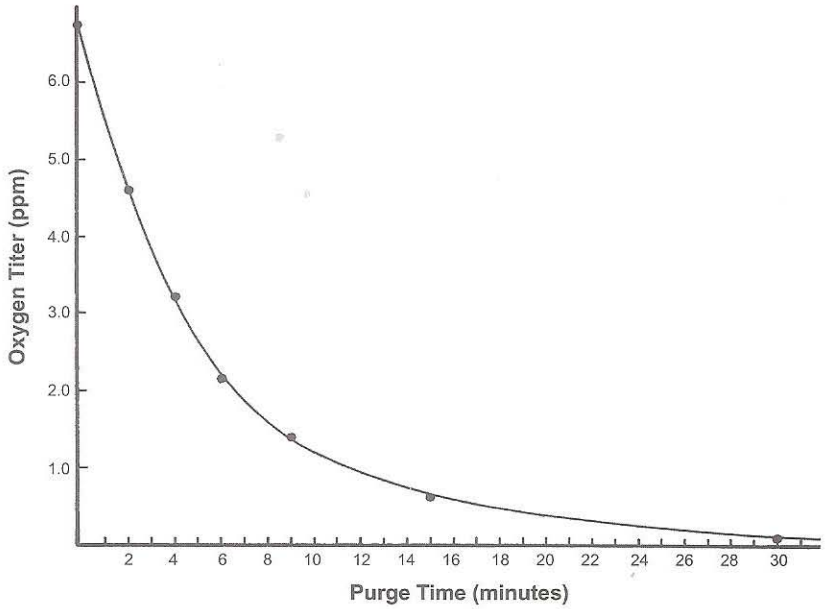

FIGURE 9-28 Reduction of dissolved oxygen concentration over time in 450 mL of distilled water at a nitrogen flow rate of 83 cc per minute.

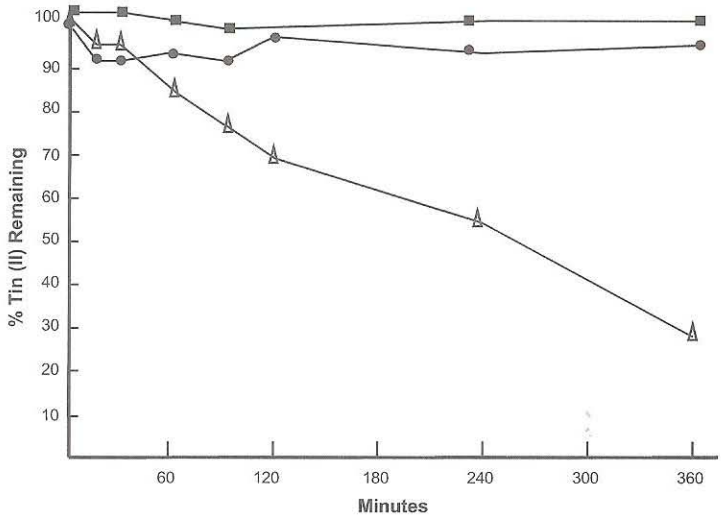

FIGURE 9-29 Influence of preparation and storage conditions on stability of stannous pyrophosphate solutions. • = oxygenated water, nitrogen atmosphere; ■ = nitrogen-purged water, nitrogen atmosphere; △ = nitrogen-purged water, room air.

the tin wire or to dissolve any stannous oxychloride present if stannous chloride crystals are used. These solutions must be kept under constant nitrogen purge to prevent oxidation. Figure 9-29 illustrates the stability of stannous pyrophosphate solution when prepared and stored under various conditions, demonstrating the lability of these solutions to the presence of oxygen. Once the tin ligand complex is formed, kits are prepared by dispensing a small aliquot, typically 1 mL, into presterilized serum vials. This process is performed under aseptic conditions in a laminar airflow environment. To retard oxidation of tin

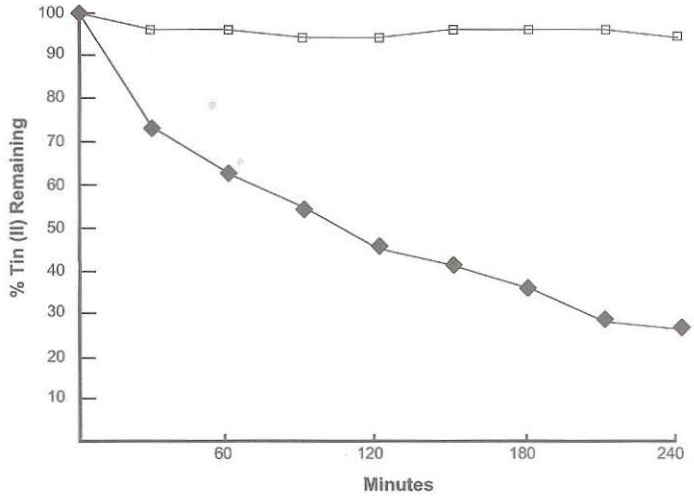

FIGURE 9-30 Effect of physical state on stability of stannous pyrophosphate exposed to room air. □ = frozen samples; ◆ = liquid samples.

during the filling process, the solutions may be kept cold before vial filling and frozen immediately after filling. Figure 9-30 illustrates the loss of Sn(II) in stannous pyrophosphate vials when the vials are filled and frozen immediately and when vial freezing is delayed for various times after filling. The Sn(II) titer falls rapidly to about 73% when freezing is delayed only 30 minutes, whereas vials frozen immediately after filling retain their Sn(II) content. After filling and freezing, vials are lyophilized and backfilled with nitrogen to maintain stability for long periods. When the solution is reconstituted with saline or sodium pertechnetate, however, oxidation can readily occur if air is not excluded from the vial.

Kits may be prepared extemporaneously on occasion for in-house use. In this situation, the key elements for success are to keep all solutions purged constantly with nitrogen during preparation and to freeze solutions immediately after vial filling to reduce the loss of Sn(II) in the kit. The vials can be chilled on a bed of dry ice prior to filling to ensure a quick freeze. Vials should be backfilled with sterile nitrogen gas. If small numbers of kits are prepared for in-house use (e.g., when kits are unavailable from suppliers) and freeze-drying equipment is not available, kits may be kept frozen.

Quantitative Assay of Tin (II)

The ease with which Sn(II) is oxidized makes it quite difficult to prepare solutions accurately unless they are of high concentration. In practice, however, the Sn(II) concentration in ^{99m}Tc radiopharmaceuticals is quite low, magnifying the problem of stability despite efforts to provide oxygen-free conditions during preparation. Kits, therefore, must be analyzed to ensure that they maintain sufficient Sn(II) content. This can be accomplished by volumetric titration with standard oxidant solutions. While ceric sulfate and potassium dichromate are standard oxidants used in redox titrations, potassium iodate appears to offer the most versatility for solutions of Sn(II) in the presence of organic complexing agents.[84] Ceric and dichromate solutions, because of their powerful oxidizing ability, may produce erroneous results by oxidizing the organic complexes present. Iodate titrations of stannous complexes can be carried out effectively for kits containing Sn(II) in the range

of 15 μg to 4 mg or more in a 10 mL volume. An alternative method, for assaying Sn(II) in the range of 2 to 10 μg/mL, is based on spectrophotometrically measuring a blue complex produced upon reduction of phosphomolybdate by Sn(II). The latter method was developed at Brookhaven to assay the small amounts of Sn(II) in its RBC kits. Details of these methods of Sn(II) analysis are reported in the literature.[84–86] Another useful method is analysis of the usable amounts of Sn(II) in kits by direct titration of kits with ^{99m}Tc-sodium pertechnetate containing known amounts of carrier-added ^{99}Tc-sodium pertechnetate.[87]

Tin Toxicity

Occasionally a question arises concerning the potential for toxicity from the administration of tin in radiopharmaceutical kits. Because information on the in vivo distribution and toxicity of tin in humans is scarce and not well documented, one must rely primarily on animal studies for determining acute toxicity. Additionally, to gain some perspective regarding safety, one can consider the amounts of tin expected to be administered to humans and compare those amounts with the normal concentrations of tin in the body from dietary sources.

Acute toxicity studies in rats demonstrate that when stannous chloride dihydrate is injected intravenously, the 24 hour lethal dose for 50% survival of the group (LD_{50}) is 15.4 mg Sn/kg.[88] Symptoms of toxicity include tremors, ataxia, muscle weakness, weight loss, and depression. At the tissue level, the most important toxic effect is renal function impairment because of pathologic changes in the kidney.

The primary route of excretion of tin is urinary, and the principal organ that concentrates tin is bone.[89] From a single intravenous dose of 2 mg Sn(II) or Sn(IV)/kg, 30% is excreted in urine, and 11% of the Sn(II) but none of the Sn(IV) is excreted in bile. Sn(IV), however, appears to show more of a preference for bone than Sn(II). Two days after an intravenous dose of tin citrate labeled with ^{113}Sn, the total skeletal ^{113}Sn activity is 35% of the administered Sn(II) and 46% of the Sn(IV). The biologic half-life in bone is calculated to be 20 to 40 days. Two days after oral or intravenous dosing, blood ^{113}Sn activity is very low and is limited entirely to the red cells. Tissue studies in humans have demonstrated the normal presence of metals in the body, including tin.[90] Most of the tin is localized in bone.

Tissue distribution of tin from radiopharmaceuticals depends on the chemical form administered. Weak chelates that undergo in vivo hydrolysis are expected to deposit tin in the RES, whereas stable chelates will distribute tin more widely in the tissues or it will be excreted in the urine.[91]

If one considers the usual concentrations of tin administered in radiopharmaceuticals, the amounts appear to be quite safe. In general the largest single dose of tin expected to be administered intravenously in nuclear medicine is 2 mg, which is equivalent to about 0.03 mg/kg for a 70 kg adult. This is one five-hundredth of the LD_{50} reported in rats. Typically, however, the dose of tin administered is one-half to one-tenth this amount, making the safety factor on the order of 1000 to 5000.

KIT-PREPARED ^{99M}TC RADIOPHARMACEUTICALS: GENERAL CONSIDERATIONS

The complexing agent (ligand) in the kit dictates the final chemical form of technetium and ultimately its biologic fate after intravenous injection. The functions of the complexing agent (ligand) are summarized in Table 9-8.

TABLE 9-8 Complexing Agent Function in ^{99m}Tc Kits

1. Complexes Sn^{2+} and Sn^{4+}
2. Complexes and stabilizes reduced ^{99m}Tc and ^{99}Tc
3. Determines technetium's biologic localization

^{99m}Tc radiopharmaceuticals are prepared by adding ^{99m}Tc-sodium pertechnetate to the kit. This causes dissolution of the lyophilized powder and initiates the labeling reaction. Subsequently the complexed stannous ion reduces the pertechnetate to a lower oxidation state and the reduced technetium binds to the ligand, producing the desired radiopharmaceutical. For most kits, the complexation reaction occurs rapidly at room temperature. Some kits need to be heated to effect a complete reaction to the final form. In most kits, the reduced technetium labels the principal ligand directly. In some kits, the reduced technetium first complexes with an intermediate weaker ligand, which transfers the reduced technetium species to the principal ligand. This exchange labeling method stabilizes reduced technetium when the reaction kinetics with the principal ligand are slow.

The reduction–oxidation reactions are shown below for reduction of pertechnetate to the Tc(IV) oxidation state. Other oxidation states of technetium may be produced, such as Tc(I), Tc(III), and Tc(V), depending on the complexing agent and reaction conditions. In the following reactions, 9-6 shows the oxidation of Sn(II), which releases six electrons (two electrons per atom), and 9-7 shows the acceptance of those six electrons by two molecules of pertechnetate, reducing it to the 4+ oxidation state.

$$3Sn^{2+} \leftrightarrow 3Sn^{4+} + 6e^- \tag{9-6}$$

$$2TcO_4^- + 12H^+ + 6e^- \leftrightarrow 2TcO^{2+} + 6H_2O \tag{9-7}$$

The sum of reactions 9-6 and 9-7 is as follows:

$$2TcO_4^- + 3Sn^{2+} + 12H^+ \leftrightarrow 2TcO^{2+} + 3Sn^{4+} + 6H_2O \tag{9-8}$$

The generalized scheme for the binding of reduced technetium in kits containing stannous ion is shown in Figure 9-31, using DTPA as an exemplary ligand. As shown in this figure, technetium can be present in three principal chemical forms: technetium bound to ligand (desired radiopharmaceutical); unreduced free pertechnetate; and reduced, hydrolyzed technetium. The latter two forms are undesirable impurities. Other forms of impurities may be present, depending on the type of radiopharmaceutical prepared, but these two may typically be present in all agents.

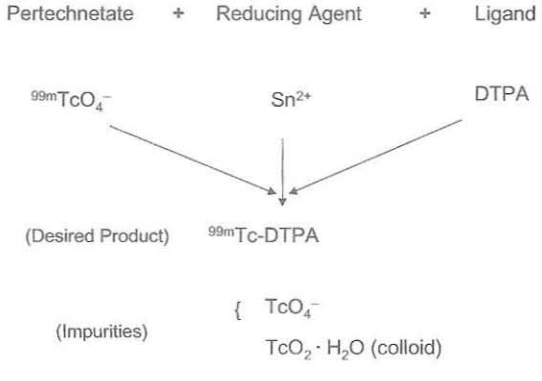

FIGURE 9-31 General scheme followed in ^{99m}Tc kit labeling using DTPA as exemplary ligand, illustrating the ^{99m}Tc-DTPA complex as the desired product and the potential radiochemical impurities that can be expected.

Pertechnetate Impurity

At least two major factors can cause the development of pertechnetate impurity: oxygen and free radicals induced by radiolysis. Each of these substances can cause oxidation of stannous ion according to the following reactions. An insufficient stannous ion concentration decreases the reducing power in the kit. The oxidation of Sn(II) by oxygen is as follows:

$$2Sn^{2+} + O_2 + 4H^+ \leftrightarrow 2Sn^{4+} + 2H_2O \quad (9\text{-}9)$$

This reaction is important during the kit production process previously discussed. It is also important during the radiolabeling reaction because of oxygen from the air or dissolved in the sodium pertechnetate saline solutions added to kits. Owanwanne et al.[92] demonstrated that oxygen has a greater effect during the radiolabeling reaction than after the reaction is complete, because it competes with pertechnetate for Sn(II). The equilibrium concentration of pure oxygen dissolved in water is 1.23×10^{-3} M at 25°C and 1 atm.[93] Thus, according to Equation 9-9, the concentration of stannous ion required for complete reaction with oxygen in a saturated solution is 2.46×10^{-3} M. Since water at ambient conditions is equilibrated with air (which contains only 20.95% O_2), these molar concentrations would be 20% less under ambient environmental conditions. As such, 1 mL of water (or saline) equilibrated with air would have the oxygen capacity to oxidize 116 μg of $SnCl_2 \cdot 2H_2O$, equivalent to 61 μg Sn(II).

Radiolysis may occur after radioactivity is added to kits, producing free radicals (see Chapter 6 for free radical production reactions). The principal radiolytic species produced in aqueous solution are the hydrated electron, e^-_{aq}, and the hydrogen radical, $H^\cdot$, which are powerful reducing agents, and the hydroxy radical, $OH^\cdot$, and hydroperoxy radical, $HO_2^\cdot$, which are powerful oxidizing agents.[94,95] The concentration of the hydroperoxy radical increases in the presence of oxygen. A free radical contains a single unpaired electron. If the electron is donated to another species, the free radical is a reducing agent. If the free radical accepts an electron from another species, it is an oxidizing agent. The following oxidizing reactions are possible with Sn(II) in radiopharmaceutical kits:[95]

$$Sn^{2+} + 2H^+ + 2OH^\cdot \leftrightarrow Sn^{4+} + 2H_2O \quad (9\text{-}10)$$

$$Sn^{2+} + 2H^+ + 2HO_2^\cdot \leftrightarrow Sn^{4+} + 2H_2O_2 \quad (9\text{-}11)$$

Free radicals may be present in the sodium pertechnetate added to the kits or may be generated in the solution once the kit is reconstituted. Free radicals are more likely to be generated if large amounts of activity are added to the kit, if kits sit for a long time, if oxygen is present, and if small amounts of Sn(II) are in the kit. Molinski[96] has shown that free radical reactions will generate hydrogen peroxide in aqueous solution at a constant rate of 33×10^{-5} μg/mCi per hour and that the principal factors that predispose to the production of hydrogen peroxide in pertechnetate solutions are increasing amounts of total activity and oxygen. Ascorbic acid added to kits will reduce peroxide to insignificant levels.

It has been shown that radiation-induced decomposition of the technetium complex is catalyzed by the presence of dissolved oxygen and that the presence of excess stannous ion acts as an inhibitor of this reaction.[97] It is therefore of utmost importance, for most technetium radiopharmaceuticals, that a sufficient level of stannous ion be maintained throughout the useful life of the technetium-labeled kit. The oxygen-catalyzed reaction

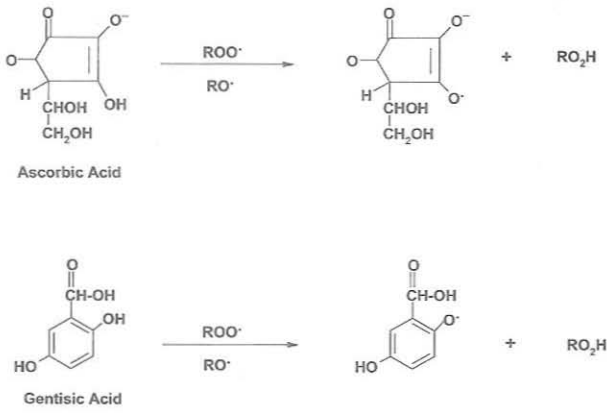

FIGURE 9-32 Mechanism of action of free radical scavengers ascorbic acid and gentisic acid.

probably occurs through the generation of two free-radical oxidation intermediates.[98] The first intermediates are alkoxy or hydroxy radicals produced by the scission of the oxygen–oxygen bond of peroxides according to Equation 9-12. The other intermediate is the peroxy radical formed from oxygen and radiolysis byproducts according to Equation 9-13:

$$RO\text{-}OH \rightarrow RO^{\cdot} + {}^{\cdot}OH \tag{9-12}$$

$$R^{\cdot} + O_2 \rightarrow RO_2^{\cdot} \tag{9-13}$$

These free radical species may then degrade the technetium complex with the generation of free pertechnetate according to the following generalized reaction:

$$\text{Tc-Ligand} \xrightarrow{RO_2^{\cdot}} \text{Ligand} + TcO_4^- \tag{9-14}$$

Some technetium-labeled chelates are more stable than others. The bone imaging agents are fairly weak chelates, and those kits containing low levels of Sn(II) can be stabilized against oxidation by adding antioxidants to the kits. Ascorbic acid and gentisic acid have been used as effective antioxidants in bone kits. As shown in Figure 9-32, they function by donating reactive hydrogen atoms to the free-radical intermediates to yield a resonance-stabilized and nonreactive molecule, RO_2H.[98] The free radical is thus neutralized to a chemical state that cannot attack the technetium complex.

Hydrolyzed–Reduced Technetium Impurity

The hydrolyzed–reduced technetium (HR-Tc) impurity is characterized by the formation of an insoluble colloidal species, as follows; (s) indicates solid.

$$TcO^{2+} + 2OH^- \rightarrow TcO_2 \cdot H_2O(s) \tag{9-15}$$

This reaction is favored at pH values that approach neutrality or greater and at low concentrations of chelating agent.[97] Hydroxyl ions present at increased concentrations will compete with the chelating agent for reduced technetium, forming the colloid. Additionally,

any uncomplexed stannous ion can also hydrolyze to form insoluble colloidal tin hydroxide, as shown in the following reaction:

$$Sn^{2+} + 2OH^- \rightarrow Sn(OH)_2(s) \quad (9\text{-}16)$$

This presents a problem because this tin colloid will also bind reduced technetium and compete with the chelating agent during the labeling reaction. These hydrolysis problems can be mitigated by ensuring that a sufficient excess of chelating agent is present and by maintaining favorable pH conditions.

Methods for analyzing ^{99m}Tc radiopharmaceuticals for pertechnetate and HR-Tc impurities are discussed in Chapter 12.

Technetium–Ligand Complexation

The character of the complexation between reduced technetium and the ligand depends on the type of ligand and the reduction conditions, although the process involves ionic, covalent, and coordinate covalent bonding. Technetium exhibits various coordination numbers that can be satisfied through a combination of binding sites on the ligand and through hydroxyl species in solution. Chelating ligands in ^{99m}Tc radiopharmaceuticals may contain negatively ionized atoms, such as oxygen, sulfur, or nitrogen, that neutralize the positive charge on technetium. Some technetium complexes are neutral while others have either a net positive or negative charge, and these charge conditions may be necessary for complex localization in vivo. Some complexes are dimeric and others polymeric in character, with a technetium atom bridging two ligand molecules. This provides stability to the complex. Figure 9-9 illustrates the binding of two N-substituted IDA ligands to hexacoordinate technetium as an example. It represents the chelation structure found in ^{99m}Tc hepatobiliary imaging agents.

Some kits contain a precursor or transfer ligand that functions to keep reduced technetium and stannous ion soluble during the labeling reaction. This technique is especially useful when the kinetics of complexation with the principal ligand is slow or when the solubility of the principal ligand or the stability of its Sn(II)-complex is lower in aqueous solution. Typical transfer ligands are EDTA, gluconate, gluceptate, and tartrate.

Summary of Technetium Kit Chemistry

Technetium can exist in a number of oxidation states, but Tc(VII) is the most stable and is the state obtained from the ^{99m}Tc generator. Technetium must be reduced to a lower oxidation state, typically Tc(I), Tc(III),Tc(IV), or Tc(V), before it will bind with complexing agents to form useful radiopharmaceuticals. Chemical reduction is usually accomplished with stannous tin. Radiopharmaceutical preparation is typically accomplished by adding ^{99m}Tc-sodium pertechnetate to a vial (kit) containing the ligand, stannous tin, and other added substances. The chemical species of technetium that form during radiolabeling are the technetium complex (desired species) and various undesirable impurities that include reduced technetium colloid and pertechnetate. Colloidal impurities can be minimized by using sufficient excess complexing agent and proper pH. Pertechnetate impurity can be minimized by excluding oxygen, maintaining sufficient stannous ion concentration, and using antioxidants and radical scavengers in the kit. The various technetium species present in technetium radiopharmaceuticals can be readily determined by simple radiochromatography procedures.

KIT-PREPARED ^{99m}TC RADIOPHARMACEUTICALS: SPECIFIC AGENTS

The following discussion addresses topics such as kit components, storage conditions, preparation considerations, stability, radiochemical purity, impurities, and general applications of technetium radiopharmaceuticals prepared from kits. The intent is to cover salient points rather than to be comprehensive. Readers can find detailed information about the properties of each kit in the USP monographs and manufacturer package inserts. The kits are listed here alphabetically by name according to the Nomenclature Committee of the USP Committee of Revision and the United States Adopted Names Council.

Sodium Pertechnetate Tc 99m Injection

Sodium pertechnetate Tc 99m injection is a sterile aqueous solution of ^{99m}Tc and ^{99}Tc as sodium pertechnetate in 0.9% sodium chloride injection obtained from the ^{99}Mo–^{99m}Tc generator. Its pH range is 4.5 to 7.5. It is the source material for reconstituting radiopharmaceutical kits. When eluted from the generator, it must be assayed in the dose calibrator to determine total ^{99m}Tc and ^{99}Mo activity and the total ^{99}Mo-to-^{99m}Tc activity ratio. This ratio must not exceed 0.15 μCi of ^{99}Mo per millicurie of ^{99m}Tc at the time of patient dose administration.[99] Sodium pertechnetate injection must also be tested for aluminum ion contamination, which must not exceed 10 μg/mL. The expiration time for sodium pertechnetate injection, and any kit prepared with it, is not later than 12 hours from the time of generator elution, since it does not contain an antimicrobial preservative. Kits that are formulated with preservatives may have an expiration time longer than 12 hours. The expiration time of any generator supplying sodium pertechnetate is 14 days after manufacture. See Chapter 8 for a detailed discussion of generator eluate tests.

Technetium Tc 99m Albumin Injection

Technetium Tc 99m albumin injection (^{99m}Tc-albumin; ^{99m}Tc-HSA, Amersham) is a sterile aqueous solution of ^{99m}Tc complexed to human serum albumin at a pH between 2.5 and 5.0. The kit contains a lyophilized mixture of human albumin (21 mg) and stannous tartrate (0.23 mg), sealed under nitrogen gas.[100] The kit contains no bacteriostatic preservative and must be stored before and after labeling at 2°C to 8°C.

The complex is prepared by first reconstituting the lyophilized powder with 1.0 mL of sterile water for injection, followed by addition of up to 3.0 mL (100 mCi max) (3700 MBq) of ^{99m}Tc-sodium pertechnetate. The vial is rolled between the hands to gently mix the contents (shaking protein solutions causes foaming) and allowed to stand for 20 minutes to achieve maximum tagging. The product is stable for 6 hours after preparation. The radiochemical purity is not less than 90%, and possible impurities are free pertechnetate and hydrolyzed–reduced technetium,[101] each of which should not exceed 5%.[99]

Early ^{99m}Tc-Sn–labeled human serum albumin preparations had significantly faster blood clearance times than the standard iodinated HSA because of the method of preparation.[102] The commercial ^{99m}Tc-HSA kit described here uses stannous tartrate as a reducing agent, and the product labeling claims that it has prolonged blood clearance with minimal background and organ interference in imaging the blood pool. Albumin (molecular weight approximately 70,000) remains confined to the vascular space because it is restricted from filtration at the glomerulus, where the molecular weight limit is 5000. ^{99m}Tc-HSA, therefore, is useful for imaging the heart blood pool. For adults, the usual administered activity of ^{99m}Tc-HSA is 5 mCi (185 MBq) by intravenous injection. The critical organ is the urinary bladder wall, with a radiation absorbed dose of 0.033 rad(cGy)/mCi.[100]

TABLE 9-9 Composition of ^{99m}Tc-MAA Kits

Component	Amount
Bracco (Macrotec)	
Human albumin aggregated	1.5 mg
Human albumin	10.0 mg
$SnCl_2 \cdot 2H_2O$	70 μg (min)
Sodium chloride	1.8 mg
CIS-US (Pulmolite)	
Human albumin aggregated	1.0 mg
Human albumin	10.0 mg
$SnCl_2$	2.4 μg (min)
Draximage MAA and Medi-Physics (MPI-MAA)	
Human albumin aggregated	2.5 mg
Human albumin	5.0 mg
$SnCl_2 \cdot 2H_2O$	0.06 mg (min) 0.11 mg (max)
Sodium chloride	1.2 mg
Mallinckrodt (TechneScan MAA)	
Human albumin aggregated	2.0 mg
Human albumin	0.5 mg
$SnCl_2 \cdot 2H_2O$	120 μg
Lactose	80.0 mg
Succinic acid	24.0 mg
Sodium acetate	1.4 mg

TABLE 9-10 Properties of ^{99m}Tc-MAA Kits

Manufacturer	Particles per Kit	Maximum Activity (Labeling Time)	Lung Half-life	Kit Storage Conditions: Before Labeling	Kit Storage Conditions: After Labeling	Expiration Time
Mallinckrodt	$8 \pm 4 \times 10^6$	60 mCi (15 min)	3.8 hr	2–8°C	2–8°C	8 hr
DraxImage	$4–8 \times 10^6$	100 mCi (15 min)	2–3 hr	2–8°C	2–8°C	6 hr
CIS-US	$3.6–6.5 \times 10^6$	50 mCi (1–2 min)	5 hr	15–30°C	2–8°C	6 hr
Bracco	$2.0–7.0 \times 10^6$	50 mCi (6 min)	2–3 hr	2–8°C	2–8°C	6 hr

Technetium Tc 99m Albumin Aggregated Injection

Technetium Tc 99m albumin aggregated injection (^{99m}Tc-albumin aggregated or ^{99m}Tc-MAA) is a sterile aqueous suspension of ^{99m}Tc labeled to human albumin aggregate particles in the pH range of 3.8 to 8.0. Kits for preparing ^{99m}Tc-MAA are available from several manufacturers and consist of a sterile lyophilized powder of nonradioactive ingredients sealed under nitrogen. Table 9-9 lists the components of various kits, and Table 9-10 lists kit properties. The stannous albumin aggregates in the kits are produced by heating human albumin in the presence of stannous chloride under controlled conditions of temperature, pH, and mixing. Not less than 90% of the aggregate particles have a diameter between 10 μm and 90 μm, and none can exceed 150 μm.[99] Figure 9-33 is a photomicrograph of ^{99m}Tc-MAA particles.

The labeled product is prepared by aseptically adding the required amount of ^{99m}Tc-sodium pertechnetate to the kit to reconstitute and disperse the particles. The kit is allowed to stand at room temperature for up to 15 minutes to ensure maximum tagging. The

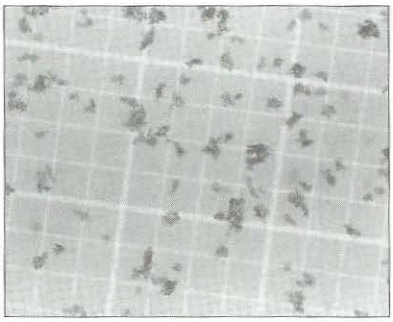

FIGURE 9-33 Photomicrograph of ^{99m}Tc-MAA particles. Distance between lines is 50 μm.

amount of activity added to the kit must be at a concentration that will permit removal of a 3 mCi (111 MBq) dose containing typically between 100,000 and 600,000 particles, as recommended by the manufacturer. The number of particles per dose may need to be lowered for pediatric patients and patients who have right-to-left cardiac shunts. ^{99m}Tc-MAA is contraindicated in patients with severe pulmonary hypertension. (See Chapter 16 for details regarding potential particle toxicity). Accordingly, the concentration of particles in the kit may require dilution with sterile saline before labeling to achieve the desired particle concentration range. The number of particles per dose will increase with time because of constantly declining specific activity. Thus, for example, adding 50 mCi (1850 MBq) to a kit containing 5 million particles will provide 300,000 particles in a 3 mCi (111 MBq) dose initially, but 6 hours later the same dose will contain 600,000 particles.

In general, ^{99m}Tc-MAA kits are stored at 2°C to 8°C before and after labeling. The expiration time after labeling ranges from 6 to 8 hours depending on the manufacturer. The radiochemical purity is not less than 90% of the total radioactivity tagged to albumin particles determined by chromatography. Not more than 10% soluble supernatant impurities may be present, as determined by centrifugation.[99]

Upon intravenous injection, ^{99m}Tc-MAA particles become trapped in obstructed blood vessels downstream from the injection site and in any vessel whose diameter is smaller than the particle size. ^{99m}Tc-MAA is therefore indicated for perfusion lung imaging to assess the presence of pulmonary emboli, for isotope venography to identify lower extremity venous thrombosis, and for assessment of peritoneovenous (LeVeen) shunt patency. The usual adult administered activity of ^{99m}Tc-MAA for perfusion lung imaging is 3 to 4 mCi (111 to 148 MBq) by intravenous injection. The critical organ is the lung, with a radiation absorbed dose of 0.22 rad(cGy)/mCi.[103]

Technetium Tc 99m Apcitide Injection

Technetium Tc 99m apcitide injection (^{99m}Tc-apcitide; AcuTect, Diatide) is a sterile aqueous solution prepared from a kit containing a lyophilized mixture of the peptide bibapcitide (100 μg), sodium glucoheptonate dihydrate (75 mg), and stannous chloride dihydrate (89 μg), adjusted to a pH of 7.4. The kit must be stored at 2°C to 8°C before labeling with ^{99m}Tc-sodium pertechnetate.

The product is prepared by bringing the kit to room temperature and adding up to 50 mCi (1850 MBq) of ^{99m}Tc-sodium pertechnetate in a volume of 1 to 3 mL. Concentrations of ^{99m}Tc-sodium pertechnetate greater than 50 mCi/mL must be diluted with preservative-free normal saline prior to reconstitution. After dissolution of the powder, the vial is placed into a shielded boiling water bath for 15 minutes to cause the labeling reaction, which proceeds as follows:

$$TcO_4^- + \text{Sn-Glucoheptonate} \rightarrow \text{Tc-Glucoheptonate}$$

$$\text{Bibapcitide} + \text{Tc-Glucoheptonate} \xrightarrow{\text{Heat}} \text{Tc-Apcitide}$$

During this time the bibapcitide molecule (Figure 9-13), composed of two apcitide monomers, is split to release apcitide. Apcitide is labeled with ^{99m}Tc by ligand exchange through ^{99m}Tc-glucoheptonate as the transfer agent.[33] The mixture is cooled and stored at 20°C to 25°C and must be used within 6 hours of preparation. The radiochemical purity must be at least 90%, as determined by instant thin-layer chromatography.[104]

^{99m}Tc-apcitide binds to the GP IIb/IIIa receptors on activated platelets via its peptide sequence (-apc-gly-asp), which mimics the -arg-gly-asp peptide sequence in fibrinogen that recognizes the platelet receptor. Platelets become activated when they encounter an injured blood vessel wall, exposing the GP IIb/IIIa receptors. These receptors attract fibrinogen to the platelets, helping to form a thrombus. ^{99m}Tc-apcitide is indicated for the detection of acute venous thrombosis in the lower extremities.[104,105] The usual adult administered activity of ^{99m}Tc-apcitide is 20 mCi (740 MBq). The critical organ is the urinary bladder wall, with a radiation absorbed dose of 0.22 rad(cGy)/mCi.[104]

Technetium Tc 99m Bicisate Injection

Technetium Tc 99m bicisate injection (^{99m}Tc-bicisate or ^{99m}Tc-ECD; Neurolite, DuPont) is a sterile aqueous solution prepared from a kit containing a lyophilized mixture of bicisate dihydrochloride (0.9 mg), disodium edetate dihydrate (0.36 mg) (to solubilize stannous ion), mannitol (24 mg), and stannous chloride dihydrate (72 μg), adjusted to pH 2.7 (pH above 3 decreases kit shelf life) and sealed under nitrogen. The kit also contains a vial of phosphate buffer at pH 7.6. The kit should be stored at 15°C to 25°C and protected from light. Bicisate is also known as ethyl cysteinate dimer (ECD). The chemical structure of the ^{99m}Tc-bicisate complex is shown in Figure 9-20.

The labeled product is prepared in a three-step process by (1) adding 100 mCi of ^{99m}Tc-sodium pertechnetate in a 2 mL volume to the phosphate buffer vial (this raises the pH to optimum for labeling reaction), (2) adding 3 mL of 0.9% sodium chloride injection to the lyophilized bicisate vial, and (3) within 30 seconds, removing 1 mL from the bicisate vial and adding it to the pertechnetate/buffer vial. This final mixture is incubated for 30 minutes at room temperature to effect labeling. Note that no less than 50 mCi should be used, or incomplete labeling may occur. If needed, the ^{99m}Tc-bicisate can be diluted with normal saline only after the product is labeled. The labeled product is stored at 15°C to 25°C and must be used within 6 hours of preparation. The radiochemical purity must be 90% or higher, as determined by instant thin-layer chromatography.[99,106]

^{99m}Tc-bicisate is indicated as an adjunctive procedure to computed tomography (CT) and magnetic resonance imaging (MRI) in the localization of stroke. The usual adult administered activity for brain imaging is 10 to 30 mCi (370 to 1110 MBq) by intravenous injection. The critical organ is the urinary bladder wall, with a radiation absorbed dose of 0.11 rad(cGy)/mCi.[106]

Technetium Tc 99m Depreotide Injection

Technetium Tc 99m depreotide injection (^{99m}Tc-depreotide; NeoTect, Diatide) is a sterile aqueous solution prepared from a kit containing a sterile lyophilized mixture of the synthetic peptide depreotide (50 μg) (Figure 9-14), sodium glucoheptonate dihydrate

(5 mg), stannous chloride dihydrate (50 μg), and disodium EDTA dihydrate (100 μg) at pH 7.4, sealed under nitrogen. The kit is stored at –10°C or lower before labeling. Labeling with ^{99m}Tc is done by bringing the kit to room temperature (20°C to 25°C) and adding from 15 mCi to a maximum of 50 mCi of ^{99m}Tc-sodium pertechnetate in a total volume of 1 mL. Dilution of ^{99m}Tc-sodium pertechnetate solutions should be made only with preservative-free 0.9% sodium chloride injection. After dissolution of the powder, the kit is placed into a boiling water bath or a heated dry block for 10 minutes to effect labeling. During the labeling reaction, the EDTA and glucoheptonate transfer ligands are labeled first, and then the technetium is exchanged with the depreotide.[71] The solution is cooled and stored at room temperature and must be used within 5 hours of preparation. Radiochemical purity must be 90% or higher, as determined by instant thin-layer chromatography.[107]

^{99m}Tc-depreotide binds to somatostatin receptors and is indicated for the localization of receptor-bearing pulmonary masses in patients with CT-identified lesions who have known or highly suspected malignancy. The usual adult administered activity of ^{99m}Tc-depreotide is 15 to 20 mCi (555 to 740 MBq) by intravenous injection. The critical organ is the kidney, with a radiation absorbed dose of 0.33 rad(cGy)/mCi.[107]

Technetium Tc 99m Disofenin Injection

Technetium Tc 99m disofenin injection (^{99m}Tc-disofenin or ^{99m}Tc-DISIDA; Hepatolite, CIS-US) is a sterile aqueous solution prepared from a lyophilized kit containing the complexing ligand disofenin (20 mg) and stannous chloride dihydrate (0.6 mg) at pH 4 to 5, sealed under nitrogen. The chemical name of disofenin is diisopropylacetanilido iminodiacetic acid; its structure is shown in Figure 9-9. The kit is stored at 15°C to 25°C before and after labeling with ^{99m}Tc.

^{99m}Tc-disofenin is prepared by adding 12 to 100 mCi (444 to 3700 MBq) of ^{99m}Tc-sodium pertechnetate in a 4 to 5 mL volume to the kit. The vial is swirled for 1 minute to dissolve the powder and then allowed to incubate at room temperature for 4 minutes to effect complexation of ^{99m}Tc with disofenin. The prepared product has a useful life of 6 hours. The radiochemical purity of the ^{99m}Tc-disofenin complex is not less than 90%.[108]

^{99m}Tc-disofenin is indicated as a hepatobiliary agent in the diagnosis of acute cholecystitis. The usual adult administered activity is 1 to 5 mCi (37 to 185 MBq) by intravenous injection in nonjaundiced patients and 3 to 8 mCi (111 to 296 MBq) in patients whose bilirubin level is greater than 5 mg/dL. The critical organ is the upper large intestinal wall, with a radiation absorbed dose of 0.35 rad(cGy)/mCi.[108]

Technetium Tc 99m Exametazime Injection

Technetium Tc 99m exametazime injection (^{99m}Tc-exametazime or ^{99m}Tc-HMPAO; Ceretec, Amersham) is a sterile aqueous solution prepared from a kit containing a sterile lyophilized mixture of exametazime (0.5 mg), stannous chloride dihydrate (7.6 μg), and sodium chloride (4.5 mg) sealed under nitrogen. Exametazime is also known as hexamethylpropyleneamine oxime, or HMPAO (Figure 9-21). The structural formula of the technetium complex is shown in Figure 9-20. The kit also contains one vial each of 1% methylene blue and a phosphate buffer that, when mixed together, act as a stabilizer. The kit is stored at 15°C to 25°C before labeling and at 20°C to 25°C after labeling with technetium.

^{99m}Tc-exametazime is prepared one of two ways: (1) with or without stabilizer for brain imaging and (2) without stabilizer for labeling leukocytes. The stabilized product is prepared by mixing 0.5 mL of methylene blue 1% with 4.5 mL of phosphate buffer. The lyophilized kit is reconstituted with 10 to 54 mCi (370 to 1998 MBq) of ^{99m}Tc-sodium

pertechnetate, followed within 2 minutes by the addition of 2 mL of the methylene blue/buffer mixture, which confers product stability for 4 hours. Because the product is blue and opaque to visualization, it must be injected through a 0.45 μm membrane filter supplied with the kit to remove any particulate matter that may be present in the solution. Unstabilized ^{99m}Tc-exametazime, which is used for labeling leukocytes, is prepared by reconstituting the lyophilized powder with 10 to 54 mCi (370 to 1998 MBq) of ^{99m}Tc-sodium pertechnetate in a volume of 5 mL. Because the methylene blue stabilizer is not mixed with this product, it has a useful life of only 30 minutes and therefore must be prepared close to the time of need.

The ^{99m}Tc-exametazime formed in the kit is the D,L-HMPAO complex, which is lipophilic and shows high brain retention because of its conversion in vivo, via reduction by glutathione, to the hydrophilic complex, which is trapped in tissue. This lipophilic-complex to hydrophilic-complex conversion can also occur in vitro, being enhanced by heat, nucleophiles (e.g., thiols), free radicals, and high stannous ion concentration, and is the reason for the limited shelf life without stabilization.[109] The kit is formulated with small amounts of stannous ion to limit in vitro decomposition. Kits in North America are stabilized with methylene blue, which acts as a free radical scavenger and as an oxidizer of the excess stannous ion remaining after the reduction/complexation reaction. Kits in Europe are stabilized with cobalt chloride ($CoCl_2$), which serves the same functions as methylene blue.[71]

Because the kit contains such a small amount of stannous chloride, it is recommended that, to obtain the highest radiochemical purity product, the ^{99m}Tc-sodium pertechnetate solution used be obtained from a generator previously eluted within 24 hours and that eluate not more than 30 minutes old be used for brain imaging and eluate not more than 2 hours old, for leukocyte labeling. These precautions will reduce the amount of radiolytic products (free radicals) and "carrier" ^{99}Tc added to the kit. The radiochemical purity of ^{99m}Tc-exametazime must be not less than 80% as determined by instant thin-layer chromatography.[99,109]

^{99m}Tc-exametazime, with or without stabilization, is indicated for the detection of altered cerebral perfusion in stroke. The usual adult administered activity is 10 to 30 mCi (370 to 1110 MBq), and the critical organ is the lacrimal glands, with an absorbed dose of 0.258 rad(cGy)/mCi. Unstabilized ^{99m}Tc-exametazime labeled to autologous leukocytes is indicated for the localization of intra-abdominal infection and inflammatory bowel disease. The usual adult administered activity is 7 to 25 mCi (259 to 925 MBq), and the critical organ is the spleen, with an absorbed dose of 0.556 rad(cGy)/mCi.[109]

Technetium Tc 99m Gluceptate Injection

Technetium Tc 99m gluceptate injection (^{99m}Tc-gluceptate or ^{99m}Tc-GH) is a sterile aqueous solution prepared from a lyophilized kit that contains gluceptate calcium (50 mg) and stannous chloride dihydrate (1.1 mg), which is adjusted to pH 6.9 to 7.1 and sealed under nitrogen. The kit, using the same formulation, is available from Mallinckrodt and Drax-Image. The kit is stored at 2°C to 30°C before labeling and at 2°C to 8°C after labeling with technetium. Gluceptate, otherwise known as glucoheptonate, is a seven-carbon carboxylic acid sugar whose chemical structure is shown in Figure 9-34.

The ^{99m}Tc-gluceptate complex is prepared by adding up to 300 mCi (11,100 MBq) in 2 to 10 mL of ^{99m}Tc-sodium pertechnetate solution to the kit and letting it stand at room temperature for 15 minutes to effect labeling. The labeled product is stable for 6 hours after preparation. The radiochemical purity, determined by instant thin-layer chromatography, is not less than 90% as the ^{99m}Tc-gluceptate complex.[99]

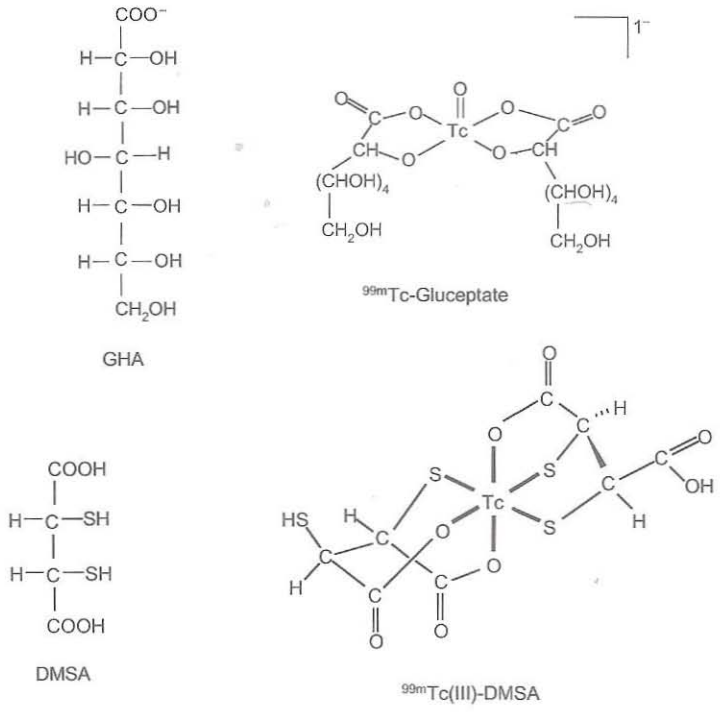

FIGURE 9-34 Chemical structures of glucoheptonic acid (GHA) and 2,3-dimercaptosuccinic acid (DMSA) ligands and their respective ^{99m}Tc complexes.

^{99m}Tc-gluceptate is indicated for use in brain and kidney imaging. The usual adult administered activity is 15 to 20 mCi (555 to 740 MBq) for brain imaging and 10 to 15 mCi (370 to 555 MBq) for kidney imaging, given intravenously. The critical organ is the renal cortex, with a radiation absorbed dose of 0.24 rad(cGy)/mCi.[110]

Technetium Tc 99m Mebrofenin Injection

Technetium Tc 99m mebrofenin injection (^{99m}Tc-mebrofenin or ^{99m}Tc-BRIDA; Choletec, Bracco) is a sterile aqueous solution prepared from a lyophilized kit sealed under nitrogen containing the complexing ligand mebrofenin (45 mg), stannous fluoride dihydrate (1.03 mg), and methylparaben (5.2 mg) and propylparaben (0.58 mg) as preservatives. The pH of the reconstituted product is 4.2 to 5.7. Mebrofenin is a methyl- and bromine-substituted acetanilido iminodiacetic acid analogue; its chemical structure is shown in Figure 9-9. The kit is stored before and after labeling with technetium at 20°C to 25°C.

^{99m}Tc-mebrofenin is prepared by adding up to 100 mCi (3700 MBq) in 1 to 5 mL of ^{99m}Tc-sodium pertechnetate solution to the kit and allowing it to stand at room temperature for 15 minutes to effect labeling. The labeled product is stable for 18 hours because it contains a preservative. The radiochemical purity of the ^{99m}Tc-mebrofenin complex is not less than 90%.[99]

^{99m}Tc-mebrofenin is indicated for use as a hepatobiliary imaging agent. The usual adult administered activity is 2 to 5 mCi (74 to 185 MBq) in nonjaundiced patients and 3 to 10 mCi (111 to 370 MBq) in patients with bilirubin levels greater than 1.5 mg/dL. The critical organ is the upper large intestinal wall, with a radiation absorbed dose of 0.248 rad(cGy)/mCi.[111]

TABLE 9-11 Properties of ^{99m}Tc-Medronate and ^{99m}Tc-Oxidronate Kits

Manufacturer	Composition[a] Component	Amount	Maximum Activity/Vol (Labeling Time)	Storage Conditions Before Labeling	After Labeling	Expiration Time
Bracco	Medronic acid	20 mg	500 mCi	20–25°C	2–8°C	6 hr
	SnF_2	0.38 mg	0.5–5 mL			
	Ascorbic acid	1.0 mg	(1 to 2 min)			
CIS-US	Medronate Na_2	10 mg	200 mCi	20–25°C	20–25°C	6 hr
	$SnCl_2 \cdot 2H_2O$	1.15 mg	2–8 mL			
			(1 to 2 min)			
DraxImage	Medronic acid	10 mg	500 mCi	2–30°C	2–30°C	6 hr
	$SnCl_2 \cdot 2H_2O$	1.21 mg	(immediate)			
	PABA	2.0 mg				
Mallinckrodt	Oxidronate Na	3.15 mg	300 mCi	20–25°C	20–25°C	8 hr
	$SnCl_2 \cdot 2H_2O$	0.297 mg	3–6 mL			
	Gentisic acid	0.84 mg	(30 sec)			
Nycomed/ Amersham	Medronic acid	10 mg	No max listed	≤25°C	≤25°C	6 hr
	$SnCl_2 \cdot 2H_2O$	0.29 mg	2–8 mL			
	Ascorbic acid	2.0 mg	(1 to 2 min)			

[a] Stannous chloride and stannous fluoride are maximum amounts (as stannous and stannic salt) per kit.

Technetium Tc 99m Medronate Injection

Technetium Tc 99m medronate injection (^{99m}Tc-medronate or ^{99m}Tc-MDP) is a sterile aqueous solution prepared from a lyophilized kit containing medronic acid and stannous chloride. Medronate is otherwise known as methylene diphosphonic acid (MDP); its chemical structure is shown in Figure 9-8. Kits are available from several manufacturers; kit properties are shown in Table 9-11.

^{99m}Tc-medronate is prepared by adding the specified amount of activity and volume of ^{99m}Tc-sodium pertechnetate to the kit and mixing for a maximum of 1 to 2 minutes to effect labeling. Several kits are formulated with antioxidant stabilizer (gentisic acid or ascorbic acid) to protect the relatively labile complex from degradation by oxygen and radiolytically generated free radicals. The radiochemical purity should be no less than 90%, as determined by instant thin-layer chromatography.[99]

^{99m}Tc-medronate is indicated as a bone-imaging agent to delineate areas of altered osteogenesis due to various causes. It is frequently used to identify metastatic bone lesions from breast and prostate cancer. The usual adult administered activity is 10 to 20 mCi (370 to 740 MBq) by intravenous injection. The critical organ is the urinary bladder wall, with a radiation absorbed dose of 0.13 rad(cGy)/mCi (2 hour void).[112]

Technetium Tc 99m Mertiatide Injection

Technetium Tc 99m mertiatide injection (^{99m}Tc-mertiatide or ^{99m}Tc-MAG3; TechneScan MAG3, Mallinckrodt) is a sterile aqueous solution prepared from a kit that contains a lyophilized mixture of betiatide (1 mg), stannous chloride dihydrate (0.2 mg), sodium tartrate dihydrate (40 mg), and lactose monohydrate (20 mg) sealed under argon. The chemical structures of the betiatide ligand and ^{99m}Tc-mertiatide are shown in Figure 9-24. The kit should be stored at 15°C to 30°C and protected from light before labeling with technetium.

^{99m}Tc-mertiatide is prepared by inserting a venting needle into the kit and then injecting 20 to 100 mCi (740 to 3700 MBq) of ^{99m}Tc-sodium pertechnetate in a 4 to 10 mL volume. The ^{99m}Tc-sodium pertechnetate should not be more than 6 hours old. The plunger on the ^{99m}Tc syringe is pulled back to remove 2 mL of argon gas and introduce air into the vial. The air is required to oxidize the excess stannous ion to ensure a high radiochemical purity, possibly by preventing further reduction of Tc(V) to Tc(IV). The vial is immediately placed into a shielded boiling water bath for 10 minutes. The vial must be placed in the water bath within 5 minutes of adding the pertechnetate solution. During the heating step, the labile ligand transfer agent Tc-tartrate is formed and the benzoyl-protecting group on betiatide is hydrolyzed, permitting transfer of reduced technetium to the mertiatide ligand. The vial is then cooled for 15 minutes before use. The pH of the reconstituted product is between 5 and 6. The labeled product is stored at 15°C to 30°C and must be used within 6 hours of preparation. The radiochemical purity must be 90% or higher, as determined with Sep-Pak C18 (Waters) reverse-phase mini-column chromatography.[99,113] Factors that can potentially reduce radiochemical purity are using more than 100 mCi (3700 MBq) and less than 4 mL to reconstitute the kit, waiting longer than 5 minutes to place the vial into the boiling water bath, and not adding air to the reaction vial.[113]

^{99m}Tc-mertiatide is indicated for renal imaging for the diagnosis of congenital and acquired abnormalities, renal failure, urinary tract obstruction, and calculi. It is a diagnostic aid in renal function and split function studies, renal angiograms, and renogram curves for whole kidney and renal cortex. The usual adult administered activity is 5 to10 mCi (185 to 370 MBq) by intravenous injection. The critical organ is the urinary bladder wall, with a radiation absorbed dose of 0.48 rad(cGy)/mCi.[114]

Technetium Tc 99m Oxidronate Injection

Technetium Tc 99m oxidronate injection (^{99m}Tc-oxidronate or ^{99m}Tc-HDP; TechneScan HDP, Mallinckrodt) is a sterile aqueous solution prepared from a kit that contains oxidronate sodium (3.15 mg) (structure shown in Figure 9-8), stannous chloride dihydrate (0.297 mg), gentisic acid (0.84 mg) as an antioxidant stabilizer, and sodium chloride (30 mg), sealed under nitrogen. The kit should be stored at 20°C to 25°C before and after labeling with ^{99m}Tc-sodium pertechnetate.

^{99m}Tc-oxidronate is prepared by adding up to 300 mCi (11,100 MBq) of ^{99m}Tc-sodium pertechnetate in 3 to 6 mL volume and mixing for 30 seconds. The pH of the reconstituted product is between 4 and 5.5, and it is stable for 8 hours after preparation. The radiochemical purity must be no less than 90%, as determined by instant thin-layer chromatography.[99]

^{99m}Tc-oxidronate is indicated as a diagnostic skeletal imaging agent used to demonstrate areas of altered osteogenesis. The usual adult administered activity is 10 to 20 mCi (370 to 740 MBq) by intravenous injection. The critical organ is the bone surface, with a radiation absorbed dose of 0.322 rad(cGy)/mCi.[115]

Technetium Tc 99m Pentetate Injection

Technetium Tc 99m pentetate injection (^{99m}Tc-pentetate or ^{99m}Tc-DTPA) is a sterile aqueous solution prepared from a kit containing a lyophilized mixture of DTPA, stannous chloride, and other adjuvants sealed under nitrogen (Table 9-12). Some kits contain calcium, which was added as a precautionary measure when DTPA preparations were first being developed for cisternographic studies; this reduces the chance of depleting this ion in CSF. One kit contains paraaminobenzoic acid (PABA) as a free-radical scavenger, which increases the shelf life of the kit. The chemical structure of DTPA is shown in Figure 9-8.

TABLE 9-12 Properies of ^{99m}Tc-Pentetate (^{99m}Tc-DTPA) Kits

Manufacturer	Composition[a]		Maximum Activity/Vol (Labeling Time)	Storage Conditions		Expiration Time
	Component	Amount		Before Labeling	After Labeling	
Bracco	Pentetate-Na_5	5 mg	No amount listed	20–25°C	20–25°C	6 hr
(Techneplex)	$SnCl_2 \cdot 2H_2O$	0.275 mg	2–8 mL			1 hr
			(1 to 2 min)			(GFR studies)
CIS-US	Pentetate-Ca-Na_3	20.6 mg	160 mCi	15–30°C	15–30°C	6 hr
(CIS-DTPA)	$SnCl_2 \cdot 2H_2O$	0.30 mg	1–8 mL			1 hr
			(1 to 2 min)			(GFR studies)
DraxImage	Pentetic acid	20 mg	500 mCi	2–25°C	2–25°C	12 hr
	$SnCl_2 \cdot 2H_2O$	0.385 mg	2–10 mL			
	PABA	5.0 mg	(15 min)			
	$CaCl_2 \cdot 2H_2O$	3.73 mg				

[a] Stannous chloride and stannous fluoride are maximum amounts (as stannous and stannic salt) per kit.

^{99m}Tc-pentetate is prepared by simply adding the required amount of ^{99m}Tc-sodium pertechnetate and allowing the kit to stand for a few minutes to effect labeling. The pH of the reconstituted product is between 3.8 and 7.5, and it is stable for 6 to 12 hours, depending on the kit. The radiochemical purity must be 90% or higher.[99]

^{99m}Tc-pentetate is indicated for use in brain and kidney imaging, to assess renal perfusion, and to estimate GFR. Although ^{99m}Tc-pentetate has a long shelf life, it must be used within 1 hour of preparation for GFR studies in accordance with FDA-approved labeling for this application. ^{99m}Tc-pentetate is also used for other applications, as an aerosol for lung ventilation studies (FDA approved) and in CSF leak studies (not FDA approved). Typical administered activities are 3 mCi (GFR measurement), 5 to 10 mCi (185 to 370 MBq) (renal perfusion), and 10 to 20 mCi (370 to 740 MBq) (brain imaging). The critical organ is the bladder wall, with a radiation absorbed dose of 0.115 rad(cGy)/mCi (2 hour void) and 0.27 rad(cGy)/mCi (4.8 hour void).[116]

Technetium Tc 99m Pyrophosphate Injection

Technetium Tc-99m pyrophosphate injection (^{99m}Tc-pyrophosphate or ^{99m}Tc-PPi) is a sterile aqueous solution prepared from a kit containing a sterile lyophilized mixture of sodium pyrophosphate and stannous chloride sealed under nitrogen. Kits are available from several manufacturers (Table 9-13). One kit (Pyrolite, CIS-US) is formulated with a trimetaphosphate that also complexes with technetium and localizes in bone.[117] The chemical structures of pyrophosphate and trimetaphosphate are shown in Figure 9-8.

^{99m}Tc-pyrophosphate is prepared by simply adding the required amount of ^{99m}Tc-sodium pertechnetate and allowing the kit to stand for a few minutes to effect labeling. The reconstituted product has a pH between 4.0 and 7.5 and is stable for 6 hours. The radiochemical purity must be 90% or higher.[99]

For use as a source of tin for labeling red blood cells for blood pool imaging, the kit is reconstituted with 0.9% sodium chloride injection, and stannous pyrophosphate is injected 5 to 60 minutes before administration of ^{99m}Tc-sodium pertechnetate for in vivo RBC labeling.

^{99m}Tc-pyrophosphate is indicated for bone and cardiac (infarct-avid) imaging with an administered activity of 15 mCi (555 MBq). The critical organ is the bladder wall, with a radiation absorbed dose of 0.23 rad(cGy)/mCi (4.8 hour void).[118]

TABLE 9-13 Properties of ^{99m}Tc-Stannous Pyrophosphate Kits

Manufacturer	Composition[a] Component	Amount	Maximum Activity/Vol (Labeling Time)	Storage Conditions Before Labeling	After Labeling	Expiration Time
Bracco	Sodium pyrophosphate	40 mg	75 mCi/4 mL	2–8°C	2–8°C	6 hr
(Phosphotec)	SnF_2	0.9 mg	(Immediate)			
CIS-US	Sodium pyrophosphate	12 mg	100 mCi/10 mL	15–30°C	15–30°C	6 hr
(CIS-PYRO)	$SnCl_2 \cdot 2H_2O$	4.9 mg	(10 minutes)			
CIS-US	Sod pyrophosphate	10 mg	200 mCi/7 mL	20–25°C	20–25°C	6 hr
(Pyrolite)	Sodium trimetaphosphate	30 mg	(1 minute)			
	$SnCl_2 \cdot 2H_2O$	1.8 mg				
Mallinckrodt	Sodium pyrophospate	11.9 mg	100 mCi/10 mL	2–8°C	20–25°C	6 hr
(TechneScan PYP)	$SnCl_2 \cdot 2H_2O$	4.4 mg	(5 minutes)			

[a] Stannous chloride and stannous fluoride are maximum amounts (as stannous and stannic salt) per kit.

Technetium Tc 99m Red Blood Cells (In Vitro Method)

The in vitro method for preparing ^{99m}Tc-labeled red blood cells (^{99m}Tc-RBCs) was perfected with a kit developed at Brookhaven.[119,120] It consisted of a 10 mL Vacutainer (Becton, Dickinson) tube containing a lyophilized mixture of stannous ion 2.0 μg, sodium citrate 3.67 mg, dextrose 5.5 mg, and sodium chloride 0.11 mg. Labeling was achieved by adding 4 mL of whole blood and isolating the "tinned" red cells by centrifugation prior to mixing with pertechnetate. This technique was eventually modified by Srivastava[121] to permit labeling in whole blood without isolating packed red cells. The method involves mixing anticoagulated whole blood with stannous citrate to "tin" RBCs, adding sodium hypochlorite to oxidize excess extracellular stannous ion, and adding ^{99m}Tc-sodium pertechnetate to label the cells. The oxidation of the excess stannous ion prevents extracellular reduction of pertechnetate and permits high labeling efficiency intracellularly (approximately 98%). A commercial kit (Ultratag RBC, Mallinckrodt) based on this method is available. The blood cells are usually autologous, but they may be donor cells if carefully typed and cross-matched and checked for viral contamination. The kit consists of three components:

1. 10 mL reaction vial: Lyophilized mixture of stannous chloride dihydrate 105 μg, sodium citrate dihydrate 3.67 mg, and dextrose anhydrous 5.5 mg at pH 7.1 to 7.2.
2. Syringe I: sodium hypochlorite 0.6 mg in 0.6 mL at pH 11 to 13.
3. Syringe II: citric acid monohydrate 8.7 mg, sodium citrate dihydrate 32.5 mg, and dextrose anhydrous 12 mg in total volume of 1.0 mL at pH 4.5 to 5.5.

The cells are labeled as follows:

1. Collect 1 to 3 mL patient's blood. Use a maximum of 0.15 mL acid citrate dextrose (ACD) or 10 to 15 units heparin per mL blood. Do not use EDTA or oxalate as anticoagulants.
2. Transfer blood to the reaction vial to dissolve crystals. Incubate 5 minutes.
3. Add contents of syringe I. Mix by gentle inversion 5 times.
4. Add contents of syringe II. Mix by gentle inversion 5 times.
5. Add 10 to 100 mCi (370 to 3700 MBq) ^{99m}Tc-sodium pertechnetate in up to 3 mL.
6. Mix gently 5 times. Incubate 20 minutes to label cells.

Adding RBCs to the reaction vial causes a portion of the stannous ion to cross the red cell membrane into the cell. Too much ACD impairs this diffusion process; this is the reason for limiting the amount used. Not all of the stannous ion enters the cells, and sodium hypochlorite is added to oxidize this extracellular stannous ion. This is effective because hypochlorite cannot cross the red cell membrane to oxidize intracellular tin. The citrate solution in syringe II is added to sequester excess extracellular stannous ion to enhance its oxidation by hypochlorite. At this point ^{99m}Tc-sodium pertechnetate is added, and it readily diffuses into the cells, encounters intracellular stannous ion, and becomes reduced and bound in the cell. If extracellular stannous ion were present, it would reduce the ^{99m}Tc-sodium pertechnetate extracellularly and prevent it from entering the cell. This would lower the labeling efficiency.

Radiochemical purity can be checked by mixing 0.2 mL of ^{99m}Tc-RBCs with 2 mL saline and centrifuging. Assay of the supernatant (unbound activity) and the red cell precipitate (bound activity) provides a measure of labeling efficiency. The labeling efficiency must be no less than 90%[99] and is typically greater than 95 %.[122]

^{99m}Tc-RBCs are a blood-pool imaging agent indicated for cardiac imaging and for the detection of gastrointestinal bleeding, with an intravenous dosage range of 10 to 20 mCi (370 to 740 MBq). The critical organ is the spleen, with a radiation absorbed dose of 0.11 rad/mCi.[122]

Technetium Tc 99m Red Blood Cells (In Vivo Method)

The in vivo method of labeling red cells was first suggested by Pavel et al.[123] and Stokely et al.[124] for use in cardiac blood pool studies. The method is based on the intravenous injection of stannous pyrophosphate (Sn-PPi) 20 minutes to 24 hours prior to intravenous administration of ^{99m}Tc-sodium pertechnetate, which then labels the tinned red cells. The Pavel technique involves reconstituting one vial of TechneScan PYP (Mallinckrodt) (which contains an average of 15.7 mg Sn-PPi and, on average, about 2 mg Sn^{2+}) with 5 mL normal saline and injecting the patient with 1.4 mg Sn-PPi per 1000 mL whole blood volume. According to these parameters, the average 70 kg adult male (with approximately 5400 mL whole blood) would receive about 7.5 mg Sn-PPi (one-half vial) per dose, equivalent to approximately 15 μg Sn(II)/kg. Within 20 to 30 minutes of injecting the Sn-PPi, 15 to 25 mCi (555 to 925 MBq) of ^{99m}Tc-sodium pertechnetate is administered intravenously to label the red cells for blood pool imaging. Hamilton et al.[125] investigated the amounts of stannous ion required to label red cells and reported that the maximal in vivo labeling efficiency is obtained with an intravenous dose of 10 μg Sn (II)/kg or greater. Although Pavel et al. reported labeling efficiencies of approximately 96%, Callahan et al.[126] noted that when this technique was used for gastrointestinal bleeding studies, variable amounts of gastric and urinary activity interfered with the study. Investigation into the possible causes of this extravascular activity led to the deduction that, immediately after intravenous injection of free pertechnetate with the in vivo method, there occurs a competition for pertechnetate between the red cells and the extracellular fluid space, gastric mucosa, thyroid, and salivary glands. This led to the development of the modified in vivo method for labeling red cells.[126]

Technetium Tc 99m Red Blood Cells (Modified In Vivo Method)

The modified in vivo method was developed to increase the labeling efficiency of ^{99m}Tc-RBCs and provide a firm label prior to intravenous injection.[126] With this technique, the patient receives approximately 500 μg of stannous ion as Sn-PPi from a Pyrolite (CIS-US) kit intravenously. Twenty minutes later, 3 mL of tinned red blood cells is withdrawn through a

heparinized winged infusion set into a shielded syringe containing 20 mCi (740 MBq) of ^{99m}Tc-sodium pertechnetate. The mixture is incubated for 10 minutes with gentle agitation and then reinjected into the patient. Labeling yields higher than 90% are achieved with this method because the red cells compete for ^{99m}Tc-sodium pertechnetate with only the plasma in the syringe.

Labeling Mechanism of ^{99m}Tc-Red Blood Cells

After incubation of stannous pyrophosphate with red blood cells, some of the stannous ion crosses the cell membrane, apparently transported by a specific transport system[127] inside the cell, where the stannous ion is believed to be associated with an intracellular protein.[128] The pertechnetate anion can readily diffuse into the cell, become reduced by the stannous ion, and subsequently bind to hemoglobin, which prevents it from diffusing back out of the cell.[128] In vitro studies have shown that within the hemoglobin molecule approximately 20% of ^{99m}Tc and 90% of tin are associated with heme, and 80% of ^{99m}Tc and 10% of tin are associated with globin.[129] Transport studies in human erythrocytes have demonstrated that the pertechnetate anion is transported across the membrane via the band-3 protein transport system in exchange for chloride or bicarbonate ion.[130] It is worth noting that dipyridamole can inhibit this transport; this may be a factor in decreasing the labeling efficiency of red cells in patients who receive therapeutic or diagnostic doses of this drug.[130]

In humans, the biologic half-life in blood of ^{99m}Tc-RBCs prepared by the in vitro technique is biexponential, with 5% of the activity having a 20 minute half-life and 95% having a 29 hour half-life.[131] Cells labeled in vivo are assumed to behave with a normal biologic half-life of red cells (i.e., about 80 days).

Technetium Tc 99m Sestamibi Injection

Technetium Tc 99m sestamibi injection (^{99m}Tc-sestamibi) is a sterile aqueous solution prepared from a kit consisting of a lyophilized mixture of tetrakis (2-methoxy isobutyl isonitrile) copper (I) tetrafluoroborate (1.0 mg), sodium citrate dihydrate (2.6 mg), L-cysteine HCl monohydrate (1.0 mg), mannitol (20 mg), and stannous chloride dihydrate (0.025 to 0.075 mg) sealed under nitrogen. ^{99m}Tc-sestamibi is prepared by adding 25 to 150 mCi (925 to 5550 MBq) of ^{99m}Tc-sodium pertechnetate in 1 to 3 mL volume to the kit and mixing vigorously to dissolve the powder. The vial is then placed into a boiling water bath for 10 minutes. During this time the following reactions take place:[71]

$$\text{Step 1.}\quad TcO_4^- + \text{citrate} \xrightarrow{Sn^{2+}} \text{Tc-citrate}$$

$$\text{Step 2.}\quad \left[Cu(I)(MIBI)_4\right]^+ + \text{Tc-citrate} \xrightarrow{\text{heat}} \left[Tc(I)(MIBI)_6\right]^+$$

The vial is allowed to cool 15 minutes before use. The labeled product is stored at 15°C to 25°C and is stable for 6 hours. Its radiochemical purity is 90% or higher.[99] The chemical structure of ^{99m}Tc-sestamibi is shown in Figure 9-18.

The sestamibi kit is sold under two trade names, Cardiolite (DuPont Merck) for heart imaging and Miraluma (DuPont Merck) for breast imaging. The composition and labeling of these kits are identical. ^{99m}Tc-sestamibi is indicated for myocardial perfusion studies in a dosage range of 10 to 30 mCi (370 to 1110 MBq) and for breast imaging to confirm the

presence or absence of malignancy in a dosage range of 20 to 30 mCi (740 to 1110 MBq). Because of its lipophilicity, the principal route of excretion is hepatobiliary, and the critical organ is the upper large intestinal wall, with a radiation absorbed dose of 0.15 rad/mCi after stress injection and 0.18 rad(cGy)/mCi after rest injection.[132]

Technetium Tc 99m Succimer Injection

Technetium Tc 99m succimer injection (^{99m}Tc-succimer or ^{99m}Tc-DMSA) is a sterile aqueous solution prepared from a kit consisting of a lyophilized mixture of DMSA (1.0 mg) and stannous chloride dihydrate (0.42 mg), ascorbic acid (0.70 mg), and inositol (50 mg) sealed under nitrogen. The kit is stored at 2°C to 8°C.

Kit labeling is accomplished by adding up to 40 mCi (1480 MBq) ^{99m}Tc-sodium pertechnetate in a 1 to 6 mL volume to the vial and incubating for 10 minutes. During this time the following reactions take place:

$$\mathrm{Sn(II)DMSA} + \mathrm{TcO_4^-} \xrightarrow{\text{fast}} \text{Tc-DMSA (Complex I)}$$

$$\text{Tc-DMSA (Complex I)} \xrightarrow{10\ \text{min}} \text{Tc-DMSA (Complex II)}$$

The resulting product has a pH between 2 and 3 and is stable for 4 hours. Its radiochemical purity must be 85% or higher.[99] The chemical structure of DMSA and proposed structure of ^{99m}Tc-DMSA are shown in Figure 9-34.[133]

Ikeda et al.[134,135] demonstrated that four possible Tc-DMSA complexes can form when pertechnetate and Sn(II) DMSA are reacted. Complex II has the highest kidney uptake. The maximum yield of Complex II is achieved at pH 2.5 in the absence of oxygen. Urinary excretion with no kidney uptake occurs at higher pH values. Kidney localization of complexes prepared at one pH is not appreciably altered if the pH is later changed.[134,136] Complex II formed at pH 2.5 will revert to Complex IV if the pH is raised, but kidney localization diminishes by only 25%.[134] Complexes formed at neutral pH do not localize in the kidney if the pH is subsequently lowered to 2.5. Ikeda et al.[134] believed that Complex I is Tc(IV)DMSA and Complex II is Tc(III)DMSA, although this has not been confirmed. A Tc(V)DMSA complex, prepared at alkaline pH,[137,138] has been shown to have an affinity for tumors. Its chemical structure has been characterized to be $[TcO(DMSA)_2]^-$ (Figure 9-35) as three possible isomers, and its properties have been shown to be the same as those of Tc(V)DMSA.[138]

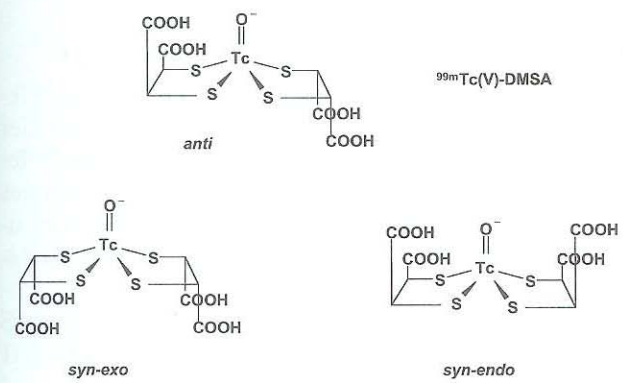

FIGURE 9-35 Geometrical isomers of $Tc^{V}O(DMSA)_2$. (Reprinted with permission from reference 138.)

The labeling reaction of ^{99m}Tc-DMSA proceeds in two steps: rapid formation of Complex I followed by a slower, rate-determining step from Complex I to Complex II, the latter being greatly affected by oxygen.[134] This is the reason for a 10 minute incubation period. Once Complex II is formed, it may revert back to Complex I by oxidation. This occurs because of the oxidation of Sn(II) to Sn(IV), which lowers the reduction potential of the system. Diminished kidney uptake occurs because Complex I is readily excreted. In addition to decreased kidney uptake, increased liver activity has been reported when a ^{99m}Tc-DMSA solution was injected 20 minutes after 1 mL of air was added to the reaction vial of an unstabilized kit.[139] The inclusion of ascorbic acid in present-day kits retards this oxidation.

^{99m}Tc-DMSA is indicated for kidney imaging for evaluation of renal parenchymal disorders. The usual adult administered activity is 5 mCi (185 MBq). The critical organ is the renal cortex, with a radiation absorbed dose of 0.85 rad(cGy)/mCi.[140]

Technetium Tc 99m Sulfur Colloid Injection

Technetium Tc 99m sulfur colloid injection (^{99m}Tc-sulfur colloid or ^{99m}Tc-SC) is a sterile colloidal dispersion of sulfur particles labeled with ^{99m}Tc and prepared from a kit (CIS-Sulfur Colloid Kit, CIS-US). The kit consists of three components: (1) a reaction vial containing a lyophilized mixture of 2.0 mg anhydrous sodium thiosulfate (the source of sulfur), 2.3 mg disodium edetate (Al^{3+} ion chelator), and 18.1 mg gelatin (protective colloid); (2) a Solution A vial with 1.8 mL of 0.148 M hydrochloric acid; and (3) a Solution B vial with 1.8 mL of 24.6 mg/mL anhydrous sodium biphosphate and 7.9 mg/mL sodium hydroxide. The kit should be stored at 15°C to 30°C.

^{99m}Tc-sulfur colloid is prepared by adding 1 to 3 mL of ^{99m}Tc-sodium pertechnetate (not more than 500 mCi [18,500 MBq] in each mL) to the reaction vial to dissolve the powder. After the addition of 1.5 mL of Solution A (acid), the vial is placed into a boiling water bath for 5 minutes. At the end of boiling, the vial is cooled, and 1.5 mL of Solution B (buffer) is added. The pH of the final mixture is between 4.5 and 7.5 and radiochemical purity must be 92% or higher.[99] The labeled product is stable for 6 hours stored at 15°C to 30°C.

The chemistry of ^{99m}Tc-sulfur colloid has been extensively reviewed.[6] During the boiling incubation step of the acidified mixture, thiosulfate is hydrolyzed, releasing elemental sulfur. The sulfur atoms aggregate to form colloid-sized particles. Gelatin, as a protective colloid, controls particle size and aggregation by coating the sulfur particles with a protective charged protein sheath that causes the particles to repel each other. Also during the incubation step, technetium heptasulfide is formed and becomes incorporated into the sulfur particles. These reactions are summarized below:

$$S_2O_3^{2-} + H^+ \xrightarrow{\text{Heat}} S + HSO_3^-$$

$$2\ TcO_4^- + 7S_2O_3^{2-} \xrightarrow{\text{Heat}} Tc_2S_7 + 7SO_4^{2-} + H_2O$$

The EDTA in the formulation chelates any aluminum ion that may be present in the ^{99m}Tc-sodium pertechnetate solution. Any free aluminum ion reacts with the phosphate buffer to form insoluble aluminum phosphate, which precipitates from solution and carries ^{99m}Tc-sulfur colloid with it. Such a product would localize in the lungs. Figure 9-36 illustrates a microscopic view of a normal ^{99m}Tc-sulfur colloid preparation and the results of formulation changes with gelatin omitted and EDTA omitted. Figure 9-37 illustrates the stabilizing effect of EDTA against aluminum phosphate flocculation.

^{99m}Tc-sulfur colloid is indicated for several uses in various dosages: imaging the RES (liver and spleen, 1 to 8 mCi [37 to 296 MBq]); in bone marrow studies, 3 to 12 mCi (111

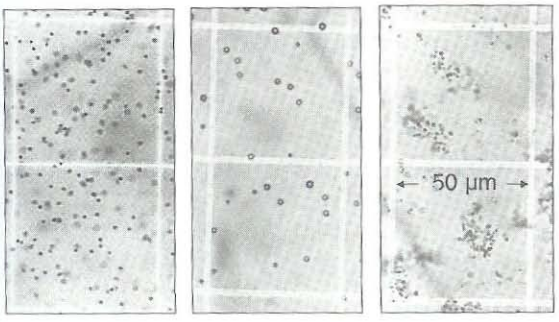

FIGURE 9-36 Photomicrographs of sulfur colloid prepared with gelatin, without gelatin, and without EDTA. Product prepared without gelatin has larger particle size. Product prepared without EDTA shows sulfur colloid particles coprecipitated with flocculated particles of aluminum phosphate. Magnification ×450.

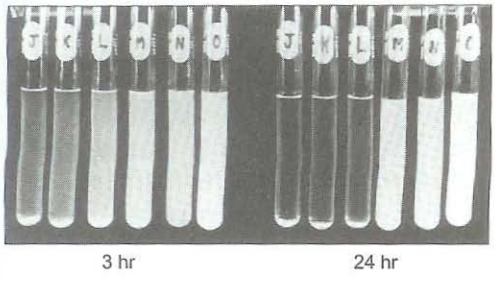

FIGURE 9-37 Stabilizing effect of EDTA against aluminum phosphate flocculation in ^{99m}Tc-sulfur colloid. EDTA-to-Al ion molar ratio: J, 0.125; K, 0.25; L, 0.5; M, 1.0; N, 2.0; O, 4.0. Note gradual improved stabilization in the 3 hour samples as the ratio increases.

to 444 MBq); to evaluate the patency of peritoneovenous (LeVeen) shunts; and in oral preparations for esophageal transit studies, gastroesophageal reflux studies, and pulmonary aspiration studies. It is also used in lymphoscintigraphy. The critical organ after intravenous injection is the liver, with a radiation absorbed dose of 0.34 rad(cGy)/mCi.[141]

Technetium Tc 99m Tetrofosmin Injection

Technetium Tc 99m tetrofosmin (^{99m}Tc-tetrofosmin; Myoview, Amersham) injection is a sterile aqueous solution prepared from a kit containing a lyophilized mixture of tetrofosmin (0.23 mg), stannous chloride dihydrate (30 μg), disodium sulfosalicylate (0.32 mg), sodium D-gluconate (1.0 mg), and sodium bicarbonate (1.8 mg) sealed under nitrogen. The kit is stored at 2°C to 8°C before reconstitution.

Labeling of tetrofosmin is accomplished by introducing a venting needle to the kit and adding up to 240 mCi (8880 MBq) of ^{99m}Tc-sodium pertechnetate (in 4 to 8 mL volume and not more than 30 mCi/mL concentration). This is followed by removal of 2 mL of gas from the vial and incubation at room temperature for 15 minutes. During this time the following reaction sequence occurs:[71]

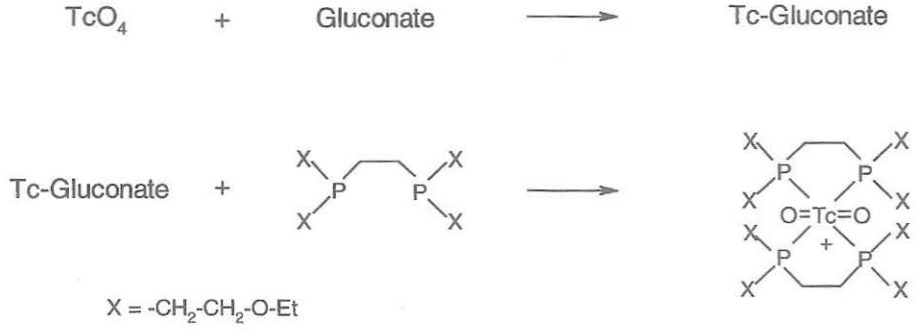

This reaction employs a gluconate transfer ligand to facilitate the complexation reaction between the technetium oxo core and tetrofosmin. Since the tetrofosmin ligand is neutral, the ^{99m}Tc-tetrofosmin complex has an overall charge of 1+ from the $O{=}Tc{=}O^{1+}$ core. The labeled product is stored at 2°C to 25°C after technetium labeling and is stable for 8 hours. Its radiochemical purity must be no less than 90%.[99]

^{99m}Tc-tetrofosmin is indicated for imaging the heart to assess myocardial perfusion. For a stress/rest study the recommended stress dose is 5 to 8 mCi (185 to 296 MBq), followed in 4 hours by a rest dose of 15 to 24 mCi (555 to 888 MBq). The critical organ is the gallbladder wall, with a radiation absorbed dose of 0.123 rad(cGy)/mCi (stress) and 0.180 rad(cGy)/mCi (rest).[142]

Technetium 99m-Labeled White Blood Cells

Several methods have been used to label leukocytes with technetium, with various levels of success.[143] One technique is to label leukocytes with ^{99m}Tc-albumin colloid, exploiting the cell's natural phagocytic function to take up the radiocolloid.[144] Another technique is to first tin the leukocytes with stannous glucoheptonate and then label them with ^{99m}Tc-sodium pertechnetate.[145] Both of these methods are able to successfully localize sites of infection. The labeling of leukocytes with technetium achieved more widespread acceptance with the development of ^{99m}Tc-exametazime (^{99m}Tc-HMPAO). Previously established methods for labeling leukocytes with ^{111}In complexes (oxine and tropolone) demonstrated that a neutral lipophilic complex is required to label leukocytes efficiently, and ^{99m}Tc-HMPAO has this property. Peters et al.[146] prepared leukocytes labeled with ^{99m}Tc-HMPAO and demonstrated that the method compared favorably with ^{111}In-tropolone-labeled leukocytes. Labeling efficiency with the method is about 50%, with 78% of the activity associated with granulocytes.[147] A significant advantage of the method, besides the convenience and physical properties of ^{99m}Tc, is that leukocytes can be labeled with ^{99m}Tc-HMPAO in the presence of plasma, which is important for maintaining leukocyte viability.[148]

All present methods for labeling leukocytes with technetium require prior separation of leukocytes from whole blood. Technique is important to maintain cell viability. In general, low-speed centrifugation is used to obtain the leukocyte button. Several methods exist for labeling leukocytes; the following method, illustrated in Figure 9-38, describes the basic process:

1. Collect 43 mL whole blood in 7 mL of ACD in a 60 mL syringe through a 19 gauge winged set.
2. Add 10 mL 6% hetastarch, mix well, and let syringe sit with needle end upright until the red cells settle to the bottom (approximately 45 minutes).
3. Transfer the leukocyte-rich plasma (LRP) layer to a sterile 50 mL centrifuge tube.
4. Centrifuge at 450*g* for 5 minutes to pellet the leukocytes. Draw off all but 0.5 to 1.0 mL of leukocyte-poor plasma (LPP). Save LPP.
5. Gently resuspend the leukocyte button in plasma.
6. Reconstitute one HMPAO (Ceretec, Amersham) vial with 30 mCi ^{99m}Tc-sodium pertechnetate in 5 mL. Mix vial for 30 seconds to dissolve contents. Immediately add the 5 mL ^{99m}Tc-HMPAO to the leukocyte suspension and swirl gently to mix.
7. Incubate the cells for 15 to 20 minutes. Swirl gently every 5 minutes.
8. At end of incubation, add 15 mL LPP (from step 4) and spin cells at 450*g* for 5 minutes. Remove supernatant to a new tube and save.
9. Resuspend the labeled cells in 10 mL LPP. Observe closely to determine that no cell clumping is present.

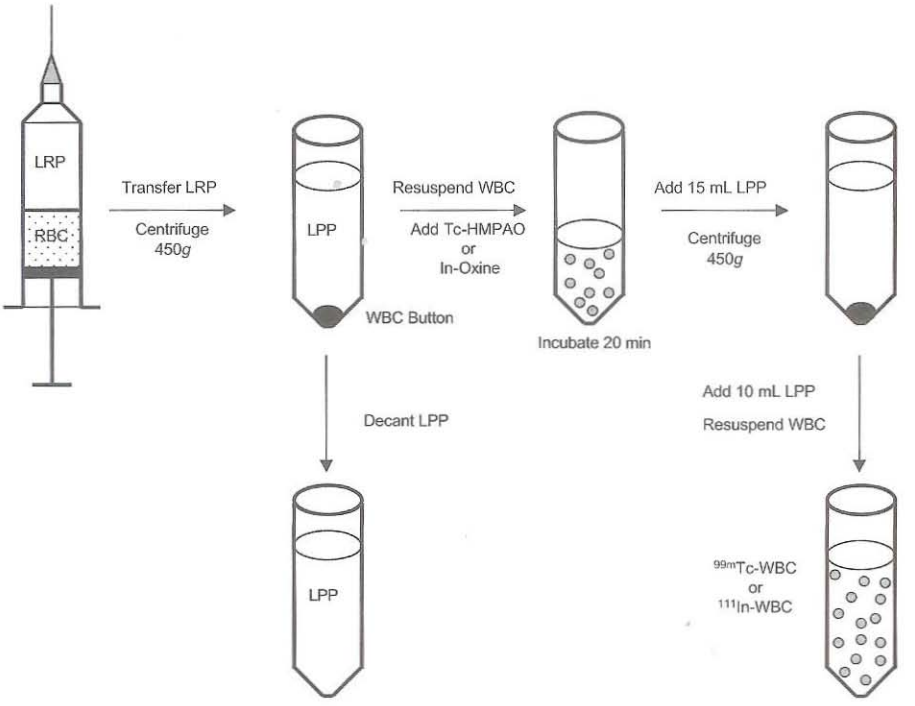

FIGURE 9-38 Procedure for labeling white blood cells with technetium or indium.

10. Assay the supernatant from step 8 and the labeled cells from step 9 in a dose calibrator. Determine the labeling efficiency.
11. Inject adult patient with 10 mCi (370 MBq) ^{99m}Tc-labeled leukocytes within 1 hour of labeling.

IODINE CHEMISTRY

The most useful radioisotopes of iodine for nuclear medicine are ^{123}I, ^{125}I, and ^{131}I. Their physical properties are shown in Table 9-14. The ultimate application determines which isotope is used. For diagnostic studies, ^{123}I and ^{131}I are the only nuclides with gamma energy suitable for imaging applications. ^{123}I is best suited for imaging because its gamma energy is abundant and efficiently detected by the sodium iodide crystal. Because of its short half-life, ^{123}I has to be purchased daily and is therefore less convenient to use. The high gamma energies of ^{131}I are less efficiently detected by the sodium iodide crystal and require heavier collimation,

TABLE 9-14 Physical Properties of Radioiodine Isotopes

Nuclide	Half-life	Decay Mode/Product	Photon MeV	Photon Abundance (%)	SA[a] mCi/μg	R/hr/mCi at 1 cm	HVL (mm Pb)
^{123}I	13.2 hours	EC/^{123}Te	0.159 (gamma)	83	1930.0	1.5	0.37
			0.027 (Te x-rays)	71			
^{125}I	59.4 days	EC/^{125}Te	0.035 (gamma)	7	17.5	0.7	0.015
			0.027 (Te x-rays)	114			
^{131}I	8.02 days	β^-/^{131}Xe	0.364 (gamma)	82	124.0	2.2	3.0
			0.637 (gamma)	7			

[a] Theoretical maximum specific activity.

which decreases sensitivity. Its beta emission, however, is useful for radiation treatment procedures in conditions such as hyperthyroidism and thyroid cancer. ^{131}I has also been used as a radiolabel for therapeutic antibodies, such as LYM-1 and tositumomab (Bexxar, Corixa Corporation), for the treatment of non-Hodgkin's lymphoma. Radiopharmaceuticals containing ^{131}I have a reasonable shelf life because of its 8-day half-life.

The photons of ^{125}I are too weak to escape from the body for external detection, and this isotope is best reserved for in vitro applications. ^{125}I-iothalamate has been useful for GFR studies, and ^{125}I-human serum albumin is used for plasma volume measurement. ^{125}I is also useful as a radiolabel for in vitro tests such as radioimmunoassays, in which its low-energy radiation and lack of beta emission make it less damaging to labeled biologic products. Although its gamma energies are too low for diagnostic imaging studies, ^{125}I is sometimes used in brachytherapy for radiation treatment of tumors in situ because its radiation is effectively absorbed over a short distance. In this regard, Iotrex (Proxima Therapeutics, Alpharetta, Ga.) is a ^{125}I intracavitary radiation therapy product for treating malignant brain tumors after tumor resection.

Radioiodine Production

131I

This isotope of iodine is obtained as a byproduct of uranium fission but can also be produced by the neutron activation of tellurium. Both methods produce ^{131}Te, which decays to ^{131}I:

$$^{235}U(n,f)\,^{131}Te \xrightarrow{\beta^-,\ 30\,hr} {}^{131}I$$

$$^{130}Te(n,\gamma)\,^{131}Te \xrightarrow{\beta^-,\ 30\,hr} {}^{131}I$$

The nuclear material is processed to yield sodium iodide as the final chemical form.

The ^{131}I nucleus is characterized by 53 protons and 78 neutrons, 4 neutrons more than the stable isotope ^{127}I. Neutron-rich ^{131}I undergoes negatron (beta-minus) decay with a half-life of 8.04 days to stable ^{131}Xe according to the following decay equation:

$$^{131}_{53}I_{78} \xrightarrow{n \rightarrow p^+ + e^- + \nu} {}^{131}_{54}Xe_{77} + 0.971\ MeV(\beta,\nu,\gamma)$$

130.906117 AMU 130.905075 AMU

The transition energy between ^{131}I and the ^{131}Xe ground state is 0.971 MeV (0.001042 AMU × 931.5 MeV/amu). Several beta transitions are possible in the decay scheme of ^{131}I (Figure 9-39), but the most frequent transition (γ_{14}) releases a 0.364 MeV gamma ray with 81% abundance.[149] It is the principal photon used in gamma-camera imaging. The remaining 0.607 MeV of transition energy is given to the beta particle and neutrino.

125I

^{125}I is produced indirectly by the neutron irradiation of ^{124}Xe to yield a short half-lived ^{125}Xe that quickly decays to ^{125}I:

$$^{124}Xe(n,\gamma)\,^{125}Xe \xrightarrow{EC,\ 17\ hr} {}^{125}I$$

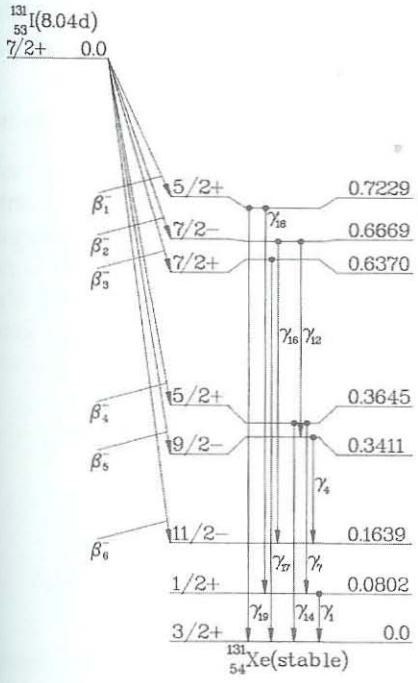

FIGURE 9-39 Decay scheme for ^{131}I. (Reprinted with permission from reference 149.)

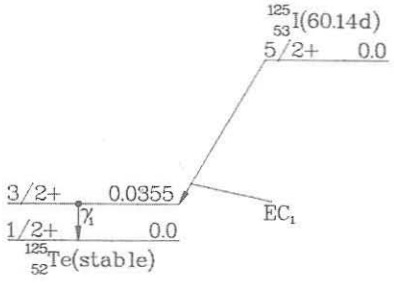

FIGURE 9-40 Decay scheme for ^{125}I. (Reprinted with permission from reference 149.)

The nucleus of ^{125}I is characterized by 53 protons and 72 neutrons, 2 neutrons less than ^{127}I. This neutron-deficient nucleus undergoes EC decay with a half-life of 60.14 days to stable ^{125}Te according to the following decay equation:

$$\underset{124.904624\ \text{AMU}}{{}^{125}_{53}I_{72}} \xrightarrow[p^+ + e^- \rightarrow n + \nu]{} \underset{124.904433\ \text{AMU}}{{}^{125}_{52}Te_{73}} + 0.178\ \text{MeV}(\nu,\gamma)$$

The transition energy for this decay is 0.178 MeV. Of this amount, the neutrino carries away 0.143 MeV to an excited state of ^{125}Te, which promptly de-excites to the ground state, releasing the remaining 0.035 MeV as a gamma ray (Figure 9-40). For every 100 atoms of ^{125}I that decay, 93 of the 0.035 MeV gammas undergo electron conversion (K-, L-, and M-shell electrons are removed), so only 7 gamma rays are detectable (7% abundance). However, a high percentage (114%) of 0.027 MeV ^{125}Te x-rays are emitted, which are used for detection. ^{125}I is easily shielded because of its weak photon energies. In fact, about 50% of its photons will be absorbed by a glass vial or container. For this reason, container geometry must be considered for the accurate measurement of ^{125}I sources. See Chapter 11 for more details on ^{125}I assay.

^{123}I

This isotope has nearly ideal properties for imaging, with a 13.2 hour half-life and a 0.159 MeV gamma ray that is efficiently detected by the sodium iodide crystal of the gamma

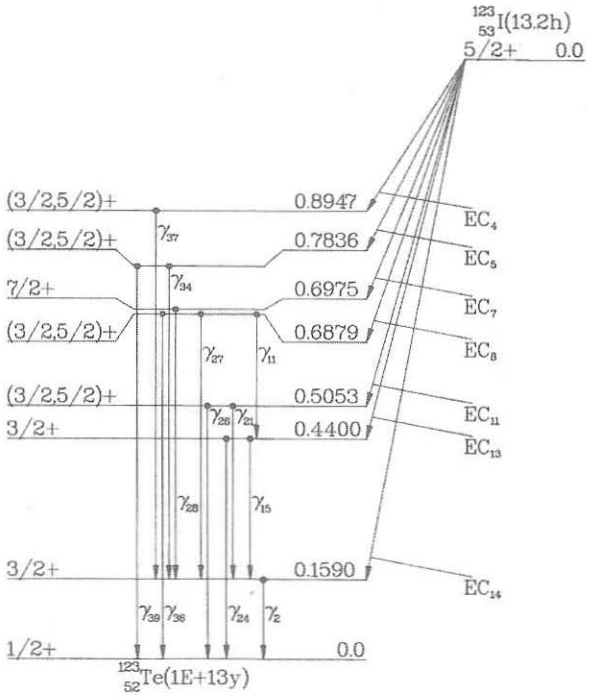

FIGURE 9-41 Decay scheme for ^{123}I. (Reprinted with permission from reference 149.)

camera. ^{123}I is produced in a cyclotron by the proton bombardment of a ^{124}Xe target. The short-lived initial product ^{123}Xe quickly decays to ^{123}I:

$$^{124}Xe(p,2n)^{123}Cs \xrightarrow{5.8\ min} {}^{123}Xe \xrightarrow{2\ hr} {}^{123}I$$

The ^{123}I nucleus is characterized by 53 protons and 70 neutrons, making it 4 neutrons less than ^{127}I. It decays by EC to ^{123}Te, which is essentially stable ($T_{1/2} = 1.2 \times 10^{13}$ years) (Figure 9-41).

$$^{123}_{53}I_{70} \xrightarrow[p^+ + e^- \rightarrow n + \nu]{} {}^{123}_{52}Te_{71} + 1.230\ MeV(\nu,\gamma)$$

122.905596 AMU 122.904276 AMU

The transition energy for this decay is 1.23 MeV, which is dissipated by several available EC transitions. The principal route (EC_{14}) proceeds to the excited state of ^{123}Te, which emits the 0.159 MeV gamma ray (γ_2). A partial loss of the 0.159 MeV gamma ray to K-, L-, and M-conversion electrons yields a photon abundance of 83%.

^{123}I is easily collimated and shielded and its gamma energy is efficiently detected by the gamma camera. Its short half-life and lack of beta radiation significantly reduce the radiation dose to the thyroid gland to one one-hundredth that of ^{131}I. The main disadvantages of ^{123}I are the requirement for daily delivery and the cost, because of its short half-life and cyclotron production.

An important point to consider in the dose calibrator assay of ^{123}I is the high abundance (71%) of 0.027 MeV x-rays emitted, which are subject to significant absorption by the ^{123}I source container. This can affect the dose measurement by more than 10%. Therefore, care must be taken to develop geometry correction factors for the different types of containers used in its radioassay. A facile technique employing a copper filter to handle this problem

has been published.[150] The technique obviates the necessity for applying geometry correction factors for different container configurations.

Solution Chemistry and Handling of Radioiodide

Iodine is a member of the group VII elements, the halogens, each having seven valence electrons. Iodine's electron configuration is $[Kr]4d^{10}5s^25p^5$. The halogens have high electronegativity and form negative halide ions typically found in ionic salts. All except fluorine also have positive oxidation states. Radioiodine is usually obtained as sodium iodide. Under favorable conditions, iodide will enter into oxidation reactions in aqueous solution, producing volatile forms that are a potential safety hazard. The significant oxidative reactions that can occur in radioiodide solutions are as follows:[151–155]

$$4I^- + O_2 + 4H^+ \leftrightarrow 2I_2 + 2H_2O \quad (9\text{-}17)$$

$$2HI + H_2O_2 \leftrightarrow I_2 + 2H_2O \quad (9\text{-}18)$$

$$2I^- + 2OH^{\cdot} \leftrightarrow I_2 + 2OH^- \quad (9\text{-}19)$$

Reaction 9-17 can be effectively retarded by buffering the radioiodide solution to an alkaline pH in the range of 7.0 to 8.5. Reducing agents such as sodium thiosulfate or bisulfites will reverse these reactions. The reaction with thiosulfate is as follows:

$$I_2 + 2S_2O_3^{2-} \rightarrow 2I^- + S_4O_6^{2-} \quad (9\text{-}20)$$

Indirect oxidation of iodide can occur by radiolytic effects that produce free radicals and peroxides, which oxidize iodide via reactions 9-18 and 9-19. Radiolytic effects are higher in ^{131}I solutions because of the significant amount of beta radiation. These radiation-induced reactions are difficult to prevent entirely but can be minimized by lowering the radioactive concentration, using radical scavengers, and adding antioxidants.[156,157] Chelating agents such as EDTA are sometimes used to retard oxidative catalysis induced by trace metal ions in solution.[151] Oxidative reactions are accelerated by heat and light, and since iodine has a low solubility in water (0.03% at 20°C) refrigerated storage will lower its volatility. The chlorine in tap water will oxidize radioiodide to volatile radioiodine; therefore, dilutions of radioiodide solutions should be made with distilled water.[158]

Upon receipt at the nuclear pharmacy, screw-top bottles of ^{131}I-sodium iodide solution should be wipe tested directly with a cotton-tipped applicator to detect any contamination on the external surface of the bottle, in addition to a wipe test of the external surface of the package. Broken bottles, bottles with loose caps, and even bottles with tight caps having grossly contaminated external surfaces can be discovered upon receipt from the supplier. Wearing disposable rubber gloves is a necessity. Inadvertent skin contamination can be removed by rinsing with water, followed by soap and water lather and another rinse. A mild scrubbing with a hand brush may be needed. Table 9-15 gives recommendations for safe handling of radioiodide solutions.

Labeling with Radioiodine

Radioiodine's importance in nuclear medicine stems from its diverse chemistry and the availability of several isotopes with different physical properties. Iodinated compounds

TABLE 9-15 Recommendations for Safe Handling of Radioiodide Solutions

1. Wear disposable gloves when handling radioiodide solutions
2. Wipe test solution vials for removable contamination upon receipt
3. Open solution vials and perform all radioiodinations in an exhaust hood
4. Dilute solutions with distilled water and with 0.2% sodium thiosulfate for prolonged storage
5. Buffer solutions to pH range of 7.0 to 8.5
6. Store solutions in a cool environment to reduce volatility
7. Perform bioassays on personnel who handle 10 mCi or more of radioiodine

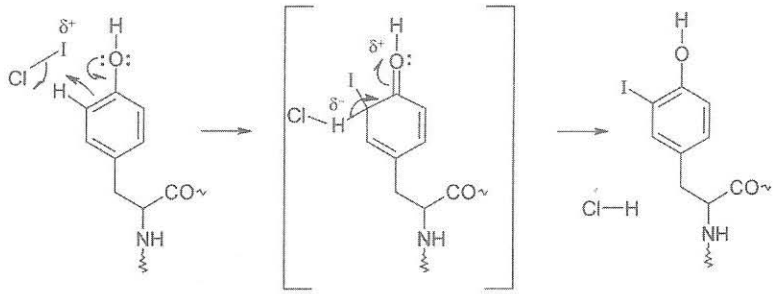

FIGURE 9-42 Mechanism of iodination of tyrosyl residues in proteins by electrophilic substitution.

can be prepared by several methods, including isotope exchange, nucleophilic substitution, electrophilic substitution, addition to double bonds, iododemetallation, and conjugation labeling with prosthetic groups. These methods have been reviewed by Lever.[159] Of these methods, electrophilic substitution, isotope exchange, and conjugation labeling have been most widely used to prepare radiopharmaceuticals.

Electrophilic Substitution

With the exception of nucleophilic substitution reactions involving substitution of I^- for a leaving group such as bromide, most radioiodinations involve substituting the electrophilic I^+ ion for a hydrogen atom in an electron-rich aromatic compound. The substitution reaction is facilitated by strong electron-donating groups (e.g., OH or NH_2) in the aromatic ring. The *p*-hydroxyl group in tyrosine is a good example (Figure 9-42). Direct iodination of proteins and antibodies into tyrosine is accomplished by this mechanism. The general substitution reaction is as follows, with asterisk indicating radioactive isotope:

$$R\text{-}H + I_2^* \leftrightarrow R\text{-}I^* + HI \qquad (9\text{-}21)$$

Isotope Exchange

Labeling can also occur by isotope exchange, in which the radioiodine atom exchanges with a stable iodine atom in the molecule. Theoretically, a 1:1 substrate-to-radioiodine molar ratio will produce a 50% labeling yield, whereas a 20:1 ratio will increase the yield to more than 95%, although specific activity will be lower.[159] Labeling reactions are typically conducted with the application of heat, either in solution or in the solid phase. Compounds that have been labeled in this manner include ^{123}I-iodoamphetamine (IMP),

^{123}I-N,N,N'-trimethyl-N'-[2-hydroxy-3-methyl-5-iodobenzyl]-1,3-propanediamine (^{123}I-HIPDM), ^{123}I- or ^{131}I-OIH, and ^{123}I- or ^{131}I-MIBG. The general exchange reaction is as follows:

$$R\text{-}I + I_2^* \leftrightarrow R\text{-}I^* + I_2 \tag{9-22}$$

In molecular iodine (I_2), the structure (I^-–I^+) is assumed. The I^+ ion does not exist alone but usually forms a complex with a nucleophilic species in aqueous solution. The following reactions are possible:

$$I_2 + H_2O \leftrightarrow H_2OI^+ + I^- \tag{9-23}$$

$$I_2 + OH^- \leftrightarrow HOI + I^- \tag{9-24}$$

It is believed that the iodinating species in labeling reactions is either the hydrated complex (H_2OI^+)[160] or hypoiodous acid (HOI).[161]

Protein iodination is one of the most important radiolabeling techniques in nuclear medicine. Typical iodination sites in protein molecules include the 3 and 5 positions of the aromatic ring of tyrosine as the primary site or the imidazole ring of histidine as a secondary site. Because the anionic form of the molecule to be labeled seems to be the reactive species with I^+, close attention must be paid to the protein's pKa and the pH of the reaction mixture. At low pH tyrosine is protonated, and labeling yields are low. Basic pH, however, promotes dissociation of tyrosine hydrogens to form the desired tyrosinate anion and also promotes the hydrolysis of I_2 according to reaction 9-24.[162] This greatly facilitates the rate of iodination into the tyrosine ring (Figures 9-42 and 9-43). Solutions of pH 7 to 9 are usually used in protein iodination. One must avoid higher pH values (>10) because of the irreversible disproportionation of HOI to iodate according to the following reaction. Some iodate, however, will still form at pH 7 to 9:

$$3HOI + 3OH^- \leftrightarrow 2I^- + IO_3^- + 3H_2O \tag{9-25}$$

The order of mixing reagents is important in achieving high iodination yield. This depends on the method of radioiodination, but in general the molecule to be labeled is added first with buffer followed by radioiodide and iodinating agent. To retard protein damage, mild iodinating conditions must be used. More attention must be paid when using iodinating agents that are fairly strong oxidizing agents because they may attack the protein. It is recommended that not more than one atom of iodine per molecule of protein on average be introduced to preserve protein integrity. However, this too depends on the protein, the iodinating method, and the ultimate use or application of the iodinated protein.[163] For example, iodinated albumin prepared by the iodine monochloride method should contain not more than one mole of iodine per mole of protein.

Iodination Methods

Several methods of iodination have been used to label radiopharmaceuticals. These include iodine monochloride, chloramine-T, lactoperoxidase, electrolysis, Iodo-Gen (Pierce, Rockford, Ill.), Iodo-Beads (Pierce), and the Bolton-Hunter reagent. A few of these methods are described here. All except the Bolton-Hunter method involve covalent attachment of cationic iodine to the aromatic ring of tyrosine residues in the protein.

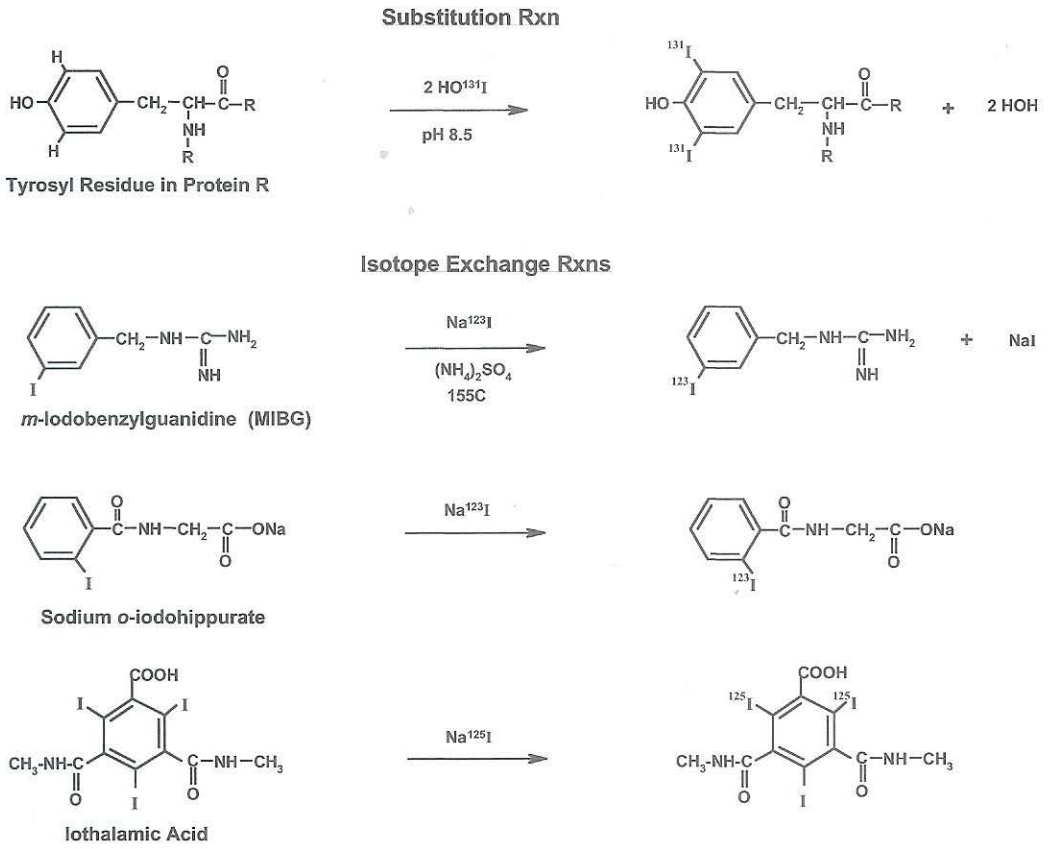

FIGURE 9-43 Radioiodination. Substitution reaction producing iodinated tyrosyl residue in a protein, and isotope exchange reactions producing *m*-iodobenzylguanidine (MIBG), *o*-iodohippurate (OIH), and iothalamic acid.

Iodine Monochloride

The iodine in iodine monochloride is in the I^+ state because of chlorine's greater electronegativity. Iodine monochloride is formed by the oxidation of iodide with iodate in strong acid according to the following reaction:

$$2\,NaI + NaIO_3 + 6\,HCl \leftrightarrow 3\,ICl + H_2O + 3\,NaCl \qquad (9\text{-}26)$$

When mixed with iodine monochloride, radioiodide undergoes isotope exchange. Because the iodine monochloride is in excess and all of its iodine is in the I^+ form, essentially all of the radioiodide is converted to I^+ accordingly:

$$ICl + NaI^* \leftrightarrow I^*Cl + NaI \qquad (9\text{-}27)$$

Subsequently, the I*Cl hydrolyzes to HOI*, which iodinates the compound.[162] Radiolabeling yields are about 75%, but specific activity of the product is low because stable iodine is also incorporated into the compound because of the excess stable iodine monochloride present. In this labeling technique radioiodide is added to the buffered compound, and

TABLE 9-16 Radioiodination of a Protein

Mixing Sequence	Typical Amounts
1. Protein	100 μg
2. Phosphate buffer	To pH 7 to 8
3. NaI*	$Na^{131}I$ 0.087 μg
4. Iodinating agent	Chloramine-T 1.25 μg
	React for 10 minutes on ice
5. Reducing agent	Sodium metabisulfite 2.5 μg

Asterisk indicates radioactive isotope.

iodine monochloride is jetted into the mixture. If iodine monochloride is added before the radioiodide, labeling yields are lowered considerably because the isotope-exchange reaction is impaired by the reaction of iodine monochloride directly with the compound. The iodine monochloride is added rapidly to disperse the mixture quickly to reduce the degree of multiple labeling within the same molecule created by localized concentrations of reactive iodine. An advantage of this method is that the amount of iodine incorporated into the compound is controlled by the amount of iodine monochloride used. This is an advantage if excessive substitution must be avoided.

Chloramine-T

This method uses the sodium salt of N-chloro-4-methyl benzene sulfonamide (chloramine-T) as the iodinating agent.[163,164] Chloramine-T undergoes hydrolysis at pH 7 to 8, liberating sodium hypochlorite, which oxidizes radioiodide to hypoiodous acid according to the following reactions:

$$CH_3-C_6H_4SO_2NaNCl + H_2O \leftrightarrow CH_3-C_6H_4SO_2NH_2 + NaOCl \quad (9\text{-}28)$$

$$NaOCl + HI^* \leftrightarrow HOI^* + NaCl \quad (9\text{-}29)$$

The general technique is to mix the compound to be labeled with buffer and radioiodide and then add the fresh chloramine-T solution. A period of incubation is required, and the reaction is stopped by adding a reducing agent. The typical labeling conditions for IgG with ^{131}I in a 1:1 molar ratio of antibody to iodine are shown in Table 9-16.

High labeling yields can be obtained, but labeling conditions must be carefully controlled because chloramine-T is a powerful oxidizing agent and may damage proteins.[165] The advantage of chloramine-T is that no carrier iodide is needed; therefore, high specific activities can be obtained. Additionally, virtually complete utilization of the isotope can be achieved. This method has been effectively used to label the LYM-1 antibody for the treatment of non-Hodgkin's lymphoma.[166]

Iodo-Gen and Iodo-Beads

Iodo-Gen (Pierce) and Iodo-Beads (Pierce) are solid-phase oxidants in a technology developed to permit iodinations to proceed in a two-phase system, with the oxidant material bound in a solid phase from which reactants can be separated by simple aspiration (Figure 9-44). The Iodo-Gen method involves dissolving the Iodo-Gen oxidizing reagent (1,3,4,6-

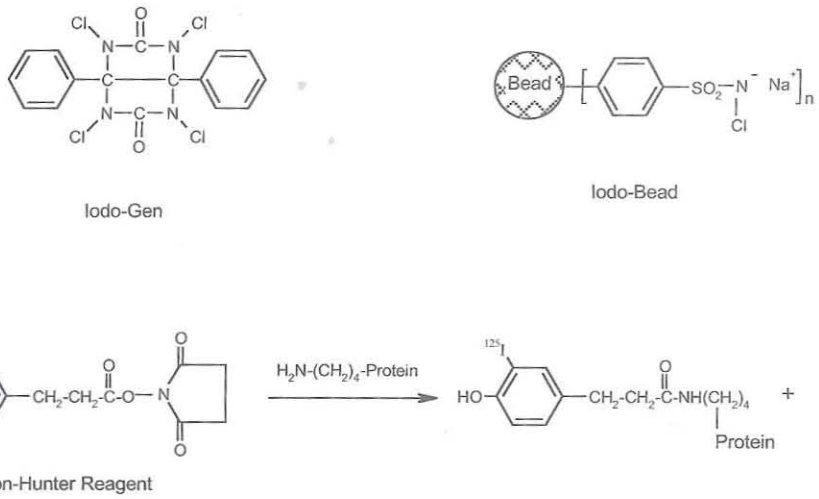

FIGURE 9-44 Chemical structures of two mild oxidizing iodinating agents: Iodo-Gen and Iodo-Beads. Radioiodination of non–tyrosine-containing proteins via the Bolton-Hunter reagent.

tetrachloro-3α,6α-diphenylglycouril) in an organic solvent such as chloroform and plating the reagent onto the sides of a glass tube after solvent evaporation. The buffered protein and radioiodide are added to the Iodo-Gen–coated tube and incubated for 10 minutes, whereupon the Iodo-Gen oxidizes the iodide. The reaction is stopped by aspirating the mixture from the tube.

Iodo-Beads are nonporous polystyrene beads to which is bonded the sodium salt of N-chloro-benzenesulfonamide as the oxidant. Labeling involves mixing radioiodide with several beads, incubating 5 minutes to allow oxidation of iodide, then adding the protein in buffer, incubating 10 minutes more, and aspirating the mixture to stop the reaction.

These solid-phase iodination techniques are claimed to provide milder oxidation conditions for the protein compared with chloramine-T and do not require the addition of a reducing agent to stop the reaction. Labeling yields are good and high specific activity labeling can be achieved.[167]

Bolton-Hunter Reagent

To circumvent the problem of protein damage by direct iodination and to be able to label proteins that lack the tyrosine moiety, indirect radioiodination using a prosthetic group can be used. An example is the Bolton-Hunter reagent.[168] This reagent is a reactive conjugate prelabeled with radioiodine that is reacted with the protein, eliminating contact with oxidizing and reducing agents. The reagent is an ^{125}I-labeled acylating agent, iodinated 3-(4-hydroxy-phenyl) propionic acid N-hydroxysuccinimide ester, which reacts with lysine amino groups in the protein (Figure 9-44). This method is mild, producing proteins that retain immunoreactivity.

IODINATED RADIOPHARMACEUTICALS

Radiopharmaceuticals labeled with ^{123}I, ^{125}I, and ^{131}I are available from several radiopharmaceutical companies. They can also be compounded at the time of use.

Sodium Iodide I 123, I 125, and I 131 Capsules or Solution

^{131}I-sodium iodide is available from commercial suppliers in hard gelatin capsules and in aqueous solution for oral administration. Capsules used for diagnostic studies are generally available in 15, 25, 50, and 100 μCi (185, 925, 1850, and 3700 kBq) strengths. Capsules may contain sodium radioiodide mixed with a granulated powder mixture or deposited as a thin film in a mixture of polyethylene glycol and thiosulfate.[169] Therapeutic capsules for treating hyperthyroidism or thyroid carcinoma are also available and made to order on 24 hour notice. These may contain sodium iodide mixed with a semisolid glob of polyethylene glycol inside the capsule or adsorbed on anhydrous sodium phosphate. Various strengths are available, up to 100 mCi (3700 MBq) per capsule.

Oral solutions of ^{131}I-sodium iodide are manufactured to maintain their stability against oxidation. Products may contain disodium phosphate to adjust pH to 7.5 to 9.0, sodium bisulfite as an antioxidant, and disodium EDTA. These stabilizers will not interfere with clinical use for thyroid studies, but such solutions cannot be used in radioiodination reactions because of the antioxidant. Solutions are available in several concentrations up to 25 mCi (925 MBq)/mL and 150 mCi (5550 MBq) per vial. Solutions of ^{131}I-sodium iodide may turn an amber color with age because of radiation-induced chromophores. This is a normal process and does not affect the quality of the radiopharmaceutical.

^{123}I-sodium iodide is available as diagnostic capsules in 100 μCi (3.7 MBq) and 200 μCi (7.4 MBq) strengths adsorbed on sucrose. ^{125}I-sodium iodide is not sold as a radiopharmaceutical.

^{123}I-, ^{125}I-, and ^{131}I-sodium iodide in sodium hydroxide solution without stabilizers are available as radiochemicals for use in radioiodinations.

Iodinated I 125 Albumin Injection

Iodinated I 125 albumin (^{125}I-HSA) injection is prepared by mild iodination of normal human albumin to introduce not more than one atom of iodine per molecule of albumin to minimize denaturation of the protein. The iodine is firmly bound and released only by metabolism of the protein in vivo. Radiolytic decomposition is minimal with the ^{125}I label, and the product has a long shelf life. Its radiochemical purity is not less than 97%. Being a biologic product, it is stored at 2°C to 8°C. The product is available in 100 μCi (3.7 MBq) multidose vials of 10 mL. ^{125}I-HSA is indicated primarily for measuring plasma volume. The usual adult administered activity for plasma volume measurement is 5 to 10 μCi (185 to 370 kBq). The critical organ is the total body, with a radiation absorbed dose of 0.0006 rad(cGy)/μCi.[170]

Iobenguane I 123 or I 131 Injection

Iobenguane sulfate (MIBG) has the chemical structure shown in Figure 9-43. It is labeled either with ^{123}I (prepared on site) or with ^{131}I, available as a commercially prepared product. The ^{131}I product (^{131}I-MIBG) is supplied to the end user as a frozen solution in a concentration of 2.3 mCi(85.1 MBq)/mL. The product should be kept frozen until use and should be used within 6 hours after thawing. ^{131}I-MIBG received FDA approval for marketing in 1994.

The radioiodinated product is labeled by the solid-phase isotope-exchange method. ^{123}I- or ^{131}I-sodium iodide in dilute sodium hydroxide and 1 mL of MIBG exchange solution, containing 2 mg MIBG sulfate and 10 mg ammonium sulfate, is heated at 155°C for 30 minutes. The dried product is redissolved in 1 mL water and reheated for an additional 30 minutes.[171] The final product is redissolved in water or saline and sterile-filtered before

use. Labeling yields are typically 98% or higher, requiring no purification step to remove unbound iodide. During the solid-phase exchange reaction, thermal decomposition of ammonium sulfate drives off ammonia and lowers the pH. The mildly acidic, oxidizing conditions ensure that I^+ will be formed to effect the electrophilic exchange reaction. High labeling yields require an absence of chloride ion; therefore, saline should not be used during the heating step.[172] Once the product is labeled, it can be reconstituted in normal saline for injection. The radiochemical purity of ^{123}I- and ^{131}I-MIBG is not less than 90%.[99]

^{131}I- or ^{123}I-MIBG is indicated for the localization of primary or metastatic pheochromocytomas, neuroblastomas, and carcinoids. The usual intravenous adult administered activity of ^{131}I-MIBG is 0.5 mCi (18.5 MBq). In patients who weigh more than 65 kg, the dose is 0.3 mCi(11.1 MBq)/m^2 up to a maximum of 1 mCi (37 MBq). Children's doses of ^{131}I-MIBG are based on 0.3 mCi(11.1 MBq)/m^2 to a maximum dosage of 0.5 mCi (18.5 MBq). Dosing of ^{123}I-MIBG is based on 0.14 mCi/kg, with a suggested maximum dose of 10 mCi (370 MBq) in adults.[173,174] A thyroid-blocking dose of potassium iodide (KI) should be administered 1 day before and 7 days after dosing with ^{131}I-MIBG.[175] The FDA-recommended thyroid-protective doses of KI daily are as follows: infants less than 1 month old, 16 mg; children age 1 month to 3 years, 32 mg; children age 3 years to 18 years, 65 mg; adults, 130 mg.

The critical organs for ^{131}I-MIBG in the adult are the urinary bladder wall and the liver, each with a radiation absorbed dose of 3 rad(cGy)/mCi.[175] For ^{123}I-MIBG the critical organ is the urinary bladder wall, with a radiation absorbed dose of 0.35 rad(cGy)/mCi.

Iodohippurate Sodium I 131 Injection

Iodohippurate sodium I 131 injection (^{131}I-iodohippurate or ^{131}I-OIH; hippuran) has been essentially supplanted by ^{99m}Tc-mertiatide (^{99m}Tc-MAG3). A brief description is included here because for more than 30 years OIH was the major agent for evaluating renal function. Its only disadvantage is that it cannot be labeled with ^{99m}Tc. The chemical structure of OIH is shown in Figure 9-43. It is prepared by isotope exchange. Its radiochemical purity is not less than 97%, with the major radiochemical impurity being radioiodide. The high purity limits are necessary because OIH's ability to measure renal function is based on its high renal extraction and elimination in the urine. Too much free radioiodide prolongs renal clearance because of radioiodide's high degree of reabsorption (approximately 70%) by the tubular cells. OIH's principal route of elimination is tubular secretion, and it has played a prime role in assessing global renal function via the renogram. It is the "gold standard" to which other renal function agents are compared. A typical dosage for renal function assessment is 75 μCi (2.775 MBq) for one kidney and 200 μCi (7.4 MBq) for two kidneys. The critical organ is the urinary bladder wall, with a radiation absorbed dose of 5.7 mrad/μCi.[176]

Iothalamate Sodium I 125 Injection

Iothalamate sodium I 125 injection (^{125}I-iothalamate; Glofil-125, Cypros Pharmaceutical) is prepared by isotope exchange. Its chemical structure is shown in Figure 9-43. It is not used for renal imaging because of the ^{125}I label. Its renal clearance after intravenous injection closely approximates that of inulin, and its primary indication is the assessment of GFR. It is supplied in a multidose vial with a radioactivity concentration of 250 to 300 μCi/mL (9.25 to 11.1 MBq/mL) in a 4 mL volume. Its radiochemical purity is not less than 98%.[99] The product should be stored at 2°C to 8°C. Dosage varies with the method used to assess GFR. A single-dose technique requires a dosage of 10 to 30 μCi (370 to 1110 kBq),

TABLE 9-17 Physical Properties of Gallium and Indium Radionuclides

Nuclide	Half-life	Decay Mode	Photons (MeV)	% Abundance
^{67}Ga	3.26 days	EC	0.093	37
			0.185	20
			0.300	17
			0.394	5
^{68}Ga	67.8 min	Positron	0.511	178
^{111}In	2.80 days	EC	0.171	90
			0.245	94
^{113m}In	1.66 hr	Isomeric transition	0.392	64

and a continuous infusion technique requires 20 to 100 μCi (740 to 3700 kBq). The critical organ is the thyroid gland, with a radiation absorbed dose of 7.8 mrad/μCi.[177]

GALLIUM AND INDIUM CHEMISTRY

The chemistry of gallium and indium is similar. In some instances the radiopharmaceuticals of these nuclides have been used for similar purposes, such as tumor and abscess localization. The most frequently used radionuclides are ^{67}Ga and ^{111}In. Both are cyclotron produced, have similar half-lives, and decay by EC to yield photons with useful imaging properties. Other radioisotopes of gallium and indium, such as ^{68}Ga and ^{113m}In, have been used in nuclear medicine over the years but are less frequently used today. The decay properties of gallium and indium isotopes are summarized in Table 9-17.

Gallium and indium are members of the group III metals in the periodic table. The electron configuration for gallium is $[Ar]3d^{10}4s^24p^1$ and for indium is $[Kr]4d^{10}5s^25p^1$. Each readily loses one, two, or three electrons but typically assumes the 3+ oxidation state in aqueous solution, which is the most relevant state for radiopharmaceuticals. In acidic aqueous solution below pH 3, gallium and indium likely exist in the ionic form as the hexaaqua complexes $[Ga(H_2O)_6]^{3+}$ and $[In(H_2O)_6]^{3+}$. When pH is higher than 3, these metals hydrolyze and form insoluble hydroxides, $Ga(OH)_3$ and $In(OH)_3$, which precipitate from solution. At tracer quantities, these hydroxides disperse as radiocolloids. Gallium is amphoteric, acting as a metal at low pH and forming the hydroxide as pH is raised toward neutrality. At high pH, gallium acts as a nonmetal, and the hydroxide dissolves in excess base to form the soluble gallate ion $Ga(OH)_4^-$. The formation of coordination complexes with indium and gallium usually occurs by ligand exchange from weak complexes such as acetate, citrate, or tartrate, which prevent hydrolysis while the higher-stability coordination complex forms. Chelating agents commonly used to stabilize indium and gallium at higher pH in vitro include citrate, EDTA, DTPA, and 8-hydroxyquinoline (oxine). Ga^{3+} and In^{3+} will undergo ligand exchange from the weaker complexes (oxine or citrate) to transferrin in plasma because of the large formation constant (K) for the transferrin complexes (Ga-transferrin, log K = 20.3; In-transferrin, log K = 18.7).[178] The DTPA complexes of indium and gallium, being hexadentate, are more stable and tend to be inert to in vivo ligand exchange with transferrin.

Production of Gallium and Indium

Gallium and indium are produced in a cyclotron. ^{67}Ga is most commonly produced by the nuclear reaction ^{68}Zn(p,2n)^{67}Ga, and ^{111}In by the nuclear reaction ^{111}Cd(p,n)^{111}In. The targets are processed by ion exchange and solvent extraction techniques, evaporated to dryness from isopropyl ether, and redissolved in 0.05 M hydrochloric acid.[179,180]

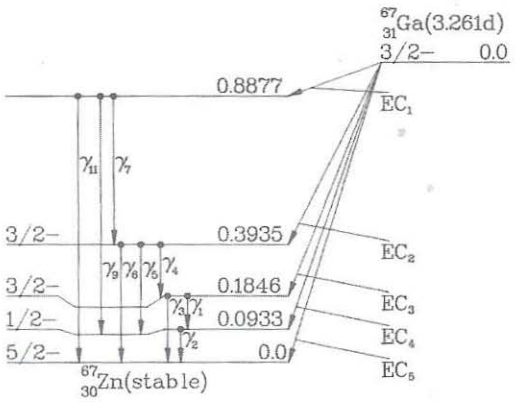

FIGURE 9-45 Decay scheme for ^{67}Ga. (Reprinted with permission from reference 149.)

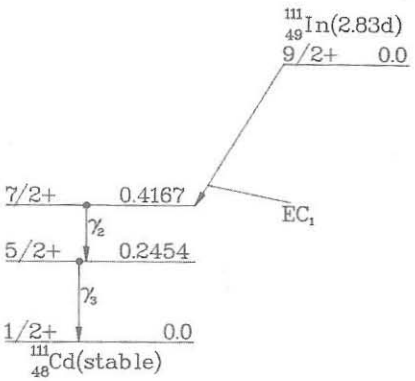

FIGURE 9-46 Decay scheme for ^{111}In. (Reprinted with permission from reference 149.)

The ^{67}Ga nucleus decays by EC with a half-life of 3.26 days to stable ^{67}Zn:

$$^{67}_{31}Ga_{36} \xrightarrow[p^+ + e^- \rightarrow n + \nu]{} {}^{67}_{30}Zn_{37} + 0.997\ MeV(\nu,\gamma)$$

66.92822 AMU 66.92715 AMU

The transition energy for this decay is 0.997 MeV, which is dissipated by several available EC transitions (Figure 9-45). Several gamma photons are emitted that are used for imaging, the principal ones being 0.093 MeV (γ_2) with 37% abundance, 0.185 MeV (γ_3) with 20% abundance, 0.300 MeV (γ_5) with 17% abundance, and 0.394 MeV (γ_6) with 5% abundance.[149]

^{68}Ga is produced from the ^{68}Ge–^{68}Ga generator. ^{68}Ga has a 68 minute half-life and ^{68}Ge a 280 day half-life, which gives this secular equilibrium generator a long useful shelf life. ^{68}Ga is a positron emitter that is not used in routine nuclear medicine practice. It is used, however, as a transmission source for attenuation correction in PET cameras.

The ^{111}In nucleus decays by EC with a half-life of 2.83 days to stable ^{111}Cd:

$$^{111}_{49}In_{62} \xrightarrow[p^+ + e^- \rightarrow n + \nu]{} {}^{111}_{48}Cd_{63} + 1.230\ MeV(\nu,\gamma)$$

110.9055 AMU 110.90418 AMU

The transition energy for this decay is 1.230 MeV, which is dissipated by a neutrino at 0.814 MeV, one gamma ray at 0.171 MeV (γ_2) with 90% abundance, and another gamma ray at 0.245 MeV (γ_3) with 94% abundance (Figure 9-46).[149]

^{113m}In is produced from the ^{113}Sn–^{113m}In generator. This isotope of indium preceded that of ^{111}In in nuclear medicine. This is another example of a long-lived secular equilibrium generator system: The ^{113}Sn parent has a half-life of 115 days and the ^{113m}In daughter's half-life is 1.66 hours. This generator is no longer used.

Gallium Citrate Ga 67 Injection

Although many potential radiopharmaceuticals can be made with gallium, the only compound that has achieved major use in nuclear medicine is ^{67}Ga-gallium citrate. It is available as a sterile aqueous solution in multidose vials (2 mCi [74 MBq]/mL, 3 to 12

mCi (111 to 444 MBq) from several manufacturers. It is prepared by neutralizing acidic NCA ^{67}Ga-gallium chloride with sodium hydroxide in the presence of 4% sodium citrate, producing a 1:1 ^{67}Ga:citrate complex. Depending on the pH, several protonated species are possible. The species at around pH 4 is $[C_3H_4OGa(OH)_2(COO)(COOH)_2]^-$ and at pH higher than 8 it is $[C_3H_4OGa(OH)_2(COO)_3]^{3-}$.[181] The injection has a pH between 5.5 and 8.0 and is preserved with 0.9% benzyl alcohol. It is stored at room temperature (20°C–25°C). Its radiochemical purity is not less than 97%.[99] At the time of calibration, it contains not more than 0.02% ^{66}Ga and 0.2% ^{65}Zn radionuclidic impurities.

^{67}Ga-gallium citrate is indicated for diagnostic imaging of Hodgkin's disease, lymphoma, bronchogenic carcinoma, and inflammatory lesions to identify fevers of unknown origin. The standard adult dosage is 3 to 8 mCi (111 to 296 MBq), administered intravenously. The critical organ is the lower large intestine, with a radiation absorbed dose of 0.9 rad(cGy)/mCi.[182]

Indium In 111 Chloride Solution

Indium In 111 chloride injection is available as a sterile aqueous solution of NCA ^{111}In-indium chloride in 0.05 M hydrochloric acid, pH 1.1 to 1.4 (Mallinckrodt) and in 0.04 M hydrochloric acid, pH approximately 1.4, as Indichlor (Amersham). Both products are available as 5 mCi (185 MBq) in 0.5 mL volume single-use vials, to be stored at room temperature (20°C to 25°C). The radiochemical purity is not less than 95% as ionic $^{3+}$In. Radionuclidic purity at the time of calibration is not less than 99.925% ^{111}In, with not more than 0.075% ^{114m}In and ^{65}Zn, combined, as radionuclidic impurities. ^{111}In-indium chloride is intended for use in labeling antibodies such as capromab pendetide (^{111}In-capromab penditide; ProstaScint, Cytogen).

Indium In 111 Oxyquinoline Solution

Indium In 111 oxyquinoline solution is a sterile aqueous solution of NCA $^{111}In^{3+}$ complexed to 8-hydroxyquinoline (oxine). The complex is a 3:1 ratio of oxine:indium (Figure 9-47). The product is available as a single-use vial at a pH range of 6.5 to 7.5. Each mL contains at calibration time 1 mCi (37 MBq) ^{111}In, 50 µg oxine, 100 µg polysorbate 80 (detergent stabilizer), and 6 mg N-2-hydroxyethyl-piperazine-N'-2-ethane sulfonic acid (HEPES) buffer in 0.75% sodium chloride solution. It is stored at room temperature. Its radiochemical purity is not less than 90%.[99] The product contains not more than 1 µCi (37 kBq) ^{114m}In impurity per 1 mCi (37 MBq) ^{111}In at the time of calibration. At the time of expiration, it contains not less than 99.75% ^{111}In and not more than 0.25% of $^{114m/114}$In impurities.

^{111}In-indium oxine is indicated for radiolabeling autologous leukocytes (see below). The usual adult dosage of ^{111}In-labeled leukocytes is 200 to 500 µCi (7.4 to 18.5 MBq) intravenously. The critical organ is the spleen, with a radiation absorbed dose of 20 rad(cGy)/500 µCi (7.4 MBq) (at the expiration date of the product).[183]

Indium In 111 Pentetate Injection

Indium In 111 pentetate injection (^{111}In-pentetate or ^{111}In-DTPA) is a sterile aqueous solution of NCA $^{111}In^{3+}$ complexed to disodium pentetate in a 1:1 molar ratio. The eight-coordinate structure for the complex is shown in Figure 9-47.[184] The single-use product, available in a 1.5 mL vial, contains in each mL of isotonic solution at the time of calibration 1 mCi (37 MBq) ^{111}In, 20 to 50 µg pentetic acid, and sodium bicarbonate with the pH adjusted to 7 to 8. It is stored at 5°C to 30°C. The radiochemical purity is not less than 90%.[99] The

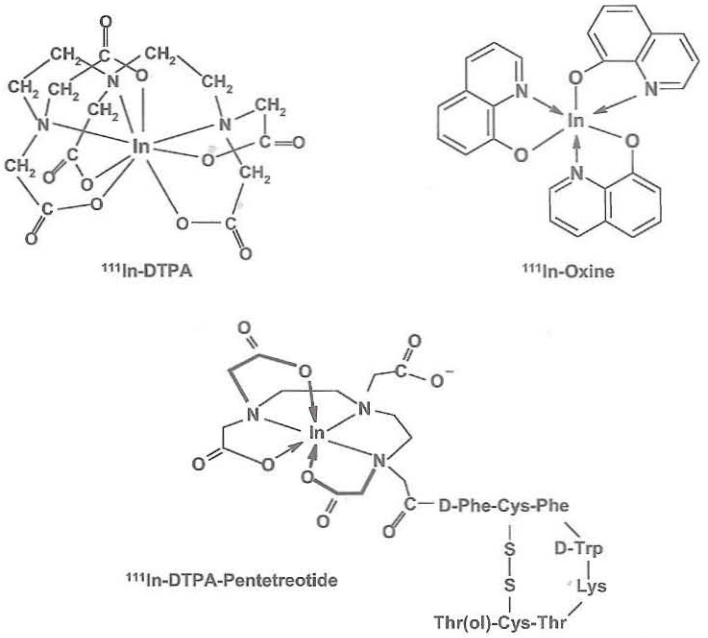

FIGURE 9-47 Chemical structures of ^{111}In-labeled DTPA, oxine, and pentetreotide.

radionuclidic purity at calibration time is not less than 99.88% ^{111}In and less than 0.06% ^{114m}In and ^{65}Zn combined.

^{111}In-DTPA is indicated for use in radionuclide cisternography. The usual intrathecal adult dosage is 500 μCi (18.4 MBq) (maximum dosage). The critical organ is the spinal cord surface, with a radiation absorbed dose of 5 rad(cGy)/500 μCi.[185]

Indium In 111 Pentetreotide Injection

Indium In 111 pentetreotide injection (^{111}In-pentetreotide; OctreoScan, Mallinckrodt) is prepared from a kit that contains a lyophilized mixture of 10 μg of pentetreotide, 2.0 mg gentisic acid, 4.9 mg anhydrous trisodium citrate, 0.37 mg anhydrous citric acid, and 10 mg inositol. The kit also contains a vial of indium In 111 chloride injection that contains, at the calibration date, 1.1 mL of $^{111}In(Cl)_3$ at 3 mCi(111 MBq)/mL in 0.02 M hydrochloric acid and 3.5 μg/mL ferric chloride. The presence of ferric chloride increases the labeling yield. The kit is stored at refrigerated temperature (2°C to 8°C) before labeling. The product is labeled by adding the ^{111}In-indium chloride to the lyophilized mixture and incubating at room temperature for 30 minutes. Once formed, the product is stored at or below 25°C and must be used within 6 hours of preparation. A proposed chemical structure is shown in Figure 9-47. The product may be diluted with up to 3 mL of normal saline immediately before injection. The radiochemical purity must be checked before patient administration and should be not less than 90%.[99,186]

^{111}In-pentetreotide is indicated for localization of primary and metastatic neuroendocrine tumors bearing somatostatin receptors. The usual adult intravenous dosage for planar imaging is 3 mCi (111 MBq); for SPECT imaging the dose is 6 mCi (222 MBq). The kit is made available a few days before the calibration date to provide sufficient activity for SPECT imaging. The critical organ is the spleen, with a radiation absorbed dose of 14.77 rad(cGy)/6 mCi.[186]

Indium In 111-Labeled Antibodies

Indium-111 is used to label antibodies for radioimmunodiagnosis in nuclear medicine. Labeling is made possible by covalent attachment of a linker molecule to the antibody away from the antigen binding site. The linker molecule contains a chelating group to complex indium. Antibody labeling is generally accomplished by first mixing ^{111}In-indium chloride with an acetate buffer and then mixing this with the antibody to effect chelation of ^{111}In to the antibody. The antibodies in current use are indium In 111 capromab pendetide (ProstaScint) for imaging prostate cancer metastases and indium In 111 ibritumomab tiuxetan (In-111 Zevalin, IDEC Pharmaceuticals) for use in conjunction with Y-90 Zevalin (IDEC Pharmaceuticals) in the treatment of patients with relapsed or refractory follicular non-Hodgkin's lymphoma. These and other radiolabeled antibodies are discussed in more detail in Chapter 21.

Indium 111-Labeled White Blood Cells

Several methods exist for labeling leukocytes with ^{111}In. The basic process, illustrated in Figure 9-38, is as follows:

1. Collect 43 mL whole blood in 7 mL of ACD in a 60 mL syringe through a 19 gauge winged set.
2. Add 10 mL 6% hetastarch, mix well, and let syringe sit with needle end upright until the red cells separate to the bottom (approximately 45 minutes).
3. Transfer the LRP layer to a sterile 50 mL centrifuge tube.
4. Centrifuge at 450*g* for 5 minutes to pellet the leukocytes. Draw off all but 0.5 to 1.0 mL of LPP. Save LPP.
5. Gently resuspend the leukocyte button in 2.5 mL saline.
6. Draw up ^{111}In-oxine solution into a 3 mL syringe. Rinse the vial with 0.5 mL of sterile normal saline and draw this up into the syringe. Add this ^{111}In-oxine solution dropwise to the leukocytes with gentle swirling.
7. Incubate the cells for 15 to 20 minutes. Swirl gently every 5 minutes.
8. At end of incubation, add 15 mL LPP (from step 4) and spin cells at 450*g* for 5 minutes. Remove the supernatant to a new tube and save.
9. Resuspend the labeled cells in 10 mL LPP. Observe closely that no cell clumping is present.
10. Assay the supernatant from step 8 and the labeled cells from step 9 in a dose calibrator. Determine the labeling efficiency.
11. Inject adult patient with 0.5 mCi (18.4 MBq) ^{111}In-labeled leukocytes within 1 hour of labeling.

THALLIUM CHEMISTRY

Thallium is a member of the group III metals, along with gallium and indium. Its electron configuration is $[Xe]5d^{10}6s^26p^1$, and it exists typically in the 1+ (thallous) or 3+ (thallic) oxidation states in its compounds. TlOH resembles alkali-metal hydroxides in being a soluble, strong base; however $Tl(OH)_3$ is quite insoluble.

^{201}Tl is produced by bombarding a target of pure natural thallium metal with protons:[187]

$$^{203}\mathrm{Tl}(\mathrm{p},3\mathrm{n})\,^{201}\mathrm{Pb} \xrightarrow{9.4\ \mathrm{hr}} {}^{201}\mathrm{Tl}$$

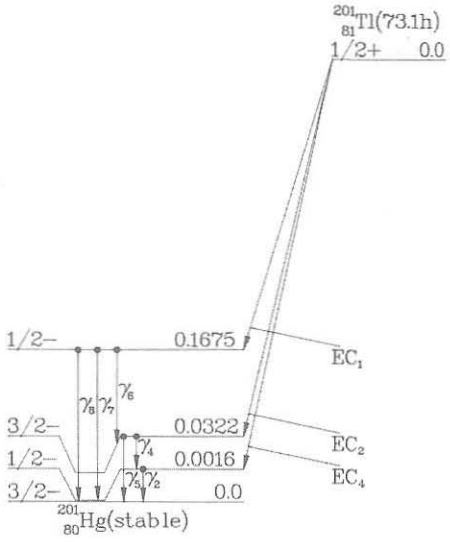

FIGURE 9-48 Decay scheme for ^{201}Tl. (Reprinted with permission from reference 149.)

After irradiation, the target is dissolved in mineral acid and the ^{201}Pb is separated by ion-exchange chromatography. After decay of the ^{201}Pb, ^{201}Tl is isolated by ion-exchange chromatography and the chloride salt is formed by dissolution in hydrochloric acid and evaporated to dryness. The ^{201}TlCl is dissolved in sodium hydroxide and adjusted to pH 7.0, sterilized, and tested to detect any carrier thallium present. Radiochromatography is done to differentiate Tl^{+} and Tl^{3+}. Radiochemical purity is not less than 95%. Gamma spectroscopy is performed to assess radionuclidic purity.

^{201}Tl decays by EC with a half-life of 73.1 hours to stable ^{201}Hg:

$$\underset{200.9708\ \text{AMU}}{{}^{201}_{81}\text{Tl}_{120}} \xrightarrow[p^{+}+e^{-}\rightarrow n+\nu]{} \underset{200.97031\ \text{AMU}}{{}^{201}_{80}\text{Hg}_{121}} + 0.456\,\text{MeV}(\nu,\gamma)$$

The transition energy for this decay is 0.456 MeV, which is dissipated by one of three EC routes to excited levels of mercury (Figure 9-48). The principal photons are 0.135 MeV (γ_6) at 2.7%, 0.167 MeV (γ_8) at 10%, and 0.0689 to 0.0803 MeV mercury x-rays at 94.4% abundance.[149]

Thallous Chloride Tl 201 Injection

Thallous chloride T1 201 injection is a sterile aqueous solution that contains at the time of calibration 1 mCi(37 MBq)/mL of ^{201}Tl-thallous chloride in 0.9% sodium chloride solution, pH adjusted to 4.5 to 7.0 and preserved with 0.9% benzyl alcohol.[188] Multidose vials in 2, 4, 8, and 9 mCi (74, 148, 296, and 333 MBq) sizes are available at different calibration times throughout the week. Its radiochemical purity is not less than 95%.[99] At the time of calibration, it contains no more than 1.0% each of ^{200}Tl and ^{202}Tl and not more than 0.25% ^{203}Pb as radionuclidic impurities, and no less than 98% ^{201}Tl as the desired radionuclide. The product is stored at room temperature.

^{201}Tl-thallous chloride is indicated for evaluation of myocardial perfusion in the diagnosis and localization of myocardial infarction and ischemic heart disease. Its other approved indication is the localization of parathyroid hyperactivity (adenoma) in patients with elevated serum calcium and parathyroid hormone levels. Thallium has also been used as a tumor marker in brain, breast, and lung cancer. Its mechanism of tumor localization is believed to

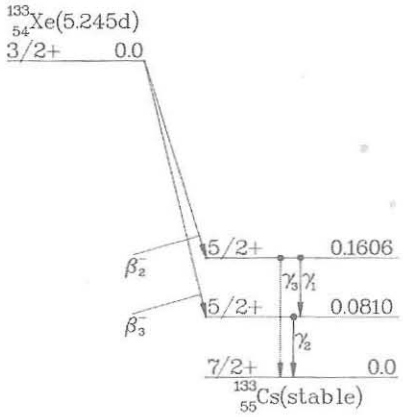

FIGURE 9-49 Decay scheme for ^{133}Xe. (Reprinted with permission from reference 149.)

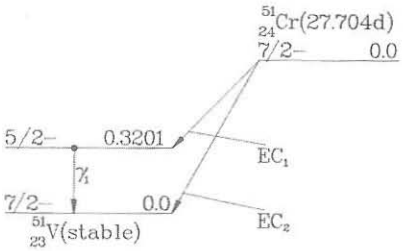

FIGURE 9-50 Decay scheme for ^{51}Cr. (Reprinted with permission from reference 149.)

^{51}Cr is produced by neutron activation of stable chromium metal or chromium oxide enriched in ^{50}Cr by the reaction $^{50}Cr(n,\gamma)^{51}Cr$.[192] The irradiated material is dissolved in hydrochloric acid and the chromic chloride is oxidized to chromate. ^{51}Cr decays by EC with a half-life of 27.7 days to stable ^{51}V as follows:

$$\underset{50.944786\ \text{AMU}}{{}^{51}_{24}Cr_{27}} \xrightarrow[p^+ + e^- \rightarrow n + \nu]{} \underset{50.943978\ \text{AMU}}{{}^{51}_{23}V_{28}} + 0.753\ \text{MeV}(\nu,\gamma)$$

The transition energy for this decay is 0.753 MeV, which is dissipated by one of two EC routes. In the case of EC_2, all of the energy is taken away by the neutrino. The EC_1 route decays to the excited level of vanadium (Figure 9-50).[149] In this route, the neutrino carries away 0.433 MeV, and a 0.320 MeV gamma ray is emitted from the excited nuclear state of vanadium. The 0.320 MeV photon has only a 10% abundance, making ^{51}Cr unsatisfactory for imaging. However, it is quite suitable for studies that involve in vitro scintillation counting procedures.

Sodium chromate Cr 51 injection (^{51}Cr-sodium chromate) is a clear, colorless sterile solution. It is available in 250 μCi (9.25 MBq) vials at a concentration of 100 μCi (3.7 MBq)/mL at the time of calibration. Its pH is between 7.5 and 8.5, and its specific activity is not less than 10 mCi (370 MBq)/mg Na_2CrO_4 at expiration.[99] The limit on specific activity is to prevent potential chromium toxicity of red blood cells. The radiochemical purity is not less than 90% as sodium chromate, which is determined by paper chromatography.[99] The presence of excess chromic impurity, $^{51}Cr^{3+}$, must be limited because it does not label erythrocytes. The product is stored at room temperature.

^{51}Cr-sodium chromate is indicated for determination of red blood cell volume or mass, study of red cell survival, and evaluation of blood loss. For determination of red cell volume, the dosage ranges from 10 to 30 μCi (370 to 1110 kBq); red cell survival studies utilize a dosage of 150 μCi (5.55 MBq). The critical organ is the spleen, with a radiation absorbed dose of 2.64 rad(cGy)/200 μCi.[192]

^{51}Cr is also available as the radiochemical chromic chloride, $^{51}CrCl_3$, for other labeling purposes and is sometimes used to label plasma proteins for assessing gastrointestinal protein loss. As ^{51}Cr-EDTA, it has been used to determine GFR.

TABLE 9-18 Physical Properties of Xenon Radioisotopes

Nuclide	Half-life	Decay Mode	Photons (MeV)	% Abundance
^{127}Xe	36.4 days	EC	0.172	26
			0.203	68
			0.375	17
^{133}Xe	5.24 days	Negatron	0.081	37

be related to tumor blood flow and permeability and active uptake via the Na-K ATPase pump as a thallium analogue. The usual adult dosage for myocardial imaging is 2 to 4 mCi (74 to 148 MBq) intravenously. The critical organ in males is the testes, with a radiation absorbed dose of 3 rad(cGy)/mCi; in females it is the thyroid gland, with a dose of 2.3 rad(cGy)/mCi.[188]

XENON XE 133 GAS

Xenon is an inert gas, and it is used in nuclear medicine in its native elemental state. Its electron configuration is $[Kr]4d^{10}5s^25p^6$. Two isotopes of xenon have been used clinically in nuclear medicine: ^{127}Xe and ^{133}Xe (Table 9-18). ^{127}Xe is cyclotron produced and was used for lung ventilation studies for several years, but it is no longer available. The principal isotope used currently is ^{133}Xe. It is produced as a fission byproduct in a nuclear reactor as follows: $^{235}U(n,f)^{133}Xe$. The product is available in unit dose vials ready for patient use in amounts of 10 mCi (370 MBq) and 20 mCi (740 MBq) from various suppliers. (The properties described here pertain to vials supplied by Mallinckrodt.) It may contain small amounts of other radioactive gas impurities, namely, ^{133m}Xe, ^{131m}Xe, and ^{85}Kr, in addition to ^{131}I.[189] It should be stored at room temperature. Xenon Xe 133 gas (^{133}Xe-xenon) is indicated for inhalation studies to evaluate lung function and for the assessment of cerebral blood flow. The usual adult dosage is 10 mCi (370 MBq) by inhalation. The critical organ is the lung. The radiation absorbed dose depends on the volume of the spirometer used to perform the study; for a 5 L spirometer it is 0.11 rad/10 mCi and for a 10 L spirometer it is 0.065 rad/10 mCi.[189]

^{133}Xe undergoes negatron (beta minus) decay with a half-life of 5.25 days to stable cesium:

$$\underset{132.9055\ \text{AMU}}{{}^{133}_{54}Xe_{79}} \xrightarrow[n \rightarrow p^+ + e^-]{} \underset{132.9051\ \text{AMU}}{{}^{133}_{55}Cs_{78}} + 0.373\ \text{MeV}(\beta,\gamma)$$

The principal photon used for imaging is 0.081 MeV (γ_2), 37% abundance (Figure 9-49).[149]

SODIUM CHROMATE CR 51 INJECTION

Chromium is another transition element. Transition elements owe their separate classification in the periodic table to belated filling of the next-to-outermost electron energy level. Chromium's electron configuration is $[Ar]3d^54s^1$. Chromium can exist in several oxidation states, the most common one in nuclear medicine being 6+ as sodium chromate, $Na_2{}^{51}CrO_4$. Sodium chromate is an oxidizing agent and can be readily reduced to the 3+ oxidation state. From the biologic perspective, chromate ion ($^{51}CrO_4^{2-}$) readily diffuses through the erythrocyte membrane, and it is used to label red blood cells. Chromate is reduced intracellularly to chromic ion ($^{51}Cr^{3+}$), which binds to hemoglobin in the red cell.[190,191]

TABLE 9-19 Physical Properties of Cobalt Radioisotopes

Nuclide	Half-life	Decay Mode	Photons (MeV)	% Abundance
^{57}Co	271.8 days	EC	0.122	86
			0.137	10
^{58}Co	70.88 days	EC, positron	0.511	30
			0.811	99
^{60}Co	5.27 yr	Negatron	1.173	100
			1.333	100

CYANOCOBALAMIN CO 57 CAPSULES

Cobalt is a transition metal whose chemistry is similar to that of iron and nickel. Its electron configuration is $[Ar]3d^74s^2$. Cobalt shows oxidation states of 2+ (cobaltous) and 3+ (cobaltic); however, unlike ferrous iron, the 2+ oxidation state is quite stable to oxidation, and its solutions can be kept indefinitely exposed to air. Cobalt is hexacoordinate. In solution Co^{2+} is likely to exist as the hydrated ion $Co(H_2O)_6^{2+}$.

The primary radioisotopes of cobalt are ^{57}Co, ^{58}Co, and ^{60}Co. Their physical properties are shown in Table 9-19. The most frequently used isotopes in nuclear medicine are ^{57}Co and ^{58}Co. ^{60}Co has the longest half-life and the most energetic photons and produces the highest radiation dose. It is no longer used as a tracer. ^{58}Co is generally prepared by neutron irradiation of a nickel target by the reaction $^{58}Ni(n,p)^{58}Co$. The irradiated target materials (nickel metal, oxides, or carbonate) are dissolved in concentrated acids, and the ^{58}Co nuclide is isolated by ion-exchange and solvent extraction methods.[193] ^{57}Co is produced in a cyclotron by four simultaneous proton-induced reactions on a nickel-58 target electroplated on a copper target holder.[194] The reactions are

$$^{58}Ni(p,2p)^{57}Co$$

$$^{58}Ni(p,pn)^{57}Ni \xrightarrow{37\ hr} {}^{57}Co$$

$$^{58}Ni(p,2n)^{57}Cu \longrightarrow {}^{57}Ni \xrightarrow{37\ hr} {}^{57}Co$$

After bombardment the nickel target is stripped from the copper with concentrated hydrochloric acid, isolated on an ion-exchange resin, and eluted with 6 M hydrochloric acid.

^{57}Co decays with a half-life of 271.8 days by EC to stable ^{57}Fe as follows:

$$^{57}_{27}Co_{30} \xrightarrow[p^+ + e^- \rightarrow n + \nu]{} {}^{57}_{26}Fe_{31} + 0.838\ MeV(\nu,\gamma)$$

56.93629 AMU 56.93539 AMU

The transition energy for this decay is 0.838 MeV, which is released by either of two EC routes, each to an excited level of ^{57}Fe followed by emission of gamma rays (Figure 9-51).[149] The most abundant gamma rays are 0.122 MeV (γ_2) at 86% and 0.137 MeV (γ_3) at 10%.

Cyanocobalamin is a water-soluble compound that crystallizes as small red needles. Its solutions are a cherry red color. Cyanocobalamin is a cobalt coordination complex in which the cobalt is trivalent and has a coordination number of six. The complex is neutral; its structure is shown in Figure 9-52. The cyanide group coordinated to the cobalt is not part of the natural vitamin but rather is an artifact caused by isolation of the vitamin on

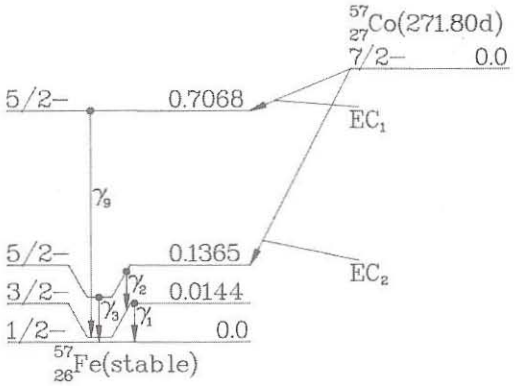

FIGURE 9-51 Decay scheme for ^{57}Co. (Reprinted with permission from reference 149.)

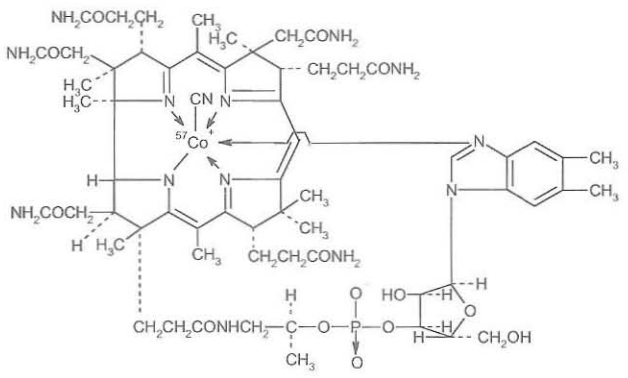

FIGURE 9-52 Chemical structure of ^{57}Co-cyanocobalamin.

charcoal. Vitamin B_{12} stored in the liver has a 5′-deoxyadenosyl anion ligand instead of cyanide.[195] By strict organic chemical definition, however, because cyanide was the first form of the vitamin to be isolated, cyanocobalamin is vitamin B_{12}.

Cyanocobalamin labeled with cobalt radionuclides is prepared biosynthetically. The radiolabeled cobalamins are isolated from a fermentation of the microorganism *Streptomyces griseus* grown in a nutrient medium containing the appropriate cobalt nuclide salt.[196]

Cyanocobalamin Co 57 capsules for oral administration contain approximately 0.5 to 1.0 μCi (18.5 to 37 kBq) in each capsule, with a specific activity not less than 0.5 μCi (18.5 kBq)/μg of cyanocobalamin.[99] The radiochemical purity is not less than 95%.[99] ^{57}Co-cyanocobalamin is indicated for the diagnosis of pernicious anemia and of other defects of intestinal absorption of vitamin B_{12}. The usual adult dosage is one capsule of 0.5 to 1.0 μCi (18.5 to 37 kBq). The capsules are typically used in the Schilling urinary excretion test of vitamin B_{12} absorption. The product is available from Bracco Diagnostics as ^{57}Co-cyanocobalamin capsules alone or as a diagnostic kit that contains the capsules, a ^{57}Co reference standard, intrinsic factor capsules (for Schilling test 2), and a 1000 μg syringe of "cold" vitamin B_{12}. Either product should be stored at room temperature. The critical organ is the liver, with a radiation absorbed dose of 0.13 rad(cGy)/μCi in normal subjects (without a flushing dose of "cold" B_{12}) and 0.026 rad(cGy)/μCi in patients with pernicious anemia.[197]

PHOSPHORUS CHEMISTRY

Phosphorus is a member of the group V elements. Members of this group have properties ranging from nonmetallic (nitrogen and phosphorus) to semimetallic (argon and antimony)

to metallic (bismuth).[198] Each of these elements has five valence electrons in its outermost energy level. The electron configuration of phosphorus is $[Ne]3s^23p^3$. Phosphorus can assume valences from 3– (by acquiring three electrons) to 5+ (by losing five electrons). It is most commonly known in pharmacy in its acid form, orthophosphoric acid (H_3PO_4). As a triprotic acid, it dissociates into three possible conjugate base forms depending on the pH of the solution. The predominant forms of phosphate present in the pH range of pharmaceutical injections are the monobasic ($H_2PO_4^-$) and the dibasic (HPO_4^{2-}) anions. The ionic equilibrium equation for these forms is

$$H_2PO_4^- \xleftarrow{\leftarrow H^+ OH^- \rightarrow} HPO_4^{2-} \left(pKa\ 7.2\right)$$

At a pH higher than 7.2, the dibasic form predominates, and the presence of excess Ca^{2+} ions in solution may cause the precipitation of dibasic calcium phosphate ($CaHPO_4$) because of its low solubility (approximately 30 mg/dL). This can be prevented by keeping the pH below 7. If Al^{3+} ions are present in a solution with phosphate, aluminum phosphate will precipitate because it is insoluble. When this is a possibility, a chelating agent such as EDTA is often used to sequester the aluminum away from the phosphate. EDTA is used in ^{99m}Tc-sulfur colloid kits for this purpose.

Among the other phosphoric acids are pyrophosphoric acid, $H_4P_2O_7$, and metaphosphoric acid, HPO_3. While pyrophosphoric acid, like orthophosphoric acid, is a discrete molecule, metaphosphoric acid is polymeric. Solutions of these acids are not stable and on standing over time will convert to orthophosphoric acid. The sodium salts of these acids are useful agents in chemistry because they will complex metal ions. Sodium trimetaphosphate ($Na_3P_3O_9$) is prepared by heating NaH_2PO_4 for several hours at 550°C. It forms soluble chelates with cations, notably Ca^{2+}, and has been used extensively as a water-softening agent under the trade name Calgon. Sodium pyrophosphate, $Na_4P_2O_7$, and sodium trimetaphosphate are used extensively in nuclear medicine as the stannous chelates in kits used for bone imaging and for tagging red blood cells. These include the stannous pyrophosphate kits (TechneScan PYP, Mallinckrodt; Phosphotec, Bracco; CIS-PYRO, CIS-US) and the stannous trimetaphosphate kit (Pyrolite, CIS-US). See Figure 9-8 for the chemical structures of these phosphates.

The radioisotope of phosphorus used in nuclear medicine is ^{32}P. It is prepared in a nuclear reactor by the capture of a fast neutron by stable sulfur according to the reaction $^{32}S(n,p)^{32}P$. ^{32}P decays by negatron emission with a half-life of 14.26 days to stable ^{32}S as follows:

$$\underset{31.973908\ AMU}{{}^{32}_{15}P_{17}} \xrightarrow[n \rightarrow p^+ + e^-]{} \underset{31.972047\ AMU}{{}^{32}_{16}S_{16}} + 1.73\,MeV\left(\beta,\nu\right)$$

^{32}P is considered to be a pure beta emitter because no gamma photons are emitted during its decay (Figure 9-53). The transition energy for this decay is 1.73 MeV, which is split between the beta particle and the neutrino. Bremsstrahlung radiation is produced during the decay of ^{32}P, but this is secondary to the decay process and is caused by the interaction of the high-speed beta particle with matter. Because it lacks any principal photon, ^{32}P is used only in therapeutic applications. The principal radiopharmaceuticals available that are labeled with ^{32}P are chromic phosphate P 32 suspension and sodium phosphate P 32 solution.

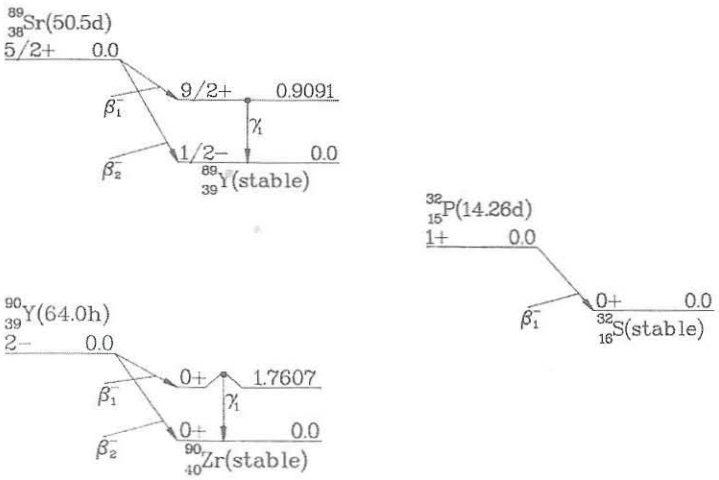

FIGURE 9-53 Decay schemes for ^{89}Sr, ^{32}P, and ^{90}Y. (Reprinted with permission from reference 149.)

Chromic Phosphate P 32 Suspension

Chromic phosphate P 32 suspension (^{32}P-chromic phosphate) is a grayish-green insoluble colloidal chromic phosphate ($Cr^{32}PO_4$). It is produced by mixing chromic nitrate solution with radiophosphoric acid. The resulting precipitate of chromic phosphate is dried in an oven and reduced to a particle size of about 1 μm in a ball mill.[198,199] A commercial product is available (Phosphocol P-32, Mallinckrodt) that is a sterile aqueous suspension in 30% dextrose and 0.1% sodium acetate, preserved with 2% benzyl alcohol. Its particle size distribution is as follows: less than 0.6 μm, 0.7%; 0.7 to 1.3 μm, 74.4%; 1.4 to 2.0 μm, 16.6%; 2.1 to 4.0 μm, 7%; more than 4.0 μm, 2.9%. Its radiochemical purity is not less than 95% and it has a pH range of 3.0 to 5.0.[99] The product is stored at room temperature. It is available in 15 mCi (555 MBq) multidose vials at a concentration of 5 mCi (185 MBq)/mL, with a specific activity of 3.3 mCi (122.1 MBq)/mg of chromic phosphate at calibration.[200]

^{32}P-chromic phosphate is administered by intracavitary instillation for the treatment of peritoneal or pleural effusions caused by metastatic disease. It has also been used in the interstitial treatment of cancer. An off-label application is radiation synovectomy in diseases involving inflamed synovial lining, such as rheumatoid arthritis. Typical adult dosage for intraperitoneal instillation is 10 to 20 mCi (370 to 740 MBq); for intrapleural instillation it is 6 to 12 mCi (222 to 444 MBq). Interstitial tumor dose is based on estimated tumor mass and is in the range of 0.1 to 0.5 mCi (3.7 to 18.5 MBq)/gram. The radiation absorbed dose depends on the tissue surface area exposed and depth; calculations for an average (70 kg) patient with 90% retention are shown in Table 9-20.[200]

Sodium Phosphate P 32 Solution

Sodium phosphate P 32 solution (^{32}P-sodium phosphate) is a clear, colorless sterile solution of sodium phosphate at pH 5.0 to 6.0. It is suitable for oral or intravenous administration. *USP 24* states that the product is dibasic sodium phosphate, but at the final pH range listed in the product monograph it is mostly the monobasic form because the pKa for the equilibrium of these two forms is 7.2 (see first reaction under Phosphorus Chemistry). The commercial product is available with a radioactive concentration of 0.67 mCi (24.79 MBq)/mL in 5 mCi (185 MBq) vials at the time of calibration. Its radiochemical purity must be 100%.[99] It is stored at room temperature.

TABLE 9-20 Radiation Dose Estimates for Chromic Phosphate P 32 Suspension[a]

		Tissue Absorbed Dose (rad) per 20 mCi (740 MBq)		
Tissue Depth (cm)	Dose Rate (rad/hr)	Pleural (4000 cm²)	Peritoneal (5000 cm²)	Prostate (16 grams)
0.004	10.2	23,000	18,000	910,000
0.008	8.58	19,000	15,000	
0.012	7.61	17,000	14,000	
0.016	6.91	15,000	12,000	
0.020	6.36	14,000	11,000	
0.10	2.41	5,400	4,300	
0.20	0.94	2,100	1,700	

[a] For 70 kg patient with 90% retention.

Source: Phosphocol P-32 package insert (Mallinckrodt; November 2000).

^{32}P-sodium phosphate is indicated for the treatment of polycythemia vera, chronic myelocytic leukemia, and chronic lymphocytic leukemia. It has also been used as a palliative treatment for skeletal metastases in the treatment of bone pain. The adult dosage for polycythemia vera, established by the Polycythemia Vera Study Group, recommends an initial intravenous dose of 2 to 3 mCi (74 to 111 MBq)/m² of body surface area, not to exceed 5 mCi (185 MBq).[201] The radiation absorbed dose to the bone marrow has been estimated to be 24 rad(cGy)/mCi, divided among marrow, 13 rad(cGy); trabecular bone, 10 rad(cGy); and cortical bone, 1 rad(cGy).[202]

STRONTIUM CHEMISTRY

Strontium is a member of the group II (alkaline-earth) elements, which include beryllium, magnesium, calcium, barium, and radium. Strontium's electron configuration is [Kr]5s². Alkaline-earth metals are so named because alchemists referred to any nonmetallic substance that was insoluble and unchanged by fire as an "earth," and the earths of group II give an alkaline reaction.[198] They are moderately strong reducing agents, and their compounds have an oxidation state of 2+. In vivo these elements have a propensity to localize in bone. Several radioisotopes of strontium have been used in nuclear medicine over the years, notably ^{85}Sr and ^{87m}Sr for bone imaging and ^{89}Sr for therapy.

Strontium Chloride Sr 89 Injection

^{89}Sr is the isotope currently used in nuclear medicine. It is produced by neutron activation of enriched ^{88}Sr by the reaction ^{88}Sr(n,γ)^{89}Sr. The target is processed into its final form as strontium chloride, $^{89}SrCl_2$. ^{89}Sr decays by beta emission with a 50.5 day half-life to stable ^{89}Y as follows:

$$\underset{88.90697\ \text{AMU}}{{}^{89}_{38}Sr_{51}} \xrightarrow[n \rightarrow p^{+}+e^{-}]{} \underset{88.9054\ \text{AMU}}{{}^{89}_{39}Y_{50}} + 1.463\,\text{MeV}(\beta,\nu)$$

The transition energy for this decay is 1.463 MeV, which is the maximum energy of the beta particle. The average energy of the beta particle is 0.583 MeV, with the remainder carried off by the neutrino. Strontium decays by one of two beta transitions, one going to the excited level of ^{89}Y (Figure 9-53). This path results in a gamma ray emission of 0.091

TABLE 9-20 Radiation Dose Estimates for Chromic Phosphate P 32 Suspension[a]

Tissue Depth (cm)	Dose Rate (rad/hr)	Tissue Absorbed Dose (rad) per 20 mCi (740 MBq)		
		Pleural (4000 cm²)	Peritoneal (5000 cm²)	Prostate (16 grams)
0.004	10.2	23,000	18,000	910,000
0.008	8.58	19,000	15,000	
0.012	7.61	17,000	14,000	
0.016	6.91	15,000	12,000	
0.020	6.36	14,000	11,000	
0.10	2.41	5,400	4,300	
0.20	0.94	2,100	1,700	

[a] For 70 kg patient with 90% retention.

Source: Phosphocol P-32 package insert (Mallinckrodt; November 2000).

^{32}P-sodium phosphate is indicated for the treatment of polycythemia vera, chronic myelocytic leukemia, and chronic lymphocytic leukemia. It has also been used as a palliative treatment for skeletal metastases in the treatment of bone pain. The adult dosage for polycythemia vera, established by the Polycythemia Vera Study Group, recommends an initial intravenous dose of 2 to 3 mCi (74 to 111 MBq)/m² of body surface area, not to exceed 5 mCi (185 MBq).[201] The radiation absorbed dose to the bone marrow has been estimated to be 24 rad(cGy)/mCi, divided among marrow, 13 rad(cGy); trabecular bone, 10 rad(cGy); and cortical bone, 1 rad(cGy).[202]

STRONTIUM CHEMISTRY

Strontium is a member of the group II (alkaline-earth) elements, which include beryllium, magnesium, calcium, barium, and radium. Strontium's electron configuration is [Kr]5s². Alkaline-earth metals are so named because alchemists referred to any nonmetallic substance that was insoluble and unchanged by fire as an "earth," and the earths of group II give an alkaline reaction.[198] They are moderately strong reducing agents, and their compounds have an oxidation state of 2+. In vivo these elements have a propensity to localize in bone. Several radioisotopes of strontium have been used in nuclear medicine over the years, notably ^{85}Sr and ^{87m}Sr for bone imaging and ^{89}Sr for therapy.

Strontium Chloride Sr 89 Injection

^{89}Sr is the isotope currently used in nuclear medicine. It is produced by neutron activation of enriched ^{88}Sr by the reaction ^{88}Sr(n,γ)^{89}Sr. The target is processed into its final form as strontium chloride, $^{89}SrCl_2$. ^{89}Sr decays by beta emission with a 50.5 day half-life to stable ^{89}Y as follows:

$$^{89}_{38}Sr_{51} \xrightarrow[n \rightarrow p^{+}+e^{-}]{} {}^{89}_{39}Y_{50} + 1.463\,MeV(\beta,\nu)$$

88.90697 AMU 88.9054 AMU

The transition energy for this decay is 1.463 MeV, which is the maximum energy of the beta particle. The average energy of the beta particle is 0.583 MeV, with the remainder carried off by the neutrino. Strontium decays by one of two beta transitions, one going to the excited level of ^{89}Y (Figure 9-53). This path results in a gamma ray emission of 0.091

MeV (γ_1), but with a very low abundance (0.009%) that is not sufficient for imaging or measuring ^{89}Sr activity in a dose calibrator. However, because the manufacturer assays its product with scintillation methods traceable to the National Institute of Standards and Technology, the product itself can be used as a source to determine a dose calibrator setting for measuring dosages after appropriate decay correction of the product.[203]

Strontium chloride Sr 89 injection (^{89}Sr-strontium chloride; Metastron, Medi-Physics/Amersham) is a sterile aqueous solution at pH 4.0 to 7.5. It is supplied in 4 mCi (148 MBq) vials at a concentration of 1 mCi (37 MBq)/mL, with a specific activity of 80 to 167 μCi (2.96 to 6.18 MBq)/mg at the time of calibration. The product is stored at room temperature (15°–25°C) and expires 28 days after calibration.

^{89}Sr-strontium chloride is indicated for the palliative treatment of bone pain in patients with skeletal metastases. The usual adult dosage is 4 mCi intravenously, and it can be dosed by weight at 40 to 60 μCi (1.48 to 2.22 MBq)/kg. The critical organ is the bone surface, with a radiation absorbed dose of 63 rad(cGy)/mCi.[204]

YTTRIUM CHEMISTRY

Yttrium is a member of the group IIIB transition elements. Its electron configuration is $[Kr]4d^15s^2$. It is quite rare naturally, but as a metal it reacts well to produce compounds in which its oxidation state is 3+. Yttrium hydrolyzes below pH 7 and thus requires buffering with sodium acetate during labeling reactions, similar to indium. To be an effective label for antibodies, yttrium must be chelated firmly with a derivatized DTPA ligand; otherwise, it will dissociate and localize in bone, where it can deliver a high radiation dose to the bone marrow.

^{90}Y is the daughter product of ^{90}Sr decay. ^{90}Y itself decays by beta emission with a half-life of 64.0 hours to stable zirconium ^{90}Zr, as follows:

$$\underset{89.9067\ \text{AMU}}{{}^{90}_{39}Y_{51}} \xrightarrow[n \rightarrow p^+ + e^-]{} \underset{89.90426\ \text{AMU}}{{}^{90}_{40}Zr_{50}} + 2.27\,\text{MeV}(\beta, \nu)$$

The transition energy for this decay is 2.27 MeV, which can be carried away by one of two possible beta transitions, but essentially the β_2 route occurs 100% to the ground state of ^{90}Zr (Figure 9-53). The maximum beta-particle energy is 2.27 MeV, and the average particle energy is 0.935 MeV, with the remainder carried off by the neutrino.

Yttrium Y 90 Chloride Solution

Yttrium Y 90 chloride is a sterile aqueous solution of yttrium chloride in 0.05 M hydrochloric acid. It is produced by solvent extraction of ^{90}Y from a ^{90}Sr generator solution and purified into the chloride form, $^{90}YCl_3$. ^{90}Y-yttrium chloride is available from MDS Nordion (Ontario, Canada) in 5, 10, 20, and 50 mCi (185, 370, 740, and 1850 MBq) amounts per vial with no more than 20 μCi of ^{90}Sr radionuclide impurity per Ci of ^{90}Y at expiration. The product is used for labeling monoclonal antibodies for radioimmunotherapy. A notable example is ibritumomab tiuxetan (^{90}Y-ibritumomab tiuxetan; Zevalin, IDEC Pharmaceuticals) for the treatment of patients with relapsed or refractory low-grade, follicular, or transformed B-cell non-Hodgkin's lymphoma. Details of this antibody are discussed in Chapter 23.

SAMARIUM CHEMISTRY

Samarium is a member of the lanthanide transition elements known as the rare earths. Its electron configuration is $[Xe]4f^6 5d^0 6s^2$, and it forms complexes in the 3+ oxidation state. ^{153}Sm has useful properties for therapeutic application in palliation of painful bone metastases. It forms coordination complexes of high thermodynamic stability with phosphonate and aminocarboxylate ligands.[205] ^{153}Sm is produced in high yield and purity by neutron irradiation of isotopically enriched ^{152}Sm oxide ($^{152}Sm_2O_3$) by the reaction $^{152}Sm(n,\gamma)^{153}Sm$. The oxide target is dissolved in 1.0 M hydrochloric acid, diluted to 0.1 M hydrochloric acid, added to a lyophilized kit of ethylenediaminetetramethylenephosphonic acid (EDTMP) for complexation, and brought to pH 7.0 to 8.5 with sodium hydroxide.[206] The ionic formula for the complex is $^{153}Sm^{3+}[CH_2N(CH_2PO_3^{2-}]_2$, and it has a molecular weight of 581.1. The chemical structure of the pentasodium salt is shown in Figure 9-54.

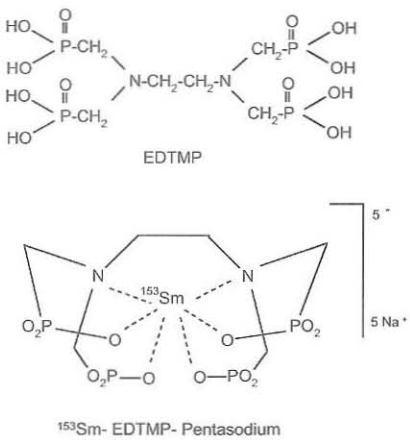

FIGURE 9-54 Chemical structures of EDTMP ligand and its ^{153}Sm coordination complex.

^{153}Sm decays by beta emission with a 46.7 hour half-life to stable ^{153}Eu according to the following decay equation:

$$^{153}_{62}Sm_{91} \xrightarrow[n \rightarrow p^+ + e^-]{} {}^{153}_{63}Eu_{90} + 0.810\ MeV(\beta,\nu,\gamma)$$

152.9217 AMU 152.92083 AMU

The transition energy for this decay is 0.810 MeV, which is dissipated by several beta-decay routes (Figure 9-55). The most abundant routes are β_{15} (20%), 0.810 MeV; β_{13} (50%), 0.710 MeV; and β_{11} (30%), 0.640 MeV. The most abundant gamma ray is γ_{11} (29%) at 0.103 MeV. The average energy released as beta particles per decay of ^{153}Sm is 0.233 MeV. This is computed by multiplying each maximum beta-particle energy listed above by its abundance and by 0.33 (the average fraction of transition energy per decay dissipated by beta particles) and then summing the individual average beta energies. Thus, we have (0.810 MeV) (0.20) (0.33) + (0.710 MeV) (0.50) (0.33) + (0.640 MeV) (0.30) (0.33) = 0.233 MeV.

Samarium Sm 153 Lexidronam Injection

Samarium Sm 153 lexidronam injection (^{153}Sm-lexidronam; Quadramet, DuPont Merck) is a sterile, aqueous, clear to light amber solution for intravenous administration. Each milliliter of solution contains, at calibration, 35 mg $EDTMP \cdot 2H_2O$; 5.3 mg Ca as $Ca(OH)_2$; 14.1 mg Na as NaOH, equivalent to 44 mg Ca/Na EDTMP (anhydrous); and 50 mCi (1850 MBq) ^{153}Sm, at a specific activity of 1.0 to 11.0 mCi (37 to 407 MBq)/μg Sm. The solution pH is 7.0 to 8.5. The product is available as a frozen solution at a concentration of 50 mCi (1850 MBq)/mL in vial sizes of 100 mCi (3700 MBq) and 150 mCi (5550 MBq). The drug expires 48 hours after the calibration time or within 8 hours of thawing.

Although the thermodynamic stability constant of ^{153}Sm-EDTMP is quite high, the complex in not kinetically inert in plasma. Therefore, ^{153}Sm-lexidronam has a ligand-to-metal ratio of approximately 250:1 to 300:l. The excess ligand prevents any samarium that dissociates from the EDTMP from forming insoluble ^{153}Sm-hydroxyl species that localize in the liver.[205]

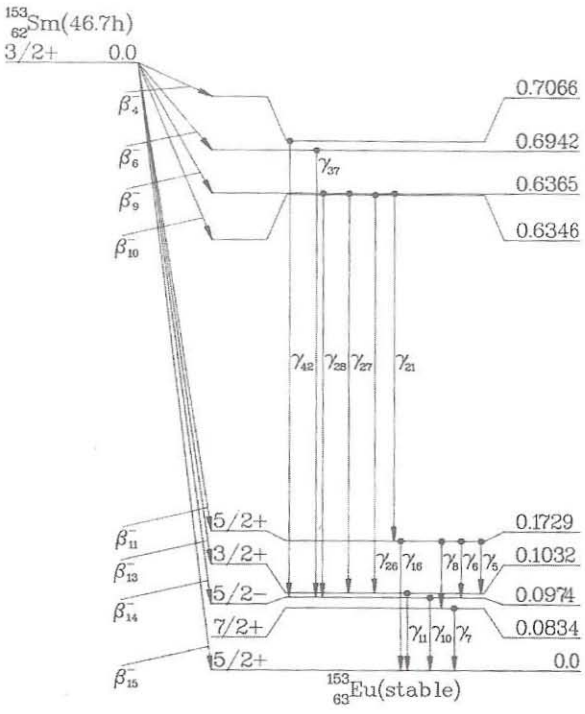

FIGURE 9-55 Decay scheme for ^{153}Sm. (Reprinted with permission from reference 149.)

^{153}Sm-lexidronam is indicated for relief of pain in patients with confirmed osteoblastic metastatic bone lesions that enhance on radionuclide bone scan.[207] Neoplastic bone disease associated with lytic-type bony metastases such as multiple myeloma may not be treatable with ^{153}Sm-lexidronam.[206] The recommended dosage is 1 mCi (37 MBq)/kg intravenously. The critical organ is the bone surface, with a radiation absorbed dose of 25 rad(cGy)/mCi.[207]

REFERENCES

1. Wolf AP. Terminology concerning specific activity of radiopharmaceuticals [reply]. *J Nucl Med.* 1981;22:392-3.
2. Pizzarello DJ, Witcofski RL. *Basic Radiation Biology.* Philadelphia: Lea & Febiger; 1967:61.
3. McAfee JG, Subramanian G. Radioactive agents for imaging. In: Freeman LM, Johnson PM, eds. *Clinical Scintillation Imaging.* 2nd ed. New York: Grune & Stratton; 1975:13-114.
4. Eckelman WC, Reba RC. The classification of radiotracers. *J Nucl Med.* 1978;19:1179-81.
5. Counsell RE, Ice RD. The design of organ imaging radiopharmaceuticals. In: Ariens EJ, ed. *Drug Design.* Vol 2. 6th ed. New York: Academic Press; 1975:172.
6. Steigman J, Eckelman WC. *The Chemistry of Technetium in Medicine.* Washington, DC: National Academy Press; 1992:16.
7. Alvarez J. Preparation of ^{113m}In radiopharmaceuticals. In: Subramanian G, Rhodes BA, Cooper JF, et al., eds. *Radiopharmaceuticals.* New York: Society of Nuclear Medicine; 1975:102-6.
8. Cooper JF, Wagner HN Jr. Preparation and control of ^{113m}In radiopharmaceuticals. In: *Radiopharmaceuticals from Generator-Produced Radionuclides.* Vienna, Austria: International Atomic Energy Agency; 1971:83-9.
9. Perrier AC, Segrè E. Some chemical properties of element 43. *J Chem Physiol* 1937;5:712.
10. Glasstone S. *Sourcebook on Atomic Energy.* 3rd ed. New York: Van Nostrand Reinhold; 1967:657-8.
11. Seaborg GR, Segrè E. Nuclear isomerism of element 43. *Phys Rev.* 1939;55:808-14.
12. Richards P. Nuclide generators. In: Andrews GA, Knisely RM, Wagner HN Jr, eds. *Radioactive Pharmaceuticals.* Oak Ridge, TN: US Atomic Energy Commission; 1965:155-63.

13. Harper PV, Lathrop KA, Gottschalk A. Pharmacodynamics of some technetium-99m preparations. In: Andrews GA, Knisely RM, Wagner HN Jr, eds. *Radioactive Pharmaceuticals*. Oak Ridge, TN: US Atomic Energy Commission; 1965:335-58.
14. Richards P, Steigman J. Chemistry of technetium as applied to radiopharmaceuticals. In: Subramanian G, Rhodes BA, Cooper JF, et al., eds. *Radiopharmaceuticals*. New York: Society of Nuclear Medicine; 1975:23-35.
15. Eckelman W, Richards P. Instant Tc-99m DTPA. *J Nucl Med*. 1970;11:761.
16. Davison A, Jones AG, Orvig C, et al. A new class of oxotechnetium(5+) chelate complexes containing a $TcON_2S_2$ core. *Inorg Chem*. 1981;20:1629-32.
17. Loberg MD, Fields AT. Chemical structure of technetium-99m-labeled N-(2,6-dimethylphenylcarbamoylmethyl)iminodiacetic acid (Tc-HIDA). *Int J Appl Radiat Isot*. 1978;29:167-73.
18. Deutsch E, Glavan KA, Sodd VJ, et al. Cationic Tc-99m complexes as potential myocardial imaging agents. *J Nucl Med*. 1981;22:897-907.
19. Loberg MD, Fields AT. Stability of ^{99m}Tc-labeled N-substituted iminodiacetic acids: ligand exchange reaction between ^{99m}Tc-HIDA and EDTA. *Int J Appl Radiat Isot*. 1977;28:687-92.
20. Ryan J, Cooper M, Loberg M, et al. Technetium-99m-labeled N-(2,6-dimethylphenyl carbamoylmethyl) iminodiacetic acid (Tc-99m HIDA): a new radiopharmaceutical for hepatobiliary imaging studies. *J Nucl Med*. 1977;18:995-1004.
21. Davison A, Orvig C, Trop HS, et al. Preparation of oxobis(dithiolato) complexes of technetium(V) and rhenium (V). *Inorg Chem*. 1980;19:1988-92.
22. Jones AG, Abrams MJ, Davison A, et al. Biological studies of a new class of technetium complexes: the hexakis(alkylisonitrile)technetium (I) complexes. *Int J Nucl Med Biol*. 1984;11:225-34.
23. Cheesman EH, Blanchette MA, Ganey MV, et al. Technetium-99m ECD: ester-derivatized diamine-dithiol Tc complexes for imaging brain perfusion [abstract]. *J Nucl Med*. 1988;29:788.
24. Nowotnik DP, Canning LR, Cumming SA, et al. Development of a Tc-99m-labelled radiopharmaceutical for cerebral blood flow imaging. *Nucl Med Commun*. 1985;6:499-506.
25. Fritzberg AR, Kasina S, Eshima D, et al. Synthesis and biological evaluation of technetium-99m MAG3 as a hippuran replacement. *J Nucl Med*. 27;1986:111-16.
26. Forster AM, Storey AE, Archer CM, et al. Structural characterization of the new myocardial imaging agent technetium-99m tetrofosmin (^{99m}Tc-P 53) [abstract]. *J Nucl Med*. 1992;33:850.
27. Jones AG, Davison A, Trop HS, et al. Oxotechnetium (V) complexes [abstract]. *J Nucl Med*. 1979;20:641.
28. Mazzi U, Nicolini M, Bandoli G, et al. Technetium coordination chemistry: development of new backbones for ^{99m}Tc radiopharmaceuticals. In: Nicolini M, Bandoli G, Mazzi U, eds. *Technetium and Rhenium in Chemistry and Nuclear Medicine 3*. Verona, Italy: Cortina International; 1990:39-50.
29. Jurisson SS, Lydon JD. Potential technetium small molecule radiopharmaceuticals. *Chem Rev*. 1999;99:2205-18.
30. Liu S, Edwards DS. ^{99m}Tc-labeled small peptides as diagnostic radiopharmaceuticals. *Chem Rev*. 1999;99:2235-68.
31. Banerjee S, Pillai MRA. Evolution of Tc-99m in diagnostic radiopharmaceuticals. *Semin Nucl Med*. 2001;31:260-77.
32. Mease RC, Lambert C. Newer methods of labeling diagnostic agents with Tc-99m. *Semin Nucl Med*. 2001;31:278-85.
33. Lister-James J, Dean RT. Technetium-99m-labeled receptor-specific small synthetic peptides: practical imaging agents of biochemical markers. In: Nicolini M, Mazzi U, eds. *Technetium, Rhenium, and Other Metals in Chemistry and Nuclear Medicine 5*. Padova, Italy: SGE Ditorioli; 1999:401-7.
34. Lister-James J, Knight LC, Maurer AH, et al. Thrombus imaging with a technetium-99m-labeled, activated platelet receptor-binding peptide. *J Nucl Med*. 1996;37:775-81.
35. Rhodes BA, Zamora PO, Newell KD, et al. Technetium-99m labeling of murine monoclonal antibody fragments. *J Nucl Med*. 1986;27;685-93.
36. Schwarz A, Steinstrabber A. A novel approach to Tc-99m labeled monoclonal antibodies. *J Nucl Med*. 1987;28:P721.
37. Thakur ML, DeFulvio J, Richard MD, et al. Technetium-99m labeled monoclonal antibodies: evaluation of reducing agents. *Nucl Med Biol*. 1991;18:227-33.
38. Eckelman WC, Paik CH, Steigman J. Three approaches to radiolabeling antibodies with ^{99m}Tc. *Nucl Med Biol*. 1989;16:171-6.
39. Childs RL, Hnatowich DJ. Optimum conditions for labeling of DTPA-coupled antibodies with technetium-99m. *J Nucl Med*. 1985;26:293-9.
40. Abrams MJ, Juweid M, tenKate CI, et al. Technetium-99m-human polyclonal IgG radiolabeled via the hydrazine nicotinamide derivative for imaging focal sites of infection in rats. *J Nucl Med*. 1990;31:2022-8.
41. Hnatowich DJ, Mardirossian G, Rusckowski M, et al. Directly and indirectly technetium-99m-labeled antibodies: a comparison of in vitro and animal in vivo properties. *J Nucl Med*. 1993;34:109-19.

42. Fritzberg AR, Abrahams PG, Beaumier PL, et al. Specific and stable labeling of antibodies with technetium-99m with a diamide dithiolate chelating agent. *Proc Natl Acad Sci USA.* 1989;85:4025-9.
43. Alberto R, Schibli R, Egli A, et al. A novel organometallic aquo complex of technetium for the labeling of biomolecules: synthesis of $[Tc(H2O)3(CO)3]^+$ from $^{99m}TcO_4^-$ in aqueous solution and its reaction with a bifunctional ligand. *J Am Chem Soc.* 1998;120:7987-8.
44. Hoepping A, Reisgys M, Brust P, et al. TROTEC-1: a new high-affinity ligand for labeling of the dopamine transporter. *J Med Chem.* 1998;41:4429-32.
45. Spradau TW, Katzenellenbogen JA. Preparation of cyclopentadienyltricarbonylrhenium complexes using a double ligand-transfer reaction. *Organometallics.* 1998;17:2009-17.
46. Spradau TW, Katzenellenbogen JA. Protein and peptide labeling with (cyclopenadienyl)tricarbonyl rhenium and technetium. *Bioconjug Chem.* 1998;9:765-72.
47. Spradau TW, Edwards WB, Anderson CJ, et al. Synthesis and biological evaluation of Tc-99m cyclopentdienyltricarbonyltechnetium-labeled octreotide. *Nucl Med Biol.* 1999;26:1-7.
48. Volkert WA, Hoffman TS, Seger RM, et al. Tc-99m propylene amine oxime (Tc-99m PnAO); a potential brain radiopharmaceutical. *Eur J Nucl Med.* 1984;9:511-6.
49. Neirinckx RD, Canning LR, Piper IM, et al. Technetium-99m d,l-HM-PAO: a new radiopharmaceutical for SPECT imaging of regional cerebral blood perfusion. *J Nucl Med.* 1987;28:191-202.
50. Neirinckx RD, Burke JF, Harrison RC, et al. The retention mechanism of technetium-99m-HM-PAO: intracellular reaction with glutathione. *J Cereb Blood Flow Metab.* 1988;8:S4-12.
51. Hung JC, Corlija M, Volkert WA, et al. Kinetic analysis of technetium-99m d,l-HM-PAO decomposition in aqueous media. *J Nucl Med.* 1988;29:1568-76.
52. Lever SZ, Burns HD, Kervitsky TM, et al. Design, preparation, and biodistribution of a technetium-99m triaminedithiol complex to assess regional cerebral blood flow. *J Nucl Med.* 1985;26:1287-94.
53. Walovitch RC, Hill TC, Garrity ST, et al. Characterization of technetium-99m-L,L-ECD for brain perfusion imaging. 1: Pharmacology of technetium-99m ECD in nonhuman primates. *J Nucl Med.* 1989; 30:1892-901.
54. Jones AG, Davison A, LaTegola MR, et al. Chemical and in vivo studies of the anion oxo[N,N'-ethylenebis(2-mercaptoacetimido)]technetate(V). *J Nucl Med.* 1982;23:801-9.
55. Fritzberg AR, Rao TN, Adhikesavalu D, el al. Synthesis and characterization of Re and Tc complexes of N_2S_2 and N_3S ligands. In: *Proceedings of the Sixth International Symposium on Radiopharmaceutical Chemistry.* New York: Wiley; 1986:95-7.
56. Eshima D, Fritzberg AR, Taylor A Jr. ^{99m}Tc renal tubular function agents: current status. *Semin Nucl Med.* 1990;20:28-40.
57. Nosco DL, Wolfangel RG, Bushman MJ, et al. Technetium-99m MAG3: labeling conditions and quality control. *J Nucl Med Technol.* 1993;21:69-74.
58. Hung J, Wilson ME, Brown M. Rapid preparation and quality control of technetium-99m MAG3. *J Nucl Med Technol.* 1991;19:176-9.
59. Kung MP, Stevenson DA, Plossl K, et al. ^{99m}Tc-TRODAT-1: a novel technetium-99m complex as a dopamine transporter imaging agent. *Eur J Nucl Med.* 1997;24:372-80.
60. Mozley PD, Stubbs JB, Plossl K, et al. Biodistribution and dosimetry of TRODAT-1: a technetium-99m tropane for imaging dopamine transporters. *J Nucl Med* 1998;39:2069-76.
61. Johannsen B, Scheunemann M, Spies H, et al. Technetium(V) and rhenium(V) complexes for 5-HT_{2A} serotonin receptor binding: structure-affinity considerations. *Nucl Med Biol.* 1996;23:429-38.
62. Seifert S, Pietzsch HJ, Scheunemann M, et al. No carrier added preparations of "3 + 1" mixed-ligand ^{99m}Tc complexes. *Appl Radiat Isot.* 1998;49:5-11.
63. Johannsen B, Berger R, Brust P, et al. Structural modification of receptor-binding technetium-99m complexes in order to improve brain uptake. *Eur J Nucl Med.* 1997;24:316-9.
64. Syhre R, Seifert S, Spies H, et al. Stability versus reactivity of "3 + 1" mixed-ligand technetium-99m complexes in vitro and in vivo. *Eur J Nucl Med.* 1998;25:793-6.
65. Sinusas AJ. The potential for myocardial imaging with hypoxia markers. *Semin Nucl Med.* 1999;29:330-88.
66. Ballinger JR. Imaging hypoxia in tumors. *Semin Nucl Med.* 2001;31:321-9.
67. Murugesan S, Shetty SJ, Noronha OPD, et al. Technetium-99m-cyclam AK 2123: a novel marker for tumor hypoxia. *Appl Radiat Isot.* 2001;54:81-8.
68. Verbruggen AM, Nosco DL, Van Neron CG, et al. Technetium-99m-L,L-ethylenedicysteine: a renal imaging agent. I: Labeling and evaluation in animals. *J Nucl Med.* 1992;33:551-7.
69. Taylor A, Hansen L, Eshima D, et al. Comparison of technetium-99m-LL-EC isomers in rats and humans. *J Nucl Med.* 1997;38:821-6.
70. Kelly JD, Forster AM, Higley B, et al. Technetium-99m-Tetrofosmin as a new radiopharmaceutical for myocardial perfusion imaging. *J Nucl Med.* 1993;34:222-7.
71. Burke J. Advances in ^{99m}Tc Radiopharmaceutical Chemistry. Paper presented at the 148th Annual Meeting of the American Pharmaceutical Association; March 2001; San Francisco, Calif.

72. Baldas J, Bonnyman J. Substitution reactions of $^{99m}TcNCl_4^-$: a route to a new class of ^{99m}Tc-radiopharmaceuticals. *Int J Appl Radiat Isot.* 1985;36:133-9.
73. Baldas J, Bonnyman J. Effect of ^{99m}Tc-nitrido group on the behavior of ^{99m}Tc-radiopharmaceuticals. *Int J Appl Radiat Isot.* 1985;36:919-23.
74. Pasqualini R, Duatti A, Bellande E, et al. Bis(dithiocarbamato) nitrido technetium-99m radiopharmaceuticals: a class of neutral myocardial imaging agents. *J Nucl Med.* 1994;35:334-41.
75. Fagret D, Pierre-Yves M, Brunotte F, et al. Myocardial perfusion imaging with technetium-99m-Tc NOET: comparison with thallium-201 and coronary angiography. *J Nucl Med.* 1995;36:936-43.
76. Liu S, Edwards DS, Looby RJ, et al. Labeling a hydrazino nicotinamide-modified cyclic IIb/IIIa receptor antagonist with ^{99m}Tc using aminocarboxylates as coligands. *Bioconjug Chem.* 1996;7:63-71.
77. Edwards DS, Liu S, Barrett JA, et al. New and versatile ternary ligand system for technetium radiopharmaceuticals: water soluble phosphines and tricine as coligands in labeling a hydrazinonicotinamide-modified cyclic glycoprotein IIb/IIIa receptor antagonist with ^{99m}Tc. *Bioconjug Chem.* 1997;8:146-54.
78. Barrett JA, Crocker AC, Damphouse DJ, et al. Biological evaluation of thrombus imaging agents utilizing water soluble phosphines and tricine as coligands when used to label a hydrazinonicotinamide-modified cyclic glycoprotein IIb/IIIa receptor antagonist with ^{99m}Tc. *Bioconjug Chem.* 1997;8:155-60.
79. Nishiyama H, Deutsch E, Adolph RJ, et al. Basal kinetic studies of Tc-99m DMPE as a myocardial imaging agent in the dog. *J Nucl Med.* 1982;23:1093-1101.
80. Treher EN, Francesconi LC, Gougoutas JZ, et al. Monocapped tris (dioxime) complexes of technetium(III): synthesis and structural characterization of $TcX(dioxime)_3$ B-R (x = Cl, Br; dioxime = dimethylglyoxime, cyclohexanedione dioxime; R = CH_3, C_4H_9. *Inorg Chem.* 1989;28:3411-6.
81. Rossetti C, Vanoli G, Paganelli G, et al. Human biodistribution, dosimetry and clinical use of technetium(III)-99m-Q12. *J Nucl Med.* 1994;35:1571-80.
82. Deutsch E, Vanderhayden J, Gerundini P, et al. Development of nonreducible technetium-99m(III) cations as myocardial perfusion imaging agents: initial experience in humans. *J Nucl Med.* 1987;28:1870-80.
83. Hendel RC, Gerson MC, Verani MS, et al. Perfusion imaging with Tc-99m furifosmin (Q12): multicenter phase III trial to evaluate safety and comparative efficacy [abstract]. *Circulation.* 1994;90:I-449.
84. Srivastava SC, Richards P. Technetium-labeled compounds. In: Rayudu GVS, ed. *Radiotracers for Medical Applications.* Boca Raton, FL: CRC Press; 1981:28-67.
85. Meinken GE, Srivastava SC, Richards P. Determination of microgram amounts of stannous tin in technetium labeling kits. *J Nucl Med.* 1980;21:P78.
86. Chervu LR, Vallabhajosyula B, Mani J. Stannous ion quantitation in Tc-99m radiopharmaceuticals kits. *Eur J Nucl Med.* 1982;7:291-3.
87. Srivastava SC, Meinken G, Smith TD. Problems associated with stannous Tc-99m radiopharmaceuticals. *Int J Appl Radiat Isot.* 1977;28:83-95.
88. Conine DL, Yum M, Martz RC. Toxicity of sodium pentafluorostannite, a new anticariogenic agent: comparison of the acute toxicity of sodium pentafluorostannite, sodium fluoride, and stannous chloride in mice and/or rats. *Toxicol Appl Pharmacol.* 1975;33:21-6.
89. Hiles RA. Absorption, distribution, and excretion of inorganic tin in rats. *Toxicol Appl Pharmacol.* 1974;27:366-79.
90. Kehoe RA, Cholak J, Story RV. A spectrochemical study of the normal ranges of concentration of certain trace metals in biological materials. *J Nutr.* 1940;19:579-92.
91. Zalutsky MR, Rayudu GVS, Friedman AM. The biological behavior of tin following administration of nine Tc-99m-Sn-complexes. *Int J Nucl Med Biol.* 1977;4:224-30.
92. Owanwanne A, Church LB, Blau M. Effect of oxygen on the reduction of pertechnetate by stannous ion. *J Nucl Med.* 1977;18:822-6.
93. *CRC Handbook of Chemistry and Physics.* 43rd ed. Cleveland: The Chemical Rubber Co; 1961:1706.
94. Steigman J. Chemistry of the alumina column. *Int J Appl Radiat Isot.* 1982;33:829-34.
95. Chase GD, Rabinowitz JL. *Principles of Radioisotope Methodology.* 3rd ed. Minneapolis: Burgess; 1967:442-7.
96. Molinski VJ. A review of Tc-99m generator technology. *Int J Appl Radiat Isot.* 1982;33:811-9.
97. Billinghurst MW, Rempel S, Westendorf BA. Radiation decomposition of technetium-99m radiopharmaceuticals. *J Nucl Med.* 1979;20:138-43.
98. Tofe AJ, Francis MD. In vitro stabilization of a low-tin bone imaging agent (Tc-99m-Sn-HEDP) by ascorbic acid. *J Nucl Med.* 1976;17:820-5.
99. *The United States Pharmacopeia 24/The National Formulary 19.* Rockville, MD: United States Pharmacopeial Convention; 2000.
100. Technetium Tc-99m HSA Multidose Kit [package insert]. Arlington Heights, IL: Medi-Physics Inc/Amersham Healthcare; 1993.
101. Robbins PJ. *Chromatography of Technetium-99m Radiopharmaceuticals—A Practical Guide.* New York: Society of Nuclear Medicine; 1984.

102. Nusynowitz ML, Straw JD, Benedetto AR, et al. Blood clearance rates of technetium-99m albumin preparations [concise communication]. *J Nucl Med.* 1978;19:1142-5.
103. TechneScan MAA Kit [package insert]. St Louis, MO: Mallinckrodt Inc; 2000.
104. Tc-99m Apcitide [package insert]. Londonderry, NH: Diatide Inc; 1998.
105. Taillefer R, Edell S, Innes G, et al. Acute thromboscintigraphy with Tc-99m-apcitide: Results of the phase-3 multicenter clinical trial comparing Tc-99m apcitide scintigraphy with contrast venography for imaging acute DVT. *J Nucl Med.* 2000;41:1214-23.
106. Tc-99m Bicisate [package insert]. Billerica, MA: DuPont Pharmaceuticals; 1998.
107. Tc-99m Depreotide [package insert]. Londonderry, NH: Diatide Inc; 1999.
108. Tc-99m Disofenin [package insert]. Bedford, MA: CIS-US Inc; 1999.
109. Tc-99m Exametazime [package insert]. Arlington Heights, IL: Medi-Physics Inc/Amersham Healthcare; 1996.
110. Tc-99m Gluceptate [package insert]. Kirkland, Quebec: DraxImage Inc; 1998.
111. Tc-99m Mebrofenin [package insert]. Princeton, NJ: Bracco Diagnostics Inc; 2000.
112. Tc-99m Medronate [package insert]. Princeton, NJ: Bracco Diagnostics Inc; 1999.
113. Nosco DL, Wolfangel RG, Bushman MJ, et al. Technetium-99m MAG3: labeling conditions and quality control. *J Nucl Med Technol.* 1993;21:69-74.
114. Tc-99m Mertiatide [package insert]. St Louis, MO: Mallinckrodt Inc; 1995.
115. Tc-99m Oxidronate[package insert]. St Louis, MO: Mallinckrodt Inc; 1995.
116. Tc-99m Pentetate [package insert]. Bedford, MA: CIS-US Inc; 1993.
117. Nelson MF, Melton RF, Van Wazer JR. Sodium trimetaphosphate as a bone-imaging agent. I: Animal studies. *J Nucl Med* 1975;16:1043-8.
118. Tc-99m Pyrophosphate [package insert]. St Louis, MO: Mallinckrodt Inc; 2000.
119. Smith TD, Richards P. A simple kit for the preparation of Tc-99m red blood cells. *J Nucl Med.* 1976;17:126-32.
120. Srivastava SC, Chervu LR. Radionuclide labeled red blood cells: current status and future prospects. *Semin Nucl Med.* 1982;14:68-82.
121. Srivastava SC, Babich JB, Richards P. A new kit method for the selective labeling of erythrocytes in whole blood with technetium-99m. *J Nucl Med.* 1983;24:P128.
122. UltraTag RBC [package insert]. St Louis, MO: Mallinckrodt Inc; 2000.
123. Pavel DG, Zimmer AM, Patterson VN. In vivo labeling of red blood cells with Tc-99m: a new approach to blood pool visualization. *J Nucl Med.* 1977;18:305-8.
124. Stokely EM, Parkey RW, Bonte FJ, et al. Gated blood pool imaging following ^{99m}Tc stannous pyrophosphate imaging. *Radiology.* 1976;120:433-4.
125. Hamilton RG, Alderson PO. A comparative evaluation of techniques for rapid and efficient in vivo labeling of red cells with Tc-99m pertechnetate. *J Nucl Med.* 1977;18:1010-3.
126. Callahan RJ, Froelich JW, McKusick KA, et al. A modified method for the in vivo labeling of red blood cells with Tc-99m [concise communication]. *J Nucl Med.* 1982;23:315-8.
127. Dewanjee MK, Rao SA, Penniston GT. Mechanism of red blood cell labeling with ^{99m}Tc-pertechnetate: the role of the cation pump at RBC membrane on the distribution and binding of Sn^{2+} and ^{99m}Tc with the membrene proteins and hemoglobin. *J Labeled Compounds Radiopharm.* 1982;19:1464-5.
128. Dewanjee MK. Binding of Tc-99m ion to hemoglobin. *J Nucl Med.* 1974;15:703-6.
129. Straub RF, Srivastava SC, Meinken GE, et al. Transport, binding and uptake kinetics of tin and technetium in the in-vitro Tc-99m labeling of red blood cells. *J Nucl Med.*1985;26:P130.
130. Callahan RJ, Rabito CA. Radiolabelling of erythrocytes with technetium-99m: role of band-3 protein in the transport of pertechnetate across the cell membrane. *J Nucl Med.* 1990;31:2004-10.
131. Larson SM, Hamilton GW, Richards P, et al. Kit-labeled technetium-99m red blood cells (Tc-99m RBCs) for clinical cardiac chamber imaging. *Eur J Nucl Med.* 1978;3:227-31.
132. Cardiolite/Miraluma [package insert]. Billerica, MA: DuPont Pharmaceuticals; 2000.
133. Moretti JL, Rapin JR, Saccavina JC, et al. 2,3-Dimercaptosuccinic-acid chelates. 1: Structure and pharmacokinetic studies. *Int J Nucl Med Biol.* 1984;11:270-4.
134. Ikeda I, Inoue O, Kurata K. Chemical and biological studies on Tc-99m DMS-II: effect of Sn(II) on the formation of various Tc-DMS complexes. *Int J Appl Radiat Isot.* 1976;27:681-8.
135. Ikeda I, Inoue O, Kurata K. Preparation of various Tc-99m dimercaptosuccinate complexes and their evaluation as radiotracers. *J Nucl Med.* 1977;18:1222-9.
136. Kubiatowicz KO, Bolles TF, Nova JC, et al. Localization of low molecular weight Tc-99m labeled dimercaptodicarboxylic acids in kidney tissue. *J Pharm Sci.* 1979;68:621-3.
137. Sampson C. Preparation of ^{99m}Tc-(V)DMSA. *Nucl Med Comm.* 1987;8:184-5.
138. Blower PJ, Singh J, Clarke SEM. The chemical identity of pentavalent technetium-99m-dimercaptosuccinic acid. *J Nucl Med.* 1991;32:845-9.

139. Taylor A Jr. Lallone RL, Hogan PL. Optimal handling of dimercaptosuccinic acid for quantitative renal scanning. *J Nucl Med.* 1980;21:1190-3.
140. DMSA kit for the preparation of Tc-99m Succimer injection [package insert]. Arlington Heights, IL: Medi-Physics Inc/Amersham Healthcare; 1993.
141. CIS-Sulfur Colloid [package insert]. Bedford, MA: CIS-US Inc; 1998.
142. Myoview [package insert]. Arlington Heights, IL: Medi-Physics Inc/Amersham Healthcare; 1996.
143. Srivastava SC, Straub RF. Blood cell labeling with ^{99m}Tc: progress and perspectives. *Semin Nucl Med.* 1990;20:41-51.
144. Marcus CS, Kuperus JH, Butler JA, et al. Phagocytic labeling of leukocytes with ^{99m}Tc-albumin colloid for nuclear imaging. *Nucl Med Biol.* 1988;15:673-82.
145. Srivastava SC, Straub RF, Modesto RR, et al. A stannous glucoheptonate kit method for ^{99m}Tc labeling of leukocytes and platelets. *J Labeled Compounds Radiopharm.* 1989;16:38-40.
146. Peters AM, Danpure HJ, Osman S, et al. Clinical experience with ^{99m}Tc-hexamethylpropylene-amine-oxime for labelling leucocytes and imaging inflammation. *Lancet.* 1986;2:946-9.
147. Roddie ME, Peters AM, Danpure HJ, et al. Inflammation: imaging with Tc-99m HMPAO-labeled leukocytes. *Radiology.* 1988;166:767-72.
148. Peters AM, Saverymuttu SH, Reavy HJ, et al. Imaging inflammation with 111-indium-tropolonate labeled leukocytes. *J Nucl Med.* 1983;24:39-44.
149. Weber DA, Eckerman KF, Dillman LT, et al. *MIRD: Radionuclide Data and Decay Schemes.* New York: Society of Nuclear Medicine; 1989.
150. Kowalsky RJ, Johnston RE. Dose calibrator assay of iodine-123 and indium-111 with a copper filter. *J Nucl Med Technol.* 1998;26:94-8.
151. Wolfangel RL. Accumulation of radioiodine in staff members [reply]. *J Nucl Med.* 1979;20:995.
152. Howard BY. Safe handling of radioiodinated solutions. *J Nucl Med Technol.* 1976;4:28-30.
153. Miller KL, Bott SM, Velkley DE, et al. Review of contamination and exposure hazards associated with therapeutic doses of radioiodine. *J Nucl Med Technol.* 1979;7:163-6.
154. Pollock RW, Meyer RD. Concentration of I-131 in the air during thyroid therapies. *Health Phys.* 1979;36:68-9.
155. Rubin LM, Miller KL, Schadt WW. A solution to the radioiodine volatilization problem. *Health Phys.* 1977;32:307-9.
156. Burgess JS, Partington EJ. *Radiation Decomposition Effects in Aqueous Solutions of Carrier-free Sodium Iodide I-131.* Amersham, Bucks, England: The Radiochemical Center; 1960. Publication RCC/R98.
157. Shubnyakova LP, Kharlamov VT, Pikaev AK. Radiolysis of dilute aqueous solutions of Na^{131}I. *Khimiya Vysokikh Energii.* 1976;10:41-5.
158. Maguire WJ. A precaution for minimizing radiation exposure from iodine vaporization. *J Nucl Med Technol.* 1980;8:90-3.
159. Lever JR. Radioiodinated compounds. In: Wagner HN Jr, Szabo Z, Buchanan JW, eds. *Principles of Nuclear Medicine.* 2nd ed. Philadelphia: WB Saunders; 1995:199-213.
160. Hughes WL. The chemistry of iodination. *Ann NY Acad Sci.* 1957;70:3-18.
161. McFarlane AS. Efficient trace-labeling of proteins with iodine. *Nature.* 1958;182:53-5.
162. Helmkemp RW, Contreras MA, Bale WF. I-131 labeling of proteins by the iodine monochloride method. *Int J Appl Radiat Isot.* 1967;18:737-46.
163. Bayly RJ, Anthony E, Evans JS, et al. Synthesis of labeled compounds. In: Tubis M, Wolf W, eds. *Radiopharmacy.* New York: Wiley; 1976:303-78.
164. Hunter WM, Greenwood FC. Preparation of iodine-131 labeled human growth hormones of high specific activity. *Nature.* 1962;194:495-6.
165. McConahey PJ, Dixon EJ. A method of trace iodination of proteins for immunological studies. *Int Arch Allergy.* 1966;29:185-9.
166. Mills SL, DeNardo SJ, DeNardo GL, et al. I-123 radiolabeling of monoclonal antibodies for in vivo procedures. *Hybridoma.* 1986;5:265-75.
167. Markwell MAK. A new solid-state reagent to iodinate proteins. *Anal Biochem.* 1982;125:427-32.
168. Bolton AE, Hunter WM. The labeling of proteins to high specific radioactivities by conjugation to a I-125 containing acylating agent. *Biochem J.* 1973;133:529-39.
169. Haney TA, Wedeking P, Morcos N, et al. A therapeutic and diagnostic I-131 capsule formulation with minimal volatility and maximal bioavailability. *J Nucl Med.* 1981;22:P74.
170. Kereiakes JG, Rosenstein M. *Handbook of Radiation Doses in Nuclear Medicine and Diagnostic X-ray.* Boca Raton, FL: CRC Press; 1980.
171. Mock BH, Weiner RE. Simplified solid-state labeling of I-123 m-iodobenzylguanidine. *Appl Radiat Isot.* 1988;39:939-42.
172. Mangner TJ, Wu J-L, Weiland DM. Solid-phase exchange radioiodination of aryl iodides. Facilitation by ammonium sulfate. *J Org Chem.* 1982;47:1484-8.

173. Gelfand MJ, Elgazzar AH, Kriss VM, et al. Iodine-123-MIBG SPECT versus planar imaging in children with neural crest tumors. *J Nucl Med.* 1994;35:1753-7.
174. Shapiro B, Gross MD. Radiochemistry, biochemistry, and kinetics of ^{131}I-metaiodobenzylguanidine (MIBG) and ^{123}I-MIGB: clinical implications of the use of ^{123}I-MIGB. *Med Pediatr Oncol.* 1987;15:170-7.
175. Iobenguane Sulfate I-131 [package insert]. Bedford, MA: CIS-US Inc; 1994.
176. Iodohippurate Sodium I-131 [package insert]. St Louis, MO: Mallinckrodt Inc; 1995.
177. Iothalamate Sodium I-125 [package insert]. Carlsbad, CA: Cypros Pharmaceutical; 1995.
178. Anderson CJ, Welch MJ. Radiometal-labeled agents (non-technetium) for diagnostic imaging. *Chem Rev.* 1999;99:2219-34.
179. Brown LC. Chemical processing of cyclotron-produced Ga-67. *Int J Appl Radiat Isot.* 1971;22:710-3.
180. Brown LC, Beets AL. Cyclotron production of carrier-free indium-111. *Int J Appl Radiat Isot.* 1972;23:57-63.
181. Dymov AM, Savostin AP. *Analytical Chemistry of Gallium.* Ann Arbor, MI: Ann Arbor Science; 1970.
182. Gallium Citrate Ga-67 [package insert]. St Louis, MO: Mallinckrodt Inc; 2000.
183. Indium In-111 Oxine [package insert]. Arlington Heights, IL: Medi-Physics Inc/Amersham Healthcare, 1996.
184. Maecke HR, Riesen A, Ritter W. The molecular structure of indium-DTPA. *J Nucl Med.* 1989;30:1235-9.
185. Indium In-111 DTPA [package insert]. Arlington Heights, IL: Medi-Physics Inc/Amersham Healthcare; 1994.
186. OctreoScan kit [package insert]. St Louis, MO: Mallinckrodt Inc; 2000.
187. Lebowitz E, Green MW, Fairchild R, et al. Thallium-201 for medical use I. *J Nucl Med.* 1975;16:151-5.
188. Thallous Chloride Tl-201 [package insert]. St Louis, MO: Mallinckrodt Inc; 2000.
189. Xenon Xe 133 Gas [package insert]. St Louis, MO: Mallinckrodt Inc; 2000.
190. Person HA. The binding of Cr-51 to hemoglobin. I: In vitro studies. *Blood.* 1963;22:218-20.
191. Gray SJ, Sterling K. The tagging of red cells and plasma proteins with radioactive chromium. *J Clin Invest.* 1950;29:1604-10.
192. Sodium Chromate Cr-51 [package insert]. St Louis, MO: Mallinckrodt Inc; 1997.
193. *Radioisotope Production and Quality Control.* Vienna, Austria: International Atomic Energy Agency; 1971:151-2. Technical Reports Series No. 128.
194. Hupf HB. Production and purification of radionuclides. In: Tubis M, Wolf W, eds. *Radiopharmacy.* New York: Wiley; 1976:225-53.
195. Kline OL, Boehne JW. Vitamins and other nutrients. In: Osol A, Hoover JE, eds. *Remington's Pharmaceutical Sciences.* 14th ed. Easton, PA: Mack Publishing Co; 1970:1011.
196. Rosenblum C. Production and metabolism of cobalt-labeled cyanocobalamin. In: Andrews GA, Knisley RM, Wagner HN Jr, eds. *Radioactive Pharmaceuticals.* Oak Ridge, TN: US Atomic Energy Commission; 1966:455-76.
197. Rubratope-57 [insert]. Princeton, NJ: Bracco Diagnostics Inc; 1996.
198. Sienko MJ, Plane RA. *Chemistry.* 2nd ed. New York: McGraw-Hill; 1961.
199. Morton ME. Colloidal chromic radiophosphate in high yields for radiotherapy. *Nucleonics.* 1952;10:92-7.
200. Phosphocol P-32 [package insert]. St Louis, MO: Mallinckrodt Inc; 2000.
201. Wasserman LR. The treatment of polycythemia vera. *Semin Hematol.* 1976;13:57-78.
202. Spiers FW, Beddoe AH, King SD, et al. The absorbed dose to bone marrow in the treatment of polycythemia vera by P-32. *Br J Radiol.* 1976;49:133-40.
203. Herold TJ, Gross GP, Hung JC. A technique for measurement of strontium-89 in a dose calibrator. *J Nucl Med Technol.* 1995;23:26-8.
204. Metastron [package insert]. Arlington Heights, IL: Medi-Physics Inc/Amersham Healthcare, 1998.
205. Volkert WA, Hoffman TJ. Therapeutic radiopharmaceuticals. *Chem Rev.* 1999;99:2269-92.
206. Singh A, Holmes RA, Farhangi M, et al. Human pharmacoknetics of samarium-153 EDTMP in metastatic cancer. *J Nucl Med.* 1989;30:1814-8.
207. Quadramet [package insert]. North Billerica, MA: DuPont Merck; 1997.

10 Radiopharmaceuticals for Positron Emission Tomography

Stephen M. Moerlein

Clinical applications of positron emission tomography (PET) have grown remarkably in recent years. Like other nuclear medicine procedures, PET imaging detects the distribution of tracers within the body. Whereas magnetic resonance imaging (MRI) and computed tomography (CT) imaging methods provide structural or anatomic information, PET imaging is intrinsically linked to function because the biologic fate of PET radiotracers is determined by the in vivo rate of the physiologic processes of the organism.

PET differs from conventional single-photon emission computed tomography (SPECT) imaging in that short-lived positron-emitting radionuclides are used as radiolabels. This has several important implications. First, because of the physics of positron decay, coincidence circuitry can be used, which facilitates acquisition of high-resolution images with accurate attenuation correction. Additionally, most of the elements used as positron-emitting labels (Table 10-1) are attached via covalent bonds and are commonly found in several biochemical and drug structures. This leads to much greater versatility in the development of novel PET radiopharmaceuticals, compared with the application of ^{99m}Tc (attached via bulky chelating linker groups) or ^{123}I (which forms a biologically unstable bond with carbon) as radiopharmaceutical labels.

PET imaging has unique applications that have proven useful for routine procedures in nuclear medicine. Given the special characteristics of PET methods and the wide range of tracer design and production, further growth in this area of nuclear medicine is anticipated, despite its higher costs. This chapter discusses the current status of PET radiopharmaceuticals used routinely for clinical imaging procedures and presents examples of clinical research applications of this powerful imaging technique.

POSITRON EMISSION TOMOGRAPHY

Positron Decay

Proton-rich nuclei decay either by positron emission or by electron capture (EC).[1] EC is a prevalent decay process for nuclides used in conventional nuclear medicine, since it generates photons that are well suited for imaging by Anger-type thallium-activated sodium iodide [NaI(Tl)] cameras. Examples of such clinically useful radiopharmaceutical labels are ^{123}I and ^{111}In. The photons emitted by these nuclides are collimated by lead collimators to determine the directionality of the photons detected by NaI(Tl) crystals used for image reconstruction.

Positron decay transforms proton-rich nuclei closer to the line of beta stability by converting the unstable nucleus to a daughter nuclide with one less proton and one more neutron, together with the emission of a positron and a neutrino. The elementary process can be written as follows:

TABLE 10-1 Radionuclides Used in Positron Emission Tomography

Nuclide	Half-life	E_{max} (MeV)
^{15}O	2 min	1.7
^{13}N	10 min	1.2
^{11}C	20 min	1.0
^{18}F	110 min	0.7
^{82}Rb	76 sec	3.4
^{68}Ga	68 min	1.9

$$p \rightarrow n + \beta^+ + \nu$$

Emission of a neutrino (ν) is necessary in this decay process to conserve momentum and angular momentum.[1] The emitted neutrino has very little interaction with matter and is of importance to PET imaging only in that, because of conservation laws, it influences the energy of the corresponding positron. Unlike the photons imaged in conventional nuclear medicine, which are monoenergetic with discrete energy groups, positrons are emitted with a continuous energy spectrum and have a median energy equal to approximately one-third of the maximum positron energy.[2] As discussed later, the range of the emitted positrons has practical impact in that it degrades image resolution in PET.

An emitted positron will lose energy through ionization and excitation of atoms along its pathway until it reaches thermal velocities and combines with an orbital electron in an annihilation reaction.[1] This elementary process is written as follows:

$$\beta^+ + e^- \rightarrow \gamma + \gamma$$

A positron is an antiparticle of an ordinary electron, so the annihilation reaction converts the entire mass of each particle into energy.

Momentum conservation in this process demands that two gamma quanta be produced with equal and opposite momenta. The two quanta are emitted almost exactly 180° apart; any deviation from colinearity derives from residual momentum in the positron at the time of annihilation (Figure 10-1). Because the rest mass of the positron and of the electron is 511 keV, the annihilation photons each have an energy of 511 keV. It is important to note that it is these annihilation photons (and not the positrons themselves) that are detected by PET imaging devices.

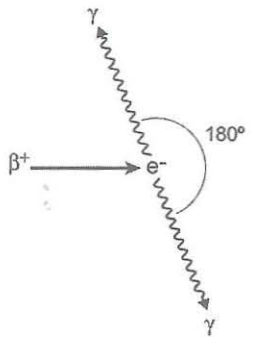

FIGURE 10-1 Positron decay with production of annihilation radiation.

Coincidence Detection

The directionality of the annihilation photons after positron detection allows the unique PET imaging method to be achieved. The key unit of PET detection is the coincidence circuit, shown in Figure 10-2, which provides for the colinearity of the two annihilation photons to be discriminated. In this method, only simultaneous events detected within the common field of view of the two detectors are registered as an annihilation event, and hence as a positron emission.

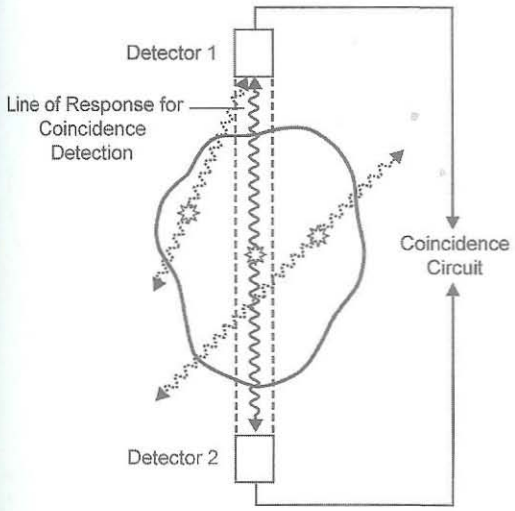

FIGURE 10-2 Coincidence circuitry for detection of annihilation radiation.

TABLE 10-2 Properties of Scintillator Crystals for PET

Property	NaI(Tl)	BGO	LSO	GSO
Efficiency (%, 12.5 mm)	34	68	64	57
Relative emission intensity	100	15	75	30
Light decay constant (nsec)	230	300	40	60
Energy resolution	8	12	12	8

This technique is based on the fact that the annihilation photons always escape at approximately 180° from one another and arrive at opposing detectors nearly simultaneously. Detection of an event at only a single detector would not be registered as a coincidence, so singles or randoms are excluded from the data collection process. This electronic collimation is a unique advantage of PET imaging; there is no need for the heavy lead shielding with collimating septa required for image definition in single-photon imaging.

Another major difference between detection in PET and in conventional nuclear medicine cameras is the type of scintillation crystals used. Whereas relatively thin (three-eighths inch standard) NaI(Tl) crystals are widely used in single-photon nuclear medicine cameras, these are inadequate for efficient stopping of the 511 keV annihilation photons imaged in PET. The crystals used for PET scanners are listed in Table 10-2. Note that although NaI(Tl) scintillators have very high light output, for application with PET these crystals have poor efficiency for detecting annihilation photons, slow response (large decay constant), and relatively poor energy resolution. The large scintillator decay constant of NaI(Tl) leads to increased dead time with high count rates, and the poor energy resolution of this crystal leads to an increased scatter component in coincidence detection.

Most commercial PET scanners utilize bismuth germanate (BGO) detectors. BGO scintillators are especially useful for PET imaging because of their efficiency in detecting 511 keV photons and their relatively high-energy resolution. BGO scintillators have two main disadvantages: a large decay constant, and thus limited capacity with high count rates; and poor light emission, which increases noise.

The future development of PET instrumentation may involve the application of lutetium oxyorthosilicate (LSO) or gadolinium orthosilicate (GSO) as detector materials.

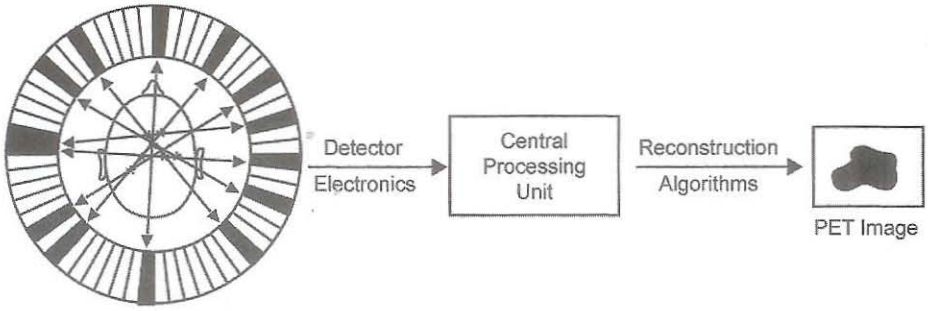

FIGURE 10-3 PET scanner design consisting of circular banks of coincidence circuits.

TABLE 10-3 Factors that Degrade PET Images

Problem	Correction
Scatter	Increase energy resolution
Attenuation	Transmission scan
Random events	Fast scintillators and electronics
Dead time	Fast scintillators and electronics
Noise	Increase signal counts
Spatial resolution	Decrease detector size

Although the efficiency for detection of 511 keV photons by these scintillators is less than that of BGO, LSO and GSO have small decay constants. Thus, these detectors should be more useful for PET imaging at high count rates than NaI(Tl) or BGO, which because of dead time are more easily paralyzed by high count rates. This characteristic is especially valuable for three-dimensional (3-D) data acquisition in PET.

PET Scanner Design

Dedicated PET scanners consist of a series of coincidence circuits assembled into a ring shape to enclose all the angles around the subject to be imaged (Figure 10-3).[3] Several rings of detectors are mounted next to one another in the transaxial direction, so that multislice image acquisition can occur simultaneously.

The PET scanner is based on coincidence detection; if a photon is detected at two detectors within the ring simultaneously, the interaction is recorded as a coincidence event. The number of coincidences for a particular line of response is thus directly proportional to the amount of positron-emitting radioactivity within the field of view of the two detectors.

The recorded coincidence counts between detectors can be expressed as sinograms, which are the collection of coincidence data expressed as an angular function. Sinograms are reconstructed from raw data into cross-sectional images using computer algorithms similar to those used in SPECT or CT.

This simplified description of PET system design is complicated by several factors that act in concert to degrade image quality.[3] These factors are summarized in Table 10-3.

Scatter is an important effect in PET, especially because electronic collimation is used instead of lead collimation. As shown in Figure 10-4, scatter can be in-plane or out-of-plane and acts to artificially increase counts within a line of response, even though no positron decay occurred there. Scatter can be decreased by using lead septa around

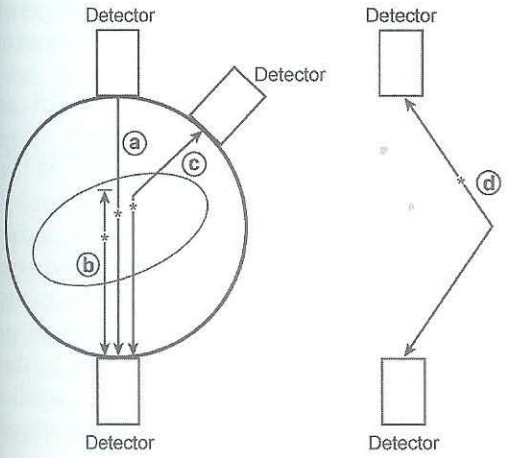

FIGURE 10-4 Factors leading to degradation of PET image resolution. (a) True coincidence; (b) tissue absorption; (c) in-plane scatter; (d) out-of-plane scatter.

scintillators to reduce access to scattered photons, by increasing energy resolution of the detectors, and by applying scatter correction algorithms.

Attenuation is another parameter that strongly influences PET image quality. Attenuation results in the loss of true counts, resulting in increased noise and inaccurate quantification in reconstructed images. The 511 keV photons detected by PET are individually attenuated to a lesser extent than the lower-energy photons used in conventional SPECT imaging, because two attenuated photons must be detected in coincidence detection, but the overall impact of attenuation is actually more important in PET imaging than in single-photon imaging.

Attenuation is proportional to tissue density and is accounted for by a measured transmission attenuation correction. The attenuation correction is determined using a transmission measurement similar to that used in CT imaging. This approach entails the use of a moving line source, with a photon energy similar to that of annihilation radiation. A common line source is a bar of ^{68}Ge, which decays to ^{68}Ga, which decays by positron emission and release of annihilation photons. The line source projects photons through the patient perpendicular to the detectors as it rotates around the ring of scintillators. The resulting transmission scan accurately measures the attenuation of photons for each detector and is used to correct the emission data for this effect. The transmission attenuation correction measurement is ideally made before administration of the PET radiopharmaceutical.

Random events degrade PET image quality because they are not true coincidences. The scintillator and its associated electronics require a finite time to detect true annihilation photons and record a coincidence; therefore, a minimum time window is required for operation of the coincidence circuits of the PET scanner. Thus, the time interval for the scanner must be optimized so that there is a window large enough to efficiently detect annihilation photons but not large enough to allow a high proportion of random events to occur. Random events can be decreased by the use of fast scintillators that have small decay constants.

Dead time is another parameter affecting PET image quality, especially with high count-rate imaging procedures. When an excessive number of events impinge upon a scintillator, the response of the scintillator may become saturated and detection efficiency may decrease. This effect is minimized with the use of faster scintillators and electronics, which permit higher levels of annihilation radiation to be accurately detected.

PET scanner noise diminishes image quality because it increases the level of background counts and thereby decreases the signal-to-background contrast. To increase the

signal counts in relation to random noise counts, higher radiopharmaceutical dosages or longer scan intervals can be used. Increasing the efficiency of the scanner for detection of annihilation radiation also increases the signal-to-noise ratio.

The spatial resolution of PET images is affected by several factors, some of which can be controlled through scanner design. Spatial resolution is affected by positron range, which is related to the positron energy, as well as by the slight noncolinearity of the two 511 keV photons from positron annihilation. Resolution is also inversely proportional to detector size; the smaller the detector, the greater the resolution. Note that this relationship is opposite that of detector efficiency, which decreases as the crystal dimensions decrease. The design of scanners with smaller detectors is ultimately limited by physical constraints, since the photomultiplier tube (PMT) and related electronics attached to scintillators are relatively bulky. To circumvent this effect, PET scanners often use detector blocks that have several detector elements etched onto a single scintillator crystal to give a smaller effective detector size. In this way, the effective detector element dimensions are decreased with no change in the actual detector crystal-to-photomultiplier tube ratio.

Two-Dimensional versus Three-Dimensional Data Acquisition

Emission data from PET can be collected in either two-dimensional (2-D) or 3-D mode. A simplified illustration of the difference between these data-acquisition modes is shown in Figure 10-5. In the 2-D mode, coincidences are collected in the direct plane or in simple cross-plane orientation in which coincidences between scintillators immediately adjacent to the direct plane are included in the database for image reconstruction. In 2-D data acquisition, lead septa are used to surround the sides of the detector elements to reduce the solid angle of detection and thereby minimize counts from scattered photons and randoms arriving from directions outside of the line of response for the specific detectors.

In the 3-D mode, the shielding septa are removed, and all possible configurations of detector elements are used as coincidence circuits for image reconstruction. The total number of coincidences analyzed in 3-D mode is clearly much larger than that in 2-D PET imaging. The advantage of applying the 3-D mode for PET data acquisition is that sensitivity is greatly increased. A disadvantage is that because the detector elements are unshielded, scatter is more prevalent and more sophisticated algorithms are needed for image reconstruction. In addition, 3-D PET imaging is especially prone to detector saturation caused by the high number of coincidence and random events that are detected. For this reason, it has been suggested that NaI(Tl) crystals may be more appropriate for 3-D mode than BGO, since the higher-energy resolution of the latter reduces the scatter

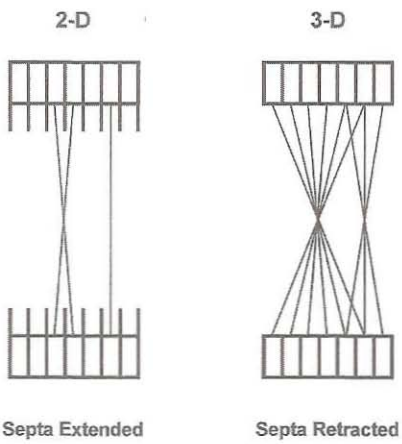

FIGURE 10-5 Two- and three-dimensional data acquisition modes in PET. With 2-D imaging, septa are extended, and only in-plane or simple cross-plane coincidences are detected. With 3-D imaging, septa are retracted, and the number of coincidences is dramatically increased.

component of data. The shorter scintillation decay time of GSO and LSO (Table 10-2) may also prove to be useful in improving the count rate performance of PET systems acquiring data in 3-D mode.

Hybrid PET Systems

The ideal manner in which to accomplish PET imaging is to use dedicated PET scanners designed as described above. Alternative technology has been examined, however, for acquiring PET data in a less expensive manner than with dedicated PET systems. The motivation behind these efforts is to promote clinical application of PET radiopharmaceuticals by lowering the capital investment required for the imaging device. These less expensive imaging devices are referred to as hybrid PET scanners.

One hybrid approach is to adapt conventional dual-head NaI(Tl) detectors to collect coincidence data as they rotate about the patient. A major modification to traditional gamma-imaging devices that is necessary to enable acquisition of PET data is that the NaI(Tl) crystal thickness must be increased from the standard three-eighths inch to between one-half and 1 inch in order to attain adequate stopping power for the 511 keV annihilation photons. In addition, coincidence triggering must be installed in the imaging equipment. Other changes include removal of lead collimators, which are not needed for the electronic collimation of PET, as well as modifications that increase the count rate capability of the scanner.

An alternative low-cost hybrid PET approach is to mount multiple gamma cameras in a ring around the patient to enable data acquisition in a coincidence mode. The same modifications apply to this system as for the conversion of a rotating gamma camera into a hybrid PET system. With this scanner design, increasing the crystal thickness for optimized detection of annihilation radiation is easier to accomplish, since the scintillators are stationary and do not have to rotate. As with the rotating-head NaI(Tl) hybrid scanner, this system has the drawback of poor detection efficiency (due to the low stopping power of the scintillator). The system also saturates easily when exposed to high count rates (due to the large decay constant of NaI[Tl]).

Another approach to reducing the cost of PET imaging tracers is the use of a partial-ring, multicrystal PET scanner. In this system design, the same technology is used as in dedicated PET scanners, but only a portion of the ring is constructed. The complete set of emission data is acquired by stepwise rotation of the partial ring around the patient. Costs are less because only a fraction of the detector elements that are used in a dedicated scanner are needed for the partial ring of these systems. Compared with dedicated PET systems, however, an obvious disadvantage of this hybrid system is poor detection efficiency as a result of not having a full ring of detectors.

PET/CT Scanners

To anatomically locate areas of increased tracer localization in PET images, it is necessary to coregister emission (PET) and transmission (CT) images. Such coregistration facilitates the mapping of functional changes (detected by PET) onto their anatomic sites (detected by CT). When the CT and PET data are obtained on individual scanners, increased scheduling time is required, causing greater patient inconvenience. Moreover, substantial technical difficulties are involved in realigning tomographic images created from nonidentical patient imaging done on two different machines.

A solution to these problems is to combine CT and PET imaging into a single scanner.[4] Such fused PET/CT devices are commercially available, and they facilitate increased patient throughput in busy imaging clinics, improving patient convenience. The fused

devices allow technical improvements in precise positioning of imaging subjects. These devices do not use the same detection instrumentation but consist of a dedicated PET scanner mounted next to a CT scanner. Although different imaging detection rings are used, they are physically mounted in close proximity, so the patient reclines on a bed that can be slid into position for imaging by each portion of the device.

Although the high-resolution CT images generated by this fused device exceed the requirements for attenuation correction and scatter correction of PET images, the clinical-quality anatomic images obtained with the CT component of the scanner are of the caliber that radiologists normally use. This has the benefit of providing radiologists, surgeons, and oncologists with the type of anatomic information they routinely apply in practice, combined with coregistered PET images, data they may not have used in the past. The combined PET/CT delivers precise information about the location and extent of tracer localization to experienced practitioners of PET and also has the valuable effect of introducing nonspecialist clinicians to the role of PET in providing information that supplements more established testing methods for patient care and disease management.[5]

IMAGING APPLICATIONS

Since its beginnings as a research tool, PET has been used over the years to study the in vivo distribution of numerous positron-emitting tracers. Studies with these tracers have provided valuable insight into the pathophysiology of diseases and the in vivo action of pharmacologic agents. However, only a few of the tracers have come into routine clinical use, partially because the field of PET imaging is new and has not yet fully developed. The primary limiting factor, however, is the stringent requirements a PET protocol must meet in order to be implemented in routine patient care. These requirements include diagnostic efficacy, imaging protocol simplicity, and radiopharmaceutical compounding efficiency. These specific clinical requirements supplement the general safety restrictions for all PET tracers administered to humans, such as limits on absorbed radiation dose and quality assurance for purity, sterility, and apyrogenicity. Its ability to meet the more stringent requirements determines whether a tracer is suitable as a radiopharmaceutical for routine patient care or is appropriate only for specialized clinical research applications.

An important criterion for clinical utility is that the radiopharmaceutical must be used in PET imaging procedures that have validated diagnostic efficacy. If a PET procedure will give clinical information that is not achievable by other, less expensive means, the cost of PET is justified within the overall scope of health care expenses.

Another requirement for routine clinical utility is that the PET imaging protocol be relatively simple. Simple procedures streamline clinical operations, facilitate rapid dissemination of answers to clinical questions, reduce costs, and minimize patient inconvenience.

Finally, clinically useful PET tracers must be prepared in an efficient, reliable manner. This ensures timely delivery of the radiopharmaceutical in quantities adequate for scheduled studies as well as for potential emergency additions to the workday schedule. Efficiency is important in preparing radiopharmaceutical dosages for unscheduled studies, which may become more prevalent as PET imaging becomes as common as other diagnostic tests used in the hospital setting.

To date, despite the many PET tracers that have been developed, only a few radiopharmaceuticals satisfy all three requirements for clinical utility. Although multisite studies over time may show the diagnostic efficacy of several tracers, other radiopharmaceuticals (especially metabolic tracers or receptor ligands) utilize complicated tracer kinetic models that are time consuming and unsuitable for rapid turnaround in the clinical setting. Such

TABLE 10-4 Radiopharmaceuticals for Clinical PET

Radiopharmaceutical	Physical Half-Life	Physiologic Parameter
Cardiovascular Tracers		
Water O 15 injection	2 min	Perfusion
Ammonia N 13 injection	10 min	Perfusion
Rubidium chloride Rb 82 injection	76 sec	Perfusion
Carbon monoxide C 11	20 min	Blood volume
Metabolic Tracers		
Fludeoxyglucose F 18 injection	110 min	Glucose utilization
Sodium acetate C 11 injection	20 min	Metabolic oxidation
Neurotransmission Tracers		
Fluorodopa F 18 injection	110 min	Dopa decarboxylase
Raclopride C 11 injection	20 min	D_2 receptors
Flumazenil C 11 injection	20 min	BZD receptors

PET tracers will probably be limited to clinical research projects unless simplified image analysis techniques can be developed and validated.

PET tracers that satisfy the stringent requirements for routine clinical use are listed in Table 10-4. Both cyclotron-based and generator-available radiopharmaceuticals are listed. The physiologic basis for the localization of these tracers is discussed here; the radiosynthesis of individual radiolabeled drugs is detailed in a later section.

Table 10-4 lists several physiologic functions that can be assessed noninvasively with PET. These are categorized as cardiovascular parameters, metabolic processes, and neurotransmission measurements. Cardiovascular parameters include perfusion and blood volume. These processes affect the delivery of nutrients and other tracers to the tissues under study. Metabolic processes assess the utilization of nutrients on a regional basis and include glycolytic and oxidative pathways. Metabolic changes occur as a direct consequence of human pathology. Neurotransmission is a complicated physiologic process that involves the synthesis and release of neurotransmitters as well as their binding to neuronal receptor sites. Changes in the subtle equilibrium of any of these components of neurotransmission can lead to disease. Pathophysiologic processes often involve changes in more than one of these categories of parameters, so multiple PET measurements are often warranted to fully evaluate patient status.

Table 10-4 lists the appropriate radiopharmaceuticals indicated for measurement of each of these physiologic processes by PET. All of these tracers and applications have evolved to a sufficient level of clinical acceptance that monographs for each are found in *The United States Pharmacopeia, 26th Revision, and The National Formulary 21st Edition (USP 26/NF 21)*.[6] The following section discusses details of these clinical PET radiopharmaceuticals, including the mechanism of localization of each radiotracer and its specific clinical imaging indication.

Cardiovascular Parameters

The major cardiovascular parameter is tissue perfusion, and several PET tracers are indicated for clinical use. Blood flow can be measured using the PET radiopharmaceuticals water O 15 injection, ammonia N 13 injection, and rubidium chloride Rb 82 injection. Each of these tracers has its individual advantages for measuring tissue perfusion by PET. Blood volume is another cardiovascular parameter that can be determined by PET imaging, with carbon monoxide C 11.

Blood Flow

Tissue perfusion was the first PET measurement to be instituted for routine clinical use. The impetus for this application is the high-resolution images and sensitivity of PET together with the prevalence of ischemic conditions in the heart and brain. Blood flow is essential for maintenance of adequate tissue oxygenation and nutrition, and suboptimal perfusion is a major cause of pathology and therapeutic failure. From the imaging perspective, perfusion is of fundamental importance because it affects delivery of tracer to the region of interest. Indications for PET perfusion measurements include evaluation of coronary artery disease, cerebrovascular defects, and organ perfusion in conjunction with PET measurement of other parameters.

Necessary characteristics of a PET perfusion tracer are that the radiopharmaceutical be deposited in tissues in proportion to blood flow and that the localized radioactivity within the region be retained for the duration of the scan. Tissue accumulation of the flow tracer can be caused by diverse mechanisms, including passive diffusion and active transport, and retention of radioactivity may be caused by dilutional effects or binding to intracellular constituents.

^{15}O-water is the most versatile perfusion tracer available. This radiopharmaceutical is freely diffusible, and tissue extraction does not substantially decrease at high flow rates. Tissue perfusion in the brain and heart can be quantified by using tracer kinetic modeling of PET data derived with ^{15}O-water. Since the physical half-life of this tracer is only 2 minutes and the turnaround time for radiopharmaceutical production is short, multiple PET measurements can be made on a single patient during a single imaging session. This is a great advantage when repeat studies are required, such as in the evaluation of resting and stressed myocardial blood flow or measurement of cerebral activation. ^{15}O-water has found widespread application in PET measurement of cerebral perfusion and is the only tracer that quantitatively measures myocardial blood flow. A disadvantage of this tracer for clinical perfusion studies of the heart is that clearance of activity from the blood is slow compared with the half-life of ^{15}O. For this reason, when myocardial perfusion measurements are undertaken, it is necessary to correct for activity in the heart chambers. Although this is readily accomplished using ^{15}O-carbon monoxide, it is an inconvenience because it necessitates the administration of a second PET tracer, and the subtraction images used to delineate myocardium tend to be statistically noisy. For this reason, alternative PET tracers may be preferred for clinical assessment of myocardial ischemia.

Ammonia N 13 injection (^{13}N-ammonia) is favored as a tracer for PET measurement of myocardial perfusion. This tracer is partially extracted, meaning that the extraction fraction decreases at high perfusion rates. The trapping mechanism for ^{13}N-ammonia involves incorporation of the radionuclide into glutamine because of the enzymatic action of glutamine synthetase. Myocardial perfusion is difficult to quantify with this tracer because of the tracer's variable extraction. However, since most clinical measurements of myocardial perfusion require only a qualitative assessment of heart perfusion, in which an ischemic zone is compared with healthy myocardium, absolute quantification of myocardial perfusion is not a prerequisite for clinical utility. A major advantage of ^{13}N-ammonia in PET imaging of myocardial perfusion is that the relatively long physical half-life (10 minutes) of the radionuclide facilitates clearance of blood background, and very high quality PET perfusion images are attained without need for an image subtraction procedure. On the other hand, the half-life of ^{13}N also creates difficulties for clinical scheduling, since repeated studies (as in rest–stress perfusion protocols) are not possible in rapid succession, in contrast to the use of perfusion tracers that have shorter half-lives.

^{82}Rb-rubidium chloride was the first radiopharmaceutical applied for clinical PET and is the only PET tracer used clinically that is available from a generator system. Rubidium

ion is an analogue of potassium and accumulates in myocardium via active transport. As with ^{15}O-water, rapid sequential perfusion measurements can be made, and imaging protocols that involve rest–stress conditions can be scheduled with minimal difficulty. Like ^{13}N-ammonia, ^{82}Rb-rubidium chloride is partially extracted, which means that quantification of myocardial perfusion is difficult. In addition, the short physical half-life of the nuclide (76 seconds) is inadequate for sufficient clearance of blood background activity from the heart chambers. Attempts have been made to correct for blood background activity for continuous-infusion or bolus-injection protocols, but the resulting data are not as easy to analyze as for longer-lived tracers. Despite these limitations, a major attraction of ^{82}Rb-rubidium chloride for clinical application is that it can be used in the absence of a cyclotron and capital investment costs are thus lower than for cyclotron-produced PET radiopharmaceuticals.

Blood Volume

Assessment of blood volume with PET is often useful because it facilitates correction of other PET data for regional disparities in blood volume. This adjunctive PET measurement can be applied to the raw data for tracers that localize via other mechanisms, providing a cleaner signal for the process of interest. A good example is correction for blood volume in flow or metabolic measurements of the heart, since the heart chambers occupy such a large fraction of the total myocardial volume.

Radiolabeled carbon monoxide is the tracer of choice for accomplishing PET blood-volume measurement. The positron-emitting gas is inhaled through a filtered mouthpiece, and the tracer rapidly binds in vivo to hemoglobin to form carboxyhemoglobin. Carboxyhemoglobin remains trapped within the plasma compartment, so the radioactivity detected by PET within a region of interest represents the blood volume for that region. Carbon monoxide C 11 can be used as a PET tracer for the measurement of blood volume. Although not listed in *USP 26/NF 21*, ^{15}O-carbon monoxide may be a more appropriate tracer for measurement of blood volume in the clinical setting. The shorter half-life of the ^{15}O label facilitates rapid PET measurement of blood volume, creates minimal scheduling difficulty, and results in a decreased radiation burden to the patient. It is thus more prudent to use ^{15}O-carbon monoxide as an adjunctive PET measurement when imaging other PET tracers than to add the longer-lived carbon monoxide C 11 to an imaging protocol.

Metabolic Processes

The radiopharmaceuticals indicated for clinical measurement of metabolic processes are fludeoxyglucose F 18 injection (^{18}F-FDG) and sodium acetate C 11 injection (^{11}C-acetate). The first is widely used for assessment of glucose utilization, and the second has found predominant application for evaluation of tissue oxidative metabolism, especially in the myocardium.

Glucose Utilization

The predominant radiopharmaceutical for clinical PET is the metabolic tracer ^{18}F-FDG. Several favorable characteristics promote its widespread use for noninvasive assessment of human pathology. These include multiple and diverse indications for use in PET imaging, the facile manner of drug preparation, and the convenient half-life of the radiolabel.

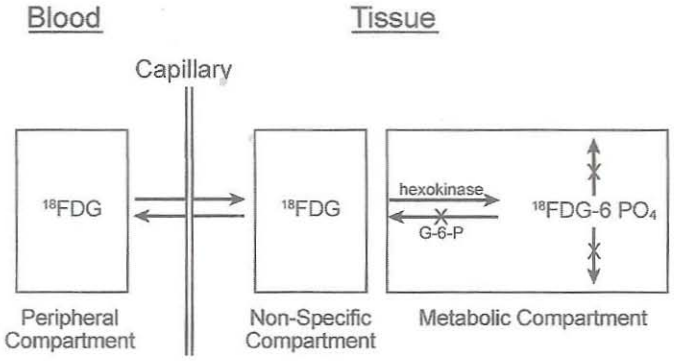

FIGURE 10-6 Metabolic trapping of ^{18}F-FDG. The tracer is phosphorylated by hexokinase but is not further metabolized and does not redistribute.

Glucose is a nutrient used by most tissues of the body, so evaluation of regional glucose utilization in vivo by PET is clinically important for assessing the vitality of organs as well as for monitoring therapeutic response to interventions. ^{18}F-FDG is thus indicated for several different applications, including PET imaging of the brain, heart, and various neoplasms.

As shown in Figure 10-6, the unique biologic property of ^{18}F-FDG that promotes its use as a radiopharmaceutical is its metabolic trapping in vivo. The radiolabeled glucose derivative participates in the initial steps of glucose metabolism (carrier-mediated transport and phosphorylation at the 6 position by the enzyme hexokinase), so the radiopharmaceutical faithfully traces aerobic or anaerobic flux. However, after these initial biochemical steps, the phosphorylated intermediate does not undergo further metabolism to glycogen or to carbon dioxide, nor is it effectively degraded by glucose 6-phosphatase. Thus, tissues accumulate radioactivity in proportion to their glucose utilization rate, and there is no complicating redistribution of radiometabolites that would weaken the image contrast of tracer accumulation. In clinical PET, images of glucose utilization are typically acquired 45 to 60 minutes after the intravenous injection of ^{18}F-FDG.

Oxidative Metabolism

Another important metabolic measurement made by PET is oxidative metabolism. This is especially pertinent in cardiology, because oxidative metabolism is the major nutritional pathway for myocardium under aerobic conditions. Under these conditions, the primary source of energy for the healthy myocyte derives from fatty acids that enter the Krebs cycle and subsequently undergo beta-oxidation.

Sodium acetate C 11 injection is the PET radiopharmaceutical used to clinically assess oxidative metabolism in the heart. ^{11}C-acetate is the smallest fatty acid, and it enters the Krebs cycle in a substrate-independent manner to be metabolized to ^{11}C-carbon dioxide at a rate dependent on the oxidative capability of the heart (Figure 10-7). The viability of heart tissue can therefore be measured by PET determination of the clearance half-life of ^{11}C-acetate from myocardium after bolus injection of the radiopharmaceutical.

PET measurement of myocardial viability using ^{11}C-sodium acetate has clinical value. It is frequently used in concert with myocardial perfusion measurements to discriminate infarction (dead myocardium) from ischemia (underperfused tissue that may be rescued through appropriate medical intervention).

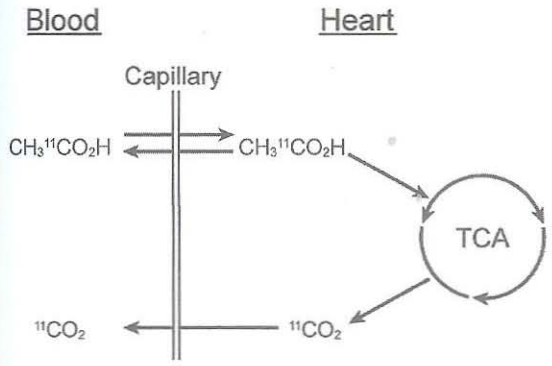

FIGURE 10-7 Oxidative metabolism of ^{11}C-acetate. In viable myocardial tissue, the tracer enters the Krebs (TCA) cycle, is converted to carbon dioxide, and clears from the heart.

TABLE 10-5 Off-Label Applications of PET Tracers

Radiopharmaceutical	Application
Sodium acetate C 11 injection	Prostate cancer
	Hepatocellular carcinoma
	Myocardial perfusion
Fluorodopa F 18 injection	Melanoma
	Thyroid cancer

More sophisticated viability studies sometimes combine PET measurement of ^{11}C-acetate with a flow measurement as well as with PET measurement of glucose utilization using ^{18}F-FDG. In these studies, ischemic zones (flow tracer) are compared with decreases in oxidative metabolism (^{11}C-sodium acetate) or increases in glucose utilization (^{18}F-FDG), the latter of which is up-regulated as anaerobic glycolysis becomes a more important source of energy for the ischemic myocytes. Note that infarcted myocardium will metabolize neither ^{11}C-acetate nor ^{18}F-FDG.

In addition to the primary indication for ^{11}C-sodium acetate in clinical PET myocardial viability measurements, there are off-label uses for this PET radiopharmaceutical (Table 10-5). These uses were identified through serendipity, and their discovery suggests that there may be other indications for alternative PET radiopharmaceuticals that have not been identified and exploited.

^{11}C-sodium acetate has also proven useful as a myocardial perfusion tracer.[7,8] Soon after bolus injection, the tracer has kinetics similar to that of a partially extracted perfusion tracer. It may streamline clinical PET protocols if the same tracer (^{11}C-sodium acetate) is used for both flow and viability measurements in patients scheduled for myocardial viability studies, rather than adding a second flow tracer to the imaging session. An added benefit of using one tracer for two measurements is that the patient is spared the additional radiation dose from a second tracer.

^{11}C-sodium acetate is also useful for PET imaging of prostate cancer and hepatocellular carcinoma.[9,10] The development of PET radiopharmaceuticals for assessment of prostate cancer has proven to be challenging; the location of the gland near the bladder makes discrimination difficult for tracers that clear through the kidneys and urinary tract. For similar reasons, tracers that clear by the hepatic route are difficult to use for discrimination of liver tumors. ^{11}C-acetate is eliminated as ^{11}C-carbon dioxide from the lungs, so there is neither bladder nor liver accumulation of activity, in contrast to the use of ^{18}F-FDG. Localization of ^{11}C-acetate within tumor sites is believed to be due to participation in lipid synthesis within lesions.

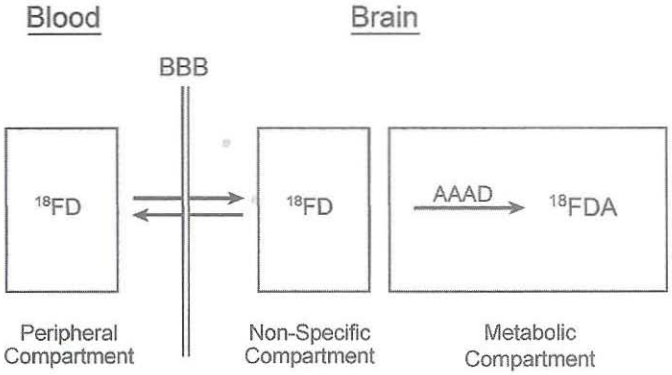

FIGURE 10-8 In vivo localization of 6-^{18}F-fluorodopa (^{18}F-FD) within dopaminergic neurons. The tracer is decarboxylated by cellular aromatic amino acid decarboxylase (AAAD) to form fluorodopamine (^{18}F-FDA), which remains within the neuron.

Neurotransmission Imaging

The third broad category of clinical PET applications is the noninvasive assessment of neurotransmission. Neuronal communication is a complicated process that involves the synthesis and release of neurotransmitters that diffuse across the synaptic cleft to bind to and activate specific receptors on postsynaptic nerve cells. Myriad neurotransmitter pathways in the brain interact in an inhibitory or excitatory fashion. Intensive worldwide research is devoted to gaining insight into the complicated manner in which these pathways interact in health and disease.

Some of the results of PET neuroscience research have been translated to clinical nuclear medicine. Three PET radiopharmaceuticals have demonstrated clinical utility (Table 10-4). Two of these, fluorodopa F 18 injection (^{18}F-FD) and raclopride C 11 injection (^{11}C-RAC), are used in the assessment of the dopaminergic nervous system. Dopamine neurotransmission is affected in degenerative diseases like Parkinson's and Huntington's, and dopamine receptors are the site of action of antipsychotic drugs.

The third PET tracer used for neurotransmission imaging is flumazenil C 11 injection (^{11}C-FMZ). Flumazenil binds to benzodiazepine (BZD) receptors in the brain. Although these drug-binding sites are not bona fide neurotransmitter receptors, BZD receptors are allosterically linked to receptors for the inhibitor neurotransmitter gamma aminobutyric acid (GABA). PET tracers for imaging GABA receptor activity are not currently available, but radiopharmaceuticals that bind to BZD receptors give in vivo data that are indicative of GABA activity.

Enzyme Activity

^{18}F-FD is useful for PET assessment of a number of cerebral dopamine neurons. As illustrated in Figure 10-8, the tracer follows the enzymatic pathway that converts levodopa to dopamine. ^{18}F-FD is used rather than an ^{18}F-labeled derivative of dopamine because dopamine is a charged species that does not partition across the blood–brain barrier to gain access to dopamine neurons in the brain. Within the brain, ^{18}F-FD is acted upon by aromatic amino acid decarboxylase to form ^{18}F-fluorodopamine and accumulates within dopaminergic neurons. There is selective localization within the basal ganglia of the brain, the area that controls movement. In degenerative diseases like Parkinson's disease, there

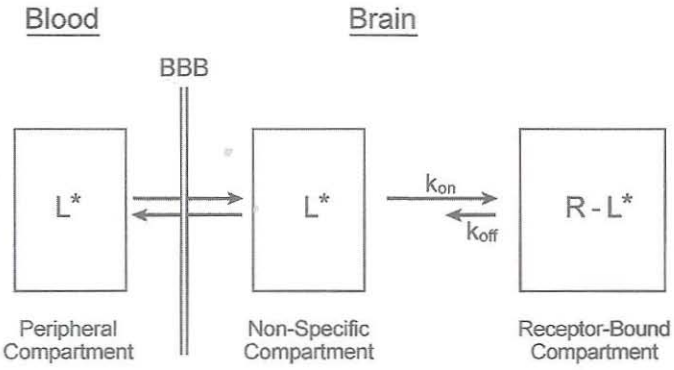

FIGURE 10-9 In vivo localization of radioligands to receptor sites. The radioligand (L*) must pass the blood–brain barrier (BBB) and have high affinity for binding to the receptor (R) and relatively low nonspecific binding.

is loss of dopaminergic neurons, so the level of accumulation of activity in the basal ganglia is less than in healthy, age-matched controls. The decrease in ^{18}F-FD localization in dopamine-rich areas of the brain has been shown to correlate with disease severity.

Like sodium acetate C 11 injection, ^{18}F-FD has an off-label application (Table 10- 5). It has been found to accumulate in vivo within tumors and has proven useful for PET evaluation of melanoma and thyroid carcinoma.[11,12] The localization mechanism is believed to be due to increased amino acid utilization by the cancerous lesions.

Neuroreceptor Binding

Both ^{11}C-RAC and ^{11}C-FMZ are examples of receptor-binding radiopharmaceuticals. Receptor-binding PET radiopharmaceuticals have high affinity and high specific activity so that primarily receptor-bound localization is detected in the PET image (Figure 10-9).

The in vivo localization of ^{11}C-RAC is anatomically similar to that of ^{18}F-FD, but the two tracers measure two different aspects of the same neurotransmitter system. ^{11}C-RAC binds to postsynaptic dopamine D_2 receptors with moderately high affinity. There are few D_2 receptors, so ^{11}C-RAC must be of very high specific activity (>500 Ci/mmol) to ensure that only a small percentage of the binding sites are occupied. Generally, D_2 receptors are up-regulated when dopamine levels in the synapse are low (as in Parkinson's disease) and down-regulated by high levels of the neurotransmitter (as in psychosis), but this relationship can be altered by receptor dysfunction. The major application of ^{11}C-RAC stems from the fact that the radioligand is displaceable by endogenous dopamine. ^{11}C-RAC binding is measured before and after an intervention that induces dopamine release, and the decrease in D_2 binding after the intervention is an index of the functional capability of the dopaminergic system. These receptor-displacement studies have been used to evaluate drug potency in vivo and to measure the effect of stimuli on dopamine release, as well as to assess the residual function of dopaminergic neurons in degenerative states.

^{11}C-FMZ binds with high affinity to BZD receptors in the brain, which are ubiquitous in cerebral tissue but are especially concentrated in the cortex. The link between the inhibitory neurotransmitter GABA and BZD binding underlies the clinical utility of ^{11}C-FMZ. Because there is decreased inhibitory GABA innervation in epileptic foci, binding of ^{11}C-FMZ is also reduced at these tissue sites. This has clinical utility in imaging the foci of intractable seizures, for which surgical intervention may be considered. Although there

is also decreased glucose utilization and thus decreased accumulation of ^{18}F-FDG in the region of the epileptic focus during the interictal period, the size of the region of decreased glucose utilization exceeds the more discriminatory area of decreased ^{11}C-FMZ binding. Thus, the application of ^{11}C-FMZ in PET can identify tissue that is possibly healthy, permitting a more conservative approach to removal of brain tissue.

REIMBURSABLE PET PROCEDURES

Reimbursement for imaging procedures is a very important issue in the advancement of PET as a clinical tool. Only when PET procedures are reimbursed is it financially feasible to apply them on a widespread basis for patient care. The key decision maker about reimbursement is the federal government's Centers for Medicare and Medicaid Services (CMS), since most third-party payers follow CMS reimbursement decisions. Although CMS uses private companies as local contractors to process and pay Medicare claims, its coverage decisions apply nationwide and specify coverage instruction, billing codes, and effective dates for payment.

Of the PET imaging procedures that have been used in research, only a select few have been approved for CMS reimbursement. This approval is an important step in technology transfer, because procedures are approved only after careful scrutiny of the scientific evidence that evaluates the effectiveness and clinical benefit of the particular imaging procedure. Professional organizations such as the Society of Nuclear Medicine (SNM) and the Academy of Molecular Imaging (AMI) play an important role by lobbying and providing expert information to CMS for approval of new PET procedures. Once a procedure is deemed worthy of CMS reimbursement, it can move from the specialized realm of medical research, with its limited number of subjects funded by a granting agency for a specific study, to the health care arena, where PET imaging can be performed routinely to benefit the population at large. Only those PET procedures that have been shown to have advantages over existing clinical test methods are granted CMS reimbursement. CMS-reimbursed PET procedures are used in oncology, neurology, and cardiology. Tables 10-6 through 10-8 list indications for which CMS has approved coverage of PET procedures. These tables reflect the influence CMS restrictions on reimbursement have had on the emergence of PET as a clinical tool.

The first PET studies approved for reimbursement by CMS were myocardial perfusion studies with ^{82}Rb-rubidium chloride (Table 10-8), in 1995. Several years later (in 2001), five indications for PET imaging with ^{18}F-FDG gained CMS approval (Table 10-7). The devices used in these approved procedures included both dedicated (full- or partial-ring) PET scanners and hybrid (coincidence) gamma cameras, because the data reviewed for approval were acquired using either type of scanner. The more recent expansion of clinical PET into further indications for imaging with ^{18}F-FDG and ^{13}N-ammonia is based on regional or whole-body imaging data acquired only with dedicated PET scanners (Table 10-6). The data show the superiority of these devices for the specific clinical applications and reflect the tendency of contemporary clinical PET facilities to use dedicated PET instrumentation rather than hybrid devices that give poorer image quality. Thus, the most recent CMS-reimbursed PET procedures require imaging with dedicated PET scanners, and only the earlier CMS authorizations (which remain in effect) allow hybrid scanners to be used for clinical imaging studies.

Oncology

The field of oncology is the biggest beneficiary of CMS reimbursement. PET studies are indicated for breast cancer, colorectal cancer, esophageal cancer, head and neck cancer,

TABLE 10-6 CMS-Approved PET Procedures (Dedicated PET Scanners)[a]

Pathology	Tracer	Indication
Oncology		
Breast cancer	^{18}F-FDG	Initial diagnosis or surgical planning
		Staging/restaging after therapy
		Evaluation of therapy response
Colorectal cancer	^{18}F-FDG	Diagnosis/initial staging/restaging
Esophageal cancer	^{18}F-FDG	Diagnosis/initial staging/restaging
Head and neck cancer[b]	^{18}F-FDG	Diagnosis/initial staging/restaging
Lung cancer (non–small-cell)	^{18}F-FDG	Diagnosis/initial staging/restaging
Lymphoma	^{18}F-FDG	Diagnosis/initial staging/restaging
Melanoma	^{18}F-FDG	Diagnosis/initial staging/restaging
Single pulmonary nodule[b]	^{18}F-FDG	Characterization
Thyroid cancer	^{18}F-FDG	Restaging, negative ^{131}I scan, elevated or rising thyroglobulin level
Neurology		
Refractory seizures[c]	^{18}F-FDG	Presurgical evaluation
Cardiology		
Myocardial viability[d]	^{18}F-FDG	Following inconclusive SPECT study
		Primary or initial diagnostic study prior to revascularization
Myocardial perfusion[d]	^{13}N-ammonia	In place of, or after inconclusive, SPECT exam

[a] Unless otherwise noted, procedures are whole-body PET imaging.
[b] Regional or whole-body imaging.
[c] Regional brain imaging.
[d] Regional heart imaging.

TABLE 10-7 CMS-Approved PET Procedures (Hybrid Scanners)[a]

Pathology	Tracer	Indication
Oncology		
Colorectal cancer	^{18}F-FDG	Recurrence of colorectal cancer or metastatic disease
Lung cancer (non–small-cell)[b]	^{18}F-FDG	Initial staging
Lymphoma	^{18}F-FDG	Staging and characterization
Melanoma	^{18}F-FDG	Recurrence of melanoma or metastatic disease
Single pulmonary nodule[b]	^{18}F-FDG	Solitary pulmonary nodule following CT

[a] Unless otherwise noted, studies are whole-body PET imaging.
[b] Regional or whole-body imaging.

TABLE 10-8 CMS-Approved Indications for PET Myocardial Perfusion Imaging Using ^{82}Rb-Rubidium Chloride[a]

Following previous PET
Following rest or stress SPECT
Following coronary angiography
Following stress planar myocardial perfusion
Following stress echocardiogram
Following stress nuclear ventriculogram
Following rest or stress ECG

[a] Single study or multiple studies, rest or stress (exercise or pharmacologic).

lymphoma, melanoma, and thyroid cancer. All of these oncologic PET studies use ^{18}F-FDG, imaged with either dedicated (Table 10-6) or hybrid (Table 10-7) scanners.

In breast cancer, whole-body ^{18}F-FDG PET scans are indicated for initial diagnosis and surgical planning, for staging or restaging of disease after prior treatment, and for evaluating the response of the patient to a given therapy (Table 10-6). PET can also be used to identify axillary nodes or distant metastatic disease, to exclude recurrence of disease, and to monitor individual patient response to medical treatment.

Another important oncologic application of PET approved by CMS is the diagnosis, initial staging, and restaging of colorectal cancer. For this indication, either dedicated (Table 10-6) or hybrid (Table 10-7) scanners can be used to image ^{18}F-FDG. Such procedures include ruling out distant metastases during preoperative evaluation of patients with potentially resectable liver or lung metastasis. ^{18}F-FDG PET imaging is also authorized for detection of locally recurrent or distant metastatic disease in patients with elevated or increasing carcinoembryonic antigen who may be candidates for surgical re-excision. Detecting regional spread to aid in staging malignancy and distinguishing cancer from scar tissue after surgical or radiation therapy are other important applications of PET in oncology.

The diagnosis, initial staging, and restaging of esophageal cancer with ^{18}F-FDG and dedicated PET scanners has also reached the level of clinical significance (Table 10-6). PET can be used to detect regional and distant spread of this malignancy and thereby facilitate medical decisions regarding surgery, surgery plus chemoradiation, or palliative therapy.

Another indication for PET imaging in oncology is head and neck cancer, for which CMS reimburses diagnosis, initial staging, and restaging (Table 10-6). In particular, ^{18}F-FDG and dedicated PET scanners can be applied for detection of the primary lesion or identification of the optimum biopsy site for squamous cell carcinoma with nodal metastasis and unknown primary source. It is also used for the detection of recurrent or residual tumor after definitive therapy and to determine the extent of local, regional, and distant disease.

PET procedures using ^{18}F-FDG are approved by CMS for the diagnosis, initial staging, and restaging of lung cancer patients. Dedicated PET can be used to characterize solitary pulmonary nodules, to distinguish malignant from benign pulmonary nodules, and to stage mediastinal or distant metastatic disease as a component of radiotherapy treatment planning (Table 10-6). It is also beneficial for detection of recurrent or residual tumors after medical therapy. Studies to evaluate single pulmonary nodules using ^{18}F-FDG and hybrid PET scanners are also reimbursable after CT examination (Table 10-7).

CMS has approved PET imaging for the diagnosis, initial staging, and restaging of lymphoma (Tables 10-6 and 10-7). ^{18}F-FDG PET has clinical value for determining the extent of disease and measuring treatment response in patients with Hodgkin's lymphoma and intermediate-grade non-Hodgkin's lymphoma.

The diagnosis, initial staging, and restaging of melanomas is another important area of oncology in which CMS has judged PET imaging as beneficial. Applications for ^{18}F-FDG PET imaging in this area are characterization of the extent of local and regional spread in patients with high-risk melanoma and evaluation of suspected recurrence of the malignancy after prior medical treatment. Both dedicated (Table 10-6) and hybrid (Table 10-7) scanner devices have been authorized for PET melanoma imaging procedures.

^{18}F-FDG imaging of thyroid cancer using dedicated PET scanners is the most recently approved PET procedure in oncology (Table 10-6). It is indicated for restaging previously treated metastatic or locally recurrent disease in patients who have had prior treatment, have a negative ^{131}I whole-body scan, and have elevated or rising serum thyroglobulin levels.

Neurology

The sole CMS-approved PET procedure in neurology is for presurgical evaluation of epilepsy. In this application, PET imaging of ^{18}F-FDG is used to localize seizure foci in patients with intractable complex seizure disorders. As with other recently approved indications, only imaging procedures that are performed with dedicated PET scanners are authorized for reimbursement.

Cardiology

CMS has concluded that PET has clinical value in the area of cardiology as well (Tables 10-6 and 10-8). PET assessment of myocardial viability using ^{18}F-FDG is one such application. PET imaging with dedicated scanners is used to distinguish viable myocardium from infarcted heart tissue in patients with suspected hibernating or stunned myocardium (Table 10-6). ^{18}F-FDG PET is also indicated for further evaluation of patients with inconclusive SPECT scan results.

Dedicated PET scanner procedures are also authorized by CMS for preoperative prognostic assessment of cardiology patients. In particular, PET imaging of ^{18}F-FDG can be used to evaluate the extent of myocardial disease in patients being considered for interventional procedures such as revascularization or heart transplantation (Table 10-6).

CMS has approved reimbursement for the use of ^{13}N-ammonia in myocardial perfusion measurements (Table 10-6). For this indication, only imaging by dedicated PET scanners is authorized. ^{13}N-ammonia is imaged in the stressed or resting state to evaluate myocardial blood flow only in place of SPECT scanning or after an inconclusive SPECT scan. CMS approval is more restrictive here than for the ^{82}Rb-rubidium chloride PET imaging procedure approved earlier (Table 10-8), the only other CMS-approved procedure for PET assessment of myocardial perfusion. Despite its restrictiveness, the approval of ^{13}N-ammonia PET is beneficial for imaging centers with access to cyclotrons, because it means that PET studies of both myocardial viability and perfusion can be performed using cyclotron-produced radiopharmaceuticals only, and the additional capital expense of generator technology for ^{82}Rb-rubidium chloride PET perfusion measurements can be avoided.

Authorized indications for PET myocardial perfusion measurements using ^{82}Rb-rubidium chloride are numerous; this was the first PET imaging procedure to be approved by CMS for reimbursement (Table 10-8). PET perfusion measurements with ^{82}Rb-rubidium chloride in both the resting and stressed (exercise or pharmacologic) states are approved. As shown in Table 10-8, these procedures are reimbursable when performed after other procedures using PET, SPECT, and other means. Comparison of ^{82}Rb-rubidium chloride PET myocardial perfusion measurements and PET estimates of myocardial viability determined by ^{18}F-FDG are especially valuable in viability–perfusion analysis. Although cyclotron-produced ^{13}N-ammonia is also approved for myocardial perfusion measurements (Table 10-6), the indications are much more limited than those authorized for ^{82}Rb-rubidium chloride.

RADIONUCLIDE PRODUCTION

Positron-emitting radionuclides lie on the proton-rich side of the line of beta stability.[1] For this reason, they are usually produced by accelerators that bombard targets with charged particles, rather than by using nuclear reactors as a source of neutrons to irradiate targets. The positron-emitting nuclides commonly used as radiolabels in clinical PET are listed in Table 10-1. Four of these cyclotron-produced radionuclides are isotopes of elements (oxygen, nitrogen, carbon, fluorine) that are frequently found in biochemical and drug structures,

TABLE 10-9 Generator-Produced PET Radionuclides

Nuclide	Half-life	E_{max} (MeV)	Parent Isotope (Half-life)
^{82}Rb	76 sec	3.35	^{82}Sr (25.6 days)
^{68}Ga	68 min	1.90	^{68}Ge (271 days)

have useful half-lives that range from 2 minutes (^{15}O) to 110 minutes (^{18}F), and are incorporated into radiopharmaceutical structures via covalent bonds. These physicochemical characteristics explain the widespread use of cyclotron-produced nuclides for labeling PET radiopharmaceuticals.

Two of the positron-emitting nuclides available from generator systems, ^{82}Rb and ^{68}Ga, do not require a cyclotron for production. Compared with the cyclotron-produced nuclides, however, the properties of these nuclides are much less versatile for labeling drug structures for PET imaging. ^{82}Rb is used solely as a perfusion tracer, and ^{68}Ga is most often used in clinical PET simply as a source of photons for transmission scans.

Radionuclide Generators

Compared with cyclotron-prepared radiopharmaceuticals, PET radiopharmaceuticals available from generators (Table 10-9) are much less commonly used in clinical practice. However, for the sake of completeness, their use in clinical PET imaging will be discussed briefly.

The ^{82}Rb generator was the first system authorized for reimbursement for clinical PET imaging (Table 10-8). The commercially available generator system consists of the parent isotope ^{82}Sr bound to a hydrous stannic oxide column and is eluted with 0.9% sodium chloride injection to isolate the ^{82}Rb daughter (Figure 10-10).[13] The versatility of

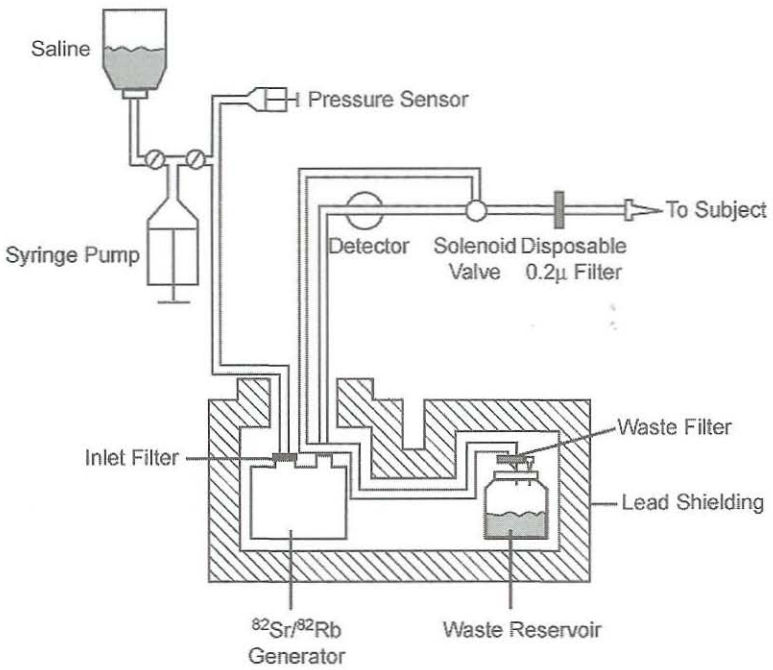

FIGURE 10-10 Diagram of the ^{82}Sr–^{82}Rb generator system. This is the only generator system used for clinical PET imaging.

the generator system is limited by the short physical half-lives of the parent nuclide and the daughter radioisotope (Table 10-9). ^{82}Sr decays by EC with a half-life of 25.6 days, which limits the useful lifetime of the generator system to only a few weeks. The very short 76 second half-life of the rubidium daughter, although useful for repeat studies in PET, prevents any coordination chemistry from being performed with the nuclide prior to patient administration.

The generator system is thus limited to the role of a source of ^{82}Rb infusate for patients undergoing cardiovascular PET measurements. The generator eluate is passed through a dosimeter and sterilizing filter and directly into the patient for myocardial blood flow measurements (Figure 10-10). A microprocessor-controlled syringe pump determines the elution profile so that either bolus or continuous infusion can be used.[13] Because of the short half-life of the radioisotope, the actual batch of ^{82}Rb injection used does not undergo any quality control testing before administration to the patient. However, the generator elution performance is carefully assessed immediately before the PET study to confirm proper functioning of the device; the total radioactivity that is eluted, the elution profile, and potential breakthrough of ^{82}Sr are measured.

Although the physical characteristics of the ^{68}Ge–^{68}Ga generator appear to be ideally suited for clinical applications, to date the use of ^{68}Ga in PET imaging has been limited to research. Nevertheless, there is great potential for future development of this generator as a source of positron-emitting radiopharmaceuticals. ^{68}Ge decays by EC with a half-life of 271 days, which translates to a useful lifetime of approximately 1 year for the generator. In addition, the 68 minute half-life of the daughter confers substantial versatility to radiopharmaceutical labeling or PET imaging procedures with ^{68}Ga. A commercially available ^{68}Ga generator system consists of the ^{68}Ge parent bound to a column of stannous oxide and is eluted with 1 N hydrochloric acid.[14] The generator is characterized by high recovery of ^{68}Ga daughter and low breakthrough of ^{68}Ge parent.

The most common application of the ^{68}Ge–^{68}Ga decay system is not for radiopharmaceutical production but for instrumentation use. The generator system is often used in PET devices as a source of 511 keV photons needed for transmission measurements and attenuation correction of emission scans. In this case, the daughter ^{68}Ga is not eluted from the generator column but instead is merely allowed to decay on the rods in situ. The long half-life of the ^{68}Ge parent is a major advantage for this application, because the source rods have to be replaced infrequently.

Charged Particle Accelerators

Most PET radionuclides are produced with cyclotrons, devices designed by physicists to accelerate charged particles. As illustrated in schematic form in Figure 10-11, the operation of the cyclotron is based on the concept that repeated application of small accelerating voltages to ions will accelerate those ions to high velocities. These accelerated particles will be constrained to circular pathways by the presence of a magnetic field induced by magnetic poles situated above and below the accelerating electrodes. As the particles pass the interface between the hollow electrodes (called "dees" because of their shape), the difference in electrical potential (controlled by a radiofrequency oscillator) imparts additional kinetic energy to the ion. As the ions increase in velocity, their radius of rotation increases until they achieve their terminal velocity, which is determined by the engineering parameters designed into the cyclotron. The beam of high-energy charged particles is then deflected away from the magnetically constrained pathway of the cyclotron to impinge upon the target. The irradiation of the target material by the cyclotron beam produces, by nuclear reaction, the radionuclides used for labeling PET radiopharmaceuticals.

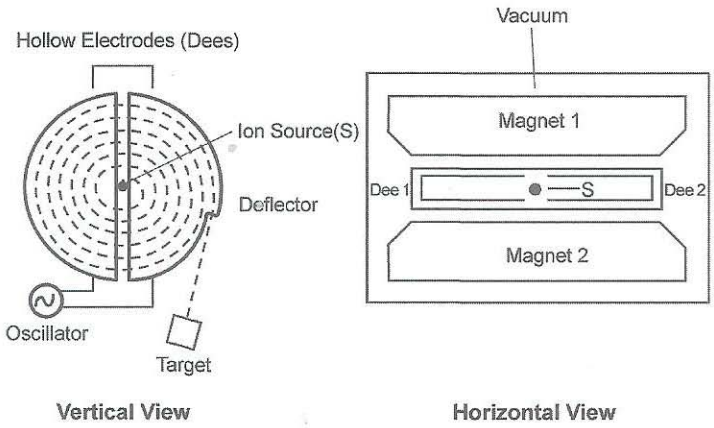

FIGURE 10-11 Diagram of cyclotron acceleration of particle beams for PET radionuclide production. Accelerated particles can be either positive or negative ions.

TABLE 10-10 Classification of Particle Accelerators

Level I	Single particle (usually p or d)
	E_p ≤10 MeV
Level II	Single or multiple particle (usually p and/or d)
	E_p ≤20 MeV
Level III	Single or multiple particle (usually p)
	E_p ≤50 MeV
Level IV	Single or multiple particle (usually p)
	E_p 70–500 MeV

Clearly, more details are involved in actual radionuclide production than are included in this simplistic description; readers are referred to more comprehensive information.[15–17] Cyclotrons are designed to many different specifications depending on their nuclear applications, and those used for medical radioisotope production generally have lower beam energy and higher beam current than corresponding machines used for physics research. Higher beam currents are desirable because the amount of radionuclide produced is proportional to the number of nuclear reactions that are induced by the beam. Also, the threshold energies for the nuclear reactions used to produce positron-emitting nuclides are relatively low compared with those used in particle physics research.

Accelerators for the production of radionuclides have been classified into four levels (Table 10-10) based on the particles accelerated and their energies.[17] The higher the energy of the accelerator, the more expensive are capital installation and subsequent operating costs. For most in-hospital production of PET radionuclides, either level I or level II machines are used; the energies of these cyclotrons are adequate for the production of needed quantities of positron emitters for PET. Level III or IV accelerators are used to produce less common radionuclides used in nuclear medicine procedures, but the radionuclides used routinely for labeling PET radiopharmaceuticals (Table 10-1) do not require the use of such large devices.

Most modern PET-based cyclotrons use negative-ion acceleration technology, although several older positive-ion machines are still in current use in the PET community. The advantage of negative-ion machines is that substantially less radiation shielding is required, so installation costs are reduced. In addition, beam extraction is greatly simplified

TABLE 10-11 Cyclotron Production of PET Radionuclides

Nuclide	Half-life	Reaction	Target	Target Product	Batch Yields
^{15}O	2 min	$^{14}N(d,n)^{15}O$	0.1% O_2/N_2	$[^{15}O]O_2$	1000 mCi
		$^{15}N(p,n)^{15}O$			1000 mCi
^{13}N	10 min	$^{16}O(p,\alpha)^{13}N$	^{16}O-water	$[^{13}N]NH_3$, $[^{13}N]NO_3^-$, $[^{13}N]NO_2^-$	200 mCi
^{11}C	20 min	$^{14}N(p,\alpha)^{11}C$	0.5% O_2/N_2	$[^{11}C]CO_2$	1000–2000 mCi
^{18}F	110 min	$^{18}O(p,n)^{18}F$[a]	^{18}O-water	$[^{18}F]F^-_{aq}$	500–2000 mCi
		$^{20}Ne(d,\alpha)^{18}F$[b]	0.5% $F_2/^{20}Ne$	$[^{18}F]F_2$	250 mCi

[a] ^{18}F produced as high specific activity fluoride ion (F^-).

[b] ^{18}F produced as moderate specific activity fluorine gas (F_2).

with negative-ion machines. With negative-ion cyclotrons, a thin graphite foil is place in the beam pathway, so the ions are stripped of their negative charge and converted to positive ions. According to the laws of electromagnetism, the positively charged particles will rotate in the direction opposite that of the original beam of negative ions, so they will impinge upon targets mounted on appropriately situated exit ports. By placing the graphite foils at different radii of the cyclotron, the energy of the beam hitting the target can be selected. Also, by adjusting the depth of foil insertion, either a fraction or the entire beam can be stripped, enabling adjustment of beam intensity so that it hits a single target or irradiates multiple targets simultaneously. This type of flexibility is a great asset when radionuclide production is scheduled for busy PET clinics.

Cyclotron Targetry

The selection of targets to be irradiated in cyclotrons for isotope production is an area that has undergone intensive research and optimization.[16,18] Cyclotron targets can be gaseous, liquid, or solid, but those used for producing routine PET radionuclides are gaseous or liquid, and their loading or unloading can be achieved by application of a pressure differential. A caution concerning the irradiation of liquid targets is that free radicals may be generated in situ. Such radicals can potentially interfere with the reactivity of the product radionuclide by creating species that interfere with subsequent radiopharmaceutical labeling reactions. However, by careful control of beam and target conditions during cyclotron irradiation, such deleterious effects can be minimized.

The nuclear reactions commonly used for radionuclide production in clinical PET centers are listed in Table 10-11. These reactions use incident particles of either protons or deuterons, which are accelerated to adequate energies in moderate beam intensities by level I or level II cyclotrons. The selection of the nuclear reaction to be used for radioisotope production is determined by the capability of the particle accelerator. More expensive multiparticle machines accelerate both deuterons and protons and have the advantage that inexpensive targets of naturally abundant nuclei can be used for radioisotope production. An exception to this generalization is the production of ^{18}F-fluoride, which requires isotopically enriched ^{18}O-water as a target, regardless of whether level I or level II accelerators are used.

Single-particle machines that produce only proton beams are less expensive than level II cyclotrons but have the disadvantage that they require expensive isotopically enriched target materials for the production of ^{15}O, since the $^{14}N(d,n)^{15}O$ nuclear reaction is not an option. However, for clinical PET centers that do not require heavy production of ^{15}O tracers, single-particle (level I) cyclotrons offer a relatively inexpensive means of radionuclide production.

TABLE 10-12 Radioactive Precursors for Labeling PET Radiopharmaceuticals

Radionuclide	Labeling Precursor
^{15}O	^{15}O-oxygen
^{13}N	^{13}N-nitrate, ^{13}N-nitrite
^{11}C	^{11}C-carbon dioxide
	^{11}C-methyl iodide
^{18}F	Reactive ^{18}F-fluoride
	^{18}F-fluorine

Labeling Precursors

It is important to consider the chemical form of the radionuclide as it leaves the target, because this dictates the chemical reactivity and hence the synthetic reactions that can be used for radiopharmaceutical preparation. In some cases, target products can be immediately applied for radiopharmaceutical synthesis. However, it is more usual for the target product to be purified, either to remove chemicals that interfere with the labeling procedure or to convert the target product to alternative chemical forms that can be more easily incorporated into the molecular structure of the desired radiopharmaceutical. The degree of chemical manipulation is thus dictated by the spectrum of radiochemicals and chemicals present in the irradiated target and is further constrained by the half-life of the product radionuclide. The predominant labeling precursors for synthesis of PET radiopharmaceuticals are listed in Table 10-12.

Gaseous ^{15}O-Oxygen

As shown in Table 10-12, the target product for ^{15}O (which has a 2 minute half-life) is gaseous ^{15}O-oxygen ($[^{15}O]O_2$). Although ^{15}O-oxygen can be used as a PET radiopharmaceutical for measuring tissue oxygen consumption, it is more commonly used to synthesize alternative radiopharmaceutical structures, such as ^{15}O-water or ^{15}O-carbon monoxide, for imaging use. Thus, it is appropriate to consider ^{15}O-oxygen a labeling precursor for these more popular ^{15}O-labeled PET radiopharmaceuticals. Because of the short half-life of ^{15}O, the target product must be rapidly converted to desired chemical forms using on-line techniques. These production techniques are described below.

Oxo Anions of ^{13}N-Nitrogen

The 10 minute half-life of ^{13}N also limits the number of radiosynthetic steps that can be used to incorporate the nuclide into a labeled drug, and to date ^{13}N-ammonia is the sole ^{13}N-labeled radiopharmaceutical of clinical significance. ^{13}N is produced in the irradiated target in a spectrum of chemical forms including ^{13}N-ammonia, ^{13}N-nitrate, and ^{13}N-nitrite. Instead of purifying the relatively modest fraction that is produced in the form of ^{13}N-ammonia, it is more efficient to convert all of the chemical forms of ^{13}N produced in the target to ^{13}N-ammonia. In this regard, ^{13}N-nitrate and ^{13}N-nitrite can be considered labeling precursors for ^{13}N-ammonia. Techniques have been developed for the rapid reduction of nitrogen oxides in the target mixture to ^{13}N-ammonia for radiopharmaceutical use, as well as for minimization of their production in the target during irradiation; these are described below.

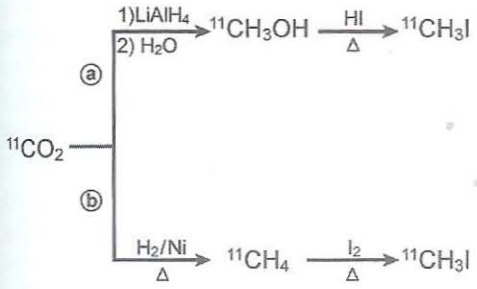

FIGURE 10-12 Radiosynthesis of the labeling precursor ^{11}C-methyl iodide. (a) Liquid-phase method; (b) gas-phase method.

^{11}C-Methyl Iodide

The relatively long 20 minute half-life of ^{11}C facilitates much greater latitude in chemical manipulation, both for preparation of the labeling precursor and during radiopharmaceutical synthesis. The target product for ^{11}C is ^{11}C-carbon dioxide, which can either be used directly as a labeling reagent or converted to a large number of synthetic precursors.[19,20] Of these diverse ^{11}C labeling reagents, ^{11}C-methyl iodide is especially valuable because of the large number of drug structures that can be labeled by N- or O-methylation.[21]

There are liquid-phase and gas-phase methods for preparing ^{11}C-methyl iodide. Liquid-phase methods were the first to be developed.[22–24] This synthetic approach involves the reduction of ^{11}C-carbon dioxide target to ^{11}C-methanol using lithium aluminum hydride and subsequent treatment of the ^{11}C-methanol intermediate with hydriodic acid to form ^{11}C-methyl iodide (Figure 10-12). The second step of this procedure can take place either by addition of hydriodic acid to the reduction vessel ("one-pot" synthesis) or after distillation of ^{11}C-methanol into a second vessel that contains hydriodic acid ("two-pot" synthesis). With either synthetic approach, the final ^{11}C-methyl iodide must be passed through purifying columns of soda lime and phosphorus pentoxide into a separate reaction vessel for radiopharmaceutical labeling. This purification step is necessary in order to remove any traces of hydrogen iodide or water, which would quench ^{11}C-methylation reactions.

Although recommendations have been proposed for standardizing production conditions for ^{11}C-methyl iodide prepared by liquid-phase methods,[21] the labeling technique is cumbersome and the radiochemical yield and specific activity are extremely sensitive to environmental conditions and reagents. Moreover, the turnaround time for production of ^{11}C-labeled PET radiopharmaceuticals in this manner is unwieldy because of the time needed for apparatus replacement and setup. This is a major impediment to the efficient operation of a clinical production center at a busy PET clinic, especially when repeated imaging scans are required in the same patient.

Gas-phase methods provide a better means of preparing ^{11}C-methyl iodide.[25,26] As shown in Figure 10-12, in this synthetic approach ^{11}C-carbon dioxide is first reduced to ^{11}C-methane by heating in the presence of hydrogen gas with nickel catalysis. The ^{11}C-methane intermediate is then converted to ^{11}C-methyl iodide by recirculation through a heated quartz tube that contains iodine crystals. The ^{11}C-methyl iodide is then trapped on a porous polymer support and subsequently released as a gas for radiopharmaceutical labeling applications.

The gas-phase approach to making ^{11}C-methyl iodide has several advantages. The system is easily automated, and commercial sources supply microprocessor-controlled devices that accomplish this radiochemistry over a 12 minute period, completely without operator intervention. The system is also capable of synthesizing multiple batches of the labeling precursor without the need for apparatus replacement or setup. Thus, sequential

batches of ^{11}C-methylated radiopharmaceuticals can be prepared without excessive radiation burden to production personnel. Moreover, the turnaround time between successive batches of ^{11}C-methyl iodide is only 20 to 30 minutes, which enables scheduling flexibility. The gas-phase synthesis of ^{11}C-methyl iodide also yields a higher specific activity product than the liquid phase approach, and the production sequence promotes greater consistency of precursor quality, which is important for radiopharmaceutical quality assurance.

Reactive ^{18}F-Fluoride

The 110 minute half-life of ^{18}F is very convenient for radiopharmaceutical synthesis. The radionuclide can be produced in two chemical forms, high specific activity ^{18}F-fluoride ion ($[^{18}F]F^-$) and moderate specific activity gaseous ^{18}F-fluorine ($[^{18}F]F_2$).

The preferred form of ^{18}F for radiopharmaceutical labeling is reactive ^{18}F-fluoride, which is used in nucleophilic substitution reactions. Aqueous ^{18}F-fluoride is produced with high specific activity in multicurie batches by proton irradiation of ^{18}O-water. Because of the high batch yields for cyclotron production of ^{18}F-fluoride, large quantities of PET radiopharmaceuticals can be synthesized from this precursor for use in the imaging clinic throughout the workday. In other situations, these high radiopharmaceutical production yields can be used to advantage because they facilitate distribution of PET tracers to off-site remote imaging locations. An additional advantage of ^{18}F-fluoride as a labeling precursor is its high specific activity, which makes possible the synthesis of PET radiopharmaceuticals for receptor-binding studies. It also minimizes the potential for pharmacologic or toxicologic effects of ^{18}F-labeled tracers, whether receptor-binding or not.

The irradiated ^{18}O-water target that contains ^{18}F-fluoride can be either used directly for nucleophilic fluorination reactions or purified by passage through a resin that separates the aqueous ^{18}F-fluoride from byproducts in the irradiated solution (Figure 10-13).[27] Heat generation during target irradiation causes byproducts to be dissolved in the target solution that can potentially interfere with subsequent labeling reactions. For this reason, resin purification has the dual advantages of facilitating recovery of expensive irradiated ^{18}O-water for reuse, as well as removing chemicals that may impede radiopharmaceutical labeling reactions with ^{18}F-fluoride.

Nucleophilic fluorination reactions are inhibited by water, so it is essential that the aqueous solution of ^{18}F-fluoride be completely dried prior to the substitution reaction that incorporates ^{18}F into the molecular structure of the radiopharmaceutical. Such chemical

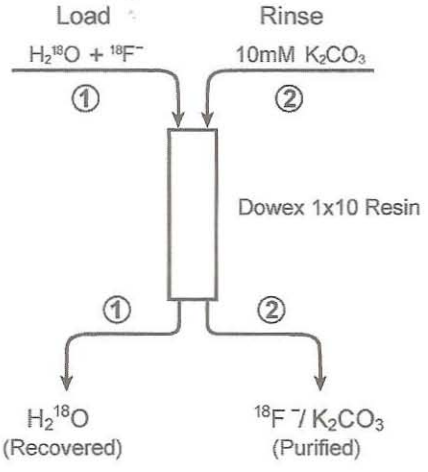

FIGURE 10-13 Resin purification of ^{18}F-fluoride and recovery of irradiated ^{18}O-water. (1) Loading of target water and ^{18}F-fluoride, with recovery of ^{18}O-water for reuse; (2) elution of purified ^{18}F-fluoride with aqueous potassium carbonate.

transformation of aqueous ^{18}F-fluoride into reactive ^{18}F-fluoride is a key aspect of radiopharmaceutical synthesis, and the major steps have been reviewed.[20,28] There are three major steps to this process. First, a cation such as potassium, complexed to an aminopolyether cryptand such as Kryptofix 2.2.2 (Sigma-Aldrich) or a tetraalkylammonium salt, is added to the aqueous solution to serve as a counterion to the fluoride anion. Second, all traces of water are removed from the solution by azeotropic distillation with acetonitrile. Finally, a dipolar, aprotic organic solvent such as dimethylsulfoxide, dimethylformamide, or acetonitrile is added to resolubilize the dried complex of ^{18}F-fluoride. The resulting anhydrous solution of radioactivity contains reactive ^{18}F-fluoride and is added to the appropriate substrate to facilitate the nucleophilic substitution reaction necessary for radiopharmaceutical labeling.

Electrophilic ^{18}F-Fluorine

Although nucleophilic reactions may give high radiochemical yields for some ^{18}F-labeled PET tracers, this is not always the case. Some drug structures cannot be fluorinated in useful quantities with nucleophilic reactions because of the electronic nature (electron-rich rather than electron-poor aromatic rings) of the labeling substrate. An example of such a PET radiopharmaceutical is ^{18}F-fluorodopa (^{18}F-FD).

For these select applications, electrophilic ^{18}F-fluorine is used as a labeling precursor. Several electrophilic ^{18}F-fluorination reagents, including ^{18}F-labeled acetyl hypofluorite and xenon difluoride, have been developed over the years,[20] but ^{18}F-fluorine is the electrophilic fluorination precursor of choice from the perspective of simplicity and efficiency of labeling procedures.

^{18}F-fluorine is produced in hundred-millicurie quantities by the irradiation of a ^{20}Ne gas target with deuterons. It is necessary for the neon target to contain 0.1% to 2% F_2 as a carrier,[29] so the radionuclide is produced in only moderate specific activity (<12 Ci/mmol).[30] Both the batch yield and the specific activity of ^{18}F-fluorine are much lower than for ^{18}F-fluoride. Nevertheless, ^{18}F-fluorine is an extremely valuable precursor for that special category of PET radiopharmaceutical that cannot be labeled via ^{18}F-fluoride and does not require high specific activity to be effective.

RADIOPHARMACEUTICAL SYNTHESIS

The preparation of a short-lived positron-emitting radiopharmaceutical has stringent requirements because of the short half-lives of the relevant radionuclides. Radiosyntheses must be rapid and must produce the desired radiopharmaceutical in high radiochemical yield and purity. Although not always essential, high specific activity is often advantageous, either to avoid saturation of the biologic process under study or to minimize potential pharmacologic and toxicologic effects.

To accomplish this, facile labeling techniques using substrates that direct the radionuclide to a specific molecular site are needed. The preparation of these substrates often requires substantial synthetic expertise, and various commercial sources specialize in supplying these labeling reagents. As explained above, rapid, efficient conversion of the target product (the chemical bearing the product radionuclide) into a labeling precursor (or reactive chemical reagent form) of the radionuclide is frequently used to facilitate radiopharmaceutical labeling efficiency.

^{15}O and ^{13}N have short half-lives that preclude time-consuming radiosynthetic or imaging procedures. Radiopharmaceuticals labeled with these nuclides are rapidly produced on line, with minimal chemical manipulation. By contrast, the longer-lived ^{11}C and ^{18}F

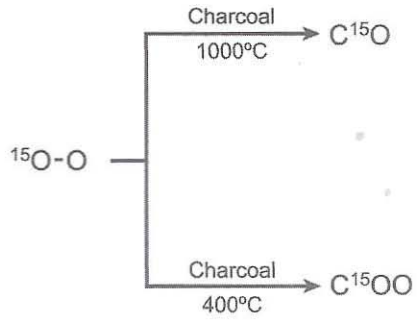

FIGURE 10-14 On-line synthesis of ^{15}O-carbon monoxide and ^{15}O-carbon dioxide from target product ^{15}O-oxygen.

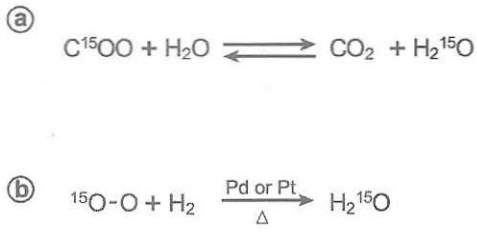

FIGURE 10-15 Radiosynthesis of ^{15}O-water. (a) Isotopic exchange method; (b) chemical reduction method.

labels allow more flexibility with radiopharmaceuticals that have more lengthy preparation or imaging requirements. Generally speaking, however, clinically used PET nuclides have short half-lives and, with the exception of ^{18}F, must be prepared on site to satisfy the needs of the PET imaging suite.

^{15}O-Labeled Gases

Because of the short half-life of ^{15}O, PET radiopharmaceuticals that are labeled with this nuclide are produced on line with little operator intervention. As illustrated in Figure 10-14, target product ^{15}O-oxygen is converted to either ^{15}O-carbon monoxide or ^{15}O-carbon dioxide by recirculation through a charcoal furnace heated to 1000°C or 400°C, respectively.[31–34] For production of ^{15}O-carbon monoxide, careful control of beam and target conditions is necessary to minimize the amount of toxic nonradioactive carbon monoxide present in the radiopharmaceutical product.[35]

^{15}O-oxygen is commonly used in PET research protocols for measuring the cerebral metabolic rate of oxygen, whereas ^{15}O-carbon monoxide is used in assessing regional cerebral blood volume. Both of these radioactive gases are administered to the subject by direct inhalation of the target gas through a disposable mouthpiece with a 0.2 μm filter.

Water O 15 Injection

^{15}O-labeled water is produced for perfusion measurements by isotopic exchange or reduction reactions. In the exchange method, ^{15}O-carbon dioxide is used as a labeling precursor that is converted to ^{15}O-water, as shown in Figure 10-15. During cyclotron bombardment of the target, the ^{15}O-carbon dioxide that is produced on line is bubbled though a sterile bag of water for injection mounted in an ionization chamber.[33] The entire apparatus is mounted within a shielded "hot" cell. When adequate exchange labeling has occurred, as monitored by the ionization chamber reading at the cyclotron control console, some of the bag contents is remotely transferred to a 12 mL sterile syringe, which is pneumatically sent to the PET suite for bolus injection into the subject. Routinely, 50 to 125 mCi is produced in this manner, with a turnaround time of only 10 to 12 minutes.[33]

^{15}O-water can also be produced by reduction of ^{15}O-oxygen, as shown in Figure 10-15. Using this production route, conversion of the target product ^{15}O-oxygen into the labeling intermediate ^{15}O-carbon dioxide is unnecessary. Hydrogen gas is instead admixed with the target stream of ^{15}O-oxygen, and the mixture is passed over palladium or platinum

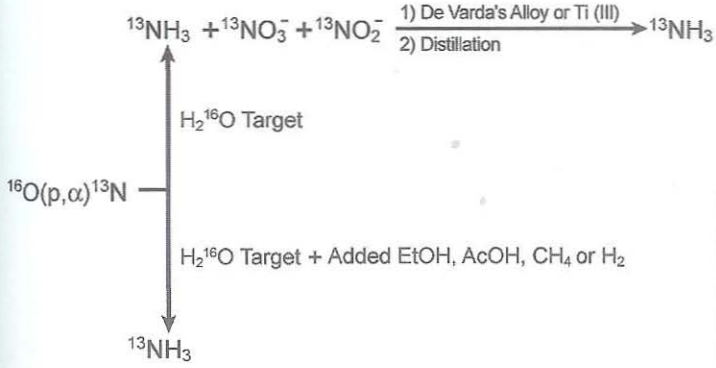

FIGURE 10-16 Radiosynthesis of ^{13}N-ammonia. Oxo anions of ^{13}N can be reduced either after irradiation or in situ during irradiation by the addition of reductants to the ^{16}O-water target.

catalyst heated to 450°C.[32,34] The reduced ^{15}O-water that results is trapped by bubbling though sterile water.

The reliable yield and short production turnaround time for preparation of ^{15}O-water make this radiopharmaceutical ideally suited for application in cerebral activation studies, in which rapidly repeated PET measurements of brain perfusion in the resting and activated state are performed.[36,37] In addition, the ease of production of this short-lived PET tracer also facilitates ancillary measurement of tissue perfusion to supplement PET imaging protocols that involve longer-lived radiopharmaceuticals.

Ammonia N 13 Injection

As shown in Table 10-11, the proton irradiation of ^{16}O-water results in ^{13}N in a variety of chemical forms.[38,39] The desired form, ^{13}N-ammonia, represents only a fraction of the total ^{13}N radioactivity that is produced. ^{13}N-ammonia ($^{13}NH_3$) is formed when ^{13}N atoms abstract hydrogen atoms from water. However, radiolytic oxidation also occurs during cyclotron irradiation of water, and ^{13}N-ammonia is converted to a large extent to oxo anions such as ^{13}N-nitrate or ^{13}N-nitrite. These radiolytically produced oxo anions can account for up to 85% of the total ^{13}N radioactivity.[40]

The oxo anions of ^{13}N can be removed from the desired ^{13}N-ammonia to yield a radiochemically pure product, but this is an inefficient use of the ^{13}N activity that is produced. Thus, most production sequences for ^{13}N-ammonia involve chemical reduction of the oxo anions to ^{13}N-ammonia (Figure 10-16). This is accomplished by using reducing agents such as DeVarda's alloy in aqueous sodium hydroxide[41] or titanium (III) salts,[42] followed by distillation of the ^{13}N-ammonia into a slightly acidic aqueous solution for product reformulation.

An alternative to chemically reducing oxidized target products from the target solution is to prevent their formation during irradiation (Figure 10-15). This is achieved by adding radical scavengers such as ethanol, acetic acid, methane, or hydrogen to the target mixture, and results in ^{13}N-ammonia only, and no oxo anions, being produced.[43–46] This slight alteration in production simplifies the overall radiopharmaceutical production process for ^{13}N-ammonia.

Sodium Acetate C 11 Injection

The preparation of sodium acetate C 11 injection for PET studies of myocardial viability involves radiosynthesis of ^{11}C-acetate from target product ^{11}C-carbon dioxide.[47] As shown in Figure 10-17, the radiosynthetic pathway is to first carbonate methylmagnesium Grignard reagent with ^{11}C-carbon dioxide, followed by acid hydrolysis to form ^{11}C-acetic acid.

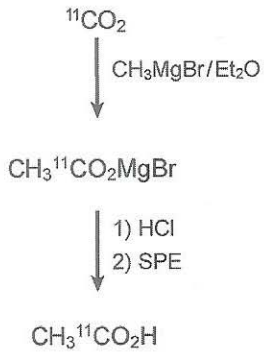

FIGURE 10-17 Radiosynthesis of ^{11}C-acetate from ^{11}C-carbon dioxide gas. This is a three-step procedure involving carbonation of a Grignard reagent, hydrolysis of the intermediate, and purification by solid phase extraction (SPE).

This two-step reaction has been adapted for several radiopharmaceutical production systems. The reaction conditions vary only slightly for these different devices; the main difference between these production systems lies in how the labeled drug is purified.

Sodium acetate C 11 injection can be purified by using solid-phase extraction,[48–51] liquid–liquid extraction,[52,53] or distillation.[54–56] Solid-phase extraction is preferred for clinical production, since it facilitates automated production of the PET radiopharmaceutical via robotics or other dedicated systems. A flexible robotic system has been described that reliably produces the labeled drug in batch yields of 220 to 300 mCi within 25 minutes.[51] Similar production results are accomplished in the clinical setting with alternative dedicated systems, and many of these production devices are available from commercial suppliers.

Fludeoxyglucose F 18 Injection

The workhorse of clinical PET imaging is ^{18}F-FDG. This radiopharmaceutical has several clinical indications and can be produced as a multidose batch suitable for use throughout the workday or for distribution to imaging sites remote from the production location. Although this radiopharmaceutical can be synthesized via electrophilic as well as nucleophilic reactions, the nucleophilic approach is preferred because of the higher production yields and the enantiomeric purity of the drug product.[57]

For clinical application, the universal method for production of this PET radiopharmaceutical is nucleophilic ^{18}F-fluoride displacement of a triflate ($-OS_2CF_3$) leaving group on a mannose precursor, followed by hydrolysis of protecting groups (Figure 10-18). Since the original description of this radiosynthetic method,[58] automation of drug production has been accomplished with only minor alteration of the original nucleophilic substitution pathway. Some of these automated systems are based on aminopolyether- or tetrabutylammonium-mediated nucleophilic fluorination,[59,60] whereas other systems utilize resin-supported ^{18}F-fluoride for the nucleophilic substitution reaction.[61] Several commercially available automated systems have been developed for routine production of the tracer and yield several curies of ^{18}F-FDG.

Recent synthetic refinements use basic rather than acidic hydrolysis to deprotect the fluorinated intermediate. The practical advantages of this change are shorter drug preparation times and avoidance of the formation of 2-chloro-2-dexoxyglucose as a chemical contaminant in the radiopharmaceutical product.[62] Studies have shown that 2-^{18}F-fluorodeoxy-D-glucose does not undergo epimerization under these alkaline conditions.[63]

^{18}F-FDG prepared in the above devices is purified via solid-phase extraction and ion exchange in a straightforward manner. The neutralized hydrolysis mixture is simply passed through cartridges bearing exchange resins that efficiently remove any traces of

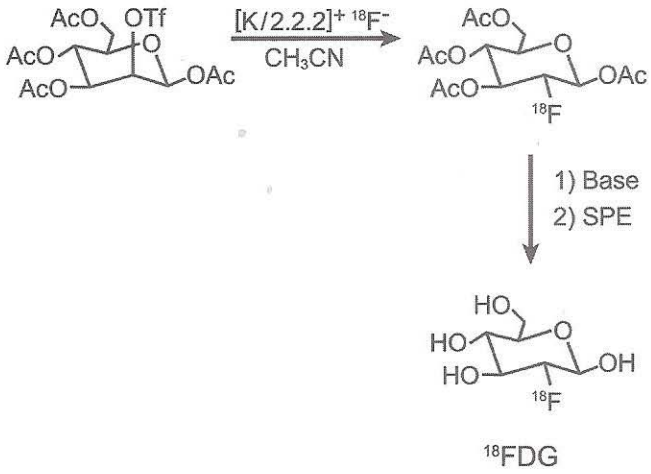

FIGURE 10-18 Radiosynthesis of 2-^{18}F-fluoro-2-deoxy-D-glucose (^{18}F-FDG) from ^{18}F-fluoride ion. This is a three-step procedure involving fluorination of a mannose triflate precursor, deprotection of the intermediate, and purification by solid phase extraction (SPE).

potential chemical and radiochemical byproducts from the final drug solution. The simplicity of these procedures enhances the reliability of automated production systems for clinical PET centers.

Fluorodopa F 18 Injection

^{18}F-fluorodopa is an example of a useful PET radiopharmaceutical that is prepared in moderate specific activity using ^{18}F-fluorine as a labeling precursor. The reaction pathway, shown in Figure 10-19, involves the region-specific electrophilic ^{18}F-fluorodemetallation of an organometallic precursor by ^{18}F-fluorine gas.[64] The fluorine displaces the metal from the aromatic site of the labeling substrate in an electrophilic substitution reaction, so only the 6-^{18}F-fluoro isomer of fluorodopa is produced. Mercuric [65,66] or stannylated [67,68] labeling precursors are used because they give high fluorodemetallation yields.

Following the fluorination step, the labeled intermediate is deprotected via acidic hydrolysis and the drug is purified using preparative reverse-phase high-performance liquid chromatography (HPLC). The purification of this radiopharmaceutical, as well as of the other tracers of neurotransmission (Table 10-4), requires HPLC, which adds an element of complexity to the overall drug production sequence that is not necessary for the other radiopharmaceuticals used in clinical PET. In the case of ^{18}F-FD, dilute acetic acid is used as the HPLC mobile phase for the purification, which simplifies product reformulation. The isolated HPLC product peak is collected and sterilized by terminal filtration into the final product container, since the HPLC solvent and its pH range are already physiologically compatible.

Flumazenil C 11 Injection and Raclopride C 11 Injection

^{11}C-FMZ and ^{11}C-RAC receptor-binding radiopharmaceuticals are examples of high specific activity tracers synthesized using ^{11}C-methyl iodide as a labeling precursor. ^{11}C-FMZ is synthesized via N-^{11}C-methylation,[69–72] whereas ^{11}C-RAC is prepared via O-^{11}C-methylation.[73–75]

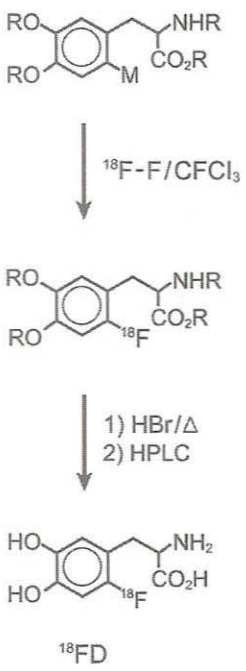

FIGURE 10-19 Radiosynthesis of 6-^{18}F-fluoro-L-dopa (^{18}F-FD) from ^{18}F-fluorine gas. This is a three-step procedure involving fluorodemetallation of an organotin- or mercury-leaving group (M), deprotection of the intermediate, and purification by HPLC.

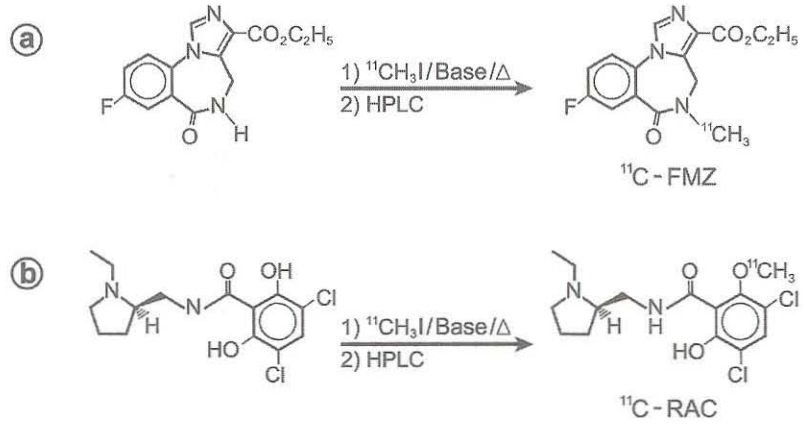

FIGURE 10-20 Radiosynthesis of ^{11}C-flumazenil (^{11}C-FMZ) and ^{11}C-raclopride (^{11}C-RAC) from ^{11}C-methyl iodide. These are two-step procedures involving N- or O-methylation, followed by purification using HPLC.

The basic procedure used for the preparation of both of these receptor ligands is the same (Figure 10-20). ^{11}C-methyl iodide is bubbled through a solution of the respective normethyl substrate and the ^{11}C-methylation reaction is promoted by heating the reaction mixture for 1 to 3 minutes. The product is then purified by HPLC, which separates the ^{11}C-labeled ligand from the unlabeled substrate and other contaminants. The typical preparation time (including HPLC purification) is 30 to 40 minutes from delivery of ^{11}C-methyl iodide to the reaction solution. This time frame is practical for use with ^{11}C, which has a 20 minute half-life.

RADIOPHARMACEUTICAL PRODUCTION SYSTEMS

Preparation of radiopharmaceuticals in multimillicurie quantities in a routine manner requires special production systems to avoid unduly hazardous conditions for production personnel. Special demands associated with the preparation of PET radiopharmaceuticals include a high radiation environment, bulky lead shielding, short production intervals due to radionuclidic half-lives, and a production capability that supplies the needs of the clinical imaging schedule. In addition to these requirements, the radiosynthesis must yield the labeled drug in a pure state on a reliable, efficient basis. Frequently, tracer radiosyntheses must be repeated multiple times within a single workday. Finally, the production system must facilitate in-process documentation of the major steps of the compounding procedure so that labeled drug production is in compliance with federal and state regulations.

To address these challenges, several PET radiopharmaceutical production systems have been developed over the years.[76,77] Although these systems have differences, they all share certain characteristics. They all use the procedural steps of fluid flow, radioactivity measurement, temperature control, solvent dispensing, and product purification, within a shielded hot cell. The systems uniformly emphasize proper selection of equipment, materials, controllers, dispensing devices, extraction hardware, and radioactivity detectors so that each of the synthetic steps is accomplished in a predictable fashion, consistently yielding a high-purity drug product in an efficient manner. Disposable equipment is used wherever possible to minimize the potential introduction of contaminants during radiopharmaceutical compounding procedures.

The various designs of PET radiopharmaceutical production systems can be broadly categorized as remotely operated systems, automated modular systems, and robotic systems. These three categories are discussed below.

Remotely Operated Systems

Remotely operated systems are the most flexible and least expensive means of high-radioactivity radiopharmaceutical syntheses, since there is no computer or microprocessor used for radiopharmaceutical compounding. These systems can thus be considered an intermediate step in the evolution of methods from low-level preclinical synthesis of tracers to optimized high-level production procedures using robotics or automated modular designs.

Remotely operated systems are collections of devices that facilitate real-time operator control over the various steps of radiopharmaceutical production. This control takes place from behind lead shielding so that radiosyntheses are carried out in a safe manner. Components such as motor-driven needles, screw-driven capping devices, and remotely pressurized fluid lines are custom designed to accomplish tasks such as fluid delivery to reaction vessels, sealing of reaction vessels, and transfer of reaction mixtures to HPLC injectors for product purification. Use of long-handled tongs for radioactivity manipulation is also common with this approach.

These systems are easy to implement for radiopharmaceutical production and require a minimum number of optimization studies prior to their application. Remotely operated systems are especially valuable for the initial high radioactivity syntheses of PET radiopharmaceuticals because of their ease of installation. The flexibility of the system design facilitates rapid configuration of the appropriate devices and components for a given radiopharmaceutical within a shielded hot cell. Also, the same hot cell can accommodate

the various components needed for preparation of several different radiopharmaceuticals. After production conditions are optimized for routine production of a given PET tracer, the decision can be made whether to continue with remotely operated production or to make a capital investment in more expensive automated modular or robotic systems.

A major disadvantage of remotely operated systems is that the drug preparation sequence relies totally on operator intervention. During routine application there is potential for great variation in production conditions, with possible variance in radiopharmaceutical product quality.

With appropriate adherence to process guidelines, however, remotely operated systems offer an adequate and inexpensive means for compounding PET tracers, and several systems have been developed for the routine production of clinically used PET radiopharmaceuticals. Systems have been described for the ^{18}F-labeled tracers ^{18}F-FDG[78,79] and ^{18}F-FD.[80,81] Remotely operated systems are also available for preparing ^{11}C-sodium acetate[54–56,82,83] and ^{13}N-ammonia.[40,41]

Automated Modular Systems

Once all of the production parameters have been optimized for preparation of a PET radiopharmaceutical, it is possible to automate the entire drug production process. This is accomplished using modular systems in which the movement of synthetic intermediates through fixed-plumbed devices and equipment is completely controlled by computer software or timing circuits. In the modular approach, all the equipment necessary for the production of a given radiopharmaceutical is mounted together, and the operation from start to finish is preprogrammed according to optimized reaction conditions. Because all of the compounding steps are programmed, deviations in the preparation conditions are minimal and the quality of the final product is thus standardized.

A major advantage of automated modular systems for the routine production of PET radiopharmaceuticals is that product consistency is enhanced. Also, the fact that the system is dedicated to the production of a single tracer simplifies maintenance and troubleshooting. For these reasons, most commercially supplied PET radiopharmaceutical production systems are of the automated modular type. In some cases, commercial systems are marketed in which all reagents are mounted on a single disposable cartridge for each production batch. Use of such disposables tends to minimize the potential for contamination of the final drug product.

A disadvantage of this drug production approach is that it is difficult to do repetitive batch production on the same workday using the same module because of the radioactivity remaining in the system after the initial synthesis. Also, hot-cell space must be allocated for the production of each tracer, since separate modular systems are used for the preparation of the individual radiopharmaceuticals. This limitation has been recognized by some research groups, which have proposed application of modular systems for the production of more than one tracer when radiosynthetic steps are similar. However, this expanded application of automated modules is possible only with research tracers. Each of the clinically applied radiopharmaceuticals listed in Table 10-4 requires a separate automated module for preparation, since the radiosynthetic steps used to prepare the different tracers do not overlap.

Several automated modular systems have been described for the production of clinical PET radiopharmaceuticals. Various modular systems are available for producing ^{18}F-FDG.[84–87] Automated production modules have also been described for ^{11}C-sodium acetate,[52,53] ^{13}N-ammonia,[42,88] ^{18}F-FD,[89] and ^{11}C-FMZ.[72]

Robotic Systems

Robotic production systems use commercially available robots to move radioactive intermediates between fixed workstations to accomplish radiopharmaceutical synthesis, purification, and reformulation. Because the robot arm and gripping device are flexible, they have capabilities similar to a human arm and hand. Because the action of the robot arm is microprocessor controlled, optimized radiopharmaceutical production sequences can be programmed into the control software. Robotic production systems thus combine the flexibility of remotely controlled systems with the standardized production parameters of automated modular production systems.

The flexibility of robotics allows synthesis of a variety of tracers with the same device. This is especially useful in research endeavors, in which the radiosynthesis of novel PET tracers must be scaled up to the radioactivity levels necessary for performance of PET studies. For this reason, the primary promoters of robotic production systems have been PET centers that emphasize clinical and preclinical imaging research.[90–94]

Robotics also has special advantages when applied in the routine production of radiopharmaceuticals for clinical PET. The flexibility of robotic systems facilitates the production of multiple PET tracers within the same shielded hot cell, which is valuable to sites with limited space for radiopharmaceutical production. The microprocessor control over production steps increases the batch-to-batch consistency of radiopharmaceutical quality and aids in the documentation of production procedures. Moreover, robotic systems can be programmed to move radioactive waste remaining from a production session to a shielded area within a hot cell, so setup for subsequent radiopharmaceutical syntheses is less problematic in terms of the radiation dose to personnel.

Robotics has the unique potential for simultaneous synthesis of two or more tracers within a single hot cell. If this potential were realized through creative software, it would be especially valuable for busy PET clinics. With this capability, the PET radiopharmaceutical production schedule would be limited only by the capability of the cyclotron to produce the starting radionuclides.

Robotic synthesis of several radiopharmaceuticals for clinical PET has been achieved. Labeled drugs prepared via robotics include ^{18}F-FDG,[60,94] ^{11}C-sodium acetate,[51] ^{11}C-FMZ,[94] and ^{18}F-FD.[93]

RADIOPHARMACEUTICAL FORMULATION

A major concern for nuclear pharmacists is the reformulation of PET radiopharmaceuticals. A PET tracer may be radiochemically pure, but the isolation process may yield the tracer dissolved in a solvent inappropriate for human administration. The solvent used for purification must then be removed and the tracer reconstituted into a physiologically compatible solution.

Liquid chromatography is generally used for purification of radiopharmaceuticals. It typically involves simple solid-phase extraction cartridges or HPLC. In either case, the basic components are the same: the impure reaction solution traverses over a stationary phase through which flows the mobile phase. The eluant solution bears the purified radiopharmaceutical dissolved in the mobile phase. These chromatographic systems are optimized so that retention times are as low as feasible without compromising product purity. This facilitates purification of the radiopharmaceutical within the temporal constraints of the short half-life of the positron-emitting label. In addition, the tracer is isolated in a minimum volume of mobile phase, which makes radiopharmaceutical reformulation less problematic.

In ideal situations, radiopharmaceutical purification involves chromatographic systems in which the mobile phase is a physiologically compatible liquid. Examples are the solid-phase extraction purification of ^{18}F-FDG, which uses sterile water for injection as the mobile phase, and the HPLC purification of ^{18}F-FD, which uses a weakly acidic (acetic acid, pH 5) aqueous solution. These purification systems are possible because the final reaction mixture contains chemical contaminants that are easily resolved from the radiopharmaceutical product.

The production of some PET radiopharmaceuticals generates byproducts that cannot be removed from the product by chromatographic systems with aqueous mobile phases. Notable examples are receptor-binding radioligands such as ^{11}C-FMZ and ^{11}C-RAC. The reaction mixture for these tracers includes the nonreacted, nor-methyl labeling substrate as well as the ^{11}C-labeled tracer. Since these tracers differ from the labeling substrate by only a single methyl substituent, the chromatographic characteristics of these two chemicals are very similar. Typically, reverse- or normal-phase HPLC is required to resolve the radioligand from the labeling substrate. In either case, toxic organic compounds are used in the HPLC mobile phase, so the radiochemically pure radioligand isolated in the product fraction of the HPLC eluant is unsuitable for human administration.

Reformulation of the radiopharmaceutical thus involves removal of the HPLC mobile phase from the purified radioligand. This can be accomplished by one of two means. The first is to remove the solvent using a rotary evaporator. The HPLC solvent is evaporated by gentle heating under reduced pressure. The radiopharmaceutical, which remains on the wall of the glass vessel after evaporation of volatiles, is then dissolved in a physiologically compatible solvent for further work-up. This approach is cumbersome, subjects the product to heat- or vacuum-related losses, and is limited to HPLC solvents that have relatively low boiling points.

The second reformulation method is more amenable to remote operation and involves solid-phase extraction. In this approach, the product fraction from the HPLC is diluted in a 25 to 250 mL volume of aqueous buffer and passed across a reverse-phase Sep-Pak (Waters) cartridge. The lipophilic radiopharmaceutical is retained on the cartridge, while the diluted organic solvents are eluted to waste. The shielded cartridge is then rinsed with additional sterile water for injection to remove residual contaminants, and the radiopharmaceutical product is subsequently eluted off the cartridge with a small volume of ethanol. The ethanol can be diluted with sterile water for injection or 0.9% sodium chloride injection to complete the reformulation procedure.

Once the radiopharmaceutical is reformulated into an appropriate injectate, it must meet further requirements for suitability for human administration. In addition to radiochemical and chemical purity, sterility is key. Because heat sterilization is impractical for these tracers, terminal sterilization via membrane filtration is the method most commonly used. Passage of the reformulated radiopharmaceutical through a 0.2 μm filter into a final product container effectively removes bacterial contamination from the reformulated tracer solution. There are important caveats with this method of compounding PET tracers, however.

First, terminal sterilization removes bacterial contamination but not pyrogenic compounds, which are capable of passing through the 0.2 μm pores of the filter. Thus, this method ensures against bacterial contamination but does not guarantee a pyrogen-free product. Absence of pyrogens in the radiopharmaceutical is best ensured by eliminating pyrogens in the production procedure. If a radiopharmaceutical product is found to be pyrogenic, it is necessary to replace any component or reagent in the production process that may act as a source of pyrogens, since there is no filter to eliminate these fever-inducing compounds from the drug solution.

Second, it is important to use membrane filters that have compatibility specifications appropriate for the solution being sterilized. Many radiopharmaceuticals require solvents

that have pH adjustments or solubilizing agents (such as ethanol) to facilitate the dissolution of otherwise poorly soluble substances. Although the filter membrane itself may be resistant to degradation by these solvents, the plastic housing or the adhesive used to hold the filter assembly together may not withstand the solvent. Commercial suppliers of filter assemblies can often recommend specific filter types for given applications.

Finally, it is essential after each terminal filtration to test for membrane integrity. If a filter has ruptured during the compounding procedure because of overpressurization, there is no guaranteed that the radiopharmaceutical product is sterile. The only way to confirm that the filter is still intact after filtration is to perform a bubble test, in which the intact, wet membrane will create resistance to a pressurized syringe. This bubble test can be performed manually immediately after filtration of the radiopharmaceutical into the final product container. Alternatively, some production systems have the membrane integrity test automated as a part of the radiolabeled drug compounding procedure.[51]

QUALITY ASSURANCE

Quality assurance of the final drug product is an important aspect of PET, just as it is in conventional nuclear medicine practice. The quality of the radiopharmaceutical must meet high standards to ensure safety of the patient and to be an effective imaging agent that results in useful diagnostic information.

Because of the greater level of sophistication of PET radiopharmaceutical compounding, however, the instrumentation used in quality control testing is more complicated than that used in conventional nuclear medicine. For example, radiochemical purity testing, which is usually performed on a prerelease basis, can involve gas chromatography (^{15}O tracers) or HPLC (^{11}C or ^{18}F tracers). In some cases (^{18}F-FDG), thin-layer radiochromatographic methods have been developed to simplify radiochemical purity testing.

Because of the synthetic methods used, testing for chemical purity is also a requirement for PET radiopharmaceuticals. This is usually accomplished using gas chromatography or HPLC techniques to quantify the amount of contaminant chemicals in the final drug product. To streamline the clinical production of PET tracers, it is sometimes possible to develop simple colorimetric tests to confirm that contaminant levels fall below official limits. An example of this is the color spot test method that was developed for the detection of Kryptofix 2.2.2 in preparations of ^{18}F-FDG.[95]

Product quality is defined in *USP 26/NF 21*, which is an official compendium of drug standards.[6] The United States Pharmacopeia (USP) publishes monographs for the major PET radiopharmaceuticals used in clinical practice. These monographs define standards of purity with regard to sterility, apyrogenicity, pH, radiochemical purity, radionuclidic purity, chemical purity, and labeling requirements. USP also sets standards for methods of assessing these aspects of purity, such as for sterility testing and for pyrogen testing with bacterial endotoxin techniques.

USP establishes detailed guidelines for the compounding of PET tracers. These guidelines define the control of components, materials, and supplies; verification of compounding procedures; stability testing and expiration dating; and steps to be taken during the compounding of PET radiopharmaceuticals for human use. Standards for quality control, sterilization, and sterility assurance are also given in these guidelines.

USP also publishes guidelines for the use of automated radiochemical synthesis apparatus for PET radiopharmaceuticals. These guidelines address such important issues as equipment quality assurance, routine quality control testing, reagent audit trail, and documentation of apparatus parameters. The guidelines also point out that any changes made in the synthesis method should be validated to confirm that there is no effect on final drug quality.

It is important to be aware that similar quality assurance guidelines exist outside the United States.[96] Many innovative PET studies are performed in foreign PET centers, and it is reassuring to know, when interpreting image results, that the PET tracer being imaged is of high quality.

REGULATORY ISSUES

As with radiopharmaceuticals in general, the oversight of PET radiopharmaceutical production, application, and disposal involves several different regulatory bodies. These include the Food and Drug Administration (FDA), Environmental Protection Agency, and Occupational Safety and Health Administration; organizations responsible for the radiation safety of the public; and organizations and agencies that promulgate the safe and effective use of drugs. Examples are the Joint Commission on Accreditation of Healthcare Organizations and federal agencies that implement laws such as the Health Insurance Portability and Accountability Act of 1996, which mandates control of protected health information. For PET radiopharmaceuticals that are transported off site, regulations of the Department of Transportation must also be adhered to. Product quality is regulated by USP, which establishes purity standards for PET radiopharmaceuticals. Finally, professional licensing bodies, such as state boards of pharmacy, play key roles in regulating activities related to PET and PET radiopharmaceuticals.

Compliance with all of these regulatory demands is important, not only because it is ethical and beneficial for the public at large but because failure to comply can have unwanted legal consequences. Furthermore, adherence to the pertinent regulations is key to financial reimbursement for PET procedures.

A major hurdle to reimbursement for PET imaging procedures has been FDA approval of the relevant radiopharmaceuticals. CMS and third-party payers are reluctant to reimburse for PET procedures that involve "experimental" imaging of radiochemicals in human subjects. However, as described above, reimbursement will be made for PET imaging procedures that involve drugs with FDA-approved indications for imaging (Tables 10-6 through 10-8). Thus, from a financial perspective, drawing a distinction between a labeled tracer and an FDA-approved radiopharmaceutical is essential.

Selecting PET radiopharmaceuticals for approval from the many existing PET tracers was an arduous task for FDA, given that the agency had no history of regulating this category of drug. Unlike conventional FDA-approved drugs, the drugs used for PET have no pharmacologic effect, disappear rapidly, and have personnel radiation safety issues associated with their manufacture. The evolution of the current FDA involvement with PET and its relationship to reimbursement have been reviewed elsewhere.[97]

The traditional route of drug approval is not applicable to PET radiopharmaceuticals, but the FDA Modernization Act of 1997 (FDAMA) allows modifications of new drug applications (NDAs) and current good manufacturing practices (CGMPs) that are relevant and enforceable for the PET community. The safety and efficacy of clinically used PET radiopharmaceuticals were evaluated by FDA with the assistance of the PET community in reviewing the literature. Although the process of evaluating PET radiopharmaceuticals and their indications is ongoing, precedent has been established for involving the PET community at large rather than requiring individual PET sites to prove the safety and efficacy of tracers.

FDA ensures compliance with manufacturing standards by requiring the filing of NDAs, adherence to CGMPs, and inspection by FDA staff. FDAMA has streamlined these requirements for PET, and FDA will adopt templates that can be used by various PET production sites in a manner that greatly simplifies regulatory compliance and standardizes the manufacture of PET radiopharmaceuticals. FDA has enlisted the assistance of the

PET community in developing templates for NDAs and CGMPs for clinically used PET radiopharmaceuticals. Under this regulatory model, PET sites will register as drug manufacturers, submit NDAs based on available templates, follow standardized CGMPs, and be inspected for compliance by FDA.

An alternative model for the production of PET radiopharmaceuticals is based on the traditional right of professional pharmacists to compound drugs upon receipt of a prescription written by a physician in the course of caring for a given patient. This model requires the PET radiopharmaceutical dispensed for the patient to meet all official standards of purity, but it differs in that the site is not registered as a drug manufacturer and an NDA has not been filed for the PET radiopharmaceutical. In this alternative model, the professional activities of the compounding pharmacist are regulated by the state board of pharmacy, and the nuclear pharmacy performing PET radiopharmaceutical compounding is licensed and inspected by the state board of pharmacy.

FUTURE OUTLOOK

Further research into the development, validation, and implementation of new radiopharmaceuticals for PET imaging is integral to the continued growth of this area of nuclear medicine practice. Efforts to discover and evaluate new radiolabeled compounds for clinical use in PET protocols are increasing our understanding of human physiology and pathophysiology. New PET imaging techniques will undoubtedly be added to the list of PET procedures used in health care. New PET radiopharmaceuticals and methods may advance medical practice by promoting the longitudinal assessment of therapy for various disorders. Future PET techniques may also have a role in the development of new therapeutic agents, since PET imaging efficiently evaluates important parameters such as dose–occupancy relationships and could help streamline clinical trials of new drugs.

PET imaging is especially well positioned for future growth because of its versatility in quantifying physiologic parameters. Substantial progress has been made in meeting the challenges associated with the radiochemical synthesis of radiopharmaceutical structures for PET.[98] Moreover, recent advances in the instrumentation of small-animal scanners now permit PET imaging of improved animal models of human disease. The capability to noninvasively validate novel radiotracers in animals yields valuable insight into new imaging techniques for drug development and for clinical diagnostic applications in humans.

Examples of these exciting new developments in PET research have been presented at meetings of the International Isotope Society and the Academy of Molecular Imaging. Abstracts from the International Isotope Society demonstrate the large pipeline of novel PET tracers that have been synthesized for preclinical evaluation.[99] Abstracts from the Academy of Molecular Imaging reveal important advances in instrumentation (Institute for Molecular Imaging), preclinical imaging in drug discovery (Society of Non-Invasive Imaging in Drug Development), and state-of-the-art diagnostic PET applications (Institute of Clinical PET).[100] This research suggests that clinical PET applications will continue to grow.

REFERENCES

1. Friedlander G, Kennedy JW, Macias ES, et al. *Nuclear and Radiochemistry.* 3rd ed. New York: Wiley-Interscience; 1981.
2. Sorenson JA, Phelps ME. *Physics in Nuclear Medicine.* 2nd ed. Philadelphia: WB Saunders; 1987.
3. Turkington TG. Introduction to PET instrumentation. *J Nucl Med Technol.* 2001;29:1-8.

4. Townsend DW, Beyer T. A combined PET/CT scanner: the path to true image fusion. *Br J Radiol.* 2002;75:S24-30.
5. Townsend DW. A combined PET/CT scanner: the choices. *J Nucl Med.* 2001;42:533-4.
6. *United States Pharmacopeia 26/National Formulary 21.* Rockville, MD: United States Pharmacopeial Convention; 2003.
7. Sciacca RR, Akinboboye O, Chou RL, et al. Measurement of myocardial blood flow with PET using 1-^{11}C-acetate. *J Nucl Med.* 2001;42:63-70.
8. Van den Hoff J, Burchert W, Berner A-R, et al. [1-^{11}C] Acetate as a quantitative perfusion tracer in myocardial PET. *J Nucl Med.* 2001;42:1174-82.
9. Oyama N, Akino H, Kanamaru H, et al. ^{11}C-Acetate PET imaging of prostate cancer. *J Nucl Med.* 2002;43:181-6.
10. Ho C-L, Yu SCH, Yeung DWC. ^{11}C-Acetate PET imaging in hepatocellular carcinoma and other liver masses. *J Nucl Med.* 2003;44:213-21.
11. Dimitriakopoulou-Strauss A, Strauss LG, Burger C. Quantitative PET studies in pretreated melanoma patients: a comparison of 6-[^{18}F] fluoro-L-dopa with ^{18}F-FDG and ^{15}O-water using compartment and noncompartment analysis. *J Nucl Med.* 2001;42:248-56.
12. Hoegerle S, Altehoefer C, Ghanem N, et al. ^{18}F-DOPA positron emission tomography for tumour detection in patients with medullary thyroid carcinoma and elevated calcitonin levels. *Eur J Nucl Med.* 2001;28:64-71.
13. Gennaro GP, Neirinckx RD, Bergner B, et al. A radionuclide generator and infusion system for pharmaceutical quality Rb-82. In: Knapp FF, Butler TA, eds. *Radionuclide Generators: New Systems for Nuclear Medicine Applications.* Washington, DC: American Chemical Society; 1984:135-50.
14. Loc'h C, Maziere B, Comar D. A new generator for ionic gallium-68. *J Nucl Med.* 1980;21:171-3.
15. Ruth TJ. Accelerators available for isotope production. In: Welch MJ, Redvanly CS, eds. *Handbook of Radiopharmaceuticals: Radiochemistry and Applications.* Hoboken, NJ: Wiley; 2003:71-85.
16. Schlyer DJ. Production of radionuclides in accelerators. In: Welch MJ, Redvanly CS, eds. *Handbook of Radiopharmaceuticals: Radiochemistry and Applications.* Hoboken, NJ: Wiley; 2003:1-70.
17. Wolf AP, Jones WB. Cyclotrons for biomedical isotope production. *Radiochim Acta.* 1983;34:1-7.
18. Qaim SM, Clark JC, Crouzel C, et al. PET radionuclide production. In: Stöcklin G, Pike VW, eds. *Radiopharmaceuticals for Positron Emission Tomography: Methodological Aspects.* Boston: Kluwer Academic Publishers; 1993:1-43.
19. Antoni G, Kihlberg T, Långström B. Aspects on the synthesis of ^{11}C-labelled compounds. In: Welch MJ, Redvanly CS, eds. *Handbook of Radiopharmaceuticals: Radiochemistry and Applications.* Hoboken. NJ: Wiley; 2003:141-94.
20. Ferrieri RA. Production and application of synthetic precursors labeled with carbon-11 and fluorine-18. In: Welch MJ, Redvanly CS, eds. *Handbook of Radiopharmaceuticals: Radiochemistry and Applications.* Hoboken, NJ: Wiley; 2003:229-82.
21. Crouzel C, Långström B, Pike VW, et al. Recommendations for a practical production of ^{11}C-methyl iodide. *Appl Radiat Isot.* 1987;38:601-4.
22. Långström B, Lundqvist H. The preparation of ^{11}C-methyl iodide and its use in the synthesis of ^{11}C-methyl-L-methionine. *Int J Appl Radiat Isot.* 1976;27:357-63.
23. Marazano C, Maziere M, Berger G, et al. Synthesis of methyl iodide-^{11}C and formaldehyde-^{11}C. *Int J Appl Radiat Isot.* 1977;28:49-54.
24. Iwata R, Ido T, Saji H, et al. A remote-controlled synthesis of ^{11}C-iodomethane for the practical preparation of ^{11}C-labeled radiopharmaceuticals. *Int J Appl Radiat Isot.* 1979;30:194-6.
25. Larsen P, Ulin J, Dahlstrom K, et al. Synthesis of [^{11}C] iodomethane by iodination of [^{11}C] methane. *Appl Radiat Isot.* 1997;48:153-7.
26. Link JM, Krohn KA, Clark JC. Production of [^{11}C] CH_3I by single-pass reaction of [^{11}C] CH_4 with I_2. *Nucl Med Biol.* 1997;24:93-7.
27. Schlyer DJ, Bastos MAV, Alexoff D, et al. Separation of [^{18}F] fluoride from [^{18}O] water using anion exchange resin. *Appl Radiat Isot.* 1990;41:531-3.
28. Snyder SE, Kilbourn MR. Chemistry of fluorine-18 radiopharmaceuticals. In: Welch MJ, Redvanly CS, eds. *Handbook of Radiopharmaceuticals: Radiochemistry and Applications.* Hoboken, NJ: Wiley; 2003:195-227.
29. Casella V, Ido T, Wolf AP, et al. Anhydrous ^{18}F labeled elemental fluorine for radiopharmaceutical production. *J Nucl Med.* 1980;21:750-7.
30. Blessing G, Coenen HH, Franken K, et al. Production of [^{18}F] F_2, H^{18}F and $^{18}F_{aq}$ using the ^{20}Ne(d,α)^{18}F process. *Appl Radiat Isot.* 1986;37:1135-40.
31. Strijckmans K, Vandecasteele C, Sambre J. Production and quality control of $^{15}O_2$ and C$^{15}O_2$ for medical use. *Int J Appl Radiat Isot.* 1985;36:279-83.
32. Clark JC, Buckingham PD. *Short-lived Radioactive Gases for Clinical Use.* London: Butterworths; 1975.

33. Welch MJ, Kilbourn MR. A remote system for the routine production of oxygen-15 radiopharmaceuticals. *J Labeled Compounds Radiopharm.* 1986;22:1193-1200.
34. Berridge MS, Terris AH, Cassidy EH. Low-carrier production of [^{15}O] oxygen, water and carbon monoxide. *Appl Radiat Isot.* 1990;41:1173-5.
35. Clark JC, Crouzel C, Meyer GJ, et al. Current methodology for oxygen-15 production and clinical use. *Appl Radiat Isot.* 1987;38:597-600.
36. Sergent T. Brain-imaging studies of cognitive functions. *Trends Neurosci.* 1994;17:221-7.
37. Cowell SF, Code C. Thinking nuclear medicine—PET activation. *J Nucl Med Technol.* 1998;26:17-22.
38. Krizek H, Lembares N, Dinwoodie R, et al. Production of radiochemically pure $^{13}NH_3$ for biomedical studies using the $^{16}O(p,\alpha)^{13}N$ reaction. *J Nucl Med.* 1973;14:629-30.
39. Tilbury RS, Dahl JR. ^{13}N species formed by proton irradiation of water. *Radiation Res.* 1979;79:22-3.
40. Parks NJ, Krohn KA. The synthesis of ^{13}N labelled ammonia, dinitrogen, nitrite and nitrate using a single cyclotron target system. *Int J Appl Radiat Isot.* 1978;29:754-6.
41. Vaalburg W, Kamphusi JAA, Beerling-van der Moles HD, et al. An improved method for the production of ^{13}N-labelled ammonia. *Int J Appl Radiat Isot.* 1975;26:316-8.
42. Ido T, Iwata R. Fully automated synthesis of $^{13}NH_3$. *J Labeled Compounds Radiopharm.* 1981;18:244-6.
43. Wieland BW, Bida G, Padgett H, et al. In-target production of ^{13}N-ammonia via proton irradiation of dilute aqueous ethanol and acetic acid mixtures. *Appl Radiat Isot.* 1991;42:1095-8.
44. Berridge MS, Landmeier BJ. In-target production of [N-13] ammonia—target design, products, and operating parameters. *Appl Radiat Isot.* 1993;44:1433-41.
45. Krasikova RN, Fedorova OS, Korsakov MV, et al. Improved [N-13] ammonia yield from the proton irradiation of water using methane gas. *Appl Radiat Isot.* 1999;51:395-401.
46. Mullholland GK, Sutorik A, Jewett DM, et al. Direct in-target synthesis of [^{13}N] NH_3 by irradiation of water under hydrogen pressure. *J Nucl Med.* 1989;30:926.
47. Moerlein SM, Gropler RJ, Welch MJ, et al. USP standards for sodium acetate C-11 injection. *Pharm Forum.* 1994;20:7523-5.
48. Meyer G-J, Günther K, Matzke K-H, et al. A modified method for ^{11}C acetate, preventing liquid phase extraction steps. *J Labeled Compounds Radiopharm.* 1993;32:182-3.
49. Kruijer PS, Ter Lindin T, Mooij R, et al. A practical method for the preparation of [^{11}C] acetate. *Appl Radiat Isot.* 1995;46:317-21.
50. Iwata R, Ido T, Tada M. Column extraction method for rapid preparation of [^{11}C] acetic and [^{11}C] palmitic acids. *Appl Radiat Isot.* 1995;46:117-21.
51. Moerlein SM, Gaehle GG, Welch MJ. Robotic preparation of sodium acetate C-11 injection for use in clinical PET. *Nucl Med Biol.* 2002;29:613-21.
52. Pike VW, Horlock PL, Brown C, et al. The remotely-controlled preparation of a ^{11}C-labeled radiopharmaceutical—[1-^{11}C] acetate. *Int J Appl Radiat Isot.* 1984;35:623-7.
53. Del Fiore G, Peters JM, Quaglia L, et al. Automated production of carbon-11 labeled acetate to allow detection of transient myocardial ischemia in man, using positron emission tomography. *J Radioanal Nucl Chem Lett.* 1984;87:1-14.
54. Norenberg JP, Simpson NR, Dunn BB, et al. Remote synthesis of [^{11}C] acetate. *Appl Radiat Isot.* 1992;43:943-5.
55. Ishiwata K, Ishii S-I, Sasaki T, et al. A distillation method of preparing C-11 labeled acetate for routine clinical use. *Appl Radiat Isot.* 1993;44:761-3.
56. Berridge MS, Cassidy EH, Miraldi F. [^{11}C] Acetate and [^{11}C] methionine: improved syntheses and quality control. *Appl Radiat Isot.* 1994;46:173-5.
57. Coenen HH, Pike VW, Stöcklin G, et al. Recommendation for a practical production of [2-^{18}F] fluoro-2-deoxy-D-glucose. *Appl Radiat Isot.* 1987;38:605-10.
58. Hamacher K, Coenen HH, Stöcklin G. Efficient stereospecific synthesis of no-carrier-added 2-[^{18}F]-fluoro-2-deoxy-D-glucose using aminopolyether supported nucleophilic substitution. *J Nucl Med.* 1986;27:235-8.
59. Hamacher K, Blessing G, Nebeling B. Computer-aided synthesis (CAS) of no-carrier-added 2-[^{18}F] fluoro-2-deoxy-D-glucose: an efficient automated system for the aminopolyether-supported nucleophilic fluorination. *Appl Radiat Isot.* 1990;41:49-55.
60. Brodack JW, Dence CS, Kilbourn MR, et al. Robotic production of 2-deoxy-2-[^{18}F] fluoro-D-glucose: a routine method of synthesis using tetrabutylammonium [^{18}F]fluoride. *Appl Radiat Isot.* 1988;39:699-703.
61. Toorongian SA, Mulholland GK, Jewett DM, et al. Routine production of 2-deoxy-2-[^{18}F] fluoro-D-glucose by direct nucleophilic exchange on a quaternary 4-aminopyridium resin. *Nucl Med Biol.* 1990;17:273-9.
62. Füchtner F, Steinbach J, Mäding P, et al. Basic hydrolysis of 2-[^{18}F] fluoro-1,3,4,6-tetra-*O*-acetyl-D-glucose in the preparation of 2-[^{18}F]fluoro-2-deoxy-D-glucose. *Appl Radiat Isot.* 1996;47:61-6.
63. Meyer G-J, Matzke KH, Hamacher K, et al. The stability of 2-[^{18}F] fluoro-deoxy-D-glucose towards epimerisation under alkaline conditions. *Appl Radiat Isot.* 1999;51:37-41.

64. Luxen A, Guillaume M, Melega WP, et al. Production of 6-[^{18}F] fluoro-L-DOPA and its metabolism in vivo: a critical review. *Nucl Med Biol.* 1992;19:149-58.
65. Luxen A, Perlmutter M, Bida GT, et al. Remote, semiautomated production of 6-[^{18}F] fluoro-L-dopa for human studies with PET. *Appl Radiat Isot.* 1990;41:275-81.
66. Adam MJ, Jivan S. Synthesis and purification of L-6-[^{18}F] fluorodopa. *Appl Radiat Isot.* 1988;39:1203-06.
67. Namavari M, Bishop A, Satyamurthy N, et al. Regioselective radiofluorodestannylation with [^{18}F] F_2 and [^{18}F] CH_3COOF: a high yield synthesis of 6-[^{18}F] fluoro-L-dopa. *Appl Radiat Isot.* 1992;43:989-96.
68. de Vries EFJ, Luurtsema G, Brüssermann M, et al. Fully automated synthesis module for the high yield one-pot preparation of 6-[^{18}F] fluoro-L-DOPA. *Appl Radiat Isot.* 1999;51:389-94.
69. Moerlein SM, Mintun MA, Perlmutter JS, et al. USP standards for flumazenil C 11 injection. *Pharm Forum.* 1998;24:6360-5.
70. Maziere M, Hantraye P, Prenant C, et al. Synthesis of ethyl 8-fluoro-5,6-dihydro-5-[^{11}C]methyl-6-oxo-4H-imidazo[1,5-a][1,4]benzodiazepine-3-carboxylate (RO 15.1788-^{11}C): a specific radioligand for the in vivo study of central benzodiazepine receptors by positron emission tomography. *Int J Appl Radiat Isot.* 1984;35:973-6.
71. Halldin C, Stone-Elander S, Thorell J-O, et al. ^{11}C-Labelling of Ro-15-1788 in two different positions, and also ^{11}C-labelling of its main metabolite Ro 15-3890, for PET studies of the benzodiazepine receptors. *Appl Radiat Isot.* 1988;39:993-7.
72. Suzuki K, Inoue O, Hashimoto K, et al. Computer-controlled large scale production of high specific activity [^{11}C] Ro 15-1788 for PET studies of benzodiazepine receptors. *Int J Appl Radiat Isot.* 1985;36:971-6.
73. Moerlein SM, Perlmutter JS, Welch MJ. USP Standards for raclopride C 11 injection. *Pharm Forum.* 1995;21:172-6.
74. Farde L, Pauli S, Hall H, et al. Stereoselective binding of ^{11}C-raclopride in living human brain: a search for extrastriatal central D2-dopamine receptors by PET. *Psychopharmacology.* 1988;94:471-8.
75. Halldin C, Farde L, Högberg T, et al. A comparative PET-study of five carbon-11 or fluorine-18 labelled salicylamides: preparation and in vitro dopamine D-2 receptor binding. *Nucl Med Biol.* 1991;18:871-81.
76. Crouzel C, Clark JC, Brihaye C, et al. Radiochemistry automation for PET. In: Stöcklin G, Pike VW, eds. *Radiopharmaceuticals for Positron Emission Tomography: Methodological Aspects.* Boston: Kluwer Academic Publishers; 1993:45-89.
77. Alexoff DL. Automation for the synthesis and application of PET radiopharmaceuticals. In: Welch MJ, Redvanly CS, eds. *Handbook of Radiopharmaceuticals: Radiochemistry and Applications.* Hoboken, NJ: Wiley; 2003:229-82.
78. Fowler JS, MacGregor RR, Wolf AP, et al. A shielded synthesis system for production of 2-deoxy-2-[^{18}F] fluoro-D-glucose. *J Nucl Med.* 1981;22:376-80.
79. Barrio JR, MacDonald NS, Robinson GD, et al. Remote, semiautomated production of F-18-labeled 2-deoxy-2-fluor-D-glucose. *J Nucl Med.* 1981;22:372-5.
80. Adam MJ, Ruth TJ, Grierson JR, et al. Routine synthesis of L-[^{18}F]6-fluorodopa with fluorine-18 acetyl hypofluorite. *J Nucl Med.* 1986;27:1462-6.
81. Luxen A, Barrio JR, Van Moffaert G, et al. Remote, semiautomated production of 6-[F-18] fluoro-L-dopa for human studies with PET. *J Labeled Compounds Radiopharm.* 1989;26:465-6.
82. Pike VW, Eakins MN, Allan RM, et al. Preparation of [1-^{11}C] acetate—an agent for the study of myocardial metabolism by positron emission tomography. *Int J Appl Radiat Isot.* 1982;33:505-12.
83. Welch MJ, Dence CS, Kilbourn MR. Remote systems for the routine production of some carbon-11 radiopharmaceuticals. *J Labeled Compounds Radiopharm.* 1982;19:1382.
84. Iwata R, Ido T, Takahashi T, et al. Automated synthesis system for production of 2-deoxy-[^{18}F] fluoro-D-glucose with computer control. *Appl Radiat Isot.* 1984;35:445-54.
85. Alexoff DL, Russell JAG, Shiue C-Y, et al. Modular automation in PET tracer manufacturing: application of an autosynthesizer to the production of 2-deoxy-2-[^{18}F] fluoro-D-glucose. *Appl Radiat Isot.* 1986;37: 1045-61.
86. Padgett HC, Schmidt DG, Luxen A, et al. Computer-controlled radiochemical synthesis: a chemistry process control unit for the automated production of radiochemicals. *Appl Radiat Isot.* 1989;40:433-45.
87. Hamacher K, Blessing G, Nebeling B. Computer-aided synthesis (CAS) of no-carrier-added 2-[^{18}F] fluoro-2-deoxy-glucose: an efficient automated system for the aminopolyether-supported nucleophilic fluorination. *Appl Rad Isot.* 1990;41:49-55.
88. Suzuki K, Tamate K, Nakayama T, et al. Development of equipment for the automatic production of $^{13}NH_3$ and L-(^{13}N)-glutamate. *J Labeled Compounds Radiopharm.* 1982;19:1374-5.
89. Ruth TJ, Adam MJ, Jivan S, et al. An automated system for the synthesis of L-6[^{18}F] fluorodopa. *J Labeled Compounds Radiopharm.* 1991;30:304.
90. Brodack JW, Kilbourn MR, Welch MJ, et al. Application of robotics to radiopharmaceutical preparation: controlled synthesis of fluorine-18 16 alpha-fluoroestradiol-17 beta. *J Nucl Med.* 1986;27:714-21.

91. Brodack JW, Kilbourn MR, Welch MJ. Automated production of several positron-emitting radiopharmaceuticals using a single laboratory robot. *Appl Radiat Isot.* 1988;39:689-97.
92. Brodack JW, Kaiser SL, Welch MJ. Laboratory robotics for the remote synthesis of generator-based positron-emitting radiopharmaceuticals. *Lab Robotics Autom.* 1989;1:285-94.
93. Brihaye C, Lemaire C, Damhaut P, et al. Robot-assisted synthesis of [^{18}F] altanserin, 4-[^{18}F] fluorotropapride, 6-[^{18}F] fluorodopa and 2-[^{18}F] fluoro-L-tyrosine. *J Labeled Compounds Radiopharm.* 1994;35:160-2.
94. Krasikova RN. Automated synthesis of radiopharmaceuticals for positron emission tomography. *Radiochemistry.* 1998;40:352-61.
95. Mock BH, Winkle W, Vavrek MT. A color test for the detection of Kryptofix 2.2.2 in [^{18}F] FDG preparations. *Nucl Med Biol.* 997;24:193-5.
96. Meyer G-J, Coenen HH, Waters SL, et al. Quality assurance and quality control of short-lived radiopharmaceuticals for PET. In: Stöcklin G, Pike VW, eds. *Radiopharmaceuticals for Positron Emission Tomography: Methodological Aspects.* Boston: Kluwer Academic Publishers; 1993:91-150.
97. Keppler JS. Federal regulations and reimbursement for PET. *J Nucl Med Technol.* 2001;29:173-9.
98. Welch MJ, Redvanly CS, eds. *Handbook of Radiopharmaceuticals: Radiochemistry and Applications.* Hoboken, NJ: Wiley; 2003.
99. Fifteenth International Symposium on Radiopharmaceutical Chemistry. *J Labeled Compounds Radiopharm.* 2003;46:S1-403.
100. Scientific Abstracts of the 2003 International Conference of the Academy of Molecular Imaging. *Mol Imaging Biol.* 2003;5:95-215.

11 The Nuclear Pharmacy

Kristina M. Wittstrom

In a nuclear pharmacy radiopharmaceuticals are procured, prepared, stored, and dispensed primarily for patient administration within a nuclear medicine facility. Large teaching and research facilities may have a complete in-house nuclear pharmacy, while smaller institutions may have a modest space within the nuclear medicine department for minimal handling procedures. It is estimated that 70% to 80% of all radiopharmaceutical doses are dispensed through commercial centralized nuclear pharmacies.[1] This chapter examines some of the unique aspects of a commercial nuclear pharmacy.

DEVELOPMENT OF NUCLEAR PHARMACY

The development of nuclear pharmacy advanced with the advent of the ^{99m}Tc generator in the late 1960s.[1,2] With the increasing availability of reagent kits, pharmacists became involved in the preparation and dispensing of short-lived radiopharmaceuticals. The first educational program in nuclear pharmacy was established in 1969 at the University of Southern California. Other early programs included those at Purdue, Michigan, Tennessee, and New Mexico.

The 1970s saw a tremendous growth in nuclear medicine, new radiopharmaceuticals, and nuclear pharmacy. The first commercial centralized nuclear pharmacy was created in 1972 by Richard Keesee at the University of New Mexico College of Pharmacy in Albuquerque. Keesee is credited with the concept of unit dose radiopharmaceuticals: dispensing a single patient dose of radioactive drug on the prescription order of a physician. Graduates of the university educational programs began to establish commercial centralized nuclear pharmacies in 1974. Nuclear pharmacies spread across the country, numbering about 50 by 1980. By 2000, an estimated 400 centralized nuclear pharmacies staffed by about 1000 nuclear pharmacists were providing radiopharmaceuticals to hospitals and clinics in the United States. Recently, centralized commercial radiopharmacies have been developed in other countries. The development of positron emission tomography (PET) imaging and PET radiopharmaceuticals has provided a new growth area for nuclear pharmacy.

FACILITIES AND EQUIPMENT

The Nuclear Regulatory Commission (NRC) requires that nuclear pharmacy facilities and equipment be adequate to protect health and minimize danger to life or property, minimize the likelihood of contamination, and keep exposures of workers and the public as low as reasonably achievable (ALARA). The requirements include documentation that the nuclear pharmacy has sufficient engineering controls and barriers to protect the public and employees. Specifically, the facility and equipment must be designed to effectively keep personnel exposures to radiation and radioactive materials ALARA, to minimize the risks from handling radioactive materials.[3]

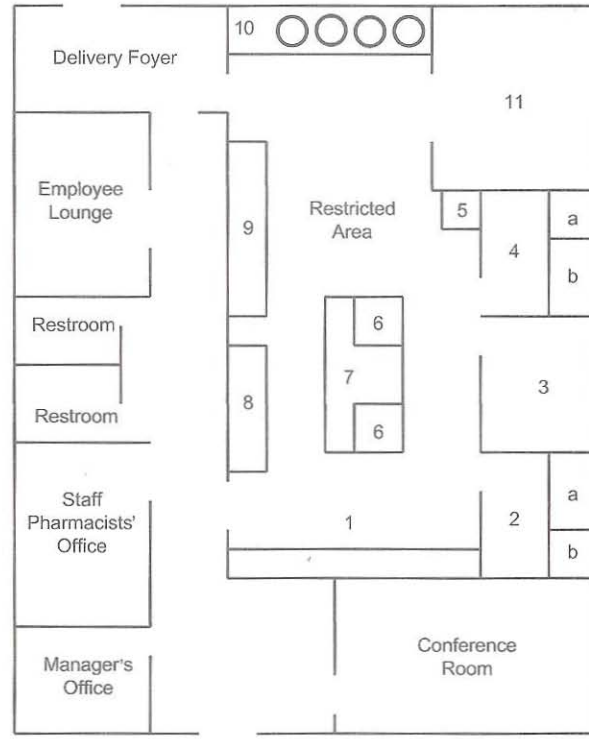

FIGURE 11-1 Nuclear pharmacy floor plan. (1) Prescription processing area, (2) labeling room with laminar flow hoods, (3) generator room, (4) radioiodine room with (a) fume hood and (b) exhausting glove box, (5) refrigerator/freezer, (6) dose drawing station in laminar flow hood, (7) wrapping area, (8) quality control area, (9) DOT area, (10) waste processing area, (11) waste storage room.

There are multiple ways to design a nuclear pharmacy to meet NRC requirements. Ideally, the pharmacy should be a free-standing structure or the end unit of a multitenant building. This minimizes common walls and reduces potential exposure of the general public. The floor plan should be arranged with areas designated for specific functions, with "hot" storage areas located away from other work areas. The physical layout can vary in size and design, but most nuclear pharmacies have some common features. Figure 11-1 is a typical floor plan with work and storage areas.

The nuclear pharmacy is divided into two areas. The unrestricted area consists of offices, conference room, and employee lounge. Access to this area by the general public and employees is not restricted. There are no radioactive materials in the unrestricted area. The restricted area consists of the storage and work areas for handling radioactive materials. Only trained radiation workers have access to this area. The restricted area is divided into several function-specific areas.

Restricted Area

The prescription processing area is where telephone orders are received by the nuclear pharmacist. These orders are transcribed and routinely entered into a computer system. Electronic prescriptions, labels, and packing slips are generated in this area.

The labeling room is sequestered from general traffic and kept as clean as possible. Open-transfer labeling processes requiring a sterile air environment are performed here. A vertical laminar flow hood (biologic safety hood) is used for all radioactive labeling procedures and is essential for open-container procedures such as blood cell labeling.

The generator room is the storage site for the many generators received in the nuclear pharmacy. A nuclear pharmacy uses many large (multicurie) generators each week. Although the generators are stored in the manufacturer's shielding, additional lead shielding

is needed to minimize employee exposure. This area is often one of the "hottest" within the restricted area.

The iodine room contains an exhausting fume hood for the storage of volatile radioactive materials, usually ^{131}I and ^{133}Xe. The fume hood ducting contains special traps to monitor the release of effluent into the atmosphere (see Chapter 5, Radiation Safety). A glove box–type unit may be used that exhausts into the main fume hood. Manipulations of volatile substances are performed within the glove box. A second trap is located near the glove box to monitor potential employee exposure.

Many radiopharmaceutical components require refrigeration or freezing to maintain product integrity. Several reconstituted radiopharmaceuticals should be refrigerated to retard microbial growth and maintain sterility. No food or drink is stored in the same refrigerator with these products. The refrigerator and freezer compartment temperatures should be monitored and recorded daily.

Each nuclear pharmacy has one or more radiopharmaceutical dose-drawing stations. These consist of a laminar flow hood with appropriate shielding and calibrators. All closed-system compounding is performed within these hoods. Unit dose radiopharmaceuticals are also prepared within a laminar flow hood. After the doses have been drawn, they are passed to a wrapping area. Unit dose shields are closed and labeled. Security shrink-wrap is often added at this point. The shields are wipe tested for removable contamination before moving to the Department of Transportation (DOT) area.

While doses are being wrapped, the compounded radiopharmaceutical is tested. Although this is not required by regulation, nuclear pharmacy standards of practice recommend that each radiopharmaceutical be tested for purity before its release for patient administration. Testing includes radionuclidic and radiochemical purity checks. A detailed discussion of these quality control tests is presented in Chapter 12.

Wrapped doses are moved to the DOT area. Here doses are packed into delivery containers. Package testing and monitoring required by DOT are then performed before the package can be released for transport and delivery. Chapter 5 contains a discussion of DOT requirements.

As a service to unit dose users, most nuclear pharmacies offer a waste management system. Spent syringes are returned in shields and DOT packaging to the nuclear pharmacy. The packages are opened and the spent syringes sorted by isotope half-life into cardboard containers stored in lead-shielded barrels such as that shown in Figure 11-2. The waste is held for decay in the waste storage area. After 10 half-lives the waste is transferred to a biohazardous waste disposal service. A more detailed discussion can be found in Chapter 5.

FIGURE 11-2 Lead-lined waste storage module. (Used with permission of Biodex Medical Systems, Shirley, NY.)

Storage and Shielding for Radioactive Materials

To minimize radiation exposure of employees, radioactive materials should be stored and handled using protective equipment. Most such equipment is made of lead in different configurations. Basic shielding equipment is listed in Table 11-1. Storage equipment is available in a variety of sizes and designs to accommodate specific needs. A nuclear pharmacy can purchase lead-lined fixtures such as those shown in Figure 11-3.

TABLE 11-1 Storage and Shielding Equipment for Radioactive Material

Lead-lined storage areas
For radiopharmaceuticals
For radioactive sealed sources
For radioactive waste
Lead L-block shields with leaded-glass viewing area
Lead bricks
Lead waste barrels
Vial shields (lead or tungsten)
Unit dose syringe delivery shields (lead or tungsten)
Dispensing syringe shields (leaded glass)
Lead sheeting of various size and thickness

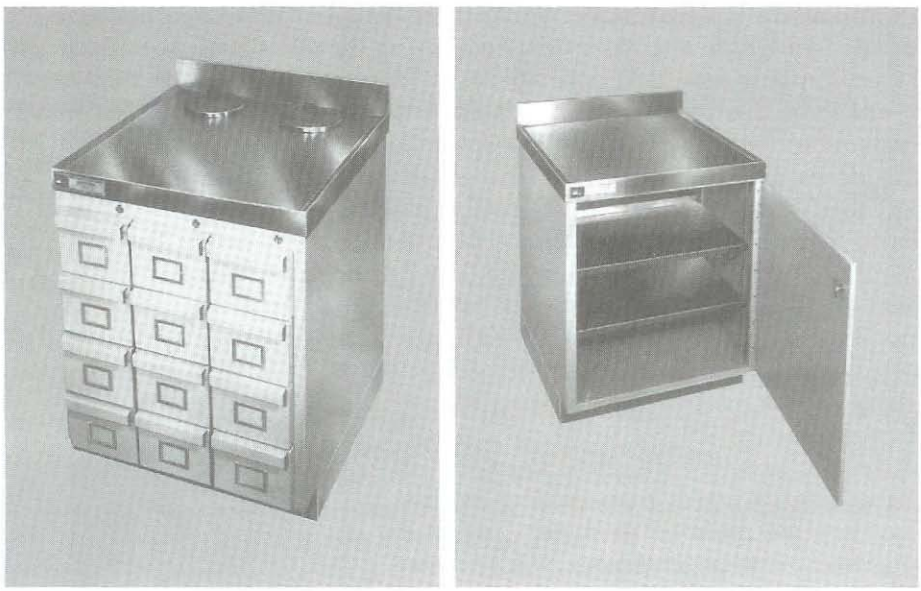

FIGURE 11-3 Lead-lined storage modules for radiopharmaceuticals and miscellaneous sources. (Used with permission of Biodex Medical Systems.)

Lead bricks, usually $2 \times 4 \times 8$ inches, are useful for providing extra shielding in areas where extemporaneous shielding is required, such as in the fume hood. Bricks provide the flexibility of a movable shield that can be changed or moved as needed. Lead bricks are available from commercial suppliers.

Vial shields of either lead or tungsten can be purchased or salvaged from manufacturer shields supplied with radiopharmaceuticals. Vial shields are used to shield generator elution vials, prepared radiopharmaceuticals, and multidose vials prepared for customers. The thickness of lead shields should match the gamma energy of the source to minimize exposure during handling and transit to the nuclear medicine facility. Adequate shielding is most important in the handling and transporting of ^{131}I and ^{18}F. Their high gamma energies require thicker lead to reduce exposure.

There are several styles of syringe shields. Some are designed for use in injecting patients. These are often made of lead with a glass inset for reading syringe markings. Figure 11-4 illustrates this type of shield. Unique to nuclear pharmacy is the dispensing

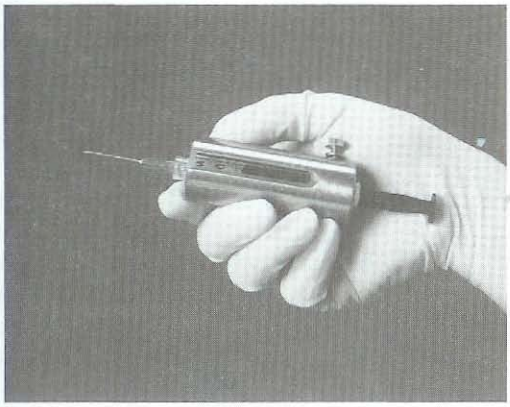

FIGURE 11-4 Syringe shield with leaded-glass viewing area. (Used with permission of Biodex Medical Systems.)

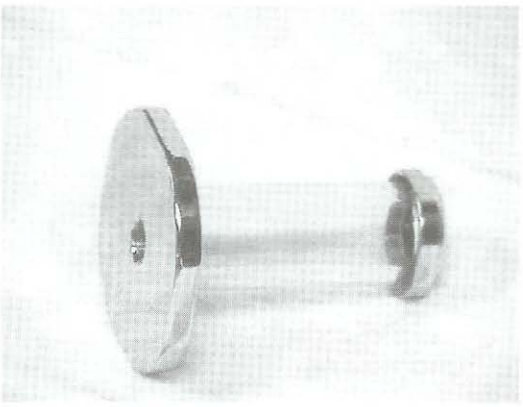

FIGURE 11-5 Dispensing syringe shield used in drawing doses from radiopharmaceutical vials.

syringe shield. This shield is made entirely of leaded glass, eliminating the need to manipulate the syringe to see the markings. The needle end of the shield is threaded to lock the syringe in place during compounding procedures. A chrome-covered lead plate is affixed to the end of the shield to protect the pharmacist's hands from the cone of radiation emitted from a bulk radiopharmaceutical preparation. This type of shield is pictured in Figure 11-5.

A lead L-block (Figure 11-6) is an L-shaped piece of lead with an inset of leaded glass to permit viewing of the work area. An L-block is routinely used in dispensing stations to protect the worker's body and face during manipulation of radioactive materials. L-blocks are also used at the quality control station, in the glove box–type exhausting fume hood, and in front of devices used to heat radiopharmaceuticals during compounding.

Work Surfaces and Sinks

Work surfaces throughout the pharmacy should be constructed of material resistant to the absorption of liquid, such as stainless steel, plastic, epoxy coating, or Formica. Surfaces over which radioactive materials are manipulated should be protected with plastic-backed absorbent sheeting. This sheeting will absorb any liquid contamination and is easy to remove. A nuclear pharmacy may have a sink within the restricted area. A sink is useful for decontaminating equipment or personnel. Sinks are most commonly used for hand washing before exiting the restricted area. Sinks are not intended for the disposal of radioactive solutions.

Hoods

As discussed earlier, it is desirable to have several types of hoods within the restricted area. Exhaust hoods are used to contain volatile radiopharmaceuticals such as iodine and xenon preparations. A traditional chemical exhaust hood is acceptable for processes that do not require a sterile air environment.

Procedures that involve the labeling of blood cells and proteins require the sterile air environment provided by a laminar flow hood. Figure 11-7 illustrates the two basic types of laminar flow hoods, the horizontal flow hood and the vertical flow hood. In general, the horizontal flow hood has no application in a nuclear pharmacy because its airflow pattern is not suitable for hazardous materials. A vertical flow biologic safety hood is

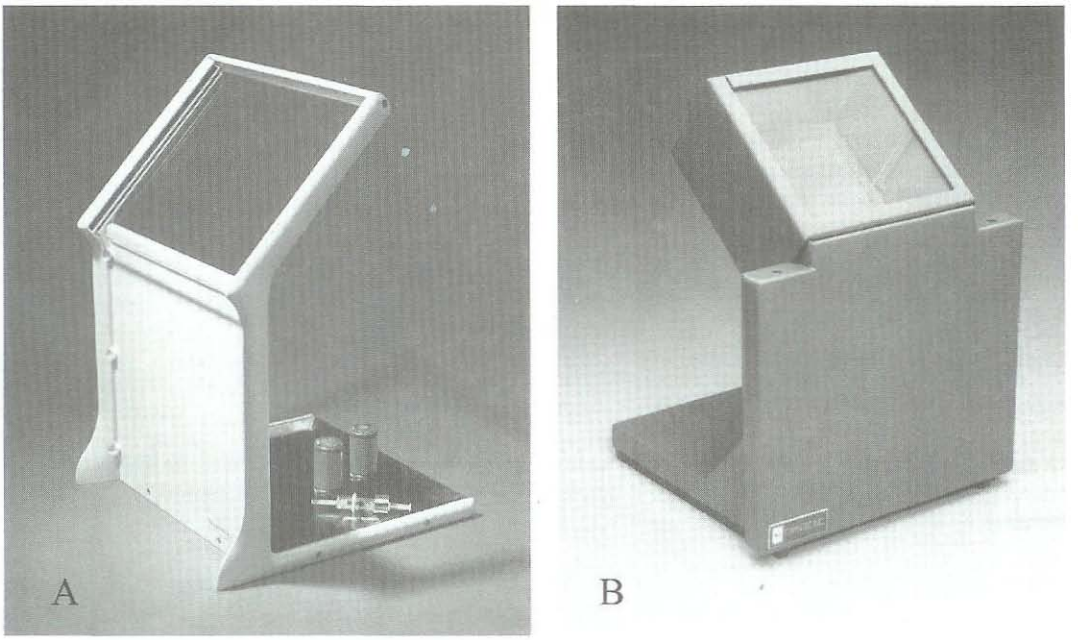

FIGURE 11-6 Lead-shielded L-block drawing stations with leaded-glass viewing area. (A) Standard L-block (½ inch thick lead) with ¼ inch thick leaded glass for single-photon-emitting radiopharmaceuticals (used with permission of Biodex Medical Systems); (B) PET 511 L-block (1 inch thick lead) with 4 inch thick leaded glass for positron-emitting radiopharmaceuticals (used with permission of Capintec Inc., Ramsey, NJ).

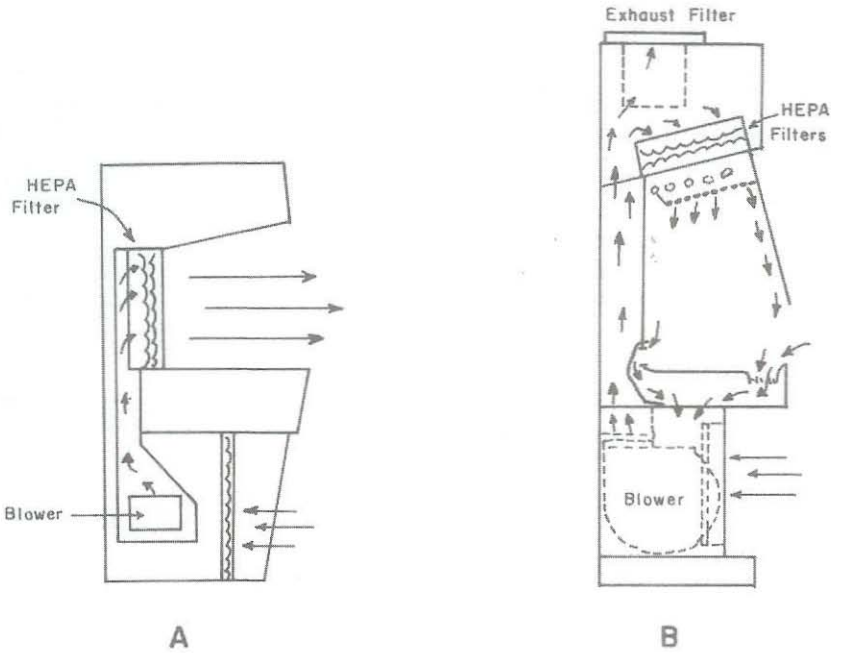

FIGURE 11-7 Laminar flow hoods. (A) Horizontal flow hood; (B) vertical flow hood.

recommended for handling any potentially biohazardous material, including radioactive material. Air entering the biologic safety hood is forced through a high-efficiency particulate air (HEPA) filter so that the quality of air is 99.9% free of particles less than 0.3 μm. Air leaving the hood passes through a second HEPA filter to prevent the release of particulate biohazardous material into the workspace. A Class II Type B-1 vertical flow hood that exhausts into the room is adequate for most types of procedures except those involving volatile radionuclides. Work with volatile agents requires a Class II Type B-2 hood that exhausts to the outside of the facility. Dispensing stations are usually placed within a vertical laminar flow hood. Ideally, the hood should be of the exhausting type to maximize protection of the worker and the environment, particularly if volatile nuclides are handled. Hoods should remain operational throughout the workday. At the beginning of a new workday, a hood should be allowed to run for at least 15 minutes before cleaning, decontamination, or use.

RADIATION DETECTION INSTRUMENTATION

The devices used to measure or detect radioactivity in a nuclear pharmacy include dose calibrators, portable Geiger-Müller (GM) survey meters, ion chambers or meters with energy-compensated probes, area monitors, and scintillation detectors with single-channel or multichannel analyzers. The principles of operation of these instruments are discussed in Chapter 3.

Dose Calibrators

The dose calibrator is an ionization chamber that is calibrated to measure the radioactivity of different isotopes used in radiopharmaceuticals (Figure 11-8). It is capable of measuring a range of activities from microcuries to curies. This easy-to-use instrument is adjusted for the radionuclide to be measured either by selecting a preset button or by adjusting a potentiometer to a specific calibration number. The source of radioactivity is placed into the chamber well and the activity is displayed on a digital readout.

FIGURE 11-8 Dose calibrator for assaying radiopharmaceuticals. (Used with permission of Capintec Inc.)

The user must be aware of geometric factors that may affect the readout on a dose calibrator. This is particularly important in measuring the activity of low photon energy nuclides, such as ^{125}I (27–35 keV) and nuclides that produce abundant low-energy characteristic x-rays, such as ^{123}I (27–31 keV) and ^{111}In (23–26 keV). Different types of containers (e.g., plastic syringe, glass vial) may exhibit different readings of the same amount of activity as a result of the difference in absorption of low-energy photons by the container. Correction factors must be applied to accurately measure certain radionuclides in different configurations. For example, measurements of ^{125}I in glass vials may be 30% to 50% less than the same amount of activity measured in a plastic syringe. The recent introduction of the ^{125}I product Iotrex (Proxima Therapeutics, Alpharetta, Ga.) for in situ brachytherapy of brain tumors is a case in point. The procedure requires the accurate measurement of multimillicurie amounts of ^{125}I. The manufacturer of this product has specified the exact type and size of syringe and the specific dose calibrator setting to use to assay the dose correctly.

Nuclides such as ^{123}I and ^{111}In emit high-energy gamma rays for imaging, but they also emit a high abundance of low-energy x-rays in the range of 23 to 31 keV that will affect the dose calibrator readout with different types of containers. A simple device using a copper filter inserted into the dose calibrator eliminates this problem by absorbing the low-energy x-rays without affecting the high-energy gamma rays.[4]

Dose calibrators are quite rugged and operate satisfactorily for many years. Daily and periodic quality control assessments are needed to ensure accurate operations. These assessments are discussed further in Chapter 12.

Geiger-Müller Survey Meters

This gas-filled detector was discussed in Chapter 3. It is a portable device for measuring radiation exposure in counts per minute (cpm) or milliroentgens per hour (mR/hr). The meter measures radiation detected by a probe. The preferred probe for use in nuclear pharmacies is the pancake probe. The front of the probe (Figure 11-9) has little shielding, allowing for a very sensitive check for contamination. The back of the probe is covered with a metal plate. Since the meters are calibrated against the back of the probe, it can be used to assess radiation fields. Other types of probes include the end-window probe suitable for contamination checks and beta probes that have a sliding beta "window," allowing for monitoring of both gamma and beta emissions.

Survey meters are the workhorses of a nuclear pharmacy. They are used in checking packages of radioactive materials, checking for contamination in work areas, monitoring personnel, and measuring radiation fields. However, a GM-type survey meter is limited in the amount of radiation exposure it can detect accurately. Most portable survey meters are accurate to 1 or 2 R/hr. Higher exposures require the use of a different instrument.

Ionization Chambers or Energy-Compensated Probes

High levels of radiation exposure such as those from multicurie ^{99m}Tc generators or high-activity ^{131}I shipments may require an instrument that can read above the levels of the GM survey meter. An ionization chamber will accurately read high levels of radiation exposure, but not as rapidly as a GM meter. An alternative to an ionization chamber is a multipurpose survey meter that not only operates with a gas-filled probe but also has an internal energy-compensated solid detector probe. A nuclear pharmacy that does not receive or ship packages containing high activity levels of radioactive materials with high radiation exposure rates does not need this additional equipment.

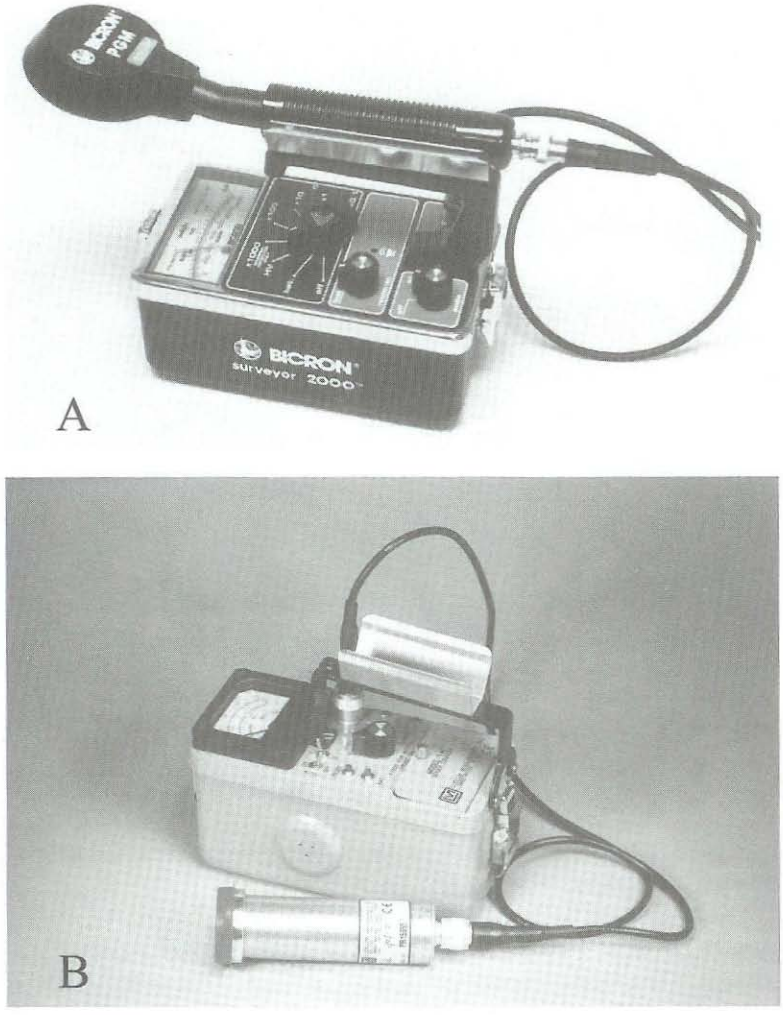

FIGURE 11-9 Geiger-Müller survey meters with (A) pancake-type probe (used with permission of Capintec Inc.) and (B) end-window-type probe (used with permission of Biodex Medical Systems).

Area Monitors

Area monitors are similar to GM survey meters except that they are usually stationary and are plugged into an electrical outlet. Area monitors are placed at the exit points of a restricted area and in other areas where ambient radiation exposure is a concern. Many monitors are equipped with an adjustable alarm that can be set to go off when a specific radiation level is exceeded. These device are sometimes equipped with two probes and are used to monitor hands, feet, and clothing before personnel exit the restricted area. A typical monitor is shown in Figure 11-10.

Scintillation Well Counters

A scintillation well counter consists of a sodium iodide crystal detector designed with a well to accept test tubes. The crystal is coupled to a photomultiplier tube. This unit detects gamma radiation and generates voltage pulses proportional to the gamma energy deposited in the

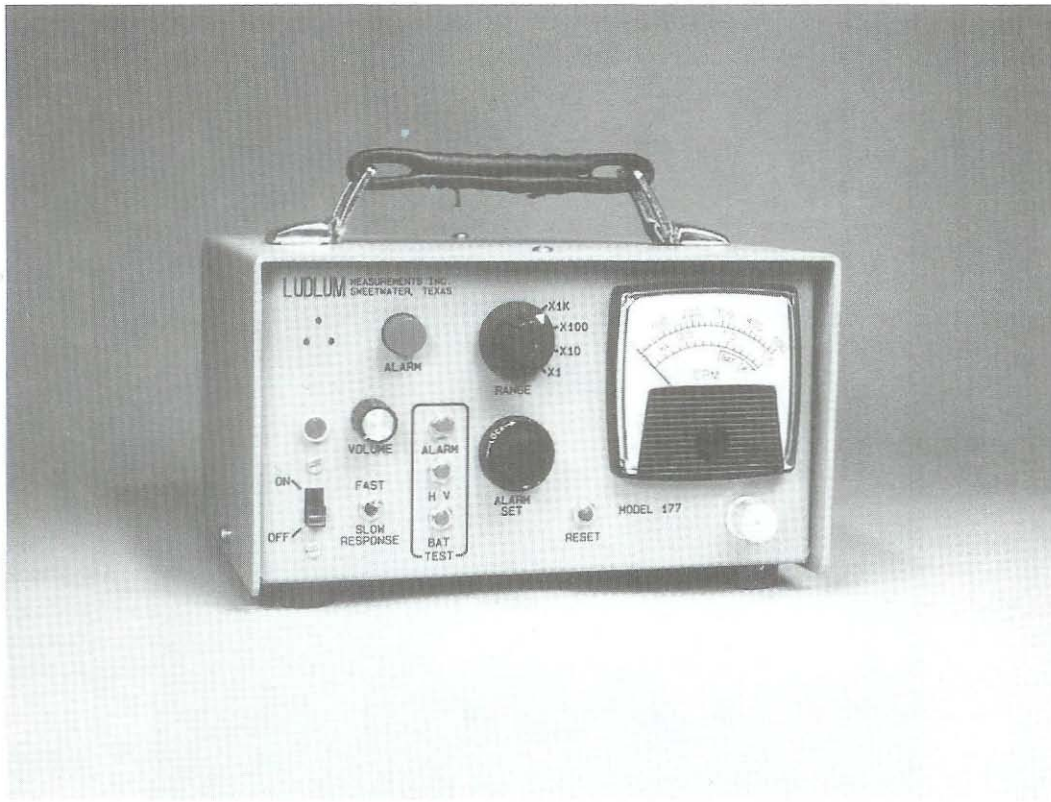

FIGURE 11-10 Geiger-Müller alarm rate meter for monitoring ambient radiation levels. (Used with permission of Biodex Medical Systems.)

crystal. The pulses are sent to a single-channel or multichannel analyzer (spectrometer) that can discriminate between the photon energy pulses. This permits the identification of unknown radionuclide samples and measurement of the amounts of radioactivity in samples containing one or more known nuclides. The well counter is primarily used to count small amounts of radioactivity (<1 μCi) present in room wipes, package wipes, and samples of biologic fluid (e.g., plasma or urine). This sensitive instrument must be located in a low-level background counting area. An example of a scintillation well counter is shown in Figure 11-11.

MISCELLANEOUS EQUIPMENT AND SUPPLIES

A number of other items are necessary in the nuclear pharmacy. A microscope and hemacytometer are used to size particulate-containing radiopharmaceuticals such as radiocolloids, macroaggregated albumin, and labeled cells. A centrifuge is necessary for separating blood cells from plasma for cell-labeling studies. Several radiopharmaceuticals require heating for periods of time. A water bath or heat block is often used to heat these products. A refrigerator and freezer are necessary for proper storage of radiopharmaceutical components. Daily temperature checks should be made on both the refrigerator and the freezer. Various types of chromatography materials and reagents are necessary to perform quality control on prepared radiopharmaceuticals. An in-depth discussion of these supplies can be found in Chapter 12.

FIGURE 11-11 Sodium iodide scintillation well counter. (Used with permission of Ludlum Measurements, Inc., Sweetwater, TX.)

PERSONNEL

A nuclear pharmacy is licensed by a state board of pharmacy. Accordingly, compounding and dispensing operations must be done under the supervision of a registered pharmacist and in accordance with all pharmacy statutes and regulations. The possession, handling, and dispensing of radiopharmaceuticals is regulated by NRC or an agreement-state regulatory body. NRC regulations require that the use and handling of radiopharmaceuticals be under the supervision and direction of an authorized nuclear pharmacist (ANP).

Authorized Nuclear Pharmacist

All activities within a nuclear pharmacy must be performed under the supervision and direction of an ANP. An ANP has completed a traditional pharmacy education, is registered as a pharmacist within the state of practice, and has completed an accredited program consisting of 200 contact hours of didactic education and 500 hours of experiential training. A handful of universities offer an undergraduate ANP program. Alternatives to the university classroom programs include university-sponsored distance education programs and on-site programs. Commercial nuclear pharmacy chains may offer internal courses for their employees.

The primary responsibility of an ANP is to prepare sterile, efficacious radiopharmaceuticals and provide the right drug in the right dose for the right patient at the right time. The ANP must have a strong knowledge base in nuclear pharmacy methods and techniques, as well as in the scientific principles that underlie the practice of pharmacy.

TABLE 11-2 Protective and Aseptic Techniques in Nuclear Pharmacy

Wear disposable gloves and a street-length lab coat.
Work behind a lead L-block when manipulating radioactive material.
Use syringe shields when preparing and dispensing doses.
Use the inverse square law to reduce radiation exposure. Use tongs to handle large amounts of unshielded radioactive material.
Cover work areas with absorbent plastic-backed paper.
Plan ahead and work quickly and efficiently. Perform dry runs for new procedures.
Work with only one radiopharmaceutical at a time.
Swab vial septa with alcohol.
Maintain negative pressure on vials containing radiopharmaceuticals.
Use correct technique for needles entering vial septa to prevent coring.
Inspect all radiopharmaceutical components, materials, devices, and solutions carefully for accuracy and integrity.
Do not eat or drink in the restricted area.

Nuclear Pharmacist Technician

As specified by the state boards of pharmacy, nonpharmacist personnel may be allowed to perform routine, nonjudgmental dispensing tasks. These individuals have received in-house training to perform specific tasks under the supervision of the ANP. Tasks commonly delegated to technicians include quality control testing, inventory control, packaging, and record keeping.

Delivery Personnel

Most nuclear pharmacies maintain a staff of delivery personnel and a fleet of vehicles. Delivery personnel are trained in the handling of packages containing radioactive material being transported to the final user (hospital or clinic). All personnel working in a nuclear pharmacy have received training in emergency procedures involving packages containing radioactive materials.

HANDLING TECHNIQUES

Nuclear pharmacy techniques can be divided into two categories: protective techniques and aseptic techniques. Protective techniques prevent or minimize radioactive contamination and unnecessary radiation exposure. Aseptic techniques prevent or minimize the chance of microbial contamination of sterile solutions and devices. Each nuclear pharmacy has an internal policies and procedures manual that details the required techniques. Common recommendations are listed in Table 11-2.

NUCLEAR PHARMACY PRACTICE

The Section on Nuclear Pharmacy of the American Pharmacists Association has developed Nuclear Pharmacy Practice Guidelines; these were initially established in 1978 and were updated most recently in 1994. The guidelines cover several domains and contain statements to aid in the description and interpretation of nuclear pharmacy practice. The nine general domains involved in nuclear pharmacy practice are procurement, compounding, quality assurance, dispensing, distribution, health and safety, provision of information and consultation, monitoring patient outcomes, and research and development.[5]

The guidelines do not consider differences in practice setting, job responsibilities, or other considerations. They may not be applicable to all nuclear pharmacists, nor are they all-inclusive. Pharmacists should use professional judgment in interpreting the guidelines.

Procurement

Procurement of radiopharmaceuticals and the associated activities are learned from experience on the job. Some tasks, such as determining product specifications, initiating purchase orders, receiving shipments, maintaining inventory, and proper storage of materials, are very similar to those involved in other areas of pharmacy practice. The art of procurement involves anticipating daily needs for short-lived radiopharmaceuticals and obtaining amounts that meet these needs with minimal waste. Procurement involves daily, and often hourly, analysis of inventory against anticipated next-day demands.

The ordering of radiopharmaceuticals requires a thorough knowledge of calibration and expiration dates and times, as well as shipping and delivery schedules. In contrast to traditional pharmaceuticals, orders for radiopharmaceuticals are placed directly with the manufacturer. A nuclear pharmacy may have daily standing orders for some products, but these orders must be constantly assessed and adjusted. Most orders are shipped by air to arrive in the early hours of the morning, often before the nuclear pharmacy opens for the day. The materials must be on hand in the pharmacy in time to get them to the hospitals and clinics before the nuclear medicine department opens.

Nuclear pharmacies have a designated delivery area for shipments that arrive when the nuclear pharmacy is closed. This may be an exterior lock box or a secured foyer for which the delivery company has a key. Package receipt involves following the regulatory procedures for opening packages. Details regarding receipt of radioactive material packages are discussed in Chapter 5.

Compounding

Although many radiopharmaceuticals are available in ready-to-use form, most must be compounded on an as-needed basis. Compounding activity can range from the relatively simple task of reconstituting reagent kits with ^{99m}Tc-sodium pertechnetate to complex tasks such as operating a cyclotron and synthesizing PET radiopharmaceuticals. Nuclear pharmacists may also perform extemporaneous compounding of commercially unavailable radiopharmaceuticals such as ^{123}I-iobenguane sulfate (^{123}I-MIBG). As in other pharmacy practice settings, a valid prescription order is needed. Other considerations include appropriate components, supplies, and equipment; a suitable environment for sterile dosage forms; and appropriate record keeping, including lot-specific information to ensure traceability and validation or verification of the radiopharmaceutical's compounding procedure, storage, and expiration date.

Most commonly, the nuclear pharmacy prepares technetium radiopharmaceuticals by reconstituting reagent kits with sodium pertechnetate. Each nuclear pharmacy has internal written procedures for the reconstitution of ^{99m}Tc kits. If no written procedure has been tested and validated, the manufacturer's package insert recommendations should be followed.

The preparation of radiopharmaceuticals labeled with technetium and other radionuclides is more complex than most drug compounding because radioactive accountability and decay, radiation protection, and radiolabeling conditions must be considered. Each radiopharmaceutical lot is assigned a radioactive concentration at a given time, for example, 50 mCi (1850 MBq)/mL at 1200 hours, and a lot number. When an order for a particular radiopharmaceutical is phoned in, prescriptions can be generated from a particular radiopharmaceutical lot. A computer-generated report of predispensing information is available

TABLE 11-3 Predispensing Worksheet for ^{99m}Tc-Medronate (MDP) 40 mCi/mL at 0600

Rx No.	Hospital	Patient	Drug	Activity	Cal Time	Volume
12345	Memorial	Smith	MDP	25 mCi	0900	0.890
12350	Community	Jones	MDP	20 mCi	0830	0.67
12371	St Jo	Adams	MDP	25 mCi	1000	1.0
12375	St Jo	Brown	MDP	25 mCi	1030	1.04
12376	St Jo	White	MDP	25 mCi	1100	1.12
12390	Holy Cross	Garcia	MDP	15 mCi	0900	0.53
12391	Holy Cross	Smith	MDP	15 mCi	0930	0.50
Total volume						5.75

UNC Hospitals Division of Nuclear Medicine
Technetium-99m Radiopharmaceutical Compounding Record

* Determined by Mo99:Tc99m Ratio or 12 hr, whichever is less.

Date	Nuclear Med Control No	Tc-99m Pertechnetate				Time	Radiopharmaceutical Kit				Saline			Total Vol	Prep By	uCi Mo99	Ratio Mo99:Tc99m
		Source	Lot No	Activity	Volume		Type	Volume	Mfr	Lot No	Mfr	Lot No	Volume			ug Al^{3+}	Expir Time *

FIGURE 11-12 ^{99m}Tc radiopharmaceutical compounding control record.

prior to the compounding of a particular radiopharmaceutical lot; it provides not only prescription traceability but compounding specifics. Table 11-3 shows a representative predispensing report for seven prescriptions totaling 5.75 mL of total volume to be compounded.

Each prepared radiopharmaceutical lot must have traceability of all components contained in the final product. Every nuclear pharmacy has some type of kit-compounding worksheet or record. This record, usually generated by hand, lists traceable information about each component used in the radiopharmaceutical's preparation, such as the manufacturer's lot number, the time and activity of reconstitution, and volumes used. These hand-generated records are converted into an electronic format as time allows. Figure 11-12 illustrates a kit-compounding worksheet.

Nontechnetium radiopharmaceuticals are commercially available as approved drugs. Some of these products are in ready-to-use form and simply require a decay calculation before a patient dose is dispensed. Examples are ^{67}Ga-gallium citrate, ^{201}Tl-thallous chloride, ^{131}I-sodium iodide, and ^{111}In-pentetate. Other products are in kit form, and their preparation requires following the instructions in the manufacturer's package insert. Examples are ^{111}In-pentetreotide (OctreoScan) and ^{111}In-capromab pendetide (ProstaScint). Record keeping for these products is similar to that for technetium radiopharmaceuticals.

Upon a written order from a physician for a specific radiopharmaceutical for a specific patient, a nuclear pharmacist may extemporaneously compound a radiopharmaceutical that is not commercially available. Standards of practice for reagent chemical purity, sterility, and apyrogenicity become the responsibility of the nuclear pharmacist. Such

compounding activities must be performed and documented in accordance with state board of pharmacy and FDA regulations.

The compounding of PET radiopharmaceuticals requires more controls, validation procedures, and record keeping than are needed for any other radiopharmaceutical. A PET radiopharmaceutical may require that the pharmacist synthesize the desired radionuclide, purify it, and chemically incorporate it into a biologic tracer form, using good manufacturing practices. Additional information on PET radiopharmaceuticals can be found in Chapter 10.

Quality Assurance

Quality assurance of radiopharmaceuticals involves the performance of appropriate chemical, physical, and biologic tests to ensure that the product is suitable for human use. Certain standards, such as sterility and apyrogenicity, may be guaranteed by the manufacturer of commercially available reagent kits. This minimizes the quality assurance demands on the nuclear pharmacist. When radiopharmaceuticals, including PET products, are compounded extemporaneously, verification of product specifications is the responsibility of the nuclear pharmacist. This responsibility includes not only performing the test(s) but also interpretation of the results, evaluation of analytical test methods, calibration or functional checks of equipment and instruments used, and appropriate record keeping. Record keeping is more than just ensuring component traceability; records must also document procedure validation and include test results and analysis. Radiopharmaceuticals must meet all specifications described in the appropriate USP monograph. These include radionuclidic purity, radiochemical purity, chemical purity, pH, particle size, sterility, apyrogenicity, and specific activity. Details on quality assurance testing can be found in Chapter 12.

Dispensing

An authorized prescription order is made by a nuclear medicine physician (or delegate) in accordance with state and local requirements. The radiopharmaceutical is dispensed to the authorized nuclear physician at an authorized location. Radiopharmaceuticals are not dispensed directly to patients, but to those professionals licensed to administer radiopharmaceuticals. Most radiopharmaceutical prescriptions are dispensed as unit doses ready for administration to a particular patient. Multidose vials of radiopharmaceuticals may be delivered to nuclear medicine departments to cover emergency or unexpected situations "per physician order."

Each state board of pharmacy and the radiation safety agency has specific requirements for the labeling of radiopharmaceuticals. The syringe or vial that contains the radioactive material must be tagged with specific information, including prescription number, patient name, radiopharmaceutical name, activity dispensed, and the date and time of calibration. The labeled syringe or vial is placed into a lead shield that also must be labeled. The shield label is larger and can accommodate additional information, such as directions for storage or administration.

The nuclear pharmacist is responsible for ensuring that the radiopharmaceutical dosage is consistent with the prescription order and is appropriate for a particular patient study. Patient considerations may include prior history, age, weight, sex, and disease state. Other considerations include adjustment for radioactive decay between preparation and dispensing times and between dispensing and administration times. For some radiopharmaceuticals, stability concerns may mandate a shorter product expiration time. The

nuclear pharmacist must have a working knowledge of product chemistry and pharmacokinetics to optimize patient care.

Most radiopharmaceuticals are injectable products and require the use of aseptic technique during compounding and dispensing operations. The nuclear pharmacist must be able to ensure maintenance of sterile controls throughout both processes. This involves the proper use of well-maintained laminar airflow hoods for both compounding and dispensing procedures.

Distribution

The distribution of radiopharmaceuticals is a major responsibility of the nuclear pharmacist. After radiopharmaceuticals have been compounded and dispensed, they must be transported to the final site of use. Radiopharmaceuticals must arrive in a timely manner so that the flow of a nuclear medicine department's operations is not disrupted. There are many regulatory and logistical considerations in the distribution process.

DOT regulates packaging, labeling, shipping papers, employee training, and actual transport. The recipient of radioactive material must meet regulatory requirements regarding where, when, and how deliveries are to be made. Other regulatory groups that may be involved include the Environmental Protection Agency (EPA) (biohazardous waste transport), hazardous materials agencies, and state law enforcement agencies (for example, the California Highway Patrol requires a special license to transport radioactive materials). A nuclear pharmacist must be knowledgeable about the applicable local, state, and federal regulations governing the transport of radioactive materials.

Nuclear pharmacies offer set deliveries at certain times throughout the day. These are often identified with production runs: The first run is the first compounding session of the day, with doses delivered prior to 0700; the second run provides doses delivered around midday; and the third run provides late afternoon products. Each run is divided into routes of several hospital deliveries in sequence. In addition, deliveries are made outside these regular runs to meet same-day orders and emergency orders. The nuclear pharmacist must have a comprehensive working knowledge of transport regulations, know the location and distance of each hospital, and efficiently juggle delivery personnel and vehicles to make timely delivery of radiopharmaceuticals. Larger nuclear pharmacies may utilize a dispatcher to handle delivery logistics.

Requests for radiopharmaceuticals do not cease at 1700. The nuclear pharmacist is available 24 hours a day, 7 days a week to provide imaging materials. After-hours requests often are of an emergency nature and require expeditious delivery. Sometimes the nuclear pharmacist not only compounds and dispenses the prescription but also delivers it.

Health and Safety

Radiation safety requirements and standards have been established and are enforced by NRC or agreement states. These requirements include limits for radiation doses, area levels of radiation, airborne concentrations of radioactivity, waste disposal, and precautionary procedures to protect the health and safety of the occupationally exposed worker and the general public. The ANP designation implies that a nuclear pharmacist not only is capable of operating a nuclear pharmacy but also is qualified to function as the site radiation safety officer. Chapter 5 reviews radiation safety issues in detail.

In addition to radiation safety concerns, other aspects of health and safety are important. The Occupational Safety and Health Administration regulates chemical safety and other personnel hazards. EPA regulates the release of radioactivity into the air (air monitoring) and the handling of biologic or biohazardous materials. The federal agencies may often have a

TABLE 11-4 Information and Consultation Topics

Biologic effects of radiation
Radiation physics
Radiopharmaceutical compounding
Quality assurance
Clinical applications of radiopharmaceuticals
Pharmacologic interventions used with radiopharmaceuticals
Drug–radiopharmaceutical interactions
Adverse reactions to radiopharmaceuticals
Patient-specific variables that alter radiopharmaceutical distribution
Radiopharmaceutical product defects
Regulatory issues

local or state equivalent with regulations that are equally or more restrictive. To prevent citations and penalties, nuclear pharmacies must be in compliance with all safety standards.

Provision of Information and Consultation

A nuclear pharmacist is part of the nuclear medicine team. Nuclear pharmacists share their expert knowledge by providing the appropriate information to physicians, technologists, patients, and others. This information ranges from regulatory requirements to patient-specific variables. Table 11-4 summarizes types of information requested from a nuclear pharmacist.

The nuclear pharmacist provides information in many different settings. Educational information may be presented to the pharmacy staff, a hospital, a local or national professional meeting, or to regulatory agencies. Organizational policies and procedures are often developed under the guidance of a group of nuclear pharmacists. These may be for a single pharmacy or a corporate structure or for the benefit of the profession. Information pertinent to the care of a specific patient (pharmaceutical care) is requested daily from physicians and technologists.

Monitoring Patient Outcomes

A nuclear pharmacist does not usually have direct contact with patients. However, nuclear pharmacists contribute to patient outcomes through patient preparation, dose calculation, development of institutional standards for the use of radiopharmaceuticals, and knowledge of proper interventional agents and imaging sequence.

Research and Development

Nuclear pharmacists may participate in the development of new radiopharmaceuticals, new compounding procedures, and quality control tests. Many nuclear pharmacists participate in clinical investigations and evaluations of new uses of radiopharmaceuticals. An important contribution of the nuclear pharmacist is the dissemination of information about new products and techniques to practicing nuclear medicine physicians and technologists.

RECORDS IN THE NUCLEAR PHARMACY

NRC and agreement-state agencies require an accounting of all transfer, disposal, or decay of radioactive material. Records substantiating daily and periodic testing must also be

TABLE 11-5 Representative List of Required Records

Generator elution records
Compounding records
Dispensing records
Radiopharmaceutical quality assurance testing
Incoming package receiving record
Outgoing package shipping papers
Room wipes and surveys
Air monitoring
Employee bioassay
Employee training documents
Employee dosimetry reports
Equipment testing—daily and periodic
Laminar flow hood cleaning
Laminar flow integrity testing
Temperature checks of refrigerator/freezer
Waste disposal records—hazardous material and radioactive materials

maintained for specific amounts of time. DOT requires that copies of shipping documents be maintained for 1 year. EPA wants "cradle to grave" traceability of biohazardous waste. Compounding and dispensing records must also be kept. Boards of pharmacy expect certain records, such as temperature checks on refrigerators and freezers. Nuclear pharmacy internal protocols and procedures may require additional records not mandated by a regulatory body. A key concept promulgated by all regulatory agencies is that if a written record is not available, the process or procedure did not occur. Table 11-5 provides a representative list of required records for a nuclear pharmacy.

REFERENCES

1. Shaw SM, Ponto JA. Nuclear pharmacy practice. In: Gennaro, AR, ed. *Remington: The Science and Practice of Pharmacy.* 20th ed. Philadelphia: Lippincott Williams & Wilkins; 2000:1781-91.
2. Brucer MA. *A Chronology of Nuclear Medicine 1600-1989.* St Louis: Heritage; 1990.
3. US Nuclear Regulatory Commission. *Consolidated Guidance about Materials Licenses: Program-Specific Guidance about Commercial Radiopharmacy Licenses.* NUREG-1556, vol 13. Washington, DC: US Nuclear Regulatory Commission; 1999.
4. Kowalsky RJ, Johnston RE. Dose calibrator assay of iodine-123 and indium-111 with a copper filter. *J Nucl Med Technol.* 1998;26:94-8.
5. American Pharmaceutical Association. *Nuclear Pharmacy Practice Guidelines.* Washington, DC: American Pharmaceutical Association; 1994.

12 Quality Control in Nuclear Pharmacy

Joseph C. Hung

The old adage that a chain is only as strong as its weakest link is applicable to nuclear medicine practice. The nuclear medicine physician must be sure that the information obtained from a radiodiagnostic procedure is a true representation of the patient's condition. The strength and conviction of a physician's diagnostic impression are based not only on his or her knowledge and experience but on trust in a nuclear diagnostic system in which all measures have been taken to prevent errors. There are several areas where problems can occur to weaken the system: competency of personnel, data collection, data processing and display systems, instrumentation, and radiopharmaceuticals. This chapter focuses on practical methods used in the nuclear pharmacy to ensure high-quality radiopharmaceuticals and proper operation of the instruments used in preparing them.

RADIOPHARMACEUTICAL QUALITY CONTROL

Because radiopharmaceuticals are intended for human administration, quality control (QC) procedures are imperative to ensure their safety and effectiveness. QC of radiopharmaceuticals has been defined by Briner[1] as "a series of tests, observations and analyses that will indicate beyond a reasonable doubt the identity, quality, and quantity of all ingredients present in a product and which will demonstrate that the technology employed in its formulation or manufacture will yield a dosage form of highest safety, purity, and efficacy." This definition implies that the QC program must be in operation continuously throughout the radiopharmaceutical preparation process.

Radiopharmaceuticals prepared by drug manufacturers are routinely monitored through a series of vigorous testing procedures. Consequently, the end user is generally not required to conduct any further QC evaluation on such products, except for certain mandated tests such as the ^{99}Mo breakthrough test on a ^{99m}Tc generator eluate.[2] However, for extemporaneously prepared ^{99m}Tc-labeled compounds, it is the responsibility of the preparer to ensure that the final product meets acceptable standards of quality and purity. Fortunately, the occurrence of defective or substandard radiopharmaceutical products has reportedly been infrequent.[3–10]

There are three basic sources of information on QC methods for radiopharmaceuticals: the *United States Pharmacopeia* (*USP*), drug product package inserts, and the scientific literature. *USP* is the official compendium of drug products manufactured in the United States. It is recognized by the federal Food, Drug, and Cosmetic Act and is referenced in numerous statutes regulating items used in medical practice.[11] USP standards for establishing a drug's identity, strength, quality, and purity, and specifications for packaging and labeling provide a guide for the quality of drug products prepared for medical use,

including radiopharmaceuticals. Package inserts, which must be approved by FDA, are supplied with radioactive drug products and include preparation and QC information for the nuclear pharmacist preparing these products. The third source of information is the scientific literature. Although journal articles, textbooks, and technical reports do not have the power of statute associated with a USP method, they are sometimes used as alternative sources for QC test methods in nuclear pharmacy practice.

The official test method for QC described in the *USP* monograph for a radiopharmaceutical does not preclude the use of alternative methods.[12] However, alternative methods must be shown to be equivalent to the USP method, which is the reference method. It is not clear whether FDA has a similar policy regarding deviations from test procedures described in package inserts. FDA permits physicians to use approved drug products for unapproved or unlisted clinical indications.[13,14] Nuclear pharmacists should also be permitted to use alternative QC testing methods in order to meet production capabilities and constraints, especially if the testing information described in the package insert is incomplete or is listed only as a recommendation.[15]

Routine radiopharmaceutical QC procedures can be broken down into four categories: radiation considerations, chemical considerations, pharmaceutical considerations, and biologic considerations.

RADIATION CONSIDERATIONS

The safe and efficacious use of radiopharmaceuticals requires that they be of the highest purity with regard to their radionuclide and chemical composition. Any nuclear medicine procedure requires the administration of a particular radionuclide in a particular chemical form. The presence of impurities, such as different radionuclides or other chemical forms of the desired radionuclide, may produce undesirable information from the diagnostic procedure. Therefore, it is important to conduct purity tests on all radiopharmaceuticals prior to patient administration.

Radionuclide Identity

A radionuclide can be identified by its mode of decay, nuclear emission energies, and half-life. The most practical method for radionuclide identification in nuclear pharmacy practice is gamma ray spectrometry. This can be readily accomplished with a multichannel analyzer (MCA) equipped with a sodium iodide [NaI(Tl)] detector or a lithium-drifted germanium semiconductor detector [Ge(Li) detector] (Figure 12-1).[16] The sodium iodide detector has a much lower energy resolution than a Ge(Li) detector but is more commonly available.

In some situations, such as when two or more positron-emitting radionuclides need to be identified (e.g., ^{18}F impurities in a ^{13}N preparation), half-life determinations can be carried out in addition to gamma spectrometry, since ^{18}F and ^{13}N demonstrate identical spectra. A dose calibrator can be used to measure half-life in radionuclide identity tests. Half-life is determined by successive counting of a radioactive sample at intervals corresponding to half of the estimated half-life for a time period equal to about three half-lives.[16–18] Half-life determinations are not required in traditional nuclear pharmacy practice but may be appropriate in certain practice settings. Such determinations are best performed as part of an ongoing quality assurance program to validate methods, because of the time required to conduct these tests.

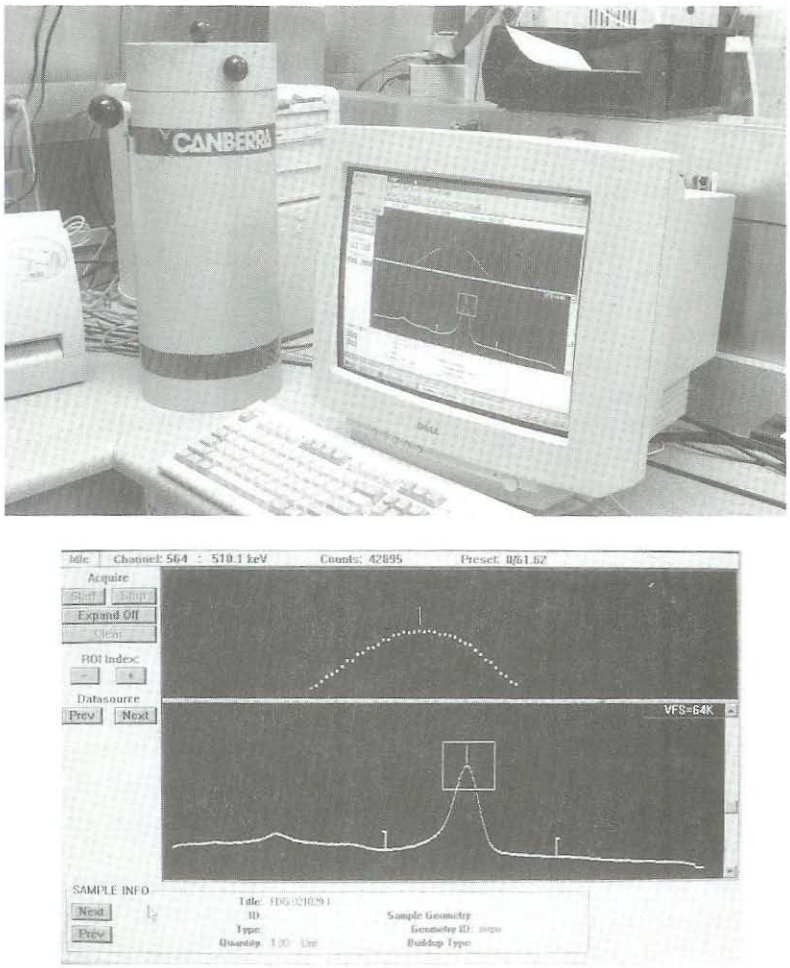

FIGURE 12-1 A multichannel analyzer with a pulse-height spectrum shown on the monitor.

Radionuclidic Purity

Radionuclidic purity of a radiopharmaceutical is defined as a ratio, expressed as a percentage, of the radioactivity of the desired radionuclide to the total radioactivity in the preparation. For example, a 100 μCi (3.7 MBq) ^{99m}Tc-sodium pertechnetate preparation containing 99.5 μCi (3.68 MBq) as ^{99m}Tc and 0.5 μCi (18.5 kBq) ^{99}Mo would have a radionuclidic purity of 99.5% with respect to ^{99m}Tc. In this example, ^{99}Mo activity would represent a 0.5% radionuclidic impurity.

Radionuclidic impurities are significant because they can contribute unnecessary radiation dose to the patient without adding to the diagnostic information obtained. Examples of radionuclidic impurities include 66 hour ^{99}Mo impurity in 6 hour ^{99m}Tc, 4 day ^{124}I impurity in 13 hour ^{123}I, and 12 day ^{202}Tl impurity in 73 hour ^{201}Tl. Relevant radionuclidic impurities and acceptable limits in radiopharmaceuticals are usually listed in package inserts or specified in *USP* monographs. Some of these are given in Table 12-1. Radionuclidic purity requirements must be fulfilled throughout the useful life of a radiopharmaceutical.

Radionuclidic impurities in radiopharmaceuticals can arise from several factors. These include the method of radionuclide production, target impurities that contribute

TABLE 12-1 Radionuclidic Purity of Commonly Used Radionuclides

Radionuclide	Half-Life (Principal Energy)	Purity	Contaminants	Half-Life (Principal Energy)	Acceptable Limits
^{67}Ga	77.9 hours (93 keV, 184 keV, 296 keV, 388 keV)	99% ^{67}Ga			
^{111}In	2.8 days (173 keV, 247 keV)		^{110m}In		<3 μCi/mCi (<111 kBq/37MBq) ^{111}In
			^{114m}In	50.0 days (192 keV, 558 keV, 724 keV)	<3 μCi/mCi (<111 kBq/37MBq) ^{111}In
			^{65}Zn	243.9 days (1.12 MeV)	<3 μCi/mCi (<111kBq/37MBq) ^{111}In
^{123}I	13.3 hours (159 keV)	85% ^{123}I			
^{99m}Tc	6.1 hours (140 keV)		^{99}Mo	66.7 hours (181 keV, 740 keV, 778 keV)	<0.15 μCi/mCi (5.55 kBq/37MBq) ^{99m}Tc
^{201}Tl	73.0 hours (60–80 keV, 135 keV, 167 keV)	95% ^{201}Tl	^{200}Tl	26.1 hours (368 keV, 579 keV, 829 keV, 1.21 MeV)	<2%
			^{203}Pb	52.0 hours (279 keV, 401 keV)	<0.3%
			^{202}Tl	12.2 days (439 keV, 522 keV, 961 keV)	<2.7%
^{133}Xe	5.3 days (31 keV, 81 keV)	95% ^{133}Xe			

Source: *The United States Pharmacopeia, 27th rev., and The National Formulary, 22nd ed.*; 2004.

to competing nuclear reactions, and incomplete radionuclide separation during radiochemical processing. A change in target material and type of nuclear reaction can reduce the level of radionuclidic impurities. An example is the production of ^{123}I by the (p,2n) reaction on a ^{124}Te target, which produces significantly more radionuclidic impurities (i.e., ^{124}I, ^{125}I, ^{130}I, and ^{131}I) than the (p,5n) reaction on an ^{127}I target, which produces only an ^{125}I impurity.

Radionuclidic purity is constantly changing. If the radionuclidic impurity has a half-life longer than that of the principal radionuclide, the concentration of the impurity will increase with time. Such a situation often forms the basis for establishing a radiopharmaceutical's expiration date. An example is ^{202}Tl ($T_{½}$ = 12 days) impurity in thallous chloride ^{201}Tl injection ($T_{½}$ = 73 hours). The highly abundant (95%) 493 keV gamma ray of ^{202}Tl may affect image quality when low-energy collimation is used during ^{201}Tl imaging. Another example is the presence of ^{99}Mo ($T_{½}$ = 66 hr) in ^{99m}Tc-sodium pertechnetate ($T_{½}$ = 6 hr). Figure 12-2 illustrates the expiration time for a ^{99m}Tc generator eluate as a function of the Mo:Tc ratio.

Measurement of radionuclidic purity can usually be accomplished using an MCA equipped with a Ge(Li) detector (Figure 12-1). The gamma-ray spectrum and corresponding half-lives can be used to identify the radionuclides present. The photopeak height and area under the curve on the gamma-ray spectrum are analyzed to assess the amount of radionuclidic purity present. Ge(Li) detectors are preferred for gamma spectrometry because of their superior energy resolution in separating gamma-ray photopeaks. When a sodium iodide detector is used, it may be impossible to resolve gamma rays with close

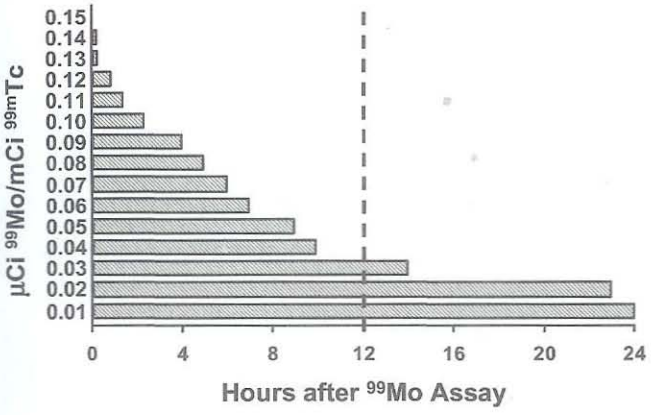

FIGURE 12-2 Expiration time of a ^{99m}Tc generator eluate based on the initial ^{99}Mo–^{99m}Tc activity ratio. The upper limit for this ratio is 0.15 µCi ^{99}Mo/mCi ^{99m}Tc. For example, an initial ratio of 0.09 will become 0.15 in about 4 hours and the eluate will expire. The dotted line indicates the default expiration time for any generator eluate (12 hours).

energies because of photopeak overlap. Other types of detectors are required if alpha- and beta-emitting impurities need to be detected.

Most radiopharmaceuticals used in nuclear medicine have their radionuclidic purity tested by the manufacturer. The only routine test required in nuclear pharmacy practice is the ^{99}Mo breakthrough test on the ^{99m}Tc generator eluate. When necessary, a gamma-ray spectrum can be easily acquired and analyzed to assess radionuclidic purity prior to release of a radiopharmaceutical preparation. If radiopharmaceuticals are compounded extemporaneously with radiochemicals, it is prudent to run a gamma-ray spectrum on the radiochemical because these sources are not sold in final-use form as radiopharmaceuticals.

Radiochemical Identity

A radiochemical is best identified by in vitro analytic methods. These methods may include electrophoresis, gas chromatography (GC), liquid chromatography, such as high-performance liquid chromatography (HPLC; also called high-pressure liquid chromatography), paper chromatography, solid-phase extraction, and thin-layer chromatography (TLC). Technical descriptions of these analytic methods are presented in *USP* General Chapter 621, Chromatography.[19] Methods commonly used in radiopharmaceutical analysis are discussed briefly below.

Gas Chromatography

GC is a valuable technique for qualitative and quantitative analysis of organic compounds (Figure 12-3). The GC system allows various components of a sample to be separated on the basis of their volatility and ability to partition between a high–boiling-point liquid stationary phase and a gaseous mobile phase. For complete analysis of complex mixtures of drug molecules, each component separated must possess a relatively high level of partitioning and volatility under the operating temperature range. The GC system usually consists of a gas supply, an injection port, a thermostat-controlled oven that contains the column, a detector system, and an integrator for recording retention time along with peak area information for the separated chemical species.

Sample Injection Port

The sample solution is introduced into the system through the injection port with a syringe. The sample volume should not be too large, and the sample should be introduced onto

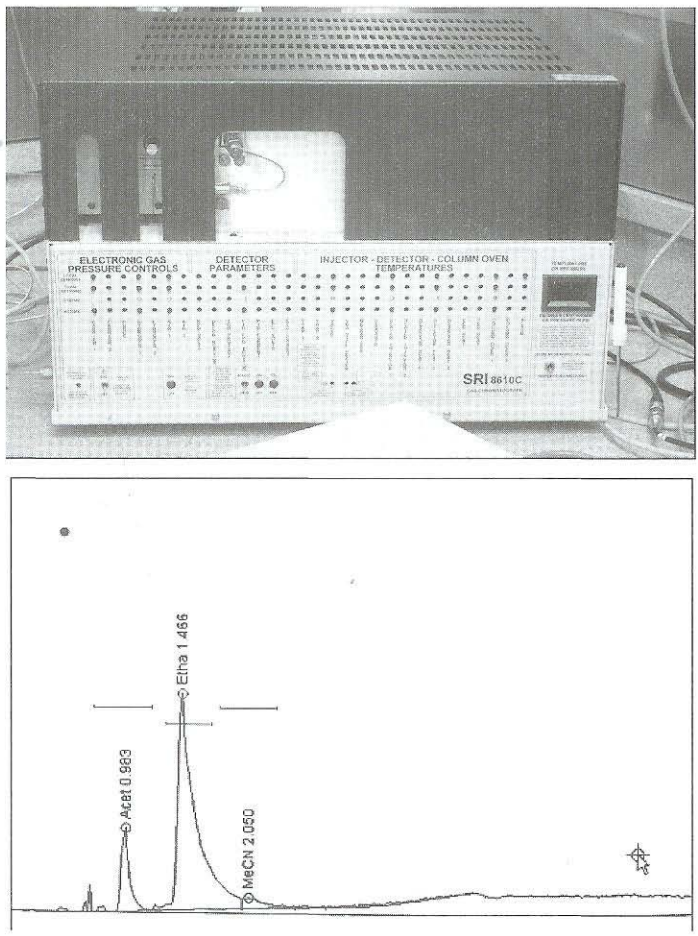

FIGURE 12-3 A gas chromatography system and a spectrum of various residual solvents detected from a preparation of fludeoxyglucose F 18 injection.

the column as a bolus to avoid loss of peak resolution. A silicone rubber septum is normally installed in the injection port to prevent leakage of the sample and mobile phase. The temperature of the sample injection port is usually set at approximately 50°C higher than the boiling point of the least volatile component of the sample, or at least 10°C to 15°C above the column oven temperature to ensure volatilization of sample components.

Mobile Phase Gases

The vaporized sample is transported through the column by the flow of inert gas (mobile phase) where separation of the sample components occurs. Nitrogen is typically used as the mobile phase, but other gases such as argon or helium are sometimes used. If necessary, the gases are filtered of impurities through special in-line absorbent cartridges. Regulator valves control the overall gas pressure from the tanks.

Columns

Two general types of columns are used for GC analysis, packed columns and capillary (open tubular) columns. A packed column contains a finely divided, inert, solid support material coated with liquid stationary phase. A capillary column has the stationary phase coated on the inside wall of a thin glass capillary tube. For precise work, column temperature

must be controlled within tenths of a degree. The optimum column temperature depends on the boiling point of the sample. As a rule, a temperature slightly above the average boiling point of the sample results in an elution time of 2 to 30 minutes. Minimal temperatures give good resolution but result in increased elution times. If a sample has a wide boiling point range, then temperature programming can be useful.

Detectors

Many types of detectors can be used in GC analysis. Mass selective detectors (MSD) are common, although electron capture, flame ionization, and thermal conductivity detectors are also used. An MSD has the added advantage of allowing identification of chemical components from the mass spectrum. With the flame ionization detector system, hydrogen and air are added to the column eluant at the detector and ignited to maintain a flame just above the column exit. When organic compounds are burned in the detector flame, ions are formed that change the voltage at the collector electrodes. As more molecules enter the detector, more ions are formed, increasing the intensity of the signal recorded by the integrator.

Chromatogram

The area under a chromatographic peak, known as the peak area, represents the total amount of analyte in a sample. The time, in minutes, between sample injection and analyte detection is referred to as retention time. It is a measure of the time an analyte spends on the column and is used qualitatively for analyte identification after comparison with a series of standards.

High-Performance Liquid Chromatography

HPLC is one of the most versatile tools used in radiopharmaceutical analysis, because it provides high-resolution component separation (Figure 12-4). HPLC can be used with organic or inorganic molecules, including nonvolatile species that cannot be analyzed by GC.

There are many different makes and models of chromatographs. The major components of any HPLC system include a mobile phase reservoir, pump, injector, column, detector, and recorder. Both the injector and the column are equipped with overflow reservoirs.

The analytic process begins with a mobile phase that is drawn up from the reservoir and propelled by the pump into the injector. Here, a sample is injected via an injection valve or by a syringe–septum arrangement and then carried through the column under pressure (up to 6000 psi) at a precisely controlled rate. The column is the heart of the system and is where component separation occurs. Separated components leave the column and enter a detector that measures the concentration of different solutes in the sample. A signal sent to a recording device (an integrator) generates a chromatogram that displays retention times and peak areas for each component.

Reservoir

The solvent reservoir holds the mobile phase required for the sample elution. Particulate matter in the mobile phase, which could clog the system, is removed by a fritted steel filter on the end of the uptake tube.

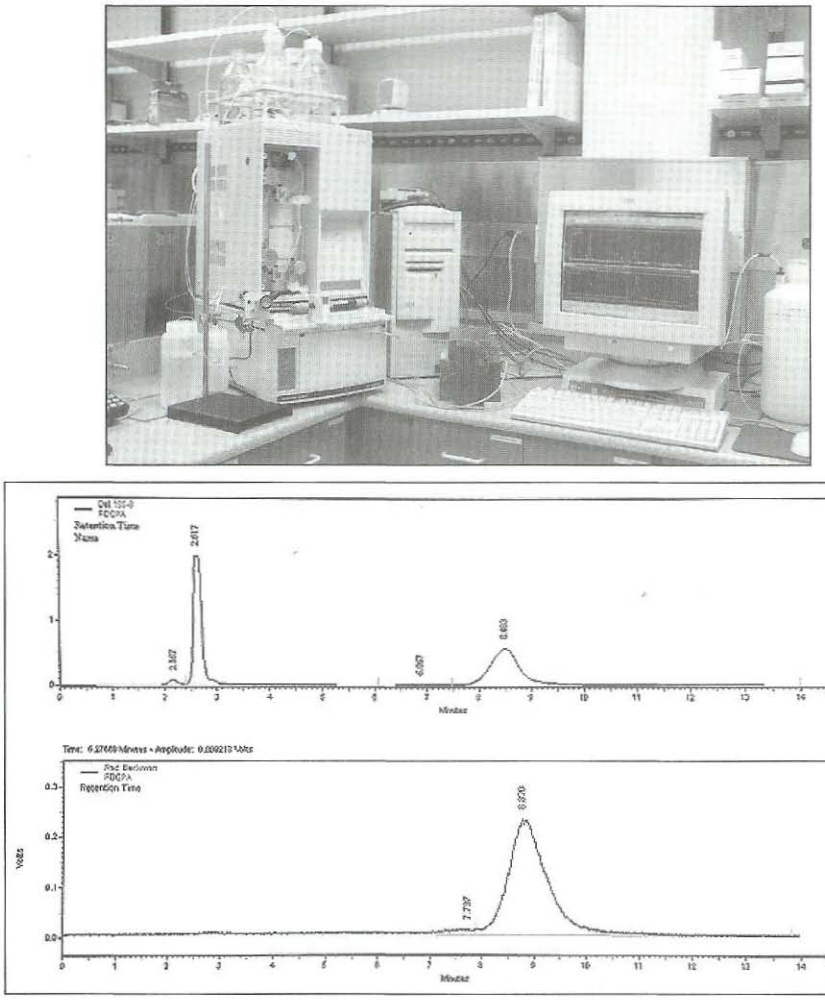

FIGURE 12-4 The upper panel illustrates a high-performance (pressure) liquid chromatography (HPLC) system coupled with a scintillation detector for analysis of fluorodopa F 18 injection. The upper spectrum, obtained with a UV detector, identifies the fluorodopa peak; the lower spectrum, generated with a radiation detector, identifies the ^{18}F activity associated with the fluorodopa peak.

Pump and Damper

A high-pressure pump draws up the mobile phase and drives it forward at a constant rate via a piston-type pump. Other pump types can also be used. The pump operates by withdrawing a piston, which creates a sudden drop in pressure in an internal chamber. To compensate, the mobile phase is drawn into the chamber through a lower one-way check valve. The upper exit valve is closed because of negative pressure. When the piston pushes back into the chamber, the pressure increases and the mobile phase is forced out. The upper check valve opens while the lower check valve blocks backflow.

A pulse damper is placed in line with the pump to reduce the pulsations caused by the action of the piston in the pump head. In this case, the pulse damper consists of a long expandable coil that smoothes out the flow of the mobile phase by stretching with each pulse of pressure from the pump and recoiling when the pressure ceases. Without the damper in place, the pulses would register as bumps on the chromatogram.

The pump should be capable of delivering a constant and pulse-free flow rate at pressures up to 6000 psi. This is achievable if the mobile phase is free of air. It is therefore essential that the solvent(s) be degassed before use. The mobile phase or eluant should be filtered free of particulate matter and should flow through an in-line filter before entering the pump head. Before analysis, the pump should always be bled of any trapped air by priming the pump head. Pump heads should be periodically inspected for leaks and pump seal wear. The check valves and pistons should also be regularly inspected for damage.

Sample Injector Port

From the pulse damper, the mobile phase travels to the injector, where it can either flow directly into the column via an internal loop or be redirected by the switching of a valve through an external loop where it picks up the sample. In the load position of the injector, the external loop is isolated from the high-pressure mobile phase, allowing the sample solution to be injected into the external loop at atmospheric pressure. Excess sample is removed via the injector overflow tube. External loops can vary in size, but the 20 µL size is common. When switched to the inject position, the mobile phase passes through the external loop, carrying the sample solution to the column at high pressure.

Injectors may become blocked, and the internal components (rotor seal, injection port seal) may wear with use. An injector should be visually inspected before use to check for leaks and to ensure that there is liquid flow through the injector loop pathway.

Columns

Columns are available in many different sizes. Some are used for analysis of small samples (i.e., analytic HPLC), while others are used for isolating large quantities of a particular component in a mixture (i.e., preparative HPLC).

HPLC analytic methods are of two types: normal-phase and reverse-phase. In normal-phase HPLC, the packing material is polar in nature (e.g., Si–O–Si–R packing), whereas the mobile phase consists of nonpolar solvent(s) (e.g., hexane, acetone, other hydrocarbons). Samples of moderate to strong polarity are well separated by normal-phase HPLC. In reverse-phase HPLC, the column uses a nonpolar stationary phase (e.g., C18 packing) and a relatively polar mobile phase (e.g., water, methanol, acetonitrile). In this system, polar analytes will elute from the column ahead of less polar analytes.

HPLC columns give little trouble if they have been properly conditioned, cleaned, and stored. End fittings should always be tight so that there are no leaks, and column frits should be replaced in the event of persistent leaks.

Detector

Analytes that are eluted from the column are monitored by a detector. A wide range of detectors are available for HPLC systems. The most common is the ultraviolet (UV) spectrophotometer. For working with radiopharmaceutical samples, a radiation detector is necessary. For the UV detector system, the analyte passes through a flow cell, altering the absorbance of UV light shone through it. This change in absorbance is recorded and printed out as a chromatogram peak. If a radiation detector is used, such as a NaI(Tl) detector, it will detect the concentration of radioactive components in the eluate. Detectors are generally very reliable; however, UV detectors should be periodically checked for cell

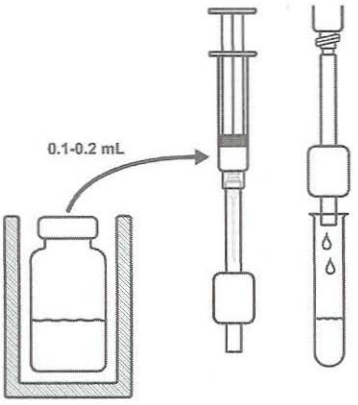

FIGURE 12-5 The Sep-Pak cartridge system for radiopharmaceutical purity determination. Radiopharmaceutical is applied to the cartridge, followed by elution of radioactive components.

gasket failure, cracked windows, leaks, and blockages in the flow cell. The source lamp of a UV detector will need to be replaced after it has reached its maximum life.

HPLC testing for radiochemical identity has some drawbacks: (1) An HPLC system is more expensive and elaborate; (2) an HPLC system is not widely available in nuclear medicine or nuclear pharmacy laboratories; and (3) completion of the test requires two HPLC runs, one with the test solution and another using the reference solution, whereas paper chromatography or TLC requires only one run for completion because the sample and reference standard are spotted on the same strip. Thus, for practical reasons, paper chromatography and TLC are the simplest and most rapid methods for routine QC testing of radiochemical species in radiopharmaceuticals.

Solid-Phase Extraction

Solid-phase extraction (SPE) is similar in principle to HPLC in that the technique involves a solid support medium coupled with a solvent mobile phase. A convenient device using this method is the Sep-Pak cartridge (Waters Chromatography, Millipore Corporation, Milford, Mass). Sep-Pak cartridges are disposable SPE devices commonly used for sample preparation (e.g., purification, trace enrichment or concentration, fractionation, solvent exchange) (Figure 12-5). They can also be used as analytic devices. Generally, the proper use of a Sep-Pak cartridge requires a five-step process: sample preparation, cartridge conditioning and equilibration, sample application, washing, and elution. However, the separation procedure for a given compound is unique, and not all of the five steps may be required for the application.

A Sep-Pak cartridge method described in the ^{99m}Tc-mertiatide (^{99m}Tc-MAG3) package insert is recommended for determining ^{99m}Tc-MAG3 radiochemical purity (RCP) and is described here to illustrate the SPE technique.[20] Reverse-phase chromatography with Sep-Pak C18 cartridges for RCP determination of ^{99m}Tc-MAG3 involves a series of steps using solvents of different polarities to separate the different radiochemical species.

1. Conditioning. The cartridge is conditioned with 6 to 10 void volumes of a moderately nonpolar, water-miscible solvent, such as methanol, ethanol, or acetonitrile, followed by a polar solvent similar to the sample solution. For ^{99m}Tc-MAG3, 10 mL of ethanol is used to prepare the cartridge, followed by 10 mL of 0.001 N hydrochloric acid. The cartridge is then drained by pushing 5 mL of air through it with the syringe; however, the cartridge should not be allowed to dry out before sample application.

2. Sample application and washing. If the less polar analyte is to be retained by the C18 sorbent and the more polar unwanted species eluted, the cartridge should be washed with a polar solvent in which the analyte has limited solubility. For ^{99m}Tc-MAG3, 0.1 mL of the ^{99m}Tc-MAG3 preparation solution is applied to the cartridge, and then the cartridge is rinsed with 10 mL of 0.001 N hydrochloric acid, whereupon ^{99m}Tc-MAG3, being the less polar analyte, is retained by the C18 sorbent while the more polar ^{99m}Tc-sodium pertechnetate and ^{99m}Tc-tartrate impurities are washed off.
3. Analyte elution. Elute the retained less polar analyte with a nonpolar or moderately polar solvent. For ^{99m}Tc-MAG3, 10 mL of ethanol is used to elute the ^{99m}Tc-MAG3.
4. When all components are recovered, discard the used cartridge in an appropriate manner. For ^{99m}Tc-MAG3, the cartridge will contain the retained hydrolyzed–reduced ^{99m}Tc (H-R ^{99m}Tc) impurity.

The separation efficiency of a Sep-Pak cartridge varies with flow rate and sample load. In general, resolution may be poor if the sample flow rate is too high, because components may not interact sufficiently with the sorbent. Overloading a sample onto the cartridge results in sample breakthrough, which later leads to variability in sample recovery or outcome interpretation.

The Sep-Pak cartridge can provide a complete chromatographic separation of ^{99m}Tc radiochemical species; however, the solvent elution process, costly cartridge, and lengthy procedure make the Sep-Pak cartridge method less than ideal for routine use in a busy nuclear medicine department or nuclear pharmacy. Possible technical errors can also occur with this cartridge method. For example, after radiopharmaceutical loading, the cartridge must be eluted slowly with an appropriate solvent; otherwise, the analyte bound to the sorbent (e.g., ^{99m}Tc-MAG3) may not be completely removed, resulting in false estimation of radiochemical identity or RCP (described in next section). Another disadvantage associated with the use of Sep-Pak cartridges for either radiochemical identification or RCP determination is the increased radiation exposure of the person performing the Sep-Pak procedure. The Sep-Pak cartridge method requires at least 0.1 mL of ^{99m}Tc radiopharmaceutical preparation to be loaded onto the cartridge. This volume may contain several millicuries (megabecquerels) of activity. For example, a regular ^{99m}Tc-MAG3 kit preparation will contain between 0.5 mCi (18.5 MBq) and 2.5 mCi (92.5 MBq) per 0.1 mL application. An alternative technique, using a two-strip paper chromatography system, requires only two 5 μL samples (50–250 μCi; 1.9–9.3 MBq) for RCP analysis and less than 3 minutes to complete the RCP determination for ^{99m}Tc-MAG3.[21]

Paper and Thin-Layer Chromatography

Paper chromatography and TLC methods are used most frequently to identify the various radiochemical species in a radiopharmaceutical preparation, especially for ^{99m}Tc-labeled radiopharmaceuticals. In each of these techniques, microliter amounts of the radiopharmaceutical are spotted at the origin of a chromatographic strip (the stationary phase). The chromatographic strip is then placed vertically in a chromatographic chamber (usually a vial or glass tube) that contains an appropriate solvent (mobile phase). The strip is placed in the solvent so that the origin of the spot is not immersed.

The stationary phase may be paper, such as Whatman 31ET or Gelman Solvent Saturation Pads. A modified thin-layer support called instant thin-layer chromatography (ITLC) is also used. This is a glass microfiber mesh impregnated with silica gel (ITLC-SG) or polysilicic acid (ITLC-SA), which results in a support resembling paper. The mobile

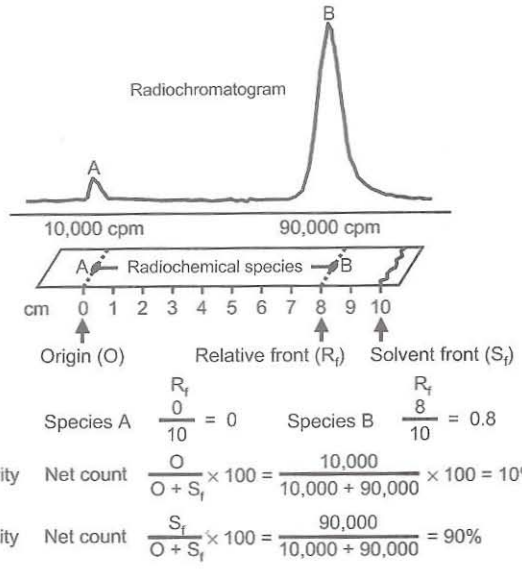

FIGURE 12-6 Radiochromatogram analysis. Species A represents the desired radiopharmaceutical; species B represents radiochemical impurity. See text for explanation of R_f and S_f.

phase is usually water, saline, or an organic solvent. The chromatographic chamber must be covered tightly to maintain a solvent-saturated atmosphere. The electrostatic forces (adsorption and capillary action) of the stationary phase tend to retard the movement of various radiochemical species, whereas the mobile phase carries each radiochemical component according to its partition between the stationary phase and the mobile phase. The partitioning of each radiochemical species between the stationary and mobile phases is determined by the solubility of the radiochemical species in the mobile phase, which is affected by the polarity of the solvent. Therefore, the electrostatic attractive forces of the stationary phase and the polarity of the mobile phase are the two determining factors in the separation of different radiochemical components in a sample.

Selection of appropriate support and solvent systems permits separation of the different chemical species in a radiopharmaceutical. After chromatogram development, the strip is removed, dried, and analyzed using a radiochromatogram scanner or another method for counting the radioactivity distribution on the strip.

The solvent front (S_f) is the distance that the solvent travels from the origin of the chromatographic strip, whereas the relative front (R_f) of a radiochemical component is the distance the component travels from the origin relative to the S_f (Figure 12-6).

R_f values for chemical components in a radiopharmaceutical are established by using known radiochemical species in a given chromatographic system. The identities of various radiochemical species present in a radiopharmaceutical are determined by comparing their R_f values with known R_f values in the same system. One of the following three methods can be used to determine R_f values and the relative amount of a radiochemical component in the radiopharmaceutical preparation for the purpose of determining RCP:

1. Scanning the strip with a radiochromatogram scanner that traces out various activity peaks (Figures 12-6 and 12-7). Peak position (its R_f) is indicative of the particular species present, and peak area corresponds to the respective amount of activity for each species.
2. Cutting the chromatogram into centimeter segments that are individually counted. Subsequently, a histogram plot of the activity distribution is made and the amount of activity in each species determined.

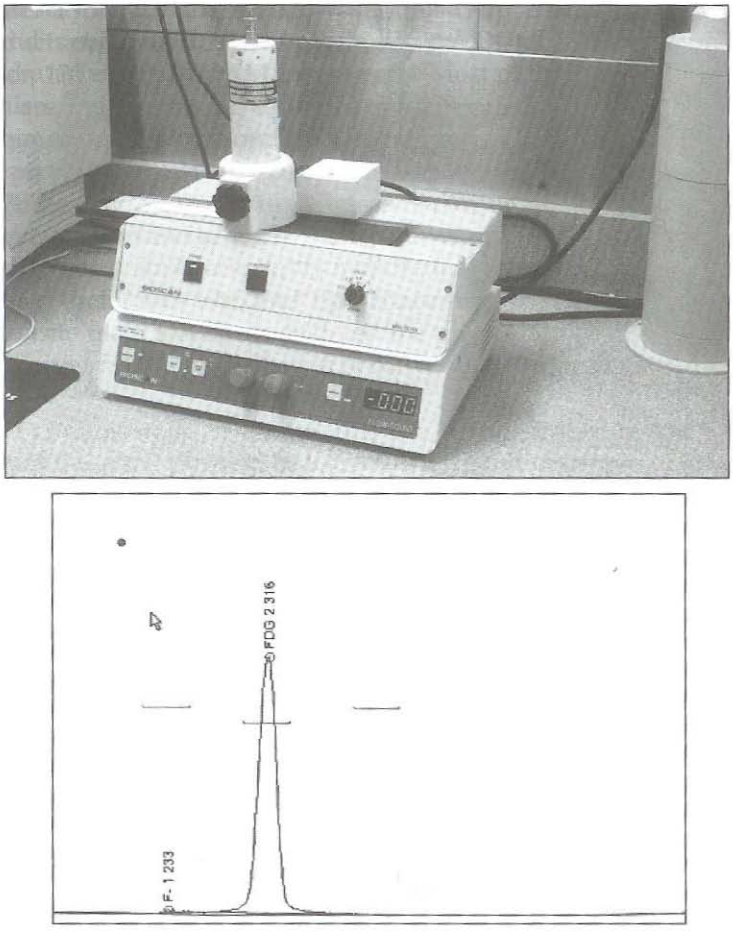

FIGURE 12-7 Radiochromatogram scanner and a spectrum of fludeoxyglucose F 18 injection.

3. Using a miniaturized chromatography system that uses a 6 cm strip. This method is used when the species are well separated on the strip so that it can be cut into two pieces and counted for analysis. This method is used routinely for ^{99m}Tc radiopharmaceuticals because it is rapid and easy to perform on a daily basis.

Paper chromatography and TLC methods are generally accurate and reliable; however, with these systems R_f values vary somewhat depending on the brand of solid support, quality of solvent, and operating conditions.[19] Consequently, radiochemical identification is best accomplished when a pure, authentic sample of the compound in question is used as a reference standard on the same chromatogram. In addition, although both test and standard (reference) solution samples are spotted on the same paper chromatography or TLC strip, the R_f values measured for the test substance may differ from the values obtained for the reference compound.[19] An acceptable range (as determined by system suitability testing described below) for this difference should be established.

To verify the resolution and reproducibility of any chromatographic system (e.g., GC, HPLC, TLC), suitability testing should be completed before sample analysis.[19,22] The difference in measured R_f values between the test and reference samples should not exceed reliability estimates as determined statistically from replicate assays.[19] These types of tests are necessary to validate a chromatographic system's precision and accuracy.

Technical Precautions in Performing Chromatography Procedures

ITLC and paper chromatography procedures are easy to perform and are usually trouble free; however, there are several procedural errors and artifactual results that can occur. Possible causes of the artifacts and errors are summarized below.[23–26]

1. Strips counted in a dose calibrator should contain at least 100 μCi (3.7 MBq) of activity to keep the counting error to 1% or less. This assumes dose calibrator sensitivity of 1 μCi (37 kBq) and, at minimum, a 1% impurity in a 100 μCi (3.7 MBq) sample. If a scintillation well counter is used for counting, the strips should be counted far enough away from the detector so that the counting rate does not exceed the dead time of the detector.[27,28] This is not a problem if the dose calibrator or radiochromatogram scanner is used for analysis.
2. The radiopharmaceutical sample spot should be placed at least 1 cm from the bottom of the strip so the spot itself does not enter the solvent but is well above its level. In this way the solvent will pass through the spot and cause soluble species to migrate in a normal manner. If the spot is even partly submerged in the solvent, these species will be retarded from migration and erroneous results will occur.[29]
3. Fresh chromatography strips and solvents should be used to ensure reproducibility in analysis.
4. To avoid incorrect analysis, care should be taken to not allow the solvent to migrate past the S_f line. If the strip is eluted significantly past the S_f line, the cut line must be changed to maintain the same R_f value.
5. Oxidation reactions or strip interactions can occur on the chromatography paper or ITLC strip. Reduced states of ^{99m}Tc are easily oxidized; therefore, the spot of radiopharmaceutical should not undergo prolonged air drying on the strip before it is placed in the solvent. ^{99m}Tc species may bind with the media or strip, which is often the cause of streaking (e.g., inadequate or no separation of free ^{99m}Tc and H-R ^{99m}Tc from the principal ^{99m}Tc complex).
6. In spotting the radiopharmaceutical, uneven spotting or splattering should be avoided.
7. Interaction of radiochemical species can occur with preparative compounds or ink markers used to visualize solvent flow.
8. Grease from fingerprints can alter migration patterns during development.
9. The chromatography strip should not be allowed to touch the side of the wet chromatography chamber, or solvent will rise up rapidly on the strip by capillary action, invalidating the analysis.
10. Cross-contamination of chromatography strips with other radiopharmaceuticals can lead to erroneous results.
11. Use of the wrong solvent or improper solvent preparation will alter results.
12. Use of the wrong chromatographic strips for a particular radiopharmaceutical will cause erroneous results.
13. Insufficient solvent in the chromatography chamber will cause solvent evaporation and incomplete development of the strip.
14. Use of contaminated tweezers or scissors when handling chromatographic paper or ITLC media can lead to spurious results.
15. Exposure of solvent to the atmosphere for too long can result in evaporation of one solvent in a mixture or absorption of water vapor in organic solvents, causing altered R_f values.
16. Mechanical factors such as chamber movement and unleveled surfaces may cause erroneous results.

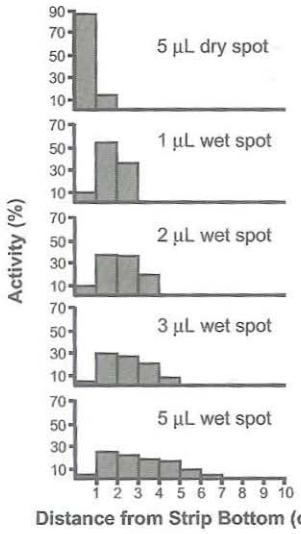

FIGURE 12-8 Demonstration of chromatogram streaking of ^{99m}Tc-DTPA with the instant thin-layer chromatography–silica gel (ITLC-SG)/acetone system as a function of wet spot size.

TABLE 12-2 Effect of Wet versus Dry Spot on Minichromatography Results (% Activity) for ^{99m}Tc-Labeled Compounds in ITLC-SG/Acetone System

	Wet Spot[a]		Dry Spot[a]	
Radiopharmaceutical	**Origin**	**Solvent Front**	**Origin**	**Solvent Front**
^{99m}Tc-gluceptate (GH)[b]	74.01	25.99	99.81	0.19
^{99m}Tc-pentetate (DTPA)[b]	60.04	39.96	99.70	0.30
^{99m}Tc-pyrophosphate (PYP or PPi)[b]	85.37	14.63	99.39	0.61
^{99m}Tc-medronate (MDP)[b]	82.60	17.40	99.82	0.18

[a] Results are means of five determinations on 5 cm ITLC-SG strips.

[b] Common chemical abbreviation.

Source: Reference 29.

Prolonged air drying of the applied sample spot on the chromatography strip is not desirable because the ^{99m}Tc complex may be oxidized.[29] Drying should be done quickly with a hot-air dryer or in a stream of nitrogen gas. Spot drying before development is important in some circumstances, however, particularly when organic solvents such as acetone are used and especially if the applied spot is 5 µL or larger. Acetone will mix freely with water. Hence, radiochemical species that are soluble in water but not soluble in acetone, such as ^{99m}Tc complexes, will streak up the strip from the origin if the spot is wet. If streaking extends into the top half of the strip, erroneous results will be obtained. This is more likely to occur with 5 cm ministrips than with standard 10 cm strips. If the applied spot is small, about 1 µL, drying of the spot may not be necessary.

Figure 12-8 shows that the extent of streaking depends on spot size, and Table 12-2 lists the results obtained with several ^{99m}Tc-labeled complexes developed on 5 cm ITLC-SG strips in acetone after application of a 5 µL wet or dried spot. It is evident from these data that significant migration (i.e., streaking) of the ^{99m}Tc-labeled complex occurs into the solvent-front half of the strip if a large wet spot is developed in acetone. During analysis

this would be interpreted as a ^{99m}Tc-sodium pertechnetate impurity, but it would be an artifact created by improper technique.[29]

Corrective Actions

If a low RCP value is obtained, one should

1. Review the RCP testing technique to ensure that the appropriate procedures to avoid errors and artifacts, as described above, have been followed. Repeat the RCP testing procedure.
2. If the RCP is still below the acceptable limit, discard the reconstituted kit and prepare another kit.
3. If several kits from the same lot number have failed RCP testing, notify the manufacturer.

The use of USP reference standards in evaluating radiochemical identity is ideal; however, reference standards for compounds of interest may not be available. A good example of this is the three reference standards for fludeoxyglucose F 18 (^{18}F-FDG) identified in the *United States Pharmacopeia* (i.e., USP Fludeoxyglucose, USP Fludeoxyglucose Related Compound A RS, and USP Fludeoxyglucose Related Compound B RS).[30] These USP-grade reference standards cannot be obtained from any commercial source. If the USP reference standard is not available, one can use a high-quality source of chemical substance, such as a substance that is listed as Food Chemicals Codes (FCC) grade, an authentic substances (AS) grade, an analytic reagent (AR), or a substance that has been certified by the American Chemical Society (ACS).[31] For non–positron emission tomography radiopharmaceuticals, the corresponding reference standard or high-quality chemical substance to the nonradioactive compound of interest usually does not exist or is not commercially available. Therefore, it may not be necessary to carry out radiochemical identity testing on reconstituted non-PET radiopharmaceuticals.

Counting Instruments for Radiochromatography

Radionuclide Dose Calibrators

The dose calibrator is often used for RCP measurements in the nuclear pharmacy because it is easy to use and results are obtained quickly. However, the accuracy of measurement with this instrument is of major concern if low amounts of radioactivity are used. In general, when a dose calibrator is used for RCP determination, the chromatography strips should contain 100 μCi (3.7 MBq) or more of activity in order to reduce the error to ≤1%.

Well Scintillation Counters

The gamma scintillation well counter is an appropriate instrument for counting chromatography strips; however, to achieve accurate assessment of radioactivity, the dead time of this instrument must not be exceeded. To avoid exceeding the maximum counting capabilities of the well counter, four different methods are recommended: (1) increasing the distance from source to detector; (2) using an attenuator on the well counter, such as an appropriately sized metal disk or coin placed over the opening of the well counter; (3) decreasing the activity of the radioactive sample; and (4) correcting for instrument dead time if the well counter is equipped with a device that automatically compensates for high amounts of radioactivity.[32]

Radiochromatogram Scanners

A radiochromatogram scanner (Figure 12-7) detects and measures the distribution of radioactivity along the intact radiochromatography strip. The scanner can analyze samples over a wide range of activities and assess the relative amounts of radiochemical species distributed over the strip; however, the procedure is time consuming and the instrument is quite expensive.

Radiochemical Purity

The RCP value of a radiopharmaceutical preparation is defined as the ratio, expressed as a percentage, of the radioactivity in the desired chemical form to the total radioactivity in the radiopharmaceutical preparation. For example, a 100 μCi (3.7 MBq) sample of ^{99m}Tc-sulfur colloid (SC) of which 95 μCi (3.5 MBq) is present as ^{99m}Tc bound to sulfur particles and 5 μCi (1.85 kBq) is ^{99m}Tc-sodium pertechnetate would have an RCP of 95%. The radiopharmaceutical product in this case contains a 5% ^{99m}Tc-sodium pertechnetate impurity.

Radiochemical impurities are undesirable because their distribution in the body differs from that of the radiopharmaceutical of interest, making it difficult to obtain useful information in nuclear medicine studies. High background counts that are due to the presence of radiochemical impurities in areas not of primary interest in the study can degrade image quality, interfere with diagnostic interpretation, and expose the patient to unnecessary absorbed radiation dose. For example, ^{99m}Tc-sodium pertechnetate present in bone imaging radiopharmaceuticals at 5% or greater impurities is readily seen as stomach and thyroid uptake on the scan, as shown in Figure 12-9.

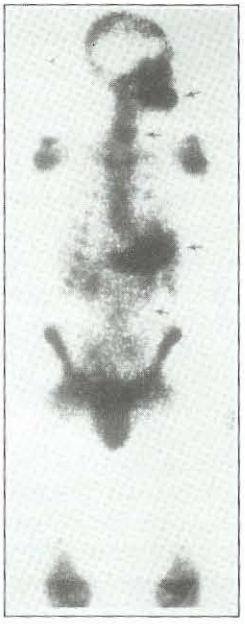

FIGURE 12-9 Whole-body bone scan with ^{99m}Tc-MDP showing ^{99m}Tc-sodium pertechnetate impurity localized in the salivary glands, thyroid, stomach, and intestinal tract (arrows).

Radiochemical impurities in radiopharmaceuticals can arise from a number of sources, including competing chemical reactions during radiolabeling, problems in preparative techniques, radiolytic decomposition of the product, oxidation–reduction reactions, and chemical changes during storage because of pH or temperature changes and exposure to light. Radiation causes decomposition of water, a major ingredient of most radiopharmaceutical preparations, leading to the production of reactive hydrogen atoms and hydroxyl radicals, hydrated electrons, hydrogen, hydrogen ions, and hydrogen peroxide. Hydrogen peroxide is formed in the presence of oxygen radicals, originating from the radiolytic decomposition of dissolved oxygen. Many radiopharmaceuticals show improved stability if oxygen is excluded. Radiation can also affect the radiopharmaceutical itself, giving rise to ions, radicals, and excited states. These species can combine with one another and with the active species formed from water. Radiation decomposition can be minimized by the use of chemical agents that act as electron or radical scavengers.

Relevant radiochemical impurities and their limits are usually listed in the package insert or in the *USP* monograph (Table 12-3). RCP requirements must be fulfilled throughout the useful life of the radiopharmaceutical. The three basic sources of information on

TABLE 12-3 Radiochemical Purity Limits of Commonly Used Radiopharmaceuticals from *USP 27* and Package Inserts

Radiopharmaceutical	USP Monograph[a]	Package Insert[a,b]
^{14}C-urea	90	NA
^{57}Co-cyanocobalamin	95	NA
^{51}Cr-sodium chromate	90	NA
^{18}F-sodium fluoride	95	NA
^{18}F-fludeoxyglucose (^{18}F-FDG)[c]	90	90
^{67}Ga-gallium citrate	97	NA
^{111}In-capromab pendetide (ProstaScint, Cytogen)[d]	90	90
^{111}In-indium chloride	95	95
^{111}In-ibritumomab tiuxetan (Zevalin, IDEC Pharmaceuticals)[d]	NA	95
^{111}In-oxyquinoline (oxine)[c]	90	NA
^{111}In-pentetate (DTPA)[c]	90	NA
^{111}In-pentetreotide (OctreoScan, Mallinckrodt)[d]	90	90
^{123}I-iobenguane (MIBG)[e]	90	NA
^{123}I-iodohippurate sodium	97	NA
^{123}I-sodium iodide	95	NA
^{125}I-iodinated albumin	97	NA
^{125}I-sodium iothalamate	98	NA
^{131}I-iobenguane	90	NA
^{131}I-iodinated albumin	97	NA
^{131}I-iodomethylnorcholesterol (NP59)[e]	NA	NA
^{131}I-sodium iodide	95	NA
^{131}I-tositumomab (Bexxar)[d]	NA	NA
^{13}N-ammonia	95	NA
^{32}P-chromic phosphate	95	NA
^{32}P-sodium phosphate	100	NA
^{82}Rb-rubidium chloride	NA	NA
^{153}Sm-lexidronam (EDTMP)[c]	99	NA
^{89}Sr-strontium chloride	NA	NA
^{99m}Tc-albumin aggregated or ^{99m}Tc-macroaggregated albumin (MAA)[c]	90	NA
^{99m}Tc-apcitide (AcuTect, Rentschler Biotechnologie)[d]	90	90
^{99m}Tc-arcitumomab (CEA-Scan, Immunomedics)[d]	95	90
^{99m}Tc-bicisate (ECD)[c] (Neurolite, Bristol Myers Squibb Medical Imaging)[d]	90	90
^{99m}Tc-depreotide (NeoTect, Rentschler Biotechnologie)[d]	90	90
^{99m}Tc-disofenin (DISIDA)[c] (Hepatolite, CIS-US)[d]	90	NA
^{99m}Tc-exametazime (HMPAO)[c] (Ceretec, Nycomed Amersham)[d]	80	80
^{99m}Tc-gluceptate (GH)[c]	90	NA
^{99m}Tc-mebrofenin (BRIDA)[c] (Choletec)[d]	90	NA
^{99m}Tc-medronate (MDP)[c]	90	NA
^{99m}Tc-mertiatide (MAG3)[c] (TechneScan MAG3, Mallinckrodt)[d]	90	90
^{99m}Tc-oxidronate (HDP)[c]	90	NA
^{99m}Tc-pentetate (DTPA)[c]	90	NA
^{99m}Tc-sodium pertechnetate	95	NA
^{99m}Tc-pyrophosphate (PYP or PPi)[c]	90	NA
^{99m}Tc-red blood cells (UltraTag, Mallinckrodt)[d]	90	NA
^{99m}Tc-sestamibi (Cardiolite and Miraluma, Bristol Myers Squibb Medical Imaging)[d]	90	90
^{99m}Tc-succimer (DMSA)[c]	85	NA
^{99m}Tc-sulfur colloid (SC)[c]	92	NA
^{99m}Tc-tetrofosmin (Myoview, Amersham Health AS)[d]	90	90
^{201}Tl-thallous chloride	95	NA
^{133}Xe-xenon gas	85	NA
^{90}Y-ibritumomab tiuxetan (Zevalin)[d]	NA	95

TABLE 12-3 Radiochemical Purity Limits of Commonly Used Radiopharmaceuticals from *USP 27* and Package Inserts (Continued)

[a] Minimum percent radiochemical purity.
[b] NA = not available.
[c] Common chemical abbreviation.
[d] Brand name of the reagent kit.
[e] Investigational new drug application (IND) with the University of Michigan required.

RCP test methods are the *United States Pharmacopeia*, package inserts, and the published literature. However, because the information provided in these sources is not always complete or practical, it can be difficult to select and perform adequate RCP testing on the prepared radiopharmaceutical.[15,33] Table 12-4 lists routinely used chromatography methods for reconstituted radiopharmaceuticals.[34–55] The methods in Table 12-4 are taken from package inserts or the published literature, and selection of various published RCP testing methods was based on the rating system described in a compilation of procedures published by the American Pharmacists Association.[56]

Radiopharmaceuticals labeled with ^{99m}Tc are widely used in nuclear medicine studies. There are four principal radiochemical species that can be present in stannous-reduced ^{99m}Tc-labeled radiopharmaceuticals: (1) the ^{99m}Tc complex, which is the desired radiochemical species; (2) free ^{99m}Tc in the form of ^{99m}Tc-sodium pertechnetate (it was not reduced initially because of low levels of divalent stannous ions [Sn^{2+}] or was reduced but then reoxidized); (3) H-R ^{99m}Tc, which includes reduced ^{99m}Tc that reacts with water to form various hydrolyzed species (e.g., $^{99m}TcO_2$) and ^{99m}Tc-Sn^{2+}colloids formed by the binding of reduced ^{99m}Tc to hydrolyzed stannous ion; and (4) ^{99m}Tc complexes of transfer ligands such as glucoheptonate and tartrate. Free ^{99m}Tc-sodium pertechnetate increases tissue background activity because of activity localized in the stomach, gut, and thyroid gland (Figure 12-9). H-R ^{99m}Tc, as TcO_2 or ^{99m}Tc-Sn colloid, not only compromises the labeling yield of the ^{99m}Tc complex but also interferes with imaging interpretation because of its localization in the reticuloendothelial system.

In general, with technetium chromatography systems, H-R ^{99m}Tc contaminants remain at the origin ($R_f = 0.0$) because they are insoluble particles, and free ^{99m}Tc-sodium pertechnetate travels to the solvent front ($R_f = 1.0$) in most solvents. The ^{99m}Tc complex may have an $R_f = 0.0$ or 1.0 or somewhere in between, depending on the system used. A simple chromatography system for RCP determination would allow the ^{99m}Tc complex to migrate to the S_f, with free ^{99m}Tc-sodium pertechnetate and H-R ^{99m}Tc remaining at the origin. This type of system is illustrated for ^{99m}Tc-sestamibi, as an example, in Figure 12-10. The RCP for the ^{99m}Tc complex is easily calculated by dividing the radioactivity on the top portion of the strip by the total activity in both sections of the chromatography strip. Many other ^{99m}Tc-labeled complexes require a two-solvent dual-strip system to determine RCP, because the ^{99m}Tc complex is always associated with one of the two radiochemical impurities (i.e., either free ^{99m}Tc or insoluble H-R ^{99m}Tc) and cannot be isolated by itself. This is illustrated in Figure 12-11 for ^{99m}Tc-apcitide, which has three impurities (free ^{99m}Tc-sodium pertechnetate, ^{99m}Tc-glucoheptonate, and insoluble ^{99m}Tc). Thus, the RCP of the ^{99m}Tc complex is determined indirectly by subtracting the percentage of each radiochemical impurity from 100% to obtain the percentage of the ^{99m}Tc complex.

Assessment of Radioactivity

The previous version of Part 35 in Title 10 of the Code of Federal Regulations (CFR) required that each radiopharmaceutical dose be assayed in a dose calibrator unless it was

TABLE 12-4 Chromatographic Systems for Reconstituted Radiopharmaceuticals

Radiopharmaceutical	Stationary Phase[a]	Mobile Phase	Relative Front (R_f) Values: Labeled Complex	Relative Front (R_f) Values: Unlabeled Radioisotope	Relative Front (R_f) Values: Other Radiochemical Impurities	Minimum RCP[b]	Special Instructions	Ref.
^{111}In-capromab pendetide (ProstaScint)[c]	ITLC-SG	0.9% NaCl	0.0–0.5	0.5–1.0	0.5–1.0	90	d	34
^{111}In-Ibritumomab tiuxetan (Zevalin)[c]	ITLC-SG	0.9% NaCl	0.0–0.5	0.5–1.0	0.5–1.0	95		35
^{111}In-pentetreotide (OctreoScan)[c]	Waters Sep-Pak C18 cartridge	e	e	e	e	90	e	36
^{99m}Tc-albumin aggregated or ^{99m}Tc-macroaggregated albumin (MAA)[f]	Whatman 31ET	Acetone	0.0	1.0	0.0	90		37
^{99m}Tc-apcitide (AcuTect)[c]	ITLC-SG	Water	0.25–1.0	0.25–1.0	0.0–0.25, 0.25–1.0[g]	90	h	38
	ITLC-SG	Saturated NaCl solution (SAS)[i]	0.0–0.75	0.75–1.0	0.0–0.75, 0.75–1.0[j]			
^{99m}Tc-arcitumomab (CEA-Scan)[c]	ITLC-SG	Acetone	0.0–0.5	0.5–1.0	0.0–0.5	90/95[k]		39
^{99m}Tc-bicisate (ECD)[f] (Neurolite)[a]	1. Bakerflex silica gel 1B-F	Ethyl acetate	1.0	0.0	0.0	90	l	40
	2. Whatman 17	Ethyl acetate	1.0	0.0	0.0	90		41
^{99m}Tc-depreotide (NeoTect)[c]	ITLC-SG	Methanol:1 M Ammonium acetate (1:1, v/v) (MAM)[f]	0.4–1.0	0.4–1.0	0.0–0.4, 0.4–1.0[m]	90	n	42
	ITLC-SG	SAS[i]	0.0–0.75	0.75–1.0	0.0–0.75, 0.75–1.0[o]			
^{99m}Tc-disofenin (DISIDA)[f] (Hepatolite)[c]	ITLC-SA	20% NaCl	0.0	1.0	0.0	90		43
^{99m}Tc-exametazime (HMPAO)[f] (Ceretec)[c]	1. ITLC-SG	Methyl ethyl ketone	0.8–1.0	0.8–1.0	0.0[p]	80		44
	ITLC-SG	0.9% NaCl	0.0	0.8–1.0	0.0			
	Whatman 31ET	50% Acetonitrile	0.8–1.0	0.8–1.0	0.8–1.0/0.0[q]			
	2. Gelman Solvent Saturation Pads	Ether	1.0	0.0	0.0	80		45,46

TABLE 12-4 Chromatographic Systems for Reconstituted Radiopharmaceuticals (Continued)

[a] ITLC-SA = instant thin-layer chromatography–polysilicic acid; ITLC-SG = instant thin-layer chromatography–silica gel; TLC = thin-layer chromatography.

[b] RCP = radiochemical purity.

[c] Brand name of the reagent kit.

[d] Before applying the test sample to the ITLC-SG strip, mix equal parts (several drops of each) of ^{111}In-capromab pendetide with 0.05 M ^{99m}Tc-DTPA solution and allow the mixture to stand at room temperature for 1 minute.

[e] Slowly push 10 mL of methanol through the longer end of a fresh Waters Sep-Pak C18 cartridge. Similarly, rinse the cartridge with 10 mL water and then with another 5 mL water. Discard the eluates. Load 0.05–0.1 mL of ^{111}In-pentetreotide on the longer end of the cartridge column, making sure the test sample migrates onto the column and not into the tube neck. With a disposable syringe, slowly push (in dropwise manner) 5 mL of water through the longer end of the cartridge, using a test tube (tube 1) to collect the eluate. Similarly, elute the cartridge with 5 mL methanol drop by drop and collect the eluate in a test tube (tube 2). Place the Sep-Pak cartridge in a test tube (tube 3). The percentages of ^{111}In-pentetreotide (tube 2), hydrophilic impurities (tube 1), and nonelutable impurities (tube 3) are calculated by dividing the radioactivity in each tube by the total of activity of all three tubes.

[f] Common chemical abbreviation.

[g] ^{99m}Tc immobile materials (R_f = 0.0–0.25), ^{99m}Tc-glucoheptonate (R_f = 0.25–1.0).

[h] RCP of ^{99m}Tc-apcitide = 100 – (% activity in the bottom piece of ITLC-SG water strip + % activity in the top piece of ITLC-SG SAS strip).

[i] Mix 5 grams of NaCl with 5 to 10 mL of water and shake periodically for 10 to 15 minutes. Add more NaCl and shake again for 10 to 15 minutes until a solid residue remains.

[j] ^{99m}Tc immobile materials (R_f = 0.0–0.75), ^{99m}Tc-glucoheptonate (R_f = 0.75–1.0).

[k] Package insert: 90%; *USP*: 95%.

[l] (1)Pre-equilibrate the chromatographic developing tank with ethyl acetate for 15 to 30 minutes. (2) The sample spot should not be greater than 10 mm; allow the spot to dry for 5 to 10 minutes. (3) The developing time is approximately 15 minutes.

[m] ^{99m}Tc nonmobiles (R_f = 0.0–0.4), ^{99m}Tc-glucoheptonate and ^{99m}Tc-edetate (R_f = 0.4–1.0).

[n] RCP of ^{99m}Tc-depreotide = 100 – (% activity in the bottom piece of ITLC-SG MAM strip + % activity in the top piece of ITLC-SG SAS strip).

[o] ^{99m}Tc nonmobiles (R_f = 0.0–0.75), ^{99m}Tc-glucoheptonate and ^{99m}Tc-edetate (R_f = 0.75–1.0).

[p] Secondary ^{99m}Tc-exametazime complex and hydrolyzed–reduced (H-R) ^{99m}Tc stay at the origin.

[q] Secondary ^{99m}Tc-exametazime complex migrates to R_f 0.8 to 1.0, whereas H-R ^{99m}Tc remains at the origin.

[r] (1) Preparation of Sep-Pak C18 cartridge. The Sep-Pak C18 cartridge is first flushed with 10 mL of 200 proof ethanol, followed by flushing with 10 mL of 0.001 N HCl. The cartridge is then drained by pushing 5 mL of air through the cartridge with a syringe. (2) Sample analysis. Apply 0.1 mL of ^{99m}Tc-mertiatide to the long end of the cartridge. The cartridge is then eluted successively with 10 mL of 0.001N hydrochloric acid and 10 mL of 1:1 ethanol/0.9% sodium chloride solution. The two fractions of sample eluates and cartridges are collected in separate culture tubes for counting. (3) Counting. The radioactivity of the first sample elution (hydrophilic ^{99m}Tc impurity plus a fraction of H-R ^{99m}Tc), the second sample elution (^{99m}Tc-mertiatide), and the cartridge (the remaining H-R ^{99m}Tc plus nonelutable impurities) is assayed in a dose calibrator. The percentages of ^{99m}Tc-mertiatide (fraction 2), hydrophilic ^{99m}Tc species (primarily H-R ^{99m}Tc), and nonelutable impurities are calculated by dividing each fraction of radioactivity by the total of activity of both sample liquid fractions and the cartridge.

[s] Hydrophilic ^{99m}Tc impurity migrates to R_f 0.5 to 1.0, whereas H-R ^{99m}Tc remains at the origin.

[t] (1) Transfer 0.2 mL of ^{99m}Tc-red blood cells (RBC) to a centrifuge tube containing 2 mL of 0.9% NaCl. (2) Centrifuge the ^{99m}Tc-RBC sample at 150*g* for 1 minute. (3) Carefully pipette off the diluted plasma. (4) Measure the radioactivity in the plasma and the RBCs separately in a dose calibrator. (5) Calculate the labeling efficiency of ^{99m}Tc-RBC as follows:

$$\% \text{ RBC labeling} = [\text{RBC activity} \div (\text{RBC activity} + \text{Plasma activity})] \times 100.$$

[u] (1) The TLC plate has to be predried in an oven at 100°C for 1 hour. (2) After two drops of ^{99m}Tc-sestamibi sample are applied side-by-side on top of the ethanol wet spot, the TLC plate is placed in a desiccator to allow the spot to dry before the plate is developed in the TLC tank. (3) This TLC system requires about 30 minutes to complete the drying and development.

[v] Slowly push 5 mL of ethanol (100% ethanol is preferable) through the longer end of a fresh Waters Sep-Pak alumina N cartridge. Load 0.05 to 0.1 mL of ^{99m}Tc-sestamibi on the longer end of the cartridge column, making sure the test sample gets on the column and not in the tube neck. With a disposable syringe, slowly push (in dropwise manner) 10 mL of ethanol through the longer end of the cartridge, using a test tube (tube 1) to collect the eluate. Follow with a few milliliters of air to collect all of the ethanol. Place the Sep-Pak cartridge in a test tube (tube 2). The percentage of ^{99m}Tc-sestamibi (tube 2) is calculated by dividing the radioactivity in tube 2 by the total activity in tubes 1 and 2.

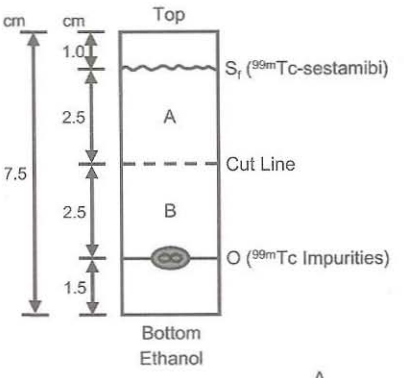

FIGURE 12-10 Single-strip thin-layer chromatography system for radiochemical purity (RCP) determination of ^{99m}Tc-sestamibi.

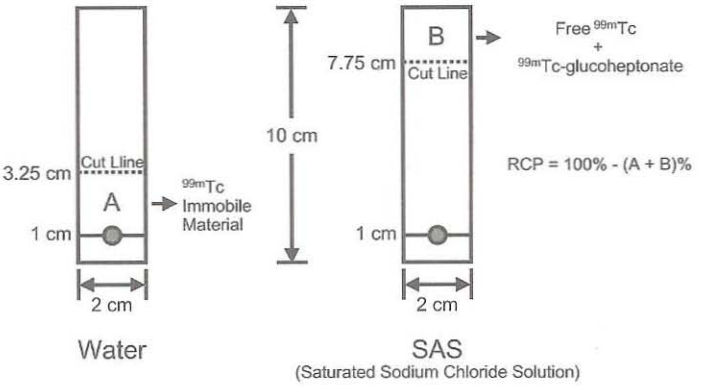

FIGURE 12-11 Dual-strip ITLC-SG systems for radiochemical purity (RCP) determination of ^{99m}Tc-apcitide (AcuTect, Rentschler Biotechnologie).

a pure beta- or alpha-emitting material.[57] Changes in 10 CFR 35.63, "Determination of dosages of unsealed byproduct material for medical use" are as follows:[58]

- For a unit dose (a radiopharmaceutical dose that is received in a unit form and is not manipulated by the licensee), the dosage may be determined by direct measurement of activity (e.g., in a dose calibrator), or based upon the reported activity by a manufacturer or a preparer licensed under 10 CFR 32.72 (e.g., a licensed nuclear pharmacy) and accounting for decay.[59]
- For a non–unit dose (anything prepared or manipulated by the licensee), the dosage may be determined by a direct measurement, a combination of measurement of dosage and mathematical calculations, or a combination of volumetric measurements and mathematical calculations based upon the measurement made by a manufacturer or preparer licensed under 10 CFR 32.72.[59]

A dose calibrator is commonly used in a nuclear pharmacy for determination of the amount of radioactivity because it permits rapid and accurate measurement of radiopharmaceutical dosages. However, accurate measurement of a dosage with a dose calibrator depends on the following factors: (1) a properly calibrated dose calibrator (see the section titled Quality Control of a Dose Calibrator), (2) adherence to the specified measurement range (i.e., maximum and minimum measurable radioactivity), (3) the type of container (e.g., syringe, vial, test tube) and the filling volume of solution in the container.

Certain radionuclides, such as ^{123}I, ^{111}In, and ^{133}Xe, not only have high-energy photopeaks but also emit substantial amounts of low-energy characteristic x-rays that produce variations in dosage measurements, especially when different container configurations or materials are used.[60,61] With the use of a copper filter (0.6 mm thickness), one can effectively reduce the low-energy component of ^{123}I and ^{111}In, even when these radionuclides are placed in various types of containers and are dispensed in different solution volumes.[62] ^{90}Y has attracted much research and clinical attention in radioimmunotherapy (especially with regard to its role in the Zevalin [ibritumomab tiuxetan] radiotherapeutic regimen) because its 64 hour half-life and pure beta emissions are very useful in cancer therapy. Although the typical dose calibrator has been designed to measure gamma-emitting radionuclides, it may also be quite useful in dosage measurement of pure beta emitters such as ^{90}Y using its readily produced bremsstrahlung radiation.[63–65]

According to the new 10 CFR 35,[58] if the dosage of a radiopharmaceutical preparation needs to be assayed, with regard to all beta- and difficult-to-measure gamma-emitting materials (e.g., ^{153}Sm), it would be sensible to use volumetric measurements and mathematical calculations. For all other radiopharmaceutical preparations, a dose calibrator can be used to directly measure the radioactivity.

The amount of radioactivity in a radiopharmaceutical is usually determined either by whole-vial assay or by counting an aliquot of the radiopharmaceutical in a dose calibrator. Radioactive concentration is usually expressed in terms of specific activity, which is defined as the activity per unit weight of the labeled compound (e.g., millicuries per gram or megabecquerels per gram), or specific concentration, which is defined as the activity per unit volume (e.g., millicuries per milliliter or megabecquerels per milliliter). The value of the radioactive concentration is usually stated on the vial label along with the calibration date and time; however, the new 10 CFR 35.69 "Labeling of vials and syringes" requires only that the identity of the radioactive drug be shown on the label.[66] Although curies or millicuries are the units of radioactivity commonly used in the United States, the becquerel is the internationally recognized unit for radioactivity. Therefore, it is sensible to include megabecquerels and megabecquerels per milliliter on the vial or syringe label. It is common practice that each vial or syringe of a radiopharmaceutical be radioassayed to confirm that activity is within ±10% of the labeled amount of activity after decay correction. It is interesting to note that the new 35.63 allows a difference of ±20% between the measured dosage and the prescribed dosage.[58]

It is important to verify the stated activity on the label of a radiopharmaceutical received by a nuclear medicine department or nuclear pharmacy. The European Association of Nuclear Medicine reported its findings with regard to defects in radiopharmaceuticals and noted instances in which incorrect radioactivities were provided by manufacturers.[3–8] Its 2000 annual report states that the measured activity of one shipment of ^{131}I therapeutic capsules was 20% to 40% higher than that stated on the labels.[8] This illustrates the importance of assaying the radioactivity of any radioactive material received. A concern raised by this finding is that without some type of assay on receipt, dosage calculations determined by volumetric measurements and mathematical calculations based on information provided by the manufacturer could result in incorrect dosing of patients. This would be particularly significant for pure beta- or alpha-emitting material, which is difficult or impossible to assay in a dose calibrator. Some method for assessing the activity of all radiopharmaceuticals should be a part of the standard of practice to avoid misadministration to patients.

Regarding the assessment of ^{18}F radioactivity, the *European Pharmacopeia* stipulates that a standardized ^{18}F solution should be used. However, this requirement can be satisfied with the use of ^{137}Cs (662 keV) standard, because its energy is close to that of ^{18}F (511 keV).[67]

Certain radionuclides, such as ^{123}I, ^{111}In, and ^{133}Xe, not only have high-energy photopeaks but also emit substantial amounts of low-energy characteristic x-rays that produce variations in dosage measurements, especially when different container configurations or materials are used.[60,61] With the use of a copper filter (0.6 mm thickness), one can effectively reduce the low-energy component of ^{123}I and ^{111}In, even when these radionuclides are placed in various types of containers and are dispensed in different solution volumes.[62] ^{90}Y has attracted much research and clinical attention in radioimmunotherapy (especially with regard to its role in the Zevalin [ibritumomab tiuxetan] radiotherapeutic regimen) because its 64 hour half-life and pure beta emissions are very useful in cancer therapy. Although the typical dose calibrator has been designed to measure gamma-emitting radionuclides, it may also be quite useful in dosage measurement of pure beta emitters such as ^{90}Y using its readily produced bremsstrahlung radiation.[63–65]

According to the new 10 CFR 35,[58] if the dosage of a radiopharmaceutical preparation needs to be assayed, with regard to all beta- and difficult-to-measure gamma-emitting materials (e.g., ^{153}Sm), it would be sensible to use volumetric measurements and mathematical calculations. For all other radiopharmaceutical preparations, a dose calibrator can be used to directly measure the radioactivity.

The amount of radioactivity in a radiopharmaceutical is usually determined either by whole-vial assay or by counting an aliquot of the radiopharmaceutical in a dose calibrator. Radioactive concentration is usually expressed in terms of specific activity, which is defined as the activity per unit weight of the labeled compound (e.g., millicuries per gram or megabecquerels per gram), or specific concentration, which is defined as the activity per unit volume (e.g., millicuries per milliliter or megabecquerels per milliliter). The value of the radioactive concentration is usually stated on the vial label along with the calibration date and time; however, the new 10 CFR 35.69 "Labeling of vials and syringes" requires only that the identity of the radioactive drug be shown on the label.[66] Although curies or millicuries are the units of radioactivity commonly used in the United States, the becquerel is the internationally recognized unit for radioactivity. Therefore, it is sensible to include megabecquerels and megabecquerels per milliliter on the vial or syringe label. It is common practice that each vial or syringe of a radiopharmaceutical be radioassayed to confirm that activity is within ±10% of the labeled amount of activity after decay correction. It is interesting to note that the new 35.63 allows a difference of ±20% between the measured dosage and the prescribed dosage.[58]

It is important to verify the stated activity on the label of a radiopharmaceutical received by a nuclear medicine department or nuclear pharmacy. The European Association of Nuclear Medicine reported its findings with regard to defects in radiopharmaceuticals and noted instances in which incorrect radioactivities were provided by manufacturers.[3–8] Its 2000 annual report states that the measured activity of one shipment of ^{131}I therapeutic capsules was 20% to 40% higher than that stated on the labels.[8] This illustrates the importance of assaying the radioactivity of any radioactive material received. A concern raised by this finding is that without some type of assay on receipt, dosage calculations determined by volumetric measurements and mathematical calculations based on information provided by the manufacturer could result in incorrect dosing of patients. This would be particularly significant for pure beta- or alpha-emitting material, which is difficult or impossible to assay in a dose calibrator. Some method for assessing the activity of all radiopharmaceuticals should be a part of the standard of practice to avoid misadministration to patients.

Regarding the assessment of ^{18}F radioactivity, the *European Pharmacopeia* stipulates that a standardized ^{18}F solution should be used. However, this requirement can be satisfied with the use of ^{137}Cs (662 keV) standard, because its energy is close to that of ^{18}F (511 keV).[67]

Specific Activity

Specific activity is defined as the radioactivity of the radionuclide per unit mass of the element or of the chemical form concerned. It is a critical specification especially for the receptor-binding radiopharmaceuticals, to ensure that adequate amounts of these radioactive drugs will be taken up by the associated receptors.

Specific activity changes with time. Therefore, the statement of the specific activity should include a date and, if necessary, a time. The requirement of the specific activity must be fulfilled throughout the period of validity.

No testing for specific activity of a radiopharmaceutical preparation is required if the radionuclide of interest is prepared by a no-carrier-added method of synthesis. If carrier-added synthesis is used for production of the radionuclide concerned, the appropriate test and acceptance criteria as well as the testing frequency for specific activity must be defined.

CHEMICAL CONSIDERATIONS

Chemical Purity

Chemical purity is a measurement of the presence of undesirable chemical species in radiopharmaceuticals. This assessment is important to ensure that the presence of any chemical substance with potential toxic, physiologic, or pharmacologic effects is within appropriate limits. Chemical purity testing should be performed on any chemical substance that is either used or formed during the synthesis of a radiopharmaceutical preparation, even though such substances may not be listed in the *USP* monograph or package insert (e.g., chemical impurities, unlabeled ingredients, reagents, and byproducts).[1]

Examples of chemical impurities significant to nuclear pharmacy are as follows:

1. Aluminum ion (Al^{3+}) in ^{99}Mo–^{99m}Tc generator eluate. Excessive Al^{3+} can induce flocculation of ^{99m}Tc-SC because Al^{3+} combines with the phosphate buffer in the product to form insoluble aluminum phosphate.[68,69] In bone scanning, liver localization and degradation of image quality have been noted when Al^{3+} concentrations exceed 10 μg per milliliter of ^{99m}Tc eluate.[69] Accordingly, *USP* limits the concentration of aluminum ion in ^{99m}Tc-sodium pertechnetate to 10 μg/mL.[70] Assessment of aluminum ion concentration in the ^{99m}Tc eluate is usually performed with a colorimetric spot test (discussed in Chapter 8) and should be done on every eluate.
2. Carrier iodine in radioiodide solution. Carrier iodine can compete with radioiodine in the radiodination process, resulting in poor labeling efficiency, and will interfere with uptake of tracer radioiodide in the thyroid gland.
3. Trace metals such as iron in ^{111}In-indium chloride solution. Trace metals have been known to significantly reduce labeling yields with ^{111}In, especially in platelet labeling with ^{111}In-oxine.

For ^{18}F-FDG injection, potential chemical impurities are aminopolyether 4,7,13,16,21,24-hexaoxa-1,10-diazabicyclo-(8,8,8)-hexacosane (Kryptofix 2.2.2. [Sigma-Aldrich], or K222), 2-chloro-2-deoxy-D-glucose (ClDG), 2-fluoro-2-deoxy-D-glucose (FDG), tetra-alkyl ammonium salts, and 4-(4-methylpiperidino)pyridine. Testing for these chemical impurities can be done by comparison of spot size and intensity shown on a developed TLC strip (K222), with a sophisticated HPLC system equipped with a UV detector (ClDG, FDG,

and tetra-alkyl ammonium salts), or with a UV spectrophotometer [4-(4-methylpiperidino)pyridine].

Residual Solvents

Similar to the chemical purity assessment, any residual solvents present in the final radiopharmaceutical preparation must be determined and found to be within USP limits.

FDA guidance for the pharmaceutical industry groups residual solvents into three classes.[71] The classification of residual solvents involves assessment of not only their potential toxicity with respect to human health concerns but also their possible deleterious effects on the environment.[71] Class 1 comprises solvents known and strongly suspected to be human carcinogens and environmental hazards. Their use should be avoided in the manufacture of drug substances, excipients, and drug products. Class 2 solvents have inherent toxicity, and their use should be limited in pharmaceutical products.[71,72] Solvents in Class 3 are those that have less toxic potential and thus pose a lower risk to human health.[71,72]

A GC system with flame ionization detection is the instrument of choice in the determination of residual solvents. In a manner similar to an HPLC system, a GC system must be validated for proper analysis of residual solvents.[19,22] According to *USP*, the resolution between standard and test solutions should be not less than 1.0, and the relative standard deviation for replicate injections should not be more than 5%.[30]

PHARMACEUTICAL CONSIDERATIONS

The basic considerations regarding the pharmaceutical aspects of a radiopharmaceutical are appearance and color, particle number and size, pH, osmolality, and stabilizers or preservatives.

Appearance and Color

Annual reports of defective radiopharmaceutical products prepared by the European Association of Nuclear Medicine frequently describe the presence of foreign substances (e.g., black particles, glass elements, fiber) in vials, coring of vial stoppers, and vial breakage or cracking before, during, and after reconstitution.[3–8] Although these occurrences are rare, they do underscore the value of inspecting the content of kit vials before and after radiopharmaceutical preparation. One should be thoroughly familiar with the normal appearance and color of every radiopharmaceutical (Table 12-5). Formulations used in nuclear medicine may be true solutions, colloidal dispersions, suspensions, or solid materials such as oral capsules; they have defined properties that allow their identification. Gross macroscopic inspection of solutions should be performed to identify any

TABLE 12-5 Appearance and Color of Radiopharmaceuticals

Radiopharmaceutical	Appearance	Color
^{99m}Tc-macroaggregated albumin (MAA)	Turbid	White
^{99m}Tc-sulfur colloid	Slightly turbid	Milky
Other ^{99m}Tc-labeled compounds	Clear	Colorless
^{131}I-sodium iodide	Clear (turns light amber with time)	Colorless
^{32}P-sodium phosphate	Clear	Colorless
^{32}P-chromic phosphate	Turbid	Bluish green
Other non-^{99m}Tc-labeled compounds	Clear	Colorless

TABLE 12-6 Particle Size of Common Particulate Radiopharmaceuticals

Radiopharmaceutical	Diameter (nm)
^{99m}Tc-sulfur colloid (thiosulfate)	100 to 1000
Filtered ^{99m}Tc-sulfur colloid (thiosulfate)	<100 to 220
^{99m}Tc-macroaggregated albumin (MAA)	10,000 to 90,000 (90%) <150,000 (100%)

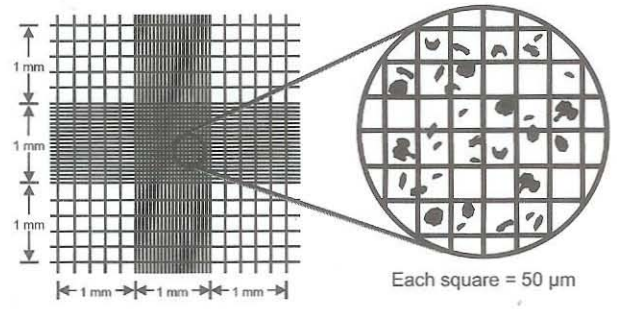

NOTE —Ruled surface is 0.1 mm below the cover glass on the slide; therefore the volume under the central square is 0.1 mm^3

QUESTION —If the central square contains 110 MAA particles seen under a microscope, calculate the total number in a vial containing 5 mL of MAA suspension

$$\frac{110 \text{ particles}}{0.1 \text{ mm}^3} \times \frac{1000 \text{ mm}^3}{1 \text{ mL}} \times \frac{5 \text{ mL}}{\text{vial}} = 5.5 \times 10^6 \text{ particles/vial}$$

FIGURE 12-12 Estimating size and number of ^{99m}Tc-MAA particles with the hemacytometer grid.

foreign material or change in appearance or color. For example, ^{131}I-sodium iodide solution is clear and colorless when freshly prepared but turns light amber with time because of radiolysis effects; this color change is not deleterious. Another example is the difference between ^{32}P-sodium phosphate, which is a colorless, clear solution, and ^{32}P-chromic phosphate, which is a bluish-green, turbid, insoluble suspension (Table 12-5). Observations should be made through leaded-glass shielding that is not tinted or fogged so as to obscure the inspection.

Particle Number and Size

Particulate radiopharmaceuticals such as ^{99m}Tc-SC and ^{99m}Tc-macroaggregated albumin (^{99m}Tc-MAA) normally have a cloudy appearance (Table 12-5). Microscopic inspection of these agents, or filtration analysis of ^{99m}Tc-SC, can be performed to confirm that particles are uniformly dispersed and of proper size (Table 12-6).

Microscopic inspection with a light microscope and hemacytometer grid can be performed to estimate particle size and number with ^{99m}Tc-MAA (Figure 12-12). According to *USP*, at least 90% of ^{99m}Tc-MAA particles should have a diameter between 10 and 90 µm, with none greater than 150 µm.[73]

pH

All radiopharmaceuticals have an optimal pH range for stability, and most radiopharmaceuticals are within a pH range of 4 to 8, with some exceptions:

1. Radioiodine solution should be kept in alkaline pH to prevent volatilization of iodine.
2. Indium chloride solution must be kept quite acid (pH 1 to 3) to remain in solution and to prevent formation of insoluble indium hydroxides. Chelated forms of indium, however, such as ^{111}In-DTPA, are very soluble at neutral pH.
3. The pH of unstabilized ^{99m}Tc-exametazime injection is in the range of 9.0 to 9.8, whereas the pH of the stabilized ^{99m}Tc-exametazime is buffered between 6.5 and 7.5 for stability.[74,75]

According to *USP* General Chapter 791, test paper may be suitable for the measurement of an approximate pH value.[76] A narrow-band pH paper is suitable for pH assessment, because USP pH limits for radiopharmaceutical products are usually quite broad. However, the accuracy and traceability of pH paper should be initially verified with standard buffers. The pH value obtained with pH paper is approximate, and the accuracy is probably no better than ±0.25 pH units.[77]

Osmolality

Because most radiopharmaceutical preparations are formulated in physiologic saline and are therefore isotonic, an osmolality test is usually not necessary for radiopharmaceutical injections. Osmolality and pH are more critical for intrathecal injections than for intravenous injections because of the high dilution and buffering capacity of the blood.

Stabilizers and Preservatives

Stabilizers may be added to radiopharmaceuticals for a number of reasons. Typically they are added to retard oxidation or to reduce radiolytic degradation in preparations with high specific concentration. A preservative is usually added to a radiopharmaceutical formulation to retard the growth of microorganisms that might be introduced into the vial during multiple penetrations. Preservatives can extend the shelf life of a ^{99m}Tc radiopharmaceutical beyond the default expiration time of 12 hours. ^{99m}Tc-mebrofenin is a good example of this. If the added stabilizer or preservative may cause toxic, physiologic, or pharmacologic effects, it must be properly evaluated before release of the drug product for patient use. The testing method, acceptance limits, and testing schedule for assay of the potentially toxic stabilizer or preservative should be established and validated. Such testing is typically the domain of the radiopharmaceutical manufacturer and is not part of the routine practice of nuclear pharmacy.

BIOLOGIC CONSIDERATIONS

Most radiopharmaceuticals are designed for parenteral administration and therefore must be prepared by aseptic processing. The goal of aseptic processing is to prepare a drug product that is free of microorganisms and toxic microbial byproducts, most notably bacterial endotoxins.

Microbiologic control (i.e., sterility testing) and bacterial endotoxin testing (BET) must be performed according to written policies and procedures for radiopharmaceuticals when these tests are required as release criteria. Retrospective sterility testing and BET should be conducted on randomly selected batches of the product to check the adequacy of aseptic technique. These tests should be conducted at regular intervals, depending on historical results and trends, and should be completed more frequently when new personnel are

involved. Sterility testing and BET should be performed according to procedures based on and adapted from those described in *USP* General Chapters 71 and 85, respectively.[78,79]

Sterility

A sterile solution is one that contains no living organisms, pathogenic or nonpathogenic. All injectable products must be sterilized by steam (autoclave) or membrane filtration. Autoclaving, with steam under pressure, is useful only for products that can withstand the severe physical conditions of 121°C under pressure at 15 pounds per square inch gauge (psig). These conditions obviously preclude autoclaving of protein and biologic products. For heat-labile products, sterilizing membrane filtration is the method of choice. Membrane porosity should be at 0.22 μm.

If radiopharmaceuticals are formulated from raw materials, sterile glassware, syringes, and other components should be used to lessen the chance of introducing microorganisms and pyrogenic material into the product. Radiopharmaceutical products with a long enough half-life should be subjected to the USP sterility test before use. The official sterility test uses fluid thioglycolate medium to test for bacterial contamination and soybean casein digest medium to test for fungi.[78] Sterility tests can usually be conducted in a hospital's microbiology laboratory. Of course, proper precautions must be taken if the product is radioactive.

The test for sterility should be carried out in accordance with *USP* General Chapter 71.[78] However, special difficulties arise with radiopharmaceutical preparations because of the short half-life of some radionuclides (especially those used for diagnostic purposes), small size batches, low production volume, and radiation hazards.

The USP sterility testing method requires observation of the tubes of media over a 14 day incubation period unless otherwise specified elsewhere in the sterility testing chapter or in the individual monograph.[78] It is common to observe the test samples at days 3, 7, and 14. In any event, the short half-lives of most radiopharmaceuticals used in nuclear medicine studies prohibit completion of the sterility testing before the release of radiopharmaceutical products. In addition, when the half-life of the radionuclide is very brief (e.g., less than 20 minutes), administration of the radiopharmaceutical preparation to the patient is generally on-line with a validated production system. It is justifiable to dispense radioactive drug products before completion of the sterility test if the radiopharmaceutical is prepared by a validated aseptic process.

For safety reasons (i.e., high levels of radioactivity), it may be not possible to use the quantity of a radiopharmaceutical preparation stipulated in the USP sterility testing chapter.[78] To limit radiation exposure of personnel, the product should be diluted or allowed to decay to a safe working level before sterility tests are conducted.

In regard to the initiation time of sterility testing, FDA regulations (preliminary draft proposed rule and draft guidance) addressing current good manufacturing practices (CGMP) for PET drug products stipulate that the sterility test may be started the next day after preparation.[22,80] Although the 24 hour window for the start of sterility testing matches that specified in FDA's draft chemistry, manufacturing, and control (CMC) section for three PET drug products (ammonia N 13 injection, fludeoxyglucose F 18 injection, and sodium fluoride F 18 injection),[81] it is not practical. It may be necessary to conduct sterility tests on the next working day when preparations are made just before or during a weekend or holiday.

In summary, radiopharmaceutical preparations should meet the requirements stated in *USP* General Chapter 71 on sterility tests, with the exception that radioactive drug products may be distributed or dispensed before completion of the tests for sterility.[78] The

sterility test must be started after an appropriate decay period following final manufacture or preparation.

Membrane Filter Integrity

Since the sterility test is completed retrospectively for most radiopharmaceuticals, the membrane filter integrity test can be considered an indicator of the microbiologic purity of the product. All membranes used for product sterilization must pass an integrity test prior to product release. "Bubble point" measurement is a simple test for membrane filter integrity.[80,81]

Bacterial Endotoxin Testing

Pyrogens are metabolic products of microorganisms that cause a pyretic response upon injection. Endotoxin is the most significant pyrogen. The response in humans is characterized by the onset of chills and fever within 45 to 90 minutes after the injection of pyrogenic material. General malaise and headache may also be present. The severity of response is dependent upon the extent of contamination.

All injectable products are required to be pyrogen free. Endotoxin is not removed by sterilizing membrane filtration methods; therefore, a solution could be sterile but pyrogenic. The most likely sources of pyrogens have been impure water and chemicals used in product preparation. Pyrogenic contamination is usually prevented by using high-quality chemicals and water for injection. Glassware can be rendered pyrogen free by dry heat at 250°C for 30 minutes, which incinerates the endotoxin. Autoclaving does not completely destroy pyrogens.

The official test for the presence of pyrogens in parenterals has been the USP rabbit test.[82] The USP rabbit pyrogen test requires intravenous administration of the drug to be tested into the marginal ear vein of three rabbits whose body temperature is monitored. Temperature is recorded each hour for 3 hours and compared with the baseline temperature before injection. The product passes the test if no rabbit shows an individual rise in temperature of 0.6°C or more above its respective control temperature and if the sum of the three individual maximum temperature rises does not exceed 1.4°C. Details of the test can be found in the *United States Pharmacopeia*. Special care and facilities are needed to house the rabbits so that the test will be valid. Rabbits are subject to temperature elevations solely from fright or excitation. Thus, sham testing must be performed to ensure reliability. Although this has been a reliable test for the presence of pyrogens in parenterals, it has limitations for use with radiopharmaceuticals, particularly those containing short-lived radionuclides. Additionally, the rabbit test appears to lack the sensitivity required to detect endotoxins in radiopharmaceuticals intended for intrathecal use.[83] Fortunately, an in vitro test has been developed that is far more sensitive to bacterial endotoxin than the rabbit test; this is the limulus amebocyte lysate (LAL) test, now officially known as the bacterial endotoxins test (BET).

The bioassay in rabbits was the first pyrogen test and was used for many years, but the BET was shown to be more sensitive.[83] Development of a viable alternative to the USP rabbit pyrogen test began with the observation by Bang[84] that gram-negative bacteria caused intravascular coagulation in the American horseshoe crab, *Limulus polyphemus*. In collaboration, Levin and Bang[85] later found that this clotting resulted from action between endotoxins and a clottable protein (a proenzyme) in the lysate of the crab's circulating blood cells, which are amebocytes. The need for a suitable pyrogen test for drugs, especially radiopharmaceuticals, led Cooper, Levin, and Wagner[86] to develop a simple method of applying this new approach to endotoxin testing of drug products. The BET (then called

TABLE 12-7 Characteristics of Limulus Amebocyte Lysate (LAL) Test

1. It is an in vitro test
2. It can be performed in-house with minimal equipment and personnel
3. Test volume can be as small as 0.1 mL
4. The test is completed within 1 hour
5. An in-process 20 minute endotoxin limit test can be used to allow for early release of an ultra-short-lived radiopharmaceutical
6. Positive and negative controls and inhibition or enhancement testing can be performed with each test
7. It is relatively inexpensive, and the test materials can be stored until needed
8. The sensitivity of the LAL test allows for substantial dilution of the test sample (except for intrathecal drug products)
9. It can be used to test drugs not amenable to the rabbit test, such as anesthetics, cancer chemotherapeutic agents, sedatives, narcotics, intrathecal drugs, and drugs that exert potent pharmacologic effects on animal systems[86]

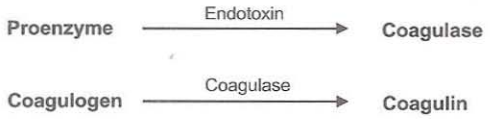

FIGURE 12-13 The activation sequence of a proenzyme in limulus amebocyte lysate catalyzed by a gram-negative bacterial endotoxin.

the LAL test), was introduced in the *United States Pharmacopeia, 20th Revision,* and assigned official status by the USP Committee of Revision in 1993.[86]

The BET for pyrogens is preferred over the rabbit test (especially for radiopharmaceutical preparations) because of simplicity, sensitivity, specificity, rapidity, and cost-effectiveness.[86] Table 12-7 lists characteristics of the BET. It is a qualitative and quantitative test for gram-negative bacterial endotoxin. A proenzyme obtained from a lysate of washed amebocytes of *L. polyphemus* blood is extremely sensitive to the presence of gram-negative bacterial endotoxin. Once the proenzyme is activated by the endotoxin (its rate of activation is determined by the concentration of endotoxin present), the activated enzyme (coagulase) hydrolyzes specific bonds within a clotting protein (i.e., coagulogen) that is also present in LAL (Figure 12-13). The hydrolyzed coagulogen then turns into coagulin and forms a gelatinous clot. Lyophilized lysate must be stored between 2°C and 8°C to maintain effectiveness.

There are two types of BET techniques: the gel-clot technique and the photometric technique (i.e., a turbidimetric method and a chromogenic method).[79] The specifications listed in the *USP* monograph for selecting a testing technique should be followed. Unless otherwise indicated in the *USP* monograph, the gel-clot technique is the method of choice in case of dispute.[79]

The LAL reaction is enzyme mediated and has an optimal pH range for proper performance of the LAL reagent. As with most enzymatic reactions, test samples for LAL testing should be done at neutrality. If necessary, pH should be adjusted with endotoxin-free acid or base. Samples to be tested may be stored at 2°C to 8°C for 24 hours or be kept frozen if the storage period is longer than 24 hours.

The validity of BET results requires an adequate demonstration that the test sample does not inhibit or enhance the reaction or otherwise interfere with the test. Interference can be overcome by suitable treatment, such as filtration, neutralization, dialysis, or heating.[79] However, most compounds are inhibitory in the undiluted state. Therefore, the easiest way to overcome inhibition is to dilute the test sample. Sample dilution must not exceed the maximum valid dilution, which is the maximum allowable dilution of a specimen at which the endotoxin limit can be determined by the BET technique.[79] In any event,

inhibition or enhancement testing should be performed on the test sample solutions to determine whether they interfere with the LAL reagent, as well as to ensure that the chosen treatment has effectively eliminated interference without loss of endotoxins. A product is said to be free of product inhibition or enhancement if the geometric mean end point of endotoxin in the product is between one-half and 2 times the labeled lysate sensitivity.[79]

Each vial of LAL is labeled with the lysate sensitivity (λ), which is obtained using the USP reference standard endotoxin (RSE) and is expressed in endotoxin units (EU) per milliliter. One EU (or USP-EU) is equal to one international unit (IU) of endotoxin. A sensitivity of not less than 0.15 EU/mL should be met for an LAL reagent to be used for routine BET.[79] Before using a new batch of LAL reagent kits, each user should confirm the labeled LAL reagent sensitivity by using the control standard endotoxin (CSE) supplied with an LAL reagent kit. This should be verified again when there is any change in test conditions that might affect the outcome of testing, such as a change in the formulation.[79] Acceptable variation of the measured sensitivity of the LAL reagent is between one-half and 2 times the stated lysate sensitivity.

According to *USP*, 5 EU/kg body weight is the endotoxin limit for a drug product administered by any route other than intrathecally (for which the limit is 0.2 EU/kg).[79] However, the endotoxin limit for radiopharmaceutical products is 175 EU/V, where V is the maximum dose in milliliters, at the expiration time. For intrathecally administered radiopharmaceuticals, the endotoxin limit is 14/V because endotoxin is most toxic by the intrathecal route. Drug products intended for intrathecal administration must be tested at a lesser dilution to meet the limit of 14 EU/V.

Because, at expiration time, the maximum administered total volume of a radiopharmaceutical may be equal to the total volume of the entire vial of the radioactive drug product, it might seem appropriate to calculate the bacterial endotoxin limit (i.e., 175 EU/V) using the total volume in the vial. This approach is simple, but it results in a stringent limit. This is because the total volume of the entire vial of radiopharmaceutical preparation, rather than a partial volume, is used as the denominator for calculation of the acceptable bacterial endotoxin limit.

The USP gel-clot limit test is used when a monograph or a package insert contains a requirement for bacterial endotoxin limit.[79] As shown in Table 12-8, the test is not valid unless both replicates of test solutions B and C are positive and those of test solution D are negative.[79] The test should be repeated when the results of replicates of test solution A are not consistent (i.e., one positive and one negative).[79] Practical procedures for applying the gel-clot limit test in pharmacy compounding were recently discussed.[87]

To quantify the endotoxin concentration of an unknown solution, serial 2-fold dilutions of sample are tested until an end point is reached (Table 12-9). The endotoxin concentration (E) is calculated by multiplying the lysate sensitivity (λ) by the reciprocal of the end point dilution. For example, a product yielded an end point at a 1:8 dilution with LAL reagent water when using an LAL reagent with $\lambda = 0.125$ EU/mL [$E = \lambda \times 8 = 0.125$ EU/mL $\times 8 = 1$ EU/mL].

TABLE 12-8 Gel-Clot Limit Test

Test Solution	Number of Replicates	Endotoxin Concentration/Test Sample or Control	Function	Results or Comments
A	2	None/sample solution	Test sample	May be positive or negative
B	2	2 λ/sample solution	Test for interference	Should be positive
C	2	2 λ/LAL reagent water	Positive control	Should be positive
D	2	None/LAL reagent water	Negative control	Should be negative

TABLE 12-9 Gel-Clot Assay

Test Solution	Number of Replicates	Endotoxin Concentration/ Test Sample or Control	Diluent	Dilution Factor	Initial Endotoxin Concentration	Results or Comments
A	2	None/sample solution	LAL reagent water	1	–	See text for calculation of endotoxin concentration of solution A
	2			2	–	
	2			4	–	
	2			8	–	
B	2	2 λ/sample solution	–	1	2 λ	Should be positive
C	2	2 λ/LAL reagent water	LAL reagent water	1	2 λ	Geometric[a] mean end point concentration is in the range of 0.5 λ to 2 λ
	2			2	1 λ	
	2			4	0.5 λ	
	2			8	0.25 λ	
D	2	None/LAL reagent water	–	–	–	Should be negative

[a] The end point is the last positive test in the series of decreasing concentrations of endotoxin.

Source: General Chapter 85, page 2025, *The United States Pharmacopeia, 26th rev., and The National Formulary, 21st ed.*; 2003.

The commonly used gel-clot technique for determining bacterial endotoxin concentration requires a 60 minute incubation period, as described in *USP* General Chapter 85.[79] This is also the endotoxin testing method recommended in FDA's draft guidance on CGMP for PET drug products.[22] Because the remainder of the required QC testing for a typical PET radiopharmaceutical (e.g., ^{18}F-FDG), with the exception of the sterility test, can be completed in 20 to 30 minutes, it is not practical and is indeed quite wasteful to delay release of the short-lived ^{18}F-FDG injection for an additional 30 to 40 minutes. Kinetic LAL methods using multitube readers are the quickest ways to complete a BET for PET radiopharmaceuticals.[88]

USP General Chapter 823 on the compounding of PET radiopharmaceuticals indicates that an in-process 20 minute endotoxin "limit test" (i.e., incorporating positive controls in the range of 5 EU per milliliter to 175 EU/*V*) can be used to allow for the possibility of early release, for human use, of an injectable PET drug radiolabeled with a radionuclide having a half-life greater than 20 minutes. However, the standard 60 minute BET must be performed and completed.[89] This two-part BET is a sensible approach, especially for the short half-lived PET drug products, because all other required QC testing procedures (with the exception of the sterility test and the 60-minute BET testing) are usually completed in 20 to 30 minutes. Nonetheless, it is interesting to note that the 20 minute BET is mentioned in neither *USP* General Chapter 85 nor *USP* General Chapter 823.[79,89] Cooper[90] proposed a test scheme for the 20 minute BET. The proposed 20 minute gel-clot limit test includes use of the standard test tubes as described in *USP* General Chapter 85, plus one additional positive product control tube that contains a test sample solution mixed with 160 λ endotoxin concentration.

INSTRUMENT QUALITY CONTROL

A nuclear pharmacy laboratory usually has a dose calibrator, a scintillation well counter, and a Geiger-Müller (GM) survey meter as standard equipment for measuring radioactivity. CGMP for PET drug products require that a PET drug production facility be

TABLE 12-10 Dose Calibrator Quality Control Requirements of 10 CFR 35.50 ("Old" Part 35)

Quality Control Test	Frequency[a]	Sources and Conditions[b]
Constancy	At beginning of each day of use	Not less than 50 μCi of a photon emitter
Accuracy	At installation and annually	Not less than 50 μCi of a photon emitter Two sources used, each within ±5% of its stated activity; one source must have a principal photon energy between 100 and 500 keV
Linearity	At installation and quarterly	Test from highest patient or research subject dosage down to 30 μCi
Geometry	At installation	Test range of volumes and configurations to be used

[a] Each test must be performed after instrument adjustment or repair.

[b] Mathematically correct dosage readings for geometry or linearity errors that exceed 10%. Repair or replace dose calibrator if accuracy or constancy error exceeds 10%.

equipped with additional instruments (e.g., HPLC, GC, MCA) for QC testing. The purpose and operating principles of these instruments have been addressed previously (the dose calibrator, scintillation well counter/MCA, and GM survey meter are discussed in Chapter 3; HPLC and GC are discussed earlier in this chapter). This section will describe routine QC procedures for the dose calibrator and survey meters.

Dose Calibrator

The dose calibrator is used in nuclear medicine and nuclear pharmacy primarily to measure the activity of radiopharmaceuticals before administration to the patient. A number of quality control tests must be conducted to ensure the proper operation of this instrument.

The revised 10 CFR 35.60, "Possession, use, and calibration of instruments used to measure the activity of unsealed byproduct material," no longer spells out the procedures for checking accuracy, constancy, geometry, and linearity for dose calibrators.[91] Instead, the regulation states that licensees must follow "nationally accepted standards" or "the manufacturer's instructions" for calibrating dose measurement systems.[91] For reference, the requirements for dose calibrator QC testing described in the previous 10 CFR 35.60 are summarized in Table 12-10. These requirements may still be enforced by agreement-state licensing agencies until the revised Part 35 regulations are adopted by the states, and they are a sound guide for dose calibrator quality control.

Dose calibrator manufacturers' instructions may vary and therefore may not be a practical option for standardized QC testing of dose calibrators. In regard to "nationally accepted standards," two documents are recognized as authoritative guidelines: the American National Standard Calibration and Usage of "Dose Calibrator" Ionization Chambers for the Assay of Radionuclides, and NCRP Report 99—Quality Assurance for Diagnostic Imaging, published, respectively, by the American National Standards Institute (ANSI) and the National Council on Radiation Protection and Measurements (NCRP).[92,93]

According to 10 CFR 35.2060, "Records of calibrations of instruments used to measure the activity of unsealed byproduct material," a record of calibration must be kept for 3 years and should include dose calibrator model and serial numbers, date of calibration, results of calibration, and the name of the individual who performed the calibration.[94]

To ensure proper dose calibrator operation, the following QC tests are required: constancy (precision), accuracy, linearity, and geometry.[95] Standard radionuclide sources, otherwise known as standard reference materials, are available for conducting the accuracy

and constancy tests. A primary standard reference material is one whose disintegrations have been determined under known geometry conditions, typically 4-pi geometry. Primary standards are prepared by the National Institute of Standards and Technology (NIST) and have an uncertainty of <1%. They are supplied as 5 mL solutions in borosilicate glass ampuls with a wall thickness of approximately 0.6 mm. A secondary standard reference material is one whose activity is determined by comparison with a primary standard. Secondary standards are prepared by commercial firms (e.g., Amersham, DuPont) and have an uncertainty of 2% to 4%. These sources are typically supplied as a solid epoxy material sealed in a polyethylene bottle.

The following discussion of QC standards and procedures is based primarily on NCRP Report 99.[93]

Constancy

A constancy (precision) test ensures that the dose calibrator can measure a source of constant activity repeatedly within a stated degree of reproducibility over a long period of time. A satisfactory response to this check indicates that the dose calibrator is operating consistently from day to day.

The constancy test is performed on the dose calibrator at the beginning of each day of use. A long-lived reference source, usually ^{137}Cs, is used. Other sources may be used as well for this test. ^{137}Cs is similar in photon energy to ^{99}Mo; ^{57}Co has a principal photon energy similar to that of ^{99m}Tc. If one uses a dose calibrator only for the measurement of ^{131}I dosages, a good reference source would be ^{133}Ba, whose photon energy is similar to that of ^{131}I. A suggested method for the constancy test is as follows:

1. Assay the reference source using the dose calibrator setting for that radionuclide (e.g., use the ^{137}Cs setting to assay a ^{137}Cs source).
2. Measure the background activity at the same setting and subtract this from the measured activity. If an automatic background subtraction circuit is used, confirm that background was correctly subtracted.
3. Record the net activity (source minus background) in the QC logbook for that dose calibrator.
4. It is advantageous to repeat the above procedure, using the same reference source, for all routinely used radioisotope settings on the dose calibrator (e.g., ^{99m}Tc, ^{201}Tl, ^{111}In) to check their response. Readings will differ from the reference source but should consistently follow the characteristic half-life of the source.

Source measurements deviating by more than ±5% of the predicted activity indicate a need for instrument adjustment or repair.

Accuracy

Accuracy is defined as the closeness of a measurement to the true value. The purpose of the dose calibrator is to measure the radioactivity of a radiopharmaceutical with a high degree of accuracy. Dose calibrator accuracy is assessed by measurement of standard reference sources of known activity traceable to NIST. Typical sources used for accuracy assessment are ^{57}Co, ^{133}Ba, and ^{137}Cs. The measured activity of a reference source must agree within ±5% of its certified activity after decay correction. Calibration checks that do not agree within ±5% indicate that the instrument must be either repaired or adjusted. This test must be performed at the time of dose calibrator installation and thereafter on

a yearly basis. It must also be performed after repair or adjustment of the dose calibrator. A suggested method for the accuracy test is as follows:

1. Assay one of the reference sources using the appropriate radioisotope setting (e.g., use the ^{57}Co setting to assay ^{57}Co). Allow sufficient time for a stable reading to be obtained.
2. Remove the reference source and measure background activity. Subtract background activity from the measured activity to obtain the net activity. Confirm proper operation of the automatic background subtraction circuit if it is used.
3. Record the net measured activity, the source geometry, and the instrument settings.
4. Repeat the previous steps for a total of three independent determinations and average the net measured activity.
5. The average value must be within ±5% of the certified radioactivity after decay corrections.

Linearity

Dose calibrator linearity implies an accurate instrument response over a wide range of activities. A nonlinear response is more likely to occur at high activities than at low activities.[96] Nonlinearity at high activities is likely due to recombination of ion pairs in the chamber before they are collected at the chamber electrodes, causing a falsely low readout of the true activity present.

A linearity test should be performed at dose calibrator installation and quarterly. For practical reasons, the linearity test need be conducted only over the activity range of patient dosages being measured. ^{99m}Tc is typically used to conduct the linearity test because it is readily available in large amounts of activity. However, if the highest dose administered to a patient is 300 mCi (11.1 GBq) of ^{131}I, the amount of ^{99m}Tc activity must be adjusted upward because of differences in the decay characteristics of these two nuclides. Thus, 430 mCi (15.9 GBq) of ^{99m}Tc should be used in place of 300 mCi (11.1 GBq) of ^{131}I to compensate for the gamma energy differences between ^{131}I and ^{99m}Tc.[97]

Two methods can be used for the linearity test. The most accurate method is the decay method, which consists of multiple measurements of the same radionuclide source over an extended time period, typically 2 to 3 days.[98] An alternative method is the attenuation method, which uses a series of lead-lined sleeves or tubes of varying thickness (Figure 12-14). A set of 6 to 8 tubes is designed to progressively increase attenuation of the ^{99m}Tc source to simulate decay from 0 through 50 hours. Tube sets are commercially available from a number of vendors.

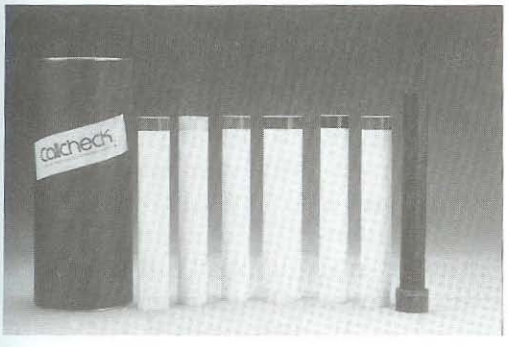

FIGURE 12-14 Lead sleeve shielding system for the dose calibrator linearity test.

Decay Method

1. Before the linearity test, properly zero the dose calibrator. A reliable and accurate clock should be used to record the time (an error of 10 minutes in the recorded time for ^{99m}Tc will result in an apparent error of 2% in the dose calibrator linearity check).
2. Obtain a ^{99m}Tc source that contains the largest activity routinely administered to a patient or routinely measured in the dose calibrator (e.g., the first elution from a new ^{99}Mo–^{99m}Tc generator).
3. Assay the ^{99m}Tc source in the dose calibrator and subtract background activity to obtain the net radioactivity in millicuries or megabecquerels. Record the date, time, and measured activity of the ^{99m}Tc source. Repeat this measurement three times and obtain the average value.
4. Repeat this process at 6, 24, 30, 48, 54, 72, and 78 hours thereafter, until the activity level of the ^{99m}Tc source has dropped to 30 μCi (111 kBq) or less.

   Using the 30 hour activity measurement (A_{30}) as a reference point, calculate the predicted activity (A_t) at the other specified times, t, using the following decay equation:

$$A_t = A_{30}\, e^{-0.1151(t-30)}$$

5. On semilog graph paper, label the logarithmic vertical axis in activity (millicuries per megabecquerel) and label the linear horizontal axis in decay time (hours). At the top of the graph, note the dose calibrator information (i.e., manufacturer, model number, and serial number), as well as the date and time of the initial assay.
6. Plot the data points and draw a best-fit straight line through the data points. Figure 12-15 shows a linearity decay graph. The linearity of the dose calibrator is determined by selecting the point that deviates furthest from the best-fit line. The deviation is calculated from the following equation:

$$\%\ \text{Deviation} = \frac{\text{Measured activity} - \text{Calculated or fitted activity}}{\text{Calculated activity}} \times 100\%$$

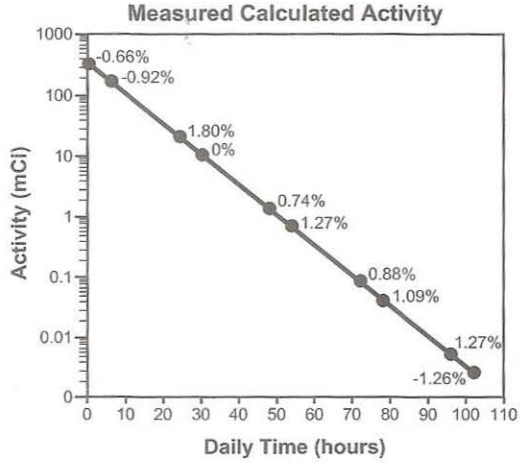

FIGURE 12-15 Dose calibrator linearity decay graph.

Attenuation Method

The set of lead sleeves must be calibrated before use for each dose calibrator and source configuration to be used routinely for the linearity test. A typical calibration method is as follows:

1. Begin the linearity test as described above in the decay method. After completing the first assay using the decay method, calibrate the lead sleeves as follows. Each measurement must be performed three times and an average value obtained. In addition, the entire calibration must be completed within 6 minutes.
2. Place the ^{99m}Tc source into a base sleeve that is not lead lined. Assay the activity of the ^{99m}Tc source using a dose calibrator and record the results.
3. Place the first lead-lined sleeve (the one with the thinnest lining) over the unlined base sleeve and record the results (Figure 12-16).
4. Remove lead sleeve 1 and place the source in lead sleeve 2. Record the measured radioactivity.
5. Repeat this process until all the lead sleeves have been used.
6. Determine the attenuation (calibration) factors for each lead-lined sleeve by dividing the activity measured in step 1 by the measured activity for the lead sleeve.
7. This procedure need be performed only once on a new set of lead sleeves. The lead-lined sleeves can now be used to test the dose calibrator for linearity.
8. Obtain a ^{99m}Tc source that contains the highest activity routinely administered to a patient or a human research subject.
9. Assay the ^{99m}Tc source in the dose calibrator and subtract background activity to obtain the net radioactivity in millicuries or megabecquerels. Record the date, time, and measured activity of the ^{99m}Tc source. Repeat this process using each of the lead sleeves. This should be done as quickly as possible to minimize errors due to decay. A maximum of 6 minutes (1% decay) is allowed before decay correction must be applied to the results.
10. Repeat step 9 three times and obtain the average value for each lead sleeve.
11. For each average activity measured, multiply the result by the appropriate calibration factor for each sleeve to obtain the factored activity. See the example in Table 12-11.
12. Sum the products from step 11 and divide by the total number of sleeves to obtain the mean factored activity. The percent deviation of each measurement from the mean is determined from the following equation:

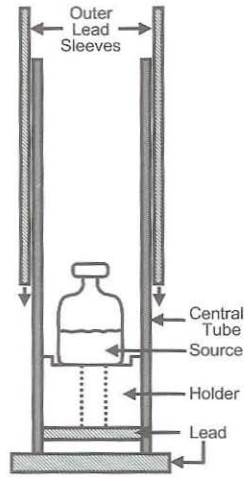

FIGURE 12-16 Diagram illustrating the shielding method for measuring dose calibrator linearity.

$$\% \text{ Deviation} = \frac{\text{Mean factored activity} - \text{Factored activity}}{\text{Mean factored activity}} \times 100\%$$

Deviations greater than ±5% between predicted and measured activity with either the decay method or the attenuation method indicate the need for repair or adjustment of the

TABLE 12-11 Example of Dose Calibrator Linearity Test Report

Tube No.	Net Measured Activity (mCi) 1	2	3	Average	Readings	×	Calibration Factor	=	Factored Activity	% Error
1	61.700	60.800	60.400	60.967			1.000		60.967	–0.36
2	35.300	34.800	34.500	34.867			1.758		61.296	–0.90
3	19.300	19.000	18.900	19.067			3.144		59.946	1.32
4	6.170	6.030	5.990	6.063			10.089		61.173	–0.70
5	2.590	2.540	2.520	2.550			23.638		60.277	0.78
6	0.441	0.437	0.434	0.437			140.456		61.426	–1.11
7	0.131	0.128	0.128	0.129			474.422		61.137	–0.64
8	0.060	0.060	0.060	0.060			1020.35		61.153	–0.66
9	0.009	0.009	0.009	0.009			6736.32		59.369	2.27

Average factored activity = 60.749
Mean + 5% = upper limit = 63.787
Mean – 5% = lower limit = 57.712
Instrument performance is within the acceptable limits of ±5% error.

dose calibrator. Alternatively, a correction factor can be applied for the specific amount of activity being measured.

Geometry

The measured activity of a radioactive source may be significantly different from its true activity, particularly in assays of radionuclides that have weak gamma emissions. In these situations the source measurement can be greatly affected by its volume or container configuration. The assayed activity can also be affected by the volume and size of the radionuclide calibrator chamber; therefore, geometry effects should be established for each type of dose calibrator.[93] The extent of these geometry effects should be ascertained for commonly used radionuclides and appropriate correction factors applied to the measurements if variations are found to be significant (>2%). Dose calibrator correction factors that are supplied by the manufacturer should be verified. In some instances differences of 200% in dose calibrator readings between glass and plastic syringes have been observed for lower-energy radionuclides such as ^{125}I. This type of situation would require a correction factor for measurements made in different types of containers. Correction factors may also need to be established for various types of syringes and for different volumes in a given syringe. An alternative technique to syringe-correction factors is to assay the stock vial before and after filling the syringe. This method maintains consistent assay geometry, and the activity in the syringe is then the difference between the two stock vial readings, with appropriate correction for any syringe volume effects if required. The geometry effects on source measurement for all types of containers should be ascertained upon installation of a dose calibrator, particularly for weak gamma emitters for which these effects may be large.

The three principal geometry considerations that may affect the accuracy of source measurement in a dose calibrator are container configuration, position of the source in the ion chamber well, and the effect of source volume.

Container Configuration

The type of source container used can greatly affect the accuracy of radionuclide measurements. This effect will be most significant with weak gamma emitters. It is important

TABLE 12-12 Effect of Container Configuration on Dose Calibrator Measurements of ^{99m}Tc, ^{131}I, and ^{125}I

	Activity Concentration in μCi/gram of Solution (% Deviation Relative to Ampul Activity)		
Radionuclide	Ampul	Serum Vial	Plastic Syringe
^{99m}Tc	44.5	44.0 (–1.1)	45.2 (+1.4)
^{131}I	37.1	35.8 (–3.5)	38.6 (+4.0)
^{125}I	39.6	20.4 (–48.4)	57.8 (+45.9)

Source: Reference 96.

to be aware that dose calibrator isotope calibration factors are established for a particular instrument by the manufacturer using reference standards in a particular container configuration, typically 5 mL of reference solution in a glass ampul. Other containers, such as glass serum vials or plastic syringes, will yield somewhat different values because of variations in photon absorption by the container. This is not a major problem with most radionuclides used in nuclear medicine, but a few exceptions do exist, such as ^{133}Xe and ^{125}I. Table 12-12 demonstrates the differences in the assay of ^{99m}Tc, ^{131}I, and ^{125}I when using standard containers and indicates a significant influence of container configuration on ^{125}I measurements.[96] For weak gamma emitters, it would be more appropriate to determine calibration factors for the specific container used to assay the radiopharmaceutical. For example, a calibration factor for ^{125}I in a plastic syringe can be determined by transferring a known amount of ^{125}I reference solution into the syringe. This can be accomplished by weighing the syringe empty and then full of the reference solution. The difference will be the weight of the reference solution. The true activity in the syringe is calculated from the known activity per unit weight of the reference solution. Subsequently, the filled syringe is assayed in the dose calibrator, and the calibration factor dial is adjusted to display the true activity on the readout meter. From that point on, all dose measurements of ^{125}I solution contained in a similar syringe utilizing that calibration factor will be accurate. This method can be applied to any radionuclide.

Ion Chamber Well Geometry

The position of a source in the ion chamber well will affect the accuracy of measurement. Each chamber has a well position where source detection sensitivity is greatest. Ideally, this position will extend over a reasonably wide range to minimize variation in measurements. Figure 12-17 illustrates typical variations in dose calibrator activity measurements of a 1.0 mCi (37 MBq) source in a 10 mL serum vial at different distances from the bottom of the ion chamber well. Note that the most accurate readings are obtained between 4 and 8 cm from the well bottom. Readings near the bottom and top of the well are lower because a significant number of photons escape from the detection volume of the chamber in these positions. Well geometry characteristics vary and should be determined for each dose calibrator.

Volume Variation

The measured activity of a radionuclide in a dose calibrator may vary with the volume of solution because of self-absorption. That is, 1 mCi (37 MBq) in a 10 mL volume may produce a different reading than if it were in a 1 mL volume. Experience has shown that this is not a significant problem with most radionuclides used in nuclear medicine except

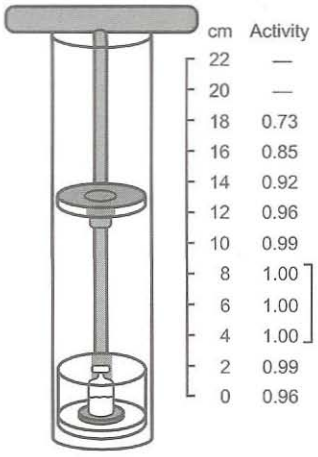

FIGURE 12-17 Ion chamber well geometry effect on activity measurements in a dose calibrator.

for weak gamma emitters such as ^{125}I. One can easily test for volume variation by placing 1 mCi (37 MBq) of any radionuclide in a 1 mL volume into a 30 mL vial. An initial reading and subsequent readings after 2 mL additions of water will indicate whether correction factors need to be applied for different volumes. Regulatory Guide 10.8, Revision 2, recommends the use of a 3 mL plastic syringe and a 30 mL glass vial for evaluation of source geometry.[99] If the error in the measured activity at any volume is greater than ±2% of the baseline activity, a correction table must be established so that the measured activity can be converted to "true activity" (i.e., true activity = measured activity × correction factor).

SURVEY INSTRUMENTS

Two types of survey instruments are used in nuclear medicine: the ionization chamber exposure rate meter and the GM survey meter (Figure 12-18). All survey instruments require routine quality control to ensure that they are operating correctly. 10 CFR 35.61, "Calibration of survey instruments," requires that survey instruments be calibrated before first use, annually, and after any repair that affects the calibration.[100] The regulations require that a licensee calibrate the instrument as follows:

1. Calibrate all scales with readings up to 10 mSv (1000 mrem) per hour using a radiation source.
2. Calibrate two separate readings on each scale or decade that will be used to show compliance.
3. Conspicuously note on the instrument the apparent exposure rate from a dedicated check source as determined at the date of calibration.

When calibrating a survey instrument, the licensee should consider a point as calibrated if the indicated exposure rate differs from the calculated exposure rate by not more than 20%, and a correction chart or graph should be conspicuously attached to the instrument. In accordance with 10 CFR 35.2061, "Records of radiation survey instrument calibrations," a licensee must maintain a record of each radiation survey instrument calibration for 3 years.[101] The record must include the model and serial number of the instrument, date of calibration, results of calibration, and name of the individual who performed the

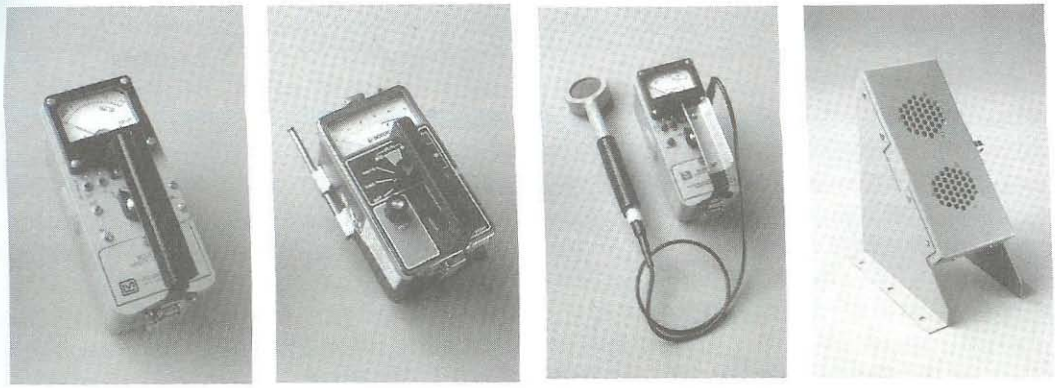

A B C D

FIGURE 12-18 Examples of ionization chamber survey instruments (A: Model 5 Geiger-Müller [GM] counter and B: RSO-50E ionization dosimeter) and GM survey meter/probe (C: Model 3 survey meter attached to Model 44-9 pancake GM detector and D: Model 44-25 pancake GM hand probe).

calibration. For mobile medical services, verification of proper instrument function must be verified with a dedicated check source before use at each client's address.[102]

Survey Meter Calibration

A model procedure for calibration of ionization chambers and GM survey instruments is as follows:

1. Calibrate each scale that reads below 1 R/hour at two points on the scale located at approximately one-third and two-thirds of full scale.
2. Calibration should be performed with a ^{137}Cs reference source of approximately 100 mCi (3.7 GBq) or greater.
3. The ^{137}Cs reference source activity should have an accuracy within ±5% of a NIST calibrated reference source. The radiation exposure from the source should be documented in terms of mR/hour at one meter and should be corrected for decay prior to the calibration procedure.
4. To obtain the appropriate scale reading, position the instrument at various distances from a ^{137}Cs source of known exposure rate at one meter (R_1). Record the distance and instrument reading. The expected reading at each distance can be determined with the inverse square law. For example, at a distance of 30 cm (0.3 m), the expected reading ($R_{0.3}$) can be calculated with the following equation:

$$R_{0.3} \times (0.3)^2 = R_1 \times (1)^2$$

5. If the measured and expected exposure rates differ by more than 10% but less than 20%, a calibration chart, graph, or response factor should be prepared and attached to the instrument.
6. If the measured and expected exposure rates differ by more than 20%, the instrument should be repaired or adjusted until the measured readings are within 10% of the expected reading.

A model procedure for calibration of GM survey meter efficiency is as follows:

1. Place a 0.5 to 1.0 inch disk-type planchette of the desired source on a countertop. This source should contain 0.1 to 0.5 μCi (3.7 to 18.5 kBq) ^{57}Co or any other radionuclide dispersed uniformly throughout the source. Ensure that all other sources of radiation have been removed from the area.
2. Place the GM survey meter either directly on top of the source or at a distance of 5 cm.
3. Measure the exposure rate in counts per minute (cpm). Note the source activity and calibration date and compute its current activity in microcuries (kilobecquerels). Divide the exposure rate by the activity to get the efficiency factor of the meter in counts per minute per microcurie (cpm per kilobecquerel). This factor should be recorded on a label affixed to the detector.

This type of calibration of a thin-window GM counter is useful for assessing removable contamination from radioactive material packages of beta-emitting radionuclides such as ^{32}P, ^{89}Sr, and ^{90}Y, since these nuclides cannot be counted in a gamma scintillation well counter.

Constancy Check

All survey meters should be checked each day before use with a long-lived reference source. The reference source is typically a plastic disk impregnated with 1 to 10 μCi (37 to 370 MBq) of ^{137}Cs, and its reading should be established at the time the survey meter is calibrated. The geometric arrangement of the source and survey meter probe should be noted and reproduced for each daily check of the meter response. Verify that the meter gives a reading within 10% of the source value documented at calibration.

QUALITY CONTROL ISSUES RELATED TO PET DRUG PRODUCTS

Section 121 of the Food and Drug Administration Modernization Act of 1997 (FDAMA) requires that FDA establish approval procedures, that is, new drug application (NDA) or abbreviated NDA (ANDA) and CGMP for PET drugs.[103] The 1997 FDAMA instituted an amendment to the federal Food, Drug, and Cosmetic Act, in which a compounded PET drug is deemed to be adulterated if it is compounded, processed, packaged, or held other than in accordance with PET compounding standards and the official monographs of USP.[103] However, the compounding of PET drug products will be subjected to NDA or ANDA and CGMP regulations 2 years after FDA establishes these requirements as stipulated in the "sunset" clause of Section 121 of 1997 FDAMA.[103]

In the process of establishing approval procedures for PET drugs, FDA issued a draft CMC section, which contains a subsection of regulatory specifications, standard testing procedures, and testing schedules.[81]

Although *USP* stipulates acceptance criteria as well as testing procedures for drugs, it does not specify the frequency for conducting the required QA tests, nor does it indicate whether drug preparations can be released for patient administration before completion of required QC testing. This may be because USP tests are commonly used either in challenges to certain claims made by consumer organizations or in evaluations of marketed drug products conducted by government regulators.[104] However, specifying testing schedules could help end users to ensure that necessary QA tests are initiated within an appropriate time frame, and to know whether a drug can be released before completion of QA tests. *USP* General Chapter 823 does give guidelines regarding testing frequency

and release criteria for PET drugs.[89] However, this chapter applies only to compounded PET drug products and will not be applicable to the QC of PET drugs once the "sunset" clause of Section 121 of 1997 FDAMA expires.[89,103]

PET drugs are unique among radiopharmaceuticals because of their short physical half-lives, ranging from a few seconds to several hours. Consequently, PET radiopharmaceuticals are typically prepared using a cyclotron that is located at or near the PET imaging facility. Most PET centers in the United States are part of an academic medical institution that has its own cyclotron and radiochemistry laboratories for producing PET radiotracers for clinical and research applications.

Notices issued by FDA in 1995 and 1997 concerning the regulation of PET radiopharmaceuticals indicate that FDA has considered the production of PET drug products to be significantly different from the production of conventional drugs in a number of important ways, as follows.[105,106]

1. Because of the short physical half-lives of PET radioisotopes,
   - Prolonged preparation time significantly erodes the useful clinical life of PET drug products;
   - PET facilities generally produce PET drug products in response to daily demand;
   - PET radiopharmaceuticals must be administered to patients shortly after production because of the short half-lives of the PET radioisotopes.
2. Only a few lots are produced per day, with one lot equaling one multiple-dose vial, for a relatively small number of patients.
3. An entire lot may be administered to one or several patients, depending upon the amount of radioactivity remaining at the time of administration. Consequently, administration of the entire quantity of a lot to a single patient should be anticipated for every lot prepared.
4. Since each multiple-dose vial contains a homogenous solution of a PET drug product and equals one lot, results from end-product testing of samples drawn from the vial may be representative not only of the entire lot but of all doses administered to patients.
5. The quantities of active ingredients contained in each lot of a PET drug generally vary from microgram to nanogram amounts.
6. PET drugs do not usually enter a general drug distribution chain. Rather, the entire lot (one vial) usually is distributed directly from the PET facility either to a single nuclear medicine department or physician for administration to patients or to a nuclear pharmacy for dispensing. Distribution to other PET centers may occur when geographic proximity allows for distribution and use within the parameters of the PET drug product's half-life.

On April 1, 2002, FDA issued a preliminary draft proposed rule, which includes proposed regulations and the rationale and intention of the draft rules on CGMP for PET drug products.[58] A companion draft guidance on CGMP for PET drugs was also released on the same day.[22] The draft guidance provides details and recommendations on compliance, based on size, scope, and complexity of PET center operations.[22] CGMP is not merely focused on identity, strength, quality, and purity of the finished PET drug products; manufacturing practices must also use adequate and validated personnel, facilities, equipment, and controls in the preparation, packaging, and holding of PET drugs in order to ensure that the drug products meet safety and quality requirements. Unique QC issues related to the preparation, packaging, and holding of PET drugs, as outlined in these two draft documents, are summarized as follows.

Personnel and Resources

A PET facility must have a sufficient number of personnel to satisfactorily complete all required tasks in a timely manner. In addition, the various stages of production and test verification must be checked by a second person. However, if a PET center is operated by one person, FDA allows that individual to perform the production and QC functions as well as to self-check his or her own work.

Quality Control Unit

Each PET drug product producer must have a QC unit to oversee its production operations to ensure the safety and quality of PET drug products. Decisions made by the QC unit to reject batches should not be subject to further review or revocation by another organizational unit or person. In large PET centers, the QC unit should be independent from the production unit. Since the QC unit in a small PET center may be indistinguishable from the production unit, an independent expert or an outside consultant should periodically audit the performance of the QC unit.

Facilities and Equipment

Critical activities involved in the production and testing of a PET drug product that expose the PET drug product or the sterile surface of a container and closure system to the environment should be conducted within an aseptic workstation with a rating of Class 100 (e.g., a laminar-airflow workstation or barrier isolator). Examples of these activities include (1) aseptic assembly of sterile components (e.g., syringe, needle, filter, vial), (2) storage of sterility samples and finished PET drug products, (3) sterility testing of the finished PET drug product, and (4) dose withdrawal for quality control or patient administration. The aseptic processing facility and the aseptic work area should be properly certified, cleaned, and validated in accordance with standard procedures, such as those listed in *USP* General Chapters 797, Pharmaceutical Compounding—Sterile Preparations, and 1208, Sterility Testing—Validation of Isolator Systems.[107,108]

Similarly, equipment used in the production and QC of a PET drug product should be adequately certified, maintained, and validated. The following reference sources (in descending order) can be used to control the usage and maintenance of such equipment: (1) manufacturer's instructions, (2) relevant *USP* general chapters, and (3) written procedures developed by each individual PET center. The warranty of any piece of equipment is normally valid if the operation procedures and maintenance schedule stated in the owner's manual are properly followed. Additionally, the manufacturer may have specific requirements for the calibration, performance, and maintenance of the machine. Hence, it may be prudent to rely primarily on the manufacturer's instructions regarding equipment issues, with the *USP* general chapter and self-established procedures as alternative sources when the manufacturer's instructions are inadequate.

Control of Components, Containers, and Closures

The components used in the production of PET drugs, including containers and closures used to package final products, must be properly controlled. Identity testing needs to be performed on each lot of a component that yields an active pharmaceutical ingredient. For the production of ^{18}F-FDG injection, the components that yield the active pharmaceutical ingredients are ^{18}O-water, mannose triflate, and ^{18}F-fluoride if it is obtained from an

outside supplier. The use of a certificate of analysis to replace identity testing is permissible in regard to (1) reagents, solvents, gases, purification columns, and other auxiliary materials, (2) containers and closures, and (3) inactive ingredients (e.g., a diluent, stabilizer, or preservative) obtained from a reliable supplier. However, if an inactive ingredient (e.g., 0.9% sodium chloride solution) is prepared on site, identity testing on the components used to prepare the inactive ingredient must be performed before its release for use.

Production and Process Controls

PET drug producers must have adequate production and process controls (i.e., master production and control record, batch production and control record) in place to ensure consistent production of a PET drug product that meets applicable standards for identity, strength, quality, and purity. The draft guidance suggests that "Corrections to paper entries should be dated and signed or initialed, leaving the original entry still readable. Corrections to electronic records should be recorded according to Part 11 (21 CFR Part 11, Electronic Records; Electronic Signatures), and there should be an audit trail to document the changes. Each batch record should be reviewed and approved for final release (signature/initials and date)."[109]

Since most PET drug products are administered to patients by injection, they must be produced by personnel who are trained in aseptic technique. An operator is initially certified to perform aseptic processing by completing three successful media-fill runs and thereafter is requalified by passing an annual media-fill run test.

Aseptic processing of PET drug products should involve microbiologic control of all components as follows: (1) Tubing and glassware should be washed and rinsed with Water for Injection USP (preferably) or purified water, wrapped in aluminum foil, and depyrogenated using a suitable dry-heat oven cycle, (2) transfer lines are suitable for reuse; however, they should be promptly cleaned after each use by rinsing with Water for Injection USP then flushing with volatile organic solvents (e.g., ethanol and acetone), and finally drying with nitrogen, (3) low-microbial grade resin column material should be used in order to limit bioburden, (4) a sample of sterilizing membrane filter should be tested before use; integrity testing of the membrane filter should be performed after filtration (i.e., bubble-point test), and (5) the environment should be periodically monitored by methods such as the use of swabs or contact plates to test the aseptic workstation surfaces and the use of settling plates or dynamic air samples to evaluate air quality of the aseptic facility and workstation.

Validation of a new process or of a significant change to an already validated process should be conducted prospectively. However, if a PET center has an established history of producing a particular PET drug, validation of the production process can be conducted retrospectively if the process has been shown to be capable of yielding batches meeting required specifications. In addition, a concurrent validation can be justified if the short half-life of the PET drug prohibits the use of either a prospective or a retrospective validation process. In any event, the draft guidance recommends the respective order of preference in regard to process validation to be prospective, retrospective, and concurrent. However, each PET drug producer should weigh the pros and cons carefully in considering which type of validation scheme to use.

Laboratory Controls

If a reference standard is obtained from an officially recognized source (e.g., *USP*), no further testing is required. However, if the reference standard is purchased from an

alternative source, a reference spectrum or other supporting data to fully confirm the identity and purity of the reference standard must either be obtained from the supplier or established by the PET center.

Stability Testing

The draft guidance suggests that establishment of the stability testing program be based on at least three production runs of the final drug product. This evaluation should be conducted under the following conditions: (1) set the radioactive concentration to be at or near the highest level, (2) store the whole batch volume in the intended container and closure system, and (3) study for a time period equal to the stated shelf life of the PET drug product.

Finished Drug Product Controls and Acceptance Criteria

The preliminary draft proposed rule indicates that PET centers must establish specifications for each batch of a PET drug product, including criteria for identity, strength, quality, purity, and if appropriate, sterility and pyrogenicity (for parenteral drug products). The proposed rule also states that the accuracy, sensitivity, specificity, and reproducibility of each testing procedure must be established and documented. These controls and acceptance criteria are requirements that must be met before a PET center may give final release to a finished PET drug product.

However, modifications to these standard guiding principles may be justifiable. For example, the prerelease of PET drug products for commercial distribution before completion of all required QC testing may be appropriate because of transportation deadlines. Reduced testing frequency (e.g., initial validation with annual testing thereafter) of certain QC procedures (e.g., radionuclidic purity, chemical purity for 2-chloro-2-deoxy-D-glucose) may be necessary because of constraints related to the costly QC equipment (e.g., MCA, special HPLC system).[110]

For a PET drug product that has a very short half-life (e.g., ^{13}N-ammonia), production usually involves multiple subbatches on the same day. The draft guidance recommends that the initial subbatch be used as the representative sample of the entire batch. Thus, the release of subsequent subbatches can be qualified for acceptance, provided the initial subbatch meets all acceptance criteria.

The preliminary draft proposed rule states that it is under consideration whether to include a provision in the CGMP regulations to allow the final release of a PET drug product if a particular required QC test cannot be completed because of equipment failure. The suggested prerequisites of such a "conditional release" include (1) previous successful completion of the incomplete test, (2) completion of the omitted test, if applicable, after the equipment is repaired, (3) notification of the receiving facility, and (4) proper calibration, operation, and maintenance of all equipment.

Labeling and Packaging

If a sticky label is not suitable for the immediate container (including the vial or syringe) because of a limited surface area or high radiation considerations, the draft guidance allows the use of a string label as long as there is a procedure in place to associate the label with the vial or syringe if the label were to come off.

Distribution

For PET centers that distribute PET drug products to affiliated institutions, outside pharmacies, and outside clients, a recall system must be in place to permit any recall notification to promptly reach the receiving facility, pharmacist, and the patient's physician, if known.

Complaint Handling

It is the responsibility of the QC unit to handle all complaints related to a specific PET drug product. An investigation must be initiated as soon as possible to collect all relevant information in a timely manner. Corrective action should be implemented immediately to avoid a similar incident in the future.

Records

All records should be kept for at least 3 years from the date of release of a PET drug product, whereas the validation reports should be kept as long as the systems are in use.

REFERENCES

1. Briner WH. Sterile kits for the preparation of radiopharmaceuticals: some basic quality control considerations. In: Subramanian G, Rhodes B, Cooper J, et al., eds. *Radiopharmaceuticals*. New York: Society of Nuclear Medicine; 1975:246-53.
2. Permissible molybdenum-99 concentration. 67 *Federal Register* 20380 (2002) (codified at 10 CFR §35.204).
3. European system for reporting adverse reactions to and defects in radiopharmaceuticals: annual report 1995. *Eur J Nucl Med*. 1996;23:BP27-31.
4. European system for reporting adverse reactions to and defects in radiopharmaceuticals: annual report 1996. *Eur J Nucl Med*. 1998;25:BP3-8.
5. European system for reporting adverse reactions to and defects in radiopharmaceuticals: annual report 1997. *Eur J Nucl Med*. 1998;25:BP45-50.
6. European system for reporting adverse reactions to and defects in radiopharmaceuticals: annual report 1998. *Eur J Nucl Med*. 1999;26:BP33-8.
7. European system for reporting adverse reactions to and defects in radiopharmaceuticals: annual report 1999. *Eur J Nucl Med*. 2001; 28:BP2-8.
8. European system for reporting adverse reactions to and defects in radiopharmaceuticals: annual report 2000. *Eur J Nucl Med*. 2002;29:BP13-9.
9. Ponto JA. Technetium-99m radiopharmaceutical preparation problems: 12 years of experience. *J Nucl Med Technol*. 1998;26:262-4.
10. Decristoforo C, Siller R, Chen F, et al. Radiochemical purity of routinely prepared ^{99m}Tc radiopharmaceuticals: a retrospective study. *Nucl Med Commun*. 2000;21:349-54.
11. Mission and preface. In: *United States Pharmacopeia 27/National Formulary 22*. Rockville, MD: United States Pharmacopeial Convention; 2004:v-xii.
12. General notices and requirements. In: *United States Pharmacopeia 27/National Formulary 22*. Rockville, MD: United States Pharmacopeial Convention; 2004:1-12.
13. Unapproved uses of approved drugs: the physician, the package insert, and the FDA. *Pediatrics*. 1978;62:262-4.
14. Kasik JE. Use of approved drugs in a non-approved way. *Iowa Medicine*. October 1987:513-5.
15. Hung JC, Ponto JA, Gadient KR, et al. Deficiencies of package insert directions for the preparation of radiopharmaceuticals. *J Am Pharm Assoc*. 2004;44:30-5.
16. Radiopharmaceutical preparation. In: *European Pharmacopeia*. 4th ed. Strasbourg, France: European Directorate for the Quality of the Medicines; 2002:1361-8.
17. Hung JC. Personal written communication with Capintec, Inc, Pittsburgh, PA, January 2002.
18. Radioactivity. In: *United States Pharmacopeia 27/National Formulary 22*. Rockville, MD: United States Pharmacopeial Convention; 2004:2374-8.

19. Chromatography. In: *United States Pharmacopeia 27/National Formulary 22.* Rockville, MD: United States Pharmacopeial Convention; 2004:2272-84.
20. TechneScan MAG3 [package insert]. St Louis, MO: Mallinckrodt Inc; 2000.
21. Hung JC, Wilson ME, Brown ML. Rapid preparation and quality control of technetium-99m MAG3. *J Nucl Med Technol.* 1991;19:176-9.
22. *Guidance: PET Drug Products—Current Good Manufacturing Practice (CGMP)* [draft]. Washington, DC: US Food and Drug Administration; 2001.
23. Levit N. *Radiopharmacy Laboratory Manual for Nuclear Medicine Technologists.* Albuquerque, NM : University of New Mexico College of Pharmacy; 1980:69-80.
24. Vivian A, Ice RD, Shen V, et al. *Procedure Manual: Radiochemical Purity of Radiopharmaceuticals Using Gelman Sepachrom (ITLC) Chromatography.* Ann Arbor, MI: Gelman Sciences; 1977:3-56.
25. Williams CC. Radiochemical purity of ^{99m}Tc-oxidronate [letter]. *J Nucl Med.* 1981;22:1015.
26. Zimmer AM, Spies SM. Quality control procedures for newer radiopharmaceuticals. *J Nucl Med Technol.* 1991;19:210-4.
27. Robbins PJ. *Chromatography of Technetium-99m Radiopharmaceuticals: A Practical Guide.* New York: Society of Nuclear Medicine; 1984.
28. Taukulis RA, Zimmer AM, Pavel DG, et al. Technical parameters associated with miniaturized chromatographic systems. *J Nucl Med Technol.* 1979;7:19.
29. Kowalsky RJ, Creekmore JR. Technical artifacts in chromatographic analysis of Tc-99m radiopharmaceuticals. *J Nucl Med Technol.* 1982;10:15.
30. Fludeoxyglucose F 18 injection. In: *United States Pharmacopeia 27/National Formulary 22.* Rockville, MD: United States Pharmacopeial Convention; 2004:815-6.
31. Introduction. In: *USP Reference Standard Catalog.* Rockville, MD: United States Pharmacopeial Convention; 2002:1-3.
32. Martinez E, Study KT. Scintillation well counter: too much activity? *Monthly Scan.* July 1980:1.
33. Hung JC, Budde PA, Wilson ME. Testing the radiochemical purity of technetium Tc 99m-labeled radiopharmaceuticals. *Am J Health Syst Pharm.* 1995;52:310-3.
34. ProstaScint [package insert]. Princeton, NJ: Cytogen; 1997.
35. Zevalin [package insert]. San Diego, CA: IDEC Pharmaceuticals; 2002.
36. Octreoscan [package insert]. St Louis, MO: Mallinckrodt Inc; 2000.
37. Zimmer AM, Pavel DG. Rapid miniaturized chromatographic quality-control procedures for Tc-99m radiopharmaceuticals. *J Nucl Med.* 1997;18:1230-3.
38. Acutect [package insert]. Wayne, NJ: Diatide/Rentschler Biotechnologie GmbH; 2001.
39. CEA-Scan [package insert]. Morris Plains, NJ: Immunomedics Inc; 1999.
40. Neurolite [package insert]. North Billerica, MA: Bristol-Myers Squibb Medical Imaging, Inc; 2001.
41. Budde PA, Hung JC, Mahoney DW, et al. Rapid quality control procedure for technetium-99m-bicisate. *J Nucl Med Technol.* 1995;23:190-4.
42. Neotect [package insert]. Londonderry, NH: Diatide/Rentschler Biotechnologie GmbH; 2000.
43. Zimmer AM, Magewski W, Spies SM. Rapid miniaturized chromatography for Tc-99m IDA agents: comparison with gel chromatography. *Eur J Nucl Med.* 1982;7:88-91.
44. Ceretec [package insert]. Amersham, England: Amersham Healthcare; 2000.
45. Jurisson S, Schlemper EO, Troutner DE, et al. Synthesis, characterization, and X-ray structual determinations of technetium (V)-oxo-tetradentate amine oxine complexes. *Inorg Chem.* 1986;25:543-9.
46. Hung JC, Taggart TR, Wilson ME, et al. Radiochemical purity testing for ^{99m}Tc-exametazime: a comparison study for three-paper chromatography. *Nucl Med Commun.* 1994;15:569-74.
47. Zimmer AM. Re: radiochemical purity of Tc-99m oxidronate [reply]. *J Nucl Med.* 1981;22:1016.
48. UltraTag [package insert]. St Louis, MO: Mallinckrodt Inc; 2000.
49. Chowdhury S, Hung JC. Optimal centrifugation parameters for labeling efficiency determination of technetium-99m labeled red blood cells [abstract]. *J Nucl Med Technol.* 1993;21:114-5.
50. Cardiolite [package insert]. North Billerica, MA: Bristol-Myers Squibb Medical Imaging; 2001.
51. Hung JC, Wilson ME, Brown ML, et al. Rapid preparation and quality control method for technetium-99m-2-methoxy isobutyl isonitrile (technetium-99m-sestamibi). *J Nucl Med.* 1991;32:2162-8.
52. Hung JC, Wilson ME, Gebhard MW, et al. Comparison of four alternative radiochemical purity testing methods for ^{99m}Tc-sestamibi. *Nucl Med Commun.* 1995;16:99-104.
53. Hammes R, Kies S, Koblenski D, et al. A better method of quality control for technetium-99m sestamibi. *J Nucl Med Technol.* 1991;19:232-5.
54. Myoview [package insert]. Arlington Heights, IL: Amersham Healthcare; 2003.
55. Metaye T, Desmarquet M, Rosenberg T. Rapid quality control for testing the radiochemical purity of ^{99m}Tc-tetrofosmin. *Nucl Med Commun.* 2001;22:1139-44.

56. American Pharmaceutical Association. *Alternative Radiochemical Purity Testing Procedures for the Compounded Radiopharmaceuticals Approved from 1988-1997*. Washington, DC: American Pharmaceutical Association; 1998.
57. Measure of dosage of unsealed byproduct material for medical use. 10 CFR §35.53 (2002).
58. Determination of dosages of unsealed byproduct material for medical use. 67 *Federal Register* 20378 (2002) (codified at 10 CFR §35.63).
59. Manufacture, preparation, or transfer for commercial distribution of radioactive drugs containing byproduct material for medical use under part 35. 10 CFR §32.72 (2002).
60. Wiarda KS. Use of a copper filter for dose calibrator measurements of nuclides emitting K x-rays. *J Nucl Med*. 1984;25:633-4.
61. Harris CC, Jaszczk RJ, Greer KL, et al. Effects of characteristic X-rays on assay of iodine-123 by dose calibrators. *J Nucl Med*. 1984;25:1367-70.
62. Kowalsky RJ, Johnston RE. Dose calibrator assay of iodine-123 and indium-111 with a copper filter. *J Nucl Med Technol*. 1998;26:94-8.
63. Salako QA, DeNardo SJ. Radioassay of yttrium-90 radiation using the radionuclide dose calibrator. *J Nucl Med*. 1997;38:723-6.
64. Zimmerman BE, Coursey BM, Cessna JT. Correct use of dose calibrator values [letter]. *J Nucl Med*. 1998;39:575.
65. Salako QA. Correct use of dose calibrator values [reply]. *J Nucl Med*. 1998; 39:575-6.
66. Labeling of vials and syringes. 67 *Federal Register* 20379 (2002) (codified at 10 CFR §35.69).
67. Fludeoxyglucose (^{18}F) injection. In: *European Pharmacopeia*. 4th ed. Strasbourg, France: European Directorate for the Quality of the Medicines; 2002;2316-9.
68. Staum MM. Incompatibility of phosphate buffer in ^{99m}Tc-sulfur colloid containing aluminum ion. *J Nucl Med*. 1972;13:386-7.
69. Study KT, Hladik WB, Saha GB. Effects of Al^{3+} ion on ^{99m}Tc sulfur colloid preparations with different buffers. *J Nucl Med Technol*. 1984;12:16-8.
70. Sodium pertechnetate Tc 99m injection. In: *United States Pharmacopeia 27/National Formulary 22*. Rockville, MD: United States Pharmacopeial Convention; 2004:1778-9.
71. US Food and Drug Administration. Classification of residual solvents by risk assessment. In: *Guidance for Industry Q3C Impurities: Residual Solvents*. Rockville, MD: US Food and Drug Administration; 1997:3. Available at: http://www.fda.gov/cder/guidance/Q3Cfnl.pdf. Accessed April 2, 2004.
72. US Food and Drug Administration. *Guidance for Industry Q3C: Tables and List*. Rockville, MD: US Food and Drug Administration; 1997. Available at: http://www.fda.gov/cder/guidance/Q3CT&Lrev1.pdf. Accessed April 2, 2004.
73. Technetium Tc 99m albumin aggregated injection. In: *United States Pharmacopeia 26/National Formulary 21*. Rockville, MD: United States Pharmacopeial Convention; 2003:1757-8.
74. Technetium Tc 99m exametazime injection. In: *United States Pharmacopeia 27/National Formulary 22*. Rockville, MD: United States Pharmacopeial Convention; 2004:1772-3.
75. Ceretec [package insert]. Arlington Heights, IL: Amersham Healthcare; 1996.
76. pH. In: *United States Pharmacopeia 27/National Formulary 22*. Rockville, MD: United States Pharmacopeial Convention; 2004:2344-5.
77. pH/px (test papers and solutions). In: *Fisher Catalog 2000/01*. Pittsburgh, PA: Fisher Scientific; 2000:1283.
78. Sterility test. In: *United States Pharmacopeia 27/National Formulary 22*. Rockville, MD: United States Pharmacopeial Convention; 2004:2157-62.
79. Bacterial endotoxins test. In: *United States Pharmacopeia 27/National Formulary 22*. Rockville, MD: United States Pharmacopeial Convention; 2004:2169-73.
80. US Food and Drug Administration. *Current Good Manufacturing Practice for Positron Emission Tomography Drugs: Preliminary Draft Proposed Rule*. Washington, DC: US Food and Drug Administration; 2002.
81. US Food and Drug Administration. *Sample Formats: Application to Manufacture Ammonia N 13 Injection Fludeoxyglucose F 18 Injection (FDG F 18) and Sodium Fluoride F 18 Injection Chemistry, Manufacturing, and Controls Section*. Rockville, MD: US Food and Drug Administration; 2000:24-6. Available at: http://www.fda.gov/cder/guidance/cmcsample.pdf. Accessed July 21, 2003.
82. Pyrogen test. In: *United States Pharmacopeia 27/National Formulary 22*. Rockville, MD: United States Pharmacopeial Convention; 2004:2194-6.
83. Cooper JF, Harbert JC. Endotoxin as a cause of aseptic meningitis after radionuclide cisternography. *J Nucl Med*. 1975;16:809-13.
84. Bang FB. A bacterial disease of *Limulus polyphemus*. *Bull Johns Hopkins Hosp*. 1956;98:325-51.
85. Levin J, Bang FB. Clottable protein in *Limulus*: its localization and kinetics of its coagulation by endotoxin. *Thromb Diath Haemorrh*. 1968;19:186-97.

86. Cooper JF. Bacterial endotoxins test. In: Prince R, ed. *Microbiology in Pharmaceutical Manufacturing*. Godalming, UK: Davis Horwood International; 2001:537-67.
87. Cooper JF, Thoma LA. Screening extemporaneously compounded intraspinal injections with the bacterial endotoxins test. *Am J Health Syst Pharm*. 2002;59:2426-33.
88. Cooper JF. BET Methods for PET Radiopharmaceuticals. Paper presented at 148th Annual Meeting of the American Pharmaceutical Association; March 2001; San Francisco, CA.
89. Radiopharmaceuticals for positron emission tomography: compounding. In: *United States Pharmacopeia 27/National Formulary 22*. Rockville, MD: United States Pharmacopeial Convention; 2004:2381-5.
90. Cooper JF. USP revision for radiopharmaceuticals for positron emission tomography (PET) takes effect June 2001. *LAL Times*. June 2001;8:1-2.
91. Possession, use, and calibration of instruments used to measure the activity of unsealed byproduct material. 67 *Federal Register* 20378 (2002) (codified at 10 CFR §35.60).
92. American National Standards Institute. *American National Standard Calibration and Usage of "Dose Calibrator" Ionization Chambers for the Assay of Radionuclides*. Washington, DC: American National Standards Institute; 1986.
93. National Council on Radiation Protection and Measurements. *Quality Assurance for Diagnostic Imaging*. NCRP Report No. 99. Bethesda, MD: National Council on Radiation Protection and Measurements; 1988.
94. Records of calibrations of instruments used to measure the activity of unsealed byproduct material. 67 *Federal Register* 20393 (2002) (codified at 10 CFR §35.20).
95. Possession, use, and calibration of instruments used to measure the activity of unsealed byproduct material. 67 *Federal Register* 20378 (2002) (codified at 10 CFR §35.60).
96. Kowalsky RJ, Johnston RE, Chan FH. Dose calibrator performance and quality control. *J Nucl Med Technol*. 1977;5:35-40.
97. Oswald WM, Herold TJ, Wilson ME, et al. Dose calibrator linearity testing using an improved attenuator system. *J Nucl Med Technol*. 1992;20:169-72.
98. Chu RY. Accuracy of dose calibrator linearity test [letter]. *Health Phys*. 1988;55:95.
99. US Nuclear Regulatory Commission. Model procedure for calibrating dose calibrator. In: *Guide for the Preparation of Applications for Medical Use Programs*. Washington, DC: US Nuclear Regulatory Commission. 1987;C-1-6.
100. Calibration of survey instruments. 67 *Federal Register* 20378 (2002) (codified at 10 CFR §35.61).
101. Records of radiation survey instrument calibration. 67 *Federal Register* 20393 (2002) (codified at 10 CFR §35.2061).
102. Records of mobile medical services. 67 *Federal Register* 20393 (2002) (codified at 10 CFR §35.2080).
103. Positron emission tomography. US Food and Drug Administration Modernization Act. Bill S. 830, Pub L No. 105-115 §121, 11 Stat 2296 (1997).
104. Briner SJ. USP monographs and tests of radiochemical purity [letter]. *Am J Health Syst Pharm*. 1995;52:1817-8.
105. Draft guidelines on the manufacture of positron emission tomography radiopharmaceutical drug products; availability. 60 *Federal Register* 10593-4 (1995).
106. Guidance for industry: current good manufacturing practices for positron emission tomographic (PET) drug products; availability. 62 *Federal Register* 19580-1 (1997).
107. Pharmaceutical compounding—sterile preparations. In: *United States Pharmacopeia 27/National Formulary 22*. Rockville, MD: United States Pharmacopeial Convention; 2004:2350-70.
108. Sterility testing: validation of isolator systems. In: *United States Pharmacopeia 27/National Formulary 22*. Rockville, MD: United States Pharmacopeial Convention; 2004:2613-6.
109. Electronic records; electronic signature. 21 CFR §11 (2002).
110. Hung JC. Comparison of various requirements of the quality assurance procedures for ^{18}F-FDG injection. *J Nucl Med*. 2002;43:1495-1506.

13 Brain

Radiopharmaceuticals for central nervous system (CNS) evaluation can be divided into five main groups: (1) nondiffusible tracers, (2) diffusible tracers, (3) metabolism markers, (4) cerebrospinal fluid (CSF) agents, and (5) receptor imaging agents.

Nondiffusible tracers were the first compounds used for brain imaging. They are generally characterized as ionized hydrophilic compounds with nonspecific mechanisms of localization in brain lesions. They are excluded from entering the normal brain by an intact blood–brain barrier (BBB). However, under conditions in which the barrier is disrupted by brain pathology, these tracers leave the vascular space and concentrate in lesions. Pathologic lesions, such as tumors, subdural hematomas, and arteriovenous malformations, typically appear as localized areas of increased uptake of radioactivity against a normal brain that is devoid of activity. Included in the nondiffusible tracer group are ^{99m}Tc-sodium pertechnetate, ^{99m}Tc-pentetate (^{99m}Tc-DTPA), ^{99m}Tc-gluceptate (^{99m}Tc-GH), and the positron emission tomography (PET) imaging agent ^{82}Rb-rubidium chloride. These agents are no longer widely used in brain imaging, primarily because anatomic brain lesions are better evaluated with other diagnostic modalities such as computed tomography (CT) and magnetic resonance imaging (MRI). However, some clinical applications for these agents still exist.

Diffusible tracers have the capacity to enter normal brain through an intact BBB. This is possible because these agents are neutral lipophilic complexes that passively diffuse through the endothelial cells of the brain's capillaries. The diffusible tracers include ^{99m}Tc-exametazime (^{99m}Tc-HMPAO) and ^{99m}Tc-bicisate (^{99m}Tc-ECD). These complexes enter normal brain tissue in proportion to regional cerebral blood flow (rCBF). Consequently, on brain images, regions of normal brain that are adequately perfused demonstrate uptake of radioactivity, whereas brain lesions (such as infarcts) that have diminished or absent blood flow appear as areas of decreased radioactivity. The development of diffusible tracers revitalized brain imaging, because nuclear medicine studies with these agents often provide functional information that complements the diagnostic findings of CT or MRI images.

Metabolism markers are agents that localize in regions of the brain that are associated with metabolic and hypermetabolic activity. The principal metabolic marker used in PET imaging is ^{18}F-fludeoxyglucose (^{18}F-FDG). As a glucose analogue, FDG localizes in tissues that use glucose as an energy substrate. Brain lesions such as seizure foci and brain tumors have elevated energy needs and demonstrate increased uptake of FDG relative to normal brain. The imaging advantage of ^{18}F-FDG, compared with radiolabeled glucose, is that FDG is only partially metabolized and becomes trapped in lesions. The accumulation of ^{18}F-FDG permits localization of the lesions with a PET camera. As a short-lived positron emitter, ^{18}F-FDG is gaining more widespread use because of the greater availability of PET cameras at nuclear medicine facilities and the availability of ^{18}F-FDG from cyclotron-based nuclear pharmacies located near hospitals and nuclear medicine clinics.

Radiopharmaceuticals for evaluation of the CSF space comprise agents that remain confined to the CSF space after a lumbar injection. These radiotracers are used to evaluate the dynamics and distribution of CSF in various disease states. Hydrocephalus is routinely evaluated with ^{111}In-pentetate (^{111}In-DTPA).

Radiopharmaceuticals for brain receptor imaging are currently used primarily in research. Receptor-avid compounds labeled with ^{99m}Tc and other radionuclides are being developed and should gain more routine application once their effectiveness in various disease states is validated and their use is approved by the Food and Drug Administration (FDA). These agents hold promise for the detection and quantitation of biochemical function in the brain. Studies have already shown that positron-emitting, isotopically labeled radiotracers such as ^{11}C-N-methylspiperone can measure the occupancy rate of dopamine receptors in the brain. Other studies have demonstrated that ^{99m}Tc-TRODAT localizes in the basal ganglia through its ability to bind to the dopamine transporter (DAT) in the brain.[1,2] A large number of receptor-binding tracers have been developed that target dopamine, β-adrenergic, steroid, and muscarinic receptors in the brain.[3] These radiotracers are expected to allow noninvasive monitoring of changes in receptors as a function of disease.

FUNCTIONAL IMAGING

The greatest strength of nuclear medicine lies in its ability to assess biologic function rather than anatomic structure. Instrumentation and radiopharmaceuticals with the ability to measure cerebral blood flow (CBF), metabolism, and biochemistry using tomographic imaging have changed the role of brain imaging from anatomic visualization to functional assessment. Functional analysis not only complements the anatomic information provided by CT and MRI but can add new information not provided by any other diagnostic modality.

Physiologic Principles

In this first clinical applications chapter, brief consideration is given to the processes involved in transport across membranes in the body. More detail can be found in basic physiology and pharmacology textbooks. The localization of drugs and radiotracer molecules depends on these processes, and transport phenomena in the brain are of great importance and complexity.

Membrane Structure and Transport Processes

The plasma membrane that surrounds a single cell in the body is composed of a phospholipid bilayer interspersed with protein molecules.[4] The individual phospholipid molecules making up each layer are composed of a hydrophilic "head" (phosphate or carboxylate portion) and a hydrophobic "tail" (fatty acid portion). The two layers of phospholipid molecules are aligned so that the head portion of one layer is oriented toward the outside of the membrane and the head portion of the other layer is oriented toward the inside (cytoplasmic side) of the membrane. The tail portions of each layer are oriented toward each other on the inside portion of the membrane. Thus, the interior of the membrane is lipoid or hydrophobic, and the exterior of the membrane is ionic or hydrophilic. The proteins in the membrane, which are mostly glycoproteins, are located on the exterior surface or protrude through the membrane. The exterior or peripheral proteins act almost entirely as enzymes.[4]

Transport across the cell membrane occurs by one of three main processes: passive diffusion, facilitated diffusion, and active transport.[4] The process of *passive diffusion* for nonelectrolytes is controlled by the relative concentrations of the substance on each side of the membrane, with the direction being from higher concentration to lower concentration.

Diffusion of charged molecules (electrolytes) is driven by the electrochemical potential across the membrane (i.e., it is affected by the difference in chemical concentration and charge concentration). Nonionic lipid-soluble molecules are favored in diffusion through the cell membrane. Their rate of diffusion is determined by the lipid solubility of the substance. Small ionic substances and water diffuse through minute pores in the membrane believed to be spaces within the protein molecules that penetrate all the way through the membrane.

Substances that are not lipid soluble but are necessary for cell viability, such as sugars and amino acids, cross the cell membrane by *facilitated diffusion*. Facilitated diffusion is a downhill transport process (high to low concentration) and is stereospecific and saturable. It involves the transport of a substance across the membrane by an enzymatic carrier. The transport of glucose into cells occurs by facilitated diffusion. The effect of the carrier is to make glucose soluble in the membrane, in which it would otherwise not be soluble because of its hydrophilicity.

Active transport across the cell membrane is an energy-dependent uphill movement from a lower concentration to a higher concentration if the substance is a nonelectrolyte and from a lower to a higher electrochemical potential if it is an electrolyte. In general, the process involves combining the substance with a carrier protein (enzyme) at the outer membrane, diffusion through the membrane, and cleavage of the substance from the enzyme at the inner membrane–cytoplasm interface. The freed substance then diffuses into the cytoplasm. Adenosine triphosphate (ATP) provides the energy required for the cleavage. The primary difference between facilitated diffusion and active transport is that active transport can move substances from low to high concentration, whereas facilitated diffusion can move substances only from high to low concentrations. The principal difference between passive diffusion and facilitated diffusion is that the latter is limited by the amount of carrier present to transport molecules. A prime example of an active transport process in the body is the sodium–potassium pump, which is present in all cell membranes of the body.[4] It carries potassium into the cell and sodium out of the cell at a net transfer rate of three sodium ions out for two potassium ions in. The carrier protein is sodium–potassium (Na-K) ATPase, which is capable of transporting ions and splitting ATP to provide energy for the pump. The pump can transport sodium ions and potassium ions against concentration gradients of 20 to 1 and 30 to 1, respectively.[4]

A fourth method of transport across cell membranes is *pinocytosis*. The mechanism of pinocytosis varies among cell types and is quite active in gastrointestinal absorption. Pinocytosis involves contact of a substance, such as a macromolecule or particle, with the outer cell membrane, which invaginates to engulf the molecule. The invagination pinches off to form a vesicle that slowly transports the substance to the inner membrane and releases it into the cytoplasm. Pinocytosis can transport substances against an electrochemical gradient, similar to active transport, but it is a much slower process. It is an important transport process for high molecular weight proteins, which cannot navigate through the small pores of the cell membrane.[4]

Nonneural Capillaries

The circulatory system supplies essential nutrients to all tissues of the body via the capillaries. Blood flow into the capillaries is controlled by the precapillary sphincter, which contracts and relaxes 5 to 10 times per minute and is autoregulated by tissue oxygen concentration.[4] With some exceptions, the walls of nonneural capillaries through which fluid and ion exchange occur in the body are composed of a unicellular layer of endothelial cells on the luminal side and a basement membrane on the abluminal side (Figure 13-1).

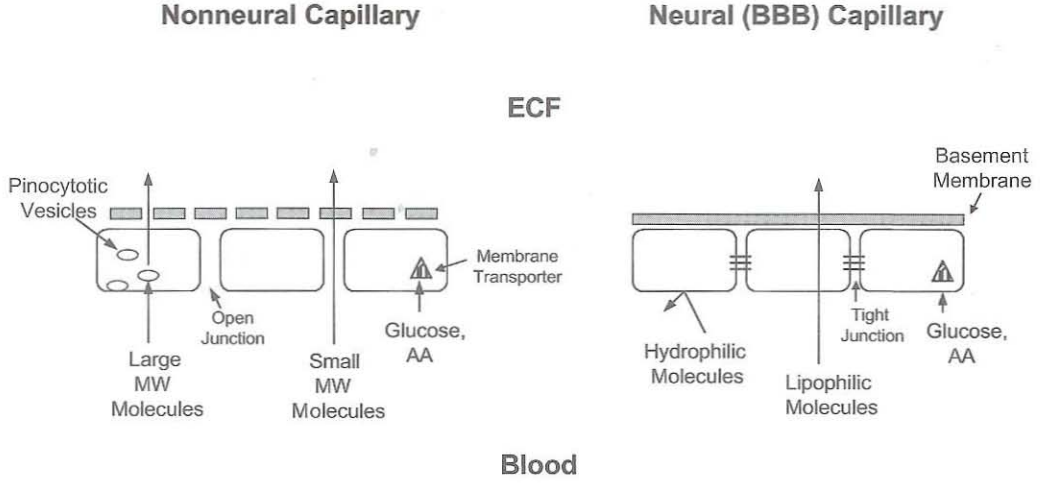

FIGURE 13-1 Transport processes through neural capillaries and nonneural capillaries from blood into extracellular fluid (ECF). See text for detailed explanation.

Intercellular clefts form a thin (6–7 nm) space between the endothelial cells, through which water and water-soluble ions can pass between the blood and the interstitial fluid.[4]

Capillary permeability to substances is a function of molecular size. Endothelial cells contain pinocytotic vesicles that serve as transporters of high molecular weight substances and small particles. Some capillaries contain fenestrae (oval windows) through the middle of the endothelial cells, through which large volumes of substances can pass by simple diffusion. These can be found in the glomerular capillaries, which allow filtration of large amounts of fluid for urine formation. Fenestrae are also found in the hepatic portal blood vessels, where they facilitate the flow of large amounts of nutrients from the blood to the liver parenchymal cells. The intercellular junction between endothelial cells is open and the basement membrane is discontinuous to allow free flow of substances. Endothelial cells also contain proteins that facilitate transport of specific substances, such as glucose and amino acids, from the blood into the tissues.

Neural Capillaries

Neural capillaries in the brain differ from standard nonneural capillaries in at least three important ways (Figure 13-1). First, the intercellular clefts or junctions are tightly apposed, limiting the free flow of substances. The tight junctions consist of fibrils that connect adjacent cell plasma membranes and occur as complete bands or belts around connected cells.[5] The fibrils surround the apical margins of epithelial cells of the choroid plexus and also form between endothelial cells of blood vessels in the brain. They are also present between barrier cells at the arachnoid membrane (Figure 13-2).[5] A second difference in neural capillaries is that they have a basement membrane that is continuous, thereby further restricting simple diffusion processes. Third, neural capillary cells have a paucity of pinocytotic vesicles to transport high molecular weight substances.

These structural differences in neural capillaries present a barrier to simple diffusion of substances between the blood and the brain extracellular space; this is known as the blood–brain barrier (BBB). Only uncharged, lipophilic molecules can diffuse across the brain endothelium as they can across other cellular membranes in the body. A few substances that are soluble in the lipid of the cell membrane as well as in water and can cross the BBB are oxygen, carbon dioxide, alcohol, and fatty acids.[4] The one similarity between

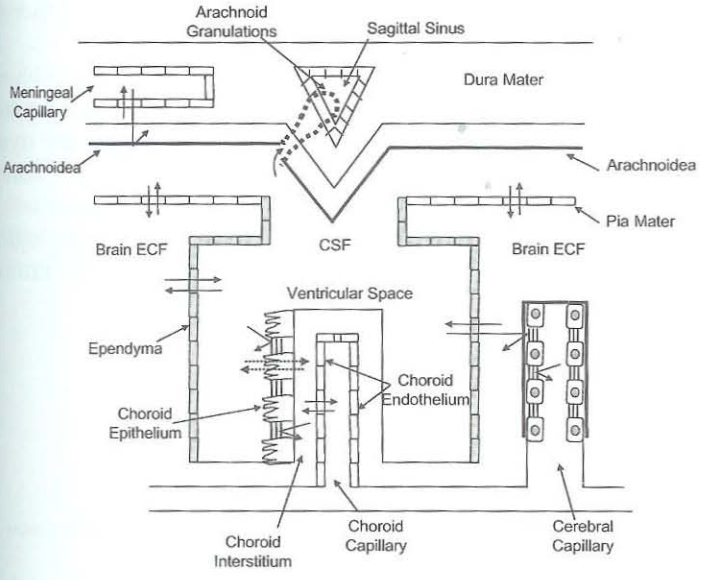

FIGURE 13-2 Sites of the blood–brain barrier in the brain are three-fold: the blood–brain extracellular fluid (ECF) barrier, the blood–cerebrospinal fluid (CSF) barrier, and the brain–CSF barrier. See text for detailed explanation.

neural and nonneural capillaries is the presence of endothelial cell membrane transport proteins for glucose and amino acids.

Blood–Brain Barrier

An understanding of drug and radiotracer localization in the brain requires knowledge of the various compartments in the brain, illustrated in Figure 13-2. The BBB separates the two main compartments of the CNS, the brain and CSF, from the third compartment, the blood, which is supplied to the brain by the cerebral capillaries, the meningeal capillaries, and the capillaries of the choroid plexus.[6]

The *blood–brain extracellular fluid (ECF) barrier* is found at the interface of the brain ECF and cerebral capillaries. Here, because of the tight junctions, water-soluble molecules are immediately restricted from crossing the endothelium into the brain ECF. This barrier's selective permeability permits the passage of only uncharged, lipid-soluble molecules.

The *blood–CSF barrier* is found at the interface of the CSF and the capillaries of the choroid plexus. The choroid endothelial cells are fenestrated and freely permeable to water-soluble molecules, which can diffuse from the choroid capillary blood into the interstitial space and between the choroid epithelial cells up to the tight junctions.[6] However, the tight junctions between the epithelial cells prevent substances from entering the CSF. Another potential site of exchange between the CSF and blood is the arachnoid membrane. The meningeal capillaries of the dura are fenestrated and permit free passage of water-soluble substances into the dural extracellular space but not into the CSF, because of tight junctions in the outermost layers of the arachnoid membrane.[6]

The *CSF–brain barrier* is at the pia mater overlying the brain surface and at the ependyma lining the ventricular system.[6] At this interface no barrier appears to exist because the ependyma and pia allow rapid equilibration of water-soluble molecules between the brain ECF and the CSF. This distribution has been demonstrated by the injection of horseradish peroxidase (molecular weight [MW] 43,000) directly into the CSF; the molecule not only penetrates the ependyma and brain parenchyma but also permeates the basement membrane and the clefts between adjacent cerebral capillary endothelial cells up to the tight junctions.[5,7] Injection directly into the CSF is therefore an effective way to deliver drugs to the brain. The CSF itself and small substances in the CSF less than

1 μm in size can egress from the CSF space through the porous arachnoid granulations into the venous blood of the superior sagittal sinus.

Historically, the concept of the BBB developed from the observation that trypan blue dye, which is bound to plasma protein, caused staining of tissues except the brain when injected intravenously into rabbits. The brain, however, could be stained when the dye was injected directly into the CSF.[5] The barrier, therefore, appears to protect the brain from various water-soluble substances present in the blood in order to maintain its homeostatic neuronal environment.[8] This barrier, however, can be disrupted by various pathologic conditions. When the BBB is disrupted, hydrophilic radiotracers are able to enter the brain and identify lesions.

Cerebral Circulation

Blood is supplied to the brain by the carotid and vertebral arteries, as shown in Figures 13-3 and 13-4. Only the major vessels are shown; the minor arteries have been omitted for clarity. The right and left vertebral arteries join to form the single basilar artery that supplies blood to the brain stem and the occipital cortex through the posterior cerebral arteries. The internal carotid arteries divide into the anterior and middle cerebral arteries and contribute communicating branches that anastomose with the posterior cerebrals. The circle of Willis at the base of the brain is formed by the interconnection of the two anterior cerebrals, the two posterior cerebrals, the two internal carotids, and the anterior and posterior communicating arteries.

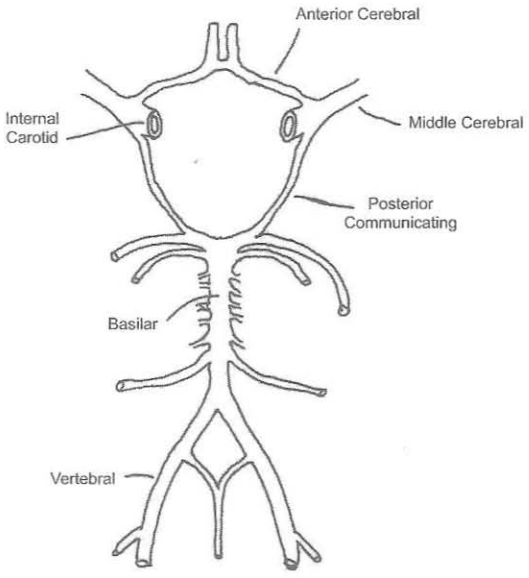

FIGURE 13-3 Arterial circulation at the base of the brain.

The right and left anterior cerebral arteries run side by side in the longitudinal fissure along the medial surface of each hemisphere and end near the terminal branches of the posterior cerebral arteries. The right and left middle cerebral arteries arise as the largest branches of the internal carotid arteries. Each runs, at first, laterally in the sylvian fissure, then back and up, where its eight discrete branches distribute blood on the lateral surface of each hemisphere.

Blood drains from the brain through large venous sinuses. The superior sagittal sinus is the large venous channel that runs posterior from the nasal cavity over the top of the brain between the two hemispheres to the occipital region, ending in the confluence of sinuses (torcula). Other major sinuses that drain into the torcula include the straight, occipital, and inferior sagittal sinuses. From the torcula, blood drains bilaterally into the right and left transverse sinuses, which run horizontally, laterally, and rostrally to terminate as the internal jugular veins, which return blood to the heart.

Brain Uptake and Extraction

Figure 13-5 illustrates the uptake of compounds in the brain. A drug in the blood may exist as free drug or drug bound to plasma protein. In general, only free drug can pass

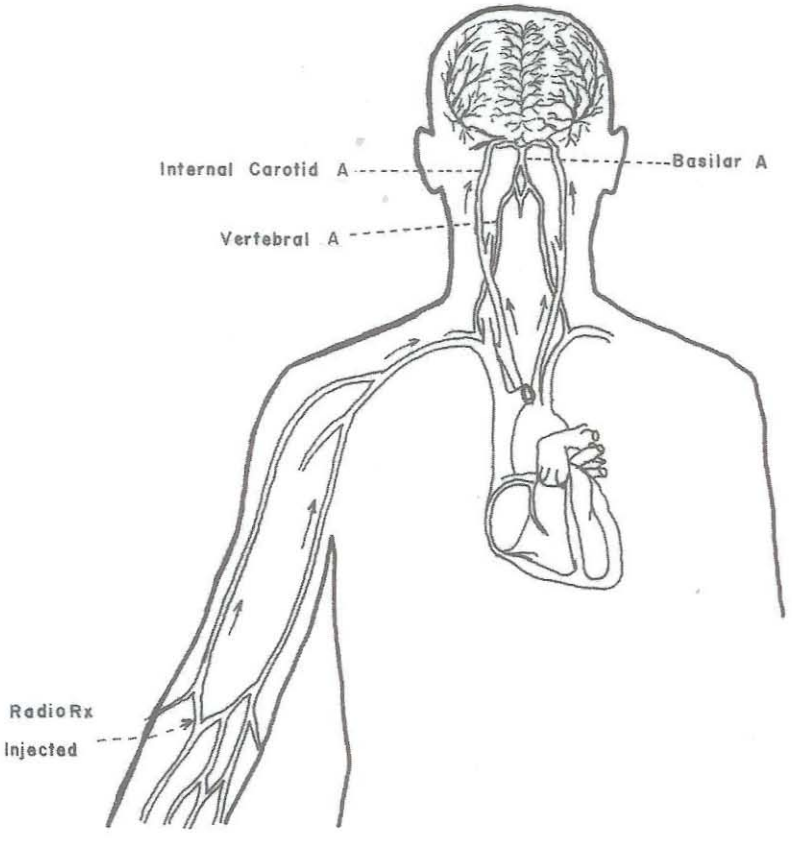

FIGURE 13-4 Cerebral delivery of radioactivity after intravenous injection of a radiopharmaceutical.

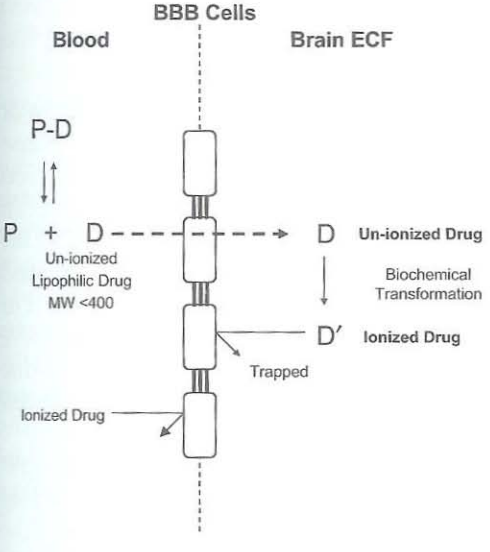

FIGURE 13-5 Mechanism of radiotracer uptake into the brain. Passive diffusion of a non–protein-bound, un-ionized, lipophilic small molecule across the neural capillary endothelium and trapping of its metabolite. D = free drug; P-D = drug bound to plasma protein.

through the capillary endothelium into the interstitial space of the brain. The amount of intravenously administered drug delivered to the brain that is taken up as the blood first passes through the brain is known as the first-pass extraction fraction. The extraction

fraction is the amount of drug extracted (difference between the arterial and venous concentration of drug) divided by the amount delivered (arterial concentration of drug). The extraction fraction of any compound that localizes by passive diffusion is influenced by several factors, including lipophilicity, protein binding, molecular size, and ionic charge. In general, neutral lipophilic molecules that are not protein bound in plasma (free drug) can passively diffuse through a biologic membrane, whereas charged hydrophilic molecules cannot. Studies conducted during the development of radiotracers for brain[9] and heart[10] imaging have demonstrated a parabolic relationship between tracer lipophilicity and organ uptake. Thus, drug uptake increases in proportion to lipophilicity but falls off at high lipophilicity because of drug binding to red blood cells and plasma protein. The optimal partition coefficient (log P_{oct}) is between 0.9 and 2.5.[9] Permeability is linear with lipophilicity up to a molecular weight of 400.[11]

Drug that enters the brain ECF is likely to diffuse back out unless it is trapped, either by undergoing a biochemical conversion to an ionized form or by becoming bound to a protein or a specific stereochemical receptor in the brain.

A compound with an extraction fraction of 1.0 will be completely extracted per pass through the brain. The standard for flow measurement in experimental animals is radiolabeled microspheres, which have an extraction fraction of 1.0 because of trapping in the small brain capillaries; microsphere uptake in the brain is thus linearly related to the amount of blood flow. Microspheres, however, are a nondiffusible marker, unlike most radiotracer molecules, whose extraction is related to diffusion across the BBB. To have high extraction, a diffusible marker must have high lipophilicity to ensure rapid permeation across the capillary membrane. If the permeability of a radiotracer is very high (extraction fraction near 1.0), then its brain uptake will be linearly proportional to blood flow, that is, brain uptake will be flow limited and reflect local pathology. Most radiopharmaceuticals for measuring CBF clinically demonstrate nonlinearity at high flows because of a diffusion limitation at these flows. Any radiotracer with low extraction will have uptake not related to flow and will not be a good marker of rCBF. No radiotracer is ideal, and none exhibits 100% extraction.

Blood Flow

The resting average blood flow to the brain is 50 mL/minute per 100 grams.[12] Most of this flow is to the gray matter, which has a high energy need. CBF changes in response to local metabolic needs (glucose and oxygen utilization), pH, and the levels of carbon dioxide. Carbon dioxide is the most potent cerebral vasodilator known. As a product of metabolism, carbon dioxide moves readily across cell membranes to lower the pH of the smooth muscle, causing vasodilation.[13] There is a direct coupling between rCBF and metabolism in the normal brain, but this does not always exist in abnormal states. For example, in acute cessation of arterial blood flow to the brain, such as in a stroke, there is reduced CBF to the ischemic area. This is the reverse of the normal response and is due to loss of carbon dioxide reactivity in the ischemic zone, with blood shunting to regions still responsive to carbon dioxide. This has been termed intracerebral steal.[13]

There are several methods for measuring CBF with radiotracers. They are complicated procedures that involve special techniques and equipment.[14] In routine nuclear medicine procedures, radiotracers are used to assess relative differences in blood flow to regions of the brain, principally in the evaluation of cerebrovascular disease, dementias, and epilepsy.

DEVELOPMENT OF BRAIN IMAGING AGENTS

Nondiffusible Tracers

Brain imaging was initially conceived to localize intracranial tumors. George Moore,[15] a neurosurgeon at the University of Minnesota, first attempted to visualize tumors during brain surgery by using ultraviolet light to detect previously injected fluorescein, which concentrated in tumors. This was followed by the use of radiolabeled ^{131}I-diiodofluorescein and then ^{131}I-labeled human serum albumin (^{131}I-HSA).[16,17] Although ^{131}I-HSA demonstrated high tumor-to-brain ratios, blood clearance was slow.

In 1959 Blau and Bender[18] introduced ^{203}Hg-chlormerodrin for brain imaging. This shortened the time between dose administration and imaging because this agent was cleared quickly from the blood by the kidney. It also had better physical properties for imaging. This was followed soon by the introduction of ^{197}Hg-chloromerodrin.[19] Both of these agents had shortcomings. The ^{203}Hg label produced a high kidney radiation dose because of its beta radiation and long effective half-life, and the 77 keV photons of ^{197}Hg were easily attenuated in brain tissue.

In the 1960s, ^{99m}Tc was introduced. The ^{99m}Tc generator was developed at Brookhaven National Laboratory and refined for medical use by Richards.[20,21] Harper et al.[22] first used the generator eluate to scan mice and found that ^{99m}Tc-pertechnetate activity localized in the stomach, salivary glands, and thyroid gland. The physical properties of ^{99m}Tc (short half-life, efficient photon detection, no particulate radiation) were more suited to the gamma camera, and large amounts of activity could be given with a smaller radiation dose. ^{99m}Tc-sodium pertechnetate soon became the agent of choice for brain scanning, requiring only prior administration of potassium perchlorate to retard its uptake in the choroid plexus. When the ^{82}Sr–^{82}Rb generator became available, the principal nondiffusible tracer for PET imaging was ^{82}Rb-rubidium chloride.

The desire to shorten the time between ^{99m}Tc-sodium pertechnetate administration and imaging, normally 3 to 4 hours, led to investigation into the use of technetium complexes with faster blood clearance.[23] ^{99m}Tc-DTPA and ^{99m}Tc-GH were compared with ^{99m}Tc-sodium pertechnetate.[24–27] Although the complexes had faster blood clearance, images obtained at early times (1.5 hours) after ^{99m}Tc-DTPA or ^{99m}Tc-sodium pertechnetate injection were less accurate than images at delayed times (3 hours). The ^{99m}Tc-GH complex had better accuracy at early and delayed times after injection and became the agent of choice for brain imaging.

The principal imaging device used with the ^{99m}Tc nondiffusible tracers is the planar gamma camera. A routine brain scan with these agents is conducted in two phases: a dynamic phase (flow study) and a static phase (delayed imaging). For the flow study, the radiopharmaceutical is injected into an arm vein. Brain perfusion is monitored with a gamma camera, which records the blood activity as it arrives and leaves the head (Figure 13-6). The major vessels seen during the arterial perfusion phase are the internal carotid arteries, the circle of Willis, the anterior cerebral arteries, and the middle cerebral arteries. After the arterial phase, there is a blush of activity throughout the head as the radiopharmaceutical distributes into the capillaries. Subsequently, venous drainage is seen by visualization of the superior sagittal sinus, the lateral (transverse) venous sinuses, and the jugular veins, which return blood to the heart. Obstructions to blood flow are seen as activity deficits in those areas. In the static phase, delayed images of the brain are taken 3 or more hours after injection to identify lesions that may concentrate activity. When nondiffusible tracers are used for brain imaging, the normal brain is devoid of activity because of BBB exclusion, whereas lesions such as tumors take up activity. Figure 13-7 illustrates two brain scans performed with a gamma camera and ^{99m}Tc-sodium pertechnetate. A similar pattern is observed with ^{99m}Tc-DTPA or ^{99m}Tc-GH. It illustrates a normal

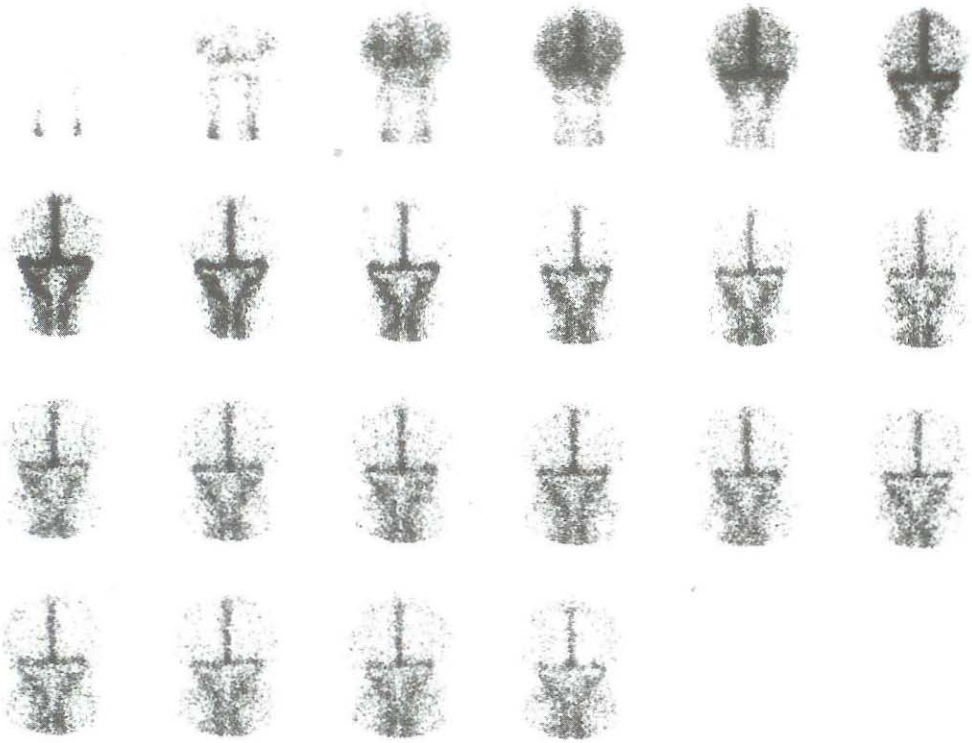

FIGURE 13-6 Normal posterior radionuclide cerebral angiogram (flow study). Images shown are made at 2 second intervals after intravenous injection of 20 mCi (740 MBq) of ^{99m}Tc-gluceptate (^{99m}Tc-GH). The arterial phase (first 2 to 6 seconds) is characterized by visualization of the two internal carotid, two middle cerebral, and paramedial posterior cerebral arteries. This is followed by a capillary "blush" phase leading quickly to the venous phase, which is recognized by the appearance of activity in the superior sagittal sinus (midline). Subsequent images show venous drainage through the lateral (transverse) venous sinuses and the jugular veins, which return blood to the heart.

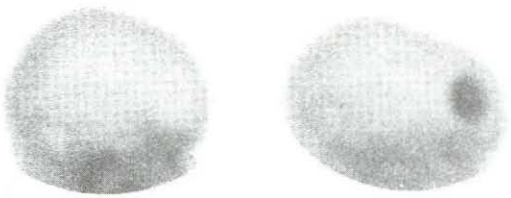

FIGURE 13-7 Brain scan (right lateral view) illustrating typical distribution pattern of a non-diffusible tracer, ^{99m}Tc-sodium pertechnetate. Normal brain, with intact BBB, is devoid of activity. Tumors, such as meningiomas, typically demonstrate increased uptake of activity.

scan devoid of cranial activity and an abnormal scan in a patient with a meningioma, showing uptake of activity in the tumor.

Brain imaging in nuclear medicine declined significantly with the introduction of CT because of CT's superior anatomic imaging capability. Brain imaging was revitalized with the development of diffusible tracers.

Diffusible Tracers

In 1978, Oldendorf[28] called attention to the decreasing number of brain scans being performed in nuclear medicine and pointed out that the lipophilic agent ^{123}I-iodoantipyrine

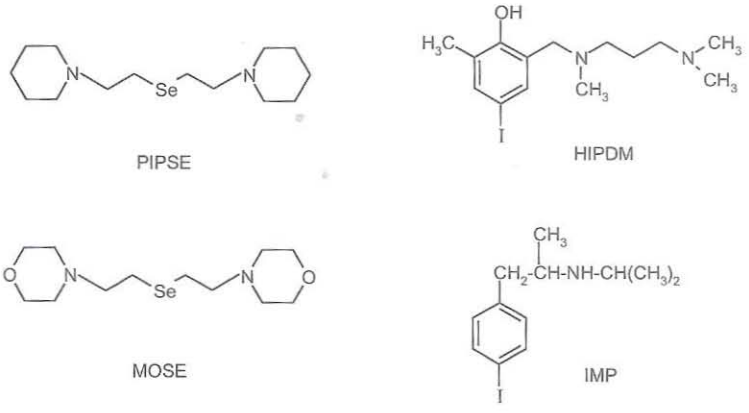

FIGURE 13-8 Chemical structures of amine-type first-generation diffusible tracers for brain imaging.

had shown brain uptake proportional to CBF.[29] Although iodoantipyrine readily crosses the BBB, it also diffuses back out and therefore has limited usefulness without a brain trapping mechanism. Oldendorf encouraged nuclear medicine scientists to direct their efforts toward the development of lipophilic ^{99m}Tc tracers that could cross the BBB so that CBF could be measured. To this end, Loberg et al.[30] prepared a series of ^{99m}Tc-labeled iminodiacetic acid analogues with varying octanol-to-water partition coefficients. They demonstrated that brain uptake was proportional to lipophilicity; however, because of high plasma protein binding, none of the agents tested had clinical potential. About the same time, Kung and Blau[31] developed two diamine compounds, di-β-(piperidinoethyl)-selenide (PIPSE) and di-β-(morpholinoethyl)-selenide (MOSE), labeled with ^{75}Se for brain localization (Figure 13-8). Their work was based on the pH-gradient hypothesis. This hypothesis assumes that an un-ionized amine species in the blood at pH 7.4 is lipophilic and will freely diffuse across the BBB. Once the amine molecule gains access to the brain's more acidic (pH 7.0) ECF, it is protonated and ionized and unable to diffuse back out.[31] Although PIPSE and MOSE never became useful brain imaging agents, their introduction led to the development of useful CBF agents. The pH-gradient concept also suggested a mechanism by which agents could become trapped in the brain, a necessary requirement for eventual tomographic imaging with SPECT.

Blood Flow Tracers

Approximately 15% of cardiac output is distributed to the brain, where it must provide substrate for the brain's metabolic needs. The brain acquires the oxygen and glucose it needs by increasing rCBF. It has been shown that blood flow and metabolism in the brain are coupled and that cerebrovascular disease can produce local changes in CBF, hence the importance of having agents in nuclear medicine that can measure rCBF.

Blood flow tracers for SPECT and PET imaging in nuclear medicine have three basic requirements: (1) They must be able to readily cross the BBB, (2) they must have brain retention long enough to acquire images (this is more critical for SPECT than PET), and (3) they must have a fixed regional distribution.[32] In the early 1980s two radioiodinated amine compounds, N-isopropyl-*p*-^{123}I-iodoamphetamine (^{123}I-IMP or iofetamine)[33] and hydroxy ^{123}I-iodobenzyl propyl diamine (^{123}I-HIPDM),[34] that had high first-pass extraction and potential for measuring regional cerebral perfusion were introduced for brain imaging (Figure 13-8). FDA originally approved ^{123}I-IMP in 1988. The manufacturer eventually withdrew it from the market for clinical reasons. The principal problem with ^{123}I-IMP was

that its original brain localization at the time of injection began to redistribute 1 hour after dosing, leading to inaccurate imaging at later times.[35] This redistribution was ascribed to continual input, as sequestered lung activity was slowly released into the circulation, and the differential washout of initially localized IMP and its metabolites from regions of the brain.[36,37] The in vivo profiles of ^{123}I-IMP and ^{123}I-HIPDM were found to be similar.[34] For a number of reasons, including uncertain brain retention mechanisms, inconvenience, and the cost of using ^{123}I, neither of these compounds became routine brain imaging agents.

In the early 1980s a number of technetium coordination compounds were also being developed for perfusion brain imaging. Significant among these were the technetium bisaminethiol complexes (^{99m}Tc-BAT) by Burns et al.[38] and Kung et al.[39] and the technetium propyleneamine oxime (^{99m}Tc-PnAO) complex by Volkert et al.[40] BAT, also known as diaminedithiol (DADT), is an N_2S_2 ligand, while PnAO is a tetraamine (N_4) ligand. The first generation of these neutral lipophilic complexes demonstrated brain uptake, but retention in brain was poor and unsuitable for SPECT imaging.[41] Subsequently, several derivatives of these ligands were prepared with amine side chains as functional groups that could potentially improve brain retention. The derivatives, however, yielded diasterioisomers that had to be separated by high-performance liquid chromatography in order to isolate the isomer with highest brain uptake. Most of the Tc-BAT derivatives that exhibited increased retention in brain had side chains containing carboxyester groups or pendent amine functionalities.[42] The most successful of these was the L,L-isomer of Tc(V)oxo-1,2-N,N'-ethylenedylbis-L-cysteine diethyl ester.[43,44] Otherwise known as ^{99m}Tc-bicisate (^{99m}Tc-ECD) (Neurolite, DuPont Merck), it is a diester derivative that undergoes in vivo hydrolysis in the brain to yield an ionized metabolite that is retained.[44]

While the ^{99m}Tc-PnAO complex showed rapid brain uptake after intravenous administration, its rapid washout precluded its use for SPECT imaging. Subsequently, several derivatives of ^{99m}PnAO were synthesized with methyl groups on the amineoxime backbone, in the hope of finding an agent that remained fixed in the brain. One of these was the hexamethyl derivative, ^{99m}Tc-hexamethylpropyleneamine oxime (^{99m}Tc-HMPAO), otherwise known as ^{99m}Tc-exametazime (Ceretec, Amersham). This complex is neutral and lipophilic but unstable in aqueous solution. The instability was found to be a conversion from the primary lipophilic complex to a secondary hydrophilic complex and was mediated by reducing agents.[45] Studies in animals and humans demonstrated that the *meso*-isomer had greater in vitro stability but little brain retention, while the D,L-isomer had poor in vitro stability but high brain retention. It was then surmised that brain uptake was caused by the lipophilic complex and brain retention was caused by its intracellular conversion to the nondiffusible hydrophilic complex. The brain conversion was shown to be caused by the intracellular reducing agent glutathione.[45]

^{99m}Tc-exametazime was eventually approved by FDA in December 1988 and ^{99m}Tc-bicisate in November 1994. Both of these agents have high first-pass extraction into the brain (^{99m}Tc-exametazime 70%[46] and ^{99m}Tc-bicisate 60%[47]). This property makes them useful markers for assessing relative CBF in the evaluation of cerebrovascular disease, particularly stroke.

Metabolic Markers

After the development of CT, interest in and the usefulness of conventional planar brain imaging with the gamma camera declined significantly. Only those studies that provided dynamic or physiologic information were of interest, and these were few because of the limited arsenal of radiopharmaceuticals. The desire for physiologic information from brain imaging led by necessity to the development of compounds labeled with carbon, nitrogen, and oxygen isotopes. However, the only practical radionuclide choices of these elements

are the short-lived positron emitters ^{11}C, ^{13}N, and ^{15}O, which require PET. Research was eventually conducted with 2-deoxy-D-glucose labeled with ^{14}C for animal studies and ^{11}C and ^{18}F for clinical studies.[47–50] The results of this work demonstrated that ^{18}F-2-deoxy-2-fluoro-D-glucose (fludeoxyglucose or FDG) was an accurate marker of glucose utilization in the brain and that it was a useful tool for studying the brain's response to normal, pathologic, and interventional stimuli.[49] These investigations were able to demonstrate further that deoxyglucose crosses the BBB and is phosphorylated similarly to glucose; however, unlike glucose, deoxyglucose-6-phosphate is retained in tissue for an extended time, which facilitates imaging studies.

FDA originally approved ^{18}F-FDG in July 1994 at the Downstate Clinical PET Center for the identification of regions of abnormal glucose metabolism associated with epileptic seizure foci. Since then, ^{18}F-FDG has shown wide applicability in cancer diagnosis in many different organ systems, for identifying primary tumors and differentiating recurrent tumor from radiation necrosis.

Receptor Imaging Agents

Another area in which radiopharmaceuticals have made important contributions to the understanding of brain function in disease is receptor imaging. A large number of receptor-based radiotracers have been investigated, but none has been approved for routine use. Because of the stereochemical specificity of receptors, many of the agents that have been investigated are labeled with ^{11}C and ^{18}F for PET imaging. SPECT agents are labeled typically with radioiodine, but some technetium-labeled agents are being developed.[2] A wide range of brain receptors exist for which imaging agents can potentially be developed. Radiotracers have been developed for brain receptors of the neurotransmitters acetylcholine, norepinephrine, dopamine, serotonin, histamine, and somatostatin. Diseases are thought to be associated with changes in the concentration of receptors (up-regulation or down-regulation), which could be measured with an appropriate receptor-binding radiotracer. For example, schizophrenia, tardive dyskinesia, and Huntington's chorea are thought to be associated with an increase in dopamine receptor concentration, while Parkinson's disease is associated with a decrease in dopamine receptors.[3] Because so many receptor-binding agents have been investigated, other references on this topic may be of interest to readers.[2,3,51–53]

BIOLOGIC PROPERTIES OF BRAIN IMAGING AGENTS

Nondiffusible Tracers

Nondiffusible tracers are no longer routinely used for brain imaging. The properties of ^{99m}Tc-sodium pertechnetate will be described in this chapter, however, because it is still used for certain nuclear medicine procedures. It is also the primary starting material for all ^{99m}Tc-labeled radiopharmaceuticals and thus may be present as an impurity in these compounds. The biologic properties of the other ^{99m}Tc complexes that were once used in brain imaging, ^{99m}Tc-DTPA and ^{99m}Tc-GH, will be discussed in other chapters.

Sodium Pertechnetate Tc 99m Injection

The clinical use of ^{99m}Tc as the pertechnetate anion, $^{99m}TcO_4^-$, began in 1961 at the University of Chicago. Many comprehensive investigations have been made with this agent, and its biologic behavior has been reviewed by Lathrop and Harper.[54] Sodium pertechnetate Tc 99m injection (^{99m}Tc-sodium pertechnetate) is usually administered by intravenous injection,

but it may be administered orally. Of the total activity circulating in the bloodstream 1 hour after injection, an average of 30% is contained in the red cell fraction and 70% in the plasma.[55] The activity is freely diffusible into and out of the red blood cells and can be removed by serial washing of cells in saline. Approximately 75% of plasma activity is protein bound, with one-third of this very loosely bound. The disappearance of activity in blood after intravenous injection is multiexponential and shows wide variation in individuals, with half-lives in the ranges of 1 to 2 minutes (50%–60%), 5 to 20 minutes (15%), and 100 to 300 minutes (20%–30%) without the coadministration of potassium perchlorate. These times are significantly prolonged if perchlorate is given.[54]

One hour after intravenous administration, ^{99m}Tc-sodium pertechnetate has the following organ distribution: 30% in gastric mucosa and juice, 2% in the thyroid gland, and 5% in salivary glands and saliva.[54] Similar to the iodide ion, pertechnetate is concentrated and secreted by the mucoid cells of the gastric glands, but not by the peptic (chief) cells or oxyntic (parietal) cells (Figure 13-9).[55,56] In the thyroid gland, pertechnetate is not metabolized as is iodide, and its accumulation is limited to the ion-concentrating mechanism of thyroid epithelial cells (i.e., it is trapped but not organified). The striated epithelial cells of the salivary glands have concentrating mechanisms for the group VII anions, including iodide and its analogues (such as pertechnetate, thiocyanate, and perchlorate).

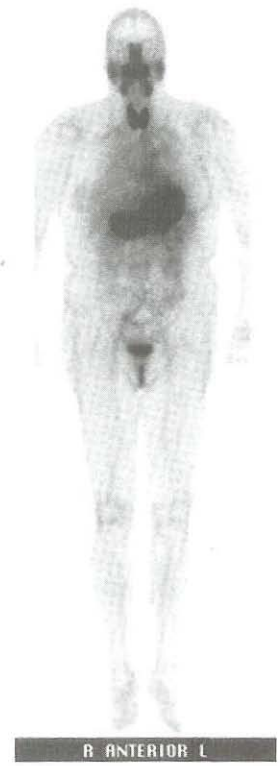

FIGURE 13-9 Total body image 2 hours after intravenous administration of 10 mCi (370 MBq) of ^{99m}Tc-sodium pertechnetate. Normal uptake of activity is seen in the salivary glands, thyroid gland, and stomach. Activity is also seen in the oral and nasopharyngeal regions and the urinary bladder.

Tissue distribution and blood clearance of ^{99m}Tc-sodium pertechnetate are similar to those of iodide, but its excretion from the body is somewhat different. The renal clearance of pertechnetate (17 mL/minute) is about half that of iodide.[57] This represents about 14% of the inulin clearance, and thus about 86% of pertechnetate is reabsorbed by the renal tubule, assuming that the filtration fractions for pertechnetate and inulin are similar. This explains why plasma clearance is so slow after intravenous administration of ^{99m}Tc-sodium pertechnetate. Another important difference between pertechnetate and iodide occurs in the bowel. Although iodide is completely absorbed by the intestine, pertechnetate is partly bound to fecal material after its secretion into the intestinal lumen and is excreted with a half-life dependent upon the movement of material out of the intestine.[58] For these reasons, by 72 hours only 50% of pertechnetate is completely eliminated from the body by urinary and fecal routes, whereas iodide excretion exclusive of thyroid activity is greater than 98% by this time.

The long-term retention of technetium in humans after ^{99m}Tc-sodium pertechnetate administration has been measured using the longer-lived isotopes ^{95m}Tc ($T_{½}$ = 60 days) and ^{96}Tc ($T_{½}$ = 43 days).[59] After oral or intravenous administration, urinary excretion of pertechnetate is rapid within the first 24 hours but drops dramatically on the second and third days, with less than 1% excreted per day thereafter. Fecal excretion begins more slowly but is the principal route of elimination 1 day after administration; it reaches a maximum by the fourth or fifth day and decreases thereafter. Cumulative urinary and

fecal excretion is 30% in 1 day (27% urine, 3% fecal), 72% in 4 days (31% urine, 41% fecal), and 90% in 8 days (34% urine, 56% fecal).[59] Long-term retention studies estimate that 77% of the dose is eliminated with a biologic half-life of 1.6 days, 19% with a half-life of 3.7 days, and 4% with a half-life of 22 days.[59]

^{99m}Tc-sodium pertechnetate has been reported to concentrate in the choroid plexus of the brain.[60] It has been shown previously that radioiodide also concentrates in the choroid plexus by a process of active transport from spinal fluid into the blood and that this process can be retarded by perchlorate. Coben et al.[61] demonstrated that perchlorate increases the blood-to-CSF transport of iodide and decreases the reverse process of CSF-to-blood transport. This phenomenon suggests that the blood–CSF barrier is due to active transport from CSF to blood rather than to membrane hindrance of transport from blood to spinal fluid.[61] That is, iodide that readily diffuses from blood to spinal fluid is rapidly transported back to blood by an active process, and this creates the blood–CSF barrier. Harper et al.[62] visualized the CSF space with ^{99m}Tc-sodium pertechnetate by pretreating the patient with perchlorate to prevent active transport of pertechnetate from the CSF to blood. Oral administration of perchlorate prevents accumulation of pertechnetate in the choroid plexus and readily displaces what has already accumulated.[60] Perchlorate may be given orally at any time before or after the injection of ^{99m}Tc-sodium pertechnetate, provided the perchlorate administration precedes imaging by at least 60 minutes.[63] The usual oral dose of sodium or potassium perchlorate is 200 to 1000 mg. Up to 450 mg of sodium perchlorate has also been given intravenously.[64] Uptake of ^{99m}Tc-sodium pertechnetate in the thyroid and stomach is also retarded by perchlorate.

^{99m}Tc-sodium pertechnetate is excreted in human milk, and it is recommended that breast-feeding be suspended for 48 hours after radionuclide studies.[65,66]

^{99m}Tc-sodium pertechnetate also undergoes placental transfer, which is reduced by perchlorate; however, posttreatment with perchlorate does not release ^{99m}Tc from the fetus.[54] ^{99m}Tc-sodium pertechnetate, like all radiopharmaceuticals, is contraindicated during pregnancy.

Technetium Tc 99m Pentetate and Technetium Tc 99m Gluceptate

Technetium Tc 99m pentetate and technetium Tc 99m gluceptate replaced ^{99m}Tc-sodium pertechnetate for brain scanning when agents that did not penetrate the BBB were routinely used for brain imaging. These agents demonstrated higher target-to-background ratios because of faster blood clearance and did not require perchlorate pretreatment. Details of their biologic properties are discussed in Chapter 18.

Mechanisms of Localization of Nondiffusible Tracers

Nondiffusible tracers typically are charged hydrophilic compounds and therefore cannot diffuse directly through the brain endothelium. They are able to enter the brain, however, when this barrier is disrupted in some way as a result of a pathologic condition. Basic mechanisms for localization of these agents in brain tumors have been described by Tator[67] and are summarized as follows (see also Figure 13-10).

Vascularity

Many tumors are highly vascularized, and a large fraction of their radioactive content is due to their increased amount of blood. Examples include hemangioblastomas, vascular meningiomas, arteriovenous malformations, and certain malignant gliomas.

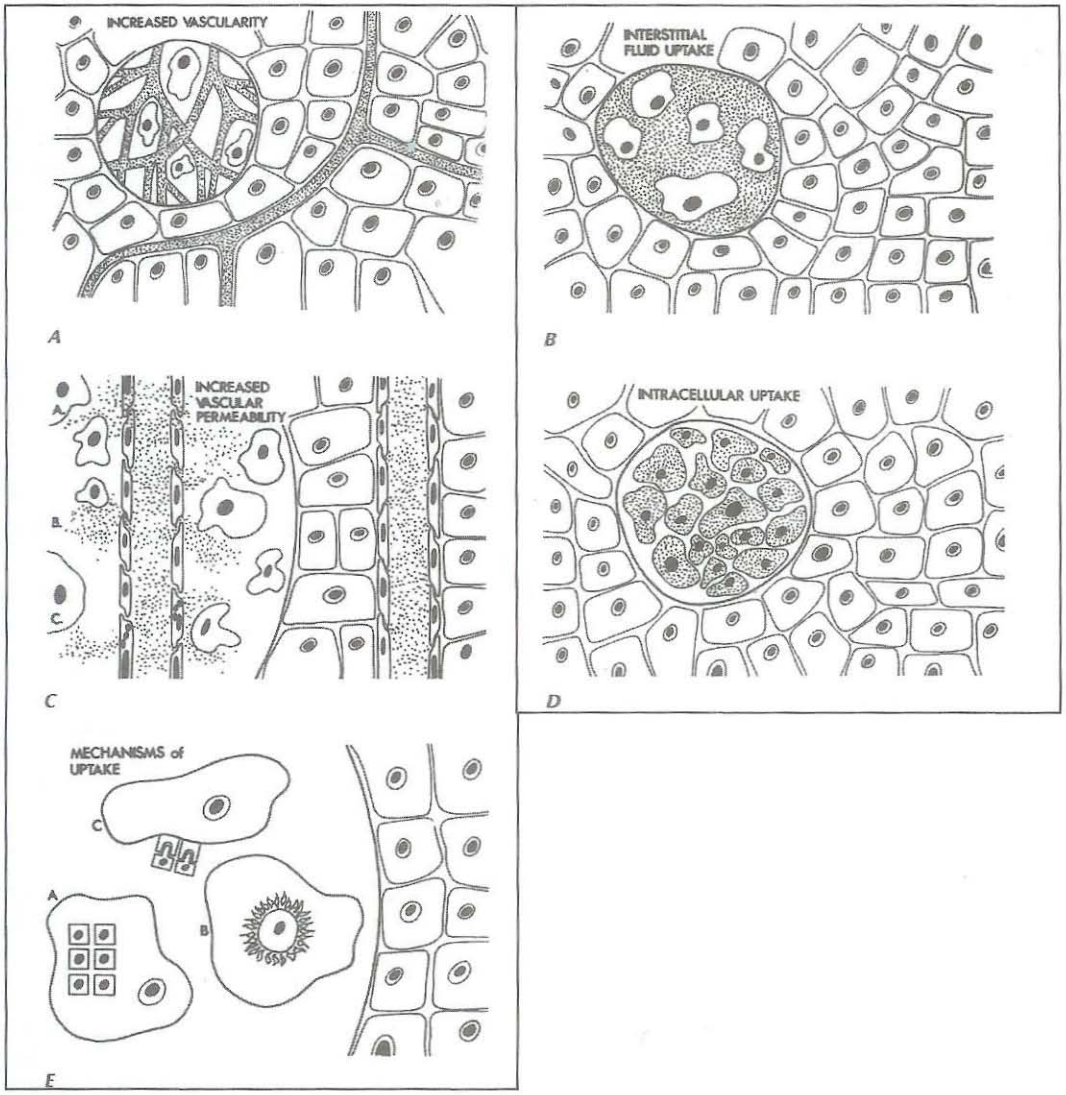

FIGURE 13-10 Basic mechanisms for the localization of radiopharmaceuticals in brain tumors. (*A*) Circumscribed neoplasm with increased vascularity surrounded by normal brain. Small dots represent radioactive tracer. (*B*) Marked accumulation of radioactive tracer in the interstitial space of neoplasm. (*C*) Increased vascular permeability of tumor capillaries, with radioactive tracer passing directly through endothelial cells (A), via gaps between endothelial cells (B), and by pinocytosis (C). In a normal brain where endothelial cells are tightly apposed, the tracer is confined to the bloodstream. (*D*) High intracellular uptake in neoplastic cells. (*E*) Neoplastic cell uptake of tracer as a substrate for growth (A) or energy (B) and adsorption of the antigen–antibody complex (C). (Reprinted with permission of the Society of Nuclear Medicine from reference 67.)

Interstitial Fluid

Almost all brain tumors contain more interstitial fluid than normal brain tissue. Many substances have a tendency to accumulate in this space, especially small molecules such as ^{99m}Tc-sodium pertechnetate and its complexes.

Capillary Permeability

The endothelial cell junctions in many tumors widen, and large molecules can readily diffuse through the open pores into the brain. Additionally, pinocytosis, not widely present in normal endothelial cells, is present to a greater extent in brain tumors. Front and Israel[68] have shown that meningiomas and glioblastomas that take up ^{99m}Tc-sodium pertechnetate and ^{57}Co-bleomycin also demonstrate, histologically, many pinocytotic vesicles and fenestrated endothelial cells, whereas tumors that exhibit no uptake of activity have normal endothelial architecture with tight junctions and few pinocytotic vesicles.

Tumor Cell Uptake

Mechanisms of uptake directly within neoplastic cells may involve substances that are substrates for energy requirements (glucose and phosphates) and for growth (amino acids). FDG localization is a good example. There may also be some intracellular protein present in tumors that binds tracer that is not present in normal cells. This has been noted with ^{67}Ga uptake in tumors outside the brain.

Diffusible Tracers

Technetium Tc 99m Exametazime Injection

Technetium Tc 99m exametazime injection (^{99m}Tc-HMPAO) is a neutral lipophilic complex with a MW of 384. Its octanol-to-water partition coefficient is 80 (i.e., log P_{oct} 1.9).[69] These properties permit ^{99m}Tc-HMPAO to readily diffuse through the BBB. The compound exists in two diastereoisomeric forms, D,L- and *meso*-.[70] However, only the D,L-isomer demonstrates significant brain uptake (Figure 13-11).[71] The two isomeric forms are separated by fractional crystallization so that the kit contains only the D,L-enantiomer. Figure 13-12 shows the chemical structure of ^{99m}Tc-D,L-HMPAO. The D,L-isomer will be referred to henceforth as ^{99m}Tc-HMPAO.

After intravenous injection, a mean of 72% of the primary lipophilic complex is extracted during the first pass into the brain at resting CBF (59 mL/minute per 100 grams), but this extraction decreases at higher flow rates.[69] Once the primary complex has crossed the BBB, its fate is determined by a competition between rapid conversion to a nondiffusible hydrophilic complex and washout to the blood. These two routes of loss of diffusible complex are of approximately equal importance, so that only about 50% of the ^{99m}Tc activity entering the brain is retained.[72] When ^{99m}Tc-HMPAO is injected into an arm vein during a clinical study, only a fraction (approximately 15%) of the injected dose (ID) reaches the brain, and a mean of 4.1% (3.5%–7.0%) of the ID actually localizes there.[71] The amount trapped in the brain reaches equilibrium by 2 minutes and remains steady over the first 8 hours. Brain retention is due to a glutathione-mediated conversion of the lipophilic complex to a hydrophilic form that cannot diffuse out of the brain.[73]

Lassen et al.[72] described a kinetic model in which ^{99m}Tc-HMPAO exists in the blood and brain compartments in an exchangeable lipophilic form and in a retained brain compartment as a nonexchangeable hydrophilic form. The model explains that the decline in extraction at high CBF is due to back diffusion of the exchangeable lipophilic complex from brain to blood. The amount that back diffuses was shown to be around 15%, and the back diffusion occurs within the first 2 minutes after injection.[69,71] When a correction is made for this back diffusion, the relationship between rCBF and ^{99m}Tc-HMPAO distribution is more linear.[72] One hundred percent extraction can never be achieved with ^{99m}Tc-HMPAO; a portion of the ID is already in the hydrophilic form because of in vitro

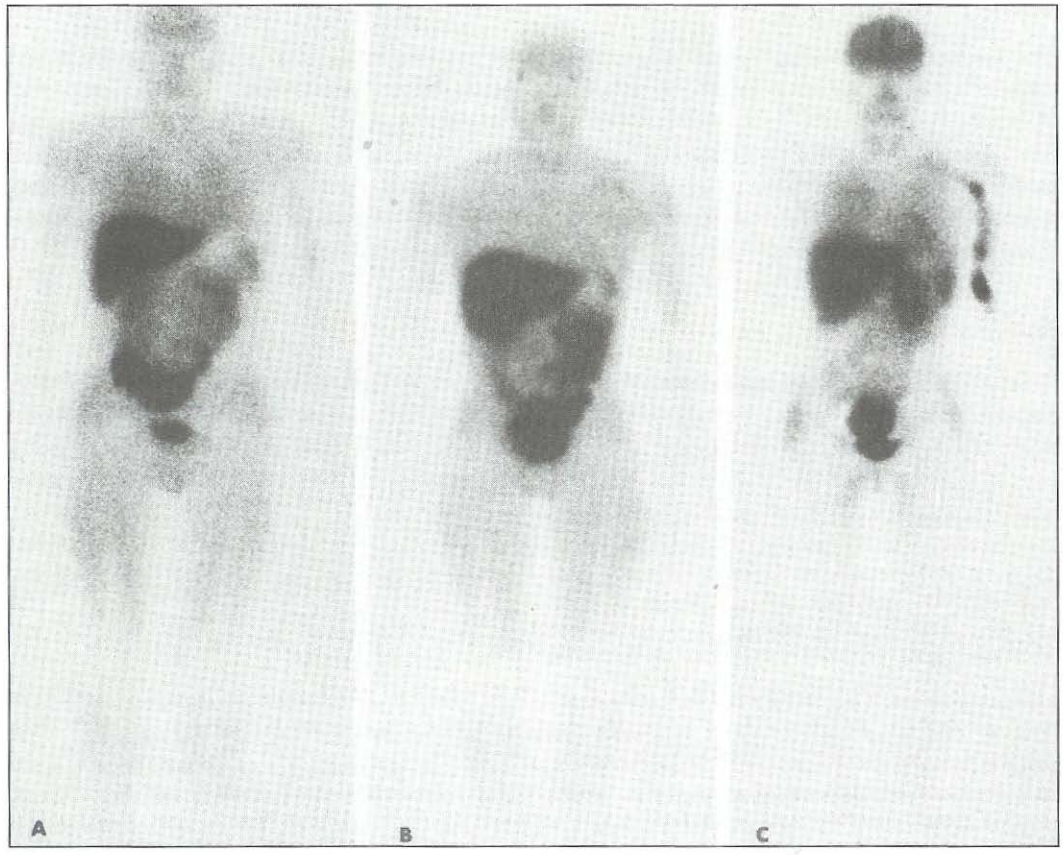

FIGURE 13-11 Anterior whole-body scans of ^{99m}Tc-HMPAO isomers 4 hours after injection. (A) Mixture of D,L- and *meso*-isomers, with uptake seen in brain, skeletal muscle, and lung. Excretion is hepatobiliary; kidneys, bladder, liver, and small intestine all are visible. (B) *Meso*-isomer, with distribution similar to the mixture but with lower lung uptake and obvious concentration of material in lacrimal glands. Brain uptake is only slightly higher than soft tissue uptake. (C) D,L-isomer, showing high uptake in brain. Uptake is also clearly seen in myocardium, subcutaneous fat of buttocks, and medial aspect of thighs. Retention of material in left brachiocephalic vein, into which material is injected, is a common feature of these materials. Activity is also seen in the urinary bladder, but amounts in the intestine are relatively small. (Reprinted with permission of the Society of Nuclear Medicine from reference 71.)

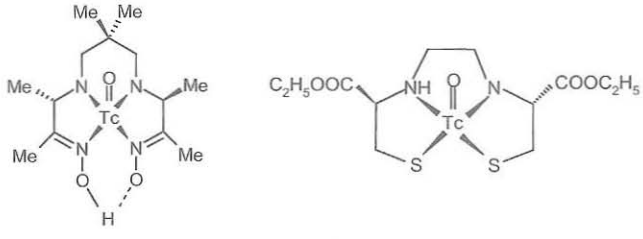

^{99m}Tc-D,L-HMPAO ^{99m}Tc-L,L-ECD

FIGURE 13-12 Chemical structures of ^{99m}Tc-D,L-HMPAO and ^{99m}Tc-L,L-ECD.

conversion prior to injection and in vivo conversion once in the blood.[74,75] The radiochemical purity of lipophilic ^{99m}Tc-HMPAO, assessed by octanol extraction, has been shown to be approximately 90% in normal saline, 40% in plasma, and 20% in whole blood by 10 minutes after tracer addition.[75] The stabilized kit reduces the chance of in vitro conversion.

^{99m}Tc-HMPAO exhibits both hepatobiliary and urinary excretion. Twenty minutes after injection, liver uptake is 10% and urinary excretion is about 2.5%, increasing to 35% in 24 hours.[71] About 30% of the ID is in the gastrointestinal tract immediately after injection, and about one-half of this is excreted via the intestinal tract by 48 hours.[76] About 40% of the ID is excreted by the kidneys into urine over 48 hours.[76] Soft-tissue distribution is predominantly in skeletal muscle. Twelve percent of activity remains in the blood 1 hour after injection.[71] The biologic half-life in the brain is estimated to be 71 hours.[77,78]

^{99m}Tc-HMPAO, with or without stabilization, is indicated for detection of altered cerebral perfusion in stroke. The usual adult administered activity is 10 to 30 mCi (370 to 1110 MBq). The critical organ listed in the package insert is the lacrimal glands, with a radiation absorbed dose of 5.6 rad(cGy)/20 mCi; however, this figure has been challenged and reported to be significantly lower (1.02 rad(cGy)/20 mCi) and to occur in only 11% of patients.[79]

Technetium Tc 99m Bicisate Injection

Technetium Tc 99m bicisate injection (^{99m}Tc-ECD) is a complex of technetium with ethyl cysteinate dimer. It is a neutral lipophilic complex with MW of 436. It can have four possible isomeric forms (D,D-, L,L-, L,D-, or D,L-) depending on whether it was synthesized with L-cysteine, D-cysteine or D,L-cysteine.[80] Both the L,L- and D,D-isomers demonstrate brain uptake, but only the L,L-isomer exhibits brain retention.[81] Brain retention is not only stereospecific but species-specific in that ^{99m}Tc-L,L-ECD (Figure 13-12) localizes only in the brains of primates (monkeys and humans). Its octanol-to-water partition coefficient is 51, and its gray-to-white matter ratio is about 4.5, demonstrating its potential usefulness in assessing rCBF.[81] The L,L-isomer will henceforth be referred to as ^{99m}Tc-ECD.

After intravenous injection, ^{99m}Tc-ECD demonstrates a high first-pass extraction into brain (47%[82], 60%[83]). Friberg et al.[84] measured brain dynamics and demonstrated that uptake and retention were triexponential, representing a vascular input spike, a back diffusion from brain to blood, and a very slow loss due to incomplete retention of hydrophilic metabolite. The distribution, however, does not change with time in the brain, and the loss appears to be the same from all regions. The retained fraction in the brain is 44%.[84] Walovitch et al.[80] demonstrated that ^{99m}Tc-ECD is rapidly metabolized in brain tissue, primarily in the cytosol, to a monoacid ester that is selectively trapped in primate brains but not in the brains of other species.

^{99m}Tc-ECD brain uptake correlates with CBF, but above 50 mL/minute per 100 grams it underestimates flow by as much as 20%.[85] Lassen and Sperling[86] compared the distribution of ^{99m}Tc-ECD and CBF measured with ^{133}Xe in patients with dementia, head trauma, epilepsy, brain tumor, and stroke. Good agreement was found in all cases except in subacute stroke patients, who failed to show reflow hyperemia in the infarct area. It was noted that this finding may be useful, particularly in subacute cases, when other SPECT methods present difficulties because of reflow masking the size and severity of the lesion.

In normal human subjects after intravenous administration, ^{99m}Tc-ECD demonstrates a maximum brain uptake of 6.5% in 5 minutes, slowly declining thereafter to 5.2% by 1 hour and 3.8% by 4 hours.[87,88] Figure 13-13 illustrates the total body distribution of ^{99m}Tc-ECD. Kinetic analysis demonstrates that 40% of brain activity washes out quickly ($T_{½}$ = 1.3 hour), while 60% clears much more slowly ($T_{½}$ = 42.3 hour).[87] Blood activity declines rapidly to 4.9% in 1 hour because of rapid plasma conversion to the monoethyl ester

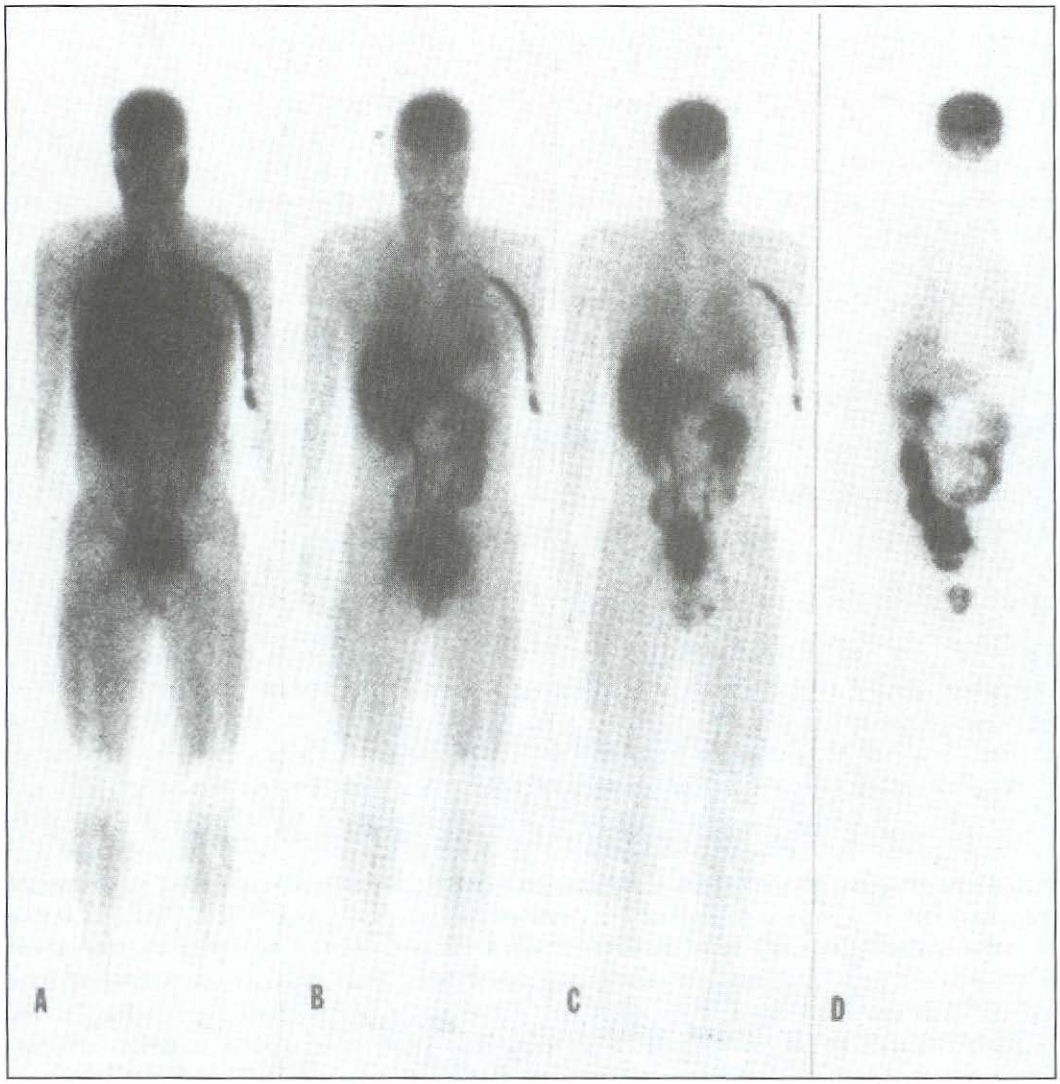

FIGURE 13-13 Whole-body distribution of ^{99m}Tc-L,L-ECD in a normal subject. Anterior views were obtained at (A) 5 minutes, (B) 1 hour, (C) 2 hours, and (D) 4 hours. (Reprinted with permission of the Society of Nuclear Medicine from reference 87.)

metabolite, which has high renal clearance (75% ID in urine within 6 hours).[89] Some of the tracer is excreted through the hepatobiliary system, with initial liver uptake of 17% at 5 minutes declining to 2.5% by 4 hours, with prominent gallbladder activity. Fecal excretion is 11% in 48 hours.[87]

The use of ^{99m}Tc-ECD in brain imaging is indicated as an adjunct to CT and MRI in localization of stroke in patients diagnosed with stroke. The usual adult administered activity for brain imaging is 10 to 30 mCi (370 to 1110 MBq) by intravenous injection. The critical organ is the urinary bladder wall, with a radiation absorbed dose of 0.11 rad(cGy)/mCi.[90]

Table 13-1 summarizes the properties of the blood flow radiotracers ^{99m}Tc-ECD, ^{99m}Tc-HMPAO, and ^{123}I-IMP. In general, ^{123}I-IMP is no longer available; it was shown to redistribute in brain at times later than 1 hour after injection and was therefore unreliable for

TABLE 13-1 Properties of SPECT Blood Flow Markers for Brain Imaging

Property	^{123}I-IMP	^{99m}Tc-HMPAO	^{99m}Tc-ECD
Molecular charge/lipophilicity	Neutral/lipophilic	Neutral/lipophilic	Neutral/lipophilic
Brain extraction efficiency	74–92%	72–80%	47–60%
Maximum brain uptake	6.5% (20 min)	4.1% (20 min)	6.5% (5 min)
Brain washout	Steady up to 1 hr Redistributes by 3 hr	15% over 2 min $T_{½}$ = 72 hr (slow component)	20% over 1 hr $T_{½}$ = 42.3 hr (slow component)
Blood levels[a]	2.5% ID (20 min)	12% ID (1 hr)	5% ID (1 hr)
Excretion	Urine (20% in 24 hr)	Urine (40% in 48 hr) Hepatobiliary (30% immediate)	Urine (72% in 24 hr) Hepatobiliary (12% in 48 hr)
Critical organ	Urinary bladder wall 1.38 rad/6 mCi	Lacrimal glands 5.16 rad/20 mCi	Urinary bladder wall 5.6 rad/20 mCi

[a] ID = injected dose.

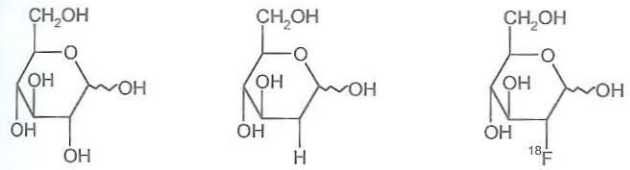

D-Glucose | 2-deoxy-D-Glucose | 2-fluoro-2-deoxy-D-Glucose (FDG)

FIGURE 13-14 Chemical structures of D-glucose, 2-deoxy-D-glucose, and 2-fluoro-2-deoxy-D-glucose (FDG).

identifying altered regional cerebral perfusion. ^{99m}Tc-HMPAO demonstrates slow blood clearance of its metabolite, causing lower target-to-background ratios than ^{99m}Tc-ECD, which exhibits rapid removal of its plasma metabolite.[91] Both agents are stable in kit form, although ^{99m}Tc-ECD is stable for a longer time (4 hours for stabilized ^{99m}Tc-HMPAO versus 6 hours for ^{99m}Tc-ECD). Neither agent redistributes in brain and both are retained long enough for SPECT imaging. ^{99m}Tc-ECD has a higher brain uptake initially than ^{99m}Tc-HMPAO, but ^{99m}Tc-ECD washes out of the brain more rapidly than ^{99m}Tc-HMPAO. However, brain washout of each agent is slow and does not appear to affect imaging.

Fludeoxyglucose F 18 Injection

Fludeoxyglucose F-18 injection (^{18}F-FDG) is a glucose analogue with a fluorine atom replacing a hydroxyl group in the C-2 position of D-glucose (Figure 13-14). ^{18}F-FDG is used to measure tissue metabolism in a variety of clinical applications. Because glucose is the primary energy substrate in brain metabolism, FDG, as a glucose analogue, will demonstrate high uptake in the brain cortex. The key difference between glucose and FDG, and the reason that ^{18}F-FDG is a useful tracer and radiolabeled glucose is not, is their different metabolism. Glucose is transported across the capillary endothelium by facilitated diffusion into the brain interstitial fluid and subsequently into the neuronal cytoplasm. In the cytoplasm, glucose undergoes enzymatic metabolism, with the first step being phosphorylation by hexokinase to glucose-6-phosphate, followed by a second step via glucose phosphate isomerase to fructose-6-phosphate. From this point it either undergoes conversion to glycogen or enters the glycolytic pathway with ultimate conversion to carbon dioxide and water. FDG is modified by substitution of the C-2 hydroxyl group of glucose

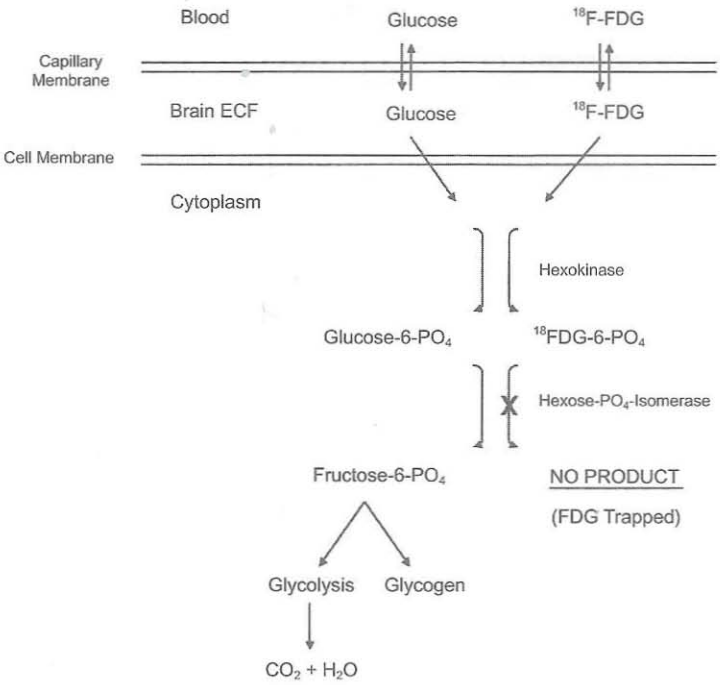

FIGURE 13-15 Metabolic scheme for glucose and FDG transport and metabolism in the brain.

with fluorine. This modification permits FDG to continue to be a substrate for the glucose transporter and for hexokinase conversion to FDG-6-phosphate, but it cannot be metabolized beyond this first step (Figure 13-15). Consequently, ^{18}F-FDG is trapped in tissue as FDG-6-phosphate and its distribution can be used to map glucose metabolism. FDG also differs from glucose in that it does not undergo tubular reabsorption and is readily excreted in the urine.

Routine procedures for brain imaging require that the patient fast for at least 4 hours before the study; if the patient has an elevated blood glucose level, poor brain uptake of FDG will occur. The patient is injected with ^{18}F-FDG in a quiet room and should remain inactive for at least 45 minutes to 1 hour to minimize uptake of ^{18}F-FDG in muscle and other tissue. The waiting time is necessary to maximize brain uptake because the first-pass extraction of FDG is low. During this time ^{18}F-FDG activity will accumulate in the urine, and the patient should void just before entering the PET scanner to reduce radiation dose to the bladder and surrounding organs.

The use of ^{18}F-FDG for measuring regional cerebral glucose utilization (rCMRglc) was validated by Phelps et al.[50] This investigation demonstrated that total ^{18}F activity, as FDG and FDG-6-phosphate, in brain tissue increases slowly after intravenous injection of 5 to 10 mCi (185 to 370 MBq) into an arm vein. Accumulation in gray and white matter reaches a plateau at about 90 minutes. The average concentration of ^{18}F in gray matter was 2.1 times that in white matter. Tissue concentration of total ^{18}F decreases after 120 minutes. The average tissue clearance half-time of FDG from brain was reported to be 9.1 hours. Within 1 hour after injection, the blood activity of ^{18}F-FDG falls to about 15% of its initial value.[50,47] For measurement of rCMRglc, the optimal time for data acquisition is between

60 and 120 minutes after injection because during this time the rCMRglc remains constant.[92]

^{18}F-FDG has fairly wide clinical application as a metabolic marker and has been used to assess brain disorders such as dementias, Parkinson's disease, and epilepsy. It has also been shown to be effective in the diagnosis and staging of several types of cancer, including brain, lung, colorectal, breast, and prostate cancer. Because tumor growth requires glucose utilization, ^{18}F-FDG can readily identify primary and metastatic lesions. ^{18}F-FDG PET can determine if a previously resected or radiation-treated brain tumor has become viable.[93–95] A patient's deterioration in the months after treatment may be due to tumor regrowth or radiation injury, and it is usually not possible to distinguish the difference by radiographic (CT) or clinical findings.[95] The differentiation is important because resection of necrotic tissue may halt deterioration and should be done at an early stage, while tumor recurrence requires early institution of chemotherapy. ^{18}F-FDG PET therefore provides functional information that improves diagnosis and facilitates patient care. At the time of diagnosis, ^{18}F-FDG PET provides information concerning the degree of malignancy and patient prognosis. After therapy, ^{18}F-FDG PET is able to assess persistence of tumor, determine degree of malignancy, monitor progression, differentiate recurrence from necrosis, and assess prognosis.[96]

The usual adult dosage of ^{18}F-FDG is 6 to 15 mCi (222 to 555 MBq). Brain imaging typically begins 45 to 60 minutes after ^{18}F-FDG injection. The principal route of elimination is urinary, with 20% of the dose excreted 2 hours after injection.[97] The critical organ is the urinary bladder wall, with a radiation absorbed dose of 7 rad(cGy)/10 mCi based on a 4.8 hour bladder voiding interval. The effective dose equivalent is 1.1 rem/10 mCi.[98]

Thallous Chloride Tl 201 Injection

Thallous chloride Tl 201 injection (^{201}Tl-thallous chloride) has been shown to be effective in localizing brain tumors with SPECT imaging. Its mechanism is believed to involve thallium's uptake by the Na-K ATPase pump in the membrane of viable tumor cells. Generally, imaging of brain tumors is begun within 5 minutes of administering 2 to 4 mCi (74 to 148 MBq) of ^{201}Tl-thallous chloride by intravenous injection. In a comparative study of ^{201}Tl-thallous chloride, ^{99m}Tc-gluceptate, and ^{67}Ga-gallium citrate with pathologic correlation in patients with gliomas, ^{201}Tl-thallous chloride identified viable tumor more accurately than the other agents and was minimally affected by concomitant corticosteroid therapy.[99] Black et al.[100] developed an index to distinguish between low-grade and high-grade intracranial tumors based on the ratio of thallium tumor uptake to normal brain uptake. An index greater than 1.5 was compatible with high-grade malignancy with 89% accuracy. Thallium is taken up in viable malignant tumors but not in areas of radiation necrosis.[101]

RADIOPHARMACEUTICALS FOR CISTERNOGRAPHY

CSF Physiology

The entire cavity enclosing the brain and spinal cord has a volume of approximately 1650 mL.[4] The major structures are shown in Figure 13-16. The brain and spinal cord are bathed in CSF. In humans, the total volume of the CSF space is about 150 mL, 30 mL of which is in the spinal canal. The rate of CSF formation is about 30 to 35 mL per hour; CSF is chiefly produced by choroid plexus secretion. Normally about 800 mL of CSF is produced each day. The composition of CSF is different from that of interstitial fluid in that CSF's concentration of sodium is 7% higher, glucose is 30% less, and potassium is 40% less.

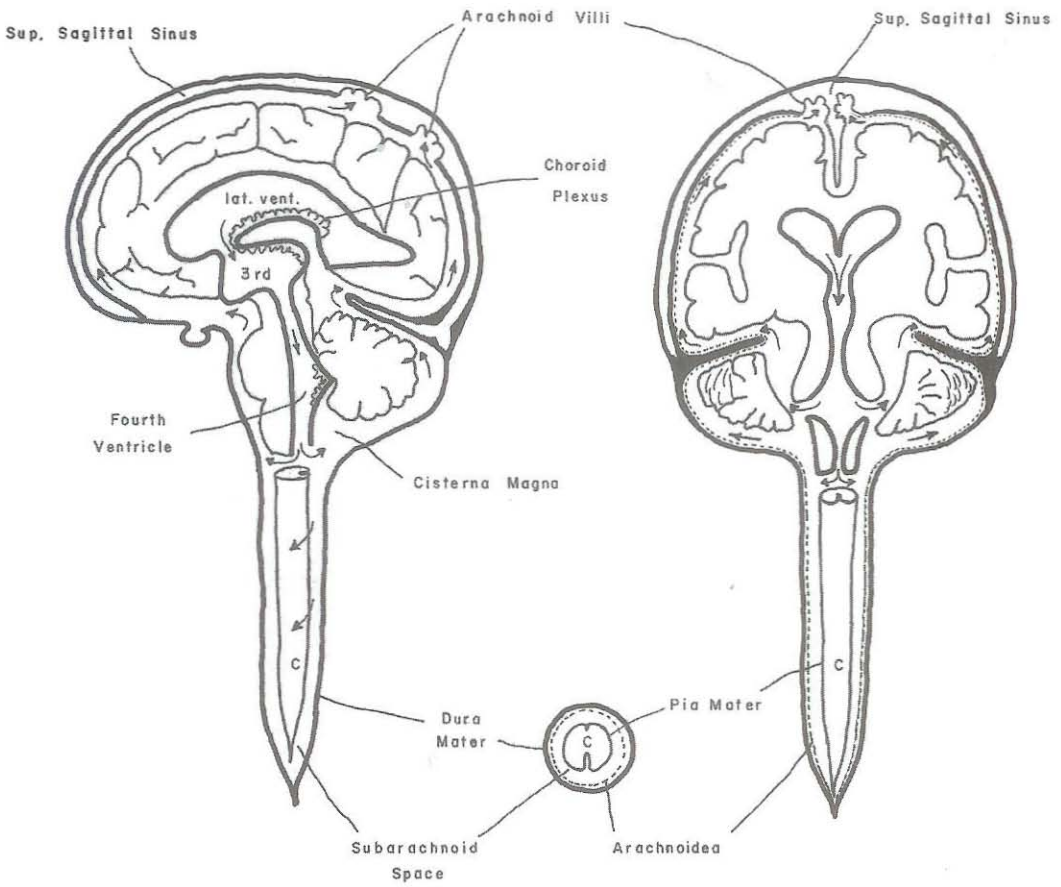

FIGURE 13-16 The brain and CSF space, showing the site of CSF production (choroid plexus) in the lateral, third, and fourth ventricles. CSF flow proceeds out of the ventricles in a caudad direction around the spinal cord and cephalad over the cerebral hemispheres and is absorbed at the arachnoid villi into the superior sagittal sinus. The cord cross-section shows the meninges and subarachnoid space.

Protein concentration is extremely low (only about 0.025%) and is similar to that of brain interstitial fluid. Normal CSF pressure is 10 mm Hg (equivalent to 135 mm H_2O), ranging from 6 to 14 mm Hg.

The choroid plexus is a cauliflowerlike tuft of infolding capillaries covered by a thin coat of ependymal cells, which elaborate the CSF. These cells also actively transport foreign substances from the CSF into the blood. The plexus projects into the temporal horns of the lateral ventricles, the posterior portions of the third ventricle, and the roof of the fourth ventricle. Fluid normally passes from the lateral ventricles through the foramen of Monro into the third ventricle and through the aqueduct of Sylvius into the fourth ventricle. Fluid escapes from the fourth ventricle through the median foramen of Magendie and two lateral foramina of Luschka to enter the cisterna magna. From the cistern it flows in the subarachnoid space through the tentorial opening and out over the cerebrum, where it passes through the arachnoid granulations into the venous sinuses of the brain. Flow through the one-way valves of the arachnoid membrane has minimal resistance; large molecules, such as proteins and other substances up to 1 μm in size, readily pass through the membrane into the sagittal sinus. As the CSF flows over the ventricular and pial surfaces of the brain, it sweeps away substances that diffuse from the brain into the CSF space.

A small quantity of CSF is formed by the blood vessels of the brain and spinal cord parenchyma and meninges. This fluid combines with that from the choroid plexus to flow through the subarachnoid space of higher levels. Most of the CSF bathing the spinal cord comes from this source.

A single layer of ependymal cells lines the walls of the ventricles and spinal cord (Figures 13-2 and 13-16). Tight junctions do not connect these epithelial cells, and the ependyma therefore is not a diffusion barrier to small solutes. Drugs placed into the ventricles readily pass into the brain extracellular space.[5] The apical microvilli of the choroid plexus facing the CSF have tight junctions that prevent diffusion of large molecules but are "leaky" to small ions (e.g., Na^+ and K^+).[5]

Development of CSF Imaging Agents

The technique of radioisotope cisternography was first described by DiChiro et al.,[102] who injected ^{131}I-radioiodinated serum albumin (RISA) into the lumbar subarachnoid space to evaluate CSF dynamics. RISA was not ideal because the ^{131}I label restricted the administered activity to 100 μCi (3.7 MBq), and there were isolated reports of aseptic meningitis that was ascribed to the amount of albumin administered.[103–105]

The desire for a higher photon yield and lower radiation dose led to the development of other radiopharmaceuticals. ^{99m}Tc-albumin was introduced for CSF rhinorrhea studies in 1968, which allowed administration of 2 mCi (74 MBq) doses.[106] However, the use of ^{99m}Tc in cisternography was limited to short-term studies, such as for CSF leaks, because of its 6 hour half-life. Routine cisternography for hydrocephalus evaluation requires imaging periods ranging from 6 to 72 hours, which necessitates a radiotracer with a longer half-life.

In 1970, ^{169}Yb-DTPA was introduced for cisternography.[107] Its advantages were a highly stable complex and a 32 day half-life that permitted strict quality control before human use. Additionally, it had a biologic half-life in the CSF compartment of about 10 hours, which was long enough for the study but short enough to keep the radiation dose low, except in patients with reduced renal clearance.

In 1971, ^{111}In was introduced for CSF studies as a transferrin complex and as a colloid.[108] The physical properties of ^{111}In (2.8 day half-life, no beta emission, and two photons) were well suited for cisternography. The colloid preparation was unsatisfactory because it collected in the basal cisterns. The transferrin complex was inconvenient because it required in-house labeling of the patient's own serum. Also, when compared with DTPA or EDTA complexes, the transferrin complex had a slower rate of clearance from the blood and the CSF space, which was attributed to its high molecular weight.[109] ^{111}In-DTPA had essentially the same biologic properties as ^{169}Yb-DTPA but significantly lower radiation absorbed dose to the spinal cord (Table 13-2). Its half-life permitted commercial production and availability with a reasonable shelf life. All of these properties made ^{111}In-DTPA the agent of choice for cisternography, and FDA approved it for routine use in 1982.

For short-term studies such as the localization of CSF leaks (rhinorrhea and otorrhea), ^{99m}Tc-DTPA has been used, although this is not an approved indication in the product labeling.[110,111]

Indium In 111 Pentetate Injection

The production and physical properties of indium In 111 pentetate injection (^{111}In-DTPA) have been well described and are discussed in Chapter 9.[112] After injection into the lumbar subarachnoid space, ^{111}In-DTPA moves slowly, with the natural flow of spinal fluid, away from the injection site toward the head (Figure 13-17). Leakage at the injection site can be

TABLE 13-2 Radiopharmaceuticals Used in Cisternography, Past and Present

Agent	Decay Mode	Physical Half-life	Effective Half-life[a]	Photon Energy keV	Photon Energy %	Administered Activity (mCi)	rad/Administered Activity[a] (spinal cord)	Study beyond 24 hr?
^{131}I-HSA	β^-	8 days	26 hr	364	83	0.1	7.1	Yes
^{169}Yb-DTPA	EC	32 days	12 hr	177	22	0.5	8.0	Yes
				198	35			
^{111}In-DTPA	EC	2.8 days	10 hr	171	91	0.5	1.9	Yes
				245	94			
^{99m}Tc-DTPA	IT	6 hr	5 hr	140	88	2.0	5.0	No

[a] Data from reference 111.

minimized by administering the radiopharmaceutical in two to three times its volume of sterile 10% dextrose injection.[113] This also improves its rate of transport cephalad. In normal human subjects, the tracer migrates first to the basal cisterns. Activity appears there in about 1 hour, achieving peak concentration at 4 hours.[114] Tracer then flows over the cerebral convexities to the parasagittal region. Activity first appears in this region at 4 hours, reaching peak levels at about 14 to 17 hours. The activity in this region then falls, decreasing to half the peak values 10 to 14 hours later, being absorbed into the blood through the arachnoid granulations. Activity does not normally enter the ventricular system; however, in certain types of hydrocephalus, activity may reflux into the ventricles.

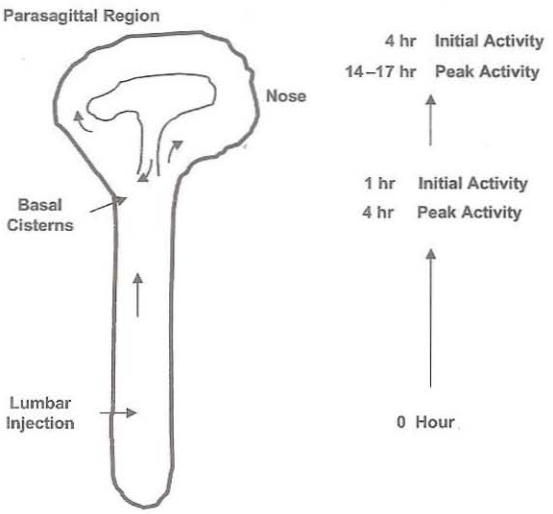

FIGURE 13-17 Right lateral view diagram of the brain and spinal canal illustrating the temporal movement of radiotracer from the lumbar injection site to the parasagittal region of the brain.

Upon absorption into the blood, ^{111}In-DTPA follows a normal urinary route of excretion through glomerular filtration. About 65% of the ^{111}In-DTPA chelate is eliminated in the urine in 1 day, increasing to 85% in 3 days.[109] The systemic distribution of ^{111}In-DTPA is described in Chapter 18.

The usual adult intrathecal dosage of ^{111}In-DTPA is 500 μCi (18.5 MBq) (maximum dosage). The critical organ is the spinal cord surface, with a radiation absorbed dose of 5 rad(cGy)/500 μCi.

Mechanisms of Drug Transport in the CSF

To remain in the CSF, a radiopharmaceutical must have certain properties, as outlined by Bell et al.[115] First, it must not be lipid soluble, or it will diffuse through the pia mater into the underlying nervous tissue. Also, CSF enzymes must not metabolize it. This may pose a problem for protein tracers, but the currently used DTPA chelates are not metabolized. Removal of substances from the CSF space occurs primarily through the arachnoid membrane

in the sagittal sinus, which, because of its porosity, permits the egress of substances with a wide range of molecular weights. Substances can also diffuse through the pia mater and ependymal cells into the brain ECF. This diffusion is favored for lipophilic molecules, but it has also been shown to occur with water-soluble molecules, such as inulin and radiographic contrast material (metrizamide).[6,116,117]

Transport of tracer molecules in the spinal fluid occurs by bulk flow or diffusion. Smaller molecules favor diffusion; proteins favor bulk flow. Theoretically, a tracer that mobilizes by bulk transport in the CSF would be a better marker of CSF flow. This would favor the use of radiolabeled proteins, but there are inherent disadvantages to their use. Albumin has been associated with aseptic meningitis and its ^{131}I label confers a high radiation dose, and labeled transferrin has to be prepared extemporaneously from patient serum. These disadvantages have favored the use of radiolabeled chelates.

^{111}In-DTPA appears to mobilize by bulk flow and diffusion.[115,118] Egress of this chelate through the arachnoid granulations is facilitated by the porosity and by the difference in pressure between the dural venous blood (about 90 mm H_2O) and the mean CSF pressure (about 135 mm H_2O).[118] Agents such as ^{111}In-DTPA may also undergo transependymal diffusion, because nearly normal clearance has been shown to occur with ^{169}Yb-DTPA during spinal canal obstruction.[118] High molecular weight molecules, such as RISA, have been shown to clear the CSF space much more slowly than chelates, leading to potentially excessive radiation dose to the spinal cord.[119]

Some agents are cleared rapidly from the CSF space by active transport through the choroid plexus epithelium. These agents include iodide, bromide, thiocyanate, phenol red, and phenolsulphonthalein.[120] Notably, ^{99m}Tc-pertechnetate clears by this mechanism, but its rate of clearance can be significantly reduced by oral perchlorate.[62]

Safety Considerations for Intrathecal Injections

Injection of foreign material into the spinal fluid, where it may come into intimate contact with the spinal nerves and the brain, deserves special attention because of potential adverse reactions. The integrity of nerve function is closely related to proper control of fluid pH, electrolyte balance, and osmolarity.[121] In addition, drug substances may have a direct effect on nerve function.[122,123] In particular, depletion of calcium ion readily causes tetany,[121] and low pH causes dilation of pial blood vessels.[121] Several cases of aseptic meningitis have been reported that were related to the chemical amounts of albumin administered during radioisotope cisternography.[103–105] Reactions believed to be associated with pyrogenic contamination in supposedly "pyrogen-free" injections have also been reported.[124] According to this report, anion exchange resins and buffers used in the manufacturing of ^{131}I-HSA and ^{111}In-DTPA were contaminated with pyrogens at levels below those detectable by the traditional rabbit pyrogen test. It was surmised that the reactions might have been due to the amount of endotoxin present in the radiotracer. Endotoxin is much more potent in producing a febrile response when administered by the intrathecal route than by the intravenous route. Limulus (bacterial endotoxin) testing is 5 to 10 times more sensitive than the rabbit test in detecting endotoxin. All radiopharmaceuticals today are tested for pyrogenic contamination with the USP bacterial endotoxins test.

Certain cisternography procedures require the injection of substantial amounts of fluid into the spinal canal.[111] For such procedures it is recommended that the fluid used have a composition similar to Elliott's B Solution (artificial CSF; Orphan Medical), to avoid possible complications arising from changes in spinal fluid pH, electrolytes, and osmolarity. Table 13-3 gives the composition of artificial CSF.

TABLE 13-3 Artificial CSF (Elliott's B Solution)

Ingredients		Instructions
1. NaCl	5.608 grams	Dissolve ingredients 1 to 5 in 970 mL SWFI. Add dropwise (with glass pipette) the acid salt solution (about 2 mL) with stirring to pH 7.4 and qs to 1000 mL. Filter through a 0.22 μm sterile membrane into vials or syringes for immediate use.
2. $Na_2CO_3 \cdot H_2O$	2.557 grams	
3. KCl	0.285 gram	
4. Na_2HPO_4	0.076 gram	
5. Glucose	0.758 gram	
6. Acid salt solution qs[a] to pH 7.4		
7. Sterile water for injection (SWFI) qs to 1000 mL		
Acid Salt Solution		
$CaCl_2$	2.0 grams	Dissolve salts in 20 mL of HCl with heating. Cool and qs to 25 mL.
$MgCl_2 \cdot 6H_2O$	1.0 gram	
HCl 12 M qs	25.0 mL	
Content of Final Preparation (mg/100 mL)		
Na^+	318.0	
Cl^-	450.0	
K^+	14.9	
Ca^{2+}	5.5	
Mg^{2+}	0.9	
P	1.7	
HCO_3^-	126.0	
Glucose	76.0	

[a] qs = Add a sufficient quantity.
Source: Reference 111.

NUCLEAR MEDICINE PROCEDURES

Nuclear medicine imaging of the CNS can be divided into two categories: imaging of the brain and imaging of the CSF. Although there continues to be an important role in nuclear medicine for brain imaging, most CNS imaging is now done by MRI or CT. These modalities offer good anatomic information. However, nuclear techniques are valuable when there is a question of abnormal regional blood flow in the brain or abnormal flow of CSF.

Normally, the BBB restricts many substances in the blood from entering the brain. Three main categories of brain imaging agents are used on the basis of this principle. One category, nondiffusible tracers, cannot cross the BBB. These radiopharmaceuticals can be used to evaluate blood flow to the brain and to determine if there is a focal abnormality or breakdown in the BBB. The second category, diffusible radiotracers, are newer and are more commonly used for brain imaging. They are typically lipophilic and readily cross the BBB to localize in brain tissue in proportion to blood flow. The third category is radiopharmaceuticals associated with PET, which are used in evaluating metabolic activity in the brain or to measure receptor density and binding affinity.[125]

RADIONUCLIDE BRAIN IMAGING

Brain Death

Rationale

Dynamic blood flow imaging of the head is obtained to determine the presence or absence of cerebral perfusion in a patient who is suspected to be brain dead. In the appropriate clinical setting, lack of cerebral perfusion can confirm the clinical diagnosis of brain death.

Procedure

The study typically consists of a cerebral radionuclide angiogram followed by static images. If a nondiffusible agent like ^{99m}Tc-DTPA is used, usually 10 mCi (370 MBq) of activity is administered intravenously into an antecubital vein in a bolus. During the angiogram portion of the study, a series of 2 to 10 second per frame anterior images of the head are obtained. Image acquisition is started just as the bolus of radiotracer is administered and is continued for 1 to 2 minutes. Static anterior and lateral blood pool images are generally obtained 5 to 10 minutes after completion of the blood flow portion of the study. It can be helpful to place an elastic band over the patient's head just above the orbits to minimize blood flow to the scalp vessels.

Pharmaceuticals

The radiopharmaceuticals most commonly used for cerebral angiography are ^{99m}Tc-DTPA and ^{99m}Tc-sodium pertechnetate. However, agents that cross the BBB, such as ^{99m}Tc-HMPAO and ^{99m}Tc-ECD, can also be used.

Interpretation

If a patient is suspected to be brain dead upon clinical evaluation and there is no evidence of cerebral perfusion on the radionuclide angiogram, the diagnosis is certain. Normally, when the radiotracer bolus is injected into a peripheral arm vein, it travels to the right side of the heart, then to the lungs and back to the left side of the heart. It is visible in the carotid arteries shortly after this. As it enters the brain, radiotracer becomes apparent in the cerebral arteries and in the sagittal sinus (Figure 13-6). If a nondiffusible tracer is used (e.g., ^{99m}Tc-GH, ^{99m}Tc-DTPA, or ^{99m}Tc-sodium pertechnetate), no radiotracer uptake will be evident in the brain on the delayed images because the tracer does not normally cross the BBB (Figure 13-7). However, if a diffusible tracer is used (^{99m}Tc-HMPAO or ^{99m}Tc-ECD), activity will accumulate in the brain over time (Figures 13-11 and 13-13).

When there is brain death, internal carotid artery blood flow ceases because of increased intracranial pressure or clotting. During the angiographic phase of the study, there is flow to both carotids, but the flow stops at this level (Figure 13-18). There is no blush of radiotracer activity in the cerebral artery territories or pooling of radiotracer in the sagittal sinus. Since blood flow is blocked in the internal carotid arteries, blood is shunted to the external carotid arteries. The increased flow in the external carotid arteries can be seen as increased flow of activity to the nasal region. This is often called the "hot nose" sign. After the angiogram phase, the blood pool images fail to demonstrate radiotracer activity in the sagittal or transverse sinuses.

Epilepsy

Epilepsy is a disorder of the brain characterized by recurring excessive neuronal discharge resulting in repeated episodes of seizures. Seizures occur when there is an abnormal focus of neuronal discharge. Epilepsy affects approximately 0.5% to 1% of the population. For patients with refractory partial seizures that cannot be adequately controlled with medication, surgery is an important treatment option if the seizure focus can be located.

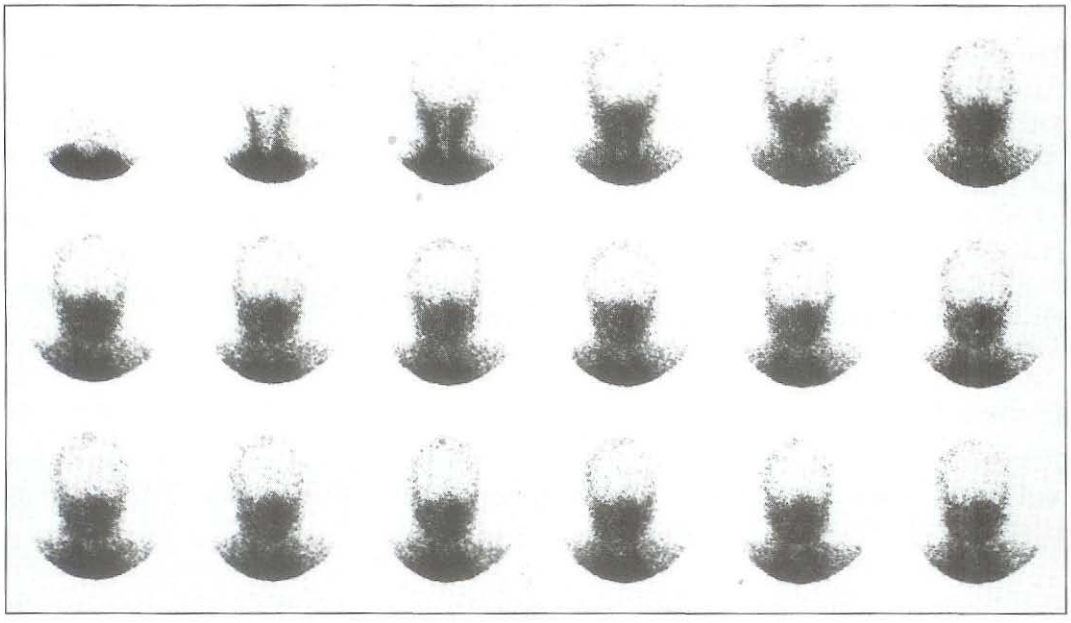

FIGURE 13-18 Brain death. Absence of cerebral perfusion after intravenous injection of ^{99m}Tc-gluceptate (^{99m}Tc-GH) is seen in this 11 month old child, a victim of smoke inhalation in a house fire.

Rationale

During a seizure, there is an increase in blood flow in the region of the neuronal discharge associated with the seizure focus.[126] In the period between seizures, there is normal or decreased blood flow to the region of the seizure focus. Thus, radiopharmaceuticals that cross the BBB and are taken up in the cortex in proportion to blood flow are useful in identifying the seizure focus. SPECT imaging with diffusible perfusion tracers such as ^{99m}Tc-HMPAO, ^{99m}Tc-ECD, and ^{18}F-FDG is most commonly used to evaluate brain perfusion for epilepsy. SPECT imaging of the brain can be done either during a seizure (ictal SPECT) or between seizures (interictal SPECT). Since blood flow can be normal between seizures, ictal SPECT is more sensitive for detecting the seizure focus.

Pharmaceuticals

The most common radiopharmaceuticals used for radionuclide cerebral perfusion imaging during the ictal period are agents that cross the BBB, such as ^{99m}Tc-HMPAO and ^{99m}Tc-ECD. These agents are lipophilic and are transported across the BBB by diffusion. They are taken up by brain cells in the cerebral cortex in proportion to blood flow and do not significantly redistribute. ^{99m}Tc-HMPAO can be reconstituted in stabilized and unstabilized forms. In the unstabilized form it should be administered intravenously no later than 30 minutes after reconstitution. This makes the unstabilized form difficult to use for an ictal study, in which the dose should be administered either during a seizure or within 30 seconds after the completion of a seizure. The stabilized form can be used for up to 4 hours after reconstitution. ^{99m}Tc-ECD can be used up to 6 hours after reconstitution.

PET with ^{18}F-FDG can also be used to localize the seizure focus. During a seizure there is increased glucose metabolism at the seizure focus.[127] Between seizures, the foci generally

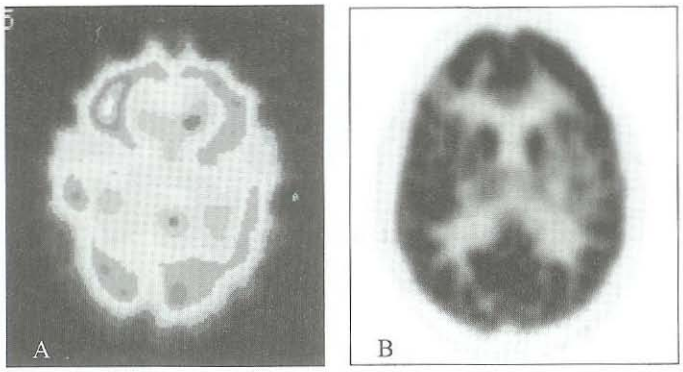

FIGURE 13-19 (A) ^{99m}Tc-HMPAO ictal brain SPECT scan showing a focal area of increased uptake in the right inferior frontal lobe in a patient with complex partial seizures. (B) ^{18}F-FDG interictal PET brain study in the same patient showing a focal area of hypometabolism in the inferior right frontal lobe that corresponds to the focus of increased uptake on the ictal scan.

demonstrate reduced glucose metabolism. Because ^{18}F has a physical half-life of only 110 minutes, it is difficult to have a dose ready and immediately available for an ictal study. Also, FDG continues to accumulate in the brain over 30 to 40 minutes, which is typically much longer than the duration of a complex partial seizure. It does not have the high first-pass extraction and retention that the ^{99m}Tc diffusible agents have. Thus, metabolic brain imaging with ^{18}F-FDG is usually performed during the interictal period. Often an ictal SPECT study done with either ^{99m}Tc-HMPAO or ^{99m}Tc-ECD is compared with an interictal ^{18}F-FDG PET study.

Procedure

Prior to either ictal or interictal imaging studies, patients are monitored by electroencephalography. If an ictal study is desired, either stabilized ^{99m}Tc-HMPAO or ^{99m}Tc-ECD is prepared for use and is kept readily available. The activity is usually between 15 and 30 mCi (555 to 1110 MBq). The patient is monitored for seizure activity. At the onset of a seizure, the dose is administered intravenously. To obtain an adequate ictal study, it is important that the dose be administered either during the seizure or within 30 seconds after completion of the seizure. SPECT imaging of the brain is usually performed 30 to 60 minutes later. Because these radiopharmaceuticals do not redistribute, imaging can be delayed as much as 4 hours after administration.

Interpretation

If an ictal SPECT study is performed, seizure foci are seen as areas of increased activity because of the increased perfusion. During interictal studies, seizure foci demonstrate either areas of decreased radiotracer uptake or normal uptake. If ^{18}F-FDG is used for an interictal study, the seizure focus may be seen as an area of decreased uptake related to hypometabolism (Figure 13-19).

Dementia

Dementia is a general mental deterioration due to organic or physiologic factors that is categorized by some degree of disorientation along with impairment in judgment, intellect,

and memory. In vascular dementias, such as multi-infarct dementia, cognitive decline is often abrupt and stepwise.[128] In Alzheimer's disease, mental deterioration is typically gradual. Although clinical evaluation along with anatomic imaging such as CT and MRI is important in screening for reversible causes of dementia, nuclear medicine techniques can often improve diagnostic accuracy.

Rationale

Several forms of dementia are treatable. For example, dementia may occur in normal-pressure hydrocephalus. Thus, it is important to try to determine the cause of new-onset dementia. Both PET and SPECT have been useful in helping to determine the cause of dementia by evaluating regional blood flow and metabolic abnormalities in the brain.

Interpretation

There is normally symmetric perfusion to the cerebral hemispheres in dementia. However, in Alzheimer's disease there is a classic pattern demonstrating decreased perfusion and metabolism in the temporoparietal regions. As mental deterioration worsens, hypometabolism in the frontal lobes is also observed.[129]

Multi-infarct dementia is caused by repeated infarcts in the brain. Brain imaging with either perfusion agents or metabolic agents typically demonstrates multiple asymmetric defects occurring in the brain. These defects can occur anywhere in the cortex.

PET Imaging for Tumor Recurrence

^{18}F-FDG is taken up into the brain tissues similarly to glucose. Normally, the gray matter, basal ganglia, and thalami show the greatest amount of uptake in the brain, with much less uptake in the white matter. The amount of uptake in the brain tissue is related to blood flow and metabolic activity.

Tumors often have increased metabolic activity compared with most tissues, which makes PET imaging very important in oncology. However, since the brain is highly metabolic, PET imaging is not always ideal for tumor imaging in the brain. An important exception to this is after a brain tumor has been surgically removed. Most often the patient has also had adjuvant radiation therapy to the tumor region. In this case, if the tumor has been removed, there should be only scar tissue in the surgical bed. Using CT or MRI, it is often difficult to determine whether the remaining tissue in the surgical bed is residual or recurrent tumor or scar tissue secondary to radiation necrosis. Scar tissue is not hypermetabolic like malignant tumor. In this scenario, if the brain is imaged with PET using ^{18}F-FDG, focal areas of hypermetabolism in the surgical bed suggest residual or recurrent tumor. Lack of significant radiotracer uptake in the surgical bed is more consistent with radiation necrosis (Figure 13-20).

CSF Imaging

Most of the CSF is formed by the choroid plexuses of the lateral, third, and fourth ventricles. The CSF produced in the lateral ventricles flows though the interventricular foramina into the third ventricle. The flow continues through the cerebral aqueduct into the fourth ventricle and from there into the subarachnoid space around the brain and spinal cord.[130] Most of the flow of CSF in the subarachnoid space is cephalad around the

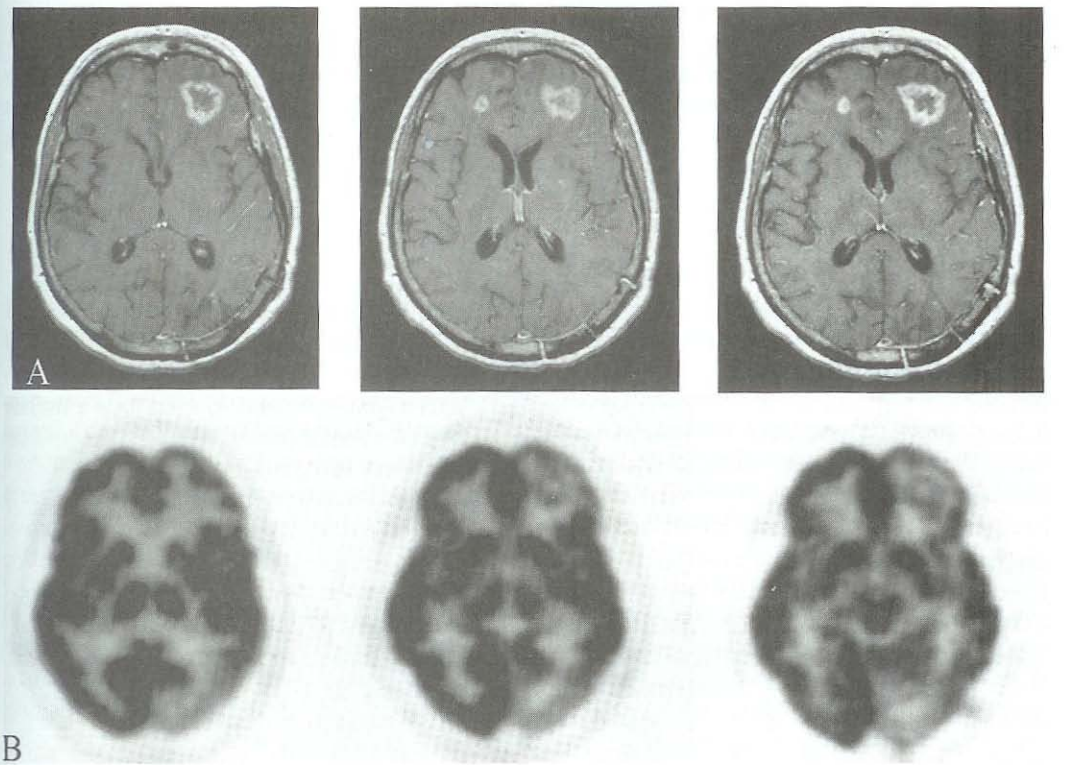

FIGURE 13-20 (A) MRI of the brain in a patient after surgery and radiation therapy for brain metastasis. There is some enhancement along the posterior aspect of the lesion in the left frontal lobe, which suggests recurrence. There is also evidence of a small metastasis in the right frontal lobe in the white matter. (B) ^{18}F-FDG PET brain study demonstrating two focal areas of hypermetabolism in the frontal lobes corresponding to the MRI findings and consistent with metastases. The focus on the left is adjacent to an area of decreased activity, likely a central area of necrosis. There is decreased metabolism in the left occipital region where the patient had surgery and radiation therapy, consistent with no evidence of recurrence in this region.

cerebral convexities toward the superior sagittal sinus. The main site of absorption of the CSF back into the venous system is through the arachnoid villi.

CSF imaging is often used to detect and evaluate normal-pressure hydrocephalus in a patient with clinical symptoms of dementia, gait disturbance, and urinary incontinence. In these patients, there is dilatation of the ventricles with normal CSF pressure. Imaging is also useful for detecting suspected CSF leaks and evaluating existing ventriculoperitoneal shunt function.

Normal-Pressure Hydrocephalus

Rationale

Hydrocephalus refers to enlargement of the ventricles caused by excessive accumulation of CSF. This can be due to overproduction of CSF by the choroid plexus, obstruction of flow to the arachnoid villi, or an abnormality in absorption. Enlargement of the ventricles can sometimes be a normal finding on MRI and CT imaging, secondary to age-related cerebral atrophy. The clinical symptoms associated with normal-pressure hydrocephalus

can show improvement after placement of a shunt to divert CSF from the ventricles back to the venous system, such as a ventriculopertioneal (VP) shunt.

Evaluation of CSF flow is usually accomplished by administering a radiopharmaceutical intrathecally. The radiotracer has to be diffusible throughout the CSF space but remain in the CSF space until it can be absorbed with the CSF using the normal pathway through the arachnoid villi.

Procedure

A lumbar puncture is performed using a small-gauge spinal needle. Typically, 500 μCi (18.5 MBq) ^{111}In-DTPA is administered intrathecally into the subarachnoid space. Initial anterior images of the head are obtained 6 hours after administration of the radiopharmaceutical. Sometimes, posterior images of the back can be obtained to evaluate whether the injection was successful. Anterior images of the head are obtained at 24 hours and 48 hours after injection. Sometimes images are also obtained at 72 hours.

Pharmaceuticals

The short physical half-life (6 hours) of ^{99m}Tc radiopharmaceuticals limits their use to shorter-duration studies such as CSF leak and VP shunt evaluation. Evaluation of normal-pressure hydrocephalus usually takes 2 to 3 days. Because of this, a radionuclide with a longer half-life is necessary for imaging. Typically, ^{111}In-DTPA is used in distinguishing normal-pressure hydrocephalus from hydrocephalus secondary to age-related atrophy. The physical half-life of 67 hours and principal photon energies of 173 keV and 247 keV make ^{111}In more appropriate for these studies.

Interpretation

After the radiopharmaceutical has been successfully injected into the lumbar subarachnoid space, it begins to ascend through the spinal canal. In adult patients, activity can normally be seen accumulating in the basal cisterns by 2 to 4 hours. Activity can also be seen in the interhemispheric and sylvian fissures at this time. Normally, radiotracer is not seen entering the lateral ventricles at any time. Over the next 24 hours, radiotracer should ascend over the cerebral convexities to the sagittal sinus, and activity in the basal cisterns should begin to clear (Figure 13-21).

Patients with normal-pressure hydrocephalus demonstrate a different flow pattern. Early on, there is reflux of radiotracer into the lateral ventricles. This will persist on the delayed images. In addition, ascent over the cerebral convexities is usually markedly delayed (Figure 13-22).

CSF Leak

Rationale

The most common cause of CSF leaks is trauma. Most CSF leaks are located in the skull base between the region of the sphenoid sinus and temporal bone. CT imaging is most often used to evaluate a CSF leak. However, when this is nondiagnostic, nuclear imaging can be useful in helping to confirm and localize the leak site.

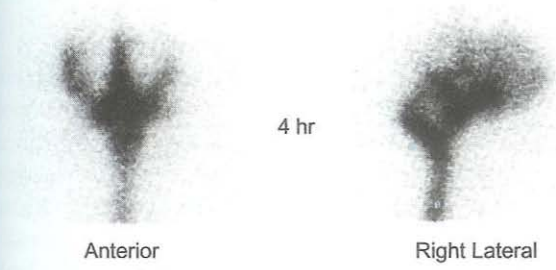

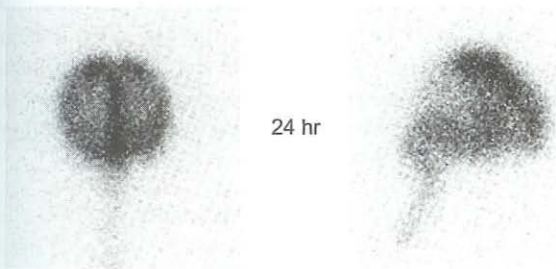

FIGURE 13-21 Normal CSF cisternogram. ^{111}In-DTPA study showing normal radiotracer accumulation in the basal cisterns and interhemispheric and sylvian fissures on the 4 hour images (trident appearance). Images at 24 hours demonstrate normal ascent of the radiotracer over the convexities to the superior sagittal sinus.

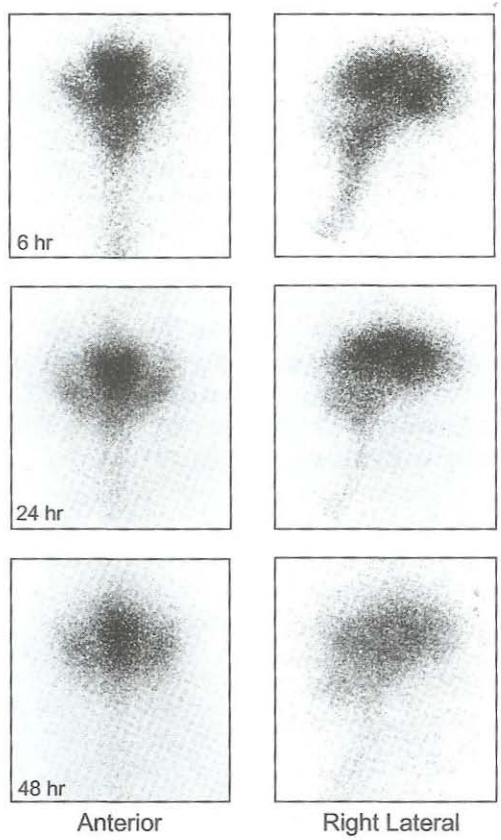

FIGURE 13-22 Normal-pressure hydrocephalus. The 6 hour images demonstrate ^{111}In-DTPA activity in the spinal subarachnoid space, basal cisterns, and lateral ventricles. At 24 hours the activity persists in the lateral ventricles, and in this patient there is very slow progression over the hemispheres. This pattern is essentially the same at 48 hours and indicates extraventricular obstruction and normal-pressure hydrocephalus.

Procedure

To evaluate a possible CSF leak, pledgets are typically placed at the suspected leak site prior to administration of the radiopharmaceutical. If the suspected leak is from the nose, pledgets are usually placed in locations near the sphenoethmoidal recess, the cribriform plate, and the middle meatus, bilaterally. If the suspected leak is from the ear, a pledget is placed in the ear canal. As in the evaluation of normal-pressure hydrocephalus, a lumbar puncture is then performed and the radiopharmaceutical is administered intrathecally. The patient is placed in the prone position or a position that most exacerbates the leak. Anterior, posterior, and lateral imaging of the head is performed, usually 2 to 4 hours later. A sample of the patient's blood is collected to measure activity in the blood or plasma. The pledgets are also collected and measured for activity using a well counter. Both pledget and plasma activity are usually measured as counts per minute per gram, and pledget-to-plasma activity ratios are calculated.

Pharmaceuticals

Because the duration of these studies is typically only about 4 hours, ^{99m}Tc radiopharmaceuticals such as ^{99m}Tc-DTPA can be used. The usual amount of administered activity is 1 to 3 mCi (37 to 111 MBq).

Interpretation

After the radiopharmaceutical has been successfully injected into the lumbar subarachnoid space, activity is usually seen in the basal cisterns by 2 to 4 hours. It is important to wait until the radiotracer accumulates in the suspected site of the leak before imaging the head and subsequently removing the pledgets. Normally, there should be no accumulation of radiotracer outside the cranial vault. Images positive for CSF leak demonstrate focal accumulations of radiotracer outside the cranium (Figure 13-23).

Radiotracer activity should not be seen in the systemic circulation until the radiotracer is absorbed into the venous system by the arachnoid villi. Thus, there should be no appreciable activity in the blood at 4 hours. Likewise, if there is no CSF leak, there should be no appreciable activity in the pledgets, and the pledget-to-plasma activity ratio should

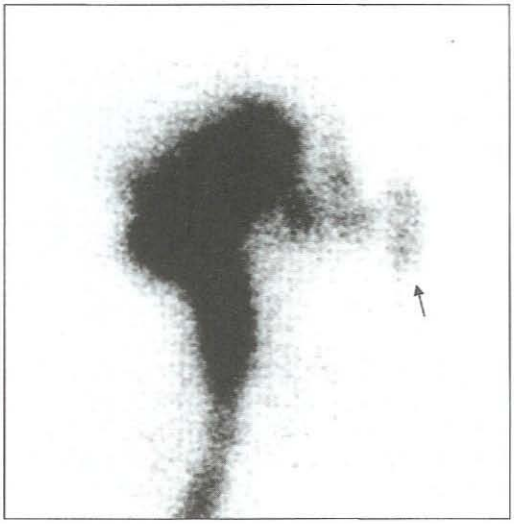

FIGURE 13-23 CSF leak in a patient with rhinorrhea after a motor vehicle accident. Lateral image of the head 1 hour after intrathecal injection of 2 mCi (74 MBq) ^{99m}Tc-DTPA at the lumbar spine level demonstrates activity in the nose consistent with a CSF leak. Pledget-to-plasma ratios (Table 13-4) show the main area of the leak to be in the left cribriform/middle meatus region.

TABLE 13-4 Nasal Pledget-to-Plasma Activity Ratios in Assessment of Positive CSF Leak with ^{99m}Tc-DTPA (see Figure 13-23)[a]

Pledget Placement	Net Counts per Minute	Pledget-to-Plasma Ratio
Right cribriform	84	0.24
Right middle meatus	590	1.7
Right sphenoid	2,627	7.5
Left cribriform	126,169	360
Left middle meatus	111,795	319
Right sphenoid	53,881	154
Plasma	350	1

[a] 2 mL of plasma, obtained at end of procedure, is counted along with each nasal pledget suspended in 2 mL of saline.

be 1. Pledget-to-plasma ratios greater than 1.5 to 1 are considered positive for CSF leak.[131] In the nose, the pledget with the highest ratio suggests the location of the leak (Table 13-4).

Shunt Evaluation

Rationale

VP and ventriculoatrial (VA) shunts are used to treat patients with obstructive hydrocephalus. If clinical symptoms begin to return or interval enlargement of the ventricles is seen on MRI or CT, the shunt may be obstructed. Anatomic studies such as plain film x-rays can determine if the shunt tubing is broken or kinked. If there is no evidence of this, nuclear medicine techniques can examine shunt function.

Procedure

To evaluate for shunt patency, radiotracer is injected into the shunt port using sterile technique (Figure 13-24). There are three parts to a VP or VA shunt: (1) the shunt port, (2) the proximal limb from the port to the ventricle, and (3) the distal limb from the port to either the atrium or the peritoneal cavity. To evaluate the proximal limb of the shunt, radiotracer is injected while manual compression is maintained on the distal limb near the port. This should force the radiotracer into the proximal limb and into the ventricle. Dynamic images of the head can be obtained by using a transmission source behind the patient to verify radiotracer accumulation in the ventricle. After radiotracer is seen in the ventricle, pressure is released from the distal limb and serial images are obtained to follow the flow of radiotracer through the distal limb.

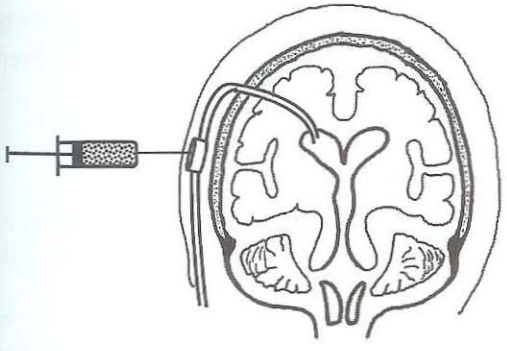

FIGURE 13-24 Diagram of the injection port for radiotracer administration during ventriculoperitoneal shunt evaluation.

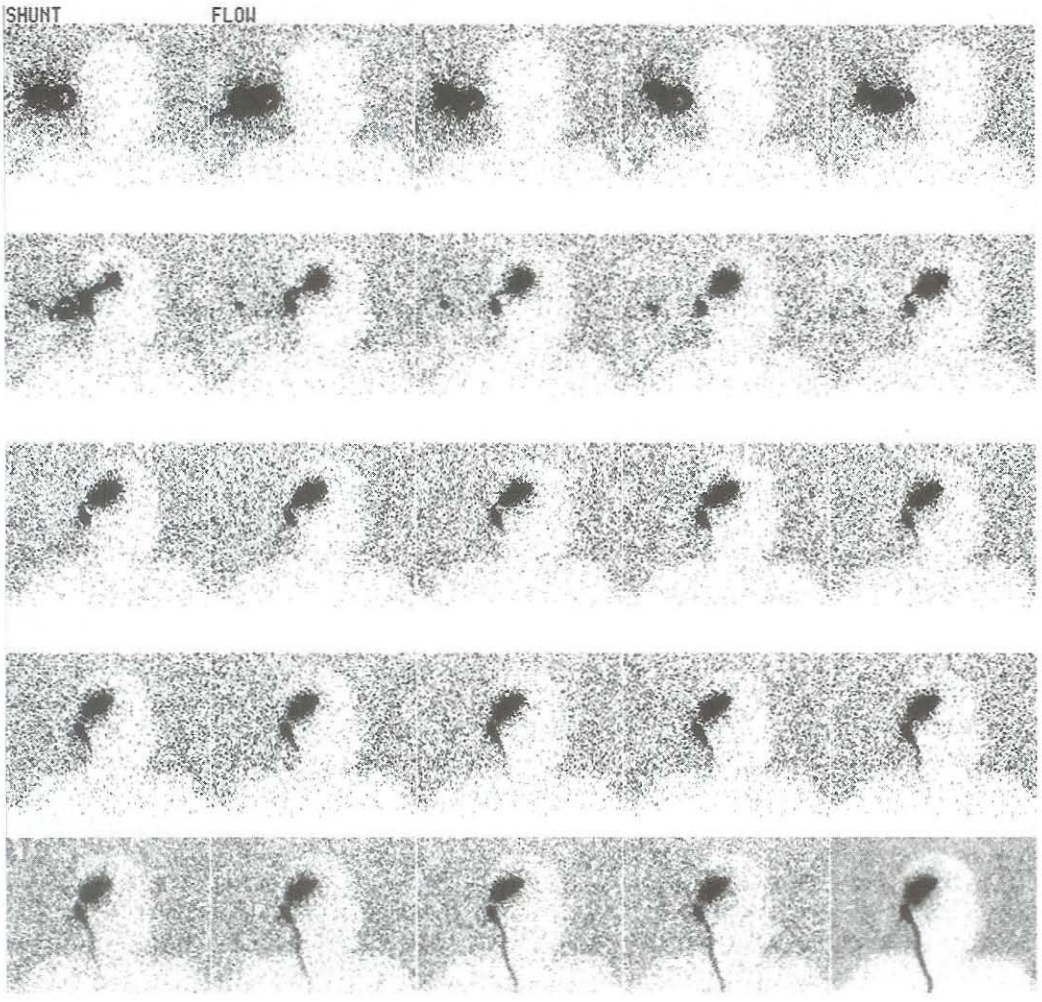

FIGURE 13-25 Ventriculoperitoneal (VP) shunt evaluation. ^{99m}Tc-DTPA study demonstrating patent VP shunt. With thumb pressure on the distal limb of the VP shunt, radiotracer is injected into the VP shunt port during the flow phase of the study. Once activity is seen in the lateral ventricle and obstruction of the proximal limb is ruled out, manual pressure is taken off the distal limb. Activity is seen to flow freely through the shunt toward the peritoneal cavity.

Pharmaceuticals

The duration of these studies is typically between 30 minutes and a few hours, so ^{99m}Tc radiopharmaceuticals such as ^{99m}Tc-DTPA can be used. The usual amount of administered activity is 1 to 2 mCi (37 to 74 MBq).

Interpretation

With proper manual pressure on the distal limb, there should be prompt visualization of activity in the ventricle after injection. If the port is accessed properly and radiotracer fails to appear in the ventricle, this is evidence of a proximal limb obstruction.

Once proximal limb patency is observed, pressure is released from the distal limb. There should be prompt passage of radiotracer through the distal limb. If the patient has

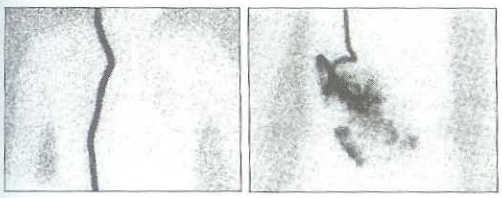

FIGURE 13-26 Patent ventriculoperitoneal shunt. Abdominal view of the same patient as in Figure 13-25 demonstrating movement of radiotracer down the patent distal limb and spilling into the peritoneal cavity.

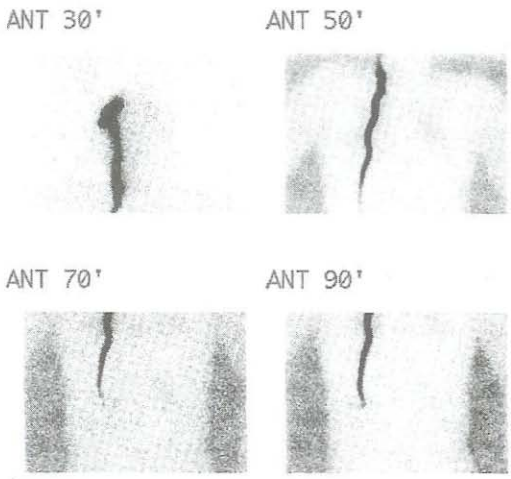

FIGURE 13-27 Obstructed ventriculoperitoneal shunt. ^{99m}Tc-DTPA study demonstrating delayed progression of radiotracer through the distal limb of the shunt. There is no evidence of tracer in the peritoneal cavity after 90 minutes.

a VP shunt, activity should be seen spilling freely into the peritoneal cavity in a few minutes to an hour (Figures 13-25 and 13-26). There is evidence of obstruction if the radiotracer fails to advance through the shunt tubing or pools at the distal tip (Figure 13-27). If the patient has a VA shunt, the radiotracer will reach the systemic circulation and will be seen in the kidneys.

REFERENCES

1. Wagner H, Burns D, Dannals R, et al. Imaging dopamine receptors in human brain by positron tomography. *Science.* 1983;221:1264-6.
2. Kung MP, Stevenson DA, Plossl K, et al. [^{99m}Tc]TRODAT-1: a novel technetium-99m complex as a dopamine transporter imaging agent. *Eur J Nucl Med.* 1997;24:372-80.
3. Eckelman WC. Clinical potential of receptor based radiopharmaceuticals. In: Fritzberg AR, ed. *Radiopharmaceuticals: Progress and Clinical Perspectives.* Vol II. Boca Raton, FL: CRC Press; 1986:89-113.
4. Guyton AC. *Textbook of Medical Physiology.* 6th ed. Philadelphia: WB Saunders; 1981:232-5.
5. Rapoport SI. *Blood-Brain Barrier in Physiology and Medicine.* New York: Raven Press; 1976:1-16.
6. Sage MR, Turski PA, Levin A. CNS imaging and the brain barriers. In: Neuwelt EA, ed. *Implications of the Blood-Brain Barrier and Its Manipulation.* Vol 2: Clinical Aspects. New York: Plenum; 1989:14-51.
7. Sage MR. Blood-brain barrier: phenomenon of increasing importance to the imaging clinician. *AJNR Am J Neuroradiol.* 1981;3:127-138.
8. Bradbury MWB. Why a blood-brain barrier? *Trends Neurosci.* 1979;2:36-8.
9. Dischino DD, Welch MJ, Kilbourn MR, et al. Relationship between lipophilicity and brain extraction of C-11-labeled radiopharmaceuticals. *J Nucl Med.* 1983;24:1030-8.
10. Dean RT, Wester DL, Nosco MD, et al. Progress in the design, evaluation and development of Tc-99m radiopharmaceuticals. In: Nicolini M, Bandoli G, Mazzi U, eds. *Technetium in Chemistry and Nuclear Medicine 2.* New York: Raven Press; 1986:147-54.
11. Levin VA. Relationship of octanol/water partition coefficient and molecular weight to rat brain capillary permeability. *J Med Chem.* 1980;23:682-4.
12. Ingvar DH, Cronqvist S, Ekbert R, et al. Normal values of regional cerebral blood flow in man, including flow and weight estimates of gray and white matter. *Acta Neurol Scand Suppl.* 1965;14:72-8.

13. Frenkel A, Front D. Clinical investigation of cerebral blood flow. In: Magistretti PL, ed. *Functional Radionuclide Imaging of the Brain.* Vol 5. New York: Raven Press; 1983:31-45.
14. Merrick MV. Xenon, red cell and transit time methods for cerebral blood flow and perfusion reserve measurement. In: Murray IPC, Ell PJ, eds. *Nuclear Medicine in Clinical Diagnosis and Treatment.* 2nd ed. Vol 1. New York, Churchill Livingstone; 1998:587-600.
15. Moore GE. Fluorescein as an agent in the differentiation of normal and malignant tissues. *Science.* 1947;106:130-1.
16. Moore GE. Use of radioactive diiodofluorescein in the diagnosis and localization of brain tumors. *Science.* 1948;107:569-71.
17. Chou SN, Aust JB, Moore GE, et al. Radioactive iodinated human serum albumin as a tracer agent for diagnosing and localizing intracranial lesions. *Proc Soc Exp Biol Med.* 1951;77:193-5.
18. Blau M, Bender MA. Radiomercury (Hg-203) labeled Neohydrin: A new agent for brain tumor localization. *J Nucl Med.* 1962;3:83-93.
19. Sodee DB. A new scanning isotope, mercury-197: a preliminary report. *J Nucl Med.* 1963;4:335-44.
20. Lindeman JF, Quinn JL III. The recent history of clinical procedures in nuclear medicine. In: Gottschalk A, Potchen EJ, eds. *Diagnostic Nuclear Imaging.* Baltimore: Williams & Wilkins; 1976:8-13.
21. Richards P. A survey of the production at the Brookhaven National Laboratory of radioisotopes for medical research. In: *5 Congresso Nucleare.* Vol 2. Rome: Comitato Nazionale Ricerche Nucleare; 1960:223-44.
22. Harper PV, Lathrop KA, Gottschalk A. Pharmacodynamics of some technetium-99m preparations. In: Andrews GA, Kniseley RM, Wagner HN Jr, eds. *Radioactive Pharmaceuticals.* Symposium 6. Washington, DC: US Atomic Energy Commission; 1966: 335-58.
23. McAfee JG, Fuegar CF, Stern HS, et al. Tc-99m pertechnetate for brain scanning. *J Nucl Med.* 1964;5:811-27.
24. Eckelman W, Richards P. Instant Tc-99m DTPA. *J Nucl Med.* 1970;11:761.
25. Wolfstein RS, Tanasescu D, Sakimura IT, et al. Brain imaging with Tc-99m DTPA: a clinical comparison of early and delayed studies. *J Nucl Med.* 1974;15:1135-7.
26. Waxman A, Tanasescu DT, Siemsen J, et al. Tc-99m glucoheptonate as a brain scanning agent: critical comparison with pertechnetate. *J Nucl Med.* 1976;17:345-8.
27. Rollo DF, Cavalieri RR, Born M, et al. Comparative evaluation of Tc-99m GH, TcO_4, and Tc-99m DTPA as brain imaging agents. *Radiology.* 1977;123:379-83.
28. Oldendorf WH. Need for new radiopharmaceuticals [letter]. *J Nucl Med.* 1978;19:1182.
29. Uzler JM, Bennett LR, Mena I, et al. Human CNS perfusion scanning with ^{123}I-iodoantipyrine. *Radiology.* 1975;115:197-200.
30. Loberg MD, Corder EH, Fields AT, et al. Membrane transport of Tc-99m-labeled radiopharmaceuticals. I: Brain uptake by passive transport. *J Nucl Med.* 1979;20:1181-8.
31. Kung HF, Blau M. Regional intracellular pH shift: a new mechanism for radiopharmaceutical uptake in brain and other tissues. *J Nucl Med.* 1980;21:147-52.
32. Kung HF. Brain radiopharmaceuticals, In: Fritzberg AR, ed. *Radiopharmaceuticals: Progress and Clinical Perspectives.* Vol II. Boca Raton, FL: CRC Press; 1986:21-39.
33. Winchell HS, Horst WD, Braun L, et al. N-isopropyl-[^{123}I] p-iodoamphetamine single-pass brain uptake and washout: binding to brain synaptosomes and localization in dog and monkey brain. *J Nucl Med.* 1980;21:947-52.
34. Kung HF, Tramposch KM, Blau M. A new brain perfusion agent: [I-123] HIPDM: N,N,N'-trimethyl-N'-[2-hydroxy-3-methyl-5-iodobenzyl]-1,3-propanediamine. *J Nucl Med.* 1983;24:66-72.
35. Creutzig H, Shober O, Gielow P, et al. Cerebral dynamics of N-isopropyl-(^{123}I) p-iodoamphetamine. *J Nucl Med.* 1986;27:178-83.
36. Yonekura Y, Fujita T, Nishizawa S, et al. Temporal changes in accumulation of N-isopropyl-p-iodoamphetamine in human brain: relation to lung clearance. *J Nucl Med.* 1989;30:1977-81.
37. Matsuda H, Tsuji S, Oba H, et al. Autoradiograph analysis of iodoamphetamine redistribution in experimental brain ischemia. *J Nucl Med.* 1990;31:660-7.
38. Burns HD, Manspeaker H, Miller R, et al. Preparation and biodistribution of neutral, lipid-soluble Tc-99m complexes of bis (2-mercaptoethyl) amine ligands [abstract]. *J Nucl Med.* 1979;20:654.
39. Kung HF, Molnar M, Billings J, et al. Synthesis and biodistribution of neutral lipid-soluble Tc-99m complexes which cross the blood brain barrier. *J Nucl Med.* 1984;25:326-32.
40. Volkert WA, Hoffman TJ, Seger RM, et al. ^{99m}Tc-Propylene amine oxime (^{99m}Tc-PnAO), a potential brain radiopharmaceutical. *Eur J Nucl Med* 1984;9:511-6.
41. Kung HF. New technetium 99m-labeled brain perfusion imaging agents. *Semin Nucl Med.* 1990;20:150-8.
42. Volkert WA. Stereoreactivity of ^{99m}Tc-chelates at chemical and physiological levels, In: Nicolini M, Bandoli G, Mazzi U, eds. *Technetium and Rhenium in Chemistry and Nuclear Medicine 3.* Verona, Italy: Cortina International; 1990:343-52.

43. Cheesman EH, Blanchette MA, Ganey MV, et al. Technetium-99m ECD: ester-derivatized diamine-dithiol Tc complexes for imaging brain perfusion [abstract]. *J Nucl Med.* 1988;29:788.
44. Walovitch RC, Hill TC, Garrity ST, et al. Characterization of technetium-99m-L,L-ECD for brain perfusion imaging. 1: Pharmacology of technetium-99m ECD in nonhuman primates. *J Nucl Med.* 1989;30:1892-8.
45. Neirinckx RD, Burke JF, Harrison RC, et al. The retention mechanism of technetium-99m-HM-PAO: Intracellular reaction with glutathione. *J Cereb Blood Flow Metab.* 1988;8:S4-12.
46. Andersen AR, Friberg H, Knudsen GM, et al. Extraction of Tc-99m d,l-HM-PAO across the blood-brain barrier. *J Cereb Blood Flow Metab.* 1988;8(suppl 1):S44-51.
47. Gallagher BM, Ansari A, Atkins H, et al. Radiopharmaceuticals XXVII. ^{18}F-labeled 2-deoxy-2-fluoro-D-glucose as a radiopharmaceutical for measuring regional myocardial glucose metabolism in vivo: tissue distribution and imaging studies in animals. *J Nucl Med.* 1977;18:990-6.
48. Kuhl D, Reivich M, Wolf A, et al. Determination of local cerebral glucose utilization by means of radionuclide computed tomography and (F-18) 2-fluoro-2-deoxy-D-glucose [abstract]. *J Nucl Med.* 1977;18:614.
49. Sokoloff L. Localization of functional activity in the central nervous system by measurement of glucose utilization with radioactive deoxyglucose. *J Cereb Blood Flow Metab.* 1981;1:7-36.
50. Phelps ME, Huang SC, Hoffman EJ, et al. Tomographic measurement of local cerebral glucose metabolic rate in humans with (F-18) 2-fluoro-2-deoxy-d-glucose: validation of method. *Ann Neurol.* 1979;6:371-88.
51. Kung HF, Ohmono Y, Kung MP. Current and future radiopharmaceuticals for brain imaging with single photon emission computed tomography. *Semin Nucl Med.* 1990;20:290-302.
52. Jurrison SS, Lydon JD. Potential technetium small molecule radiopharmaceuticals. *Chem Rev.* 1999;99:2205-18.
53. Verhoeff NPLG. Ligands for neuroreceptor imaging by single photon emission tomography (SPECT) or positron emission tomography (PET). In: Murray IPC, Ell PJ, eds. *Nuclear Medicine in Clinical Diagnosis and Treatment.* Vol 1. 2nd ed. New York: Churchill Livingstone; 1998:521-62.
54. Lathrop KA, Harper PV. Biologic behavior of Tc-99m from Tc-99m pertechnetate ion. *Prog Nucl Med.* 1972;1:145-62.
55. McAfee JG, Fueger CF, Stern HS, et al. Tc-99m pertechnetate for brain scanning. *J Nucl Med.* 1964;5:811-27.
56. Brown-Grant K. Extrathyroidal iodide concentrating mechanisms. *Physiol Rev.* 1961;41:189-213.
57. Dayton DA, Maher FT, Elveback LR. Renal clearance of technetium (Tc-99m) as pertechnetate. *Mayo Clin Proc.* 1969;44:549-51.
58. Andros G, Harper PV, Lathrop KA, et al. Pertechnetate-99m localization in man with application to thyroid scanning and the study of thyroid physiology. *J Clin Endocrinol.* 1965;25:1067-76.
59. Beasley TM, Palmer HE, Nelp WB. Distribution and excretion of technetium in humans. *Health Phys.* 1966;12:1425-35.
60. Witcofski RL, Janeway R, Maynard CD, et al. Visualization of the choroid plexus on the technetium-99m brain scan: clinical significance and blocking by potassium perchlorate. *Arch Neurol.* 1967;16:286-9.
61. Coben LA, Loeffler JD, Elsasser JC. Spinal fluid iodide transport in the dog. *Am J Physiol.* 1964;206:1373-8.
62. Harper PV, Lathrop KA, Jiminez F, et al. Technetium-99m as a scanning agent. *Radiology.* 1965;85:101-9.
63. Alazraki N, Littenberg RL, Hurwitz S, et al. Diffferences in choroid plexus concentration of pertechnetate produced by varying time of perchlorate administration and brain imaging. *J Nucl Med.* 1974;15:884-6.
64. Scheu JD, Tetalman MR, Araujo O, et al. The efficacy of intravenous sodium perchlorate in choroid plexus blocking [abstract]. *J Nucl Med.* 1976;17:528.
65. Rumble WF, Aamodt RL, Jones AE, et al. Accidental ingestion of Tc-99m in breast milk by a 10 week-old child. *J Nucl Med.* 1978;19:913-5.
66. Vagenakis AG. Duration of radioactivity in the milk of a nursing mother after Tc-99m administration [abstract]. *J Nucl Med.* 1971;12:188.
67. Tator CH. Radiopharmaceuticals for tumor localization with special emphasis on brain tumors, In: Subramanian G, Rhodes BA, Cooper JF, et al., eds. *Radiopharmaceuticals.* New York: Society of Nuclear Medicine; 1975: 474-81.
68. Front D, Israel O. Scintigraphy and ultrastructure of the blood-brain and blood-tissue barriers of human brain tumors: radionuclides as in vivo indicators of tumor permeability, In: Magistretti PL, ed. *Functional Radionuclide Imaging of the Brain.* Vol 5. New York: Raven Press; 1983:47-59.
69. Andersen AR, Friberg H, Knudsen KBM, et al. Extraction of [^{99m}Tc]-d,l-HM-PAO across the blood-brain barrier. *J Cereb Blood Flow Metab.* 1988;8:S44-51.
70. Neirinckx RD, Canning LR, Piper IM, et al. Technetium-99m d,l-HM-PAO: A new radiopharmaceutical for SPECT imaging of regional cerebral blood perfusion. *J Nucl Med.* 1987;28:191-202.
71. Sharp PF, Smith FW, Gemmell HG, et al. Technetium-99m HM-PAO sterioisomers as potential agents for imaging cerebral blood flow: human volunteer studies. *J Nucl Med.* 1986;27:171-7.

72. Lassen NA, Andersen AR, Friberg L, et al. The retention of [^{99m}Tc]-*d,l*-HM-PAO in the human brain after intracarotid bolus injection: a kinetic analysis. *J Cereb Blood Flow Metab.* 1988;8:S13-22.
73. Neirinckx RD, Burke JF, Harrison RC, et al. The retention mechanism of technetium-99m-HM-PAO: intracellular reaction with glutathione. *J Cereb Blood Flow Metab.* 1988;8:S4-12.
74. Hung JC, Volkert WA, Holmes RA. Stabilization of technetium-99m-D,L-hexamethylpropyleneamine oxime (^{99m}Tc-D,L-HMPAO) using gentisic acid. *Nucl Med Biol.* 1989;16:675-80.
75. Andersen AR, Friberg H, Lassen NA, et al. Assessment of the arterial input curve for [^{99m}Tc]-*d,l*-HM-PAO by rapid octanol extraction. *J Cereb Blood Flow Metab.* 1988;8:S23-30.
76. Tc-99m Exametazime [package insert]. Arlington Heights, IL: Medi-Physics Inc/Amersham Healthcare; 1996.
77. DeJong BM, VanRoyen EA. Uptake of SPECT radiopharmaceuticals in neocortical brain cultures. *Eur J Nucl Med.* 1989;15:16-20.
78. Nakamuira K, Tukatani Y, Kubo A, et al. The behavior of ^{99m}Tc-hexamethylpropyleneamineoxime (^{99m}Tc-HMPAO) in blood and brain. *Eur J Nucl Med.* 1989;15:100-7.
79. Villanueva-Meyer J, Thompson D, Mena I, et al. Lacrimal gland dosimetry for the brain imaging agent technetium-99m-HM-PAO. *J Nucl Med.* 1990;31:1237-9.
80. Walovitch RC, Cheesman EH, Maheu LJ, et al. Studies of the retention mechanism of the brain perfusion imaging agent ^{99m}Tc-bicisate (^{99m}Tc-ECD). *J Cereb Blood Flow Metab.* 1994;14(suppl 1):S4-11.
81. Walovitch RC, Hill TC, Garrity ST, et al. Characterization of technetium-99m-L,L-ECD for brain perfusion imaging. 1: Pharmacology of technetium-99m ECD in nonhuman primates. *J Nucl Med.* 1989;30:1892-1901.
82. Knudsen GM, Andersen AR, Somnier FE, et al. Brain extraction and distribution of ^{99m}Tc-bicisate in humans and rats. *J Cereb Blood Flow Metab.* 1994;14(suppl 1):S12-18.
83. Ishizu K, Yonekura Y, Magata Y, et al. Extraction and retention of technetium-99m-ECD in human brain: dynamic SPECT and oxygen-15-water PET studies. *J Nucl Med.* 1996;37:1600-4.
84. Friberg L, Andersen AR, Lassen NA, et al. Retention of ^{99m}Tc-bisicate in the human brain after intracarotid injection. *J Cereb Blood Flow Metab.* 1994;14(suppl 1):S19-27.
85. Greenberg JH, Araki N, Karp A. Correlation between ^{99m}Tc-bicisate and regional CBF measured with iodo-[^{14}C] antipyrine in a primate focal ischemia model. *J Cereb Blood Flow Metab.* 1994;14(suppl 1):S36-43.
86. Lassen NA, Sperling B. ^{99m}Tc-bicisate reliably images CBF in chronic brain diseases but fails to show reflow hyperemia in subacute stroke: report of a multicenter trial of 105 cases comparing ^{133}Xe and ^{99m}Tc-bicisate (ECD, Neurolite) measured by SPECT on same day. *J Cereb Blood Flow Metab.* 1994;14(suppl 1):S44-8.
87. Vallabhajosula S, Zimmerman RE, Picard M, et al. Technetium-99m ECD: A new brain imaging agent: in vivo kinetics and biodistribution studies in normal human subjects. *J Nucl Med.* 1989;30:599-604.
88. Holman BL, Hellman RS, Goldsmith SJ, et al. Biodistribution, dosimetry, and clinical evaluation of technetium-99m ethyl cysteinate dimer in normal subjects and in patients with chronic cerebral infarction. *J Nucl Med.* 1989;30:1018-24.
89. Walovitch RC, Franceschi M, Picard M, et al. Metabolism of ^{99m}Tc-L,L-ethyl cysteinate dimer in healthy volunteers. *Neuropharmacology.* 1991;30:283-92.
90. Tc-99m Bicisate [package insert]. Billerica, MA: Dupont Pharmaceuticals; 1998.
91. Léveillé J, Demonceau G, Walovitch RC. Intrasubject comparison between technetium-99m-ECD and technetium-99m-HMPAO in healthy human subjects. *J Nucl Med.* 1992;33:480-4.
92. Lucignani G, Schmidt KC, Moresco RM, et al. Measurement of regional cerebral glucose utilization with fluorine-18-FDG and PET in heterogeneous tissues: theoretical considerations and practical procedure. *J Nucl Med.* 1993;34:360-9.
93. DiChiro G, Oldfield E, Wright DC, et al. Cerebral necrosis after radiotherapy and/or intra-arterial chemotherapy for brain tumors. *AJR Am J Roentgenol.* 1988;150:189-97.
94. Doyle WK, Budinger TF, Valk PE, et al. Differentiation of cerebral radiation necrosis from tumor recurrence by [^{18}F]FDG and ^{82}Rb positron emission tomography. *J Comput Assist Tomogr.* 1987;11:563-70.
95. Valk PE, Budinger FT, Levin VA, et al. PET of malignant cerebral tumors after interstitial brachytherapy: demonstration of metabolic activity and correlation with clinical outcome. *J Neurosurg.* 1988;69:830-8.
96. Coleman RE, Hoffman JM, Hanson MW, et al. Clinical application of PET for the evaluation of brain tumors. *J Nucl Med.* 1991;32:616-22.
97. Jones SC, Alavi A, Christman D, et al. The radiation dosimetry of 2-[F-18] Fluoro-2-deoxy-D-glucose in man. *J Nucl Med.* 1982;23:613-7.
98. Radiation Internal Dose Information Center. *Radiation Dose Estimates for F-18 FDG.* Oak Ridge, TN: Oak Ridge Institute for Science and Education; 1992.
99. Kaplan WD, Takvorian T, Morris JH, et al. Thallium-201 brain tumor imaging: a comparative study with pathologic correlation. *J Nucl Med.* 1987;28:47-52.

100. Black KL, Hawkins RA, Kim KT, et al. Use of thallium-201 SPECT to quantitate malignancy grade of gliomas. *J Neurosurg.* 1989;71:342-6.
101. Yoshi Y, Satou M, Yamamoto T, et al. The role of thallium-201 single photon emission tomography in the investigation and characterization of brain tumors in man and their response to treatment. *Eur J Nucl Med.* 1993;20:39-45.
102. DiChiro G, Reames PM, Matthews WB Jr. RISA-ventriculography and RISA-cisternography. *Neurology.* 1964;14:185-91.
103. Detmer DE, Blocker HM. A case of aseptic meningitis secondary to intrathecal injection of I-131 human serum albumin. *Neurology.* 1965;15:642-3.
104. Nicol CP. A second case of aseptic meningitis after isotope cisternography using I-131 human serum albumin. *Neurology.* 1967;17;199-200.
105. Oldham RK, Staab EV. Aseptic meningitis after the intrathecal injection of radioiodinated serum albumin. *Radiology.* 1970;97:317-21.
106. Ashburn WL, Harbert JC, Briner WH, et al. Cerebrospinal fluid rhinorrhea studied with the gamma scintillation camera. *J Nucl Med.* 1968;9:523-9.
107. Wagner HN Jr, Hosain F, DeLand FH, et al. A new radiopharmaceutical for cisternography: chelated ytterbium 169. *Radiology.* 1970;95:121-5.
108. Matin P, Goodwin DA. Cerebrospinal fluid scanning with In-111. *J Nucl Med.* 1971;12:668-72.
109. Goodwin DA, Song CH, Finston R, et al. Preparation, physiology, and dosimetry of In-111 labeled radiopharmaceuticals for cisternography. *Radiology.* 1973;108:91-8.
110. Som P, Hosain F, Wagner HN Jr, et al. Cisternography with chelated complex of Tc-99m. *J Nucl Med.* 1972;13:551-3.
111. Curnes JT, Vincent LM, Kowalsky RJ, et al. CSF rhinorrhea: detection and localization using overpressure cisternography with Tc-99m DTPA. *Radiology.* 1985;154:795-9.
112. Welch MJ, Welch TJ. Solution chemistry of carrier-free indium. In: Subramanian G, Rhodes BA, Cooper JF, et al., eds. *Radiopharmaceuticals.* New York: Society of Nuclear Medicine; 1975:73-9.
113. Alazraki NP, Halpern SE, Ashburn WL, et al. Hyperbaric cisternography: experience in humans. *J Nucl Med.* 1973;14:226-9.
114. Partain CL, Alderson PO, Donovan RL, et al. Regional kinetics of indium-111 DTPA in CSF imaging of normal volunteers. In: Cloutier RJ, Coffey JL, Synder WS, et al., eds. *Radiopharmaceutical Dosimetry Symposium.* Rockville, MD: US Department of Health, Education, and Welfare, Public Health Service, Food and Drug Administration, Bureau of Radiological Health; 1976:404-9. HEW Publication (FDA) 76-8044.
115. Bell EG, Maher B, McAfee JH, et al. Radiopharmaceuticals for gamma cisternography, In: Subramanian G, Rhodes BA, Cooper JF, et al., eds. *Radiopharmaceuticals.* New York: Society of Nuclear Medicine; 1975:399-410.
116. Drayer BP, Rosenbaum AE. Metrizamide brain penetrance. *Acta Radiol Suppl.* 1977;355:280-93.
117. Sage MR, Wilcox J, Evill CA, et al. Brain parenchyma penetration by intrathecal ionic and non-ionic contrast media. *AJNR Am J Neuroradiol.* 1982;3:481-3.
118. DeLand FH, Simmons GH. Spinal cord and cerebrospinal fluid. In: Cloutier RJ, Coffey JL, Synder WS, et al., eds. *Radiopharmaceutical Dosimetry Symposium.* Rockville, MD: US Department of Health, Education, and Welfare, Public Health Service, Food and Drug Administration, Bureau of Radiological Health; 1976:390-7. HEW Publication (FDA) 76-8044.
119. Harbert JC, McCullough D, Zeiger LS, et al. Spinal cord dosimetry in I-131 HSA cisternography. *J Nucl Med.* 1970;11:534-41.
120. McAfee JG, Subramanian G. Radioactive agents for imaging. In: Freeman LM, Johnson PM, eds. *Clinical Scintillation Imaging.* 2nd ed. New York: Grune & Stratton; 1975:13-114.
121. Elliott KAC, Jasper HH. Physiological salt solutions for brain surgery. *J Neurosurg.* 1949;6:140-52.
122. Mahaley MS Jr, Odom GL. Complication after intrathecal injection of fluorescein. *J Neurosurg.* 1966;25:298-9.
123. Huggins CB, Hastings AB. Effect of calcium and citrate injections into cerebrospinal fluid. *Proc Soc Exp Biol Med.* 1933;30:459-60.
124. Cooper JF, Harbert JC. Endotoxin as a cause of aseptic meningitis after radionuclide cisternography. *J Nucl Med.* 1975;16:809-13.
125. Meegalla S, Plossl K, Kung MP, et al. ^{99m}Tc labeled tropanes as dopamine transporter imaging agents. *Bioconjug Chem.* 1996;7:421-9.
126. Hougaard K, Oikawa T, Sveinsdottir E, et al. Regional cerebral blood flow in focal cortical epilepsy. *Arch Neurol.* 1979;33:527-35.
127. Kuhl D, Engel J, Phelps M, et al. Epileptic patterns of local cerebral metabolism and perfusion in humans determined by emission computed tomography of ^{18}FDG and $^{13}NH_3$. *Ann Neurol.* 1980;8:47-60.

128. Butler CRE, Costa DC, Walker Z, et al. PET and SPECT imaging in the dementias. In: Murray IPC and Ell PJ, eds. *Nuclear Medicine in Clinical Diagnosis and Treatment*. London: Churchill Livingstone; 1998:713-28.
129. Faulstich ME. Brain imaging in dementia of the Alzheimer type. *Int J Neurosci*. 1991;57:39-49.
130. Moore KL. *Clinically Oriented Anatomy*. Baltimore: Williams & Wilkins; 1980:941-6.
131. Ommaya A, O'Tuama L, Lorenzo A. Hydrocephalus, shunts and cerebrospinal fluid leaks. In: Wagner H, Szabo Z, Buchanan J, eds. *Principles of Nuclear Medicine*. Philadelphia: WB Saunders;1995:576-84.

14 Thyroid

Radionuclide applications to the thyroid gland include all types of nuclear medicine procedures. Radionuclides are used in the radioactive iodine uptake (RAIU) test to assess thyroid gland function, in treatments for hyperthyroidism and thyroid cancer, and in imaging studies to detect disease within the thyroid gland and scans of the total body to detect thyroid metastases.

PHYSIOLOGIC PRINCIPLES

The thyroid gland is composed of a large number of follicles, each lined with epithelial cells and filled with a substance called colloid.[1] The major constituent of the colloid is thyroglobulin, which is the base for production and storage of thyroid hormone. Ingested iodide is taken up from the blood by the thyroid epithelial cells. Within these cells, iodide is rapidly oxidized to iodine by peroxidase enzymes and hydrogen peroxide. The iodine then reacts with tyrosine residues in thyroglobulin to form thyroid hormone, which is stored in the colloid.

Trapping of iodide by epithelial cells is the rate-limiting step in hormone production. This active transport process is capable of concentrating iodide to 40 times the plasma concentration under normal circumstances, and this may increase 10-fold in the hyperthyroid state. The binding of one atom of iodine to tyrosine forms monoiodotyrosine (MIT), and addition of a second atom forms diiodotyrosine (DIT). The thyroid hormones are formed by coupling reactions in which one molecule each of MIT and DIT form triiodothyronine (T_3) and two molecules of DIT form thyroxine (T_4). This metabolic scheme is shown in Figure 14-1.

The daily turnover of iodine in the body is shown in Figure 14-2. Iodine metabolism has a three-compartment kinetic model: compartment I, the extrathyroidal iodide pool (75 μg iodine); compartment II, the thyroid iodine pool (6000 μg iodine); and compartment III, the extrathyroidal iodine hormone pool (500 μg iodine).[2,3] The average daily intake of iodide is about 300 μg, but this value can vary widely according to geographic location and dietary habits. Iodide intake is balanced by a urinary loss of 285 μg and a fecal loss of 15 μg. About 75 μg of iodide is made into thyroid hormone and released into the blood. Of this amount, 15 μg is metabolized in the liver and excreted in the feces. The remaining hormone undergoes enzymatic deiodination in tissues, with recycling of 60 μg of iodide back into compartment I for reuse or renal excretion. During an average day, about 20% of the ingested iodide is organified into hormone and 80% is excreted.

A number of substances either promote or block the synthesis of thyroid hormone. Thyroid-stimulating hormone (TSH, or thyrotropin) released from the anterior pituitary gland controls several of these functions, including iodide trapping, the coupling reactions between MIT and DIT, and hormone release from the colloid into the blood. Excess plasma iodide suppresses thyroid gland uptake of iodide.

The drugs methimazole (Tapazole, Lilly) and propylthiouracil block the binding of iodine with tyrosine as well as the coupling reactions. Several halogen oxyanions and thiocyanate are capable of inhibiting the iodide-trapping mechanism and also cause discharge of iodide from the propylthiouracil-blocked gland. Of the halogenated oxyanions,

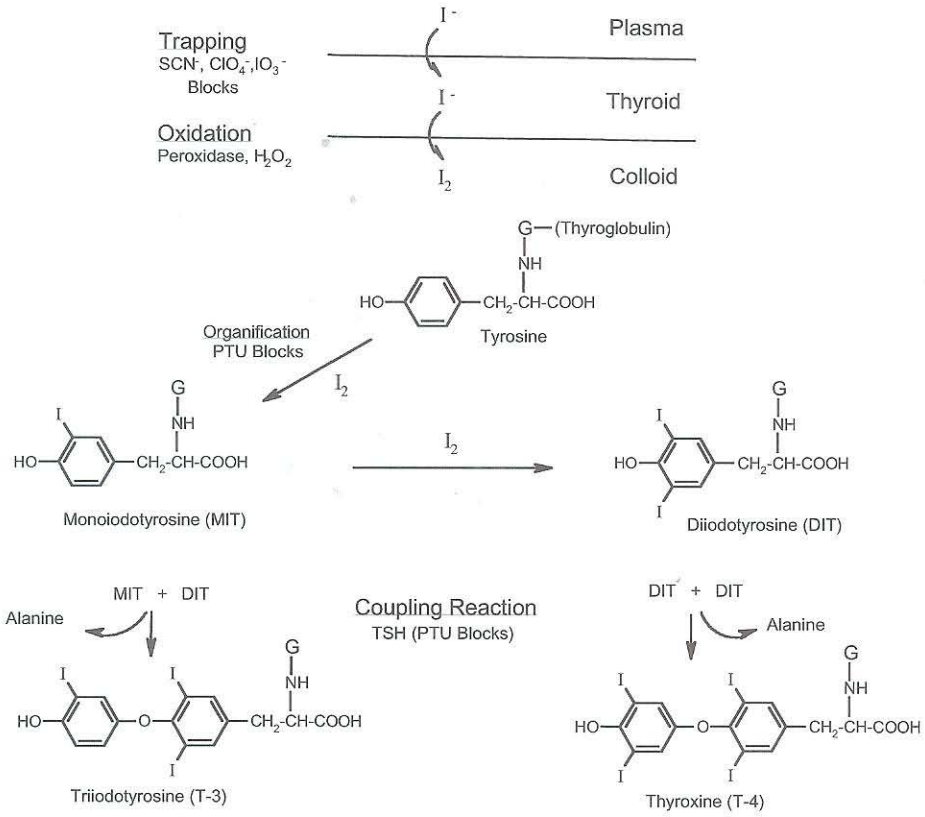

FIGURE 14-1 Schematic representation of iodine metabolism in the thyroid gland.

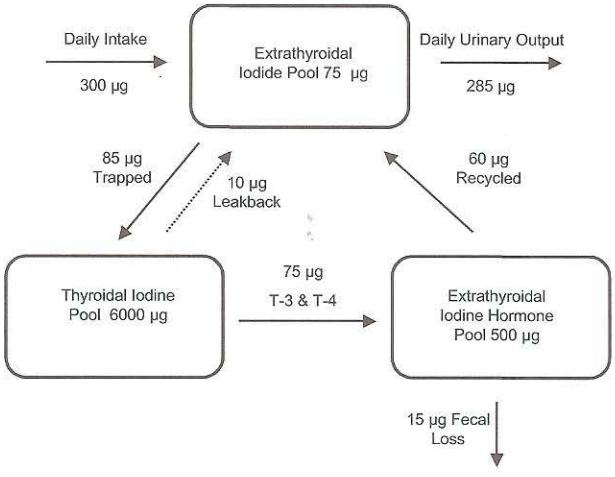

FIGURE 14-2 Daily turnover of iodine in the body.

perchlorate (ClO_4^-) is the most effective agent in discharging trapped iodide and is 10 times more potent than thiocyanate.[4]

Thyroid gland function is controlled by the hypothalamic–pituitary axis through a feedback mechanism. When the levels of circulating thyroid hormone decrease, thyrotropin-releasing factor is secreted from the hypothalamus, causing release of TSH from the

anterior pituitary, which stimulates the thyroid gland to produce more hormone. Excess circulating thyroid hormone reverses this process through negative feedback to the hypothalamus, which causes TSH levels to fall and thyroid hormone production to decrease. In the absence of disease, this process maintains thyroid gland homeostasis.

THYROID PATHOPHYSIOLOGY

Nuclear medicine procedures can be used in the diagnosis of several diseases of the thyroid gland, the most common being hyperthyroidism, thyroiditis, and thyroid nodules. In addition, hyperthyroidism and thyroid cancer can be treated with radioiodine.

Hyperthyroidism

Hyperthyroidism is characterized by hyperplastic thyroid tissue. The gland is increased in size 2 to 3 times and secretes excessive amounts of thyroid hormone, as much as 5 to15 times normal.[1] Plasma TSH levels are far below normal or essentially zero because of the suppressive feedback effect on the anterior pituitary gland. A common cause of hyperthyroidism is Graves' disease, in which the gland is a diffusely enlarged goiter. This disease has an autoimmune origin; thyroid-stimulating immunoglobulins stimulate the TSH receptors on thyroid cells, causing hyperthyroidism. Another cause of hyperthyroidism is toxic nodular goiter, in which the gland is enlarged either with multiple hyperfunctioning nodules (Plummer's disease) or with a solitary nodule that is a hyperfunctioning adenoma. In each of these conditions, the hyperfunctioning tissues demonstrate increased accumulation of radioiodine or pertechnetate on a thyroid scan.

Thyroiditis

Thyroiditis is an inflammation of the thyroid gland. Subacute thyroiditis is a benign, self-limiting condition thought, but not proven, to be of viral origin.[5,6] Initially there is a hyperthyroid phase, lasting for weeks to several months. This phase is caused by inflammation-induced release of stored thyroid hormone from the gland. RAIU is also reduced because of impairment of the trapping mechanism. Hypothyroidism may develop, which can be treated with thyroid hormone. Upon resolution of the disease, most patients return to normal thyroid function.

Chronic thyroiditis, also known as lymphocytic or Hashimoto's thyroiditis, is an autoimmune inflammatory disease with evidence of elevated circulating antithyroid antibodies similar to those associated with Graves' disease.[6,7] The thyroid parenchymal cells are increasingly replaced by lymphocytes and plasma cells and eventually by fibrosis. Hypothyroidism is the end result. In the initial stages of the disease, TSH levels are elevated but thyroid hormone levels are low normal. The gland is diffusely enlarged, but the condition differs from Graves' disease in that patients in the latter stages of thyroiditis often exhibit hypothyroidism, and thyroid scans demonstrate reduced, nonhomogeneous uptake of activity.

Thyroid Nodules

A frequent indication for thyroid scanning is the presence of one or more palpable nodules in the thyroid gland. Nodules are usually benign, but they must be evaluated to rule out the presence of cancer. Nodules that accumulate radioiodine or pertechnetate and appear "hot" on the thyroid scan are called functioning nodules. Functioning nodules may or

may not be under the control of TSH. A nodule that is not controlled by TSH is called an autonomous nodule. Sometimes, an autonomous nodule can achieve large size and produce enough thyroid hormone to supply the entire needs of the body. It may also produce excessive amounts of hormone, causing the patient to become thyrotoxic (hyperthyroid). Such a toxic nodule can suppress TSH release from the pituitary and cause suppression of the remaining normal thyroid tissue.[7] Functioning or hot nodules occur with low frequency (approximately 10%) and typically are benign. Most nodules are nonfunctioning (i.e., they do not take up radiotracer); however, some nonfunctioning nodules may be cancerous, so further studies are needed to establish a diagnosis.

HISTORICAL PERSPECTIVES

The first production of radioiodine for clinical application was at the Massachusetts Institute of Technology in 1937, when Robley Evans produced ^{128}I by neutron irradiation of ethyl iodide.[8] Intravenous injection of ^{128}I into rabbits clearly demonstrated, for the first time, the rapid accumulation of radioiodide by the thyroid gland.[9]

After the discovery of artificial radioactivity in 1934, cyclotrons were built at several research centers in the United States to produce radionuclides, mainly for medical research. Collaboration between institutions led to the rapid discovery of several iodine isotopes. Large quantities of ^{128}I were produced at Berkeley, but its 25 minute half-life was too short for metabolic studies. In 1938, ^{126}I ($T_{½}$ 13.3 days) was produced at Michigan by Tape and Cork,[10] while ^{131}I ($T_{½}$ 8.04 days) was made by Livingood and Seaborg[11] at Berkeley. Hamilton and Soley[12] reported on the first use of ^{131}I in human subjects with thyroid disease. Keston et al.[13] first reported on the uptake of radioiodine in thyroid metastasis in 1942. Probably the most significant application of ^{131}I, which heralded the value of radioisotopes in medicine, was use of the ^{131}I "atomic cocktail" in the treatment of metastatic thyroid cancer, reported by Seidlin et al.[14] in 1946. Before that, ^{131}I had been used to treat Graves' disease,[15] but a "cancer cure" had a much more dramatic impact than a treatment for hyperthyroidism. Strong public and monetary support for the fledgling discipline of nuclear medicine began with this experience.

RADIOPHARMACEUTICALS FOR THYROID STUDIES

Sodium Iodide I 123 and I 131 Capsules and Solution

^{131}I is the standard radionuclide used for routine thyroid studies. It is relatively inexpensive to produce, and its 8 day half-life allows it to be available when needed in the nuclear medicine clinic. ^{131}I-sodium iodide is available from commercial suppliers in hard gelatin capsules and in aqueous solution for oral administration. Capsules for diagnostic studies are generally available in 15, 25, 50, and 100 μCi (555, 925, 1850, and 3700 MBq) sizes. The capsules contain sodium radioiodide, either mixed with polyethylene glycol and thiosulfate as a thin film on the inside surface of the capsule or mixed with a granulated powder. Therapeutic capsules for use in hyperthyroidism and thyroid carcinoma are also available, made to order on 24 hour notice. ^{123}I-sodium iodide capsules are available in 100 and 200 μCi (3.7 and 7.4 MBq) sizes for diagnostic studies.

In thyroid uptake studies to determine thyroid function, a capsule is given to the patient and thyroid gland counts are compared with activity in a standard capsule. To minimize error in thyroid uptake measurements, it is important that the activity of capsules within a given lot vary by no more than a few percentage points from the mean capsule activity in the lot used as the standard. The *United States Pharmacopeia, 24th Revision,* required manufacturers to ensure that at least 19 of 20 capsules in a lot of ^{123}I- or ^{131}I-sodium

^{131}I-Sodium Iodide Capsule Counting Worksheet

Lot Number 300732F Date Counted 1-15-02

Activity 22 μCi Color Orange

Procedure: Count each capsule collecting at least 100,000 counts per capsule. Subtract background and determine the mean count. Discard any capsule whose count does not fall within 96.5% and 103.5% of the mean count. Save as a standard the capsule whose count is closest to the mean.

Net Capsule Counts	Net Capsule Counts
1. 112,919	11. 117,510
2. 115,374	12. 113,388
3. 113,590	13. 112,316
4. 112,782	14. 114,124
5. 111,568	15. 115,102
6. 111,546	16. 110,983
7. 110,635	17. 114,949
8. 114,117	18. 115,342
9. 113,380	19. 116,830
10. 114,417	20. 115,182

Mean Count = 113,802 × 0.965 = 109,820 (lower limit)

× 1.035 = 117,786 (upper limit)

FIGURE 14-3 Capsule-counting worksheet for statistical analysis of ^{131}I-sodium iodide capsules.

iodide contain activity between 96.5% and 103.5% of the mean capsule activity in the lot. Figure 14-3 illustrates a method that can be used to ensure that capsules are within these limits.

Some models of uptake probes for counting thyroid gland activity have programs specifically set up for the RAIU study. The capsule given to the patient is counted before administration, establishing the standard counts. The counts are stored in the computer and are automatically decay-corrected to the time of patient counting. The counts in the patient's thyroid gland are then compared with the standard count. Thus, each capsule given to the patient acts as its own standard.

Chapter 9 includes a detailed discussion of radioiodine chemistry and dosage forms.

Biologic Properties of Radioiodide

After oral administration of sodium radioiodide, the rate of gastrointestinal absorption is rapid, on the order of 5% per minute, and absorption is nearly complete within 1 to 2 hours.[16] The absorption rate may be delayed if food is present, and it is directly influenced by thyroid function, being increased in hyperthyroidism and decreased in hypothyroidism.

Iodide is cleared from the plasma primarily by the thyroid gland but also by the salivary glands, gastric mucosal cells, mammary glands, and kidneys. It is widely distributed in the body after administration. Most is excreted within the first 24 hours, and the remainder is localized mainly in the thyroid gland. Bodily distribution of radioiodide between 1 hour and 80 days is summarized in Figure 14-4.

Renal Excretion

Renal clearance of iodide is by glomerular filtration at a mean rate of 34 mL/minute, or 27% of the normal glomerular filtration rate. Thus about 73% of filtered iodide is reabsorbed by the tubule. Iodide is not bound in the kidney. Renal clearance of iodide is fairly constant over a wide range of plasma concentrations. After a dose of 10 μCi (370 kBq) of ^{131}I-sodium iodide with carrier doses of 0.001, 0.1, 1.0, and 10.0 mg of stable iodide, no

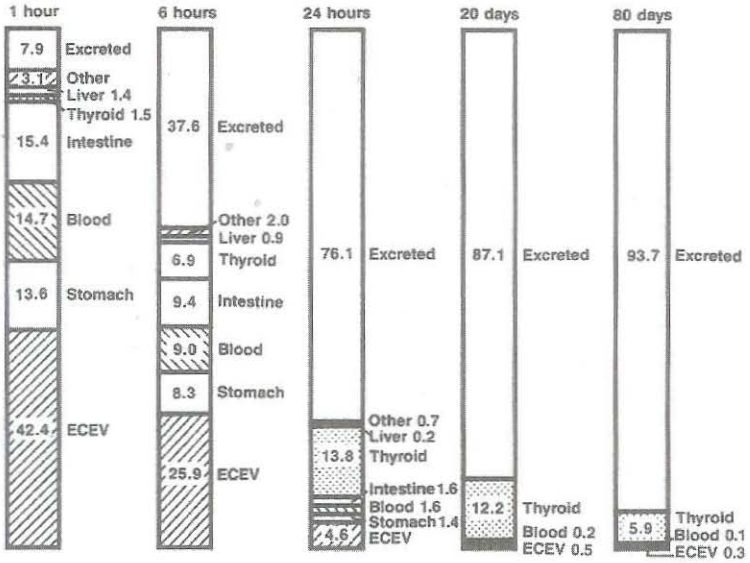

FIGURE 14-4 Estimated percentages of administered radioiodine in tissues of the body at various times after a single oral dose of radioiodide corrected for radioactive decay. The maximum thyroid uptake is assumed to be 15%. ECEV = extracellular extravascular space. (Reprinted with permission from reference 21.)

TABLE 14-1 FDA-Recommended Dose of Potassium Iodide for Thyroid Gland Protection

Age Group	Threshold Dose of Predicted Thyroid Exposure (rad or cGy)	Potassium Iodide Dose per Day (mg)
Adults over 40 yr	≥500	130[a]
Adults 18 to 40 yr	≥10	130
Adolescents ≥70 kg	≥5	130
Pregnant or lactating women	≥5	130
3 yr to 18 yr	≥5	65
1 month to 3 yr	≥5	32
Birth to 1 month	≥5	16

[a] 130 mg of potassium iodide is contained in each of the following: One 130 mg potassium iodide tablet, 0.8 mL Lugol's solution, 0.13 mL saturated solution of potassium iodide (SSKI).

Source: www.fda.gov/cder/guidance/4825fnl.htm.

difference in renal clearance of iodide occurs; however, a significant reduction of thyroid uptake occurs with the 1.0 and 10.0 mg doses, with uptakes similar to euthyroidism and the athyroid state, respectively.[17] In some instances it is necessary to administer stable iodide to protect the thyroid gland from unnecessary radiation exposure from free radioiodide, such as may occur from radioiodide released by metabolized radioiodinated radiopharmaceuticals or from accidental ingestion of radioiodide.

Thyroid-blocking doses of potassium iodide recommended by the Food and Drug Administration, based on studies after the Chernobyl nuclear reactor disaster, are shown in Table 14-1.[18] Doses are based on subject weight and predicted thyroid exposure dose. A single dose protects the thyroid gland for 24 hours. The dose of potassium iodide should be administered with milk, fruit juice, or a large volume of water to minimize gastric irritation. These doses of potassium iodide can block 90% of radioiodine absorption if the first dose is given a few hours before or immediately after intake of radioiodine; the drug can still block 50% of radioiodine absorption if the first dose is administered within 4 hours after exposure.[19] Potassium iodide (KI) is available as potassium iodide tablets, 65 mg and 130 mg (equivalent to 50 mg and 100 mg iodine, respectively), as saturated solution of potassium iodide (SSKI), 1 gram KI per mL, or as Lugol's solution, 130 mg KI per 0.8 mL. Potential adverse effects of potassium iodide include gastrointestinal disturbances, allergic reactions, and minor rashes.[18]

The fraction of an administered dose of radioiodide excreted by the kidneys over 24 hours is inversely related to thyroid gland function.[20] Seventy-six percent of a dose of radioiodide is excreted in 24 hours in normal subjects with a thyroid uptake of 15% (Figure 14-4).[21]

Thyroid Gland Uptake

Measurement of thyroid gland function with radioiodide is predicated on an amount of radiotracer that is physiologic (i.e., will not alter the gland's normal function). The amount administered in thyroid studies easily meets this requirement; the average daily dietary intake of iodide is 300 μg, and a 10 μCi (370 kBq) diagnostic dose of ^{131}I-sodium iodide contains only 8×10^{-5} μg of iodine (one eighty-millionth of total body iodine).

The RAIU study is one of the oldest in vivo function studies performed in nuclear medicine. It is based on physiologic incorporation of radioiodide tracer into the thyroid gland followed by determination of the fraction of the dose taken up in the gland over a given time period. This study is described later in the chapter. For a successful test, it is important that no substance be present in the blood that will interfere with thyroid uptake of radioiodide, and patients must be questioned before the test to identify any interfering substances. Suppression of RAIU by stable iodide has been reported.[22] Table 14-2 lists common interfering substances.[23,24] The table does not list all of the radiographic contrast agents available, but all of them contain large amounts of iodine, and several weeks should elapse before the RAIU test is conducted in a patient who has received contrast material.

Salivary Glands

A significant amount of iodide is secreted by the salivary glands. Most of this is swallowed, but expectoration of saliva is a potential source of clothing contamination after therapeutic dosing of ^{131}I. This may lead to artifacts on whole-body images. Similar artifacts are more likely to result from urinary contamination; therefore, it is wise to provide clean hospital gowns before any imaging studies. The concentration of radioiodide in salivary glands can produce a metallic taste in the mouth within a few hours after administration of a therapeutic dose of ^{131}I. Additionally, radiation sialadenitis may occur after large therapeutic doses of 150 mCi (5550 MBq), producing dry mouth and swelling and tenderness of the submaxillary glands.[25] Chewing gum or using lozenges that promote salivation can shorten the residence time of ^{131}I in the salivary glands and may reduce the incidence of sialadenitis.

TABLE 14-2 Drugs and Chemical Substances that Decrease 24-hour Thyroid Uptake

Substance	Average Duration of Effect
Iodide-Containing Drugs	
SSKI, Lugol's solution	1–4 weeks
Vitamin and mineral products	
Pima Syrup (Fleming)	
Isopropamide iodide	
Amiodarone, benziodarone	
Calcium iodide in Calcidrine syrup (Abbott)	
Hydriodic acid syrup	
Topical Iodide Products	
Iodochlorhydroxyquin—Clioquinol (Clay-Adams)	1–9 months
Iodine tincture	2 weeks
X-Ray Contrast Media	
Hypaque Meglumine, Hypaque Sodium (Winthrop)	1–2 weeks
Lipiodol, Ethiodol (Fougera)	1 year or more
Cholografin Meglumine (Bracco)	3 months
Telepaque (Nycomed)	2 months
Antithyroid Drugs	
Propylthiouracil, methimazole	2–8 days
Thyroid Medication	
Thyroid hormone, thyroxine, liothyronine	1–2 weeks
Other Drugs	
Phenylbutazone, sulfonamides	1 week
Adrenal and gonadal steroids, ACTH	8 days

Sources: References 23 and 24.

Gastric Glands

Radioiodide is highly concentrated in the gastric mucosa. Plasma clearance of iodide by the gastric glands is on the order of 25 mL/minute, and gastric juice-to-plasma ratios may be as high as 40.[26] This high concentration is inhibited by stable iodide and by perchlorate, suggesting an active transport process by the gastric cells. This gastric activity is associated with the mucoid cells rather than the parietal cells. The significance of the gastric concentrating mechanism is not known. Secretion of iodide into the gastric juice at high concentration increases the apparent iodide space of the body, but the iodide is normally rapidly reabsorbed after passing into the small intestine.[23]

Mammary Glands

Clearance of iodide by the mammary glands may achieve milk-to-plasma ratios up to 33 to 1.[27] Radioiodide and other radiopharmaceuticals are known to be excreted in human milk.[28,29] Precautions must be taken to prevent a nursing infant from ingesting contaminated milk from a mother who has received radioactive material. This is especially important in regard to ^{131}I because of the potentially high radiation dose to the infant's thyroid gland. Estimated radiation doses to newborns and 1 year old infants from radioiodide administered orally or intravenously are listed in Table 14-3.[30] It is important for a nursing

TABLE 14-3 Estimated ^{131}I and ^{123}I Radiation Dose to Newborns and Infants and Time until Breast-feeding Can Resume[a]

Radiopharmaceutical	Radiation Dose, rem/μCi[b] (^{131}I = thyroid dose) (^{123}I = effective dose) Newborn	1 Year Old	Time until Breast-feeding Resumes[c]
^{131}I sodium iodide	20	14	8 weeks after 5 μCi
^{123}I sodium iodide	0.0059	0.0041	2–3 days after 10 to 30 μCi

[a] After mother has received radioiodide.
[b] Data from reference 30.
[c] Data from reference 28.

TABLE 14-4 Radiation Absorbed Dose from Radioiodines

Target Organ	Rad(cGy)/mCi of Radioiodine Administered ^{123}I	^{124}I	^{125}I	^{131}I
Thyroid gland	13.0	890	790.0	1300.0
Total body	0.029	0.83	0.49	0.71

Source: Reference 21; values assume a 25% maximum uptake by the thyroid.

mother who receives radioiodide to know when she can resume breast-feeding her infant. Table 14-3 also gives recommended times to wait before safely resuming breast-feeding.[28]

Placental Transport of Iodide

Several studies reviewed by Brown-Grant[26] indicate that placental transport of radioiodide occurs and high fetal-to-maternal thyroid ratios are achieved near term in many instances. Studies in humans have demonstrated that the fetal thyroid gland has the ability to accumulate ^{131}I iodide by the 12th to 14th week of gestation.[31,32] Consequently, the use of radioiodine and any radioactive material during pregnancy is contraindicated.

Radiation Dose from Radioiodines

The critical organ for radioiodine is the thyroid gland. The magnitude of the radiation dose to the gland and other organs and the total body depends on the radionuclide administered and the uptake by the gland. Estimates of radiation dose to the thyroid and the total body from ^{123}I, ^{124}I, ^{125}I, and ^{131}I are shown in Table 14-4. The ^{124}I and ^{125}I isotopes are included in the table because they may occur as radionuclidic contaminants in radioiodine preparations.

Sodium Pertechnetate Tc 99m Injection

After intravenous administration of sodium pertechnetate Tc 99m injection (^{99m}Tc-sodium pertechnetate), the pertechnetate anion is trapped by the thyroid epithelial cells in a manner similar to iodide because of its similar ionic charge and volume. Its accumulation in the gland is limited to the trapping mechanism and is metabolized no further. The normal thyroid gland handles pertechnetate in the same manner that the propylthiouracil-blocked gland handles iodide, that is, pertechnetate is discharged from the gland by

TABLE 14-5 Radiopharmaceuticals for Thyroid Imaging

Radiopharmaceutical	Administered Activity	Route	Time from Dose to Image	Thyroid Dose[a] rad(cGy)/ μCi Administered
^{131}I-sodium iodide	50–100 μCi	Oral	24 hr	1.30
^{123}I-sodium iodide	200–400 μCi	Oral	24 hr	0.013
^{99m}Tc-sodium pertechnetate	2–10 mCi	IV	20–30 min	0.0002

[a] Based on 25% thyroid uptake. ^{123}I dose does not include any contribution from ^{125}I or ^{124}I radiocontaminants.

Source: Reference 21.

perchlorate.[33] Uptake of ^{99m}Tc-sodium pertechnetate by the thyroid gland is between 1% and 2% of the administered activity in euthyroid subjects but may be 10 times greater in thyrotoxicosis.[33] Multimillicurie amounts of ^{99m}Tc-sodium pertechnetate can be administered because the radiation dose to the gland is low compared with the dose from radioiodines (Table 14-5). ^{99m}Tc-sodium pertechnetate is administered intravenously for thyroid imaging at a dose of 2 to 10 mCi (74 to 370 MBq). Imaging is begun at the time of maximal uptake, which occurs in 20 to 30 minutes. The oral route may be used for imaging done at 1 hour. Chapter 13 contains more complete biologic information on ^{99m}Tc-sodium pertechnetate.

NUCLEAR MEDICINE PROCEDURES

Two nuclear medicine procedures are commonly used to evaluate patients with suspected thyroid abnormalities: the RAIU test and the thyroid scan. In addition, ^{131}I therapy is used to treat patients with known thyroid gland disease. These procedures are well established and have been used in nuclear medicine for over 50 years.[34]

Radioactive Iodine Uptake

Rationale

The thyroid gland both traps iodine and organifies it into thyroid hormone. Epithelial cells of the thyroid gland have an iodide pump that enables the thyroid gland to concentrate iodide to levels higher than those in the plasma (trapping).[35] The iodide is then used to synthesize thyroid hormone (organification). RAIU is a measure of iodine metabolism in the thyroid gland. Determination of the fraction of a dose of radioactive iodine that accumulates in the thyroid gland at specific times after oral administration can be used to estimate thyroid function. This can be helpful in evaluating both hypothyroid and hyperthyroid conditions. In hyperthyroid conditions, the 4 and 24 hour thyroid uptake values are commonly used in determining iodine metabolism and turnover rates in the thyroid. These uptake measurements can assist in the diagnosis of hyperthyroidism and are useful in determining appropriate ^{131}I therapeutic dosages. RAIU along with a thyroid scan is also useful in differentiating causes of hyperthyroidism, such as Graves' disease, Plummer's disease (toxic multinodular goiter), and subacute thyroiditis.

Procedure

Patient preparation is important. Many substances can interfere with the uptake of iodine in the thyroid gland (Table 14-2). Patients who are taking these interfering substances should not be scheduled for RAIU testing until the effects of these substances have cleared.

Administration of antithyroid drugs such as propylthiouracil and methimazole should be stopped at least 4 to 5 days before an RAIU test. Iodine-containing medications and food rich in iodine can also decrease radioiodine uptake in the thyroid gland. Prior imaging procedures such as computed tomography or angiography that use iodinated contrast agents can affect uptake of iodine in the thyroid for weeks. The patient should take nothing by mouth for 4 hours before administration of radioiodine to ensure adequate intestinal absorption. Food in the stomach can interfere with early iodine uptake.

Pharmaceuticals

To measure radioiodine uptake, a small amount of radioiodine is administered orally. Either ^{123}I- or ^{131}I-sodium iodide can be used. ^{131}I-sodium iodide is used more often, because it is inexpensive and readily available.

Uptake measurements are usually taken at 4 hours and 24 hours after administration of the radiotracer. The dose is usually 4 to 10 μCi (148 to 370 kBq) of ^{131}I-sodium iodide. The patient is placed in front of a thyroid probe and counts are obtained at the neck. Patient background counts are measured at the thigh. Counts are also obtained in a neck phantom, either from a calibrated standard capsule representing the patient dose or from the actual capsule given to the patient. Background counts are also obtained. The resulting RAIU is expressed as a percentage.

$$\text{RAIU} = \frac{\text{Neck (cpm)} - \text{Thigh (cpm)}}{\text{Administered dose (cpm)} - \text{Background (cpm)}} \times 100$$

Interpretation

The normal range for these values is different for populations with different iodine intakes, and results should be interpreted in the context of other clinical information. In general, the normal range is considered to be 5% to 15% for 4 hour uptake and 10% to 35% for 24 hour uptake.[36]

In certain hyperthyroid individuals, 4 hour uptake will be higher than 24 hour uptake. For these individuals who demonstrate more rapid than normal turnover of iodine in the thyroid gland, it may be appropriate to use a higher ^{131}I dose in radioiodine therapy.

Thyroid Scan

Rationale

Thyroid scanning can be used to relate the structure of the gland to its function. Thyroid scans are often obtained to evaluate a single palpable nodule, multiple nodules, or an enlarging gland. The scan is useful in determining the functional nature of a palpable thyroid abnormality and is often useful in distinguishing benign from malignant disease.

In patients with hyperthyroidism, thyroid scans can be useful in distinguishing Graves' disease from toxic adenoma or toxic multinodular goiter. This information helps to determine the amount of ^{131}I-sodium iodide needed for appropriate thyroid therapy.

Scanning is useful in determining if a thyroid nodule is functional. Although the majority of thyroid nodules are benign, hypofunctioning or "cold" nodules are at increased risk for malignancy.[37]

Scanning is also useful in differentiating Graves' disease from subacute thyroiditis, postpartum thyroiditis, and factitious thyroiditis. Graves' disease causes prominent diffuse

radiotracer uptake throughout the thyroid gland, whereas the other conditions demonstrate low radiotracer uptake and poor visualization of the thyroid gland.

Thyroid scans can also be used to locate ectopic thyroid tissue, such as in substernal goiter or lingual thyroid.

Procedure

Just as in RAIU testing, attention should be paid to patient preparation. The patient should not be pregnant or lactating, especially if radioiodine therapy is being considered. The patient should avoid interfering medications such as antithyroid drugs, iodine-rich foods such as kelp products, and iodine-containing medications such as amiodarone for an appropriate period of time. In many instances, the thyroid scan is obtained after the RAIU, and patient preparation has already been considered.

The patient is positioned supine with the neck extended. This is usually accomplished by placing a pillow or blanket under the patient's shoulders. Images of the neck are obtained using a gamma camera equipped with a pinhole collimator. Time to imaging varies with the radiopharmaceutical used.

Images are usually obtained 15 to 30 minutes after intravenous administration of ^{99m}Tc-sodium pertechnetate. The usual administered dose is between 2 and 10 mCi (74 to 370 MBq). Anterior, right anterior oblique, and left anterior oblique images typically are obtained. If there is a palpable nodule, imaging may be repeated with a lead marker or point source placed on the patient's skin overlying the palpable abnormality. This can be used to confirm that the palpable abnormality corresponds to a cold, hot, or warm nodule.

If ^{123}I-sodium iodide is administered orally for the thyroid scan, images are usually obtained 16 to 24 hours later. The administered dose is usually between 200 and 600 μCi (7.4 to 22.2 kBq) ^{123}I.

Pharmaceuticals

Both ^{123}I-sodium iodide and ^{99m}Tc-sodium pertechnetate are used for thyroid imaging. Both of these are trapped by the thyroid gland (i.e., transported into follicular cells of the thyroid). However, only the iodine is organified or synthesized into thyroid hormone. Both ^{99m}Tc-sodium pertechnetate and ^{123}I-sodium iodide are adequate for anatomic imaging, but ^{123}I is more accurate for functional imaging. ^{131}I can also be used for imaging the thyroid, but it is not preferred because of its higher radiation dose to the gland, which is the result of a long half-life of 8.04 days and beta particle emission.

^{123}I-sodium iodide is the imaging agent of choice because of its excellent imaging characteristics. It has a short half-life of approximately 13 hours, a gamma energy (159 keV) that is efficiently detected with the gamma camera, and absence of beta emissions. However, it is more expensive than ^{99m}Tc-sodium pertechnetate and is produced in a cyclotron, making it harder to obtain. ^{99m}Tc-sodium pertechnetate is readily available from a ^{99}Mo–^{99m}Tc generator and is much lower in cost. Thus, in most institutions, ^{99m}Tc-sodium pertechnetate is the imaging agent of choice for thyroid scanning.

Interpretation

The thyroid gland is a bilobed structure that normally demonstrates homogeneous radiotracer uptake throughout both lobes (Figure 14-5). The two lobes are joined, inferiorly and medially, by the thyroid isthmus. The isthmus often demonstrates less uptake of radioactivity than the remainder of the gland. Commonly, patients have a pyramidal lobe,

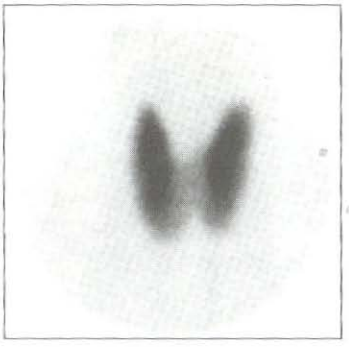

FIGURE 14-5 Normal thyroid gland in a 25 year old woman. Anterior pinhole image obtained approximately 30 minutes after administration of ^{99m}Tc-sodium pertechnetate 10 mCi.

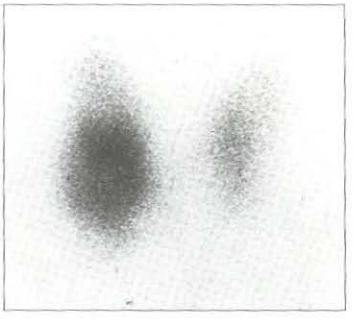

FIGURE 14-6 Large, toxic thyroid adenoma (hot nodule). Anterior image of the thyroid gland 30 minutes after intravenous administration of ^{99m}Tc-sodium pertechnetate 10 mCi demonstrates a hyperfunctioning nodule in the right lobe of the thyroid with suppression of the remaining gland.

which arises from the isthmus or the medial aspect of one of the thyroid lobes, extending medially and superiorly. In adults, the thyroid gland usually weighs between 15 and 25 grams. The right thyroid lobe is often larger than the left, extending more superiorly and inferiorly.

Palpable thyroid nodules are the most common indication for thyroid scanning. Imaging of the thyroid demonstrates the functional status of the palpable nodule and will sometimes identify other nodules. Nodules that correspond to focal areas of increased radiotracer accumulation in the thyroid gland are referred to as "hot" or hyperfunctioning nodules. Nodules that correspond to focal areas of absent radiotracer accumulation in the thyroid gland are referred to as "cold" or hypofunctioning nodules. Nodules that demonstrate some activity or activity similar to the rest of the gland are often called indeterminate or "warm" nodules. The main role of thyroid scintigraphy is to determine which nodules should undergo fine-needle aspiration biopsy.

Hot nodules are almost always benign hyperfunctioning thyroid adenomas. Autonomous functioning nodules can produce enough thyroid hormone to block the secretion of TSH from the pituitary gland, causing suppression of the remaining normal thyroid tissue (Figure 14-6).

About 85% to 90% of palpable thyroid nodules are cold nodules. Cold nodules are most commonly benign colloid cysts or other benign lesions (Figure 14-7). However, some 6% to 10% of cold nodules are malignant.[38] Therefore, cold nodules demand further evaluation, such as by ultrasonography or fine-needle aspiration biopsy. Warm nodules can be cold nodules that are embedded in the gland with overlying normal thyroid tissue. Warm nodules are approached procedurally as if they were cold nodules.

Multinodular goiter is usually seen as an enlarged gland with heterogeneous radiotracer uptake throughout the gland with hot, cold, and warm nodules (Figure 14-8). Cold nodules in multinodular goiter are less likely to be cancerous. However, a dominant cold nodule in a multinodular goiter also warrants further investigation (Figure 14-9).

Patients with Graves' disease usually have some degree of thyromegaly along with suppressed TSH. Thyroid scan usually demonstrates prominent, homogeneous radiotracer uptake throughout the thyroid gland. Many times there is a prominent pyramidal lobe (Figure 14-10).

Thyroid scanning can also be useful in hypothyroid states. An example of this is documenting the lack of thyroid tissue in a newborn with elevated TSH levels (Figure 14-11).

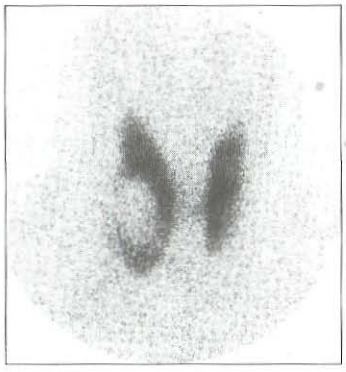

FIGURE 14-7 Cold nodule. Palpable right thyroid nodule in a 30 year old woman. Anterior pinhole image of the neck obtained 30 minutes after intravenous administration of ^{99m}Tc-sodium pertechnetate 10 mCi demonstrates a focal area of absent radiotracer accumulation in the right thyroid lobe consistent with a cold nodule.

FIGURE 14-8 Multinodular goiter. Sixty-seven year old woman with hyperthyroidism and an enlarged, nodular thyroid by palpation. Anterior pinhole image of the neck obtained 30 minutes after intravenous administration of ^{99m}Tc-sodium pertechnetate 10 mCi demonstrates multiple focal areas of both increased and decreased radiotracer accumulation consistent with toxic multinodular goiter.

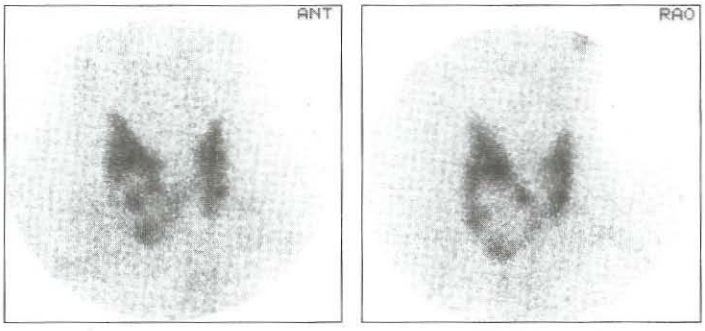

FIGURE 14-9 Thyroid scan demonstrating heterogeneous uptake in the thyroid gland with multiple focal areas of increased uptake in both lobes compatible with multinodular goiter. There is also a dominant focal area of decreased uptake involving the mid to lower right thyroid lobe, which correlated with a palpable nodule. Although most "cold" nodules in a multinodular goiter are benign, dominant cold nodules are usually investigated further with ultrasound or fine-needle aspiration biopsy. This cold nodule was found to be a Hürthle cell neoplasm.

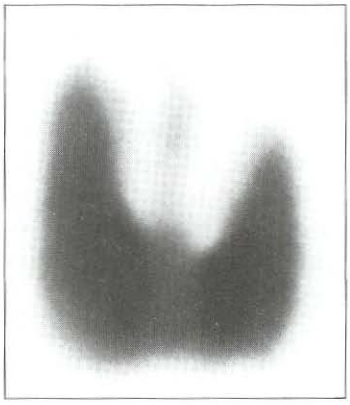

FIGURE 14-10 Graves' disease. Twenty-nine year old man with hyperthyroidism. Anterior pinhole image of the neck obtained 30 minutes after intravenous administration of ^{99m}Tc-sodium pertechnetate. Scan demonstrates prominent homogeneous uptake in an enlarged thyroid gland. Uptake is also seen in a prominent pyramidal lobe.

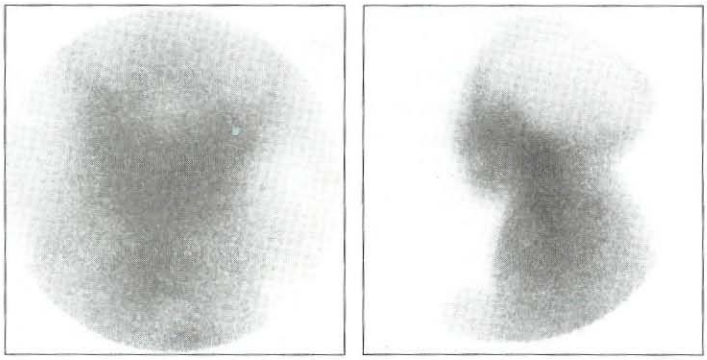

FIGURE 14-11 Agenesis of the thyroid. Twelve day old girl with elevated TSH. Anterior and left lateral pinhole images obtained after intravenous administration of ^{99m}Tc-sodium pertechnetate. There is no evidence of radiotracer accumulation in the thyroid gland.

Radioiodine Therapy

Rationale

Radioiodine therapy is an important option in the treatment of hyperthyroidism associated with Graves' disease, toxic thyroid adenoma, and toxic multinodular goiter or Plummer's disease. The options for treating hyperthyroidism include antithyroid medications, surgery, and ^{131}I-sodium iodide ablation therapy. Before radioiodine therapy is administered, it is important to confirm that the patient has hyperthyroidism both clinically and biochemically. The nature of the hyperthyroidism should also be determined. RAIU and thyroid scanning can help in differentiating thyroiditis from other conditions. Special considerations must be made if the patient is pregnant or is at high risk for thyroid storm.

Radioiodine therapy is also an option in nontoxic or euthyroid multinodular goiter in a patient with dysphagia who is not a good surgical candidate. ^{131}I therapy is also used as adjuvant treatment after surgery for papillary or follicular cell–type thyroid cancers. Controversies still exist regarding the administered dosage of ^{131}I-sodium iodide in each of these conditions.

Procedures

Graves' Disease

There are several approaches to selecting the dose of ^{131}I-sodium iodide for the treatment of Graves' disease. One of the most common methods of dose determination involves estimating the size of the thyroid gland and determining the 4 and 24 hour thyroid uptake values. The administered oral therapy dose of ^{131}I-sodium iodide is calculated by the following formula:

$$^{131}\text{I dose (mCi)} = \frac{\text{Estimated gland weight (grams)} \times \text{No. } \mu\text{Ci desired per gram of tissue}}{\%\text{ uptake at 24 hr} \times 10}$$

There is wide variation in the recommended dose in activity per gram of tissue. Generally, this varies between 55 and 200 μCi (2.035 and 7.4 kBq) per gram of tissue.[39–41] The higher doses are used for patients with severe hyperthyroid symptoms or underlying cardiac

problems, for whom it would be advantageous to induce clinical hypothyroidism as soon as possible.

β-Adrenergic blockers such as atenolol are administered to help control hyperthyroid symptoms until the patient becomes euthyroid. A single ^{131}I dose of 10 mCi (370 MBq) will induce a euthyroid or hypothyroid state in 90% of patients, with a relapse rate of only 10% to 25%.[42]

Uninodular and Multinodular Goiter

Most hot or hyperfunctioning thyroid nodules are benign.[43] Toxic autonomously functioning thyroid adenomas are relatively radioresistant, and larger doses of radioiodine are used. Toxic multinodular goiters also require a larger dose of ^{131}I than is used for Graves' disease. Typically, the maximum outpatient dose that has been used to treat these conditions is around 30 mCi (1110 MBq) of ^{131}I-sodium iodide.

Well-Differentiated Thyroid Carcinoma

Thyroid carcinomas typically start out as cold nodules on thyroid scans. Well-differentiated thyroid carcinomas such as papillary, follicular, and mixed tumors will concentrate radioiodine. However, thyroid cancer does not concentrate iodine as well as normal thyroid tissue. Because of this, it is necessary to surgically remove as much normal thyroid tissue as possible before definitive ^{131}I therapy for thyroid cancer. When most of the normal thyroid tissue is absent, TSH will rise, which will increase the function of the thyroid cancer cells.

Therapy for thyroid cancer starts with near-total thyroidectomy. The patient is not started on thyroid hormone replacement therapy after surgery. Replacement therapy is withheld for 6 weeks to allow the endogenous TSH to rise. When the TSH is high (>30 μIU/mL), a ^{123}I total-body scan is done to visualize the remaining functional thyroid tissue. The administered dose is usually around 2 mCi (74 MBq) of ^{123}I-sodium iodide, and imaging is performed the next day.

Depending on the amount of residual thyroid tissue or tumor and the location and extent of disease, an appropriate dose of ^{131}I-sodium iodide is administered. Typically, doses range from 150 to 200 mCi (5550 to 7400 MBq). Scans are often obtained a few days after treatment to further evaluate the extent of disease (Figure 14-12).

Follow-up ^{123}I total-body scans are usually done 1 year after ^{131}I therapy to assess for residual or recurrent thyroid cancer after the patient has been off thyroid hormone replacement for 6 weeks (Figure 14-13). Thyroglobulin (Tg) levels are also used to evaluate for recurrent disease.

Sometimes there is recurrent thyroid carcinoma, as evidenced by rising Tg, but the ^{123}I or ^{131}I whole-body scan is negative. In this subset of patients, positron emission tomography using ^{18}F-fludeoxyglucose has shown some value in identifying and localizing recurrent disease.[44,45]

SAFETY CONSIDERATIONS IN RADIOIODINE THERAPY

Patients who receive ^{131}I radioiodine therapy need to take precautions to minimize radiation exposure of others. In the United States, anyone who uses radioiodine must be licensed by the Nuclear Regulatory Commission (NRC). Until recently, patients treated with more than 30 mCi (1110 MBq) ^{131}I needed to be hospitalized in a private room with a private toilet and monitored until the administered activity fell below 30 mCi (1110 MBq).

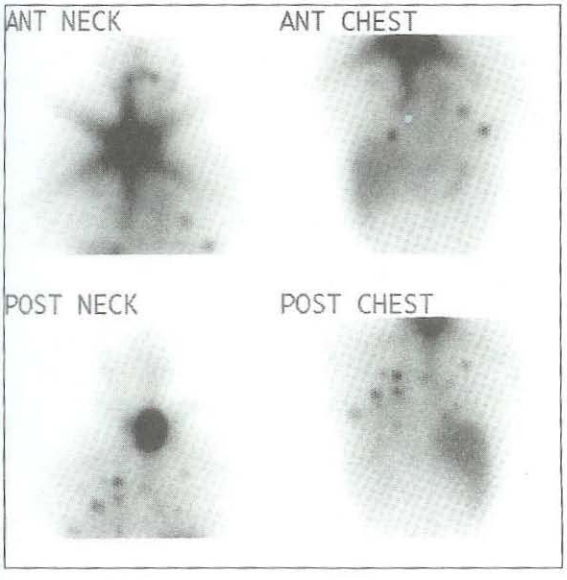

FIGURE 14-12 Metastatic thyroid cancer in a patient after thyroidectomy. Scan obtained 5 days after oral administration of ^{131}I-sodium iodide 175 mCi. The prominent focus of activity in the neck in the region of the thyroid bed is consistent with uptake in residual thyroid tissue or thyroid cancer. There is a starlike artifact associated with the prominent focus of activity in the neck. The high-energy photons of ^{131}I penetrate the collimator septa, causing this star artifact, known as septal penetration. The multiple focal areas of accumulation in the lungs are consistent with metastatic thyroid cancer.

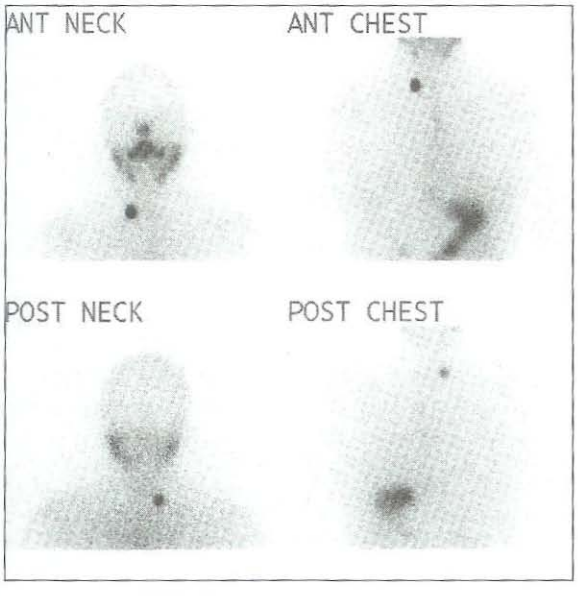

FIGURE 14-13 Thyroid cancer after therapy. ^{123}I scan of the same patient as in Figure 14-12, obtained 1 year after ^{131}I therapy. Scan shows only a single focus of residual cancer in the anterior neck. The patient subsequently underwent a second treatment with ^{131}I-sodium iodide.

However, this guideline is no longer in effect, and patients now are frequently released after having received much larger doses, even cancer therapy doses of 150 to 200 mCi (5550 to 7400 MBq) ^{131}I. In accordance with Title 10 of the Code of Federal Regulations, Part 35.75, NRC now permits a licensee to "authorize the release from its control of any individual who has been administered radiopharmaceuticals or permanent implants containing radioactive material if the total effective dose equivalent to any other individual from exposure to the released individual is not likely to exceed 5 millisievert (0.5 rem)."[46] The licensee must "provide the released individual with instructions, including written instructions, on actions recommended to maintain doses to other individuals as low as reasonably achievable if the total effective dose equivalent to any other individual is likely to exceed 1 millisievert (0.1 rem)."[46] These authorizations for release are based

TABLE 14-6 Release Criteria, Instructions, and Records Required for Patients Treated with ^{131}I

Patient Group	Basis for Release	Criteria for Release	Instructions Needed?	Records Needed?
All patients, including	Administered activity	If ≤33 mCi is given	Yes, if >7 mCi is given	No
patients who are breast-feeding	Retained activity	If ≤33 mCi is retained	Yes, if >7 mCi is retained	Yes
	Measured dose rate	If ≤7 mR/hr @ 1 m	Yes, if >2 mR/hr @ 1 m	Yes
	Patient-specific calculations	If EDE[a] is ≤0.5 rem to any individual	Yes, if EDE is >0.1 rem	Yes
Patients who are breast-feeding	All the above bases for release apply		Added instructions[b] required if >0.4 μCi given or if calculated dose to child is >0.1 rem	Need record that instructions were provided if >2.0 μCi given or calculated dose to child is >0.5 rem

[a] Effective dose equivalent.

[b] NRC recommends discontinuance or interruption of breast-feeding.

Source: Reference 46.

on patient-specific calculations. In most cases, NRC requires that records of the basis for authorizing patient release be maintained for 3 years.[46] A summary of release criteria, instructions, and records required for patients who receive ^{131}I is given in Table 14-6.

REFERENCES

1. Guyton AC. *Textbook of Medical Physiology.* 6th ed. Philadelphia; WB Saunders; 1981:931-43.
2. Hoffer PB. Gottschalk A, Quinn J III. Thyroid in vivo studies. In: Gottschalk A, Potchen EJ, eds. *Diagnostic Nuclear Medicine.* Baltimore: Williams & Wilkins; 1976:255-77.
3. Rapoport B, DeGroot LJ. Current concepts of thyroid physiology. *Semin Nucl Med.* 1971;1:265-86.
4. Wyngaarden JB, Wright BM, Ways P. The effect of certain anions upon the accumulation and retention of iodide by the thyroid gland. *Endocrinology.* 1952;50:537-49.
5. Volpe R. Thyroiditis: current views of pathogenesis. *Med Clin North Am.* 1975;59:1163-75.
6. Sandler MP, Martin WH, Powers TA. Thyroid imaging. In: Sandler MP, Coleman RE, Wackers FJ, et al., eds. *Diagnostic Nuclear Medicine.* 3rd ed. Baltimore: Williams & Wilkins; 1996:911-42.
7. Palmer EL, Scott JA, Strauss HW. *Practical Nuclear Medicine.* Philadelphia: WB Saunders; 1992:311-41.
8. Brucer M. The genesis of thyroid-iodine. In: *Vignettes in Nuclear Medicine.* No. 90. St Louis, MO: Mallinckrodt Inc; 1978.
9. Hertz S, Roberts A, Evans RD. Radioactive iodine as an indicator in the study of thyroid physiology. *Proc Soc Exp Biol Med.* 1938;38:510-3.
10. Tape GF, Cork JM. Induced radioactivity in tellurium [abstract]. *Phys Rev.* 1938;53:676.
11. Livingood JJ, Seaborg GT. Radioactive isotopes of iodine. *Phys Rev.* 1938;54:775-82.
12. Hamilton JG, Soley MH. Studies in iodine metabolism by use of a new radioactive isotope of iodine. *Am J Physiol.* 1939;127:557-8.
13. Keston AS, Ball RP, Frantz VK. Storage of radioactive iodine in a metastasis from thyroid carcinoma. *Science.* 1942;95:362-3.
14. Seidlin SM, Marinelli LD, Oshry E. Radioactive iodine therapy: effect of functioning metastasis of adenocarcinoma of the thyroid. *JAMA.* 1946;132:838.
15. Hertz S, Roberts A. Application of radioactive iodine in therapy of Graves' disease [abstract]. *J Clin Invest* 1942;21:624.
16. Keating FR Jr, Albert A. The metabolism of iodine in man as disclosed with the use of radioiodine. *Recent Prog Horm Res.* 1949;4:429-81.

17. Childs DS Jr, Keating FR Jr, Rall JE, et al. The effect of varying quantities of inorganic iodide (carrier) on the urinary excretion and thyroidal accumulation of radioiodine in exophthalmic goiter. *J Clin Invest.* 1950;29:726-38.
18. Center for Drug Evaluation and Research. *Guidance for Potassium Iodide as a Thyroid Blocking Agent in Radiation Emergencies.* Washington, DC: US Department of Health and Human Services, Food and Drug Administration, Center for Drug Evaluation and Research; November 2001.
19. US Food and Drug Administration. *Final Recommendations on Potassium Iodide for Radiation Emergencies.* Washington, DC: US Department of Health and Human Services, Food and Drug Administration; 1982. Bureau of Radiological Health Bulletin, vol 16, no. 7.
20. Skanse B. Radioactive iodine: its use in studying the urinary excretion of iodine by humans in various states of thyroid function. *Acta Med Scand.* 1948;131:251-68.
21. Loevinger R, Budinger TF, Watson EE. *MIRD Primer for Absorbed Dose Calculations.* New York: Society of Nuclear Medicine; 1988:53.
22. Sternthal E, Lipworth L, Stanley B, et al. Suppression of thyroid radioiodine uptake by various doses of stable iodide. *N Engl J Med.* 1980;303:1083-8.
23. Magalotti MF, Hummon IF, Hierschbiel E. The effect of disease and drugs on the twenty-four hour I-131 thyroid uptake. *AJR Am J Roentgenol.* 1959;81:47-60.
24. Hladik WB III, Nigg KK, Rhodes BA. Drug-induced changes in the biologic distribution of radiopharmaceuticals. *Semin Nucl Med.* 1982;12:184-218.
25. Sisson JC. Treatment of thyroid cancer. In: Wagner HN Jr, Szabo Z, Buchanan JW, eds. *Principles of Nuclear Medicine.* 2nd ed. Philadelphia: WB Saunders; 1995:629-37
26. Brown-Grant K. Extrathyroidal iodide concentrating mechanisms. *Physiol Rev.* 1961;41:189-213.
27. Honour AJ, Myant NB, Rowlands EN. Secretion of radioiodide in digestive juices and milk in man. *Clin Sci.* 1952;11:447-62.
28. Romney BM, Nickoloff EL, Esser PD, et al. Radionuclide administration to nursing mothers: mathematically derived guidelines. *Radiology.* 1986;160:549-54.
29. Nurnberger C, Lipscomb A. Transmission of I-131 to infants through human maternal milk. *JAMA.* 1952;150:1398-1400.
30. Toohey RE, Stelson AT. *Guidelines for Breastfeeding Mothers in Nuclear Medicine.* Oak Ridge, TN: Radiation Internal Dose Information Center; 1996.
31. Chapman EM, Corner GW, Robinson D, et al. The collection of radioactive iodine by the human fetal thyroid. *J Clin Endocrinol.* 1948;8:717-20.
32. Hodges RE, Evans TC, Bradbury JT, et al. The accumulation of radioiodine by human fetal thyroids. *J Clin Endocrinol.* 1955;15:661-7.
33. Andros G, Harper PV, Lathrop LA, et al. Pertechnetate-99m localization in man with applications to thyroid scanning and the study of thyroid physiology. *J Clin Endocrinol.* 1965;25:1067-76.
34. Chapman EM, Maloof F. The use of radioactive iodine in the diagnosis and treatment of hyperthyroidism; ten years' experience. *Medicine.* 1955;34:261-70.
35. Wolff J. Transport of iodide and other anions in the thyroid gland. *Physiol Rev.* January 1964;44:45-90.
36. Balon H, Dworkin H. In vivo nonimaging studies. In: Henkin RE, Boles MA, Dillehay GL, et al., eds. *Nuclear Medicine.* St Louis, MO: Mosby-Year Book; 1996:445-71.
37. Attie JN. The use of radioactive iodine in the evaluation of thyroid nodules. *Surgery.* 1959;47:611-4.
38. Freitas JE, Freitas AE. Thyroid and parathyroid imaging. *Semin Nucl Med.* 1994;24:234-45.
39. Kaplan MM, Meier DA, Dworkin HJ. Treatment of hyperthyroidism with radioactive iodine. *Endocrinol Metab Clin North Am.* March 1998;27:205-22.
40. Cooper DS. Treatment of thyrotoxicosis. In: Braverman LE, Utiger RD, eds. *Werner and Ingbar's The Thyroid: A Fundamental and Clinical Text.* 7th ed. Philadelphia: Lippincott-Raven; 1996:708-34.
41. Becker DV, Hurley JR. Radioiodine treatment of hyperthyroidism. In: Sandler MP, Coleman RE, Wackers FJ, et al., eds. *Diagnostic Nuclear Medicine.* New York: Williams & Wilkins; 1996:943-58.
42. Caruso DR, Mazzaferri EL. Intervention in Graves' disease: choosing among imperfect but effective treatment options. *Postgrad Med.* December 1992;92:117-34.
43. Ross DS. Evaluation of the thyroid nodule. *J Nucl Med.* 1991;32:2181-92.
44. Hooft L, Hoekstra OS, Deville W, et al. Diagnostic accuracy of ^{18}F-fluorodeoxyglucose positron emission tomography in the follow-up of papillary or follicular thyroid cancer. *J Clin Endocrinol Metab.* 2001;86:3779-86.
45. Wang W, Macapinlac H, Larson S, et al. [^{18}F]-2-fluoro-2-deoxy-D-glucose positron emission tomography localizes residual thyroid cancer in patients with negative diagnostic ^{131}I whole body scans and elevated serum thyroxine levels. *J Clin Endocrinol Metab.* 1999;84:2291-2302.
46. US Nuclear Regulatory Commission, Office of Nuclear Regulatory Research. *Release of Patients Administered Radioactive Materials.* Washington, DC: US Nuclear Regulatory Commission; April 1997. Regulatory Guide 8.39.

15 Heart

Coronary artery disease (CAD) is the third-ranking cause of years of potential life lost before age 65 in the United States, behind accidents and cancer.[1] CAD arises principally from a gradual narrowing of coronary arterial lumen caused by atherosclerotic deposits. The progressive narrowing of lumen diameter eventually predisposes the patient to myocardial ischemia, a condition in which coronary blood flow decreases to a level below that needed to meet oxygen demand. When coronary arterial lumen diameter is reduced by 50%, perfusion abnormalities can be detected but patients are usually asymptomatic.[2] When lumen diameter is reduced by 70%, clinical symptoms (angina) occur during myocardial stress because tissue oxygenation is temporarily below that required for adequate function. In advanced ischemic CAD, in which blood flow and tissue oxygenation are too low to sustain cardiac function at rest, myocardial infarction (MI) results, and the affected muscle dies. It is important to be able to distinguish between ischemic and infarcted myocardium, because ischemic, viable myocardium can be restored to health by medical and surgical intervention.

Cardiac imaging plays a key role in the diagnostic work-up of patients with CAD. While the goals of cardiac imaging are broad, encompassing assessment of the cardiac chambers, myocardial perfusion, metabolism, and infarction, the major focus is the assessment of myocardial perfusion. Precise measurement of regional myocardial perfusion in humans has clinical applicability for identifying ischemia, defining the extent and severity of disease, assessing myocardial viability, establishing the need for medical and surgical intervention (revascularization), and monitoring the effects of treatment.

Most clinical nuclear medicine studies today use single-photon emission computed tomography (SPECT) methods for data acquisition; however, positron emission tomography (PET) methods are increasing as PET centers become established. Approximately one-third of all nuclear medicine procedures involve heart studies. Most (84%) of these studies involve myocardial perfusion imaging (MPI), 15% are radionuclide ventriculography, and the remainder are miscellaneous studies such as infarct imaging and metabolism studies.[2] Myocardial perfusion imaging provides information about coronary artery blood flow, an indirect measure of oxygenation and metabolism in the myocardium, whereas ventriculography provides information about cardiac function.

The radiopharmaceuticals used to evaluate heart disease fall into four main groups: (1) perfusion agents (SPECT and PET) for evaluating coronary artery blood flow and ischemia, (2) blood pool agents for evaluating heart function, (3) infarct-avid agents for assessing MI, and (4) metabolism agents for assessing myocardial viability (Table 15-1). The principal agents used in SPECT imaging are ^{99m}Tc-labeled red blood cells for blood pool studies and ^{201}Tl-thallous chloride, ^{99m}Tc-sestamibi, and ^{99m}Tc-tetrofosmin for myocardial perfusion studies. ^{18}F-fludeoxyglucose (^{18}F-FDG) is the main PET agent used for myocardial viability studies. Its reasonably long half-life allows it to be available from regional PET nuclear pharmacies. The other agents used in PET imaging are ^{82}Rb-rubidium chloride, ^{15}O-water, and ^{13}N-ammonia for perfusion studies and ^{11}C-acetate and ^{11}C-palmitate for metabolism studies. These agents, because of their very short half-lives, are primarily used at facilities that have their own cyclotron and radiochemistry laboratories.

TABLE 15-1 Myocardial Imaging Agents

Planar and SPECT Agents	PET Agents
Blood pool markers	Perfusion agents
^{99m}Tc-albumin	^{82}Rb-rubidium chloride
^{99m}Tc-red blood cells	^{15}O-water
Infarct-avid agents	^{13}N-ammonia
^{99m}Tc-pyrophosphate	Metabolism agents
^{111}In-imciromab pentetate[a]	^{11}C-acetate
Perfusion agents	^{11}C-palmitate
^{201}Tl-thallous chloride	^{18}F-fludeoxyglucose
^{99m}Tc-sestamibi	
^{99m}Tc-tetrofosmin	
^{99m}Tc-teboroxime[a]	
^{99m}Tc-nitrido dithiocarbamate [Tc-N-(NOEt)$_2$]	

[a] No longer marketed in the United States.

Infarct-avid agents for localizing MI, such as ^{99m}Tc-pyrophosphate, are now infrequently used; however, newer agents are being developed for this application.

PHYSIOLOGIC PRINCIPLES

Blood Flow to the Heart

Blood flow to the normal heart varies, with the greatest flow per gram to the left ventricle and the least flow to the atria. Because of its greater mass compared with other heart chambers, the left ventricle receives about 80% of blood flow to the heart. Because of its greater thickness, the left ventricle is the predominant region seen in cardiac imaging, while the right ventricular wall is faintly visualized (Figure 15-1).

Resting myocardial blood flow to most regions of the left ventricular myocardium ranges from 0.6 to 0.8 mL/minute per gram.[3] At rest, the oxygen extraction efficiency of the heart is about 70%, compared with 20% for skeletal muscle.[4] An increased myocardial need for oxygen necessitates increased coronary blood flow. Coronary blood flow can increase in almost direct proportion to the metabolic consumption of oxygen by the heart. Under normal conditions and after appropriate stimuli, such as exercise or the administration of specific pharmacologic agents, blood flow can increase 5- to 6-fold, or up to 3 to 4 mL/minute per gram.[3] However, in the clinical setting with healthy volunteers and patients, maximal induced flows are typically in the range of 2 to 4 times baseline.[5-7] The difference between baseline flow and maximal flow is known as coronary flow reserve. This reserve is progressively lost as vessels become stenosed and hardened by atherosclerosis.

Studies in dogs have shown that resting coronary blood flow does not change until coronary diameter stenosis exceeds 85%, whereas maximal coronary blood flow begins to decrease when diameter stenosis exceeds 45% (Figure 15-2).[8] Thus, only the most severe coronary obstruction is likely to be detected by perfusion imaging under resting conditions. It follows, then, that assessment of regional myocardial perfusion under conditions of cardiac stress substantially increases the sensitivity for detecting obstructive CAD.

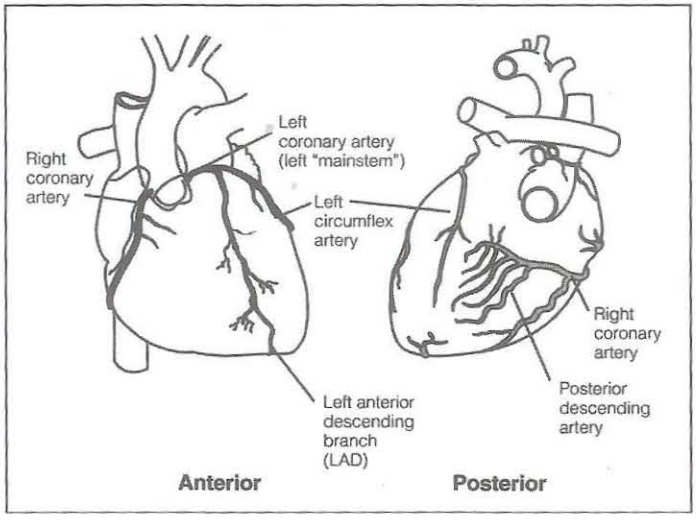

FIGURE 15-1 Anterior and posterior projections of the two main coronary arteries arising from the aorta. The right coronary artery supplies the lateral and posterior walls of the right ventricle and inferior wall of the left ventricle; the left anterior decending branch supplies the anterior wall of the right ventricle and the septum, apex, and anterior wall of the left ventricle; the left circumflex artery supplies the lateral and posterior wall of the left ventricle. (Reprinted with permission of Bristol-Myers Squibb Medical Imaging Inc. from *Introduction to Nuclear Cardiology*, 3rd ed. North Billerica, MA: DuPont Pharma Radiopharmaceuticals; 1993:75.)

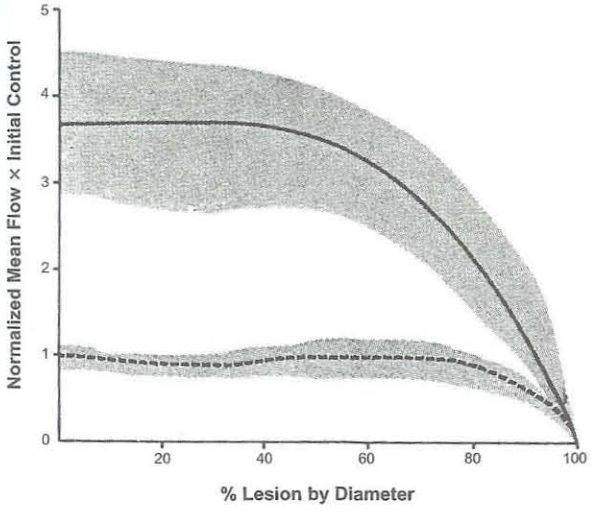

FIGURE 15-2 Relationship of coronary artery stenosis (x-coordinate) to alteration in coronary blood flow (y-coordinate) at resting flow (bottom curve) and at hyperemic flow (top curve). (Reprinted with permission of Excerpta Medica Inc. from reference 8.)

Nuclear medicine procedures are typically conducted in conjunction with cardiac stress induced by either exercise or the use of pharmacologic agents in order to identify regions of subcritical coronary stenosis.

During induced maximal coronary dilatation after exercise or pharmacologic stress, a greater portion of the increased blood flow to the heart goes to normally perfused myocardial regions, with lesser amounts going to myocardium supplied by stenosed coronary vessels because of their limited vasodilatory reserve.[8] The basis for detecting CAD with

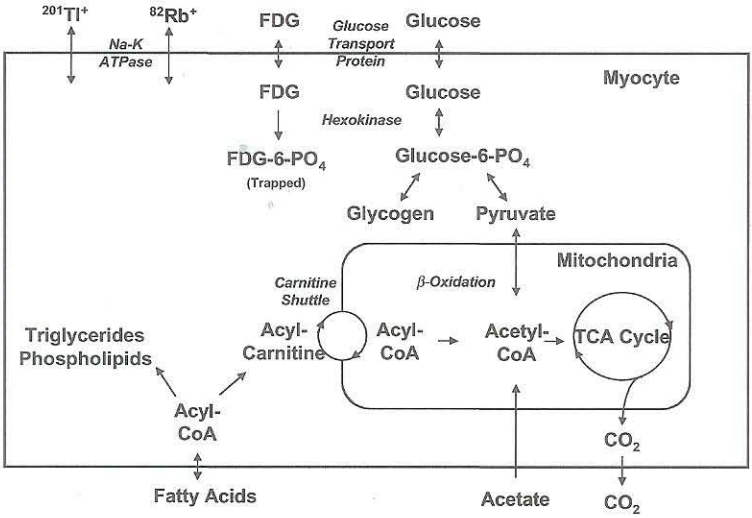

FIGURE 15-3 Metabolic processes occurring in the myocyte, illustrating the membrane uptake mechanisms for monovalent cations ($^{201}Tl^+$ and $^{82}Rb^+$) via Na-K ATPase and FDG and glucose via the glucose transporter. While glucose is metabolized completely, FDG is trapped as FDG-6-phosphate after enzymatic conversion by hexokinase. Fatty acids, as the preferred metabolic substrate for energy, can be converted into triglycerides or phospholipid stores or shunted via the carnitine shuttle into mitochondria for beta oxidation. (Reprinted with permission of W.B. Saunders from Schwaiger M, Hutchins GD. Evaluation of coronary artery disease with positron emission tomography. *Semin Nucl Med.* 1992;22:210-23.)

cardiac stress imaging is the ability to assess the difference in flow between well-perfused and poorly perfused myocardium. Early on, it was shown with ^{201}Tl-thallous chloride that imaging defects are detectable during induced hyperemia when flow into normal coronary vessels exceeds that into stenotic vessels by a ratio of 2.4 or greater.[9] The stressing methods used in nuclear medicine procedures are capable of achieving this blood flow differential.

Metabolism

Under resting conditions, the myocardium derives most of its energy from aerobic metabolism of fatty acids (Figure 15-3).[4] More than 95% of the energy liberated during metabolism is in the form of adenosine triphosphate (ATP). However, during hypoxia or ischemia, glucose becomes an important source of energy. This mechanism is less efficient, requiring tremendous amounts of blood glucose with the formation of large amounts of lactic acid in cardiac tissue.[4] Accumulation of lactate in tissue inhibits glycolysis, leading to a reduction in ATP. During coronary ischemia, ATP degrades to adenosine diphosphate (ADP), adenosine monophosphate (AMP), and adenosine. Adenosine readily diffuses through the cell membrane and is one of the principal substances that causes dilatation of the coronary arterioles during hypoxia. Its loss from the cell is much faster than its resupply under severe hypoxic conditions. Thus, within a short period of time after MI or cardiac arrest (around 30 minutes), myocardial cells begin to die.

Viability

Myocardial cells are considered to be nonviable when some basic aspect of cell behavior no longer functions.[10] When CAD is present, the progression of atherosclerosis causes

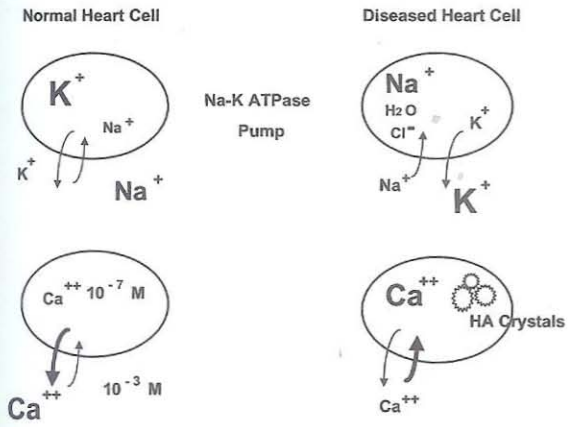

FIGURE 15-4 Sodium, potassium, and calcium ion transport between myocyte cytoplasm and interstitial fluid, demonstrating alterations in ion concentration in normal and necrotic cells.

arterial stenosis and a gradual loss of arterial compliance, resulting in a temporary reduction in blood flow and oxygen supply to meet demand (myocardial ischemia).[11] A principal symptom is chest pain upon exertion, believed to be caused by lactate accumulation. Other changes include electrical conduction abnormalities and loss of contractile function in the affected muscle. The loss of functional integrity in ischemic but viable myocardium can be reversed if blood flow is restored to the ischemic regions. However, when flow is not restored, insufficient oxygenation eventually causes the cells to die (MI).

Two primary cellular functions can be used to measure viability: membrane ion transport and intermediary metabolism.[10] Under normal circumstances the sodium–potassium (Na-K) ATPase membrane pump maintains cell function and volume through high extracellular sodium ion concentration and high intracellular potassium ion concentration (Figure 15-4).[4] It is believed that the energy available for the pump is decreased during ischemia, so that sodium ions along with chloride ions and water accumulate within the cell and potassium ions leak out into the extracellular space. This process decreases the intracellular–extracellular potassium ion concentration ratio and produces a marked effect on membrane polarity and heart muscle function. This disparity in ion shift is the basis for using potassium analogues such as $^{201}Tl^{+}$ and $^{82}Rb^{+}$ for imaging. These agents participate in the ion transport process in a manner similar to potassium and are able to assess membrane integrity and cellular viability.[10]

Several functions involved in intermediary metabolism can be exploited for assessing myocardial viability. They include glucose utilization measured by ^{18}F-FDG uptake, fatty acid metabolism measured by ^{11}C-palmitate uptake, and oxygen consumption measured by ^{11}C-acetate uptake.[11] Each of these agents has been used with PET, but the most useful is ^{18}F-FDG. ^{201}Tl as a membrane viability agent has been compared with ^{18}F-FDG as a metabolism marker. Both agents have been shown to be equivalent under the right conditions and correct protocol for assessing myocardial viability.[12]

PERFUSION IMAGING

Two conditions must exist for the measurement of coronary blood flow deficits: (1) coronary blood flow must be elevated to near maximum levels, and (2) a radiotracer whose myocardial extraction is proportional to coronary artery blood flow must be used. The key aspect of perfusion imaging is the induction of a disparity of flow between well-perfused and poorly perfused myocardium. Under these circumstances, radiotracer uptake is increased in normally perfused regions of the heart, whereas regions supplied by stenosed arteries demonstrate decreased uptake of radiotracer (Figure 15-5). The current

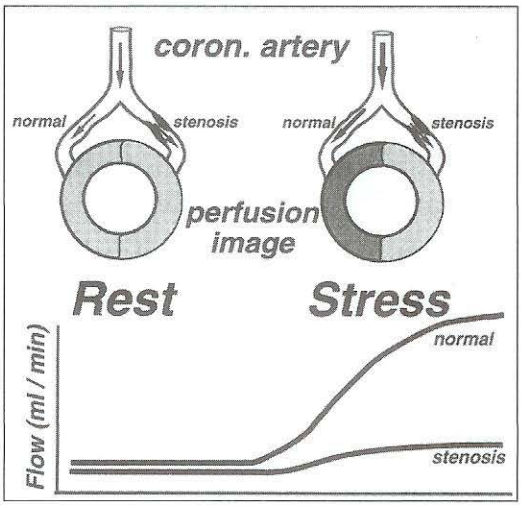

FIGURE 15-5 Schematic representation of the principle of rest–stress myocardial perfusion imaging. Top: Rest and stress diagrams of two branches of a coronary artery, one normal (left) and one stenotic (right). Middle: Myocardial perfusion images of the territories supplied by the two branches. Bottom: Coronary blood flow in the branches at rest and during stress. At rest, myocardial blood flow is equal in both coronary artery branches. When a myocardial radiotracer is injected at rest, uptake is homogeneous (normal image). During stress, coronary blood flow increases 2.0 to 2.5 times in the normal branch, but not to the same extent in the stenosed branch, resulting in heterogeneous distribution of blood flow. This heterogeneity of blood flow can be visualized with ^{201}Tl-thallous chloride, ^{99m}Tc-sestamibi, or ^{99m}Tc-tetrofosmin as an area with decreased uptake (abnormal image with a myocardial perfusion defect). (Adapted from reference 17 and used with permission of the Society of Nuclear Medicine.)

methods used to achieve maximal coronary dilatation are intense exercise and administration of pharmacologic agents that increase blood flow through either coronary vasodilatation or increased cardiac output.

Exercise Stress

Exercise is a natural method of stress that increases cardiac work and metabolic demand on the heart. When challenged by an increased physical workload, segments of the myocardium perfused by stenotic arteries are likely to become ischemic because of inadequate blood flow to meet oxygen demand. Ischemic cells lose their ability to retain ion-transport radiotracers (e.g., $^{201}Tl^{+}$) because of altered membrane integrity. Therefore, ischemia is readily detected after exercise as less tracer is localized in these regions because of reduced tracer delivery (low blood flow) and reduced tracer extraction (leaky cells).

In general, treadmill exercise is used with a modified Bruce protocol. In this method, speed and grade of the treadmill are increased in a stepwise manner to achieve the required workload on the heart.[13] End points that have been used for achieving adequate levels of cardiac stress are 85% of an age-related maximal predicted heart rate determined by the formula 220 minus the patient's age in years and a pressure–rate product (systolic blood pressure times heart rate) of 25,000 or higher. Heart rate[14] and the pressure–rate product[15] have been shown to increase linearly with workload, and coronary blood flow is closely related to the pressure–rate product.[16] In general, exercise stress under this protocol increases blood flow to about 2 times the resting flow, which is adequate for diagnostic evaluation. Exercise stress provides important prognostic information. Experience has shown that patients with CAD have a better survival rate if they can exercise longer than stage IV of the Bruce protocol (at least 12 minutes), achieve a heart rate higher than 160 beats per minute (bpm) at peak exercise, and show no ST-segment depression on the exercise electrocardiogram (ECG).[17]

A maximal increase in coronary blood flow after exercise is often difficult to achieve clinically, because many patients suspected of having heart disease cannot exercise at the intense level required to produce maximal coronary dilatation. Furthermore, exercise cannot be used in some patients because of claudication, cerebrovascular accidents, arthritis, amputation, severe anxiety, or current use of β-blocking medications.

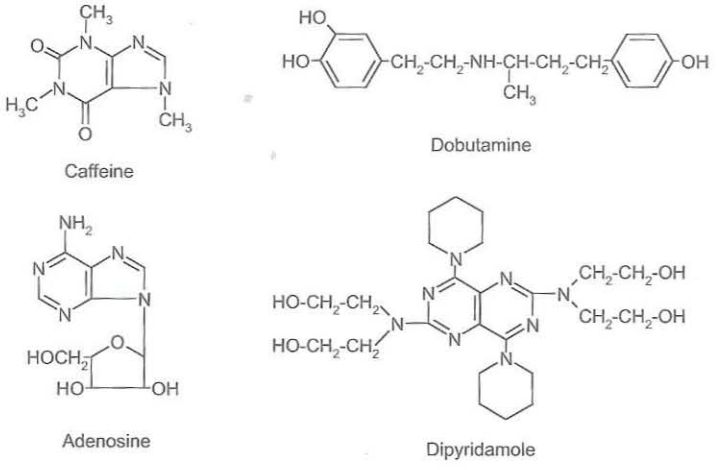

FIGURE 15-6 Chemical structures of caffeine and the pharmacologic interventional agents adenosine, dipyridamole, and dobutamine.

Pharmacologic Stress

An alternative to exercise stress is pharmacologic stress with agents such as dipyridamole, adenosine, or dobutamine (Figure 15-6).[18–23] Dipyridamole and adenosine are coronary vasodilators. After administration of either of these agents, normal vessels dilate maximally, but stenosed, noncompliant vessels fail to dilate sufficiently, creating a perfusion deficit. Hence, a heterogeneity of blood flow to the heart is created relative to the severity of CAD. True ischemia may develop with these agents but is not necessary to produce the disparity in flow. Maximal coronary dilatation is more consistently achieved with these agents than with exercise.

Dobutamine is a predominant β_1-agonist, increasing heart rate and myocardial contractility and systolic blood pressure.[23] Consequently, dobutamine increases myocardial oxygen demand, being more akin to exercise. Normal coronary arteries dilate to increase perfusion in order to meet the demand, while stenotic arteries may not be able to increase flow to the same degree as normal vessels, creating a perfusion deficit as in exercise stress.

Adenosine

Adenosine is an endogenous nucleoside present in all cells of the body, including the myocardium. It is produced by enzymatic dephosphorylation of ATP by 5′ nucleotidase (Figure 15-7). Interstitial concentrations of adenosine rise in response to increased metabolic oxygen requirements or ischemia in the heart.[24] Adenosine readily diffuses into the interstitial space, where it causes vasodilation by activating the adenosine type 2 (A_2) receptors on coronary endothelial cells and by increasing intracellular cAMP. Its half-life is very short, reported to be between 4 and 10 seconds.[25,26]

Adenosine's stimulatory effect on A_2-receptors is blocked by methylxanthine compounds such as caffeine, theophylline, and aminophylline.[27] Thus, food or beverages containing caffeine and methylxanthine medications must be discontinued for at least 12 hours before adenosine administration. Because of potentiation, patients taking oral dipyridamole should discontinue this medication for 12 hours before adenosine stress testing.[19]

Adenosine also activates A_1-receptors on myocardial cells, causing a slowing of electrical conduction through the atrioventricular node, potentially causing first-, second-, and

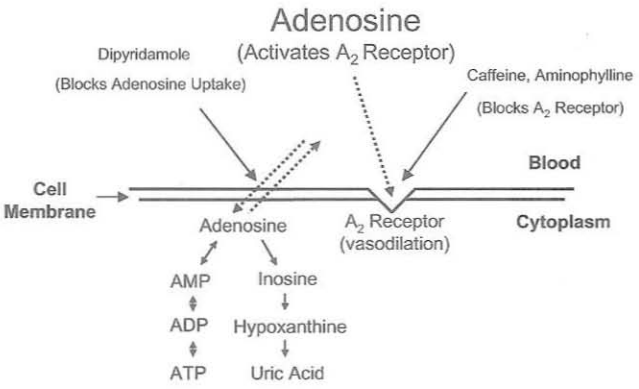

FIGURE 15-7 Mechanisms of adenosine production and interaction in tissues. Adenosine is produced by myocytes and other cells upon demand by dephosphorylation of ATP. Adenosine causes vasodilatation by activation of A_2 receptors on vascular endothelial cells. Receptor activation is blocked by methylxanthine compounds such as caffeine and aminophylline. Adenosine is rapidly absorbed into cells, where it is converted back to ATP or metabolized to uric acid. This reuptake mechanism is blocked by dipyridamole.

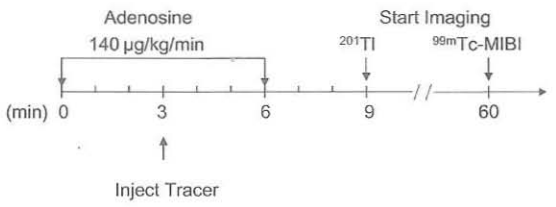

FIGURE 15-8 Adenosine dosing, radiotracer injection, and imaging protocol during pharmacologic stress imaging.

third-degree heart block. Thus, the use of adenosine (and dipyridamole) in patients with these conditions should be approached with caution and may be contraindicated.[28] Adenosine has been shown to cause bronchospasm in asthmatic patients, and both it and dipyridamole are contraindicated in these patients.[29,30]

For cardiac imaging, adenosine is administered at a standard dosage of 0.140 mg/kg per minute for 6 minutes to achieve maximal coronary vasodilation (Figure 15-8). Radiotracer is injected at 3 minutes, when vasodilation is maximal. Adenosine infusion is continued for 3 additional minutes to facilitate tracer uptake and localization in the myocardium under the stress condition. Upon cessation of adenosine infusion, imaging can begin within a few minutes with ^{201}Tl-thallous chloride, or at later times (30 to 60 minutes) with ^{99m}Tc-sestamibi or ^{99m}Tc-tetrofosmin to allow for hepatobiliary clearance of these agents.[31] Thallium imaging must commence and be completed before significant redistribution occurs, whereas the technetium agents are more firmly fixed in the heart and imaging can begin once background activity clears. With the standard dosage of adenosine, 84% of normal patients achieve an average coronary vasodilation equal to 4.4 times the resting coronary blood flow.[24] The average time from onset of infusion until maximal vasodilation is 84 ± 46 seconds. The time from cessation of infusion until coronary blood flow velocity returns to baseline levels is 145 ± 67 seconds. In normal patients the heart rate rises 24 ± 14 beats/minute, and mean arterial pressure falls 6 ± 7 mm Hg.[24]

Dipyridamole

Dipyridamole increases plasma adenosine levels indirectly by inhibiting adenosine's metabolism by adenosine deaminase and phosphodiesterase. The standard dosage of dipyridamole is 0.56 mg/kg administered over 4 minutes. Because its action is indirect, dipyridamole achieves a maximum dilator effect 6 to 8 minutes after the start of infusion, indicated by a drop in blood pressure and a rise in heart rate.[32] It increases coronary blood

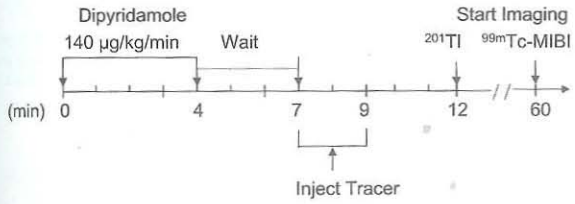

FIGURE 15-9 Dipyridamole dosing, radiotracer injection, and imaging protocol during pharmacologic stress imaging.

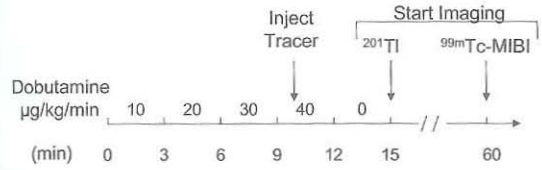

FIGURE 15-10 Dobutamine dosing, radiotracer injection, and imaging protocol during pharmacologic stress imaging.

flow about 4 times baseline, similar to adenosine. Radiotracer should be injected at the time of maximal effect, approximately 7 minutes from the start of the infusion (Figure 15-9). Imaging is begun with ^{201}Tl-thallous chloride at about 12 to 15 minutes from the start of infusion and at later times (60 minutes) with ^{99m}Tc-sestamibi or ^{99m}Tc-tetrofosmin. The plasma half-life of dipyridamole is about 30 minutes.[29] Therefore, patients must be monitored for at least 20 minutes after the test because ischemia may be provoked.[18] Some institutions routinely administer 50 to 100 mg of aminophylline intravenously 5 minutes after tracer injection to reduce the occurrence of adverse effects. If a patient complains of shortness of breath or wheezes, dipyridamole administration should be halted and aminophylline administered immediately.[18]

Splanchnic uptake of radiotracer (more with ^{99m}Tc agents than with ^{201}Tl) is greater with dipyridamole stress than with exercise stress. When dipyridamole stress is used, mild hand-grip exercises or walking, to stimulate the release of catecholamines, helps reduce blood flow and activity accumulation in the splanchnic area.[18]

Dobutamine

Principally a β_1-agonist, dobutamine causes a combined increased inotropic and chronotropic effect on the myocardium, thereby increasing contractility and oxygen demand and causing coronary vasodilation. A general imaging protocol is to administer the dosage slowly, ramping up in 10 µg/kg per minute steps every 3 minutes for 12 minutes to a maximal dose of 40 µg/kg per minute (Figure 15-10).[23] Radiotracer is injected 1 minute after the highest dose is begun (10 minutes from start of infusion), and dobutamine infusion is continued for 2 minutes more while tracer is localizing in the myocardium. If heart rate is less than 85% of the predicted rate after the maximal dose of dobutamine, intravenous atropine 0.2 to 1 mg may be administered.[33] Imaging with ^{201}Tl is begun at about 3 minutes from cessation of infusion, while imaging with ^{99m}Tc agents is begun in 60 minutes. The plasma half-life of dobutamine is 2 minutes.

Dobutamine should not be mixed in solutions containing sodium bicarbonate, sodium bisulfite, or ethanol. It is typically diluted with 0.9% sodium chloride injection. Dilutions should be used within 24 hours.

Precautions, Adverse Effects, and Contraindications

Adenosine, dipyridamole, and dobutamine are potent pharmacologic agents that should be administered with caution and with full awareness of their adverse effects and potential

TABLE 15-2 Contraindications for Use of Pharmacologic Agents in Stress Testing

Contraindication	Dipyridamole	Adenosine	Dobutamine
Unstable angina or resting ischemia	x	x	x
Poor LV function (EF <15%)	x	x	x
Hypertension (>200 mm Hg systolic)		x	x
Hypotension (<90 mm Hg systolic)	x	x	
Severe aortic stenosis			x
History of asthma	x	x	
Active bronchospastic disease	x	x	
History of tachyarrhythmias			x
Second-degree AV block		x	
Oral dipyridamole		x	
Xanthine compounds	x	x	
Atrial fibrillation with rapid ventricular response			x

Reprinted with permission from Blust JS, Boyce TM, Moore WH. Pharmacologic cardiac intervention: comparison of adenosine, dipyridamole, and dobutamine. *J Nucl Med Technol.* 1992;20:53-61.

TABLE 15-3 Percentages of Patients Experiencing Adverse Effects of Pharmacologic Agents Used in Stress Testing

Effect	Adenosine	Dipyridamole	Dobutamine
Flushing	36.5	3.4	14
Dyspnea	35.2	2.6	14
Chest pain	34.6	19.7	31
Gastrointestinal	14.6	5.6	–
Headache	14.2	12.2	14
Dizziness	8.5	11.8	4
Palpitation	–	–	29

Sources: References 35, 33, and 36 for adenosine, dipyridamole, and dobutamine, respectively.

toxicities. Blood pressure, heart rate, and a 12-lead ECG should be monitored continuously. An electronic infusion pump should be used to administer these agents to provide precise control of the dosage.[34] Contraindications for these agents are summarized in Table 15-2.

The relative merits of adenosine and dipyridamole have been compared[35] and their adverse effects have been reported.[36–38] The most common adverse effects of dipyridamole and adenosine are chest pain, headache, dizziness, flushing, dyspnea, ST-T changes on ECG, and ventricular extrasystoles. Other effects occurring less frequently include nausea, hypotension, and tachycardia (Table 15-3). These effects are related to the plasma level of vasodilator and can be readily reversed, in the case of dipyridamole by giving intravenous aminophylline (50 to 100 mg), or for adenosine by simply stopping the infusion, because of its short plasma half-life. Patients who receive aminophylline should be monitored for drug-induced ischemia before being released from the nuclear medicine department. These agents should be used with caution in patients with heart block, and both agents are contraindicated in asthma and chronic obstructive pulmonary disease.

The distribution of cardiac output to various organs is different with adenosine and dipyridamole than with exercise stress.[3] The relative blood flow to abdominal viscera increases with these agents, whereas with exercise it decreases. Thus, perfusion imaging agents, particularly ^{99m}Tc-sestamibi and ^{99m}Tc-tetrofosmin, tend to accumulate in the liver and spleen area to a greater extent with adenosine and dipyridamole than with exercise.

This visceral activity may interfere with assessing perfusion of the inferior wall of the left ventricle.[3] Additionally, adenosine and dipyridamole do not work effectively if patients have taken caffeine or other methylxanthine substances (as noted above); these substances are contraindicated for vasodilator studies.

Dobutamine is not affected by caffeine or methylxanthine drugs and is an alternative agent if adenosine or dipyridamole is contraindicated. The principal adverse effects of dobutamine are chest pain, palpitation, headache, flushing, and dyspnea (Table 15-3).[39] These effects should readily abate with cessation of the infusion. However, the β_1-blocking agent esmolol should be available in case problems arise; its recommended loading dose is 0.5 mg/kg per minute for 1 minute followed by 0.05 mg/kg per minute for 4 minutes as a maintenance dose. Dobutamine is contraindicated for the same conditions that apply to exercise stress.

Myocardial Extraction and Retention

The principal uptake mechanisms of perfusion tracers are active transport via the Na-K ATPase pump by monovalent cations and passive diffusion of lipophilic compounds. Key requirements for a useful myocardial perfusion tracer are high extraction efficiency proportional to blood flow over the range of flows seen clinically and heart retention long enough to conduct imaging studies. Myocardial extraction versus flow has been measured for several perfusion tracers.[40–42] Ideally, when the radiotracer's extraction fraction is 1.0, (i.e., 100% at any rate of flow), regional differences in myocardial tracer concentration depend solely on regional blood flow. Only labeled microspheres exhibit this property, having 100% first-pass extraction at any flow rate. Most diffusible tracers used clinically have extraction fractions less than 1.0 at resting flow, declining further as blood flow increases. This decline in extraction at normal flows occurs because radiotracer that is not fixed in the myocardium back-diffuses and washes away. As blood flow increases, capillary recruitment occurs, increasing the surface area for exchange between the blood and interstitial space and making more tracer available for extraction (i.e., an increase in the capillary permeability surface area product occurs). However, permeability, or the rate of tracer flux through the capillary membrane, is independent of surface area. Thus, while more tracer is made available for exchange at higher flows and more tracer is taken up into the heart, the fraction of total tracer extracted declines because the time available for tracer exchange at the capillary surface is shortened. Thus, tracer uptake becomes diffusion-limited at higher flows (Figure 15-11).[41–44]

Once a radiotracer is localized it must remain fixed for the period of time required for imaging; if it does not, a correction must be made for back-diffusion of tracer. For example, imaging with ^{201}Tl-thallous chloride must be completed within 45 minutes after injection because of its redistribution over time. ^{99m}Tc-teboroxime required completion of imaging within 10 to 15 minutes of injection because of its rapid back-diffusion; this agent is no longer marketed. ^{99m}Tc-sestamibi and ^{99m}Tc-tetrofosmin have relatively long myocardial retention, which is an advantage if repeat imaging is required.

Uptake of activity by the myocardium is a function of tracer delivery and extraction. Retention of activity is a function of tracer back-diffusion and binding to myocytes. Each of these processes can be affected by disease. The mechanism of localization of perfusion imaging agents differs. Thallium is taken up by active transport via the membrane pump, similar to potassium, but is retained longer than potassium. Thallium is not bound to myocytes, however, and eventually diffuses back out of these cells in proportion to blood flow.[45] ^{99m}Tc-sestamibi, as a lipophilic monovalent cation, is taken up into myocytes by passive diffusion associated with negative plasma and mitochondrial membrane potentials. Sestamibi retention is dependent on maintenance of these membrane potentials.[46]

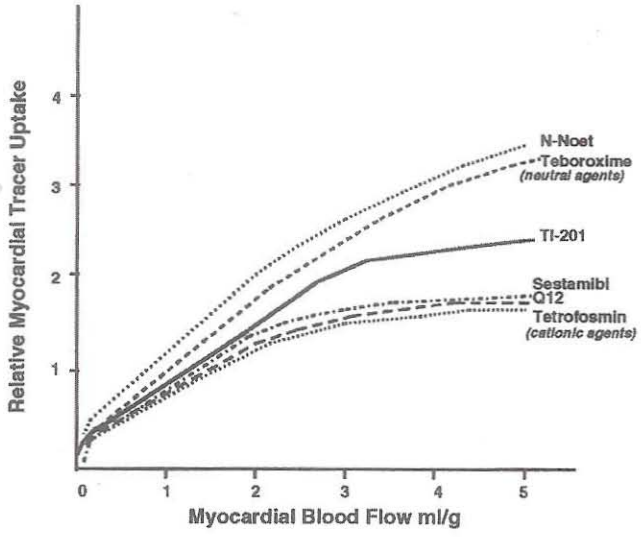

FIGURE 15-11 Relationship between myocardial blood flow and uptake of various perfusion tracers. (Reprinted with permission of W.B. Saunders from reference 85.)

TABLE 15-4 Properties of Monovalent Cations for Myocardial Perfusion Imaging

	Nuclide Property				Myocardial Property				
Radionuclide	Decay Mode	$T_{½}$ (hr)	keV	Ionic Radius (Å)	Blood Clearance $T_{½}$ (min)	Extraction (%)	Uptake (% injected dose)	Uptake Plateau (min)	Clearance $T_{½}$ (hr)
^{43}K	β^-	22.4	373, 619	1.38	2.0	71	2–3	10–20	1
^{129}Cs	EC	32.1	375, 412	1.70	9.0	22	1–2	60–120	5
^{81}Rb	EC, β^+	4.7	511, 190	1.49	2.2	70	2–3	15–45	6
^{201}Tl	EC	73	69, 80	1.50	2.9	88	4–5	5–15	4.4

Source: Reference 48.

^{99m}Tc-teboroxime, although no longer marketed, is a neutral, lipophilic tracer that diffuses rapidly across phospholipid membranes. It is not known if the compound enters the myocardial cell or is incorporated into the phospholipid layers of the membrane.[47] It rapidly back-diffuses from the heart and is not bound.

SPECT Perfusion Imaging Agents

MPI agents are otherwise known as "cold spot" markers because they demonstrate decreased accumulation of activity in poorly perfused regions of myocardium. Historically, several radioisotopes of potassium and its monovalent cation analogues have been investigated for myocardial perfusion studies.[48] Table 15-4 compares the properties of these agents. ^{43}K had the disadvantages of beta particle decay and high photon energy that degraded image resolution. Of the potassium analogues, ^{129}Cs was not ideal because of slow blood clearance and poor myocardial extraction. ^{81}Rb had good blood clearance and myocardial extraction but presented technical and logistical problems for nuclear medicine laboratories without PET capability. ^{201}Tl gained clinical acceptance because it has rapid blood clearance, high myocardial extraction, and a reasonable shelf life. However, its low-energy photons produce poor quality images compared with ^{99m}Tc agents, and its long retention time in the body limits the amount of activity that can be administered safely.

The limitations of ^{201}Tl led to the development of ^{99m}Tc-labeled complexes that would allow administration of larger amounts of activity with improved image quality and lower radiation dose. This began with the development of several cationic complexes of Tc(III), namely, *trans*-[^{99m}Tc(DIARS)$_2$X$_2$]$^+$, where DIARS represents the *o*-phenylenebis(dimethylarsine) ligand and the X represents chloride or bromide.[49] The high lipophilicity of the DIARS complex led to the less lipophilic *trans*-[^{99m}Tc(DMPE)$_2$Cl$_2$]$^+$ complex, where DMPE represents the 1,2-bis(dimethylphosphino)ethane ligand. Studies of the DMPE complex in dogs and humans showed that although the complex could image the human myocardium, intense liver uptake obscured the cardiac apex, and heart-to-liver ratios in humans were much less than in dogs. Thus, heart images obtained with the DMPE complex were inferior to those with thallium. In 1982, Jones et al.[50] prepared the hexakis(isonitrile) Tc(I) complex [^{99m}Tc(CNR)$_6$]$^+$, where R could be one of several alkyl groups, the most successful being 2-methoxy isobutyl. This Tc(I) complex, ^{99m}Tc-sestamibi, was easy to prepare, was stable, and achieved myocardial uptake proportional to blood flow when compared with thallium.[51] In 1989, ^{99m}Tc-teboroxime was developed.[52] It is a complex of Tc(III) known as a boronic acid adduct of technetium dioxime (BATO). The complex is neutral and lipophilic, with very high extraction by the myocardium proportional to blood flow. Subsequently, ^{99m}Tc-tetrofosmin was developed. It is a phosphine complex of Tc(V) that exhibits biologic properties similar to those of ^{99m}Tc-sestamibi.[53,54]

The sestamibi and tetrofosmin agents were shown to be comparable to ^{201}Tl-thallous chloride in MPI, but their heart activity was fixed and did not redistribute readily as did thallium. ^{99m}Tc-teboroxime was also shown to be comparable to ^{201}Tl-thallous chloride, but its heart uptake and washout were very rapid. Thus, while a thallium stress–rest imaging protocol can be accomplished with one dose of thallium because of its redistribution in the myocardium, two separate doses of the technetium agents must be administered, one during stress and one during rest, because these agents are bound and do not redistribute.

Thallous Chloride Tl 201 Injection

Thallium is a potassium analogue that localizes in the heart in proportion to myocardial blood flow. After intravenous administration of ^{201}Tl-thallous chloride, thallium disappears rapidly from the blood, with only 5% to 8% remaining in the blood 5 minutes after injection.[55] In the resting state, 90% of the plasma activity disappears in 20 minutes, but under stress the same percentage of activity disappears within 1.5 minutes. Maximum myocardial uptake occurs in 10 to 30 minutes in the resting state and within 5 minutes after exercise stress. In humans, approximately 4% of the injected dose (ID) is localized in the heart. Thallium heart activity is sustained long enough after exercise stress that imaging can be performed; however, imaging should be completed by 30 minutes after injection because by this time thallium begins to redistribute, being released from the heart at the same rate that it is lost from the blood.[45] Under experimental conditions after intracoronary injection of ^{201}Tl-thallous chloride in the presence of very low levels of ^{201}Tl activity in the blood, the half-life of heart release was found to be rapid (about 90 minutes).[45] The half-life from the heart after intravenous injection in clinical studies was found to be much slower (4.5 to 8 hours) because of equilibration of heart activity with ^{201}Tl activity in the blood pool and other organs.

Thallium's myocardial uptake measured in dogs at resting blood flow was found to be 0.0385% of the ID per gram, rising to 0.0614% after dipyridamole administration.[56] The fact that the increased uptake with dipyridamole was only 60% higher when blood flow increased to 3 to 4 times normal indicates a nonlinear extraction of ^{201}Tl with increased blood flow. Linearity of extraction of thallium with flow begins to fall off when blood flow is 2 to 2.5 times normal, which is about the level at which flow increases with exercise

stress.[56] A similar nonlinear relationship was shown with adenosine treatment.[57] This study in dogs also demonstrated that the extraction fraction of thallium under normal coronary blood flow was 88% but that it fell linearly with increased flow after vasodilation. The authors suggested that the drop in extraction fraction occurred because coronary flow was in excess of myocardial demand.

Total body elimination of thallium is slow, with a biologic half-life of 10 days.[55] Only 5% is excreted in the urine by 24 hours, and insignificant fecal excretion occurs. These factors plus the long physical half-life (73 hours) are undesirable properties of ^{201}Tl and contribute to its high radiation absorbed dose. The critical organs are the thyroid (2.3 rad[cGy]/mCi) and the testes (3 rad[cGy]/mCi), and the effective dose is 1.3 rem(cSv)/mCi.

After transcapillary diffusion from blood into the interstitial space, thallium is taken up into myocytes by the membrane-bound Na-K ATPase pump. Factors cited for the similarity of action between K^+ and its biologic analogues are a monovalent cationic charge and similar hydrated ionic radii. Cation uptake by the membrane pump is known to be partially inhibited by ouabain and hypoxia.[57–59] While there is a close relationship between thallium uptake and blood flow, adequate tissue oxygenation to support cellular metabolism is also required for uptake.[60] Figure 15-4 illustrates sodium and potassium ion transport in myocardial cells. There are high intracellular potassium and high extracellular sodium ion concentrations in normal cells, and conditions are reversed when cells are damaged. A significant reduction in blood flow and an oxygen deficit leading to necrosis impair this function. Since uptake of thallium depends on adequate blood flow for delivery to the myocardium and active transport across an intact sarcolemma, thallium is well suited as a marker of viability.

Chronology of Thallium Use

Thallium has been used as a marker of myocardial perfusion and viability for many years, beginning in the mid 1970s.[61] The first thallium procedures were conducted with two separate injections: one for the exercise stress study and one for the rest study. The rest study was conducted 1 to 2 weeks after the stress study because of thallium's long effective half-life in the body. The thallium procedure changed to a 1 day protocol when it was observed that thallium redistributed in the heart over time. By 3 to 4 hours after an exercise study, normal myocardial regions demonstrated a decrease in thallium activity while ischemic regions increased in activity.[62] Subsequently, the standard procedure became a 1 day thallium protocol (exercise study followed by a 3 to 4 hour redistribution study) to differentiate ischemia from infarction. This procedure was shown to provide an accurate assessment of myocardial viability when perfusion defects on the exercise study showed redistribution on delayed imaging.

Although this procedure had high sensitivity for predicting viability of reversible defects, its specificity for predicting nonviability of irreversible defects was low. This became apparent when the size of irreversible defects decreased in a number of patients who had a resting thallium study the next day.[63,64] This indicated that incomplete redistribution of thallium had occurred on the initial redistribution image, causing an overestimation of infarct size at that time. Henceforth, late (8 to 24 hour) redistribution imaging was instituted to allow more time for thallium to redistribute.[65] Kiat et al. demonstrated that 61% of irreversible thallium defects on 3 to 4 hour images reversed on late redistribution at 18 to 72 hours.[66] Late redistribution imaging improved diagnosis, but study specificity was still low. This study also demonstrated that a high percentage of patients (37%) with apparent irreversible defects had perfusion restored after myocardial revascularization

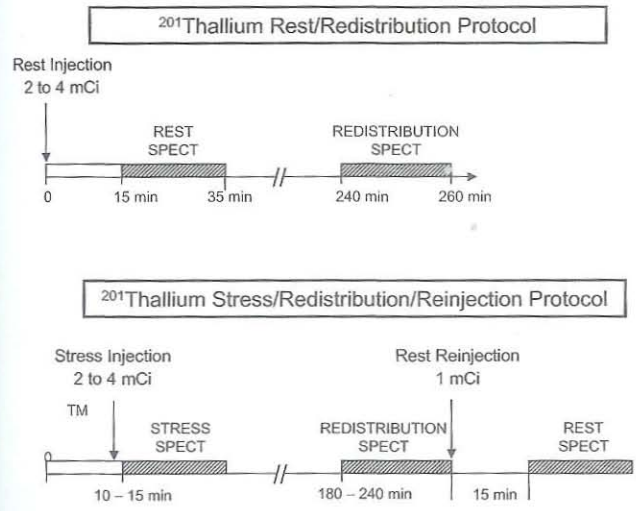

FIGURE 15-12 Thallium rest–redistribution imaging protocol and stress–redistribution–reinjection imaging protocol.

procedures. Thus, although late imaging improved diagnosis, it still overestimated the frequency and severity of myocardial fibrosis.[66]

To improve specificity, a thallium reinjection technique was introduced to increase plasma levels of thallium during the redistribution phase of the study. Reinjection of 1 mCi (37 MBq) of ^{201}Tl-thallous chloride, either after the standard 3 to 4 hour redistribution study or after a late 24 hour redistribution study, facilitates uptake of thallium into many viable regions of myocardium with apparently irreversible defects. With this technique, up to 49% of apparent irreversible defects on the 4 hour redistribution study[67] and 39% of such defects on the 24 hour redistribution study[68] were shown to have improved or normal uptake after thallium reinjection. A number of studies have also shown the ability of thallium reinjection to predict improved ventricular function after revascularization.[67,69–71] Thus, the thallium stress–redistribution–reinjection protocol has become a standard procedure for evaluating myocardial perfusion and viability.

A routine perfusion study with thallium is conducted in two parts. One of two protocols is typically used, depending on the information required (Figure 15-12). If only viability information is sought in a patient with known CAD and left ventricular dysfunction, a rest–redistribution protocol utilizing a quantitative method of reversibility assessment is preferred. If inducible ischemia and viability is the goal, a stress–redistribution–reinjection protocol is preferred for assessment of the extent and severity of myocardial ischemia.

In the rest–redistribution protocol, the thallium dose is injected into a patient who has fasted for at least 4 hours. Imaging is begun in 15 to 20 minutes and proceeds for about 20 minutes. Perfusion deficits seen on the resting study that reverse on the 4 hour redistribution study may result from clearance of ^{201}Tl from normal regions and accumulation of ^{201}Tl in the defect region during the redistribution time. Reversibility of perfusion deficits indicates viable myocardium.

The first part of the stress–redistribution–reinjection protocol is designed to produce near maximal dilatation of the coronary vessels just before administration of a 2 to 4 mCi (74 to 148 MBq) thallium dose. Dilatation is achieved through either exercise or administration of a pharmacologic agent (dipyridamole, adenosine, or dobutamine). Exercise stress should continue for 30 to 60 seconds after tracer injection to ensure heart uptake. Imaging should commence as soon as possible after tracer injection and by no later than 15 minutes. With pharmacologic stress, tracer injection and the start of imaging should follow the protocols given in Figures 15-8 through 15-10. Under these conditions, thallium ion is

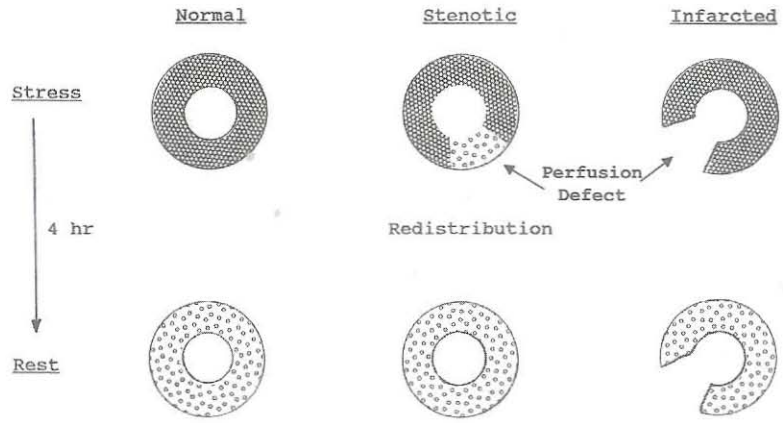

FIGURE 15-13 Model of the left ventricle (short-axis view) during stress and at rest after 4 hour redistribution of ^{201}Tl in normal, stenotic, and infarcted heart. During stress, heart activity is at high count density in normal well-perfused myocardium, at less density in stenotic regions that are poorly perfused, and absent in infarcted regions that are scarred. At rest (redistribution), normal myocardium washes out thallium more quickly than stenotic regions, with the appearance of "filling in" the stress defect in stenotic areas. A persistent defect remains in areas of infarct.

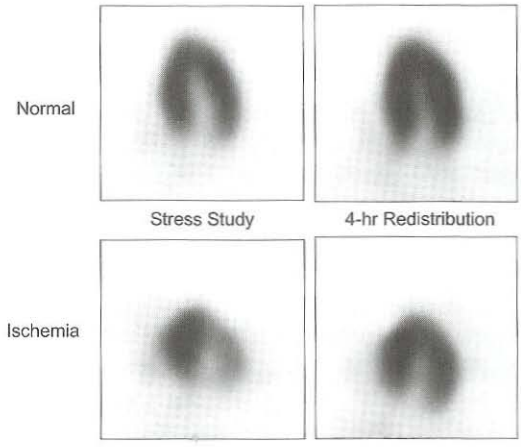

FIGURE 15-14 Adenosine stress and rest redistribution study after injection of 3 mCi ^{201}Tl-thallous chloride. Horizontal long-axis views demonstrate normal perfusion evidenced by uniform uptake of activity throughout the left ventricle during stress and rest. Ischemia is indicated by reduced perfusion and uptake of activity in the lateral ventricular wall during the stress image that fills in at the 4 hour rest redistribution image.

extracted by the myocardium in proportion to regional blood flow. Normally perfused myocardium takes up the radiotracer well, whereas poorly perfused (ischemic) or nonperfused (infarcted) myocardium shows decreased or absent radiotracer uptake, which appears as a perfusion defect (Figure 15-13). After a 3 to 4 hour period of rest, the redistribution study is performed. At this time, the heart is imaged again to assess myocardial redistribution of the ^{201}Tl activity administered during the stress study. During the rest phase, ^{201}Tl ion redistributes in the myocardium, washing out of normally perfused myocardium well, but less well from areas of compromised flow during the stress. Thus, the redistribution image of the heart demonstrates "filling-in" of activity (reversibility) in ischemic areas (Figure 15-14). When a stress perfusion defect does not reverse, thallium reinjection is used to improve specificity of the study. The heart is reimaged 15 minutes after the reinjection. The reinjection study can also be done the next day. Lack of reversibility on the reinjection image indicates MI.

^{99m}Tc-sestamibi is extracted by the myocardium in proportion to blood flow up to 2.5 mL/minute per gram, or approximately 3 times resting flow.[72] In canine myocardium at rest, its extraction fraction is about 65%, but above resting flow it decreases.[72] In comparison, the extraction of ^{201}Tl was 82% in the same canine model. In a rabbit perfused heart model, ^{201}Tl also shows higher extraction than ^{99m}Tc-sestamibi.[44] The higher extraction of thallium relative to ^{99m}Tc-sestamibi is due to higher transcapillary exchange (i.e., the plasma-to-interstitial space transport of thallium is greater). However, ^{99m}Tc-sestamibi has a higher parenchymal cell permeability and volume of distribution, contributing to a slower cellular washout compared with thallium.[44]

Myocardial uptake studies indicate that ^{99m}Tc-sestamibi enters the myocardium by passive diffusion because of its lipophilicity and is retained for a prolonged period of time. Uptake is related to the integrity of the plasma and mitochondrial membrane potentials in myocytes.[73] Subcellular distribution studies in rat heart demonstrate that approximately 90% of ^{99m}Tc-sestamibi is associated with mitochondria in an energy-dependent manner as a free cationic complex.[74] The attraction of ^{99m}Tc-sestamibi to mitochondria is promoted by a negative potential generated in the mitochondrial membrane of viable myocytes, implying that ^{99m}Tc-sestamibi is a marker of myocardial viability and perfusion.[74] Other studies show that the uptake of ^{99m}Tc-sestamibi by the heart is not affected by ouabain and thus it is not extracted by the Na-K ATPase membrane pump.[58] Therefore, sestamibi is not a potassium analogue.

In humans, the mean heart retention of ^{99m}Tc-sestamibi is 1% ± 0.4% of the ID 60 minutes after intravenous injection at rest and 1.4 ± 0.3% after exercise.[51] The activity that is fixed in the myocardium demonstrates insignificant redistribution.[75–77] After intravenous injection, over 90% of ^{99m}Tc-sestamibi clears from the blood in less than 5 minutes. Blood levels immediately after injection with ^{99m}Tc-sestamibi are higher than those after injection with ^{201}Tl-thallous chloride, presumably because of lower extraction, whereas late blood levels are lower, presumably because of lack of redistribution.[51] ^{99m}Tc-sestamibi is excreted intact principally by the kidneys and the hepatobiliary system. By 24 hours, urinary excretion is 30% and 24% of the ID after rest and exercise studies, respectively. By 48 hours, fecal excretion is 37% at rest and 29% after exercise.[51] This difference in fecal excretion via the hepatobiliary system is due to reduced splanchnic blood flow and lower liver uptake during exercise. The highest activity is achieved in gallbladder and liver, followed by the heart, spleen, and lungs. However, activity in the liver, lungs, and spleen decreases more rapidly with time than heart activity and more so with exercise studies than at rest. The biologic half-life from the heart is 6 hours and from the liver 0.5 hours after rest or exercise.[78] Thus, the heart-to-liver ratios at 30, 60, and 120 minutes are 0.5, 0.6, and 1.1, respectively, after rest injection and 1.4, 1.89, and 2.3 after exercise injection. Rest imaging thus is best begun 60 minutes or more after injection of ^{99m}Tc-sestamibi; however, some practitioners shorten the dose-to-image time to 15 to 30 minutes for SPECT exercise studies because of higher heart-to-liver ratios. Dose-to-image time should be 45 to 60 minutes if adenosine or dipyridamole stress is used to allow more time for splanchnic activity to clear.

The critical organ after rest injection is the upper large intestinal wall (3.7 rad[cGy]/20 mCi), and the effective dose is 1.11 rad(cGy)/20 mCi.[79]

Imaging is typically begun 60 minutes after rest injection and 30 minutes after exercise injection. Because ^{99m}Tc-sestamibi does not redistribute appreciably, separate rest and stress injections are required to differentiate myocardial ischemia from scar. The study can be performed as a 2 day or a 1 day protocol. There is no significant difference in diagnostic accuracy between these protocols.[31,80] With the 2 day protocol, the patient is stressed, injected with 20 to 25 mCi (740 to 925 MBq), and imaged. The rest study is performed the next day with a similar dosage. This protocol has appeal for a patient whose pretest likelihood of CAD is low, because the rest study can be canceled if the stress study is

TABLE 15-5 Comparison of ^{201}Tl and ^{99m}Tc for Myocardial Perfusion Imaging

Property	^{201}Tl	^{99m}Tc
Photon energy	69–80 keV	140 keV
	Scatter and absorption	Less scatter and absorption
	Low resolution	High resolution
Half-life	73 hr	6 hr
	Low dosage (2–3 mCi)	High dosage (20–30 mCi)
	Long collection times	Short collection times
	Low count densities	High count densities
Effective dose	1.3 rad(cGy)/mCi	1.1 rad(cGy)/mCi
Availability	Cyclotron—commercial mfr	Generator—local
First-pass study	No	Yes

TABLE 15-6 Myocardial Perfusion Imaging Agent Properties

Property	^{201}Tl-Thallous Chloride	^{99m}Tc-Sestamibi	^{99m}Tc-Tetrofosmin
Chemistry	+1 cation	+1 cation	+1 cation
	Hydrophilic	Lipophilic	Lipophilic
Shelf life	6 days after calibration	6 hours	12 hours
Photon energy (abundance)	68–80 keV (94%)	140 keV (88%)	140 keV (88%)
Uptake mechanism	Active	Passive diffusion	Passive diffusion
	Na-K ATPase pump	(associated with intact membrane potentials)	(associated with intact membrane potentials)
Extraction fraction	~ 85%	~ 66%	~ 60%
Heart uptake (% injected dose)	~ 4%	~ 1.2%	~ 1.0%
Administered activity	2–4 mCi	10–30 mCi	10–30 mCi
Heart distribution	Redistributes	Fixed (mitochondria associated)	Fixed (cytosol associated)
Effective dose	1.3 rad/mCi	0.056 rad/mCi	0.041 rad/mCi

Technetium Tc 99m Sestamibi Injection

Technetium Tc 99m sestamibi injection (^{99m}Tc-sestamibi) is a monovalent cationic lipophilic complex composed of one atom of Tc(I) and six ligand molecules of 2-methoxy isobutyl isonitrile (MIBI). Its chemistry is discussed in Chapter 9.

After intravenous injection, ^{99m}Tc-sestamibi clears rapidly from the blood and remains relatively fixed in the myocardium with a resting heart uptake of 1% of the ID. This amount is about one-fourth the uptake of ^{201}Tl, but the 10 to 30 mCi (370 to 1110 MBq) administered activity of ^{99m}Tc-sestamibi is larger, resulting in a much higher count density in the heart with ^{99m}Tc-sestamibi. The low photon energy of ^{201}Tl (69 to 80 keV) is easily attenuated in tissue, causing a low count rate from photon absorption and poor resolution caused by scatter. This can present imaging problems in obese patients and particularly in women because of potential breast attenuation artifacts. Back-scatter of thallium photons causes images to have a fuzzy appearance. By contrast, the 140 keV photons of ^{99m}Tc have less tissue attenuation, are detected efficiently, and produce sharper, higher contrast images. Table 15-5 compares the general properties of ^{201}Tl and ^{99m}Tc for myocardial imaging studies, and Table 15-6 compares the properties of MPI agents.

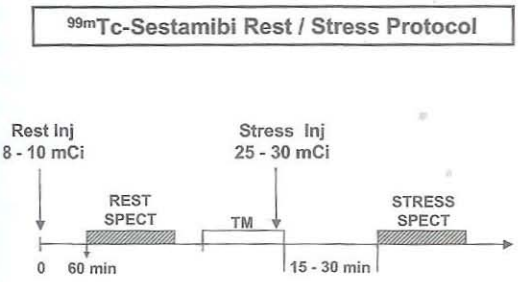

FIGURE 15-15 ^{99m}Tc-sestamibi 1 day rest–stress imaging protocol. (Reprinted with permission of the Society of Nuclear Medicine from reference 31.)

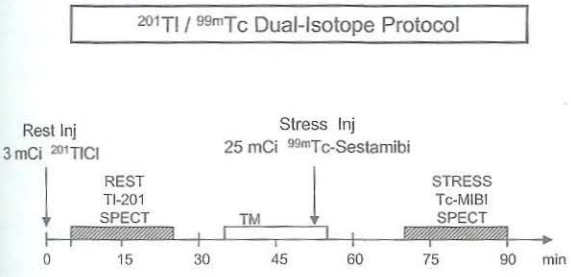

FIGURE 15-16 ^{201}Tl–^{99m}Tc dual-isotope imaging protocol. (Reprinted with permission of the Society of Nuclear Medicine from reference 31.)

normal.[31] If the 1 day protocol is used, a rest–stress sequence is preferred (Figure 15-15). A rest dose of 8 to 10 mCi (296 to 370 MBq) is injected and imaging is begun in 45 to 60 minutes. After the rest dose imaging procedure, treadmill exercise is performed and a stress injection of 25 to 30 mCi (925 to 1110 MBq) is given, followed by imaging in 15 to 30 minutes. The activity in the heart during the stress study overwhelms the residual activity from the rest dose because of the increased blood flow to the heart and the large stress dose administered. The 1 day procedure may take up to 2 to 3 hours to complete depending on the time required for acquisition of patient images. This protocol is useful when a rapid diagnosis is needed, especially in a patient with high pretest likelihood of CAD, but it may present a problem with diabetic patients because of the prolonged fasting requirements.[31]

A 1 day stress–rest procedure was proposed to speed patient throughput; however, compared with the rest–stress procedure, it had a greater likelihood of misinterpreting reversible defects as fixed.[81] This problem was attributed to stress dose crosstalk interfering with the later resting study[82] and to a lower count density from the low-activity stress dose.[31] This procedure should be reserved for patients with a low likelihood of disease, in whom a normal initial stress study is anticipated.[82]

To improve patient throughput, a dual-isotope procedure has been developed (Figure 15-16).[31] In this procedure, ^{201}Tl-thallous chloride is injected at rest and a ^{201}Tl-SPECT acquisition is made. The patient is then stressed on a treadmill, and 25 to 30 mCi (925 to 1110 MBq) of ^{99m}Tc-sestamibi is injected. A SPECT stress image is acquired 15 minutes after this injection. The entire procedure can be completed in 1.5 to 2.0 hours, making this a rapid method.

Several advantages are afforded by ^{99m}Tc-sestamibi's lack of redistribution. One is the ability to repeat image acquisition in the event of a positioning error, patient motion, or instrument malfunction. A second is the ability to inject a patient during an acute ischemic event and perform imaging later, at a more convenient time or after patient treatment. An example is ruling out myocardial ischemia in patients with unstable angina who have spontaneous chest pain.[83] ^{99m}Tc-sestamibi is injected at the time of pain. A few hours later, when the patient has stabilized, a cardiac scan is obtained. A normal scan strongly suggests

that the pain is not of coronary origin. An abnormal scan suggests significant coronary disease. A subsequent study in the absence of chest pain that demonstrates decreased size of an initial perfusion defect supports the diagnosis of a transient coronary flow disturbance. Another example is evaluation of an acute infarction to determine the amount of myocardium salvaged after thrombolytic therapy.[84] In this situation the patient is injected upon admission, thrombolytic therapy is begun, and imaging is performed within 4 to 6 hours to identify infarcted plus jeopardized myocardium at the time of the event. A repeat study at a later date identifies only infarcted myocardium. Analysis of the two studies identifies the amount of muscle salvaged.

A third advantage of ^{99m}Tc-sestamibi is the ability to evaluate myocardial perfusion and ventricular function with a single injection of tracer by means of ECG gating. This permits the simultaneous evaluation of exercise perfusion with resting ventricular function, for an estimate of myocardial viability. An exercise perfusion defect with preserved regional wall motion at rest implies ischemia, whereas regional akinesis could be associated with either scar or severely ischemic or stunned myocardium.[82]

Technetium Tc 99m Tetrofosmin Injection

Technetium Tc 99m tetrofosmin injection (^{99m}Tc-tetrofosmin) or $[^{99m}\text{Tc-(tetrofosmin)}_2\text{O}_2]^+$ is a monovalent cationic lipophilic complex of the Tc(V) dioxo core, $O{=}Tc{=}O^+$, and two bis(2-ethoxyethyl)phosphino]ethane ligands.[53] Its chemistry is described in Chapter 9.

After intravenous injection in humans, ^{99m}Tc-tetrofosmin clears rapidly from the blood; by 10 minutes, less than 5% of the ID remains, with less remaining after exercise.[54] Uptake in skeletal muscle is the main reason for high background clearance after exercise. After rest injection, heart activity declines slowly over time; it is 1.2%, 1.0%, and 0.7% of the ID at 1, 2, and 4 hours, respectively. Values are slightly higher after exercise injection. Liver uptake at these same times is 2.1%, 0.9%, and 0.3% of the ID. Heart-to-liver ratios at 30 and 60 minutes after dosing, respectively, are 0.6 and 1.2 at rest and 1.2 and 3.1 after exercise, reflecting high and rapid hepatobiliary clearance. The rapid clearance of ^{99m}Tc-tetrofosmin from abdominal organs allows imaging to be performed soon after injection.[85]

^{99m}Tc-tetrofosmin's uptake in the heart is proportional to coronary blood flow up to 2 mL/minute per gram.[86] This is similar to the uptake and flow relationship seen with ^{99m}Tc-sestamibi[76] and ^{201}Tl-thallous chloride.[56] All the SPECT agents underestimate flow at high flow rates and overestimate flow at very low flow rates, which is a function of the time tracer is available for extraction.[86] When compared with thallium extraction in the rabbit heart, tetrofosmin exhibits a myocardial extraction 60% that of thallium, but heart uptake of both tracers is correlated with blood flow.[87]

Approximately 66% of the injected activity is excreted in 48 hours, about 40% in urine and 26% in feces.[88] The critical organ is the gallbladder wall, with a radiation absorbed dose of 0.123 rad(cGy)/mCi (stress) and 0.180 rad(cGy)/mCi (rest).[88]

The mechanism of ^{99m}Tc-tetrofosmin uptake in myocytes has been investigated. Data indicate that uptake is by a metabolism-dependent process that does not involve cation channel transport. The most likely mechanism for this is potential-driven diffusion of the lipophilic cation across the sarcolemmal and mitochondrial membranes.[89] ^{99m}Tc-tetrofosmin appears to be associated more with the cytosol than within mitochondria, whereas ^{99m}Tc-sestamibi demonstrates a higher concentration within the mitochondria.[90] Quantitative analysis of ^{99m}Tc-tetrofosmin retention in the heart demonstrates that washout is very slow (4% per hour after exercise and 0.6% per hour after rest).[91] Ischemic-to-normal myocardium ratios of ^{99m}Tc-tetrofosmin range only from 0.75 to 0.72 from 5 minutes to 4 hours after injection, indicating insignificant redistribution of this agent over time. ^{99m}Tc-sestamibi, however, has been shown to exhibit a small degree of redistribution between

1 and 3 hours after dosing because of faster clearance rates from normal segments.[92] Ischemic-to-normal wall ratios with ^{99m}Tc-sestamibi were statistically higher at 3 hours (0.84) than at 1 hour (0.73), which may affect detection of CAD in cases where the ischemic defect is slight or mild.

Technetium Tc 99m Teboroxime Injection

Technetium Tc 99m teboroxime injection (^{99m}Tc-teboroxime) is a boronic acid adduct of technetium dioxime (BATO). It is a neutral lipophilic complex of Tc(III). The first-pass myocardial extraction of teboroxime (80%–90%) is higher than with sestamibi (40%–60%) and thallium (75%–85%).[93] Consequently, teboroxime has less diffusion limitation and can more reliably assess higher blood flow levels than sestamibi or thallium. However, teboroxime is not fixed in the myocardium and rapidly diffuses out shortly after injection. Its myocardial kinetics are so rapid that imaging must be started within 2 minutes of tracer injection and be completed by 6 to 9 minutes after injection.[93] Imaging protocols have been worked out to successfully conduct perfusion imaging with ^{99m}Tc-teboroxime, but the logistic problems limit its practical usefulness. The product is no longer on the market.

PET Perfusion Imaging Agents

PET imaging in myocardial disease offers several advantages over SPECT imaging. The major advantage of PET over SPECT is the ability to provide attenuation-corrected images, which decrease the occurrence of attenuation artifacts and increase specificity.[94] Other advantages include increased sensitivity and spatial resolution (PET, 6–10 mm; SPECT, 10–15 mm), which translates into a higher degree of accuracy of PET versus SPECT in the detection of CAD with perfusion tracers.[94] Quantification of blood flow is possible with PET. Additionally, metabolism studies can be done with ^{18}F-FDG, ^{11}C-acetate, and ^{11}C-palmitate. ^{18}F-FDG is considered the gold standard for evaluating myocardial viability. The principal disadvantages of PET are availability and cost.

Ammonia N 13 Injection

Radiolabeled microspheres are the standard for quantitating organ blood flow. They are nondiffusible tracers and therefore have an extraction fraction of 1.0 at all blood flow levels.[42] In the nuclear medicine clinic, however, perfusion measurements are typically made with diffusible tracers, and diffusible tracers have extraction fractions less than 1.0 because of diffusion limitations at high blood flow rates. High-extraction diffusible tracers are desirable for performing myocardial perfusion studies. Ammonia N 13 injection (^{13}N-ammonia) has proven to be one of the most effective perfusion tracers in PET. Its first-pass extraction is high (>90%) because of the rapid diffusion of uncharged lipophilic ammonia across the capillary endothelium and sarcolemma of the myocyte (Figure 15-17). However, back-diffusion of unfixed tracer occurs, so the amount retained decreases as coronary blood flow increases. At coronary blood flows of 1 and 3 mL/minute per gram, the average first-pass retention is 83% and 60%, respectively.[42] Once taken up into the myocyte, ammonia is rapidly fixed as ^{13}N-glutamine by the enzymatic conversion of *glutamic acid by glutamine synthetase.*

^{13}N-ammonia is cyclotron-produced, and its 10 minute half-life restricts its use to facilities with an onsite cyclotron. The production of ^{13}N and other positron emitters and their chemistry is discussed in Chapter 10.

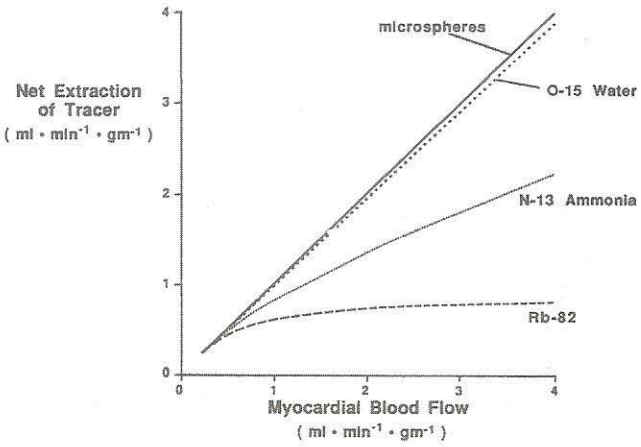

FIGURE 15-17 Myocardial extraction of PET tracers versus coronary artery blood flow. (Reprinted with permission of W.B. Saunders from reference 42.)

^{13}N-ammonia is used for evaluating myocardial blood flow. Typically 10 to 20 mCi (370 to 740 MBq) is administered intravenously, with imaging starting about 5 minutes later to allow clearance of excess tracer from the blood. The 10 minute half-life of ^{13}N requires about a 30 minute wait between rest and stress injections to allow for decay.[94]

Rubidium Chloride Rb 82 Injection

Rubidium chloride Rb 82 injection (^{82}Rb-rubidium chloride) is a generator-produced nuclide with a half-life of 75 seconds. ^{82}Rb is eluted from the generator with 0.9% sodium chloride injection as rubidium chloride. ^{82}Rb is the daughter nuclide of ^{82}Sr, which has a 25 day half-life, giving the generator a useful life of 4 to 6 weeks. After intravenous injection of ^{82}Rb-rubidium chloride, the rubidium cation is taken up across the sarcolemmal membrane via the Na-K ATPase pump. A substantial amount of nontransported tracer back-diffuses from the interstitial space and is washed away in increasing amounts nonlinearly as coronary blood flow increases.[42] The mean extraction fraction at 1 and 3 mL/minute per gram is 59% and 26%, respectively (Figure 15-17).[42,95]

Administration of ^{82}Rb-rubidium chloride for perfusion imaging is typically automated, and 40 to 60 mCi (1480 to 2220 MBq) is injected intravenously, with imaging beginning after a 90 to 120 second wait to achieve satisfactory heart-to-blood ratios after blood clearance of tracer. The rapid decay of ^{82}Rb permits multiple studies to be performed about every 10 minutes. A disadvantage of ^{82}Rb is its high-energy positron (maximum energy 3.15 MeV), which travels farther from its site of origin before annihilation than lower-energy positrons. This effectively decreases intrinsic resolution.[95]

Water O 15 Injection

^{15}O ($T_{½}$ 2 minutes) as labeled water is a freely diffusible tracer whose first-pass extraction is 95%. It is independent of blood flow and metabolically inert, and therefore appears to be an ideal tracer for perfusion studies. However, water O 15 injection (^{15}O-water) also distributes into tissues adjacent to the heart (lung and heart blood pool), which complicates imaging by requiring the use of background subtraction techniques.[42] ^{15}O-water is administered as an intravenous bolus of 30 mCi (1110 MBq), with imaging beginning immediately. Alternatively, patients inhale ^{15}O-labeled carbon dioxide for 3 to 4 minutes with continuous imaging. In vivo, the ^{15}O-carbon dioxide is converted to ^{15}O-water by carbonic anhydrase.[42] After imaging, and allowing for complete decay, the blood pool is labeled by a single-breath dose of ^{15}O-carbon monoxide, which labels red blood cells by forming

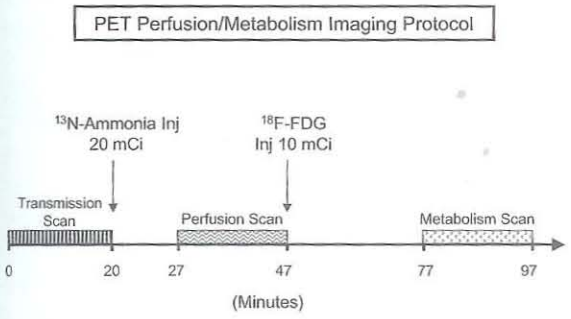

FIGURE 15-18 PET perfusion–metabolism imaging protocol to assess myocardial viability. (Reprinted with permission of the Society of Nuclear Medicine from reference 96.)

^{15}O-carboxyhemoglobin. Blood pool images are taken and subtracted from heart perfusion images to assess net myocardial perfusion.

PET Metabolism Agents

Fludeoxyglucose F 18 Injection

Fluorine F 18 ($T_{½}$ 110 minutes) labeled as 2-fluoro-2-deoxyglucose (fludeoxyglucose, or FDG) is the premier metabolic marker for glucose metabolism. Fludeoxyglucose F 18 injection (^{18}F-FDG), a hydrophilic molecule, is taken up into cells via facilitated diffusion similarly to glucose, but its metabolism is different (Figure 15-3). In the first step of glucose metabolism, hexokinase converts glucose and FDG into glucose-6-phosphate and FDG-6-phosphate, respectively. While glucose-6-phosphate participates further as a substrate for glycolysis or glycogen synthesis, FDG-6-phosphate is not a substrate for these pathways. Because it cannot readily diffuse back out of the cell, FDG-6-phosphate becomes trapped and accumulates in cells that are in active metabolism.

Under normal aerobic fasting conditions, the heart primarily uses fatty acids for its energy needs. After a glucose load, elevated insulin levels in blood cause an increase in glucose metabolism in preference to fatty acids. In the ischemic heart, areas of ischemic muscle switch to anaerobic glycolysis with glucose as the principal substrate. These areas demonstrate increased uptake of FDG. This is the basis for using FDG as a marker of myocardial metabolism and cell viability. FDG is not a useful tracer of myocardial blood flow because its uptake is not related to flow but to phosphorylation. The phosphorylation step is dependent on the rate of glucose metabolism, which is independent of blood flow.

^{18}F-FDG is supplied as an injection and is used for assessing myocardial viability. A typical protocol is to perform a perfusion/metabolism study, perfusion being evaluated first with ^{13}N-ammonia, ^{82}Rb-rubidium chloride, or ^{15}O-water (Figure 15-18). Because of the difference in physical half-lives, ^{13}N-ammonia is frequently used; it allows longer imaging times with higher count density images compared with ^{82}Rb-rubidium chloride or ^{15}O-water.[96] The metabolism phase of the study involves intravenous injection of 10 mCi (370 MBq) of ^{18}F-FDG after a loading dose of glucose to facilitate transport of FDG into the myocardial cells. The loading dose of glucose is important because fatty acids are the principal substrate for myocyte energy requirements in the fasting state and FDG is taken up very little under these conditions. Compared with subjects who have fasted for 12 hours, subjects given 50 grams of glucose orally before the FDG study demonstrate heart-to-blood activity ratios 2.5 times higher.[97] The pattern of activity uptake between the perfusion and metabolism images is key to the diagnosis. If the ammonia and FDG activity distributions are identical in the region of a perfusion defect (a match), the defect is likely caused by lack of both perfusion and active metabolism and is likely due to scar. If there is increased uptake of FDG in a region seen as a perfusion deficit with ammonia

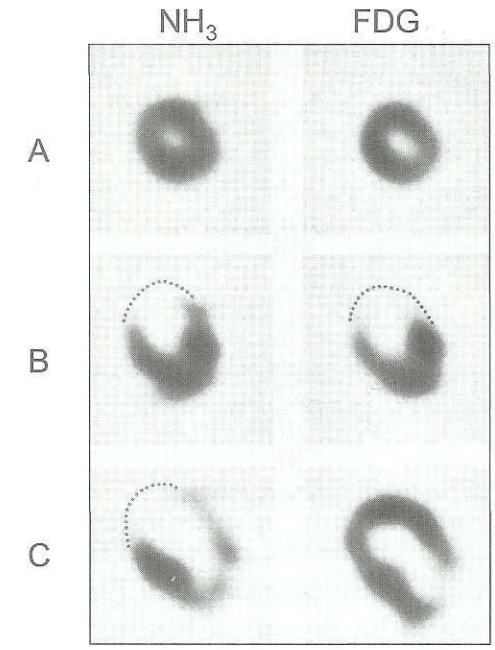

FIGURE 15-19 Regional myocardial blood flow and glucose utilization in a normal volunteer (A) and two patients with ischemic heart disease (B and C), evaluated with ^{13}N-ammonia and ^{18}F-FDG and PET. Only one midventricular cross-sectional image of blood flow (left) and glucose utilization (right) is shown per subject. Note the homogeneous tracer uptake in the normal subject. In patient B, blood flow is decreased in the anterior wall (broken line), associated with a proportional decrease in FDG uptake. This pattern reflects scar tissue. In patient C, blood flow is markedly decreased in the anterior wall and the anterior septum, while glucose utilization in the hypoperfused segment is markedly enhanced. Preservation of glucose utilization in hypoperfused and dysfunctional segments represents tissue viability. (Reprinted with permission of W.B. Saunders from Schelbert HR. Current status and prospects of new radionuclides and radiopharmaceuticals for cardiovascular nuclear medicine. *Semin Nucl Med.* 1987;17:145-81.)

(a mismatch), the interpretation is that the region represents hibernating myocardium that is active metabolically and therefore viable (Figure 15-19).

Carbon C 11 Palmitate

Carbon 11 palmitate is used to provide information about myocardial fatty acid metabolism (see Figure 15-3). The free fatty acid is largely distributed in the myocardium in proportion to blood flow, whereupon it crosses the sarcolemmal membrane, presumably by passive diffusion or possibly facilitated transport.[42] Retention or trapping of ^{11}C-palmitate requires energy-dependent esterification to ^{11}C acyl-CoA, which can enter either of two routes. In one fraction it moves via the carnitine shuttle to the inner mitochondrial membrane, where β-oxidation cleaves two carbon fragments off the long carbon chain, directing acetyl CoA to the tricarboxylic acid (TCA) cycle for complete oxidation to carbon dioxide and water. The other fraction of acyl-CoA is further esterified and deposited as triglyceride and phospholipid stores.

After intravenous administration of 15 to 20 mCi (555 to 740 MBq) of ^{11}C-palmitate and image acquisition, stored images of the ventricles are used to identify regions of interest, from which time–activity curves are generated for analysis of uptake and clearance kinetics. The slopes of these curves can then be used to assess regional metabolism in the myocardium.[42]

Sodium Acetate C 11 Injection

Sodium acetate C 11 injection (^{11}C-acetate) is avidly extracted by the myocardium and activated to acetyl-CoA, which is oxidized in the mitochondria to ^{11}C-carbon dioxide and water (see Figure 15-3). ^{11}C-acetate permits evaluation of flux through the TCA cycle and overall myocardial oxygen consumption because of its close link to oxidative phosphorylation.[42] Myocardial oxidative capacity can be measured by analyzing uptake and clearance curves. These curves change with regional abnormalities in blood flow and metabolism.

Thus, in ischemic regions, the initial uptake of ^{11}C-acetate decreases in proportion to myocardial blood flow, and clearance curves are reduced significantly.[42]

^{18}F-FDG and ^{11}C-palmitate are tracers that measure specific substrates in myocardial metabolism, whereas ^{11}C-acetate measures overall oxidative metabolism. ^{18}F-FDG measures the initial steps of exogenous glucose utilization, whereas ^{11}C-palmitate traces the entire pathway of fatty acid metabolism. In the fasted state, when fatty acid metabolism is highest in the myocardium, ^{18}F-FDG demonstrates very little uptake in the heart, but ^{11}C-palmitate uptake and clearance curves reflect rapid kinetics. The combination of ^{11}C-palmitate or ^{18}F-FDG with ^{11}C-acetate permits assessment of the contribution of fatty acid or glucose metabolism to overall oxidative metabolism or, in the ischemic condition, assessment of anaerobic versus oxidative glucose metabolism.[42]

VIABILITY ASSESSMENT

A principal reason for MPI is to predict whether ischemic dysfunctional myocardial segments are viable and therefore restorable to normal function after revascularization. The four principal conditions that can cause left ventricular dysfunction are (1) transmural MI, which involves full-thickness myocardial necrosis; (2) nontransmural MI, in which necrosis is limited to the subendocardium or scattered throughout the myocardium; (3) myocardial stunning; and (4) hibernating myocardium.[96] Revascularization is not expected to be beneficial for the first two conditions. Myocardial stunning results from severe acute ischemia followed by reperfusion, both of which cause myocardial injury and dysfunction.[98] Myocardial hibernation results in dysfunction caused by chronic reduction in coronary blood flow. In stunning, reduced contraction is mismatched with increased perfusion; in hibernation, reduced contraction is matched by reduced perfusion.[98] In both situations, the dysfunction is reversible and will resolve after restoration of myocardial perfusion. Time is required in the case of stunning to restore muscle; improved blood flow is required in the case of hibernation.

Nuclear medicine studies have been shown to be valuable in predicting viability of stunned and hibernating myocardium. Thallium viability studies have been reviewed by Maddahi et al.[96] The terms positive predictive accuracy (PPA) and negative predictive accuracy (NPA) are often used in viability assessment studies. PPA predicts the percentage of myocardial regions with reversible defects that will improve after revascularization, and NPA predicts the percentage of myocardial regions without reversibility that will not improve after revascularization. In three independent studies of rest–redistribution thallium imaging, the mean PPA was found to be 72% (range, 57% to 92%), and the mean NPA was found to be 70% (range, 62% to 77%).[99–101] In three additional studies, after exercise–redistribution–reinjection thallium imaging, NPAs in studies conducted without ^{201}Tl reinjection were 43%, 53%, and 48%, but with reinjection these values improved to 100%, 75%, and 75%, respectively, demonstrating the benefit of thallium reinjection in improving diagnostic accuracy.[67,70,102] For this reason, thallium reinjection is now a standard technique in SPECT imaging for assessing myocardial viability.

PET's ability to predict recovery of left ventricular function after revascularization procedures has been assessed with myocardial perfusion/metabolism studies using ^{15}O-water, ^{13}N-ammonia, ^{11}C-acetate, and ^{18}F-FDG. In seven studies reviewed by Maddahi et al.,[96] the average reported PPA for a PET myocardial perfusion/FDG metabolism mismatch pattern was 83% (range, 72% to 95%), and the average NPA for a matching pattern was 84% (range 75% to 100%). Thus, while both ^{201}Tl SPECT and PET imaging methods have high accuracies, PET perfusion/metabolism imaging appears to have greater diagnostic power than thallium SPECT in predicting improvement of left ventricular function in patients with CAD.

Most institutions now use a ^{99m}Tc agent (^{99m}Tc-sestamibi or ^{99m}Tc-tetrofosmin) for myocardial perfusion studies. The question remains, in the situation of chronic left ventricular dysfunction, whether ^{99m}Tc-sestamibi can distinguish between viable hibernating myocardium and fibrosis, as has been shown with the ^{201}Tl rest–reinjection technique.[12,67] Several studies indicate that ^{99m}Tc-sestamibi has limitations in identifying viability in hibernating myocardium. Cuocolo et al.[103] compared ^{99m}Tc-sestamibi and ^{201}Tl-thallous chloride in chronic CAD, demonstrating that approximately 60% of myocardial regions identified as viable by thallium reinjection were categorized as nonviable by a resting ^{99m}Tc-sestamibi study. In a comparison of ^{99m}Tc-sestamibi with FDG PET in patients with CAD, ^{99m}Tc-sestamibi was found to underestimate myocardial viability.[104] Five percent to 11% of severe defects, with ^{99m}Tc-sestamibi uptake at rest 30% or less of peak activity, were viable by FDG PET, whereas 13% to 61% of moderate to severe defects (31% to 70% of peak activity) were found to be viable by FDG PET. A case report comparing ^{201}Tl exercise–redistribution with reinjection and ^{99m}Tc-sestamibi exercise–rest in a patient with multivessel chronic CAD evaluated before and after revascularization demonstrated that thallium could distinguish between viable and nonviable regions, whereas sestamibi could not.[105] It appears that ^{99m}Tc-sestamibi, as a perfusion marker, may be able to assess viability in stunned myocardium in which perfusion is adequate, such as after reperfusion therapy for acute MI, but that it is not able to adequately identify viability in hibernating myocardium in chronic CAD, in which there is sustained reduction in blood flow.[98] Thus, in those clinics without FDG PET capability, the thallium rest–redistribution protocol or the thallium stress–redistribution–reinjection protocol would be the procedure of choice for assessing myocardial viability.

Clinical studies have shown that ^{99m}Tc-tetrofosmin accurately detects CAD when compared with ^{201}Tl-thallous chloride[106–108] and ^{99m}Tc-sestamibi.[109] The heart-to-liver ratios at rest and after dipyridamole stress indicate higher ratios for tetrofosmin compared with sestamibi, but no significant difference has been found in the quality of images or diagnostic interpretation of these two agents.[110] In a qualitative comparison for viability assessment in CAD after exercise–rest studies, tetrofosmin imaging was found to underestimate myocardial viability compared with thallium reinjection, and the difference correlated with severity of the persistent defect on rest images.[110]

Intact membrane function and metabolic processes are required for myocyte viability. Thus, markers of membrane integrity and metabolic function should be equally effective in assessing myocardial viability. The differences in the reported accuracies between SPECT and PET imaging agents for assessing viability may reside in the different abilities of these modalities to detect physiologic processes that are occurring. PET seems to have the advantage currently because of its better resolution, ability to correct for photon attenuation, and ability to assess metabolic function independent of perfusion.[111]

BLOOD POOL IMAGING AGENTS

The essential requirements for a blood pool imaging radiopharmaceutical for evaluating dynamic heart function include (1) slow blood clearance to provide steady blood pool activity during the time of data acquisition, (2) minimal localization of radioactivity in nearby organs and extravascular space that would interfere with measurements of the heart blood pool, and (3) high photon flux, which is necessary for high-resolution and high-sensitivity measurements of dynamic heart function with the gamma camera. The latter requirement is most easily met by ^{99m}Tc, and the first two requirements are met by labeling ^{99m}Tc to either human serum albumin or red blood cells.

Technetium Tc 99m Albumin Injection

Early ^{99m}Tc-human serum albumin (^{99m}Tc-HSA) preparations labeled with stannous ion had significantly faster blood clearance than radioiodinated HSA as well as high lung background activity, making them unsatisfactory for delineating the cardiac blood pool.[112] The present day ^{99m}Tc-HSA kit produces a product with a slower blood clearance and minimal background and organ interference in imaging the blood pool. Albumin (MW approximately 70,000) remains confined to the vascular space, being restricted from filtration at the glomerulus. ^{99m}Tc-HSA, therefore, is useful for imaging the heart blood pool. The usual adult administered activity of ^{99m}Tc-HSA is 5 mCi (185 MBq) by intravenous injection, and the critical organ is the urinary bladder wall, with an absorbed radiation dose of 0.033 rad(cGy)/mCi.

Technetium Tc 99m Red Blood Cells

The various methods of labeling red blood cells (RBCs) with technetium are discussed in Chapter 9. A popular labeling method for cardiac blood pool imaging is the in vivo method. With this method, a dose of "cold" stannous pyrophosphate (Sn-PPi) is injected intravenously and allowed to equilibrate for 20 to 30 minutes to "tin" the RBCs in vivo.[113] Subsequently, ^{99m}Tc-sodium pertechnetate is injected, whereupon the pertechnetate enters the RBCs, becomes reduced by the intracellular stannous ion, and is bound to hemoglobin. This provides a fixed blood pool of activity with minimal background interference from other organs around the heart. A common technique involves reconstituting one vial of Mallinckrodt TechneScan PYP (which contains an average of 15.7 mg of Sn-PPi and, on average, about 2 mg of stannous ion) with 5 mL of saline and injecting the patient with 7.5 mg of Sn-PPi (one-half vial) per dose, equivalent to approximately 15 μg Sn(II)/kg. Within 20 to 30 minutes of injecting the Sn-PPi, 20 to 30 mCi (740 to 1110 MBq) of ^{99m}Tc-sodium pertechnetate is administered intravenously to label the RBCs for blood pool imaging. Although much of the administered stannous ion in Sn-PPi is localized in other organs, the small percentage that becomes associated with the RBC hemoglobin component is sufficient to label the cells with technetium at about a 75% labeling efficiency.[114,115] The in vivo labeled cells are assumed to have a biologic half-life of about 80 days (the same as normal RBCs).

Ventriculography

A principal application of blood pool imaging agents is myocardial ventriculography for the assessment of wall motion abnormalities and measurement of ventricular ejection fraction and volume. The assessment is made with a two-part study: the first-pass study and the equilibrium study. The first-pass study permits assessment of right and left chamber function after administration of a 20 to 30 mCi (740 to 1110 MBq) intravenous bolus of ^{99m}Tc-pertechnetate activity. Subsequently, the injected pertechnetate labels RBCs in vivo, permitting an ECG-gated equilibrium study. The equilibrium study is conducted to assess left ventricular function. The equilibrium study is also known as the multigated acquisition study because the activity labeled to the red cell blood pool is monitored as it passes through the heart by acquiring images triggered or gated on the R wave of the ECG. Total activity passing through the heart during one cardiac cycle is divided into frames of activity that are stored in a computer (Figure 15-20). Typically, 32 or more frames are acquired during each cycle, so that incremental changes in left ventricular activity can be stored from end-diastole (ED) to end-systole (ES). Many cardiac cycles (and frames) of data are stored over a long image acquisition time so that a statistically significant amount

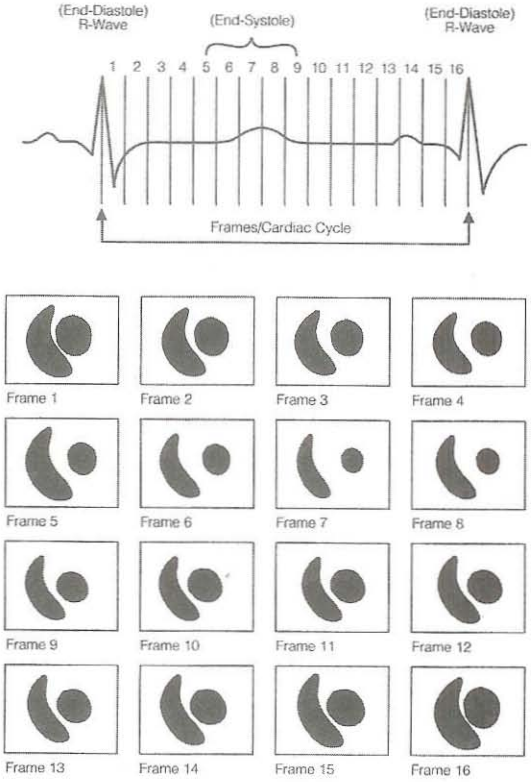

FIGURE 15-20 Gating mechanism to obtain serial single-frame images of left ventricle contraction through one cardiac cycle. See text for explanation. (Reprinted with permission of Bristol-Myers Squibb Medical Imaging, Inc. from *Introduction to Nuclear Cardiology,* 3rd ed. North Billerica, MA: DuPont Pharma Radiopharmaceuticals; 1993:226.)

of activity is accumulated in each frame. The total amount of activity stored in the frames at each gated time point is then plotted versus total cycle time to obtain a time–activity curve of blood flowing through the left ventricle. From this plot the left ventricular ejection fraction (LVEF) can be determined from ED and ES activities in the chamber as follows:

$$\text{LVEF} = \frac{(\text{ED} - \text{Bkg}) - (\text{ES} - \text{Bkg})}{(\text{Ed} - \text{Bkg})} = \frac{\text{ED} - \text{ES}}{\text{ED} - \text{Bkg}}$$

Figure 15-21 illustrates two patient studies for determination of LVEF, one normal (LVEF = 73%) and one abnormal (LVEF = 30%). Normal LVEF is 55% or greater.

INFARCT-AVID IMAGING AGENTS

Infarct-avid agents, otherwise known as "hot spot" markers, demonstrate an increased accumulation of radiotracer activity in regions of infarcted myocardium. Several types of radiolabeled agents have been developed for infarct imaging based on the pathophysiologic changes that occur in the infarct region. Some of these mechanisms have been well elucidated, while others are still being pursued in the continued development of new radiotracers for imaging MI.

Technetium Tc 99m Pyrophosphate Injection

Technetium-labeled bone agents were first used for infarct localization after the serendipitous finding of heart uptake on bone scans in patients who had recent infarcts. In the

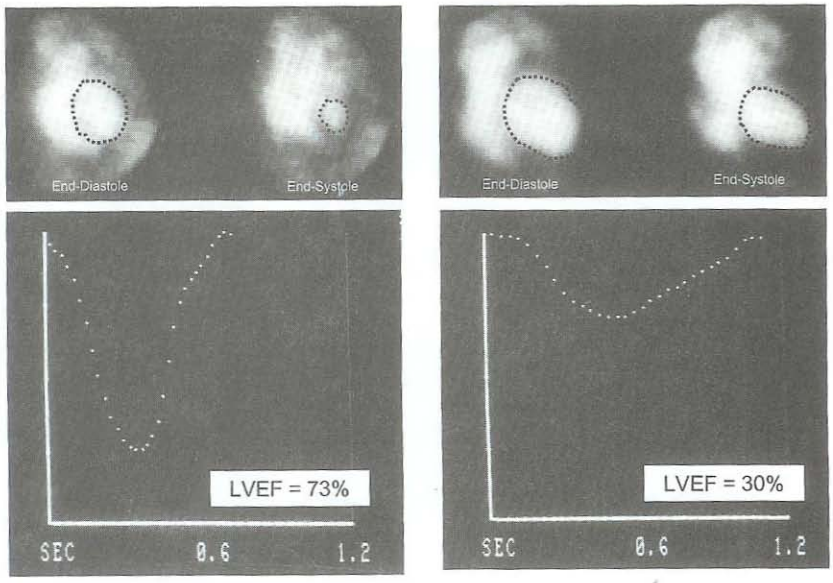

FIGURE 15-21 Left ventricular ejection fraction (LVEF) assessment. Images of the heart at end-diastole and end-systole with time–activity curves demonstrating (left) normal LVEF of 73% and (right) abnormal LVEF of 30%.

1970s, these agents proved useful because at that time there was a lack of sensitive enzyme assays for early diagnosis of MI. Investigations led to the discovery that, physiologically, ischemic damage to the myocardial cell membrane produces an imbalance in the myocyte's intracellular–extracellular calcium ion concentration. Under normal conditions, the calcium ion concentration intracellularly is about 10^{-7} M, and in extracellular fluid it is about 10^{-3} M (Figure 15-4). After infarction with disruption of the myocyte membrane, calcium ions diffuse into the infarcted cells, providing a focus for the uptake and binding of technetium-labeled agents.

In 1974, Bonte et al.[116] introduced the use of technetium Tc 99m pyrophosphate injection (^{99m}Tc-pyrophosphate or ^{99m}Tc-PPi) for imaging MI. Several other agents have been investigated for the detection of MI in animal and human studies.[48] Of the agents tested, ^{99m}Tc-pyrophosphate demonstrated the highest percentage of ID per gram in the myocardium (2.2%) and an infarct-to-normal myocardium ratio of 25:1 at 1 hour after dosing. Its mechanism of localization is related to residual blood flow to the infarcted region, calcium ion influx, and deposition of intracellular hydroxyapatite in infarcted cells.[117,118]

Membrane damage occurs after MI, which permits an influx of plasma proteins and calcium ions, some of which deposit in mitochondria, where hydroxyapatite crystals form. The proposed mechanism of ^{99m}Tc-pyrophosphate localization is sorption to various forms of tissue calcium stores, including amorphous calcium phosphate, crystalline hydroxyapatite, and calcium complexed with various macromolecules at the infarction site. Maximal concentrations occur in peripheral zones of the infarct where there is adequate blood flow, with considerably less uptake in central zones of the infarct where blood flow is reduced.[118] Temporally, after fixed coronary occlusion, ^{99m}Tc-pyrophosphate begins to localize in the infarcted tissue within 12 to 24 hours. Scintigrams become more positive during 24 to 72 hours and remain abnormal for 6 days after infarction, fading thereafter and becoming negative by day 14 (Figure 15-22). A standard dose for myocardial infarct imaging is 15 mCi (555 MBq), with imaging in 3 to 4 hours.

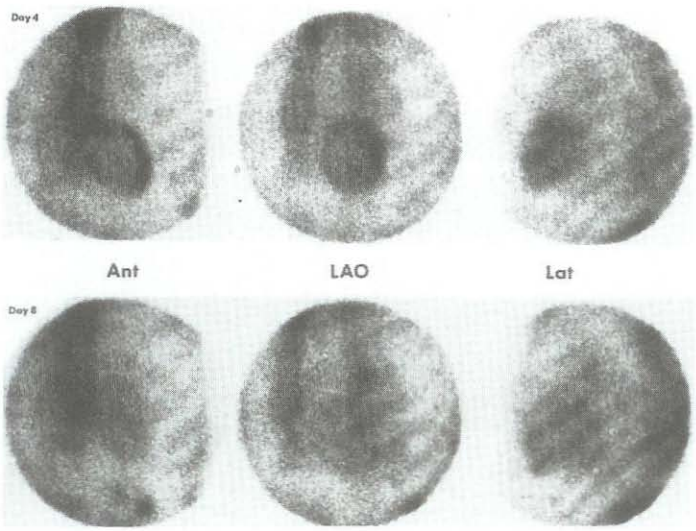

FIGURE 15-22 Infarct-avid scans obtained 4 and 8 days after extensive acute left ventricle infarction. Images obtained 2 hours after intravenous injection of 15 mCi of ^{99m}Tc-pyrophosphate.

The sensitivity of ^{99m}Tc-pyrophosphate for detecting transmural infarcts is about 90%, but only about 40% for subendocardial infarcts.[119] The overall specificity was found to be 64% in a multicenter study. Its lack of specificity is due in part to myocardial uptake in patients with stable angina without infarct and in regions of old infarcts several months after the acute episode. Additionally, the long time required before ^{99m}Tc-pyrophosphate uptake is positive after infarction (24 to 48 hours) precludes its use for early diagnosis.

Indium In 111 Imciromab Pentetate

Indium In 111 imciromab pentetate (Myoscint, Centocor), otherwise known as ^{111}In-antimyosin, is a monoclonal antibody Fab fragment with specificity for myosin. Its localization is based on disruption of the sarcolemmal membrane of dying myocytes, exposing myosin filaments that are normally segregated from the extracellular fluid. Once exposed, the myosin can bind the radiolabeled antimyosin antibody. After dosing of ^{111}In-antimyosin, imaging is performed after 24 hours or more to allow background activity to clear. Although this agent has demonstrated high sensitivity and specificity for localizing myocardial infarcts, it is no longer on the market.[120,121]

Technetium Tc 99m Glucaric Acid

Technetium Tc 99m glucaric acid (^{99m}Tc-glucarate) is a six-carbon sugar that was serendipitously found to localize in MIs during the development of a technetium label for the antimyosin antibody.[122] ^{99m}Tc-glucarate is taken up into irreparably damaged myocytes, where it is associated with highly basic histones.[122] In one investigation, it was taken up rapidly into infarcted myocardium early after the event, with best identification occurring when the radiotracer was administered within 9 hours of the infarction.[123] Because it is taken up soon after infarction, ^{99m}Tc-glucarate has a potentially significant advantage over ^{99m}Tc-pyrophosphate and ^{111}In-antimyosin. Further studies will better define its usefulness.

Technetium Tc 99m Annexin V

Technetium Tc 99m annexin V (^{99m}Tc-annexin V) is a radiolabeled form of annexin V, an endogenous protein that has a high affinity for exposed phosphatidylserine on apoptotic cells.[124] Apoptotic cells have been identified in areas of severe ischemia and infarction. During natural apoptosis (programmed cell death) in the body, an enzymatic process is initiated that causes the phospholipid phosphatidylserine to become expressed on the outer membrane surface of dying cells, where it is able to bind the annexin V ligand. The purpose of this interaction is unknown, but the binding affinity between annexin V and phosphatidylserine is high, making ^{99m}Tc-annexin V a potentially good imaging agent.[125] Further studies with this agent are needed to determine whether it has any diagnostic role in cardiac imaging.[126]

^{99m}Tc-Labeled Nitroimidazoles

Hypoxic cell markers are of interest for localizing ischemic tissues and tumors. A number of ^{99m}Tc-labeled hypoxic markers have been developed and are described in more detail in Chapter 9. Much work needs to be done on these agents because of the difficulty in measuring tissue hypoxia and defining the levels of hypoxia that are significant in pathology.

NUCLEAR MEDICINE PROCEDURES

There have been many advances in MPI since it was first introduced by Zaret et al.[127] in 1973, using ^{43}K to evaluate for the presence or absence of CAD. Since that time, advances in hardware and the development of new cardiac perfusion agents have allowed for excellent gated cardiac imaging. The main nuclear medicine applications of cardiac imaging are MPI to assess the distribution of coronary blood flow to the myocardium and gated equilibrium radionuclide ventriculography (RNV) to assess left ventricular performance. First-pass techniques can also be used to evaluate right and left ventricular performance.

MPI is now well established as an effective tool in the evaluation and management of CAD. It is commonly used in patients with known or suspected CAD to assess for the presence of significant ischemia as well as to determine the location and severity of the lesions. MPI can also be used to assess myocardial viability. For patients with known MI, both the size and the severity of the infarct territory can be evaluated. LVEF and left ventricular volumes can also be determined with gated MPI. Event-free cardiac survival has been found to be directly proportional to the LVEF after MI.[128,129] Information obtained during MPI can be used to stratify risk and help determine prognosis.

Gated equilibrium RNV is useful in evaluating ventricular function in patients with congestive heart failure and in patients undergoing chemotherapy with cardiotoxic drugs. Variables such as LVEF, regional wall motion, ES and ED volumes, and peak filling rate can be estimated. If first-pass imaging is performed, right ventricular performance can also be evaluated.

Myocardial Perfusion Imaging

Rationale

MPI uses intravenously administered radiopharmaceuticals to assess coronary blood flow to the myocardium. The radiopharmaceuticals used in MPI are taken up into the myocardium in proportion to blood flow. They can be used to evaluate areas in the myocardium

with reduced blood flow associated with ischemia or scarring. If there is significant coronary artery stenosis, there will be an area or areas of reduced radiotracer uptake in the territory supplied by the affected arteries.

Experiments by Gould et al.[8] in the 1970s, which evaluated mean blood flow in coronary arteries with increasing percent diameter coronary stenosis, demonstrated that coronary blood flow at rest was preserved until the degree of coronary stenosis was severe (Figure 15-2). Normal coronary blood flow is maintained by coronary vascular autoregulation. At rest, the coronary vessels dilate to maintain flow until the degree of stenosis reaches an advanced level of around 90% of the vessel's diameter. During times of stress, such as during exercise, normal coronary vessels can dilate to increase blood flow 3 to 5 times the level at rest. Under these conditions, augmentation of coronary blood flow can be maintained only to an approximately 50% diameter stenosis.[8]

Patients who have significant coronary artery stenosis will have an area of reduced radiopharmaceutical uptake in the myocardium corresponding to the area of reduced perfusion. If the area of reduced uptake in the myocardium is worse during conditions of stress than at rest, the perfusion abnormality is most likely due to ischemia. Information gained during the MPI study can be used not only to identify significant CAD but also to give insight into the patient's prognosis, such as the probability of a hard cardiac event (i.e., MI or cardiac-related death). MPI can help to distinguish low-risk from high-risk cardiac patients, which is important in their clinical management.

Pharmaceuticals

The radiopharmaceuticals currently used for radionuclide MPI are the single-photon–emitting radiotracers ^{99m}Tc-sestamibi, ^{99m}Tc-tetrofosmin, and ^{201}Tl-thallous chloride. The positron emitter ^{82}Rb-rubidium chloride is approved for PET MPI. PET imaging with ^{18}F-FDG can be used to evaluate myocardial viability.

Procedures

Myocardial perfusion studies are obtained to assess coronary ischemia. Studies are obtained both during stress, either exercise induced or pharmacologic, and at rest. The imaging protocol depends on the type of radiopharmaceutical administered and whether the study is done on a single day or over 2 days.

A medical history should be obtained before the stress study. This should include the reason for the exam, symptoms that led to the exam, risk factors for CAD, cardiac history, respiratory history, medications, allergies, and results of any prior studies. A 12-lead ECG should be examined to evaluate for left bundle-branch block, significant arrhythmias, and acute ischemia. Patients should fast for a minimum of 4 hours before the stress exam. The contraindications to both exercise and pharmacologic stress should be reviewed before the study.[130]

If there are no contraindications to exercise stress, it is generally the preferred method. Exercise stress gives further information about the patient, such as the degree of exercise tolerance, time to maximal heart rate, and blood pressure response. If feasible, medications that would interfere with the heart-rate and blood-pressure response, such as β-blockers, should be stopped for an appropriate time before the test.

Often exercise is not an alternative for the patient. In these cases, pharmacologic stress with either a vasodilator such adenosine or an inotropic/chronotropic agent such as dobutamine can be used. There are contraindications for each of these agents. The major contraindications for adenosine include second- or third-degree atrioventricular block, sick sinus syndrome, asthma, wheezing, pulmonary hypertension, or a systolic blood

pressure of less than 90 mm Hg. Dobutamine should not be used if the patient has a ventricular tachyarrhythmia. Neither type of agent should be used just after an acute MI or with unstable angina.

An intravenous line is placed before the stress portion of the exam. If the patient is to undergo exercise stress on a treadmill, the intravenous access must be secure and easily accessible for radiopharmaceutical administration at peak stress.

Thallous Chloride Tl 201 Injection

When ^{201}Tl-thallous chloride is administered intravenously, approximately 4% of the radiotracer is taken up by the myocardium.[57] The first-pass extraction fraction is in the range of 85%. Uptake in the myocardial regions is in proportion to blood flow, and the extraction fraction of the myocardium is linear at normal flow rates. However, the extraction fraction increases at very low blood flow and decreases at very high blood flow rates.[57] ^{201}Tl is a cation that is actively transported into the myocardial cell and depends on the Na-K ATPase pump.[131] Active uptake into the myocardial cells implies that the cells have intact cell membranes and are viable.[132] Thallium is not bound intracellularly. After the initial uptake of thallium into the myocardial tissue, it begins to redistribute. The regional concentration of thallium in the myocardium eventually comes into equilibrium, with the ratio of thallium entering the cell to that leaving the cell becoming constant. However, the rate of redistribution is prolonged in hypoperfused myocardium. Complete redistribution of ^{201}Tl can sometimes take 24 hours or more.[66]

Generally, 2 to 4 mCi (74 to 148 MBq) of ^{201}Tl-thallous chloride is administered intravenously at peak exercise or peak pharmacologic stress. The patient is maintained at peak stress for 1 to 2 more minutes. SPECT imaging is performed as soon as possible after stress. If patients undergo treadmill exercise, they are imaged as soon as deep breathing in response to exercise normalizes to prevent motion artifacts, usually 5 to 10 minutes after the end of stress. The net washout rate of ^{201}Tl-thallous chloride after exercise has a half-life of about 4 hours.[133] SPECT imaging of the heart is usually repeated 4 hours after the stress images for comparison. Images of the heart are usually displayed in three planes as short axis, vertical long axis, and horizontal long axis views (Figure 15-23), with the stress images on top and the corresponding rest images below. Regional defects seen on the stress images are compared with the same regions on the rest images. The stress defects are usually described as fixed, reversible, or partially reversible. If the defect appears fixed or only partially reversible, delayed imaging at 24 hours can be useful to further evaluate the extent of reversibility. An alternative is to reinject the patient with 1 mCi (37 Mbq) of ^{201}Tl-thallous chloride immediately after obtaining the redistribution images to overcome poor count statistics. The reinjection images help to normalize perfusion defects, as does the 24 hour imaging.[67] Reinjection can also be done at 24 hours. Fixed defects seen on the 4 hour redistribution images that show normal or improved ^{201}Tl uptake after reinjection are consistent with ischemic and viable myocardium (Figure 15-24). ^{201}Tl MPI studies are usually not gated in standard practice because of the low photon energies associated with thallium and the long half-life, which limits the administered dose to 2 to 4 mCi (74 to 148 MBq).

^{99m}Tc Agents

Because of the short 6 hour half-life of ^{99m}Tc, a much larger dose of ^{99m}Tc agents than of ^{201}Tl-thallous chloride can be administered. Also, there is less attenuation and scatter compared with ^{201}Tl because of the higher 140 keV photopeak of ^{99m}Tc. These properties result in a larger photon flux, which allows for gated imaging to evaluate regional ventricular wall

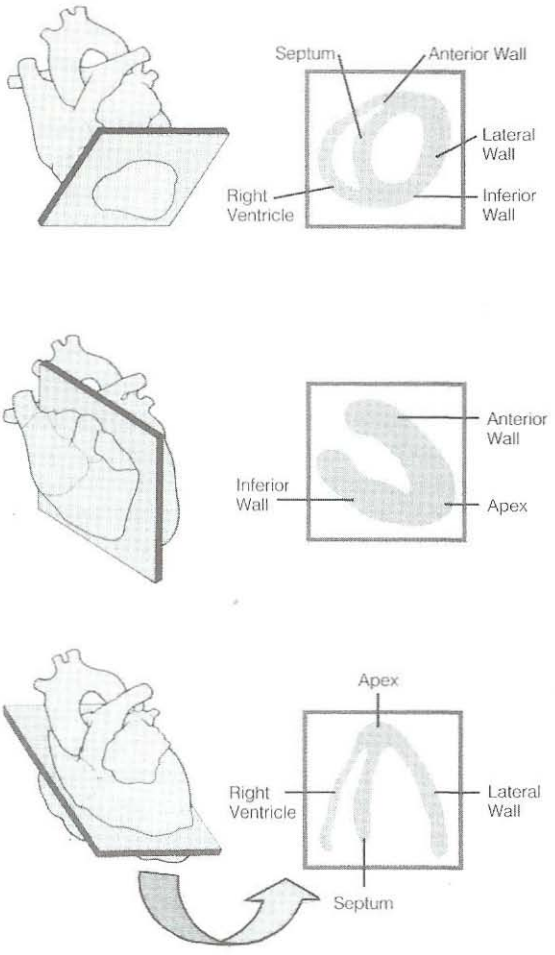

FIGURE 15-23 Cardiac tomography. Diagram of short-axis (top), vertical long-axis (middle), and horizontal long-axis (bottom) views of myocardial walls on SPECT imaging. (Reprinted with permission of Bristol-Myers Squibb Medical Imaging, Inc. from *Introduction to Nuclear Cardiology*, 3rd ed. North Billerica, MA: DuPont Pharma Radiopharmaceuticals; 1993:261.)

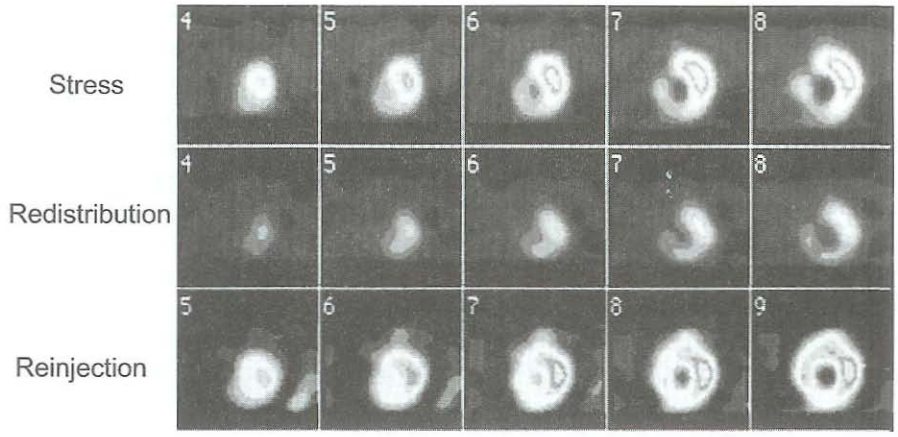

FIGURE 15-24 Adenosine ^{201}Tl stress–rest–reinjection myocardial perfusion study. Short-axis stress images (top row) and redistribution images obtained 4 hours later (second row) demonstrate perfusion defects involving the septum and inferior walls of the heart with poor washout over the 4 hour period. Images obtained 24 hours later just after reinjection with 1 mCi (37 MBq) ^{201}Tl at rest (bottom row) show improvement in the septum and inferior walls consistent with ischemia and viable myocardium in these regions.

motion. The higher administered dose also improves resolution of the images. The most commonly used compounds are ^{99m}Tc-sestamibi and ^{99m}Tc-tetrofosmin. Like ^{201}Tl-thallous chloride, these compounds are taken up in the myocardium in proportion to blood flow. Unlike ^{201}Tl-thallous chloride, they passively diffuse across the cell membrane, bind to mitochondria, and exhibit limited redistribution. Because of the limited redistribution, ^{99m}Tc-agent protocols are different from ^{201}Tl-thallous chloride protocols.

Several injection/imaging protocols can be used. One day protocols are most frequently used. However, if the patient is obese, 2 day protocols can be used to maximize the radiotracer dose both at rest and during stress. A common 1 day protocol is the rest–stress protocol (Figure 15-15). Typically 8 to 10 mCi (296 to 370 MBq) of a ^{99m}Tc agent is injected at rest, and the patient is imaged 1 hour later. One to four hours after the rest images, 25 to 30 mCi (925 to 1110 MBq) of the ^{99m}Tc agent is injected at peak stress. Imaging is repeated 30 minutes later if the patient underwent exercise stress or 60 minutes later if the stress was pharmacologic. If a 2 day protocol is used, 25 to 30 mCi (925 to 1110 MBq) of the ^{99m}Tc agent is administered both at rest and during stress, and either the rest or the stress measurements can be done on the first day.

Dual-Isotope Protocols

Some nuclear medicine clinics use a dual-isotope protocol to decrease the overall study time. In this protocol 3 to 4 mCi (111 to 148 MBq) of ^{201}Tl-thallous chloride is administered at rest, and images are obtained about 15 minutes later (Figure 15-16). About 30 minutes after the rest images are completed, the patient is stressed with exercise or pharmacologically, and 25 to 30 mCi (925 to 1110 MBq) of a ^{99m}Tc agent is administered at peak stress. The stress images are obtained 30 to 60 minutes later, depending on whether the patient underwent exercise or pharmacologic stress, respectively.

PET Myocardial Perfusion Imaging

As PET technology continues to advance and the number of clinical PET scanners increases, PET MPI is also increasing. Currently ^{82}Rb-rubidium chloride is approved for PET MPI. ^{82}Rb is a positron-emitting cation that is taken up into the myocardial cells in relation to coronary artery blood flow similar to both potassium and ^{201}Tl.[134] ^{82}Rb can be obtained from an ^{82}Sr–^{82}Rb generator, which has a shelf life of about 4 to 6 weeks. There are advantages to using this agent because of its very short half-life (only 75 seconds) and high photon energy (511 keV). The short half-life allows for a larger administered dose, faster protocols, and lower radiation exposure of the patient. The 511 keV photon energy offers better attenuation correction and higher sensitivity as the result of electronic collimation. A typical ^{82}Rb-rubidium chloride protocol involves injecting 60 mCi (2220 MBq) ^{82}Rb-rubidium chloride at rest, followed by gated imaging. After rest imaging is completed, the patient is stressed with either exercise or a pharmacologic agent. Sixty mCi of ^{82}Rb-rubidium chloride is again injected at peak stress and repeat gated imaging is done. The length of the protocol is often less than 1 hour.

PET cardiac imaging with FDG is valuable in the assessment of myocardial viability. FDG is increased in ischemic viable myocardium but decreased in infarcted myocardium.

Interpretation

Normally, when there is increased demand on the heart secondary to exercise or pharmacologic stress, blood flow increases in the coronary vessels and there is increased

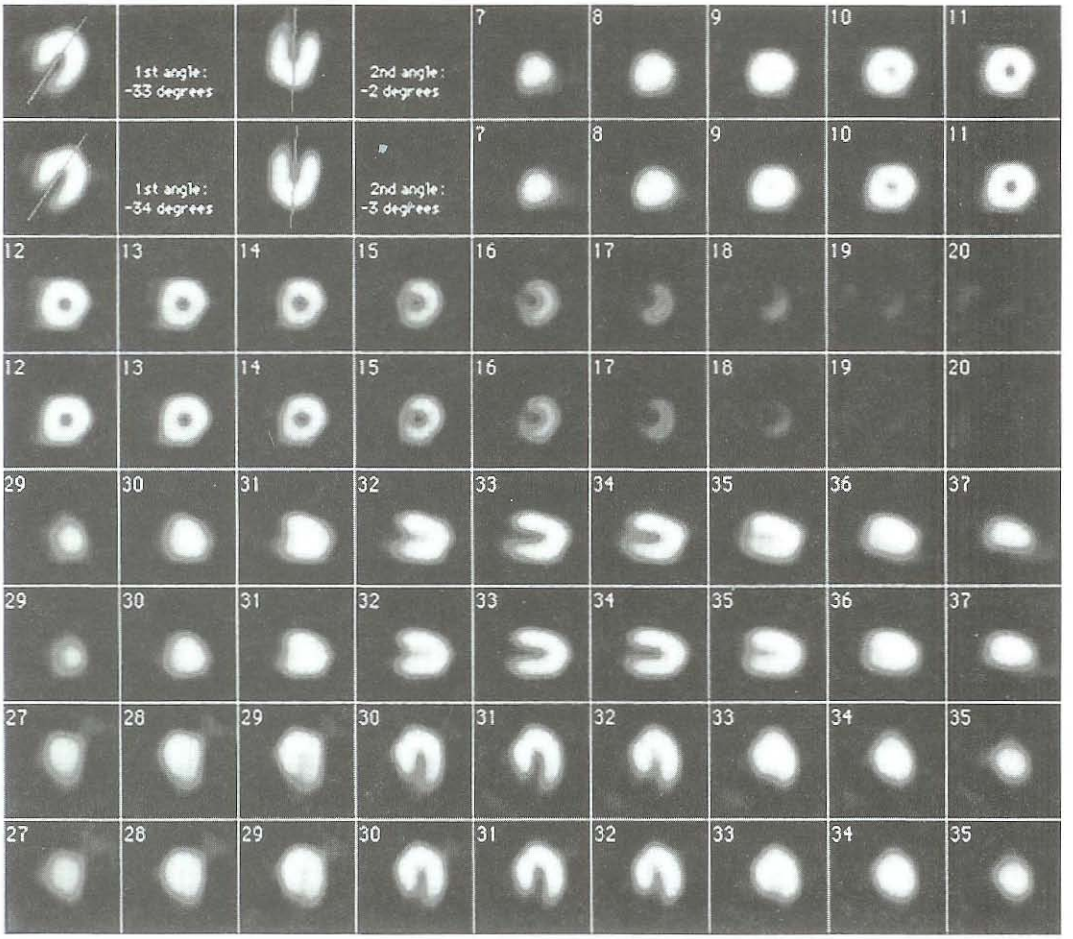

FIGURE 15-25 Normal ^{99m}Tc-sestamibi myocardial perfusion study. Images of the heart are shown in three planes. The top row represents short-axis views of the heart from apex on the left to midheart on the right at stress. Matching views on the rest portion of the study are shown in the next row. The third and fourth rows are continuation of the short-axis views at stress and rest from the midheart to the base or valve plane. The next two rows (frames 29 to 37) are the vertical long-axis views, stress on top and rest below; these views are from the septum on the left to the lateral wall on the right. The last two rows are the horizontal long-axis views, stress on top and rest below; these views run from the inferior wall on the left to the anterior wall on the right. No significant perfusion defects are seen either during stress or at rest to suggest flow-limiting coronary artery disease.

radiotracer uptake in the myocardium related to the increased blood flow. If there are no perfusion abnormalities during stress, there is homogeneous radiotracer uptake throughout the myocardium. In a normal study using a ^{99m}Tc agent, no perfusion abnormalities are seen on either the stress or rest images (Figure 15-25). If ^{201}Tl-thallous chloride is used, there are no perfusion defects seen in the stress images and there is appropriate washout from the myocardium 4 hours later on the redistribution images (Figure 15-26).

Myocardial regions with reduced radiopharmaceutical uptake on the stress portion of the myocardial perfusion study that normalize or partially normalize on the rest study represent regions of stress-induced ischemia associated with flow-limiting CAD (Figure 15-27). Myocardial regions with fixed perfusion defects on both the stress and rest portions

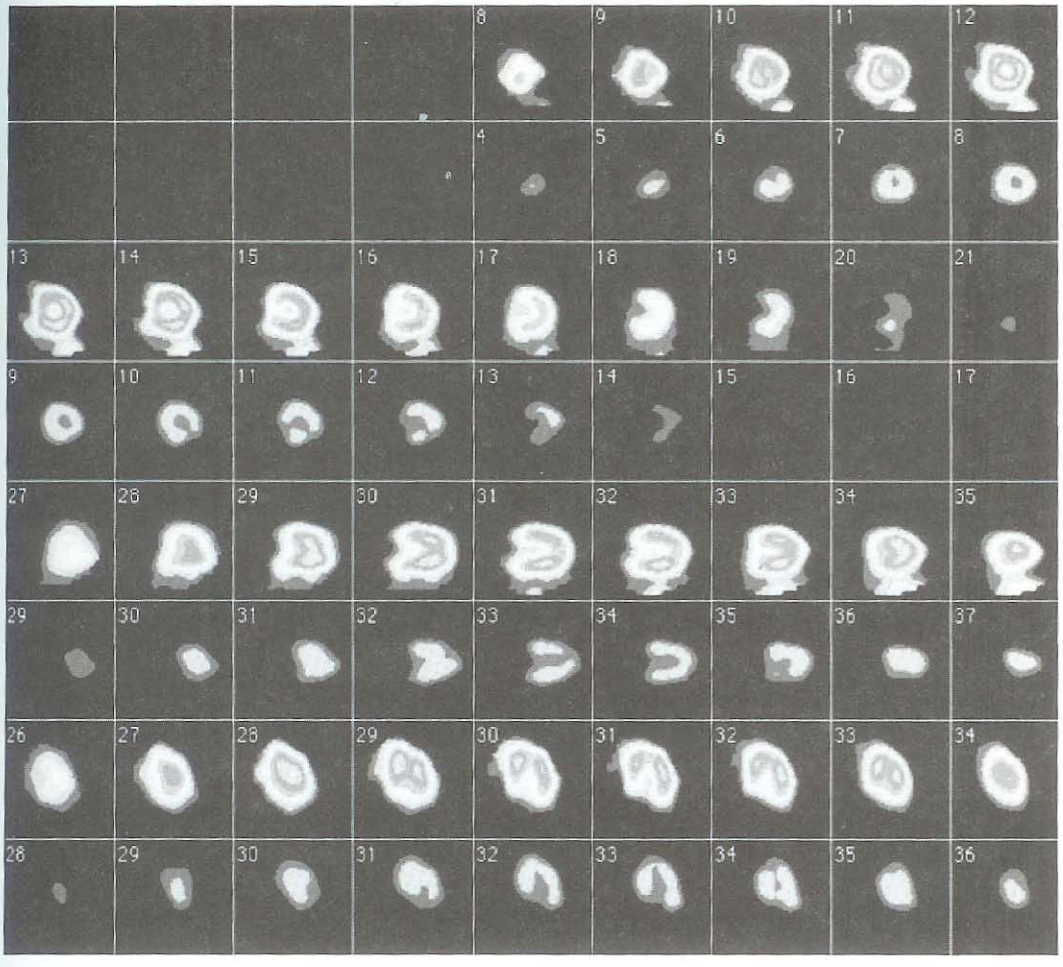

FIGURE 15-26 Normal ^{201}Tl-thallous chloride myocardial perfusion study. Stress images are on top and rest images below. Again, images of the heart are shown in three planes. The top four rows are the short-axis views from apex on the left to base on the right. The next two rows are the vertical long-axis views, stress on top and rest below. The last two rows are the horizontal long-axis views, stress on top and rest below. This study shows no significant perfusion defects during stress and good washout of the radiotracer on the redistribution images obtained 4 hours after stress.

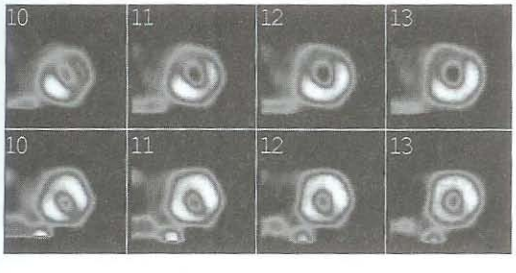

FIGURE 15-27 ^{99m}Tc-sestamibi study demonstrating myocardial ischemia. Short-axis views during stress (top row) and at rest (bottom row). Significant perfusion defects are seen on the stress portion of the study that are not present at rest, consistent with multivessel flow-limiting coronary artery disease.

of the exam can represent either scarring from prior MI (Figures 15-28 and 15-29) or possibly an attenuation artifact, usually caused by the diaphragm or breast. Gated SPECT allows further evaluation of fixed perfusion defects by examination of wall motion and

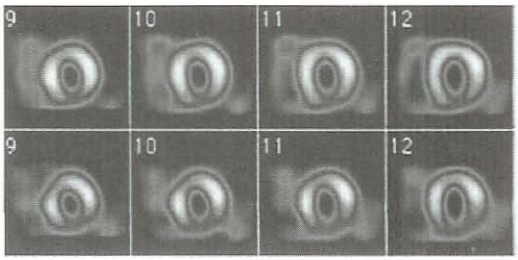

FIGURE 15-28 ^{99m}Tc sestamibi study demonstrating a fixed defect in the inferior wall both during stress and at rest. There was hypokinesis in the inferior wall on the gated images as well as decreased thickening in the inferior wall during systole most consistent with scarring from a prior myocardial infarction.

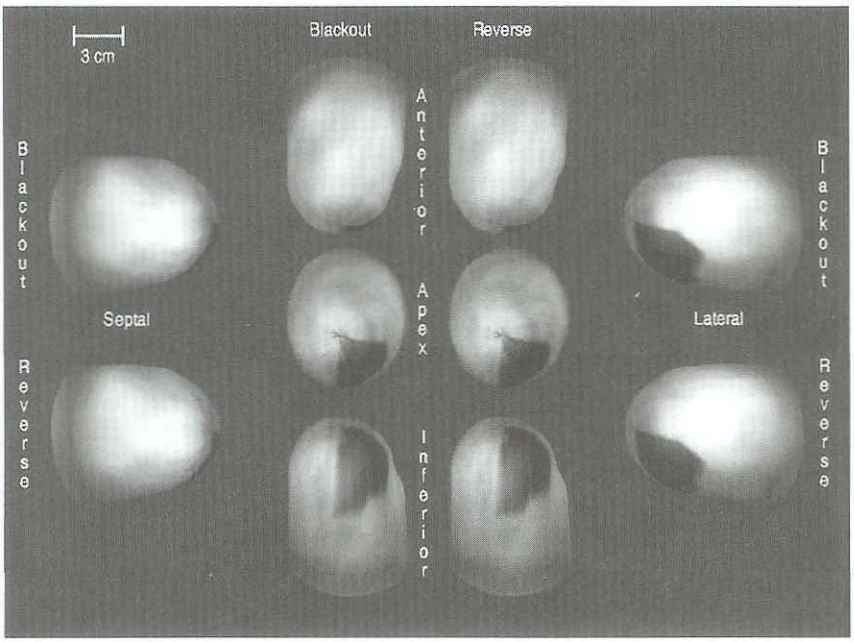

FIGURE 15-29 Three-dimensional blackout–reversibility map for the study shown in Figure 15-28, demonstrating a fixed perfusion defect (black area) in the inferior wall. Significant reversibility or ischemia would be seen as a white area in the blackout region on the reverse images but is not seen in this case.

myocardial thickening. Fixed perfusion defects with normal wall motion and thickening are likely related to attenuation artifacts. Fixed defects with abnormal focal wall motion abnormalities and decreased thickening are generally associated with scar.

Gated Equilibrium Radionuclide Ventriculography

Gated equilibrium RNV, also known as gated blood pool imaging or multigated acquisition (MUGA), is an imaging technique in which the patient's red blood cells are labeled and then gated cardiac image data are collected. The technique was developed in the early 1970s.[135] First, radiotracer must be used to label the blood pool in a stable manner. Then electrocardiographic gating of the acquisition is done based on the R wave of the ECG. Image data are collected and analyzed by computer.

Rationale

The RNV is a noninvasive way of evaluating left ventricular performance. LVEF is calculated from the data, and other parameters such as left ventricular ED and ES volumes and

peak filling rate, which is a measure of left ventricular compliance, can be estimated. These values can be used to assess performance after an acute MI. They can also serve to determine baseline function as well as follow-up after treatment in cardiomyopathies and congestive heart failure. One of the most common indications is following the performance of the heart after administration of cardiotoxic drugs such as doxorubicin used in chemotherapy. Usually a baseline RNV is obtained before the first chemotherapy treatment. An RNV is then performed just before each cycle of chemotherapy to determine if there has been a significant decrease in cardiac performance and if it is safe to administer another cycle.

Pharmaceuticals

Although any radiopharmaceutical that compartmentalizes into the intravascular space can be used for RNV, the most common technique is to use ^{99m}Tc-labeled autologous RBCs. Three methods are commonly used to label the patient's RBCs: the in vivo method, the modified in vivo method, and the in vitro method. The in vivo method involves initially injecting the patient with 0.5 to 1.0 mg stannous ion as Sn-PPi. Twenty minutes after injection of Sn-PPi, 20 to 30 mCi (740 to 1110 MBq) ^{99m}Tc-sodium pertechnetate is administered intravenously. The intracellular stannous ion acts as a reducing agent, which enables binding of ^{99m}Tc to the β-chain of hemoglobin, thus labeling the RBC. More efficient labeling can be obtained with the modified in vivo technique. In this method, 10 mL of the patient's blood is drawn into a syringe containing 20 to 30 mCi (740 to 1110 MBq) of ^{99m}Tc-sodium pertechnetate 20 minutes after intravenous injection of Sn-PPi. The mixture is incubated for 10 minutes and then injected into the patient.

The most efficient method for labeling RBCs is the in vitro technique. In this method, the patient's RBCs are labeled outside the body using a ^{99m}Tc Ultratag (Mallinckrodt) kit. All of these methods are adequate for autologous RBC labeling with ^{99m}Tc. In general practice, the in vivo technique is most commonly used because it is the easiest and there is no chance of accidentally injecting a patient with another person's labeled RBCs.

Procedure

In the in vivo labeling method, the patient is first injected with Sn-PPi to tin the RBCs. About 20 minutes later, the patient is injected with 20 to 30 mCi (740 to 1110 MBq) of ^{99m}Tc-sodium pertechnetate. The patient is usually positioned in the left anterior oblique (LAO) position for visualization of the heart. Sometimes a craniocaudal tilt is necessary to visualize the left ventricle and septum. If a craniocaudal tilt is applied, this is called a modified LAO position. Gated images of the heart are then obtained. Gating of the images is based on the R-R cardiac interval. The R-R interval is divided into 16 to 32 segments, and the computer begins data collection at the beginning of the R wave (Figure 15-20). Data are collected in these time bins over several cardiac cycles. The images can then be played back as a set of dynamic images to visualize cardiac contraction and evaluate for regional wall motion abnormalities. Regions of interest can be drawn around the left ventricle in diastole and in systole to determine the LVEF using the formula previously described.

Interpretation

The cardiac images are played back in a cinematic loop to visually evaluate regional left and right ventricular wall motion. The ventricular walls should contract and the septum

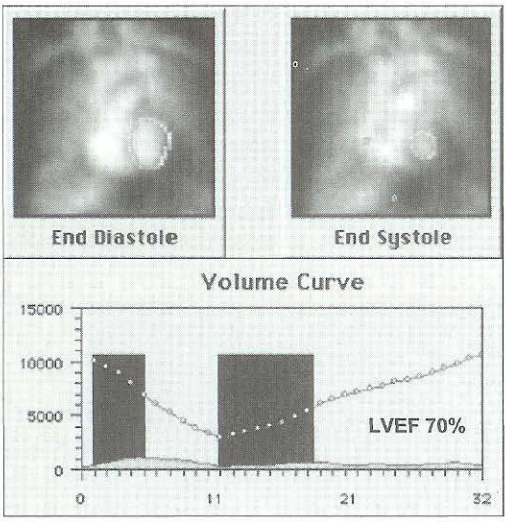

FIGURE 15-30 Normal multigated acquisition (MUGA) study. Left anterior oblique (LAO) images of the heart. Regions of interest drawn around the left ventricle at end-diastole and end-systole gave a calculated left ventricular ejection fraction of 70%. There were no regional wall motion abnormalities on the gated images.

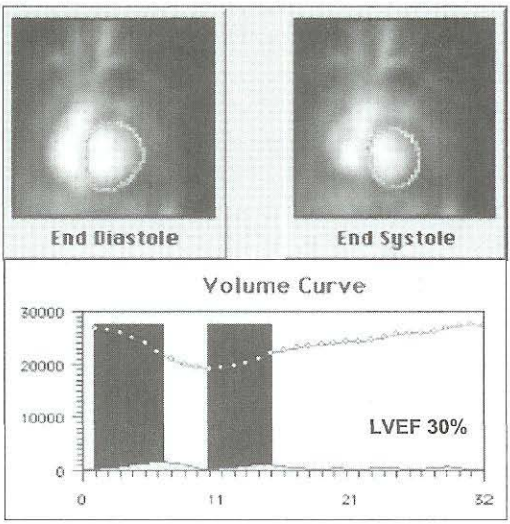

FIGURE 15-31 Abnormal MUGA study in a patient with congestive heart failure. LAO images of the heart. Regions of interest drawn around the left ventricle at end-diastole and end-systole gave a calculated left ventricular ejection fraction of only 30%. Although no focal wall motion abnormalities were noted, there was global left ventricular hypokinesis.

should thicken during systole (Figure 15-30). Cardiac wall motion is referred to as normal, hypokinetic, akinetic, or dyskinetic. Hypokinesis refers to diminished wall motion compared with normal (Figure 15-31). Akinetic means lack of wall motion, and dyskinetic refers to paradoxical wall motion as might be seen with an aneurysm. Normally the septum moves less than the other walls, with the greatest motion usually seen in the anterior, lateral, and posterior walls. The septum should thicken during systole. Dyskinetic septal motion can be seen with scarring from an MI. It can also be seen secondary to prior coronary artery bypass surgery.

First-Pass Radionuclide Angiocardiography

First-pass radionuclide angiocardiography involves imaging a bolus of radiopharmaceutical as it passes through the heart. The technique allows for evaluation of both the right and left ventricular ejection fraction. Since a bolus of activity is followed through the heart, the acquisition can be performed in just a few seconds. The technique can be used either at rest or during stress.

Rationale

The first-pass technique can be used to evaluate both right and left heart performance. However, because the configuration of the right ventricle makes it difficult to evaluate with equilibrium techniques, first-pass is a practical technique for determining right ventricular ejection fraction. Right heart function may be of value in assessing cardiomyopathies and pulmonary-related cardiac disease.

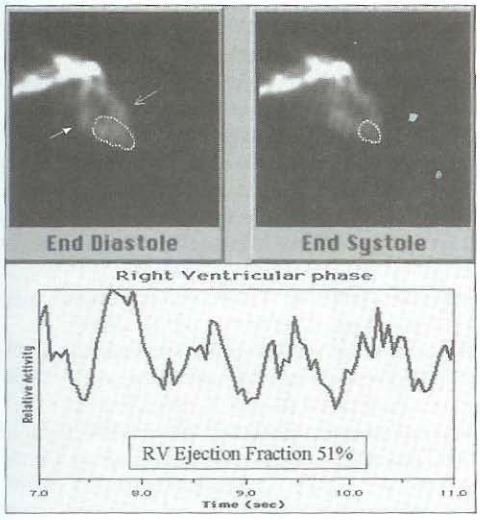

FIGURE 15-32 Normal first-pass study to evaluate right ventricular performance. Shortly after injection of a 30 mCi (1110 MBq) bolus of ^{99m}Tc-sodium pertechnetate into a right arm vein, radiotracer can be seen in the superior vena cava, right atrium (left arrow), right ventricle (dotted region), and pulmonary outflow tract (left arrow). The right ventricle can be isolated because radiotracer has not yet advanced to the lungs or left ventricle. A time–activity curve for the right ventricle was used to determine right ventricular end-diastole and end-systole. Regions of interest drawn around the right ventricle during end-diastole and end-systole gave a normal estimated right ventricular ejection fraction of 51%.

Procedure

In the first-pass technique, a small-volume, high-concentration radiotracer bolus (typically 20 to 30 mCi [740 to 1110 MBq] of ^{99m}Tc-sodium pertechnetate) is administered rapidly into a vein near the heart. Some people prefer to use the external jugular vein for this purpose. However, in most nuclear clinics a large antecubital vein is used. The patient is imaged in the 30° right anterior oblique position or anterior position over several heart cycles. Rapidly acquired image frames are obtained to observe the bolus as it passes through the heart. Ejection fraction measurements for both the right and left ventricles can be obtained by measuring the change in activity over time in each of these regions.

Interpretation

When the radiotracer bolus is administered into a large antecubital vein such as the median basilic vein, serial images show progression of the bolus front from the basilic vein into the subclavian vein, then to the superior vena cava and into the right atrium. When the right atrium contracts, the bolus advances through the tricuspid valve into the right ventricle. Next, when the right ventricle contracts, radiotracer enters the pulmonary outflow tract and moves into the lungs, left atrium, left ventricle, and aorta. During the first couple of beats, the right ventricle can be isolated on the images (Figure 15-32). Regions of interest can be drawn around the right ventricle during diastole and systole and a right ventricular ejection fraction can be estimated using the following formula:

$$\text{RVEF} = \frac{(\text{ED counts}) - (\text{ES counts})}{(\text{ED counts}) - (\text{Bkg counts})}$$

REFERENCES

1. Davidson, DM. *Preventive Cardiology.* Baltimore: Williams & Wilkins; 1991.
2. Bianco JA, Wilson MA. Myocardial ischemia and viability. In: Wilson MA, ed. *Textbook of Nuclear Medicine.* Philadelphia: Lippincott-Raven; 1998:33-66.

3. Marcus ML, Harrison DG. Physiologic basis for myocardial perfusion imaging. In: Marcus ML, Skorton DH, Schelbert HR, et al., eds. *Cardiac Imaging*. Philadelphia: WB Saunders; 1991.
4. Guyton AC. *Textbook of Medical Physiology*. 6th ed. Philadelphia: WB Saunders; 1981.
5. Holmberg S, Serzysko W, Varnauskas E. Coronary circulation during heavy exercise in control subjects and patients with coronary heart disease. *Acta Med Scand*. 1971;190:465-80.
6. Heiss HW, Barmeyer J, Wink K, et al. Studies on the regulation of myocardial blood flow in man. I: Training effects on blood flow and metabolism of the healthy heart at rest and during standardized heavy exercise. *Basic Res Cardiol*. 1976;71:658-75.
7. Brown GB, Josephson MA, Petersen RB, et al. Intravenous dipyridamole combined with isometric handgrip for near maximal acute increase in coronary flow in patients with coronary artery disease. *Am J Cardiol*. 1981;48:1077-82.
8. Gould KL, Lipscomb K, Hamilton GW. Physiologic basis for assessing critical coronary stenosis. *Am J Cardiol*. 1974;33:87-94.
9. Gould KL. Noninvasive assessment of coronary stenoses by myocardial perfusion imaging during pharmacologic coronary vasodilation. I: Physiologic basis and experimental validation. *Am J Cardiol*. 1978;41:267-78.
10. Gould KL. Myocardial viability: what does it mean and how do we measure it? *Circulation*. 1991;83:333-5.
11. Schelbert HR, Buxton D. Insights into coronary artery disease gained from metabolic imaging. *Circulation*. 1988;78:496-505.
12. Bonow RO, Dilsizian V, Cuocolo A, et al. Myocardial viability in patients with chronic coronary artery disease and left ventricular dysfunction: thallium-201 reinjection versus 18F-fluorodeoxyglucose. *Circulation*. 1991;83:26-37.
13. Bruce RA. Multi-stage treadmill test of submaximal and maximal exercise. In: *Exercise Testing and Training of Apparently Healthy Individuals: A Handbook for Physicians*. New York: American Heart Association; 1972.
14. Wolthuis RA, Froelicher VF, Fischer J, et al. The response of healthy men to treadmill exercise. *Circulation*. 1977;55:153-7.
15. Kariv I, Kellerman JJ. Effects of exercise on blood pressure. *Mal Cardiovasc*. 1969;10:247-52.
16. Holmberg S, Serysko W, Varnauskas E. Coronary circulation during heavy exercise in control subjects and patients with coronary heart disease. *Acta Med Scand*. 1971;190:465-80.
17. Wackers FJ. Exercise myocardial perfusion imaging. *J Nucl Med*. 1994;35:726-9.
18. Leppo JA. Dipyridamole myocardial perfusion imaging. *J Nucl Med*. 1994;35:730-3.
19. Iskandrian AS. Adenosine myocardial perfusion imaging. *J Nucl Med*. 1994;35:734-6.
20. Leppo JA. Dipyridamole-thallium imaging: the lazy man's stress test. *J Nucl Med*. 1989;30:281-7.
21. Verani MS, Mahmarian JJ, Hixson JB, et al. Diagnosis of coronary artery disease by controlled coronary vasodilation with adenosine and thallium-201 scintigraphy in patients unable to exercise. *Circulation*. 1990;82:80-7.
22. Wackers FJ. Adenosine or dipyridamole: which is preferred for myocardial perfusion imaging? *J Am Coll Cardiol*. 1991;17:1295-6.
23. Verani MS. Dobutamine myocardial perfusion imaging. *J Nucl Med*. 1994;35:737-9.
24. Wilson RF, Wyche K, Christensen BV, et al. Effects of adenosine on human coronary arterial circulation. *Circulation*. 1990;82:1595-1606.
25. Möser GH, Schrader J, Deussen A. Turnover of adenosine in plasma of human and dog blood. *Am J Physiol*. 1989;256:C799-806.
26. Klabunde RE. Dipyridamole inhibition of adenosine metabolism in human blood. *Eur J Pharmacol*. 1983;93:21-6.
27. Smits P, Aengevaeren WRM, Corstens FHM, et al. Caffeine reduces dipyridamole-induced myocardial ischemia. *J Nucl Med*.1989;30:1723-6.
28. Lee J, Heo J, Ogilby JS, et al. Atrioventricular block during adenosine thallium imaging. *Am Heart J*. 1992;123:1569-73.
29. Taviot B, Pavheco Y, Coppere B, et al. Bronchospasm induced in an asthmatic by the injection of adenosine. *Presse Med*. 1986;15:1103.
30. Holgate ST, Mann JS, Cushley MJ. Adenosine as a bronchoconstrictor mediator in asthma and it antagonism by methylxanthines. *J Allergy Clin Immunol*. 1984;74:302-6.
31. Berman DS, Kiat HS, Van Train KF, et al. Myocardial perfusion imaging with technetium-99m-sestamibi: comparative analysis of available imaging protocols. *J Nucl Med*. 1994;35:681-8.
32. Brown G, Josephson MA, Petersen RD, et al. Intravenous dipyridamole combined with isometric handgrip for near maximal coronary flow in patients with coronary artery disease. *Am J Cardiol*. 1981;48:1077-85.
33. McNeil AJ, Fioretti PM, El-Said ME-S, et al. Enhanced sensitivity for detection of coronary artery disease by addition of atropine to dobutamine stress echocardiography. *Am J Cardiol*. 1992;70:41-6.

34. Kowalsky RJ, Perry JR. Evaluation of intravenous infusion systems for adenosine. *J Nucl Med Technol.* 1992;20:215-9.
35. Wackers FJ. Adenosine or dipyridamole: which is preferred for myocardial perfusion imaging? *J Am Coll Cardiol.* 1991;17:1295-6.
36. Ranhosky A, Kempthrone-Rawson J. The safety of intravenous dipyridamole thallium myocardial perfusion imaging. *Circulation.* 1990;81:1205-9.
37. Wackers FJ. Adenosine-thallium imaging: faster and better? *J Am Coll Cardiol.* 1990;16:1384-6.
38. Miller DD, Labovitz AJ. Dipyridamole and adenosine vasodilator stress for myocardial imaging: vive la difference! *J Am Coll Cardiol.* 1994;23:390-2.
39. Hays JT, Mahmarian JJ, Cochran AJ, et al. Dobutamine thallium-201 tomography for evaluating patients with suspected coronary artery disease unable to undergo exercise or vasodilator pharmacologic stress testing. *J Am Coll Cardiol.* 1993;21:1583-90.
40. Weich H, Strauss WH, D'Agostino R, et al. Determination of extraction fraction by a double-tracer method. *J Nucl Med.* 1977;18:226-30.
41. Leppo JA, Meerdink DJ. Comparative myocardial extraction of two technetium-labeled BATO derivatives (SQ30217, SQ32014) and thallium. *J Nucl Med.* 1990;31:67-74.
42. Schelbert HR. Principles of positron emission tomography. In: Marcus ML, Skorton DH, Schelbert HR, et al., eds. *Cardiac Imaging.* Philadelphia: WB Saunders; 1991;1140-68.
43. Berman DS, Kiat H, Leppo J, et al. Technetium-99m myocardial perfusion imaging agents. In: Marcus ML, Skorton DH, Schelbert HR, et al., eds. *Cardiac Imaging.* Philadelphia: WB Saunders; 1991:1097-1109.
44. Leppo JA, Meerdink DJ. Comparison of the myocardial uptake of a technetium-labeled isonitrile analogue and thallium. *Circ Res.* 1989;65:632-9.
45. Pohost GM, Alpert NM, Ingwall JS, et al. Thallium redistribution: mechanisms and clinical utility. *Semin Nucl Med.* 1980;10:70-93.
46. Chiu ML, Kronauge JF, Piwnica-Worms D. Effect of mitochondrial and plasma membrane potentials on accumulation of hexakis(2-methoxyisobutylisonitrile) technetium(I) in cultured mouse fibroblasts. *J Nucl Med.* 1990;31:1646-53.
47. Stewart RE, Schwaiger M, Hutchins GD, et al. Myocardial clearance kinetics of technetium-99m–SQ30217: a marker of regional myocardial blood flow. *J Nucl Med.* 1990;31:1183-90.
48. Chervu LR. Radiopharmaceuticals in cardiovascular nuclear medicine. *Semin Nucl Med.* 1979;9:241-56
49. Deutsch E, Glavan KA, Sodd VJ, et al. Cationic Tc-99m complexes as potential myocardial imaging agents. *J Nucl Med.* 1981;22:897-907.
50. Jones AG, Abrams MJ, Davison A, et al. Biological studies of a new class of technetium complexes: the hexakis (alkylisonitrile) technetium (I) complexes. *Int J Nucl Med Biol.* 1984;11:225-34.
51. Wackers FJ, Berman DS, Maddahi J, et al. Technetium-99m hexakis 2-methoxyisobutyl isonitrile: human biodistribution, dosimetry, safety, and preliminary comparison to thallium-201 for myocardial perfusion imaging. *J Nucl Med.* 1989;30:301-11.
52. Narra RK, Nunn AD, Kuczynski BL, et al. A neutral technetium-99m complex for myocardial imaging. *J Nucl Med.* 1989;30:1830-7.
53. Kelly JD, Forster AM, Higley B, et al. Technetium-99m-tetrofosmin as a new radiopharmaceutical for myocardial perfusion imaging. *J Nucl Med.* 1993;34:222-7.
54. Higley B, Smith FW, Smith T, et al. Technetium-99m-1,2-bis[bis(2-ethoxyethyl)phosphino]ethane: human biodistribution, dosimetry, and safety of a new myocardial perfusion imaging agent. *J Nucl Med.* 1993;34:30-8.
55. Atkins HL, Budinger TF, Lebowitz E, et al. Thallium-201 for medical use. 3: Human distribution and physical imaging properties. *J Nucl Med.* 1977;18:133-40.
56. Hamilton GW, Narahara KA, Yee H, et al. Myocardial imaging with thallium-201: effect of cardiac drugs on myocardial images and absolute tissue distribution. *J Nucl Med.* 1978;19:10-16.
57. Weich HF, Strauss WH, Pitt B. The extraction of thallium-201 by the myocardium. *Circulation.* 1977;56:188-91.
58. Meerdink DJ, Leppo JA. Comparison of hypoxia and ouabain effects on the myocardial uptake kinetics of technetium-99m hexakis 2-methoxyisobutyl isonitrile and thallium-201. *J Nucl Med.* 1989;30:1500-6.
59. Maublant JC, Gachon P, Moins N. Hexakis (2-methoxyisobutylisonitrile) technetium-99m and thallium-201 chloride: uptake and release in cultured myocardial cells. *J Nucl Med.* 1988;29:48-54.
60. Ritchie JL, Hamilton GW. Biologic properties of thallium. In: Ritchie JL, Hamilton GW, Wackers FJ, eds. *Thallium-201 Myocardial Imaging.* New York: Raven Press; 1978:9-28.
61. Dilsizian V, Bonow RO. Current diagnostic techniques of assessing myocardial viability in patients with hibernating and stunned myocardium. *Circulation.* 1993;87:1-20.
62. Pohost GM, Zir LM, Moore RH, et al. Differentiation of transiently ischemic from infarcted myocardium by serial imaging after a single dose of thallium-201. *Circulation.* 1977;55:294-302.

63. Blood DK, McCarthy DM, Sciacca RR, et al. Comparison of single-dose and double-dose thallium-201 myocardial perfusion scintigraphy for the detection of coronary artery disease and prior myocardial infarction. *Circulation.* 1978;58:777-8.
64. Ritchie JL, Albro PC, Caldwell JH, et al. Thallium-201 myocardial imaging: a comparison of the redistribution and rest images. *J Nucl Med.* 1979;20:477-83.
65. Gutman J, Berman DS, Freeman M, et al. Time to completed redistribution of thallium-201 in exercise myocardial scintigraphy: relationship to the degree of coronary artery stenosis. *Am Heart J.* 1983;106:989-95.
66. Kiat H, Berman DS, Maddahi J, et al. Late reversibility of tomographic myocardial thallium-201 defects: an accurate marker of myocardial viability. *J Am Coll Cardiol.* 1988;12:1456-63.
67. Dilsizian V, Rocco TP, Freedman NMT, et al. Enhanced detection of ischemic but viable myocardium by the reinjection of thallium after stress-redistribution imaging. *N Engl J Med.* 1990;323:141-6.
68. Kayden DS, Sigal S, Soufer R, et al. Thallium-201 for assessment of myocardial viability: quantitative comparison of 24-hour redistribution imaging with imaging after reinjection at rest. *J Am Coll Cardiol.* 1991;18:1480-6.
69. Bonow RO. Identification of viable myocardium. *Circulation.* 1996;94:2674-80.
70. Ohtani H, Tamaki N, Yonekura Y, et al. Value of thallium-201 reinjection after delayed SPECT imaging for predicting reversible ischemia after coronary artery bypass grafting. *Am J Cardiol.* 1990;66:394-9.
71. Kitsiou AN, Srinivasan G, Quyyumi AA, et al. Stress-induced reversible and mild-to-moderate irreversible thallium defects: are they equally accurate for predicting recovery of regional left ventricular function after revascularization? *Circulation.* 1998;98:501-8.
72. Mousa SA, Cooney JM, Williams SJ. Relationship between regional myocardial blood flow and the distribution of Tc-99m sestamibi in the presence of total coronary artery occlusion. *Am Heart J.* 1990;119:842-7.
73. Piwnica-Worms D, Kronauge JF, Chiu ML. Uptake and retention of hexakis (2-methoxyisobutyl isonitrile) technetium(I) in cultured chick myocardial cells: mitochondrial and plasma membrane potential dependence. *Circulation.* 1990;5:1826-38.
74. Carvalho PA, Chiu ML, Kronauge JF, et al. Subcellular distribution and analysis of technetium-99m-MIBI in isolated perfused rate hearts. *J Nucl Med.* 1992;33:1516-21.
75. Okada RD, Glover D, Gaffney T, et al. Myocardial kinetics of technetium-99m-hexakis-2-methoxy-2-methylpropyl-isonitrile. *Circulation.* 1988;77:491-8.
76. Glover DK, Okada RD. Myocardial kinetics of Tc-MIBI in canine myocardium after dipyridamole. *Circulation.* 1990;81:628-37.
77. Li QS, Solot G, Frank TL, et al. Myocardial redistribution of technetium 99m-hexakis-2-methoxy-2-methylpropyl-isonitrile (SESTAMIBI). *J Nucl Med.* 1990;31:1069-76.
78. Cardiolite [package insert]. Billerica, MA: Dupont Pharmaceuticals; 2000.
79. Radiation Internal Dose Information Center. *Radiation Dose Estimates for Radiopharmaceuticals*. Oak Ridge, TN: Radiation Internal Dose Information Center, 1996.
80. Taillefer R, Laflamme L, Dupras G, et al. Myocardial perfusion imaging with Tc-99m-methoxy-isobutyl-isonitrile (MIBI): comparison of short and long time intervals between rest and stress injections: preliminary results. *Eur J Nucl Med.* 1988;13:515-22.
81. Taillefer R. Gagnon A, Laflamme L, et al. Same day injections of Tc-99m methoxy isobutyl isonitrile (hexamibi) for myocardial tomographic imaging: comparison between rest-stress and stress-rest injection sequences. *Eur J Nucl Med.* 1989;5:113-7.
82. Leppo JA, DePuey GE, Johnson LL. A review of cardiac imaging with sestamibi and teboroxime. *J Nucl Med.* 1991;32:2012-22.
83. Gregoire J, Theroux P. Detection and assessment of unstable angina using myocardial perfusion imaging: comparison between technetium-99m-sestamibi SPECT and 12-lead electrocardiogram. *Am J Cardiol.* 1990;66:42-47E.
84. Wackers FJ. Thrombolytic therapy for myocardial infarction: assessment of efficacy by myocardial perfusion imaging with technetium-99m-sestamibi. *Am J Cardiol.* 1990;66:36-41E.
85. Jain D. Technetium-99m labeled myocardial perfusion imaging agents. *Semin Nucl Med.* 1999;29:221-36.
86. Sinusas AJ, Shi O, Saltzberg MT, et al. Technetium-99m-tetrofosmin to assess myocardial blood flow: experimental validation in an intact canine model of ischemia. *J Nucl Med.* 1994;35:664-71.
87. Dahlbert ST, Gilmore MP, Leppo JA. Effect of coronary blood flow on the "uptake" of tetrofosmin in the isolated rabbit heart [abstract]. *J Nucl Med.* 1992;33:846.
88. Myoview [package insert]. Arlington Heights, IL: Nycomed-Amersham, 1998.
89. Platts EA, North TL, Pickett RD, et al. Mechanism of uptake of technetium-tetrofosmin. I: Uptake into isolated adult rat ventricular myocytes and subcellular localization. *J Nucl Cardiol.* 1995;2:317-26
90. Arbab AS, Koizumi K, Toyama K, et al. Technetium-99m-tetrofosmin, technetium-99m-MIBI and thallium-201 uptake in rat myocardial cells. *J Nucl Med.* 1998;39:266-71.

91. Sridhara BS, Braat S, Rigo P, et al. Comparison of myocardial perfusion imaging with ^{99m}Tc-tetrofosmin versus ^{201}Tl in coronary artery disease. *Am J Cardiol.* 1993;72:1015-9.
92. Taillefer R, Primeau M, Costi P, et al. Technetium-99m-sestamibi myocardial perfusion imaging in detection of coronary artery disease: comparison between initial (1-hour) and delayed (3-hour) postexercise images. *J Nucl Med.* 1991;32:1961-5.
93. Leppo JA, DePuey EG, Johnson LL. A review of cardiac imaging with sestamibi and teboroxime. *J Nucl Med.* 1991;32:2012-22.
94. Schwaiger M. Myocardial perfusion imaging with PET. *J Nucl Med.* 1994;35:693-8.
95. Budinger TF, Yano Y, Derenzo SE, et al. Myocardial extraction of Rb-82 vs. flow determined by positron emission tomography [abstract]. *Circulation.* 1983;68:III-81.
96. Maddahi J, Schelbert J, Brunken R, et al. Role of thallium-201 and PET imaging in evaluation of myocardial viability and management of patients with coronary artery disease and left ventricular dysfunction. *J Nucl Med.* 1994;35:707-15.
97. Berry JJ, Baker JA, Pieper KS, et al. The effect of metabolic milieu on cardiac PET imaging using fluorine-18-deoxyglucose and nitrogen-13-ammonia in normal volunteers. *J Nucl Med.* 1991;32:1518-25.
98. Bonow RO, Dilsizian V. Thallium-201 and technetium-99m-sestamibi for assessing viable myocardium. *J Nucl Med.* 1992;33:815-8.
99. Mori T, Minamiji K, Kurongane H, et al. Rest-injected thallium-21 imaging for assessing viability of severe asynergic regions. *J Nucl Med.* 1991;23:1718-24.
100. Alfieri O, LaCanna G, Guibbini R, et al. Recovery of myocardial function. *Eur J Cardiothorac Surg.* 1993;7:325-30.
101. Ragosta M, Beller GA, Watson DD, et al. Quantitative planar rest-redistribution Tl-201 imaging in detection of myocardial viability and prediction of improvement in left ventricular function after coronary bypass surgery in patients with severely depressed left ventricular function. *Circulation.* 1993;87:1630-41.
102. Tamaki N, Ohtani H, Yamashita K, et al. Metabolic activity in the areas of new fill-in after thallium-201 reinjection: comparison with positron emission tomography using fluorine-18-deoxyglucose. *J Nucl Med.* 1991;32:673-8.
103. Cuocolo A, Pace L, Ricciardelli B, et al. Identification of viable myocardium in patients with chronic coronary artery disease: comparison of thallium-201 scintigraphy with reinjection and technetium-99m methoxyisobutyl isonitrile. *J Nucl Med.* 1992;33:505-11.
104. Altehoefer C, vom Dahl J, Biedermann M, et al. Significance of defect severity in technetium-99m-MIBI SPECT at rest to assess myocardial viability: comparison with fluorine-18-FDG PET. *J Nucl Med.* 1994;35:569-74.
105. Maurea S, Cuocolo A, Nicolai E, et al. Improved detection of viable myocardium with thallium-201 reinjection in chronic coronary artery disease: comparison with technetium-99m-MIBI imaging. *J Nucl Med.* 1994;35:621-4.
106. Zaret BL, Rigo P, Wackers FJ, et al. Myocardial perfusion imaging with ^{99m}Tc-tetrofosmin: comparison to ^{201}Tl imaging and coronary angiography in phase III multicenter trial. *Circulation.* 1995;91:313-9.
107. Takahashi N, Tamaki N, Tadamura E, et al. Combined assessment of regional perfusion and wall motion in patients with coronary artery disease with ^{99m}Tc-tetrofosmin. *J Nucl Cardiol.* 1994;1:29-38.
108. Rigo P, Leclercq B, Itti R, et al. Technetium-99m-tetrofosmin myocardial imaging: a comparison with ^{201}Tl and angiography. *J Nucl Med.* 1994;35:587-93.
109. Flamen P, Bossuyt A, Franken PR. Technetium-99m-tetrofosmin in dipyridamole-stress myocardial SPECT imaging: intraindividual comparison with technetium-99m-sestamibi. *J Nucl Med.* 1995;36:2009-15.
110. Matsunari I, Fujino S, Taki J, et al. Myocardial viability assessment with technetium-99m-tetrofosmin and thallium-201 reinjection in coronary artery disease. *J Nucl Med.* 1995;36:1961-7.
111. Bonow RO. Assessment of myocardial viability. In: Sandler MP, Coleman RE, Patton JA, et al., eds. *Diagnostic Nuclear Medicine.* 4th ed. Philadelphia: Lippincott Williams & Wilkins; 2003:319-32.
112. Nusynowitz ML, Straw JD, Benedetto AR, et al. Blood clearance rates of technetium-99m albumin preparations [concise communication]. *J Nucl Med.* 1978;19:1142-5.
113. Pavel DG, Zimmer AM, Patterson VN. In vivo labeling of red blood cells with Tc-99m: a new approach to blood pool visualization. *J Nucl Med.* 1977;18:305-8.
114. Dewanjee MK, Rao SA, Penniston GT. Mechanism of red blood cell labeling with ^{99m}Tc-pertechnetate: the role of the cation pump at RBC membrane on the distribution and binding of Sn^{2+} and ^{99m}Tc with the membrane proteins and hemoglobin. *J Labeled Compounds Radiopharm.* 1982;19:1464-5.
115. Dewanjee MK, Anderson GS, Wahner HW. Pharmacodynamics of stannous-chelates administered with technetium-99m chelates for radionuclide imaging. In: Sodd VS, Hoogland DR, Allen DR, et al., eds. *Radiopharmaceuticals II.* New York: Society of Nuclear Medicine; 1979:421-34.
116. Bonte FJ, Parkey RW, Graham KD, et al. A new method for radionuclide imaging of acute myocardial infarction. *Radiology.* 1974;110:473-4.

117. Willerson JT, Parkey RN, Bonte FJ, et al. Pathophysiologic considerations and clinicopathological correlates of technetium-99m stannous pyrophosphate myocardial scintigraphy. *Semin Nucl Med.* 1980;10:54-69.
118. Buja LM, Tofe AJ, Kulkarni PV, et al. Sites and mechanisms of localization of technetium 99m phosphorous radiopharmaceuticals in acute myocardial infarcts and other tissues. *J Clin Invest.* 1977;60:724-40.
119. Holman LB. Radioisotopic examination of the cardiovascular system. In: Braunwald E, ed. *Heart Disease: A Textbook of Cardiovascular Medicine.* Philadelphia: WB Saunders; 1980:363-409.
120. Volpini M, Giubbini R, Gei P, et al. Diagnosis of acute myocardial infarction by indium-111 antimyosin antibodies and correlation with the traditional techniques for the evaluation of extent and localization. *Am J Cardiol.* 1989;63:7-13.
121. Johnson LL, Seldin DW, Becker LC, et al. Antimyosin imaging in acute transmural myocardial infarctions: results of a multicenter clinical trial. *J Am Coll Cardiol.* 1989;13:27-35.
122. Khaw BA, Nakazawa A, O'Donnell SM, et al. Avidity of technetium-99m glucarate for the necrotic myocardium: in vivo and in vitro assessment. *J Nucl Cardiol.* 1997;4:283-90.
123. Mariani G, Villa G, Rossettin PF, et al. Detection of acute myocardial infarction by ^{99m}Tc-labeled D-glucaric acid imaging in patients with acute chest pain. *J Nucl Med.* 1999;40:1832-9.
124. Johnson LL. Myocardial hotspot imaging, In: Sandler MP, Colemen RE, Patton JA, et al., eds. *Diagnostic Nuclear Medicine.* 4th ed. Philadelphia: Lippincott Williams & Wilkins; 2003:333-41.
125. Tait JF, Brown DS, Gibson DF, et al. Development and characterization of annexin V mutants with endogenous chelation sites for (99m) Tc. *Bioconjug Chem.* 2000;11:918-25.
126. Hofstra L, Liem IH, Dumont EA, et al. Visualization of cell death in vivo in patients with acute myocardial infarction. *Lancet.* 2000;356:209-12.
127. Zaret BL, Strauss HW, Martin WD, et al. Noninvasive regional myocardial perfusion with radioactive potassium. *N Engl J Med.* 1973;288:809-12.
128. Gaudron P, Eilles C, Kugler I, et al. Progressive left ventricular dysfunction and remodeling after myocardial infarction: potential mechanisms and early predictors. *Circulation.* 1993;87:755-63.
129. The Multicenter Postinfarction Research Group. Risk stratification and survival after myocardial infarction. *N Engl J Med.* 1983;309:331-6.
130. Strauss HW, Miller DM, Wittry MD, et al. Procedure guideline for myocardial perfusion imaging 2.0. In: *Procedure Guidelines Manual 2001-2002.* Reston, VA: Society of Nuclear Medicine; 2001:7-14.
131. McCall D. Cation exchange and glycoside binding in cultured rat heart cells. *Am J Physiol.* 1979;236:C87-95.
132. Goldhaber SZ, Newell JB, Alpert NM, et al. Effects of ischemic-like insult on myocardial 201 thallium accumulation. *Circulation.* 1983;67:778-86.
133. Garcia E, Maddahi J, Berman D, et al. Space-time quantitation of ^{201}Tl myocardial scintigraphy. *J Nucl Med.* 1981;22:309-17.
134. Bergman SR. Positron emission tomography of the heart. In: Gerson M, ed. *Cardiac Nuclear Medicine.* 3rd ed. New York: McGraw-Hill; 1996:299-335.
135. Strauss W, Zaret BL, Hinley RJ, et al. A scintiphotographic method for measuring left ventricular ejection fraction in a man without cardiac catheterization. *Am J Cardiol.* 1971;28:757.

16 Lung

Radiopharmaceuticals for lung imaging can be divided into two main groups: (1) lung perfusion agents and (2) lung ventilation agents. Perfusion agents typically are radiolabeled particles that are temporarily trapped in the lung's arterioles and capillaries after intravenous injection and provide diagnostic information about regional blood flow to the lung. Ventilation agents are radioactive gases or radioaerosols that, after inhalation, demonstrate patency of the airways and alveolar system.

PHYSIOLOGIC PRINCIPLES

The lungs are perfused by pulmonary arteries and veins, which distribute blood to and remove blood from the capillary beds where gas exchange occurs. The airways of the lung are divided into three functional zones: the conducting zone, the respiratory zone, and the intermediate or transition zone.[1] The intermediate zone links the conducting zone and respiratory zone. The conducting zone of the airways, consisting of the bronchi and bronchioles, delivers inspired air via the transition zone to the alveoli. In the respiratory zone, which consists of a complex of alveoli and capillaries, air and blood come into close contact to facilitate the exchange of oxygen and carbon dioxide. This zone is sometimes called the gas exchange apparatus.

The airway conduction system has a branching pattern from the trachea to the alveolar sacs (Figure 16-1).[2] The bronchi and bronchioles conduct air to the more peripheral zones. After inspiration, fresh air moves into the lungs by bulk flow as far as the respiratory bronchioles, where the transition zone begins, but from that point the movement of air into the alveolar ducts and alveoli occurs by diffusion. Higher tidal volumes of air penetrate deeper but never reach the end of the alveolar system by bulk flow.[3]

Lung Ventilation

Under normal conditions, airway resistance is minimal and air moves freely into and out of the airways and respiratory zone. In the presence of disease, airway resistance may increase significantly, affecting inspiration and expiration. In less severe cases of asthma or emphysema, for example, air may enter the bronchioles and alveoli readily because chest expansion and the inflow of air inflate these structures. Expiration, however, is more difficult because the weakened, diseased bronchioles collapse from the pressure of the thoracic cage against the lungs, causing air to be trapped in the alveoli. In advanced airway disease, air intake also may be obstructed because of inflamed bronchi and bronchioles and the presence of mucus plugs, often found in bronchial asthma. These alterations in air distribution can be observed with the use of radioactive gases and aerosols.

Lung Perfusion

The pulmonary artery has 22 to 26 branches. At about the 24th branch, a short connector artery of 125 μm diameter divides at right angles to form two distribution arteries (Figure 16-2). The smallest-diameter distribution arteries range in size from 60 to 100 μm, and

from these vessels short precapillary arterioles of 25 μm diameter arise at right angles. These vessels then divide into alveolar capillary beds. The basic elements of the alveolar capillary bed are the capillary segments, which have the shape of short cylindrical tubes. The segments are modified at their ends to form wedges that allow each segment to join at either end with two adjacent segments. The average internal diameter of a capillary segment is 8 μm (range, 6 to 10 μm).[2]

It is clear from the structure of the alveolar capillary network that blood entering each precapillary arteriole has alternative routes to reach the postcapillary venule. This capillary arrangement is important during lung scanning, because pulmonary hemodynamics are not appreciably affected by the temporary occlusion of a small percentage of capillary segments by radiolabeled particles unless there is advanced lung disease and pulmonary hypertension.

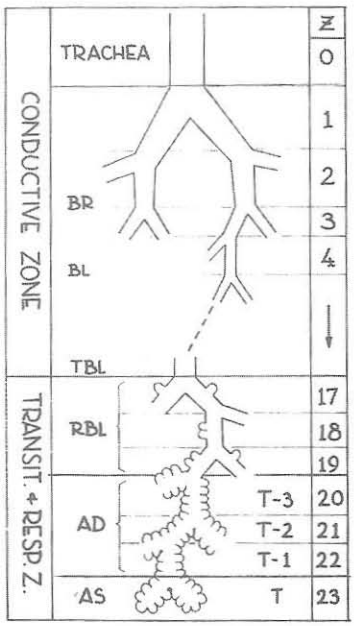

FIGURE 16-1 Branching pattern of the airways from the trachea to the alveolar sacs. BR, bronchi; BL, bronchioles; TBL, terminal bronchioles; RBL, respiratory bronchioles; AD, alveolar duct; AS, alveolar sac. (Reprinted with permission of Academic Press from reference 2.)

Normal blood flow in the lung is influenced by hydrostatic pressure. In the upright position, the mean pulmonary arterial pressure is 3 mm Hg at the apex of the lung, 13 mm Hg in the midzone, and 21 mm Hg at the base of the lung. This pressure difference alters blood distribution between the upper and lower parts of the lung. Studies conducted with the injection of xenon 133 gas dissolved in saline have shown that, in normal subjects, a change from the upright to the supine position results in a doubling of blood perfusion to the upper lung zones at the cost of the lower zones, with the midzones recording no change.[4] This equalization in hydrostatic pressure is the reason that radiolabeled particles for lung scanning are injected while the patient is supine, which evens the distribution of radioactivity in the lung.

Blood flow to the lung is affected by various pathologic conditions. In the case of pulmonary embolism (PE), the embolus not only mechanically impedes blood flow to the lung area distal to the blockage but also may cause local vasospasm, which further decreases blood flow to the region.[5] In the case of airway disease such as emphysema, destruction of many alveolar walls also causes destruction of their capillaries, resulting in increased vascular resistance to blood flow. Additionally, a physiologic decrease in local blood perfusion occurs in emphysema because emphysematous alveoli exhibit poor gas exchange. The resulting alveolar hypoxia causes reflex vasoconstriction of local blood vessels, shunting blood to areas of the lung that have better aeration.[5] For these reasons, ventilatory disease may cause perfusion defects to appear on the lung scan.

DEVELOPMENT OF LUNG PERFUSION AGENTS

Site-specific localization of radioactivity in the lungs began with the therapeutic application of gold; ^{198}Au was labeled to 50 μm carbon particles to irradiate tumor tissue.[6] The diagnostic utility of radioactive particles for lung scanning was initially investigated in

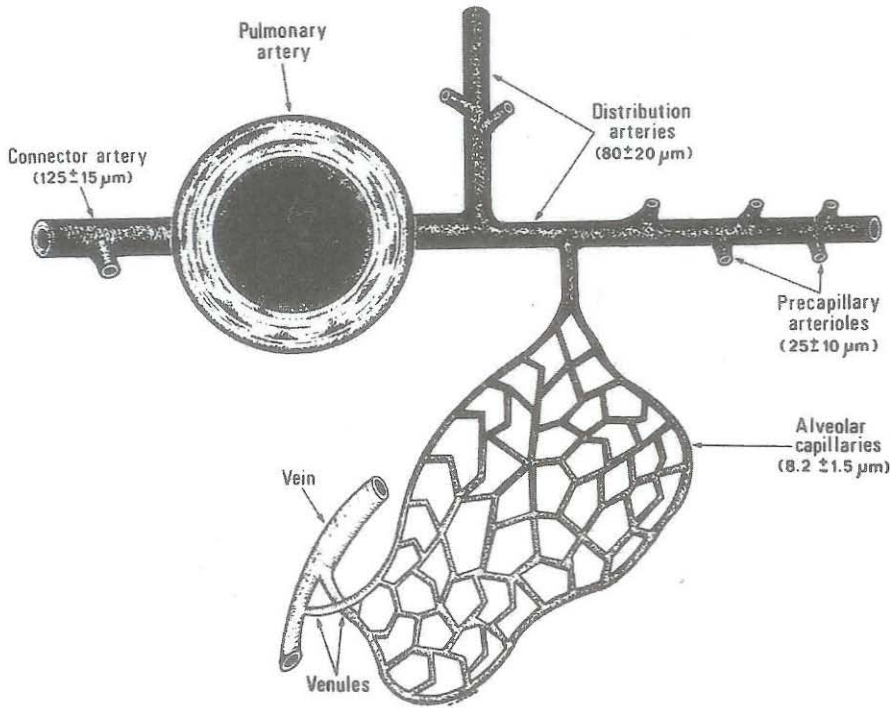

FIGURE 16-2 Schematic representation of pulmonary vasculature, emphasizing the alveolar capillary network and the anastomotic nature of the capillary bed. (Reprinted with permission of the Society of Nuclear Medicine from reference 15.)

1963 by Taplin et al., who prepared ^{131}I-labeled human serum albumin macroaggregates (^{131}I-MAA). Their studies demonstrated that these particles could be trapped and eventually cleared from the lungs.[7–9] These investigators also performed the first toxicity studies to demonstrate the safety of injecting large numbers of particles intravenously. After these studies, which occurred from 1965 to 1970, ^{131}I-MAA became the agent of choice for imaging the presence of suspected pulmonary emboli.

The search for an imaging agent with properties more favorable than ^{131}I led to the development of particles labeled with radionuclides that have shorter half-lives. These included ^{113m}In-labeled ferric hydroxide and ^{99m}Tc-labeled ferrous hydroxide macroaggregates; however, toxic reactions associated with these preparations led to their disuse.[10,11]

In 1969, ^{99m}Tc-labeled human albumin microspheres (^{99m}Tc-HAM) were developed by Zolle et al.[12] and Rhodes et al.[13] ^{99m}Tc-HAM could be microsieved to control particle size and were biodegradable in vivo. A ^{99m}Tc-HAM kit using sodium thiosulfate as the tagging agent became available from the 3M Company.[13] Labeling efficiency was only 60% to 70%, however, and insonation was necessary to break up any potential microsphere aggregations. Labeling efficiency of the ^{99m}Tc-HAM kit improved when stannous chloride was used as the reducing agent. The kit was used for several years before the company stopped its manufacture.

Subramanian et al.[14] developed technetium Tc 99m albumin aggregated injection (^{99m}Tc-MAA) as an "instant kit" using stannous chloride as the tagging agent. Labeling yields were quantitative, and the kit became commercially available in the mid-1970s. It is still the agent of choice for perfusion lung imaging.

Kits for routine preparation of ^{99m}Tc-MAA are available from several manufacturers (see Tables 9-9 and 9-10 in Chapter 9). In general, nonradioactive stannous MAA kits are

prepared by mixing sterile solutions of human serum albumin and stannous chloride in acetate buffer at a pH of around 5. The resulting solution is heated at controlled temperature and mixed to form the aggregated particles, which can be sieved to remove large aggregates. The particle size in commercial kits is in the range of 10 to 90 μm. Aliquots of the suspension are then lyophilized under nitrogen in sterile vials. The number of particles in commercial kits varies but averages about 5 million. Labeling of the MAA particles with ^{99m}Tc is accomplished by adding the required amount of ^{99m}Tc-sodium pertechnetate to a kit to achieve the desired particle concentration and specific activity. Dilution may be required to adjust the particle concentration for pediatric patients or patients with pulmonary hypertension. Chapter 9 contains a detailed discussion of ^{99m}Tc-MAA chemistry and kit preparation.

The typical lung scan dosage in adults is 3 mCi (111 MBq) by intravenous injection. The patient should be supine during the injection to ensure uniform distribution of particles within the lung. The ^{99m}Tc-MAA dose in the syringe should be gently mixed just before injection to ensure uniform particle dispersion. Blood drawn into the syringe during injection should not be allowed to stand too long, or clotting may occur. A delay may occur if there is some difficulty during the injection, and a new dose should be used if clotting is suspected. Injection of clotted particles will result in spurious information on the lung scan.

Physical Properties of ^{99m}Tc-MAA Particles

A number of factors are important in the preparation of ^{99m}Tc-MAA particles for perfusion lung imaging, including particle size, number, hardness, and chemical composition. These factors influence the biodistribution, metabolic fate, and potential toxicity of the lung perfusion agent.

Particle Size

The first criterion for localization in the lung is a particle size large enough to be trapped in the pulmonary arterioles and capillaries. Because the smallest capillaries have an internal diameter of 6 to 10 μm, particles smaller than 10 μm are unsatisfactory because they will readily pass through the lung. Particles too large will obstruct larger arterioles, of which there are fewer, potentially producing a serious reduction in blood flow and elevation of pulmonary arterial pressure. Davis investigated particle size and concluded that the capillary segments were the ideal vessels to block in the lung because they are highly anastomotic and blockade of one or even several capillary segments will not substantially alter blood flow or pressure.[15] The particle size recommended for achieving high extraction efficiency into the capillary bed was 13.5 ± 1.5 μm. However, it was also concluded that this limited size range was impractical to produce and that the tracer would clear the lung too rapidly to be useful for lung imaging. For these reasons, commercial MAA kits contain particles in the 10 to 90 μm range, with most particles between 20 and 60 μm (Figure 16-3).

Particle Number

In response to early reports of acute toxicity from administering too many particles for lung scans, several investigators set out to determine the ideal number of particles for a satisfactory lung scan. Heck and Duley,[16] working with ^{99m}Tc-albumin microspheres in the 15 to 30 μm range, reported that having too few particles (15,000 to 30,000) produced

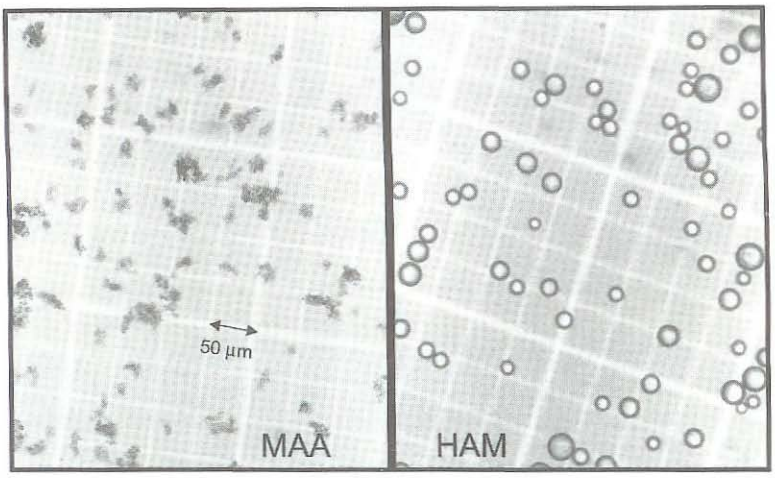

FIGURE 16-3 Photomicrograph of macroaggregated albumin (MAA) particles and human albumin microspheres (HAM).

patchy-looking lung scans, particularly at the lung periphery. They determined that the minimum number of particles for a satisfactory lung scan was 60,000.

Dworkin et al.[17] used 10 to 50 μm particles of ^{99m}Tc-MAA in dogs, confirming the work of Heck and Duley. They concluded that the minimum number of particles required for a satisfactory lung scan was 60 particles per gram of lung, which translates into 60,000 particles if the average weight of adult human lung tissue is 1000 grams. An upper limit of 250,000 particles for a lung scan was suggested because little is gained above this number and the chance of toxicity is increased. In practice it is difficult to determine the exact number of particles administered because of the wide range of particle numbers per kit. If an accurate particle number is needed for an individual kit, this can be assessed by counting methods that use a microscope and hemacytometer, discussed in Chapter 12.

Particle Hardness and Composition

Ideally, particles that lodge in the pulmonary blood vessels should be biodegradable and not produce local tissue reactions. For these reasons, human serum albumin (HSA), a natural body constituent, is routinely used. Additionally, HSA can be heated to the desired hardness to achieve proper clearance from the lung.

In the early days of lung scanning, there was concern about the potential antigenic effects of the denatured protein particles. After extensive testing, Iio and Wagner[18] found no evidence to prove that aggregated human albumin is antigenic to humans. This finding was corroborated by Taplin et al.[8]

Generally, for a given particle size, a higher heating temperature will produce a harder particle that will take longer to break up and clear from the lung. Zolle et al.[12] demonstrated that albumin microspheres prepared at 118°C, 146°C, and 165°C had biologic half-lives in dog lungs of 2.4, 7.2, and 144 hours, respectively.

Although albumin particles demonstrated absence of tissue reactions, pathologic changes were reported with ^{99m}Tc-labeled iron hydroxide MAA.[15] Flushing reactions were reported, suggesting that chemical composition was a causative factor. The use of iron hydroxide products was discontinued.

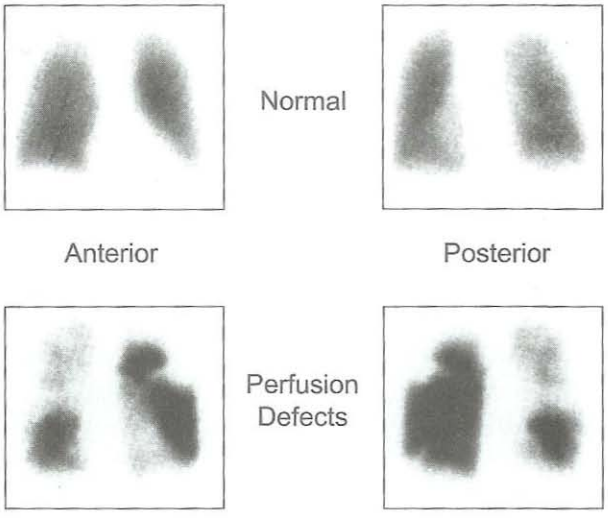

FIGURE 16-4 Perfusion lung scan with ^{99m}Tc-MAA. Normal scan and scan demonstrating multiple segmental defects due to pulmonary embolism.

Biologic Properties of ^{99m}Tc-MAA

After intravenous injection of ^{99m}Tc-MAA, more than 90% of the dose is extracted by the pulmonary arterial bed on the first pass through the lung. The mechanism of localization is physical entrapment of particles larger than the blood vessel diameter. The distribution of particles and activity in the lung is related to regional blood flow; in a normal lung, distribution is uniform over the entire lung field. Particle activity is diminished distal to any obstruction and appears as a perfusion defect on the scan (Figure 16-4). Big emboli will occlude larger vessels and produce more extensive perfusion defects.

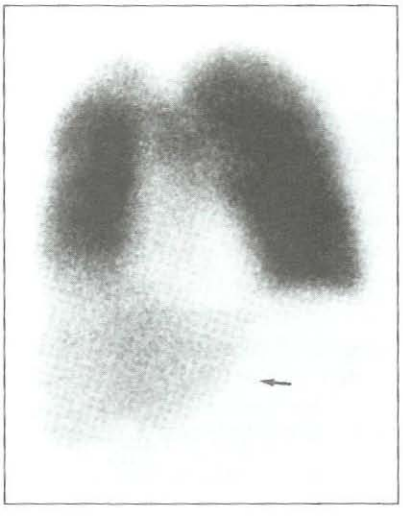

FIGURE 16-5 Anterior perfusion lung scan with ^{99m}Tc-MAA. Liver activity (arrow) is evident because of phagocytosis of particles that pass through the lung capillaries.

Biodegradation of MAA particles in the lung is slow enough to allow ample time for imaging. Using an in vivo cinemicroscopic technique, Taplin and MacDonald[19] demonstrated that the mechanism of MAA clearance from the lungs is particle fragmentation by blood cell bombardment and by continuous forward and backward movement within arterioles until aggregates are small enough to traverse the capillary lumen. Albumin microspheres do not fragment but undergo dissolution, probably through the enzymatic action of pulmonary phagocytes.[20]

The rate of particle clearance from the lung is a function of particle size, distribution, and number; method of preparation (related to particle hardness); and the state of lung health. Smaller particles are expected to have faster clearance. Taplin and MacDonald[19] demonstrated in dogs that ^{131}I-MAA doses with particle sizes of 5 to 25 μm, 10 to 70 μm, and 10 to 150 μm had biologic half-lives of 30 minutes, 4 to 6 hours, and 18 to 24 hours, respectively. Particles that are too soft because of inadequate heating or are too small readily pass through the lungs and become localized in the liver, potentially interfering with the lung scan (Figure 16-5).

The patient's condition may affect lung clearance of particles. Davis[21] determined that the average clearance half-life of ^{99m}Tc-iron hydroxide particles from the lung was 19 hours in normal subjects but was significantly slower in various degrees of PE (105 hours) and chronic lung disease (222 hours). Busse et al.[22] demonstrated that the lung clearance rate of ^{131}I-MAA was slower in asthmatics and in patients receiving corticosteroid and immunosuppressive therapy, with viral pneumonia, and with chronic interstitial lung disease. The lung half-lives of several radiolabeled particles used in perfusion lung imaging are shown in Table 9-10 in Chapter 9. An important point in this regard is that the rate of activity loss and the rate of particle loss from the lungs are not identical; a particle may partially break up and release a portion of its activity but still remain in the lung until it is small enough to pass through.[15]

Once the particles are cleared from the lungs, they are phagocytized by the reticuloendothelial system (RES), primarily by the liver (Figure 16-5). Taplin and MacDonald[19] demonstrated that ^{131}I-MAA particles undergo proteolytic digestion in Kupffer's cells, evidenced by the presence of ^{131}I-labeled tyrosine, peptides, and free radioiodide in the plasma and urine a few hours after injection. The biologic half-life in the liver was reported to be 9 to 10 hours. ^{99m}Tc-MAA is also metabolized in the liver, with urinary excretion of 30% to 75% of the dose in 24 hours, depending on the kit. These particles are also most likely digested by liver enzymes, with the release of ^{99m}Tc-labeled amino acids and pertechnetate, which are excreted in the urine. A fraction of the activity also remains in the liver, probably as insoluble ^{99m}Tc-TcO_2 colloid. The biologic fate of dual-labeled ^{99m}Tc-HSA colloid labeled with ^{14}C and ^{99m}Tc supports this mechanism.[23] Such an agent used for liver imaging demonstrated a biologic half-life of ^{14}C activity in the liver of 4 hours and of ^{99m}Tc activity of 11 hours.

Particle Toxicity

Safety and effectiveness considerations with particulate lung-scanning agents have been reviewed.[24] In the early days of lung scanning with ^{131}I-MAA, a typical lung scanning dose (LSD) contained 10^6 particles. Studies performed by Taplin and MacDonald in normal dogs demonstrated that a wide margin of safety exists when such doses are administered. These studies showed that the first sign of acute toxicity, observed as a rise in pulmonary arterial pressure (PAP), occurred at a dose of 20 mg/kg body weight (1000 times the average LSD). Such a large safety factor is possible because in the normal lung less than 1% of the arterioles and capillaries are blocked by such doses.[15]

Despite this wide margin of safety in normal subjects, several deaths have been reported after the administration of ^{131}I-MAA for lung scanning.[25–28] An evaluation of these cases revealed that these patients suffered from severe pulmonary hypertension and that their underlying diseases had caused narrowing and occlusion of pulmonary blood vessels. In each case, immediately after injection of the ^{131}I-MAA dose, clinical deterioration occurred, manifested by respiratory distress, cyanosis, hypertension, and eventual death. Each of these reports discussed the need in such cases to decrease the number of particles injected and to restrict their size to less than 50 μm, preferably to the 10 to 30 μm range.

The primary cause of cardiopulmonary toxicity associated with lung-scanning agents is the size and number of particles injected.[29,30] Large particles, when compared with the same size dose of small particles, are more effective in raising PAP. This inverse relationship between particle size and number in producing an acute toxic response is derived from the fact that larger particles block larger arterioles, of which there are fewer in the lung.

Allen et al.[31] demonstrated that the safety factor for a LSD of 10^6 particles of ^{99m}Tc-MAA (30 to 50 μm) was 125, based on an elevation of PAP of 10% to 20%.[31] This safety

TABLE 16-1 Dilution Procedure for Preparing Reduced Particle Concentration of ^{99m}Tc-MAA

1. Add 10 mL saline to 5 million particle MAA kit (500,000 particle/mL)
2. Remove 8.8 mL (4.4 million particles) and discard
3. Add 30 mCi $Na^{99m}TcO_4^-$ to the remaining 600,000 particles in the kit
4. Incubate for 15 minutes
5. Add saline to make 5 mL final volume
6. Final concentration: 3 to 6 mCi (60,000 to 120,000 particles)/0.5 to 1.0 mL

TABLE 16-2 MAA Particles per Pediatric Dose (in thousands)[a]

Variable	Newborn	1 Year	5 Years	10 Years	15 Years
Weight (kg)	3.5	12.1	20.3	33.5	55.0
Activity (mCi)	0.2	0.4	0.6	1.0	1.7
Range of particles given	10–50	50–100	200–300	200–300	200–700

[a] The suggested average pediatric dose is based on 30 μCi/kg body weight, except for newborns. A minimum dose of 200 μCi of ^{99m}Tc-MAA should be used for the lung scan procedure.

Source: Macrotec package insert, Bracco Diagnostics, Princeton, NJ.

factor increases to 1250 if only 100,000 particles are administered, which emphasizes why it is desirable to administer only as many particles as are needed for a satisfactory scan (not more than 250,000). It should be pointed out that these safety factors are for normal patients. Patients with pulmonary hypertension should be administered a minimum number of particles (60,000) for safety reasons.

Pediatric patients also require special consideration regarding number of particles in the LSD. Heyman[32] noted that a significant increase in the number of alveoli and pulmonary arteries occurs during the first few years of life, reaching adult levels at about 8 years of age. The number is 10% to 30% of adult values during the first year of life and up to 50% the adult number at 3 years. Heyman suggested limiting the number of particles to 50,000 in the newborn infant and 165,000 in children up to 1 year old. A technique has been described for preparing pediatric doses whereby excess particles from ^{99m}Tc-MAA kits are discarded and the number remaining are radiolabeled with ^{99m}Tc-sodium pertechnetate to achieve the desired concentration for pediatric lung doses.[33] An example of a dilution procedure for reducing particle concentration is shown in Table 16-1. Manufacturer package inserts for ^{99m}Tc-MAA kits contain a table of recommended dosages of particles for pediatric patients (Table 16-2).

It is important to allow sufficient time for MAA particles to be tagged with technetium during the labeling process. It may take a while longer for complete labeling when particles are diluted. It may be necessary to make the dilutions of stannous MAA with nitrogen-purged saline, to limit the amount of free pertechnetate that may occur if the majority of the stannous ion is removed during kit preparation. As little as 5% to 10% free pertechnetate will be evident as thyroid uptake on lung scans (Figure 16-6).

Another concern that arose when lung scanning was first established was the potential threat of cerebral microembolization from particles that enter the systemic circulation either after degradation in the lung or through a right-to-left cardiac shunt. In this regard, Taplin et al.[8] reported that suspensions of albumin particles, which show initial pulmonary

retention, are subsequently cleared from the lungs and transposed to the liver and spleen. It was stated that if small particles were able to traverse the pulmonary capillaries they would also traverse cerebral vessels without significant danger of microembolization. In other studies Taplin and MacDonald[19] estimated the margin of safety for particles that were not degraded into smaller sizes in the lungs but entered the systemic circulation directly through a right-to-left cardiac shunt. Studies were performed in monkeys receiving direct carotid arterial injections of MAA. After repeated injections of aggregates (10 to 100 μm), there was no evidence of histologic or observable lesions in brain tissue at administered doses less than 6 mg MAA per 100 grams of brain tissue. On the basis of these data, Taplin and MacDonald estimated that the margin of safety for a 1 mg MAA dose for a lung scan was greater than 2000. This safety margin was based on the assumption that 50% of the dose was shunted to the general circulation, of which 10% went to the head and 3% went to each hemisphere.

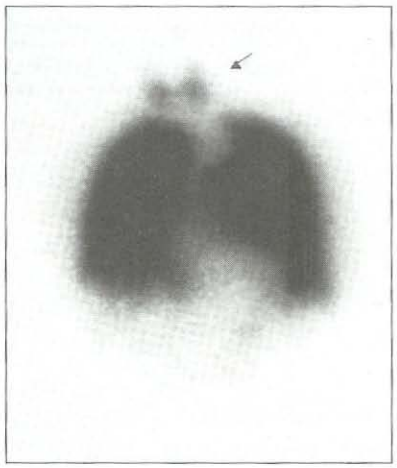

FIGURE 16-6 Perfusion lung scan demonstrating thyroid gland uptake of free pertechnetate activity present as an excessive impurity in the ^{99m}Tc-MAA preparation.

LUNG VENTILATION IMAGING AGENTS

The ventilation lung scan became an important diagnostic tool because it improved the specificity of the perfusion lung scan in the diagnosis of PE. Taplin and Chopra[34] reviewed combined perfusion–ventilation lung scanning. Before the ventilation lung scan was established as a routine procedure, a diagnosis of PE was based on clinical suspicion and on the finding of one or more segmental or lobar perfusion defects on a normal chest radiograph. When it became evident that a normal chest radiograph could not exclude all nonembolic causes of perfusion defects, particularly in cases involving chronic obstructive pulmonary disease, the ventilation lung scan (V) gained acceptance as a method for evaluating regional ventilation. It was shown to have diagnostic value in the early detection of obstructive pulmonary disease, for which chest radiographs are relatively insensitive. More important, it added specificity to lung perfusion scanning (Q) by demonstrating that perfusion defects of embolic origin (proven angiographically) were nearly always well ventilated, whereas those caused by parenchymal or obstructive airway disease were neither perfused nor ventilated (VQ matching). The finding of poorly perfused but well-ventilated regions (VQ mismatch) in radiographically normal lung was thus considered strong evidence for PE.

Inert Radioactive Gases

The most widely used agents for lung ventilation studies are the radioactive noble gases. Their use is based on the premise that these gases are relatively insoluble in body fluids, so their distribution in the lung is proportional to the regional differences in ventilation caused by localized disease in the lung. The noble gases are inert and poorly soluble in aqueous media, and several possess the physical properties to be of potential use in ventilation imaging (Table 16-3). However, only ^{133}Xe is routinely used today because of logistic or production limitations associated with the other gases.

TABLE 16-3 Radioactive Gases for Lung Ventilation Imaging

Gas	Production	Half-life	Gamma keV	Abundance %
^{133}Xe	$^{235}U(n,f)^{133}Xe \xrightarrow{\beta^-} {}^{133}Cs$	5.3 days	81	36
^{135}Xe	$^{235}U(n,f)^{135}Xe \xrightarrow{\beta^-} {}^{135}Cs$	9.1 hr	250	95
^{127}Xe	$^{133}Cs(p,2p5n)^{127}Xe \xrightarrow{EC} {}^{127}I$	36.4 days	172 203 375	25 68 18
^{81m}Kr	$^{81}Rb \xrightarrow{4.5\ hr} {}^{81m}Kr \xrightarrow{IT} {}^{81}Kr$	13 sec	191	66

^{133}Xe

^{133}Xe was first used for ventilation imaging in the mid-1960s and became more widely used clinically in the 1970s because it could be produced inexpensively and in large quantities. It is produced commercially as a byproduct of uranium fission in a nuclear reactor. It is packaged in individual patient dose vials of 10 mCi and 20 mCi (370 and 740 MBq) sizes. It has also been available in bulk (curie) amounts for in-house packaging. ^{133}Xe, with a half-life of 5.3 days, can be stored in the nuclear medicine lab ready for use. It is typically replenished by weekly shipments from the supplier.

The primary disadvantages of ^{133}Xe are poor image quality because of its low photon abundance (35%) and low tissue penetration of the 81 keV gamma ray. Additionally, the low-energy photon requires that the ventilation scan be performed prior to the ^{99m}Tc-MAA perfusion lung scan. However, some institutions perform xenon ventilation imaging after the ^{99m}Tc-MAA perfusion scan by administering 20 to 25 mCi (740 to 925 MBq) of ^{133}Xe to override the technetium activity in the lung.

^{135}Xe

^{135}Xe was introduced for ventilation studies in 1968 by Newhouse et al.[35] Its advantage was a 250 keV gamma with 95% abundance that was ideal for performing ventilation studies after the ^{99m}Tc-MAA perfusion study. However, it was not cost-effective because of its short half-life, precluding its ready supply in the clinic except through daily shipments.

^{127}Xe

In 1973, Hoffer et al.[36] reported that better quality images could be obtained with ^{127}Xe than with ^{133}Xe. This was due to the higher photon energies and abundances, the primary gamma being 203 keV at 68% abundance. This permitted ventilation imaging to follow the ^{99m}Tc-MAA perfusion scan. Other benefits of ^{127}Xe were lower radiation dose because of absent beta radiation and a longer shelf life because of its 36.4 day half-life. Other reports documented the advantages of ^{127}Xe, making it the agent of choice for several years.[37–40] Disadvantages were the requirement for heavy shielding because of high-energy gammas (375 keV) and the potential long-standing contamination hazard because of the long physical half-life. ^{127}Xe was produced from the mid-1970s into the 1980s at Brookhaven National Laboratory, the Los Alamos Meson Production Facility, and the Tri University Meson Facility in Vancouver, British Columbia. After a short period of commercial production by the radiopharmaceutical industry, ^{127}Xe was removed from the market.

TABLE 16-4 Biologic Distribution of Xenon

Body Compartment	% Distribution in Body	Biologic Half-life
Lung (air)	68	22 sec
RBC (hemoglobin)	9	3 min
Muscle	11	0.4 hr
Fat	8	2.7 hr
Other tissue	4	7.6–17 hr

Source: Reference 41.

^{81m}Kr

In the mid-1970s, ^{81m}Kr gas became available as the daughter product of ^{81}Rb decay in a generator system ($^{81}Rb \xrightarrow{4.5\ hr} {}^{81m}Kr$). The advantage of ^{81m}Kr is a 190 keV gamma of 66% abundance that allows postperfusion imaging. When a perfusion defect is seen during the ^{99m}Tc study, the patient immediately inhales ^{81m}Kr. This permits viewing of the patient in the best projection so that perfusion–ventilation match–mismatch combinations can be visualized. The 13 second half-life of ^{81m}Kr permits ventilation imaging only on wash-in; no equilibrium or washout gas trapping images are possible. One advantage of the short half-life is insignificant radiation contamination risk. This system also has the disadvantage of requiring daily delivery because the ^{81}Rb parent has only a 4.5 hour half-life.

Biologic Distribution of Xenon

The amount of xenon that enters the body during a ventilation study is directly related to the lung air concentration, the duration of exposure, and xenon's solubility in tissue fluid. The poor solubility of xenon in water (12% at 25°C) is the reason for its slow absorption into the body. About 30 hours of rebreathing is required for xenon to reach an equilibrium concentration in other tissues.[41] Within the short time of 10 minutes required for a ventilation study, only about one-third of the administered activity of xenon enters the body, assuming a lung volume of 2.5 L and a ventilation system volume of 10 L. About two-thirds of this amount is in the lung and the remainder in other tissues (Table 16-4).

The amount of xenon distributed to various tissues and their subsequent rates of clearance are related to blood flow, tissue mass, and the tissue-to-blood partition coefficient. For example, the fat-to-blood coefficient is 7.9, whereas the skeletal muscle-to-blood coefficient is only 0.7.[42] Therefore, all things being equal, fatty tissue will concentrate far more xenon than muscle, and its rate of clearance will be slower. A greater fraction of the administered dose is distributed in muscle, however, because of its larger mass and greater blood flow. Activity in the liver is sometimes seen on xenon washout studies because of the organ's fatty content.

The clearance rate of xenon from the tissues varies considerably, being fastest from the lungs ($T_{½}$ = 22 seconds) and slowest from fat ($T_{½}$ = 8 to 17 hours).[41] Obese people will therefore retain xenon for longer periods of time than lean people.

Radioaerosols

Radioaerosol lung imaging predates the use of radioactive gases for ventilation imaging, because the radioaerosol image is essentially static and can be obtained with a rectilinear scanner. The dynamic nature of the wash-in and washout phases of current ventilation imaging requires the speed of a gamma camera. Radioaerosol imaging was only slowly

accepted, and one reason was the inability to generate aerosol droplets small enough for adequate diffusion into the lung periphery. Droplets larger than 3 to 5 μm in diameter cause hyperdeposition of aerosol in the trachea and major airways in subjects without airway obstruction, leading to false-positive scans. A droplet size smaller than 2 μm is necessary for good distribution and minimal large airway deposition.

A significant development revitalized the use of radioaerosol ventilation imaging.[43] This technique employed a settling bag between the nebulizer and the patient's mouthpiece. The bag removed most of the droplets larger than 2 μm by sedimentation, impaction, and turbulence, providing a more desirable particle-size range for ventilation imaging. Further research led to the development of nebulization systems that could efficiently generate aerosol droplet particles 1 μm or less, obviating the need for a settling bag. Commercially produced disposable devices are now available for routine use in radioaerosol inhalation studies. Figure 16-7 illustrates the essential components of these devices.

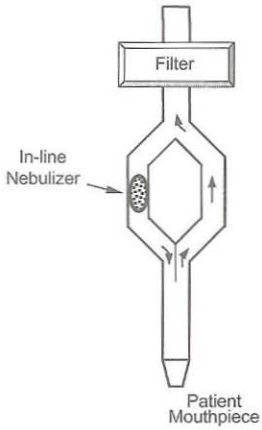

FIGURE 16-7 Diagram of a typical ^{99m}Tc-DTPA aerosol breathing unit.

A typical radioaerosol procedure involves placing 30 to 50 mCi (1110 to 1850 MBq) of ^{99m}Tc-pentetate (^{99m}Tc-DTPA) in a 2 to 3 mL volume into the nebulizer. Aerosol droplets are generated by forcing air or oxygen through the nebulizer at 8 to 10 L/minute at 25 to 50 psi. The patient inhales the radioaerosol during normal breathing through the mouth with the nose clamped shut. Radioaerosol that is not used by the patient or is exhaled during the procedure is trapped in a particle-retentive filter. The amount of radioactivity that is deposited in the patient's lungs depends on the initial nebulizer concentration, the length of breathing time, and the patient's condition. Generally, with a normal subject and an initial ^{99m}Tc-DTPA concentration of 30 mCi (1110 MBq) in 3 mL, the lung deposition of activity is approximately 0.1 mCi (3.7 MBq) per minute of breathing time. A typical study requires between 5 and 10 minutes of breathing time to acquire sufficient activity to perform inhalation imaging. The efficiency of delivering activity from the nebulizer to the lungs is only about 2% to 5%, which is why such a large amount of activity is placed in the nebulizer. After inhalation of radioaerosol, the unit is removed and the patient is transported to the gamma camera for imaging.

The technetium agent of choice for radioaerosol imaging is ^{99m}Tc-DTPA. Its rate of lung clearance into the blood is somewhat slower than that of ^{99m}Tc-sodium pertechnetate because of DTPA's larger molecular weight.[44] The clearance rate across the pulmonary epithelium into the blood is 1.5% per minute for ^{99m}Tc-DTPA and 5.1% per minute for ^{99m}Tc-pertechnetate.[44] ^{99m}Tc-DTPA also has faster and more complete elimination from the body by urinary excretion.

Technegas

A unique technetium aerosol called Technegas was developed in 1986.[45] Technegas particles are hexagonal platelets of metallic technetium encapsulated within a thin layer of graphite. The aerosol is produced by heating ^{99m}Tc-sodium pertechnetate solution to high temperature (2550°C for 15 seconds) in a graphite crucible. According to the following reaction, during the heating process pertechnetate is reduced to metallic technetium by carbon and encased in graphite a few nanometers thick, preventing its reoxidation:[46]

$$2NaTcO_4 + 3C \longrightarrow CO_2\uparrow + 2CO\uparrow + 2NaTcO_2 \longrightarrow 2NaO_2\uparrow + 2Tc$$

The average particle is 30 to 60 nm wide and 5 nm thick, with 80% of the particles below 100 nm.[46] The particles are hydrophobic and not subject to increases in size in the airways during inhalation, enabling them to penetrate deep into the lung.

Technegas is manufactured by an Australian firm, and a Technegas generator is marketed by MDS Nordion, Kanata, Ontario, Canada, for use in Europe, Africa, the Middle East, and South America. The product is not licensed in the United States.

VENTILATION–PERFUSION IMAGING METHODS

The general procedure used in ventilation imaging with radioactive gas has three parts: gas wash-in, equilibrium, and gas washout. The patient is attached to a closed-circuit breathing system supplied with oxygen (Figures 16-8 and 16-9). The study begins by having the patient inhale a bolus of ^{133}Xe gas (wash-in). A standard adult dosage is 10 mCi (370 MBq). Subsequently the patient rebreathes from the system for about 5 minutes to equilibrate the gas between the system and the lung. During this time xenon gas diffuses throughout the lung parenchyma and the count rate in the lung reaches a plateau (equilibrium). At this point the patient inhales room air and exhales the xenon activity into a

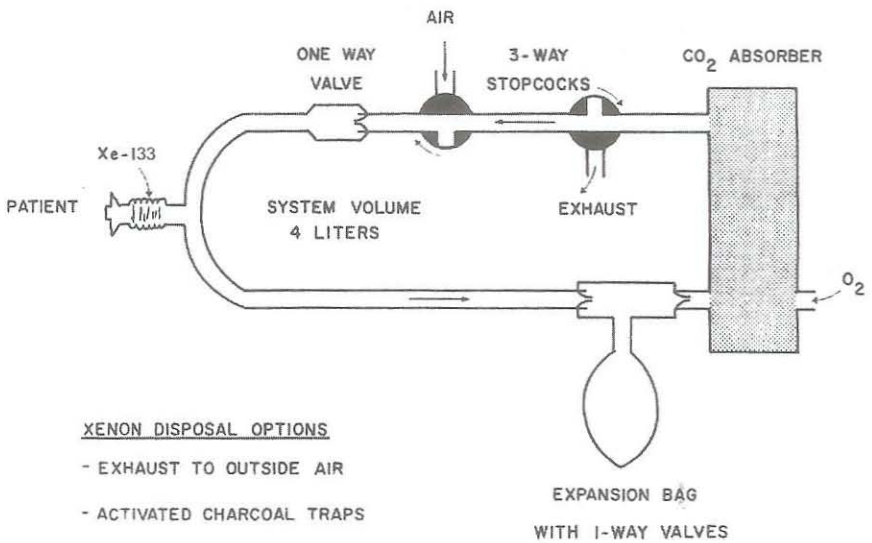

FIGURE 16-8 Diagram of a closed-circuit breathing device for administering radioactive xenon gas for lung ventilation imaging. The charcoal trap, moisture absorber, bacterial filter, and motorized blowers are omitted for simplicity.

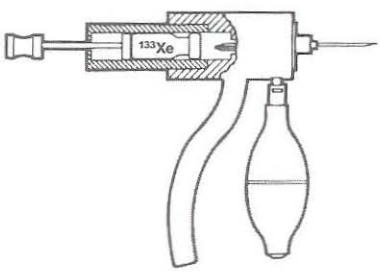

FIGURE 16-9 Hand-held device for administration of xenon gas. Forced air from the squeeze bulb transfers gas from the unit dose vial to the patient breathing system.

trap (washout). In the normal lung, inhaled gas will diffuse readily into all areas of lung parenchyma and, upon exhalation, the radioactive gas will wash out readily from the lung. In a lung where airflow and diffusion are impaired by obstructive airway disease, gas wash-in will be restricted and exhibit delayed accumulation in obstructed areas. During the equilibrium phase, when the patient rebreathes the radioactive gas, the gas atoms eventually diffuse into partially obstructed areas. Upon washout, normal areas lose activity readily, whereas poorly ventilated areas clear gas more slowly and appear as regions of trapped activity. Thus, xenon gas studies are a sensitive and quantifiable indicator of obstruction, especially in peripheral airways.[34] When the ventilation scan is abnormal and regions of gas trapping coincide with regions of perfusion defects seen on the ^{99m}Tc-MAA scan (a VQ match), the probability of PE is low and that of obstructive airway disease is high. When the ventilation scan is normal but the perfusion scan is abnormal (a VQ mismatch), the probability of PE is high.

Under ideal circumstances, in a patient with suspected PE the perfusion lung scan is performed first, because if it is normal there is no need for further evaluation. If perfusion defects are found, a subsequent ventilation scan with radioxenon will aid in obtaining a more definitive diagnosis. An important consideration when the perfusion study is performed first is that ^{99m}Tc activity will be present in the lung during the ventilation study because the ^{99m}Tc-MAA particles will not have cleared sufficiently from the lungs. Performing the ventilation study second requires that radioxenon have a photon energy higher than 140 keV to discriminate it from ^{99m}Tc activity present in the lungs. However, because ^{133}Xe has an 81 keV photon, the ventilation study is typically done first, obviating the problem of Compton-scattered ^{99m}Tc background activity in the ventilation image. A disadvantage of the study sequence in which ^{133}Xe is used first, followed by ^{99m}Tc-MAA, is that patients who have a normal perfusion study will have undergone an unnecessary ventilation study. A second potential disadvantage is that the mechanics of a radioxenon study limit it to a single viewing angle. Thus, patients are typically ventilated in the posterior projection. Although this projection best depicts most of the lung field, it may not be the best angle for viewing a particular defect seen on the perfusion scan.

When ^{127}Xe was available it was possible to perform the ^{99m}Tc-MAA perfusion study first, because the 203 keV of ^{127}Xe could be easily discriminated from the 140 keV of ^{99m}Tc. If a perfusion defect was found, the patient could be positioned with the best viewing projection in the ^{99m}Tc window and then imaged with ^{127}Xe in the higher-energy window. This procedure is also possible with ^{81m}Kr, but only the wash-in phase of the ventilation study can be viewed because of ^{81m}Kr's short half-life. Although the ideal viewing angle could be obtained with ^{81m}Kr, the inability to observe gas trapping during a washout phase reduces the study sensitivity.

Radioaerosols provide an alternative to xenon gas for ventilation imaging. Although aerosols may not be as effective as gases for penetrating deeply into the lung, they provide sufficient functional information to compare with perfusion scans. Aerosols have the inherent advantage of ready availability of technetium and DTPA kits and do not require special facilities and equipment to control a radioactive gas. Additionally, it is possible to record aerosol images in multiple projections because the aerosol particles are fixed in the lungs. Although the washout phase of the xenon study is the most sensitive method for detecting localized obstructive airway disease, radioaerosol studies provide a useful method if xenon is not available. Because both the perfusion and ventilation agents employ a ^{99m}Tc label, a potential interference problem occurs during imaging. This can be overcome by using different amounts of activity for the two studies. One method requires that the ^{99m}Tc-MAA perfusion scan be done with 1 mCi (37 MBq) and the aerosol study with 3 mCi (111 MBq).[34,47] The rationale is that embolic perfusion defects will demonstrate fill-in on the aerosol study. Complete fill-in, however, requires that the activity of the ^{99m}Tc aerosol

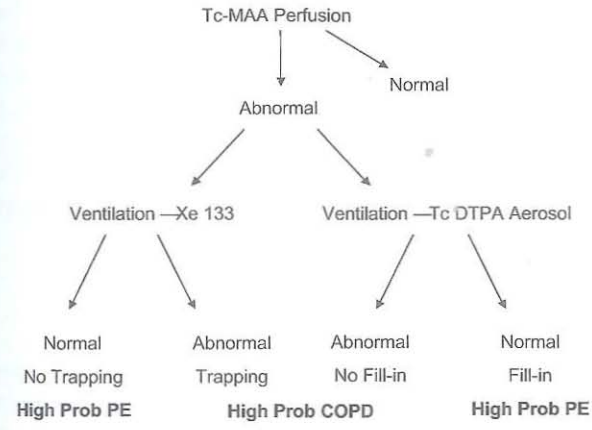

FIGURE 16-10 Perfusion–ventilation algorithm for VQ lung imaging.

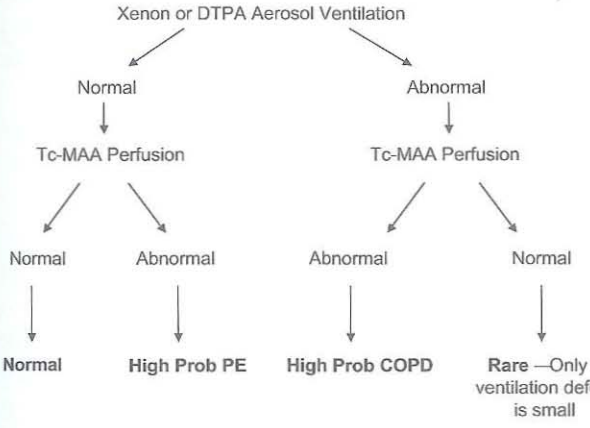

FIGURE 16-11 Ventilation–perfusion algorithm for VQ lung imaging.

present in the lung exceed that of the ^{99m}Tc-MAA injected by 2 to 3 times. A simple technique is to record the maximum count rate over the lungs from the ^{99m}Tc-MAA dose and then administer the aerosol with the patient supine until the lung count rate doubles or triples. Another technique is to perform the ^{99m}Tc-DTPA aerosol study first with about 1 mCi (37 MBq) and the ^{99m}Tc-MAA study second with 3 to 4 mCi (111 to 148 MBq).

Two simplified algorithms for distinguishing PE from chronic obstructive pulmonary disease (COPD) in patients after either a perfusion first/ventilation second or a ventilation first/perfusion second protocol are shown in Figures 16-10 and 16-11.

Xenon Administration Systems

A ventilation study with ^{133}Xe is performed with the patient attached to a closed breathing system. Several systems are available commercially. The essential components, illustrated in Figure 16-8, include a leak-resistant breathing circuit, a carbon dioxide absorber, a moisture absorber (essential for efficient charcoal trap function), an expansion device (spirometer or breathing bag), a bacterial filter (to protect the system), appropriate valves to control airflow and to admit oxygen on demand, and a device to trap the xenon when a study is complete.

Once the patient is acclimated to the breathing system, the xenon gas is flushed into the system near the patient's mouth during an inspired breath (the wash-in phase). Xenon is flushed from the vial with a special device (Figure 16-9). A double needle punctures

the vial stopper; air is pumped into the vial through one needle, and xenon activity exits through the other needle into the breathing system. The study continues to the equilibrium phase. At this point a valve in the breathing system is adjusted to permit room air to enter the system and flush xenon into a charcoal trap. The trap contains activated charcoal that retains the xenon atoms long enough to allow them to decay significantly before exiting the trap. A trap that contains moisture from the patient's breath will not retain xenon efficiently and must be replaced. Hence, silica gel or Drierite (W.A. Hammond) is used in the breathing system to absorb moisture.

Safety Control of Xenon

Federal and state regulations have been established to limit the concentration of radioactive material that can be expelled into water and air so that the total effective dose equivalent (TEDE) to the public does not exceed 0.1 rem per year and the dose rate from an external source to an unrestricted area does not exceed 2 mrem in any 1 hour. The regulations that relate to xenon release in effluents are described in Chapter 5, which contains specific calculations regarding release of ^{133}Xe so that the release does not exceed the derived air concentration. Chapter 5 also presents an example of how to determine the evacuation time in an imaging room if an accidental spill of xenon occurs.

NUCLEAR MEDICINE PROCEDURES

Rationale

Nuclear medicine functional imaging of the lungs is done to evaluate lung ventilation and perfusion. Lung ventilation is evaluated by imaging the lungs during inspiration of an inert gas such as xenon ^{133}Xe or a radiolabeled aerosol such as ^{99m}Tc-DTPA. Evaluation of perfusion involves intravenous administration of particles such as ^{99m}Tc-MAA and is based on capillary blockade. The most common indication for ventilation and perfusion lung imaging is evaluation of suspected acute PE. Other indications include evaluation of patients for lung transplantation (e.g., patients with cystic fibrosis), evaluation of patients with suspected chronic pulmonary emboli as a cause for pulmonary hypertension, preoperative evaluation of patients with COPD, and evaluation of differential lung function prior to surgical lobectomy or pneumonectomy.

Pulmonary Embolism

At least 94,000 new cases of PE are diagnosed in the United States each year; 25% of these patients die within 7 days, even with the availability of heparin prophylaxis.[48] Treatment involves timely identification of PE, appropriate anticoagulant therapy, and possible interventional therapies such as vena cava filter placement.

Clinically, PE is suspected when a patient experiences sudden-onset shortness of breath and pleuritic chest pain. This is even more worrisome in a person who is at high risk for PE. Many factors can lead to increased risk for PE; they include a history of previous PE or deep-vein thrombosis, use of oral contraceptives,[49] malignant neoplasms, surgery, trauma, immobilization, paralysis, long airplane flights, and certain blood factors.

VQ lung scans represent a safe, noninvasive means of evaluating patients with suspected PE. These studies are especially effective if the patient has a normal chest x-ray. In patients with normal chest x-rays, VQ scans have been shown to yield a definitive diagnosis of either PE or no PE in 83% of studies.[50] However, in many cases chest x-rays are

abnormal, which can lead to an increase in intermediate-probability scans. In these cases, helical computed tomography (CT) and multichannel CT have proven useful in evaluating suspected PE.

Procedure

The first step is to examine a current chest x-ray. If the patient is experiencing acute changes in symptoms, the chest x-ray should be performed and evaluated just before the VQ scan. Otherwise, a chest x-ray performed within 24 hours of the VQ scan is generally acceptable. If there are significant abnormalities on the chest x-ray that would warrant further anatomic imaging, such as a suspected tumor, then CT may be the more appropriate test for PE as well as for other abnormalities on the film. However, if there are no significant abnormalities on the chest x-ray, ventilation–perfusion imaging is an effective test for PE.

Before performing the ventilation or perfusion study, a clinical history should be obtained to evaluate the likelihood of PE. Also, special considerations should be made for certain patients. The radiation dose should be minimized in pregnant women. The number of ^{99m}Tc-MAA particles should be reduced in pediatric patients and patients with severe pulmonary hypertension or a known right-to-left ventricular shunt.

With the patient in the upright position, the dependent or lower lung zones usually demonstrate better ventilation and perfusion. This is more obvious on perfusion images than on ventilation images.[51] To compensate for the effects of gravity, patients are usually injected with ^{99m}Tc-MAA particles in the supine position. For the ventilation study, the patient can be in either upright or supine position during administration of the gas or aerosol.

The ventilation study is usually performed before the perfusion study. If the perfusion study is done first, activity from ^{99m}Tc-MAA will add background activity to the ^{133}Xe or ^{99m}Tc-DTPA ventilation study. If the ventilation study is done first with ^{133}Xe, the lower photon energy of ^{133}Xe will not contribute to the background activity in the higher-energy window of ^{99m}Tc. If the ventilation study is performed with ^{99m}Tc-DTPA aerosol prior to the perfusion study, a smaller amount of activity, in the range of 0.5 to 1 mCi (18.5 to 37 MBq), should be used so that at least 3 to 4 times this amount of activity can be used in the subsequent ^{99m}Tc-MAA perfusion study.

For the ventilation study, the patient is positioned either upright or supine in front of the camera. If ^{133}Xe is used, the ventilation study is usually done in three phases. The first phase is the first-breath or wash-in imaging phase. The second is the equilibrium phase, and the final part is the washout phase. The wash-in image is obtained when the patient first takes in a deep breath of the ^{133}Xe and holds it in for several seconds. The next set of images (the equilibrium phase) occurs while the patient is breathing into a closed system containing the ^{133}Xe and some oxygen. After this, the ^{133}Xe gas is either exhausted into the atmosphere or trapped using an activated charcoal filter, and images are obtained as the patient breathes fresh air or oxygen while the xenon clears from the lungs. Posterior or anterior and posterior images of the lungs are obtained during the wash-in, equilibrium, and washout phases of the study.

For the perfusion study, the patient is first instructed to cough and take a couple of deep breaths. The dose is administered intravenously while the patient is in the supine position. Since ^{99m}Tc-MAA particles may clump or settle out in the syringe, the syringe contents should be thoroughly mixed before administration to prevent focal hot spots on the images due to clumping. Anterior, posterior, lateral, and oblique views of the lungs are obtained.

Pharmaceuticals

For the ventilation study, radioactive inert gases such as ^{133}Xe or radiolabeled aerosols like ^{99m}Tc-DTPA are used. The most commonly used inert gas is ^{133}Xe, which has a physical half-life of approximately 5.3 days and principal gamma photon energy of 81 keV. The usual administered dose for adults is 5 to 20 mCi (185 to 740 MBq) using a facemask or mouthpiece connected to a xenon gas delivery system. Gas delivery and imaging are done in a room with negative pressure to exhaust the xenon gas.

Aerosol ventilation imaging can be performed with ^{99m}Tc-DTPA administered through a mouthpiece using a nebulizer. The usual administered dose is 0.5 to 1 mCi (18.5 to 37 MBq). One advantage of aerosol imaging is that the patient can be placed in the same positions as those used in the perfusion study for a more direct comparison.

For perfusion imaging, ^{99m}Tc-MAA is the agent of choice. The adult dosage range is 1 to 5 mCi (37 to 185 MBq), and the number of injected particles is typically between 200,000 and 700,000.[52] The number of particles should be reduced in patients with known severe pulmonary hypertension or right-to-left ventricular shunt. After administration of ^{99m}Tc-MAA, images are obtained in the anterior, posterior, right anterior oblique, left anterior oblique, right posterior oblique, left posterior oblique, right lateral, and left lateral projections.

Interpretation

In a normal ventilation study, homogeneous radiotracer activity is seen in both lungs in the first-breath or wash-in image (Figure 16-12A). During the washout phase, activity usually clears quickly from both lungs, within 2 to 3 minutes. Xenon is fat soluble and is often seen accumulating in the right upper quadrant during the washout phase in a patient with a fatty liver. Wash-in defects that normalize during the equilibrium phase and fail to clear normally in the washout phase (gas trapping) are often associated with obstructive pulmonary disease.

A normal perfusion study demonstrates homogeneous perfusion to both lungs (Figure 16-12B). A PE is typically seen as a wedge-shaped, pleural-based defect on perfusion images of the lungs secondary to obstruction of the associated segmental pulmonary arterial flow distal to the embolus. However, ventilation to this region is usually not affected. This results in a perfusion defect with no corresponding ventilation abnormality (a ventilation–perfusion mismatch).

Analysis of the perfusion portion of the study involves looking at the type of defects (classifying them as either segmental or nonsegmental), the number of defects, and the size of the defects. Segmental defects are associated with bronchopulmonary segmental territories. Subsegmental defects are associated with a portion or subset of a bronchopulmonary segmental territory. The size of a segmental perfusion defect is usually described as large, moderate, or small. A large segmental defect is defined as a perfusion defect that involves more than 75% of an anatomic lung segment. A moderate segmental defect involves 25% to 75% of a pulmonary segment, and a small segmental defect involves less than 25% of a segment. Nonsegmental defects are perfusion defects that do not correspond to any of the anatomic lung segments. Examples of nonsegmental perfusion defects include a large cardiac silhouette, tumor, pleural effusion, or elevation of a hemidiaphragm. Nonsegmental defects are not usually associated with pulmonary emboli. Once the perfusion defects have been categorized, they are compared with corresponding areas on the ventilation study. Matching ventilation–perfusion defects are usually not associated with PE.

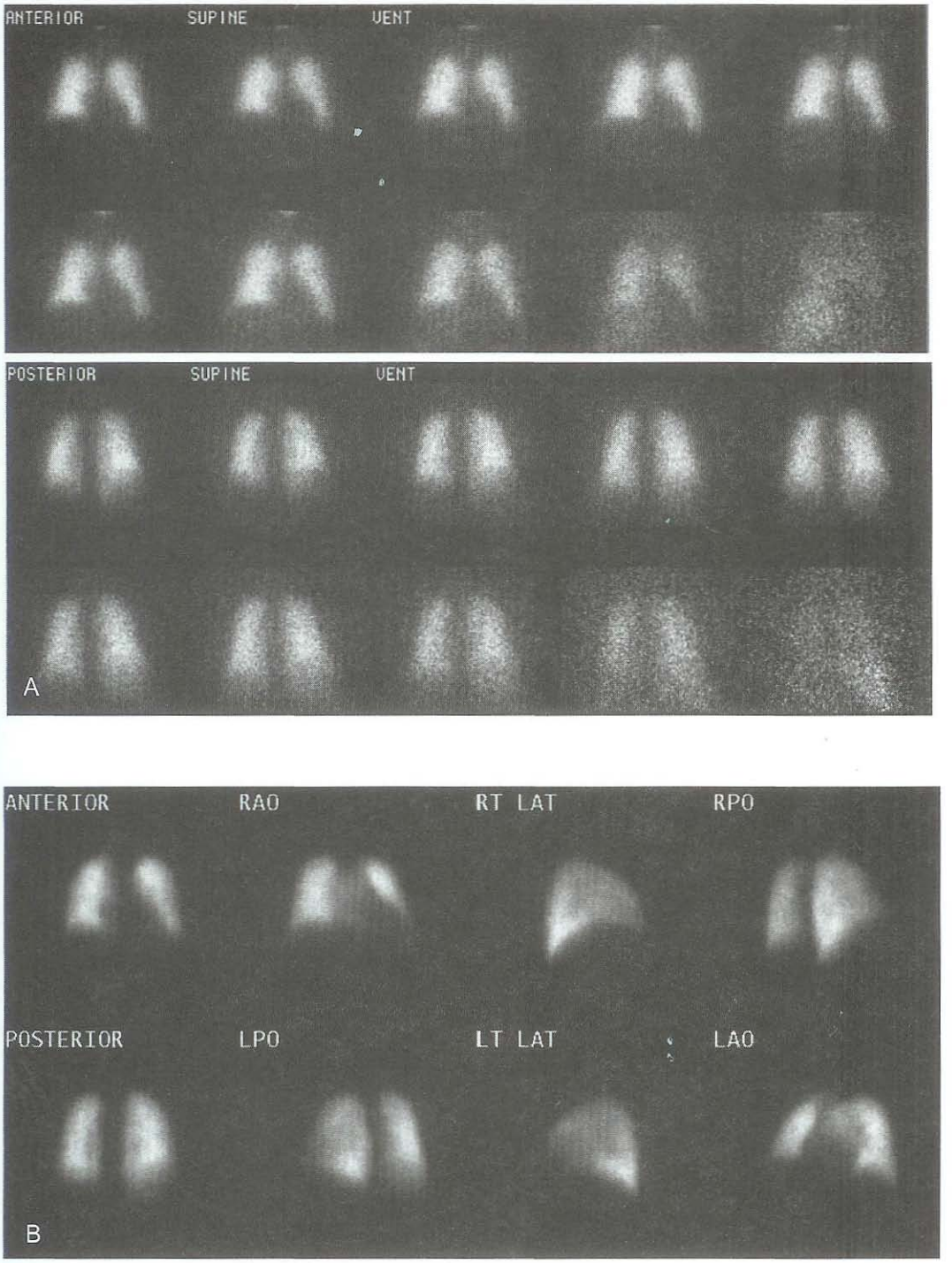

FIGURE 16-12 Normal ventilation/perfusion study. (A) Anterior and posterior ventilation images of the lungs obtained after administration of 8.6 mCi ^{133}Xe gas by facemask. No significant ventilation defects are seen in either the wash-in or washout phase. There is evidence of ^{133}Xe accumulation in the liver, likely representing some degree of fatty infiltration. (B) Anterior, posterior, lateral, and oblique images of the lungs obtained after intravenous administration of 3 mCi (111 MBq) of ^{99m}Tc-MAA. No perfusion defects are seen to suggest pulmonary emboli.

A normal perfusion study is one in which there are no perfusion defects and pulmonary perfusion matches the shape of the lungs seen on the chest x-ray (Figure 16-12B). A normal perfusion study essentially rules out the diagnosis of PE, regardless of any abnormalities on the ventilation study. In perfusion scans that demonstrate abnormalities, a set of diagnostic criteria is used to determine the probability of PE. These criteria are based on a large study, the Prospective Investigation of Pulmonary Embolism Diagnosis (PIOPED),[53] and were later redefined on the basis of retrospective analysis of the data.[54] The modified PIOPED criteria define high probability (≥80%), intermediate probability (20%–79%), and low probability (≤20%) for PE on the basis of combined results from the ventilation and perfusion studies.

Using these criteria, if two or more large segmental perfusion defects are seen without a corresponding ventilation abnormality (ventilation–perfusion mismatch), the probability of PE is considered high. The probability is also considered high with any combination of moderate or large mismatches that are the equivalent of two large segmental defects. Two moderate defects are considered equivalent to one large defect. In the PIOPED study, the specificity of a high-probability ventilation–perfusion study for PE was 97% (Figure 16-13).

The probability of PE is low if the study shows only small perfusion defects, matched perfusion and ventilation defects with a normal chest x-ray, nonsegmental perfusion defects, or any perfusion defect with a substantially larger chest x-ray abnormality. Studies that are difficult to categorize as either high or low probability are considered to show an intermediate probability for PE. An example of this would be a study with one or two moderate mismatched segmental perfusion defects.

Matching ventilation and perfusion defects can be seen with a number of conditions, including COPD, congestive heart failure, pleural effusion, lung tumors, bullous disease, and mucus plugs (Figure 16-14).

Differential Lung Perfusion

Surgical resection of tumors is a consideration in patients with non–small-cell lung carcinoma that has not advanced to stage IIIb or stage IV. The surgeon's decision to perform surgery for lung cancer depends on the patient's ability to tolerate the procedure. Differential perfusion studies along with pulmonary function studies can help to determine if the patient will be able to tolerate lobectomy or pneumonectomy. Surgical resection of all or a portion of the lung can lead to significant patient disability if the forced expiratory volume at 1 second (FEV_1) is reduced to less than 0.8 L.[55] Differential lung perfusion along with pulmonary function measurement has been found to be an accurate predictor of postoperative lung function.[56]

Anterior and posterior images of the lungs are obtained after intravenous administration of 1 to 5 mCi (37 to 185 MBq) of ^{99m}Tc-MAA. Regions of interest are drawn around each lung in both the anterior and posterior images. Counts are obtained for the anterior and posterior regions and geometric means are calculated to determine differential lung perfusion. If partial lobectomy is a consideration, the lungs can be further divided into upper, middle, and lower lung zones for a more complete evaluation of function. The differential perfusion values, along with pulmonary function test data, can be used to estimate postoperative lung function (Figure 16-15).

Right-to-Left Shunt Evaluation

Radionuclide imaging can be used to detect and quantify right-to-left shunting in congenital heart disease. Imaging can also be useful for follow-up evaluation of a right-to-left shunt to

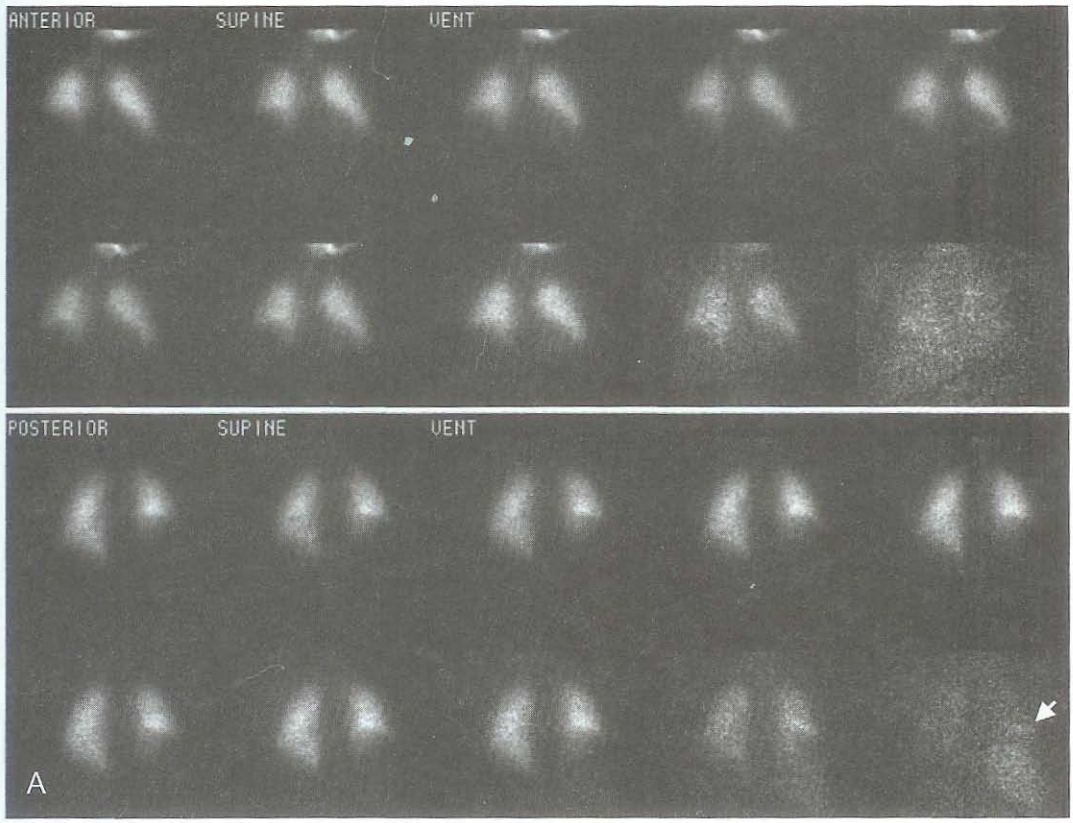

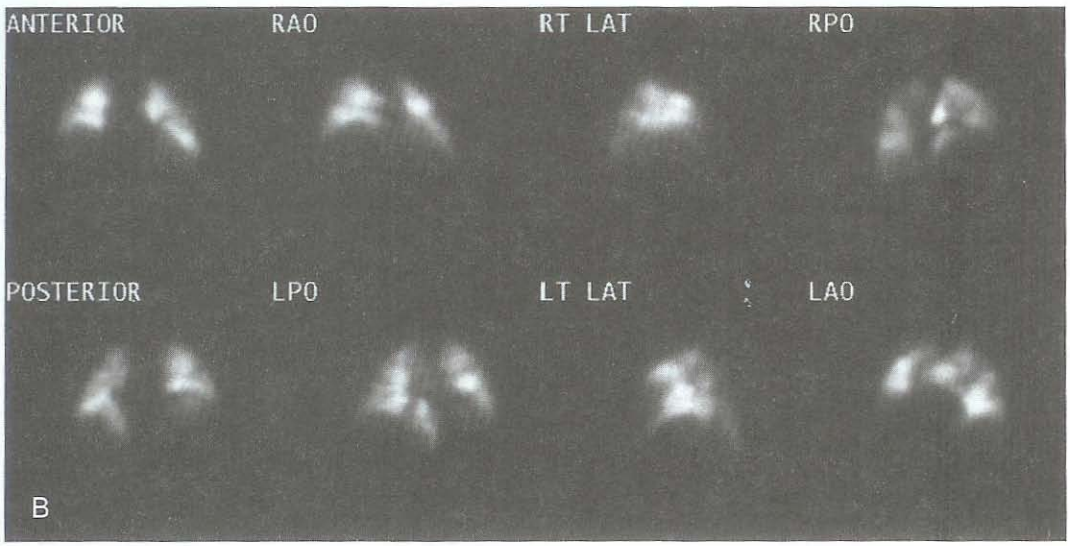

FIGURE 16-13 High probability for pulmonary emboli. (A) ^{133}Xe ventilation study with no significant ventilation defects seen on the initial first-breath or wash-in image. There is evidence of mild gas trapping at the right base (arrow) in the washout phase. Also notice ^{133}Xe uptake in the liver below the region of mild gas trapping. (B) A ^{99m}Tc-MAA perfusion study done immediately after the ventilation study demonstrated multiple wedge-shaped, pleural-based perfusion defects consistent with a high probability for pulmonary embolism.

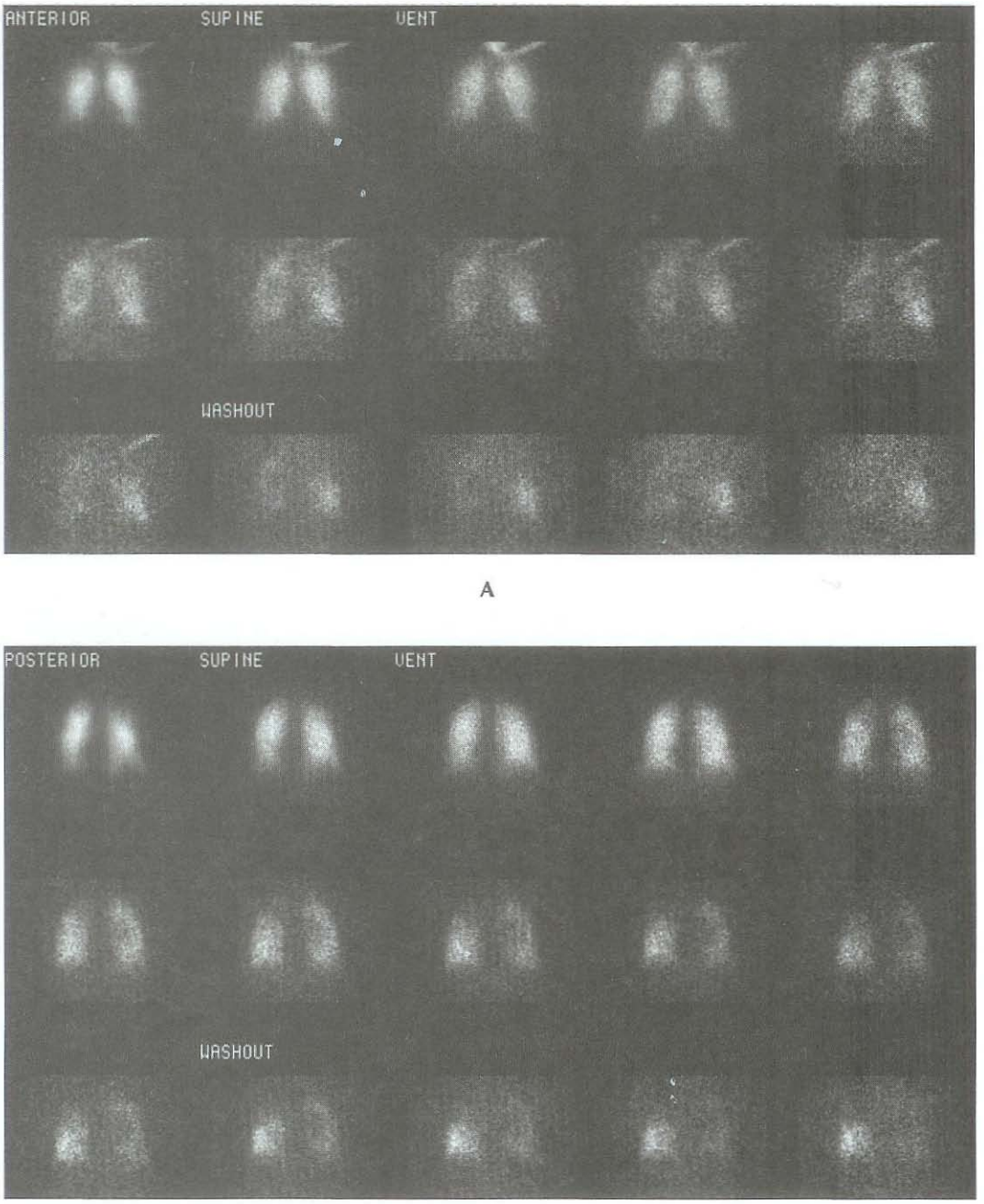

FIGURE 16-14 Obstructive pulmonary disease. (A) Anterior and (B) posterior images from a ^{133}Xe ventilation study demonstrating defects at both lung bases and the right lung apex on the first-breath image. These defects fill in during the equilibrium phase of the study and then demonstrate gas trapping during the washout phase. (C) On the ^{99m}Tc-MAA perfusion study, there is heterogeneous perfusion in both lungs with matching perfusion defects seen at the right lung apex and both bases. Matching ventilation and perfusion defects are most likely related to obstructive pulmonary disease and not to pulmonary emboli.

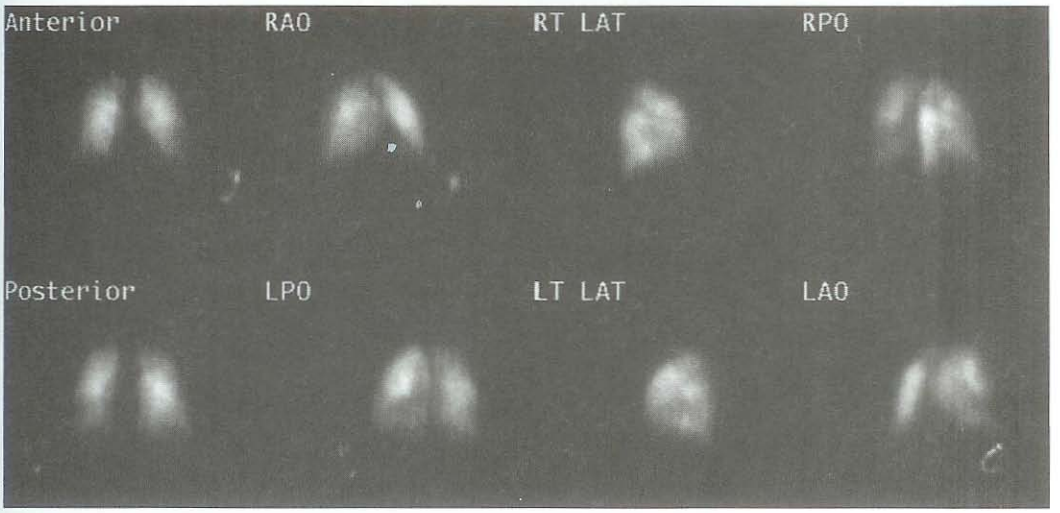

C

FIGURE 16-14 (Continued)

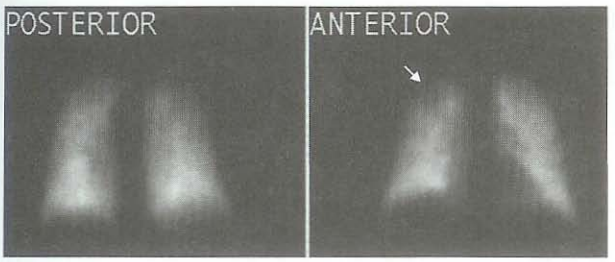

A

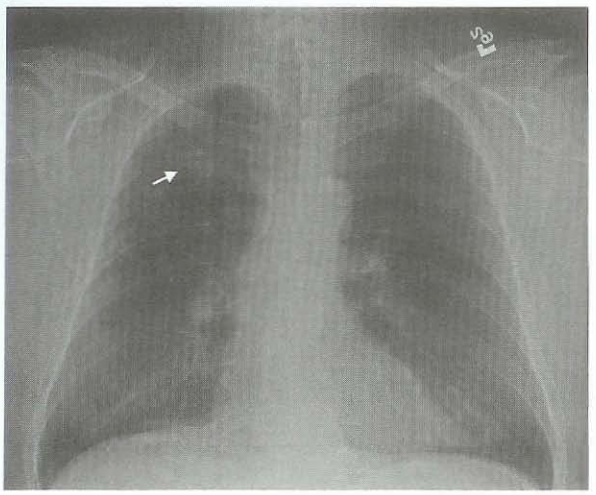

B

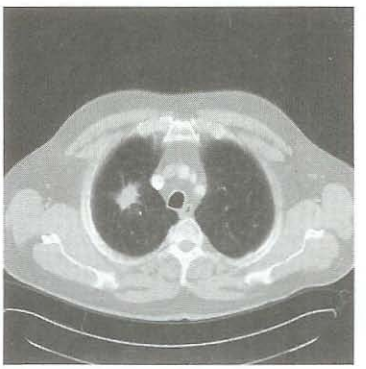

C

FIGURE 16-15 Differential lung perfusion study in a person with lung cancer. (A) Anterior and posterior images of the lungs were obtained after intravenous administration of 3 mCi (111 MBq) of ^{99m}Tc-MAA. There is a perfusion defect seen in the right upper lobe that corresponds to the patient's lung mass seen on chest x-ray (B) and chest CT (C). Regions of interest were drawn around each lung in the anterior and posterior perfusion images, and geometric means were calculated to determine the differential lung perfusion (D, page 584), which was equal in this study.

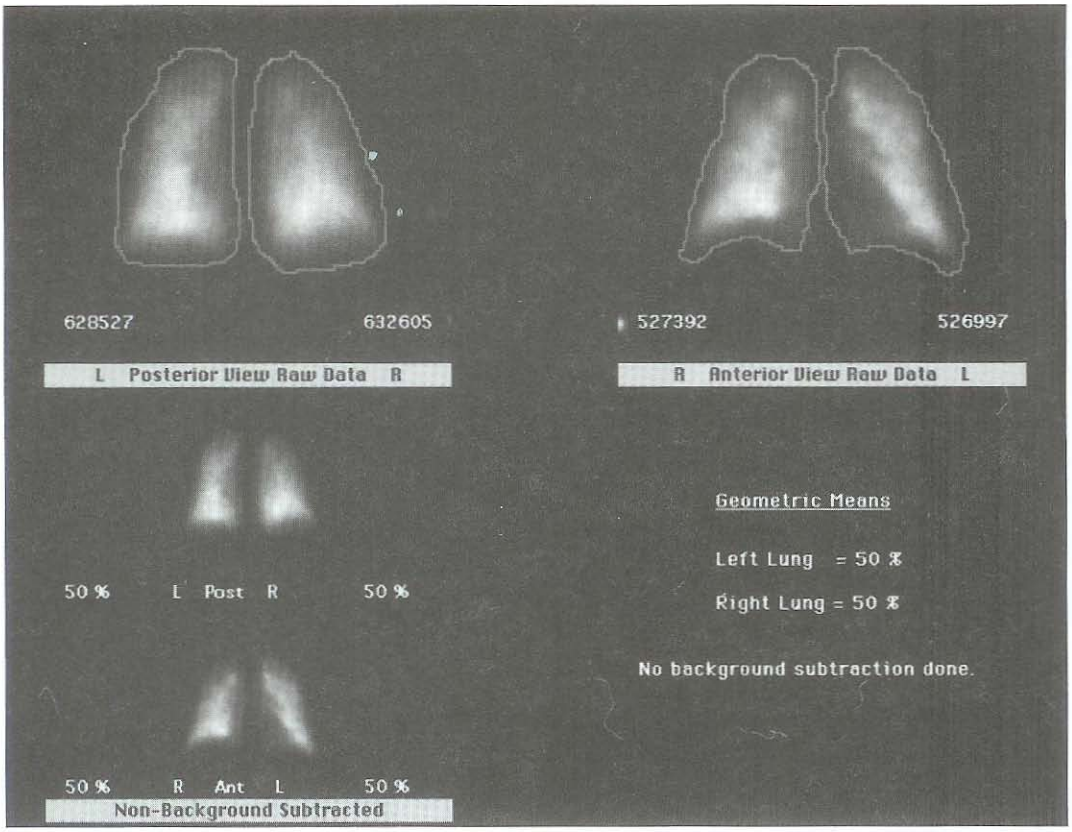

D

FIGURE 16-15 (Continued)

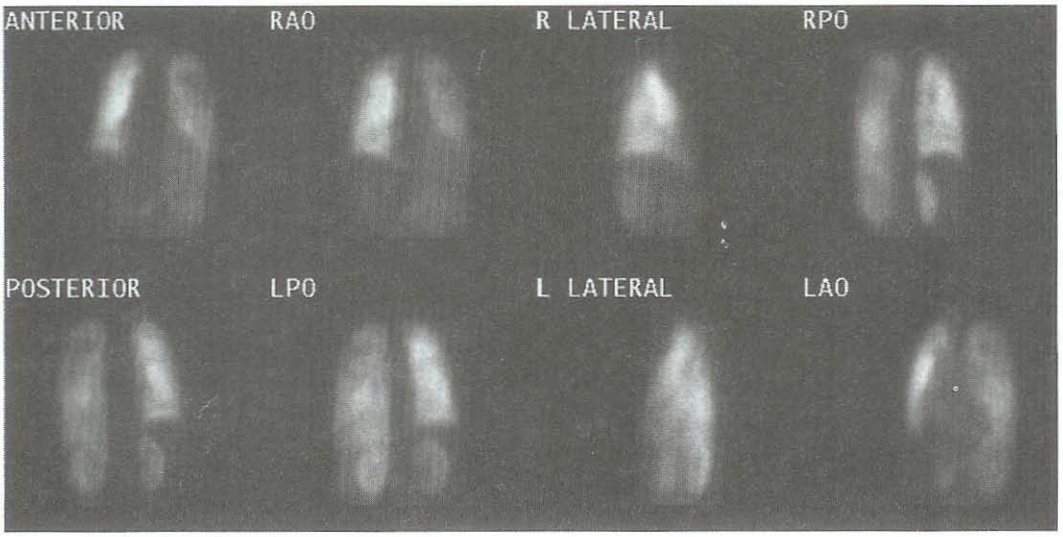

FIGURE 16-16 Right-to-left shunt in a patient with ventricular septal defect and left pulmonary atresia. ^{99m}Tc-MAA perfusion images demonstrate decreased perfusion to the left lung consistent with the patient's history of left pulmonary atresia. Radiotracer activity is seen outside the lungs in the kidneys, consistent with a right-to-left shunt.

determine worsening or improvement and after corrective surgery. The most common method is to use ^{99m}Tc-MAA.[57] In a normal perfusion scan, intravenous administration of ^{99m}Tc-MAA results in the particles being trapped in the lungs by capillary blockade. Normally, about 95% of the ^{99m}Tc-MAA particles become trapped in the pulmonary capillary bed and the remainder escape into the systemic circulation via normal anatomic shunting. When there is a right-to-left shunt, some of the intravenous particles will bypass the lungs and increase the amount entering the systemic circulation (Figure 16-16). Once in the systemic circulation, they will become trapped in systemic capillary beds. Total body scanning after administration of ^{99m}Tc-MAA permits determination of the percentage of particles trapped in the lungs versus those diverted into the systemic circulation:

$$\% \text{ Right-to-left shunt} = \frac{(\text{Total body counts} - \text{Total lung counts}) \times 100}{\text{Total body counts}}$$

REFERENCES

1. Weibel ER. Morphological basis of alveolar-capillary gas exchange. *Physiol Rev.* 1973;53:419-95.
2. Weibel ER. *Morphometry of the Human Lung*. New York: Academic Press; 1963:73-86.
3. Weibel ER. Morphological basis for V/Q distribution. In: Hutas I, Debreczeni LA, eds. *Advances in Physiological Sciences. Vol 10: Respiration*. Budapest: Pergamon Press; 1980:179-189.
4. Bryan AC, Bentivoglio LG, Beerel F, et al. Determination of regional variations in ventilation and perfusion in normal subjects using xenon 133. *J Appl Physiol.* 1964;19:395-402.
5. Guyton AC. *Textbook of Medical Physiology.* 6th ed. Philadelphia: WB Saunders; 1981:296.
6. Muller JH, Rossier PH. A new method for the treatment of cancer of the lungs by means of artificial radioactivity. *Acta Radiol.* 1951;35:449-68.
7. Haynie TP, Calhoon JD, Nasjleti CE, et al. Visualization of pulmonary artery occlusion by photoscanning. *JAMA.* 1963;185:306-8.
8. Taplin GV, Johnson DE, Dore EK, et al. Suspensions of radioalbumin aggregates for photoscanning the liver, spleen, and lung and other organs. *J Nucl Med.* 1964;5:259-75.
9. Lindeman JF, Quinn JL III. The recent history of clinical procedures in nuclear medicine. In: Gottschalk A, Potchen EJ, eds. *Diagnostic Nuclear Medicine.* Baltimore: Williams & Wilkins; 1976:8-13.
10. Stern HS, Goodwin DA, Wagner HN Jr, et al. In-113m—a short-lived isotope for lung scanning. *Nucleonics.* 1966;24:57-60.
11. Robinowitz M, Mathew J, Eckelman W, et al. Fatal reactions after Tc-99m ferrous hydroxide lung scans [abstract]. *J Nucl Med.* 1973;14:445.
12. Zolle I, Rhodes BA, Wagner HN Jr. Preparation of metabolizable radioactive human serum albumin microspheres for studies of the circulation. *Int J Appl Radiat Isot.* 1970;21:155-67.
13. Rhodes BA, Stern HS, Buchannan JA, et al. Lung scanning with Tc-99m microspheres. *Radiology.* 1971;99:613-21.
14. Subramanian G, Arnold RW, Thomas FD, et al. Evaluation of an instant Tc-99m labeled lung scanning agent [abstract]. *J Nucl Med.* 1972;13:790.
15. Davis MA. Particulate radiopharmaceuticals for pulmonary studies. In: Subramanian G, Rhodes BA, Cooper JF, et al., eds. *Radiopharmaceuticals.* New York: Society of Nuclear Medicine; 1975:267-81.
16. Heck LL, Duley JW. Statistical considerations in lung imaging with Tc-99m albumin particles. *Radiology.* 1974;113:675-9.
17. Dworkin HJ, Gutkowski RF, Porter W, et al. Effect of particle number on lung perfusion images. *J Nucl Med.* 1977;18:260-2.
18. Iio M, Wagner HN Jr. Studies of reticuloendothelial system (RES). I: Measurement of the phagocytic capacity of the RES in man and dog. *J Clin Invest.* 1963;42:417-26.
19. Taplin GV, MacDonald NS. Radiochemistry of macroaggregated albumin and newer lung scanning agents. *Semin Nucl Med.* 1971;1:132-52.
20. Burdine JA, Sonnemaker RE, Ryder LA, et al. Perfusion studies with technetium-99m human albumin microspheres (HAM). *Radiology.* 1970;95:101-7.
21. Davis MA. Long-term retention and biologic fate of Tc-99m iron hydroxide aggregates. In: *Radiopharmaceuticals and Labeled Compounds.* Vol 2. Vienna, Austria: International Atomic Energy Agency; 1973:43-63.

22. Busse W, Reed C, Tyson I, et al. Prolonged retention of radioactivity after perfusion lung scan in asthmatic patients. *J Nucl Med.* 1973;14:837-9.
23. Gallagher BM. Personal communication. North Billerica, MA: New England Nuclear Corp; 1983.
24. Kowalsky RJ. Safety and effectiveness considerations with particulate lung scanning agents. *J Nucl Med Technol.* 1982;10:223-7.
25. Dworkin HJ, Smith JR, Bull FE. A reaction after administration of macroaggregated albumin (MAA) for a lung scan. *AJR Am J Roentgenol.* 1966;98:427-33.
26. Vincent WR, Goldberg SJ, Desilets D. Fatality immediately after rapid infusion of macroaggregates of Tc-99 albumin (MAA) for lung scan. *Radiology.* 1968;91:1181-4.
27. Williams JO. Death after injection of lung scanning agent in a case of pulmonary hypertension. *Br J Radiol.* 1974;47:61-3.
28. Child JS, Wolfe JD, Tashkin D, et al. Fatal lung scan in a case of pulmonary hypertension due to obliterative pulmonary vascular disease. *Chest.* 1975;67:308-10.
29. Davis MA, Taube RA. Pulmonary perfusion imaging: acute toxicity and safety factors as a function of particle size. *J Nucl Med.* 1978;19:1209-13.
30. Allen DR, Ferens JM, Cheney FW, et al. Critical evaluation of acute cardiopulmonary toxicity of microspheres. *J Nucl Med.* 1978;19:1204-8.
31. Allen DR, Nelp WB, Hartnett DE, et al. Critical assessment of changes in the pulmonary circulation after injection of lung scanning agent (MAA). In: *Radiopharmaceuticals and Labeled Compounds.* Vol 2. Vienna, Austria: International Atomic Energy Agency; 1973:37-41.
32. Heyman S. Toxicity and safety factors associated with lung perfusion studies with radiolabeled particles [letter]. *J Nucl Med.* 1979;20:1098-9.
33. Davis MA, Taube RA. Toxicity and safety factors associated with lung perfusion studies with radiolabeled particles [reply]. *J Nucl Med.* 1979;20:1099.
34. Taplin GV, Chopra SK. Lung perfusion-ventilation scintigraphy in obstructive airway disease and pulmonary embolism. *Radiol Clin North Am.* 1978;16:491-513.
35. Newhouse MT, Wright FJ, Ingham GK, et al. Use of scintillation camera and xenon-135 for study of topographic pulmonary function. *Respir Physiol.* 1968;4:141-53.
36. Hoffer PB, Harper PV, Beck RN, et al. Improved xenon images with Xe-127. *J Nucl Med.* 1973;14:172-4.
37. Atkins HL, Susskind H, Klopper JF, et al. A clinical comparison of Xe-127 and Xe-133 for ventilation studies. *J Nucl Med.* 1977;18:653-9.
38. Chilton HM, Cooper JF, Friedman BI. Xe-127 ventilation imaging immediately after Tc-99m perfusion studies. *Clin Nucl Med.* 1977;2:152-4.
39. Goddard BA, Ackery DM. Xenon-133, Xe-127, and Xe-125 for lung function investigations: a dosimetric comparison. *J Nucl Med.* 1975;16:780-6.
40. McCartney WH, Perry JR, Staab EV, et al. Comparison of Xe-127 and Xe-133 in ventilation-perfusion imaging in diagnosis of pulmonary embolus [abstract]. *J Nucl Med.* 1978;19:675.
41. Susskind H, Atkins HL, Cohn SH, et al. Whole-body retention of radioxenon. *J Nucl Med.* 1977;18:462-71.
42. Ponto RA, Loken MK. Radioactive gases: production, properties, handling and uses. In: Subramanian G, Rhodes BA, Cooper JF, et al., eds. *Radiopharmaceuticals.* New York: Society of Nuclear Medicine; 1975:296-403.
43. Hayes M, Taplin GV, Chopra SK, et al. Improved radioaerosol administration system for routine inhalation lung imaging. *Radiology.* 1979;131:256-8.
44. Rinderknecht J, Shapiro L, Krouthhammer M, et al. Accelerated clearance of small solutes from the lungs in interstitial lung disease. *Am Rev Respir Dis.* 1980;121:105-17.
45. Burch W, Sullivan P, McLaren C. Technegas: a new ventilation agent for lung scanning. *Nucl Med Commun.* 1986;7:865-71.
46. Senden TJ, Moock KH, Fitz Gerald J, et al. The physical and chemical nature of technegas. *J Nucl Med.* 1997;38:1327-33.
47. Hayes M, Taplin GV. Lung imaging with radioaerosols for the assessment of airway disease. *Semin Nucl Med.* 1980;10:243-51.
48. Gray HW. The natural history of venous thromboembolism: impact on ventilation/perfusion scan reporting. *Semin Nucl Med.* 2002; 32:159-72.
49. Koster T, Small RA, Rosendaal FR, et al. Oral contraceptives and venous thromboembolism: a quantitative discussion of the uncertainties. *J Intern Med.* 1995;238:31-7.
50. Gottschalk A. New criteria for ventilation-perfusion lung scan interpretation: a basis for optimal interaction with helical CT angiography. *Radiographics.* 2000;20:1206-10.
51. Elgazzar AH, Khadada M. Respiratory system. In: Elgazzar AH, ed. *The Pathophysiologic Basis of Nuclear Medicine.* New York: Springer-Verlag; 2001:189-99.
52. Parker JA, Coleman RE, Siegel BA, et al. Procedure guideline for lung scintigraphy. In: *Procedure Guidelines Manual 2001-2002.* Reston, VA: Society of Nuclear Medicine; 2001:181-6.

53. PIOPED Investigators. Value of the ventilation/perfusion scan in acute pulmonary embolism: results of the Prospective Investigation of Pulmonary Embolism Diagnosis (PIOPED). *JAMA*. 1990;263:2753-9.
54. Gottschalk A, Sostman HD, Coleman RE, et al. Ventilation-perfusion scintigraphy in the PIOPED study. II: Evaluation of the scintigraphic criteria and interpretations. *J Nucl Med*. 1993;34:1119-26.
55. Williams CD, Brenowitz JB. "Prohibitive" lung function and major surgical procedures. *Am J Surg*. 1976;132:763-6.
56. Wernly JA, DeMeester TR, Kirchner PT, et al. Clinical value of quantitative ventilation-perfusion lung scans in the surgical management of bronchogenic carcinoma. *J Thorac Cardiovasc Surg*. 1980;80:535-43.
57. Gates GF, Orme HW, Dore EK. Measurement of cardiac shunting with technetium-labeled albumin aggregates. *J Nucl Med* 1971;12:746-9.

17 Liver, Spleen, and Gastrointestinal System

One of the first organs to be studied with radiopharmaceuticals was the liver. Soon after the introduction of ^{99m}Tc-sodium pertechnetate for imaging of the thyroid gland and the brain, ^{99m}Tc-sulfur colloid (^{99m}Tc-SC) was developed for liver imaging. This radiopharmaceutical has remained a key radiotracer in nuclear medicine, and its use has been expanded to other applications, including lymphoscintigraphy and gastrointestinal (GI) studies.

The liver, spleen, and bone marrow make up a major part of the reticuloendothelial system (RES). The venous sinuses of these organs are lined with reticular cells that remove from the blood foreign particles or degraded endogenous substances, such as effete red blood cells, bacteria, endotoxins, and denatured proteins. In addition, the liver excretes certain substances into the bile. Understanding these normal functions was essential in designing radioactive drugs to evaluate them.

Over the years, new techniques have been developed for using radiopharmaceuticals to evaluate organ systems. Technetium radiopharmaceuticals that were originally designed to study the liver and spleen are now used in studies of GI function, including evaluation of gastroesophageal reflux and gastric emptying and localization of GI bleeding sites.

LIVER

Two principal types of radiopharmaceuticals have been used to study the liver: particulate agents (radiocolloids) and hepatobiliary agents. Radiocolloids are trapped within the liver sinusoids, permitting morphologic evaluation of the liver, while hepatobiliary agents undergo hepatocyte extraction and excretion into bile, permitting functional assessment of the liver.

Physiologic Anatomy

A diagram of the liver and hepatobiliary system is shown in Figure 17-1. The two principal types of liver cells are the hepatocytes and the sinusoidal cells. The hepatocytes, also called polygonal cells because of their shape, account for 85% of the cells in the liver and are responsible for its major metabolic functions. The sinusoidal cells constitute the remaining 15% of liver cells.

The functional units of the liver are the lobules, which number between 50,000 and 100,000.[1] Each lobule consists of a segment of the central vein surrounded by a number of sinusoids in an arrangement similar to spokes around the hub of a wheel (Figure 17-2). The sinusoids transport blood from the portal vein to the lobule. Blood is then directed to the central vein and ultimately to the hepatic vein.

Two main types of cells make up the sinusoids: endothelial cells and Kupffer's cells. Endothelial cells form the main structure, the sinusoidal conduit, which transports blood through the lobule. Kupffer's cells, which are dispersed along the sinusoid, are macrophages

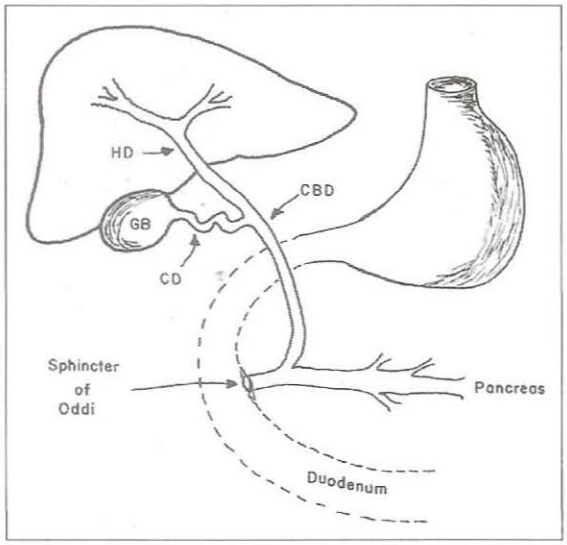

FIGURE 17-1 Liver and hepatobiliary system. Hepatic duct (HD), gallbladder (GB), cystic duct (CD), common bile duct (CBD).

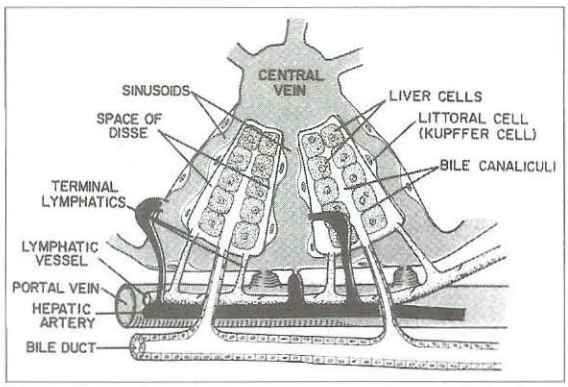

FIGURE 17-2 Basic structure of a liver lobule showing the hepatic cellular plates, the blood vessels, the bile-collecting system, and the lymph flow system composed of the space of Disse and the interlobular lymphatics. (Reprinted with permission of Elsevier Science from reference 1.)

that remove foreign substances from the blood as it passes through the liver. Surrounding the sinusoids are the hepatocytes. Between the sinusoid and the hepatocytes is the space of Disse. This space ranges from 0.25 μm to 2.0 μm in depth and contains a reinforcing network of collagen fibers. Features of liver microanatomy are depicted in Figure 17-3 and have been described by Elias and Serrick.[2]

Sinusoidal Cells

Endothelial cells are flat, irregularly shaped cells characterized by numerous pores (fenestrae) that appear throughout their cytoplasm. The pores are approximately 0.1 μm in diameter. Molecular substances and small particles can leave the sinusoidal blood through the pores to enter the space of Disse, where they have access to the underlying hepatocytes. Larger particles can enter the space through the 0.02 to 1.0 μm wide slits between the endothelial cells. In addition to this sievelike function, endothelial cells contain pinocytotic vesicles that can sequester particles less than 0.1 μm in size. This process has been observed with antimony sulfide particles.

Kupffer's cells vary in shape but are basically stellate. They lie on or embedded in the endothelial lining and can also lie at least partly in the space of Disse, where their microvilli

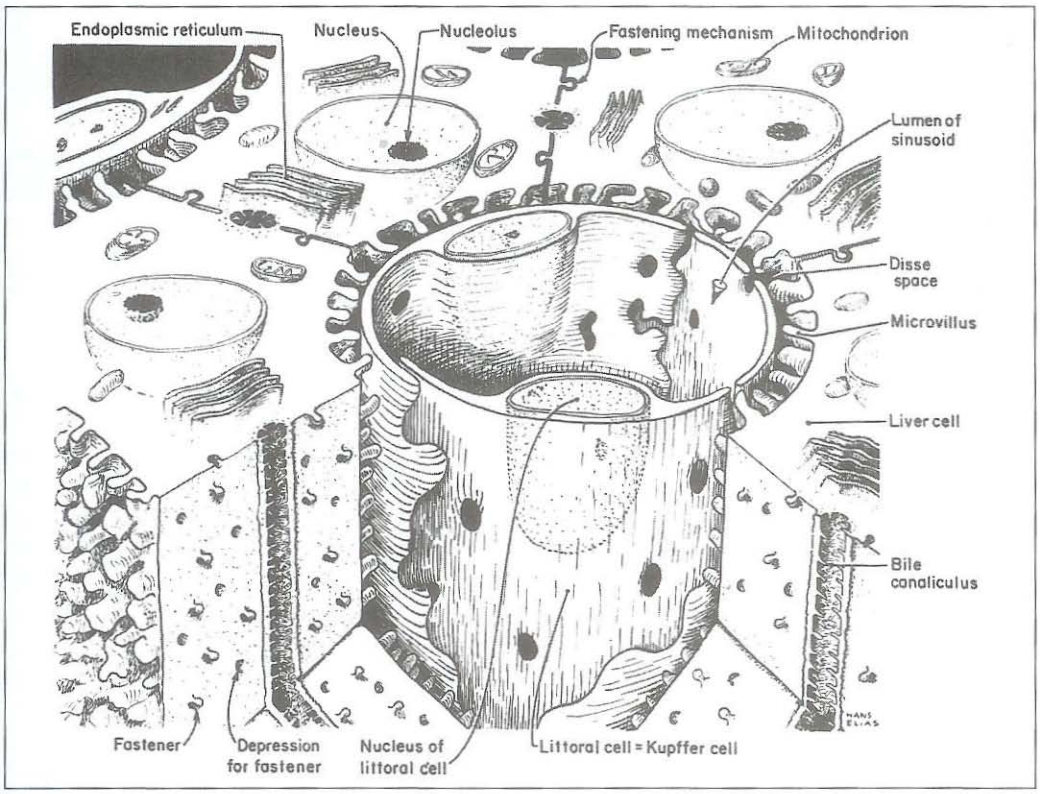

FIGURE 17-3 Ultrastructure of the mammalian liver. (Reprinted with author permission from Elias H, Pauly JE. *Human Microanatomy.* Chicago: DaVinci Publishers; 1960:135. [Publication is out of print.])

intermingle with the microvilli of the hepatocytes. They also tend to accumulate near the branches of the portal vein. Their variability in shape and position suggests that Kupffer's cells are mobile. Kupffer's cells have bulky cytoplasm that is rich in lysosomes, indicating their ability to digest various substances. Their membrane is covered with a 70 nm thick, fuzzy coat of proteinlike material that contains pinocytotic structures capable of trapping particles less than 0.1 μm in size. Additionally, Kupffer's cells are capable of phagocytosis, having pseudopodia that engulf particles larger than 0.1 μm.

Some general properties of phagocytosis by Kupffer's cells have been observed. Microscopic studies have shown in several instances, although not with all types of substances, that intravenously injected particles become coated with a serum protein (opsonin). This coating is believed to resemble fibrin, because heparin prevents the reaction. The coating frequently causes the particles to adhere to each other and to the walls of the liver sinusoids. Thus, because of aggregation, particle size in vivo can be much larger than the preinjection size. A coated particle that adheres to the fuzzy coat of a Kupffer's cell induces the phagocytic process. Once particles are inside the cell, lysosomes digest metabolizable particles and dispose of them by reutilization or excretion. Indigestible particles may be stored in lysosomes or distributed over their daughter cells or to other organs by the migration of loaded Kupffer's cells. Sinusoidal cell function has been described in detail by Wisse.[3,4]

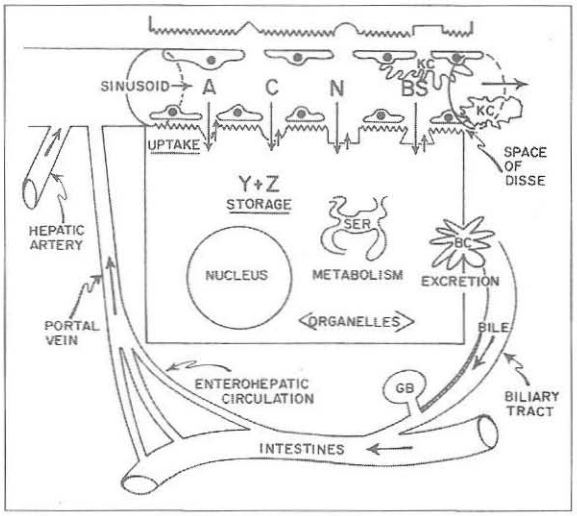

FIGURE 17-4 Schematic representation of the hepatocyte. Substrates in the blood diffuse through pores in the endothelial lining of the sinusoids and bind to the hepatocyte at one of four membrane-bound carriers: anionic (A), cationic (C), nonionic (N), and bile salt (BS). Within the hepatocyte a substrate may be stored at specific binding sites such as Y and Z proteins, and it also may undergo metabolic conversion at other sites, including the smooth endoplasmic reticulum (SER). Biliary excretion occurs at a biliary canaliculus (BC). Subsequently, the substrate in the bile may be stored and concentrated in the gallbladder (GB) or excreted into the intestine. Some biliary components are reabsorbed from the intestine into the portal vein and reextracted by the hepatocyte (enterohepatic circulation). The sinusoids are lined by Kupffer's cells (KC), which are a part of the reticuloendothelial system. (Reprinted with permission of the Society of Nuclear Medicine from reference 6.)

Hepatocytes

Hepatocytes are polygonal and about 30 μm in diameter, with eight or more surfaces. The cells are arranged in plates one cell thick that form an irregular wall surrounding the sinusoids. The hepatocyte has three physiologic surfaces: a surface that contacts neighboring hepatocytes, a grooved surface that delimits bile canaliculi, and a sinusoidal surface that projects numerous microvilli into the space of Disse.[5]

Soluble substances that leave the sinusoidal blood and enter the space of Disse may reenter the blood through the sinusoidal pores, or they may interact with specific receptor sites on the hepatocyte membrane. This membrane is capable of four independent carrier-mediated transport pathways that can accommodate organic anions, organic cations, neutral compounds, or conjugated bile salts (Figure 17-4).[6] Any substance transported at these membrane sites exhibits a transport maximum, being inhibited competitively by other substances with similar transport properties. Bilirubin is excreted by the anionic pathway. Hyperbilirubinemia, therefore, can slow the rate of radiotracer excretion by this pathway. Within the hepatocyte are various protein storage sites and metabolizing organelles that can process substances before transport into bile at the biliary canaliculus. The rate-limiting step for the transport of compounds from the blood into the bile is the excretory process at the bile canaliculus. Bile flow is a function of two active transport processes: bile salt transport and the sodium pump.[6]

Radiocolloids

Development

Several radioactive agents have been used to study the liver. Investigators in the 1950s used colloidal ^{32}P-chromic phosphate to study liver blood flow.[7] Human serum albumin (HSA) labeled with ^{131}I and colloidal gold (^{198}Au) were used to perform the first liver scans with the newly developed rectilinear scanner.[8,9] An interesting approach to liver scanning was the administration of ^{99}Mo as the molybdate anion that localized in hepatocytes by

TABLE 17-1 Radiocolloids Used for Liver Imaging

Agent	Particle Size (nm)	Half-life		Decay Mode	Gamma (keV)	Administered Activity (mCi)	Liver Dose rad(cGy)/mCi
		Physical	Biologic				
^{198}Au-colloidal gold	5–50	2.8 days	Very long	β^-	411	0.3	40
^{99m}Tc-SC	100–1000	6 hr	Very long	IT	140	5.0	0.34
^{131}I-HSA colloid	10–20	8 days	60 min	β^-	364	0.2	0.8
^{113m}In-indium hydroxide colloid	10–20	1.7 hr	30 days	IT	393	2.0	0.5
^{99m}Tc-HSA colloid	200–1000 (80%) <200 (15%)	6 hr	11 hr	IT	140	5.0	0.34

incorporation into xanthine oxidase.[10] Scans were obtained in 24 hours by detection of accumulated ^{99m}Tc activity in the liver. In 1956 Benacerraf et al.[11] developed colloidal particles of ^{131}I-HSA to study liver phagocytosis, but this agent was rapidly metabolized and cleared from the liver and thus was not satisfactory for slow-moving rectilinear scanners.

In 1963, ^{99m}Tc-SC was developed by Richards.[12] Tagging ^{99m}Tc to sulfur particles was accomplished by air oxidation of hydrogen sulfide gas bubbling through an acidified solution of ^{99m}Tc-sodium pertechnetate and gelatin. The preparation was sterilized by filtration through a 0.22 μm membrane. The particle size was estimated to be 0.05 to 0.15 μm.[13] Soon thereafter, sulfur colloid preparation was greatly simplified by use of a sodium thiosulfate kit developed by Stern et al.[14]

Other radiocolloids were developed for diagnostic studies, but none have supplanted the clinical utility of ^{99m}Tc-SC. ^{99m}Tc-antimony sulfide colloid prepared from preformed particles in the 8 to 12 nm range became more useful for studying the lymphatic system.[15] ^{113m}In-hydroxide colloid was useful as an alternative for laboratories with ^{113}Sn–^{113m}In generators.[16] ^{99m}Tc-phytate (inositol hexaphosphate), which forms an insoluble calcium chelate in the blood, was investigated as a means of altering biologic localization among liver, spleen, and bone marrow.[17] ^{99m}Tc-stannous albumin colloid was developed to reduce radiation dose to the liver because of its hepatic metabolism, but it never achieved widespread use.

^{99m}Tc-SC remains the agent of choice for RES imaging because of its ready availability, ease of preparation, and long history of use. Its method of preparation, chemistry, and kit formulation are described in Chapter 9. Table 17-1 summarizes the properties of several radiocolloids that have been used for liver imaging.

Biologic Properties of ^{99m}Tc-Sulfur Colloid

After intravenous administration to humans, ^{99m}Tc-SC leaves the vascular space rapidly, with a clearance half-life of 2 to 3 minutes, and localizes in the liver, spleen, and bone marrow.[13] About 97% of the dose is removed from the blood within 10 to 15 minutes, and liver imaging can then begin. In patients with severely diseased livers, the start of imaging may need to be delayed because of slow blood clearance. By 92 hours, 4% of the injected activity is excreted in the urine and 3% in the feces.[13] The remaining activity is retained in the body with an effective half-life of 6 hours.

Imaging of the liver can begin about 15 minutes after intravenous administration of a 5 mCi (185 MBq) dose of ^{99m}Tc-SC. Most of the radiocolloid distributes uniformly throughout the normal liver, and spleen activity is also evident (Figure 17-5). Space-occupying lesions, such as tumors and cysts, appear as areas of decreased activity.

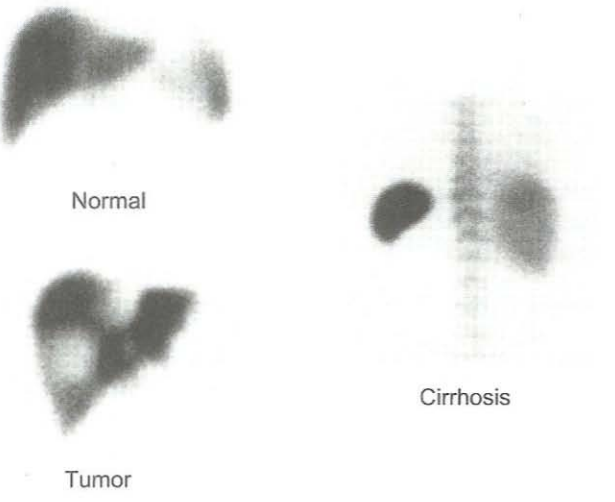

FIGURE 17-5 ^{99m}Tc-sulfur colloid liver scans. Anterior view of a normal liver and spleen, anterior liver scan with a tumor mass in the right lobe, and posterior liver–spleen scan in a patient with hepatocellular dysfunction secondary to alcoholic cirrhosis, demonstrating decreased uptake of radiotracer in the liver with compensatory increased uptake in the spleen and bone marrow.

Several factors have been shown to influence the blood clearance and distribution of radiocolloids.[18] The most important of these are organ blood flow, disease state, particle size and dose, and serum factors.

Blood Flow

Extraction of tracer doses of radiocolloids by the liver is directly related to the volume of blood flow through the organ. In a healthy individual, about 85% of a ^{99m}Tc-SC dose localizes in the liver, 4% to 8% in the spleen, and the remainder in the bone marrow.[19] This disproportionate localization is primarily because the liver receives about 30% of the cardiac output, compared with only about 5% for the spleen.[20]

Disease State

Liver disease injures or destroys a significant number of cells, and this diminishes the amount of radiocolloid deposited in the liver. Severe cirrhosis produces backpressure in portal blood flow, which also influences radiocolloid distribution. In this situation, reduced liver uptake occurs, with shunting of excess colloid to the spleen and bone marrow (Figure 17-5).

Using metabolizable microaggregates of radioiodinated albumin, Wagner and Iio[21] demonstrated that bacterial infections may cause increased RES functional capacity in humans. This effect is due to high levels of endotoxin, which stimulates overall RES activity in the body. This may lead to uptake of radiocolloid in organs that do not normally demonstrate uptake. Increased lung uptake of ^{99m}Tc-SC has been demonstrated in endotoxin-treated animals compared with nontreated controls.[22] This phenomenon may be responsible for the occasional increased lung uptake of ^{99m}Tc-SC seen in patients during a liver scan.

Particle Size

^{99m}Tc-SC prepared by the original hydrogen sulfide method produces an essentially monodispersed colloidal preparation, with 90% of the particles being 0.09 ± 0.01 μm.[23] The thiosulfate method used with commercial kits gives a less uniform size distribution. Using

Nuclepore (Whatman) filtration analysis, Davis et al.[24] have shown size distribution of thiosulfate-generated particles as follows: less than 0.1 μm, 15%; less than 0.4 μm, 70%; 0.1 to 1.0 μm, 80%; and greater than 1.0 μm, 5%.

In general, larger particles are cleared faster from the blood and have greater deposition in the liver and spleen and less in the bone marrow. Atkins et al.[25] compared small particles of ^{99m}Tc-SC produced by the hydrogen sulfide method with particles of ^{99m}Tc-SC 10 times larger produced by the thiosulfate method. Their studies demonstrated that as the dose of smaller particles is increased the percentage of uptake in the liver decreases, uptake in bone marrow increases, and spleen uptake is unaffected.

Blood Clearance and Opsonization

When colloidal particles of ^{198}Au are administered to rats in small numbers ($<1 \times 10^{13}$ particles/kg body weight), the rate of blood clearance is constant and half-life is 2.5 minutes.[26] Similar clearance half-lives have been reported for ^{99m}Tc-SC.[13] In these situations, the rate of liver uptake is related to blood flow rather than RES capacity. When the dose of radiocolloid administered is greater than 1×10^{13} particles/kg, the rate of blood disappearance decreases with increasing dose, suggesting RES depression. This phenomenon has also been observed in humans. It has been suggested that the depression is due to saturation of the reticuloendothelial cell capacity, but experimental studies reveal that it may also be due to depletion of a specific serum opsonin pool for that particular colloid.[18] Supporting the role of opsonins is the fact that RES depression in animals and humans appears to be particle-specific; the injection of one type of colloid induces a state of RES depression relative to the subsequent blood clearance of that particular colloid, whereas the clearance of a dissimilar colloid is less affected.[21] It can be inferred that the localization of particles by phagocytosis may be controlled by both antibodylike opsonins in the blood and specific macrophages that recognize a specific opsonin–particle complex. Recognition may be influenced by particle charge or other chemical properties of the particle surface.

Localization and Metabolic Fate

A common belief is that colloidal particles are localized primarily in Kupffer's cells. Although this is true, it may not explain the process entirely. Reports indicate that other mechanisms of localization may be involved. Using autoradiography, Chaudhuri et al.[27] demonstrated in mice that although colloidal ^{198}Au was primarily engulfed by Kupffer's cells, ^{99m}Tc-SC maintained a generalized distribution throughout the liver with no apparent concentration in Kupffer's cells. This may be due to differences in particle size of these two colloids or to their chemical properties. According to Brucer,[28] phagocytosis of small colloids (<0.1 μm) is a primary function of Kupffer's cells, whereas larger particles (0.1 to 1.0 μm), which leave the sinusoidal blood through the slits between endothelial cells, may become trapped in the network of hepatocellular microvilli and collagen fibrils in the space of Disse. Other studies demonstrate that a size distribution of sinusoidal cells exists.[29] There is preferential localization of small colloids (0.005 to 0.05 μm) such as ^{198}Au in the smaller cells, which are in the majority, whereas larger colloids (0.8 to 1.5 μm), such as ^{99m}Tc-SC, localize primarily in the larger sinusoidal cells, which make up only 15% to 25% of all cells.

Particles trapped in the space of Disse are presumed to drain into portal and hepatic lymph nodes, a process requiring weeks to months.[28] Although no experimental evidence supports this, it seems reasonable at least for the smaller colloids, which are readily transported in lymph. Similarly, no firm evidence is available to demonstrate the fate of particles engulfed by phagocytes. Unless specific enzyme systems are present to transform

these inert sulfur particles into chemically excretable forms (e.g., SO_4^{2-}), these particles are probably stored in the cytoplasm of Kupffer's cells. Because these cells are eventually replaced by new cells, the particles may simply be transferred from cell to cell with each succeeding generation. One study demonstrated that colloidal particles in the liver can enter the systemic circulation and migrate to the lungs, where they can pass into the airways and be expelled in the saliva or swallowed and excreted in the feces.[30]

Adverse Reactions and Toxicity

When a substance is retained for an indefinite period of time in the body, toxicity is a concern. However, chronic and acute toxicity is of little concern with diagnostic radiocolloids because they are usually administered only once or twice to the same patient and in extremely small amounts. Additionally, when the RES is challenged with high doses of colloids, recovery from RES depression is rapid and complete because of the system's regenerative capacity.[21] Colloidal indium hydroxide has been shown to produce hepatocyte toxicity in mice, but only at doses 10,000 times larger than typical doses used in nuclear medicine studies.[31]

One circumstance in which adverse effects may be serious is the potential misadministration of ^{32}P radiopharmaceuticals for therapeutic use. A serious situation may occur if the wrong salt form of ^{32}P is used. If an intracavitary injection of insoluble ^{32}P-chromic phosphate colloid is required for the treatment of peritoneal effusions and the soluble ^{32}P-sodium phosphate salt is used instead, severe bone marrow depression may result.[32] The problem occurs because the soluble sodium salt is readily absorbed into the bloodstream from the peritoneal cavity and is translocated to the bone marrow, where the beta radiation can cause severe bone marrow depression.

No toxic reactions with ^{99m}Tc-SC have been observed in mice given intravenous doses 1000 times the usual adult dose.[33] However, pyrogenic or allergic reactions have been reported with the use of ^{99m}Tc-SC; these were attributed to stabilizers used in the formulations.[32] Such reactions are rare.

Radiation Dose

Radiation dose estimates for ^{99m}Tc-SC are shown in Table 17-2.[34] The doses listed are for normal individuals and those with advanced parenchymal disease. As with all radiopharmaceuticals, the radiation dose to organs may be altered by disease. In the case of severe liver disease, radiocolloid is shifted to other organs and their radiation dose is increased while the dose to the liver is decreased. For example, when diffuse parenchymal disease (cirrhosis) is present, the radiation dose to the liver may be halved while the dose to the spleen is doubled.[35]

HEPATOBILIARY SYSTEM

Physiologic Anatomy

In addition to its metabolic functions, the liver is also an exocrine gland, secreting bile. Bile has two principal functions: (1) to dispose of waste products, such as bilirubin, and xenobiotics, such as drugs, and (2) to secrete bile salts into the intestinal tract to aid digestion. Bile is produced continuously by the hepatocytes.

The hepatobiliary system (Figures 17-1 to 17-3) consists of the biliary canaliculi, the ductal system (hepatic, cystic, and common bile ducts), the gallbladder, and the sphincter of Oddi.[36] Bile formed in the hepatocytes drains into the canaliculi, collecting in the right

TABLE 17-2 Radiation Dose Estimates for ^{99m}Tc-Sulfur Colloid

Organ	Dose after IV Administration (rad[cGy]/5 mCi)		Dose after Oral Administration (rad[cGy]/mCi)
	Normal Liver	Advanced Parenchymal Disease	
Liver	16.9	8.1	–
Spleen	10.6	21.3	–
Bone marrow	1.4	3.9	–
Testes	0.055	0.16	0.005
Ovaries	0.281	0.600	0.096
Total body	0.94	0.88	0.018
Stomach wall	–	–	0.140
Small intestine	–	–	0.260
Upper lg intestine	–	–	0.480
Lower lg intestine	–	–	0.330

Source: Reference 34 (package insert).

and left hepatic ducts. These two ducts form the common hepatic duct, which becomes the common bile duct distally. The cystic duct of the gallbladder branches from this ductal pathway. The common bile duct is the segment between the cystic duct and the ampulla of Vater, where the common bile duct and the pancreatic duct join.

The muscular sphincter of Oddi in the ampulla maintains a high tone during fasting, directing bile into the gallbladder. This sphincter also regulates bile delivery to the duodenum as it relaxes in response to peristalsis and endogenous cholecystokinin (CCK) released when food (gastric chyme) enters the duodenum. It also prevents reflux of intestinal contents into the bile and pancreatic ducts. Substances that relax the sphincter include CCK, anticholinergics, β-adrenergics, calcium channel blockers, and glucagon. Agents that increase sphincter tone include opiates, gastrin, cholinergics, α-adrenergics, and motilin.[36]

The gallbladder wall has smooth muscle that relaxes to allow filling and contracts to empty the gallbladder. The epithelial cells of the gallbladder absorb sodium, bicarbonate, chloride, and water, to concentrate the bile. This mechanism has a high capacity; the gallbladder's nominal volume is only 40 to 70 mL, while the volume of bile delivered to it from the liver is 800 to 1000 mL per day. Bile enters the gallbladder when common duct pressure is greater than intraluminal pressure in the gallbladder. The gallbladder does not fill continuously; filling is interrupted periodically by partial emptying of concentrated bile and aspiration of diluted bile. In the fasting state, about 25% of gallbladder contents is released every 2 hours in response to late phase 2 of the migratory myoelectric complex.[37] In response to gastric chyme released from the stomach into the duodenum, the gallbladder empties more than 75% of its contents into the duodenum. The gallbladder refills with bile in about 3 to 4 hours.[37]

Hepatobiliary Agents

In 1955, an interest in hepatic reticuloendothelial function led George Taplin to investigate the excretion of rose bengal dye into the biliary system. It was presumed at the time that excretion of the dye was through Kupffer's cells. However, further investigation with ^{131}I-labeled rose bengal led to the discovery that the dye was excreted by hepatocytes and was not absorbed by the bowel. This information eventually led Taplin and his colleagues[38] to introduce ^{131}I-rose bengal as the radiopharmaceutical for studying hepatobiliary excretion. It remained in use for nearly 20 years.

In the mid 1970s, a serendipitous event occurred as Loberg et al.[39] were attempting to develop a technetium-labeled heart imaging agent based on structure–distribution relationships. They chose to work with a molecule similar in structure to lidocaine. The first two agents studied were ^{99m}Tc-methyl-iminodiacetic acid (^{99m}Tc-MIDA) and ^{99m}Tc-2,6-dimethylacetanilido-iminodiacetic acid (^{99m}Tc-HIDA). Biodistribution studies in animals demonstrated that ^{99m}Tc-MIDA had rapid excretion into the urine, whereas ^{99m}Tc-HIDA was excreted primarily into bile.[39] This excretory pattern was not completely unpredictable; MIDA is quite hydrophilic, and the HIDA compound has lipophilic properties because of its substituted ring system. The high liver extraction prompted the acronym HIDA, for hepatobiliary-IDA. Since no good technetium-labeled agent for hepatobiliary imaging was available at the time, the course of development shifted away from heart agents to hepatobiliary agents.

Several ^{99m}Tc-IDA analogues were produced by alkyl substitution into the aromatic ring. The dimethyl analogue HIDA (lidofenin) has rapid hepatic uptake and a specificity of about 80%. The diethyl analogue DIDA (etifenin) also has rapid hepatic kinetics with specificity over 90%, while the paraisopropyl analogue PIPIDA (iprofenin) and the parabutyl analogue BIDA (butilfenin) have similar specificity but longer hepatocyte transit times.[40] The diisopropyl analogue 2,6-diisopropylacetanilido-iminodiacetic acid (DISIDA, or disofenin) demonstrates similar hepatic specificity to DIDA and slightly faster biliary excretion, properties also exhibited by the trimethylbromo analogue 2,4,6-trimethyl, 5-bromoacetanilido-iminodiacetic acid (BRIDA, or mebrofenin).[41,42] Three of these compounds were eventually marketed in the United States: ^{99m}Tc-lidofenin, ^{99m}Tc-disofenin, and ^{99m}Tc-mebrofenin. The latter two are the only agents currently on the market. The labeling chemistry of these analogues and their chemical structures are described in Chapter 9.

Physicochemical Properties of ^{99m}Tc-IDA Analogues

An interesting finding from the original work with ^{99m}Tc-HIDA was the discovery that the final complex formed with technetium was a dimer, with two molecules of the chelating agent (HIDA) reacting with one atom of ^{99m}Tc (Figure 17-6). The complex was technetium-essential; without the technetium atom the ^{14}C-labeled HIDA ligand itself had less than 1% hepatobiliary excretion, whereas ^{99m}Tc-HIDA had greater than 70% excretion.[43] The dimeric structure of the complex also confers stability. In vivo/in vitro ligand exchange experiments between ^{99m}Tc-HIDA and ^{99m}Tc-EDTA demonstrated that at physiologic pH, technetium release from HIDA is very slow. Thus, while ^{99m}Tc-HIDA does not possess the thermodynamic stability of ^{99m}Tc-EDTA, it is kinetically inert and quite stable in vivo.[44] This fact has been borne out in dogs injected with ^{99m}Tc-HIDA in procedures in which the contents of the urinary bladder and gallbladder were obtained and reinjected.[39] The results showed an excretory pattern similar to that of the original compound, suggesting that ^{99m}Tc-HIDA is excreted in its original radiochemical form, minimally dissociated or metabolized. Other ^{99m}Tc-IDA analogues should behave similarly.

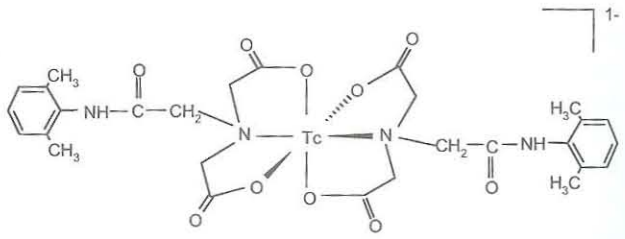

FIGURE 17-6 Chemical structure of ^{99m}Tc-2,6-dimethylacetanilido-iminodiacetic acid (^{99m}Tc-lidofenin).

The hepatobiliary excretion of a substance has been shown to be related to several physicochemical properties.[45,46] These include (1) a molecular weight between 300 and 1000; (2) the presence of a strong polar group, usually ionized at plasma pH and typically anionic; (3) the presence of nonpolar groups, usually as aromatic rings; (4) a lipophilic character enhanced by ring substitution; and (5) binding to plasma albumin, which may promote transfer into the hepatocyte and limit urinary excretion. The ^{99m}Tc-IDA complexes appear to satisfy these requirements. In a review of structure–distribution relationships for hepatobiliary agents, Nunn and Loberg[47] described how the alkyl substitution pattern on the phenyl ring modifies receptor binding of the complex to plasma protein, the hepatocyte membrane, and the intracellular hepatocyte proteins.

Biodistribution of ^{99m}Tc-IDA Analogues

After intravenous injection of either ^{99m}Tc-disofenin or ^{99m}Tc-mebrofenin, liver uptake in normal individuals is evident within 5 minutes, peaking at around 10 minutes. Gallbladder visualization is generally evident within 10 to 15 minutes, peaking in 30 to 60 minutes, with intestinal activity also evident at this time. The radiotracer is extracted from blood by active transport via the anionic site on the hepatocyte membrane and is excreted into the bile unconjugated.

The ideal hepatobiliary agent should have high hepatocyte extraction and transit and low renal excretion and should be an effective competitor for bilirubin excretion.[48] Because the ^{99m}Tc-IDA analogues are extracted at the same site as bilirubin, liver extraction is reduced competitively during hyperbilirubinemia and renal excretion increases. In this situation the best tracer to use is one that has high specificity for the hepatocyte transporter. Some institutions increase the administered activity when serum bilirubin is high. A typical dosing scheme is less than 2 mg/dL bilirubin, 5 mCi (185 MBq); 2 mg/dL to 10 mg/dL bilirubin, 7.5 mCi (277.5 MBq); and more than 10 mg/dL bilirubin, 10 mCi (370 MBq).

Lidofenin is effectively extracted up to 5 mg/dL of plasma bilirubin concentration, whereas disofenin and mebrofenin are effective at higher levels. Mebrofenin uptake into hepatocytes is less affected by bilirubin than is disofenin. In studies of isolated rat hepatocytes, disofenin uptake decreased to 36% at 10 mg/dL bilirubin, whereas mebrofenin uptake decreased only to 71%.[49] The latter two agents exhibit similar hepatocyte extraction efficiency (disofenin 60%, mebrofenin 66%) and parenchymal transit time ($T_{½}$ liver clearance: disofenin, 19 minutes; mebrofenin, 17 minutes), but mebrofenin exhibits less renal excretion than disofenin.[50] At 3 hours postinjection, 7% of disofenin and 1% of mebrofenin appear in the urine of patients with normal bilirubin levels, rising to about 30% for disofenin and 6% for mebrofenin at 24 mg/dL bilirubin.[50] Thus, mebrofenin demonstrates a greater hepatic specificity than disofenin and therefore should be more effective in patients with reduced hepatocellular function.

After intravenous administration of the ^{99m}Tc-IDA tracer, the appearance of liver activity during the arterial phase is normally delayed relative to the kidney and spleen because its principal blood supply is from the portal vein. The normal structures seen sequentially are liver parenchyma, hepatic ducts, common bile duct, gallbladder, and intestine (Figure 17-7). ^{99m}Tc-disofenin and ^{99m}Tc-mebrofenin display rapid hepatocyte kinetics and high ductal concentration, producing superior images of the hepatic ducts.[49] However, despite fast kinetics, there is delayed transit of tracer to the intestinal tract when hepatocellular disease or partial biliary obstruction is present.

In acute cholecystitis, gallbladder activity is absent (Figure 17-8). In chronic cholecystitis, the appearance of gallbladder activity may be delayed for several hours. When the common bile duct is obstructed with gallstones, radiotracer activity clears slowly from the blood, liver uptake is decreased and its clearance delayed, and kidney activity is

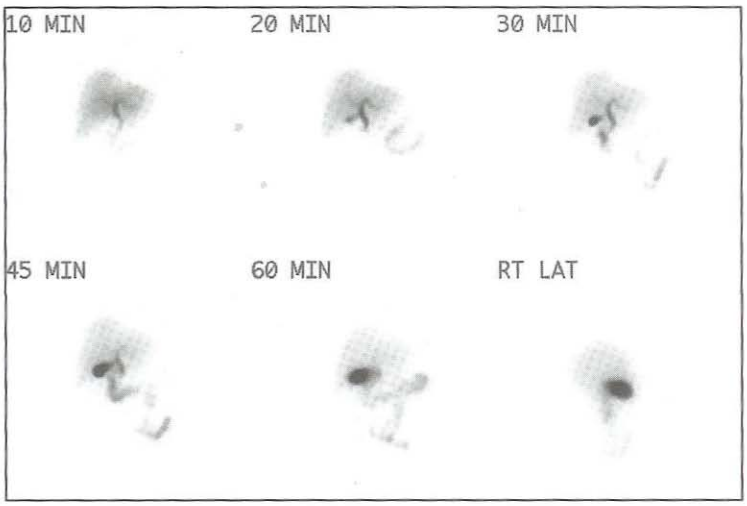

FIGURE 17-7 Normal hepatobiliary study after intravenous injection of 5 mCi of ^{99m}Tc-disofenin. On the initial image taken at 10 minutes, radiotracer accumulation is seen in the liver, biliary tree, common bile duct, and duodenum. Radiotracer is seen in the gallbladder on the 20 minute image. During the 60 minute study there is prompt clearance of radiotracer from the liver with increasing accumulation in the gallbladder and advancement through the bowel.

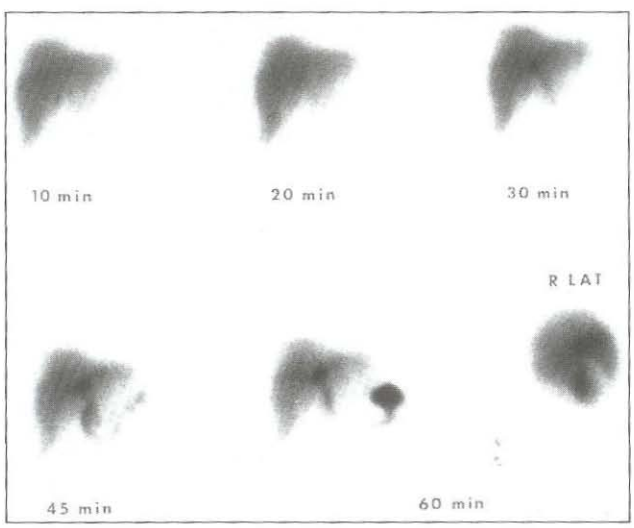

FIGURE 17-8 Acute cholecystitis. After a 5 mCi (185 MBq) intravenous dose of ^{99m}Tc-disofenin there is visualization of tracer material in the common bile duct and proximal bowel at 45 minutes. Nonvisualization of the gallbladder at 60 minutes and 3 hours (image not shown) is consistent with cystic duct obstruction and acute cholecystitis.

evident. Obstruction of bile flow in the common duct prevents activity from being excreted into the intestine (Figures 17-9 and 17-10).

Radiation Dose

Radiation dose estimates for ^{99m}Tc-disofenin and ^{99m}Tc-mebrofenin are listed in Table 17-3.[51,52] In jaundiced patients these dose estimates change because of altered tracer kinetics.

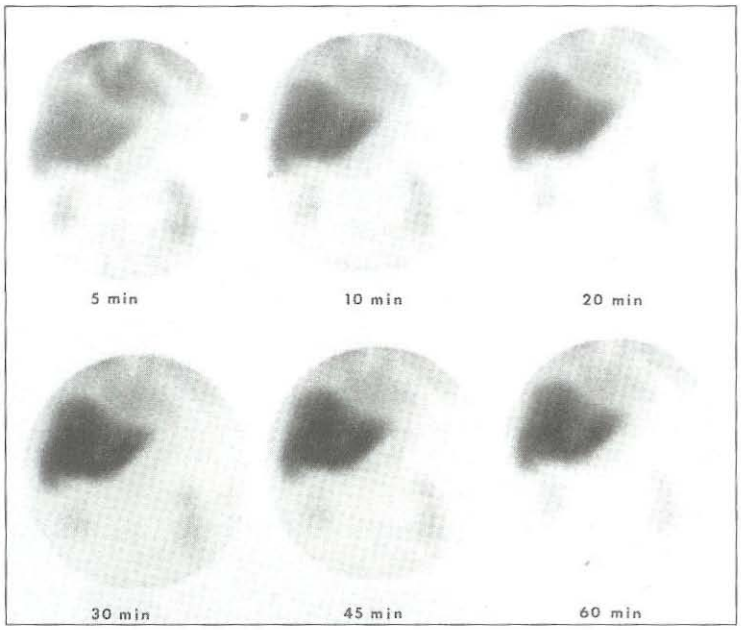

FIGURE 17-9 Biliary obstruction. Common bile duct obstruction decreases clearance of radiotracer from the blood and liver. Kidney activity is evident as well, because of decreased hepatobiliary clearance of tracer from the blood.

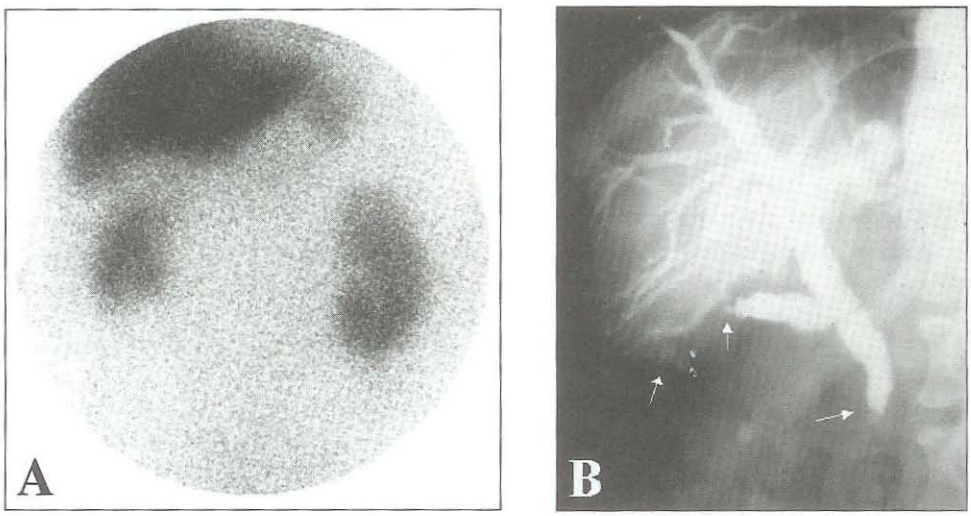

FIGURE 17-10 Five-hour delayed image (A, left) of the same patient shown in Figure 17-9, demonstrating lack of bowel excretion and prominent kidney activity. A 24 hour image (not shown) was similar to the 5 hour image, consistent with complete obstruction. Transhepatic cholangiogram in this patient (B, right) demonstrates stone obstruction in the common bile duct and cystic duct (arrows). Two stones are also evident in the gallbladder.

Pharmacologic Interventions

Several pharmacologic agents have become quite useful for augmenting hepatobiliary studies in nuclear medicine. The principal agents used are CCK, a cholecystagogue that

TABLE 17-3 Radiation Dose Estimates for ^{99m}Tc-Disofenin and ^{99m}Tc-Mebrofenin

Organ	Radiation Dose Estimate (rad[cGy]/5 mCi)	
	^{99m}Tc-Disofenin	^{99m}Tc-Mebrofenin
Upper lg intestine wall	1.75	1.24
Lower lg intestine wall	1.25	0.99
Urinary bladder wall	0.45	1.21
Small intestine	0.9	0.8
Gallbladder wall	0.7	0.63
Liver	0.15	0.40
Ovaries	0.39	0.32
Testes	0.03	0.06
Total body	0.07	0.08

Source: References 51 and 52.

increases bile flow to the intestine by causing contraction of the gallbladder and relaxation of the sphincter of Oddi; morphine sulfate, which enhances the normal constrictor tone of the sphincter of Oddi, increasing intraluminal pressure in the common bile duct; and phenobarbital, which induces enzyme production in immature hepatocytes to improve conjugation and excretion of bilirubin and other substances transported via the same pathway. Each of these substances has a role in particular clinical situations.

Cholecystokinin

CCK is an endogenous 33 amino acid polypeptide hormone released from the intestinal mucosa in response to the presence of fats and protein substances in the intestinal contents. After its release, CCK is absorbed into the blood and transported to the gallbladder, causing it to contract. CCK also stimulates the pancreas to release its digestive enzymes and relaxes the sphincter of Oddi so that bile and enzymes can enter the duodenum to participate in the digestive process.

Sincalide is the synthetic C-terminal octapeptide of CCK. It is marketed as a sterile lyophilized powder (5 μg/vial) under the trade name Kinevac (Bracco). After reconstitution with sterile water for injection to a concentration of 1 μg/mL, sincalide injection is stable for 24 hours at room temperature. It has pharmacologic actions similar to those of CCK and a plasma half-life of about 2.5 minutes.

There are two principal reasons for using CCK in hepatobiliary imaging.[53] One reason is to empty the gallbladder of its contents in situations that might lead to a false-positive study (nonvisualization of the gallbladder despite a patent cystic duct). A full gallbladder interferes with radiotracer uptake because of biliary stasis and sludge. Patients suspected to have acute cholecystitis who have a full gallbladder because of fasting 24 hours or more, are receiving total parenteral nutrition, or are anorexic should have their gallbladder emptied before the study. To facilitate gallbladder uptake of radiotracer after CCK emptying of the gallbladder, a waiting period of 30 to 60 minutes should elapse before injection of the ^{99m}Tc-IDA tracer to allow the gallbladder to relax.

The second reason for CCK cholescintigraphy is to measure gallbladder ejection fraction (GBEF), which is useful in the diagnostic work-up of patients with chronic acalculous cholecystitis (cholecystitis without stones).[53,54] The rationale for CCK cholescintigraphy is based on the hypothesis that a partially obstructed, functionally impaired gallbladder will

respond differently to exogenous CCK than a normal gallbladder.[53] The GBEF provides an objective test to preoperatively confirm a clinician's impression of acalculous disease.

The dosing of CCK for GBEF studies is critical.[54] The dose for these studies (0.02 μg/kg) was originally recommended to be given over 1 to 3 minutes; this has been modified to 30 minutes.[54] The longer dosing time is reported to provide more reliable gallbladder contraction with less variability among normals and fewer adverse effects. A shorter infusion time (1 to 3 minutes) has the potential of causing gallbladder neck spasm with inadequate gallbladder contraction and a falsely low GBEF. Additionally, abdominal cramping, nausea, and occasional vomiting may occur when the infusion rate is too rapid.

Morphine Sulfate

In a typical hepatobiliary study, 5 mCi (185 MBq) of ^{99m}Tc-labeled disofenin or mebrofenin is administered to a patient who has had no oral intake for 4 hours. Routine images are obtained every 10 minutes for 1 hour. If the gallbladder is visualized within this time, the study is normal. If the gallbladder has not been visualized by this time, delayed imaging may be conducted for up to 4 hours to distinguish chronic cholecystitis from acute cholecystitis. The time delay is necessary to allow radiotracer to penetrate the viscous sludge present in the cystic duct and gallbladder, which occurs in 20% of patients with chronic cholecystitis.[55] To shorten the time from 4 hours to about 1.5 hours, morphine sulfate (0.04 mg/kg in 10 mL normal saline infused intravenously over 3 minutes) can be administered, provided radiotracer is seen within the small bowel. Morphine enhances sphincter of Oddi tone, causing increased intraluminal pressure in the common bile duct, facilitating the flow of tracer into the gallbladder.[53] If the gallbladder is visualized during the delayed study, cystic duct obstruction and acute cholecystitis can be ruled out. If it is not visualized within 30 minutes after morphine administration, acute cholecystitis is deemed present. The specificity of delayed hepatobiliary imaging is 93% to 96%.[56] Before morphine is administered, it is important to view images to ensure that sufficient radiotracer is present within the biliary radicals; otherwise a false-positive study may result. If there is insufficient activity, 1.5 mCi (55.5 MBq) of additional tracer should be given before administering the morphine.

Phenobarbital

Phenobarbital is an enzyme inducer that promotes the conjugation and excretion of bilirubin. It is a useful adjunct in hepatobiliary imaging for differentiating neonatal hepatitis from biliary atresia. Neonatal hepatitis manifests itself at 1 to 4 weeks of age. It may be caused by hepatocytes that are unable to conjugate bilirubin as a result of infection, toxins, or unknown causes.[53] Atresia is an obstructive condition caused by sclerosing cholangitis or by the absence of intrahepatic or extrahepatic bile ducts. Neonatal hepatitis requires medical management and is self-limiting, whereas biliary atresia requires surgical intervention. Hence, the differential diagnosis is critical.

Prior to the ^{99m}Tc-IDA hepatobiliary study, the patient is pretreated with phenobarbital 5 mg/kg per day orally in two divided doses for 5 consecutive days.[53] After injection of ^{99m}Tc-disofenin or ^{99m}Tc-mebrofenin at 5 mCi (185 MBq)/1.7 m^2, images are obtained every 10 minutes for 1 hour. Delayed images may be required for up to 24 hours. If biliary excretion of the radiotracer occurs within that time frame, biliary atresia can be excluded, and the patient is treated for neonatal hepatitis. If no excretion occurs, biliary atresia is the likely cause.

SPLEEN

Physiologic Anatomy

The spleen consists of two main compartments: the white pulp, composed of small lymphocytes and plasma cells, and the red pulp, a swampy mass of vascular spaces (sinuses) separated by a supporting structure (cords) that contains phagocytic cells of the RES. The spleen has two main functions: antibody production in the white pulp and particle filtration in the red pulp. There is no significant storage of red or white blood cells in the human spleen as there is in certain animal species; however, about 30% of the body's platelets are sequestered by slow transit in the spleen and can be immediately released into the circulation when needed.[57]

Blood entering the spleen through the splenic arterioles empties first into the white pulp, where plasma skimming occurs to remove soluble antigens. Passing through the white pulp, blood enters the red pulp through an open meshwork of large oval cells at the junction of the white and red pulp, termed the marginal zone. This cellular maze appears to serve as an initial filter that removes abnormal cells and allows normal cells to proceed unhindered. Upon entering the red pulp proper, blood cells may enter either the sinuses or the cords. Blood that enters the sinuses directly passes out easily from the spleen through the efferent veins. Blood cells that enter the cords, however, must pass through a fenestrated, screenlike basement membrane separating the cords from the sinus before gaining access to the venous drainage system. Thus, they are delayed to varying degrees in their transit. Because these fenestrae are only 3 μm in diameter, the blood cells must squeeze through and are deformed in their passage. It is at this point that abnormal, misshapen, and chemically altered cells are detained or destroyed. The macrophages that line the cord side of the sinus basement membrane can then phagocytize the cellular debris. The spleen's physiologic function has been described in detail by Williams et al.[58]

Spleen-Imaging Agents

Two basic types of radioactive agents are used to image the spleen: (1) radiocolloids, which are localized by splenic phagocytes; and (2) denatured radiolabeled red blood cells (RBCs). ^{99m}Tc-SC is used to image the spleen because of convenience, but it lacks specificity because the liver sequesters most of the radiopharmaceutical. Heat-denatured radiolabeled RBCs are more spleen-specific, but their use requires isolation of the cells from whole blood, radiolabeling, and treatment prior to reinjection.

Heat-Denatured ^{99m}Tc-Red Blood Cells

Techniques for labeling and heat-denaturing RBCs were developed by Smith and Richards[59] at Brookhaven National Laboratory. The method involved a stannous citrate kit to "tin" the RBCs prior to labeling with pertechnetate. The ^{99m}Tc-labeled red blood cells (^{99m}Tc-RBCs) were then mixed with saline and heated for 15 minutes at 49°C to 50°C. The unique feature of this method was that excess tin, not associated with the cells, was removed before the addition of pertechnetate. This maximized the labeling yield at more than 97%. A commercial kit now on the market (UltraTag-RBC, Mallinckrodt) is based on the Brookhaven kit. It has been modified to allow labeling to occur in whole blood, obviating the need for a centrifugation step to remove excess stannous ion from the tinned RBCs prior to pertechnetate addition. The UltraTag kit is not approved for spleen imaging, but the method could easily be adapted for this purpose with a heat-treating step after the RBCs are labeled. An alternative is use of the stannous pyrophosphate in vivo or in

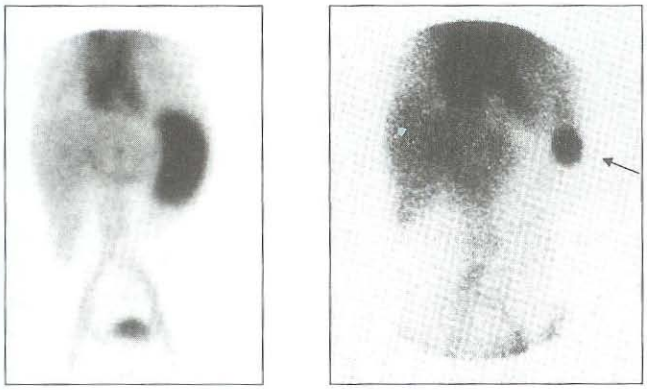

FIGURE 17-11 Spleen scans after injection of ^{99m}Tc-labeled heat denatured red blood cells. Normal anterior spleen scan (left), and spleen scan in the left anterior oblique projection (right) identifying an accessory spleen in a patient who underwent a splenectomy 10 years earlier.

vitro RBC labeling method (see Chapter 9), modified by adding a heating step once the cells are labeled with technetium.

^{99m}Tc-labeled heat-denatured RBCs prepared with the Brookhaven kit have been evaluated for splenic sequestration in humans.[60] The blood clearance of the cells is rapid ($T_{½}$, 6.3 minutes), and splenic uptake reaches a plateau by 30 minutes. Uptake varies among patients, with the lowest value at 42% of the administered activity and the mean at 72%. Two hours after dosing, 5% of the administered activity is excreted in the urine. The reliability of splenic uptake with this method has been attributed to two factors: (1) The small volume of cells (4 mL) during the heating step provides more uniform heating so that adequate cell preparation is achieved in a short time, and (2) the small volume of cells administered reduces the possibility of overloading the spleen's sequestering ability, compared with a larger volume of cells.[60]

Mechanism of Localization

Heating RBCs changes their shape from normal biconcave disks to spherocytes. Heat-denatured spherocytes have an altered cell membrane with knobby projections.[61] The changes in the membrane make it fragile. When the weakened cells squeeze through the 3 μm pores in the cords of the red pulp they are lysed, releasing their radioactive contents within the spleen. Splenic removal of RBCs is a more selective process than removal by the liver and other RES tissue. Insufficient heating of cells produces incomplete denaturation and decreased sequestration by the spleen, whereas overheating causes localization in the liver due to cell lysis in the bloodstream. Heating must be controlled carefully to produce a spleen-specific agent. Figure 17-11 illustrates a normal spleen scan and the localization of an accessory spleen using ^{99m}Tc-labeled heat-denatured RBCs.

GASTROINTESTINAL STUDIES

Several useful procedures have been developed to evaluate the GI system with radiopharmaceuticals. Procedures are routinely performed to evaluate gastroesophageal reflux and gastric emptying, detect a GI bleeding site, and localize a Meckel's diverticulum. An in vitro procedure to evaluate GI protein loss is used occasionally.

Radiopharmaceuticals for Gastroesophageal Reflux

^{99m}Tc-SC is typically used in gastroesophageal reflux studies because it is insoluble in gastric juices. Significant amounts of soluble ^{99m}Tc-sodium pertechnetate are undesirable

because its systemic absorption may contribute to increased background activity in the esophageal region. ^{99m}Tc-SC is usually given as an acidified liquid meal, which tends to aggravate reflux because an acid load in the stomach appears to delay gastric emptying and lower the resting pressure gradient of the lower esophageal sphincter.[62]

Radiopharmaceuticals for Gastric Emptying

Radionuclide gastric emptying studies measure the rate of removal of radiolabeled liquids and solids from the stomach. Such studies provide a noninvasive method of evaluating gastric physiology. Under normal conditions, liquids clear in an exponential manner and at a faster rate than solids. Although gastric emptying studies are relatively simple to perform, accurate quantitation requires attention to several aspects of the study:

1. Radionuclide markers must have high labeling efficiency and remain stable in vivo during the study.
2. Meal size and composition should be standardized.
3. A standard patient position and posture should be maintained for imaging times.
4. Correction techniques should be applied when needed to compensate for radionuclide decay, multiple radionuclide interference, geometry changes, septal penetration, and scatter from high-energy gamma rays.

The ideal tracer should not be absorbed through nor bound to the gastric mucosa, should have no effect on gastric emptying, and should mix evenly with ingested food. The two types of radioactive markers used in gastric emptying studies are liquid markers and solid markers. Liquid markers are soluble radiopharmaceuticals that are miscible with aqueous liquids and will trace the movement of liquids from the stomach. They must be nonabsorbable and stable and not localize in the stomach. Commonly used liquid markers include ^{111}In-DTPA, ^{99m}Tc-DTPA, and ^{99m}Tc-SC. ^{99m}Tc-sodium pertechnetate cannot be used because it localizes in the gastric mucosa.

Solid food markers are radionuclides incorporated into food. Various techniques have been explored to bind radionuclides to solid food. It is important that the radiolabel remain bound to the solid during the course of study; otherwise, gastric emptying of solids will be erroneously shortened because of radionuclide leaching into stomach fluid.

Various methods have been used to bind ^{99m}Tc to solid food. One method involves binding ^{99m}Tc to an inert resin and incorporating it with oatmeal.[63] A method that is widely used is to mix 1 mCi (37 MBq) of ^{99m}Tc-SC with an egg and scramble the mixture to incorporate the ^{99m}Tc-SC into the egg solid. The radiolabeled egg can be eaten as is or in a sandwich between two slices of bread. The radioactive meal is then followed by a chaser of water to rinse the esophagus.

In some instances a solid–liquid marker meal may be given as 1 mCi (37 MBq) of ^{99m}Tc-SC in scrambled egg and 100 μCi (3.7 MBq) of ^{111}In-DTPA, chased with 4 oz of water. If a solid–liquid marker is given and the ^{99m}Tc-to-^{111}In activity ratio is 6 to 1 or greater, downscatter of ^{111}In counts into the ^{99m}Tc window is minimized.[64]

To obtain meaningful results, a standard institutional protocol must be established for performing gastric emptying studies. The size of the meal and its composition will affect emptying rates. Liquids empty from the stomach monoexponentially and at a faster rate than solids, which tend to empty at a constant rate, being restricted by the pylorus.[64,65] The emptying rate is also influenced by the type of food and the amount. In general, large meals and high-calorie and fatty meals empty more slowly. An institution should use a standard meal for its gastric emptying studies and establish its own parameters for normal gastric emptying rate.

TABLE 17-4 Radiopharmaceuticals for Detection of Gastrointestinal Bleeding

^{99m}Tc-Sulfur Colloid	^{99m}Tc-Red Blood Cells
Fast blood clearance	Slow blood clearance
High target-to-background ratio	Low target-to-background ratio
Requires active bleeding	Best for intermittent bleeding

Radiopharmaceuticals for GI Bleeding

Successful management of acute GI bleeding depends upon accurate localization of the bleeding site. Most GI bleeding occurs intermittently, which presents a problem for using invasive diagnostic methods such as angiography for localizing the site. Angiography requires active bleeding during the procedure to accurately localize the site. The significant morbidity associated with this procedure led to the development of scintigraphic methods using radiopharmaceuticals.

Two radiopharmaceuticals have been found to be useful for localizing GI bleeding sites. The first agent used was ^{99m}Tc-SC, and the current agent is ^{99m}Tc-RBCs. Each agent has unique properties related to its use for detecting GI bleeding (Table 17-4). An ideal agent for detection of GI bleeding would extravasate into the bleeding site and be cleared from the blood and excreted rapidly. This would provide a high target-to-background ratio to facilitate localization of the site. Neither ^{99m}Tc-SC nor ^{99m}Tc-RBCs meets these stringent requirements. ^{99m}Tc-SC clears rapidly from the blood after intravenous injection and therefore requires active bleeding at the time of injection. Additionally, its localization in the liver and spleen may obscure bleeding sites in these areas of the abdomen. The advantage of ^{99m}Tc-RBCs is that the radiopharmaceutical's prolonged circulation time provides a reservoir of radioactive blood when bleeding occurs and is thus ideal for intermittent bleeding. This is a double-edged sword, because the prolonged blood clearance creates high tissue background. However, this has not appeared to interfere significantly with the detection of bleeding sites. The use of both these agents has been reviewed.[66–68]

^{99m}Tc-RBCs are now the agent of choice for this procedure. A comparison between ^{99m}Tc-SC and ^{99m}Tc-RBCs has been made.[68] The study involved injection of both agents into the same patient, ^{99m}Tc-SC first, followed by image acquisition for 15 to 20 minutes, followed by ^{99m}Tc-RBCs with imaging for 90 minutes. Continuous 1 minute computer-acquired images were made along with 5 minute scintiphotos in each phase of the study. Of 100 patients studied, 41 had active bleeding; 38 of these cases were accurately identified by ^{99m}Tc-RBCs. Only five cases were identified by ^{99m}Tc-SC, and in no instance did ^{99m}Tc-SC demonstrate active hemorrhage that was not subsequently identified by ^{99m}Tc-RBCs.

A key requirement for using ^{99m}Tc-RBCs is a high tagging efficiency, because any significant free pertechnetate is localized in the gastric mucosa, where it can potentially interfere with diagnostic interpretation. A kit for the in vitro preparation of ^{99m}Tc-RBCs (UltraTag-RBC, Mallinckrodt) permits labeling in whole blood and routinely produces yields in excess of 95%. The method for labeling RBCs with this kit is described in Chapter 9.

Radiopharmaceuticals for Meckel's Diverticulum

Meckel's diverticulum is the most frequent congenital malformation of the GI tract in humans.[69] It is found in 1% to 2% of people, most commonly in children, although it has been diagnosed at every age from birth onward. The most common symptom of Meckel's

diverticulum is rectal bleeding that results from peptic ulceration of the bowel by acid secreted from the gastric mucosa in the diverticulum.[70] The frequent presence of gastric mucosa in a Meckel's diverticulum led to the use of ^{99m}Tc-sodium pertechnetate for scintigraphic studies because of its inherent biologic localization in gastric mucosa. Its use in this application has shown a sensitivity of 85% and a specificity of 95% in cases of surgically proven Meckel's diverticula with ectopic mucosa.[71,72] The procedure does not directly detect diverticula that do not contain gastric mucosa.

Radiopharmaceuticals for GI Protein Loss

Under normal circumstances, large amounts of protein (approximately 100 grams) enter the GI tract daily as a result of digestive secretory processes; however, this protein is largely reabsorbed after intestinal catabolism. Protein-losing enteropathy (PLE) is characterized by excessive protein loss in the stool. Several diseases that produce inflammation and ulceration of the GI tract may cause excessive protein loss.

The test for protein loss involves recovering and measuring radiolabeled albumin that leaks into the GI tract.[73] Ideally, the radiolabel should remain firmly bound to the protein and not be excreted in the urine, because urine can contaminate stool samples. The labeled protein should be excreted into the intestinal tract only through abnormal leakage sites and not be reabsorbed.

^{131}I-HSA was one of the first agents used to study PLE. However, it had the disadvantage of being catabolized in the gut, with reabsorption of the radioiodine. Studies using ^{51}Cr-labeled albumin or ^{51}Cr-chromic chloride demonstrated that these agents could be recovered almost completely from the stool after oral administration, indicating no reabsorption of the radiolabel.[74,75] Consequently, ^{51}Cr-labeled products have become the agents of choice for PLE. ^{51}Cr-albumin demonstrated less urinary excretion (13%) than ^{51}Cr-chromic chloride (60%) 3 days after dosing and therefore was the preferred agent, with less chance of urinary contamination of stool samples during the study.[74] However, ^{51}Cr-albumin is no longer on the market. When given intravenously, ^{51}Cr-chromic chloride labels plasma albumin in vivo and is effective for this study, but it must be prepared in a sterile form. Also, ^{51}Cr-chromic chloride must be prepared carefully because it adheres tenaciously to glass; loss can be minimized by maintaining the solution at or below pH 4 and using plastic or siliconized glass containers. The final preparation must be sterilized by 0.22 μm membrane filtration before intravenous administration.

Test Procedure for PLE

A dose of 0.25 to 0.5 μCi (9.25 to 18.5 kBq) ^{51}Cr-chromic chloride per pound of body weight is administered intravenously. All stools passed during the next 4 days are collected by the patient. Patients with some conditions (e.g., Crohn's disease) may need multiple containers because of the large volume of liquid stool. Empty metal paint cans containing 10 mL phenol preservative are satisfactory for collecting stool specimens. Each sample is adjusted to a standard weight with water and assayed for radioactivity with a scintillation counter. A ^{51}Cr standard, identical to the patient dose administered, and a background can are prepared and counted along with the stool specimens. The percentage of the dose excreted in the cumulative stool samples is calculated. Normal subjects excrete 1% or less of the administered dose in 4 days.[73,74] Patients with PLE have been shown to excrete 2% to 40% of the dose. Care must be taken to instruct patients not to contaminate stool samples with urine.

NUCLEAR MEDICINE PROCEDURES

Magnetic resonance imaging (MRI), computed tomography (CT), and ultrasound are commonly used to evaluate the anatomy of the liver, hepatobiliary system, and spleen. However, imaging with radionuclides can offer more information about the physiology and function of these organs. Several radiopharmaceuticals with different mechanisms of uptake can be used to image these organ systems.

Liver–Spleen Imaging

Rationale

Liver–spleen imaging uses radiolabeled colloids that are taken up by the RES. These radiopharmaceuticals are phagocytized by RES cells in the liver, spleen, and bone marrow. Most of the particles (80% to 90%) are taken up by Kupffer's cells in the liver. About 5% are taken up in the spleen and a small percentage in the bone marrow. This allows for functional imaging of the RES and can be useful for evaluation of hepatocellular disease such as cirrhosis, hepatomegaly, splenomegaly, and certain hepatic or splenic lesions seen in an anatomic imaging study such as CT. Liver–spleen nuclear imaging studies can also be useful to localize splenic tissue.

In patients with hepatic metastatic disease, hepatic artery infusion pumps are surgically placed to deliver strong chemotherapy directly to the liver. Proper placement is essential so that the chemotherapy drugs are delivered only to the liver and not to other organs. Imaging evaluation of pump function is accomplished with ^{99m}Tc-albumin aggregated (^{99m}Tc-MAA). Once injected via the pump, these small particles are trapped in the liver by capillary blockade. If radiotracer accumulation is seen outside the liver, the position of the pump catheter needs to be adjusted or collateral circulation to these other areas needs to be identified and ligated. ^{99m}Tc-SC liver–spleen imaging can be performed for comparison if there is a question about the results of the ^{99m}Tc-MAA study. This is especially true in patients who have had liver surgery prior to pump placement. In these patients, the liver may have an abnormal contour that can be difficult to evaluate (Figure 17-12).

Blood-pool studies with ^{99m}Tc-RBCs can be used to evaluate suspected cavernous hemangiomas in the liver. Because there is sluggish blood flow in hemangiomas, these are typically seen as focal defects on the early flow images that demonstrate increased uptake on delayed images (Figure 17-13).

Splenic imaging is useful for evaluating abdominal masses thought to be residual functional splenic tissue in patients who have had surgical splenectomy for thrombocytopenia, for confirming suspected splenosis in patients who have undergone splenectomy after trauma, and for diagnosing congenital abnormalities such as asplenia or polysplenia in children. Splenic imaging can be accomplished with colloid agents as part of the liver–spleen scan. More specific imaging of the spleen can be accomplished with autologous heat-denatured ^{99m}Tc-RBCs; this is useful in determining the presence of functioning splenic tissue. Heat-denatured ^{99m}Tc-RBCs are sequestered by the functioning splenic tissue, which allows for its identification with imaging (Figure 17-14). The red blood cells are not sequestered by the liver, so the liver is not imaged as in a colloid liver–spleen scan. This can be helpful in differentiating spleen from adjacent structures, especially in patients with a liver that has a large left lobe adjacent to the spleen or in a patient with questionable situs inversus.

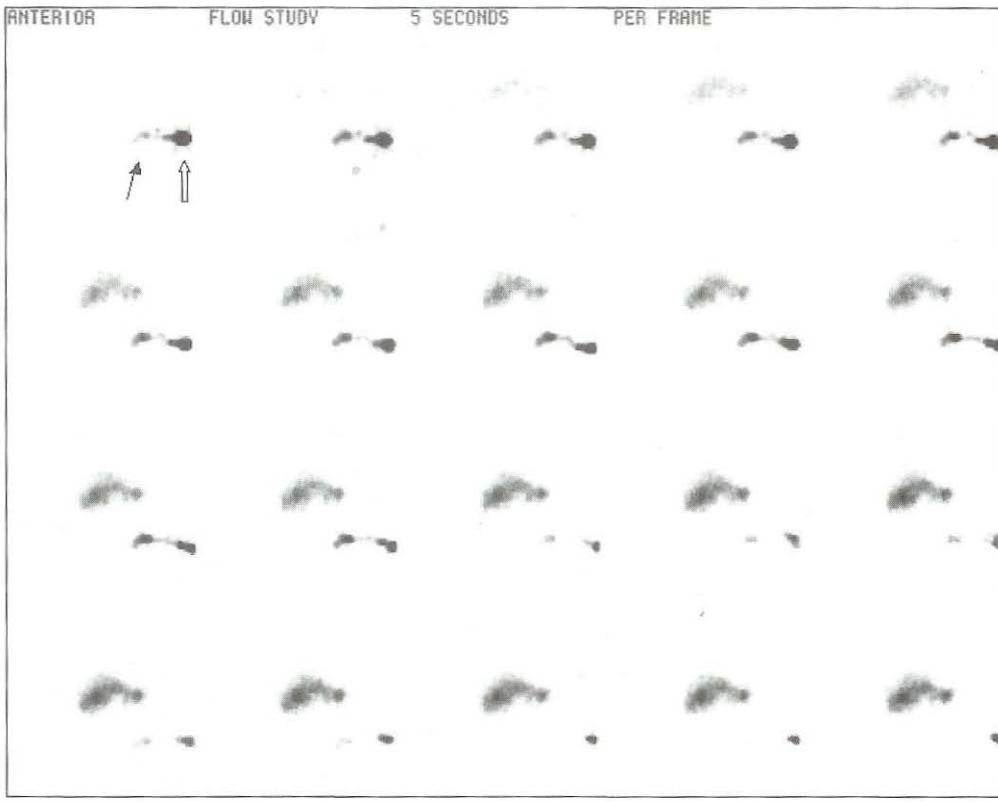

A

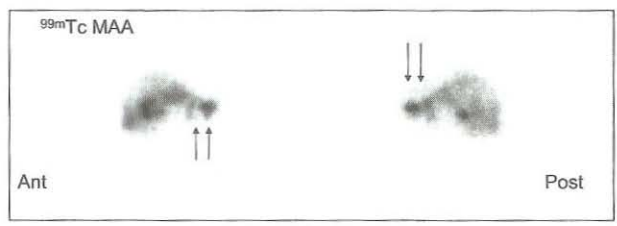

B

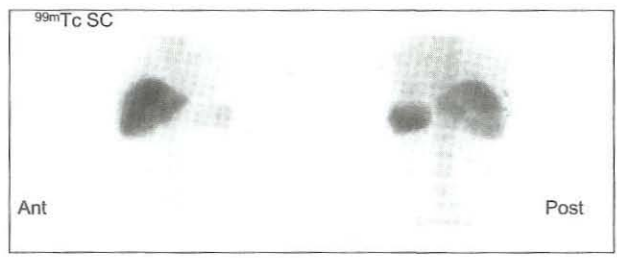

C

FIGURE 17-12 Hepatic artery infusion pump study. The patient has had a left hepatic lobectomy and placement of a hepatic artery infusion pump because of metastatic involvement by colon cancer. (A) Anterior 5-second-per-frame images from a ^{99m}Tc-MAA study. On the initial image, radiotracer is seen in the injection syringe (block arrow) and in the hepatic artery infusion pump (solid arrow). As the dose is injected, uptake is seen in the liver. (B) Anterior and posterior images of the liver from the ^{99m}Tc-MAA study showing patchy uptake in the liver with apparent uptake in the left lobe (double arrows). (C) Anterior and posterior images from a ^{99m}Tc-SC study done the next day demonstrate absence of a left lobe, indicating that the ^{99m}Tc-MAA activity seen the previous day in this region is outside the liver parenchyma in bowel.

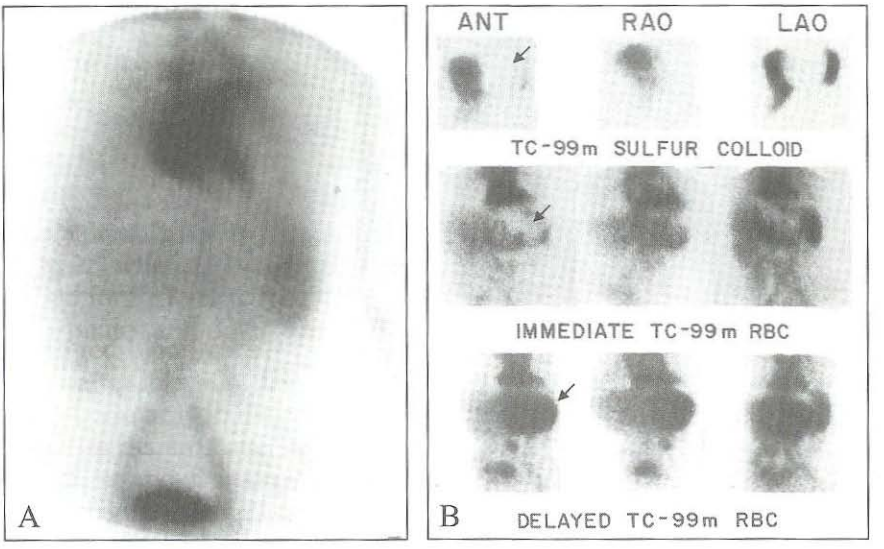

FIGURE 17-13 ^{99m}Tc-RBC liver scans. (A) Normal anterior planar liver scan demonstrating prominent activity in the heart blood pool, spleen, and urinary bladder, with no focal uptake in the liver. (B) Hemangioma. Liver scintigraphy in anterior, right anterior, and left anterior oblique views. ^{99m}Tc-sulfur colloid study shows a large focal defect in the left lobe (arrow). Immediate ^{99m}Tc-RBC study shows a focal defect in the left lobe with some increased activity in the periphery. Late ^{99m}Tc-RBC study shows a large blood pool of activity in the left lobe consistent with hemangioma. (17-13B reprinted with permission of the Society of Nuclear Medicine from Front D, Royal HD, Israel O, et al. Scintigraphy of hepatic hemangiomas: the value of Tc-99m-labeled red blood cells: concise communication. *J Nucl Med.* 1981;22:684-7.)

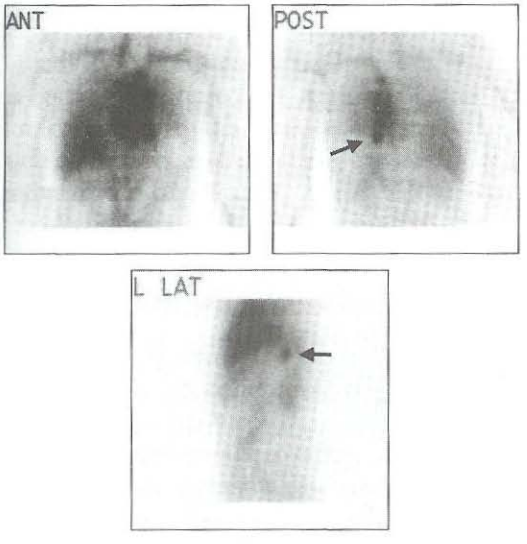

FIGURE 17-14 ^{99m}Tc-labeled heat-denatured RBC study in a patient with a history of splenectomy. Anterior, posterior, and left lateral views of the abdomen show a small focal area of ^{99m}Tc-RBC accumulation posteriorly in the left upper quadrant consistent with an accessory spleen.

Procedure

Liver–spleen imaging requires no specific patient preparation. The adult patient receives an intravenous injection of 4 to 6 mCi (148 to 222 MBq) of ^{99m}Tc-SC. A large field-of-view

camera with a low-energy all-purpose (LEAP) or low-energy high-resolution (LEHR) collimator is used for imaging. If blood flow imaging of the liver is desired, the patient is injected under the camera and 1 or 2 second frames can be obtained over the first minute to evaluate variations in blood flow to the liver (Figure 17-15A). Usually, static images are obtained 15 to 20 minutes after administration of the radiotracer. Images of the abdomen are usually obtained in the anterior, posterior, lateral, and oblique positions (Figure 17-15B).[76] Delayed images of the liver are obtained 1 to 2 hours later. SPECT imaging can sometimes be helpful if suspected lesions are small or there are several lesions.

Hepatobiliary Scintigraphy

Rationale

Hepatobiliary scintigraphy is accomplished with radiopharmaceuticals that are taken up by hepatocytes and excreted into the bile. Radiotracers are excreted into the bile canaliculi and advance through the biliary tree and common bile duct into the small intestine. Some of the radiotracer also enters the cystic duct and accumulates in the gallbladder. Hepatobiliary function can be estimated by the amount and timing of liver uptake and clearance. Patency of the hepatobiliary system can be evaluated by following the flow of radiotracer through the biliary tree and intestines. Radionuclide imaging of the hepatobiliary system is commonly used to evaluate acute cholecystitis, GBEF, common bile duct obstruction, bile leak, and congenital anomalies such as biliary atresia.

The most common indication for hepatobiliary scintigraphy is evaluation of suspected acute cholecystitis. Most cases of acute cholecystitis are caused by obstruction of the cystic duct by a gallstone. It is important to obtain a pertinent patient history before performing this exam. The history should include details of any prior GI surgeries (such as cholecystectomy), when the last meal was eaten, whether the the patient is taking opioid medications for pain, if the patient has had recent ultrasonography, and if the patient has had recent laboratory tests to determine liver enzyme levels.

The liver makes bile continuously. Normally, about two-thirds of the bile flows through the common bile duct into the duodenum. Approximately one-third flows up the cystic duct into the gallbladder, where it is stored.[77] The gallbladder contracts and empties its contents into the duodenum in response to endogenous CCK, which is produced by duodenal mucosal cells in response to fats and proteins in the intestinal contents. If the patient has recently eaten a meal, circulating endogenous CCK will prevent the gallbladder from filling. The patient should fast for 4 hours before beginning this exam. However, if the patient has not eaten for more than 24 hours or has been receiving total parenteral nutrition (TPN), the gallbladder may be full of thick, viscous bile. In this case the gallbladder may not accumulate radiotracer. Both of these conditions can result in false-positive studies (absence of gallbladder uptake of radiotracer activity).

If the patient is currently taking opioid drugs, this may interfere with the exam. The administration of opioids such as morphine sulfate results in constriction of the sphincter of Oddi, which increases the intraluminal pressure in the common bile duct and can prevent bile from entering the duodenum. Although the gallbladder may be visualized, failure of the radiotracer to enter the small bowel may be interpreted as obstruction of the common bile duct. Therefore, the study should be delayed for 4 hours after opioid administration.

If the patient's liver enzymes are elevated, the hepatocytes may not be able to concentrate enough radiotracer to visualize the gallbladder. Higher dosage of the radiopharmaceutical may be needed if the patient has marked hyperbilirubinemia.

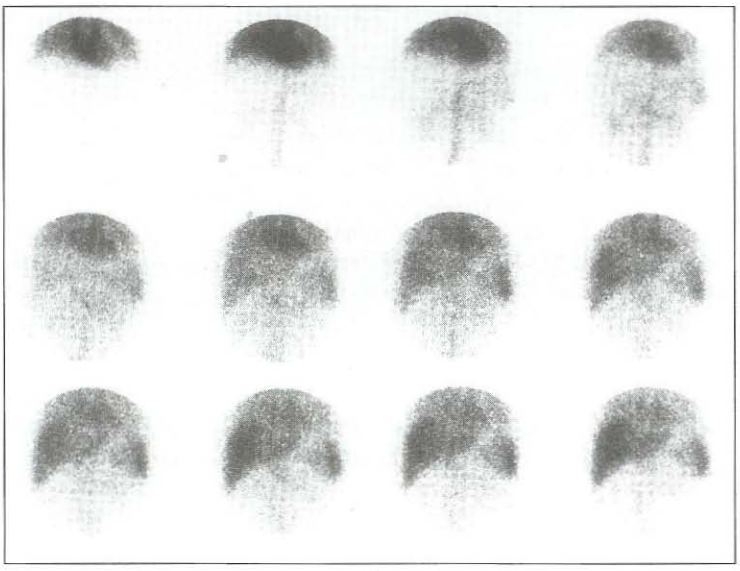

A

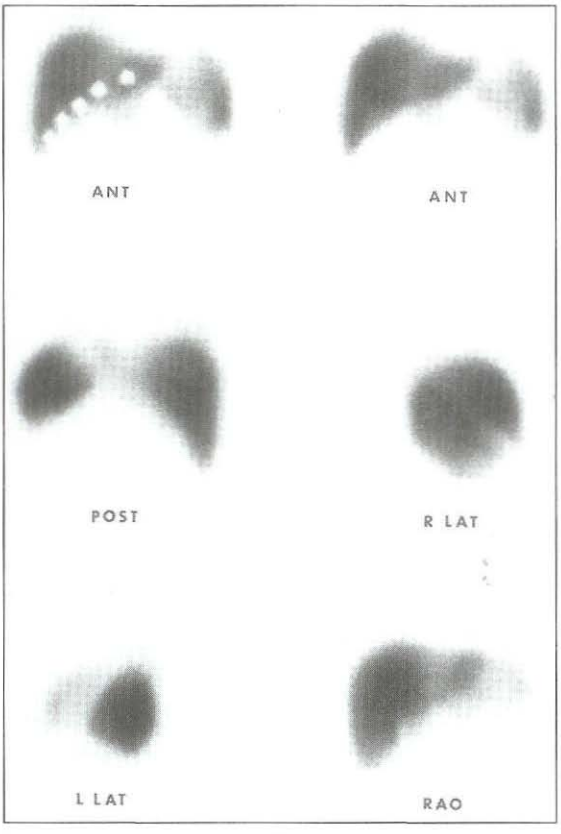

B

FIGURE 17-15 (A) Normal anterior liver blood flow study in a patient after intravenous injection of 5 mCi (185 MBq) of ^{99m}Tc-sulfur colloid. Sequential images taken at 5 second intervals demonstrate the normal distribution of activity in the heart, abdominal aorta, liver, and spleen. (B) Normal static liver–spleen scan in the same patient obtained 15 minutes after the liver flow study. Four standard views (anterior, right lateral, posterior, and left lateral) and a right anterior oblique view are shown.

Procedure

The patient should fast for about 4 hours before administration of the radiotracer. If the patient has not eaten for more than 24 hours or is receiving TPN, the patient may be pretreated with sincalide, a synthetic C-terminal octapeptide of CCK. The usual pretreatment dose of sincalide is 0.02 μg/kg. This is sometimes given as a slow intravenous infusion over 3 minutes but is preferably given as a slow drip over 20 to 30 minutes to lessen the possibility of adverse effects. Sincalide should not be administered as a bolus because it can cause gallbladder spasm and abdominal discomfort. Sincalide should also not be used if the patient is currently receiving morphine, which acts to constrict the sphincter of Oddi. If pretreatment with sincalide is considered appropriate, the hepatobiliary radiotracer is usually administered 30 to 60 minutes after the sincalide infusion is over.

Typically 1.5 to 5 mCi (55.5 to 185 MBq) of a ^{99m}Tc-labeled IDA compound (disofenin or mebrofenin) is administered to an adult. Images are obtained using a large field-of-view gamma camera with a LEAP or LEHR collimator. Anterior spot images of the abdomen can be obtained every 10 minutes, or continuous 1-minute-per-frame images of the abdomen can be obtained until radiotracer is seen in both the proximal small bowel and the gallbladder.[78] In most normal studies, the gallbladder and small bowel are visualized within 60 minutes (Figure 17-7). If there is questionable activity in the region of the gallbladder fossa, which may be either gallbladder accumulation or pooling in the proximal duodenum, a right lateral view can be helpful. The gallbladder is usually an anterior structure. If the focal accumulation is still questionable and the patient can have some water by mouth, this will clear the activity if it is in the duodenum.

If the gallbladder is not visualized after 60 minutes, delayed imaging should be performed after 4 hours. If there is activity in the proximal bowel, an alternative to 4 hour delayed imaging is augmentation with morphine sulfate. Morphine sulfate administration constricts the sphincter of Oddi, which increases the intraluminal pressure in the common bile duct. This forces radiotracer into the cystic duct and into the gallbladder if there is not an obstruction. Usually, a morphine dose of 0.04 mg/kg is given intravenously and imaging is continued for another 30 minutes. If there is very little radiotracer activity in the liver and a decision is made to administer morphine sulfate, a "booster dose" of ^{99m}Tc-IDA should be given 10 to 20 minutes before morphine administration. The booster dose is usually 1 to 1.5 mCi (37 to 55.5 MBq).

In some patients with a history of right upper quadrant pain, no evidence of gallstones on ultrasound, and a normal-appearing hepatobiliary scan, it can be useful to evaluate the GBEF. A poor ejection fraction can be seen in conditions such as chronic acalculous cholecystitis, biliary dyskinesia, cystic duct syndrome, and sphincter of Oddi dysfunction. Sincalide administration is used to assess GBEF after the gallbladder is maximally filled with the radiotracer and most of the radiotracer has cleared from the liver. Usually, sincalide 0.02 to 0.04 μg/kg is administered over 20 to 30 minutes. Anterior 1-minute-per-frame images of the gallbladder can be obtained over the 20 to 30 minute interval. Regions of interest are drawn around the gallbladder and the adjacent liver to determine background (Figure 17-16). GBEF is calculated as

$$\text{GBEF}\,\% = \frac{\text{Net maximum GB counts} - \text{Net minimum GB counts} \times 100}{\text{Net maximum GB counts}}$$

In general, a GBEF less than 35% is considered abnormal. Because sincalide has a plasma half-life of only about 2.5 minutes, it can be used both for pretreatment in patients who have fasted longer than 24 hours and for GBEF. However, sincalide should not be used in patients who required morphine stimulation to visualize the gallbladder. In these

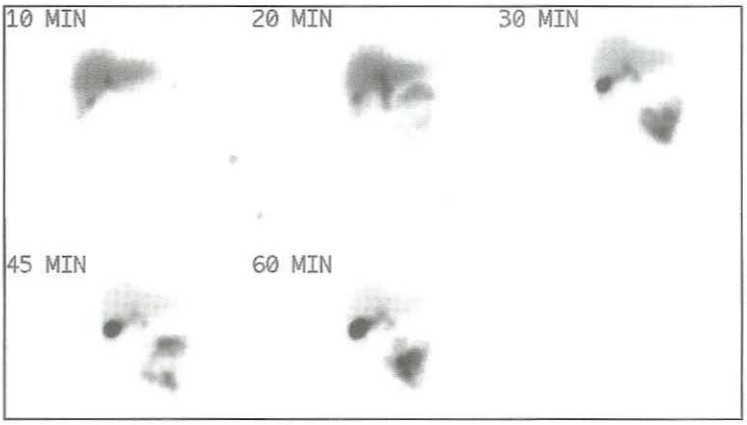

A

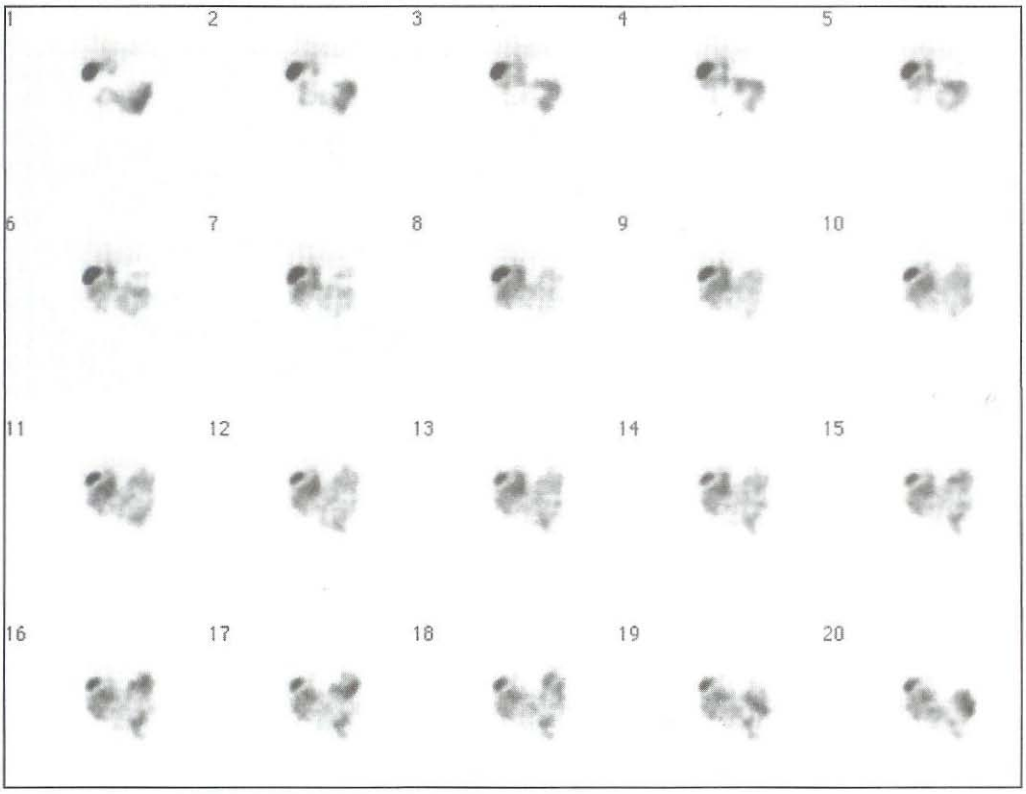

B

FIGURE 17-16 Normal hepatobiliary study after intravenous injection of 5 mCi (185 MBq) of ^{99m}Tc-disofenin. (A) On the initial image taken at 10 minutes, radiotracer accumulation is seen in the liver, biliary tree, and gallbladder. Radiotracer is seen in the proximal bowel on the 20 minute image. During the 60 minute study there is good clearance of radiotracer from the liver, with increasing accumulation in the gallbladder and advancement through the bowel. (B) After this, serial 1-minute-per-frame images of the abdomen were obtained during intravenous administration of cholecystokinin (CCK). There is normal gallbladder emptying during the 20 minute CCK administration. (C, page 616) A gallbladder time–activity curve shows prompt emptying of the gallbladder, with 74% emptying at 14 minutes. (D, page 616) Another patient with an abnormal gallbladder ejection fraction (GBEF). During the 20 minute CCK administration there is very little change in the appearance of the gallbladder (arrows). GBEF was only 5%.

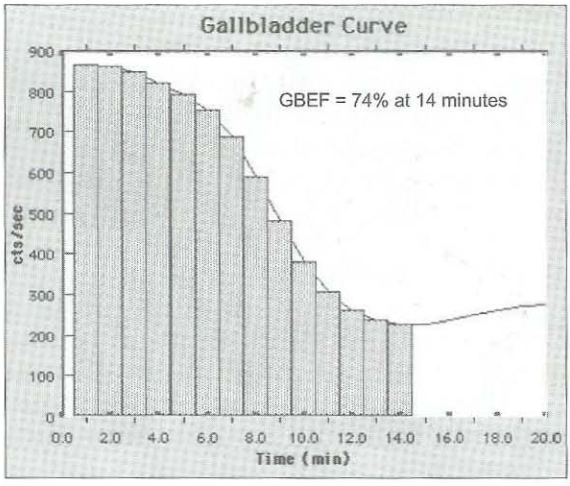

C

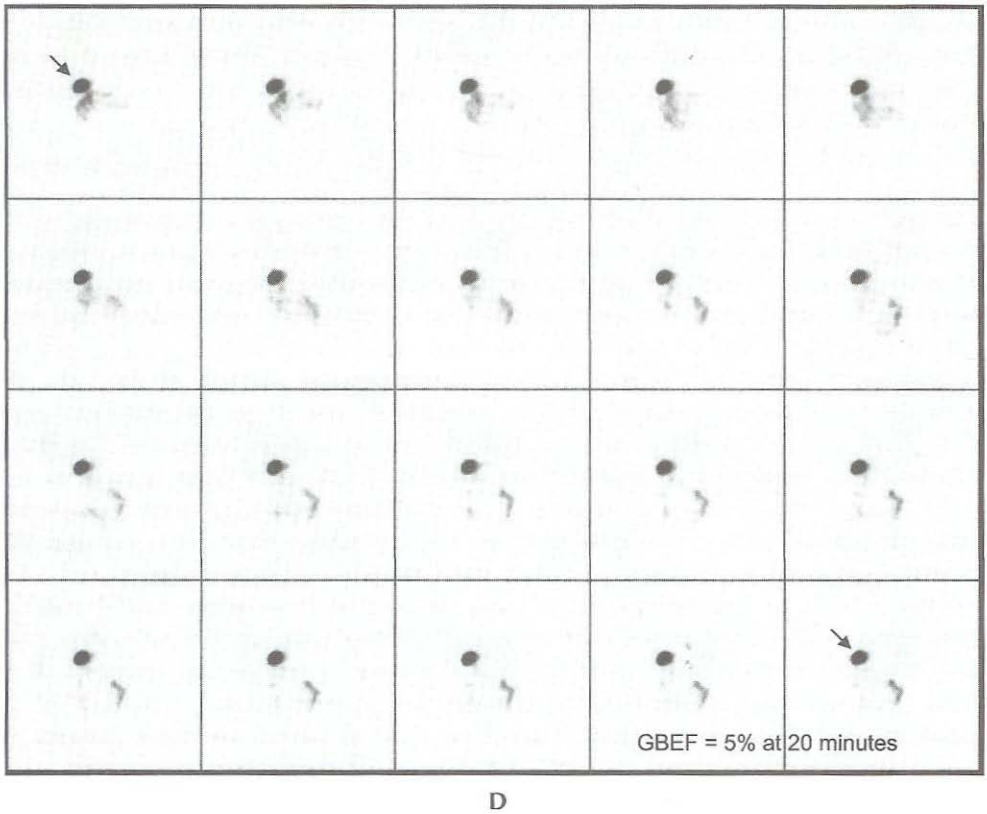

D

FIGURE 17-16 (Continued)

patients, the sphincter of Oddi is contracted because of morphine administration. Sincalide will cause the gallbladder to contract against a closed sphincter.

Radiopharmaceuticals

Hepatobiliary imaging is performed with ^{99m}Tc-IDA compounds. When these compounds are introduced into the blood, they are bound to albumin, which minimizes clearance

from the kidneys. They are actively taken up into the hepatocytes by a carrier-mediated mechanism similar to that of bilirubin uptake. Once in the hepatocytes, they are excreted unchanged into the bile canaliculi by active and passive membrane transport mechanisms.[79] The two radiopharmaceuticals currently in use in the United States are ^{99m}Tc-disofenin and ^{99m}Tc-mebrofenin. ^{99m}Tc-mebrofenin has a higher hepatic extraction and lower renal excretion than ^{99m}Tc-disofenin and may be more useful in patients with high bilirubin levels.

Interpretation

If blood flow images of the abdomen are obtained, the liver is normally seen a few seconds after the kidneys and spleen. This is because most of the blood flow to the liver comes from the portal circulation. In a normal study, there is prompt, homogeneous uptake of the radiotracer in both lobes of the liver. After only about 5 minutes there should be good clearance from the blood pool and visualization of the liver parenchyma. Delay in clearance of the blood pool is seen with hepatic insufficiency. After about 10 minutes there should be evidence of radiotracer accumulation in the biliary tree (biliary excretion). Next there should be radiotracer in the common bile duct, followed by accumulation in the gallbladder and the proximal bowel. Normally, radiotracer activity should be seen in the gallbladder and bowel within 1 hour (Figure 17-7).

Acute Cholecystitis

The most common cause of acute cholecystitis is a stone in the cystic duct that causes an obstruction. In the proper clinical setting (i.e., the patient has fasted for 4 hours, has been pretreated with sincalide if he or she has fasted for more than 24 hours, and has not had a cholecystectomy), nonvisualization of the gallbladder by 4 hours is consistent with acute cholecystitis. If morphine augmentation is used, nonvisualization 30 minutes after morphine administration is considered consistent with acute cholecystitis. In some cases of acute cholecystitis, there is a rim of increased activity in the gallbladder fossa along the inferior hepatic edge with nonvisualization of the gallbladder. This is referred to as the rim sign and is secondary to inflammation and hyperemia around the gallbladder (Figure 17-17).

Chronic Cholecystitis

Most patients with chronic cholecystitis have normal hepatobiliary scans. Some may show delayed gallbladder filling or delayed appearance of activity in the bowel. Many people with symptoms associated with either calculous or acalculous chronic gallbladder disease have reduced GBEF. In these patients GBEF after sincalide administration can be clinically useful.

Common Duct Obstruction

If there is a high-grade common duct obstruction, radiotracer will not be able to enter the bowel. Early on, there is good visualization of the liver parenchyma but no evidence of accumulation in the biliary tree or bowel (see Figures 17-9 and 17-10). If the obstruction is prolonged, there will eventually be decreased hepatic function. Partial common duct obstruction will cause a delayed or prolonged biliary-to-bowel transit time. Nonvisualization of activity in the bowel after 1 hour suggests partial common duct obstruction.

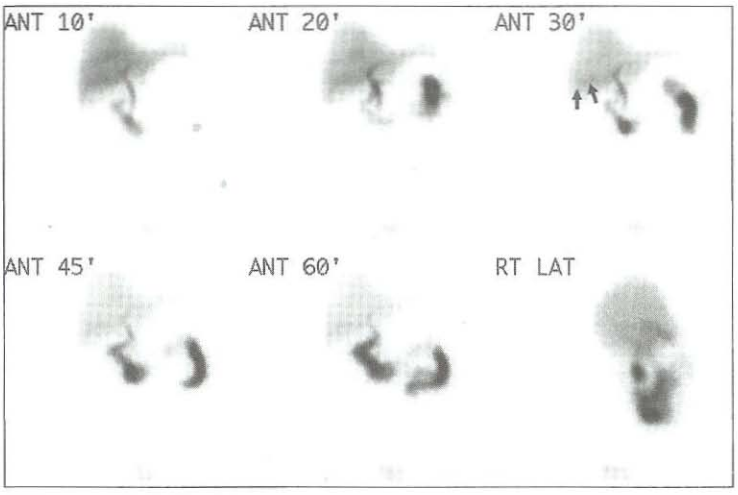

A

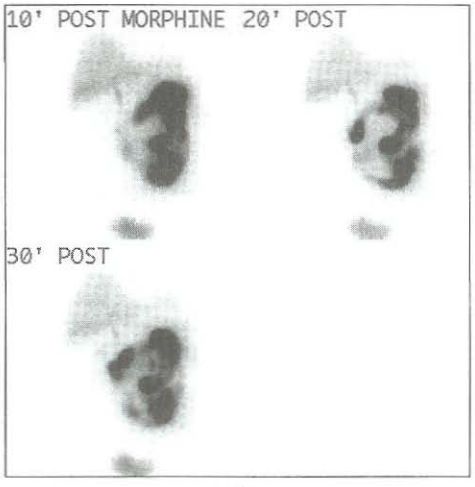

B

FIGURE 17-17 Acute cholecystitis. (A) Serial anterior images of the abdomen were obtained for 60 minutes after intravenous administration of 5 mCi (185 MBq) of ^{99m}Tc-disofenin. On the initial image at 10 minutes, there is radiotracer in the liver, biliary tree, common bile duct, and proximal bowel. Radiotracer is not seen in the gallbladder at 60 minutes. A rim of parenchymal activity is seen in the area of the gallbladder fossa on these images, which is often associated with acute cholecystitis (arrows). It is evident in about 25% of acute cholecystitis patients who are at an advanced stage of the disease. (B) Activity was not seen in the gallbladder even after augmentation with morphine to constrict the sphincter of Oddi.

However, delayed visualization of radiotracer in the bowel can be normal in some people (20% to 25%). In partial obstruction, there is often persistent accumulation of radiotracer in the common duct proximal to the obstruction.

Bile Gastritis

During the hepatobiliary scan, radiotracer can reflux from the duodenum into the stomach (bile reflux). This can sometimes be a cause of the patient's symptoms (Figure 17-18).

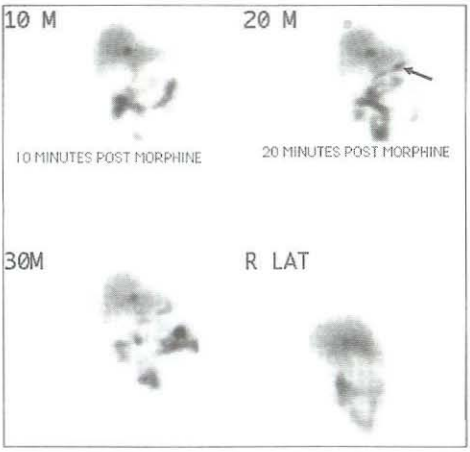

FIGURE 17-18 Acute cholecystitis with reflux gastritis. ^{99m}Tc-disofenin study with morphine augmentation. The gallbladder was not visualized during the first 60 minutes of the study, so morphine sulfate was administered. There was still no radiotracer accumulation in the gallbladder 30 minutes after morphine in this patient with acute cholecystitis. The linear area of radiotracer accumulation just inferior to the left lobe of the liver is bile reflux of the radiotracer into the stomach.

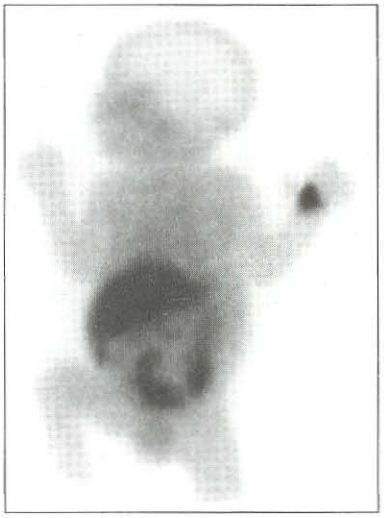

FIGURE 17-19 Neonatal hepatitis. Normal anterior hepatobiliary study in a child 2 hours after ^{99m}Tc-disofenin following 5 days of pretreatment with phenobarbital. Excretion of radiotracer into the intestinal tract confirms the presence of neonatal hepatitis and rules out biliary atresia.

Biliary Atresia

Hepatobiliary imaging can be useful in a jaundiced infant with suspected biliary atresia. The main differential diagnosis in a neonate with prolonged hepatic dysfunction and hyperbilirubinemia is neonatal hepatitis versus biliary atresia. Biliary atresia requires prompt surgical intervention before irreversible damage to the liver occurs. If biliary atresia is suspected, the infant is usually pretreated with oral phenobarbital 2.5 mg/kg twice daily for 5 to 7 days prior to the hepatobiliary scan to stimulate liver excretion. After administration of the radiopharmaceutical, imaging is performed until definite bowel activity is seen. Demonstrating radiotracer in the extrahepatic biliary tree and bowel rules out the diagnosis of biliary atresia (Figure 17-19). If definite bowel activity is not seen after several hours, a delayed 24 hour image can be helpful. If there is no evidence of bowel activity after 24 hours, the findings likely represent biliary atresia (Figure 17-20).

Bile Leak

Hepatobiliary imaging is useful in evaluating patients with suspected bile leak after either trauma (hepatic laceration) or surgery (such as laparoscopic cholecystectomy, liver transplant, or hepatectomy). If fluid collection in the abdomen is detected by another imaging modality such as ultrasound or CT, hepatobiliary imaging can be used to evaluate for clinically significant leaks, as well as obstruction that may require further surgery (Figure 17-21). Small leaks often are clinically insignificant and can be watched.

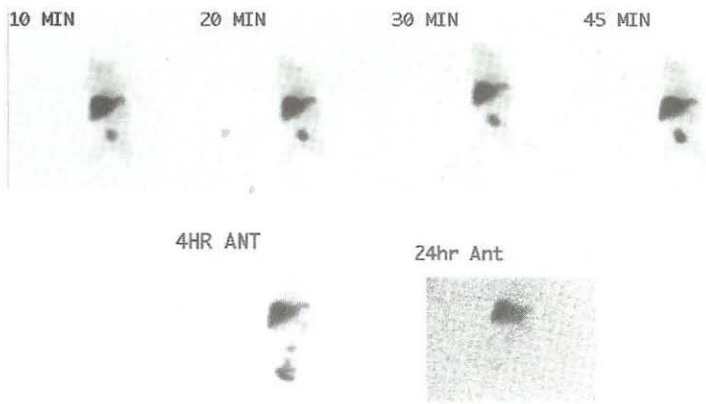

FIGURE 17-20 Biliary atresia. Anterior images of the body taken out to 24 hours after administration of 500 μCi (18.5 MBq) of ^{99m}Tc-disofenin. On the initial image taken at 10 minutes after injection of the radiopharmaceutical, there is uptake in the liver. Activity is also seen in the bladder and (faintly) in the kidneys. There was no evidence of radiotracer accumulation in the bowel or gallbladder after 24 hours in this 8 week old patient.

Gastrointestinal Studies

Several other nuclear medicine studies involve the GI tract. Some of the more common studies involve evaluation of GI bleeding, suspected Meckel's diverticulum, gastroesophageal reflux, and gastric emptying.

Gastrointestinal Bleeding

Effective management of patients suspected of having active GI bleeding often depends on identifying the bleeding site. Upper GI bleeding, which originates from the GI tract proximal to the ligament of Treitz, is successfully evaluated with endoscopy. The lower GI tract is much more difficult to evaluate with endoscopy. Many patients bleed only intermittently, making it difficult to identify the bleeding site with angiography. Nuclear imaging using ^{99m}Tc-RBCs is the method of choice for evaluation of active lower GI bleeding. Labeled RBCs remain in the intravascular space and can be imaged for up to 24 hours. This increases the chances of detecting an intermittent hemorrhage site.

Procedure

A sample of the patient's blood is removed for radiolabeling using an in vitro technique. Dosage is typically 20 to 30 mCi (740 to 1100 MBq) autologous ^{99m}Tc-labeled autologous RBCs. With the patient supine, dynamic 60-second-per-frame anterior images of the abdomen and pelvis are obtained for 60 to 90 minutes using a large field-of-view camera with a LEAP parallel hole collimator. The images can then be played back in cine mode for evaluation. Sometimes, if there is no evidence of bleeding during the 90 minute study, a delayed image at 16 to 24 hours can be useful. Activity seen within loops of bowel on the delayed images indicates that there has been active GI bleeding and may suggest the severity of the bleeding. However, delayed imaging may not be able to demonstrate the intermittent bleeding site. Activity seen in the bowel may be downstream from the bleeding site because of peristalsis.[80]

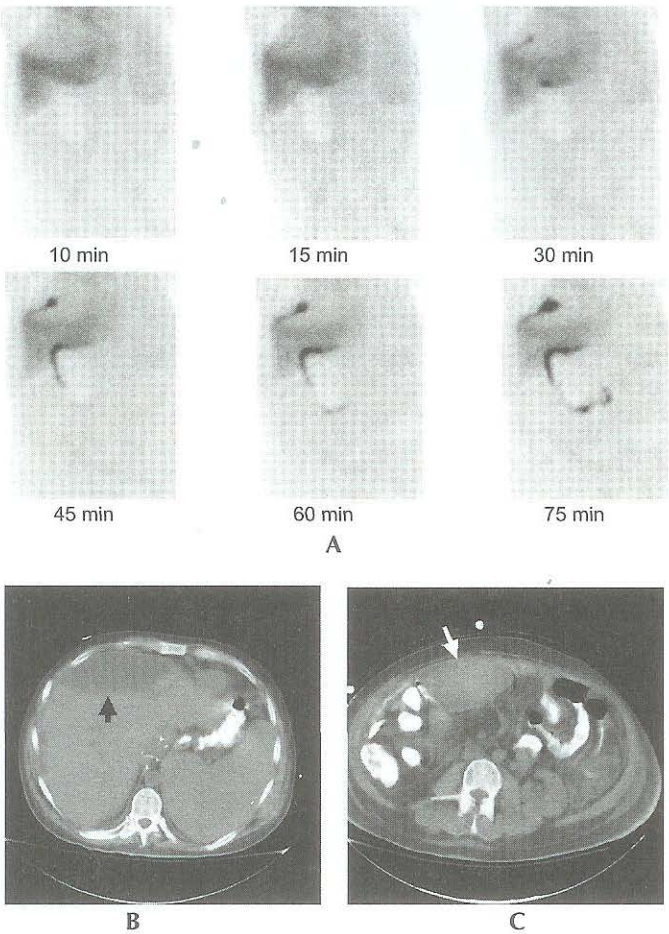

FIGURE 17-21 Bile leak. (A) Serial anterior images of the abdomen were obtained for 75 minutes after intravenous administration of 5 mCi (185 MBq) of ^{99m}Tc-disofenin in this patient after liver transplant. The images show a large photopenic defect at the dome of the liver. On the 30 minute image a linear accumulation of radiotracer is seen in the middle of the defect, which grows during the study and is consistent with an active bile leak. There is another large photopenic area below the liver. Between 45 and 75 minutes there was radiotracer accumulation in the proximal small bowel, which borders this photopenic area. (B) An axial CT image showing a low-density fluid collection anterior to the liver (black arrow). (C) Another axial CT image inferior to the liver shows a large fluid collection in the abdomen (white arrow).

Interpretation

Normally, ^{99m}Tc-labeled RBCs remain in the circulation. After administration, they come into equilibrium in the intravascular space. In a normal RBC study, activity can be seen in the heart, great vessels, liver, and spleen. It is normal to see some activity in the urine. Active GI bleeding is identified as an area of radiotracer accumulation within the bowel that increases and moves with time (Figures 17-22 to 17-24).

Meckel's Diverticulum

A Meckel's diverticulum is a blind-ending tube a few centimeters long arising from the antimesenteric border of the terminal ileum about 50 to 80 cm from the ileocecal valve. It

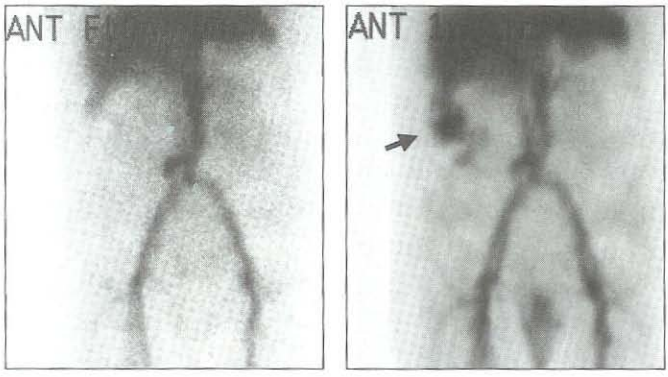

FIGURE 17-22 Abnormal GI bleeding study. Anterior images of the abdomen and pelvis from a ^{99m}Tc-RBC study in a patient with a history of passing bright red blood per rectum. (A) An early blood flow image shows activity in the heart, great vessels, and liver. (B) By 10 minutes, an abnormal focal area of accumulation is seen in the ascending colon near the hepatic flexure (arrow), demonstrating the active GI bleeding site.

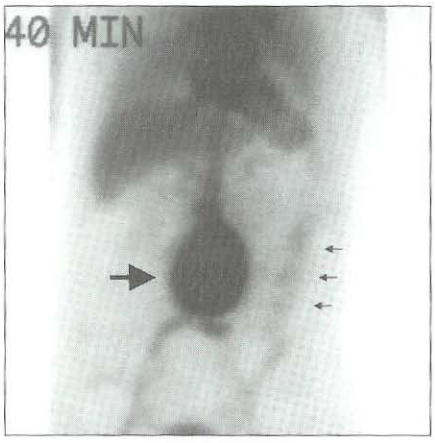

FIGURE 17-23 Abnormal GI bleeding study demonstrating a large abdominal aortic aneurysm (large arrow). During the study some radiotracer accumulation was also seen in the descending colon (small arrows), consistent with active GI bleeding. Normal activity is seen in the heart, liver, and spleen.

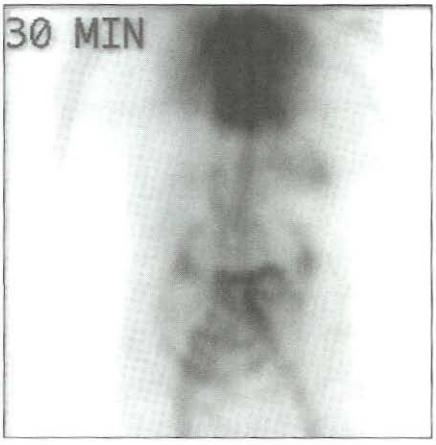

FIGURE 17-24 GI bleeding study showing active small bowel bleeding site. Anterior image taken 30 minutes after intravenous administration of ^{99m}Tc-RBCs. Activity can be seen more centrally in loops of small bowel.

is a vestigial remnant of the omphalomesenteric duct that is present in approximately 2% of the population. About half of these can contain ectopic gastric mucosa or pancreatic cells that can lead to ulceration from acid secretion and can become clinically apparent as rectal bleeding. Most of the cases of rectal bleeding resulting from a Meckel's diverticulum occur before the age of 2 years, and almost all of the diverticula responsible for rectal bleeding contain ectopic gastric mucosa.[81] ^{99m}Tc-sodium pertechnetate is the agent of choice for imaging Meckel's diverticula containing ectopic gastric mucosa because it concentrates in the mucous cells of the gastric mucosa.

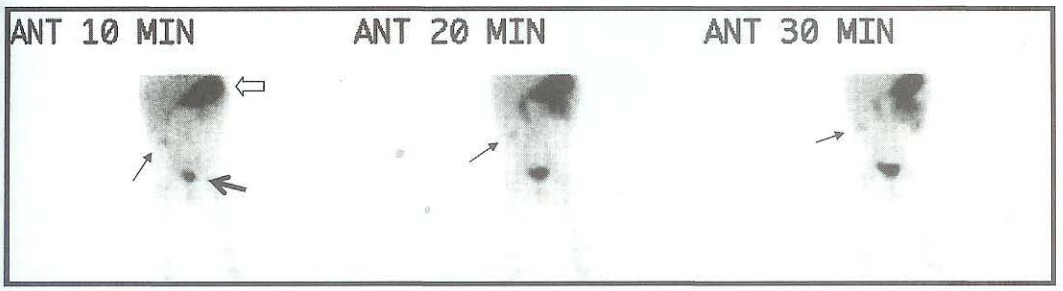

FIGURE 17-25 Meckel's diverticulum. Anterior images of the abdomen and pelvis of a 14 month old girl with intermittent GI bleeding, obtained at 10, 20, and 30 minutes after intravenous administration of 1 mCi (37 MBq) of ^{99m}Tc-sodium pertechnetate. Radiotracer accumulation is seen in the stomach (white arrow) and bladder (black arrow). There is also a small focal area of radiotracer accumulation in the right abdomen (small arrows) which was found to be a Meckel's diverticulum containing ectopic gastric mucosa.

Procedure

With the patient supine, dynamic 60 second-per-frame anterior images of the abdomen and pelvis are obtained for 60 to 90 minutes using a large field-of-view camera with a LEAP parallel hole collimator. In children, about 200 to 300 uCi/kg (7.4 to 11.1 MBq/kg) of ^{99m}Tc-sodium pertechnetate is administered intravenously. In adults, the dose is usually 10 to 15 mCi (370 to 555 MBq).[77] Pretreatment with various pharmaceuticals can increase the sensitivity of a Meckel's scan. Histamine$_2$ (H_2)-blockers such as cimetidine block secretion from the gastric mucosa cells, resulting in increased uptake. In children, oral cimetidine can be given for 2 days prior to the study at a dose of 20 mg/kg per day. In adults the dose is 300 mg four times daily for 2 days before the study. Pretreatment with pentagastrin is an alternative to H_2-blockers. Pentagastrin stimulates gastric secretion and increases gastric mucosa uptake.[80]

Interpretation

Initial anterior images of the abdomen and pelvis show activity in the intravascular space, including the heart, great vessels, liver, spleen, and kidneys. After a few minutes, physiologic activity appears in the gastric mucosa of the stomach. Over time the stomach activity becomes intense as the background activity in the heart, liver, and spleen decreases. Radiotracer uptake in a Meckel's diverticulum containing ectopic gastric mucosa should appear at about the same time activity appears in the stomach. This usually is identified as a focal area of radiotracer accumulation in the right lower quadrant or mid abdominal region (Figure 17-25). However, it can appear anywhere in the abdomen. On lateral views of the abdomen, this focus is anterior.

Gastroesophageal Reflux

Nuclear medicine imaging can be used to evaluate the presence and degree of gastroesophageal reflux, reflux of stomach contents into the esophagus manifested as a burning sensation in the chest referred to as heartburn. If this becomes severe and frequent, it is referred to as gastroesophageal reflux disease (GERD). The three different mechanisms thought to be responsible for esophageal reflux are transient relaxation of the lower esophageal sphincter, transient increase in intra-abdominal pressure, and low resting

pressure of the lower esophageal sphincter.[82] GERD can lead to respiratory complications resulting from aspiration of gastric bacteria.[83]

The radionuclide gastroesophageal reflux study is a sensitive, noninvasive test that is able to detect reflux in 90% of symptomatic patients.[62,84] Additionally, the study permits quantitation of the extent of reflux into the esophagus and can be extended to detect pulmonary aspiration of gastric contents.[85,86]

The procedure is well tolerated by children. Two hundred microcuries (7.4 MBq) of ^{99m}Tc-SC is administered orally in 30 mL of apple juice followed by additional juice or formula until the patient is sated. Abdominal pressure measurements are performed using a blood pressure cuff in small children to demonstrate reflux. The value of the radionuclide gastric reflux study in children was demonstrated in a study that showed an 80% rate of detection in subjects with gastroesophageal reflux previously documented by other acid reflux methods.[87]

Gastroesophageal reflux is a common problem in infants and children but also occurs in adults. It frequently leads to respiratory complications, presumably resulting from aspiration of gastric contents.[85] The reflux study can be extended to detect pulmonary aspiration as a consequence of gastroesophageal reflux and has been shown to be more sensitive than conventional nonradionuclide procedures.[86] The dose of ^{99m}Tc-SC given as a liquid meal at bedtime with lung scanning the following day can identify lung aspiration of refluxed gastric contents.

Adult patients should fast for 4 to 6 hours before the reflux study. The radiopharmaceutical most often used is ^{99m}Tc-SC. Typically 0.3 mCi (11.1 MBq) ^{99m}Tc-SC is added to 300 mL of acidic orange juice, which is a combination of 150 mL of orange juice and 150 mL of 0.1 N hydrochloric acid. Prior to administration of the radiotracer, the patient is fitted with an abdominal binder that can be inflated to increase pressure around the upper abdomen. The patient drinks the radiolabeled orange juice and then is positioned supine under the gamma camera. The field of view should include the entire esophagus and as much of the stomach as possible. If there is activity in the esophagus on the initial image, it may be residual swallowed activity. A small amount of water can be given to the patient to clear this activity. Typically, dynamic anterior 30 second-per-frame images are obtained during the study. If there is no evidence of activity in the esophagus, pressure is increased in the abdominal binder in 20 mm Hg increments up to 100 mm Hg. Serial 30 second-per-frame images are obtained at each increment.[88]

Normally, there should be no activity above the stomach during the study. Activity visualized in the esophagus is considered abnormal and is consistent with esophageal reflux (Figure 17-26). The degree of reflux can be calculated using the formula:

$$R = \frac{E_t - E_b}{G_0} \times 100$$

where:
R = the percent of gastroesophageal reflux
E_t = the esophageal counts at time t when the reflux is maximal
E_b = the esophageal background counts at the beginning of the study
G_0 = the stomach counts at the beginning of the study

The upper limit of normal is considered to be 3% reflux. Over 4% is considered abnormal.[84] Attention should also be paid to the lungs. If aspiration is present during the study, there will be radiotracer accumulation in the lungs.

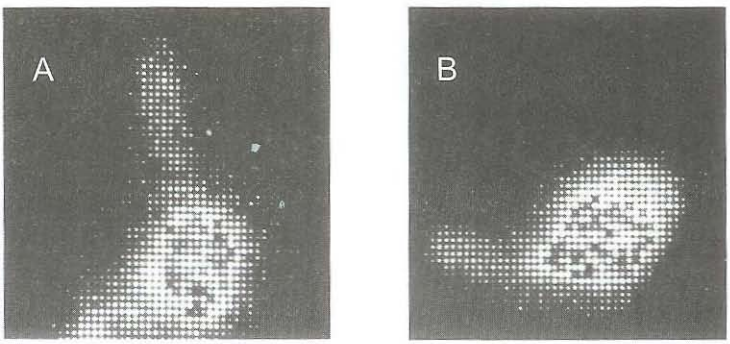

FIGURE 17-26 Gastroesohageal scintigraphy displayed on an oscilloscope of a data processor. (A) This study demonstrates reflux above the stomach into the esophagus. (B) An asymptomatic normal volunteer demonstrating gastric activity and filling of the pylorus but no reflux cephalad. (Reprinted with permission of Elsevier Science from Malmud LS, Fisher RS. Radionuclide studies of esophageal transit and gastroesophageal reflux. *Semin Nucl Med.* 1982;12:104-15.)

Gastric Emptying

The stomach can be divided into four regions: the fundus, body, antrum, and pylorus. The fundus and proximal body of the stomach predominantly serve as a storage reservoir for food. The distal stomach and antrum demonstrate peristaltic contractions that break down the food into small particles and mix them with gastric secretions. The pyloric sphincter acts as a sieve, allowing particles smaller than 1 mm to enter the duodenum with each peristaltic contraction.[89] Liquids empty from the stomach in an exponential fashion. However, solids demonstrate a lag phase while the food is being broken down into smaller particles. The lag phase is then followed by a more linear emptying phase.

Gastric emptying disorders fall into two different categories: delayed emptying and abnormally fast emptying (dumping). Delayed gastric emptying symptoms can include nausea, vomiting, abdominal discomfort, bloating, and early satiety. There are many potential causes for delayed gastric emptying, including endocrine disorders such as diabetes mellitus, mechanical obstruction, postsurgical effects, certain drugs, and idiopathic factors. Nuclear medicine gastric emptying studies are commonly ordered to evaluate for diabetic gastroparesis. Dumping can be associated with gastric surgery such as gastrectomy, antrectomy, and pyloroplasty that allows the passage of larger particles into the small bowel. In these patients, a dumping syndrome can occur after eating, with symptoms of dizziness, weakness, nausea, vomiting, sweating, and palpitations.

Scintigraphic evaluation of gastric emptying can be done with solids, liquids, or a combination of the two. In practice, gastric emptying studies are almost always done with a solid meal because the solid phase is more sensitive than the liquid phase for detecting delayed gastric emptying. The patient should fast for 8 hours before the study. Often patients are instructed to fast after midnight and the study is done in the morning. Typically, 1.0 mCi (37MBq) ^{99m}Tc-SC is mixed with an egg, which is subsequently cooked and served scrambled. This is served either alone or as an egg sandwich. For infants 0.5 mCi (18.5 MBq) of ^{99m}Tc-SC can be added to milk or formula. The patient should eat the radiolabeled food quickly, and imaging should start immediately after completion of the meal. The patient is positioned so that anterior images of the abdomen that include the distal esophagus, stomach, and small bowel can be obtained.[88] The patient can be standing

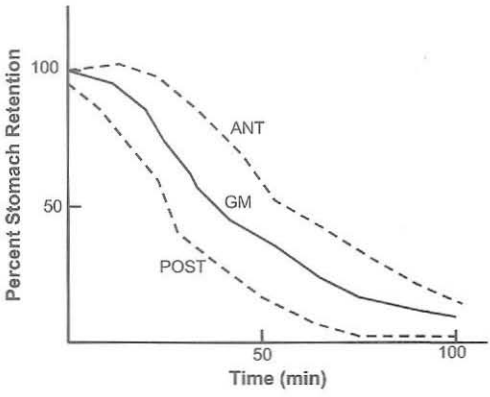

FIGURE 17-27 Gastric emptying curve. Stomach activity after a radioactive meal (1 mCi [37 MBq] of ^{99m}Tc-SC with scrambled egg), acquired by simultaneous recording of anterior and posterior counts over time. The geometric mean curve (GM) corrects for differences in depth attenuation of counts acquired from the anterior and posterior projections.

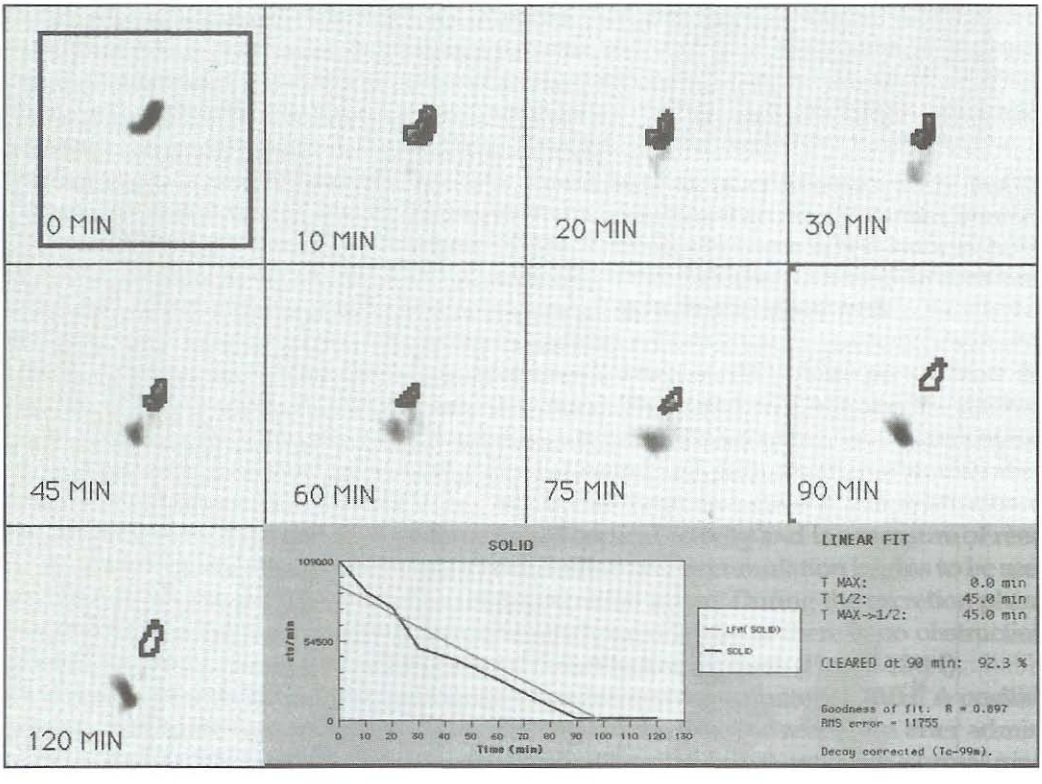

FIGURE 17-28 Normal gastric emptying study in a 2 month old girl. Serial anterior images of the abdomen were obtained for 120 minutes after oral administration of 0.5 mCi (18.5 MBq) of ^{99m}Tc-SC in 50 mL of formula. In the initial image, labeled 0 min, all of the radiolabeled formula is seen in the stomach. Regions of interest are drawn around the stomach in the subsequent images to obtain a gastric time–activity curve (inset). There was 92.3% gastric emptying by 90 minutes.

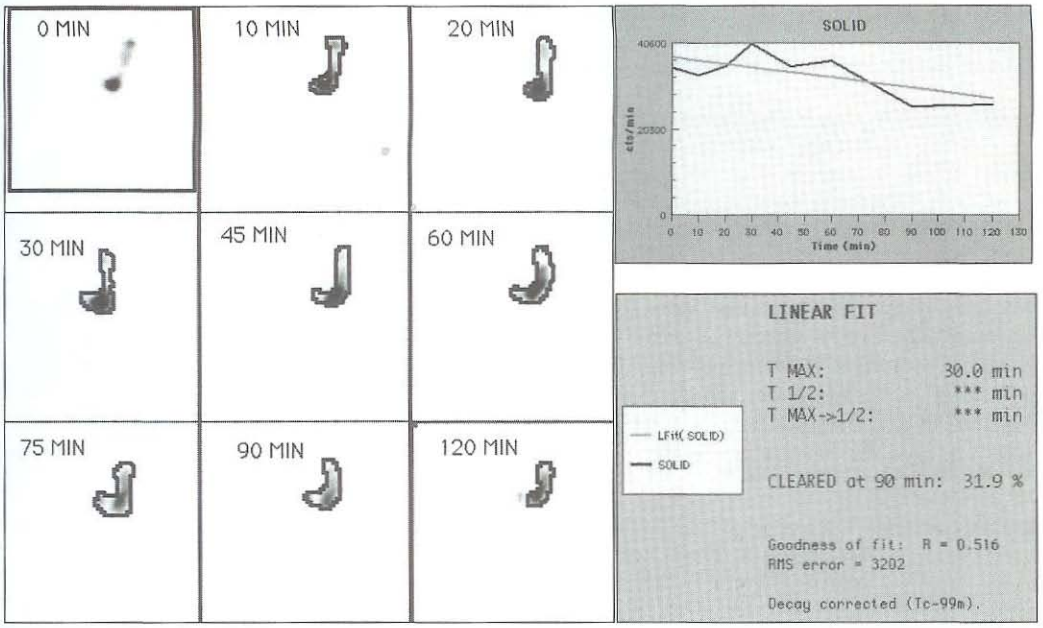

FIGURE 17-29 Delayed gastric emptying in a 50 year old patient. Serial anterior images of the abdomen were obtained out to 120 minutes after the patient ingested a radiolabeled egg. On the initial image, labeled 0 min, all of the radiolabeled egg is in the stomach. Regions of interest drawn around the stomach in the subsequent images show delayed gastric emptying, with only 31.9% gastric emptying by 90 minutes.

or supine during the study. If geometric means of the stomach counts are to be calculated, a dual-headed camera can be used to obtain anterior and posterior images of the stomach. The geometric mean ($\sqrt{\text{anterior counts} \times \text{posterior counts}}$) corrects for attenuation differences between the anterior and posterior counts (Figure 17-27). Alternatively, the left anterior oblique (LAO) viewing angle can be used to acquire images. In this projection, the stomach contents move roughly parallel to the head of the gamma camera, minimizing the effect of attenuation. This method has the advantages of simple acquisition and no need for mathematical correction; however, it is not as accurate as the geometric mean method.[90] Dynamic 1-minute-per-frame images can be obtained for at least 90 minutes. Alternatively, static images can be obtained every 15 minutes. Regions of interest are drawn around the stomach in each of the images, and a gastric time–activity curve is obtained to calculate percentage of gastric emptying.

The rate of gastric emptying depends on many variables and on the type of meal, patient position, and protocol used. Ideally, normal curves should be established in the institution performing the study. In general, for a solid gastric emptying study, there should be at least 50% emptying by 90 minutes (Figures 17-28 to 17-30).[81]

Dietary changes, including the reduction of extra fat and bulk and frequent small meals, can be useful in the treatment of both diabetic and nondiabetic gastroparesis. Therapy with prokinetic drugs such as cisapride can improve gastric emptying. Metoclopramide is a reasonable option if cisapride is ineffective.[91] Erythromycin can also be used to increase gastric emptying in both diabetic and nondiabetic gastroparesis (Figure 17-31).[92,93] Follow-up gastric emptying studies can be performed after initiation of medical therapy to assess the effectiveness of treatment.

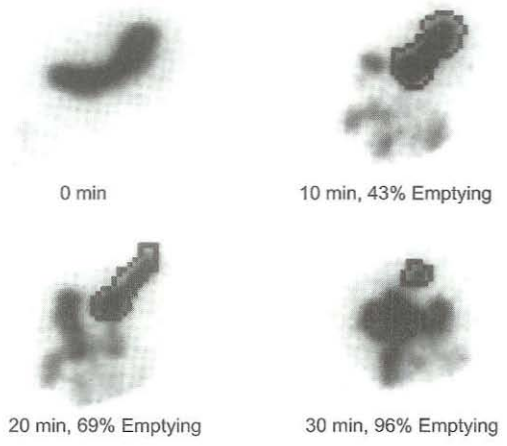

FIGURE 17-30 Rapid gastric emptying after 1 mCi (37 MBq) of ^{99m}Tc-sulfur colloid/scrambled egg meal. Regions of interest drawn around the stomach at various times represent activity remaining in the stomach, which is subtracted from the baseline stomach activity at time zero (100%) to give the percent emptying.

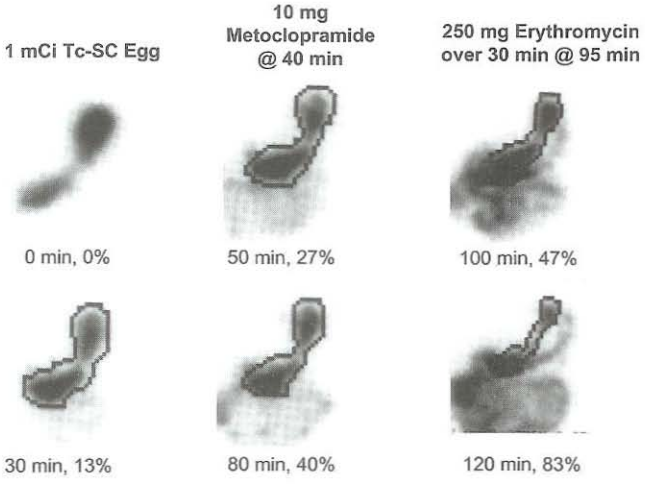

FIGURE 17-31 Delayed gastric emptying with pharmacologic intervention. Images at various time points represent percent gastric emptying.

REFERENCES

1. Guyton AC. *Circulatory Physiology II: Dynamics and Control of the Body Fluids*. Philadelphia: WB Saunders; 1975.
2. Elias H, Sherrick JC. *Morphology of the Liver*. New York: Academic Press; 1969.
3. Wisse E. Ultrastructure and function of Kupffer cells and other sinusoidal cells. In: Wisse E, Knook DL, eds. *Kupffer Cells and Other Liver Sinusoidal Cells*. Amsterdam: Elsevier North Holland; 1977:33-60.
4. Wisse E, DeZanger RB. On the morphology and other aspects of Kupffer cell function: observations and speculations concerning pinocytosis and phagocytosis. In: Liehr H, Grun M, eds. *The Reticuloendothelial System and the Pathogenesis of Liver Disease*. Amsterdam: Elsevier North Holland; 1979:3-9.
5. Rouiller CH. *The Liver: Morphology, Biochemistry, Physiology*. Vol 1. New York: Academic Press; 1963.
6. Loberg MD, Porter DW, Ryan JW. Review and current status of hepatobiliary imaging agents. In: Sorenson JA, ed. *Radiopharmaceuticals II: Proceedings of the Second International Symposium on Radiopharmaceuticals*. New York: Society of Nuclear Medicine; 1979:519-43.
7. Dobson EL, Jones HB. The behavior of intravenously injected particulate material: Its rate of disappearance from the blood stream as a measure of liver blood flow. *Acta Med Scand*. 1952;144 (suppl 273):1-71.
8. Stirrett LA, Yuhl ET, Libby RL. The hepatic radioactivity survey. *Radiology* 1953;61:930-3.

9. Stirrett LA, Yuhl ET, Cassen B. Clinical applications of hepatic radioactivity surveys. *Am J Gastroenterol.* 1954;21:310-7.
10. Sorensen LB, Archambault M. Visualization of the liver by scanning with Mo-99 (molybdate) as tracer. *J Lab Clin Med.* 1963;62:330-40.
11. Benacerraf B, Biozzi G, Halpern B, et al. A study of phagocytic activity of the reticuloendothelial system toward heat denatured human serum albumin tagged with I-131. *Res Bull.* 1956;2:19-29.
12. Richards P. A survey of the production at Brookhaven National Laboratory of radioisotopes for medical research. In: *V. Congresso Nucleare.* Vol 2. Rome: Comitato Nazionale Ricerche Nucleari; 1960:223-44.
13. Harper PV, Lathrop KA, Richards P. Tc-99m as a radiocolloid [abstract]. *J Nucl Med.* 1964;5:382.
14. Stern HS, McAfee JG, Subramanian G. Preparation, distribution and utilization of technetium Tc-99m sulfur colloid. *J Nucl Med.* 1966;7:665-75.
15. Ege GN, Warbick A. Lymphoscintigraphy: a comparison of Tc-99m antimony sulfide colloid and Tc-99m stannous phytate. *Br J Radiol.* 1979;52:124-9.
16. Goodwin DA, Stern HS, Wagner HN Jr, et al. In-113m colloid: a new radiopharmaceutical for liver scanning. *Nucleonics.* 1966;24:65-9.
17. Subramanian G, McAfee JG, Mehta A, et al. Tc-99m stannous phytate: a new in-vivo colloid for imaging the reticuloendothelial system [abstract]. *J Nucl Med.* 1973;14:459.
18. Saba TM. Physiology and physiopathology of the reticuloendothelial system. *Arch Intern Med.* 1970;126:1031-52.
19. Nelp WB. An evaluation of colloids for RES function studies. In: Subramanian G, Rhodes B, Cooper JF, et al., eds. *Radiopharmaceuticals.* New York: Society of Nuclear Medicine; 1975:349-56.
20. Guyton AC. *Textbook of Medical Physiology.* 6th ed. Philadelphia: WB Saunders; 1981.
21. Wagner HN, Iio M. Studies of the reticuloendothelial system (RES). III: Blockade of the RES in man. *J Clin Invest.* 1964;43:1525-32.
22. Quinones JD. Localization of technetium-sulfur colloid after RES stimulation [abstract]. *J Nucl Med.* 1973;14:443-4.
23. Srivastava SC, Richards P. Technetium-labeled compounds. In: Rayudu GUS, ed. *Radiotracers for Medical Applications.* Boca Raton, FL: CRC Press; 1981:90-2.
24. Davis MA, Jones AG, Trindade H. A rapid and accurate method for sizing radiocolloids. *J Nucl Med.* 1974;15:923-8.
25. Atkins HL, Hauser W, Richards P. Factors affecting distribution of Tc-99m sulfur colloid. *J Nucl Med.* 1969;10:319-20.
26. Cohen Y, Ingrand J, Caro RA. Kinetics of the disappearance of gelatin protected radiogold colloids from the blood stream. *Int J Appl Radiat Isot.* 1968;19:703-5.
27. Chaudhuri TK, Evand TC, Chaudhuri TK. Autoradiographic studies of distribution in the liver of Au-198 and Tc-99m sulfur colloids. *Radiology.* 1973;109:633-7.
28. Brucer M. *Liver Scans, Clearances, and Perfusions.* New York: Krieger; 1977.
29. Bissell DM, Hammaker L, Schmid R. Liver sinusoidal cells: identification of a subpopulation for erythrocyte catabolism. *J Cell Biol.* 1972;54:107-19.
30. Easton TW. The role of macrophage movements in the transport and elimination of intravenous thorium dioxide in mice. *Am J Anat.* 1952;90:1-33.
31. Castronovo FP, Wagner HN. Comparative toxicity and pharmacodynamics of ionic indium chloride and hydrated indium oxide. *J Nucl Med.* 1973;14:677-82.
32. Atkins HL. Adverse reactions. In: Rhodes BA, ed. *Quality Control in Nuclear Medicine.* St Louis: Mosby; 1977:263-7.
33. Haney TA, Ascanio I, Gigliotti JA, et al. Physical and biological properties of a Tc-99m sulfur colloid preparation containing disodium edetate. *J Nucl Med.* 1971;12:64-8.
34. CIS-Sulfur Colloid [package insert]. Bedford, Ma: CIS-US Inc; 1998.
35. MIRD report no. 3: summary of current radiation dose estimates to humans with various liver conditions from Tc-99m sulfur colloid. *J Nucl Med.* 1975;16:108A.
36. Shaffer EA. Gallbladder motility in health and disease. In: Feldman M, LaRusso NF, eds. *Gastroenterology and Hepatology.* Vol 6: Gallbladder and Bile Ducts. Philadelphia: Current Medicine; 1997:5.1-33.
37. Marzio L, Neri M, Capone F, et al. Gallbladder contraction and its relationship to interdigestive duodenal motor activity in normal human subjects. *Dig Dis Sci.* 1988;33:540-4.
38. Taplin GV, Meredith OM, Kade H. The radioactive (I-131 tagged) rose bengal uptake: excretion test for liver function using external gamma-ray scintillation counting techniques. *J Lab Clin Med.* 1955;45:665-75.
39. Loberg MD, Cooper M, Harvey E, et al. Development of new radiopharmaceuticals based on N-substitution of iminodiacetic acid. *J Nucl Med.* 1976;17:633-8.
40. Wistow BW, Subramanian G, Van Heertum RL, et al. An evaluation of Tc-99m labeled hepatobiliary agents. *J Nucl Med.* 1977;18:455-61.

41. Wistow BW, Subramanian G, Gagne GM, et al. Experimental and clinical trials of new Tc-99m-labeled hepatobiliary agents. *Radiology.* 1978;128:793-4.
42. Nunn AD, Loberg MD, Conley RA, et al. The development of a new cholescintigraphic agent, Tc-SQ 26,962, using a structure-distribution relationship approach. *J Nucl Med.* 1981;22:P51.
43. Ryan J, Cooper M, Loberg M, et al. Technetium-99m-labeled N-(2,6-dimethylphenyl carbamoylmethyl) iminodiacetic acid (Tc-99m HIDA): a new radiopharmaceutical for hepatobiliary imaging studies. *J Nucl Med.* 1977;18:997-1004.
44. Loberg MD, Fields AT. Stability of Tc-99m labeled N-substituted iminodiacetic acids: ligand exchange reaction between Tc-99m HIDA and EDTA. *Int J Appl Radiat Isot.* 1977;28:687-92.
45. Firnau G. Why do Tc-99m chelates work for cholescintigraphy? *Eur J Nucl Med.* 1976;1:137-9.
46. Hirom PC. The physicochemical factors required for the biliary excretion of organic cations and anions. *Biochem Soc Trans.* 1974;2:327-9.
47. Nunn AD, Loberg MD. Hepatobiliary agents. In: Spencer RP, ed. *Radiopharmaceuticals: Structure-Activity Relationships.* New York: Grune & Stratton; 1981:539-48.
48. Fritzberg AR, Klingensmith WC III. Quest for the perfect hepatobiliary radiopharmaceutical. *J Nucl Med.* 1982;23:543-6.
49. Krishnamurthy S, Krishnamurthy T. Quantitative assessment of hepatobiliary diseases with Tc-99m-IDA scintigraphy. In: Freeman LM, Weissmann HS, eds. *Nuclear Medicine Annual 1988.* New York: Raven Press; 1988:309-30.
50. Klingensmith WC III, Fritzberg AR, Spitzer VM, et al. Work in progress: clinical evaluation of Tc-99m-trimethylbromo-IDA and Tc-99m-diisopropyl-IDA for hepatobiliary imaging. *Radiology.* 1983;146:181-4.
51. Tc-99m Disofenin [package insert]. Bedford, MA: CIS-US Inc; 1999.
52. Tc-99m Mebrofenin [package insert]. Princeton, NJ: Bracco Diagnostics Inc, 2000.
53. Fink-Bennett, D. Augmented cholescintigraphy: its role in detecting acute and chronic disorders of the hepatobiliary tree. *Semin Nucl Med.* 1991;21:128-39.
54. Ziessman HA. Cholescystokinin cholescintigraphy: victim of its own success? *J Nucl Med.* 1999;40:2038-42.
55. Weissman HS, Sugarman LA, Freeman LM. The clinical role of technetium-99m iminodiacetic acid cholescintigraphy. In: Freeman LM, Weissman HS, eds. *Nuclear Medicine Annual 1981.* New York: Raven Press; 1981:35-90.
56. Fink-Bennett D. Hepatobiliary imaging. In: Sandler MP, Patton JA, Coleman RE, et al., eds. *Diagnostic Nuclear Medicine.* 3rd ed. Baltimore: Williams & Wilkins; 1997:759-72.
57. Erslev AJ, Gabuzda TG. *Pathophysiology of Blood.* 2nd ed. Philadelphia: WB Saunders; 1979:15-18.
58. Williams WJ, Beutler E, Erslev AJ, et al. *Hematology.* New York: McGraw-Hill; 1972:13-14.
59. Smith TD, Richard P. A simple kit for the preparation of Tc-99m labeled red blood cells. *J Nucl Med.* 1976;17:126-32.
60. Atkins HL, Goldman AG, Fairchild RG, et al. Splenic sequestration of Tc-99m labeled, heat treated red blood cells. *Radiology.* 1980;136:501-3.
61. Wagner HJ Jr, Razzak MA, Gaertner RA, et al. Removal of erythrocytes from the circulation. *Arch Intern Med.* 1962;110:90-7.
62. Malmud LS, Fisher RS. Radionuclide studies of esophageal transit and gastroesophageal reflux. *Semin Nucl Med.* 1982;12:104-15.
63. Wirth N, Swanson D, Shapiro B, et al. A conveniently prepared Tc-99m resin for semi-solid gastric emptying studies. *J Nucl Med.* 1983;24:511-4.
64. Christian PE, Datz FL, Sorenson JA, et al. Technical factors in gastric emptying studies: teaching editorial. *J Nucl Med.* 1983;24:264-8.
65. Malmud LS, Fisher RS, Knight LC, et al. Scintigraphic evaluation of gastric emptying. *Semin Nucl Med.* 1982;12:116-25.
66. Alavi A. Detection of gastrointestinal bleeding with Tc-99m sulfur colloid. *Semin Nucl Med.* 1982;12:126-38.
67. Winzelberg GG, McKusick KA, Frolich JW, et al. Detection of gastrointestinal bleeding with Tc-99m labeled red blood cells. *Semin Nucl Med.* 1982;12:139-46.
68. Bunker S, Lull R, Tanasescu D, et al. Scintigraphy of gastrointestinal hemorrhage: superiority of Tc-99m red blood cells over Tc-99m sulfur colloid. *Am J Roentgenol.* 1984;143:543-8.
69. Anderson WAD, Scatti TM. *Synopsis of Pathology.* St Louis: Mosby; 1968:638.
70. Kilpatrick ZM. Scanning in diagnosis of Meckel's diverticulum. *Hosp Pract.* 1974;9:131-8.
71. Sfakianakis GN, Conway JJ. Detection of ectopic gastric mucosa in Meckel's diverticulum and in other aberrations by scintigraphy. I: Pathophysiology and 10 year experience. *J Nucl Med.* 1981;22:647-54.
72. Sfakianakis GN, Conway JJ. Detection of ectopic gastric mucosa in Meckel's diverticulum and in other aberrations by scintigraphy. II: Indications and methods—a 10 year experience. *J Nucl Med.* 1981;22:732-8.

73. Stanley MM, Cerniak G. Protein-losing enteropathy. In: Rothfeld D, ed. *Nuclear Medicine In Vitro*. Philadelphia: JB Lippincott; 1974:341.
74. Mabry CC, Greenlaw RH, DeVore WD. Measurements of gastrointestinal loss of plasma albumin: a clinical and laboratory evaluation of chromium-51 labeled albumin. *J Nucl Med*. 1965;6:93-108.
75. Rubini ME, Sheehy TW, Johnson CR. Exudative enteropathy. 1: A comparative study of Cr-51 chloride and I-131 PVP. *J Lab Clin Med*. 1961;58:892-901.
76. Royal HD, Brown ML, Drum DE, et al. Procedure guideline for hepatic and splenic imaging. In: *Procedure Guidelines Manual 2001-2002*. Reston, VA: Society of Nuclear Medicine; 2001:53-7.
77. Mettler FA, Guiberteau MJ. Gastrointestinal tract. In: *Essentials of Nuclear Medicine Imaging*. 4th ed. Philadelphia: WB Saunders, 1988:237-84.
78. Balon HR, Brill DR, Fink-Bennet DM, et al. Procedure guideline for hepatobiliary scintigraphy. In: *Procedure Guidelines Manual 2001-2002*. Reston, VA: Society of Nuclear Medicine; 2001:59-64.
79. Kim CK, Yun M and Machac J. Liver and biliary tract. In: Elgazzar AH, ed. *The Physiologic Basis of Nuclear Medicine*. New York: Springer-Verlag, 2001.
80. Ford PV, Bartold SP, Fink-Bennett DM, et al. Procedure guideline for gastrointestinal bleeding and Meckel's diverticulum scintigraphy 1.0. In: *Procedure Guidelines Manual 2001-2002*. Reston, VA: Society of Nuclear Medicine; 2001:41-8.
81. Hassan F, Naddaf S, Al-Enizi E, et al. Gastrointestinal tract. In: Elgazzar AH, ed. *The Pathophysiologic Basis of Nuclear Medicine*. New York: Springer-Verlag; 2001:284-93.
82. Dodds WJ, Dent J, Hogan WJ, et al. Mechanisms of esophageal reflux in patients with reflux esophagitis. *N Engl J Med*. 1982;307:1547-52.
83. DuMoulin GC, Paterson DG, Hedley-White J, et al. Aspiration of gastric bacteria in antacid-treated patients: a frequent cause of postoperative colonization of the airway. *Lancet*. 1982;1:242-5.
84. Fisher RS, Malmud LS, Roberts GS, et al. Gastroesophageal (GE) scintiscanning to detect and quantitate GE reflux. *Gastroenterology*. 1976;70:301-8.
85. Chernow B, Johnson LF, Janowitz WR, et al. Pulmonary aspiration as a consequence of gastroesophageal reflux. *Dig Dis Sci*. 1979;24:839-44.
86. Heyman S, Kirkpatrick JA, Winton HS, et al. An improved radionuclide method for the diagnosis of gastroesophageal reflux and aspiration in children (milk scan). *Radiology*. 1979;131:479-2.
87. Rudd TG, Christie DL. Demonstration of gastroesophageal reflux in children by radionuclide gastroesophagography. *Radiology*. 1979;131:483-6.
88. Donohoe KJ, Maurer AH, Ziessman HA, et al. Procedure guideline for gastric emptying and motility 1.0. In: *Procedure Guidelines Manual 2001-2002*. Reston, VA: Society of Nuclear Medicine; 2001;37-40.
89. Meyer JH, Ohashi H, Jehn D, et al. Size of liver particles emptied from the human stomach. *Gastroenterology*. 1981;80:1489-96.
90. Fahey FH, Ziessman HA, Collen MJ, et al. Left anterior oblique projection and peak-to-scatter ratio for attenuation compensation of gastric emptying studies. *J Nucl Med*. 1989;30:233-9.
91. McCallum RW, Brown RI. Diabetic and nondiabetic gastroparesis. *Curr Treat Options Gastroenterol*. December 1998;1:1-7.
92. Urbain JLC, Vantrappen G, Janssens J, et al. Intravenous erythromycin dramatically accelerates gastric emptying in gastroparesis diabeticorum and normals and abolishes the emptying discrimination between solids and liquids. *J Nucl Med*. 1990;31:1490-3.
93. Urbain JLC, Vehemans MCM, Malmud LS. Esophageal transit, gastroesophageal reflux, and gastric emptying. In: Sandler MP, Patton JA, Coleman RD, et al., eds. *Diagnostic Nuclear Medicine*. 3rd ed. Baltimore: Williams & Wilkins; 1997:733-47.

18 Kidney

The kidney is the organ primarily responsible for eliminating metabolic waste products as well as drugs and their metabolites from the body. The renal excretion of radiopharmaceuticals provides an effective noninvasive means of assessing kidney function. A unique feature of renal nuclear medicine studies is that the function of each kidney can be measured. This is particularly useful in assessing kidney transplants. Scintigraphic methods have been developed to assess glomerular and tubular function, to detect the presence of space-occupying lesions such as tumors and cysts, and to measure relative function between the left and right kidneys. Genitourinary problems, including ureteral obstruction, residual urine after voiding, and vesicoureteral reflux, can also be evaluated. Pharmacologic agents are used to improve the diagnostic power of some renal studies. Although structural abnormalities of the kidney are best evaluated by other diagnostic modalities, kidney function is best assessed by radionuclide techniques.

PHYSIOLOGIC ANATOMY

The functional unit of the kidney is the nephron, illustrated in Figure 18-1.[1] It consists of the glomerulus, proximal convoluted tubule, loop of Henle, distal convoluted tubule, and a collecting duct that empties into the renal pelvis. Tubular urine flows through the nephron in that order. There are approximately 1.5 million nephrons in each kidney. About 85% of the nephrons reside in the kidney cortex, with their glomeruli located in the outer two-thirds; about 15% of the nephrons are juxtamedullary, with glomeruli in the corticomedullary junction; and no glomeruli are found in the kidney medulla. In cortical nephrons, the loops of Henle penetrate only a short distance into the medulla and have thin descending and thick ascending limbs; in juxtamedullary nephrons, the loops of Henle are long, penetrate deep into the medulla, and return to the cortex.

Approximately 20% to 25% (about 1200 mL) of the cardiac output flows through the kidneys. About 20% of this amount is filtered by the glomeruli, producing a filtrate that is essentially identical to plasma minus the protein. Blood enters the nephron through the afferent arteriole, which branches off the interlobular artery, subsequently flows through the glomerular capillaries, exits the glomerulus through the efferent arteriole, and enters the peritubular capillaries that bathe the tubules. Blood then leaves the nephron through the cortical venule, which flows into the interlobular vein. About 85% of renal blood perfuses the cortex and bypasses the medulla, 10% perfuses the corticomedullary junction, 2% perfuses the medulla, and 3% flows through arteriovenous shunts that bypass the cortical glomerular and peritubular capillary systems and does not contribute to glomerular filtration or tubular secretion and reabsorption.

Renal Excretion Mechanisms

Renal elimination of drug substances from the blood and into urine involves the transport processes that typically occur across biologic membranes: passive diffusion, facilitated diffusion, and active transport. These processes are described in Chapter 13. Renal excretion mechanisms have been discussed in depth by Gottschalk and Nielsen.[2,3] In general, substances are removed from the blood by glomerular filtration and tubular secretion.

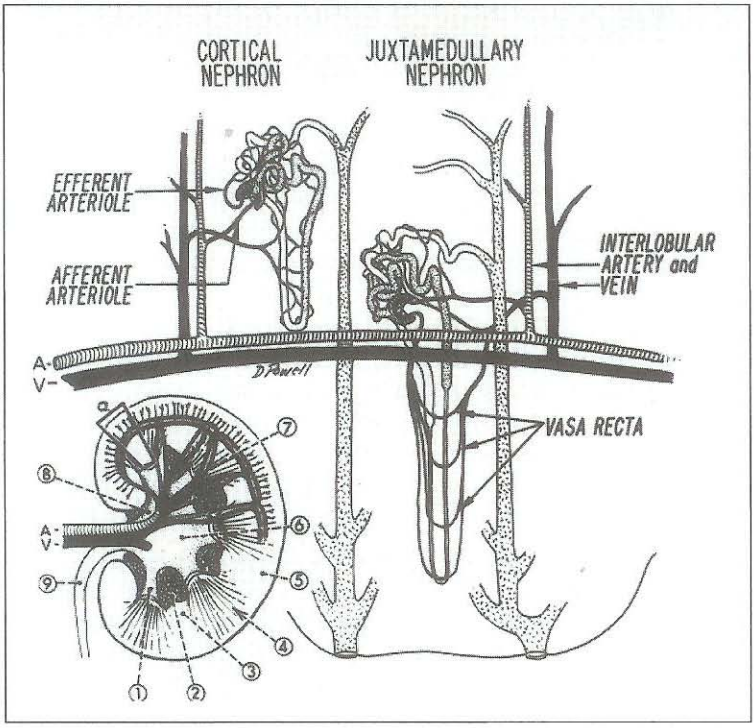

FIGURE 18-1 Diagram of the sagittal surface of a bisected kidney (lower left). Numbers 1 through 9 indicate the following: 1, minor calyx; 2, fat in sinus; 3, renal column of Bertin; 4, medullary ray; 5, cortex; 6, pelvis; 7, interlobar artery; 8, major calyx; and 9, ureter. The letter A indicates the renal artery, and the letter V indicates the renal vein. Insert (a) from the upper pole is enlarged to illustrate the relationships between the juxtamedullary and the cortical nephrons and the renal vasculature. (Reprinted with permission of Elsevier Science from reference 1.)

Reabsorption processes also occur in the tubule, where essential substances in the glomerular filtrate, such as glucose, electrolytes, and water, are reabsorbed into the blood.

A substance must satisfy two basic criteria to enter the glomerular filtrate: It must be non–protein bound and it must have a small molecular size. The glomerular capillaries are about 100-fold more permeable to water and salt than capillaries in general; however, substances with molecular weights greater than 50,000 are almost completely excluded from the glomerular filtrate. Non–protein-bound drugs with molecular weights less than 5000 are freely filterable.[4]

Any drug that enters the glomerular filtrate will be excreted in the urine if it is not reabsorbed into the blood. In general, un-ionized, lipid-soluble drugs are freely diffusible, whereas ionized, water-soluble species remain in the urine unless they are reabsorbed by a carrier-mediated transport process.[5] Therefore, substances used to assess the glomerular filtration rate (GFR) should possess strong polar properties that favor urinary excretion, as opposed to nonpolar properties that favor passive tubular reabsorption.

The degree of ionization of a drug depends on its pKa and the urinary pH, in accordance with the Henderson-Hasselbalch equation. For drugs that are weak organic acids, this equation is expressed as follows:

$$\text{pH} = \text{pKa} + \log \frac{\text{ionized drug}}{\text{un-ionized drug}}$$

Consider, for example, a weak-acid drug with a pKa of 6. At a urinary pH of 5 it is 90% un-ionized, favoring passive tubular reabsorption, whereas at a urinary pH of 7 it is 90% ionized, favoring urinary excretion. Since most drugs are either weak acids or weak bases, their renal elimination is affected by the urine's pH.

Active tubular secretion is known to occur by at least two independent pathways involving either organic anions or cations. These pathways are utilized by endogenous compounds such as choline, creatinine, epinephrine, and dopamine and by drugs such as atropine, cimetidine, and morphine.[5,6] Of importance to nuclear medicine is the active tubular secretion of organic anions such as ^{131}I-*o*-iodohippurate (^{131}I-OIH) and ^{99m}Tc-mertiatide (^{99m}Tc-MAG3). Several compounds that are secreted by the anionic pathway fit a general structural requirement proposed by Despopoulos:[7] possession of a primary anionic binding site such as a carboxylic acid (CO_2^-) or a sulfonic acid (SO_3^-) group and a secondary site provided by a carboxyl oxygen or hydroxyl group.[8] A few compounds that meet these requirements include *p*-aminohippurate (PAH), hydroxybenzoates, fatty acids, penicillin, probenecid, salicylates, and the renal radiopharmaceuticals ^{131}I-OIH and ^{99m}Tc-MAG3.

Glomerular filtration of a drug requires that it be non–protein bound and freely distributed in plasma water, but elimination of a drug by active tubular secretion is less affected by protein binding, provided the binding is reversible.[5] If a drug exhibits reversible protein binding, all of the drug will be available for tubular transport because as free drug is removed from plasma by the tubular cells, bound drug dissociates rapidly into plasma water and becomes immediately available for elimination.

Renal Clearance

Extraction of a drug from blood by the kidney can be quantitated by measuring renal clearance of the drug, defined as the minimal volume of plasma required to supply the amount of drug excreted in the urine in a given period of time.[2] The clearance concept is applicable to all substances excreted in the urine and is expressed by the formula

$$Cl_x = \frac{U_x \cdot V}{P_x} \qquad (18\text{-}1)$$

where:
U_x = urine concentration of drug
P_x = plasma concentration of drug
V = urine volume per unit time
Cl_x = renal clearance in milliliters per unit time

Consider, for example, the clearance of Na^+. Given that V = 1 mL/minute, U_{Na} = 280 mEq/L, and P_{Na} = 140 mEq/L, the clearance of sodium (Cl_{Na}) is 2 mL/minute. In other words, an amount of sodium ion equal to that contained in 2 mL of plasma (0.28 mEq) is excreted into the urine each minute. Another way to describe clearance, therefore, is that it is the volume of plasma that has its amount of drug (Na^+ in this case) completely removed per unit time. The clearance volume is virtual, however, not real, and one should not infer that all of a drug (Na^+ in this case) is removed from each 2 mL of plasma passing through the kidney. On the contrary, only some of the sodium is removed from a much larger volume of plasma perfusing the kidney.

Drug clearance occurs by glomerular filtration, tubular secretion, or a combination of these processes. Reabsorptive processes work against clearance. If a drug is known to be cleared by only one particular process, such as glomerular filtration, then the drug can be

used to measure that function. Normal GFR is about 125 mL/minute per 1.73 m^2 in humans and represents about 20% of the renal plasma flow (RPF). The mean RPF is about 650 mL/minute. A small molecular weight substance that is not bound to plasma protein can enter the glomerular filtrate. If it is not metabolized, reabsorbed, or secreted by the tubule, it will remain in the urine with a clearance of 125 mL/minute. The polysaccharide inulin best satisfies these requirements and is the standard substance used to measure GFR. Thus, during steady-state intravenous infusion of inulin, when GFR is normal the amount of inulin contained in 125 mL of plasma will appear in the urine each minute as a result of glomerular filtration. A disease process that affects glomerular function will change the inulin clearance. Hence, inulin clearance can be used to assess kidney function in a variety of conditions.

Although the clearance of a drug does not delineate a specific mechanism involved in its renal excretion, some idea of the processes involved can be gained. For example, if a freely filterable drug has a clearance less than the GFR, then it must undergo some degree of tubular reabsorption. Glucose is such a substance, being completely reabsorbed by the tubule. Its clearance, therefore, in the normal individual is zero. On the other hand, if a substance has a clearance greater than the GFR, it must undergo tubular secretion as well. PAH is an example of such a substance because its renal clearance is nearly equal to the RPF.

Extraction Efficiency

Renal clearance provides information only about the amount of drug removed from the blood that appears in the urine. It is not applicable to substances that are stored, synthesized, or metabolized by the kidney.[9] On the other hand, the extraction efficiency or extraction ratio (ER) is a measure of the amounts of drug eliminated into the urine and retained by the kidney. ER is defined by Smith[10] as the fraction of a substance removed from plasma during one circulation through the kidney. It is expressed as follows:

$$ER = \frac{A - V}{A} \tag{18-2}$$

where:
A = the renal arterial concentration of a substance
V = the renal venous concentration of a substance

Consider, for example, a drug that has an ER of 1.0. It will be completely removed in a single pass through the kidney. If none of the drug appears in the urine, then all of it is retained by the kidney. A radiopharmaceutical with this property would be an ideal renal imaging agent because all of the injected activity would end up being bound in the kidney. No radiopharmaceutical comes close to having these properties, but ^{99m}Tc-succimer (^{99m}Tc-DMSA) has a significant amount of the injected dose retained in the kidney. On the other hand, if all of the drug appears in the urine, none is retained in the kidney and its clearance is equal to the RPF (650 mL/minute). A radiopharmaceutical with this property would be an ideal agent for measuring renal plasma flow and tubular function, because most of the activity entering the urine would occur by tubular secretion. Two radiopharmaceuticals that closely approximate these properties are ^{131}I-OIH and ^{99m}Tc-MAG3.

If a drug has an ER of 0.2 and none of it is bound, secreted, or reabsorbed, it will have a clearance of 125 mL/minute, making it a good GFR agent. ^{125}I-iothalamate and ^{99m}Tc-pentetate (^{99m}Tc-DTPA) are radiopharmaceuticals that have essentially these properties,

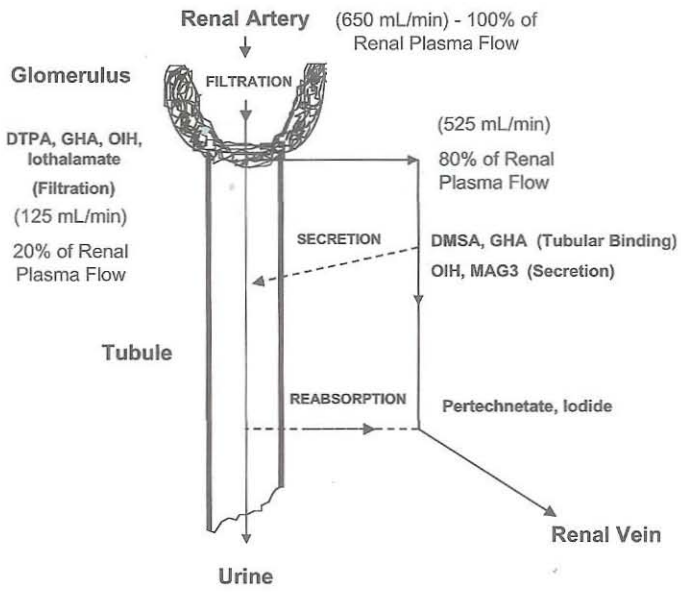

FIGURE 18-2 Schematic of the nephron, demonstrating the sites of radiopharmaceutical processing in the kidney.

TABLE 18-1 Ideal Properties of Renal Radiopharmaceuticals

Extraction Ratio	Clearance (mL/min)	Significance
1.0	0	All bound in kidney (good renal imaging agent)
1.0	650	None bound in kidney (good renal function agent)
0.2	125	None bound, secreted, or reabsorbed (good GFR agent)

and they both are used to quantitate GFR. Figure 18-2 and Table 18-1 summarize these concepts.

In renal physiology, the clearance of PAH (Cl_{PAH}) is used to estimate the renal plasma flow. However, its clearance is not equal to the renal plasma flow, because its ER (E_{PAH}) is about 0.92. Therefore, the clearance of PAH measures only the effective renal plasma flow (ERPF).[10] The ERPF of PAH in humans averages 600 mL/minute. RPF can be determined from the clearance and extraction ratio of PAH by the following relationship:

$$RPF = \frac{Cl_{PAH}}{E_{PAH}} = \frac{600\,mL/min}{0.92} = 650\,mL/min$$

Renal blood flow (RBF) can be determined from RPF and the hematocrit by the relationship RPF/(1 – hematocrit).[10] Hence, an average individual with a hematocrit of 45% would have RBF of approximately 1200 mL/minute.

The reasons for incomplete extraction of PAH have been examined. Wesson[11] lists several possible causes: (1) parenchymal bypass, in which a small amount of blood that enters the renal vein does not pass through the tubules; (2) red blood cell transport, in which drug that enters red blood cells does not readily diffuse out during blood transit through the cortical tubules; (3) incomplete cortical extraction due to incomplete drug

dissociation from plasma protein; and (4) unavailability of drug from blood that passes through the medulla.

OIH also exhibits renal extraction of less than 100% for reasons similar to those given for PAH. Because of free iodide present in OIH, which undergoes tubular reabsorption, clearance of OIH is less than clearance of PAH. OIH, however, offers the advantage of external detection for imaging and quantitation, which is not possible with PAH. OIH has been used to measure ERPF after pharmacokinetic analysis of its plasma disappearance over time.

Drug Elimination

The renal clearance tells us the amount of drug that is excreted in the urine per unit time, but it tells us nothing about the fraction of total drug that is eliminated by the kidney. For this we need to know the drug's volume of distribution (V).[5] Consider, for example, a hypothetical class of drugs that are eliminated solely by renal excretion. After an intravenous bolus injection of a dose (I_0), the rate of change in plasma concentration with respect to time (dC/dt) is given by the equation

$$\frac{dC}{dt} = k \cdot C \tag{18-3}$$

where k is the elimination rate constant determined by the ratio of clearance to apparent volume of distribution:

$$k = \frac{Cl_R}{V} \tag{18-4}$$

The plasma concentration of drug immediately after injection (C_0) is

$$C_0 = \frac{I_0}{V} \tag{18-5}$$

Integration of Equation 18-3 yields

$$C = C_0 e^{-kt} \text{ or } C = \frac{I_0}{V} e^{-kt} \tag{18-6}$$

This relationship between plasma concentration and time can be linearized by taking the natural logarithm of both sides of the equation:

$$\ln C = \ln C_0 - k \cdot t \tag{18-7}$$

The clearance of a drug (Cl_R) is the product of renal extraction efficiency (ER) and renal plasma flow (Q_p):

$$Cl_R = Q_p \cdot ER \tag{18-8}$$

This set of equations forms the basis for determining a drug's elimination rate and the influence that clearance and volume of distribution have on the rate.

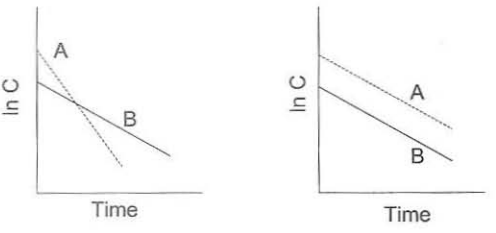

FIGURE 18-3 Plasma elimination rates for two hypothetical drugs, A and B, eliminated entirely by renal excretion and administered in equimolar doses. Left: Drugs A and B have identical renal extraction efficiencies (identical clearances) but drug A has a smaller volume of distribution than B. The elimination rate of drug A is higher because its initial plasma concentration is higher because of a smaller volume of distribution. Right: Drug A has a lower extraction efficiency than drug B (i.e., lower clearance) and the ratio of extraction efficiencies (B to A) is equal to the ratio of the distribution volumes (B to A). Drug A is now eliminated at the same rate as drug B. Even though the extraction of drug A is less than for drug B, its plasma concentration is higher (because of a smaller distribution volume), which compensates for its lower clearance.

Consider, for example, two hypothetical drugs, A and B, that are excreted entirely in the urine. V is smaller for drug A than for drug B, but the extraction efficiencies of the two drugs are identical (i.e., renal clearance is identical). If equimolar doses of the two drugs are administered, Equation 18-5 predicts that the initial concentration of A will exceed that of B. On the other hand, Equations 18-4 and 18-7 predict that the plasma concentration of A will decline more rapidly than that of B. The result of this situation is shown on the left in Figure 18-3. Now, consider a case in which the extraction efficiency (and renal clearance) of A is decreased (e.g., because of high plasma protein binding) such that the ratio of extraction efficiencies (B to A) is equal to the ratio of distribution volumes (B to A). Equations 18-4 and 18-7 then predict that the plasma concentration of A will decline at the same rate as the plasma concentration of B. The result of this situation is shown on the right in Figure 18-3. Thus, it can be shown that the rate of decline in plasma concentration (slope of k) is determined by both the volume of distribution and the clearance.

These concepts, particularly the second hypothetical situation described, explain why the elimination rates of ^{131}I-OIH and ^{99m}Tc-MAG3 are similar even though their biologic properties are different. A comparison of these agents is made later in the chapter.

Often, elimination rates are discussed in terms of a drug's half-life. Substituting $0.693/T_{½}$ for k and rearranging Equation 18-4 yields

$$T_{½} = \frac{0.693 \cdot V}{\text{Cl}} \tag{18-9}$$

This relationship demonstrates that as the volume of distribution of a drug increases, its half-life of elimination increases proportionately (i.e., its excretion rate declines). Goldstein et al.[5] have shown that, theoretically, if a drug is distributed only in plasma water (V = 3 L) and is completely cleared per pass through the kidney (ER = 1.0, Cl = 650 mL/minute), its plasma elimination half-life would be 3 minutes. If its distribution were in extracellular fluid (V = 12 L) or the total body water (V = 41 L), its half-life would be 13 minutes or 44 minutes, respectively. Hence, any radiotracer distributed only in plasma water and having a high renal extraction will be cleared most rapidly from the bloodstream.

DEVELOPMENT OF KIDNEY IMAGING AGENTS

A large number of radiopharmaceuticals have been investigated for renal imaging studies. The chemical structures and properties of the agents routinely used in renal scintigraphy

are described in Chapter 9. Several review articles have compared renal imaging agents.[6,8,12–14]

The radioisotope renogram was introduced by Taplin et al.[15] in 1956 in response to the need for a method of evaluating unilateral kidney disease in a noninvasive manner. The original method used a two-channel detection system, each kidney having its own scintillation detector connected to a rate meter and recorder. After intravenous injection of an agent cleared primarily by tubular secretion, time–activity curves were recorded over each kidney. The first agent used was ^{131}I-iodopyracet. Its main drawback was liver uptake, which interfered with right kidney evaluation. PAH was a good agent to use for physiologic reasons, but no satisfactory method could be developed to label it with a suitable gamma-emitting nuclide. However, attempts to label PAH led to the development of ^{131}I-OIH (hippuran) in 1960 by Tubis et al.[16] OIH is structurally similar to PAH but can be labeled with radioiodine. It is eliminated primarily by tubular secretion, and for over 30 years it was the agent of choice for assessing renal function. OIH is not bound in the kidney, however, and therefore cannot be used as a renal imaging agent.

The lack of an agent that would remain fixed in the kidney for imaging space-occupying lesions led to the development of ^{203}Hg-chlormerodrin. This mercury compound was bound 5% to 10% to sulfhydryl-containing proteins in tubular cells, with an effective half-life of 28 days.[17] It permitted visualization of kidney morphology and the detection of lesions, which appeared as focal areas of decreased activity. The high radiation dose from the beta-emitting ^{203}Hg nuclide (117 rad/mCi), however, prompted its replacement with ^{197}Hg, which decays by electron capture and had a radiation dose of only 6 rad/mCi. However, its low-energy photons (77 keV) yielded scans with lower resolution than ^{203}Hg. These problems stimulated the pursuit of a ^{99m}Tc-labeled agent.

In 1966, Harper et al.[18] developed a ^{99m}Tc-iron ascorbate complex for renal imaging. This complex provided the advantages of ^{99m}Tc for imaging, namely the ability to administer large amounts of activity with improved sensitivity and resolution and low radiation dose. This agent was followed by several ^{99m}Tc-labeled complexes with diethylenetriaminepentaacetic acid (DTPA) with either iron-ascorbate or stannous ion as the reducing agent.[19,20] Comparison studies determined that the iron-reduced complexes did not behave biologically as true chelates and should not be used for GFR studies.[20] Stannous-reduced ^{99m}Tc-pentetate (^{99m}Tc-DTPA) became the agent of choice for GFR studies.

In 1973, ^{99m}Tc-gluceptate (^{99m}Tc-GH), a complex of technetium with glucoheptanoic acid, was developed at New England Nuclear Corporation, and ^{99m}Tc-DMSA was developed at Medi-Physics by Lin, Khentigen, and Winchell.[21] ^{99m}Tc-DMSA reaches high concentrations in the renal cortex, making it a good choice for imaging the renal parenchyma. Its clearance from blood into urine is slow, however, because of high plasma protein binding, making it a poor agent for evaluating the pelvocaliceal collecting system. ^{99m}Tc-GH is not so highly protein bound and has a faster renal clearance than ^{99m}Tc-DMSA, but the fraction bound in kidney is lower. Early images after injection of ^{99m}Tc-GH demonstrate the collecting system well, similar to ^{99m}Tc-DTPA, whereas later images show renal parenchyma alone, similar to ^{99m}Tc-DMSA.[13]

Inulin clearance is regarded as the standard for measuring GFR. Attempts to prepare radioactive inulin have been successful in that hydroxymethyl ^{14}C-inulin shows a high degree of correlation to standard inulin for GFR measurements. However, it requires liquid scintillation counting of the ^{14}C label. Attempts to prepare inulin with a suitable gamma emitter have not been successful.

In 1965 Sigman et al.[22] used ^{131}I-iothalamate to measure GFR. This agent was subsequently shown to have renal clearance identical to that of inulin.[23] Iothalamate labeled

with ^{125}I has remained the radioactive agent of choice for quantitative assessment of GFR over the years, although ^{99m}Tc-DTPA is also used for this purpose.

Several metal chelates of EDTA and DTPA have been investigated for GFR studies. Noteworthy are ^{51}Cr-EDTA, ^{111}In-DTPA, and ^{99m}Tc-DTPA. The ^{51}Cr complex is not ideal for imaging studies because of low photon abundance of its 320 keV gamma ray. ^{111}In-DTPA and ^{99m}Tc-DTPA have similar biologic properties in humans but are not identical.[24] The ^{111}In complex has a slightly faster total-body clearance. The slightly greater retention of ^{99m}Tc-DTPA in tissues probably represents ^{99m}Tc not chelated with DTPA. ^{99m}Tc-DTPA also slightly underestimates GFR (by a few percentage points); this is related to its small amount of protein binding. Corrections for this binding have made ^{99m}Tc-DTPA a useful agent for quantitative GFR measurements.

The first technetium complex designed to replace ^{131}I-OIH was ^{99m}Tc-N,N'-bis(mercaptoacetyl) ethylenediamine (^{99m}Tc-DADS).[25] While it demonstrated significant renal excretion, biodistribution studies in animals using renal transport inhibitors (probenecid and 2,4-dinitrophenol) demonstrated that the excretion of ^{99m}Tc-DADS was decreased more than that of ^{131}I-OIH, suggesting that ^{99m}Tc-DADS has a lower affinity for the renal transport proteins.[26] Studies also demonstrated hepatobiliary excretion with ^{99m}Tc-DADS in patients with increased creatinine levels.[27] A series of substituent modifications demonstrated that addition of a carboxylate group to the ethylenediamine backbone improved renal excretion.[6] This modification, however, created an asymmetric carbon atom and resulted in two chelate ring stereoisomers, ^{99m}Tc-CO_2-DADS-*A* and ^{99m}Tc-CO_2-DADS-*B*. The *A* isomer had renal excretion properties similar to those of ^{131}I-OIH, but the *B* isomer did not. Biodistribution studies demonstrated that, 30 minutes after intravenous injection, the renal excretion of ^{99m}Tc-CO_2-DADS-*A* isomer was 81% of ^{131}I-OIH, compared with 40% for ^{99m}Tc-DADS (mixed isomers). Although this was a significant improvement, the requirement for high-performance liquid chromatographic (HPLC) purification to separate the *A* and *B* isomers precluded development of an easily usable kit, which limited the potential usefulness of ^{99m}Tc-CO_2-DADS in the nuclear medicine clinic.

The development work with ^{99m}Tc-DADS demonstrated that a carboxylate group was necessary for high specificity of the renal tubular transport system. To prevent the formation of stereoisomers from substituents placed on the N_2S_2 backbone of DADS, the ligand was changed to N_3S or triamide monomercaptide. Changing the core donor ligand and placement of the carboxyl group on the third amido nitrogen produced a radiochemically pure product without an asymmetric carbon.[28] The simplest ligand having the necessary groups for renal excretion was mercaptoacetyltriglycine. The absence of stereoisomers permitted a kit formulation that could be easily used in the nuclear medicine clinic. See Chapter 9 for details on the chemistry of ^{99m}Tc-MAG3.

Animal and clinical studies with ^{99m}Tc-MAG3 have shown its renal excretion profile to be essentially identical to that of ^{131}I-OIH. Because of its biologic properties and technetium label, ^{99m}Tc-MAG3 has replaced ^{131}I-OIH as the renal function agent of choice in routine nuclear medicine studies.

BIOLOGIC PROPERTIES OF RENAL RADIOPHARMACEUTICALS

Radiopharmaceuticals for renal studies belong to two principal groups: (1) renal clearance agents, which can be subdivided into GFR agents and tubular function agents; and (2) renal imaging agents, which are used to assess renal morphology and relative function. Agents currently used in nuclear medicine are listed in Table 18-2.

TABLE 18-2 Renal Radiopharmaceuticals

Renal Clearance Agents
1. GFR[a] agents
   a. ^{125}I-iothalamate
   b. ^{99m}Tc-pentetate (^{99m}Tc-DTPA)
2. ERPF[b] agents
   a. ^{131}I-o-iodohippurate (^{131}I-OIH)
   b. ^{99m}Tc-mertiatide (^{99m}Tc-MAG3)

Renal Imaging Agents
1. ^{99m}Tc-gluceptate (^{99m}Tc-GH)
2. ^{99m}Tc-succimer (^{99m}Tc-DMSA)

[a] Glomerular filtration rate.
[b] Effective renal plasma flow.

Technetium Tc 99m Pentetate Injection

Technetium Tc 99m pentetate injection (^{99m}Tc-DTPA) is a complex of Tc(IV) with diethylenetriaminepentaacetic acid (DTPA). ^{99m}Tc-DTPA was originally developed because its route of excretion offered potential for renal imaging studies. After intravenous injection, ^{99m}Tc-DTPA distributes into the extracellular space. Because it has low plasma protein binding (around 5%) and has no significant binding to red blood cells, renal excretion of ^{99m}Tc-DTPA is rapid, with 50% of the dose appearing in the urine 2 hours after injection and 96% excreted by 24 hours.[13,24] The complex is quite stable and is excreted unchanged in the urine. It is excreted by glomerular filtration, is not secreted or reabsorbed by the kidney tubule, and has no appreciable binding to the renal parenchyma. ^{99m}Tc-DTPA is useful in evaluating gross blood flow to the kidneys and in visualizing obstructions to urine flow in the collecting system and ureters because its renal distribution is restricted to the renal vascular space initially and the tubular urine thereafter. In this regard, ^{99m}Tc-DTPA has principal application in the assessment of renal perfusion, relative kidney function, and obstructive uropathy.

The renal clearance of ^{99m}Tc-DTPA is approximately 20% of renal plasma flow (i.e., 125 mL/minute), making it useful for the quantitative assessment of GFR.[29–34] Methods that measure GFR by plasma clearance of ^{99m}Tc-DTPA are reliable when GFR is greater than 30 mL/minute.[33] The method used should employ a correction for plasma protein binding of ^{99m}Tc-DTPA.[30,31] While most methods are relatively simple in principle, they require careful attention to technique. Additionally, it is important to report GFR values that are normalized to body surface area of 1.73 m^2.[34]

Technetium Tc 99m Succimer Injection

Technetium Tc-99m succimer injection (^{99m}Tc-DMSA) is a complex of Tc(III) with 2,3-dimercaptosuccinic acid (DMSA). Several ^{99m}Tc-DMSA complexes can be formed, depending on the labeling conditions.[35,36] Complex I is formed with an acid pH of 2.5, a DMSA:Sn ratio of 3, and the absence of oxygen. It reverts to complex II within 10 minutes of incubation. Complex II is the agent that localizes in the renal cortex. If ^{99m}Tc-DMSA is prepared at a higher pH, renal cortical concentration decreases.[37] Unstabilized preparations of ^{99m}Tc-DMSA are useful for 30 minutes, while the product prepared from a stabilized kit is useful for 4 hours. See Chapter 9 for details on chemistry and preparation.

After intravenous injection in humans, ^{99m}Tc-DMSA becomes loosely bound to plasma protein (75% at 1 hour after injection, increasing to 90% by 24 hours), with little or no

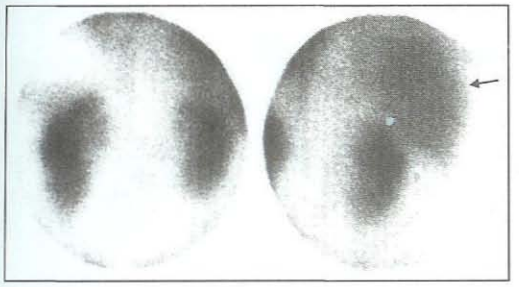

FIGURE 18-4 Renal scan with ^{99m}Tc-succimer (^{99m}Tc-DMSA), demonstrating liver uptake (arrow) secondary to renal failure.

diffusion into red blood cells.[13,38] Renal excretion is slow, with only 16% of the dose in urine 2 hours after injection. The tracer accumulates slowly in the renal cortex, where it becomes fixed, primarily in the cells of the proximal convoluted tubule.[21,39] Kidney micropuncture studies demonstrate that its mechanism of localization is via extraction from peritubular blood and fixation within the cortical cells.[40,41] Evidence suggests that this occurs by an active process that is not inhibited by probenecid; thus, ^{99m}Tc-DMSA apparently localizes by a transport system different from that of other tubular agents (e.g., ^{131}I-OIH and ^{99m}Tc-MAG3).[41,42] Although a small amount of non–protein-bound ^{99m}Tc-DMSA is filtered, this fraction is not believed to be reabsorbed.[40] Subcellular localization within cortical cells has been reported to be primarily within cytosol proteins[43] and microsomes.[44] In rats with acidic urine[42] and patients with proximal tubular acidosis,[45] renal uptake of ^{99m}Tc-DMSA declines significantly.

A maximum of about 40% of an injected dose of 5 mCi (185 MBq) is eventually bound in the two kidneys 6 hours after injection.[13] Since the uptake half-life for renal accumulation of ^{99m}Tc-DMSA is 1 hour, imaging is best performed 4 to 5 hours after injection, but it can be done as early as 2 hours. The high degree of protein binding limits the amount of activity that is filtered, precluding visualization of the collecting system. The low urinary excretion and high cortical binding of ^{99m}Tc-DMSA make it an excellent agent for detecting focal abnormalities in the renal cortex, and it is useful for assessing relative function between right and left kidney. Normal distribution in the kidney demonstrates high uptake of activity within the cortical regions. Extension of the relatively active cortical columns of Bertin into the colder regions of the medulla gives the kidneys a unique pattern of hot/cold activity distribution that must be appreciated in reading DMSA scans. Lesions such as tumors and cysts appear as cold areas within an otherwise hot kidney. An alternative route of elimination for ^{99m}Tc-DMSA is the hepatobiliary system, which can be visualized in renal failure patients studied with this agent (Figure 18-4).

Technetium Tc 99m Gluceptate Injection

Technetium Tc-99m gluceptate injection (^{99m}Tc-GH) is a complex of Tc(V) and the complexing agent glucoheptonic acid. Its chemical structure and method of preparation are discussed in Chapter 9.

After intravenous injection, ^{99m}Tc-GH distributes into the extracellular space. It is loosely bound to plasma protein (50% to 75% 1 to 6 hours after injection) with no significant binding to red blood cells.[13] Renal excretion is rapid, with 50% of the dose in urine 2 hours after injection and 71% excreted by 24 hours. Its renal mechanism is glomerular filtration and tubular secretion.[46] Soon after injection, the renal distribution of ^{99m}Tc-GH resembles that of ^{99m}Tc-DTPA, being limited to the vascular space initially, followed by a significant amount of activity accumulating in the collecting system. In later images, ^{99m}Tc-GH differs from ^{99m}Tc-DTPA in that about 12% of the injected dose is retained in the cortex because

of tubular binding.[13] Thus, ^{99m}Tc-GH has the versatility of visualizing the collecting system early after injection, similar to ^{99m}Tc-DTPA, and the renal parenchyma at later times, similar to ^{99m}Tc-DMSA. Compared with ^{99m}Tc-DMSA, however, a smaller fraction of the injected dose of ^{99m}Tc-GH localizes in the kidney, and thus its 10 to 15 mCi (370 to 555 MBq) dosage is proportionately larger. Clinically, therefore, ^{99m}Tc-GH is useful for evaluating renal perfusion, obstructive uropathy, relative kidney function, and renal masses. An alternative route of elimination for ^{99m}Tc-GH is via the hepatobiliary system, but this is not typically seen except in patients with severe renal insufficiency (Figure 18-5).

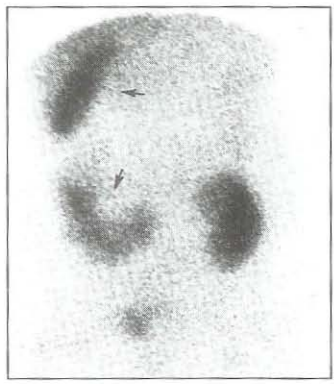

FIGURE 18-5 Hepatobiliary excretion (arrows) of ^{99m}Tc-gluceptate (^{99m}Tc-GH) in a renal transplant patient.

Technetium Tc 99m Mertiatide Injection

Technetium Tc-99m mertiatide injection (^{99m}Tc-MAG3) is a complex of Tc(V) and mercaptoacetyltriglycine.[28,47] Its chemical structure and a detailed method of preparation are discussed in Chapter 9. The primary advantage of ^{99m}Tc-MAG3 is that it exhibits the rapid excretion of ^{131}I-OIH but has the more desirable imaging properties of ^{99m}Tc.

After intravenous injection, approximately 90% of ^{99m}Tc-MAG3 is bound to plasma protein.[14,48,49] The high degree of protein binding restricts the amount that is filtered at the glomerulus, but the binding is reversible because rapid renal excretion of the radiotracer occurs via tubular secretion. Plasma disappearance curves of ^{99m}Tc-MAG3 and ^{131}I-OIH demonstrate that ^{99m}Tc-MAG3 plasma concentrations are around 1.5 times higher than those of ^{131}I-OIH; however, both agents exhibit similar rates of loss from the blood over time and therefore have the same elimination half-lives.[49] The mean plasma clearance of ^{99m}Tc-MAG3 in human subjects is 55% to 65% that of ^{131}I-OIH, but its urinary excretion profile is identical.[14] Accordingly, about 70% of the dose appears in urine 30 minutes after injection and greater than 90% by 180 minutes. Although ^{99m}Tc-MAG3's clearance is less than that of ^{131}I-OIH because of a lower extraction efficiency, its plasma concentration is higher because of a smaller volume of distribution.[49] The lower clearance is balanced by the smaller volume of distribution (Equation 18-4), giving ^{99m}Tc-MAG3 an elimination rate equal to that of ^{131}I-OIH.[48,49]

The renogram curves for ^{99m}Tc-MAG3 and ^{131}I-OIH are similar, with a mean time to peak of 3 to 5 minutes for both agents.[50] The tracer is not bound by the kidney, nor does it have significant red blood cell uptake. Properties of ^{131}I-OIH and ^{99m}Tc-MAG3 are listed in Table 18-3, and properties of all renal imaging radiopharmaceuticals are summarized in Table 18-4.

Because of its mechanism of excretion, ^{99m}Tc-MAG3 is an excellent agent for visualizing the renal collecting system, evaluating urinary obstruction, and assessing renal tubular function. Studies have shown that, in general, ^{99m}Tc-MAG3 clearance is proportional to that of ^{131}I-OIH but that some disproportionate differences occur clinically.[14,49] Thus, it has been suggested that clearances of the two agents should be reported directly and not be related to each other by a conversion factor when these agents are used to quantitate ERPF.[14] Although the renogram curves of the two agents are similar, superior image quality and anatomic detail are achieved with ^{99m}Tc-MAG3 because of its ^{99m}Tc label. In the past, renal perfusion in kidney transplants was evaluated with a combination of ^{99m}Tc-DTPA for RBF and ^{131}I-OIH for tubular function. The use of ^{99m}Tc-MAG3 allows both determinations to be made with one agent, simplifying the procedure and improving overall image

TABLE 18-3 Properties of ^{99m}Tc-MAG3 and ^{131}I-OIH

Property	^{99m}Tc-MAG3	^{131}I-OIH	^{99m}Tc-MAG3/^{131}I-OIH Ratio	Ref
Plasma protein binding (%)	87.5 ± 2.6	66.2 ± 6.9	1.32	46
	90.1 ± 2.8	70.7 ± 5.0	1.27	47
RBC uptake (%)	5.1 ± 3.3	15.3 ± 4.1	0.33	47
Tubular extraction coefficient[a]	0.55	0.83	0.66	47
Plasma clearance, Cl (mL/min)	420 ± 120	600 ± 100	0.70	46
	265 ± 98	412 ± 169	0.64	47
Volume of distribution, V (mL)	5210	7030	0.74	46
	3380	5540	0.62	47
Elimination rate, k (min^{-1})	0.0806	0.0853	0.94	46
	0.0784	0.0744	1.05	47

[a] Fraction of drug extracted as a function of its clearance and protein binding.

TABLE 18-4 Biologic Properties of Renal Imaging Radiopharmaceuticals

Property	^{99m}Tc-DTPA	^{99m}Tc-GH	^{99m}Tc-DMSA	^{99m}Tc-MAG3	^{131}I-OIH
Glomerular filtration	Yes	Yes	Not significant[a]	Not significant[a]	Yes
Tubular transport	No	Yes (cortical binding)	Yes (cortical binding)	Yes (secretion)	Yes (secretion)
Tubular reabsorption	No	No	No	No	No
Collecting system	Yes	Yes	No	Yes	Yes
Cortical binding	No	Yes (~15% ID[b])	Yes (~45% ID[b])	No	No
Dosage	10 mCi (blood flow) 3 mCi (renogram)	10 mCi (blood flow) 15 mCi (static)	5 mCi (static)	5 mCi (blood flow) 1–3 mCi (renogram)	75 μCi (1 kidney) 200 μCi (2 kidneys) (renogram)
Critical organ	Bladder wall	Bladder wall	Kidney cortex	Bladder wall	Bladder wall
Rad(cGy)/mCi (4.8 hr void)	0.27	0.28	0.85	0.48	5.71

[a] 85% to 90% plasma protein binding.

[b] Injected dose.

quality. The relatively high renal extraction of ^{99m}Tc-MAG3 (around 50%) compared with ^{99m}Tc-DTPA (around 20%) provides superior images in patients with impaired renal function.

Iothalamate Sodium I 125 Injection

Iothalamate sodium I 125 injection (^{125}I-iothalamate; Glofil-125, Cypros Pharmaceutical) has been used for many years as a diagnostic agent for measuring GFR. Its renal clearance closely approximates that of inulin, and ^{125}I-iothalamate is cleared by glomerular filtration without tubular reabsorption or secretion. ^{125}I-iothalamate is not a renal imaging agent, because ^{125}I photons (27 to 35 keV) are almost entirely absorbed by the tissues.

Iodohippurate Sodium I 131 Injection

After intravenous administration, iodohippurate sodium I 131 injection (^{131}I-OIH) rapidly disappears from the blood by diffusion into the extracellular space and through renal

elimination. It is not metabolized in the body and is excreted unchanged in the urine.[51] It is not bound to renal tubular cells.[9] In the normal hydrated subject, 70% of a single dose of ^{131}I-OIH is excreted in the urine 30 minutes after injection.[52]

Renal excretion of ^{131}I-OIH is primarily by active tubular secretion, although a significant amount of glomerular filtration also occurs. The exact fraction of injected activity excreted by each process is not well defined. Theoretically, 20% should be filtered and 80% secreted if the drug was not protein bound and had 100% renal extraction. Approximately 70% of ^{131}I-OIH is protein bound in plasma.[49] The overall renal extraction efficiency is less than 100%; it varies between 65% and 85%.[9] The wide range of reported values depends on the conditions of measurement and several intrinsic factors, such as binding to blood components, the presence of radioiodide or other impurities in the injected dose, and reabsorption by the tubule.[9]

In addition to plasma protein binding, OIH also exhibits some degree of red blood cell binding, and these factors reduce the amount extracted by the kidney.[10,49,53] Additionally, any free radioiodide present in the injected dose will be filtered and undergo reabsorption, thereby reducing clearance. As a consequence of such factors, the clearance of OIH underestimates the renal plasma flow and, as with PAH, measures only ERPF. A comparison of OIH-to-PAH clearance ratios demonstrated that the ratio varies inversely with free radioiodide in OIH preparations, ranging from 0.91 with less than 2% iodide to 0.80 with greater than 5% iodide.[51] When radioiodide impurity is high, the rate of blood clearance and urinary accumulation of radioactivity decreases substantially and produces renogram curves with flattened peaks of diminished height followed by a slowed excretory segment.[54]

^{131}I-OIH has been used to measure ERPF. The method has been simplified from a multiple blood sampling procedure to one requiring only one or two blood samples.[33,34,52] Nevertheless, the procedure demands attention to technique. Technical errors, such as inaccuracy in dose preparation, incomplete injection of the dose, inattention to the plasma sampling time, and inaccurate sample dilutions, must be avoided.[55]

A simpler study for routine assessment of renal function is the renogram. This procedure has been performed for over 30 years with ^{131}I-OIH, but it is now done primarily with ^{99m}Tc-MAG3. The parameters associated with the renogram and the measurement of GFR and ERPF are discussed below.

Technetium Tc 99m Ethylenedicysteine Injection

Technetium-99m ethylendicysteine injection (^{99m}Tc-EC) is the diacid metabolite of the deesterification of ^{99m}Tc-ethylenecysteinate dimer (^{99m}Tc-EC). When compared with ^{99m}Tc-MAG3 in human volunteers, ^{99m}Tc-EC demonstrates 31% protein binding (two-thirds less than ^{99m}Tc-MAG3), 25% higher plasma clearance, and a larger volume of distribution. Renogram curves are similar, but ^{99m}Tc-EC has a slightly higher kidney-to-background ratio.[56,57] At present ^{99m}Tc-EC is not approved by the Food and Drug Administration for renal imaging. The chemistry of ^{99m}Tc-EC is described in Chapter 9.

THE RENOGRAM

The renogram measures the time course of activity of a renal clearance agent passing through the kidney. A plot of kidney activity versus time after intravenous injection of the radiopharmaceutical yields a renogram curve (Figure 18-6). Both kidneys can be imaged simultaneously with the gamma camera and the activity in each kidney analyzed. The renogram procedure provided the first method of evaluating individual kidney function noninvasively.

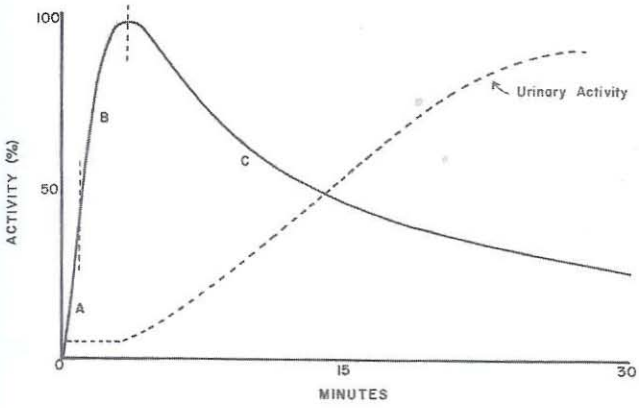

FIGURE 18-6 Normal renogram curve. See text for explanation.

Immediately after intravenous injection, ^{131}I-OIH is confined to three spaces: the blood, the extracellular space, and the kidney. ^{99m}Tc-MAG3's distribution is similar, but less activity enters the extracellular space because of its higher plasma protein binding. The initial spike of activity recorded in the renogram curve (part A in Figure 18-6) occurs during the first 30 to 60 seconds after injection and represents the simultaneous detection of radioactivity in the blood, extracellular space, and kidney. Part B of the renogram curve represents transport of radiotracer through the renal parenchyma. It is an extension of the initial spike, which continues to rise as activity is extracted from the blood into the kidney. During these two portions of the curve, no radioactivity above tissue background is detectable in the urinary bladder. In the normal hydrated subject, peak renal activity is reached 3 to 5 minutes after injection, just before the initial appearance of bladder activity. The time to peak reflects both the average linear rate of movement through the tubular system and the patency of the renal pelvis.[58] A prolonged time to peak is seen in various conditions, including low RBF states (e.g., dehydration, renal artery stenosis), parenchymal damage (e.g., interstitial nephritis or tubular necrosis), or urinary tract obstruction. The decline of the renogram curve, represented by part C in Figure 18-6, correlates temporally with an abrupt rise in bladder radioactivity as radiotracer leaves the kidney. The curve continues to fall because the amount of radioactivity leaving the kidney region is greater than that being extracted from the blood.

The time from peak curve amplitude to half this value on the falling segment of the curve in normal subjects is in the range of 12 to 15 minutes. Half-life is prolonged in renal disease and measures the same physiologic events as the time to peak, but it is less dependent on the injection technique.[58]

The ^{131}I-OIH renogram is a complex representation of multiple physiologic phenomena and, as such, is best used as a unique parameter of renal function. Relative functional differences between kidneys or within comparable segments are more easily evaluated than marginal changes in overall function. If the physiologic state is comparable, serial studies can be used to evaluate the relative overall renal function while monitoring temporal changes. Figure 18-7 illustrates several renogram curves demonstrating these temporal changes.

Since the introduction of ^{99m}Tc-MAG3, the use of ^{131}I-OIH in nuclear medicine has essentially stopped. The parameters of ^{99m}Tc-MAG3 renograms are the same as those of ^{131}I-OIH renograms. A principal advantage of ^{99m}Tc-MAG3 over ^{131}I-OIH is that the quality of kidney images is superior because of the ^{99m}Tc label. ^{99m}Tc-MAG3 is superior to ^{99m}Tc-DTPA for renograms because its higher renal extraction provides higher target-to-background ratios on kidney images, which is especially important with decreasing renal function.

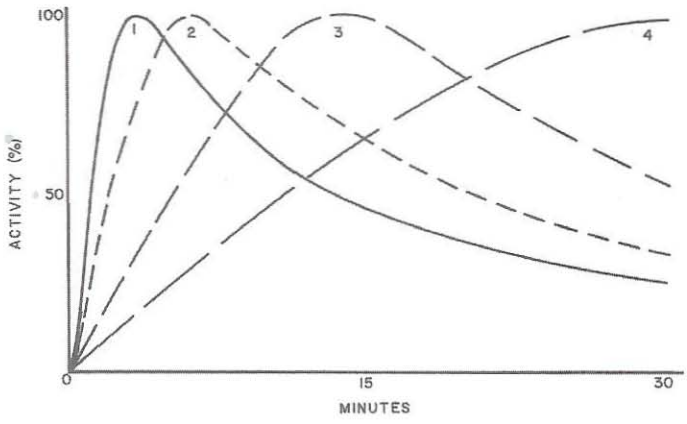

FIGURE 18-7 Normal renogram curve (1) and curves depicting progressive kidney deterioration (2, 3, and 4).

Interventional Renograms

The utility of renograms to assess kidney function can be extended further with the use of pharmacologic agents. Two such studies are the diuretic renogram and the captopril renogram.

Diuretic Renogram

The diuretic renogram is a useful test for investigating dilatation of the urinary tract.[59,60] Dilatation refers to any increase in the size of the renal calices, pelvis, or ureter detected by intravenous urography or ultrasound. These modalities detect the dilatation but cannot determine whether it is caused by an obstruction; the diuretic renogram can help determine this.

In the past the diuretic renogram was performed with ^{99m}Tc-DTPA. However, better images and easier interpretation are achieved with ^{99m}Tc-MAG3 because of its higher renal extraction. The patient should be well hydrated prior to the study. A 500 mL drink of water or orange juice 15 to 30 minutes before the study is recommended. The diuretic renogram is performed in two phases.[59] The first phase is a standard renogram, obtained for 20 minutes after intravenous injection of ^{99m}Tc-MAG3 (2 to 3 mCi [74 to 111 MBq] in adults; the pediatric dose is based on body surface area but is not less than 10% of the adult dose). The renal image in the first phase will demonstrate pooled activity in the dilated collecting system. Furosemide (1 mg/kg in infants, 0.5 mg/kg in children age 1 year to 16 years, and 40 mg in adults) is then given intravenously 20 minutes after the ^{99m}Tc-MAG3 dose. The furosemide stimulates tubular function and increases urine flow. Peak diuretic response occurs in 10 to 15 minutes. A prompt washout of pooled renal activity indicates no obstruction (Figure 18-8). Lack of washout or continued accumulation of activity strongly suggests the presence of obstruction. In patients without obstruction but with low GFR (<15 mL/minute), a false-positive study (poor diuretic response) is likely. These patients may require additional interventions.[59,60]

Captopril Renogram

Renovascular hypertension (RVH) is defined as an elevation in blood pressure caused by stenosis of the renal artery or one of its major branches.[61] Because the hypertension can be cured or ameliorated by a revascularization procedure, a noninvasive diagnostic technique such as the captopril renogram plays an important role in defining its presence in

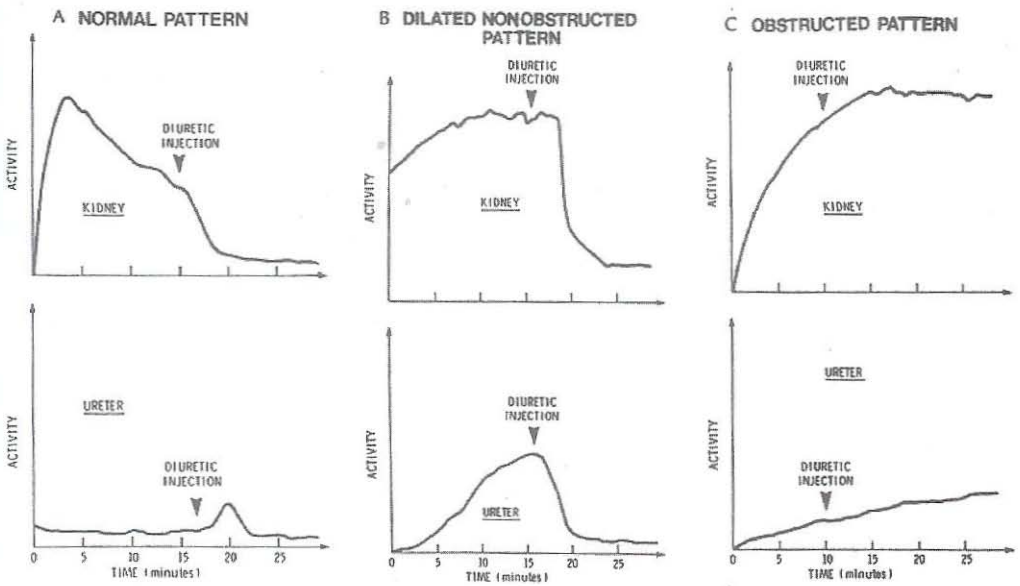

FIGURE 18-8 Representative furosemide renograms showing time–activity curves in a normal patient (A) and in patients with dilated nonobstruction (B) and obstruction (C) of the urinary collecting system. (Reprinted with permission of Elsevier Science from Thrall JH, Koff SA, Keyes JW Jr. Diuretic radionuclide renography and scintigraphy in the differential diagnosis of hydroureteronephrosis. *Semin Nucl Med.* 1981;11:89-104.)

patients with moderate to high risk of RVH. The test helps define which patients should have angiography.

The effect of captopril on split renal function in patients with unilateral renal artery stenosis was reported by Wenting et al.[62] in 1984. In 7 of 14 patients, 50 mg of captopril significantly reduced the renal extraction ratios of ^{131}I-OIH and ^{125}I-iothalamate in the affected kidney, and uptake of ^{99m}Tc-DTPA was almost zero, indicating a severe reduction in GFR. Captopril had little effect on the contralateral normal kidney. These findings eventually led to the use of captopril as an interventional pharmacologic agent in diagnostic nuclear medicine.

Under normal circumstances, GFR is proportional to the difference between the afferent and efferent arteriolar capillary pressures in each kidney. When renal artery stenosis is present in a kidney, such as occurs in RVH, a fall in renal arterial pressure stimulates the renin–angiotensin system. Renin, a polypeptide hormone secreted by specialized cells in the juxtaglomerular apparatus, stimulates the enzymatic conversion of angiotensinogen to angiotensin I. Angiotensin I, a decapeptide, is then converted to angiotensin II, an octapeptide, by angiotensin-converting enzyme (ACE) in the lung parenchyma and plasma (Figure 18-9). Angiotensin II has two main effects: vasoconstriction and stimulation of aldosterone secretion from the zona glomerulosa in the adrenal gland. It causes constriction of the efferent arteriole in the stenotic kidney, helping to restore filtration pressure and GFR (Figure 18-10). There is little effect on the normal kidney. Because of the compensating effects of angiotensin II on glomerular filtration pressure, the renogram curve for the stenotic kidney tends to appear normal. Captopril, an ACE inhibitor, competitively inhibits the conversion of angiotensin I to angiotensin II. Captopril therefore causes a drop in angiotensin II in the plasma, resulting in relaxation of the efferent arteriole of the stenotic kidney (Figure 18-10C). This effect causes a drop in the stenotic kidney's filtration pressure and a reduced extraction of radiotracer (^{99m}Tc-MAG3, ^{131}I-OIH, or ^{99m}Tc-DTPA). The normal

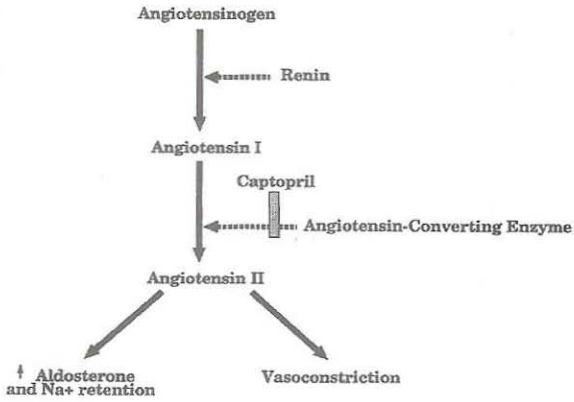

FIGURE 18-9 Schematic of the renin–angiotensin–aldosterone system showing the cascade of events leading to vasoconstriction. (Reprinted with permission of Elsevier Science from Nally JV, Black HR. State-of-the-art review: captopril renography—pathophysiological considerations and clinical observations. *Semin Nucl Med.* 1992;22:85-97.)

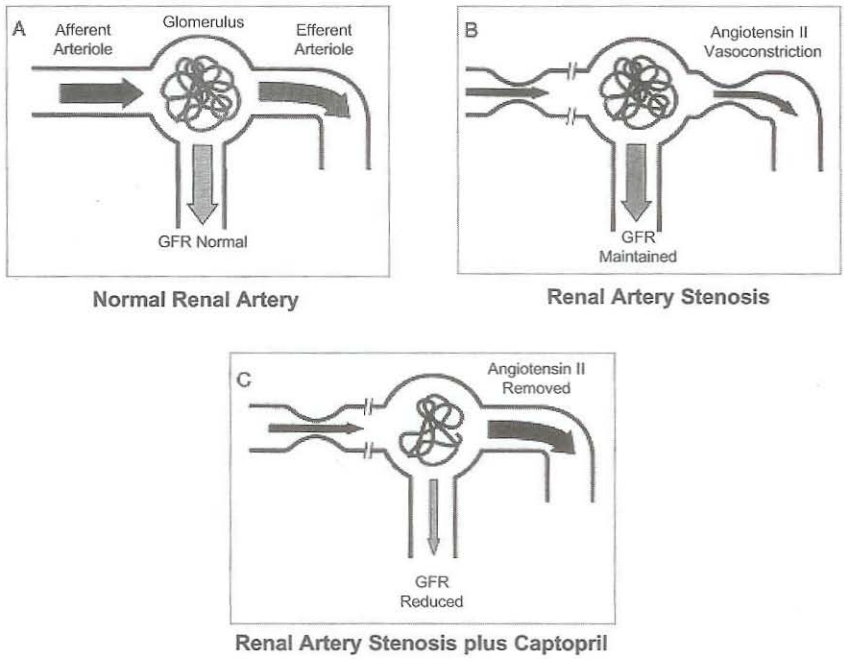

FIGURE 18-10 Schematic of captopril's effect on renal function. (A) normal renal artery and normal GFR; (B) renal artery stenosis, causing angiotensin II-mediated constriction of the efferent arteriole, with GFR maintained; (C) renal artery stenosis plus captopril, demonstrating relaxation of efferent arteriole due to ACE inhibition. (Reprinted with permission of Elsevier Science from Nally JV, Black HR. State-of-the-art review: captopril renography—pathophysiological considerations and clinical observations. *Semin Nucl Med.* 1992;22:85-97.)

kidney is less affected. Consequently, little change occurs in the renogram of the normal kidney, but the stenotic kidney demonstrates a prolonged time to peak and increased retention of radiotracer. Hence, a differential diagnosis can be made (Figure 18-11).

The patient should be hydrated with 8 oz of water 30 to 60 minutes before the study. ACE inhibitors should be discontinued for at least 2 days, preferably 3 to 5 days. Study sensitivity declines about 20% if medication is not stopped before the study.[61] No solid food should be eaten within 4 hours of the study, because food decreases absorption of captopril by 30% to 40%. Blood pressure should be measured before the start of the study

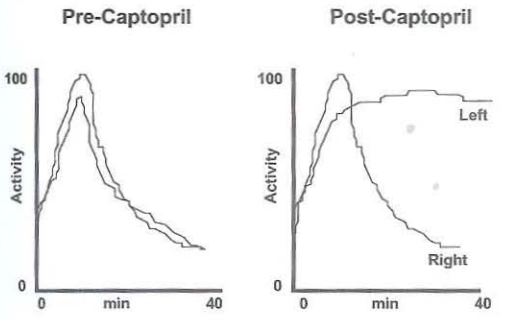

FIGURE 18-11 Effect of captopril on the renogram in patients with unilateral renovascular hypertension. The precaptopril renogram shows normal time course of activity in right and left kidneys. In the postcaptopril renogram, the right kidney is normal but radiopharmaceutical uptake in the left kidney, affected by renal artery stenosis, is greatly diminished because of the reduced filtration pressure induced by captopril's inhibition of angiotensin II production.

and every 5 to 10 minutes during the study. An intravenous line should be inserted to facilitate control of blood pressure, if necessary, and for administration of intravenous enalaprilat in lieu of oral captopril. Imaging the patient in the supine position during the study helps reduce the occurrence of hypotensive episodes. At the end of the procedure the patient's standing blood pressure should be monitored to ensure a stable reading before allowing the patient to leave the department.

A typical 1 day protocol involves performing a baseline study by first injecting 1 mCi (37 MBq) ^{99m}Tc-MAG3 and obtaining a 20 minute renogram. After a 1 hour wait (or 1 day for the 2 day protocol), 50 mg of captopril is given orally. The tablet should be crushed and administered with 8 oz of water to enhance the rate of absorption from the gastrointestinal tract. After a 60 minute wait to achieve peak captopril blood levels, the patient is injected with 3 mCi (111 MBq) ^{99m}Tc-MAG3 and a second 20 minute renogram is acquired.

The data are then analyzed, comparing the right and left kidney renograms to assess low, intermediate, or high probability for RVH. The most important criterion for the diagnosis of RVH is unilateral parenchymal retention of activity after administration of captopril.[61] Typical renogram curve patterns demonstrating temporal changes associated with parenchymal retention are shown in Figure 18-7.[61,63] For example, a diagnosis of high probability for unilateral RVH can be made if the ^{99m}Tc-MAG3 baseline (before captopril) renogram pattern changes from pattern 1 to 3 or from pattern 2 to 4 in Figure 18-7. Other types of changes have also been used in making the diagnostic interpretation.[61,63]

CLEARANCE PROCEDURES

Assessment of renal function is quite useful because so many factors affect kidney function, notably disease processes and the effects of nephrotoxic drugs. Renal clearance of radiotracers has been used for many years to obtain a measure of renal function through the assessment of GFR and ERPF. ^{99m}Tc-DTPA and ^{131}I-OIH are the primary agents used for these measurements. Since the introduction of ^{99m}Tc-MAG3, a procedure for assessment of tubular function has been developed, because ^{99m}Tc-MAG3 is excreted almost exclusively by tubular secretion.[34]

GFR measurement is the most familiar to clinicians and is the clearance measurement most widely sought. The best estimate of GFR and ERPF is made with procedures that employ multiple plasma sampling and simultaneous urine collection, following the classic clearance method. The most accurate measures are achieved if a measurement of residual bladder urine is made.[33] The complexity of this method has stimulated the development of simpler methods that rely on plasma sampling alone, using one or two plasma samples to estimate renal clearance. It is important to understand that plasma clearance methods for measuring renal clearance will work only if the radiotracer is cleared solely by kidney excretion. Scintillation gamma camera methods have also been developed for measuring

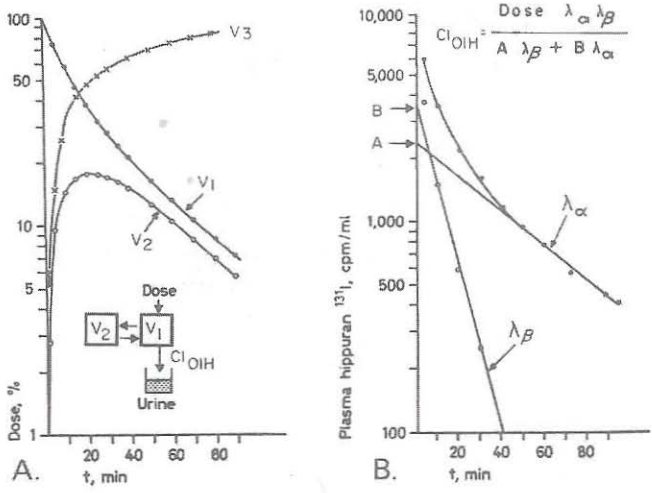

FIGURE 18-12 (A) Theoretical open two-compartment mammalian model closely approximates the human body's handling of injected ^{131}I-OIH. V_1 designates the volume into which the injection is made, V_2 the interchangeable volume, and V_3 the end volume into which the activity is excreted. The V_1 curve (expressed as percentage of injected dose) is constructed from plasma samples, and the V_2 and V_3 volumes can then be calculated. Intercompartmental flow from V_1 to V_3 is equal to the OIH clearance. (B) Bi-exponential plasma disappearance curve of OIH obtained by multiple sampling and plotted on semilog paper. The late slow component (λ_α) is subtracted from the curve to derive the early fast component (λ_β), and the intercepts A and B are determined. The curve satisfies the equation $X = Ae^{-\lambda_\alpha t} + Be^{-\lambda_\beta t}$. (Reprinted with permission of Elsevier Science from reference 52.)

clearance and have been validated against plasma methods, but in general plasma methods are more accurate.

ERPF Measurement

When a radiotracer is injected intravenously, it distributes into various body compartments as shown in Figure 18-12.[52] ^{131}I-OIH and other radiotracers (^{99m}Tc-DTPA and ^{125}I-iothalamate) distribute primarily into the plasma space and the extravascular space, yielding a biexponential plasma disappearance curve (Figure 18-12A). Radiotracer is removed from the central compartment (V_1), into which the tracer was injected, by kidney excretion into the urine compartment (V_3). Removal of tracer from compartment V_1 (plasma) to compartment V_3 (urine) represents the clearance of radiotracer. If the radiotracer is ^{99m}Tc-DTPA or ^{125}I-iothalamate, the clearance is a measure of GFR; if the radiotracer is ^{131}I-OIH, the clearance is a measure of ERPF. The curve shown in Figure 18-12 is for ^{131}I-OIH. The peripheral compartment (V_2) is not well defined and represents radiotracer that cannot be removed from the plasma into the urine because it is either in the extravascular space or bound (e.g., within red blood cells).

When radiotracer is injected and blood samples are obtained at various time points (5, 10, 15, 20, 30, 40, 60, and 90 minutes) and their respective plasma activities in counts per minute per milliliter are plotted, the biexponential plasma disappearance curve B is obtained. Subtraction of the slow component from the whole curve yields the fast component. From these curves the elimination rate constants of the fast (λ_β) and slow (λ_α) components and their respective y-intercepts, B and A, can be determined. The biexponential disappearance curve satisfies the equation $x = Ae^{-\lambda_\alpha t} + Be^{-\lambda_\beta t}$ from which the following clearance formula is derived:

$$Cl_{OIH} = \frac{(Dose)\lambda_\alpha \cdot \lambda_\beta}{A\lambda_\beta + B\lambda_\alpha} \quad (18\text{-}10)$$

In terms of half-life, Equation 18-10 can be rewritten as

$$Cl_{OIH} = \frac{Dose(0.693)}{AT_{½\alpha} + BT_{½\beta}} \quad (18\text{-}11)$$

These equations can be used to calculate the renal clearance (ERPF) of ^{131}I-OIH.[52]

A simplification of the ERPF measurement using one plasma sample taken at 44 minutes after injection of ^{131}I-OIH has been developed. Tauxe et al.[64,65] validated the single-sample method against the whole-curve method of measuring ERPF and demonstrated that the single-sample method was able to estimate ERPF with an error of ± 30 mL/minute. This has become the recommended single-sample technique for measurement of effective renal plasma flow.[33]

GFR Measurement

The primary agents recommended for GFR determination in the United States are ^{99m}Tc-DTPA and ^{125}I-iothalamate. The same pharmacokinetic principles described above for ERPF measurement apply to GFR measurement. GFR can be estimated from a single injection of either of these agents using Equation 18-10, except that later blood samples must be taken because of the slow clearance of these agents. Thus, in addition to the early blood samples noted above, late samples are collected at 120, 150, and 180 minutes after injection. Again, from the plotted biexponential curves, the slow and fast elimination rate constants are derived, along with their respective y-intercepts, which are applied to Equation 18-10 to calculate GFR.[33] If ^{99m}Tc-DTPA is used, ultrafiltration of the plasma samples must be done because ^{99m}Tc-DTPA has around 5% plasma protein binding. Because normal human plasma is 94% water and 6% protein, when the protein is filtered out of 1 mL of plasma, only 0.94 mL of ultrafiltrate remains. Therefore, ultrafiltrate counts must be multiplied by 0.94 to give the appropriate correction. This correction is not needed with ^{125}I-iothalamate.

A simplified two-sample method for GFR measurement with ^{99m}Tc-DTPA has been developed and validated,[30,31] as well as a single-sample method.[32]

NUCLEAR MEDICINE PROCEDURES

Anatomic imaging using ultrasound, CT, and MRI has an important role in evaluations of the genitourinary system. However, renal scintigraphy continues to play an important role in the evaluation of renal perfusion, renal function, and, in certain cases, anatomic abnormalities. Imaging with radionuclides can provide a combination of both anatomic and physiologic information about the kidneys. In most cases, it is the functional information that makes nuclear imaging unique and important.

Rationale

Renal scintigraphy is performed to provide information about renal perfusion, renal parenchymal function, or function of the collecting system. Hydronephrosis is one of the most common indications for scintigraphic evaluation of the kidneys. Hydronephrosis or obstructive uropathy is dilatation of the pelvis and calices of one or both kidneys, usually

identified on an anatomic study. Hydronephrosis can be acute, such as in passage of a calculus with impaction in the ureter, or it may be chronic or congenital. Other common indications for renal and genitourinary scintigraphy include evaluation of acute or chronic renal failure, renal function after trauma, renovascular disease, acute pyelonephritis, cortical scarring in patients with vesicoureteral reflux, differential renal function, postoperative perfusion, RBF, renal agenesis, congenital abnormalities, vesicoureteral reflux, and acute testicular pain, as well as evaluation of potential kidney donors and of kidney transplants.

Procedures

The choice of procedure for evaluation of the kidneys and genitourinary system depends on the indication. The type of study and radiopharmaceutical are chosen to specifically answer questions about the renal or urologic problem being investigated.

Perfusion Studies

Renal perfusion studies are obtained to evaluate blood flow to the kidneys. The patient is placed in the supine position with the gamma camera facing the patient's lower back. A large field-of-view camera is used so that the kidneys and bladder can be visualized. If a ^{99m}Tc or ^{123}I agent is administered, a low-energy, high-resolution parallel hole collimator is used. The radiotracer is administered as a bolus, usually into an antecubital vein. One- to five-second-per-frame images are obtained for the first minute.

Renogram

Renography refers to a recording of the amount of radioactivity in the kidney or kidneys over time after administration of a radiopharmaceutical. A renogram graphically displays the uptake and clearance of the radiotracer in the kidneys in the form of a renal time–activity curve. Time–activity curves are calculated by obtaining multiple serial images of the kidneys over 20 to 40 minutes. Regions of interest are drawn around the kidneys, the renal cortices, and the renal pelves in each of the images to calculate the amount of activity in each of these structures at different time points over the length of the study. Renograms are used to evaluate suspected renal obstruction, renal artery stenosis, acute tubular necrosis, and transplant rejection.

Before the study, the patient should be well hydrated. Poor hydration can result in delayed radiotracer uptake and clearance, suggesting poor renal function. The patient should void before the start of the study. Normally, the patient is placed in the supine position and posterior images are obtained for native kidneys. If a transplanted kidney is being evaluated, anterior images are obtained because a transplanted kidney is usually located anteriorly in the iliac fossa.

A perfusion study is typically obtained for the first minute. After this, static 1- to 5-minute-per-frame images of the abdomen and pelvis are obtained for the next 20 to 40 minutes to evaluate both uptake and clearance of the radiotracer in the kidneys.

Diuresis Renography

Once hydronephrosis has been established by another imaging modality such as ultrasound, nuclear medicine evaluation of the dilated upper urinary tract is usually accomplished with diuresis renography. During the renogram, if there is poor clearance from one or both of the collecting systems after 20 minutes, a diuretic such as furosemide can

be given to determine if the poor clearance is caused by either a functional or mechanical obstruction. In the adult patient, 40 mg of furosemide is administered intravenously. If the obstruction is functional, there is typically a good response to the administration of a diuretic. If the obstruction is mechanical, there is poor response or no response to the diuretic.

Renovascular Hypertension

Normally, systemic blood pressure is controlled by the renin–angiotensin system. When there is a drop in systemic blood pressure, there is an associated drop in GFR in both kidneys. As a response to the drop in GFR, there is release of renin from the juxtaglomerular cells in the kidneys. Renin then converts circulating angiotensinogen, which is made in the liver, into angiotensin I. Angiotensin I is then converted to the potent vasoconstrictor angiotensin II by ACE, predominantly found in vascular endothelium in the lungs. Angiotensin II increases GFR by constricting the efferent glomerular arterioles in the kidneys. The resultant increase in GFR leads to an inhibition of renin release in the juxtaglomerular apparatus. Angiotensin II increases the systemic blood pressure not only by vasoconstriction but also by increasing salt and water reabsorption by the renal tubular cells.[66]

Most patients with hypertension have what is referred to as essential hypertension—hypertension of unknown origin that is treated with lifelong medical management. However, a small subset of patients have hypertension secondary to stenosis of one of the renal arteries. Many of these patients have new-onset hypertension that is difficult to control with medications. If the degree of renal artery stenosis is great enough to significantly decrease GFR, the renin–angiotensin system is activated, resulting in increased systemic blood pressure. An elevation in blood pressure that is caused by renal artery stenosis is referred to as RVH. Renal artery stenosis is often caused by either atherosclerosis or fibromuscular dysplasia. If the patient's hypertension is secondary to renal artery stenosis, revascularization procedures such as balloon angioplasty and stent placement can cure or improve the hypertension.

Radionuclide evaluation of RVH is accomplished with captopril renography. Captopril is an ACE inhibitor that works by blocking the conversion of angiotensin I to the potent vasoconstrictor angiotensin II. If significant renal artery stenosis is the cause of the patient's hypertension, inhibiting the effect of angiotensin II on the efferent arterioles in the kidneys will decrease GFR in the affected kidney. The drop in GFR will result in delayed uptake of the radiopharmaceutical as well as increased cortical retention in the affected kidney.

Captopril renography can be done as either a 1 day or a 2 day study. The study usually consists of two renograms, one with captopril and a baseline study without captopril. If the patient or ordering physician agrees to a 2 day study, the captopril renogram is done first. If the captopril renogram is normal, there is little chance that the patient has RVH and there is no need to obtain a baseline study. However, if the captopril study is abnormal, a baseline study with the patient off ACE inhibitors is needed for comparison. For a 1 day study, a baseline renogram is usually performed first with a small amount of radiotracer. Typically, 1 mCi (37 MBq) of ^{99m}Tc-MAG3 is used. ^{99m}Tc-DTPA can also be used. After the baseline renogram, there should be a delay of about 1 hour before beginning the captopril study. The delay allows time to clear out possible interfering residual activity in the kidneys from the baseline study. The patient is then given 25 to 50 mg of captopril by mouth. The captopril is crushed and dissolved in water before administration. Patients should be well hydrated for the study. However, except for fluids, patients should not eat for 4 hours before the study to enhance absorption of the captopril. The patient is then monitored for an hour while the blood level of captopril comes to peak, because significant hypotension can be associated with captopril administration. The renogram is then repeated with a larger amount of activity, usually 3 mCi (111 MBq) of ^{99m}Tc-MAG3. The

With the patient in the supine position, the testicles must be positioned properly for anterior imaging. Usually, a lead shield is placed behind the testicles to shield underlying activity from the thighs. This can be an appropriately sized piece of lead wrapped in a towel. The penis is taped to the abdomen so that it does not overlay the testicles, and the testicles are positioned on the shield so that side-to-side comparison can be made. Once in position, 2-seconds-per-frame blood flow images are obtained for the first minute after administration of the radiopharmaceutical. In an adult, the dose is usually 10 mCi (370 MBq) of ^{99m}Tc-sodium pertechnetate. Static blood pool images are obtained after the flow phase of the study.

Radiopharmaceuticals

Radiopharmaceuticals used in the evaluation of renal morphology and function fall into three main categories: glomerular filtration agents, tubular secretion agents, and tubular fixation agents.

Glomerular filtration agents are used to evaluate GFR. The most common radiopharmaceuticals used for measuring GFR are ^{99m}Tc-DTPA and ^{125}I-sodium iothalamate. Measurement of GFR with both of these agents corresponds well to inulin measurements. The total GFR is evaluated by obtaining blood samples after administration of the radiopharmaceutical and comparing the blood activity against a known standard. Although both agents do well in estimating total GFR, there is a disadvantage to the use of ^{125}I-sodium iothalamate in that it cannot be used for imaging. If ^{99m}Tc-DTPA is used to evaluate GFR, a gamma camera can be used to image the kidneys during the initial part of the study. Regions of interest can be drawn around each kidney to determine the activity in each, and this can be used to estimate the differential GFR.

Tubular secretion agents can also be used for renography; these include ^{99m}Tc-MAG3 and either ^{123}I- or ^{131}I-OIH. OIH was introduced in 1960 and was one of the first radiotracers used to evaluate renal failure.[16] OIH is chemically similar to PAH. OIH can be used not only to image the kidneys but also to determine the plasma clearance or ERPF.[69] OIH is secreted primarily by the proximal tubular cells (80%), with only about 20% filtered by the glomeruli.[70]

There are drawbacks to the use of either ^{123}I- or ^{131}I-OIH in the evaluation of renal function. ^{131}I has a high photon energy of 364 keV, which is not ideal for gamma camera imaging, and has a long physical half-life of 8 days. It also decays by beta emission. Even though ^{131}I-OIH is rapidly cleared by the kidneys, the absorbed dose can be high, especially in renal failure. Because of this, the administered dose must be low, usually between 0.2 to 0.3 mCi (7.4 to11.1 MBq). ^{123}I-OIH is preferred because ^{123}I has a better photon energy for imaging (159 keV). Because ^{123}I does not have particulate radiation, a higher dose can be administered, 0.4 to 0.5 mCi (14.8 to 18.5 MBq). However, ^{123}I is expensive and not as readily available as ^{131}I.

^{99m}Tc-MAG3 is currently the tubular secretion agent of choice for evaluating RBF and function. It can also be used to evaluate plasma clearance or ERPF.[69,71] After intravenous administration, ^{99m}Tc-MAG3 clears quickly from the blood pool in a biphasic pattern. The first component of the biphasic pattern has a $T_{½}$ of 3.18 minutes, and the second component has a $T_{½}$ of 16.9 minutes.[48] ^{99m}Tc-MAG3 is highly protein bound and is secreted by the proximal tubular cells.[72] The 140 keV energy of ^{99m}Tc is excellent for imaging, and ^{99m}Tc has a short physical half-life of only 6 hours and no particulate radiation. Because of these characteristics, a higher dose can be administered, resulting in a greater photon flux and better imaging.

The last category of renal radiopharmaceuticals is the tubular fixation agents. These agents are used to image the renal parenchyma. The two agents currently in use are

^{99m}Tc-DMSA and ^{99m}Tc-GH. These agents localize in the kidney primarily by tubular transport processes. After intravenous administration, accumulation in the renal parenchyma is related to the amount of functioning renal tissue. There is good clearance from the urine and the blood pool, with prolonged accumulation in the renal cortex. This allows for excellent imaging of the cortex to assess for abnormalities such as scarring. Regions of interest can be drawn around both kidneys in the anterior and posterior images, and geometric means can be calculated to determine differential renal function.

Interpretation

To evaluate renal perfusion, the radiotracer is given as a bolus, usually into an antecubital vein. With the patient in the supine position, posterior 1- to 5-second-per-frame images of the abdomen are obtained for the first minute. Imaging is started just as the bolus of radiotracer is administered. The bolus of activity advances through the subclavian vein into the superior vena cava and then into the right heart. After this, radiotracer is seen in the lungs, and then in the left heart and the aorta. Blood flow to the kidneys should be seen approximately 1 second after the bolus of radiotracer in the abdominal aorta passes the renal arteries. Normally, there should be prompt, symmetric blood flow to both kidneys seen at approximately the same time the abdominal aorta is visualized (Figure 18-13).

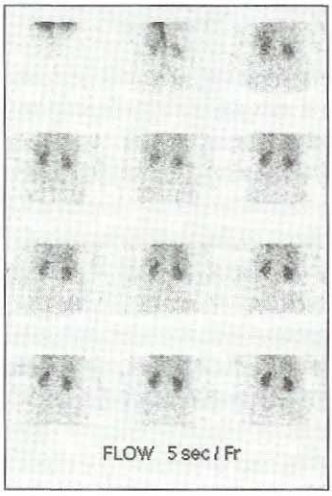

FIGURE 18-13 Normal ^{99m}Tc-MAG renal blood flow study. Prompt, symmetric activity is seen in both kidneys. Activity in the kidneys is seen at the same time as in the abdominal aorta.

There are three distinct phases to the normal renogram. Initially, after administration of the radiotracer there is uptake in the kidneys related to blood flow. Radiotracer is seen in the kidneys within about 1 second after the injected radiotracer in the abdominal aorta passes the renal arteries. This phase occurs over the first minute and is referred to as the vascular phase. The next 2 to 4 minutes are referred to as the parenchymal phase, in which radiotracer is concentrated in the renal parenchyma. Maximal parenchymal activity is usually seen between 3 to 5 minutes after administration of the radiopharmaceutical. The time to peak is the duration between administration of the radiopharmaceutical and the maximum renal cortical activity and is a measure of renal function. At the end of the parenchymal phase, radiotracer accumulation begins to be seen in the collecting systems. The next phase is the excretion phase. During the excretion phase there should be continued clearance from the renal parenchyma. If there is no obstruction there also should be continued clearance from the collecting systems (Figure 18-14).

A captopril (or ACE inhibitor) renogram is performed to evaluate for RVH. A positive study is one that demonstrates a significant change in the baseline renogram after administration of an ACE inhibitor such as captopril or enalaprilat. In patients with normal renal function, radiotracer retention in one kidney after administration of captopril is consistent with a high probability for RVH (Figure 18-15). Many of these patients can be cured or significantly improved through balloon angioplasty or stent placement.

When there is a question of obstructive uropathy, a diuretic renogram is performed. When patients present with a dilated collecting system, it is important to determine if the collecting system is obstructed. Hydronephrosis can be the result of mechanical obstruction

higher dose is used to compensate for any residual activity from the baseline study. Th renal time–activity curves for the studies done before and after captopril administratio are then compared.

Cortical Scintigraphy

Acute pyelonephritis in children usually results from vesicoureteral reflux of infecte urine. Renal cortical scintigraphy using tubular fixation agents such as ^{99m}Tc-DMSA ^{99m}Tc-GH has been shown to be a sensitive technique for diagnosis of acute pyelonephrit and assessment of renal scarring. After intravenous administration of either of thes agents, accumulation in the renal parenchyma is related to the amount of functionir renal tissue. In acute pyelonephritis there is decreased radiotracer accumulation in th affected renal parenchyma as a result of both ischemia and tubular cell dysfunction.[67] acute pyelonephritis is detected early and treated with appropriate antibiotics, the infe tion can be healed without scar formation. Repeated infections can lead to renal scarrir and eventually to renal failure. Cortical scintigraphy can also be used to evaluate th relative functioning of renal tissue.

There is no specific patient preparation for administration of the radiotracer. Th typical dose of ^{99m}Tc-DMSA in children is 0.04 to 0.05 mCi/kg (1.48 to 1.85 MBq/k administered intravenously.[68] Anterior and posterior images of the kidneys are usual obtained approximately 4 hours later. However, delayed imaging can be obtained up 24 hours. Oblique images or single-photon emission computed tomography (SPEC images of the kidneys can also be obtained to help evaluate for cortical defects.

Radionuclide Cystography

Radionuclide cystography is generally accepted as a sensitive test for vesicoureteral reflu Urinary tract infection (UTI) with vesicoureteral reflux can lead to renal infections th result in scarring and hypertension. Although vesicoureteral reflux can be evaluated wi conventional radiographic techniques such as the voiding cystourethrogram, radionuclic cystography results in significantly less gonadal radiation. Radionuclide cystography considered the technique of choice for evaluating UTI in young girls. Radionuclide cy tography can also be used for follow-up after surgical intervention or medical manageme of vesicoureteral reflux.

The most common method for evaluating vesicoureteral reflux involves catheterizatio of the bladder and instillation of 1 mCi (37MBq) of ^{99m}Tc-sodium pertechnetate throug the catheter into the bladder. The catheter is then attached to a saline drip and the bladd is passively filled to capacity. For the filling phase of the study, the patient is supine wi the camera under the patient. Serial posterior 5-second-per-frame images of the abdome and pelvis are obtained during the filling, maximal fill, and voiding phases of the stud In an older, more cooperative child, the voiding phase is usually accomplished with th child sitting on a bedpan with the camera positioned behind the patient. An image obtained after voiding. Regions of interest can be drawn around the bladder and th ureters to obtain an estimate of the relative amount of vesicoureteral reflux.

Scrotal Scintigraphy

Although ultrasound is more commonly used to evaluate acute scrotal pain, scrotal sci tigraphy can be used as an alternative method. Scrotal scintigraphy can be useful differentiating acute pain from inflammation (e.g., in epididymitis) from testicular torsio which is a surgical emergency.

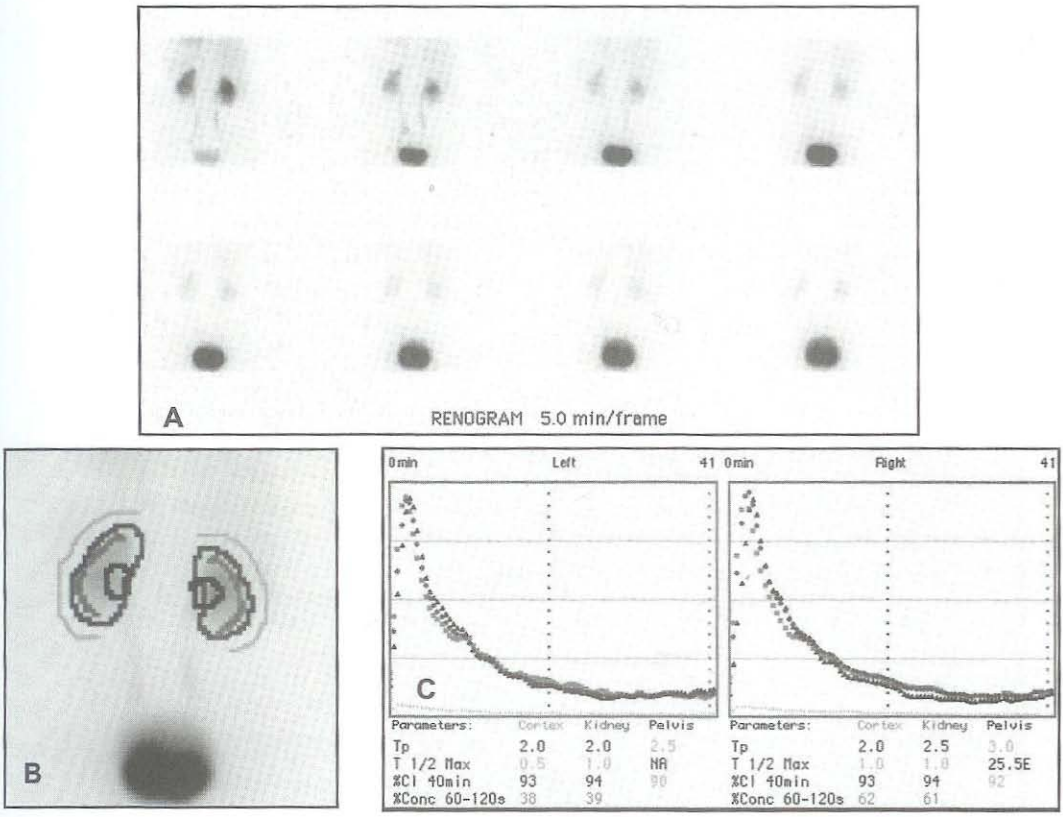

FIGURE 18-14 Normal ^{99m}Tc-MAG3 renogram. (A) Static posterior 5-minute-per-frame images of the kidneys were obtained for 40 minutes. There is good clearance in both kidneys. (B) Regions of interest were drawn around the renal cortex, the kidney, and the pelvis of each kidney to measure activity over time in these regions, as well as background activity. (C) Renal time–activity curves demonstrate the maximum parenchymal phase activity at approximately 2 minutes. There is good clearance from both kidneys during the study.

which can lead to loss of renal function, or it can be secondary to functional abnormality such as muscle atony. In either the mechanically obstructed kidney or the functionally dilated but nonobstructed kidney, there is a delayed time to peak for the radiotracer as well as little to no clearance prior to administration of a diuretic. In the obstructed kidney, administration of the diuretic has little to no effect on the renal time–activity curve. However, in the case of nonobstructed hydronephrosis, there is usually prompt response to the administration of the diuretic (Figure 18-16). After administration of the diuretic, the kidney usually clears half the radioactivity in less than 10 minutes when there is no significant obstruction. If the time to half-maximum radiotracer is greater than 20 minutes after diuretic administration, the kidney is obstructed. A time to half-maximum between 10 and 20 minutes is indeterminate for partial obstruction.

Kidney transplants are placed in the anterior iliac fossa. Renograms are sometimes obtained shortly after surgery to determine if the transplanted kidney is functioning. A complication that is often present soon after transplant is ischemic damage to the donor kidney. This presents as poor renal function and poor urine output but with good renal perfusion. This is referred to as acute tubular necrosis and usually resolves over the first three weeks. On the renogram it is seen as a delayed time to peak and poor clearance (Figure

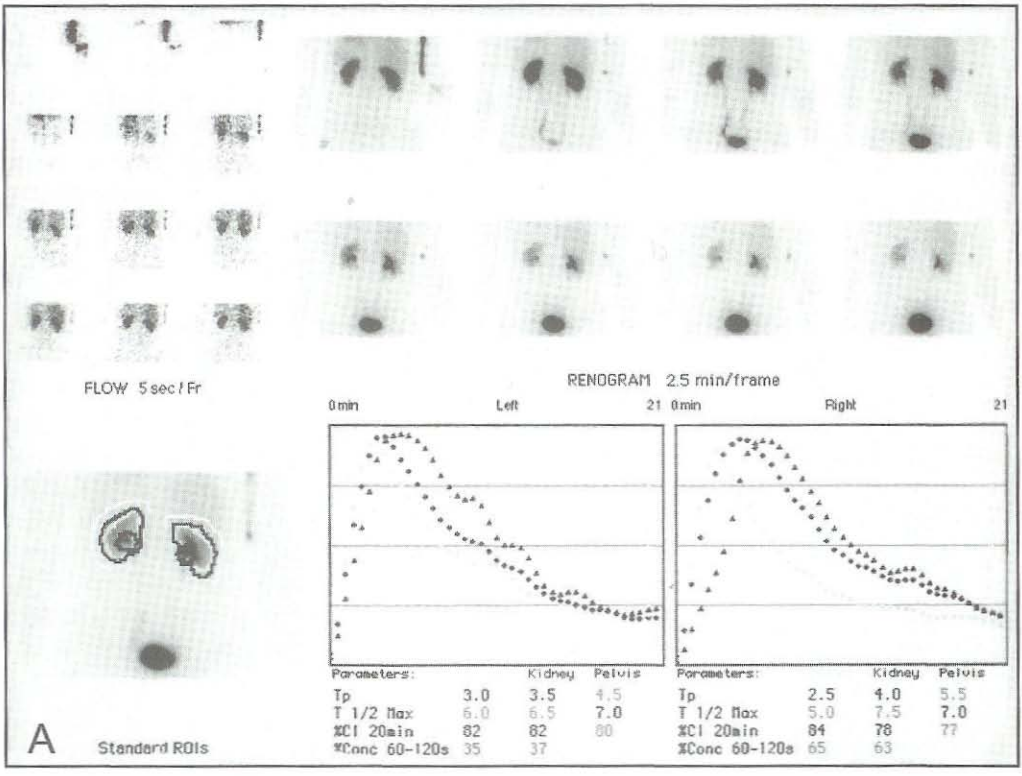
FLOW 5 sec / Fr
RENOGRAM 2.5 min/frame
0 min
Left
21
0 min
Right
21
Parameters:
Kidney
Pelvis
Tp 3.0 3.5 4.5
T 1/2 Max 6.0 6.5 7.0
%CI 20min 82 82 80
%Conc 60-120s 35 37
Parameters:
Kidney
Pelvis
Tp 2.5 4.0 5.5
T 1/2 Max 5.0 7.5 7.0
%CI 20min 84 78 77
%Conc 60-120s 65 63
A
Standard ROIs

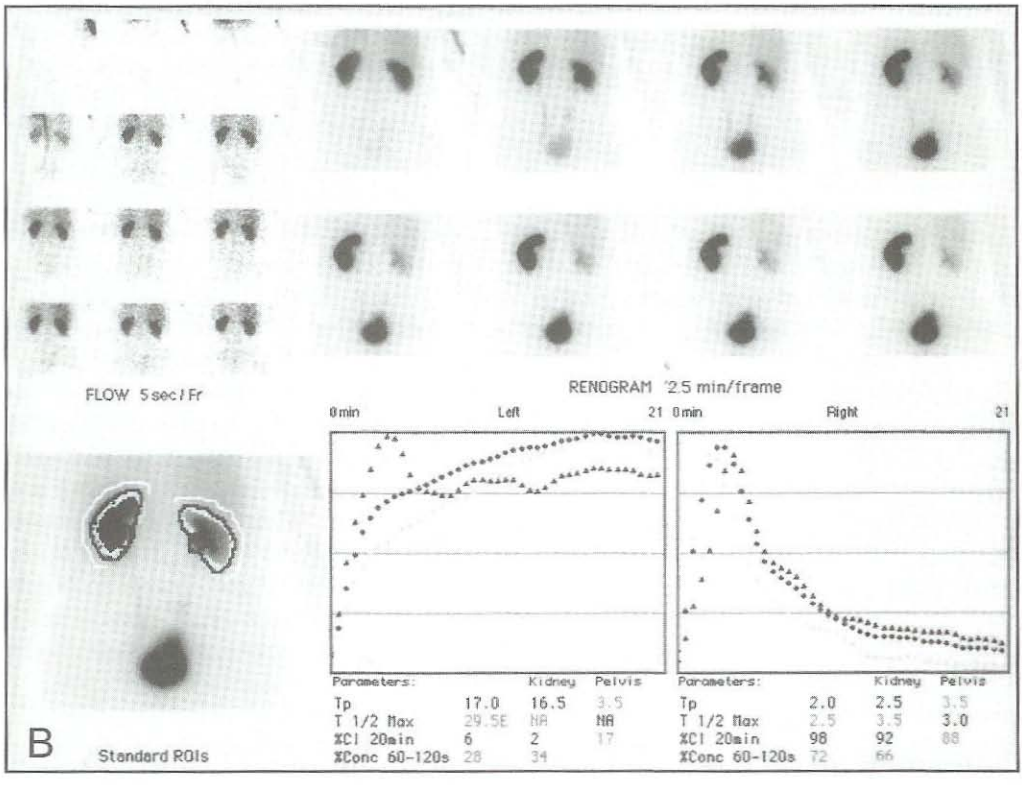
FLOW 5 sec / Fr
RENOGRAM 2.5 min/frame
0 min
Left
21
0 min
Right
21
Parameters:
Kidney
Pelvis
Tp 17.0 16.5 3.5
T 1/2 Max 29.5E NA NA
%CI 20min 6 2 17
%Conc 60-120s 28 34
Parameters:
Kidney
Pelvis
Tp 2.0 2.5 3.5
T 1/2 Max 2.5 3.5 3.0
%CI 20min 98 92 88
%Conc 60-120s 72 66
B
Standard ROIs

FIGURE 18-15

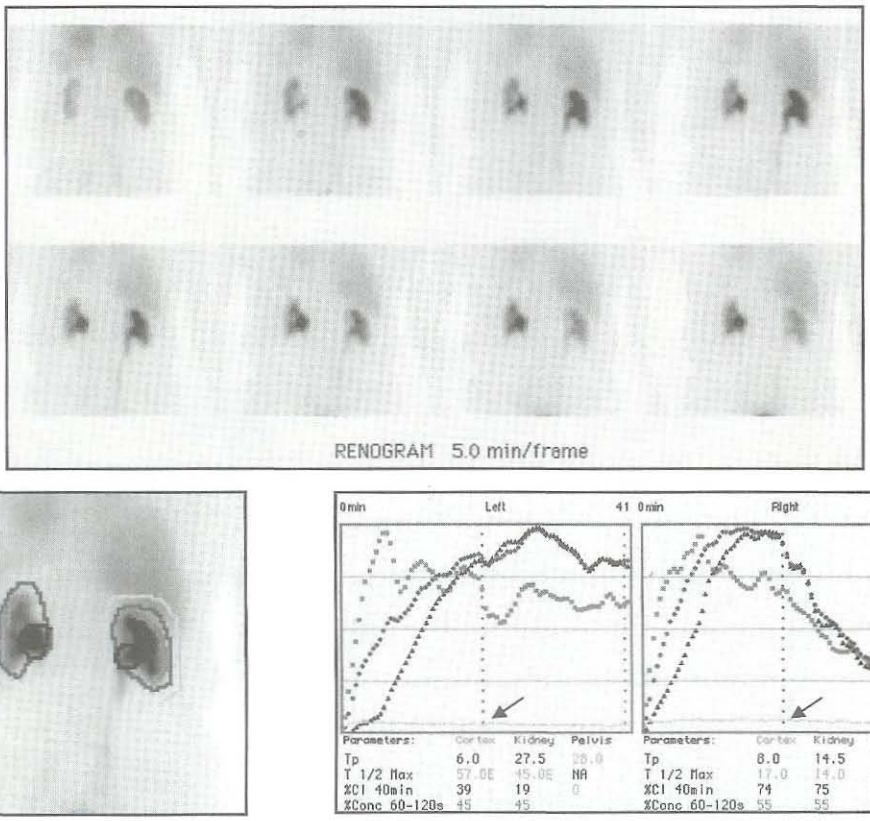

FIGURE 18-16 Diuretic renogram with ^{99m}Tc-MAG3 in a patient with bilateral hydronephrosis. There is a delayed time to peak in both kidneys and no significant clearance from either kidney 20 minutes into the study. A diuretic was administered at 20 minutes (arrows). There is prompt response to the diuretic in the right kidney with 75% clearance at 40 minutes and little to no response in the left kidney in this patient with partial obstruction in the left kidney and nonobstructed hydronephrosis in the right kidney.

18-17). After the first week and most commonly during the first 3 months after transplantation, acute rejection is a concern. On the renogram, acute rejection is seen as delayed renal uptake and reduced excretion with worsening renal perfusion on the flow images.

In a normal renal cortical scan, there is homogeneous radiotracer accumulation in the renal parenchyma of both kidneys. Both kidneys should demonstrate reniform shape. Normal differential renal function can vary from 50% in each kidney to 44% and 56% (Figure 18-18). Defects sometimes can be associated with nonfunctioning renal tissue. Figure 18-19 demonstrates a cortical defect associated with a renal cell carcinoma. Infection such as acute pyelonephritis can be seen as a single cortical defect in one kidney or multiple cortical defects involving one or both kidneys. Scarring is usually associated with volume loss. Scarring may appear as a wedge-shaped cortical defect, a flattening of the renal contour, or a concave defect (Figure 18-20).

FIGURE 18-15 (Opposite) Captopril renogram with ^{99m}Tc-MAG3. (A) Precaptopril renogram with 1 mCi (37 MBq) of ^{99m}Tc-MAG3 shows normal renal time–activity curves in both kidneys. (B) Postcaptopril study demonstrates a significant increase in the time to peak and delayed clearance in the left kidney consistent with renal artery stenosis.

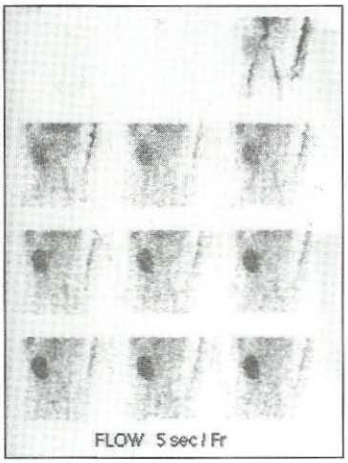

A

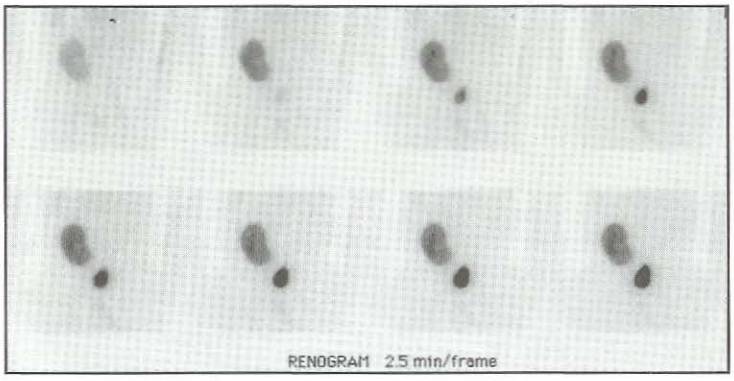

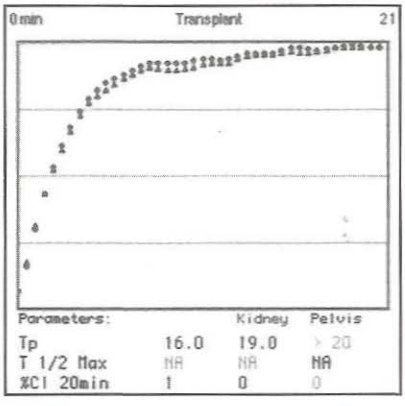

B

FIGURE 18-17 Renal transplant evaluation using ^{99m}Tc-MAG3. (A) Anterior 5-second-per-frame blood flow images of the transplant kidney in the right iliac fossa. There is prompt blood flow to the transplant kidney. Activity is seen in the kidney at the same time as in the iliac vessels. (B) Static anterior 2.5-minute-per-frame images over the next 20 minutes and the associated renal time–activity curve demonstrate a delayed time to peak in the kidney and poor clearance, although there is some excretion into the bladder. The patient's transplant surgery was only a few days earlier. These findings are most consistent with acute tubular necrosis.

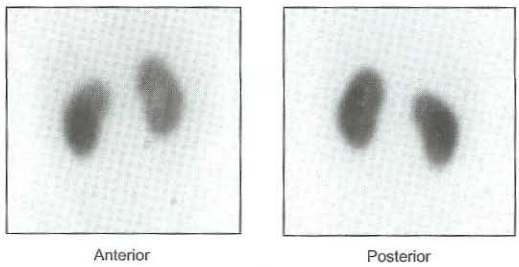

A

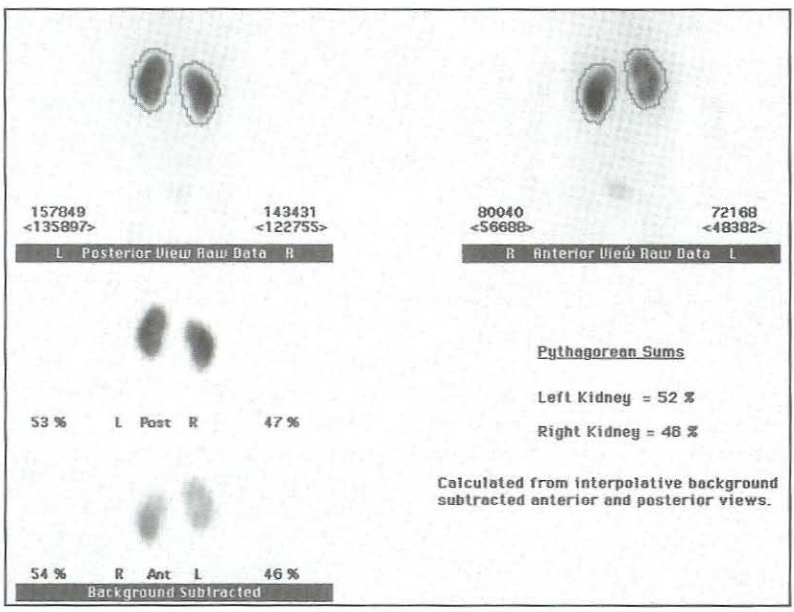

B

FIGURE 18-18 Normal renal cortical scan using ^{99m}Tc-DMSA. (A) There is relatively homogenous radiotracer accumulation in both kidneys. There are no cortical defects to suggest infection or scarring. (B) Regions of interest were drawn around each kidney in both the anterior and posterior projections, and geometric means were calculated to determine differential renal function. The differential function was calculated to be 52% on the left and 48% on the right, which is considered normal.

Although not routinely used for renal imaging, positron emission tomography with ^{18}F-fludeoxyglucose (^{18}F-FDG) has been used to image renal masses and to assess for distant metastatic involvement. Since ^{18}F-FDG is normally excreted by the kidneys, a diuretic such as furosemide can be used to clear activity from the kidneys prior to imaging (Figure 18-21).

Renal cortical scintigraphy can also be useful in evaluating renal function in congenital renal abnormalities. Figure 18-22 demonstrates lack of function in a multicystic dysplastic kidney. Figure 18-23 shows a horseshoe kidney joined at the lower poles.

A normal radionuclide cystogram will show radiotracer activity in a normally shaped bladder only during the filling, full bladder, and voiding stages of the exam. On the postvoid image, there should be no significant residual activity in the bladder. In the presence of vesicoureteral reflux, there will be evidence of radiotracer accumulation in one or both of the ureters during the exam. If radiotracer refluxes only into the distal portion of the ureter, this is considered mild or grade 1 reflux. There is moderate or grade 2 reflux if radiotracer is seen to the level of the renal pelvis of what appears to be a

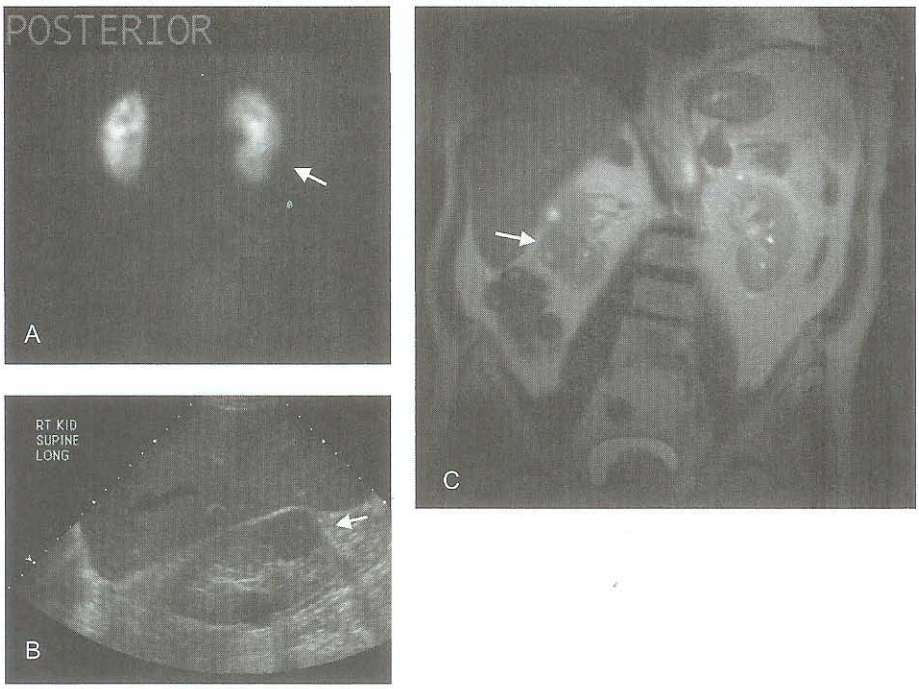

FIGURE 18-19 Renal cell carcinoma. (A) Posterior renal cortical scan with ^{99m}Tc-DMSA demonstrating a concave cortical defect in the lateral lower pole of the right kidney (arrow). (B) Renal ultrasound long-axis image of the right kidney showing a corresponding hypoechoic mass in the right kidney (arrow). (C) Coronal magnetic resonance image also demonstrating the mass in lateral lower pole of the right kidney (arrow).

nondilated renal collecting system (Figure 18-24). If there is reflux into a dilated renal collecting system, the reflux is severe or grade 3.

Scrotal imaging is performed to evaluate acute-onset scrotal pain. In the normal scan, there is symmetric, diffuse, mild perfusion to both testicles as well as symmetric blood pooling on the delayed images. Acute epididymitis is seen as increased blood flow and pooling in the region of the epididymis (Figure 18-25). Early in testicular torsion there may be decreased blood pooling in the torsed testicle. After several hours, there can be increased blood flow and pooling to the scrotum around the torsed testicle. The testicle appears as a photopenic defect surrounded by increased radiotracer (Figure 18-26).

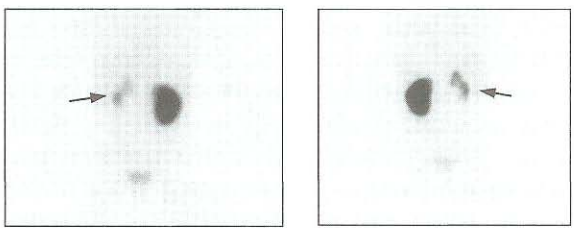

FIGURE 18-20 Renal cortical scan of a 5 year old girl with a history of urinary tract infections obtained 6 hours after intravenous administration of 2 mCi (7.4 MBq) of ^{99m}Tc-DMSA. (A) Anterior and posterior images show a small scarred right kidney (arrows) with a normal-appearing left kidney. (B) The differential renal function was calculated to be only 8% in the right kidney.

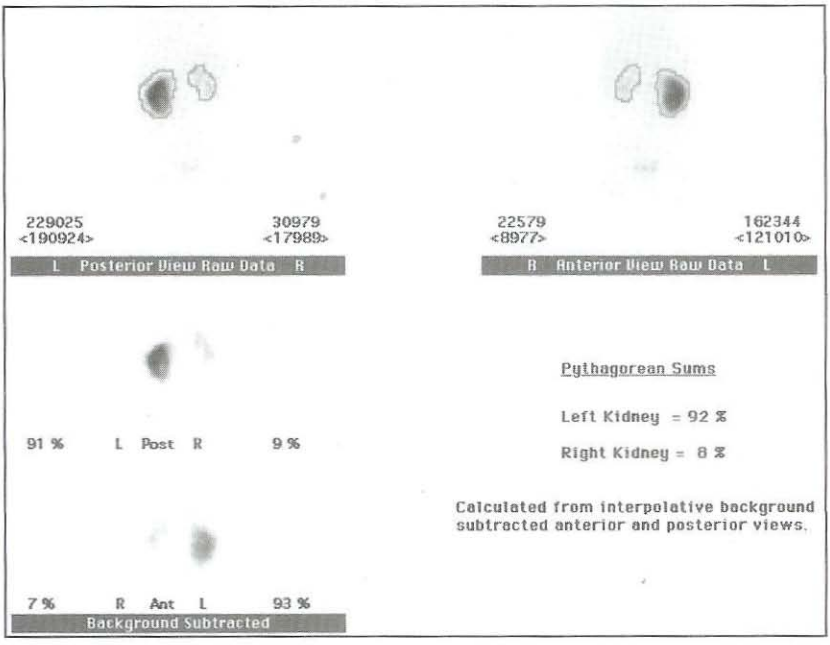

B

FIGURE 18-20 (Continued)

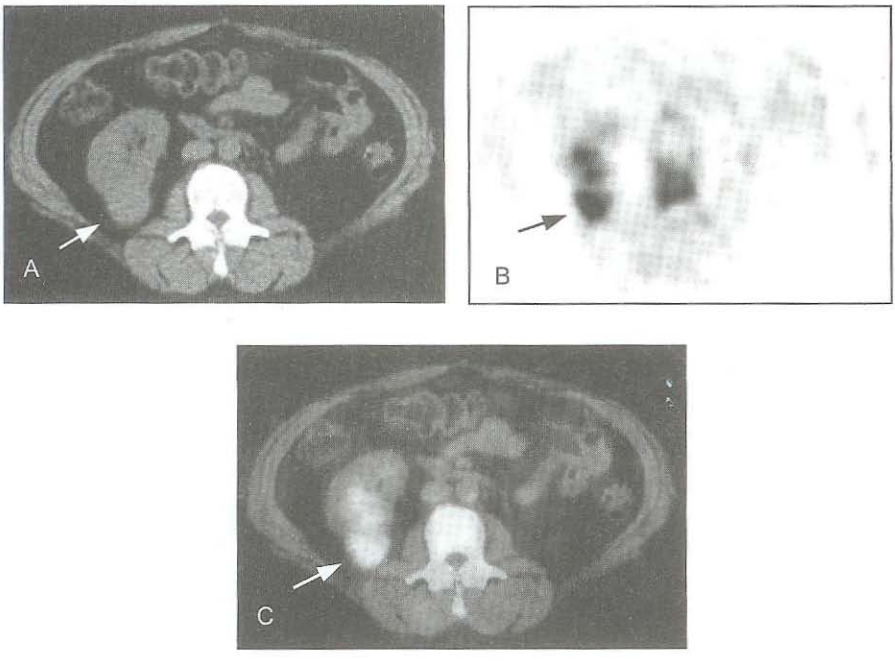

FIGURE 18-21 Renal sarcoma. (A) Axial noncontrast computed tomography (CT) image through the right kidney shows an exophytic soft tissue mass in the posterior aspect of the right kidney (white arrow). (B) A corresponding axial positron emission tomography (PET) image using ^{18}F-fludeoxyglucose shows a focal area of hypermetabolism in the same region (black arrow). (C) Axial PET/CT fusion image demonstrates that the focal area of hypermetabolism corresponds to the exophytic mass (white arrow). The mass was found to be a renal sarcoma.

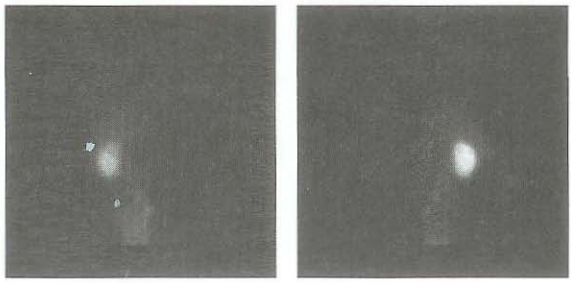

A

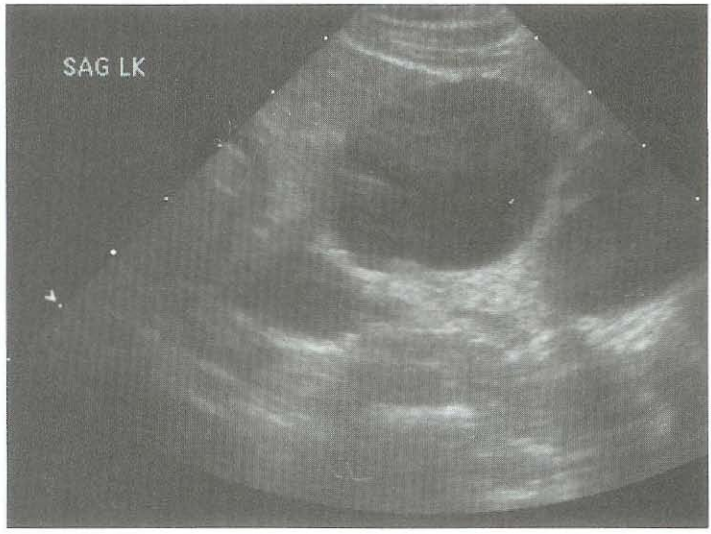

B

FIGURE 18-22 Multicystic dysplastic kidney in a 5 month old child. (A) ^{99m}Tc-DMSA renal cortica scan shows normal-appearing right kidney with no evidence of a functioning left kidney. (B) Sagitta ultrasound image of the left kidney shows multiple cysts in this patient with multicystic dysplasti kidney.

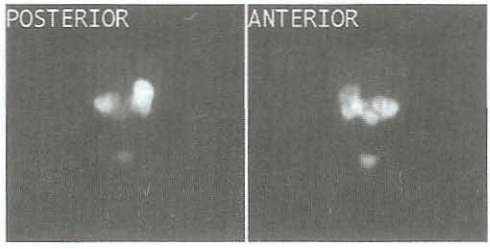

FIGURE 18-23 Horseshoe kidney. Anterior and posterior images from a renal cortical ^{99m}Tc-DMS. study demonstrating a union of the lower poles of the kidneys in this patient with a horseshc kidney.

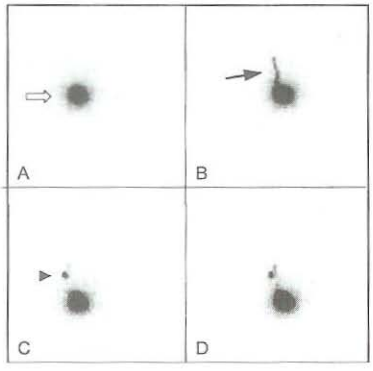

FIGURE 18-24 Vesicoureteral reflux. After catheterization of the bladder, 1 mCi (37 MBq) of ^{99m}Tc-sodium pertechnetate was administered into the bladder. (A) Radiotracer is seen in the bladder (open arrow). (B) On a subsequent image there is reflux of radiotracer into the left ureter on this posterior image of the abdomen and pelvis (black arrow). (C) On a later image there is accumulation in the left renal pelvis (black arrowhead). (D) Radiotracer is seen in the left renal pelvis and ureter. There is no evidence of reflux into the right ureter.

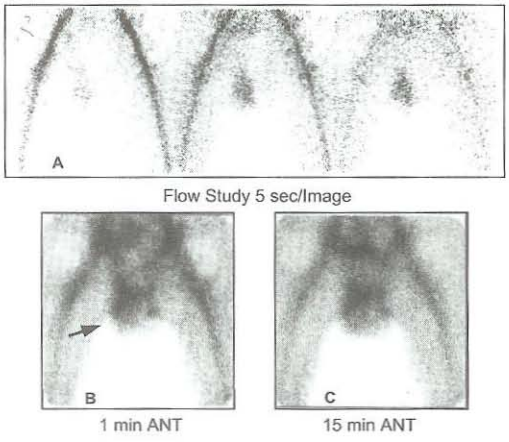

FIGURE 18-25 Scrotal imaging with ^{99m}Tc-sodium pertechnetate. (A) Blood flow, (B) blood pool, and (C) 15 minute delayed anterior images of the pelvis demonstrate increased blood flow and blood pool to the superior and lateral right scrotum in this patient with acute-onset right scrotal pain. The pattern is most consistent with acute epididymitis.

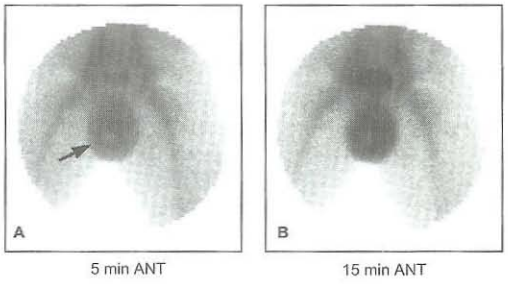

FIGURE 18-26 Delayed testicular torsion. Anterior images of the scrotum taken at (A) 5 and (B) 15 minutes after intravenous administration of ^{99m}Tc-sodium pertechnetate. Images show increased scrotal activity on the right with a photopenic central area corresponding to the ischemic right testicle (arrow). The patient's right scrotal pain began the day before the study.

REFERENCES

1. Brenner BM, Rector FC Jr. *The Kidney.* Philadelphia: WB Saunders; 1976.
2. Gottschalk CW, Lassiter WE. Mechanisms of urine formation. In: Mountcastle VB, ed. *Medical Physiology.* Vol 2. 14th ed. St Louis: Mosby; 1980.
3. Nielson P, Rasmussen F. Relationships between molecular structure and excretion of drugs. *Life Sci.* 1975;17:1495-512.
4. McAfee JG, Subramanian G. Radioactive agents for imaging. In: Freeman LM, Johnson PM, eds. *Clinical Scintillation Imaging.* 2nd ed. New York: Grune & Stratton; 1975:13-114.
5. Goldstein A, Aronow L, Kalman SM. *Principles of Drug Action.* New York: Harper & Row; 1969.

6. Fritzberg AR. Advances in renal radiopharmaceuticals. In: Fritzberg AR, ed. *Radiopharmaceuticals: Progress and Clinical Perspectives.* Vol 1. Boca Raton, FL: CRC Press; 1986:61-87.
7. Despopoulus A. A definition of substrate specificity in renal transport of organic anions. *J Theoret Biol.* 1965;8:163-92.
8. Fritzberg AR. Current status of renal radiopharmaceuticals. *J Nucl Med Technol.* 1984;12:177-89.
9. McAfee JG, Grossman ZD, Gagne G, et al. Comparison of renal extraction efficiencies for radioactive agents in the normal dog. *J Nucl Med.* 1981;22:333-8.
10. Smith HB. *The Kidney: Structure and Function in Health and Disease.* New York: Oxford University Press; 1951:154.
11. Wesson LG. *Physiology of the Human Kidney.* New York: Grune & Stratton; 1969.
12. Chervu RL, Blaufox MD. Renal radiopharmaceuticals: an update. *Semin Nucl Med.* 1982;12:224-45.
13. Arnold RW, Subramanian G, McAfee JG, et al. Comparison of Tc-99m complexes for renal imaging. *J Nucl Med.* 1975;16:357-67.
14. Eshima D, Fritzberg AR, Taylor A Jr. Tc-99m renal tubular function agents: current status. *Semin Nucl Med.* 1990;20:28-40.
15. Taplin GV, Meredith OM Jr, Kade H, et al. The radioisotope renogram. *J Lab Clin Med.* 1956;48:886-901.
16. Tubis M, Posnick E, Nordyke RA. Preparation and use of I-131 labeled sodium iodohippurate in kidney function tests. *Proc Soc Exp Biol Med.* 1960;103:497-8.
17. McAfee JG, Wagner HN Jr. Visualization of renal parenchyma: scintiscanning with Hg-203 Neohydrin. *Radiology.* 1960;75:820-1.
18. Harper PV, Lathrop KA, Hinn GM, et al. Technetium-99m iron complex. In: Andrews GA, Kniseley RM, Wagner HN Jr, eds. *Radioactive Pharmaceuticals.* USAEC Symposium Series 9. Oak Ridge, TN: US Atomic Energy Commission; 1966:347-51.
19. Eckelman W, Richards P. Instant Tc-99m DTPA. *J Nucl Med.* 1970;11:761.
20. Atkins HL, Cardinale KG, Eckelman WC, et al. Evaluation of Tc-99m DTPA prepared by three different methods. *Radiology.* 1971;98:674-7.
21. Lin TH, Khentigen A, Winchell HS. A Tc-99m chelate substitute for organoradiomercurial renal agents. *J Nucl Med.* 1974;15:34-5.
22. Sigman EM, Elwood CM, Knox F. The measurement of glomerular filtration rate in man with sodium iothalamate I-131 (Conray). *J Nucl Med.* 1965;7:60-8.
23. Elwood CM, Sigman EM. The measurement of glomerular filtration and effective renal plasma flow in man by iothalamate I-131 and iodpyracet I-131. *Circulation.* 1967;36:441-8.
24. McAfee JG, Gagne G, Atkins HL, et al. Biological distribution and excretion of DTPA labeled with Tc-99m and In-111. *J Nucl Med.* 1979;20:1273-8.
25. Jones AG, Davison A, LaTegola MR, et al. Chemical and in vivo studies of the anion oxo[N,N'-ethylenebis(2-mercaptoacetimido)]technetate(V). *J Nucl Med.* 1982;23:801-9.
26. Fritzberg AR, Whitney WP, Kuni CC, et al. Biodistribution and renal excretion of ^{99m}Tc-N,N'-bis(mercaptoacetyl) ethylenediamine: effect of renal tubular transport inhibitors. *Int J Nucl Med Biol.* 1982;9:79-82.
27. Klingensmith WC III, Gerhold JP, Fritzberg AR, et al. Clinical comparison of Tc-99m N,N'-bis(mercaptoacetyl) ethylenediamine and ^{131}I-orthoiodohippurate for evaluation of renal tubular function. *J Nucl Med.* 1982;23:377-80.
28. Fritzberg AR, Kasina S, Eshima D, et al. Synthesis and biological evaluation of technetium-99m MAG3 as a hippuran replacement. *J Nucl Med.* 27;1986:111-16.
29. Gates GF. Split renal function testing using Tc-99m DTPA: a rapid technique for determining differential glomerular filtration. *Clin Nucl Med.* 1982;8:400-7.
30. Russell CD, Bischoff PG, Kontzen FN, et al. Measurement of glomerular filtration rate: single injection plasma clearance method without urine collection. *J Nucl Med.* 1985;26:1243-7.
31. Rowell KL, Kontzen FN, Stutzman ME, et al. Technical aspects of a new technique for estimating glomerular filtration rate using technetium-99m-DTPA. *J Nucl Med Technol.* 1986;14:196-8.
32. Ham HR, Piepsz A. Estimation of glomerular filtration rate in infants and in children using a single-plasma sample method. *J Nucl Med.* 1991;32:1294-7.
33. Blaufox MD, Aurell M, Bubeck B, et al. Report of the radionuclides in nephrourology committee on renal clearance. *J Nucl Med.* 1996;37:1883-90.
34. Bubeck B. Renal clearance determination with one blood sample: improved accuracy and universal applicability by a new calculation principle. *Semin Nucl Med.* 1993;23:73-86.
35. Ikeda I, Inoue O, Kurata K. Chemical and biological studies on Tc-99m DMS-II: effect of Sn(II) on the formation of various Tc-DMS complexes. *Int J Appl Radiat Isot.* 1976;27:681-88.
36. Ikeda I, Inoue O, Kurata K. Preparation of various Tc-99m dimercaptosuccinate complexes and their evaluation as radiotracers. *J Nucl Med.* 1977;18:1222-9.
37. Kubiatowicz KO, Bolles TF, Nova JC, et al. Localization of low molecular weight Tc-99m labeled dimercaptodicarboxylic acids in kidney tissue. *J Pharm Sci.* 1979;68:621-3.

38. Dewanjee MK. Binding of diagnostic radiopharmaceuticals to human serum albumin by sequential and equilibrium dialysis. *J Nucl Med.* 1982;23:753-4.
39. Hosokawa S, Kawamura J, Yoshida O, et al. Basic studies on intrarenal localization of renal scanning agent ^{99m}Tc-DMSA. *Acta Urol Jap.* 1978;24:61-5.
40. Suur-Müller R, Gutsche HU. Tubular reabsorption of technetium-99m-DMSA. *J Nucl Med.* 1995;36:1654-8.
41. Goldraich NP, Alvarenga AR, Goldraich IH, et al. Renal accumulation of ^{99m}Tc-DMSA in the artificially perfused isolated rat kidney. *J Urol.* 1985;134:1282-6.
42. Yee CA, Lee HB, Blaufox MD. Tc-99m DMSA renal uptake: influence of biochemical and physiologic factors. *J Nucl Med.* 1981;22:1054-8.
43. Razumeni NV, Petrovi J. Biochemical studies of the renal radiopharmaceutical compound dimercaptosuccinate. II: Subcellular localization of ^{99m}Tc-DMS complex in the rat kidney in vivo. *Eur J Nucl Med.* 1982;7:304-7.
44. Moretti JL, Rapin JR, Saccavini JC, et al. 2,3-Dimercaptosuccinic acid chelates-2: renal localization. *Int J Nucl Med Biol.* 1984;11:275-9.
45. Van Luyk WHJ, Ensing GJ, Piers DA. Low renal uptake of ^{99m}Tc-DMSA in patients with proximal tubular dysfunction. *Eur J Med.* 1983;8:404-5.
46. Lee HB, Blaufox MD. Mechanism of renal concentration of technetium-99m glucoheptonate. *J Nucl Med.* 1985;26:1308-13.
47. Nosco DL, Wolfangel RG, Bushman MJ, et al. Technetium-99m MAG3: labeling conditions and quality control. *J Nucl Med Technol.* 1993;21:69-74.
48. Taylor A Jr, Eshima D, Fritzberg AR, et al. Comparison of iodine-131 OIH and technetium MAG3 renal imaging in volunteers. *J Nucl Med.* 1986;27:795-803.
49. Bubeck B, Brandau W, Weber E, et al. Pharmacokinetics of technetium-99m-MAG3 in humans. *J Nucl Med.* 1990;31:1285-93.
50. Jafri RA, Britton KE, Nimmon CC, et al. Technetium-99m MAG3, a comparison with iodine-123 and iodine-131 orthoiodohippurate, in patients with renal disorders. *J Nucl Med.* 1988;29:147-58.
51. Burbank MK, Tauxe WN, Maher FT, et al. Evaluation of radioiodinated Hippuran for the estimation of renal plasma flow. *Proc Staff Mayo Clin.* 1961;36:372-86.
52. Dubovsky EV, Russell CD. Quantitation of renal function with glomerular and tubular agents. *Semin Nucl Med.* 1982;12:308-29.
53. Maher FT, Tauxe WN. Renal clearance in man of pharmaceuticals containing radioactive iodine: influence of plasma binding. *JAMA.* 1969;207:97-104.
54. Magnusson G. Influence of varying amounts of I-131 in radiohippuran on the radioactivity measurements. *Acta Med Scand.* 1962;(suppl 378):111-5.
55. Kontzen FN, Tobin M, Dubovsky EV, et al. Comprehensive renal function studies: technical aspects. *J Nucl Med Technol.* 1977;5:81-4.
56. Verbruggen AM, Nosco DL, Van Neron CG, et al. Technetium-99m-L,L-ethylenedicysteine: a renal imaging agent. I: Labeling and evaluation in animals. *J Nucl Med.* 1992;33:551-7.
57. Eshima D, Taylor A Jr. Technetium-99m (^{99m}Tc) mercaptoacetyltriglycine: update on the new ^{99m}Tc renal tubular function agent. *Semin Nucl Med.* 1992;22:61-73.
58. Farmelant MH, Burrows BA. The renogram: physiologic basis and current clinical use. *Semin Nucl Med.* 1974;4:61-73.
59. O'Reilly P, Aurell M, Britton K, et al. Consensus on diuresis renography for investigating the dilated upper urinary tract. *J Nucl Med.* 1996;37:1872-6.
60. Blaufox MD. Procedures of choice in renal nuclear medicine. *J Nucl Med.* 1991;32:1301-9.
61. Taylor A, Nally J, Aurell M, et al. Consensus report on ACE inhibitor renography for detecting renovascular hypertension. *J Nucl Med.* 1996;37:1876-82.
62. Wenting GJ, Tan-Tjiong HL, Derkx FHM, et al. Split renal function after captopril in unilateral renal artery stenosis. *BMJ.* 1984;288:886-90.
63. Fommei E, Ghione S, Hilson AJW, et al. Captopril radionuclide test in renovascular hypertension: a European multicenter study. *Eur J Nucl Med.* 1993;20:625-44.
64. Tauxe WN, Maher FT, Taylor WF. Effective renal plasma flow: estimation from theoretical volumes of distribution of intravenously injected ^{131}I-orthoiodohippurate. *Mayo Clin Proc.* 1971;46:524-31.
65. Tauxe WN, Dubovsky EV, Kidd T Jr, et al. New formulae for the calculation of effective renal plasma flow. *Eur J Nucl Med.* 1982;7:51-4.
66. Sarkar SD, Singhal PG. Basis of renal scintigraphy. In: Elgazzar AH, ed. *The Pathophysiologic Basis of Nuclear Medicine.* New York: Springer-Verlag; 2001:154-68.
67. Majd M, Rushton HG. Renal cortical scintigraphy in the diagnosis of acute pyelonephritis. *Semin Nucl Med.* 1992;22:98-111.
68. Mandell GA, Eggli DF, Gilday DL, et al. Procedure guideline for renal cortical scintigraphy in children 2.0. In: *Procedure Guidelines Manual 2001-2002.* Reston, VA: Society of Nuclear Medicine; 2001:157-60.

69. Blaufox MD, Mattias A, Bubeck B, et al: Report of the Radionuclides in Nephrourology Committee on Renal Clearance. In: Taylor A, Nally J, Thomsen H, eds. *Radionuclides in Nephrourology.* Reston, VA: Society of Nuclear Medicine; 1997:22-36.
70. Saha GB. *Fundamentals of Nuclear Pharmacy.* 4th ed. New York: Springer-Verlag; 1998:271.
71. O'Reilly P, Aurell M, Britton K, et al. Consensus on diuresis renography for investigating the dilated upper urinary tract. In: Taylor A, Nally J, Thomsen H, eds. *Radionuclides in Nephrourology.* Reston, VA: Society of Nuclear Medicine; 1997:1-7.
72. Taylor AJ, Nally JV. Clinical applications of renal scintigraphy. *AJR Am J Roentgenol.* 1995;164:31-41.

19 Bone

Bone imaging is performed for many reasons, including the evaluation of metastatic disease, infection, and traumatic injury. An important benefit of bone imaging is its sensitivity. On a standard x-ray exam, bone mineral content must be altered significantly before a lesion can be detected. In comparison, it takes only a few metabolically active cells undergoing osseous remodeling to attract bone-avid radiolabeled complexes that "light up" on the bone scan. Bone imaging, therefore, is useful for assessing pathologic lesions in bone at an early stage of disease. However, regions of bone remodeling demonstrate increased accumulation of activity regardless of the cause. Thus, bone imaging lacks specificity because the bone scan does not detect a particular type of pathology; it reveals only the effects of that pathology.

PHYSIOLOGIC ANATOMY

Bone is composed of minute crystals of hydroxyapatite (HA) associated with collagen fibers. The crystals are continually being produced and reabsorbed in the bone remodeling process. The surface area of bone mineral is quite large because of the small size of bone crystals. Bone mineral is composed mainly of calcium, phosphate, and hydroxyl ions. The presence of these ions on the large adsorptive surface of bone creates a chemically reactive site for many radionuclidic substances that have an affinity for bone. This provides a mechanism for studying bone physiology and for performing diagnostic imaging procedures to detect disease associated with bone.

Living bone consists of a variety of tissues, as shown in Figure 19-1.[1] The outer layer of bone, which imparts its shape and strength, is cortical bone. Internal to the cortical bone is spongy cancellous (trabecular) bone. Cancellous bone contains the marrow, which is composed of fat and hematopoietic elements. The articulating surfaces of bone are covered with a layer of cartilage. Tendons, ligaments, and muscle attachments are inserted into cortical bone. Blood vessels penetrate the cortex and permeate the cancellous bone. A fibrous and cellular envelope covers the bone tissue surfaces. This envelope, consisting of the periosteum externally and the endosteum internally, contains the osteocytes, which are pluripotent in bone remodeling.

Bone Composition

Fresh compact bone is composed of 9% water, 11% organic matrix, and 69% inorganic salts.[1] The organic matrix consists of a noncollagenous or ground substance (10%) and collagen fibers (90%). The noncollagenous matrix consists of multiple substances, including mucopolysaccharides, glycoproteins, phosphoproteins, and phospholipids. It serves as mineralization nucleator and inhibitor and as a "glue" that occupies the space between collagen fibers. Little else is known about the precise distribution and function of the noncollagenous matrix in bone.

Collagen fibers give bone its tensile strength and provide nucleation centers for the deposition of inorganic salts. These salts, composed essentially of calcium and phosphate, give bone its compressional strength. The principal inorganic salts found in bone are

amorphous calcium phosphate (ACP) and HA. ACP is believed to be the precursor to HA, the predominant crystalline form found in mature bone. Bone composition is summarized in Figure 19-2.

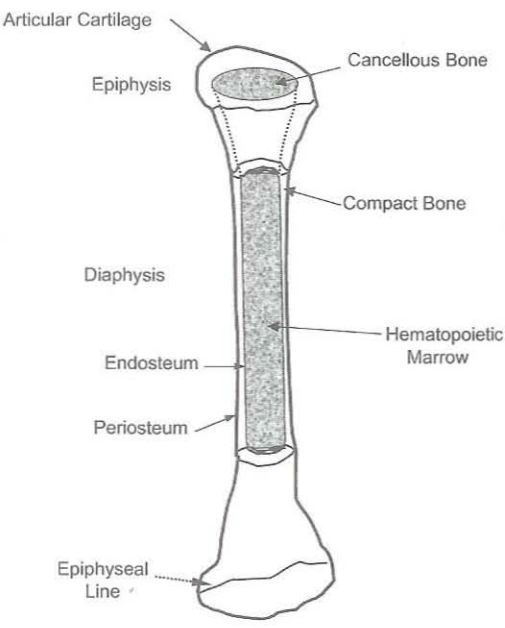

FIGURE 19-1 Diagram of bone showing the principal tissues.

Bone Formation

Osteocytes function as osteoblasts or osteoclasts. Osteoclasts are instrumental in bone resorption. Osteoblasts are bone-forming cells that lie directly on bone surfaces; they are responsible for synthesizing the organic matrix, called osteoid, that occupies the space between osteoblasts and the underlying calcified bone. Soon after collagen fibers are formed by osteoblasts, ACP precipitates on their surfaces at periodic intervals to form minute nidi that rapidly multiply and grow over days and weeks to form HA crystals. The ACP is not crystalline but is a mixture of hydrated calcium phosphates of varying Ca/P molar ratios consisting mainly of calcium monohydrogen phosphate ($CaHPO_4$, Ca/P = 1.0), octacalcium phosphate ($Ca_4H(PO_4)_3$, Ca/P = 1.33), and tricalcium phosphate ($Ca_3(PO_4)_2$, Ca/P = 1.5).[2] By a process of substitution and addition of atoms, or resorption (through osteoclastic activity) and reprecipitation, these ACP salts are converted into the well-crystallized HA ($Ca_{10}(OH)_2(PO_4)_6$, Ca/P = 1.66).

It is not known precisely what causes calcium salts to deposit in osteoid, but at least two theories have been suggested.[3] Osteoblast mitochondria can concentrate large quantities of calcium and phosphate into vesicles. The first theory is that the vesicles then migrate to the cell wall and extrude minute calcium phosphate crystals onto the osteoid to serve as nucleation centers for HA crystal growth. Another theory is that the osteoblast secrete a substance into the osteoid to neutralize an inhibitor substance (perhaps pyrophosphate) that normally prevents HA crystallization. Once the inhibitor is neutralized, the natural affinity of collagen fibers for calcium salts supposedly causes the precipitation.

HA crystals are a very stable end product of bone mineralization and do not redissolve readily. Additionally, the crystals formed are microcrystalline in nature; under physiologic conditions HA almost never forms crystals that are larger than a few hundred angstroms

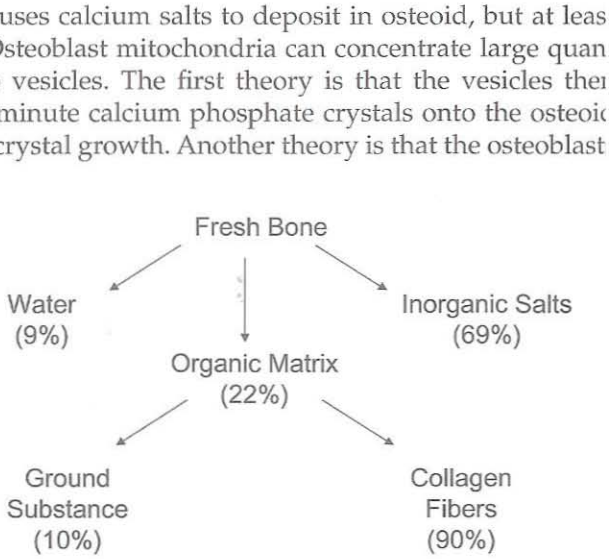

FIGURE 19-2 Bone composition.

in length, breadth, or thickness. Consequently, the HA system has a large surface area (200 m^2/gram) that provides an enormous opportunity for adsorption and surface exchange of a variety of ions. Prominent examples include Sr^{2+}, Pb^{2+}, Ra^{2+}, and Mg^{2+}, which exchange with Ca^{2+}; F^-, which exchanges with OH^-; and CO_3^{2-}, citrate, phosphate esters, diphosphonates, and pyrophosphate, which exchange with phosphate. It is precisely for this reason that radionuclide species of these substances have been used successfully to study and image the skeleton in humans and animals.

DEVELOPMENT OF BONE IMAGING AGENTS

The use of self-luminous radium paint on watch dials began in 1908, after an earlier discovery that alpha particles striking a zinc sulfide surface produced luminescence. Radium paint was made by mixing radium chloride and zinc sulfide with a binder. The first hint that radioactive material localized in bone came in 1924, when a radium dial painter developed severe osteonecrosis of the mandible and maxilla. Several other reports followed this initial discovery of the so-called "radium jaw," and the cause was traced to isotope localization in bone after chronic inhalation of radon gas, which is the radioactive daughter of radium decay, and ingestion of radium paint by licking the tip of the paint brush.

Many radionuclides have been used to study bone, but few of the earlier ones had desirable physical properties for bone imaging. The earliest use of bone-seeking radionuclides was for the treatment of bone disease and metastatic lesions. These radionuclides included ^{32}P, ^{45}Ca, ^{47}Ca, ^{89}Sr, and ^{72}Ga. In 1949, ^{72}Ga was one of the first radionuclides used to detect bone metastases, but it was unacceptable because of its high 2.5 MeV gamma energy.[4] Investigations were switched to ^{68}Ga and then to ^{67}Ga in the early 1950s, but the serendipitous finding by Edwards and Hayes[5] in 1969 that carrier-free gallium localized in soft-tissue tumors all but terminated gallium's potential for becoming a bone-imaging agent. Additionally, bone localization of radiotracer gallium required the coadministration of stable carrier gallium, which was thought to be potentially toxic.

Around 1961, clinical bone scanning had its true beginning when Charkes and Sklaroff[6] at the Einstein Medical Center in Philadelphia began to use ^{85}Sr bone scans to locate metastases for the rational application of radiotherapy. Strontium was selected because its metabolism simulated that of calcium and the gamma emission of ^{85}Sr could be measured by external detection. Additionally, bone metastasis could be detected with ^{85}Sr before it was evident on x-ray exam. According to one report in 1961, radiographic changes were demonstrated in only 56% of breast cancer patients who had shown abnormal vertebral uptake with ^{85}Sr.[7] That report noted a French study performed in 1948 whose investigators reported that a bone lesion must be 30% to 50% decalcified to be visible on x-ray.

^{85}Sr was available as the nitrate or chloride salt and was administered intravenously. Its long biologic and physical half-lives limited the adult dose to 100 μCi (3.7 MBq), which resulted in prolonged scanning times and poor counting statistics. Although the rate of bone uptake was rapid (90% of maximum in 1 hour), its slow excretion required at least a 2 day delay before scanning to improve the bone-to-background ratio. In 1964, Meckelnburg[8] introduced ^{87m}Sr-strontium citrate for bone imaging. The short 2.8 hour half-life and decay by isomeric transition lowered the radiation dose significantly below that of ^{85}Sr; this favored the use of ^{87m}Sr in children. However, its short half-life required bone scans to be performed before adequate excretion occurred, which increased the potential for false-positive and false-negative interpretation.

In 1962, Blau et al.[9] introduced ^{18}F as sodium fluoride for bone scanning. Its principal advantage was high bone-to-background ratios because of its rapid blood clearance after

intravenous injection. However, a significant logistic problem was created; its 1.8 hour half-life required that the user be located close to the ^{18}F production site. In the late 1960s and early 1970s transportation problems improved, but the isotope cost was high. ^{18}F gradually gained clinical acceptance, but then the introduction of ^{99m}Tc-labeled phosphate compounds for bone imaging brought ^{18}F use to a virtual halt.

On the basis of the prior finding that ^{32}P-labeled polyphosphate localized in the mineral phase of bone,[10] Subramanian and McAfee[11] successfully prepared a stannous chloride–reduced ^{99m}Tc-tripolyphosphate (^{99m}Tc-STPP) complex that localized in bone. This was a key contribution to the field of nuclear medicine, because it meant that the desirable properties of ^{99m}Tc could be used for studying bone. The report indicated that ^{99m}Tc-STPP achieved a skeletal uptake 65% that of ^{85}Sr only 3 hours after injection. A few months later Subramanian and colleagues[12] reported on an improved agent using synthetic long-chain polyphosphate (46 phosphate units). Other investigators also worked with polyphosphates, and a Harvard group[13] confirmed the finding by Subramanian's group that the average chain length of 40 phosphate units produced the highest bone uptake. The Harvard group, however, achieved a bone uptake of only 25% of the injected dose (ID), compared with Subramanian's reported 50% uptake. This discrepancy led to further investigation. About the same time, two studies comparing bone uptake as a function of phosphate chain length indicated that bone uptake was inversely related to chain length. This was in direct contradiction to previous reports. Several other reports were published on the use of ^{99m}Tc complexed to pyrophosphate (PPi), a two-unit phosphate chain with high bone uptake. The Harvard group reanalyzed its polyphosphate preparation as well as that of Subramanian, to find a changed composition. They found appreciable amounts of orthophosphate and pyrophosphate present. Further analyses led to the conclusion that the desirable bone-localizing property of the original long-chain polyphosphates was due to the presence of PPi, either as an impurity or as a degradation product. The formal introduction of ^{99m}Tc-pyrophosphate (^{99m}Tc-PPi) came in 1972 by Perez and co-workers[14] in Paris, France. ^{99m}Tc-PPi had high chemical purity, labeling yields with ^{99m}Tc-sodium pertechnetate were high (>90%), and its blood clearance was more rapid than that of polyphosphate.

Also in 1972, a different class of ^{99m}Tc-labeled phosphorus compounds was introduced for bone imaging. These were the diphosphonates, which are organophosphorus compounds characterized by a phosphorus-to-carbon (P–C–P) bond, in contrast to the phosphorus-to-oxygen (P–O–P) bond characteristic of polyphosphates and pyrophosphates. The diphosphonates had previously been found to inhibit dissolution of bone and crystal growth of HA in certain bone diseases. Other studies indicated that the phosphorus-to-carbon bond was more stable in vivo, because it was not broken down by phosphatases as were the phosphates.

Three groups reported almost simultaneously on ^{99m}Tc-labeled ethane-1-hydroxy-1-diphosphonate (^{99m}Tc-etidronate, or ^{99m}Tc-EHDP) for bone imaging.[15–17] The advantages claimed for ^{99m}Tc-EHDP compared with ^{99m}Tc-PPi were a slightly greater bone concentration (50% to 55% of ID for ^{99m}Tc-EHDP versus 45% to 50% of ID for ^{99m}Tc-PPi), improved in vivo stability (although this was implied), and faster blood clearance, which was its primary advantage. The blood clearance, however, was still not as rapid as that of ^{18}F.

In 1975 Subramanian et al.[18] introduced ^{99m}Tc-labeled methylene disphosphonate (^{99m}Tc-medronate, or ^{99m}Tc-MDP) for bone imaging and compared it with ^{99m}Tc-EHDP, ^{99m}Tc-PPi, and ^{99m}Tc-labeled polyphosphate. Their findings in humans indicated that diphosphonates are cleared more rapidly from the blood than pyrophosphates or polyphosphates. ^{99m}Tc-labeled polyphosphates were found to be slowest; ^{99m}Tc-MDP was found to be fastest and equivalent to ^{18}F-fluoride clearance. The slower clearance of polyphosphates and pyrophosphates was attributed in part to their higher plasma protein binding

and diffusion into red blood cells (RBCs). The fraction associated with RBCs 24 hours after injection was 22% for ^{99m}Tc-labeled polyphosphate, 60% for ^{99m}Tc-PPi, and negligible amounts for ^{99m}Tc-EHDP and ^{99m}Tc-MDP. Each agent produced excellent bone images, but high-quality images could, as a rule, be obtained 2 hours after injection with ^{99m}Tc-MDP, whereas 3 to 4 hours was often required for ^{99m}Tc-EHDP and 4 hours for pyrophosphates and polyphosphates.

In addition to achieving higher blood clearance for bone agents, higher bone affinity can also increase the bone-to-soft-tissue ratio. When one of the methylene hydrogen atoms in MDP is replaced by a hydroxyl group, hydroxymethylene diphosphonate (HMDP) is formed. The technetium complex is known as ^{99m}Tc-oxidronate (^{99m}Tc-HDP). The presence of the hydroxyl group on the carbon atom appears to increase the bone uptake of diphosphonates because it provides the opportunity for tridentate binding to calcium on the growing surface of HA crystals.[19] Experimental work in animals demonstrated that ^{99m}Tc-HDP has a higher binding affinity for apatite crystals than do ^{99m}Tc-EHDP and ^{99m}Tc-MDP.[20]

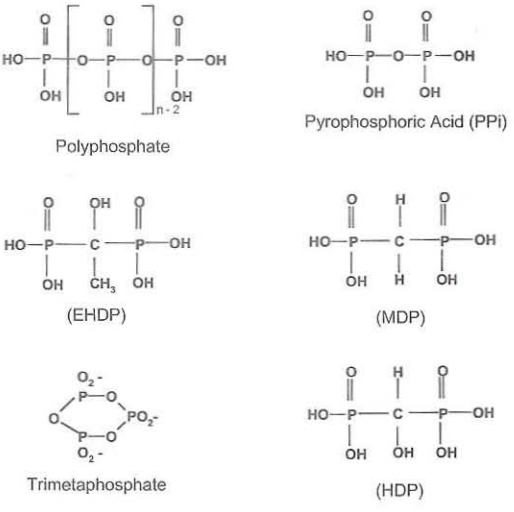

FIGURE 19-3 Chemical structures of ligands used in preparing ^{99m}Tc bone agents.

Also in 1975, a ^{99m}Tc-trimetaphosphate complex was introduced for bone imaging.[21] This cyclic phosphate was reported to have bone uptake equivalent to that for ^{99m}Tc-EHDP and tripolyphosphate. Optimum bone uptake, with minimal liver uptake, was observed when 25 to 50 mg trimetaphosphate per milligram of stannous chloride was used.

The structures of the various phosphate and diphosphonate ligands for preparing ^{99m}Tc bone agents are shown in Figure 19-3. Of these complexes, the only ones currently on the market for bone imaging are ^{99m}Tc-MDP and ^{99m}Tc-HDP. Two pyrophosphate (PPi) kits, one containing trimetaphosphate, are also approved for bone imaging, but they are used mostly for in vivo labeling of RBCs and for myocardial infarct-avid imaging.

PHYSICAL PROPERTIES OF ^{99M}TC BONE AGENTS

The ^{99m}Tc bone complexes are prepared by simply adding the required amount of pertechnetate to a sterile lyophilized kit containing a mixture of stannous ion and the appropriate ligand. The composition of various commercial kits is shown in Table 9-11 (Chapter 9). Radiochemical purity is checked by instant thin-layer chromatography for the presence of free pertechnetate and hydrolyzed–reduced technetium colloid. Formation of the colloidal impurity is favored if the ratio of phosphate to tin is too low and the pH of the reaction mixture is too high.[21] Liver uptake on clinical images has been observed when the colloid impurity is significant (Figure 19-4). Excess pertechnetate impurity is evident on the bone scan as uptake in the thyroid gland and stomach (Figure 19-5).

Technetium bone complexes can degrade over time, producing free pertechnetate.[22] While this can be counteracted by adding excess stannous ion to the kits, large amounts of Sn(II) in bone kits have been shown to interfere with the activity distribution in pertechnetate brain scans for up to 2 weeks after the administration of bone agents containing high levels of Sn(II).[23] Some bone kits were developed with low amounts of tin, but this created a stability problem because free pertechnetate was generated over time in reconstituted kits.

The oxidative degradation is promoted by atmospheric and dissolved oxygen and radiolytically generated free radicals. Nitrogen purging of ^{99m}Tc-sodium pertechnetate solutions and kits helps rid them of gaseous and dissolved oxygen, but it does not provide satisfactory protection against oxidation by free radicals. The problems associated with low-tin kits was significantly reduced by the addition of ascorbic acid or gentisic acid as antioxidants to diphosphonate bone kits (Figure 19-6).[24,25] Only gentisic acid can be used in pyrophosphate kits, because the presence of ascorbic acid causes the formation of a ^{99m}Tc-ascorbate complex that results in renal images.[26]

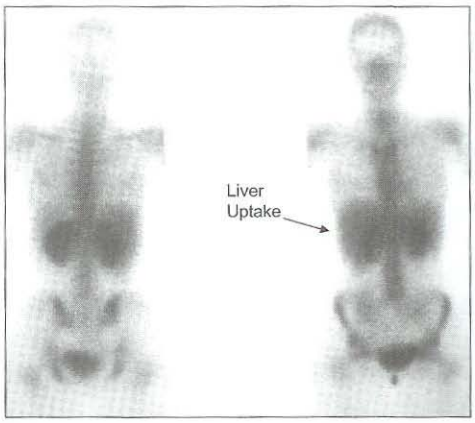

FIGURE 19-4 ^{99m}Tc-pyrophosphate (^{99m}Tc-PPi) bone scan demonstrating liver uptake due to hydrolyzed–reduced technetium impurity in the administered dose.

The antioxidants in kits are free radical scavengers that stabilize by retarding free radical reactions with the ^{99m}Tc bone complex. Radiolytically produced alkoxy ($RO^{\cdot}$) and peroxy ($RO_2^{\cdot}$) radicals can be stabilized by ascorbate or gentisate through the transfer of an H atom from the antioxidant molecule to the free radical, yielding a resonance-stabilized and nonreactive molecule, (RO_2H). This reaction is shown in Figure 9-32 (Chapter 9). Elimination of the intermediate radical by ascorbate (or gentisate) is believed to provide in vitro stability by inhibition of the slow oxidation of TcO_2 to TcO_4^-.[24] The mechanism of bone complex degradation to yield pertechnetate has been suggested to occur by initial dissociation of Tc(IV) from the stable chelate and hydrolysis into TcO_2 with subsequent oxidation to TcO_4^-, rather than by a direct interaction of the chelate with oxygen.[27]

Other kit formulation factors important to the clinical performance of technetium bone complexes include proper ligand-to-tin ratio and the amount of bone agent injected. Tofe and Francis[28] found that the optimum EHDP-to-stannous chloride weight ratio was between 5:1 and 50:1 based on binding affinity to HA in vitro. Ratios of 12:1 and 50:1 gave the same biodistribution in animals. Subramanian et al.[18] obtained optimal skeletal localization with MDP-to-tin ratios of 10:1 at doses between 0.01 and 0.5 mg MDP per kilogram of body weight, with no significant difference in distribution. Bevan et al.[29] found that liver uptake of ^{99m}Tc activity occurred when the Na_2HMDP load was above 0.1 mg per kilogram of body weight in rats, guinea pigs, and dogs. These findings were taken into consideration when HMDP kits were formulated for human use. Ponto[30] has compiled an

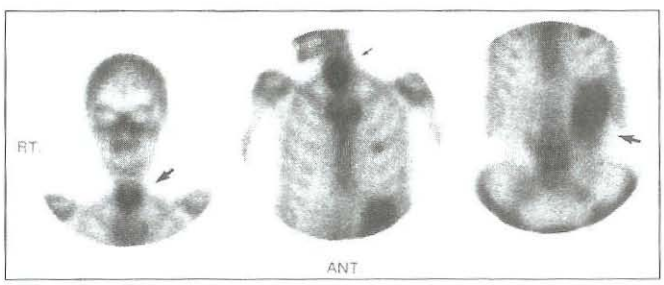

FIGURE 19-5 Bone scan demonstrating thyroid and stomach activity resulting from excess pertechnetate impurity in the bone agent injected.

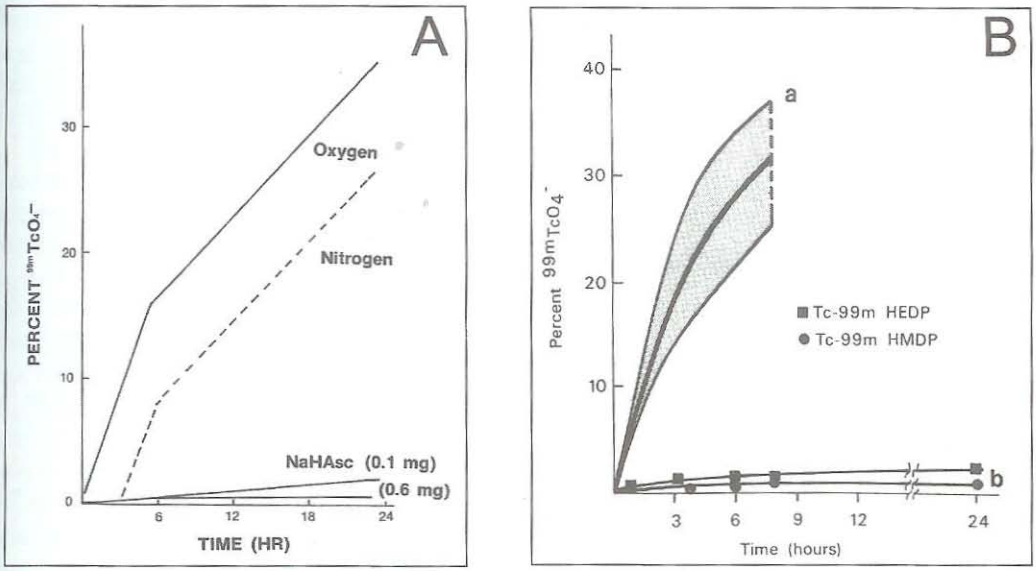

FIGURE 19-6 (A) In vitro stability of ^{99m}Tc-HEDP (^{99m}Tc-EHDP) without stabilizer, in vials under oxygen (air) and nitrogen atmosphere (top two curves); and with stabilizer (0.1 mg and 0.6 mg sodium ascorbate) under either oxygen (air) or nitrogen atmosphere (bottom two curves). (Reprinted with permission of the Society of Nuclear Medicine from reference 24.) (B) In vitro stability of ^{99m}Tc-HEDP and ^{99m}Tc-HMDP under (a) oxygen (no stabilizer) or (b) nitrogen or oxygen (with stabilizer). Stabilizer was 0.56 mg of either ascorbic acid or gentisic acid. (Reprinted with permission of the Society of Nuclear Medicine from reference 25.)

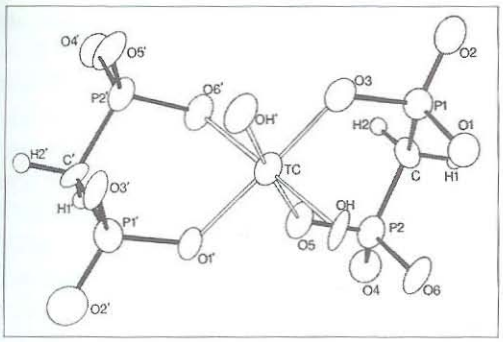

FIGURE 19-7 Perspective view of a portion of the $[Tc(OH)(MDP)^-]_n$ infinite polymer (MDP represents methylene diphosphonate in an unknown protonation state). Hydrogen atoms bonded to oxygen, lithium counterions, and waters of hydration are omitted for clarity. (Reprinted with permission of the Society of Nuclear Medicine from reference 31.)

excellent review of how formulation factors of ^{99m}Tc bone agents and other technetium compounds affect their biodistribution.

Analysis of technetium bone complexes indicates that they are not a single well-defined chemical species but are probably mixtures of short- and long-chain polymers.[31] The polymeric structure of $[Tc(OH)MDP^-]_n$ is characterized by technetium atoms bridged by MDP and OH ligands, and the MDP ligands are in turn bridged by technetium atoms, as shown in Figure 19-7. High-performance liquid chromatographic (HPLC) analysis of preparations with varying concentrations of technetium has shown that polymeric complexes, evidenced by multiple HPLC peaks, are formed when millimolar concentrations of technetium are present, whereas preparations made with no-carrier-added technetium produce only one peak.[32] It has been suggested that multiple complex formation may affect the biodistribution and elimination of ^{99m}Tc-diphosphonate complexes.

BIOLOGIC PROPERTIES OF ^{99m}TC BONE AGENTS

The biodistribution of ^{99m}Tc bone agents in humans and animals has been compared.[18] After intravenous administration these agents are rapidly distributed in the body, and by 3 hours most of the activity is located in the skeleton, urine, and blood. The whole-blood activity as a fraction of the ID at this time is 8% for ^{99m}Tc-PPi, 5% for ^{99m}Tc-EHDP, and 3% for ^{99m}Tc-MDP. For Tc-PPi the blood activity is primarily found in plasma protein (43%) and RBCs (30%). The blood activity of the diphosphonates is primarily associated with protein, with no significant binding to RBCs. Consequently, the blood clearance rates for ^{99m}Tc-EHDP and ^{99m}Tc-MDP are significantly faster than those of ^{99m}Tc-PPi, with ^{99m}Tc-MDP being the most rapid (Figure 19-8). The blood clearance rate of ^{99m}Tc-HDP is similar to that of ^{99m}Tc-MDP.[29] The 3 hour urine accumulation in humans is 43% for PPi, 56% for ^{99m}Tc-EHDP, and 59% for ^{99m}Tc-MDP. The absolute average bone concentration of the diphosphonates in rabbits has been shown to be 1.6 times higher than that of ^{99m}Tc-PPi. No statistically significant difference has been found between the bone concentration of ^{99m}Tc-EHDP and ^{99m}Tc-MDP.[18] In humans, approximately 45% to 55% of the injected activity of ^{99m}Tc-EHDP and ^{99m}Tc-MDP localizes in bone within 3 hours.[13]

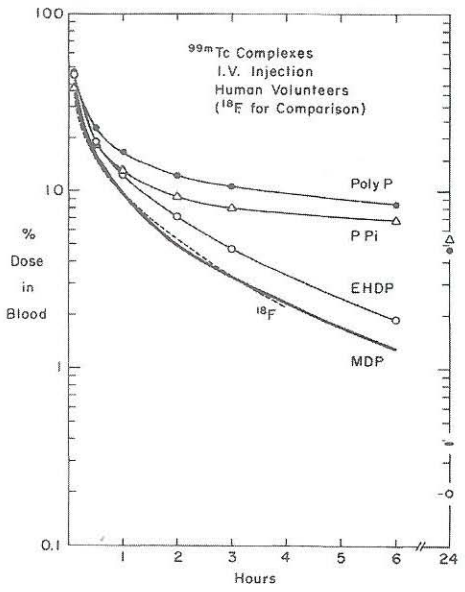

FIGURE 19-8 Blood clearance of ^{99m}Tc-MDP in humans compared with three other ^{99m}Tc complexes and ^{18}F-sodium fluoride (corrected for physical decay). (Reprinted with permission of the Society of Nuclear Medicine from reference 18.)

In a comparison between diphosphonates, the blood clearance of ^{99m}Tc-HDP was similar to ^{99m}Tc-MDP up to 3 hours but faster thereafter.[29] In vitro and in vivo bone uptake experiments have demonstrated that ^{99m}Tc-HDP has significantly higher bone affinity than ^{99m}Tc-EHDP and ^{99m}Tc-MDP.[33] Indirect whole-body retention measurements in humans have demonstrated that ^{99m}Tc-HDP has a 20% higher skeletal uptake than ^{99m}Tc-MDP.[34] Despite these differences, clinical comparisons of ^{99m}Tc-HDP, ^{99m}Tc-EHDP, and ^{99m}Tc-MDP have shown no significant difference in lesion detection.[35–37] Earlier comparisons between ^{99m}Tc-MDP and ^{99m}Tc-PPi showed higher-quality bone scans with ^{99m}Tc-MDP but no obvious difference in diagnostic sensitivity.[38]

In summary, several ^{99m}Tc bone agents have been developed since 1971. The first was ^{99m}Tc-STPP, then ^{99m}Tc-polyphosphate, followed by ^{99m}Tc-PPi, ^{99m}Tc-etidronate (^{99m}Tc-EHDP), ^{99m}Tc-medronate (^{99m}Tc-MDP), and finally ^{99m}Tc-oxidronate (^{99m}Tc-HDP). In general, each successive agent yielded improved scan quality because of higher bone-to-soft-tissue ratio. Although there appears to be no significant difference in lesion detection with the last four agents, ^{99m}Tc-MDP and ^{99m}Tc-HDP are preferred because of their higher-quality, cleaner-looking bone images. ^{99m}Tc-EHDP is no longer marketed.

Localization Mechanisms

Bone localization of the ^{99m}Tc complexes requires adequate blood flow to bone and the absence of any diffusional barrier during transit from blood to the bone surface.[39] The

chemical composition of the bone surface and the structural properties of the bone agent itself are important factors in the binding of ^{99m}Tc complexes to bone.

The fluoride anion (F^-) reacts with bone by isomorphous exchange of fluoride with hydroxyl (OH^-) in HA. An additional factor that made ^{18}F-fluoride a useful bone imaging agent was its high bone-to-background ratio because of its low protein binding (around 5%) and lack of RBC binding at physiologic pH.[40]

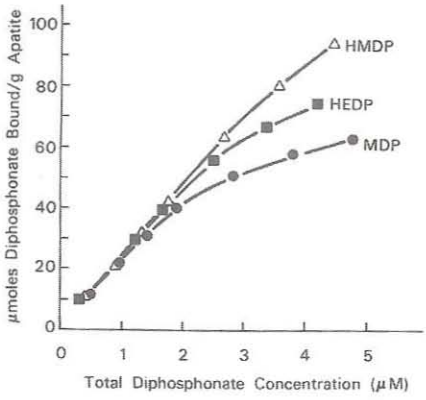

FIGURE 19-9 Adsorption of ^{14}C-labeled MDP, HEDP, and HMDP (HDP) on crystalline hydroxyapatite. (Reprinted with permission of the Society of Nuclear Medicine from reference 20.)

The anionic ^{99m}Tc-labeled phosphate and phosphonate complexes are believed to interact with bone by binding to Ca^{2+} ions in bone crystals. The process is referred to as chemisorption. Localization occurs primarily in the mineral phase of bone, with insignificant binding to the organic matrix.[20] In vitro and in vivo experiments have shown that ^{99m}Tc-diphosphonates bind to ACP to a higher degree than to crystalline HA.[20,33] The hypothesis for this is that ACP contains newly formed apatite crystallites that have a crystal-growing face with a chemical configuration of calcium ions best suited for binding to oxygen atoms in the diphosphonate ligand.[20] As bone matures, this configuration is altered so that less uptake of bone agent occurs in mature bone. The difference in binding between ACP and HA is the basis for detecting bone lesions, because areas of increased osteogenic activity contain higher concentrations of ACP relative to HA. It is important to note that the bone scan does not identify a specific pathologic process (e.g., trauma, infection, or cancer) but rather shows the effect of a pathologic process on normal bone. However, characteristic patterns of activity distribution do occur in certain conditions such as Paget's disease.

The mechanism of localization of ^{99m}Tc-diphosphonate complexes in bone is not entirely known but appears to depend on the chemical structure of the ligand in the complex. The ligands EHDP, MDP, and HDP are geminal diphosphonates, which means that both phosphonate moieties are attached to the same carbon atom. This places the oxygen atoms on the phosphonate groups at a distance and position conducive to binding with calcium in bone.[19] The type of substitution at the two remaining sites on the central carbon atom can also influence the agent's binding to bone. Binding to calcium in bone is highest when one of these substituents is hydroxyl and the other is hydrogen, as in HDP.[20] This is illustrated in Figures 19-9 and 19-10. It is proposed that the triangular face of the HDP ligand allows optimal tridentate binding to calcium through both geminal diphosphonate oxygen atoms and the hydroxyl group. Binding of EHDP to calcium, which also has three oxygen-binding groups, is less likely because of steric hindrance by the methyl group. MDP has lower binding affinity because it can undergo only bidentate binding. An additional factor that may contribute to binding affinity is the relative solubilities of the complex's calcium salts formed when they react at the bone surface. In this regard the decreasing order of solubility has been determined to be MDP > EHDP > HMDP ≥ PPi.[20]

Dosing and Biodistribution

The typical adult dose of ^{99m}Tc-HDP or ^{99m}Tc-MDP for bone imaging is 20 mCi (740 MBq) given intravenously. Imaging is generally performed 2 to 3 hours after injection to allow

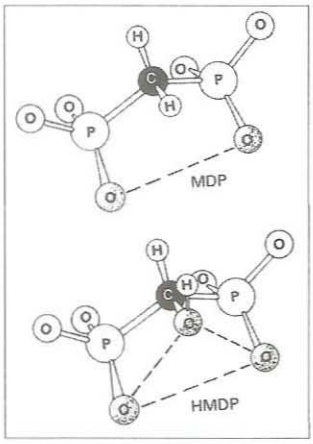

FIGURE 19-10 Comparison of HMDP (HDP) and MDP structures, indicating the potential of tridentate binding in hydroxylated molecules such as HMDP. (Reprinted with permission of the Society of Nuclear Medicine from reference 29.)

plasma and tissue background activity to be excreted. Approximately 40% to 50% of the injected activity localizes in bone, with the remainder excreted in the urine.

On the bone image the normal skeleton demonstrates uptake of radioactivity, and there may be some evidence of activity in the kidneys and urinary bladder. Bone lesions generally appear as focal areas of increased activity. Diffusely increased concentration in the entire skeleton may be seen in patients with hyperparathyroidism, which causes a generalized increase in osseous remodeling.[41]

In contrast to these patterns are the cold lesions seen with vaso-occlusive disease, metal prostheses, and the occasional site where tumor has replaced most of the bone. Often, cool areas or areas of mildly diminished activity concentration demarcate a site of external radiation therapy where radiation-induced vascular changes have occurred and osteocytes have been destroyed.

The pattern of tracer distribution after injection often provides diagnostic information in certain types of disease, such as infection, where local blood flow patterns and bone uptake (or lack thereof) provide the information necessary to distinguish soft-tissue infection from bone infection. For example, early in the course of osteomyelitis standard radiographs are usually normal, but the sensitivity of bone scanning is frequently helpful. A three-phase bone scan is typically done in this situation. The three-phase study includes a perfusion phase, an equilibrium or "blood pool" image, and a delayed 2 hour image showing bone metabolic activity. A typical perfusion study involves 5 second images for 90 seconds to observe blood flow to the affected area. This is followed by a blood pool image at 3 minutes to demonstrate extracellular accumulation of tracer. The delayed image demonstrates if there is any bone involvement (osseous remodeling). The interpretation of the three-phase bone scan is shown in Table 19-1.

TABLE 19-1 Activity Distribution in a Three-Phase Bone Scan

	Activity Accumulation		
Disease	**Phase 1: Blood Flow Image**	**Phase 2: Blood Pool Image**	**Phase 3: Delayed Image**
Cellulitis	↑	↑	Normal
Osteomyelitis	↑	↑	↑
Noninflammatory[a]	Normal	Normal	↑

[a] For example, degenerative joint disease, chronic inactive osteomyelitis.

TABLE 19-2 Radiation Dose Estimates for ^{99m}Tc Bone Complexes

Tissue	Adult Radiation Absorbed Dose (rad[cGy] per 20 mCi)		
	^{99m}Tc-HDP	^{99m}Tc-MDP	^{99m}Tc-PPi
Bone surfaces	3.80	2.60	2.80
Urinary bladder wall	1.60	2.40	1.80
Red marrow	0.56	0.40	0.46
Kidneys	0.44	0.64	0.48
Ovaries	0.26	0.24	0.28
Testes	0.17	0.17	0.20
Effective dose equivalent (rem)	0.46	0.44	0.44

Source: Reference 42 (dosimetry tables).

Dosimetry

Estimates of radiation dose to selected organs from ^{99m}Tc bone agents are listed in Table 19-2.[42] The dose to the skeleton is an average adult dose that assumes uniform skeletal distribution; however, bone distribution often is not uniform, with higher concentrations in the vertebrae and ribs than in long bones.[18] Additionally, bone activity has been shown to be two to three times higher in the epiphyseal region than in the diaphysis of growing long bones. This distribution is evident particularly in pediatric patients; the growth plate has a much higher concentration than in adults. The radiation dose to the pediatric growth plate has been estimated to be as much as 6 to 8 times higher than the dose to the adult skeleton.[43] The critical organ is bone, and the next highest dose is to the urinary bladder, reflecting the high urinary excretion of the injected dose. The bladder dose is typically based on either a 2.4 hour or 4.8 hour voiding interval. The dose can be reduced if the patient voids more frequently; frequent voiding should be recommended to the patient at the time of dose administration. Dosimetry estimates reported in the literature and product package inserts differ somewhat because of variations in the biokinetic models used for calculating absorbed dose.

Adverse Effects

No significant toxic effects have been reported for ^{99m}Tc bone agents at the dose normally administered. The usual dose range for ^{99m}Tc-PPi is 0.02 to 0.2 mg PPi per kilogram of body weight; for ^{99m}Tc-diphosphonate it is one-fifth to one-half that amount. A first level of potential toxic effect is related to the complexing of bone agents with serum calcium. With PPi, tetany in rats is produced by 22 mg/kg and electrocardiographic changes indicative of hypocalcemia are seen at 12 mg/kg intravenous doses.[44] If these doses are extrapolated to humans, the safety factor between a diagnostic dose and the lowest dose for minimally detectable hypocalcemia as noted by electrocardiogram is 55.[18]

Few adverse reactions to the administration of ^{99m}Tc bone complexes have been noted. The frequency of reactions to ^{99m}Tc-MDP reported in 1984 was 0.5 per 100,000.[45] Reported adverse effects of ^{99m}Tc-MDP include skin rash and transient symptoms of headache, dizziness, nausea, myalgia, and fever.[46]

Altered Biodistribution of Bone-Imaging Agents

Altered biodistribution of bone-imaging agents labeled with ^{99m}Tc has been associated with drugs and treatment regimens.[47,48] Intense renal parenchymal uptake of bone agent has been reported in children treated with vincristine, doxorubicin, and cyclophosphamide. The

mechanism of renal uptake is unknown. Long-term steroid therapy induces bone mineral depletion and has been shown to cause a generalized decrease in skeletal uptake of bone-imaging agents. Bilateral breast uptake of ^{99m}Tc-PPi has been reported in a man treated with diethylstilbestrol for prostate cancer. Several reports have demonstrated abnormal distribution and localization of ^{99m}Tc bone agents because of iron. Localized activity has occurred at sites where intramuscular iron–dextran has been injected; this may be due to localized hyperemia or complexation of the bone agent with iron. Plasma iron overload has been associated with decreased skeletal uptake of bone agents in several cases. Technetium diphosphonates have shown splenic uptake in sickle cell disease, which may be related to increased iron concentration. Increased liver uptake of ^{99m}Tc-diphosphonates has been shown to occur with increased levels of plasma aluminum; this has also been documented in controlled animal experiments. A so-called sickle sign, an area of diffuse activity around the calvaria, has been observed on bone scans in 56% of breast cancer patients receiving intensive cytotoxic therapy.

Other maldistributions have been described and more detail provided by Hladik et al.[47] and Lentle et al.[48] Although it is difficult to determine the exact causes of these maldistributions, it is important to know that they can occur for many reasons that may not be associated with the particular disease being evaluated by the bone scan.

NUCLEAR MEDICINE PROCEDURES

Rationale

Bone scanning continues to be a mainstay of general nuclear medicine imaging. The most common indication for a whole-body bone scan is in the work-up of metastatic disease. However, there are many other indications for bone imaging, including the evaluation of trauma or occult fractures, osteomyelitis, bone pain, bone tumors, bone infarcts, avascular necrosis, arthritic disease, reflex sympathetic dystrophy, certain metabolic disorders, viability of bone grafts, suspected loosening or infection of an orthopedic prosthesis, and heterotopic bone formation.

Bone scans have a very high sensitivity for detecting metastasis to bone. Bone lesions can usually be detected much earlier than with plain film x-rays, because bone scans demonstrate focal areas of increased osseous remodeling that often precede the structural changes seen on plain films. The degree of radiopharmaceutical uptake in bone depends on several factors. The most important are thought to be blood flow and extraction efficiency.[49] An increase in either blood flow or extraction efficiency leads to increased radiotracer uptake in bone. There is decreased radiotracer accumulation in areas of decreased blood flow, such as a bone infarct. Decreased focal accumulation of radiotracer is sometimes seen with metal prostheses and in the occasional site where tumor has replaced most of the bone.

Procedure

Before administration of the radiopharmaceutical, it is important to understand the reason for the exam and to obtain a relevant patient history. If the problem is localized or there is a question of infection, a three-phase bone scan may be useful in evaluating blood flow and blood pooling in the region in addition to standard delayed imaging to detect the presence of osseous remodeling. This requires that the patient be positioned and imaged with the gamma camera during intravenous administration of the radiopharmaceutical. Also, the site of radiopharmaceutical injection should be away from the site of suspected

injury or pathology. Often there is partial extravasation of the radiotracer in the soft tissue at the site of administration, which can make this area difficult to evaluate.

Although bone scans are very sensitive for osseous remodeling, they are not very specific. A patient history can help increase the specificity of the exam. The patient should be asked about any history that might affect the bone scan results. This could include prior fractures, surgeries that have involved bone, recent trauma, cancer history, known bony lesions or metastatic disease to bone, prosthetic implants, radiation therapy, and osteomyelitis. If there is question of a fracture in a younger person, localized spot imaging of the suspected area is usually performed. Whole-body bone scans are performed if there is a suspicion or history of cancer. Single-photon emission computed tomography (SPECT) can be used to improve detection or rule out bony lesions in patients with localized pain, such as in the lower back.

Once the history is obtained, the reason for the exam is understood, and the appropriate imaging procedure has been selected, the adult patient is usually injected with 20 to 30 mCi (740 to 1110 MBq) of a ^{99m}Tc-diphosphonate compound intravenously. If blood flow imaging is to be performed, the region of interest is positioned on the gamma camera prior to injection. One- to two-second-per-frame images of the region are obtained for 30 to 60 seconds during administration of the radiotracer. After this, blood-pool images of the region are obtained within 10 minutes after administration of the radiotracer. Standard imaging is usually done 2 to 4 hours after injection. Diphosphonates are rapidly cleared from the blood and accumulate in the skeleton and in the urine. Two to four hours after administration, approximately 50% of the diphosphonate radiotracer should be adsorbed onto the mineral phase of bone; most of the rest is cleared by the kidneys. After administration of the radiopharmaceutical and before imaging, the patient is encouraged to drink fluids. Unbound diphosphonates are rapidly cleared by the kidneys. Having the patient drink fluids and void just prior to imaging helps reduce soft-tissue retention and minimize radiation dose to the bladder.

Radiopharmaceuticals

The most commonly used radiopharmaceuticals for bone scanning are the ^{99m}Tc-diphosphonates such as ^{99m}Tc-MDP and ^{99m}Tc-HDP. In adults, the administered dose is usually between 20 and 30 mCi (740 to 1110 MBq) given intravenously. In children, the dose is determined by weight, usually 250 to 300 μCi/kg (9.25 to 11.1 MBq/kg) with a minimum of 1 to 2.5 mCi (37 to 92.5 MBq).[49] Unless there are contraindications, patients should be well hydrated after injection.

Interpretation

The normal whole-body bone scan varies with the age of the patient. In the child, there is normally intense, symmetric radiotracer uptake in the growth plate regions of the long bones (Figure 19-11). These become less intense in the older child and teenager (Figure 19-12). Once growth plate fusion is complete in the adult, the symmetric increased epiphyseal uptake is no longer present (Figure 19-13).

In the adult, focal areas of increased uptake in the cervical spine that have a lateral and posterior location typically represent degenerative change. Areas of more prominent skeletal uptake are normally seen in the acromioclavicular joints, sternoclavicular joints, sternum, and iliac crests. There is increased activity in the nasopharyngeal region in the skull. In general, the distribution of the radiopharmaceutical should be symmetric from side to side in the skeleton. Focal areas of increased activity represent areas of increased osseous remodeling or repair. Asymmetric focal areas of either increased or decreased

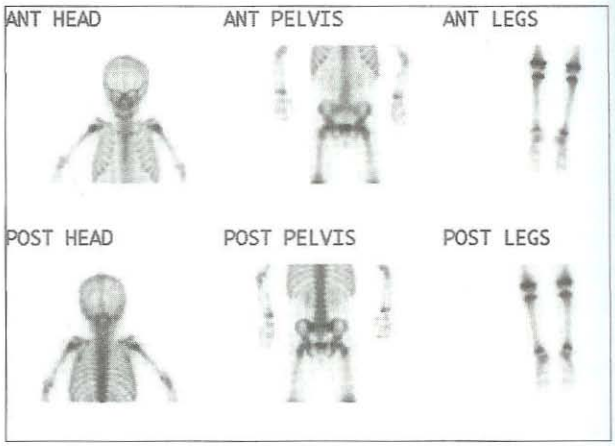

FIGURE 19-11 Normal bone scan in a 2 year old girl. Note the symmetric, increased uptake in the epiphyseal and metaphyseal growth plate regions, which is normal in this age group.

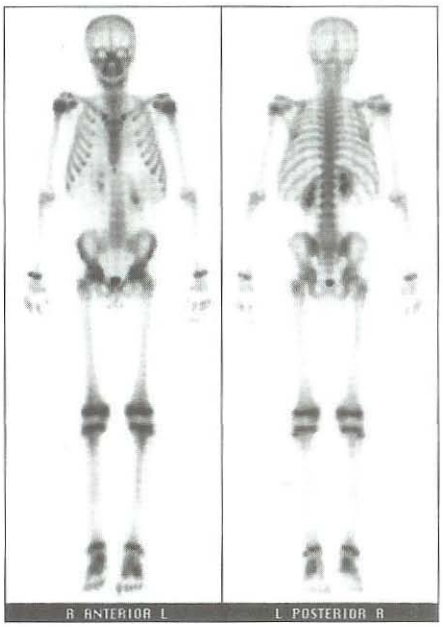

FIGURE 19-12 Normal bone scan in a 13 year old boy. There continues to be increased physiologic uptake in the growth plates, which is normal.

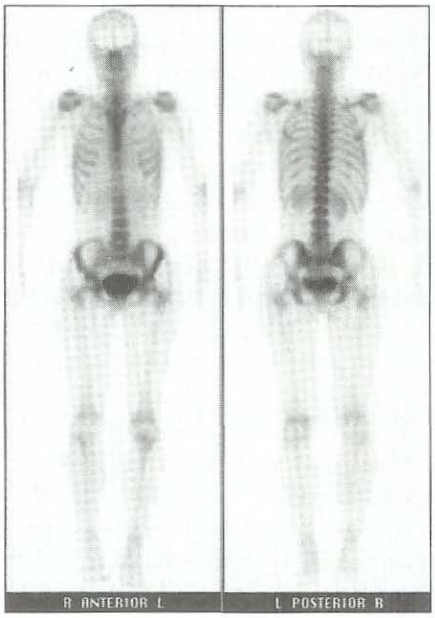

FIGURE 19-13 Normal bone scan in an adult. The epiphyseal growth centers have fused and no longer demonstrate increased uptake. The activity in the fused growth centers is now similar to that in the adjacent bone.

radiotracer uptake are abnormal and should be analyzed in the context of the patient's history.

Most fractures can be detected as focal areas of increased radiotracer uptake within 24 hours after injury.[50] Early on, the increased radiotracer uptake in bone is secondary to hyperemia. In the first few weeks after injury, there is generalized increased activity in the region of the fracture. The fracture becomes more prominent and focal over the next 2 to 3 months. After this, diphosphonate uptake at the fracture site gradually decreases to the same intensity as in the normal surrounding bone. Most fractures return to normal on the bone scan within 3 years.

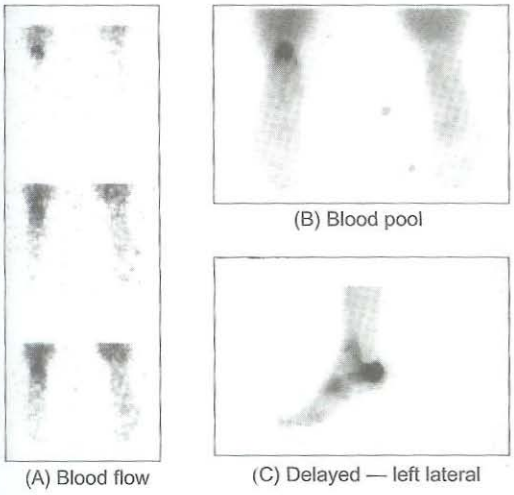

FIGURE 19-14 Stress fracture in a patient with pain in the left foot after trauma. Three-phase bone scan of the feet demonstrates increased blood flow (A) and increased blood pool (B) in the posterior left foot. Delayed images (C) obtained 3 hours after administration of ^{99m}Tc-HDP demonstrate increased osseous remodeling in this patient with a calcaneal fracture. An x-ray obtained earlier was read as negative.

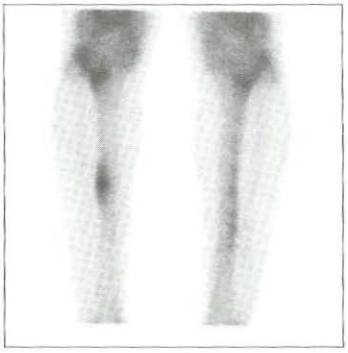

FIGURE 19-15 Anterior image of the tibias in a jogger with bilateral tibial pain. The mild, patchy increased cortical uptake seen along the left tibia represents shin splints. The more focal area of increased osseous remodeling in the right tibia represents a stress fracture.

Many traumatic fractures, such as displaced fractures, are easily seen on plain x-rays. However, some fractures can be subtle or show no abnormality on plain film x-ray. Stress fractures or fatigue fractures are the result of repeated trauma and are common in athletes. These fractures begin as microfractures that are painful but show no abnormality on plain film. It usually takes a week to 14 days to demonstrate an anatomic abnormality on x-rays after a stress fracture. If there is continued trauma, the stress fracture can progress to a complete fracture. In a bone scan, a stress fracture is typically seen as a focal area of increased osseous remodeling at the fracture site. On a three-phase bone scan there is also increased blood flow and blood pooling to the area (Figure 19-14).

Shin splints, a painful periosteal reaction to stress along muscle insertions, are common in runners. Unlike stress fractures, shin splints do not progress to fracture. Shin splints are usually seen as increased radiotracer uptake along the cortical shaft of the tibia. They frequently involve more than one-third of the length of the tibial shaft. On a three-phase bone scan, they do not demonstrate increased blood flow and blood pooling of radiotracer. Shin splints and tibial stress fractures commonly coexist in the same patient, and it is important to differentiate between them to determine the proper therapy (Figure 19-15). If a delay in diagnosis is acceptable, plain film imaging after 10 to 14 days can be done. However, if a delay in diagnosis is not acceptable, such as in a marathon runner in training, three-phase bone scanning is a sensitive means of evaluating for stress fracture.[51]

Osteomyelitis, infection of the bone, can be related to a penetrating injury such as a puncture wound or to spread of infection from the adjacent soft tissues or via the blood. Early diagnosis is important for successful treatment. Osteomyelitis is more difficult to treat than soft-tissue infection (cellulitis). Usually, cellulitis responds to short-term treatment with antibiotics, whereas osteomyelitis requires long-term antibiotic therapy and possibly surgery. Thus, distinguishing between the two is important. Bone scanning will demonstrate increased osseous remodeling secondary to acute osteomyelitis before there

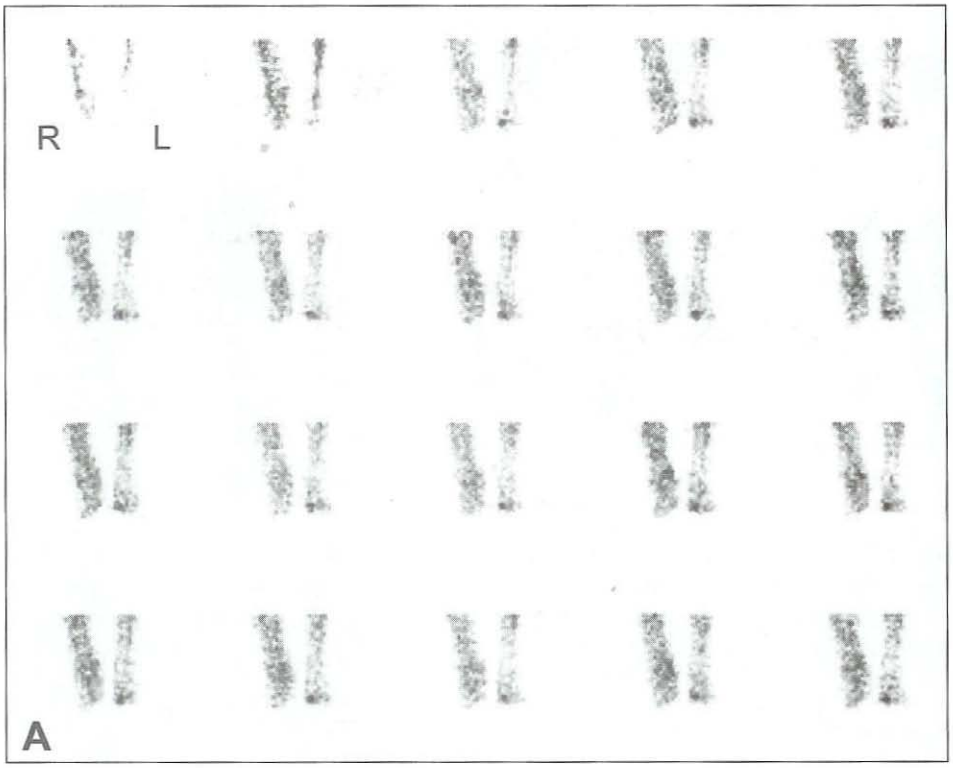

FIGURE 19-16 A patient with an ulcer on the right heel. Anterior (A) and posterior (B) blood flow images demonstrate increased blood flow to the right heel. There is also increased blood flow to the left great toe. Increased blood pooling (C) is also seen in these regions. On the delayed images (D) of the feet, there is increased osseous remodeling in these areas as well. Increased blood flow, blood pool, and osseous remodeling in the calcaneus was consistent with osteomyelitis. There was no associated ulceration on the left great toe. The similar pattern in the toe was likely due to trauma.

are anatomic changes that can be seen on plain film x-rays. Improvements in bone scanning along with antibiotics and surgical techniques have helped reduce the morbidity associated with osteomyelitis.[52] In general, osteomyelitis will demonstrate increased blood flow, increased blood pool, and prominent delayed uptake in the bone within 48 to 72 hours of the onset of infection in a three-phase bone scan (Figure 19-16).[53] Evidence of bone destruction on x-rays is not appreciated for 10 to 14 days.[54] Cellulitis will demonstrate increased blood flow and blood pool but will not demonstrate prominent uptake in the bone on the delayed imaging.

One of the most common indications for a whole-body bone scan is evaluation of metastatic involvement in bone for cancer staging. Also, serial bone scintigraphy in patients with known metastatis to bone can be helpful in planning radiation treatment and monitoring response. Bone scintigraphy has a high sensitivity for detecting metastatic disease to bone and evaluating the extent of involvement. Bone scanning is particularly useful in patients with nonosseous cancers that have a high tendency to metastasize to bone, such as malignancies of the prostate, breast, lung, kidney, and thyroid gland (Figure 19-17). Bone metastases most frequently involve the axial skeleton (skull, spine, and thoracic girdle). When there is extensive involvement of the skeleton, metastases to the appendicular skeleton, the pelvis, and upper and lower extremities may also be seen. When there is diffuse involvement of the skeleton in widespread metastatic disease, the

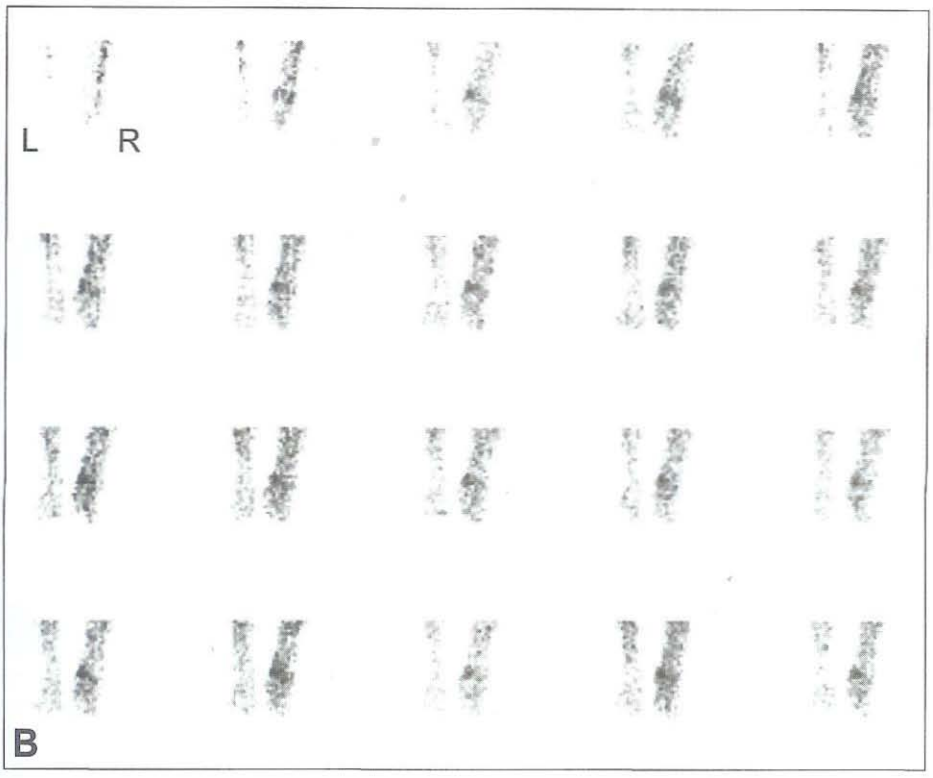

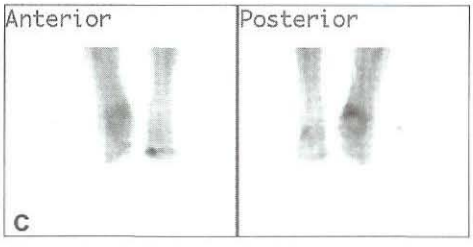

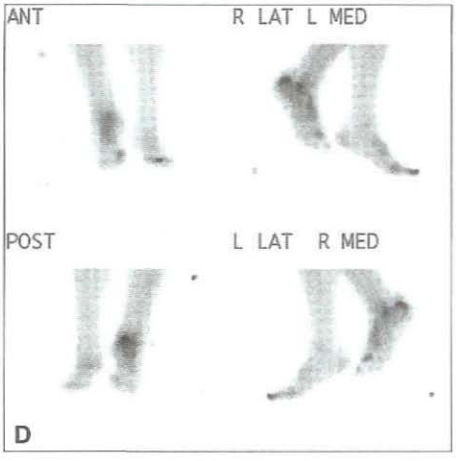

FIGURE 19-16 (Continued)

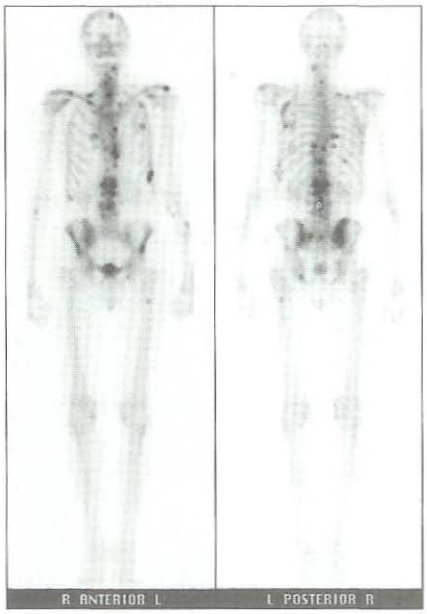

FIGURE 19-17 Anterior and posterior whole-body images demonstrating multiple abnormal focal areas of osseous remodeling in a patient with prostate cancer and metastatic disease to bone.

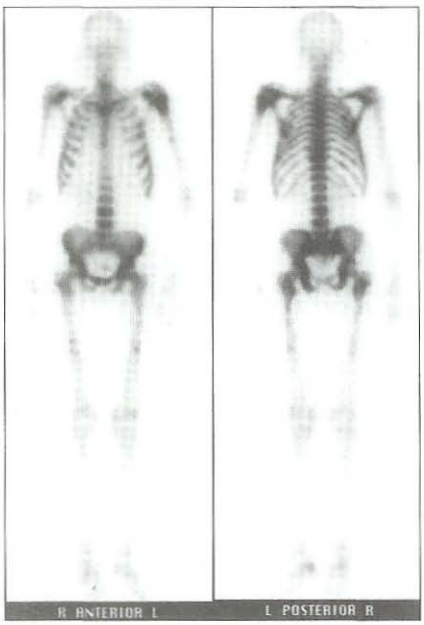

FIGURE 19-18 "Superscan" in a patient with prostate carcinoma and widespread metastatic disease to bone. The skeleton is diffusely involved with metastatic disease. There is a high bone-to-soft tissue background ratio and the kidneys are barely visualized.

lesions can become confluent, resulting in a deceptively normal-appearing bone scan called a "superscan." In such a scan there is little to no renal uptake, a high bone-to-background soft tissue ratio, and greater uptake in the axial skeleton than in the appendicular skeleton (Figure 19-18). Superscans can also be seen with metabolic conditions such as hyperparathyroidism.

Hypertrophic pulmonary osteoarthropathy is a nonneoplastic process often seen with lung cancer. Intense, often patchy, pericortical uptake is seen in the long bones; this is sometimes referred to as the "tramtrack sign" (Figure 19-19). These skeletal manifestations often regress after excision of the pulmonary lesion.[55]

Primary bone tumors can often display prominent radiotracer uptake on bone scans (Figure 19-20). Computed tomography and magnetic resonance imaging are most useful for evaluating the extent of the tumor margin in bone and extension into the soft tissues. However, bone scintigraphy can be useful in determining whether there are distant metastases (Figure 19-21).

Bone scanning can also be useful in evaluating metabolic bone disease.[56] A bone scan can determine the extent of the disease and help evaluate response to therapy. Sometimes the bone scan can even be diagnostic. Paget's disease (osteitis deformans) is a disease of unknown etiology that begins with active resorption of bone. This is followed by a mixed phase of both resorption and bone formation and then a sclerotic phase of bone formation. It is relatively common in temperate climates, with a prevalence of 3% to 4% in people over 55 years of age.[57] The disease has a classic appearance on a bone scan. There is often very prominent uptake of the radiotracer in bone, involving the pelvis, segments of long bones, and the skull (Figure 19-22).

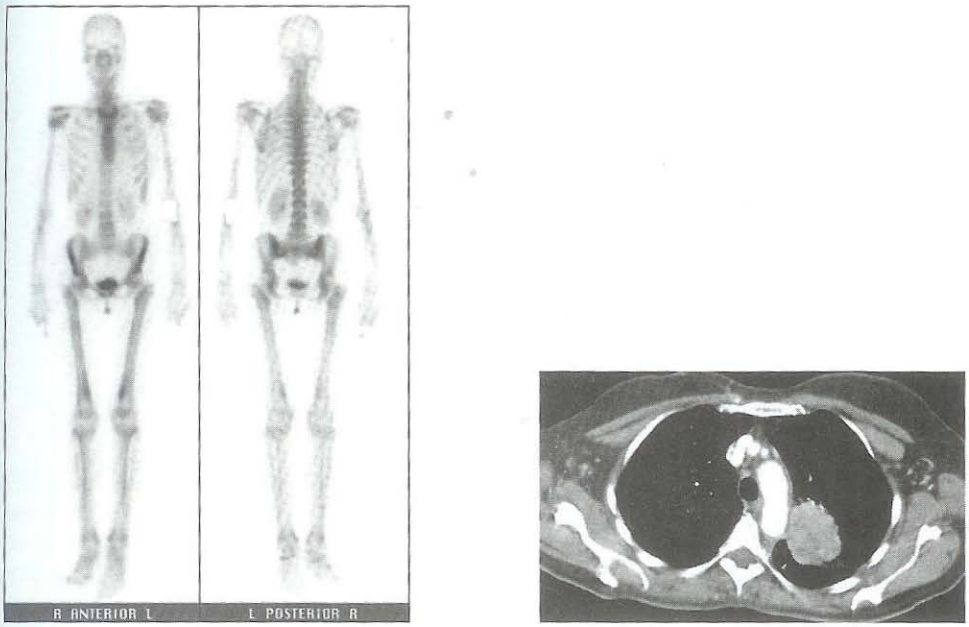

A B

FIGURE 19-19 Hypertrophic pulmonary osteoarthropathy in a patient with lung cancer. (A) There is diffusely increased osseous remodeling along the cortical shafts of the femurs, which is secondary to lung cancer in this case. Note the focal area of increased soft tissue uptake in the left chest on the posterior whole-body image between the fifth and sixth ribs, representing uptake in the patient's lung mass. (B) CT image demonstrating left apical lung mass.

Gouty arthritis is a recurrent arthritis of the peripheral joints that occurs as a result of monosodium urate crystal deposition in joints and tendons. Hyperuricemia is most commonly associated with decreased renal clearance of urate. The initial symptom is acute monoarticular or polyarticular pain that is often nocturnal. Over time, insoluble crystals precipitate into joints, which can evolve to permanent joint deformities (Figure 19-23).

Avascular necrosis of bone is an uncommon condition characterized by occlusion of the nutrient artery to bone. The most common sites include the femoral head, distal femoral condyles, and humeral head, which are vulnerable because of poor collateral blood supply. In the early stages of avascular necrosis, decreased blood activity and osseous uptake at the site appear as a cold spot on the bone scan (Figure 19-24). In later stages of the disease, collateral circulation causes increased blood activity with osseous remodeling and evidence of increased uptake at the site.

As seen in the preceding examples, an area of increased osseous remodeling or a focal hot spot on a bone scan typically catches a clinician's attention. Bone scintigraphy offers information not only about increased osseous remodeling but about normal, decreased, or absent osseous remodeling. Areas of decreased osseous remodeling can be seen in regions where a patient received prior radiation therapy. Areas of absent uptake in bone can be associated with bone infarctions, avascular necrosis, or metal prostheses, or may occur where tumor has replaced the bone. Diffusely increased soft tissue uptake in the body can be seen with poor renal function. More localized soft tissue uptake can be seen in certain tumors or in areas with poor venous return, such as areas of edema in an extremity. Metabolic information about osseous remodeling obtained through bone scanning continues to have an important place in clinical decision making.

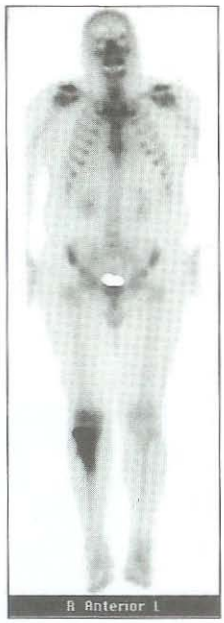

FIGURE 19-20 Adult male with knee pain. There is prominent, abnormal, increased osseous remodeling in the proximal one-third of the right tibia in this patient with chondrosarcoma.

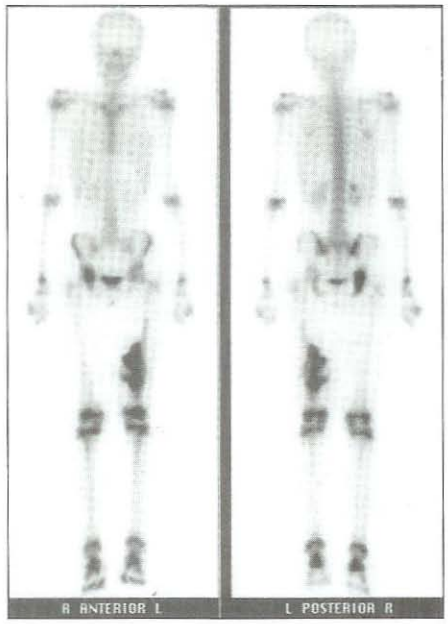

FIGURE 19-21 There is a large, expansile-appearing focal area of increased osseous remodeling involving the mid to distal left femur in this 14 year old patient with osteosarcoma. There is also metastatic involvement of the right acetabulum extending into the ischium. Note the physiologic increased uptake in the growth plates.

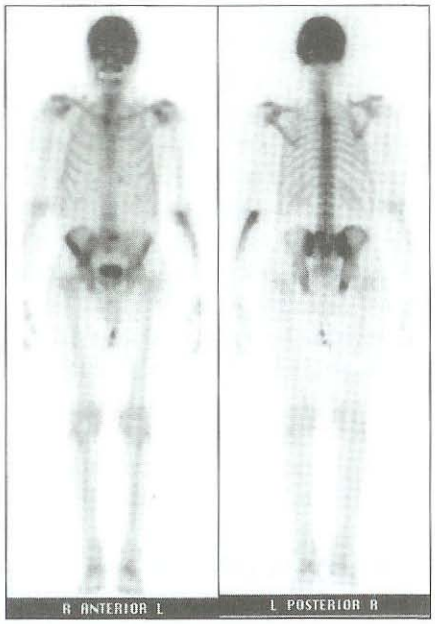

FIGURE 19-22 Anterior and posterior whole-body bone scan demonstrating prominent uptake in the skull, pelvis, and left ulna in a patient with Paget's disease.

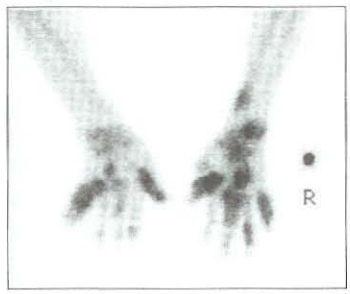

FIGURE 19-23 Bone scan of the hands demonstrating multiple abnormal focal areas of osseous remodeling in a patient with gout.

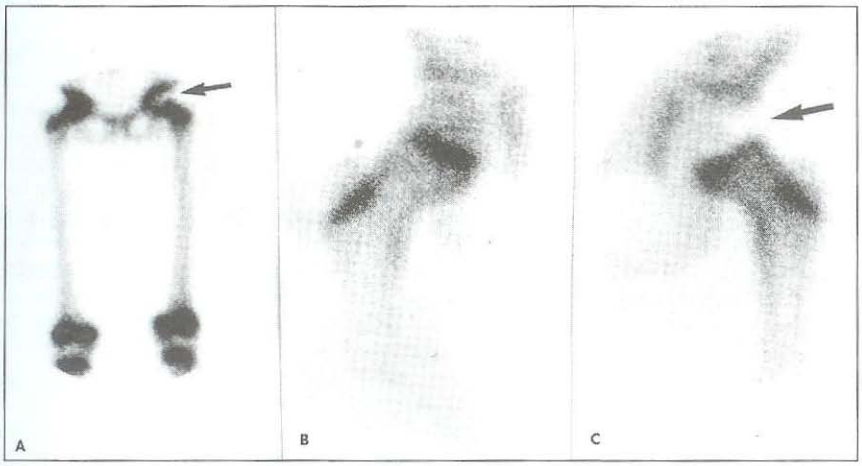

FIGURE 19-24 Avascular necrosis. Anterior bone scan on a young child illustrating the pelvis and thighs (A), right hip (B), and left hip (C). Note the absence of tracer in the left femoral head because of arterial occlusion to bone. Also evident is the increased concentration of activity normally seen in the epiphyseal growth plates of a child.

REFERENCES

1. Trifflitt JT. The organic matrix of bone tissue. In: Urist MR, ed. *Fundamental and Clinical Bone Physiology.* Philadelphia: JB Lippincott; 1980:45-82.
2. Neuman WF. Bone material and calcification mechanisms. In: Urist MR, ed. *Fundamental and Clinical Bone Physiology.* Philadelphia: JB Lippincott; 1980:83-107.
3. Guyton AC. *Textbook of Medical Physiology.* 6th ed. Philadelphia: WB Saunders; 1981:977-81.
4. Dudley HC, Maddox GE, LaRue HC. Studies of the metabolism of gallium. *J Pharmacol Exp Ther.* 1949;96:135-8.
5. Edwards CL, Hayes RL. Tumor scanning with Ga-67 citrate. *J Nucl Med.* 1969;10:103-5.
6. Charkes ND, Sklaroff DM. Early diagnosis of metastatic bone cancer by photoscanning with strontium-85. *J Nucl Med.* 1964;5:168-79.
7. Gynning I, Langeland P, Lindberg S, et al. Localization with Sr-85 of spinal metastasis in mammary cancer and changes in uptake after hormone and roentgen therapy: a preliminary report. *Acta Radiol.* 1961;55:119-28.
8. Meckelnburg RI. Clinical value of generator produced 87m-strontium. *J Nucl Med.* 1964;5:929-35.
9. Blau M, Nagler W, Bender WA. Fluorine-18: a new isotope for bone scanning. *J Nucl Med.* 1962;3:332-4.
10. Fels IG, Kaplan E, Greco J. Incorporation in vivo of P-32 from condensed phosphates. *Proc Soc Exp Biol Med.* 1959;100:53-5.
11. Subramanian G, McAfee JG. A new complex of Tc-99m for skeletal imaging. *Radiology.* 1971;99:192-6.
12. Subramanian G, McAfee JG, O'Mara RE, et al. Tc-99m polyphosphate PP_{46}: a new radiopharmaceutical for skeletal imaging. *J Nucl Med.* 1971;12:399-400.
13. Davis MA, Jones AG. Comparison of Tc-99m labeled phosphate and phosphonate agents for skeletal imaging. *Semin Nucl Med.* 1976;6:19-31.
14. Perez R, Cohen Y, Henry R, et al. A new radiopharmaceutical for Tc-99m bone scanning [abstract]. *J Nucl Med.* 1972;13:788.
15. Yano Y, McRae J, Van Dyke DC, et al. Technetium-99m labeled stannous ethane-1-hydroxy-1, 1-diphosphonate: a new bone scanning agent. *J Nucl Med.* 1973;14:73-8.
16. Castronovo FP, Callahan RJ. New bone scanning agent: Tc-99m-labeled 1-hydroxyethylidene-1, 1-disodium phosphonate. *J Nucl Med.* 1972;13:823-7.
17. Subramanian G, McAfee JG, Blair RJ, et al. Tc-99m EHDP: a potential radiopharmaceutical for skeletal imaging. *J Nucl Med.* 1972;13:947-50.
18. Subramanian G, McAfee JG, Blair RJ, et al. Technetium-99m methylene diphosphonate: a superior agent for skeletal imaging: comparison with other technetium complexes. *J Nucl Med.* 1975;16:744-55.

19. Barnett BL, Strickland LC. The structure of disodium dihydrogen-1-hydroxyethylidene diphosphonate tetrahydrate: a bone growth regulator. *Acta Crystallogr B.* 1979;B35:1212-4.
20. Francis MD, Tofe AJ, Benedict JJ, et al. Imaging the skeletal system. In: Sorenson JA, ed. *Radiopharmaceuticals II.* New York: Society of Nuclear Medicine; 1979:603-14.
21. Nelson MF, Melton RF, Van Wazer JR. Sodium trimetaphosphate as a bone-imaging agent. I: Animal studies. *J Nucl Med.* 1975;16:1043-8.
22. Kowalsky RJ, Dalton DR. Technical problems associated with the production of technetium Tc-99m tin (II) pyrophosphate kits. *Am J Hosp Pharm.* 1981;38:1722-6.
23. Chandler WM, Shuck LD. Abnormal technetium-99m pertechnetate imaging following stannous pyrophosphate bone imaging. *J Nucl Med.* 1975;16:518-9.
24. Tofe AJ, Francis MD. In vitro stabilization of low-tin bone-imaging agent (Tc-99m-Sn-HEDP) by ascorbic acid. *J Nucl Med.* 1976;17:820-25.
25. Tofe AJ, Bevan JA, Fawzi MD, et al. Gentisic acid: a new stabilizer for low tin skeletal imaging agents: concise communication. *J Nucl Med.* 1980;21:366-70.
26. Ballinger J, Der M, Bowen B. Stabilization of Tc-99m pyrophosphate injection with gentisic acid. *Eur J Nucl Med.* 1981;6:153-4.
27. Hambright P, McRae J, Valk PE, et al. Chemistry of technetium radiopharmaceuticals: exploration of the tissue distribution and oxidation state consequences of technetium (IV) in Tc-Sn-gluconate and Tc-Sn-EHDP using carrier ^{99}Tc. *J Nucl Med.* 1975;16:478-82.
28. Tofe AJ, Francis MD. Optimization of the ratio of stannous tin:ethane-1-hydroxy-1-diphosphonate for bone scanning with Tc-99m pertechnetate. *J Nucl Med.* 1974;15:69-74.
29. Bevan J, Tofe AJ, Benedict JJ, et al. Tc-99m HMDP (hydroxymethylene diphosphonate): a radiopharmaceutical for skeletal and acute myocardial infarct imaging. 1: Synthesis and distribution in animals. *J Nucl Med.* 1980;21:961-6.
30. Ponto JA. A review of radiopharmaceutical formulation problems and their clinical manifestations. In: Hladik W B III, ed. *Continuing Education Course for Nuclear Pharmacists and Nuclear Medicine Professionals.* Vol II, no. 3. Albuquerque, NM: Pharmacy Continuing Education, University of New Mexico; 1993.
31. Deutsch E. Inorganic radiopharmaceuticals. In: Sorenson JA, ed. *Radiopharmaceuticals II.* New York: Society of Nuclear Medicine; 1979:129-46.
32. Pinkerton TC, Ferguson DL, Deutsch E, et al. In vivo distributions of some component fractions of Tc($NaBH_4$)-HEDP mixtures separated by anion-exchange high performance liquid chromatography. *Int J Appl Radiat Isot.* 1982;33:907-15.
33. Francis MD, Ferguson DL, Tofe AJ, et al. Comparative evaluation of three diphosphonates: in vitro adsorption (C-14 labeled) and in vivo osteogenic uptake (Tc-99m complexed). *J Nucl Med.* 1980;21:1185-9.
34. Fogelman I, Pearson DW, Bessent RG, et al. A comparison of skeletal uptake of three diphosphonates by whole body retention: concise communication. *J Nucl Med.* 1981;22:880-3.
35. Silberstein EB. A radiopharmaceutical and clinical comparison of Tc-99m-Sn-hydroxy-methylene diphosphonate with Tc-99m-Sn-hydroxyethylidene diphosphonate. *Radiology.* 1980;136:747-51.
36. Littlefield JL, Rudd TG. Tc-99m hydroxy-methylene diphosphonate (HMDP) versus Tc-99m methylene diphosphonate (MDP): biological and clinical comparison [abstract]. *Clin Nucl Med.* 1980;5:S28.
37. Rosenthall L, Arzoumanian A, Damtew B, et al. A crossover study comparing Tc-99m labeled HMDP and MDP in patients. *Clin Nucl Med.* 1981;6:353-5.
38. Rudd TG, Allen DR, Hartnett DE. Tc-99m methylene diphosphonate versus Tc-99m pyrophosphate: biologic and clinical comparison. *J Nucl Med.* 1977;18:872-6.
39. Fogelman I, Citrin DL, McKillop JH. A clinical comparison of Tc-99m HEDP and Tc-99m MDP in the detection of bone metastasis. *J Nucl Med.* 1979;20:98-101.
40. Jones AG, Francis MD, Davis MA. Bone scanning: radionuclidic reaction mechanisms. *Semin Nucl Med.* 1976;6:3-18.
41. King MA, Weber DA, Casarett GW, et al. A study of irradiated bone. II: Changes in Tc-99m pyrophosphate bone imaging. *J Nucl Med.* 1980;21:22-30.
42. Stabin MG, Stubbs JB, Toohey RE. *Radiation Dose Estimates for Radiopharmaceuticals.* Oak Ridge, TN: Radiation Internal Dose Information Center, Oak Ridge Institute for Science and Education (ORISE); 1996.
43. Thomas SR, Gelfand MJ, Kerades JG, et al. Dose to the metaphyseal growth complexes in children undergoing Tc-99m EHDP bone scans. *Radiology.* 1978;126:193-5.
44. Stevenson JS, Eckelman WC, Sobocinski PZ, et al. The toxicity of Sn-pyrophosphate: clinical manifestations prior to acute LD-50. *J Nucl Med.* 1974;15:252-6.
45. Atkins HL. Reported adverse reactions to radiopharmaceuticals remain low in 1984. *J Nucl Med.* 1986;27:327.
46. Hoving J, Roosjen HN, Brouwers JRBJ. Adverse reactions to technetium-99m methylene diphosphonate. *J Nucl Med.* 1988;29:1302-3.

47. Hladik WB III, Nigg KK, Rhodes BA. Drug induced changes in the biologic distribution of radiopharmaceuticals. *Semin Nucl Med.* 1982;12:184-218.
48. Lentle BC, Scott JR, Noujaim AA, et al. Iatrogenic alterations in radionuclide biodistributions. *Semin Nucl Med.* 1979;9:131-43.
49. Donohoe KJ, Henkin RE, Royal HD, et al. Procedure guideline for bone scintigraphy 2.0. In: *Procedure Guidelines Manual 2001-2002.* Reston, VA: Society of Nuclear Medicine; 2001.
50. Matin P. Appearance of bone scans following fractures: including immediate and long-term studies. *J Nucl Med.* 1979;20:1227-31.
51. Matin P. Basic principles of nuclear medicine techniques for detection and evaluation of trauma and sports medicine injuries. *Semin Nucl Med.* 1988;18:90-112.
52. Waldvogel FA, Vasey H. Osteomyelitis: the past decade. *N Engl J Med.* 1980;303:360-70.
53. Van der Wall H. Assessment of infection. In: Murray IPC, Ell PJ, eds. *Nuclear Medicine in Clinical Diagnosis and Treatment.* 2nd ed. Edinburgh: Churchill Livingstone; 1998:1185-1207.
54. Handmaker H, Leonards R. The bone scan in inflammatory osseous disease. *Semin Nucl Med.* 1976;6:95-105.
55. Rosenthall L, Kirsh J. Observations of radionuclide imaging in hypertrophic pulmonary osteoarthropathy. *Radiology.* 1976;120:359-62.
56. Hain SF, Fogelman I. Nuclear medicine studies in metabolic bone disease. *Semin Musculoskelet Radiol.* 2002;6:323-30.
57. Elgazzar AH, Shehab D, Malki A, et al. Musculoskeletal system. In: *The Physiologic Basis of Nuclear Medicine.* New York: Springer-Verlag; 2001:88-126.

20 Total-Body and Miscellaneous Procedures

The previous chapters have focused on radiopharmaceuticals for evaluation of the major organ systems in the body. This chapter discusses radiopharmaceuticals in total-body soft-tissue imaging, with particular focus on radiopharmaceuticals for infection and tumor imaging. Miscellaneous nuclear medicine procedures are also addressed.

INFECTION IMAGING AGENTS

The Inflammatory Process

Infection stimulates an acute inflammatory process in the body, and agents having an affinity for inflamed tissue have been very useful in localizing active sites of infection. The inflammatory process is characterized by an accumulation of leukocytes, or white blood cells (WBCs), at the site of infection. The most useful agents for infection imaging include ^{67}Ga-gallium citrate and ^{111}In- and ^{99m}Tc-labeled WBCs. ^{99m}Tc-labeled antibodies have also been investigated for infection imaging.

The adult human has approximately 7000 WBCs per cubic millimeter (micoliter) of blood. WBCs comprise polymorphonuclear neutrophils (62%), eosinophils (2.3%), and basophils (0.4%), collectively called "polys" or granulocytes because of their granular appearance; monocytes (5.3%); and lymphocytes (30%).

Once released from the bone marrow, granulocytes have a normal life span of 6 to 8 hours in circulation and 2 to 3 days in tissues. Circulation time is shortened during serious infection. Monocytes have a short life span in blood but may exist in tissues as macrophages for months. Lymphocytes have a prolonged life span of several months.

Neutrophils and monocytes are the main types of WBCs involved in an inflammatory response to invading microorganisms. An inflammatory response may be caused by a noxious stimulus, such as infection, heat, chemical insult, or trauma. It may also be caused by a disease process, such as rheumatic or allergic conditions. The inflammatory reaction is characterized by a vascular response and occurs in two phases: a fluid phase and a cellular phase.[1]

After the initial injury, histamine, bradykinin, and serotonin are liberated by the damaged tissue. These substances cause localized hyperemia and increased capillary permeability, which allows proteins and fluids to leak into the affected tissue, causing edema. This constitutes the fluid phase. The presence of fibrinogen in the fluid leads to the formation of clots that wall off the injured area, delaying the spread of bacteria and toxic products.

The cellular phase of the inflammatory reaction has three stages. The first involves phagocytic activity of local macrophages. The second is characterized by neutrophilia, with a large increase in circulating neutrophils in response to chemical mediators released in the inflamed tissues. The number of neutrophils can increase from 15,000 to 25,000 per microliter within a few hours. Neutrophils migrate to the inflamed area and localize by diapedesis through the porous capillary walls. They are attracted by bacterial toxins and

cellular products (chemotaxis), whereupon they become attached and exert their phagocytic function. The third stage of the cellular response is slower but longer. It involves migration of lysosome-rich monocytes to the injured area over a period of 8 to 12 hours. Monocytes also exert a phagocytic function. WBCs eventually die and collect in the area to form an abscess, which can be localized by radiopharmaceuticals.

Gallium Citrate Ga 67 Injection

Gallium citrate Ga 67 injection (^{67}Ga-gallium citrate) was originally investigated as a bone imaging agent; however, early studies demonstrated, serendipitously, that carrier-free ^{67}Ga-gallium citrate preferentially localized in soft-tissue lesions.[2] The first patient studied with ^{67}Ga-gallium citrate had Hodgkin's disease, and ^{67}Ga localized in the affected lymph nodes. Soon thereafter, it was discovered that ^{67}Ga also localized in inflammatory processes.[3,4] Even though it lacks specificity for tumor imaging, ^{67}Ga-gallium citrate has been used for over 30 years to image certain tumors and inflammatory processes.[5]

After intravenous injection of ^{67}Ga-gallium citrate, the complex dissociates in blood, with ^{67}Ga becoming bound to plasma transferrin.[6] About 80% of the injected ^{67}Ga activity is protein bound.[7] The plasma clearance of ^{67}Ga activity is biphasic, with half-lives of 30 hours and 25 days for 17% and 85% of the injected activity, respectively.[8] Its excretion from the body is slow, with 15% to 25% appearing in the urine within 24 hours. By 7 days, 35% has been excreted in urine and feces combined, and 65% remains in the body.[9] At 24, 48, and 72 hours after injection, about 20%, 10%, and 5%, respectively, still remains in the blood.[10]

The principal organs that localize gallium are the liver, spleen, gastrointestinal (GI) tract, kidney, skeleton, and bone marrow (Figure 20-1).[8,11] Gallium's nonspecific uptake in the GI tract is the major disadvantage of this radiopharmaceutical for imaging infection in the abdominal region. The difficulties with planar imaging in distinguishing bowel content of ^{67}Ga from abnormal foci in the abdomen or pelvis can be greatly alleviated by single-photon emission computed tomography (SPECT) imaging of this area 48 hours after injection. SPECT images, under these circumstances, can precisely define the locations of ^{67}Ga concentration in bowel lumen or nonlumen (e.g., pancreas, kidney, and peritoneum) (Figure 20-2).

Significant kidney activity beyond 24 hours should be investigated to rule out causes other than normal clearance. Occasional uptake of activity occurs in the lacrimal and salivary glands and in the breasts during menarche, pregnancy, and lactation.[12–14] The high concentration of lactoferrin in many normal tissues is believed to be responsible for the localization of gallium in these tissues. Transferrin and lactoferrin are metabolized in the liver and could account for the uptake of gallium in normal liver.

Whole-body x-irradiation can alter the normal distribution of carrier-free ^{67}Ga-gallium citrate, producing increased excretion and bone deposition together with decreased soft-tissue uptake.[15] This pattern is similar to the effect produced by iron saturation of transferrin.[16] The finding of elevated serum iron levels after irradiation of animals strongly suggests this mechanism.[17]

Although ^{67}Ga-gallium citrate was used extensively in the past for infection imaging, ^{111}In- or ^{99m}Tc-labeled WBCs are now the primary choices for localizing acute infection.[18,19] ^{111}In-WBCs or ^{67}Ga-gallium citrate can be used for imaging chronic infection; however, ^{67}Ga-gallium citrate has been shown to have less specificity for this condition.[19,20] A principal application of ^{67}Ga-gallium citrate is in patients with fever of unknown origin, a condition characterized by fever (38.3°C) of greater than 3 weeks' duration with no cause identified during 1 week of hospitalization.[18,19] ^{67}Ga-gallium citrate is the agent of choice in nonbacterial infections, opportunistic respiratory infections, and lymph node abnormalities

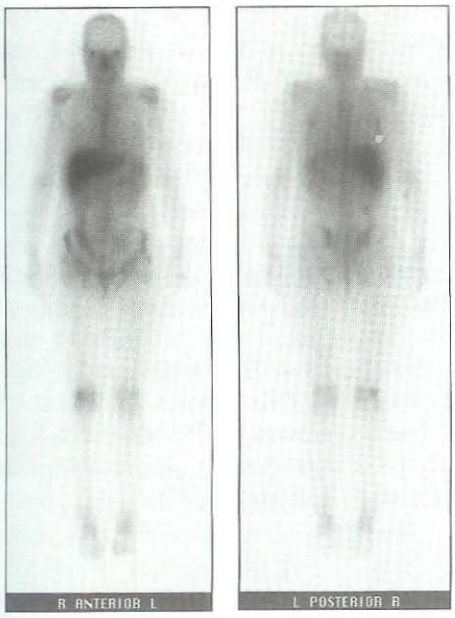

FIGURE 20-1 Normal total body ^{67}Ga scan. Anterior and posterior whole-body images were obtained 48 hours after intravenous administration of 8 mCi (296 MBq) of ^{67}Ga-gallium citrate. In the head, normal radiotracer accumulation is seen in the lacrimal glands and nasopharynx. *Physiologic uptake is seen in the skeleton. In the* abdomen, the most prominent uptake is seen in the liver, with a lesser amount in the spleen. Activity is often present in the colon.

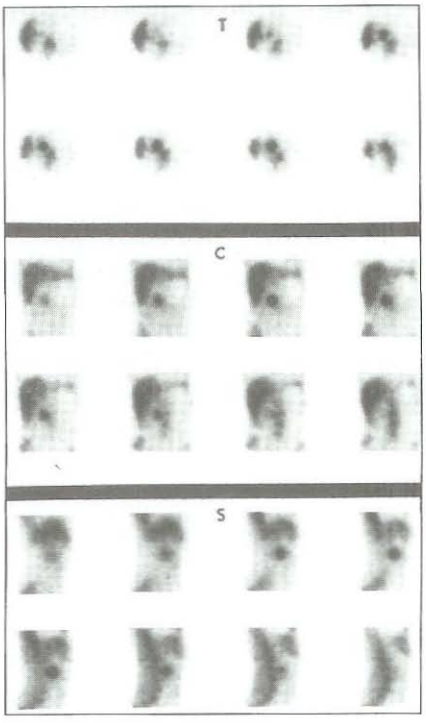

FIGURE 20-2 ^{67}Ga infection scan. Gallium SPECT transaxial (T), coronal (C), and sagittal (S) images *demonstrating an abscess in the head of the pancreas.* SPECT 3-D definition allowed differentiation of the pancreatic focus from bowel activity.

in immunocompromised patients such as those with acquired immunodeficiency syndrome (AIDS).[21]

Although its uptake in infectious processes has been investigated extensively, the exact mechanism of ^{67}Ga localization is not clear. ^{67}Ga may bind to WBCs that subsequently migrate to the inflammatory lesion, or it may bind to WBCs that have already localized in the lesion. The theory is that ^{67}Ga bound to transferrin passes into the leukocyte, where it is bound to intracellular lactoferrin, which has a higher binding affinity for gallium.[22] Localization in infections may also be due to translocation of ^{67}Ga from transferrin to bacterial siderophores, macrophage ferritin, and polymorphonuclear lactoferrin, all of which bind gallium more firmly than transferrin.[23]

The standard adult dosage is 3 mCi (111 MBq) for infection localization, with imaging at 4 hours and 24 hours if prompt information is required. Delaying imaging for 48 to 72 hours provides better quality images because of less background activity. The critical organ is the lower large intestine, with a radiation absorbed dose of 0.9 rad/mCi.

Radiolabeled WBCs

The nonspecific localization of ^{67}Ga-gallium citrate when used for infection imaging stimulated an investigation into methods for labeling WBCs. McAfee and Thakur[24,25] examined the use of both soluble and particulate agents to determine which methods offered the greatest promise for routine preparation. Particulate agents were found to be ineffective

because of the inability to completely remove loosely attached radioactive particles from leukocyte surfaces after radiolabeling. Methods that used soluble agents demonstrated that only nonpolar, lipid-soluble chelates labeled cells effectively. The most effective agents were ^{111}In chelates of oxine, tropolone, and acetylacetone.[26,27] These ligands form neutral, lipid soluble 3:1 chelates with indium. McAfee and Thakur[24] chose to use oxine over acetylacetone because the latter complex with indium tended to elute from WBCs and had a higher degree of erythrocyte (red blood cell, or RBC) labeling. Both ^{111}In-indium oxine and ^{111}In-indium tropolone have been shown to be effective labeling agents for WBCs and platelets; however, the only complex available commercially for routine use is ^{111}In-indium oxine. The chemical structures of these two complexes are shown in Figure 20-3.

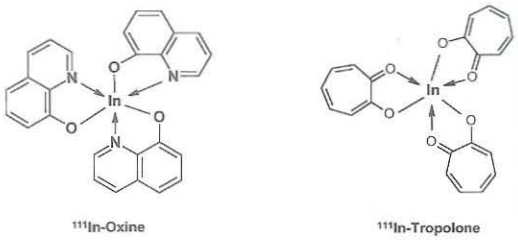

^{111}In-Oxine ^{111}In-Tropolone

FIGURE 20-3 Chemical structures of ^{111}In-indium oxine and ^{111}In-indium tropolone.

WBC Labeling Methods

The routine methods for labeling WBCs with ^{111}In and ^{99m}Tc have been reported.[28–33] A general stepwise procedure is given in Chapter 9. Because all blood cellular elements are labeled indiscriminately with lipophilic indium or technetium complexes, it is necessary to separate WBCs from whole blood before labeling. This is accomplished by gravity settling of anticoagulated whole blood (43 mL whole blood + 7 mL acid citrate dextrose [ACD] anticoagulant solution) to which 10 mL of 6% hetastarch has been added. The hetastarch promotes aggregation of RBCs, facilitating their rate of settling. This agent may be omitted in patients with leukocytosis who inherently have a high RBC sedimentation rate. RBCs do not separate well in patients with sickle cell anemia. If leukocyte labeling is attempted in sickle cell patients, the blood should be separated into two tubes and up to 50% hetastarch added to settle RBCs.

Normally, cell separation takes 45 to 60 minutes.The RBCs form a bottom layer, and the top layer (buffy coat) of leukocyte-rich plasma (LRP) contains most of the platelets and about 70% of the WBCs.[29] A small portion of the RBCs (2% to 4%) remain in the buffy coat, giving it a slightly pink appearance. This low concentration of RBCs does not interfere with infection imaging.[30] ^{111}In-indium oxine does not bind to RBCs as it does to WBCs, which have a protein that binds indium. Gentle centrifugation of the LRP (450*g* for 5 minutes) concentrates the WBCs into a button. The leukocyte-poor plasma (LPP) is withdrawn and the WBC button resuspended in a small amount of saline to which the ^{111}In-indium oxine or ^{99m}Tc-exametazime (^{99m}Tc-HMPAO) is added. This is followed by a 15 to 20 minute incubation to effect cell labeling.

In general, WBCs maintain their viability best in the presence of plasma. However, the relatively weak ^{111}In-indium oxine complex (stability constant approximately 10^{10}) is prone to release the indium to transferrin (stability constant approximately 10^{30}) present in plasma.[28] This will reduce cell labeling yields. The WBCs can be washed once with saline to remove the plasma transferrin prior to labeling. This results in higher labeling yields, but leukocyte viability may suffer. Another approach is to concentrate a large number of WBCs in a small amount of plasma. This technique enables a large number of cells to compete effectively with plasma transferrin during labeling and at the same time sustains leukocyte viability.[27] One advantage of using ^{111}In-tropolone for labeling WBCs is its ability to label in the presence of plasma.[29] ^{99m}Tc-HMPAO is also not affected by transferrin; WBCs can be labeled efficiently in up to 20% plasma.[33] As a general rule,

radiolabeled WBCs should be reinjected back into the patient within 3 hours of removal to ensure satisfactory viability.

During the incubation period, the neutral, lipophilic ^{111}In-oxine complex penetrates the leukocyte cell membrane and dissociates intracellularly, with subsequent binding of indium to cytoplasmic proteins (Figure 20-4).[29] During ^{99m}Tc-HMPAO labeling, the lipophilic complex diffuses into the leukocyte and is converted into a nondiffusible hydrophilic complex that becomes trapped within the cell.[18] Subcellular binding studies have shown that ^{99m}Tc-HMPAO preferentially labels eosinophils and is predominantly stored in the secretory granules.[34]

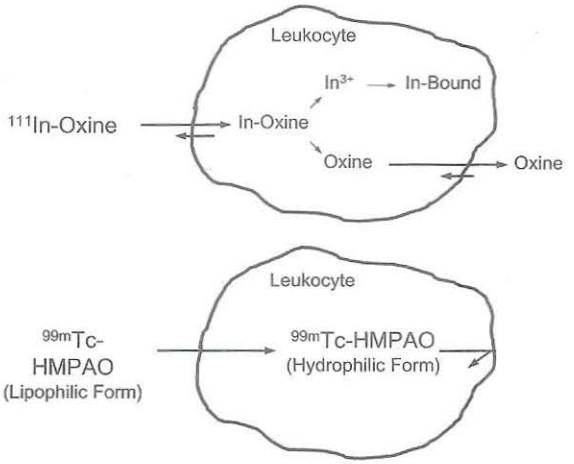

FIGURE 20-4 Proposed mechanism for labeling of leukocytes (WBCs) with ^{111}In-indium oxine and ^{99m}Tc-HMPAO.

McAfee and Thakur[24] demonstrated that labeling yields of WBCs increased linearly from approximately 35% to 75% as the number of cells increased from 3.6×10^7 to 1.3×10^8.[24] Using an average of 10^8 cells, Goodwin et al.[35] achieved a labeling efficiency of 84% ± 9%, and in patients with WBC counts above 15,000 per microliter in peripheral blood yields were usually 90% or more.[35] Coleman et al.[36] reported a 34% labeling efficiency in dilute plasma compared with 87% in saline. The mean number of WBCs in normal adult whole blood is 7000/μL or 7×10^6/mL. On the basis of this value, the number of WBCs in 43 mL of normal whole blood is about 3×10^8. The minimum number of WBCs required for efficient labeling is 10^8 cells, as noted above.

Indium In 111 White Blood Cells

The maximum adult administered activity of ^{111}In-WBCs is 0.5 mCi (18.5 MBq), with a useful range of 0.2 to 0.5 mCi (7.4 to 18.5 MBq). The plasma half-life is about 7 hours.[35] Imaging usually is performed 18 to 24 hours after injection but may be done at 1 to 4 hours if urgent information is needed. Imaging at 1 to 4 hours, however, is associated with lower sensitivity for abscess detection (33%) than 24 hour images (95%).[19] Beyond 24 hours, radioactivity is normally present in the liver, spleen, and bone marrow, but body background is generally low (Figure 20-5). Early images after injection show transient lung activity, which is mostly cleared by 4 hours. The intense spleen activity is due to labeled platelets and WBCs damaged during preparation. This distribution is the reverse of ^{67}Ga-gallium citrate scans, in which liver activity is more intense than spleen activity. Areas of infection appear as focal regions of increased uptake of activity similar to that seen with ^{67}Ga-gallium citrate (Figure 20-6). Because of the appearance of early lung activity with ^{111}In-WBCs, some physicians prefer ^{67}Ga-gallium citrate when imaging chest inflammatory conditions such as sarcoidosis, diffuse pneumonia, and interstitial inflammatory reactions.[19] Suspected infections in the abdomen and pelvis, however, are best imaged with ^{111}In-WBCs because of the lack of activity in the bowel. In the bones and joints, there is little accumulation of ^{111}In-WBCs in noninflammatory regions of increased bone turnover, such as those caused by osteoarthritis. This is an advantage over ^{67}Ga-gallium citrate in patients with complicated orthopedic problems. In suspected osteomyelitis, ^{111}In- or

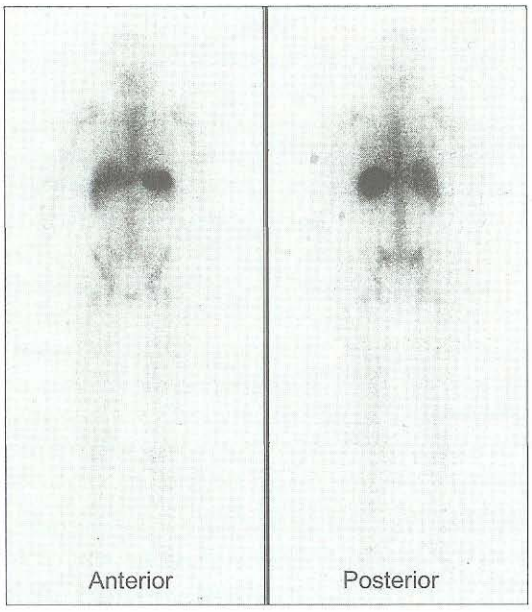

FIGURE 20-5 Normal ^{111}In-WBC scan. Anterior and posterior whole-body images were obtained 24 hours after intravenous administration of 500 μCi (18.5 MBq) of ^{111}In-indium oxine-labeled WBCs. Radiotracer accumulation is seen in the liver, spleen, and bone marrow.

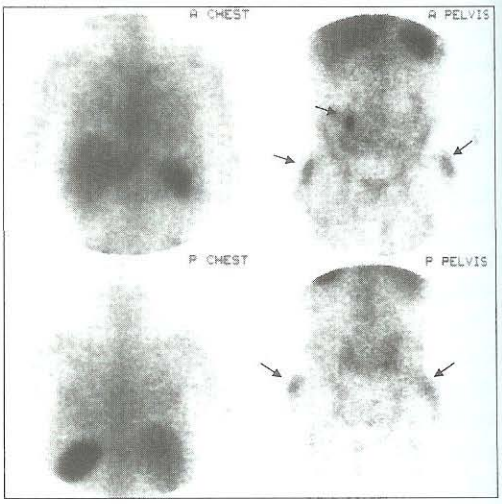

FIGURE 20-6 ^{111}In-WBC scan demonstrating infection. Anterior and posterior spot images of the chest, abdomen, and pelvis were obtained 24 hours after intravenous administration of 500 μCi (18.5 MB) of ^{111}In-oxine-labeled WBCs. There are several abnormal focal areas of radiotracer accumulation; the most prominent are in the right pelvis and in the soft tissues lateral to both hips (arrows). There is also abnormal diffuse uptake in the lungs.

^{99m}Tc-WBCs have been used to confirm or exclude the diagnosis, in conjunction with a three-phase bone scan.

The critical organ with ^{111}In-WBCs is the spleen, with a radiation absorbed dose of 20 rad(cGy)/0.5 mCi. This includes the dose due to ^{111}In (99.75%) and ^{114m}In/^{114}In (0.25% impurities) at the time of expiration of the ^{111}In-indium oxine.

Technetium Tc 99m White Blood Cells

The usual adult administered activity of ^{99m}Tc-WBCs is 10 mCi (370 MBq), with a suggested range of 7 to 25 mCi (259 to 925 MBq). The plasma half-life is approximately 4 hours.[18] The biologic distribution of ^{99m}Tc-WBCs differs slightly from that of ^{111}In-WBCs, demonstrating some biliary excretion with bowel activity and activity in the renal collecting system and bladder.[18] These accumulations are attributed to release of secondary hydrophilic complexes of ^{99m}Tc-HMPAO.[18] Occasionally, gallbladder activity is seen. The nonspecific bowel activity does not appear until at least 2 hours after injection and increases beyond 4 hours after injection. It presents a problem in imaging inflammatory bowel disease (IBD) and abdominal infection. Typically, in imaging soft-tissue sepsis, sequential imaging at 1 to 4 hours is necessary to delineate abscess from nonspecific bowel activity. Infections localized away from the abdomen are more easily identified (Figure 20-7). Imaging can be done up to 24 hours after dosing, but significant bowel activity may interfere at this time and result in false-positive diagnosis. As with ^{111}In-WBCs, there is significant liver and spleen activity with ^{99m}Tc-WBCs. ^{99m}Tc-WBCs are the agent of choice for IBD and acute sepsis, in which an early diagnosis is mandatory.[18] Diagnostic accuracy in these conditions is considered equivalent to that of ^{111}In-WBCs.[18] Most forms of chronic sepsis are imaged better with ^{111}In-WBCs. ^{67}Ga-gallium citrate is the agent of choice for

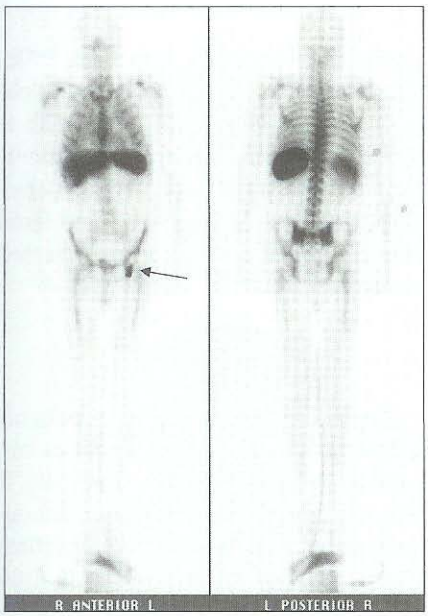

FIGURE 20-7 Femoral graft infection. Anterior and posterior whole-body images were obtained approximately 4 hours after intravenous administration of 10 mCi (370 MBq) ^{99m}Tc-HMPAO-labeled autologous WBCs. On the anterior image there is an abnormal focal accumulation of radiotracer in the left groin region that extends from the surface of the skin to the patient's femoral graft, consistent with infection at the graft insertion site (arrow).

TABLE 20-1 Comparison of ^{67}Ga-Gallium Citrate and ^{99m}Tc- and ^{111}In-Labeled Leukocytes (WBCs) for Infection Imaging

Property	^{99m}Tc-WBCs	^{111}In-WBCs	^{67}Ga-Gallium Citrate
Availability	Same day as request	Next day after request	Same day as request
Administered activity	10 mCi	0.5 mCi	3 mCi
Target-to-background ratio	Fair	Good	Poor
Collimation	LEAP[a]/high-resolution	Medium energy	Medium energy
Labeling	In ≤20% plasma	Remove plasma	None
EDE[b]	0.74 rem/10 mCi	1.2 rem/0.5 mCi	1.23 rem/3 mCi
Plasma $T_{½}$	~ 4 hr (^{99m}Tc label elutes)	~ 7 hr	30 hr (17%) 25 days (83%)
Imaging time	1 to 4 hr	18 to 24 hr	24 to 72 hr
Normal activity distribution	Liver, spleen, bone marrow, bowel, kidney, gallbladder	Liver, spleen, bone marrow	Liver, spleen, bone marrow, bowel, kidney, skeleton
General applications	Acute infection, inflammatory bowel disease, osteomyelitis	Acute and chronic infection, inflammatory bowel disease, osteomyelitis	Fever of unknown origin, nonbacterial infections

[a] Low-energy all-purpose.

[b] Effective dose equivalent data from Radiation Internal Dose Information Center, Oak Ridge Institute for Science and Education, Oak Ridge, TN 37831-0117.

diagnosis of fever of unknown origin, since it detects many types of inflammatory processes.

The critical organ with ^{99m}Tc-WBCs is the spleen, with a radiation absorbed dose of 13.9 rad(cGy)/25 mCi (925 MBq) maximum administered activity. Table 20-1 compares the properties of ^{67}Ga-gallium citrate, ^{99m}Tc-WBCs, and ^{111}In-WBCs for infection imaging.

Antibodies for Infection Imaging

Two technetium-labeled antibodies have been investigated for localizing infection: ^{99m}Tc-sulesomab (^{99m}Tc-LeukoScan, Immunomedics) and ^{99m}Tc-labeled anti-CD15 immunoglobulin M monoclonal antibody (^{99m}Tc-LeuTech, Palatin Technologies). ^{99m}Tc-sulesomab is indicated for the diagnostic localization of infection and inflammation in bone in patients with suspected osteomyelitis. ^{99m}Tc-LeuTech has been evaluated in humans for the detection of appendicitis. These investigational agents are discussed in Chapter 21. Compared with radiolabeled WBCs, they are simpler to use and safer because they are injected directly into the patient without the need for leukocyte separation and labeling.

Clinical Considerations in Infection Imaging

It can be difficult to diagnose and localize a site of occult infection, particularly in patients who cannot cooperate or have no localizing signs. If detected early, most infections can be cured with proper treatment; delayed diagnosis is associated with higher mortality. If localizing signs are present, anatomic imaging with ultrasonography or computed tomography (CT) is often used first. However, these modalities cannot usually differentiate between infection, such as an abscess, and a noninfectious process, such as a sterile fluid collection or inflammation. Indications for nuclear medicine imaging in infection include fever of unknown origin, suspected occult abscess, postoperative infection, suspected infection of a vascular graft, osteomyelitis, disk space infection, and suspected infections in immunocompromised patients. One advantage of a nuclear medicine study is that the whole body can be imaged. This is particularly important when there are no localizing signs.

Currently, the three most common agents used to localize foci of infection are ^{67}Ga-gallium citrate, ^{111}In-oxine labeled autologous WBCs, and ^{99m}Tc-HMPAO labeled autologous WBCs. Positron emission tomography (PET) has shown promise for evaluation of infection and inflammation. The appropriate choice of radiopharmaceutical for imaging infection depends on the clinical setting. Several factors should be considered in deciding which radiopharmaceutical to use, including whether the infection is acute or chronic, the suspected anatomic location, history of recent surgery, chemotherapy, blood transfusions, severe leukopenia, and existing malignancy.

Although ^{67}Ga-gallium citrate is sensitive for detecting foci of infection, it is less specific than labeled WBCs because it is also taken up in several tumors such as lymphoma and lung cancer and by sterile inflammation such as in a healing wound. Whole-body imaging is usually done 24 to 48 hours after administration. Accumulation in the colon can be significant, which may interfere with evaluation of the abdomen. Thus, laxatives are usually administered the day before imaging to reduce activity in the bowel. If the patient is receiving chemotherapy, blood transfusions, or iron therapy, ^{67}Ga-gallium citrate can sometimes demonstrate an altered biodistribution that resembles a bone scan (Figure 20-8). This can also be seen if the patient has received gadolinium for a magnetic resonance imaging (MRI) study just before ^{67}Ga-gallium citrate administration. A study comparing imaging with ^{67}Ga-gallium citrate and with ^{111}In-WBCs in the same patients for diagnosis of occult sepsis showed that false-negatives with ^{67}Ga tended to occur in patients with infections of less than 1 week's duration, whereas false-negatives with ^{111}In-WBCs were more likely to occur in infections more than 2 weeks old.[37] Thus, ^{67}Ga-gallium citrate may be a better choice for chronic infections. ^{67}Ga-gallium citrate is preferred over labeled autologous WBCs for disk space infection and imaging of the spine.[38] ^{67}Ga-gallium citrate is also more useful for evaluation of pulmonary disorders, such as evaluating response to therapy in AIDS patients with *Pneumocystis carinii* pneumonia,[39] drug-induced pulmonary

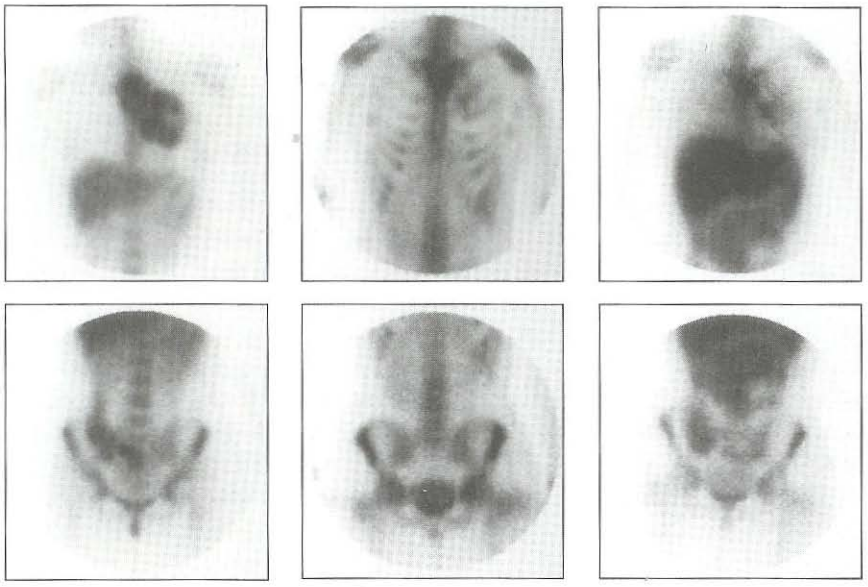

FIGURE 20-8 Lymphoma. (Left) Initial anterior spot images of the chest and abdomen were obtained 48 hours after intravenous administration of 10 mCi (370 MBq) of ^{67}Ga-gallium citrate to a patient with lymphoma. The images demonstrate prominent abnormal focal accumulation of the radiotracer in the chest in the patient's tumor. (Center) A follow-up ^{67}Ga-gallium citrate scan after treatment, demonstrating altered biodistribution resembling a diphosphonate bone scan. The patient had received chemotherapy and blood transfusions before the follow-up scan. With this altered distribution, neoplastic lesions can be missed. (Right) Another follow-up study in this patient at a later date demonstrated residual tumor in the chest.

toxicity in patients receiving amiodarone,[40] and granulomatous inflammatory processes such as sarcoidosis.[41] ^{67}Ga-gallium citrate may also be appropriate in evaluating fever of unknown origin in patients with suspected tumor or autoimmune disease.

Radiolabeling WBCs is a somewhat tedious procedure compared with a ^{67}Ga-gallium citrate injection. However, labeled WBCs are more specific for infection than ^{67}Ga-gallium citrate. With ^{111}In-WBCs, physiologic uptake is seen in the liver, spleen, and bone marrow. There is normally no uptake in the urinary tract or the bowel. This can be useful for evaluating IBD or suspected urinary tract infection. Early imaging can be obtained 4 hours after administration. However, delayed imaging at 24 hours should be obtained if the early images are negative. Also ^{111}In-WBCs have a higher target-to-background ratio than ^{67}Ga-gallium citrate in acute pyogenic infections.[29]

Imaging with ^{99m}Tc-HMPAO labeled WBCs can be performed 2 to 4 hours after administration, offering an earlier diagnosis than with ^{67}Ga-gallium citrate or ^{111}In-WBCs. This is the agent of choice if an early diagnosis is urgently needed. Because of the higher photon flux of the ^{99m}Tc dose, better anatomic localization is sometimes possible. In contrast to ^{111}In-WBCs, there is physiologic bowel activity and urinary tract activity that can complicate imaging of the abdomen.

Comparing ^{111}In-WBCs and ^{99m}Tc-HMPAO labeled WBCs, Peters[42] preferred ^{99m}Tc-labeled WBCs when an early diagnosis is essential. However, in more chronic processes such as fever of unknown origin or an infected hip prosthesis, where the turnover of granulocytes is slower, ^{111}In 24-hour imaging is preferred.

PET imaging with ^{18}F-FDG has proven to be clinically useful in the diagnosis and management of several malignancies. ^{18}F-FDG has also been shown to accumulate in a

variety of infectious and inflammatory processes.[43] As PET imaging becomes more widely used in clinical medicine, it will undoubtedly prove to be a valuable tool in the diagnosis of infection and response to therapy.[44]

TUMOR IMAGING AGENTS

Traditionally, anatomic imaging modalities such as CT, MRI, and ultrasonography have been the primary methods used in tumor detection. One limitation of these modalities is that they cannot distinguish between benign and malignant tumors or between pretherapeutic and posttherapeutic anatomic alterations such as scarring, inflammation, or necrosis and neoplastic processes.[45] Functional information is needed in tumor diagnosis, and radiopharmaceuticals can meet this need because certain radiotracers have an avidity for viable tumor tissue. The principal agent in this regard is ^{18}F-fludeoxyglucose (^{18}F-FDG). The proven diagnostic effectiveness of fusing high spatial-resolution CT images with functional information provided by ^{18}F-FDG PET led to the development of a hybrid single-unit CT/PET camera. Fusion imaging has superior diagnostic power because it permits the acquisition and coregistration of anatomic and functional images during a single patient visit.

Tumor imaging outside specific organs began in the 1960s with the discovery of ^{67}Ga uptake in lymphomas. ^{67}Ga-gallium citrate, originally approved for lymphoma imaging, still maintains its place as a valuable tumor imaging agent. The growth of tumor imaging has increased substantially in recent years. This is attributed, in part, to the development of new radiopharmaceutical agents, such as *meta*-iodobenzylguanidine (MIBG) and radiolabeled antibodies and peptides designed to target specific receptors on tumor cells.

Another significant advance in tumor detection has been the emergence of ^{18}F-FDG PET imaging. This followed the validation of ^{18}F-FDG uptake in many types of tumors, increased availability of ^{18}F-FDG through regional nuclear pharmacies, increased acquisition of PET cameras for clinical studies at imaging centers, and approval for Medicare reimbursement for the diagnosis and staging of a number of tumor types.

Another application in tumor diagnosis came with the discovery that certain tumors have an avidity for radiopharmaceuticals originally approved for other uses. Two examples are ^{99m}Tc-sestamibi and ^{201}Tl-thallous chloride, which have been useful for localizing parathyroid adenomas and other types of tumors.

Radiopharmaceuticals have been found useful for tumor imaging in three areas: staging tumors to assess the extent of involvement, assessing response to tumor treatment, and evaluating tumor recurrence.

Gallium Citrate Ga 67 Injection

Gallium citrate Ga 67 injection (^{67}Ga-gallium citrate) was approved originally for the detection and staging of Hodgkin's and non-Hodgkin's lymphoma, and it still has value for these applications. It is particularly useful for identifying suspected recurrence of lymphoma and monitoring the effects of therapeutic regimens.

The normal biodistribution of ^{67}Ga-gallium citrate after intravenous injection is discussed above under infection imaging. For tumor imaging, the standard dosage is 8 to 10 mCi (296 to 370 MBq), an amount necessary for good sensitivity with SPECT imaging. The three principal photopeaks, 93 keV (38%), 185 keV (24%), and 300 keV (16%), should be used for imaging to improve counting statistics. Because of gallium's slow excretion, imaging is typically done 48 to 72 hours or more after injection to improve the tumor-to-background ratio. Image interpretation is more difficult in regions of normal gallium

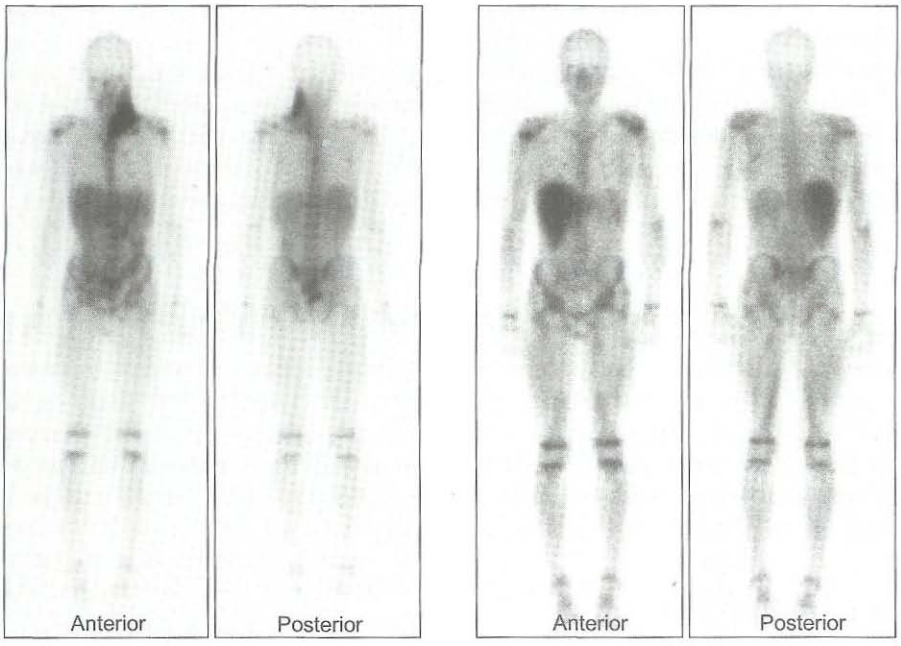

FIGURE 20-9 Hodgkin's lymphoma. (Left) Anterior and posterior whole-body images of a 14 year old boy with Hodgkin's lymphoma of the neck, obtained 48 hours after administration of 8 mCi (296 MBq) of ^{67}Ga-gallium citrate. There is a prominent area of abnormal tracer uptake in the left neck that extends into the superior mediastinum. (Right) A follow-up ^{67}Ga-gallium citrate whole-body scan obtained 2 months later demonstrates interval resolution of Hodgkin's lymphoma after chemotherapy.

uptake (liver, spleen, bone, bone marrow, and bowel). Delayed imaging of the abdomen *is often necessary to distinguish tumor (fixed activity) from normal bowel accumulation* that will clear over time. Laxatives can be used to facilitate bowel elimination.

^{67}Ga-gallium citrate has been useful in evaluating the effectiveness of tumor therapies because its uptake is a measure of tumor viability. If tumor treatment with chemotherapy or radiation therapy is followed by ^{67}Ga-gallium citrate imaging, gallium should be administered as late as possible (preferably 3 weeks) after the last treatment and 48 hours before the next treatment, because these treatments are known to alter gallium's biodistribution. It is important to establish the tumor's avidity for gallium before chemotherapy or other treatment. Once this is done, the response to therapy can be followed because gallium uptake diminishes or disappears after successful treatment (Figure 20-9). Similarly, the appearance of new foci of gallium uptake is a sensitive predictor of disease recurrence. A residual soft-tissue mass may be evident on CT in some patients after chemotherapy or radiation therapy. CT is not able to distinguish the functional status of a mass, for example, whether it is residual tumor or fibrosis. However, if the tumor has been previously established as being gallium avid, ^{67}Ga-gallium citrate imaging can be used to make the distinction, since it is taken up in tumor but not in fibrotic scar. Thus, the functional data from ^{67}Ga-gallium citrate images add clinical relevance to CT or MRI findings.

The exact mechanism of gallium's localization in tumors remains unclear. Gallium is taken up in viable tumor cells and not in necrotic or scarred regions of tumor. One theory is that Ga-transferrin in blood is taken up by tumor cell receptors and intracellular gallium

dissociates and binds to lactoferrin or to a specific tumor protein or is localized in tumor cell organelles.[46–48]

The sensitivity of SPECT imaging using ^{67}Ga-gallium citrate for tumor detection is high in Hodgkin's disease (>90%), non-Hodgkin's lymphoma (85%), hepatocellular carcinoma (90%), and soft-tissue sarcomas (93%). Other tumors that have shown gallium avidity, but with lower sensitivities for detection, include malignant melanomas (82%), lung tumors (85%), head and neck tumors (75%), and abdominal and pelvic tumors (55%).[49]

PEPTIDE RECEPTOR IMAGING AGENTS

The development of peptide receptor imaging agents is still in its infancy; this area should see tremendous growth in the future. Some of the first agents in this category are somatostatin receptor imaging agents. The widespread presence of somatostatin receptors in the body has led to the imaging of many types of tumors that possess these receptors. Because the tissues containing somatostatin receptors are part of the neuroendocrine system, this system is reviewed briefly.

Neuroendocrine System

The neuroendocrine system includes a diverse group of tissues whose cells have common features in their cytochemistry and ultrastructure.[50] Endocrine system cells have the ability to take up amine precursor substances such as dihydroxyphenylalanine (L-DOPA) and 5-hydroxytryptophan (5-HTP) and decarboxylate them, producing the corresponding biogenic amines dopamine and 5-hydroxytryptamine. This gave endocrine system cells their early designation as amine precursor uptake and decarboxylation (APUD) cells. APUD cells also have high levels of particular enzymes and the capacity to produce peptide hormones. They display prominent rough endoplasmic reticulum and Golgi complex and are rich in free ribosomes, but their most characteristic feature is the presence of round secretory granules that store amine substances.[50] The "classic" APUD system included all peptide-producing cells of the stomach, duodenum, intestine, pancreatic islets, adrenal medulla, extra-adrenal paraganglia, anterior pituitary, parafollicular thyroid cells, and melanoblasts.[51] Observations over the years have changed and expanded the APUD cell concept. First, the same amines and peptides found in classic APUD cells are also present in the central nervous system, in peripheral nerves, and in more widely dispersed endocrine cells in organs of the GI and respiratory tracts. Studies have shown that some of these cells are derived during embryogenesis from the neural crest and some from the endoderm. The term neuroendocrine, therefore, has slowly replaced APUD, to reflect the close association between the neural and endocrine systems.

Somatostatin Receptors

Somatostatin, a 14-amino-acid peptide, is found principally in the hypothalamus, but it also occurs in the GI system, other parts of the brain, the spinal cord, peripheral nerves, placenta, retina, thymus, and adrenal medulla.[52] Physiologically, somatostatin plays a key role in the modulation of neuroendocrine cells. In the pituitary gland it acts as a neurohormone, inhibiting the release of growth hormone, adrenocorticotropic hormone (ACTH), and thyroid-stimulating hormone (TSH). In the nervous system it is a neurotransmitter or neuromodulator. Outside the brain it can act directly on cells (paracrine function) or as a true hormone. For example, circulating in the blood, it can act on the pancreas or GI tract to inhibit the release of intestinal peptides such as insulin, gastrin, and glucagon.

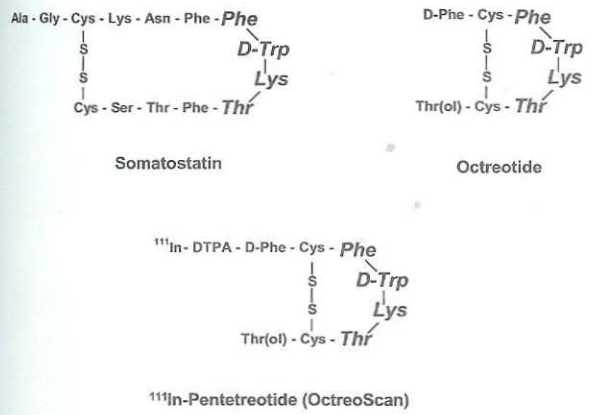

FIGURE 20-10 Chemical structures of somatostatin, octreotide, and ^{111}In-pentetreotide.

Somatostatin receptors have also been demonstrated on a variety of human tumors of neuroendocrine tissue, such as pituitary tumors, endocrine pancreatic tumors, carcinoids, paragangliomas, small cell lung cancers, medullary thyroid carcinomas, and pheochromocytomas, as well as meningiomas, astrocytomas, neuroblastomas, and some breast cancers.[53,54] Mechanistically, somatostatin is known to inhibit secretion of hormones and growth factors that regulate tumor growth, inhibit angiogenesis, modulate immunologic activity, and exhibit direct antimitotic effects via somatostatin receptors on tumor cells. Because of these actions, somatostatin should be a useful agent in the treatment of neuroendocrine tumors. From a practical point of view, however, the short plasma half-life (about 2 minutes) of somatostatin necessitated the development of a longer-acting derivative that could be used as a therapeutic agent.[52,55] This was eventually accomplished by chemical modification of the molecule, eliminating the amino acids responsible for somatostatin's rapid metabolism and retaining the cyclic amino acid configuration required for receptor binding (Figure 20-10). The result was a synthetic 8-amino-acid sequenced peptide known as octreotide, which is currently marketed as Sandostatin (Novartis).

Indium In 111 Pentetreotide Injection

The high density of somatostatin receptors on primary and metastatic tumor cells permits their detection with radionuclide markers of octreotide analogues. One such agent is indium In 111 pentetreotide injection (^{111}In-pentetreotide, or OctreoScan [Mallinckrodt]), which has specific affinity for somatostatin receptors on tumors. Positive scans of such tumors are useful in optimizing decisions about primary treatment and have been shown to predict good response to long-term therapy with somatostatin analogues (octreotide) for symptoms related to hormonal hypersecretion.

^{111}In-pentetreotide is prepared from a kit that contains a lyophilized mixture of pentetreotide and appropriate adjuvants for labeling. The kit also contains a separate vial of ^{111}In-indium chloride injection, which is added to the lyophilized pentetreotide at the time of use. The preparation and chemical properties of ^{111}In-pentetreotide are discussed in Chapter 9. The labeled product should be used within 6 hours of preparation. If necessary, the labeled product may be diluted to a maximum volume of 3 mL with normal saline immediately before use. Dilution should not be done before the labeling reaction.

^{111}In-pentetreotide is indicated for diagnostic localization of primary and metastatic neuroendocrine tumors bearing somatostatin receptors.[55] After intravenous injection, ^{111}In-pentetreotide distributes rapidly into the tissues, with only about one-third of the injected dose remaining in the blood pool 10 minutes after injection. It is excreted primarily by the kidney. About 50% is eliminated in the urine by 6 hours and 90% by 48 hours. Minor

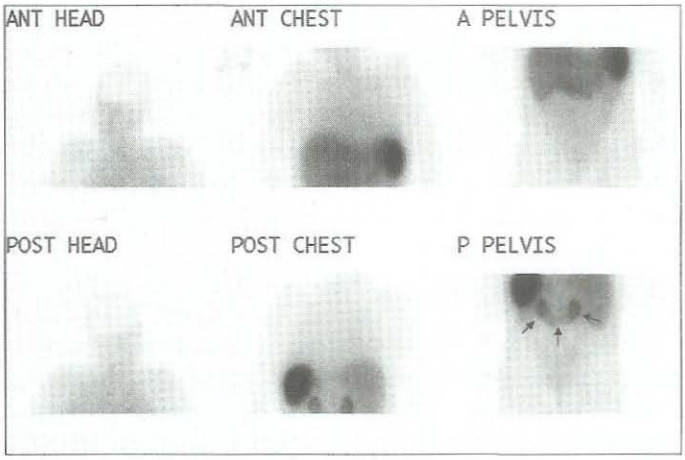

FIGURE 20-11 Normal ^{111}In-pentetreotide scan. Anterior and posterior spot images of the body were obtained 24 hours after intravenous administration of 5 mCi (185 MBq) of ^{111}In-pentetreotide. Physiologic radiotracer accumulation is seen in the liver, spleen, and kidneys. Note the curvilinear uptake in the kidneys in the posterior image of the pelvis in this patient with a horseshoe kidney (arrows).

amounts (<2%) undergo hepatobiliary excretion. The usual adult dosage for SPECT imaging is 6 mCi (222 MBq). Organs receiving the highest radiation absorbed dose are the spleen (14.8 rad), kidneys (10.8 rad), and urinary bladder (6 rad) per 6 mCi (222 MBq) dose.

The following precautions should be noted.[55] ^{111}In-pentetreotide should not be injected into intravenous lines used for parenteral nutrition because the sugars present may cause a glycosyl–^{111}In-pentetreotide conjugate to form. Patients receiving octreotide therapy should suspend this medication for 72 hours before administration of ^{111}In-pentetreotide. The patient should maintain good hydration (two 8 oz glasses of water prior to injection) to increase renal elimination and thus reduce background activity. Bowel cleansing is recommended before imaging to promote elimination of normal bowel accumulation of activity. Suggested bowel preparation agents are Dulcolax, magnesium citrate, and Metamucil.[56] Standard octreotide therapy may cause hypoglycemia in patients with insulinoma; therefore, as a precaution, an intravenous infusion of glucose should be given just before and during administration of ^{111}In-pentetreotide in patients with insulinoma.

Imaging is performed in 24 hours and may be repeated at 48 hours if needed to rule out suspected bowel accumulation of activity localized in the abdominal region. Uptake of ^{111}In-pentetreotide will be evident in tumors rich with somatostatin receptors. Uptake is also expected to occur in the normal pituitary gland, thyroid gland, liver, spleen, kidneys, and urinary bladder (Figure 20-11).[54] Many tumors have a high number of somatostatin receptors and will bind ^{111}In-pentetreotide (Figures 20-12 and 20-13). Krenning and colleagues[53,54] have comprehensively discussed ^{111}In-pentetreotide scintigraphy. Table 20-2 gives a partial list of tumors with their somatostatin receptor density, the detection rate of these tumors by ^{111}In-pentetreotide scintigraphy, and the correlation of ^{111}In-pentetreotide scintigraphy with other diagnostic methods. Fairly good agreement exists between the density of receptors present in tumors measured by positive ^{111}In-pentetreotide uptake and their detection by CT, MRI, ultrasonography, angiography, surgery, or biopsy. ^{111}In-pentetreotide may detect small tumors and metastatic lesions not found by CT, MRI, or ultrasonography. In a multicenter trial, 28% of tumors detected by ^{111}In-pentetreotide were missed by other methods.[56]

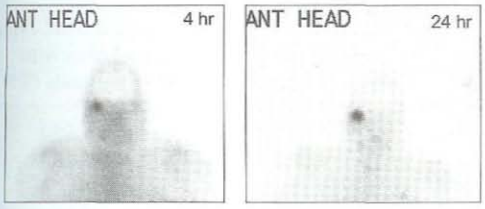

FIGURE 20-12 Abnormal ^{111}In-pentetreotide scan demonstrating a somatostatin receptor-positive tumor in the head. Anterior and posterior spot images of the head obtained at 4 and 24 hours after intravenous administration of 5 mCi (185 MBq) of ^{111}In-pentetreotide demonstrate an abnormal focal accumulation in the region of the right ear that corresponded to a right postauricular mass seen on a CT study.

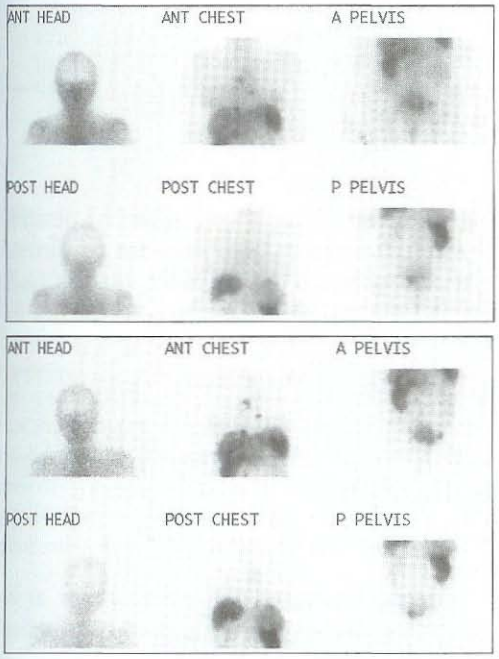

FIGURE 20-13 Abnormal ^{111}In-pentetreotide scan with multiple areas of increased uptake in a patient with metastatic carcinoid tumor. Anterior and posterior spot images of the head, chest, abdomen, and pelvis were obtained at 4 hours (top) and 24 hours (bottom) after intravenous administration of 5 mCi (185 MBq) of ^{111}In-pentetreotide. The images demonstrate multiple focal areas of abnormal accumulation in the chest, abdomen, and pelvis consistent with metastatic carcinoid.

^{111}In-pentetreotide is helpful in selecting a patient's treatment. For example, surgical treatment is more favorable when there is a solitary localized tumor. Widespread metastatic lesions are better treated with drugs. Posttreatment scans with ^{111}In-pentetreotide can also be used to monitor the effectiveness of treatment of receptor-positive tumors. Clinicians can better predict the response to octreotide therapy if tumors are receptor-positive as shown by positive ^{111}In-pentetreotide uptake. Therapy and expense can be spared in patients who have negative scans, indicative of receptor-negative tumors.

Technetium Tc 99m Depreotide Injection

Technetium Tc 99m depreotide injection (^{99m}Tc-depreotide, or NeoTect [Diatide]) is a radiolabeled peptide that binds to somatostatin receptors in normal and malignant tissue. Its preparation and chemical properties are described in Chapter 9. ^{99m}Tc-depreotide is indicated for the localization of receptor-bearing pulmonary masses in patients with CT-identified lesions who have known or highly suspected malignancy. The usual adult administered activity of ^{99m}Tc-depreotide is 15 to 20 mCi (555 to 740 MBq) by intravenous injection. Imaging is performed between 2 and 4 hours after injection. Approximately 12% of the injected activity is excreted in the urine by 4 hours.

Clinical studies comparing the value of ^{99m}Tc-depreotide with histologic examination in detecting malignant solitary pulmonary nodules showed a sensitivity of around 70%

TABLE 20-2 ^{111}In-Pentetreotide (OctreoScan) Correlation in Tumor Detection

Tumor Type	In Vitro Receptor Prevalence (%)[a]	Scintigraphy Detection Rate (%)[a]	Correlation with Other Methods (%)[b]
Carcinoid	55/62 (88)	74/78 (95)	190/237 (80)
Gastrinoma	6/6 (100)	13/14 (93)	40/42 (95)
Insulinoma	18/27 (67)	13/28 (46)	4/13 (31)
Medullary thyroid carcinoma	10/26 (38)	24/35 (69)	12/22 (54)
Paraganglioma	11/12 (92)	42/42 (100)	6/7 (86)
Pituitary adenoma	45/46 (98)	21/28 (75)	24/30 (80)
Small cell lung carcinoma	4/7 (57)	38/38 (100)	2/2 (100)
Pheochromocytoma	38/52 (73)	13/15 (87)	9/9 (100)

[a] Data from reference 45.

[b] Data from reference 46.

and a specificity of 79% to 86%.[57–59] The false-negative rate (negative images in positive biopsies) was 29% and the false-positive rate (positive images in patients with confirmed acute and chronic inflammatory processes or infections) was 17%. Other studies have shown ^{99m}Tc-depreotide to be comparable to ^{18}F-FDG PET in sensitivity and accuracy for evaluation of malignant solitary pulmonary nodules.[50,51] Thus, SPECT imaging with ^{99m}Tc-depreotide appears to offer a convenient imaging modality at facilities where ^{18}F-FDG PET is not available.

FDG-PET TUMOR IMAGING

Fludeoxyglucose F 18 Injection

Fludeoxyglucose F 18 injection (^{18}F-FDG) is a glucose analogue with a fluorine atom replacing the hydroxyl group in the C-2 position of D-glucose. Its method of production is discussed in Chapter 10. Its biologic properties and mechanism of tissue uptake are described in detail in Chapters 10 and 13. Briefly, FDG uptake into tissues is similar to that of glucose, except that FDG is trapped as FDG-6-phosphate because it cannot be metabolized further. The trapped activity permits imaging of any tissue that metabolizes glucose. Because tumors have metabolic rates greater than those in normal tissues, they can be localized by their higher accumulation of FDG activity compared with normal tissue.

After intravenous injection of ^{18}F-FDG in a normal fasting patient, the brain cortex demonstrates high uptake of FDG because glucose is the primary energy substrate in brain. Therefore, total-body images demonstrate prominent activity in the brain. Uptake of FDG by the myocardium depends primarily on the glucose load in the blood. In the fasting state, the heart uses primarily fatty acids as its energy source, but in the postprandial state or after administration of a glucose load, heart uptake of FDG is increased.

For tumor imaging, the patient must fast for at least 4 hours to lower blood glucose concentration and maximize uptake in tumor tissue. The patient should limit physical activity for 45 to 60 minutes after dosing to minimize FDG uptake in skeletal muscle while the dose is localizing in tumor. The patient should also void just prior to imaging to eliminate urinary accumulation of FDG. The administered activity ranges from 5 to 20 mCi (185 to 740 MBq) and depends partly on the type of scanner. Typical bismuth germanate PET scanners in the two-dimensional mode require doses of 10 to 15 mCi (370 to 555 MBq).[60] The injection technique is critical because dose extravasation will cause avid uptake of FDG in the lymph nodes draining the area. Thus, imaging of the right axillary

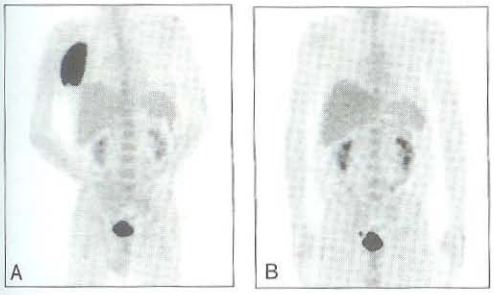

FIGURE 20-14 ^{18}F-FDG PET. Hodgkin's lymphoma before and after chemotherapy. (A) Patient with large right axillary mass diagnosed as Hodgkin's lymphoma. Anterior PET image shows a prominent abnormal focal area of hypermetabolism in the right axilla. (B) Follow-up PET scan demonstrates interval resolution of the focal area of hypermetabolism in the right axilla after completion of chemotherapy. There is no evidence of active lymphoma on the follow-up scan.

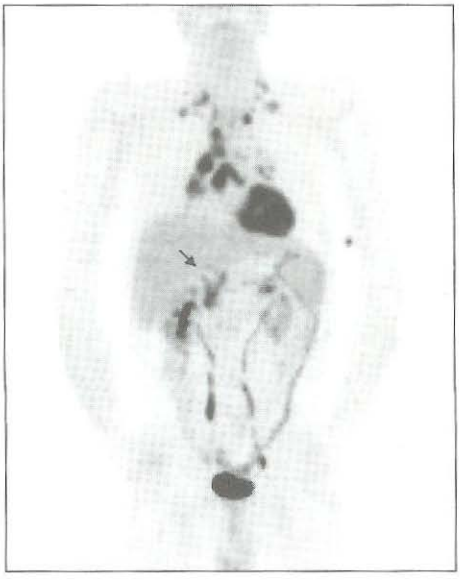

FIGURE 20-15 ^{18}F-FDG PET. Hodgkin's lymphoma. Anterior PET image obtained 1 hour after intravenous administration of 12 mCi (444 MBq) of ^{18}F-FDG. There are multiple abnormal focal areas of hypermetabolism in the chest. An abnormal focal area of hypermetabolism is also seen in the abdomen medial to the right kidney (arrow).

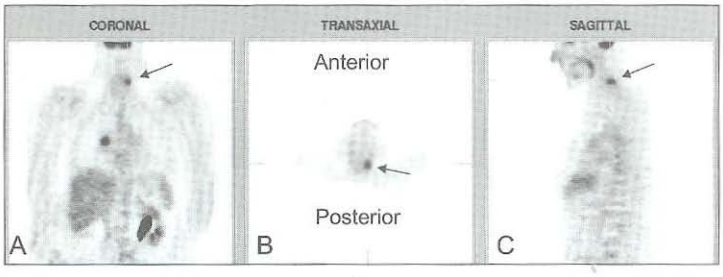

FIGURE 20-16 ^{18}F-FDG PET. Metastatic renal cell carcinoma. (A) Coronal PET image of the chest and abdomen demonstrating two abnormal focal areas of hypermetabolism. One is in the right hilar region. The other is in the right neck (arrow). There is no radiotracer uptake in the right kidney. The patient has had a prior right nephrectomy for renal cell carcinoma. (B) An axial image through the neck shows this focus to be in the right posterior paramidline region (arrow). (C) A sagittal image through the neck lesion helps confirm that this is in a vertebral body (arrow).

region, for example, requires intravenous injection into the left arm or a foot vein to minimize potential interference.[60]

^{18}F-FDG has broad application in cancer diagnosis. The Food and Drug Administration (FDA) has approved FDG PET for all cancers, and Medicare reimbursement for use in the diagnosis and staging of a number of tumors has been approved.[45] (See Chapter 10, Tables 10-6, 10-7, and 10-8, for approved PET procedures.) Figures 20-14 through 20-19 demonstrate the value of FDG PET imaging in a variety of tumor types.

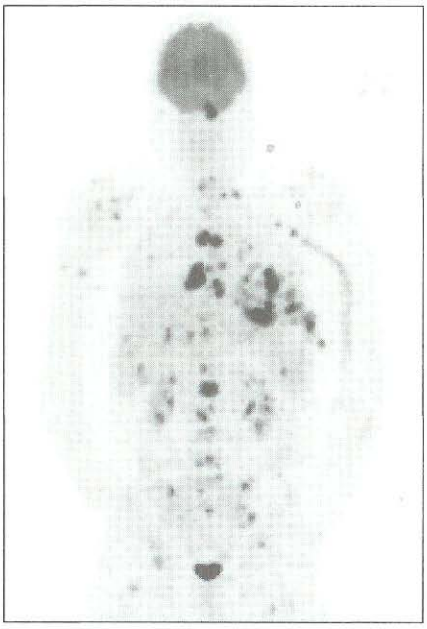

FIGURE 20-17 ^{18}F-FDG PET. Melanoma. Anterior PET image demonstrating multiple abnormal focal areas of hypermetabolism in this patient with widespread metastatic disease from melanoma.

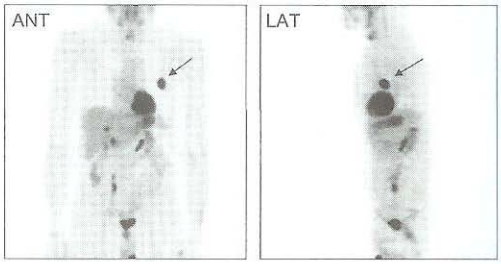

FIGURE 20-18 ^{18}F-FDG PET. Single pulmonary nodule. Anterior and lateral images demonstrating a focal area of hypermetabolism in the left lung in this patient with non–small-cell lung carcinoma (arrow). On this study, prominent uptake in the left ventricle of the heart is likely due to insufficient fasting before the exam.

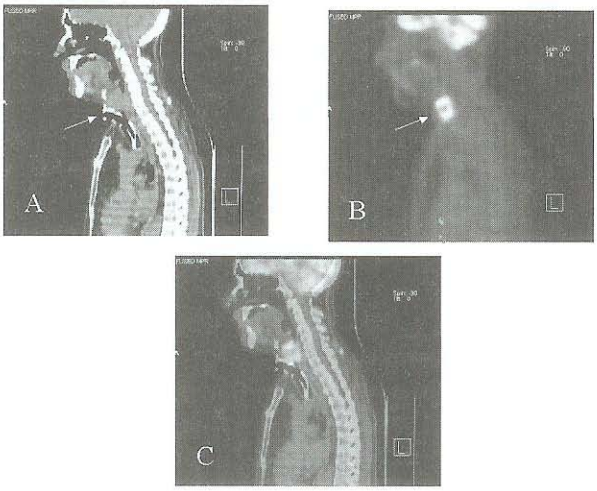

FIGURE 20-19 ^{18}F-FDG PET. PET/CT fusion study. Sagittal images of the neck of a patient with recurrent squamous cell carcinoma. (A) Sagittal noncontrast CT image of the neck. The patient has a tracheostomy tube in place (arrow). (B) Sagittal PET image through the same plane demonstrates an abnormal focal area of hypermetabolism consistent with recurrent tumor (arrow). (C) PET/CT fusion image demonstrating the location of the recurrent tumor above the endotracheal tube.

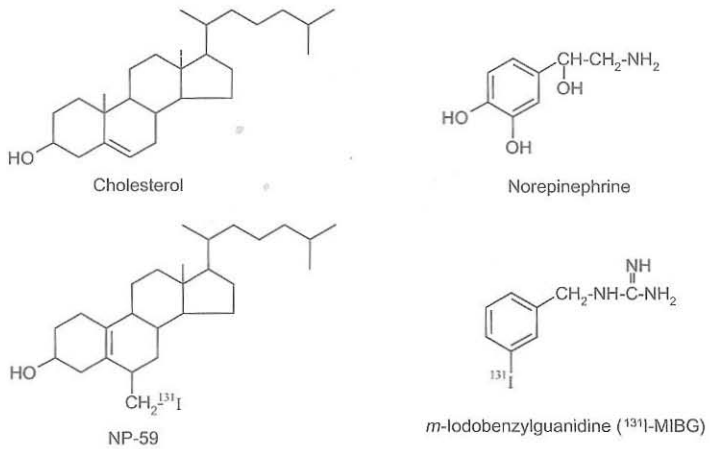

FIGURE 20-20 Chemical structures of cholesterol, NP-59, norepinephrine, and ^{131}I-*meta*-iodobenzylguanidine (^{131}I-MIBG).

ADRENAL GLAND IMAGING AGENTS

The body has two adrenal glands, each weighing about 5 grams, normally situated on the upper pole of each kidney. Each adrenal gland has two zones. The adrenal cortex (outer zone) is responsible for producing mineralocorticoids, the primary one being aldosterone, and glucocorticoids, primarily cortisol. The cortex also produces androgenic hormones. The adrenal medulla (inner zone) produces epinephrine and norepinephrine, the pressor amines associated with stimulation of the sympathetic nervous system.

Radiopharmaceutical agents have been developed to image the adrenal cortex and medulla on the basis of normal biochemical processes that occur in these tissues.

Cortical Imaging Agents

Because cholesterol is the main precursor substance in the production of adrenocortical steroids, radiolabeled cholesterol analogues were developed to study the adrenal gland. The principal agent to achieve success for imaging the adrenal cortex is ^{131}I-6-β-iodomethyl-19-norcholesterol (NP-59) (Figure 20-20).[61] It has been used to evaluate several conditions that affect the adrenal glands, such as Cushing's syndrome, primary aldosteronism, hyperandrogenism, and adrenal masses; its use has been reviewed by Thrall et al.[62]

Medullary Imaging Agents

The role of the adrenal medulla in the synthesis and storage of catecholamines was key to the development of adrenal medullary imaging agents. Dopamine is the immediate precursor to norepinephrine, which is synthesized in the chromaffin cells of the adrenal medulla (Figure 20-21). One approach to developing an adrenal imaging agent was to radiolabel dopamine and its analogues. Although uptake of ^{14}C-labeled dopamine and ^{35}S-labeled dopamine analogues into the adrenals was demonstrated, no satisfactory gamma-emitting dopamine analogue could be prepared.[63]

A successful approach was eventually found when radioiodinated benzylguanidines were investigated because of their potent antiadrenergic activity.[64] The ability to halogenate the aromatic ring in benzylguanidine led Wieland et al.[65] to investigate the *ortho-*, *meta-*, and *para*-iodinated derivatives. Further studies demonstrated that the *meta*-iodinated isomer

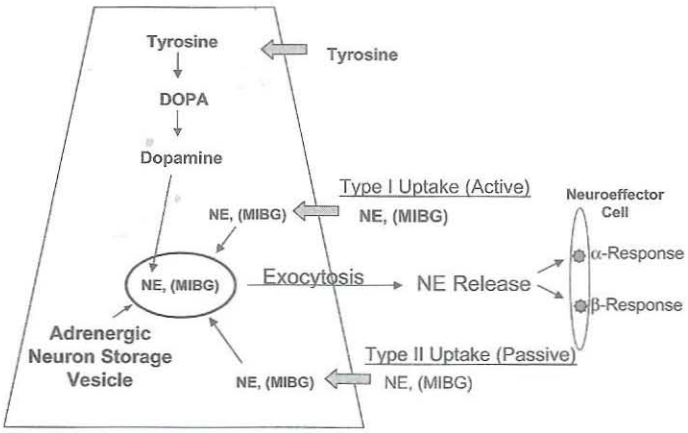

FIGURE 20-21 Mechanism of localization of *m*-iodobenzylguanidine (^{123}I- or ^{131}I-MIBG) in adrenergic neurons and adrenomedullary cells.

(Figure 20-20) was superior for imaging by virtue of its resistance to in vivo deiodination and its lower concentration in liver compared with the other isomers.[66]

Iobenguane I 123 or I 131 Injection

Radioiodinated *meta*-iodo-benzylguanidine (iobenguane sulfate, or MIBG) is labeled by the solid-phase isotope exchange method described in Chapter 9. ^{131}I-MIBG is available commercially as a frozen product, while ^{123}I-MIBG is prepared extemporaneously. ^{131}I-MIBG has been shown to be effective in localizing neuroendocrine tumors derived from the APUD system. It has approved indications for scintigraphic localization of pheochromocytomas and neuroblastomas.[67,68] ^{131}I-MIBG has also been shown to be useful in carcinoid tumors and medullary carcinoma of the thyroid.[69,70]

Uptake Mechanism, Inhibition, and Biologic Properties

Tumors that take up ^{131}I-MIBG are believed to do so by a specific uptake mechanism, with storage in intracellular granules (Figure 20-21). Experimental evidence indicates that ^{131}I-MIBG is taken up into sympathetic neuroeffector cells similar to norepinephrine by a specific catecholamine type I active uptake mechanism and stored in adrenergic storage vesicles.[71] Reserpine, a drug known to inhibit the uptake of norepinephrine by chromaffin granules and to deplete stores of catecholamines in the adrenal medulla, has been shown to deplete 90% of MIBG stores in the adrenal medulla in dogs previously administered ^{131}I-MIBG.[66] ^{131}I-MIBG's uptake mechanism is similar to that of norepinephrine, but unlike norepinephrine it does not interact with postsynaptic α- and β-adrenergic receptors.

A number of drugs that participate in the same mechanisms of uptake or depletion of epinephrine as ^{131}I-MIBG have been shown to reduce the uptake of ^{131}I-MIBG in neuroendocrine tumors. Drugs that are known to interfere with ^{131}I-MIBG scintigraphy or are expected to reduce ^{131}I-MIBG uptake because of their known pharmacologic actions are listed in Table 20-3.[72] The length of time a patient should refrain from using the drug before ^{131}I-MIBG administration is also given.

After intravenous injection, ^{131}I-MIBG is found to localize normally in tissues with extensive sympathetic innervation (salivary glands, nasopharynx, and heart) and tissues involved in metabolism and excretion (liver, spleen, and urinary bladder) (Figure 20-22).[71,73] Normal

TABLE 20-3 Drugs Known or Expected to Reduce MIBG Uptake in Sympathetic Neuroeffector Cells

Group 1 (should not be taken for 6 weeks prior to MIBG administration)	Group 2 (should not be taken for 2 weeks prior to MIBG administration)
Tricyclic Antidepressants Amitriptyline, amoxapine, desipramine, doxepin, imipramine, maprotiline, nortriptyline, protriptyline, trazodone, trimipramine	*Tranquilizers* Acetophenazine, chlorpromazine, chlorprothixene, droperidol, fluphenazine, haloperidol, mesoridazine, perphenazine, pimozide, prochlorperazine, promazine, thioridazine, thiothixene, trifluoperazine, triflupromazine *Sympathomimetics* Albuterol, amphetamine, benzphetamine, cocaine, dextroamphetamine, diethylpropion, dobutamine, dopamine, fenfluramine, isoetharine, isoproterenol, mazindol, metaproterenol, metaraminol, methamphetamine, methylphenidate, phendimetrazine, phenmetrazine, phentermine, phenylephrine, phenylpropanolamine, pseudoephedrine, terbutaline *Antihypertensive/Cardiovascular Drugs* Bretylium, diltiazem, guanethidine, labetalol, nifedipine, reserpine, verapamil

Source: Reference 72.

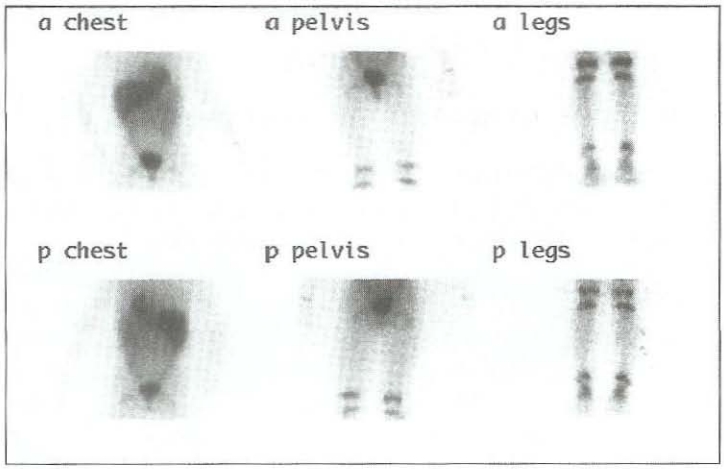

FIGURE 20-22 Normal MIBG scan. Anterior and posterior spot images of the chest, abdomen, and pelvis were obtained 24 hours after intravenous administration of 2.5 mCi (92.5 MBq) of ^{123}I-MIBG. Normal uptake is seen in the liver, bladder, and growth plates.

adrenal medulla is seen only occasionally, because of its small size and depth in the body. Most of the ^{131}I-MIBG is excreted unchanged in the urine: 55% in 24 hours and 90% in 4 days.[74] The stability of ^{131}I-MIBG in vivo is attributed to the guanidine side chain. A small amount of in vivo metabolism does occur, however, with release of 2% to 6% free iodide. This requires administration of potassium iodide to protect the thyroid gland.

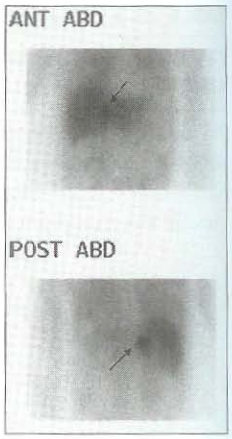

FIGURE 20-23 MIBG scan. Pheochromocytoma. Anterior and posterior images of the abdomen taken 24 hours after intravenous administration of 10 mCi (370 MBq) of ^{123}I-MIBG in this patient with history of pheochromocytoma. There is an abnormal focal area of accumulation in the region of the right adrenal gland (arrow) consistent with the patient's history of pheochromocytoma.

The usual intravenous adult administered activity of ^{131}I-MIBG is 0.5 mCi (18.5 MBq). In patients over 65 kg the dose is 0.3 mCi/m^2 (11.1 MBq/m^2) up to a maximum of 1 mCi (37 MBq). Children's doses of ^{131}I-MIBG are based on 0.3 mCi/m^2 (11.1 MBq/m^2) to a maximum dosage of 0.5 mCi. Dosing of ^{123}I-MIBG is based on 0.14 mCi/kg (5.18 MBq/kg), with a suggested maximum dose of 10 mCi (370 MBq) in adults.[75,76] A thyroid-blocking dose of potassium iodide should be administered 1 day before dosing and 7 days after dosing with ^{131}I-MIBG.[77] The FDA-recommended thyroid-protective doses of potassium iodide daily are as follows: infants less than 1 month old, 16 mg; children 1 month to 3 years, 32 mg; children 3 years to 18 years, 65 mg; and adults, 130 mg.

The critical organs for ^{131}I-MIBG in the adult are the urinary bladder wall and the liver, each with a radiation absorbed dose of 3 rad(cGy)/mCi.[77]

Figures 20-23 through 20-26 illustrate the value of MIBG in the diagnosis of pheochromocytoma, neuroblastoma, and paraganglioma.

PARATHYROID GLAND IMAGING AGENTS

Normally there are four parathyroid glands in the human body, one located behind each upper and lower pole of the thyroid. Ectopic locations of parathyroid glands can occur, particularly in the region of the thymus gland and mediastinum.

The parathyroid glands secrete parathormone (PTH), which regulates calcium and phosphorus metabolism in the body. PTH promotes calcium and phosphate resorption from bone, increased renal tubular reabsorption of calcium, and a diminished rate of phosphate reabsorption. Hypersecretion of PTH may be caused by a parathyroid adenoma (primary hyperparathyroidism) or through an indirect feedback mechanism initiated by hypocalcemia due to renal failure. The latter process results in parathyroid hyperplasia (secondary hyperparathyroidism) that can progress, leading to autonomous activity of one or more of the parathyroid glands (tertiary hyperparathyroidism). Serum calcium levels routinely monitored in blood screens are an important diagnostic parameter in identifying parathyroid disease.

There is no clear way to differentiate a hyperplastic gland from an adenoma. In general, an enlarged gland is classified as an adenoma if the remaining three glands are found to be normal. If all four parathyroids are enlarged, a diagnosis of hyperplasia is made.[78] About 85% of cases of hyperparathyroidism are caused by a solitary parathyroid adenoma that can be effectively cured by surgery. The success rate for resection of parathyroid adenomas is 95%, which would appear to obviate the need for a presurgical scan of the parathyroids. However, scintigraphy is helpful in directing surgical exploration to the site

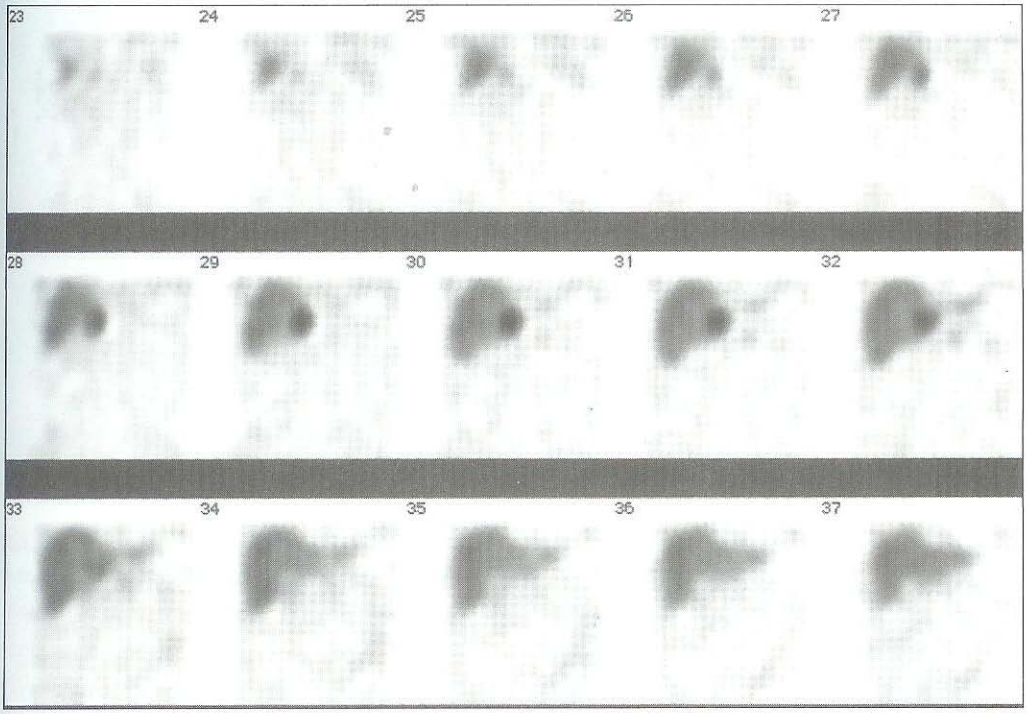

FIGURE 20-24 ^{123}I-MIBG SPECT. Pheochromocytoma. Coronal SPECT images through the abdomen of the patient in Figure 20-23 demonstrate a prominent abnormal focus in the region of the right adrenal gland.

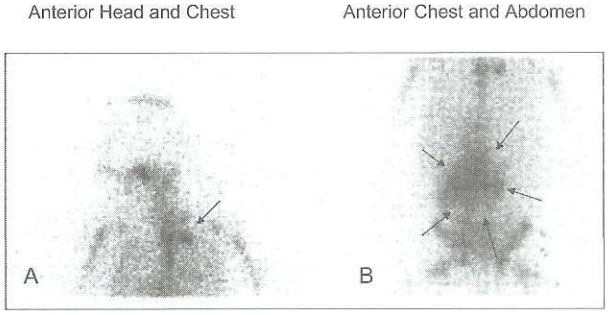

FIGURE 20-25 MIBG scan. Neuroblastoma. Anterior spot images of the head, chest, and abdomen taken 48 hours after intravenous administration of 2.2 mCi (81.4 MBq) of ^{123}I-MIBG. (A) Small focal area of abnormal radiotracer accumulation is seen near the manubrium (arrow). (B) There is a large focal area of abnormal accumulation in the abdomen and pelvis (arrows) representing uptake in neuroblastoma.

of the adenoma, particularly if it is ectopic, and scanning is also useful in localizing suspected residual adenoma after a previous parathyroidectomy.

No radiopharmaceutical specifically targets the parathyroid glands, and so special imaging techniques have been devised to localize parathyroid adenomas. After an initial report that ^{201}Tl-thallous chloride was taken up in parathyroid glands,[79] purportedly because of the increased cellular density and vascularity of parathyroid adenomas, a dual-isotope

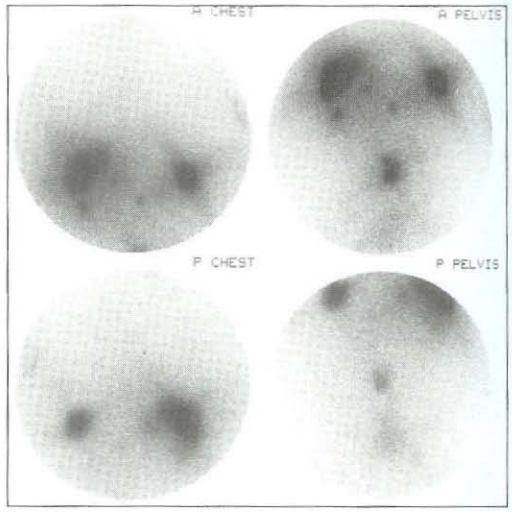

FIGURE 20-26 MIBG scan. Paraganglioma. Anterior and posterior spot images of the chest, abdomen, and pelvis taken 24 hours after intravenous administration of 475 μCi (17.58 MBq) of ^{131}I-MIBG in a patient who was treated for paraganglioma with metastases to liver and bone. There are abnormal focal areas of radiotracer uptake in the liver and left upper quadrant. Multiple smaller focal areas of abnormal uptake are identified in the abdomen. There is also a focus of radiotracer uptake in the midline lower abdomen that is more anteriorly located. These are all consistent with metastatic involvement. Radiotracer uptake was also noted in the right femur and left humerus (images not shown).

method was described to localize adenomas.[80] This technique used two agents, ^{201}Tl-thallous chloride and ^{99m}Tc-sodium pertechnetate. The original method involved administration of pertechnetate first, followed by thallium. Others have reversed this order, acquiring the lower-energy thallium scan first to facilitate separation of the two photon energies by gamma spectrometry. Because thallium localizes in both parathyroid and thyroid tissue but pertechnetate localizes only in thyroid tissue, subtraction of the thyroid image isolates the parathyroid adenoma. If ^{99m}Tc-sodium pertechnetate is administered first, the 140 keV pertechnetate thyroid image is stored as a matrix in the computer. A downscatter image from ^{99m}Tc is also stored in the 75 keV ^{201}Tl window. The ^{99m}Tc 140 keV thyroid and 75 keV downscatter images are typically of 5 minutes' duration each. ^{201}Tl-thallous chloride is injected, and the thyroid/parathyroid images are obtained in the 75 keV window. These images are acquired as an accumulation of 1 minute images for 25 minutes so that part of them can be discarded if patient motion occurs. During processing, the technetium downscatter image matrix is first subtracted from the thallium cumulative image. The ^{99m}Tc 140 keV thyroid image is then subtracted serially from the thyroid/parathyroid image until the enlarged or hyperplastic parathyroid tissue becomes apparent in the image (Figure 20-27). Usually 2 mCi (74 MBq) of each tracer is used for this procedure.

In 1989, Coakley et al.[81] introduced the use of ^{99m}Tc-sestamibi for imaging parathyroid adenoma. Subsequently, a report on preoperative localization of adenoma with this agent demonstrated its equivalency to ^{201}Tl-thallous chloride.[82] The method involved acquisition of ^{123}I thyroid images, which were then subtracted from ^{201}Tl-thallous chloride or ^{99m}Tc-sestamibi thyroid/parathyroid images to isolate the parathyroid adenoma. Sestamibi was found to wash out of parathyroid tissue more slowly than thallium. The slower washout of sestamibi was attributed to its avidity for the increased number of mitochondria in parathyroid adenomas.

To simplify the method of parathyroid adenoma scintigraphy, Taillefer et al.[83] described a double-phase differential washout technique. The method is based on the time-dependent variation in washout rates of ^{99m}Tc-sestamibi from the thyroid gland and parathyroid adenomas. The imaging technique consists of administration of 20 to 25 mCi (740 to 925 MBq) of ^{99m}Tc-sestamibi with images made at 15 minutes (early phase) and 2 hours (late phase). With this method 90% (19 of 21) of parathyroid adenomas are localized on the basis of more rapid washout of sestamibi from thyroid tissue compared with slower washout from parathyroid adenoma. The parathyroid adenoma-to-thyroid activity ratio

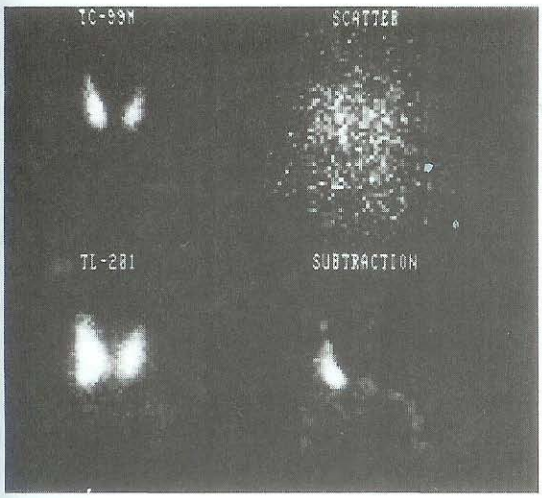

FIGURE 20-27 $^{201}Tl/^{99m}Tc$-pertechnetate parathyroid imaging using a subtraction technique. The technetium thyroid image was subtracted from the thallium thyroid/parathyroid image to demonstrate the location of the parathyroid adenoma.

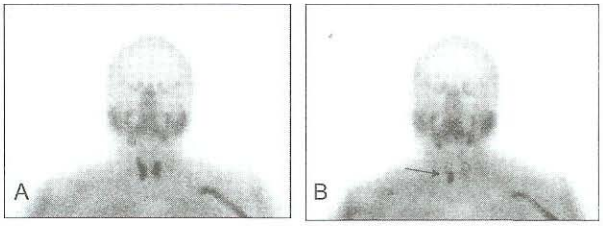

FIGURE 20-28 ^{99m}Tc-sestamibi parathyroid scan demonstrating a parathyroid adenoma. Anterior spot images of the neck were obtained 15 minutes and 2 hours after intravenous administration of 20 mCi (740 MBq) of ^{99m}Tc-sestamibi to this patient with hyperparathyroidism. (A) On the 15 minute image radiotracer accumulation is seen in both lobes of the thyroid gland. (B) On the 2 hour image there has been clearance of radiotracer from the thyroid gland. However, an abnormal focal area of residual radiotracer accumulation is seen in the region of the lower pole of the right lobe of the thyroid gland consistent with a right inferior parathyroid adenoma.

was reported to be 1.24 in early-phase imaging, increasing to 1.46 in late-phase imaging, where the adenoma was clearly seen (Figure 20-28).

MISCELLANEOUS IMAGING PROCEDURES

Lymphoscintigraphy

The typical interstitial location of solid tumors predisposes their spread systemically via the lymphatic system. This concept was introduced in the 18th century by Le Dran, who described the progression of breast cancer to regional lymph nodes via the lymphatics.[84,85] Le Dran postulated that cancer metastasized systemically by this mechanism, and his work provided an early foundation from which the sentinel node concept has developed over the past 20 years.

The Sentinel Node Concept

The sentinel node concept postulates that the first lymph node, or sentinel node (SN), that receives lymph drainage from a tumor bed will contain cancer cells if the primary tumor has spread via the lymphatics. If this is true, then finding a sentinel node that is cancer free is strong evidence that the tumor has not spread. The SN concept presupposes an

orderly spread of cancer within the lymphatic chain beginning with the sentinel lymph node. The possibility exists that more than one lymph node bed may drain a tumor site, and thus more than one sentinel node may be identified. Therefore, the mapping techniques that are used must be able to identify all lymph node basins draining a tumor site.

Morton and Chan[85] have described the application of the SN concept to malignant melanoma, tracing the concept from its early beginnings to the current methods of SN identification: lymphoscintigraphy, vital blue dye, and gamma probe counting during surgery. The rationale for the current diagnostic approach is that, of those patients with intermediate-thickness primary melanoma who undergo lymph node dissection, only about 20% are expected to have metastasis in regional lymph nodes. Thus about 80% of patients will undergo an unnecessary procedure that is costly and fraught with morbidity, including risk of acute wound problems, chronic lymphedema, and nerve injury. The finding of cancer-free SNs can spare many patients the expense and problems associated with lymph node dissection.

The SN concept was brought to the forefront of cancer management around the same time by Cabanas[86] and Holmes et al.[87] Cabanas, in the management of patients with penile cancer, introduced the term sentinel node and applied the SN concept to 43 penile carcinoma patients, finding that 31 patients with SNs negative for tumor had a 5 year survival rate of 90%.[88] SN identification was accomplished by a manual surgical technique. Holmes et al.[87] used lymphoscintigraphy in applying the SN concept to map lymph node basins and introduced the concept of selective lymphadenectomy in primary cutaneous melanomas. On the basis of their experience with radiopharmaceutical mapping, vital blue dye as a visual marker was introduced to facilitate localization of the lymphatic basin during surgery.[89] With the dye technique, they were able to identify SNs in 194 (82%) of 237 lymphatic basins. Of those nodes that were positive for tumor, only two SNs were negative when a nonsentinel node in the same basin was found to be positive (<1% false-negative rate), demonstrating the high accuracy rate of this procedure.

In 1993, Alex et al.[90] introduced the use of ^{99m}Tc-sulfur colloid (^{99m}Tc-SC) for melanoma lymphoscintigraphy. They initially compared lymphoscintigraphy and the use of a gamma scintillation probe with vital blue dye to identify sentinel lymph nodes in cats, demonstrating equal sensitivities of the two techniques. These findings were subsequently corroborated in patients with malignant melanoma.[91]

Melanoma Lymphoscintigraphy

Lymphoscintigraphy has been shown to improve the accuracy of staging patients with malignant melanoma.[92–94] The generally accepted staging for malignant melanoma is summarized in Table 20-4. Approximately 85% of patients with malignant melanoma present with stage I or II disease.[92] Identification of nodal involvement in these patients is key to staging and treatment because positive nodal involvement accurately predicts spread of disease via the lymphatics. Conversely, negative SN involvement removes the necessity

TABLE 20-4 Staging Criteria for Malignant Melanoma

Melanoma Stage	Staging Criteria
Stage I	Thin (<1.5 mm) primary tumor
Stage II	Thicker (>1.5 mm) primary tumor
Stage III	Regional spread of disease to skin more than 5 cm from primary tumor or to regional lymph nodes
Stage IV	Evidence of distant metastases

Source: Reference 84.

for extensive nodal dissection and the associated morbidity. The value of vital blue dye combined with lymphoscintigraphy is that it allows accurate identification of not only the SNs but also the true nodal basins that drain from the melanoma lesions. This improves the localization of positive nodes in beds that would not have been predicted to receive lymphatic drainage from the primary melanoma on the basis of conventional estimates by surgeons.[95] The significant advantage from a pathology standpoint is that there is a higher probability of discovering cancer cells in a few thoroughly examined high-risk SNs than in less thorough examination of several nodes from an entire nodal basin.[85,92]

Variations in methods are reported in the literature, but a current recommended technique for localizing SNs in melanoma involves preoperative lymphoscintigraphy 1 to 4 hours before surgery with filtered ^{99m}Tc-SC injected intradermally at a dosage of 0.5 to 0.8 mCi (18.5 to 29.6 MBq) around the melanoma site.[94] Gamma-camera imaging is performed to document the drainage pattern from the primary tumor area through the dermal lymphatics to the regional lymph nodes. The skin overlying the SN is then marked. The SN is usually identified within 30 minutes after injection. At the time of surgery, 1 to 2 mL of vital blue dye (patent blue or isosulfan blue) is injected around the primary tumor. A surgical incision with skin flaps is made in the lymph node basin to allow visual identification of the blue-stained lymphatic channel from the edge of the wound to the SN. Blue dye SN identification is corroborated by intraoperative gamma-probe counting. A node-to-background ratio of 2 or greater is used for positive identification. Blue-stained SNs are excised for histochemical assessment of metastasis. The rate of SN identification was found to be 99.1% when isosulfan blue dye was combined with radiocolloid lymphoscintigraphy, compared with 95.2% when isosulfan blue dye alone was used.[94]

The SN concept has been validated for melanoma, and it is in the process of being validated in breast and penile cancer, cancer of the vulva, and head and neck cancer.[96]

Breast Lymphoscintigraphy

The success that has been achieved in identifying SNs with melanoma has generated great interest in applying this concept to the staging of breast cancer. Alazraki et al.[96] summarized the findings of several studies using lymphoscintigraphy and other techniques. While no standard procedure or preferred method for breast lymphoscintigraphy has been defined, the general techniques used have been described.

Both unfiltered and filtered ^{99m}Tc-SC have been used with success; however, unfiltered colloid requires larger administered activities (1 mCi [37 MBq]) to achieve adequate penetration within the lymphatics. This is attributed to the poor migration of larger particles in the unfiltered preparation. Filtered ^{99m}Tc-SC can be given in smaller amounts of 0.4 to 0.6 mCi (14.8 to 22.2 MBq) because a greater fraction of the particles injected are able to migrate through the lymphatic channels. The radiocolloid is typically injected either intradermally or interstitially around the tumor site (peritumoral injection).[96] One technique involves the injection of 450 μCi (16.65 MBq) in 6 mL, divided into six 1 mL aliquots injected in separate sites around the tumor. Another technique involves administering a total of 600 μCi (22.2 MBq): four 100 μCi (3.7 MBq) peritumoral injections and one 200 μCi (7.4 MBq) intradermal injection.

Imaging the area surrounding the injection site has been shown to be effective in locating SNs, providing a visual guide for the surgeon. Early sequential imaging reveals the pattern of radiocolloid progress in the lymphatic channels and helps to distinguish the first nodes to receive radioactivity, the SNs, from secondary nodes in the lymphatic chain that appear at later imaging times. The sensitivity of various techniques for finding SNs in breast cancer (blue dye alone; intraoperative probe alone; blue dye plus probe; imaging plus probe; and blue dye, imaging, and probe combined) have demonstrated that

lymphoscintigraphic imaging combined with blue dye and the intraoperative probe is the most successful.[96]

Radiopharmaceuticals for Lymphoscintigraphy

Early diagnostic attempts to evaluate the lymphatic system were made by contrast lymphography after injection of radiographic contrast material (ethiodized oil) into cannulated lymphatic vessels. Later attempts, using ^{198}Au-colloidal gold by interstitial injection,[97] demonstrated the simplicity of radionuclide lymphoscintigraphy, with minimal complications and excellent correlation with contrast lymphography.[98,99] Because the radiocolloid did not require lymphatic vessel cannulation, the technique provided a means of evaluating lymphatic drainage in previously inaccessible areas.

Much of the early information on the ideal properties of radiocolloids for lymphoscintigraphy was gained from studies of internal mammary lymphoscintigraphy by Ege et al.[100] These investigations demonstrated that a uniform dispersion of small particles (<100 nm) was necessary for colloid to translocate from the interstitial injection site to the lymphatic channels and nodes. Large particles (500 to 2000 nm) remained trapped at the injection site. Although larger particles migrate through the lymphatics after intralymphatic injection, this precludes the advantage of interstitial administration.

A number of radiocolloid preparations have been investigated for use in lymphoscintigraphy. Early investigations demonstrated that ^{198}Au-colloidal gold had ideal particle size (5 to 50 nm), but its high radiation dose was unsatisfactory for routine diagnostic use. Important ^{99m}Tc agents that were evaluated included sulfur colloid, stannous phytate, and antimony sulfide. ^{99m}Tc-SC produced by the thiosulfate kit method was found to be unsatisfactory because of inadequate migration from the injection site as a result of the relatively large particle size range (100 to 1000 nm).[101] ^{99m}Tc-SC produced by the hydrogen sulfide method has smaller particles (<100 nm) with satisfactory lymph node scans, but the method of preparation is cumbersome.[102] A kit for the preparation of ^{99m}Tc-antimony sulfide produces particles in an ideal size range (3 to 30 nm), and this agent was shown to be satisfactory for mammary lymphoscintigraphy.[103,104] ^{99m}Tc-stannous phytate forms an in vivo colloid about the same size as ^{99m}Tc-antimony sulfide but was found to be inferior to it in clinical studies.[104] However, the ^{99m}Tc-antimony sulfide kit never achieved approval for routine use in the United States and is no longer available.

The resurgence in lymphoscintigraphy and the SN concept focused attention again on the preparation of satisfactory ^{99m}Tc-labeled agents for this application. The only agents available in the United States with possible application to lymphoscintigraphy are ^{99m}Tc-albumin (^{99m}Tc-HSA) and ^{99m}Tc-SC. Bergqvist et al.[105] revisited the particle size requirements for interstitial lymphoscintigraphic agents, reconfirming that a particle size less than 100 nm is necessary for adequate migration and uptake into lymph nodes after interstitial injection. They further noted that ^{99m}Tc-HSA, which is not a particulate agent, shows less retention within lymph nodes and that its rapid transit in the lymphatic channels may lead to missed detection of SNs. A ^{99m}Tc-HSA nanocolloid kit is available in Europe and has been found to provide good results in identifying SNs. Approximately 95% of the colloidal albumin particles in this kit are less than 80 nm in size.[106,107]

The relatively high proportion of large particles in traditionally prepared ^{99m}Tc-SC led to the use of filtration techniques to remove larger particles.[108–110] Dragotakes et al.[100] demonstrated, by laser light scattering analysis, that filtration of a standard preparation of ^{99m}Tc-SC through a 0.1 μm membrane filter yielded particles with a bimodal size distribution; the particles predominantly were 10 ± 2 nm in size, but a small portion (<0.1%) were in the 89 to 173 nm size range. Hung et al.[109] found that ^{99m}Tc-SC filtered through a 0.1 μm membrane filter produced about 90% of particles between 15 and 50 nm

TABLE 20-5 Particle Size Distribution of ^{99m}Tc-Sulfur Colloid

^{99m}Tc-Sulfur Colloid Preparation Method	Particle Size (nm)	% of Total
Standard method (5 minute heating)	<100	15 to 20
	100 to 600	70 to 80
	700 to 5,000	2 to 4
	>5,000	0.5 to 1.5
Modified method (3 minute heating)	<30	47
	30 to 50	0
	50 to 80	1
	80 to 200	5
	200 to 400	21
	400 to 800	16
	800 to 2,000	5
	2,000 to 5,000	1
	5,000 to 10,000	0
	>10,000	5

as determined by Nuclepore (Whatman) polycarbonate filter analysis, with a mean size of 38 ± 3.3 nm by electron microscopy. Laser light-scatter analysis showed the particles to be bimodal with mean particle sizes of 7.5 nm (minor peak) and 53.9 nm (major peak). The differences in particle size distribution reported for 0.1 μm membrane filtered SC by these investigators may be due to differences in kit composition during the initial preparation of ^{99m}Tc-SC.

Eshima et al.[111] have shown that smaller colloidal particles are generated when ^{99m}Tc-SC is prepared using increased amounts of carrier ^{99}Tc from long ingrowth generator eluates and a heating time that is shortened from 10 minutes to 3 minutes. The optimal preparation conditions were reported to be addition of 150 mCi (5550 MBq) of ^{99m}Tc-sodium pertechnetate from a 72 hour ingrowth generator in 3 mL to a lyophilized sulfur colloid kit (CIS-US). After addition of 1.5 mL 0.148 M hydrochloric acid, the vial is placed immediately into a boiling water bath for 1.5 minutes, removed and agitated, reheated for an additional 1.5 minutes, removed, and then cooled for 2 minutes at room temperature before addition of 1.5 mL of buffer. Nuclepore polycarbonate filter analysis demonstrated a shift to smaller particle sizes by this method of preparation. Table 20-5 shows the particle size distribution of sulfur colloid prepared by the standard method and by the modified heating method described by Eshima et al.[111] SC prepared by this modified heating method followed by filtration through a 0.22 μm membrane filter was shown to be more effective in visualizing lymphatic channels and identifying sentinel lymph nodes than SC filtered through a 5.0 μm membrane filter.[110] It is worth noting that 0.22 μm membrane filtration after a standard heating method (5 minute boil) in the preparation of ^{99m}Tc-SC also results in satisfactory lymphoscintigraphy. The key point for success in lymphoscintigraphy is removal of larger particles that have a slowed migration rate from the interstitial space to the lymphatic channels. Figures 20-29 and 20-30 are lymphoscintigrams identifying sentinel lymph nodes after ^{99m}Tc-SC administration and imaging with a gamma camera.

Dacryoscintigraphy

Dacryoscintigraphy is a useful method for assessing nasolacrimal drainage of tears.[112,113] Under normal conditions, the lacrimal glands release tear fluid to maintain a thin protective film over the cornea through the blinking reflex (Figure 20-31). Excess tear fluid collects in the conjunctival sac and is cleared through the lacrimal puncta, located one each in the

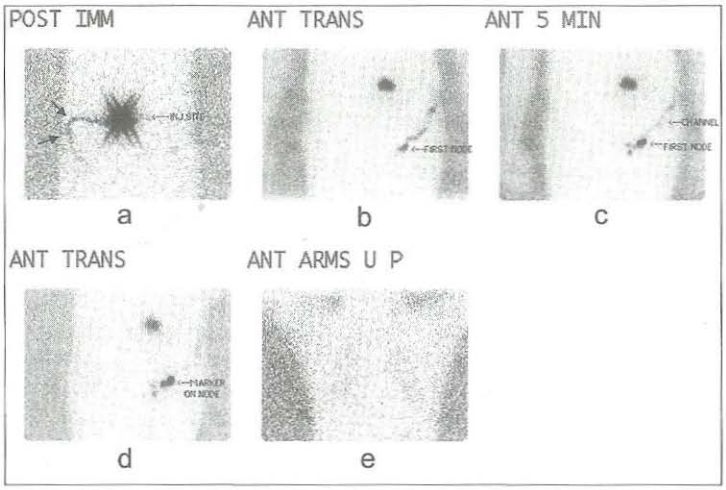

FIGURE 20-29 Lymphoscintigraphy for localization of the sentinel lymph node. (a) Posterior transmission image taken shortly after four intradermal injections of 250 μCi (9.25 MBq) of ^{99m}Tc-sulfur colloid were made around a melanoma lesion on the patient's lower left back. There is already radiotracer uptake in a draining lymph channel (arrows). (b) An anterior image of the pelvis shows the lymph channel leading to a focal accumulation in the left groin consistent with accumulation in the sentinel lymph node. (c) Shortly after this, two other smaller foci are seen in the left groin. (d) A ^{99m}Tc point source was used to locate the position on the patient's skin overlying the sentinel node, and a felt marker pen was used to mark the location on the patient's skin. (e) A transmission scan of the chest demonstrates no migration to the axillary regions.

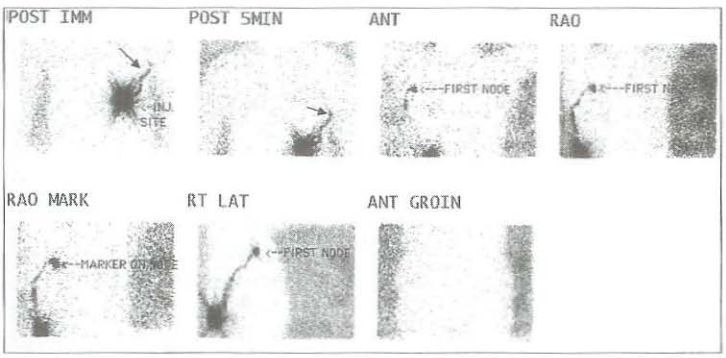

FIGURE 20-30 Lymphoscintigraphy in another patient with a melanoma lesion on the right mid back. Posterior transmission images taken immediately and 5 minutes after four intradermal injections of 250 μCi (9.25 MBq) of ^{99m}Tc-SC were made around the melanoma lesion. In this patient, the draining lymph channel courses toward the right axilla (arrows). Anterior, right anterior oblique (RAO), and right lateral (RT LAT) images clearly show the lymph channel and a focal accumulation in the right axilla consistent with accumulation of radiotracer in the sentinel node. A ^{99m}Tc point source was used to locate the position on the patient's skin overlying the node, and a felt marker pen was used to mark the patient's skin prior to surgery. An anterior transmission image of the pelvis showed no migration of the radiotracer to either groin region.

upper and lower eyelid in the region of the medial canthus. Tear fluid entering the puncta drains through the upper and lower canaliculi into the nasolacrimal sac and down the nasolacrimal duct through the valve of Hasner, emptying into the nasal cavity.

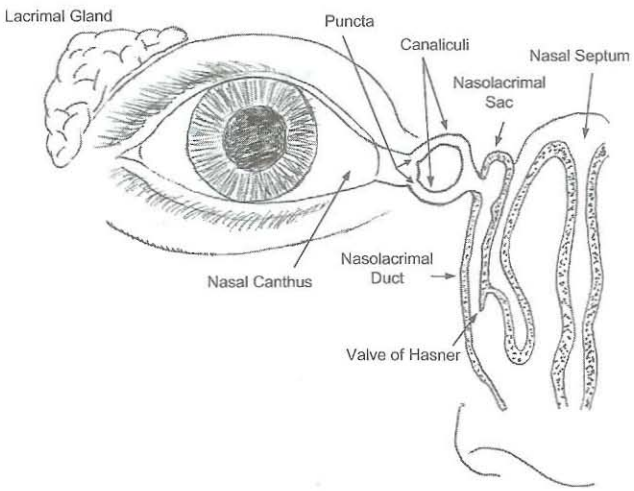

FIGURE 20-31 Principal structures in the nasolacrimal system.

Epiphora is a disorder of tear drainage through the nasolacrimal system. Obstruction of tear drainage can have many causes, such as trauma, inflammation, degenerative changes, and diseases of the nasal sinus. The technique of dacryoscintigraphy involves application of 100 μCi (3.7 MBq) of ^{99m}Tc-sodium pertechnetate solution in a volume of 10 to 30 μL to the eye in the region of the nasal canthus.[113] Normal human lacrimal fluid volume is around 7 μL, but up to 30 μL can be added without overflow provided the subject does not blink.[114] Blinking facilitates movement of tear fluid through the nasolacrimal system, and a smaller drop size would preclude overflow of activity from the conjunctival sac during blinking.[115]

The asymptomatic eye is examined first to familiarize the patient with the procedure and to provide a normal control for comparison. A specially constructed pinhole collimator with a 1 mm aperture is used, which gives the best balance between resolution and sensitivity. After placement of a drop of ^{99m}Tc-sodium pertechnetate in the eye, serial scintigrams are obtained every 30 seconds for 5 minutes. Normal transit time from the conjunctiva to the nasolacrimal sac is less than 1.5 minutes.[112] Longer times indicate delay and provide a sensitive means for detecting obstruction to drainage. Partial obstruction can be demonstrated with a negative Valsalva's maneuver (pinching the nostrils while attempting to draw in air). Dacryoscintigrams demonstrating normal and abnormal drainage patterns are shown in Figure 20-32.

The radiation dose to the lens of a normally draining eye is estimated to be 0.014 to 0.021 rad (cGy) per 100 to 150 μCi (3.7 to 5.55 MBq), whereas in total obstruction the worst case would be 0.4 to 0.6 rad (cGy).[116] The radiation absorbed dose from this procedure is quite safe, since the threshold dose for initiating cataract formation in the eye is 200 rad (2 Gy).[117] Application of normal saline after a study facilitates clearance of radioactivity from the nasolacrimal system and lowers the radiation dose.

BONE MARROW IMAGING

In adults, active bone marrow normally resides in the axial skeleton, primarily in the vertebral bodies, pelvis, sternum, ribs, and scapulae, and to a variable extent in the skull.[118] Its distribution in the appendicular skeleton is limited to the proximal one-third of the femurs and humeri.

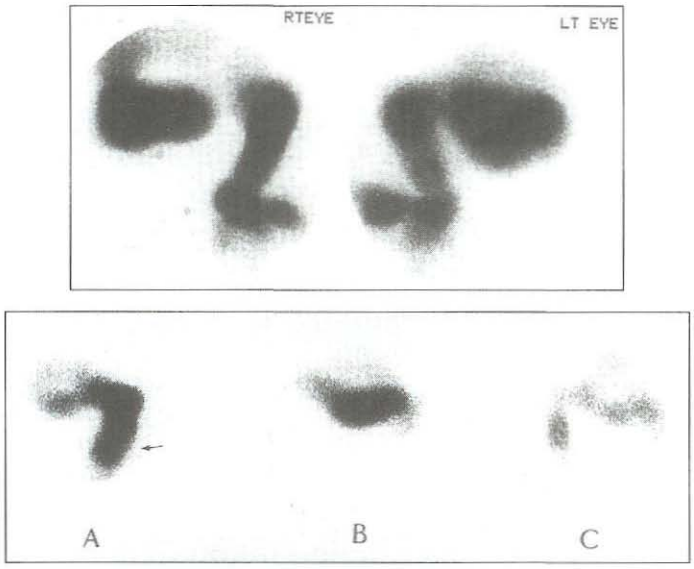

FIGURE 20-32 Dacryoscintigrams obtained with a pinhole collimator and scintillation camera after instillation of 100 μCi (3.7 MBq) of ^{99m}Tc-sodium pertechnetate into the lateral canthus of each eye. Upper panel: Normal dacryoscintigram demonstrating normal tear drainage from the right and left eyes. Lower panel: (A) The right eye exhibits normal drainage into the lacrimal duct (arrow); (B) the left eye demonstrates a lack of drainage under normal conditions, but drainage into the lacrimal duct is induced (C) after a negative Valsalva maneuver, which indicates a stenotic condition rather than complete obstruction.

Blood is supplied to the bone marrow through nutrient arteries that run longitudinally in the central portion of the marrow cavity and send out lateral branches that terminate in capillary beds within bone or at the periphery of the marrow space.[119] The arteriolar capillary blood is drained by postcapillary venules that reenter the marrow cavity and coalesce to form large venous sinuses in which the blood flow is back toward the center of the cavity to the central vein.[119] The erythropoietic marrow is in the form of cords that lie between the venous sinuses. The wall of the venous sinus is primarily composed of a unicellular layer, but in its fullest development it is trilaminar, consisting of a lining cell, basement membrane, and adventitial cells.[120] The wall is fenestrated, requiring blood cells leaving the erythropoietic tissue to squeeze through pores to enter the venous circulation. The adventitial cells, being phagocytic, remove foreign particles from the blood as it passes into the sinuses. They are responsible for trapping radiocolloids in the bone marrow.

Radiopharmaceuticals for imaging studies target cells in the erythropoietic, reticuloendothelial, or granulopoietic marrow.[118,121,122] The ideal radiotracer for the erythropoietic marrow is one that participates in RBC production. From a physiologic perspective, radionuclides of iron are ideal because erythropoiesis is responsible for 80% to 90% of plasma iron turnover in the body.[118] However, radionuclides of iron have potential imaging limitations. ^{52}Fe is a positron emitter with an 8.2 hour half-life and has been used for quantitative assessment of erythropoiesis in bone marrow expansion, but it requires a PET camera.[123] Additionally, ^{52}Fe has the practical limitations of expense and availability because it is produced in a cyclotron. ^{59}Fe, with a half-life of 45 days, produces high-energy gamma rays of 1.1 MeV and 1.3 MeV that are unsatisfactory for imaging. Its use has been limited to ferrokinetic studies of erythropoietic bone marrow activity. Indium has chemical properties similar to iron and, after intravenous injection, ^{111}In-indium chloride labels

plasma transferrin similarly to iron. However, indium's biologic properties are significantly different from those of iron. Studies in humans have demonstrated that the plasma clearance half-life of ^{111}In-labeled transferrin (6.1 hours) is much slower than the plasma half-life of ^{59}Fe-labeled transferrin (1 to 2 hours), and liver uptake of ^{111}In-labeled transferrin is greater.[124] Animal studies demonstrate much less uptake of indium into erythrocytes compared with iron.[124] Other studies have shown that the distribution of indium is more like that of radiocolloids than that of iron.[118] Thus, although ^{111}In-indium chloride has been used for bone marrow imaging studies, it is not a true tracer of erythrogenesis.

These limitations of iron and indium nuclides led to the use of radiocolloids for bone marrow scintigraphy. ^{99m}Tc-SC is widely used, although in Europe, ^{99m}Tc-microaggregated human serum albumin nanocolloid is frequently used for bone marrow scintigraphy. A typical intravenous dose of ^{99m}Tc-SC for bone marrow imaging is 10 to 12 mCi, with imaging commencing in 20 to 30 minutes. This dose is larger than the typical liver-scanning dose but is necessary to provide an excess of particles and activity to visualize the marrow. The particle size range of standard ^{99m}Tc-SC preparations is 0.1 to 1.0 μm. However, Atkins et al.[125] demonstrated that greater localization of ^{99m}Tc-SC in bone marrow occurs if smaller particles (around 0.1 μm) are used and if large doses are administered. Apparently, smaller particles are less likely to be trapped in the liver than larger particles, and larger doses decrease the efficiency of the liver and spleen in removing particles, so that extra particles localize in the marrow.

Radiocolloids are a practical choice for studying the bone marrow because in normal individuals the erythropoietic marrow and the reticuloendothelial marrow distributions are similar. An exception to this coincident marrow distribution pattern has been shown to occur mainly in diseases that cause ineffective erythropoiesis, in which the reticuloendothelial marrow expands but the erythropoietic marrow does not. This disparity has been demonstrated by comparing the activity distribution pattern between ^{52}Fe in erythropoietic marrow and radiocolloids in the reticuloendothelial marrow.[126] A similar disparity has been shown to occur after chemotherapy or irradiation of bone marrow; erythropoietic cells are depleted with little effect on reticuloendothelial cells.[127,118] A practical limitation of radiocolloids is that they are not useful for the evaluation of bone marrow in the lower thoracic and upper lumbar spine because of interfering radiocolloid accumulation in the liver and spleen. This type of interference does not occur with the use of iron radionuclides, which have insignificant activity uptake in liver and spleen. Despite these caveats, ^{99m}Tc-SC is convenient and quite useful for bone marrow imaging in many clinical situations. An example is myelofibrosis, in which axial marrow is replaced by fibrous tissue, causing compensatory hyperplasia of marrow with peripheral expansion.[128] Additionally, the spleen is enlarged, compensating for the loss of normal erythropoietic tissue (Figure 20-33).

Imaging the granulopoietic marrow became possible with the introduction of an antigranulocyte antibody labeled with ^{99m}Tc. The murine monoclonal antibody is an IgG_1 isotype anti-carcinoembryonic antigen that cross-reacts with NCA-95 (a nonspecific cross-reacting antigen) that is present on the cellular membrane of human granulocytes. This antibody is designated in the literature as NCAA or BW 250/183.[121,129] The radiolabeled antibody is prepared from a kit by premixing ^{99m}Tc-sodium pertechnetate with a transfer ligand and stannous chloride and transferring this mixture to the lyophilized antibody. A gentle mixing process is required to limit the amount of liver uptake of the labeled antibody.[130] For clinical use in bone marrow imaging, 8 mCi (300 MBq) of the technetium-labeled antibody is administered intravenously and total body images are obtained in 3 to 4 hours. The use of this antibody for bone marrow imaging in several pathologic conditions has been described.[121,122]

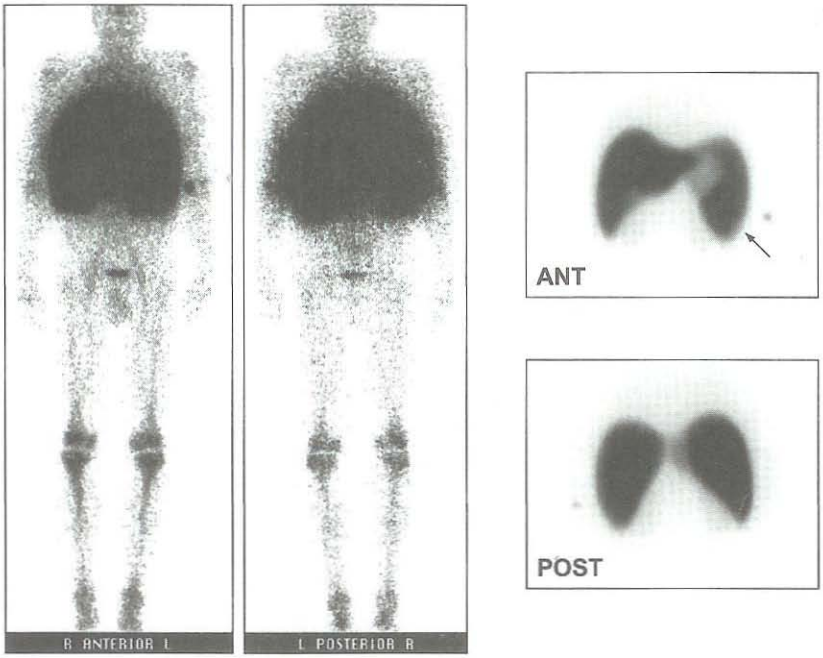

FIGURE 20-33 Bone marrow scan in a 55 year old man with pancytopenia and splenomegaly being evaluated for myelofibrosis. Anterior and posterior total body images (left panels) obtained 30 minutes after intravenous injection of 10 mCi (370MBq) of ^{99m}Tc-SC, showing absence of normal red marrow activity within the axial and proximal appendicular skeleton. Instead, there is abnormally increased radiotracer uptake within the distal femora and proximal tibias, reflecting red marrow expansion. Anterior and posterior liver–spleen scans (right panels) demonstrate splenomegaly with increased radiocolloid uptake, likely reflecting extramedullary hematopoiesis. (Photo courtesy of Dr. Amy Maszkiewicz, University of North Carolina Hospitals.)

REFERENCES

1. Spector WG, Willoughby DA. The inflammatory response. *Bact Rev.* 1963;27:117-54.
2. Edwards CL, Hayes RL. Tumor scanning with Ga-67 citrate. *J Nucl Med.* 1969;10:103-5.
3. Bell EG, O'Mara RE, Henry CA, et al. Non-neoplastic localization of Ga-67 citrate. *J Nucl Med.* 1971;12:338-9.
4. Lavender JP, Lowe J, Barker JR. Gallium-67 citrate scanning in neoplastic and inflammatory lesions. *Br J Radiol.* 1971;44:361-6.
5. Staab EV, McCartney WH. Role of gallium-67 in inflammatory disease. *Semin Nucl Med.* 1978;8:219-34.
6. Larson SM, Allen DR, Rasey JS, et al. Kinetics of binding of carrier-free Ga-67 to human transferrin. *J Nucl Med.* 1978;19:1245-9.
7. Watson EE, Cloutier RJ, Gibbs WD. Whole-body retention of Ga-67 citrate. *J Nucl Med.* 1973;14:840-2.
8. Hnatowich DJ, Kulprathipanja S, Beh R. The importance of pH and citrate concentration on the in vitro and in vivo behaviour of radiogallium. *Int J Appl Radiat Isot.* 1977;28:925-31.
9. Nelson B, Hayes RL, Edwards CL, et al. Distribution of gallium in human tissues after intravenous administration. *J Nucl Med.* 1972;13:92-100.
10. Larson SM. Mechanisms of localization of gallium-67 in tumors. *Semin Nucl Med.* 1978;8:193-203.
11. Larson SM, Hoffer PB. Normal patterns of localization. In: Hoffer PB, Bekerman C, Henkin RE, eds. *Gallium-67 Imaging.* New York: Wiley; 1978:23.
12. Mishkin FS, Maynard WP. Lacrimal gland accumulation of Ga-67. *J Nucl Med.* 1975;15:630-1.
13. Larson SM, Schall GL. Gallium-67 concentration in human breast milk [abstract]. *JAMA.* 1971;218:257.
14. Bekerman C, Hoffer PB. Salivary gland uptake of Ga-67 citrate following radiation therapy. *J Nucl Med.* 1976;17:685-7.

15. Fletcher JW, Herbig FK, Donati RM. Ga-67 citrate distribution following whole-body irradiation or chemotherapy. *Radiology.* 1975;117:709-12.
16. Hayes RL, Rafter JJ, Byrd BL, et al. Studies of the in vivo entry of Ga-67 into normal and malignant tissue. *J Nucl Med.* 1981;22:325-32.
17. Bradley WP, Alderson PO, Eckelman WC, et al. Decreased tumor uptake of gallium-67 in animals after whole-body irradiation. *J Nucl Med.* 1978;19:204-9.
18. Peters AM. The utility of ^{99m}Tc-HMPAO-leukocytes for imaging infection. *Semin Nucl Med.* 1994;24:110-27.
19. Datz FL. Indium-111-labeled leukocytes for the detection of infection: current status. *Semin Nucl Med.* 1994;24:92-109.
20. McDougall IR, Goodwin DA. Gallium scans vs ^{111}In-labeled oxyquinoline WBC scan. *Arch Intern Med.* 1982;142:1407-8.
21. Palestro CJ. The current role of gallium imaging in infection. *Semin Nucl Med.* 1994;24:128-41.
22. Hoffer PB. Mechanisms of localization. In: Hoffer PB, Bekerman C, Henkin RE, eds. *Gallium-67 Imaging.* New York: Wiley; 1978:3.
23. Weiner RE, Schreiber GJ, Hoffer PB, et al. Compounds which mediate gallium-67 transfer from lactoferrin to ferritin. *J Nucl Med.* 1985;26:908-16.
24. McAfee JG, Thakur ML. Survey of radioactive agents for in vitro labeling of phagocytic leukocytes. I: Soluble agents. *J Nucl Med.* 1976;17:480-7.
25. McAfee JG, Thakur ML. Survey of radioactive agents for in vitro labeling of phagocytic leukocytes. II: Particles. *J Nucl Med.* 1976;17:488-92.
26. Sinn H, Silvester DJ. Simplified cell labeling with indium-111 acetylacetone. *Br J Radiol.* 1979;52:758-9.
27. Danpure HJ, Osman S, Brady F. The labeling of blood cells in plasma with In-111 tropolonate. *Br J Radiol.* 1982;55:247-9.
28. Thakur ML, Coleman RE, Welch MJ. Indium-111-labeled leukocytes for the localization of abscesses: preparation, analysis, tissue distribution, and comparison with gallium-67 citrate in dogs. *J Lab Clin Med.* 1977;82:217-28.
29. McAfee JG, Subramanian G, Gagne G. Technique of leukocyte harvesting and labeling: problems and perspectives. *Semin Nucl Med.* 1984;14:83-106.
30. Gobuty AH. Technologic, clinical, and basic science considerations for In-111-oxine-labeled leukocyte studies. *J Nucl Med Technol.* 1983;11:190-5.
31. Baker WJ, Datz FL. Preparation and clinical utility of In-111 labeled leukocytes. *J Nucl Med Technol.* 1984;12:131-8.
32. Peters AM, Danpure HJ, Osman S, et al. Clinical experience with ^{99m}Tc-hexamethylpropyleneamineoxime for labeling leucocytes and imaging inflammation. *Lancet.* 1986;946-9.
33. Roddie ME, Peters AM, Danpure HJ, et al. Inflammation: imaging with Tc-99m HMPAO-labeled leukocytes. *Radiology.* 1988;166:767-72.
34. Moberg L, Karawajczyk M, Venge P. ^{99m}Tc-HMPAO (Ceretec) is stored in and released from the granules of eosinophil granulocytes. *Br J Haematol.* 2001;114:185-90.
35. Goodwin DA, Doherty PW, McDougall IR. Clinical use of indium-111 labeled white cells: an analysis of 312 cases. In: Thakur ML, Gottschalk A, eds. *Indium-111 Labeled Neutrophils, Platelets, and Lymphocytes.* New York: Trivirum; 1981:131.
36. Coleman RE, Welch DM, Baker W, et al. Clinical experience using indium-111 labeled leukocytes. In: Thakur ML, Gottschalk A, eds. *Indium-111 Labeled Neutrophils, Platelets, and Lymphocytes.* New York: Trivirum; 1981:103.
37. Sfakianakis GN, Al-Skeikh W, Heal A, et al. Comparison of scintigraphy with In-111 leukocytes and Ga-67 in the diagnosis of occult sepsis. *J Nucl Med.* 1982;23:618-26.
38. Seabold JE, Palestro CJ, Brown ML, et al. Procedure guideline for gallium scintigraphy in inflammation 2.0. In: *Procedure Guidelines Manual 2001-2002.* Reston, VA: Society of Nuclear Medicine; 2001:87-91.
39. Woolfenden JM, Carrasquillo JA, Larson SM, et al. Acquired immunodeficiency syndrome: Ga-67 citrate imaging. *Radiology.* 1987;162:383-7.
40. Moinuddin M, Rackett J. Gallium scintigraphy in the detection of amiodarone lung toxicity. *Am J Radiol.* 1986;147:607-9.
41. Line BR, Hunninghake GW, Koegh BA, et al. Gallium-67 scanning to stage the alveolitis in sarcoidosis: correlation with clinical studies, pulmonary function studies and bronchoalveolar lavage. *Am Rev Resp Dis.* 1981;123:440-6.
42. Peters AM. Imaging inflammation: current role of labeled autologous leukocytes. *J Nucl Med.* 1992;33:65-7.
43. Zhuang H, Alavi A. 18-fluorodeoxyglucose positron emission tomographic imaging in the detection and monitoring of infection and inflammation. *Semin Nucl Med.* 2002;32:47-59.
44. Chacko TK, Zhuang H, Nakhoda KZ, et al. Applications of fluorodeoxyglucose positron emission tomography in the diagnosis of infection. *Nucl Med Commun.* 2003;24:615-24.

45. Czernin J, Phelps ME. Positron emission tomography scanning: current and future applications. *Annu Rev Med.* 2002;53:89-112.
46. Hayes RL. The tissue distribution of gallium radionuclides. *J Nucl Med.* 1977;18:740-2.
47. Hayes RL. Chemistry and radiochemistry of metal-ion nuclides commonly employed in radiopharmaceuticals. In: Heindel ND, Burns HD, Honda T, et al., eds. *The Chemistry of Radiopharmaceuticals.* New York: Masson; 1977:155.
48. Brown DH, Byrd BL, Carlton JE, et al. A quantitative study of the subcellular localization of Ga-67. *Cancer Res.* 1976;36:956-63.
49. Thrall JH, Ziessman HA. *Nuclear Medicine: The Requisites.* 2nd ed. St Louis: Mosby; 2001:193-227.
50. DeGroot LJ, ed. *Endocrinology.* Vol 2. 3rd ed. Philadelphia: WB Saunders; 1995:1278.
51. Sherwood LM. Paraneoplastic endocrine disorders (ectopic hormone syndromes). In: DeGroot LJ, ed. *Endocrinology.* Vol 3. 3rd ed. Philadelphia: WB Saunders; 1995:2754-802.
52. DeGroot LJ, ed. *Endocrinology.* Vol 1. 2nd ed. Philadelphia: WB Saunders; 1989:250.
53. Krenning EP, Kwekkeboom DJ, Bakker WH, et al. Somatostatin receptor scintigraphy with [^{111}In-DTPA-D-Phe^1]- and [^{123}I-Tyr^3]-octreotide: the Rotterdam experience with more than 1000 patients. *Eur J Nucl Med.* 1993;20:716-31.
54. Krenning EP, Kwekkeboom DJ, Pauwels S, et al: Somatostatin receptor scintigraphy. In: Freeman LM, ed. *Nuclear Medicine Annual.* New York: Raven Press; 1995:1-50.
55. Somatostatin Receptor Imaging for Neuroendocrine Tumors [product monograph]. St Louis: Mallinckrodt Inc; 1994.
56. Olsen JO, Pozderac RV, Hinkle G, et al. Somatostatin receptor imaging of neuroendocrine tumors with indium-111 pentetreotide (OctreoScan). *Semin Nucl Med.* 1995;25:251-61.
57. NeoTect [package insert]. Londonderry, NH: Diatide Inc, 1999.
58. Blum J, Handmaker H, Lister-James J, et al. A multicenter trial with a somatostatin analog ^{99m}Tc depreotide in the evaluation of solitary pulmonary nodules. *Chest.* 2000;117:1232-8.
59. Goldsmith SJ, Kostakoglu L. Role of nuclear medicine in the evaluation of the solitary pulmonary nodule. *Semin Ultrasound CT MR.* 2000;21:129-38.
60. Wahl RL. Principles of cancer imaging with fluorodeoxyglucose. In: Wahl RL, Buchanan JW, eds. *Principles and Practice of Positron Emission Tomography.* Philadelphia: Lippincott Williams & Wilkins; 2002:100-10.
61. Blair RS, Beierwaltes WH, Lieberman LM, et al. Radiolabeled cholesterol as an adrenal scanning agent. *J Nucl Med.* 1971;12:176-80.
62. Thrall JH, Frietas JE, Beierwaltes WH. Adrenal scintigraphy. *Semin Nucl Med.* 1978;8:23-41.
63. Ice RD, Wieland DM, Beierwaltes WH, et al. Concentration of dopamine analogs in the adrenal medulla. *J Nucl Med.* 1975;16:1147-51.
64. Short JH, Darby TD. Sympathetic nervous system blocking agents. III: Derivations of benzylguanidine. *J Med Chem.* 1967;10:833-40.
65. Wieland DM, Wu JJ, Brown LE, et al. Radiolabeled adrenergic neuron-blocking agents: adrenomedullary imaging with I-131 iodobenzylguanidine. *J Nucl Med.* 1980;21:349-53.
66. Wieland DM, Brown LE, Tobes MC, et al. Imaging the primate adrenal medulla with I-123 and I-131 meta-iodo-benzylguanidine [concise communication]. *J Nucl Med.* 1981;22:358-64.
67. Shapiro B, Copp JE, Sisson JC, et al. Iodine-131 meta-iodobenzylguanidine for the locating of suspected pheochromocytoma: experience in 400 cases. *J Nucl Med.* 1985;26:576-85.
68. Geatti O, Shapiro B, Sisson JC, et al. 131-I-metaiodobenzylguanidine (131-I-MIBG) scintigraphy for the location of neuroblastoma: preliminary experience in 10 cases. *J Nucl Med.* 1984;26:736-62.
69. Fischer M, Kamanabroo D, Sonderkamp H, et al. Scintigraphic imaging of carcinoid tumours with 131-I-metaiodobenzylguanidine. *Lancet.* 1984;2:165.
70. Sonew T, Funkunaga M, Otsuka N, et al. Metastatic medullary thyroid cancer: localization with iodine-131-metaiodobenzylguanidine. *J Nucl Med.* 1985;26:604-8.
71. McEwan AJ, Shapiro B, Sisson JC, et al. Radioiodobenzylguanidine for the scintigraphic location and therapy of adrenergic tumors. *Semin Nucl Med.* 1985;15:132-53.
72. Petry NA, Shapiro B. Radiopharmaceuticals for endocrine imaging: adrenomedullary imaging. In: Swanson DP, Chilton HM, Thrall JH, eds. *Pharmaceuticals in Medical Imaging.* New York: Macmillan; 1990:343-93.
73. Nakajo M, Shapiro B, Copp J, et al. The normal and abnormal distribution of the adrenomedullary imaging agent m-[I-131]-iodobenzylguanidine (I-131-MIBG) in man: evaluation by scintigraphy. *J Nucl Med.* 1983;24:672-82.
74. Mangner TJ, Tobes MC, Wieland DM, et al. Metabolism of meta-I-131-iodobenzylguanidine in patients with metastatic pheochromocytoma: concise communication. *J Nucl Med.* 1986;27:37-44.
75. Gelfand MJ, Elgazzar AH, Kriss VM, et al. Iodine-123-MIBG SPECT versus planar imaging in children with neural crest tumors. *J Nucl Med.* 1994;35:1753-7.

76. Shapiro B, Gross MD. Radiochemistry, biochemistry, and kinetics of ^{131}I-metaiodobenzylguanidine (MIBG) and ^{123}I-MIGB: clinical implications of the use of ^{123}I-MIGB. *Med Ped Oncol.* 1987;15:170-7.
77. Iobenguane Sulfate I-131 [package insert]. Bedford, MA: CIS-US Inc; 1994.
78. Gerald D, Marx SJ, Spiegel AM. Parathyroid hormone, calcitonin, and the calciferols. In: Wilson JD, Foster DW, eds. *Williams Textbook of Endocrinology.* 8th ed. Philadelphia: WB Saunders; 1992:1398-1476.
79. Fukunaga M, Morita R, Yonekura Y, et al. Accumulation of ^{201}Tl-chloride in a parathyroid adenoma. *Clin Nucl Med.* 1979;4:229-30.
80. Ferlin G, Borsato N, Camerani M, et al. New perspectives in localizing enlarged parathyroids by technetium-thallium subtraction scan. *J Nucl Med.* 1983;24:438-41.
81. Coakley AJ, Kettle AG, Wells CP, et al. ^{99m}Tc-sestamibi: a new agent for parathyroid imaging. *Nucl Med Commun.* 1989;10:791-4.
82. O'Doherty MJ, Kettle AG, Wells P, et al. Parathyroid imaging with technetium-99m-sestamibi: preoperative localization and tissue uptake studies. *J Nucl Med.* 1992;33:313-8.
83. Taillefer R, Boucher Y, Potvin C, et al. Detection and localization of parathyroid adenomas in patients with hyperparathyroidism using a single radionuclide imaging procedure with technetium-99m-sestamibi (double-phase study). *J Nucl Med.* 1992;33:1801-7.
84. Kardinal CG, Yarbro JW. A conceptual history of cancer. *Semin Oncol.* 1979;6:396-408.
85. Morton DL, Chan AD. The concept of sentinel node localization: how it started. *Semin Nucl Med.* 2000;30:4-10.
86. Cabanas RM. An approach for the treatment of penile carcinoma. *Cancer.* 1977;39:456-66.
87. Holmes EC, Moseley HS, Morton DL, et al. A rational approach to the surgical management of melanoma. *Ann Surg.* 1977;186:481-90.
88. Cabanas RM. Anatomy and biopsy of sentinel lymph nodes. *Urol Clin North Am.* 1992;19:267-76.
89. Morton DL, Wen DR, Wong JH, et al. Technical details of intraoperative lymphatic mapping for early stage melanoma. *Arch Surg.* 1992;127:392-9.
90. Alex JC, Krag DN. Gamma probe guided localization of lymph nodes. *Surg Oncol.* 1993;2:137-43.
91. Alex JC, Weaver DL, Fairbank JT, et al. Gamma probe guided lymph node localization in malignant melanoma. *Surg Oncol.* 1993;2:303-8.
92. Berman CG, Choi J, Hersh MR, et al Melanoma lymphoscintigraphy and lymphatic mapping. *Semin Nucl Med.* 2000;30:49-55.
93. Morton DL, Chan AD. Current status of intraoperative lymphatic mapping and sentinel lymphandenectomy for melanoma: is it standard of care? *J Am Coll Surg.* 1999;189:214-23.
94. Morton DL, Thompson JF, Essner R, et al. Validation of the accuracy in a multicenter trial of intraoperative lymphatic mapping and sentinel lymphadenectomy for early-stage melanoma. *Ann Surg.* 1999;230:453-65.
95. Alazraki NP, Eshima D, Eshima LA, et al. Lymphoscintigraphy, the sentinel node concept, and the intraoperative gamma probe in melanoma, breast cancer, and other potential cancers. *Semin Nucl Med.* 1997;27:55-67.
96. Alazraki NP, Styblo T, Grant SF, et al. Sentinel node staging of early breast cancer using lymphoscintigraphy and the intraoperative gamma-detecting probe. *Semin Nucl Med.* 2000;30:56-64.
97. Sherman AL, Ter-Pogossian M. Lymph node concentration of radioactive colloidal gold following interstitial injection. *Cancer.* 1953;6:1238-40.
98. Kazem I, Antionaides J, Brady LW, et al. Clinical evaluation of lymph node scanning utilizing colloidal gold 198. *Radiology.* 1968;90:905-11.
99. Kazem I, Nedwich A, Mortel R, et al. Comparative histological changes in the normal lymph node following ethiodol lymphography and colloidal gold-198 lymph scanning. *Clin Radiol.* 1971;22:382-8.
100. Ege GN. Internal mammary lymphoscintigraphy: the rationale, technique, interpretation and clinical application: a review. *Radiology.* 1976;118:101-7.
101. Warbick A, Ege GN, Henkelman RM, et al. An evaluation of radiocolloid size technique. *J Nucl Med.* 1977;18:827-34.
102. Dunson GL, Thrall JH, Stevenson JS, et al. Tc-99m minicolloid for radionuclide lymphoscintigraphy. *Radiology.* 1973;109:387-92.
103. Ege GN, Warbick A. Lymphoscintigraphy: a comparison of Tc-99m antimony sulfide colloid and Tc-99m stannous phytate. *Br J Radiol.* 1979;52:124-9.
104. Kaplan WD, Davis MA, Rose CM. A comparison of two technetium-99m-labeled radiopharmaceuticals for lymphoscintigraphy [concise communication]. *J Nucl Med.* 1979;20:933-7.
105. Bergqvist L, Strand S-E, Perssom BRR. Particle sizing and biokinetics of interstitial lymphoscintigraphic agents. *Semin Nucl Med.* 1983;12:9-19.
106. Solco NANOCOLL [package insert]. Eidhoven, The Netherlands: Amersham Cygne; 1966.
107. Wilhelm AJ, Mijnhout GS, Franssen EJ. Radiopharmaceuticals in sentinel lymph node dissection: an overview. *Eur J Nucl Med.* 1999;26(suppl):S36-42.

108. Dragotakes SC, Callahan RJ, LaPointe LC, et al. Particle size characterization of a filtered ^{99m}Tc-sulfur colloid preparation for lymphoscintigraphy [abstract]. *J Nucl Med.* 1995;36:80P.
109. Hung JC, Wiseman GA, Wahner HW, et al. Filtered technetium-99m-sulfur colloid evaluated for lymphoscintigraphy. *J Nucl Med.* 1995;36:1895-1901.
110. Goldfarb LR, Alazraki NP, Eshima D, et al. Lymphoscintigraphic identification of sentinel lymph nodes: clinical evaluation of 0.22-μm filtration of Tc-99m sulfur colloid. *Radiology.* 1998;208:505-9.
111. Eshima D, Eshima LA, Gotti NM, et al. Technetium-99m-sulfur colloid for lymphoscintigraphy: effects of preparation parameters. *J Nucl Med.* 1996;37:1575-8.
112. Brown M, El Gammal TAM, Luxenberg MN, et al. The value, limitations, and applications of nuclear dacryocystography. *Semin Nucl Med.* 1981;11:250-7.
113. Brizel HE, Sheils WC, Brown M. The effects of radiotherapy on the nasolacrimal system as evaluated by dacryoscintigraphy. *Radiology.* 1975;116:373-81.
114. Mishima S, Gasset A, Klyce SD, et al. Determination of tear volume and tear flow. *Invest Ophthalmol.* 1966;5:264-76.
115. Daubert J, Nik N, Chandeyssoun PA, et al. Tear flow analysis through upper and lower systems. *Ophthal Plast Reconstr Surg.* 1990;6:193-6.
116. Robertson JS, Brown ML, Colvard DM. Radiation absorbed dose to the lens in dacryoscintigraphy with pertechnetate. *Radiology.* 1979;113:747-50.
117. Merriam GR, Szechter A, Focht EF. The effects of ionizing radiations on the eye. *Front Radiat Ther Oncol.* 1972;6:346-85.
118. Datz FL, Taylor A, Jr. The clinical use of radionuclide bone marrow imaging. *Semin Nucl Med.* 1985;15:239-59.
119. Weiss L, Chen LT. The organization of hematopoietic cords and vascular sinuses in bone marrow. *Blood Cells.* 1975;1:617-38.
120. Weiss L. The structure of bone marrow. *J Morphol.* 1965;117:467-537.
121. Reske SN. Recent advances in bone marrow scanning. *Eur J Nucl Med.* 1991;18:203-21.
122. Yum M, Kim C, Sam J, et al. Bone marrow scintigraphy. In: Sandler MP, Coleman RE, Patton JA, et al., eds. *Diagnostic Nuclear Medicine.* 4th ed. Philadelphia: Lippincott Williams & Wilkins; 2003:565-87.
123. Ferrant A, Rodhain J, Leners N, et al. Quantitative assessment of erythropoiesis in bone marrow expansion areas using ^{52}Fe. *Br J Haematol.* 1986;62:247-55.
124. McIntyre PA. Agents for bone marrow imaging: an evaluation. In: Subramanian G, Rhodes B, Cooper JF, et al., eds. *Radiopharmaceuticals.* New York: Society of Nuclear Medicine; 1975:343-8.
125. Atkins HL, Hauser W, Richards P. Factors affecting distribution of ^{99m}Tc-sulfur colloid. *J Nucl Med* 1969;10:319-20.
126. McIntyre PA. Newer developments in nuclear medicine applicable to hematology. In: Brown EB, ed. *Progress in Hematology.* Vol 10. Orlando, FL: Grune and Stratton; 1977:361-409.
127. Nelp WB, Gohil MN, Larson SM, et al. Long-term effects of local irradiation of the marrow on erythron and red cell function. *Blood.* 1970;36:617-22.
128. Dibos PE, Judisch JM, Spaulding MB. Scanning the reticuloendothelial system (RES) in hematological diseases. *Johns Hopkins Med J.* 1972;130:68-81.
129. Duncker CM, Carrió I, Berná L, et al. Radioimmune imaging of bone marrow in patients with suspected bone metastases from primary breast cancer. *J Nucl Med.* 1990;31:1450-5.
130. Reske S, Buell U. Reduced technetium-99m labeled NCA-95/CEA-antibody uptake in the liver due to gentle antibody reconstitution: technical note. *Eur J Nucl Med.* 1990;17:38-41.

21 Monoclonal Antibodies

The development of clinically useful radiolabeled antibodies has been a long and arduous process. The specificity of an antibody for an antigen was initially regarded by drug-targeting scientists as another "magic bullet" in the diagnosis and treatment of disease. However, early studies in humans demonstrated that while radiolabeled antibodies target tumor cells well in vitro, targeting of tumor cells in vivo is tumor associated rather than tumor specific. The nonspecific in vivo uptake of antibodies in normal tissue made them less than ideal for clinical use. Although success with radiolabeled antibodies was limited initially, persistent efforts by scientists and clinicians led to techniques for improving uptake in target tissue, diminishing nonspecific uptake, and reducing adverse immune reactions.

Site-specific localization of monoclonal antibodies became more attainable with the identification of a deletion-mutant form of epidermal growth factor receptor that exists in several tumor cell populations but not in normal tissues.[1] Monoclonal antibodies specific for this receptor have been developed, and this may lead to improved targeting in tumor tissue. Additionally, research has shown radiolabeled antibodies to be useful adjuncts to conventional therapy, especially in diseases that have become refractory to chemotherapy. This application has been particularly beneficial in the treatment of non-Hodgkin's lymphoma and likely will be extended to other conditions.

In conventional medical practice, the successful diagnosis of cervical cancer through periodic cytomorphologic evaluation has shown that early identification and treatment of cancer can markedly reduce morbidity and mortality. Early identification and treatment can prevent metastasis and its often dismal prognosis. One major problem, however, has been the availability of specific, sensitive methods for detecting cancerous tissue at an early stage. The potential for sensitive radioactive methods of detection, coupled with the immunologic specificity of antibodies in vivo, has driven the development of radiolabeled antibodies for identifying the presence of tumors (radioimmunodiagnosis, or RID) and delivering lethal doses of ionizing radiation to tumors while sparing normal tissue (radioimmunotherapy, or RIT).

Before discussing specific radiolabeled antibodies used in nuclear medicine, this chapter briefly reviews the immune system, antibody structure and properties, and methods used to produce and radiolabel antibodies.

THE IMMUNE SYSTEM

The human immune system originates from lymphocytic stem cells present in the bone marrow at birth. These stem cells give rise to precursor cells that ultimately develop into mature T-lymphocytes and B-lymphocytes. Precursor "T" cells, or pre-T cells, undergo differentiation in the thymus gland, where they acquire the characteristics of T-lymphocytes. Precursor "B" cells are differentiated in the bone marrow, where they acquire the mature characteristics of B-lymphocytes. In birds, where this process was first studied, lymphocyte differentiation occurs in the bursa of Fabricius, which is the reason for the designation "B" cell. T-lymphocytes confer cellular immunity, whereas B-lymphocytes confer humoral immunity (Figure 21-1). The mature cells leave the primary lymphoid tissue of the thymus gland and bone marrow to take up residence in the secondary

lymphoid tissues of the body, composed mainly of the spleen, lymph nodes, and mucous-associated lymphoid tissues. In these places they wait, like armed warriors, to be activated by specific antigen invaders. Once activated, a sensitized T-lymphocyte can recognize and destroy specific antigens or cells directly, whereas activated B-lymphocytes are sensitized to become plasma cells that produce antibodies against specific antigens.

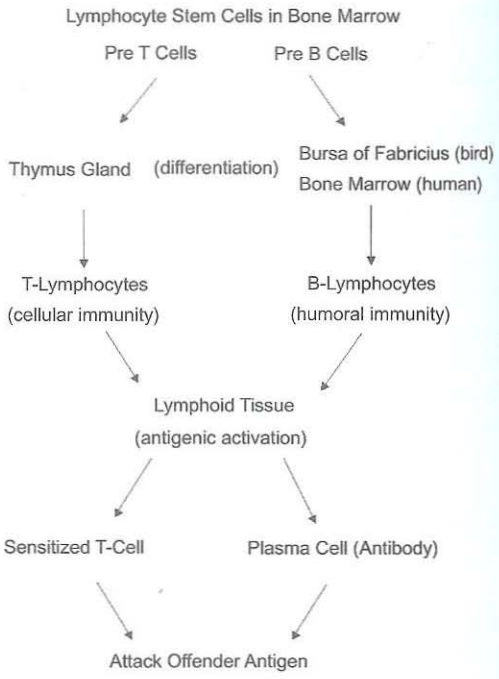

FIGURE 21-1 Schematic of immune system development.

Antibody Structure

Enzyme digestion studies of the gamma globulin fraction of serum helped to determine the basic structure of the antibody, shown in Figure 21-2.[2,3] The antibody has a Y-shaped configuration consisting of two heavy-chain polypeptides (450 amino acid residues per chain) and two light-chain polypeptides (220 amino acid residues per chain) linked together by disulfide bonds and noncovalent forces (H-bonding, van der Waals, ionic, and hydrophobic interactions). Thus, a whole antibody consists of approximately 1340 amino acids. The disulfide bonds between the heavy chains occur in an area called the hinge region.

The antibody has two main functional regions. The fragment antigen-binding region (Fab) contains the antigen recognition site (paratope), which is responsible for binding of the antibody with a specific antigenic determinant (epitope) on the antigen (e.g., tumor cell). Epitopes occur on the surface of the cell membrane of an invader cell. This region of the antibody is sometimes referred to as the amino terminus. The other main functional region of the antibody is the fragment crystallizable (Fc) region, which is sometimes referred to as the carboxyl terminus. The Fc region is responsible for linking the antibody to other molecules involved in the immunologic response. For example, when an antibody binds with an antigen on an invading cell, certain effector functions are brought into play to eliminate the invader. This involves binding sites in the Fc region of the antibody, which initiate effects such as complement-dependent cytotoxicity (CDC), binding to mononuclear cells with phagocytosis, or binding to Fc receptors on natural killer (NK) cells to effect destruction by antibody-dependent cell-mediated cytotoxicity (ADCC). The Fc region also contains oligosaccharides that reside just below the hinge region. Modifications can be made to carbohydrates located in this region to attach linker groups for antibody labeling.

In the original work on determining antibody structure, pepsin digestion of whole antibody cleaved it below the hinge region, producing one bivalent $F(ab')_2$ fragment and two Fc fragments. When papain digestion was used, two monovalent Fab fragments were produced, each carrying a paratope at the end farthest from the cleavage site, demonstrating that there were two paratopes for each antibody molecule. A single Fc fragment, connected by disulfide bonds, was also produced in papain digestion because the cleavage occurred above the hinge region. This process is summarized in Figure 21-3.

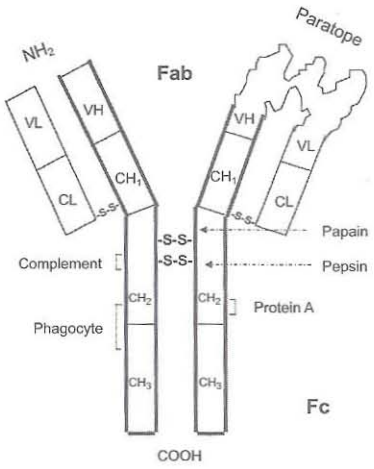

FIGURE 21-2 IgG antibody structure and key components. (Fab) antigen-binding region; (Fc) fragment crystallizable; (VL) variable light chain; (VH) variable heavy chain; (CL) constant light chain; (CH) constant heavy chain. See text for description of enzyme effects and Fc region functionalities.

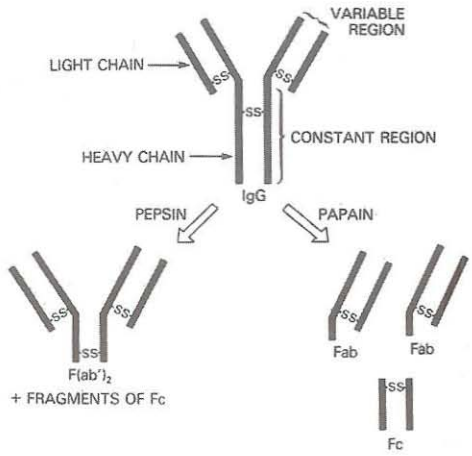

FIGURE 21-3 IgG molecules consist of two heavy and two light protein chains held together by disulfide bonds. Two variable regions can bind to specific antigenic sites, and the constant region interacts with the host immune system. Enzymatic digestion with pepsin removes part of the constant region to produce an $F(ab')_2$ fragment, whereas papain splits the molecule into an Fc fragment and two Fab fragments. (Reprinted with permission of the Society of Nuclear Medicine from reference 8.)

TABLE 21-1 Antibody Classification

Class (Isotype)	Serum Conc (mg/100 mL)	Molecular Weight (× 1000)	Chains	
			Light	Heavy
IgG	800–1600	150–180	2 λ or κ	2 γ
IgA	150–400	160	2 λ or κ	2 α
IgM	50–200	900	10 λ or κ	10 μ
IgD	0.3–40	180	2 λ or κ	2 δ
IgE	0.03	200	2 λ or κ	2 ε

Antibody Classification

There are five major immunoglobulin (Ig) classes in the blood: IgG, IgA, IgD, IgE, and IgM. The properties of these classes are summarized in Table 21-1. IgG is the most abundant class, having the highest serum concentration. It has been shown that the four-chain antibody structure described above is basic for all immunoglobulin classes and that while the light chains are similar between classes, composed of either kappa (κ) or lambda (λ) chains, the heavy chains are specific for each class. The far right column of the table indicates that the IgG class contains two gamma (γ) heavy chains, the IgA class two alpha (α) heavy chains, and so forth. IgM is a composite of five basic antibody units, and has five times the number of heavy and light chains of other antibody classes.

Studies involving enzymatic treatment of immunoglobulins revealed that some of the fragments contained regions along the polypeptide chains where amino acid sequences

Antibody Development

Antibodies against human tumor cell lines can easily be produced in the spleens of animals injected with tumor cells. Tumor cells as antigens, however, contain several different determinants or epitopes on their cell membranes. Upon antigenic challenge, splenic B-lymphocytes develop antibodies against each of the different epitopes on the tumor cells. The result is diverse antibodies (polyclonal antibodies) all specific to the same antigen but with varying degrees of avidity. A key point in the development of antibodies for diagnosis and therapy is identification and isolation of the B-lymphocyte that produces the particular antibody (monoclonal antibody) that has the highest avidity for the tumor cell. Monoclonal antibodies are antibodies that possess identical specificities and recognize the same epitope on the antigen.[5] The potential advantage of monoclonal antibodies is that they should react more predictably and exclusively with the tumor antigenic sites and have less interaction with nonspecific sites in the body.

A major problem discovered in early studies was that antigenically stimulated lymphocytes could not be grown alone in cell culture. The ability to grow these cells was essential for identifying desirable clones of B-lymphocytes and producing a specific monoclonal antibody. In 1975, Kohler and Milstein[6] made a discovery that solved this problem. They developed a method of producing monoclonal antibodies in vitro by fusing splenic lymphocytes from immunized mice with mouse myeloma cells. The result was clones of hybrid cells called hybridomas. The myeloma cell provided the immortality needed for the hybrid cell to reproduce itself, and the lymphocyte enabled the hybrid cell to produce the desired monoclonal antibody.[7] Hybridomas can be grown in tissue culture, providing the ability to isolate the desired monoclonal antibodies in buffer. Hybridomas can also be grown in mouse peritoneum, whereupon antibodies are harvested from ascites fluid. Commercial production of antibodies is carried out in mice and through the use of hybridoma technology (Figures 21-4 and 21-5).[8]

Although all of the antibody a hybridoma clone secretes is genetically derived from a single cell, it is not a monoclonal antibody in the immunologic sense because each cell of the clone has some chromosomes from the myeloma cell parent and some from the spleen cell parent.[8] As a result, the hybridoma antibody is frequently a mix of heavy and light chains of both parent cells. Because the aim is to find a clone with only heavy and light chains of the specifically immune spleen cell, hundreds of fusions and reclonings may be required before a single hybrid that secretes the desired antibody is formed (Figure 21-5). Once the desired clone is found, it can be frozen for long-term storage. At any time thereafter a sample of the clone can be injected into animals of the same strain as those that provided the original cells for fusing.[7] The injected hybridomas will grow and secrete the specific monoclonal antibody in high concentration in the animal's serum. Alternatively, a clone can be grown in mass culture in vitro and the antibody harvested from the medium.

Antibody Modification

Antibodies can be modified to remove undesirable characteristics and to change their kinetic properties. Hybridomas produce whole antibodies with the Fab and Fc regions intact. Antibodies for clinical use are of the IgG type having a molecular weight of about 150,000. The $F(ab')_2$ fragment has a molecular weight of about 100,000 and the Fab fragment about 50,000. Whole antibodies have properties distinctly different from antibody fragments. Because of their large molecular weight, whole antibodies have slower blood clearance, have a greater chance of being taken up into tumor, achieve a lower tumor-to-background ratio, and are more suited for longer-lived radionuclides such as ^{131}I and ^{111}In. Additionally, whole antibodies have a higher rate of human antimouse antibody (HAMA)

TABLE 21-2 Antibody Subclassification

	Subclass	
Class	Human	Mouse
IgG	IgG1, IgG2, IgG3, IgG4	IgG1, IgG2a, IgG2b, IgG3
IgA	IgA1, IgA2	None
IgM	None	None
IgD	None	None
IgE	IgE1, IgE2	None

either were relatively constant or varied between different antibody molecules. Such regions are referred to as the constant and variable domains within the antibody molecule. IgG has one variable domain and one constant domain on the light and heavy chains in the Fab fragment and two constant domains in the Fc fragment of the heavy chains (Figure 21-2). The variable domains on the heavy and light chains extend from the amino terminus to approximately residue 120, and the constant domains extend from residues 121 to 220 on the light chain and from 121 to 450 on the heavy chain. By comparison, IgE and IgM each have one variable and four constant domains (three are in the Fc fragment).

Each variable domain contains amino acid positions with exceptional degrees of variability, termed the hypervariable regions or complementarity-determinant regions (CDRs) because these sites complement specific sites on the antigen. Sequence analysis has shown that CDRs occur along heavy and light chains at about residue 30, between residues 50 and 60, and between residues 90 and 100, with relatively constant "framework" regions between them.[4] The heavy chain has an additional CDR between residues 80 and 90. Each CDR consists of a peculiar amino acid sequence that determines the antibody's uniqueness. In the tertiary structure of the antibody, the heavy and light chains loop together in such a way that three of these hypervariable regions are exposed at the tip of each Fab fragment, forming the antigen-binding site (paratope). The CDR between residues 80 and 90 does not seem to participate in paratope formation.

Structural variation, particularly within the heavy chains, determines the immunoglobulin isotype or class (e.g., IgG versus IgA). Within each class are subclasses determined by specific amino acid sequence differences in the heavy chains and particularly by the number of disulfide bonds present in the hinge region. For example, human IgG contains four subclasses, IgG1, IgG2, IgG3, and IgG4 (Table 21-2). Subclasses of an immunoglobulin differ in their ability to fix complement or react with microbial proteins in the immunologic process. The subclass of an antibody available for clinical use is often listed in the product labeling.

The subclass or isotypic markers are constant within a given species but have distinct differences between species. For example, mouse IgG subclasses are IgG1, IgG2a, IgG2b, and IgG3. There are also allotypic determinants (genetic markers) that identify immunologic differences between IgG molecules within a given species. For example, blood from two individuals with different allotypic markers may be incompatible. Allotypic determinants are regions of variation found in the constant heavy domains, CH_1 and CH_2. In addition, the blood of individuals having identical allotypic markers may exhibit incompatibility because of differences in idiotypic markers. Idiotypes are specific markers found in the variable regions of the antibody and are likely to be associated with the hypervariable regions.[4]

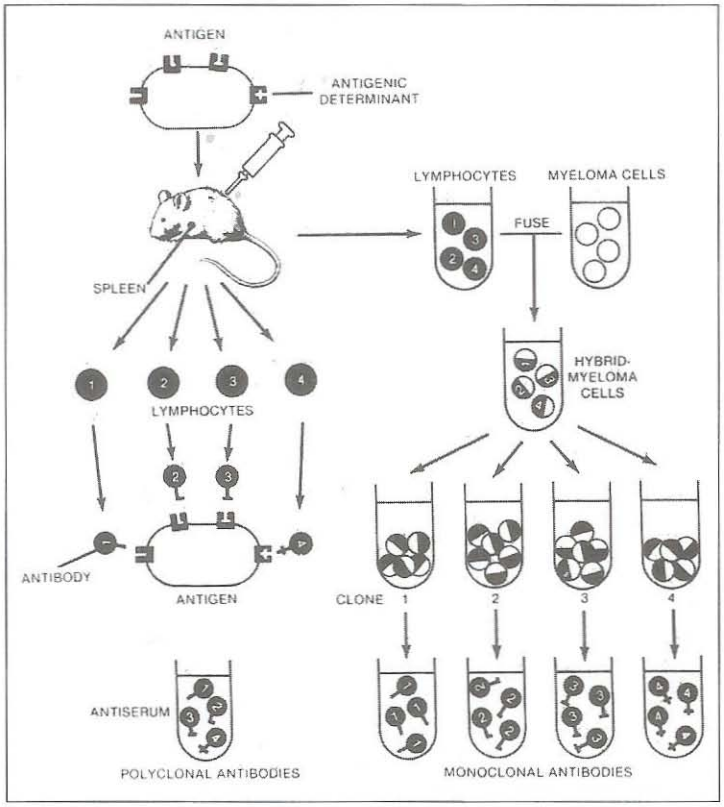

FIGURE 21-4 Injection of antigen into a mouse or other higher animal elicits a heterogeneous antibody response because of the stimulation of several B-lymphocytes by various determinants on the antigen, which results in polyclonal antibodies in the serum (left). If sensitized lymphocytes are removed from the spleen of an immunized animal and induced to fuse with myeloma cells, individual hybrid cells can be cloned, each producing monoclonal antibodies to a single antigenic determinant (right). (Reprinted with permission of the Society of Nuclear Medicine from reference 8.)

response because they retain the Fc portion. The HAMA response is an undesirable immunologic reaction that results from human antibodies being produced against the injected mouse antibody as the foreign antigen. This response is more probable after multiple exposures to the antibody.

Antibody fragments are parts of the antibody produced by enzymatic cleavage with pepsin or papain. Fragmentation makes the antibody's kinetic properties different from those of whole antibodies. Fragments have faster blood clearance because of their smaller molecular weight. Because of this, a lower percentage of the injected dose is taken up in tumor, but the tumor-to-background ratio is higher. The faster clearance means a shorter time from dose to imaging, so antibody fragments are particularly suited for labeling with shorter-lived radionuclides such as ^{99m}Tc or ^{123}I. Additionally, because the Fc portion of the antibody is removed during enzymatic cleavage, the HAMA response occurs less freqently with fragments. Elimination of the Fc portion also reduces binding of the antibody to Fc receptors in the liver and uptake of the metabolized antibody by macrophages.[5]

Antibody fragments are produced either by enzyme digestion or through genetic engineering. Pepsin digestion of whole antibody results in one $F(ab')_2$ fragment with bivalent antigen-binding capability. Papain digestion results in two Fab fragments capable of monovalent antigen binding. Despite removal of the Fc portion during enzyme digestion,

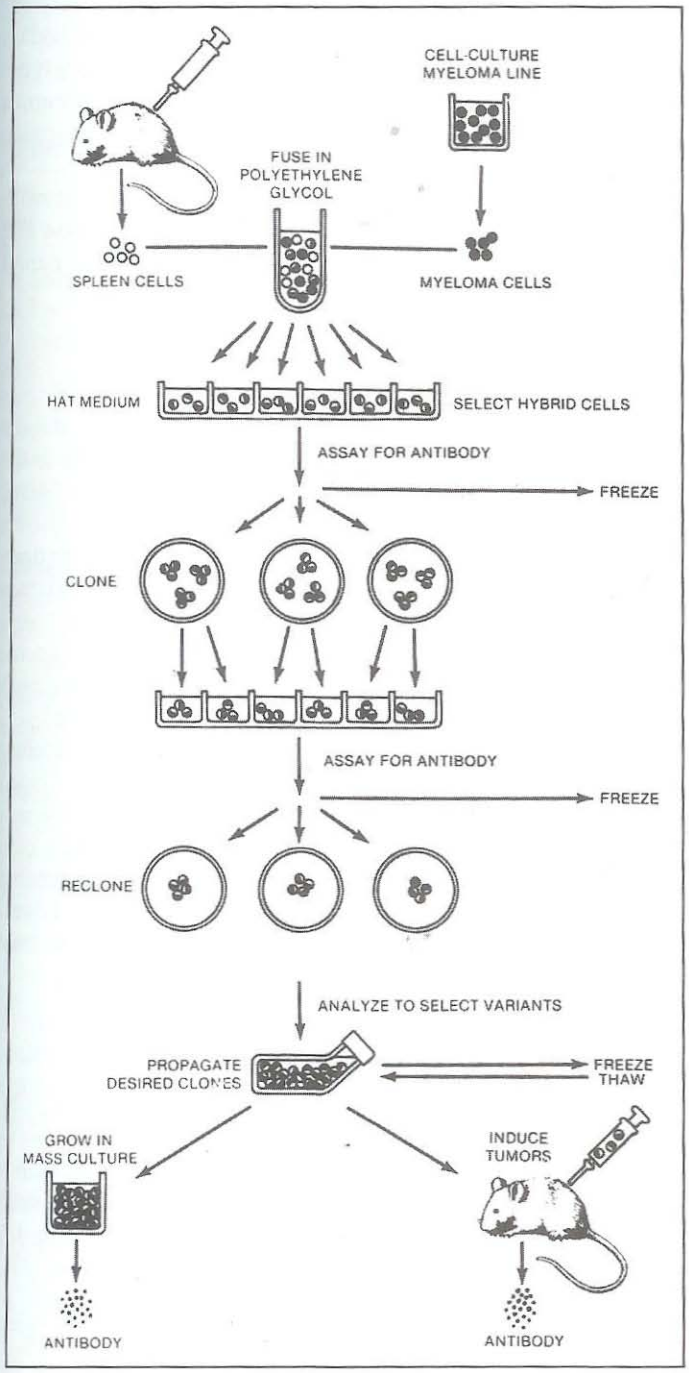

FIGURE 21-5 Fusion of antigen-stimulated spleen cells with myeloma cells in polyethylene glycol results in hybrid cells that can be cloned in hypoxanthine–aminopterin–thymidine (HAT) medium. Those clones that generate immunoglobulin are further propagated, and those producing antibodies to the desired antigen are selected to find the variant that produces antibody with the desired specificity and binding properties. Hybridomas can be maintained in mass culture or mouse ascites fluid, and clones at any stage of development can be frozen for later use. (Reprinted with permission of the Society of Nuclear Medicine from reference 8.)

antibody fragments can still elicit a HAMA response because they contain amino acid sequences unique to the mouse. Consequently, genetic engineering techniques have been developed to reduce the HAMA response.[9] Several types of modifications can be made. A *chimeric* antibody contains a murine variable domain and a human constant domain; a *humanized* antibody goes one step further and has only a murine CDR, with the remainder being human. Two other modifications can be made to shorten the time between antibody injection and imaging: single-chain antigen-binding proteins that consist of a variable

heavy chain and a light chain linked together by a disulfide bond, and molecular recognition units that consist of the CDR alone. Despite these efforts to "humanize" antibodies, antimouse antibodies can still be induced because the CDR is of mouse origin. These types of antibodies are called human antichimeric antibodies (HACA) or human antihuman antibodies (HAHA), depending on whether the modified antibody is chimeric or humanized.

In addition to reducing HAMA response, another advantage of chimeric and humanized antibodies is that they possess a much more potent immune effector function and are therefore more capable of inducing CDC and ADCC than are their murine parent antibodies, making them potentially more effective antitumor agents.[10]

Antibody–Antigen Interaction

A whole antibody has two antigen-binding sites, making it a bivalent ligand. Each of these sites can interact with a single epitope on the antigen. The *affinity* of an antibody is the strength of binding between a single antigen-binding site on the antibody and its antigenic epitope.[11] Antibody affinity is typically determined by equilibrium dialysis with known amounts of antigen and antibody. A smaller fraction of antibody associated with an antigen indicates a low binding affinity. Because an antibody is bivalent, it may interact with two epitopes on the antigen. The probability of this occurring increases if the substrate (e.g., tumor cell) antigen density is high. The overall strength of binding of an antibody molecule to an antigen is called its *avidity*. Antibody avidity is greater than affinity because both binding sites on the antibody must dissociate for it to be released from the antigen.

When an antibody is radiolabeled, its antigen-binding site may be altered, affecting its ability to react with the antigen. The immunoreactivity of an antibody can be tested by measuring its ability to react with cells that express the specific antigenic determinant on their surface. A typical way to assess a radiolabeled antibody's immunoreactivity is to incubate it with an excess of antigen (tumor cells) and measure the fraction of labeled antibody bound to the cells. Raji cells, which bear the antigenic determinants for lymphoma, have been used to assess the immunoreactivity of labeled antibodies used to treat non-Hodgkin's lymphoma.

Antibody Nomenclature

A variety of terms are used to describe antibodies and their antigenic markers (Table 21-3). The name of an antibody reveals some of its characteristics. The generic name given to an antibody (e.g., ibritumomab or rituximab) is derived as follows.[12,13] The suffix *mab* is used for monoclonal antibodies and antibody fragments. Preceding the suffix is one or more letters identifying the antibody source (e.g., *o* = mouse, *u* = human, *xi* = chimeric). Preceding the antibody source designation is a letter code identifying the disease state subclass (e.g., *vir* = viral, *bac* = bacterial, *lim* = immunomodulator, *cir* = cardiovascular) or area of tumor involvement (e.g., *col* = colon, *mel* = melanoma, *mar* = mammary, *tum* or *tu* = miscellaneous tumor). Preceding the disease code is a unique prefix selected by the antibody manufacturer. If the antibody is radiolabeled, the antibody name is preceded by the name of the radionuclide, its elemental symbol, and its mass number. For example, the Zevalin (Biogen Idec) antibody labeled with ^{90}Y or ^{111}In is written as yttrium Y 90 ibritumomab or indium In 111 ibritumomab, and Bexxar (GlaxoSmithKline) is written as iodine I 131 tositumomab.

In addition to the generic name of an unconjugated antibody is a number/letter code designation for the antibody (e.g., B1 for tositumomab and 2B8 for ibritumomab). If an antibody is a conjugate, the conjugate name follows its generic name. For example, Zevalin

TABLE 21-3 Antibody Nomenclature

Disease[a]	Trade Name	Generic Name	Unconjugated Monoclonal Antibody Designation	Antigenic Marker
NHL	Zevalin	^{90}Y- or ^{111}In-ibritumomab tiuxetan	2B8	CD20
NHL	Bexxar	^{131}I-tositumomab	B1	CD20
NHL	Rituxan	Rituximab	C2B8	CD20
CR cancer	CEA Scan	^{99m}Tc-arcitumomab	IMMU-4	CEA
CR/OV cancer	OncoScint CR/OV	^{111}In-satumomab pendetide	B72.3	TAG72
Prostate cancer	ProstaScint	^{111}In-capromab pendetide	7E11-C5.3	PSA
NHL	–	^{131}I-LYM-1	LYM-1	HLA-DR
NHL	Lymphocide	^{90}Y-epratuzumab	hLL2	CD22
Infection	LeukoScan	^{99m}Tc-sulesomab	IMMU-MN3	NCA-90
Infection	LeuTech	^{99m}Tc-LeuTech	Anti-SSEA-1	CD15

[a] NHL = non-Hodgkin's lymphoma; CR = colorectal; OV = ovarian.

labeled with ^{90}Y or ^{111}In is a conjugate of the monoclonal antibody ibritumomab and the bifunctional chelating agent tiuxetan. The full names, thus, are yttrium Y 90 ibritumomab tiuxetan and indium In 111 ibritumomab tiuxetan.

Specific surface molecules on the lymphocyte cell membrane that are recognized by groups of monoclonal antibodies are called *clusters of differentiation* (CD). The CD designation is followed by an arbitrarily assigned number. These CD antigens are expressed on the surface of malignant B-lymphocytes in tumors and normal B-lymphocytes in the blood, spleen, lymph nodes, bone marrow, and some of their precursors in the marrow, depending on the antigen.[10] For example, the CD20 antigen, targeted by unconjugated rituximab, ^{111}In- or ^{90}Y-ibritumomab, and ^{131}I-tositumomab, is found on all cells, including pre-B cells of the bone marrow, but not on the stem cells.

ANTIBODY LABELING

A variety of radionuclides, mainly radiohalogens and radiometals, are used to label antibodies.[14–18] At present, the antibodies used in nuclear medicine practice are labeled with ^{131}I, ^{99m}Tc, ^{111}In, and ^{90}Y, although other nuclides are being studied. A list of radionuclides for RID and RIT is given in Table 21-4.

Radionuclide Considerations

Radiolabeled antibodies are used for both diagnosis and therapy. Currently, therapeutic applications are receiving much attention. Radionuclides for RID must necessarily emit gamma radiation, while those for RIT emit particulate radiation, typically beta particles. The development of alpha-particle emitters in RIT is under investigation.

For RIT, the radionuclide properties should be compatible with the size and location of the tumor. In general, large solid tumors and those that do not internalize antibody (e.g., CD20 antigens) require more energetic, penetrating radiation, while metastatic lesions, composed of only a few hundred cells, can be treated with short-range radiations. Tumors that internalize antibodies (e.g., CD22 antigens) can be more effectively killed by radionuclides that emit short-range radiation, such as Auger electrons (e.g., ^{125}I and ^{77}Br) and alpha particles (e.g., ^{211}At and ^{212}Bi). Low-energy Auger electrons have high linear energy transfer and possess the advantage of depositing their energy close to the cell

TABLE 21-4 Properties of Radiolabels for Diagnostic and Therapeutic Antibodies

			Radiation Properties			
			Particles		Photons	
Radionuclide	Half-life	Decay Mode	Max keV	Mean Range (mm)	keV	Abundance (%)
^{67}Cu	61.9 hr	β^-	570	0.27	92	11
					185	49
^{90}Y	64.08 hr	β^-	2280	2.76	–	
^{99m}Tc	6.01 hr	IT	–	–	140.5	88
^{123}I	13.2 hr	EC	–	–	159	84
^{125}I	59.4 days	EC	–	–	27	115
					35	6.7
^{131}I	8.02 days	β^-	606	0.4	364	82
					637	6.5
^{186}Re	89.2 hr	β^-	1070	0.92	137	9
^{188}Re	17 hr	β^-	2120	2.43	155	15
^{211}At	7.2 hr	Alpha	5866	0.06	–	42
			7450	0.08		58

nucleus. They also have the potential of sparing normal tissue surrounding the tumor. Larger tumors and those that bind antibodies on surface receptors are more effectively treated with more energetic beta emitters, such as ^{90}Y, ^{131}I, ^{186}Re, and ^{188}Re.

In general, the half-life of a radionuclide should be matched with the antibody's in vivo kinetics. Whole or intact antibodies, which have prolonged circulation times, are best labeled with longer half-lived nuclides, such as ^{131}I, ^{111}In, and ^{90}Y. Antibody fragments, which clear more quickly from the bloodstream, are preferably labeled with shorter-lived nuclides, such as ^{99m}Tc and ^{123}I. Ideally, a therapeutic radionuclide should also emit photons to permit imaging of antibody distribution in vivo. This greatly facilitates quantitative distribution studies for estimating radiation dosimetry. In some instances (e.g., with ibritumomab), the antibody is labeled with a beta emitter (^{90}Y) for therapy, but it can also be labeled with a gamma emitter (^{111}In) to facilitate dosimetry calculations.

Ideally, the radionuclide should not dissociate from the antibody in vivo, because this would result in an undesirable radiation dose to normal tissues and a reduced dose to the tumor. In general, the radioiodines are prone to enzymatic deiodination with uptake in the thyroid gland and stomach, while metallic radionuclides released from antibodies are taken up into bone. Significant effort has been directed toward the development of radiolabeling methods that mitigate these problems.

Radioiodine Labeling

Antibodies and proteins have been labeled with a variety of radiohalogens, including ^{123}I, ^{125}I, ^{131}I, ^{77}Br, ^{18}F, and ^{211}At.[14] Most antibody labeling, however, is done with the radioiodines. Both direct and indirect methods of labeling are used.

With direct iodination (via electrophilic substitution), radioiodide (I^-) is oxidized to I^+, which binds to hydroxylbenzyl moieties of tyrosyl residues in the antibody polypeptide chains, as follows:

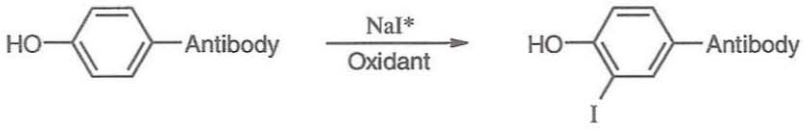

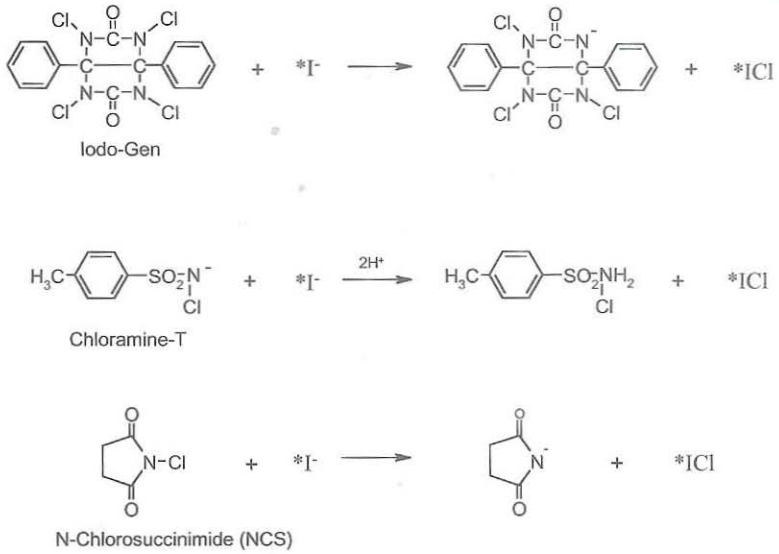

FIGURE 21-6 Oxidants used in the radioiodination of proteins and antibodies.

The direct method has the advantage of relatively easy iodine chemistry (see Chapter 9). Common oxidants for iodination are chloramine-T and the milder Iodo-Gen (Pierce), which is claimed to be less damaging to the antibody (Figure 21-6).[5] N-chlorosuccinimide (NCS) has been used as an oxidant with indirect methods of iodination. Iodo-Gen is preferred for labeling $F(ab')_2$ fragments because this method does not use sodium metabisulfite, which has the capacity to reduce $F(ab')_2$ fragments to Fab.[17]

Indirect methods of labeling antibodies involve attaching the radiohalogen to an intermediate compound that conjugates with the antibody. The principal functional groups on antibodies involved in conjugation reactions are amines, sulfhydryls, and oxidized sugars. However, most conjugations are via acylation reactions between ε-amino groups in lysine and an activated N-hydroxysuccinimide ester (NHS). The classic agent of this type is the Bolton-Hunter reagent (N-succinimidyl 3-iodo-4-hydroxyphenylpropionate).

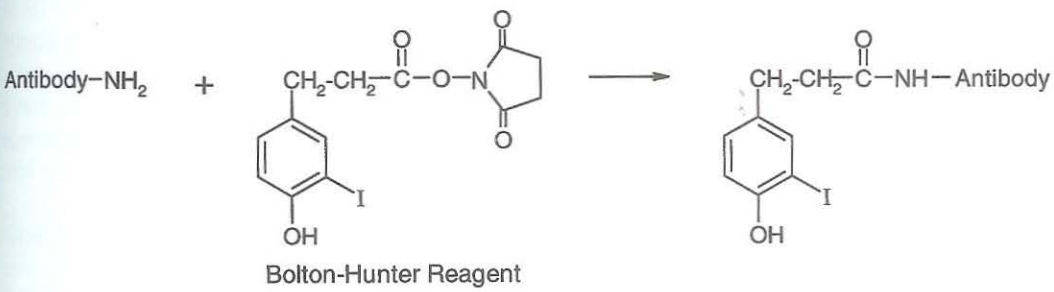

The principal advantages offered by this agent are its ability to label proteins that do not contain tyrosyl residues or are particularly sensitive to the oxidizing and reducing conditions of direct iodination. Labeling yields, however, are lower with the Bolton-Hunter reagent because competing aqueous hydrolysis reactions of the active ester group occur during the radiolabeling. A significant problem with antibodies labeled directly or with the Bolton-Hunter reagent is that the radioiodine label is positioned *ortho* to the hydroxyl

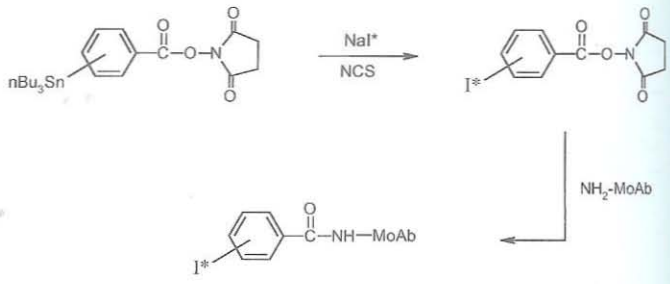

FIGURE 21-7 Synthesis of N-succinimidyl 3- or 4-^{131}I-iodobenzoate (SIB) from the corresponding N-succinimidyl (tri-n-butylstannyl)benzoate precursor via iododestannylation followed by conjugation of SIB to lysine ε-amino groups on the antibody.

group in the aromatic ring. This makes it prone to in vivo deiodination by deiodinase enzymes similar to the metabolism of thyroid hormone.

Other active ester intermediates for indirect iodination have been developed.[14–17] The prototypical method for iodination of an antibody by these intermediates occurs in two steps. The initial step involves synthesis of N-succinimidyl 3- or 4-^{131}I-iodobenzoate (SIB) from the corresponding N-succinimidyl (tri-n-butylstannyl)benzoate precursor via iododestannylation. This is followed by conjugation of SIB to lysine ε-amino groups on the antibody (Figure 21-7).[16,19] This method results in placement of the radioiodine atom in an aromatic ring without a hydroxyl group. Its position within the ring is *meta* or *para*, depending on the precursor used. Although it is more difficult to radiohalogenate nonphenolic aryl ring benzoates, they are more stable to dehalogenation in vivo. When compared with the Bolton-Hunter reagent or directly labeled antibody, the N-succinimidyl 3-iodobenzoate ester was shown to produce radiolabeled antibody most stable toward dehalogenation in vivo. Distribution studies in mice demonstrated that thyroid uptake of activity (a monitor of dehalogenation) of the iodobenzoyl conjugate was about one-half that of the Bolton-Hunter–labeled antibody and only 7% that of antibody iodinated directly with Iodo-Gen.[20] Additional reports demonstrated enhanced tumor uptake, therapeutic efficacy, and in vivo stability against dehalogenation with iodobenzoyl antibody conjugates.[21,22]

Many other methods can be used to radiolabel antibodies, as reviewed by Wilbur.[14]

Radiometal Labeling

The labeling of antibodies with radiometals advanced significantly with the development of bifunctional chelating agents (BFCAs). A number of methods have been used to label proteins and antibodies with radiometals.[22–32] For chelation with ^{111}In and ^{90}Y particularly, derivatives of ethylenediamine tetraacetic acid (EDTA), diethylenetriamine pentaacetic acid (DTPA), and 1,4,7,10-tetraazacyclododecane-1,4,7,10-tetraacetic acid (DOTA) have been explored. Antibodies currently approved for routine use in nuclear medicine use DTPA as the chelating ligand. They are labeled with the postlabeling approach, using kits that contain the antibody–BFCA conjugate.

Two principal approaches have been used to link BFCAs to antibodies. One approach is to conjugate the BFCA with the ε-amino group of lysine within the antibody. However, because lysine is present throughout the antibody molecule, site-specific conjugation is not possible with this approach. Depending on the labeling conditions, this approach may result in reduced antibody specificity if conjugation occurs in proximity to the Fab region.

Another approach involves conjugation of the BFCA to oxidized oligosaccharide moieties within the antibody. Virtually all immunoglobulins contain carbohydrates that are linked to the constant regions of the heavy chains in the Fc region of the antibody. Consequently, conjugation and labeling of BFCAs in this region should result in less likelihood of interference with the antigen-binding site.

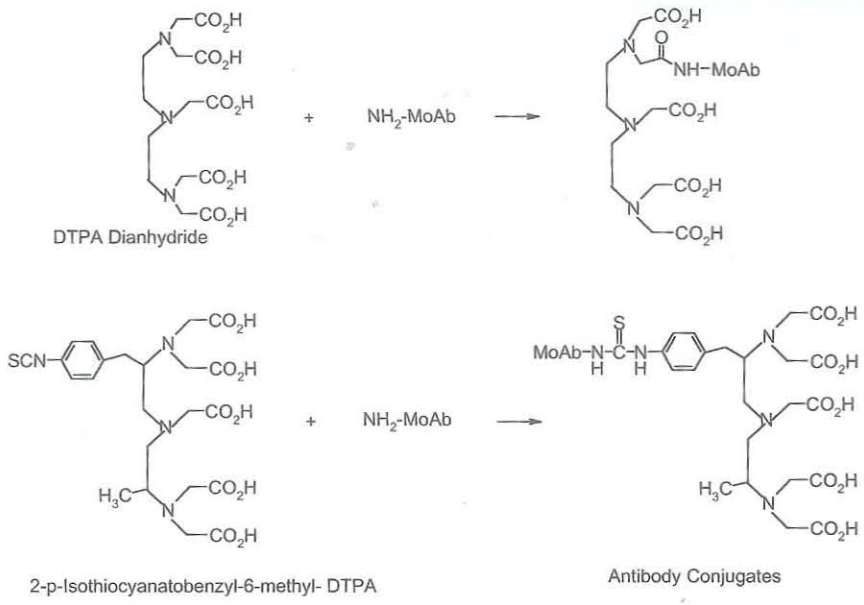

FIGURE 21-8 Antibody conjugation methods involving the use of DTPA dianhydride to covalently attach DTPA to the antibody via lysine acylation (top reaction) and by way of the DTPA derivative, 1-p-isothiocyanatobenzyl-DTPA (bottom reaction), which forms a stable thiourea bond with the antibody. (MoAb is monoclonal antibody.)

Initial antibody conjugation methods used DTPA dianhydride to covalently attach DTPA to the antibody via lysine acylation (Figure 21-8). The labeling of antibodies conjugated in this manner with ^{90}Y, for example, demonstrated that yttrium slowly leaches from the antibody in vivo, with radionuclide localization in bone.[33,34] It was thought that the loss of one DTPA carboxyl group to acylation rendered it unavailable for chelation and made the radiometal bond vulnerable.

Another labeling approach uses DTPA derivatives. With this technique, a benzyl moiety containing an antibody-coupling group is covalently bound to a methylene carbon in the DTPA backbone (Figure 21-8).[24,27,28] A typical example is 1-p-isothiocyanatobenzyl-DTPA, which forms a stable thiourea bond with the antibody according to the following reaction, where MoAb is monoclonal antibody:

$$\text{DTPA-Benzyl-N=C=S} + \text{H}_2\text{N-LYS-MoAb} \longrightarrow \text{DTPA-Benzyl-NH-}\overset{\overset{\text{S}}{\|}}{\text{C}}\text{-NH-LYS-MoAb}$$

This technique of conjugation frees all five DTPA carboxyl groups for chelation with the radiometal, significantly increasing the chelate's thermodynamic stability. Additional functional groups can be attached at other sites on the backbone to sterically hinder the release of the radiometal, improving stability further. An example is 2-p-isothiocyanatobenzyl-6-methyl-DTPA (1B4M-DTPA) (Figure 21-8). This BFCA, designated MX-DTPA, is conjugated with ibritumomab for labeling with ^{111}In or ^{90}Y, forming a stable 1:1 octadentate chelate with these metals.[28,29,35]

Another ligand that has been explored to improve chelation stability is DOTA. DOTA is a macrocyclic chelating agent known to produce exceedingly inert chelates with lanthanides. This significantly reduces radiometal dissociation and localization in bone. A

major drawback to the clinical practicality of DOTA, however, is its slow reaction kinetics during chelation. This poses a problem during antibody labeling because of the detrimental radiolytic effects of hard beta emitters, such as ^{90}Y, on antibody immunoreactivity. Thus, new derivatives of DOTA have been sought to speed up its chelation kinetics.[18]

Oligosaccharide conjugation technology in antibody labeling involves the oxidation of sugar moieties in the Fc region to aldehydes, typically with sodium periodate ($NaIO_4$). The aldehyde group can selectively react with compounds containing amines, hydrazines, hydrazides, and semicarbazides.[36] This permits the selective attachment of BFCAs to the Fc region of the antibody, where radiolabeling will occur away from the antigen-binding site. A typical conjugation reaction between an amino derivative of DTPA and antibody aldehyde groups involves formation of an imine or Schiff base with the antibody, which is then reduced to the stable secondary amine as follows:

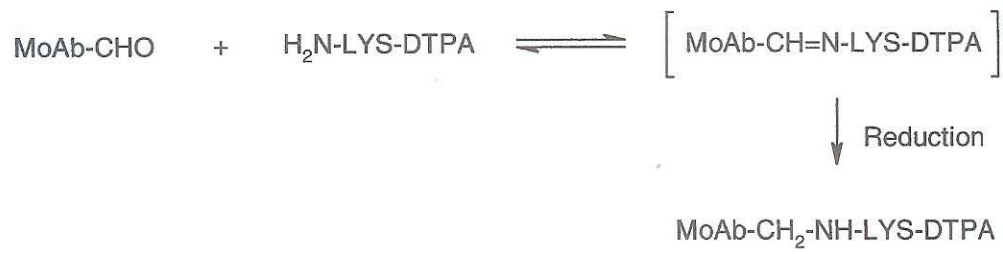

The BFCA used in the production of ^{111}In-satumomab pendetide and ^{111}In-capromab pendetide (ProstaScint, Cytogen) is glycyl-tyrosyl-(N-ε-DTPA)-lysine or GYK-DTPA. It is the linker molecule attached to oxidized sugars in the Fc region that chelates ^{111}In to the antibody.

Bifunctional chelation technology makes antibody labeling amenable to kit preparation; only the buffered radiometal must be added to the antibody conjugate in the kit. The labeling yield in commercially available products is typically greater than 90%. Radiolabeling via bifunctional chelation is discussed in Chapter 9.

Several approaches have been used to label antibodies with ^{99m}Tc.[30–32] A direct method relies on the reduction of disulfide bridges within the antibody to generate endogenous sulfhydryl groups. These groups are attachment sites for reduced technetium (see Figure 9-15, Chapter 9). An indirect method of labeling antibodies involves first conjugation of DTPA to the antibody and then addition of reduced technetium to the conjugate. This method is similar to the postlabeling approach described above for ^{111}In and ^{90}Y labeling. A third approach to labeling antibodies with technetium is to employ a prelabeled ligand (prelabeling approach).[32] In this method, dithionite-reduced technetium is complexed to an N_2S_2 ligand functionalized with a carboxylate group. This is then activated with an ester group through which it is bound efficiently to the antibody via an acylation reaction with lysine amine residues (see Figure 9-16, Chapter 9). This labeling approach obviates nonspecific binding of technetium to the antibody, which has been found to occur with direct labeling by the postlabeling approach. Although this method produces a stable antibody label without nonspecific binding, it is somewhat cumbersome and less adaptable to simple kit formulation.

RADIOLABELED ANTIBODIES

Five radiolabeled antibodies for diagnosis and two antibodies for therapy have received FDA approval for routine use in nuclear medicine. The ^{99m}Tc diagnostic antibodies are

^{99m}Tc-arcitumomab (CEA-Scan, Immunomedics) and ^{99m}Tc-nofetumomab merpentan (Verluma; no longer marketed). The ^{111}In diagnostic antibodies are ^{111}In-satumomab pendetide (OncoScint CR/OV), ^{111}In-imciromab pentetate (Myoscint), and ^{111}In-capromab pendetide (ProstaScint). OncoScint CR/OV and Myoscint are no longer marketed. The therapeutic antibodies are ^{90}Y-ibritumomab tiuxetan (Zevalin) and ^{131}I-tositumomab (Bexxar). Several other radiolabeled antibodies are in development, including ^{99m}Tc-sulesomab (^{99m}Tc-LeukoScan, Immunomedics) and ^{99m}Tc-LeuTech (Palatin) for imaging infection, ^{90}Y-epratuzumab, and ^{131}I- and ^{67}Cu-LYM-1 for treating non-Hodgkin's lymphoma. The diagnostic antibodies are discussed in this chapter and the therapeutic antibodies, in Chapter 23.

Diagnostic Antibodies

Technetium Tc 99m Arcitumomab

^{99m}Tc-arcitumomab (CEA-Scan) is a murine Fab fragment of IMMU-4 monoclonal antibody of the IgG1 subclass. IMMU-4 specifically reacts with carcinoembryonic antigen (CEA), a 200 kDa antigen expressed predominantly on the cell surface of a variety of carcinomas, particularly of the gastrointestinal (GI) tract, but also found in fetal GI tissues and certain inflammatory conditions, such as Crohn's disease and inflammatory bowel disease. It is prepared from whole antibody, which is isolated from mouse ascitic fluid and subsequently digested with pepsin to produce the $F(ab')_2$ fragments, and then further reduced to produce the Fab fragments.

The kit consists of a single vial of lyophilized antibody with stannous chloride and other adjuvants. It is stored in the refrigerator before use. Labeling is accomplished by adding 30 mCi (1110 MBq) in 1 mL of ^{99m}Tc-sodium pertechnetate. After incubation for 5 minutes at room temperature, 1 mL of sterile saline is added. Technetium binds to the reduced sulfhydryl groups present in the Fab fragment.

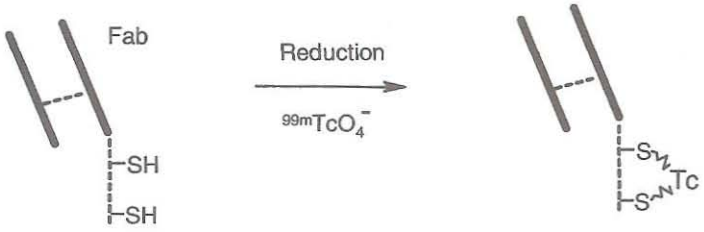

Radiochemical purity is achieved with instant thin-layer chromatograpy with silica gel (ITLC-SG) in acetone, with the ^{99m}Tc-labeled antibody remaining at the origin and the free pertechnetate migrating to the solvent front. Radiochemical purity must be 90% or higher. The labeled product should be stored at room temperature and used within 4 hours after preparation. The labeled antibody does not require filtration before administration to the patient.

^{99m}Tc-arcitumomab is used to detect recurrent or metastatic colorectal cancer involving the liver, abdomen, and pelvis in patients with confirmed colorectal carcinoma. It is also used in patients whose CEA levels are rising to determine if the patient has disease amenable to surgery. The dosage of ^{99m}Tc-arcitumomab is 20 to 30 mCi intravenously, with no restrictions on rate of infusion. Its HAMA response is reported to be less than 1%. Planar or SPECT images are done at 2 to 5 hours after dosing, with delayed images at 24 hours if needed. The critical organ is the kidney, sustaining a radiation absorbed dose of 0.074 rad per 20 mCi (740 MBq).

Indium In 111 Capromab Pendetide

^{111}In-capromab pendetide (ProstaScint) is an intact antibody 7E11-C5.3 of the IgG1 subclass. It reacts with prostate-specific antigen, a glycoprotein expressed by the prostate epithelium.

The antibody is labeled with ^{111}In via GYK-DTPA linker technology. The linker is covalently bound to a carbohydrate in the Fc portion of the antibody.

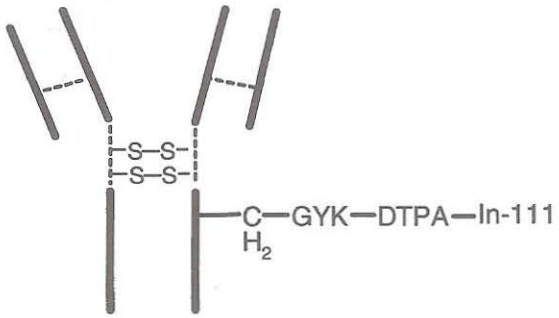

The kit is composed of the antibody in 1 mL of phosphate-buffered saline (PBS), which is stored in the refrigerator before use, a vial of acetate buffer, and a Millex-GV (Millipore) filter. ^{111}In-indium chloride is available from Amersham and Mallinckrodt. Labeling is accomplished in a three-step process. First, 0.1 mL of acetate buffer is added to the indium chloride. This step produces the intermediate species, indium acetate, which keeps indium soluble at the pH necessary for antibody labeling. This is followed by addition of 6 to 7 mCi (222 to 259 MBq) of indium acetate to the antibody and incubation for 30 minutes at room temperature to effect complexation of ^{111}In to the antibody. At this point the remaining 1.9 mL of acetate buffer is added to the mixture to complete the preparation. Radiochemical purity is checked by spotting this mixture on an ITLC-SG strip and developing it in normal saline. The antibody remains at the origin and the free indium migrates to the solvent front. Radiochemical purity must be 90% or higher. The labeled antibody is drawn up through the Millex filter before use, and the product is stable for 8 hours at room temperature.

^{111}In-capromab pendetide is indicated for use in patients with biopsy-proven and clinically localized prostate cancer who are at high risk for metastasis, to help clinicians decide on a course of therapy. ^{111}In-capromab pendetide is also indicated for use in postprostatectomy patients with a high clinical suspicion of occult recurrent or residual prostate cancer (Figures 21-9 and 21-10). The usual administered dosage is 5 mCi (185 MBq) given intravenously over 5 minutes. Whole-body planar imaging is done of the pelvis, abdomen, and thorax between 72 and 120 hours after dosing. The patient should be prepared with a cathartic the night before and a cleansing enema and bladder void 1 hour before imaging. SPECT imaging is done, with a blood pool image acquired 30 minutes after dosing followed by pelvis and abdomen images at 72 to 120 hours after dosing. Lesions are seen as increased focal accumulations of activity (Figure 21-10). Some normal activity is seen in the liver, spleen, bone marrow, and genitalia. The critical organ is the liver, sustaining a radiation absorbed dose of 18.5 rad/5 mCi (185 MBq) administered activity.

Technetium Tc 99m Sulesomab

^{99m}Tc-sulesomab (LeukoScan) is a murine Fab fragment of IMMU-MN3 antigranulocyte monoclonal antibody. It reacts with a 90 kDa glycoprotein, nonspecific cross-reactive

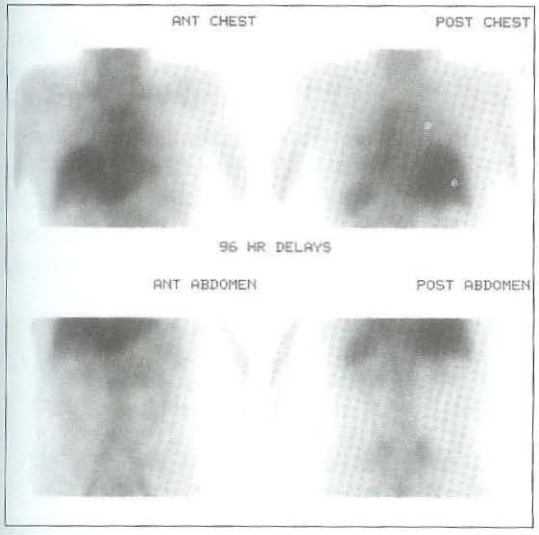

FIGURE 21-9 Normal scan in a 79 year old man with prostate cancer, obtained 96 hours after injection of 5 mCi (185 MBq) of ^{111}In-capromab pendetide. Increased activity is seen in the region of the prostate gland, consistent with the patient's known prostate cancer, but there is no evidence of metastasis in the central abdominal region.

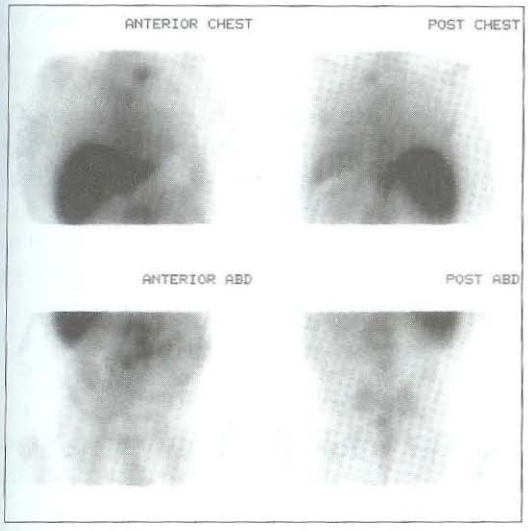

FIGURE 21-10 Prostate metastases in a 68 year old man with prostate cancer and elevated prostate-specific antigen level. Images obtained 30 minutes after injection of 4.7 mCi (174 MBq) of ^{111}In-capromab pendetide demonstrate evidence of metastatic lesions, seen as a focus of increased tracer accumulation in the left side of the neck and multiple foci of tracer accumulation in the central abdominal region.

antigen (NCA-90), on the surface of granulocytes.[37] LeukoScan cross-reacts with CEA and may interact with CEA-producing tumors.

^{99m}Tc-sulesomab is prepared from a kit containing 0.31 mg of the antibody sulesomab, 0.22 mg stannous chloride, and other adjuvants, at pH 5 to 7. The kit is stored at 2°C to 8°C prior to labeling. The lyophilized powder is reconstituted with 0.5 mL of sterile saline, followed by the addition of 30 to 40 mCi (1110 to 1480 MBq) ^{99m}Tc-sodium pertechnetate in a volume of 1.0 mL. The product is ready for use after a 5 minute incubation. The labeled antibody should be stored at room temperature and used within 4 hours after preparation. Its radiochemical purity must be 90% or higher, as determined by ITLC-SG in acetone. The labeled antibody remains at the origin and the free pertechnetate travels to the solvent front.

^{99m}Tc-sulesomab is indicated for the diagnostic localization of infection and inflammation in bone in patients with suspected osteomyelitis, including patients with diabetic foot ulcers. A typical administered dose is 20 to 30 mCi (740 to 1110 MBq) containing 0.25 mg

of antibody. Imaging is performed 1 to 8 hours after injection as desired; there is no difference in detection of the presence or absence of osteomyelitis between 1 to 2 hour and 5 to 8 hour imaging times. Several studies have shown the value of ^{99m}Tc-sulesomab for diagnosing infection, compared with ^{111}In-oxine-labeled autologous leukocytes. Becker et al.[38] reported the sensitivity, specificity, and accuracy, respectively, of ^{99m}Tc-sulesomab as 90%, 84.6%, and 87.9% compared with 83.9%, 76.5%, and 81.3% for autologous leukocytes, whereas Hakki et al.[39] reported 93%, 89%, and 90% for ^{99m}Tc-sulesomab and 85%, 75%, and 79% for autologous leukocytes. Thus, ^{99m}Tc-sulesomab appears to be a better agent than ^{111}In-oxine leukocytes, requires less preparation time, and does not raise the safety concerns of labeling autologous leukocytes.

There have been no reports of positive HAMA response with a single dose of ^{99m}Tc-sulesomab. The critical organ is the kidney, with a radiation absorbed dose of 4.15 rad/25 mCi (925 MBq). The effective dose equivalent is 0.95 rem.

Technetium Tc 99m LeuTech

^{99m}Tc-LeuTech (Palatin) is a ^{99m}Tc-labeled IgM murine monoclonal antibody (anti–stage-specific embryonic antigen-1 [SSEA-1]) that has a specificity for the glycoprotein lacto-N-fucopentaeose-III (CD15) expressed on human neutrophils, eosinophils, and lymphocytes.[40] ^{99m}Tc-LeuTech binds avidly to circulating polymorphonuclear leukocytes and has been reported to localize rapidly in infectious processes after injection. It has been evaluated in humans for detection of appendicitis. The antibody is labeled by addition of ^{99m}Tc-sodium pertechnetate, followed by incubation for 15 minutes at room temperature or 30 minutes at 37°C, and stabilized with ascorbic acid. After administration of ^{99m}Tc-LeuTech to patients with suspected acute appendicitis, imaging was reported to be positive in all 26 patients who had appendicitis (100% accuracy) and negative in 19 of 23 patients without appendicitis (83% specificity).[41] This product, similar to ^{99m}Tc-sulesomab, if approved for routine use, will provide a simple, safe method for labeling leukocytes in vivo for the diagnosis of infection.

Therapeutic Antibodies

Several antibodies have been developed for therapy, particularly for the treatment of non-Hodgkin's lymphoma. The properties of these antibodies and the results of clinical studies with them are discussed in Chapter 23.

REFERENCES

1. Wikstrand CJ, Hale LP, Batra SK, et al. Monoclonal antibodies against EGFRvIII are tumor specific and react with breast and lung carcinomas and malignant gliomas. *Cancer Res.* 1995;55:3140-8.
2. McCullough KC, Spier RE. *Monoclonal Antibodies in Biotechnology: Theoretical and Practical Aspects.* London: Cambridge University Press; 1990.
3. Steward MW. *Antibodies: Their Structure and Function.* New York: Chapman and Hall; 1984.
4. vanOss CJ, vanRegenmortal MHV, eds. *Immunochemistry.* New York: Marcel Dekker; 1994:12, 31.
5. Lyster DM, Alcorn LN. Antibody imaging and therapy in human cancer. In: Fritzberg AR, ed. *Radiopharmaceuticals: Progress and Clinical Perspectives.* Vol 1. Boca Raton, FL: CRC Press; 1986:41-59.
6. Kohler G, Milstein C. Continuous culture of fused cells secreting antibody of predefined specificity. *Nature.* 1975;256:495-7.
7. Milstein C. Monoclonal antibodies. *Sci Am.* 1980;243:66-74.
8. Keenan AM, Harbert JC, Larson SM. Monoclonal antibodies in nuclear medicine. *J Nucl Med.* 1985;26:531-7.
9. Mayforth RD, Quintans J. Designer and catalytic antibodies. *N Engl J Med.* 1990;323:173-8.

10. Juweid ME. Radioimmunotherapy of B-cell non-Hodgkin's lymphoma: from clinical trial to clinical practice. *J Nucl Med.* 2002;43:1507-29.
11. Janeway CA Jr, Travers P. *Immunobiology.* 3rd ed. New York: Garland Publishing; 1997:2:19-2:21.
12. Augustine SC, Norenberg JP. The treatment of low grade B-cell non-Hodgkin's lymphomas with radiopharmaceuticals. Correspondence Continuing Education Program, University of New Mexico, May 2002.
13. USAN Council. List no. 351, monoclonal antibodies. *Clin Pharmacol Ther.* 1993;54:114-6.
14. Wilbur DS. Radiohalogenation of proteins: an overview of radionuclides, labeling methods, and reagents for conjugate labeling. *Bioconjug Chem.* 1992;3:433-70.
15. Fritzberg AR, Meares CF. Metallic radionuclides for radioimmunotherapy. In: Abrams PG, Fritzberg AR, eds. *Radioimmunotherapy of Cancer.* New York: Marcel Dekker; 2000:57-79.
16. Zalutsky MR. Radiohalogens for radioimmunotherapy. In: Abrams PG, Fritzberg AR, eds. *Radioimmunotherapy of Cancer.* New York: Marcel Dekker; 2000:81-106.
17. Griffiths GL. Radiochemistry of therapeutic radionuclides. In: Goldenberg DM, ed. *Cancer Therapy with Radiolabeled Antibodies.* Boca Raton, FL: CRC Press; 1995:47-61.
18. Gansow OA, Wu C. Advanced methods for radiolabeling monoclonal antibodies with therapeutic radionuclides. In: Goldenberg DM, ed. *Cancer Therapy with Radiolabeled Antibodies.* Boca Raton, FL: CRC Press; 1995:63-76.
19. Wilbur DS, Hadley SW, Grant LM, et al. Radioiodinated iodobenzyl conjugates of a monoclonal antibody Fab fragment: in vivo comparisons with chloramine-T labeled Fab. *Bioconjug Chem.* 1991;2:111-6.
20. Vaidyanathan G, Zalutsky MR. Protein radiohalogenation: observations on the design of N-succimidyl ester acylation agents. *Bioconjug Chem.* 1990;1:269-73.
21. Zalutsky MR, Noska MA, Colapinto EV, et al. Enhanced tumor localization and in vivo stability of a monoclonal antibody radioiodinated using N-succinimidyl 3-(tri-n-butylstannyl) benzoate. *Cancer Res.* 1989;49:5543-9.
22. Schuster JM, Garg PK, Bigner DD, et al. Improved therapeutic efficacy of a monoclonal antibody radioiodinated using N-succinimidyl 3-(tri-n-butylstannyl) benzoate. *Cancer Res.* 1991;51:4164-9.
23. Eckelman WC, Paik CH, Steigman J. Three approaches to radiolabeling antibodies with ^{99m}Tc. *Nucl Med Biol.* 1989;16:171-6.
24. Westerberg DA, Carney PL, Rogers PE, et al. Synthesis of novel bifunctional chelators and their use in preparing monoclonal antibody conjugates for tumor targeting. *J Med Chem.* 1989;32:236-43.
25. Meares CF, McCall MJ, Reardan DT, et al. Conjugation of antibodies with bifunctional chelating agents: isothiocyanate and bromoacetamide reagents, methods of analysis, and subsequent addition of metal ions. *Anal Biochem.* 1984;142:68-78.
26. Meares CF. Chelating agents for the binding of metal ions to antibodies. *Nucl Med Biol.* 1986;13:311-8.
27. Brechbiel MW, Gansow OA, Atcher RW, et al. Synthesis of 1-(p-isothiocyanatobenzyl) derivatives of DTPA and EDTA: antibody labeling and tumor imaging studies. *Inorg Chem.* 1986;25:2272-7.
28. Cummins CH, Rutter EW Jr, Fordyce WA. A convenient synthesis of bifunctional chelating agents based on diethylenetriaminepentaacetic acid and their coordination chemistry with yttrium (III). *Bioconjug Chem.* 1991;2:180-6.
29. Chinn PC, Leonard JE, Rosenberg J, et al. Preclinical evaluation of ^{90}Y-labeled anti-CD 20 monoclonal antibody for treatment of non-Hodgkin's lymphoma. *Int J Oncol.* 1999;15:1017-25.
30. Hnatowich DJ, Mardirossian G, Rusckowski M, et al. Directly and indirectly technetium-99m-labeled antibodies: a comparison of in vitro and animal in vivo properties. *J Nucl Med.* 1993;34:109-19.
31. Eckelman WC, Paik CH, Steigman J. Three approaches to radiolabeling antibodies with ^{99m}Tc. *Nucl Med Biol.* 1989;16:171-6.
32. Fritzberg AR, Abrahams PG, Beaumier PL, et al. Specific and stable labeling of antibodies with technetium-99m with a diamide dithiolate chelating agent. *Proc Natl Acad Sci USA.* 1989;85:4025-9.
33. Washburn L, Sun T, Lee Y-CC, et al. Comparison of five bifunctional chelate techniques for ^{90}Y-labeled monoclonal antibody CO17-1A. *Nucl Med Biol.* 1991;18:313-21.
34. Harrison A, Walker C, Parker D, et al. The in vivo release of ^{90}Y from cyclic and acyclic ligand-antibody conjugates. *Nucl Med Biol.* 1991;18:469-76.
35. Maecke HR, Riesen A, Ritter W. The molecular structure of indium-DTPA. *J Nucl Med.* 1989;30:1235-9.
36. Rodwell JD, Alvarez VL, Lee C, et al. Site-specific covalent modification of monoclonal antibodies: In vitro and in vivo evaluations. *Proc Natl Acad Sci USA.* 1986;83:2632-6.
37. Hansen HJ, Goldenberg DM, Newman ES, et al. Characterization of second-generation monoclonal antibodies against carcinoembryonic antigen. *Cancer.* 1993;71:3478-85.
38. Becker W, Palestro CJ, Winship J, et al. Rapid imaging of infections with a monoclonal antibody fragment (LeukoScan). *Clin Orthoped.* 1996;329:263-72.
39. Hakki S, Harwood SJ, Morrissey MA, et al. Comparative study of monoclonal antibody scan in diagnosing orthopaedic infection. *Clin Orthoped.* 1997;335:275-85.

40. Thakur ML, Marcus CS, Henneman P, et al. Imaging inflammatory diseases with neutrophil-specific technetium-99m-labeled monoclonal antibody anti-SSEA-1. *J Nucl Med.* 1996;37:1789-95.
41. Kipper SL, Rypins EB, Evans DG, et al. Neutrophil-specific ^{99m}Tc-labeled anti-CD15 monoclonal antibody imaging for diagnosis of equivocal appendicitis. *J Nucl Med.* 2000;41:449-55.

22 In Vivo Function Studies

In vivo function studies use radiotracers to measure physiologic processes in the body. The term *tracer* is particularly applicable to these studies. Simply defined, a tracer is a species that follows or outlines something else, the "tracee."[1] In nuclear medicine, a patient's bodily functions are assessed by measuring the absorption, dilution, concentration, or excretion of a radioactive tracer. An effective radiotracer is processed by the body system of interest in the same way as its tracee. In general, this means the tracer should be chemically identical to the tracee or should function as the tracee in the system and not interfere with the process being studied.

Tracers commonly used in biomedical studies can divided into three groups: (1) contrast material (dyes), (2) nonradioactive (stable) isotopes, and (3) radioactive isotopes. This chapter discusses radioisotopic tracers routinely used in nuclear medicine studies.

BLOOD VOLUME MEASUREMENT

Blood consists of a fluid fraction (plasma) and the cellular elements: red cells (erythrocytes, or RBCs), white cells (leukocytes, or WBCs), and platelets (thrombocytes). Each microliter (mm^3) of adult human blood contains an average of 5×10^6 RBCs, 7×10^3 WBCs, and 3×10^5 platelets. Most of the cellular volume is therefore composed of RBCs. When anticoagulated whole blood is centrifuged, it is separated into a volume of packed cells and supernatant plasma. The volume of RBCs, expressed as a percentage of the whole blood sample, is the hematocrit. It averages 45% in adult males and 42% percent in females.

Theoretically, whole blood volume can be determined from either the hematocrit or the plasmacrit (percentage of the blood volume occupied by plasma) and a measurement of the RBC volume or plasma volume, as follows:

$$\text{Whole blood volume} = \frac{\text{Red cell volume}}{\text{Hematocrit}} \text{ or } \frac{\text{Plasma volume}}{\text{Plasmacrit}} \qquad (22\text{-}1)$$

Some error is associated with such a measurement, however, because of small differences between the large-vessel hematocrit (LVH) and the mean whole-body hematocrit (WBH). The WBH, which is the average distribution of RBCs in blood throughout the body, is calculated from independent measurements of the RBC volume and the plasma volume as follows:[2]

$$\text{Mean whole-body hematocrit} = \frac{\text{Red cell volume}}{\text{Red cell volume} + \text{Plasma volume}} \qquad (22\text{-}2)$$

The mean WBH is generally lower than the LVH. The mean WBH-to-LVH ratio is 0.915, ranging from 0.89 to 0.94.[2]

The LVH is determined by obtaining a sample of blood from an arm vein and centrifuging it in a capillary tube 75 mm long and 1.2 to 1.4 mm in diameter. A standard microhematocrit centrifuge spins the tube at 13,000 rpm for 4 to 5 minutes. The LVH is the ratio of the height of the packed RBCs to the height of the RBCs plus plasma. The

LVH is somewhat exaggerated because of the amount of plasma trapped between the cells. The amount of trapped plasma varies with centrifugal force, spinning time, viscosity of the blood, and volume of RBCs present.[2] In general, a standard microhematocrit reading should be multiplied by 0.96 to correct for trapped plasma.[2] Thus, if the height of the RBC fraction in a microhematocrit tube is 24 mm and the height of the RBC and plasma fractions is 60 mm, the hematocrit is 40%. Correcting the microhematocrit for trapped plasma and LVH yields an approximate WBH, as follows:

$$0.40(\text{Hct\%}) \times 0.96 = 38.4\%(\text{LVH}) \times 0.915 = 34.94\%(\text{WBH})$$

A more accurate measurement of blood volume is made by measuring RBC volume and plasma volume independently and then adding them together to arrive at the whole blood volume.

Isotope Dilution Analysis

Measurements of blood volume and plasma volume are based on the principle of isotope dilution analysis. Following this principle, a radioactive tracer of known volume (V_1) and concentration (C_1) is added to an unknown volume (V_2). The tracer is allowed to equilibrate with the system and a sample is then removed for analysis to determine the new tracer concentration (C_2) (Figure 22-1). The unknown volume is calculated from the following relationship:

$$V_2 = \frac{C_1 \cdot V_1}{C_2} \tag{22-3}$$

An accurate determination of blood volume is predicated on the requirements that (1) the tracer does not degrade in or significantly leak from the compartment during the time of measurement and (2) the volume of tracer does not significantly change the volume of the compartment being measured. For routine nuclear medicine procedures, the second requirement is not a problem; however, the first requirement may be a concern in some circumstances, and corrections must be applied if necessary.

RBC Volume

RBC volume is routinely measured by labeling a sample of autologous RBCs with ^{51}Cr. An accurate volume of ^{51}Cr-labeled RBCs of known concentration (cpm/mL) is injected intravenously into an arm vein and allowed to reach equilibrium in the circulation, typically in 15 to 30 minutes. At this time a sample of blood is removed from the opposite arm. Samples are counted in a scintillation well counter, corrected for background count, and expressed as net counts per minute per milliliter. From Equation 22-3, the RBC volume is calculated as follows:

$$\text{Red cell volume}\,(\text{mL}) = \frac{\text{Injected } ^{51}\text{Cr-RBC cpm}}{\text{Removed } ^{51}\text{Cr-RBC cpm/mL}}$$

Even though the ^{51}Cr activity elutes from RBCs (approximately 1% per day), this small amount will not affect the results of the study, which is completed in 1 to 2 hours.

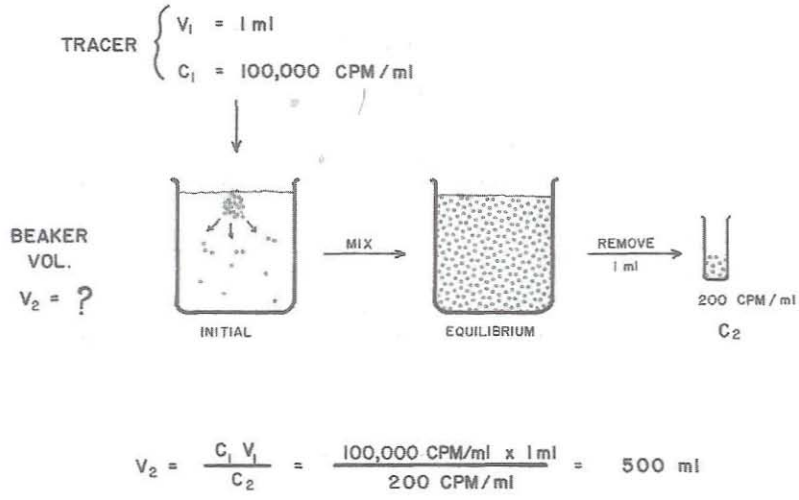

FIGURE 22-1 Determination of the unknown volume of a compartment (beaker) using the principle of isotope dilution analysis.

The following example illustrates a routine procedure for labeling RBCs with ^{51}Cr. Forty milliliters of whole blood from a patient's arm vein is drawn into a syringe containing 8 mL of acid citrate dextrose (ACD) anticoagulant solution. From this mixture, 14 mL is used to prepare background RBC and plasma samples. The remaining 34 mL is added to a sterile vented serum vial, followed by 150 μCi (5.55 MBq) of ^{51}Cr-sodium chromate. This mixture is allowed to incubate for 20 to 30 minutes, with gentle mixing every 5 minutes. During the labeling reaction, the chromate anion ($^{51}CrO_4^{2-}$) diffuses into the RBCs and is reduced intracellularly to chromic ion ($^{51}Cr^{3+}$), which becomes bound to hemoglobin.[3–5] The maximum amount of chromium that labels RBCs is less than 0.5 μg/mL of RBCs and is nontoxic to the cells. Labeling efficiency is 85% to 90%. At the end of incubation, the blood can be centrifuged to separate the labeled cells from the unlabeled plasma activity or, alternatively, ascorbic acid (100 mg) can be added to the blood–chromate mixture and incubated for 5 minutes. The latter method is preferred by some investigators because it spares the cells from centrifuge and manipulation trauma. The ascorbic acid reduces the unlabeled chromate ion to chromic ion, preventing the in vivo labeling of RBCs when the labeled blood mixture is reinjected into the patient. When the ascorbic acid technique is used, however, plasma activity must be subtracted from whole blood measurements in the final analysis because chromic ion labels plasma protein. The labeling method is shown in Figure 22-2.

At completion of the labeling procedure, 1 mL of tagged blood is diluted to 100 mL with water. This 1:100 dilution is the ^{51}Cr-RBC standard, which is used to determine the total activity injected into the patient. After this, 20 mL of labeled blood containing about 80 μCi (2.96 MBq) of ^{51}Cr activity is injected intravenously into the patient. After a 30 minute equilibration time, a 15 mL sample of blood is removed from the opposite arm into a heparinized syringe. This represents the equilibrium concentration of the injected dose uniformly distributed in the unknown volume of blood. Two milliliters of the following samples is counted in a scintillation counter: standard whole blood (1:100 dilution), standard plasma (1:25 dilution), 30 minute whole blood, 30 minute plasma, whole blood background, and plasma background. Counts are adjusted for background, and dilution factors are applied where required. Corrections are made for large vein-to-whole body

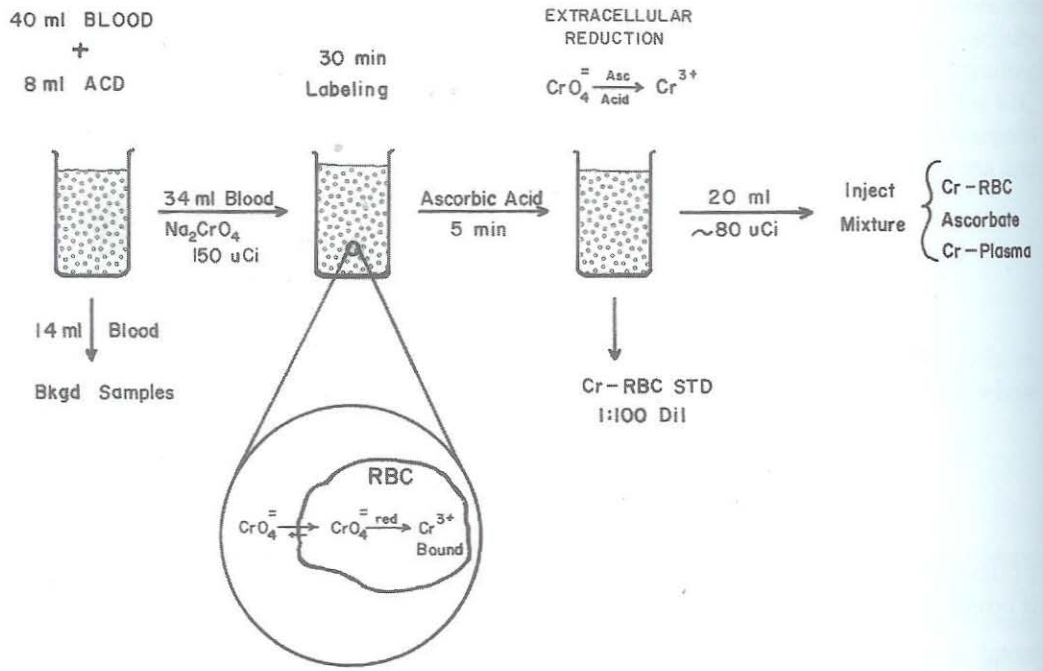

FIGURE 22-2 Method of labeling red blood cells with ^{51}Cr-sodium chromate for determining RBC volume by isotope dilution analysis.

hematocrit and for trapped plasma (see Table 22-1). The RBC volume is then calculated. Blood volume measurement is explained in detail in standard textbooks.[2,6,7]

Plasma Volume

Plasma volume is measured with ^{125}I-human serum albumin (^{125}I-HSA). Typically, 5 to 10 μCi (185 to 370 kBq) of ^{125}I-HSA is injected intravenously and allowed to reach equilibrium in the body (in about 15 minutes). A blood sample is then removed from the opposite arm and the plasma activity is determined by sample counting in a scintillation counter. The plasma volume is then calculated from the total activity injected and the concentration of activity per milliliter of plasma at the time of injection (C_0), using Equation 22-3:

$$\text{Plasma volume (mL)} = \frac{\text{Injected cpm } ^{125}\text{I-HSA}}{C_0 \text{ sample cpm/mL}}$$

Because ^{125}I-HSA slowly leaks out of the plasma compartment, plasma samples analyzed at different times after injection yield increasingly larger plasma volumes; in other words, the volume of ^{125}I-HSA distribution increases over time because the concentration in plasma is decreasing. Therefore, the initial equilibrium concentration (C_0) must be determined from the following equations, which are derived from a graphical plot of the natural logarithm of plasma activity versus time (Figure 22-3):

$$\ln C_0 = \frac{\ln C_2 t_1 - \ln C_1 t_2}{t_1 - t_2}$$

$$\text{and } C_0 = e^{\ln C_0}$$

TABLE 22-1 ^{51}Cr Red Blood Cell Volume Analysis Worksheet

Patient name: NS	Unit no:	Date:
Height: 59 in × 2.54 cm/in = 149.86 cm	Weight: 139 lb ÷ 2.2 lb/kg = 63.18 kg	
Sex: Female	Age: 75	Dose ^{51}Cr-sodium chromate injected: 80 μCi
Sample volumes:	Whole blood (WB) adm: 20 mL	Counting vol: 2 mL
Counting time: 1 min	Dilutions: Whole blood 1:100	Plasma 1:25
Hematocrits	Standard whole blood (std Hct) 0.41	30-min patient vein (30 min Hct_v) 0.50

	(A) Gross Sample Cts (2 mL volume)	(B) Net Sample Cts (A – Relevant Bkg)	(C) Dilution Factor	(D) Net Corrected Cts (B × C)	
Std WB	6716	6684	100	668,400	(WBs)
Std plasma	2657	2625	25	65,625	(Pls)
30-min Pt WB	4143	4111	–	–	(WBp)
30-min Pt plasma	156	127	–	–	(Plp)
WB bkg	32	–	–	–	–
Plasma bkg	29	–	–	–	–

Corrected std Hct[a] (Hct_s) = Std Hct 0.41 × 0.88 = 0.36

Corrected std plasmacrit (Pct_s) = (1.0 – Hct_s) = 0.64

Corrected 30-min Pt Hct (Hct30) = 30-min Hct_v 0.50 × 0.88 = 0.44

Corrected 30-min Pt plasmacrit (Pct30) = (1.0 – Hct30) = 0.56

Red blood cell volume calculation

$$\text{Formula: } \frac{\left[WB_s - \left(Pl_s \times Pct_s\right)\right] \times \left(\text{mL WB Adm}\right) \times \left(Hct30\right)}{WB_p - \left(Pl_p \times Pct30\right)}$$

$$\frac{\left[668{,}400 - \left(65{,}625 \times 0.64\right)\right] \times 20 \text{ mL} \times 0.44}{4{,}111 - \left(127 \times 0.56\right)} = 1364 \text{ mL RBC volume}$$

Parameter	Predicted Formula[b]	Predicted Value	Measured
WB vol (mL)	Females: 24.8 H $(cm)^{0.725}$ W $(kg)^{0.425}$ – 1954 Males: 23.6 H $(cm)^{0.725}$ W $(kg)^{0.425}$ – 1229	3504	2665
RBC vol (mL)	Predicted WB vol × 0.4	1402	1364
RBC mass (mL/kg)	–	21.0	21.6
Plasma vol (mL)	Predicted WB vol × 0.6	2103	1301
Plasma mass (mL/kg)	–	31.5	20.6

[a] The hematocrit correction factor (0.88) is derived from the product of the correction for whole-body hematocrit (0.92) and trapped plasma (0.96). Source: Early PJ, Sodee DB. *Principles & Practice of Nuclear Medicine*. Baltimore: Mosby; 1984:832.

[b] Source: Reference 8.

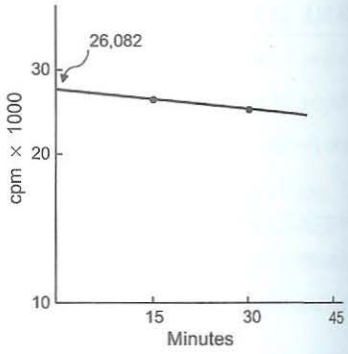

FIGURE 22-3 Graphical method of determining the zero-time plasma concentration of ^{125}I-human serum albumin in the measurement of plasma volume by isotope dilution analysis. Extrapolation of the line drawn through the 15 and 30 minute time points intersects the y-axis at the C_0 plasma activity (26,082 cpm).

where C_1 is the plasma cpm of the first sample time point (15 minutes) and C_2 is the plasma cpm at the second sample time point (30 minutes).

The following example illustrates the procedure for measuring plasma volume. An intravenous line is established and an infusion set attached, and a 5 mL sample of blood is obtained for background baseline measurement. Then 5 to 10 μCi (185 to 370 kBq) of ^{125}I-HSA is injected intravenously into the opposite arm and the exact time is recorded. From the initial arm, 5 mL samples of blood are removed into heparinized syringes at 15 and 30 minutes after the time of injection. These samples and the background sample are centrifuged and the net activity (cpm/mL) in the plasma samples is determined in a scintillation counter. These timed sample activity concentrations are plotted on semilog graph paper, and the resulting straight line is extrapolated to zero time to obtain the plasma concentration (C_0) of the injected dose at the time of injection (Figure 22-3).

Alternatively, the C_0 plasma concentration can be calculated from Equation 22-4. Its derivation is shown in Figure 22-4.

$$C_0 = \frac{(C_1)^2}{C_2} \tag{22-4}$$

This equation is valid only if the second plasma sample is taken at a time that is exactly twice the sampling time of the first plasma sample (e.g., t_1 of 10 minutes and t_2 of 20 minutes, or t_1 of 15 minutes and t_2 of 30 minutes). This facilitates the determination of C_0.

The total activity of ^{125}I-HSA in the injected dose is determined by counting a standard dilution (1:4000) of the injected dose prepared from the same lot of ^{125}I-HSA. The values and calculations for a typical patient study are shown in Table 22-2.

Combined RBC–Plasma Volume Measurement

For convenience, ^{51}Cr-RBC volume and ^{125}I-HSA plasma volume studies are typically performed together. Using this approach, ^{125}I-HSA is injected first, and samples of blood for plasma volume measurement are obtained while the RBCs are being labeled with ^{51}Cr-sodium chromate. After the 15 minute and 30 minute samples are obtained for the plasma volume study, the tagged ^{51}Cr-RBCs are injected. A sample of blood is obtained 30 minutes later for the RBC volume determination. Although the blood sample for the RBC measurement will contain both ^{125}I and ^{51}Cr, the ^{125}I counts (photon E = 27 to 35 keV) are easily discriminated from the ^{51}Cr counting window (photon E = 320 keV) of the scintillation spectrometer. An example of a combined study in the same patient is shown in Tables 22-1 and 22-2.

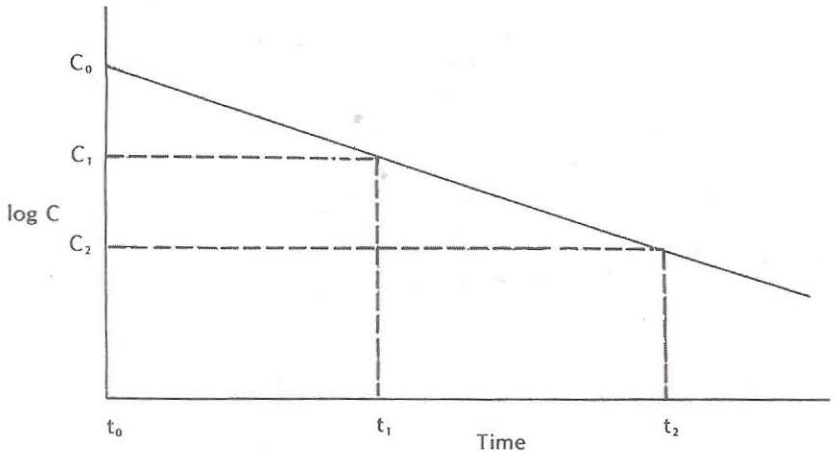

$$C_0 = C_2 + 2(C_1 - C_2)$$

or

$$C_0 = 2\,C_1 - C_2$$

$$\log C_0 = 2 \log C_1 - \log C_2$$

or

$$C_0 = \frac{(C_1)^2}{C_2}$$

FIGURE 22-4 Derivation of the simplified equation for determining C_0 in plasma volume analysis. Assumptions: first-order exponential rate of loss of ^{125}I-HSA from plasma compartment, and t_2 equals $2 \times t_1$.

TABLE 22-2 ^{125}I-HSA Plasma Volume Analysis Worksheet

Patient name: NS Unit no:	Date: 6-3-02
Height: 59 in × 2.54 cm/in = 149.86 cm	Weight: 139 lb ÷ 2.2 lb/kg = 66.18 kg
Sex: F	Age: 75
Dose (μCi ^{125}I-HSA): 7.0	
Std dilution factor (DF): 1:4000	
Counting time: 2 min	Counting vol: 2 mL
15-min plasma gross counts: 25,285	Net counts (gross cts – bkg 1): 25,250
30-min plasma gross counts: 24,480	Net counts (gross cts – bkg 1): 24,445
Plasma background counts (bkg 1): 35	
Room background counts (bkg 2): 35	
Standard counts gross: 8520	Net counts (gross cts – bkg 2): 8485

Formulas: C_0 counts $= \dfrac{(\text{Net } C_{15})^2}{\text{Net } C_{30}} = \dfrac{(25{,}250)^2}{24{,}445} = 26{,}082$

$$\text{Plasma vol} = \frac{\text{Net Std Cts} \times \text{DF}}{C_0 \text{ counts}} = \frac{(8485) \times (4000)}{26{,}082} = 1301 \text{ mL}$$

Predicted normal values for whole blood volume are either determined from standard tables or calculated by a formula based on body surface area.[8] The predicted normal RBC volume or mass and plasma volume or mass are then calculated (see Table 22-1). The normal average values (mL/kg) for total blood volume (mass), RBC mass, and plasma mass for males and females are as follows:[9]

	Females	*Males*
Total blood mass	66	72
RBC mass	24	28
Plasma mass	42	44

RBC SURVIVAL

The ability to measure the survival of RBCs in the circulation is helpful for several reasons: (1) It provides information about the compatibility and suitability of donor blood used in transfusions, (2) it is helpful in validating whole blood collection and storage methods, and (3) in patients with hemolytic anemia, RBC survival studies may provide insight into the rate and mechanism of hemolysis.

A shortened half-life of disappearance of labeled RBCs from the circulation supports the diagnosis of intravascular hemolysis or hypersplenism. Because the spleen is the normal site for destruction of senescent RBCs, a splenic sequestration study may also yield useful information. The normal spleen-to-liver ratio of activity from ^{51}Cr-labeled RBCs is 1 to 1. In cases of hypersplenism, it is greater than 2 to 1. Increased liver activity is indicative of intravascular hemolysis, because hemoglobin is metabolically processed by the liver.

The application of radiotracer techniques has proven to be an important advance in determining RBC survival. With this method, the patient's own blood, as well as donor blood, can be labeled with a radionuclide (e.g., ^{51}Cr or ^{99m}Tc), and survival of the cells in the circulation can be monitored by radioactive counting of blood samples obtained periodically over time.

Cohort and Random Labeling of RBCs

Radionuclide methods of labeling RBCs can be divided into two groups: cohort labeling and random labeling.[10] In cohort labeling, the radiotracer is incorporated into cells as they are newly formed, and the survival of this group or cohort of cells of similar age is studied by monitoring their passage into and removal from the circulation. Although cohort labeling is the ideal method for studying RBC survival, it requires that labeling be accomplished within a short window of time, that the label remain within the cell throughout its life span, and that the label not be reused after destruction of the cell. Because no radiolabel meets all of these requirements, cohort labeling is not routinely used.

In random labeling, cells are labeled in such a way that the age distribution of the labeled sample reflects the age distribution of the parent population. Survival is studied by monitoring the disappearance of the labeled sample from the circulation. ^{51}Cr-sodium chromate is routinely used for random labeling of RBCs. The advantages of this agent are that the labeling is simple and convenient, the label is not reused, and external gamma counting can be performed with in vitro samples and, if necessary, in vivo detection to localize areas of RBC sequestration in the body. The latter is important for assessing the relative roles of different sites of RBC destruction in known cases of hemolytic anemia. One disadvantage of ^{51}Cr-sodium chromate is that the ^{51}Cr label elutes from the cells in

vivo at an exponential rate of about 1% per day.[11] This elution requires a correction to obtain clinically satisfactory approximations of the mean RBC life span.

RBC Survival Method

The RBC survival method is useful for measuring the life span of RBCs in patients with known or suspected hemolytic anemia and for validating new procedures for collecting and storing whole blood. Survival is determined by monitoring the disappearance of ^{51}Cr-labeled RBCs from the circulation. The half-life of ^{51}Cr-labeled RBCs in normal subjects measured by this method is about 30 days.[6] This value is about twice the normal rate of removal by RBC destruction alone of 1% per day for senescent cells. The increased rate with ^{51}Cr-RBCs is due to an additional 1% loss per day from elution of the ^{51}Cr label. Consequently, ^{51}Cr-RBC survival data bear no simple relationship to the mean cell life span, which is the parameter required in clinical practice. If, however, as recommended by the International Committee for Standardization in Hematology, the ^{51}Cr-RBC survival data are corrected for ^{51}Cr elution, and the patient is in a steady state of RBC production and destruction during the course of study, then the corrected half-life value is a measure of RBC destruction only. Furthermore, multiplying this corrected half-life value by 1.443 gives the mean life of RBC survival.

A summary of the procedure follows; greater detail can be found elsewhere. Autologous RBCs are labeled with ^{51}Cr as described previously for RBC volume determination. This method conforms to the recommended methods established for labeling RBCs with ^{51}Cr. Labeled blood is then injected into the patient. On day 1 after injection, a sample of blood is withdrawn and the net count rate in the RBCs is determined. This procedure is repeated three times per week for 2 weeks. The percentage of the day 1 sample RBC activity that is present in each subsequent sample is determined as follows:

$$\%\ \text{Survival of labeled red cells} = \frac{\text{Net cpm of sampled red cells} \times 100}{\text{Net cpm of red cells on day 1}}$$

These data are then corrected for ^{51}Cr decay and elution and plotted on semilog graph paper. The mean RBC life span is calculated as the reciprocal of the slope of the plotted line, or 1.443 times the half-life of disappearance over time (Figure 22-5). The normal mean RBC life span determined by this method is 115 days.

TESTS FOR VITAMIN B_{12} DEFICIENCY

Vitamin B_{12} (cyanocobalamin) is an essential nutrient for all cells of the body because it is required for the synthesis of DNA.[12] Lack of this vitamin causes failure of nuclear maturation and cell division. Because tissues that produce RBCs are among the most rapidly proliferating in the body, a lack of vitamin B_{12} particularly inhibits the rate of RBC production. This is manifested, in part, by adult erythrocytes that have flimsy membranes and are large, oval, and irregularly shaped instead of having the usual biconcave disk shape. Such cells have a normal amount of hemoglobin and are quite capable of carrying oxygen, but their fragility causes them to have a short life span, measured in weeks rather than months. Vitamin B_{12} deficiency thus causes maturation failure in the process of erythropoiesis.

The most common cause of maturation failure is not lack of vitamin B_{12} in the diet but failure to absorb it from the gastrointestinal tract. This often occurs in pernicious anemia,

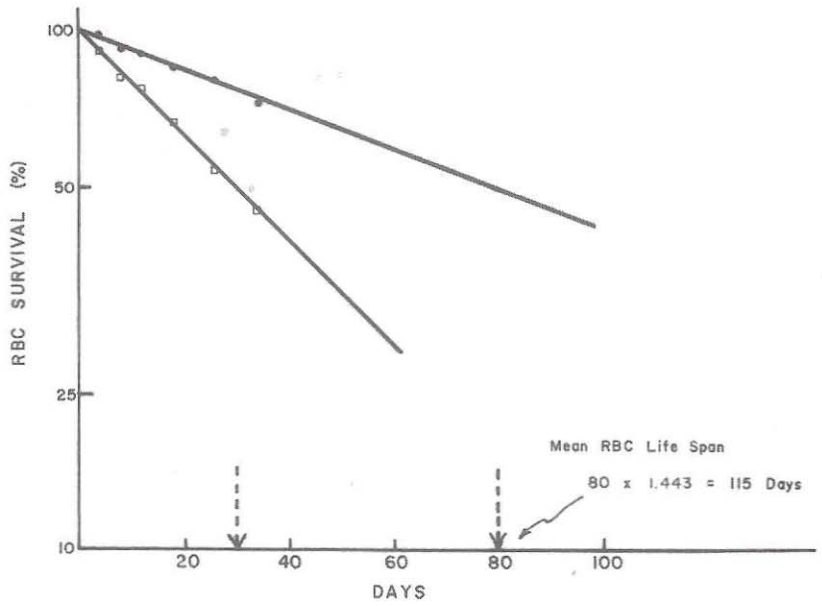

FIGURE 22-5 Determination of mean RBC life span from the in vivo survival of ^{51}Cr-labeled RBCs. □ = survival related to RBC destruction and ^{51}Cr elution; • = survival related to RBC destruction only, corrected for ^{51}Cr elution.

in which the basic disorder is a failure of the gastric mucosa to secrete intrinsic factor, a substance necessary for vitamin B_{12} absorption. Intrinsic factor is a glycoprotein secreted by the parietal cells of the gastric glands. It combines with vitamin B_{12} in food and makes the vitamin available for absorption across the intestinal mucosa. Intrinsic factor binds tightly with vitamin B_{12}, which protects the vitamin from digestion by gastrointestinal enzymes. The vitamin–intrinsic factor complex binds to specific receptors on the brush-border membranes of the ileum's mucosal cells. The complex is then transported into the cells by pinocytosis, and within about 4 hours the vitamin is released into the bloodstream. Once in the blood, vitamin B_{12} is bound to a plasma β-globulin, transcobalamin II, which transports it to the tissues, primarily the liver, where it is stored. The vitamin is slowly released from the liver when needed by the body. The normal amount required for the maturation of RBCs is about 1 μg per day. The normal amount stored in the liver is about 1000 μg. Figure 22-6 illustrates the absorption and distribution of vitamin B_{12}.

Besides the lack of intrinsic factor as a cause for vitamin B_{12} deficiency, any number of intestinal diseases or defects can interfere with the absorption of the vitamin–intrinsic factor complex.[12] Antibodies to intrinsic factor or to the B_{12}–intrinsic factor complex may play a role in impaired uptake by the ileal cells. Bacterial overgrowth or certain intestinal parasites can prevent an adequate supply of vitamin B_{12} from reaching the ileum. Additionally, any damage to ileal mucosal cells by disease or surgical procedures can interfere with absorption. Finally, pure vegetarianism may be a cause, because vitamin B_{12} is found only in animal protein.

Normal individuals have plasma concentrations of vitamin B_{12} between 200 and 900 pg/mL, whereas a deficiency state is usually present when the level falls below 200 pg/mL.[13]

Once a diagnosis of vitamin B_{12} deficiency is made on the basis of low serum B_{12} and clinical signs and symptoms, the question is whether the deficiency is due to a lack of intrinsic factor or to ileal dysfunction. A number of methods, all using radioactive vitamin labeled with ^{57}Co, ^{58}Co, or ^{60}Co, have been used to measure absorption of vitamin B_{12} from

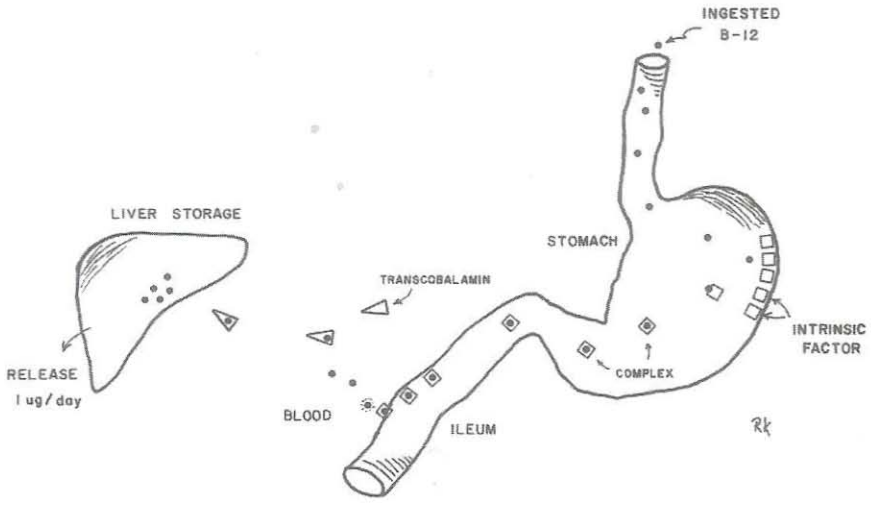

FIGURE 22-6 Pathways of vitamin B_{12} metabolism. See text for explanation.

the gastrointestinal tract; current studies use ^{57}Co. The properties of these isotopes are listed in Table 9-19, Chapter 9. Early methods analyzed either blood samples, to measure the amount of an oral dose of radiolabeled vitamin that was absorbed, or stool samples, to measure the amount that was not absorbed.[14,15] The urinary excretion method, or Schilling test, measures the fraction of the administered dose that is excreted in the urine in 24 hours.[16] Of these three methods, the Schilling test is the procedure of choice.

Schilling Test

The first step of the Schilling test is the administration of an oral dose of radiolabeled *vitamin B_{12} containing about 0.5 μCi (18.5 kBq)* of ^{57}Co and between 0.5 and 1.0 μg of vitamin. The patient must fast for at least 8 hours before the test. The amount of vitamin in the dose must be physiologic, no more than might be present in a normal meal, because quantities above this level may be absorbed by mechanisms not dependent on intrinsic factor.[17] Within 2 hours of the oral dose, 1000 μg of stable vitamin B_{12} is administered intramuscularly. This is known as a "flushing dose" because this amount of vitamin temporarily saturates B_{12} binding sites in the tissues and enables a significant fraction of the absorbed radioactive dose to be excreted in the urine. Vitamin B_{12} is excreted by glomerular filtration. A complete 24 hour urine collection must be made and the volume accurately measured. Equal volumes of urine and a ^{57}Co standard, representing 20% of the administered dose, are counted in a scintillation counter. The fraction of the dose excreted is calculated as follows:

$$\%\ ^{57}\text{Co-B}_{12}\text{ dose excreted} = \frac{\text{Net counts in urine} \times 100}{\text{Net counts in } ^{57}\text{Co std} \times 5}$$

In normal subjects, more than 7% of the dose is excreted in 24 hours. A value less than 7% is indicative of absorption abnormality. The procedure just described is known as the Schilling test I.

If the amount of dose excreted is less than 7%, a Schilling test II is indicated. Within 3 to 5 days of the first test, a repeat test is conducted that includes a 60 mg capsule of

intrinsic factor given along with another dose of ^{57}Co-vitamin B_{12}. Under these test conditions, if the patient has pernicious anemia the 24 hour urine excretion becomes normal. If some other malabsorption problem exists, however, no change from the first test is observed. Below-normal excretion of ^{57}Co-vitamin B_{12} measured by a Schilling test II may indicate that inadequate intestinal absorption is caused by bacterial overgrowth competing for the vitamin–intrinsic factor complex in the intestine. In this situation, a third test is conducted after a 2 week course of broad-spectrum antibiotic to sterilize the bowel. If such bacterial overgrowth is the cause of malabsorption, urinary excretion should then become normal on a third Schilling test.

One disadvantage of the Schilling test is the necessity for complete 24 hour urine collection. Maximal excretion of vitamin B_{12} occurs between 8 and 12 hours after an oral dose, and loss of specimen during this time can produce a falsely low result in a normal subject. Erroneously low results can also occur in subjects with delayed urinary excretion, such as patients with renal failure. It is therefore wise to procure two separate 24 hour urine collections in succession. An initial low 24 hour excretion rate due to renal disease can be readily uncovered by this method, and if there is a gross discrepancy between the urine volumes collected during the first and second day, one can suspect that a significant loss of urine has occurred.

An alternative approach to performing the sequential Schilling tests I and II is the dual-isotope technique.[18] This technique involves simultaneous administration of one capsule containing ^{57}Co-cyanocobalamin bound to intrinsic factor and a second capsule of ^{58}Co-cyanocobalamin alone. The 24 hour urine is counted and the ratio of ^{57}Co to ^{58}Co excreted is measured. This test accomplishes the Schilling tests I and II simultaneously, and it does not rely on a complete 24 hour urine collection because the ratio of isotopes is measured. A commercial kit (Dicopac, Amersham/Searle) was once available for conducting this test, but it has been removed from the market.

REFERENCES

1. Welch TJC, Potchen EJ, Welch MJ. *Fundamentals of the Tracer Method.* Philadelphia: WB Saunders; 1972.
2. Albert SN. *Blood Volume and Extracellular Fluid Volume.* 2nd ed. Springfield IL: Charles C Thomas; 1971.
3. Gray SJ, Sterling K. The tagging of red cells and plasma proteins with radioactive chromium. *J Clin Invest.* 1950;29:1604-13.
4. Person HA. The binding of Cr-51 to hemoglobin. I: In vitro studies. *Blood.* 1963;22:218-30.
5. Ebaugh FG, Samuels AJ, Dobrowlski P, et al. The site of the CrO_4-hemoglobin bond as determined by starch electrophoresis and chromatography [abstract]. *Fed Proc.* 1961;20:70.
6. Albert SN, Sodee DB. In vivo and in vitro studies of hemopoietic production and components. In: Sodee DB, Early PJ, eds. *Mosby's Manual of Nuclear Medicine Procedures.* 3rd ed. St Louis: Mosby; 1981:269.
7. Arnold JE. Blood volume. In: Gottschalk A, Potchen EJ, eds. *Diagnostic Nuclear Medicine.* Baltimore: Williams & Wilkins; 1976:130-8.
8. Hidalgo JU, Nadler SB, Bloch T. The use of the electronic digital computer to determine best fit of blood volume formulas. *J Nucl Med.* 1962;3:94-9.
9. Early PJ, Razzak MA, Sodee DB. *Textbook of Nuclear Medicine Technology.* 3rd ed. St Louis: Mosby; 1979:351.
10. Bentley SA. Red cell survival studies reinterpreted. *Clin Haematol.* 1977;6:601-23.
11. Ebaugh FG Jr, Emerson CP, Ross JF. The use of radioactive chromium-51 as an erythrocyte tagging agent for the determination of red cell survival in vivo. *J Clin Invest.* 1953;32:1260-76.
12. Guyton AC. *Textbook of Medical Physiology.* 6th ed. Philadelphia: WB Saunders; 1981:59.
13. Hillman RS. Vitamin B-12, folic acid, and the treatment of megaloblastic anemias. In: Gilman AG, Goodman LS, Gilman A, eds. *The Pharmacological Basis of Therapeutics.* 6th ed. New York: Macmillan; 1980:1331.
14. Nelp WB, McAfee JG, Wagner HN Jr. Single measurement of plasma radioactive vitamin B-12 as a test for pernicious anemia. *J Lab Clin Med.* 1963;61:158-65.
15. Heinle RW, Welch AD, Scharf V, et al. Studies of excretion (and absorption) of Co-60 labeled vitamin B-12 in pernicious anemia. *Trans Assoc Am Physicans.* 1952;65:214-22.

16. Schilling RF. Intrinsic factor studies. II: The effect of gastric juice on the urinary excretion of radioactivity after the oral administration of radioactive vitamin B-12. *J Lab Clin Med.* 1953;42:860-6.
17. McIntyre PA. The blood and blood-forming organ. In: Wagner HN Jr, ed. *Nuclear Medicine: A Hospital Text.* New York: HP Publishers; 1975:185.
18. Katz JH, Dimase J, Donaldson RM Jr. Simultaneous administration of gastric juice bound and free radioactive cyanocobalamin: rapid procedure for differentiating between intrinsic factor deficiency and other causes of vitamin B-12 malabsorption. *J Lab Clin Med.* 1963;61:266-9.

23 Therapeutic Radiopharmaceuticals

The development of new radioactive agents and treatment methods has led to an increase in therapeutic applications of radiopharmaceuticals over the past 10 years. Therapeutic applications include cancer radioimmunotherapy (RIT), palliation of painful bone metastases, treatment of malignant effusions, radiation synovectomy, treatment of hyperthyroidism and thyroid cancer, and treatment of brain tumors. This chapter discusses these applications, except for thyroid therapy, which was covered in Chapter 14.

RADIOIMMUNOTHERAPY

The introduction of monoclonal antibody technology stimulated the development of immunologic methods of destroying malignant tissue. The rationale for the use of antibody therapy for tumor destruction was based on the natural mechanisms of antibody immune effector functions, namely, lysis of tumor cells by complement-mediated cytotoxicity (CMC) and antibody-dependent cell-mediated cytotoxicity (ADCC) or induction of apoptosis (programmed cell death).

Initial clinical experience using unmodified antibodies to treat cancer was disappointing, but specific problems were identified that led to new approaches to the use of antibodies. Significant problems included difficulties in delivering antibody to tumors and in penetrating into bulky tumors, the inability of murine antibodies to adequately exert cytotoxic effects through human immune effector functions, the development of immunogenic responses to mouse antibody (human antimouse antibody, or HAMA), and the development of antigen-negative tumor cells that render the tumor refractory to further treatment.[1]

Efforts in the field of genetic engineering led to the creation of chimeric and humanized antibodies; this improved therapy significantly, because murine antibodies interacted poorly with complement and human effector cells in vivo. A good example of successful genetic engineering is the development of the chimeric monoclonal antibody rituximab (Rituxan, Genentech), which targets the CD20 antigen on malignant B-lymphocytes. This antibody contains murine variable regions and human constant regions. Studies have demonstrated this antibody's ability to lyse B-cells by CMC and ADCC. Additionally, its chimeric structure significantly reduces its immunogenicity compared with its murine parent.[2] Rituximab has been shown to be effective in the treatment of non-Hodgkin's lymphoma (NHL).[3,4] It produces objective tumor responses in approximately 50% of patients with relapsed or refractory low-grade or follicular NHL. It was the first antibody approved by the Food and Drug Administration (FDA) for treating cancer.

The desire for more effective therapy with antibodies led to the development of radiolabeled monoclonal antibodies. Studies indicated that NHL can be treated effectively by RIT for several reasons, including the inherent radiosensitivity of lymphocytes, the vascular accessibility of these malignancies, and the large number of target antigens on the surface of lymphocytes. For example, the B-cell antigens CD19, CD20, and CD22 are

and the radiation absorbed dose to various organs is calculated by standard pharmacokinetic and Medical Internal Radiation Dose (MIRD) techniques. The cumulated activity ($\tilde{A}$) and the volume or mass of tumor and normal tissue needed for the "S" value calculation are the essential pieces of information required for dose estimates. Gamma-camera imaging provides a measure of tissue activity over time, while computed tomography (CT) or magnetic resonance imaging (MRI) is used to define tumor volumes. If the therapeutic radionuclide is a pure beta emitter, a photon-emitting surrogate with similar pharmacokinetic properties and physical half-life is labeled to the antibody for dosimetry estimates. This approach works well with ^{90}Y- and ^{111}In-labeled ibritumomab tiuxetan, which have similar biologic properties and decay half-lives. A half-life match between the surrogate tracer nuclide and the therapy nuclide is important. A surrogate tracer having a shorter half-life than the therapy nuclide may miss important late pharmacokinetic data, resulting in unreliable time–activity curves and dosimetry estimates.

Two different approaches have been used to deliver a cytotoxic dose of radiation to tumors: (1) the nonmyeloablative or low-dose approach and (2) the myeloablative or high-dose approach.[6,8] Nonmyeloablative RIT is designed to spare bone marrow from toxicity. Consequently, dose escalation studies are required to determine the maximum tolerated dose (MTD). Dose-limiting toxicity in RIT usually occurs 2 to 3 weeks after therapy, with a nadir at about 4 to 8 weeks and full recovery usually within 12 weeks after therapy.[6] Myelotoxicity is typically manifested by thrombocytopenia and neutropenia.[8] The myelotoxicity response depends on patient-specific conditions and whether prior chemotherapy or immunotherapy has been received, in which case patients are more vulnerable to toxicity. In myeloablative RIT, the radiation dose is almost certain to result in bone marrow ablation and requires a hematopoietic stem cell transplant (HSCT). The treatment dose is designed to deliver not more than the MTD to the dose-limiting normal tissues, those being the lung, kidney, liver, and gastrointestinal tract.[6,8]

Dosing Methods

Two dosing methods have been used in RIT: the radiation dose method and the radionuclide dose method.[6,8] In the radiation dose method, the amount of administered activity for the therapeutic dose is based on a prescribed radiation dose to the critical dose-limiting organ (red marrow or total body) in the case of nonmyeloablative RIT or the critical dose-limiting second organ (lung, kidney, liver, gastrointestinal tract) in the case of myeloablative RIT.[6] In the radionuclide dose method, the amount of radioactivity administered is based on body weight or body surface area, (i.e., mCi per kg or m^2).

Nonmyeloablative therapy in NHL has been conducted using both the radiation dose method and the radionuclide dose method.[6] In the radiation dose method, the amount of radioactivity to be administered is calculated by dividing the prescribed radiation dose (cGy) to the critical organ (red marrow or total body) by the radiation dose per unit activity (cGy/mCi) to the critical organ, estimated by a pretherapy tracer dose. The total-body dose is used as a marrow dose surrogate for ^{131}I-monoclonal antibodies because of its penetrating gamma radiation component, which contributes significantly to the red marrow dose.[9] This is the method used for dosing ^{131}I-tositumomab. The MTD for ^{131}I-tositumomab in nonmyeloablative therapy of NHL is 75 rad(cGy) to the total body. This was determined from a dose-escalation study beginning with a 25 rad(cGy) total-body dose, increasing in increments of 10 rad(cGy).[10]

With the radionuclide dose method in nonmyeloablative therapy, the amount of radioactivity administered is based on the maximum allowed activity per kilogram of body weight. This method does not require a tracer dose to calculate the administered activity, but tracer studies are typically done before therapy as a safety measure to ensure normal

biodistribution to organs. This method has been used with ^{90}Y-ibritumomab tiuxetan. The MTD for ^{90}Y-ibritumomab tiuxetan in nonmyeloablative therapy of NHL is 0.4 mCi/kg (14.8 MBq/kg) in patients with platelet counts 150,000/μL or higher and 0.3 mCi/kg (11.1 MBq/kg) with platelet counts 100,000 to 149,000/μL. The maximum allowed dose per patient treatment is 32 mCi (1184 MBq) regardless of body weight, based on critical threshold doses of 300 rad(cGy) to the marrow and 2000 rad(cGy) to any secondary organ (lungs, liver, or kidneys). The MTD was determined from a dose escalation study beginning at a dose of 0.2 mCi/kg (7.4 MBq/kg) with increasing increments of 0.1 mCi/kg (3.7 MBq/kg).[11] The total-body dose method that is used for ^{131}I-tositumomab cannot be used with ^{90}Y-ibritumomab tiuxetan because the red marrow dose does not correlate well with total-body dose. The reason is the residualizing of ^{90}Y in the body and its lack of gamma emissions.[6]

Myeloablative therapy has also been used in NHL patients. The amount of administered activity in these patients is determined by the radiation dose method. In this approach, a Phase I dose-escalation study was conducted beginning at 1000 rad(cGy) to the lungs as the critical organ, with incremental increases to 3075 rad(cGy).[12] The MTD was determined to be 2725 rad(cGy). Patients also received HSCT in this treatment regimen because of the resulting bone marrow ablation. The results of this type of treatment regimen in a Phase II trial and of nonmyeloablative treatment studies in RIT are described below in the discussion of individual antibodies.

THERAPEUTIC ANTIBODIES

^{90}Y- and ^{111}In-Ibritumomab Tiuxetan

Ibritumomab tiuxetan is an antibody conjugate of ibritumomab, an intact IgG1 kappa murine monoclonal antibody, and tiuxetan (MX-DTPA), an isothiocyanatobenzyl-derivatized DTPA linker, covalently bound to lysine and arginine amino groups in the antibody by a stable thiourea bond (see Figure 21-8, Chapter 21). ^{90}Y or ^{111}In is labeled to the antibody by chelation with the DTPA ligand. The radiolabeled antibody targets the CD20 antigen present on the surface of normal B-lymphocytes and the malignant B-lymphocytes of NHL.

The therapeutic regimen of ibritumomab tiuxetan is supplied as two separate identical kits, one for preparing a single dose of ^{111}In-labeled diagnostic antibody and the other for a single dose of ^{90}Y-labeled therapeutic antibody. The kits should be stored in the refrigerator prior to use.

Antibody labeling follows specific steps that differ between ^{111}In and ^{90}Y in the amounts of activity and antibody used and the length of incubation. The labeling steps for each radionuclide are summarized in Table 23-1. In general, shaking and foaming of the antibody during labeling must be avoided because this denatures the antibody. ^{90}Y-yttrium chloride for labeling is supplied directly from MDS Nordion when the antibody kit is ordered from Biogen Idec. The ^{111}In-indium chloride must be obtained separately from either Amersham Health or Mallinckrodt.

Radiochemical purity of the labeled antibody is assessed by instant thin-layer chromatography with silica gel (ITLC-SG) in normal saline. The unbound nuclide travels to the solvent front and labeled antibody remains at the origin. Its purity must be 95% or higher. Labeled antibody is stored at 2°C to 8°C. ^{90}Y-ibritumomab tiuxetan should be used within 8 hours and ^{111}In-ibritumomab tiuxetan within 12 hours after radiolabeling.

Developmental studies have shown that the immunoreactivity of ^{111}In-ibritumomab tiuxetan incubated for 15 minutes during radiolabeling is essentially conserved while that of ^{90}Y-labeled antibody is about 60%.[13] The incubation time for ^{90}Y-ibritumomab tiuxetan is therefore limited to 5 minutes to minimize the effects of radiolysis and to maintain

TABLE 23-1 Radiolabeling of Ibritumomab Tiuxetan with ^{111}In and ^{90}Y

^{111}In Labeling Steps	^{90}Y Labeling Steps
1. Add required volume of 50 mM sodium acetate buffer to the reaction vial. (Buffer volume = 1.2 times the volume of 5.5 mCi $^{111}InCl_3$). Coat entire surface of reaction vial with buffer.	1. Add required volume of 50 mM sodium acetate buffer to the reaction vial. (Buffer volume = 1.2 times the volume of 40 mCi $^{90}YCl_3$). Coat entire surface of reaction vial with buffer.
2. Add 5.5 mCi $^{111}InCl_3$ to the reaction vial and mix the solutions.	2. Add 40 mCi $^{90}YCl_3$ to the reaction vial and mix the solutions.
3. Add 1.0 mL of the antibody to the reaction vial and roll/mix solutions gently. Do not cause foaming of the antibody.	3. Add 1.3 mL of the antibody to the reaction vial and roll/mix solutions gently. Do not cause foaming of the antibody.
4. Incubate at room temperature for 30 minutes.	4. Incubate at room temperature for 5 minutes.
5. Add the formulation buffer (FB) to quench the labeling. (FB volume = 10 mL minus the volumes of $^{111}InCl_3$ + acetate buffer + antibody)	5. Immediately add the formulation buffer to quench the labeling. (FB volume = 10 mL minus the volumes of $^{90}YCl_3$ + acetate buffer + antibody)

immunoreactivity at around 75%. Antibody degradation is caused by the high-energy beta emission of ^{90}Y. The formulation buffer contains human serum albumin (HSA), which stabilizes the labeled antibody against radiolytic damage.[13] HSA was found to be effective in preserving antibody structure and immunoreactivity. The formulation buffer also contains DTPA to ensure that the small amount of ^{90}Y or ^{111}In not labeled to the antibody will be chelated and eliminated by renal excretion.

Ibritumomab tiuxetan is indicated for the treatment of patients with relapsed or refractory low-grade, follicular, or transformed B-cell NHL, including patients with rituximab-refractory follicular NHL.[14]

The ibritumomab tiuxetan dosage schedule proceeds in two steps, each requiring a predose of rituximab prior to administration of either ^{111}In-ibritumomab tiuxetan or ^{90}Y-ibritumomab tiuxetan. The rituximab predose is given initially to block accessible CD20 sites in the peripheral circulation and prevent indiscriminate uptake of the radiolabeled antibody in the reticuloendothelial system. The pretreatment facilitates optimum biodistribution of the radiolabeled antibody to tumor sites.

Rituximab was the first monoclonal antibody approved by FDA for the treatment of cancer. It is a genetically engineered chimeric monoclonal antibody specific for the CD20 antigen on B-lymphocytes. It contains murine light- and heavy-chain variable region sequences and human constant region sequences. Ibritumomab is the murine antibody parent of rituximab. Rituximab alone in standard immunotherapy produces objective tumor responses. However, its effectiveness is significantly less than that of ^{90}Y-ibritumomab tiuxetan. In a prospective randomized Phase III trial comparing ^{90}Y-ibritumomab tiuxetan with rituximab in relapsed or refractory low-grade, follicular, or transformed NHL, the overall response rates for ^{90}Y-ibritumomab tiuxetan and rituximab were 80% and 56%, respectively.[15] The complete remission rate was 30% for ^{90}Y-ibritumomab tiuxetan and only 16% for rituximab.

Dosing Regimen

Figure 23-2 illustrates a typical ibritumomab tiuxetan administration schedule. The first step of the therapeutic regimen involves intravenous infusion of rituximab 250 mg/m^2. It is infused initially at a rate of 50 mg/hour, escalating in 50 mg/hour increments every 30 minutes to a maximum rate of 400 mg/hour, provided no hypersensitivity reactions occur. The major adverse effects are fever and chills, which can be controlled by reducing the

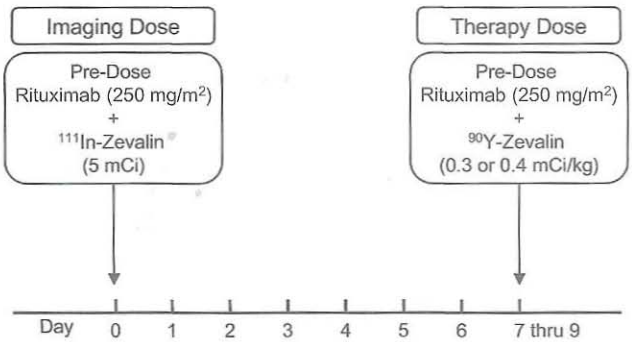

FIGURE 23-2 Dosing schedule for ^{111}In- and ^{90}Y-ibritumomab tiuxetan (Zevalin).

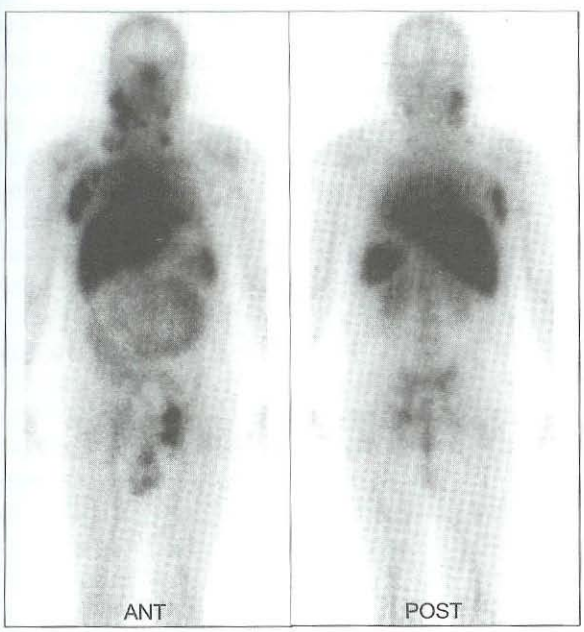

FIGURE 23-3 Fifty-seven-year-old man with low grade non-Hodgkin's lymphoma.^{111}In-ibritumomab tiuxetan scan 48 hours after radiopharmaceutical administration showing multiple focal areas of accumulation in the neck, right axilla, and left inguinal region. The patient went on to have ^{90}Y-ibritumomab tiuxetan therapy 1 week later.

infusion rate. Rituximab should be infused within 4 hours before the administration of either ^{111}In-ibritumomab tiuxetan or ^{90}Y-ibritumomab tiuxetan. Rituximab infusion is followed by 5 mCi (185 MBq) of ^{111}In-ibritumomab tiuxetan, given intravenously over 10 minutes. ^{111}In-ibritumomab tiuxetan permits gamma-camera imaging to confirm normal biodistribution of antibody prior to ^{90}Y-ibritumomab tiuxetan administration (Figure 23-3).[16] It predicts the behavior of ^{90}Y-ibritumomab tiuxetan and ensures that normal tissue dose limits will not be exceeded, which would preclude administration of ^{90}Y-ibritumomab tiuxetan. Abnormal distribution would be evident from more intense lung activity relative to the cardiac blood pool in the 24 hour image or relative to liver on the 48 hour image, or kidney activity more intense than liver activity on the 48 hour posterior image, or areas of bowel activity equal to liver activity on the 48 hour image.

The second step occurs in 7 to 9 days, consisting of a second infusion of rituximab 250 mg/m^2, followed by 0.4 mCi/kg (14.8 MBq/kg) or 0.3 mCi/kg (11.1 MBq/kg) of ^{90}Y-ibritumomab tiuxetan given intravenously over 10 minutes. The infusion line should be flushed with 10 mL of saline after each antibody administration.

The principal adverse effects of ^{90}Y-ibritumomab tiuxetan are hematologic: thrombocytopenia and neutropenia. These effects occur less frequently when platelet counts are greater than 150,000 cells/μL. The dose of ^{90}Y-ibritumomab tiuxetan should be reduced to 0.3 mCi/kg (11.1 MBq/kg) in patients with a baseline platelet count between 100,000 and 149,000 cells/μL. No patient with a platelet count less than 100,000 should be treated. The maximum allowable dose of ^{90}Y-ibritumomab tiuxetan is 32.0 mCi (1184 MBq) regardless of the patient's weight. The dose limit is to ensure that no patient receives radiation absorbed doses to any normal organ greater than 2000 rad(cGy) or greater than 300 rad(cGy) to the red marrow.[16] The median absorbed radiation doses per 32 mCi to selected organs are spleen, 1113 rad(cGy); liver, 568 rad(cGy); lung, 237 rad(cGy); kidney, 12 rad(cGy), red marrow, 154 rad (cGy), and total body, 59 rad(cGy).[14] The median effective half-life of ^{90}Y-ibritumomab tiuxetan in the blood in clinical trials was 27 hours (range, 14 to 44 hours).[13] The frequency of HAMA response is 2.4%, and human antichimeric antibody (HACA) response is 2%.[14]

From a therapeutic standpoint, ^{90}Y has a wider range of effectiveness than ^{131}I because of its higher beta energy. For example, the effective path lengths (χ_{90}) of ^{90}Y and ^{131}I are about 5 mm and 1 mm, respectively, meaning that 90% of their beta-particle energies are absorbed within a sphere of 5 mm or 1 mm radius, respectively.[16] A 5 mm path length corresponds to about 100 to 200 cell diameters. Thus, ^{90}Y betas bound to surface cells on a tumor can deliver radiation dose to non–antibody-bound tumor cells located deep within the tumor (the crossfire effect). This consideration is important in bulky or poorly vascularized tumors.

Radiation Safety

Caution should be exercised in handling ^{90}Y during radiolabeling. The exposure rate per millicurie from the mouth of an open vial of ^{90}Y is 32 R/hour.[14] Its average beta particle range in air is about 3.7 m, unshielded. Although the beta particle energy is quite high, it can be completely absorbed by 1 cm of low-Z material such as Plexiglas or Lucite (see Table 4-4, Chapter 4). Syringe shields should be constructed of these materials to limit bremsstrahlung production. A thin layer of lead may be used over the plastic shield to absorb any bremsstrahlung produced. Geiger-Müller survey meters are extremely efficient for detecting low-energy photons but could give erroneously high readings unless they have been calibrated for ^{90}Y bremsstrahlung.[17]

^{90}Y exposure of family members and members of the public from patients treated with ^{90}Y-ibritumomab tiuxetan is very low. The specific bremsstrahlung dose constant for ^{90}Y in soft tissue from a 70 kg patient is 0.00564 R-cm^2/mCi-hr (1.52 μGy-cm^2/MBq-hr).[17] Based on the Nuclear Regulatory Commission (NRC) threshold for exposure of members of the public (0.5 rem), excluding self-absorption of bremsstrahlung, a patient would need to be dosed above 38,500 mCi (1.42×10^6 MBq) of ^{90}Y to exceed this limit.[17] Since the maximum dose of ^{90}Y-ibritumomab tiuxetan is 32 mCi (1184 MBq), therapy with this antibody is safe and requires no restrictions to prevent exposure of members of the public. The only recommendation for family members is to avoid contamination from body excretions, mainly urine, although this is not likely to be a safety issue because urinary excretion is quite low, about 7.3% per week. The recommended instructions for patients released after treatment with ^{90}Y-ibritumomab tiuxetan are as follows: [17] For 3 days after treatment, clean up any contaminated body fluid and urine and flush it down the toilet or place it in a plastic bag in household trash, and wash hands thoroughly after using the toilet. For 1 week after treatment, use condoms during sexual relations.

^{131}I-Tositumomab

Tositumomab, otherwise known as B1, is an IgG2a kappa murine monoclonal antibody. ^{131}I-tositumomab targets the CD20 antigen present on the surface of normal B-lymphocytes and the malignant B-lymphocytes of NHL. It is prepared by the Iodo-Gen method of radioiodination and is supplied as a frozen product that is thawed at the time of use.

A number of studies have involved nonmyeloablative treatment of NHL with ^{131}I-tositumomab. Phase I, II, and III trials with ^{131}I-tositumomab have demonstrated that it is safe and effective for the treatment of low-grade and transformed NHL in patients previously treated with chemotherapy or immunotherapy and in those not previously treated.[6] Kaminski et al.,[10] in a Phase I trial, treated patients with low-grade and intermediate-grade NHL who were chemotherapy resistant or who had large tumor burdens. ^{131}I-tositumomab dosages ranged from 34 to 161 mCi (1258 to 5957 MBq). Of those treated, 79% achieved a tumor response and 50% had complete remission with a median duration greater than 13 months. The MTD was determined to be 75 rad(cGy) total body.

Phase II and III studies have also been completed with nonmyeloablative doses of ^{131}I-tositumomab. Vose et al.[18] reported the results of a multicenter Phase II study in patients with chemotherapy-relapsed/refractory low-grade and transformed low-grade NHL. Patients received a 450 mg predose of unlabeled tositumomab followed by a 5 mCi dosimetric dose of ^{131}I-tositumomab and a 75 rad(cGy) whole-body therapeutic dose 1 to 2 weeks later. The overall response rate of the 45 patients treated was 57% for low-grade and 60% for transformed NHL, with a median response duration of 9.9 months. Complete remission was achieved in 32% of patients, with a median duration of 19.9 months. Kaminski et al.[19] reported on a pivotal study in patients who had received a prior median course of four chemotherapy regimens and who were either treated or not treated with 75 rad(cGy) ^{131}I-tositumomab. Of patients treated with RIT, 65% had complete or partial remission, compared with only 28% of patients with chemotherapy alone. Wahl et al.[20] evaluated the effectiveness of RIT alone in NHL patients previously untreated with chemotherapy. All patients had stage III or IV disease; 65% had lymphomatous bone marrow involvement and 29% had high tumor burdens. Patients received ^{131}I-tositumomab at a total body dose of 75 rad(cGy). Ninety-seven percent of patients demonstrated a partial or complete remission, with 63% achieving complete remission. No hematologic support was needed, but the HAMA response (flulike symptoms) was high (64%), probably because of the unsuppressed immune system in these patients, since no chemotherapy had been given prior to RIT.

One study involved myeloablative treatment of NHL with ^{131}I-tositumomab.[21] In this Phase II study, 25 patients with relapsed B-cell NHL were given a myeloablative MTD combined with autologous HSCT after a 5 mCi (185 MBq) predose to assess normal biodistribution. Twenty-one patients received a therapeutic dose of ^{131}I-tositumomab designed to deliver 2700 rad(cGy) to the lungs as critical secondary organ, followed by HSCT. Of these 21 patients, 18 (86%) had an objective response and 16 (76%) achieved a complete remission. A follow-up study that included more patients treated with myeloablative doses of ^{131}I-tositumomab showed a very high overall response rate and complete remission rate, suggesting that the myeloablative approach may produce better results than nonmyeloablative therapy.[22]

These clinical trials demonstrate that ^{131}I-tositumomab is safe and effective for the treatment of NHL either alone or in combination with chemotherapy. A reduction in the HAMA response will be necessary if RIT is to become a front-line approach to treating NHL without prior chemotherapy. This may become possible if humanized antibody is used to reduce the murine component.

^{90}Y-Epratuzumab

Epratuzumab (hLL2), the humanized monoclonal antibody of the murine IgG2a antibody (mLL2), reacts with the CD22 antigen on the surface of NHL B-cells. This antibody does not react with normal peripheral blood cells but does react with germinal B-cells of normal lymph nodes and the white pulp of the spleen.[23] It has been labeled with ^{131}I, ^{111}In, ^{90}Y, and ^{186}Re.

LL2 is an interesting antibody because, in contrast to antibodies reacting with the CD20 antigen, it becomes internalized rapidly within the cell after its CD22 interaction.[24] Subsequently, the CD22 antigen is resynthesized and re-expressed on the cell so that additional antibody can be localized and internalized. The rate of lysosomal catabolism of an internalized antibody is usually much higher than the rate of decay of its radiolabel. This may shorten the radiation dose delivered to the tumor cell if the radionuclide metabolite is readily excreted from the cell. If the radiolabel is residualized in the tumor cell, its longer residence time will produce higher tumor-to-background ratios and radiation dose delivered to the tumor.[25]

Studies have shown that ^{111}In- and ^{90}Y-labeled antibodies have longer residence times in tumors than conventionally iodinated antibodies.[26,27] This is apparently due to trapping of the radiolabeled metabolites of ^{111}In and ^{90}Y within tumor cell lysosomes after catabolism. Conventionally iodinated antibodies, labeled via chloramine-T or Iodo-Gen, release iodotyrosine as a principal metabolite, which readily diffuses out of lysosomes and the tumor cell.[27,28] After release, iodotyrosine undergoes deiodination by tyrosine deiodinase.[29] All antibodies bound to tumor cells are slowly released over time after their degradation; however, those bound to surface antigens are released more slowly than are rapidly internalized antibodies. Thus, the effectiveness of a radiolabeled antibody in delivering radiation dose to tumor depends on the type of radiolabel and its retention by the tumor after catabolism. It has been shown that antibodies iodinated with a residualizing radioiodine conjugate, such as dilactitol iodotyramine, have a longer residence time in tumors.[26,30] This is attributed to the inability of the metabolized conjugate to diffuse out of lysosomes. It appears that tumor cells that rapidly internalize antibodies would be more effectively killed if the antibody was labeled with a residualizing radiometal conjugate or a radioiodine conjugate than with a conventional radioiodine label. Juweid et al.[31] have compared hLL2 radiolabeled with ^{131}I (by Iodo-Gen) and ^{111}In and ^{90}Y (via the benzyl-DTPA-hLL2 conjugate) in patients with relapsed refractory NHL. After therapeutic doses of ^{131}I-hLL2 or ^{90}Y-hLL2 to deliver 50 to 100 rad(cGy) to bone marrow, the estimated radiation dose to tumors larger than 3 cm was 2.4 ± 1.9 rad(cGy) for ^{131}I-hLL2 versus 21.5 ± 10.0 rad(cGy) for ^{90}Y-hLL2. Objective tumor response was seen in 2 of 13 patients given ^{131}I-hLL2 and 2 of 7 patients given ^{90}Y-hLL2.

^{131}I-LYM-1

LYM-1 is an IgG2a murine monoclonal antibody that targets HLA-DR expressed on the surface of most malignant B-lymphocytes.[32] The LYM-1 antibody was initially developed against the Raji cell line that originated from a patient with African Burkitt's lymphoma. The antibody–antigen complex is not internalized.

RIT of NHL with ^{131}I-LYM-1 was initiated because of the high radiosensitivity of B-lymphocytes. The first clinical trial of RIT for lymphoma was conducted with ^{131}I-LYM-1. Initial trials demonstrated that it was necessary to use a predose of unlabeled "cold" antibody before administration of the radiolabeled antibody in order to prolong its blood clearance and increase tumor uptake. The "cold" predose of LYM-1 (5 mg) was able to achieve this effect by saturating nonspecific receptors in the liver.[33]

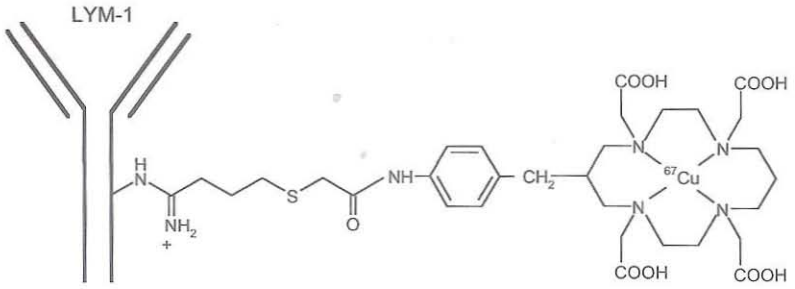

FIGURE 23-4 Chemical structure of ^{64}Cu-2-iminothiolane bromoacetamido benzyl TETA (^{67}Cu-2IT-BAT-LYM-1).

Two radiolabels have been used to label LYM-1: ^{131}I by standard chloramine-T iodination to yield ^{131}I-LYM-1, and ^{67}Cu in the form of the BFCA 2-iminothiolane bromoacetamido benzyl TETA (^{67}Cu-2IT-BAT) to yield the antibody conjugate ^{67}Cu-2IT-BAT-LYM-1. TETA (1,4,8,11-tetraazacyclotetradecane-1,4,8,11-tetraacetic acid) is the macrocyclic chelator (Figure 23-4). It was specifically designed to produce a stable chelate with Cu(II).[34,35] The TETA chelator contains the functionality of iminothiolane to link it to the antibody. ^{67}Cu is a potentially effective radionuclide for RIT. As the TETA chelate it is quite stable (about 1% loss per day in in vitro studies),[34] and there is no biologic mechanism for its uptake in bone marrow to increase myelosuppression.[36] It has a half-life (2.58 days) that is similar to the residence time of a typical antibody on the tumor.[34] It emits beta particles of moderate energy with a mean range of 0.27 mm, and it has a useful photon energy (185 keV) for imaging and dosimetry estimation.

Clinical studies of LYM-1 RIT for NHL have been summarized by DeNardo and DeNardo.[32] Fifty-five patients who were refractory to multiple-drug chemotherapy were treated with ^{131}I-LYM-1 in fractionated doses. Thirty-one patients received low-dose therapy of 30 to 60 mCi (1110 to 2220 MBq). Of these, 1 patient did not respond to treatment and 17 of 30 responding patients had remission of their disease, 3 with complete remission (CR) and 14 with partial remission (PR). Of 24 patients treated with an MTD protocol of 40 to 100 mCi/m^2 (1480 to 3700 MBq/m^2), 13 responded, 8 with CR and 5 with PR. Of these patients, 17 (30%) developed HAMA. Myelosuppression was the only significant radiation-induced toxicity.

The fractionated dose approach to RIT with LYM-1 was chosen in the belief that a single large dose could not completely permeate all of the tumor and multiple smaller doses would cause partial destruction of tumor that would lead to vascularization of other parts of the tumor and more effective treatment.[34] This strategy has been demonstrated to be effective in mice.[37] In these fractionated RIT studies, an overall response rate (complete and partial remission) of 55% was achieved in 57 patients treated with ^{131}I-LYM-1.

Patients with advanced lymphoma treated with the ^{67}Cu-2IT-BAT-LYM-1 conjugate have shown a 48% response within several days of dosing with 3.4 to 14.4 mCi (125.8 to 532.8 MBq).[38] The mean radiation dose ratios were 32:1 tumor-to-marrow, 24:1 tumor-to-total-body, and 1.5:1 tumor-to-liver because of the long residence time of the ^{67}Cu-LYM-1 conjugate in tumor. When compared with ^{131}I-LYM-1, the ^{67}Cu-LYM-1 conjugate had a mean tumor concentration 2.8 times that of ^{131}I-LYM-1 and resulted in tumor-to-marrow indices of 29 for the ^{67}Cu-LYM-1 conjugate and 9.7 for ^{131}I-LYM-1.[39] These results suggest that the ^{67}Cu-LYM-1 conjugate may be superior to ^{131}I-LYM-1 for RIT.

PRETARGETED RADIOIMMUNOTHERAPY

Despite the success achieved with the treatment of NHL and other tumors, tumor targeting is fraught with problems. The amount of radiolabeled antibody taken up by tumors is typically only 0.001% to 0.1% of the injected dose because of heterogeneous antigen density, the development of antigen-negative tumor cells, nonuniform vascularity, and other factors such as circulating antigen, which prevents injected antibody from reaching peripheral sites. All of these factors lead to low tumor-to-background ratios.

To overcome some of the causes of low tumor uptake of radiolabeled antibody, pretargeting methods have been developed. These techniques involve the administration of "cold" antibody derivatized to carry a secondary receptor that can bind a subsequently injected radiolabeled ligand. To enhance uptake of the radiolabeled ligand at tumor sites, a clearance technique is used to remove excess residual antibody in the circulation before the radiolabeled ligand is administered. These methods have been reviewed.[40–42]

A pretargeting modality that has been studied widely is the avidin–biotin system. Avidins are small oligomeric proteins made up of four identical subunits, each having a specific binding site for biotin. The affinity of biotin for avidins is very high, with the complex having a dissociation constant of 10^{-15} M. Avidins are isolated either from hen egg white (avidin) or from *Streptomyces avidinii* (streptavidin). Biotin is a 244 Da molecule that can be activated with a variety of functional groups to covalently attach it to proteins or chelating agents that bind radionuclides. One approach is to biotinylate an antibody by covalently attaching a biotin molecule to it. This conjugate can then be used to pretarget the tumor, followed by administration of radiolabeled streptavidin to deliver radioactivity to the tumor. Alternatively, the streptavidin can be covalently linked to the antibody as the pretargeting agent, followed by administration of radiolabeled biotin. In this case the biotin has been previously functionalized with a chelating agent to bind a radionuclide. The latter approach is being investigated with a DOTA–biotin conjugate labeled with ^{90}Y.[43,44]

Two approaches are used in pretargeted therapy: the two-step method and the three-step method.[40] In the two-step method, biotinylated monoclonal antibody (or streptavidin monoclonal antibody) is administered first, followed in 1 to 2 days by administration of radiolabeled streptavidin (or radiolabeled biotin). This approach has appeal when tumor is confined to a small space, such as the peritoneal cavity. When disease is widespread and systemic administration is required, the three-step method is preferred. In this situation, a biotinylated monoclonal antibody is administered first to target the tumor. This is followed 1 day later by the injection of avidin, which removes excess circulating biotinylated monoclonal antibody, and streptavidin, which targets the tumor cells. After this step, radiolabeled biotin is injected, which targets the tumor-bound streptavidin, thus delivering the radioactivity to the tumor.

RADIOTHERAPY OF BONE PAIN

Bone metastases eventually develop in 50% of patients with breast or prostate cancer.[45] Radiopharmaceutical treatment of bone pain caused by metastatic cancer has provided much relief for patients with this condition, ameliorating pain 40% to 80% of the time.[46] Pain relief may last for a few weeks to several months. The goal of treatment is to preserve function and improve quality of life for the patient by relieving pain, reducing the amounts of narcotics needed for pain relief, and improving ambulation. Several modalities have been used to treat bone pain, including analgesics, hormone therapy, chemotherapy, surgery, radiopharmaceuticals, and external beam radiation. These modalities have been reviewed.[47] Of radiation treatment methods, external beam radiation has been effective in

TABLE 23-2 Radiopharmaceuticals for Painful Bone Metastases

Radiopharmaceutical	Half-life (days)	Beta Max (MeV)	Beta Mean (MeV)	Mean Range (mm)	Gamma *E* (MeV) (abundance)
^{32}P-sodium phosphate	14.3	1.71	0.7	3.0	None
^{89}Sr-strontium chloride	50.5	1.46	0.58	2.4	0.910 (0.009%)
^{186}Re-etidronate (^{186}Re-HEDP)	3.8	1.07	0.35	1.1	0.137 (9%)
^{153}Sm-lexidronam (^{153}Sm-EDTMP)	1.9	0.81	0.23	0.6	0.103 (28%)
^{117m}Sn-pentetate (^{117m}Sn-DTPA)	13.6	0.13[a]	–	0.2	0.159 (86%)
		0.15[a]		0.3	

[a] Conversion electrons.

reducing pain from metastases, but its application is limited to treating localized sites in the body. More generalized external radiation treatments have debilitating adverse effects such as nausea and vomiting. Because metastases are often widespread, systemic radionuclide therapy is a better choice, providing more general and long-lasting relief with minimal adverse effects. Palliative treatment of bone pain currently is restricted to patients with incurable disease who are expected to live several months.

To be effective in reducing bone pain, a radiopharmaceutical must have certain characteristics.[48] First, it must have a high affinity for reactive bone; second, it must emit beta or electron radiation; third, the radiation must have sufficient energy to reach the cells responsible for the pain; and fourth, the half-life must be long enough to deliver damaging or lethal radiation to the cells.

Table 23-2 lists several radiopharmaceuticals that are approved for routine use or are under investigation. In general, all of these agents have an intrinsic affinity for mature bone (hydroxyapatite), with a particular affinity for regions of osteoblastic activity where amorphous calcium phosphate is being deposited. Thus, their sites of uptake in bone can be predicted by a standard bone scan with ^{99m}Tc-medronate (^{99m}Tc-MDP) or ^{99m}Tc-oxidronate (^{99m}Tc-HDP). ^{32}P and ^{89}Sr undergo biologic incorporation into bone similar to calcium, ^{186}Re and ^{153}Sm phosphonate complexes localize by chemisorption, and ^{117m}Sn is deposited in bone as a hydrated oxide after hydrolysis at the bone surface. A similar hydrolysis reaction may be involved with ^{186}Re and ^{153}Sm as well. These radiopharmaceuticals have widely varying half-lives and mean particle energies in the range of 0.13 to 0.70 MeV, but the response rate for all of these agents, measured by pain reduction, is in the range of 40% to 80% over a wide range of administered activities.[46] No dose–response effect has been demonstrated to occur with these agents.[48] The mechanism of action of any of these agents in relieving bone pain is not known. Only ^{32}P-sodium phosphate, ^{89}Sr-strontium chloride, and ^{153}Sm-lexidronam are approved by FDA for routine use. Clinical trials of ^{117m}Sn-pentetate (^{117m}Sn-DTPA) and ^{186}Re-etidronate (^{186}Re-HEDP) are no longer active in the United States.

Sodium Phosphate P 32 Solution

Sodium phosphate P 32 solution (^{32}P-sodium phosphate) is a clear, colorless sterile solution at pH 5.0 to 6.0 suitable for oral or intravenous administration. The commercial product is available at a radioactive concentration of 0.67 mCi/mL (24.8 MBq/mL) in 5 mCi (185 MBq) vials at the time of calibration. ^{32}P-sodium phosphate was the earliest agent used for treating painful bone metastases.[49] A review of ^{32}P-sodium phosphate for this indication showed effective pain response ranging from 60% to 90%.[50] One concern with ^{32}P as the phosphate is its involvement in many metabolic processes in the body, particularly in the

hematopoietic system. Its principal toxicity has been bone marrow depression caused by its high-energy beta particle. When compared with ^{89}Sr-strontium chloride for the treatment of painful bone metastases, ^{32}P-sodium phosphate was equally effective in reducing pain (90%) but caused a higher level of myelosuppression.[51] Pain reduction may be seen in 5 to 14 days after administration of ^{32}P-sodium phosphate.

Strontium Chloride Sr 89 Injection

Strontium chloride Sr 89 injection (^{89}Sr-strontium chloride; Metastron, Amersham) was approved by FDA in June 1993 for the treatment of bone pain in patients with skeletal metastases. It is supplied as a sterile injection of ^{89}Sr-strontium chloride in water at a concentration of 1 mCi/mL (37 MBq/mL) with a total of 4 mCi (148 MBq) in a 10 mL vial. Its expiration date is 28 days after calibration. The dosage range is 40 to 60 μCi/kg (1.48 to 2.22 MBq/kg), with an average dose of 4 mCi (148 MBq) given intravenously. The dose is administered over 1 to 2 minutes to minimize any "flushing" reaction. Administration can be repeated, but an interval of not less than 90 days is recommended. A single injection of 4 mCi (148 MBq) relieves pain in 65% to 80% of patients, with complete relief of pain in 20%. The time to response is 1 to 3 weeks, and the median duration of benefit is 4 to 6 months. Retreatment is possible at approximately 3 month intervals on up to eight occasions. ^{89}Sr-strontium chloride is generally not recommended in patients with an expected survival of less than 3 months and in patients with disseminated intravascular coagulation.[47]

Because ^{89}Sr suppresses bone marrow, at initial treatment the patient's platelet count should be greater than 60,000 and white blood cell count greater than 2400. A complete blood and platelet count should be obtained at least every other week to monitor the hematologic effects. The usual hematologic response is a 20% to 30% decrease in platelet count; the lowest point occurs at 5 to 6 weeks, with complete recovery by 12 weeks. The use of ^{89}Sr-strontium chloride should be avoided in patients who have received previous chemotherapy with bone marrow suppression, because of the additive toxicity that may ensue.

Serafini[47] has reviewed several studies performed with ^{89}Sr. In general, these studies indicated that pain relief was quite good, ranging from 60% to 85%, and that the degree of relief was independent of administered activity, which ranged from 1 to 10 mCi (37 to 370 MBq). Thus, a dose–response effect was not seen. Mild to moderate myelotoxicity (thrombocytopenia) was reported in most trials, with more severe toxicity occurring with higher doses.

The mechanism of ^{89}Sr uptake into bone is similar to that for calcium and occurs at sites of active osteogenesis. Increased uptake of longer duration occurs in metastases, compared with normal bone.[47] About 70% of the dose is retained in the skeleton, ranging from up to 88% retention with extensive metastases to 11% with few metastases. Of the fraction excreted, two-thirds is urinary and one-third is fecal.

Patients who are to receive ^{89}Sr-strontium chloride should be advised that their pain may worsen in the 2 to 3 days after dosing. This so-called flare response, which occurs in 10% to 20% of patients, is transient and readily treated with nonaspirin analgesics. The type of analgesic is important because thrombocytopenia is exacerbated with anticlotting drugs like aspirin. Patients should be told that the onset of pain relief may take 1 to 3 weeks and that ^{89}Sr-strontium chloride does not cause nausea, vomiting, or hair loss, which they might expect from chemotherapy or other forms of radiation treatment.

The critical organ is the bone surface, with a radiation dose of 63 rad (cGy)/mCi, equivalent to a 250 rad (cGy) dose from 4 mCi (148 MBq).

^{89}Sr is considered to be a pure beta emitter, despite its 910 keV gamma ray of very low abundance (0.009%). Therefore, its assay in a dose calibrator relies on the measurement of bremsstrahlung, which can vary considerably depending on the assay geometry. Consequently, a method has been developed for the radioassay of ^{89}Sr dosages in the radionuclide dose calibrator.[52] The method is as follows: First, calculate the activity in the vial at the time and date of dispensing based on the label calibration data. Second, assay the vial in the dose calibrator, adjusting the calibration dial to read the calculated activity. Because of the insensitivity of the dose calibrator to beta emitters, an empiric calibration factor must be selected, typically a setting around 600, using the adjustable potentiometer dial, and a correction factor of 100 applied to the reading to get the correct value. Third, calculate the volume needed to obtain the patient dosage, and withdraw this amount into a syringe. Next, reassay the vial. The difference between the two readings is the activity in the syringe. Now assay the syringe and adjust the calibration dial to read the activity in the syringe. After injecting the patient, reassay the syringe for any residual activity. The difference between the two syringe readings is the activity injected into the patient.

Samarium Sm 153 Lexidronam Injection

Samarium Sm 153 lexidronam injection (^{153}Sm-lexidronam; Quadramet, Berlex) is a sterile, aqueous, clear to light amber solution for intravenous administration. The solution pH is 7.0 to 8.5. The product is available as a frozen solution at a concentration of 50 mCi/mL (1850 MBq/mL) in vial sizes of 100 mCi (3700 MBq) and 150 mCi (5550 MBq). It expires 48 hours after the calibration time or within 8 hours of thawing. It is indicated for the relief of pain in patients with confirmed osteoblastic metastatic bone disease.

^{153}Sm is a beta and gamma emitter, and its 103 keV gamma ray permits bone imaging if desired. The biologic localization in lesions and normal bone of ^{153}Sm-lexidronam is similar to that of ^{99m}Tc-medronate.[53] Its half-life is 46.3 hours. It has been suggested that this short half-life results in a high dose rate over a short period of time, which should provide a rapid onset of pain relief and a limited amount of bone marrow suppression, but this has not been proven. After intravenous administration, ^{153}Sm-lexidronam localizes in bone metastases similar to ^{99m}Tc-diphosphonate bone imaging agents; however, ^{153}Sm undergoes a hydrolysis reaction at the bone surface.[54] By 4 to 6 hours after dosing, urinary excretion is essentially complete and uptake in bone is related to the extent of metastases present, not the dose administered.[55,56] Total bone uptake averages 65% of the injected dose. The critical organ is bone surface, with a radiation absorbed dose of 25 rad(cGy)/mCi.[56]

^{53}Sm-lexidronam suppresses bone marrow in a manner similar to ^{89}Sr-strontium chloride. Platelet counts reach a nadir in 3 to 5 weeks with recovery by 8 weeks; with ^{89}Sr-strontium chloride the nadir occurs in 5 to 6 weeks with recovery in 12 weeks.[55] The standard dosage is 1 mCi/kg (37 MBq/kg) body weight. At this dosage, relief of bone pain occurs 1 week after dosing in 35% of patients, increasing to 70% by the fourth week.[55] By the 16th week, 39% of patients still note effective pain relief. After dosing at 1 mCi/kg (37 MBq/kg), the rate of "flare" response is low (7%, compared with 5.6% in untreated control subjects).[56] Retreatment with additional doses of ^{153}Sm-lexidronam has been shown to be safe and efficacious.[57]

Dose calibrator calibration factors must be established with ^{153}Sm-lexidronam because of the geometry dependence of activity measurements with beta emitters, despite the gamma emission of ^{153}Sm. This is typically done before the first dose is administered by assay of a 15 mCi (555 MBq) calibration standard supplied by the manufacturer. Typically, calibration factors are determined by assaying ^{153}Sm in its glass vial and in 3 mL and 5 mL plastic syringes used for patient dosing.

Rhenium Re 186 Etidronate Injection

The similarities of rhenium and technetium chemistry, their ability to label bone-seeking diphosphonates, and the beta–gamma emissions of ^{186}Re, which permit radiation therapy and gamma-camera imaging, prompted the development of ^{186}Re-etidronate (^{186}Re-HEDP). The short half-life (89 hours) is thought to permit relatively high dose rates for treatment of metastases and allow for repeated treatments. Dosimetry studies have demonstrated a high tumor-to-marrow dose ratio (mean, 34:1).[58] This radiopharmaceutical is approved for use in Europe but not in the United States.

Initial studies with ^{186}Re-HEDP identified the need for purification, because formulations contained a mixture of complexes that contributed to soft tissue uptake.[59]

One kit used in clinical studies requires stannous ion reduction of ^{186}Re-perrhenate and heating for 10 minutes to effect complexation with HEDP, followed by a purification step accomplished by passage through a Sep-Pak Accell QMA (Waters) anion exchange cartridge to isolate the desired complex.[59] Patients with metastatic disease from prostate cancer (32 of 44), breast cancer (7 of 44), and other cancer types (5 of 44) who were treated with this product demonstrated a 77% response after a single dose of 34 mCi (1258 MBq), and a 50% response was seen in patients who received a second injection. Patients experienced an average reduction in pain of 60%.

Another kit preparation involves heating the perrhenate, stannous ion, and HEDP mixture for 10 minutes, followed by pH adjustment with sodium acetate solution. The product is not subjected to a purification step.[60] Thirty-seven prostate cancer patients treated with doses ranging from 35 to 95 mCi (1295 to 3515 MBq) of ^{186}Re-HEDP prepared by this method achieved a 54% response rate (20 of 37). There appeared to be a dose–response relationship with higher doses, but it did not reach statistical significance because of the small number of subjects. The lower response rate in this study may have been due to the strict guidelines used to evaluate pain relief.

^{186}Re-HEDP appears to have merit for providing pain relief from bone metastases, but it is not certain whether this agent will eventually be approved for routine use in the United States, because clinical studies have not continued.

Tin Sn 117m Pentetate Injection

^{117m}Sn-pentetate (^{117m}Sn-DTPA) is produced by a neutron elastic scattering reaction on ^{117}Sn metal, ^{117}Sn(n,n'γ)^{117m}Sn.[61] ^{117m}Sn decays by isomeric transition, emitting a 159 keV gamma ray (86%) and conversion electrons of 127 to 129 keV and 152 keV (114%). Preliminary dosimetry calculations in bone and bone marrow estimate a bone-to-bone-marrow radiation dose ratio of 9 to 1, primarily because of its low-energy conversion electron radiation.[61] These estimates indicate that ^{117m}Sn might be effective in the palliative treatment of metastatic bone pain without significant bone marrow toxicity. When compared with ^{32}P-sodium phosphate in a murine model to quantitate radiation dose to bone and bone marrow, the low-energy conversion electrons of ^{117m}Sn-DTPA demonstrated an 8-fold therapeutic advantage over the high-energy beta particles of ^{32}P.[62]

In a clinical study of bone pain, ^{117m}Sn-DTPA was administered to five groups of patients in a wide range of activities (from 71 to 286 μCi/kg [2.63 to 10.58 MBq/kg]).[63] The overall response rate for pain relief was 75% in 40 patient treatments. No apparent dose–response relationship was observed; however, the time of onset of pain relief was shorter with higher dosages. Only one patient exhibited a mild grade of leukocyte toxicity. The investigators stated that ^{117m}Sn-DTPA warrants further large-scale trials to compare it with other agents.

^{32}P THERAPY

In addition to the treatment of painful bone metastases, ^{32}P in its two principal chemical forms, ^{32}P-sodium phosphate and ^{32}P-chromic phosphate, has applications in polycythemia vera, effusion therapy (peritoneal and pleural), and radiation synovectomy.

Polycythemia Vera

Polycythemia vera is a rare disease characterized by an elevation of the red blood cell mass, total blood volume, and peripheral leukocyte and platelet counts.[64] Hematocrits may be 50% to 60% or more, white blood cell counts greater than 12,000/μL, and platelets in excess of 400,000/μL. The high viscosity of blood leads to sluggish blood flow through organs. If untreated, thrombosis and hemorrhage that can lead to death may result.[65] The condition has been treated with phlebotomy, chemotherapy (chlorambucil, hydroxyurea), and ^{32}P-sodium phosphate therapy. The treatment of choice is hydroxyurea, with ^{32}P-sodium phosphate therapy as a second choice if hydroxyurea therapy fails or patients cannot comply with the requirements of hydroxyurea therapy.[66]

The dose of ^{32}P-sodium phosphate recommended by the Polycythemia Vera Study Group is 2 to 3 mCi/m^2 (7.4 to 11.1 MBq/m^2) given intravenously after phlebotomy to achieve a hematocrit level of 42% to 47%.[67] The dose should not exceed 5 mCi (185 MBq). This is usually sufficient to produce a remission. If remission does not occur in 3 months, the dose should be increased by 25%. Another dose increase by 25%, but not exceeding 7 mCi (259 MBq), may be tried as a third dose after a period of another 3 months. Retreatment is usually restricted for 6 months thereafter.

When soluble radiophosphate enters the miscible body phosphate pool, it is concentrated by rapidly proliferating tissue. Its use in polycythemia vera and other bone marrow diseases is based on the fact that blood cell precursors in the bone marrow divide and proliferate rapidly in health and to an even greater extent in these diseases. The radiophosphate selectively concentrates in the mitotically active cells of the bone marrow and in trabecular and cortical bone. The radiation dose to the bone marrow has been estimated to be 24 rad(cGy)/mCi divided among marrow, 13 rad(cGy); trabecular bone, 10 rad(cGy); and cortical bone, 1 rad(cGy).[68] An increased rate of neoplasia (leukemia) occurs with bone marrow doses greater than 100 rad(cGy).[69] This is likely to occur with typical therapy; however, median survival has been reported to be better with ^{32}P-sodium phosphate (12 years) than with phlebotomy (8 years).[70]

Effusion Therapy

Malignant peritoneal and pleural effusions are complications that may arise from cancer. Intracavitary instillation of insoluble ^{32}P-chromic phosphate suspension into the peritoneal cavity or pleural cavity has been effective in the palliative treatment of painful symptoms resulting from the accumulation of fluid in these cavities. The insoluble colloidal particles of chromic phosphate, mostly in the 1 to 2 μm range, are engulfed by floating macrophages and eventually by fixed tissue macrophages lining the wall of the serous cavity. The beta radiation from ^{32}P causes fibrosis of the mesothelium and small blood vessels, which leads to reduced fluid production.[71] The dosage range for intraperitoneal instillation is 10 to 20 mCi (370 to 740 MBq), and for intrapleural instillation it is 6 to 12 mCi (222 to 444 MBq). ^{32}P-chromic phosphate can be dispersed in 30 to 50 mL of sterile saline before instillation. A patent route of instillation can be ascertained before administration of ^{32}P-chromic phosphate suspension by introducing ^{99m}Tc-sulfur colloid and imaging the cavitary distribution with a gamma camera. The accumulated cavitary fluid is removed prior to

^{32}P-chromic phosphate administration because large volumes of fluid will reduce the radiation dose delivered to the tissue.

Studies have shown that the rate of recurrence of ovarian cancer is decreased after radical surgery if ^{32}P-chromic phosphate is administered during the second-look operation. Second-look patients treated with ^{32}P-chromic phosphate have shown higher survival rates (85%) than untreated patients (50%).[72,73]

Radiation Synovectomy

Diseases such as rheumatoid arthritis cause synovial inflammation in the joints. The inflammatory process involves increased secretion of synovial fluid and the release of enzymes and cell factors that result in cartilage degradation and eventual joint destruction. The disadvantages associated with surgical synovectomy (hospitalization, physical therapy, and cost) led to the use of radiation synovectomy. Radiation synovectomy involves the injection of a nondiffusible radioactive agent into the involved joint space.[74] Ideally, the agent should not leak out of the joint space. Local irradiation of the inflamed synovial lining decreases fluid production and the pain associated with intra-articular pressure. There is also destruction of the cells responsible for releasing enzymes and cytokines that mediate joint destruction.

The ideal agent for radiation synovectomy should have a beta energy with a range of 5 to 10 mm in tissue to effectively destroy the synovium but spare the cartilage and a dose rate that limits the production of an acute inflammatory response.[74] ^{32}P-chromic phosphate appears to possess ideal properties in that its maximum beta range in tissue is 7.9 mm and its half-life of 14.3 days permits administration of a smaller amount of radioactivity, ranging from 1 to 2 mCi (37 to 74 MBq), to bring about a slow destruction of tissue without inducing an acute inflammatory response.[74] The ^{32}P-chromic phosphate particles are phagocytized by synovial macrophages, helping to retain the particles within the joint space.

^{125}I-IOTREX

The GliaSite Radiation Therapy System (RTS, Proxima) was designed for intracavitary brachytherapy of malignant gliomas in the brain.[75] The RTS is an inflatable balloon catheter that is placed into a resection cavity in the brain after surgical removal of a brain tumor (Figure 23-5). During treatment planning, the balloon is filled with saline containing contrast material, and an MRI image is made for assessment of the required radiation dose and tissue depth. After this, the required ^{125}I-Iotrex activity, dwell time, and dose rate are determined for a specified balloon volume. At the time of treatment, the saline is removed from the balloon and ^{125}I-Iotrex in the prescribed volume is instilled into the balloon, where it remains for 3 to 6 days. The exact dwell time is determined by the prescribed radiation dose required for treatment. Doses range from 40 to 60 rad(cGy). ^{125}I-Iotrex in the balloon delivers radiation to the margins of brain cavities created by tumor resection. Radiation dose is typically applied over a tissue depth of 0.5 to 2 cm.

^{125}I-Iotrex is a sterile solution containing sodium 3-^{125}I-iodo-4-hydroxybenzenesulfonate (Figure 23-6). It is available from MDS Nordion in a conical glass vial in a 1 mL volume with a nominal activity of 195 mCi/mL (7215 MBq/mL). The ^{125}I is organically bound and is readily excreted in the urine in the event that it inadvertently leaches from the balloon during treatment.[76] Under normal operating conditions, the balloon is expected to release about 1% of the ^{125}I-Iotrex. The radiation dose to all organs is estimated to be below the thresholds for deterministic effects in the unlikely event of a release of a maximum dose of 450 mCi (16,650 MBq) systemically.[76] The effective dose from this

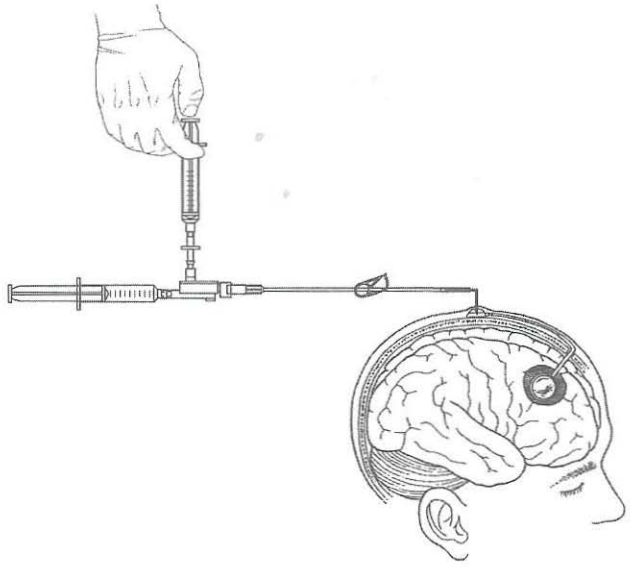

FIGURE 23-5 Administration technique for ^{125}I-Iotrex in malignant glioma brachytherapy. (Used with permission of Proxima Therapeutics Inc., Alpharetta, GA.)

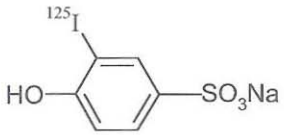

FIGURE 23-6 Chemical structure of ^{125}I-Iotrex.

amount if 1% is released is estimated to be 0.24 rad(cGy); if 100% is released, the effective dose is 24 rad(cGy).[77]

Radioassay of ^{125}I-Iotrex requires specific attention to geometry considerations because of the low-energy photons emitted from ^{125}I. The correct procedure is described in the product brochure and package insert. In general, dose calibration factors for Capintec dose calibrators have been established for measuring the dose in a 5 mL BD (Becton, Dickinson) plastic syringe fitted with a 1.5 inch needle. Calibration factors for dose calibrators of other manufacturers must be determined using an ^{125}I standard. The dose should be assayed with no air space between the liquid surface and the rubber plunger, because of a substantial difference in the readings. Typically, residual activity in the syringe is assayed after dose administration to determine the exact amount of activity injected into the balloon. Again, because of sensitive geometry considerations, a volume of saline equal to the original dose volume must be introduced into the empty syringe to obtain an accurate assay of residual activity.

REFERENCES

1. Krieger MS, Weiden PL, Breitz HB, et al. Radioimmunotherapy in the treatment of non-Hodgkin's lymphoma. In: Abrams PG, Fritzberg AR, eds. *Radioimmunotherapy of Cancer.* New York: Marcel Dekker; 2000:245-63.
2. Reff ME, Carner K, Chambers KS, et al. Depletion of B cells in vivo by a chimeric mouse human monoclonal antibody to CD20. *Blood.* 1994;83:435-45.

3. Maloney DG, Grillo-Lopez AJ, White CA, et al. IDEC-C2B8 (Rituximab) anti-CD20 monoclonal antibody therapy in patients with relapsed low-grade non-Hodgkin's lymphoma. *Blood.* 1997;90:2188-95.
4. McLaughlin P, Grillo-Lopez AJ, Link BK, et al. Rituximab chimeric anti-CD20 monoclonal antibody therapy for relapsed indolent lymphoma: half of patients respond to a four-dose treatment program. *J Clin Oncol.* 1998;16:2825-33.
5. Mattes MJ. Pharmacokinetics of antibodies and their radiolabels. In: Goldenberg DM, ed. *Cancer Therapy with Radiolabeled Antibodies.* Boca Raton, FL: CRC Press; 1995:89-99.
6. Juweid ME. Radioimmunotherapy of B-cell non-Hodgkin's lymphoma: from clinical trial to clinical practice. *J Nucl Med.* 2002;43:1507-29.
7. Zalutsky MR. Radiohalogens for radioimmunotherapy. In: Abrams PG, Fritzberg AR, eds. *Radioimmunotherapy of Cancer.* New York: Marcel Dekker; 2000:81-106.
8. DeNardo GL, Juweid ME, White CA, et al. Role of radiation dosimetry in radioimmunotherapy planning and treatment dosing. *Crit Rev Oncol Hematol.* 2001;39:203-18.
9. Juweid M, Dunn R, Zhang CH, et al. The contribution of whole-body radiation to red marrow dose in patients receiving radioimmunotherapy with ^{131}I-labeled anti-carcinoembryonic antigen monoclonal antibodies [abstract]. *Cancer Biother Radiopharm.* 1998;13:319.
10. Kaminski MS, Zasadny KR, Francis IR, et al. Iodine-131-anti-B1 radioimmunotherapy for B-cell lymphoma. *J Clin Oncol.* 1996;14:1974-81.
11. Witzig T, White CA, Wiseman G, et al. Phase I/II trial of IDEC-Y2B8 radioimmunotherapy for treatment of relapsed or refractory CD20+ B-cell non-Hodgkin's lymphoma. *J Clin Oncol.* 1999;17:3793-3803.
12. Press OW, Eary JF, Appelbaum FR, et al. Radiolabeled-antibody therapy of B-cell lymphoma with autologous bone marrow support. *N Engl J Med.* 1993;329:1219-24.
13. Chinn PC, Leonard JE, Rosenberg J, et al. Preclinical evaluation of ^{90}Y-labeled anti-CD 20 monoclonal antibody for treatment of non-Hodgkin's lymphoma. *Int J Oncol.* 1999;15:1017-25.
14. Zevalin [package insert]. San Diego, CA: Idec Pharmaceuticals; 2002.
15. Witzig TE, Gordon LI, Cabanillas F, et al. Randomized controlled trial of yttrium-90-labeled ibritumomab tiuxetan radioimmunotherapy versus rituximab immunotherapy for patients with relapsed or refractory low-grade, follicular, or transformed B-cell non-Hodgkin's lymphoma. *J Clin Oncol.* 2002;20:2453-63.
16. Wiseman GA, White CA, Stabin M, et al. Phase I/II ^{90}Y-Zevalin (yttrium-90 ibritumomab tiuxetan, IDEC-Y2B8) radioimmunotherapy dosimetry results in relapsed or refractory non-Hodgkin's lymphoma. *Eur J Nucl Med.* 2000;27:766-77.
17. Wagner HN Jr, Wiseman GA, Marcus CS, et al. Administration guidelines for radioimmunotherapy of non-Hodgkin's lymphoma with ^{90}Y-labeled anti-CD20 monoclonal antibody. *J Nucl Med.* 2002;43:267-72.
18. Vose JM, Wahl RL, Saleh M, et al. Multicenter phase II study of iodine-131 tositumomab for chemotherapy-relapsed/refractory low-grade and transformed low-grade B-cell non-Hodgkin's lymphoma. *J Clin Oncol.* 2000;18:1316-23.
19. Kaminski MS, Zelenetz AD, Press OW, et al. Pivotal study of iodine I-131 tositumomab for chemotherapy-refractory low-grade or transformed low-grade B-cell non-Hodgkin's lymphomas. *J Clin Oncol.* 2001;19:3918-28.
20. Wahl RL, Zasadny KR, Estes J, et al. Single center experience with iodine ^{131}I tositumomab radioimmunotherapy for previously untreated follicular lymphoma (FL) [abstract]. *J Nucl Med.* 2000;41(suppl):79P.
21. Press O, Eary JF, Appelbaum FR, et al. Phase II trial of ^{131}I-B1 (anti-CD20) antibody therapy with autologous stem cell transplantation for relapsed B-cell lymphomas. *Lancet.* 1995;346:336-40.
22. Liu SY, Eary JF, Petersdorf SH, et al. Follow-up of relapsed B-cell lymphoma patients treated with iodine-131-labeled anti-CD20 antibody and autologous stem-cell rescue. *J Clin Oncol.* 1998;16:3270-8.
23. Juweid M, Sharkey RM, Markowitz A, et al. Treatment of non-Hodgkin's lymphoma with radiolabeled murine, chimeric, or humanized LL2, an *anti*-CD22 monoclonal antibody. *Cancer Res.* 1995;55:5899-907s.
24. Shih LB, Lu HH, Xuan H, et al. Internalization and intracellular processing of an anti-B-cell lymphoma monoclonal antibody, LL2. *Int J Cancer.* 1994;56:538-45.
25. Sharkey RM, Behr TM, Mattes MJ, et al. Advantage of residualizing radiolabels for an internalizing antibody against the B-cell lymphoma antigen, CD22. *Cancer Immunol Immunother.* 1997;44:179-88.
26. Shih LB, Thorpe SR, Griffiths GL, et al. The processing and fate of antibodies and their radiolabels bound to the surface of tumor cells in vitro: a comparison of nine radiolabels. *J Nucl Med.* 1994;35:899-908.
27. Naruki Y, Carrasquillo JA, Reynolds JC, et al. Differential cellular catabolism of ^{111}In, ^{90}Y, and ^{125}I radiolabeled T101 anti-CD5 monoclonal antibody. *Nucl Med Biol.* 1990;17:201-7.
28. Geissler F, Anderson SK, Venkatesan P, et al. Intracellular catabolism of radioiodinated anti-μ antibodies by malignant B-cells. *Cancer Res.* 1992;52:2907-15.
29. Dumas P, Maziere B, Autissoer N, et al. Specificite de l'iodotyrosine desiodase des microsomes thyroidiens et hepatiques. *Biochim Biophys Acta.* 1973;293:36-47.
30. Stein R, Goldenberg DM, Thorpe SR, et al. Effects of radiolabeling monoclonal antibodies with a residualizing iodine radiolabel on the accretion of radioisotope in tumors. *Cancer Res.* 1995;55:3132-9.

31. Juweid ME, Stadtmauer E, Hajjar G, et al. Pharmacokinetics, dosimetry, and initial therapeutic results with ^{131}I- and ^{111}In/^{90}Y-labeled humanized LL2 anti-CD22 monoclonal antibody in patients with relapsed, refractory non-Hodgkin's lymphoma. *Clin Cancer Res.* 1999;5(suppl):3292-3303s.
32. DeNardo GL, DeNardo SJ. Treatment of B-lymphocyte malignancies with ^{131}I-LYM-1 and ^{67}Cu-2IT-BAT-LYM-1 and opportunities for improvement. In: Goldenberg DM, ed. *Cancer Therapy with Radiolabeled Antibodies.* Boca Raton, FL: CRC Press; 1995: 217-27.
33. O'Grady LF, DeNardo GL, DeNardo SJ. Radiolabeled monoclonal antibodies for the detection of cancer. *Am J Physiol Imag.* 1986;1:44-9.
34. Fritzberg AR, Meares CF. Metallic radionuclides for radioimmunotherapy. In: Abrams PG, Fritzberg AR, eds. *Radioimmunotherapy of Cancer.* New York: Marcel Dekker; 2000:57-79.
35. Griffiths GL. Radiochemistry of therapeutic radionuclides. In: Goldenberg DM, ed. *Cancer Therapy with Radiolabeled Antibodies.* Boca Raton, FL: CRC Press; 1995:47-61.
36. Linder MC, Hazegh-Azam M. Copper biochemistry and molecular biology. *Am J Clin Nutr.* 1996;63:797s-811s.
37. Schlom J, Molinolo A, Simpson JF, et al. Advantage of dose fractionation in monoclonal antibody-targeted radioimmunotherapy. *J Natl Cancer Inst.* 1990;82:763-71.
38. DeNardo SJ, DeNardo GL, Kukis DL, et al. ^{67}Cu-2IT-BAT-Lym-1 pharmacokinetics, radiation dosimetry, toxicity and tumor regression in patients with lymphoma. *J Nucl Med.* 1999;40:302-10.
39. DeNardo GL, Kukis DL, Shen S, et al. ^{67}Cu- versus ^{131}I-labeled Lym-1 antibody: comparative pharmacokinetics and dosimetry in patients with non-Hodgkin's lymphoma. *Clin Cancer Res.* 1999;5:533-41.
40. Chinol M, Grana C, Gennari R, et al. Pretargeted radioimmunotherapy of cancer. In: Abrams PG, Fritzberg AR, eds. *Radioimmunotherapy of Cancer.* New York: Marcel Dekker; 2000:169-193.
41. Theodore LJ, Fritzberg AR, Schultz JE, et al. Evolution of a pretarget radioimmunotherapeutic regimen. In: Abrams PG, Fritzberg AR, eds. *Radioimmunotherapy of Cancer.* New York: Marcel Dekker; 2000:195-221.
42. Paganelli G, Magnani P, Siccardi AG, et al. Clinical application of the avidin-biotin system for tumor targeting. In: Goldenberg DM, ed. *Cancer Therapy with Radiolabeled Antibodies.* Boca Raton, FL: CRC Press; 1995:239-54.
43. Paganelli G, Grana C, Chinol M, et al. Antibody guided three-step therapy for high grade glioma with yttrium-90 biotin. *Eur J Nucl Med.* 1999;26:348-57.
44. Breitz HB, Weiden PL, Beaumier PL, et al. Clinical optimization of pretargeted radioimmunotherapy (PRIT™) with antibody–streptavidin conjugate and ^{90}Y-DOTA-biotin. *J Nucl Med.* 2000;41:131-40.
45. Robinson RG, Preston DF, Spicer JA, et al. Radionuclide therapy of intractable bone pain: emphasis on strontium-89. *Semin Nucl Med.* 1992;22:28-32.
46. Silberstein EB. Systemic radiopharmaceutical therapy of painful osteoblastic metastases. *Semin Radiat Oncol.* 2000;10:240-9.
47. Serafini AN. Therapy of metastatic bone pain. *J Nucl Med.* 2001;42:895-906.
48. Silberstein EB. Dosage and response in radiopharmaceutical therapy of painful osseous metastases. *J Nucl Med.* 1996;7:249-52.
49. Friedell HL, Storaasli JP. The use of radioactive phosphorus in the treatment of carcinoma of the breast with widespread metastases to bone. *AJR Am J Roentgenol.* 1950;64:559-75.
50. Silberstein EB. The treatment of painful osseous metastases with phosphorus-32-labeled phosphates. *Semin Oncol.* 1993;20(suppl 2):10-21.
51. Nair N. Relative efficacy of ^{32}P and ^{89}Sr in palliation in skeletal metastases. *J Nucl Med.* 1999;40:256-61.
52. Herold TJ, Gross GP, Hung JC. A technique for measurement of strontium-89 in a dose calibrator. *J Nucl Med Technol.* 1994;22:110.
53. Eary JF, Collins C, Stabin M, et al. Samarium-153-EDTMP biodistribution and dosimetry estimation. *J Nucl Med.* 1993;34:1031-36.
54. Goeckeler WF, Troutner DE, Volkert WA, et al. ^{153}Sm radiotherapeutic bone agents. *Nucl Med Biol.* 1986;13:479-82.
55. Resche I, Chatal J-F, Pecking A, et al. A dose-controlled study of ^{153}Sm-ethylenediaminetetramethylene-phosphonate (EDTMP) in the treatment of patients with painful bone metastases. *Eur J Cancer.* 1997;33:1583-91.
56. Quadramet [package insert]. North Billerica, MA: Dupont-Merck; 1997.
57. Menda Y, Bushnell DL, Williams RD. Efficacy and safety of repeated samarium-153 lexidronam treatment in a patient with prostate cancer and metastatic bone pain. *Clin Nucl Med.* 2000;25:698-700.
58. Maxon HR, Deutsch EA, Thomas SR, et al. Re-186 (sn) HEDP for treatment of multiple metastatic foci in bone: human biodistribution and dosimetric studies. *Radiology.* 1988;166:501-7.
59. Maxon HR III, Thomas SR, Hertzberg VS, et al. Rhenium-186 hydroxyethylidene diphosphonate for the treatment of painful osseous metastases. *Semin Nucl Med.* 1992;22:33-40.
60. de Klerk JMH, van Dijk A, van het Schip AD, et al. Pharmacokinetics of rhenium-186 after administration of rhenium-186-HEDP to patients with bone metastases. *J Nucl Med.* 1992;33:646-51.

61. Atkins HL, Mausner LF, Srivastava SC, et al. Tin-117m(4+)-DTPA for palliation of pain from osseous metastases: a pilot study. *J Nucl Med.* 1995;36:725-9.
62. Bishayee A, Rao DV, Srivastava SC, et al. Marrow-sparing effects of ^{117m}Sn(4+) diethylenetriaminepentaacetic acid for radionuclide therapy of bone cancer. *J Nucl Med.* 2000;41:2043-50.
63. Srivastava SC, Atkins HL, Krishnamurthy GT, et al. Treatment of metastatic bone pain with tin-117m stannic diethylenetriaminepentaacetic acid: a phase I/II clinical study. *Clin Cancer Res.* 1998;4:61-8.
64. Hoffman R, Wasserman LR. Natural history and management of polycythemia vera. *Adv Intern Med.* 1979;24:255-85.
65. Chievitz E, Thiede T. Complications and causes of death in polycythemia vera. *Acta Med Scand.* 1962;172:513-23.
66. Shastri KA, Logue GL. Polycythemia vera. In: Rakel RE, ed. *Conn's Current Therapy.* Philadelphia: WB Saunders; 1993.
67. Wasserman LR. The treatment of polycythemia vera. *Semin Hematol.* 1976;13:57-78.
68. Spiers FW, Beddoe AH, King SD. The absorbed dose to bone marrow in the treatment of polycythemia by P-32. *Br J Radiol.* 1976;49:133-40.
69. Silberstein EB. Radionuclide therapy of hematologic disorders. *Semin Nucl Med.* 1979;9:100-7.
70. Osgood EE. Polycythemia vera: age relationships and survival. *Blood.* 1965;26:243-56.
71. Hazra TA, Howells R. Use of beta emitters for intracavitary therapy. In: Spencer RP, ed. *Therapy in Nuclear Medicine.* New York: Grune & Stratton; 1978:307-12.
72. Varia M, Rosenman J, Venkataraman S, et al. Intraperitoneal chromic phosphate therapy after second-look laparotomy for ovarian cancer. *Cancer.* 1988;61:919-27.
73. Rogers L, Varia M, Halle J, et al. ^{32}P following negative second-look laparotomy for epithelial ovarian cancer. *Gynecol Oncol.* 1993;50:141-6.
74. Shortkroff S, Sledge CB. Radiation synovectomy. In: Wagner HN Jr, Szabo Z, Buchanan JW, eds. *Principles of Nuclear Medicine.* Philadelphia: WB Saunders; 1995:1021-8.
75. Stubbs J, Frankel R, Schultz K, et al. Preclinical evaluation of a novel device for delivering brachytherapy to resected brain tumor cavity margins. *J Neurosurg.* 2002;96:335-43.
76. Stubbs JB, Strickland AD, Frank RK, et al. Biodistribution and dosimetry of an aqueous solution containing sodium 3-[^{125}I] iodo-4-hydroxybenzenesulfonate (Iotrex) for brachytherapy of resected malignant brain tumors. *Cancer Biother Radiopharm.* 2000;15:645-56.
77. Iotrex [package insert]. Alpharetta, GA: Proxima Therapeutics Inc, 2001.

Index

Page numbers followed by *t* or *f* refer to tables or figures, respectively.

F

T

U

V

W

X

Y

Z